HANDBOOK OF NATURAL GAS TRANSMISSION AND PROCESSING

PRINCIPLES AND PRACTICES

FOURTH EDITION

SAEID MOKHATAB, WILLIAM A. POE, AND JOHN Y. MAK

G P
P

Handbook of Natural Gas Transmission and Processing

Principles and Practices

Fourth Edition

Saeid Mokhatab
Gas Processing Consultant, Canada

William A. Poe
Senior Principal Technical Consultant, AVEVA, USA

John Y. Mak
Senior Fellow and Technical Director, Fluor, USA

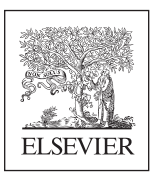

Gulf Professional Publishing
An imprint of Elsevier

Gulf Professional Publishing is an imprint of Elsevier
50 Hampshire Street, 5th Floor, Cambridge, MA 02139, United States
The Boulevard, Langford Lane, Kidlington, Oxford, OX5 1GB, United Kingdom

Notices
Knowledge and best practice in this field are constantly changing. As new research and experience broaden our understanding, changes in research methods, professional practices, or medical treatment may become necessary.

Practitioners and researchers must always rely on their own experience and knowledge in evaluating and using any information, methods, compounds, or experiments described herein. In using such information or methods they should be mindful of their own safety and the safety of others, including parties for whom they have a professional responsibility.

To the fullest extent of the law, neither the Publisher nor the authors, contributors, or editors, assume any liability for any injury and/or damage to persons or property as a matter of products liability, negligence or otherwise, or from any use or operation of any methods, products, instructions, or ideas contained in the material herein.

Library of Congress Cataloging-in-Publication Data
A catalog record for this book is available from the Library of Congress

British Library Cataloguing-in-Publication Data
A catalogue record for this book is available from the British Library

ISBN: 978-0-12-815817-3

Publisher: Joe Hayton
Acquisition Editor: Katie Hammon
Editorial Project Manager: Ali Afzal-Khan
Production Project Manager: Bharatwaj Varatharajan
Cover Designer: Greg Harris

Typeset by TNQ Technologies

Disclaimer

This book is intended to be a learning tool. The materials discussed in this book are presented solely for educational purposes and are not intended to constitute design specifications or operating procedures. While every effort has been made to present current and accurate information, the authors assume no liability whatsoever for any loss or damage resulting from using them.

This book is dedicated to all professionals that preceded us: researchers, scientists, engineers, operators, and educators in the natural gas industry, who inspire us to assemble their knowledge and experience, manifesting this book that is much needed in today's changing landscape of natural gas.

With Contribution by

Jean-Noël Jaubert, Romain Privat (Université de Lorraine, France) and **Epaminondas Voutsas** (National Technical University of Athens, Greece)
Authors of Chapter 2, Phase Behavior of Natural Gas Systems

Wim Van Wassenhove (Billington Process Technology AS, Norway)
Author of Chapter 19, Process Modelling and Simulation of Gas Processing Plants

Laura A. Pellegrini, Giorgia De Guido, and **Stefano Langé** (Politecnico di Milano, Italy)
Authors of Chapter 22, Energy and Exergy Analyses of Natural Gas Processing Plants

About the Authors

Saeid Mokhatab is one of the most recognizable names in the natural gas community through his contributions to advancing the technologies in the natural gas processing industry. He has been actively involved in different aspects of several large-scale gas processing projects, from conceptual design through plant startup and operations support. He has presented on gas processing technologies worldwide and has published 300 technical papers and two renowned Elsevier's handbooks in collaboration with leading experts from the largest international engineering companies and prominent process licensors. His numerous publications, which are widely read and highly respected, have set the technical standards in the natural gas processing industry and are considered by many as major references to be used for any gas processing/LNG project in development. He founded the world's first peer-reviewed journal devoted to natural gas science and engineering (published by Elsevier, the United States) and has held editorial positions for many scientific journals/book publishing companies in the hydrocarbon processing industry. He has also served as a member of technical committees for several professional societies and acclaimed gas processing conferences worldwide. As a result of his outstanding work in the natural gas industry, he has received a number of international awards and medals, and his biography has been listed in highly prestigious directories.

William A. "Bill" Poe is a Senior Principal Technical Consultant at AVEVA, the United States. He has over 35 years of international business and industrial experience in design, operations, and project management of gas processing plants with a special focus on automation, multivariable predictive control (MPC), advanced process control (APC), optimization design and implementation, and real-time performance monitoring. Bill started his career at Shell Oil Company, USA, in 1981, working over a decade in natural gas processing plants operations and engineering as well as management of multimillion-dollar projects. In 1993, he joined Continental Controls to lead the process engineering department in support of executing contracts with the Gas Research Institute, USA, where he developed new multivariable control applications in the natural gas industry. After joining GE as part of the Continental Controls acquisition, he became vice president of this division of GE where his responsibilities included direction of product development, projects, technical sales support, and customer service for multivariable control and optimization applications in the natural gas industry. In 2001, Bill joined Invensys Process Systems, USA, where he has developed APC and Optimization Master Plans for international companies such as Saudi Aramco, ADNOC, Statoil, and PDVSA, as well as automation and advanced process control feasibility studies for over 100 natural gas processing plants worldwide. After Schneider Electric acquired Invensys Process Systems in 2014 and merged its software division with AVEVA in 2018, he has continued to work with the top gas processing companies. Bill is an Associate Editor of the *Journal of Natural Gas Science & Engineering*, has authored or coauthored more than 60 technical papers, and made numerous technical presentations at prestigious international conferences. He received the GE Innovators Award in 1999 and attained the Invensys Circle of Excellence in 2011.

John Y. Mak is a Senior Fellow and Technical Director at Fluor, the United States, and leads the technology and design development for Fluor chemical and energy division. He is the technical expert and SME with Fluor for over 40 years and has been leading major oil and gas, petrochemical and refinery projects from conceptual designs, feasibility studies, FEED development, detailed engineering,

to plant start-up and performance testing. John has made contributions to innovations in natural gas treating and processing, NGL recovery, LNG liquefaction and regasification, synthesis gas purification, and carbon capture methods. John is the coauthor of the *Handbook of Liquefied Natural Gas*, first edition (2013) published by Elsevier, the United States. He has published over 80 technical papers and has frequently presented his findings at technical conferences such as GPA Midstream Convention, GPA Europe, Laurance Reid Gas Conditioning Conference, LNG Summit, Offshore Technology Conference, GASTECH, and China Coal Forum. John is the inventor of over 90 patents and patent pending processes. John is specializing in more complex NGL recovery designs for conventional and unconventional gases, treating high CO_2 content gases using physical solvents, acid gas removal with amines, cryogenic nitrogen rejection, and helium recovery.

Preface to the Fourth Edition

Natural gas is an abundant global resource and is a clean burning fuel that offers important environmental benefits compared to other fossil fuels. Natural gas is a versatile and safe source of energy that is necessary to bridge us to the future of renewable sources. The surge of natural gas production from unconventional sources is remarkable and further underscores the importance of gas processing. In this regard, it is fitting that the most up-to-date technical materials covering these subjects be well-known to gas producers, gas processors, technical specialists, and project developers. While many publications and books are available, there is a lack of a comprehensive book that captures the complete natural gas value chain from well-head to the end-user. This updated book provides the basic theoretical and practical background, while also covering innovations and new developments in the subject areas.

Many interesting and exciting developments in the natural gas industry have emerged since the publication of the third edition in 2015 that provoked us to add and update several sections. We reviewed published materials and selected the most appropriate and viable innovations, combined with our own research and practical experience for updating. The result is a more complete and comprehensive reference that fully covers the ranges of today's challenging gas processing problems. Six new chapters have been added to include detailed discussion of the thermodynamic and energy efficiency of relevant processes, and innovations in processing super-rich gas, high CO_2 content gas, and high nitrogen content gas with other contaminants.

This book is a major contribution to the professional literature as we have attempted to concentrate on what we perceive to be an acceptable design and proven practices. The organization of content addresses the design aspects that are important to students in the engineering curricula, and the operating and trouble-shooting facets for plant operators. We hope this handbook provides the design reference and conveys valuable experience to both the beginners and the experienced.

The preparation of a book that covers such a broad subject requires different sources of information. We gratefully acknowledge our indebtedness to all of the individuals who contributed to the development of this book. An invaluable contribution to this edition is the insight by experts in their specialties and applications. Special thanks are due to friends and colleagues, who encouraged, assessed, and made this book possible. Among them are Dr. Louis Mattar and Dr. Mehran Pooladi-Darvish of the Fekete Associates Inc., Canada, who prepared the section on 'Natural Gas Exploration and Production' in Chapter 1. We also appreciate Mr. Cris Heijckers of Kranji Solutions Pte Ltd., Singapore, for preparing a section on 'Practical Design of Separation Systems' in Chapter 5. We deeply acknowledge the greatest help of Dr. Rainer Kurz of Solar Turbines Inc., USA, in updating Chapter 14. We thank Mr. Sidney P. Santos of At Work Rio Engineering and Consulting Ltd., Brazil, for his constructive comments and suggestions on Chapter 15. We also express our sincere appreciation to Dr. Scott Northrop of ExxonMobil Upstream Research Company, USA, and Mr. Michael Mitariten of Air Liquide, USA, who provided valuable comments for the betterment of the book. Finally, we appreciate the editorial staff members of Elsevier who have been an excellent source of strong support during the preparation and publication of this book.

The accelerated delivery of information contained in this handbook is important as we all strive to adapt to the latest technology in gas processing for a greener and safer environment. Our mission is to continuously follow the progress, add new materials in the future editions, and update the fundamental and practical materials already in this edition.

Saeid Mokhatab
William A. Poe
John Y. Mak

Endorsements for the Fourth Edition

This handbook is a valuable reference that covers all aspects of the natural gas transmission and processing industries. It contains much needed design, operation, and optimization information, all in a single source and does an excellent job of highlighting the key considerations for any gas processing project, as well as providing innovative solutions in natural gas liquids recovery and treating high nitrogen and carbon dioxide content gases in unconventional gas plants. It is a key addition to any gas processing professional's library.

Jason Kraynek, Vice President of Business Transformation & Innovations, Fluor, USA.

This handbook is a valuable reference that covers all aspects of natural gas processing and handling. It has been fully updated in this fourth edition to also cover the recent developments in dealing with more sour gases and gases that contain all kinds of contaminants. It provides a good insight into the operational and technical aspects of handling of natural gases. A great reference for students, operators, and engineers working in the natural gas industry.

Frank Scheel, Director of Technology, Jacobs—Comprimo Sulfur Solutions, the Netherlands.

This well-balanced book is a must read for anyone in the natural gas business due to its completeness in the coverage of all aspects of the natural gas transmission and processing industry. In addition to covering some topics rarely discussed and hard to find in the literature, it fully addresses the complex elements of the gas processing industry as well as practical advices for the safe design and operation of gas plants in a straightforward fashion, which makes the book appealing to all parties who are involved in the natural gas field development projects.

Philip Hunter, Senior Vice President—Global LNG/FLNG/GTL Technology & Development, KBR, UK.

This high quality, comprehensive book gives an accurate picture of where the natural gas transmission and processing industry stands today, and describes some relatively new technologies that could become important in the future. I recommend this book for any professional gas processing engineer and technologist.

David Messersmith, Bechtel Fellow and Manager of LNG Technology and Services Group, Bechtel OG&C, USA.

This is a valuable handbook to both an experienced engineer and a graduate just commencing in natural gas engineering. It provides practical advice for design and operation based on sound engineering principles and established techniques as well as introducing process solutions based on new and emerging technologies.

Adrian Finn, Manager of Process Technology, Costain Natural Resources, UK.

This is a wide ranging book providing the reader with much more information than that necessary to just support the engineering of a gas plant. Having introduced the fundamental science of natural gas, it covers sources, products, transportation, and economics of natural gas production, before covering all the unit operations involved in gas treatment to meet product specifications. Additional sections are included covering control systems, dynamic simulation, maximizing gas plant profitability, and gas plant project management, and these contribute to what is a holistic handbook that will educate all those who wish to learn about the subject.

Jon Lewis, Vice President of Gas Processing and Sulfur Recovery,
Advisian, WorleyParsons Group, UK.

This book comes at a critical time when many nations are shifting to an increasingly higher percentage of natural gas use within their range of energy sources. Giving the reader a comprehensive insight into the natural gas transmission and processing industry, this book will prove invaluable in orienting the newcomer and extending the scope of understanding of the veteran.

Lorenzo Micucci, Manager of Technology and Markets Research, Siirtec Nigi, Italy.

This comprehensive reference book covers all technical aspects of natural gas transmission and processing in a very practical manner. Contrary to other books, it is pleasant to read, and the information, always accurate, can be found easily. Very importantly, it also describes emerging trends and helps to understand what the future of gas processing could look like.

Alexandre Terrigeol, Sales and Technical Manager, CECA Molecular Sieves, France.

A very useful handbook that covers topics that others have missed. Highly recommended for any professionals who are involved with the natural gas transmission and processing industry. The authors are experts in their field and provide high quality coverage of subjects that are current and of practical use to long time professionals as well as newcomers. The material is quite comprehensive and covers all aspects of natural gas making this a need to have reference book.

Dr. Thomas H. Wines, Director of Applications Development, Pall Corporation, USA.

The reader will find the information on gas handling from the wellhead to the consumer to not only be informative, but be presented with an eye toward practical applications and with an operations understanding. The comprehensive coverage of the subjects makes it a useful guide to those new to the natural gas transmission and processing industry and a ready reference for more experienced engineers.

Michael J. Mitariten, Senior Director, Natural Gas and Biogas Separations,
Air Liquide, USA.

This excellent handbook gives a comprehensive insight into the complete natural gas transmission and processing industry. As such, it is the perfect companion for young process engineering graduates just starting to learn the business, as well as for more experienced engineers looking for a desktop reference book. I enjoyed especially the fine balance the authors found between the introduction of each process step, the description of the most important process design principles (including safety and environmental), and the so important (and sometimes forgotten) operational aspects of efficiently and safely running the plant. I especially liked the chapter on "Real-Time Optimization of Gas Processing Plants" as it covers the practical requirements of advanced process control, real time optimization, and the underlying process models and it rounds it all up with a detailed description of a successful real-life example.

Dr. Michael Brodkorb, EMEA Software Consulting Manager, Honeywell Process Solutions, Spain.

This comprehensive book provides in-depth coverage of all technical aspects of natural gas transmission and processing, beyond those addressed in other books. This is a "must addition" to library of anyone working in the midstream and downstream sectors of natural gas utilization to achieve higher career goals. I commend the authors' continuous effort to make it an excellent source book for all professionals, engineers, and scientists in the natural gas industry.

Dr. Suresh C. Sharma, ONEOK Chair Professor and Director of Natural Gas Engineering and Management, University of Oklahoma, USA.

This book is a major contribution to the professional literature and will serve as a valuable desk reference for scientists, researchers, and engineers working in the upstream, midstream, and downstream sectors of natural gas industry. Literature references for in-depth study enhance the reference aspect of this comprehensive work. The organization of materials also permits flexibility in designing courses in the gas processing field for university students in chemical/petroleum engineering curricula.

Dr. Kenneth R. Hall, Professor of Chemical Engineering and Associate Dean for Research and Graduate Studies, Texas A&M University at Qatar, Qatar.

This comprehensive book provides a state-of-the-art treatment of the different aspects of natural gas transmission and processing from the fundamental principles to the latest technology developments. It is a unique reference for all professionals involved in natural gas industry and an excellent textbook for graduate programs on the subject.

Dr. Valerio Cozzani, Professor of Chemical Engineering and Director of Postgraduate Program on Oil and Gas Process Design, University of Bologna, Italy.

Natural gas transmission and processing industry requires engineers to be provided with books and materials that would help them put their best effort towards understanding the many complex concepts. In spite of the tremendous pressure experienced by the professionals, there is a lack of adequate support material. This comprehensive book, which is the first example of its kind with a massive coverage of subjects, is a great step towards this endeavor. An impressive feature of this book is the high competence of authors who are perfectly versed in their areas of specialization.

Dr. Jean-Noël JAUBERT, Professor of Chemical Engineering and Head of the Thermodynamics and Energy Research Group, University of Lorraine, France.

This unique handbook, written by internationally renowned gas-engineering experts, is a major contribution to the professional and scholarly literature, offering an excellent coverage of key topics in the natural gas supply chain. It addresses the principles, practices, advanced technologies, new issues, and challenges related to the natural gas transmission and processing industry, which have not been addressed in depth in any existing books. I recommend it highly, as a reference and textbook.

Dr. Brian F. Towler, Professor and Chair of Petroleum Engineering, University of Queensland, Australia.

This is a comprehensive handbook that provides a wide and detailed coverage of the different aspects of natural gas transmission and processing, representing a valuable guide for scientists, researchers, university students, and engineers working in the relevant fields. It is the reference book for my research group when we need some tips on natural gas processing.

Dr. Laura A. Pellegrini, Professor of Chemical Plants and Director of Graduate and Postgraduate Program in Chemical Engineering, Politecnico di Milano, Italy.

CHAPTER

NATURAL GAS FUNDAMENTALS 1

1.1 INTRODUCTION

Natural gas is the most energy efficient fossil fuel—it offers important energy saving benefits when it is used instead of oil or coal. Although the primary use of natural gas is as a fuel, it is also a source of hydrocarbons for petrochemical feedstocks and a major source of elemental sulfur, an important industrial chemical. Its popularity as an energy source is expected to grow substantially in the future because natural gas can help achieve two important energy goals for the 21st century—providing the sustainable energy supplies and services needed for social and economic development and reducing adverse impacts on global climate and the environment in general. Natural gas consumption and trade have been growing steadily over the past two decades and natural gas has strengthened its position in the world energy mix. Although the demand for natural gas declined in 2009, as a result of the economic slowdown, it is expected to resume growth in both emerging and traditional markets in the coming decades. Such increase in the near future will be driven because of additional demand in current uses, primarily power generation. There is yet a little overlap between the use of natural gas and oil in all large markets. However, there are certain moves in the horizon, including the electrifying of transportation, which will push natural gas use to ever higher levels.

This chapter gives the reader an introduction to natural gas by describing the origin and composition of natural gas, gas sources, phase behavior and properties, and transportation methods.

1.2 NATURAL GAS HISTORY

The discovery of natural gas dates back to ancient times in the Middle East. It was considered by ancients to be a supernatural manifestation. Noticed only when ignited, it appeared as a mysterious fire bursting from fissures in the ground. Natural gas seeps were discovered in Iran between 6000 and 2000 BC. The practical use of natural gas dates back to the Chinese 2500 years ago, who used bamboo pipes to collect it from natural seeps and convey it to gas-fired evaporators, where it was used to boil ocean water for salt. Apparently, natural gas was unknown in Europe until its discovery in England in 1659. However, since manufactured gas (coal gas) was already commercially available, natural gas remained unpopular. In 1815, natural gas was discovered in the United States during digging of a salt-brine well in Charleston, West Virginia. In 1821, an American gunsmith named William Aaron Hart drilled the first natural gas well in the United States. It was covered with a large barrel, and the gas was

Handbook of Natural Gas Transmission and Processing. https://doi.org/10.1016/B978-0-12-815817-3.00001-0

directed through wooden pipes that were replaced a few years later with lead pipe. One of the earliest attempts of monetization occurred in 1824 in Fredonia, New York, which led to the formation of the first natural gas company in the United States, the Fredonia Gas Light Company, in 1858.

The 19th century is considered as the starting point of the gas industry. In the early 1900s, huge amounts of natural gas were found in Texas and Oklahoma, and in the 1920s a modern seamless steel pipe was introduced. The strength of this new pipe, which could be welded into long sections, allowed gas to be carried under higher pressures and, thus, in greater quantities. As the technology to create a seamless steel pipe and related equipment advanced, the size and length of pipelines increased, as did the volumes of gas that could be transported easily and safely over many miles. The first natural gas pipeline longer than 200 miles was built in 1925, from Louisiana to Texas.

A steady growth in the use of gas was marked in the early and mid-twentieth century. However, it was the shortages of crude oil in the late 1960s and early 1970s that forced major industrial nations to seek energy alternatives. Since those events, gas has become a central fossil fuel energy source. Today, natural gas has become extremely important as a concentrated, clean fuel for home heating and cooking and electrical power generation, and is sought after almost as much as oil.

1.3 NATURAL GAS ORIGIN AND SOURCES

There are different theories as to the origins of fossil fuels. The most widely accepted theory of the origin of natural gas asserts that it came from organic matter (the remains of land and aquatic plants, animals, and microorganisms) that was trapped within sediments as they were deposited and transformed over long periods of time into their present form. Two main mechanisms, namely biogenic and thermogenic, are responsible for the degradation of the original fossil organic material in sediments (Rojey et al., 1997). Biogenic gas is formed at shallow depths and low temperatures due to the action of bacteria on the organic debris accumulating in the sediments. In contrast, thermogenic gas is formed at greater depths by degradation of organic matter, called kerogen, accumulated in fine-grained sediments, especially clays and shales. This degradation occurs through the combined effects of temperature and pressure. Thermogenic gas is believed to be produced through two mechanisms, namely, direct thermal cracking of sedimentary organic matter and secondary thermal cracking of oil that is formed in the first stage. The former is called the primary thermogenic gas that coexists with oil, while the latter is called secondary thermogenic gas that coexists with an insoluble solid matter, called pyrobitumen. Both mechanisms involve thermal cracking with some degree of sustained pressure, mainly through the weight of the sedimentary formation. Little information is available on the time required to generate thermogenic gas other than the general belief that it is a very long time.

Hydrocarbons are generated in “source rock” and often migrate to subsurface formations called “reservoir rock.” The quality of a reservoir rock is determined by its two principal properties: porosity and permeability. Porosity is the void space between the grains, and indicates the rock’s capacity to contain liquid or gaseous hydrocarbons. Permeability is the measurement of the rock’s ability to transmit the oil or gas.

Natural gas resources differ by the geological characteristics of their reservoir rock. In fact, natural gas comes from both “conventional” and “unconventional” geological formations (Fig. 1.1).

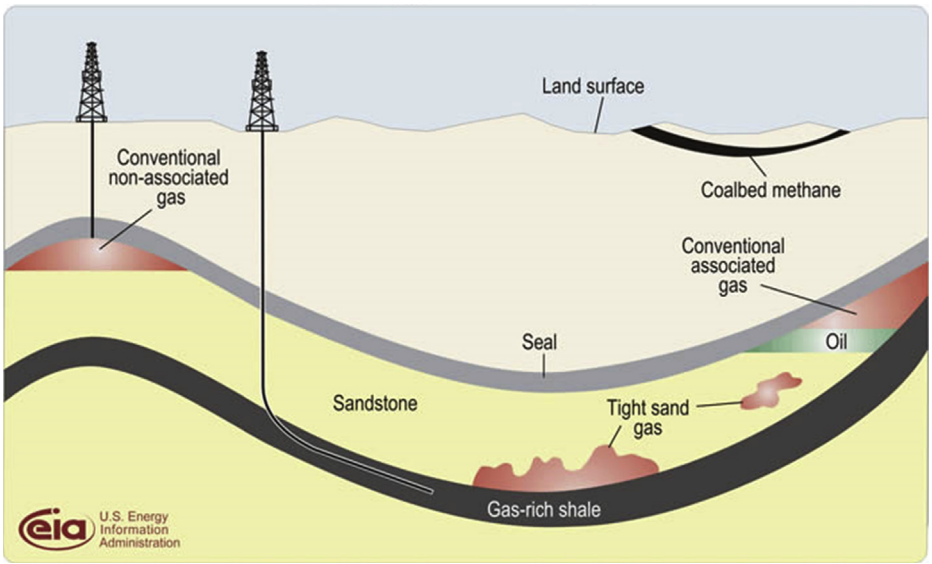

FIGURE 1.1

Schematic geology of natural gas resources.

1.3.1 CONVENTIONAL GAS

Conventional gas is typically "free gas" trapped in multiple porous zones in naturally occurring rock formations such as carbonates, sandstones, and siltstones. Conventional natural gas generally occurs in deep reservoirs, either associated with crude oil (associated gas[1]) or in reservoirs that contain little or no crude oil (nonassociated gas[2]).

Conventional gas is typically found in medium to highly porous reservoirs with a permeability greater than 1 millidarcy (mD). Pressure moves the gas towards the production wells (i.e., natural flow). As such, it can be extracted via traditional techniques that are relatively easy and inexpensive (Speight, 2013).

1.3.2 UNCONVENTIONAL GAS

Unconventional gas is the collective term for natural gas held in formations that are different from conventional reservoirs. Natural gas resources such as shales, tight gas sands, coal (also known as coalbed methane), geopressurized aquifers, and gas hydrates[3] are often referred to as unconventional gas resources. However, the three main types of unconventional natural gas resources are: *shale gas*, *tight gas*, and *coalbed methane*.

[1]Associated gas is produced with the oil and is sometimes separated at the casing head or wellhead. Gas produced in this fashion is also referred to as casing head gas or oil well gas.
[2]Nonassociated gas is sometimes referred to as gas well gas.
[3]Gas hydrates are ice-like structures of water and gas located under the permafrost, or under the sea.

Shale gas is extracted from shales (source rock, usually at depths greater than about 1500 m), which have naturally low permeability. The gas that shale contains (mainly methane) is either adsorbed onto the organic matter or left in a free state in the tiny void spaces (pores) of the rock. The only way to produce commercially meaningful quantities of gas from shale is by generating large hydraulic fractures in the formation through a process commonly known as "fracking." Large volumes of water and sand (proppant) are pumped downhole to open fractures in the shale formation. The sand fills the fractures so that the soft shale does not "heal" when the well is put on production. Initially, the well produces a substantial portion of the injected water. After that, gas will be produced at initially high rates, but those rates generally fall off over time.

Tight gas is trapped in ultra-compacted reservoirs characterized by relatively high porosity but with very low permeability (due to their laminated structures). Interconnections between the rock pores in the sandstone that contains the gas are very small, so the gas migrates through them with great difficulty.

Coalbed methane (also known as coal seam gas) is trapped in coal deposits, often near the surface. Most of the gas (primarily methane) is adsorbed on the lamellar surfaces of the coal, which is an excellent "storage medium." The permeability of the coal decreases with increasing depth, meaning that deeper wells have a lower production rate. As such, it is easy to drill and complete the coal deposit at shallow depths ($<$1000 m) at relatively low costs. However, there is an initial period of production where water must be unloaded from the well before gas production can commence.

A common characteristic of the different types of unconventional gas resources is that they contain large quantities of natural gas, but it is usually more difficult to produce this gas as compared to conventional reservoir rocks. In fact, unconventional gas is found in reservoirs with a relatively low permeability ($<$1 mD) and therefore, cannot be extracted by conventional methods (Speight, 2013). To extract natural gas at cost-effective rates, artificial pathways must be created. The key extraction technologies are horizontal drilling and hydraulic fracturing as described previously. Because of the relatively rapid decline rate of these wells, many more must be drilled compared to the number of wells needed for a conventional reservoir.

A large proportion of the gas produced globally to date was by conventional means (Speight, 2013). However, with improving extraction technology, many of the unconventional gas resources have either become viable or show promise to become economically viable in the future (Kelkar, 2008). In gas exporting regions, unconventional resources might complement conventional gas production; however, in gas importing regions, unconventional gas production can lead to falling gas prices and a reduction of gas imports (Korn, 2010).

1.4 NATURAL GAS COMPOSITION AND CLASSIFICATION

Natural gas is a complex mixture of hydrocarbon and nonhydrocarbon constituents and exists as a gas under atmospheric conditions. Virtually hundreds of different compounds may be present in natural gas in varying amounts. Even two wells producing from the same reservoir may produce gases of different composition as the reservoir is depleted.

While natural gas is formed primarily of methane (CH_4), it can also include significant quantities of ethane (C_2H_6), propane (C_3H_8), butane (C_4H_{10}), and pentane (C_5H_{12}) as well as traces of hexane (C_6H_{14}) and heavier hydrocarbons. Many natural gases often contain nitrogen (N_2), carbon dioxide

(CO_2), hydrogen sulfide (H_2S), and other sulfur components such as mercaptans (R−SH),[4] carbonyl sulfide (COS), and carbon disulfide (CS_2). Trace quantities of argon, hydrogen, and helium may also be present. Trace quantities of metallic substances are known to exist in natural gases including arsenic, selenium, mercury, and uranium.

According to the proportion of hydrocarbons heavier than methane, different types of natural gas (dry, wet, and condensate) can be considered. Natural gas is considered "dry" when it is almost pure methane, having had most of the other commonly associated hydrocarbons removed. When other hydrocarbons are present, the natural gas is "wet," where it forms a liquid phase during production under surface conditions. 'Condensate' gases have a high content of hydrocarbon liquids and form a liquid phase in the reservoir during production, during the depletion process.

Natural gases are commonly classified according to their liquid contents as either lean or rich and according to the sulfur content as either sweet or sour.

The lean and rich terms refer to the amount of potentially recoverable liquids. The term usually applies to ethane and heavier components but sometimes applies instead to propane and heavier components (if ethane is not regarded as a valuable liquid component). To quantify the liquid contents of a natural gas mixture, the industry uses GPM, or gallons of liquids recoverable per 1000 standard cubic feet (Mscf[5]) of gas. Lean natural gas has a liquid content less than 2 GPM. Moderately rich natural gas has between 2 and 5 GPM, and very rich natural gas has greater than 5 GPM (Ewan et al., 1975).

The sweet and sour terms refer to the H_2S content. Strictly speaking, "sweet" and "sour" refer to both acid gases (H_2S and CO_2) but are usually applied to H_2S alone. A sweet gas contains negligible amounts of H_2S, whereas a sour gas has unacceptable quantities of H_2S. The terms are relative, but generally, sweet means the gas contains less than 4 ppmv of H_2S. Carbon dioxide can be tolerated to much higher levels, say 3−4 mol%, as long as the heating value of the sales gas is satisfactory.

1.5 NATURAL GAS PHASE BEHAVIOR

Natural gas is a naturally occurring hydrocarbon mixture that is found underground and at elevated conditions of pressure and temperature. Therefore, there is an essential need to know a priori how the gas fluid will behave under a wide range of pressure and temperature conditions, particularly in terms of its volumetric and thermophysical properties that are required in simulating reservoirs, evaluating reserves, forecasting production, designing production facilities, and designing gathering and transportation systems. In fact, an accurate knowledge of hydrocarbon fluid phase behavior is crucial in designing and operating the gas-engineering processes efficiently and optimally. This means, having advanced predictive tools for the characterization of hydrocarbon phase behavior with the highest accuracy possible is the key to mastering the economics of natural gas systems.

The natural gas phase behavior is a plot of pressure versus temperature that determines whether the natural gas stream at a given pressure and temperature consists of a single gas phase or two phases, gas and liquid. The phase behavior of natural gas with a given composition is typically displayed on a phase diagram, an example of which is shown in Fig. 1.2. The left-hand side of the curve is the bubble point line and divides the single-phase liquid region from the two-phase gas−liquid region. The

[4]R signifies an organic group such as a methyl, ethyl, propyl or other group.
[5]In the petroleum industry, 1000 is usually abbreviated by the Roman numeral "M".

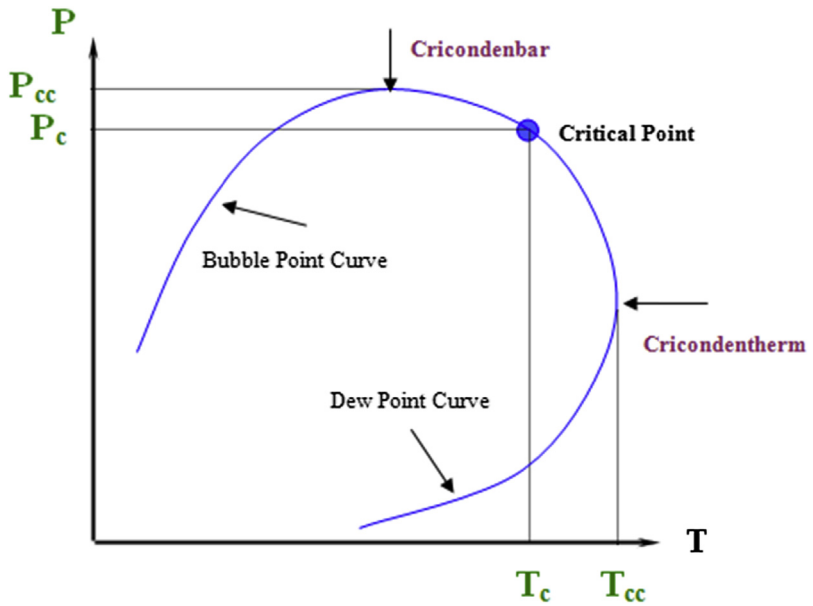

FIGURE 1.2

Pressure–temperature diagram for a typical natural gas mixture.

right-hand side of the curve is the dew point line and divides the two-phase gas–liquid region and the single-phase gas region. The bubble point and dew point lines intersect at the critical point, where the distinction between gas and liquid properties disappears. The maximum pressure at which liquids can form is called the cricondenbar (P_{CC}), and the maximum temperature at which liquids can form is called the cricondentherm (T_{CC}). However, there is something very interesting going on within the region $T_c < T < T_{cc}$, where we will be moving from a 0% liquid to another 0% liquid condition (both on the dew point curve) in an isothermal compression. This different behavior of a vapor under compression is called retrograde (contrary to expectation) condensation. It is also important to see that a similar behavior is to be expected within the region $P_c < P < P_{cc}$. In this case, we talk about retrograde vaporization since we will be moving from a 100% liquid to another 100% liquid condition (both on the bubble point curve) in an isobaric heating.

The natural gas phase behavior is a function of the composition of the gas mixture and is strongly influenced by the concentration of the heavier hydrocarbons, especially hexane plus.[6] The presence of heavier hydrocarbons will increase the phase envelope and failure to include them in a phase calculation will underpredict the phase envelope. There is also an essential need for proper characterization of the heavy ends. In fact, although some different fluid descriptions match to some extent the behavior of the reservoir fluids at reservoir conditions, they exhibit larger variations once surface simulators are used and the fluids are subjected to process conditions.

[6]Hexane plus or C_6^+ is a terminology used in natural gas engineering which indicates a grouping of heavier hydrocarbons including the hexane and heavier hydrocarbons such as heptane, octane, nonane, etc.

1.6 NATURAL GAS PROPERTIES

1.6.1 CHEMICAL AND PHYSICAL PROPERTIES

Natural gas is colorless, odorless, tasteless, shapeless, and lighter than air (see Table 1.1). The natural gas after appropriate treatment for acid gas reduction, and moisture and hydrocarbon dew point adjustment, would then be sold within prescribed limits of pressure, heating value, and possibly *Wobbe Index* (often referred to as the *Wobbe Number*).

One of the principal uses of natural gas is as a fuel, and consequently, pipeline gas is normally bought and sold on the basis of its heating value that can be produced by burning the gas. The heating value of natural gas is variable and depends on its accumulations which are influenced by the amount and types of gases they contain.[7] The gas industry always uses the gross heating value (frequently called higher heating value) in custody transfer. Obviously, the numerical difference between the two net and gross heating values is the heat of condensation of water at the specified conditions. Heating values for custody transfer are determined either by direct measurement, in which calorimetry is used, or by computation of the value on the basis of gas analysis (Gas Processors Association, 1996). The heating value of natural gas is measured in British thermal unit (Btu). A British thermal unit is the energy required to raise the temperature of 1 pound of water by 1°F. For larger industrial customers, the abbreviations MBtu (1000 Btu) or MMBtu (million Btu) are more commonly used. Since meters measure volume and not energy content, a conversion factor of 1000 Btu/ft^3 is commonly used by gas companies to convert the volume of gas used to its heat equivalent, and thus calculate the actual energy use.

The Wobbe Index (defined as the gross heating value of the gas divided by the square root of the specific gravity) gives a measure of the heat input to an appliance through a given aperture at a given gas pressure. Using this as a vertical coordinate and the flame speed factor as the horizontal coordinate, a combustion diagram can be constructed for an appliance, or a whole range of appliances, with the aid of appropriate test gases. This diagram shows the area within which variations in the Wobbe Index and flame speed factor of gases may occur for the given range of appliances without resulting in either incomplete combustion, flame lift, or the lighting back of preaerated flames. This method of prediction of combustion characteristics is not sufficiently accurate to eliminate entirely the need for the practical testing of new gases.

Since natural gas as delivered to pipelines has practically no odor, the addition of an odorant is required by most regulations in order that the presence of the gas can be detected readily in case of accidents and leaks. This odorization is provided by the addition of trace amounts of some organic sulfur compounds to the gas before it reaches the consumer. The sulfur compound, a chemical odorant (a *mercaptan* also called a *thiol* with the general formula R−SH and the odor of rotten eggs) is added to natural gas so that it can be smelled if there is a gas leak. The standard requirement is that a user will be able to detect the presence of the gas by odor when the concentration reaches 1% of gas in air. Since the lower limit of flammability of natural gas is approximately 5%, this requirement is equivalent to one-fifth the lower limit of flammability. The combustion of these trace amounts of odorant does not create any serious problems of sulfur content or toxicity.

[7]Since the heat energy of the natural gas is related to the relative proportion of "lighter" methane versus "heavier" ethane, propane, butane, pentane, and other components, heat energy is not a constant value between different natural gas sources (Chandra, 2006).

Table 1.1 Properties of Natural Gas

Properties	Value
Relative molar mass	17−20
Carbon content, weight%	73.3
Hydrogen content, weight%	23.9
Oxygen content, weight%	0.4
Hydrogen/carbon atomic ratio	3.0−4.0
Relative density, 15°C	0.72−0.81
Boiling point, °C	−162
Autoignition temperature, °C	540−560
Octane number	120−130
Methane number	69−99
Stoichiometric air/fuel ratio, weight	17.2
Vapor flammability limits, volume %	5−15
Flammability limits	0.7−2.1
Lower heating/calorific value, MJ/kg	38−50
Stoichiometric lower heating value, MJ/kg	2.75
Methane concentration, volume %	80−99
Ethane concentration, volume %	2.7−4.6
Nitrogen concentration, volume %	0.1−15
Carbon dioxide concentration, volume %	1−5
Sulfur concentration, weight% ppm	<5
Specific CO_2 formation, g/MJ	38−50

In the following section we discuss important gas properties including specific gravity, compressibility factor, formation volume factor, density, isothermal compressibility, and viscosity.

1.6.1.1 Gas Specific Gravity

Specific gravity of a natural gas is defined as the ratio of gas density to the density of air, both defined at the same pressure and temperature. These densities are usually defined at standard conditions (14.7 psia and 60°F). Therefore, specific gravity of gas is defined as:

$$\gamma_g = \frac{M}{M_{air}} \tag{1.1}$$

where M is the molecular weight of gas and M_{air} is the molecular weight of air that is equal to 29. Once we can calculate the value of molecular weight of a mixture, we can calculate the specific gravity of the mixture. For a gas mixture, we can calculate the molecular weight as:

$$M = \sum_{i=1}^{n} y_i M_i \tag{1.2}$$

where M_i is the molecular weight of component i, y_i is the mole fraction of component i, and n is the total number of components.

Various gas properties, including the molecular weights for pure components, are given in Table 1.2.

1.6.1.2 Gas Compressibility Factor

The volume of a real gas is usually less than what the volume of an ideal gas would be, and hence a real gas is said to be super-compressible. The ratio of the real volume to the ideal volume, which is a measure of the amount the gas deviates from perfect behavior, is called the super compressibility factor, sometimes shortened to the compressibility factor. It is also called the gas deviation factor, and given the symbol "Z". The gas deviation factor is by definition the ratio of the volume actually occupied by a gas at a given pressure and temperature to the volume it would occupy if it behaved ideally.

The real gas equation of state is then written as:

$$PV = ZnRT \tag{1.3}$$

where P is the pressure, V is the volume, T is the absolute temperature, Z is the compressibility factor, n is the number of kilomoles of the gas, and R is the gas constant.

The gas deviation factor, Z, is close to 1 at low pressures and high temperatures which means the gas behaves as an ideal gas at these conditions. At standard or atmospheric conditions the gas Z factor is always approximately 1.

Empirical correlations for Z-factor for natural gases were developed before the advent of digital computers. Although their use is in decline, they can still be used for rapid estimates of the Z-factor. Chart look-up is another means of determining Z-factor of natural gas mixtures. These methods are invariably based on some type of corresponding states development. According to the theory of corresponding states, substances at corresponding states will exhibit the same behavior. The theory of corresponding states dictates that the Z factor can be uniquely defined as a function of reduced pressure and reduced temperature. The reduced pressure and reduced temperature are defined as:

$$P_r = \frac{P}{P_c} \quad \text{and} \quad T_r = \frac{T}{T_c} \tag{1.4}$$

where P_r and T_r are reduced pressure and reduced temperature, respectively; and P_c and T_c are critical pressure and critical temperature of the gas, respectively. The values of critical pressure and critical temperature can be estimated from the following equations if the composition of the gas and the critical properties of the individual components are known.

$$P_c = \sum_{i}^{n} P_{Ci} y_i \quad \text{and} \quad T_c = \sum_{i}^{n} T_{ci}\, y_i \tag{1.5}$$

where P_{ci} and T_{ci} are the critical pressure and critical temperature of component i, respectively; and y_i is the mole fraction of component i.

Once critical properties of the mixture are calculated as stated in Eq. (1.5), we can use Eq. (1.4) to calculate the reduced properties of the mixture.

Table 1.2 Physical Constants for Pure Components (Whitson and Brule, 2000)

Compound	Formula	Molecular Weight	Critical Constants			
			P_c psia [kPa]	T_c °R[°K]	V_c $ft^3/lb[m^3/kg]$	Z_c
Methane	CH_4	16.043	667.8 [4604]	343 [190.6]	0.0991 [0.0062]	0.2884
Ethane	C_2H_6	30.070	707.8 [4880]	549.8 [305.4]	0.0788 [0.00492]	0.2843
Propane	C_3H_8	44.097	616.3 [4249]	665.7 [369.8]	0.0737 [0.0046]	0.2804
n-Butane	C_4H_{10}	58.124	5 50.7 [3797]	765.3 [425.2]	0.0702 [0.00438]	0.2736
Isobutane	C_4H_{10}	58.124	529.1 [3648]	734.7 [408.2]	0.0724 [0.00452]	0.2824
n-Pentane	C_5H_{12}	72.151	488.6 [3369]	845.4 [469.7]	0.0675 [0.00422]	0.2623
Isopentane	C_5H_{12}	72.151	490.4 [3381]	828.8 [460.4]	0.0679 [0.00424]	0.2701
Neopentane	C_5H_{12}	72.151	464.0 [3199]	781.11	0.0674 [0.00421]	0.2537
n-Hexane	C_6H_{14}	86.178	436.9 [3012]	913.4 [507.4]	0.0688 [0.0043]	0.2643
n-Heptane	C_7H_{16}	100.205	396.8 [2736]	972.5 [540.3]	0.0691 [0.00432]	0.2633
n-Octane	C_8H_{18}	114.232	360.6 [2486]	1023.9 [568.8]	0.0690 [0.0043]	0.2587
n-Nonane	C_9H_{20}	128.30	332 [2289]	1070.3 [594.6]	0.0684 [0.00427]	0.2536
n-Deeane	$C_{10}H_{22}$	142.30	304 [2096]	1111.8 [617.7]	0.0679 [0.00424]	0.2462
Ethylene	C_2H_4	28.054	729.8 [5032]	508.6 [282.6]	0.0737 [0.0046]	0.2765
Propene	C_3H_6	42.081	669 [4613]	656.9 [364.9]	0.0689 [0.0043]	0.2752
Acetylene	C_2H_2	26.038	890.4 [6139]	555.3 [308.5]	0.0695 [0.00434]	0.2704
Carbon dioxide	CO_2	44.010	1071 [7382]	547.6 [304.2]	0.0342 [0.00214]	0.2742
Hydrogen sulfide	H_2S	34.076	1306 [9005]	672.4 [373.6]	0.0459 [0.00287]	0.2831
Sulfur dioxide	SO_2	64.059	1145 [7894]	775.5 [430.8]	0.0306 [0.00191]	0.2697
Nitrogen	N_2	28.013	493 [3399]	227.3 [126.3]	0.0514 [0.00321]	0.2916
Water	H_2O	18.015	3208 [22,105]	1165.0 [647.2]	0.0500 [0.00312]	0.2350

The values of critical pressure and critical temperature can be estimated from its specific gravity if the composition of the gas and the critical properties of the individual components are not known. The method uses a correlation to estimate pseudo-critical temperature and pseudo-critical pressure values from the specific gravity. There are several different correlations available. The most common is the one proposed by Sutton (1985), which is based on the basis of 264 different gas samples. Sutton (1985) used regression analysis on the raw data to obtain the following second order fits for the pseudo-critical properties.

$$P_{pc} = 756.8 - 131.07\,\gamma_g - 3.6\,\gamma_g^2 \tag{1.6}$$

$$T_{pc} = 169.2 + 349.5\,\gamma_g - 74.0\,\gamma_g^2 \tag{1.7}$$

These equations are valid over the range of specific gas gravities with which Sutton (1985) worked $0.57 < \gamma_g < 1.68$.

The most commonly used method to estimate the Z factor is the chart provided by Standing and Katz (1942). The Z-factor chart is shown in Fig. 1.3. The chart covers the range of reduced pressure from 0 to 15, and the range of reduced temperature from 1.05 to 3. This chart is generally reliable for sweet natural gases with minor amounts of nonhydrocarbons. It was developed using data for binary mixtures of methane with propane, ethane, butane, and natural gases having a wide range of composition. None of the gas mixtures had molecular weight in excess of 40. For low molecular weight gases, it was found that the Z-factor estimated from Standing and Katz (1942) chart has error in the order of 2%−3%. However, for gas mixtures whose components differ greatly in molecular weight from 40, this chart provides inaccurate Z-factors (Elsharkawy et al., 2001).

Wichert and Aziz (1972) have developed a correlation to account for inaccuracies in the Standing and Katz chart when the gas contains significant fractions of acid gases specifically carbon dioxide (CO_2) and hydrogen sulfide (H_2S). The Wichert and Aziz (1972) correlation modifies the values of the pseudo-critical temperature and pressure of the gas. Once the modified pseudo-critical properties are obtained, they are used to calculate pseudo-reduced properties and the Z-factor is determined from Fig. 1.3. The Wichert and Aziz (1972) correlation first calculates a deviation parameter "ε":

$$\varepsilon = 120(A^{0.9} - A^{1.6}) + 15(B^{0.5} - B^4) \tag{1.8}$$

where: A: sum of the mole fractions of CO_2 and H_2S in the gas mixture; B: mole fraction of H_2S in the gas mixture

Then, "ε" is used to determine the modified pseudo-critical properties as follows:

$$T'_{pc} = T_{pc} - \varepsilon \tag{1.9}$$

$$P'_{pc} = \frac{P_{pc}T'_{pc}}{[T_{pc} - B(1-B)\varepsilon]} \tag{1.10}$$

The correlation is applicable to concentrations of $CO_2 < 54.4$ mol % and $H_2S < 73.8$ mol%. Wichert and Aziz (1972) found their correlation to have an average absolute error of 0.97% over the following ranges of data: 154 psia $< P <$ 7026 psia and 40°F $< T <$ 300°F.

Methods of direct calculation using corresponding states have also been developed, ranging from correlations of chart values to sophisticated equation sets based on theoretical developments (Elsharkawy et al., 2001 and Heidaryan et al., 2010). However, the use of equations of state (EOS) to

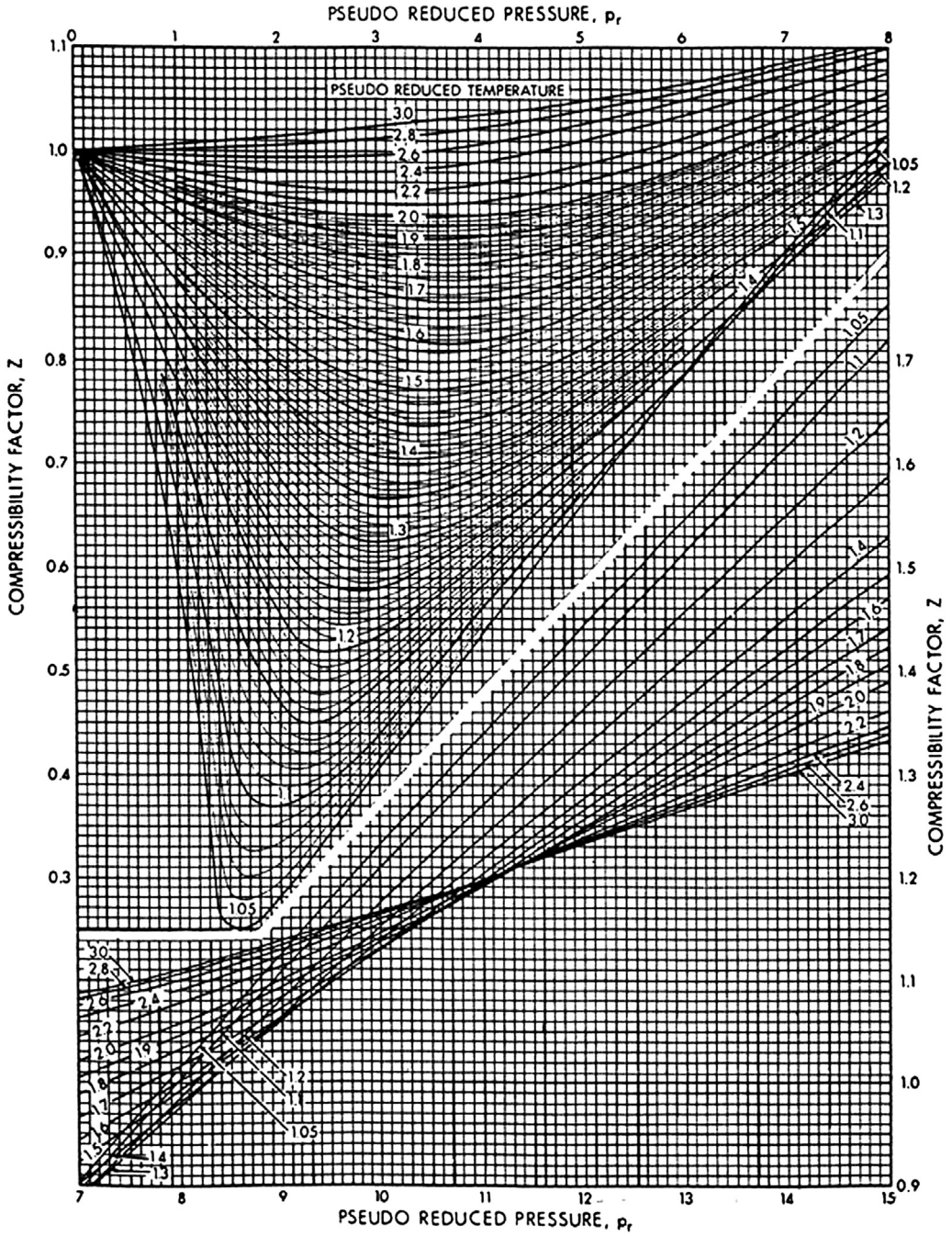

FIGURE 1.3

Compressibility of natural gases as a function of reduced pressure and temperature (Standing and Katz, 1942).

determine Z-factors has grown in popularity as computing capabilities have improved. Equations of state represent the most complex method of calculating Z-factor, but also the most accurate.

1.6.1.3 Gas Formation Volume Factor

The formation volume factor for gas is defined as the ratio of volume of 1 mol of gas at reservoir conditions to the volume of 1 mol of gas at standard conditions (P_s and T_s). Using the real gas law and assuming that the Z factor at standard conditions is one, the equation for formation volume factor (B_g) can be written as:

$$B_g = \frac{V_R}{V_s} = \frac{nZRT}{P}\frac{P_s}{nZ_sRT_s} = \frac{P_sZT}{T_sP} \tag{1.11}$$

when P_s is 1 atm (14.6959 psia or 101.325 kPa) and T_s is 60°F (519.67°R or 288.71°K) this equation can be written in three well known standard forms:

$$B_g = 0.0283\frac{ZT}{P} \tag{1.12}$$

where B_g is in ft^3/SCF, P is in psia, and T is in °R. Alternately,

$$B_g = 0.3507\frac{ZT}{P} \tag{1.13}$$

where B_g is in m^3/Sm^3, P is in KPa, and T is in °K.

In some cases, it is more convenient to define the value of B_g in bbl/SCF. The equation can be written as:

$$B_g = 0.005\frac{ZT}{P} \tag{1.14}$$

where T is in °R and P is in psia.

1.6.1.4 Gas Density

The gas density is defined as mass per unit volume and so can also be derived and calculated from the real gas law:

$$\rho_g = \frac{m}{V} = \frac{PM}{ZRT} \tag{1.15}$$

Knowing that molecular weight of gas is the product of specific gravity and molecular weight of air, and the value of R is 10.73 in field units [8.314 in SI units], we can write the equation for density as:

$$\rho_g = 2.7\,\frac{P\,\gamma_g}{ZT} \tag{1.16}$$

where ρ_g is in lbm/ft^3, P is in psia, and T is in °R. Alternately,

$$\rho_g = 3.49\,\frac{P\,\gamma_g}{ZT} \tag{1.17}$$

where ρ_g is in kg/m^3, P is in kPa, and T is in °K.

The density can also be written as:

$$\rho_g = 0.0764\frac{\gamma_g}{B_g} \tag{1.18}$$

where ρ_g is in lbm/ft^3 and B_g is in ft^3/SCF. Alternately,

$$\rho_g = 1.224\frac{\gamma_g}{B_g} \tag{1.19}$$

where ρ_g is in kg/m^3 and B_g is in m^3/Sm^3.

1.6.1.5 Isothermal Compressibility of Gases

The isothermal gas compressibility, which is given by the symbol c_g, is a useful concept that will be used extensively in determining the compressible properties of the reservoir. The isothermal compressibility is also called the bulk modulus of elasticity. Gas usually is the most compressible medium in the reservoir. However, care should be taken so that it is not confused with the gas deviation factor, Z, which is sometimes called the super-compressibility factor:

$$c_g = -\frac{1}{V_g}\left(\frac{\partial V_g}{\partial P}\right)_T \tag{1.20}$$

where V and P are volume and pressure, respectively, and T is the absolute temperature. For ideal gas, we can define the compressibility as:

$$c_g = \frac{1}{P} \tag{1.21}$$

Whereas, for nonideal gas, compressibility is defined as:

$$c_g = \frac{1}{P} - \frac{1}{Z}\left(\frac{\partial Z}{\partial P}\right)_T \tag{1.22}$$

If the relationship between the Z factor and pressure at a given temperature is known, we can calculate the compressibility of gas. Since we already know the relationship between Z and P, we can numerically calculate the derivative and, hence, the value of the compressibility.

1.6.1.6 Gas Viscosity

A number of methods have been developed to calculate gas viscosity. The method of Lee et al. (1966) is a simple relation which gives quite accurate results for typical natural gas mixtures with low nonhydrocarbon content. The Lee et al. (1966) correlation was evaluated by Jeje and Mattar (2004) and has the following form:

$$\mu_g = 1.10^{-4}K\exp\left[X\left(\frac{\rho_g}{62.4}\right)^Y\right] \tag{1.23}$$

where:

$$K = \frac{(9.4 + 0.02M_g)T^{1.5}}{209 + 19M_g + T} \tag{1.24}$$

$$X = 3.5 + \frac{986}{T} + 0.01M_g \tag{1.25}$$

$$Y = 2.4 - 0.2X \tag{1.26}$$

In this expression, temperature is given in (°R), the density of the gas in lbm/ft^3 (calculated at the pressure and temperature of the system), and the resulting viscosity is expressed in centipoises (c_p).

The viscosity of gas mixtures at 1 atm and reservoir temperature can be determined from the gas mixture composition:

$$\mu_{ga} = \frac{\sum_{i=1}^{N} y_i \mu_i \sqrt{M_{gi}}}{\sum_{i=1}^{N} y_i \sqrt{M_{gi}}} \tag{1.27}$$

where μ_{ga} is the viscosity of the gas mixture at the desired temperature and atmospheric pressure, y_i is the mole fraction of the ith component, μ_{ga} is the viscosity of the ith component of the gas mixture at the desired temperature and atmospheric pressure, M_{gi} is the molecular weight of the ith component of the gas mixture, and N is the number of components in the gas mixture.

This viscosity is then multiplied by the viscosity ratio to obtain the viscosity at reservoir temperature and pressure.

1.6.2 THERMODYNAMIC PROPERTIES

The principles of thermodynamics find very wide application in predicting the properties of hydrocarbons. The properties of greatest interest are specific heats of natural gas and its Joule−Thomson coefficient.

1.6.2.1 Specific Heat

Specific heat is defined as the amount of heat required to raise the temperature of a unit mass of a substance through unity. It is an intensive property of a substance. It can be measured at constant pressure (C_p), or at constant volume (C_v), resulting in two distinct specific heat values. In terms of basic thermodynamic quantities:

$$C_p = \left(\frac{\partial H}{\partial T}\right)_p \tag{1.28}$$

$$C_v = \left(\frac{\partial U}{\partial T}\right)_v \tag{1.29}$$

where H is the molal enthalpy (BTU/lbmole), U is the molal internal energy (Btu/lbmole), C_p is the molal specific heat at constant pressure (BTU/lbmole-^oR), and C_v is the molal specific heat at constant volume (Btu/lbmole-^oR).

Both heat capacities are thermodynamically related. It can be proven that this relationship is controlled by the P−V−T behavior of the substances through the following relationship:

$$C_p - C_v = T\left(\frac{\partial V}{\partial T}\right)_p \left(\frac{\partial P}{\partial T}\right)_v \tag{1.30}$$

For ideal gases:

$$C_p - C_v = R \tag{1.31}$$

where R is the universal gas constant.

1.6.2.2 Joule−Thomson Coefficient

When a nonideal gas suddenly expands from a high pressure to a low pressure there is often a temperature change. Note that this is far from a reversible effect. It is however an adiabatic effect due to the fact that the pressure change occurs too quickly for a significant heat transfer to occur. Thermodynamically, the Joule−Thomson coefficient is defined as:

$$\eta = \left(\frac{\partial T}{\partial P}\right)_H \tag{1.32}$$

Using thermodynamic relationships, alternative expressions can be written. For example, using the cycling rule we may write:

$$\eta = \frac{RT^2}{PC_p}\left(\frac{\partial Z}{\partial T}\right)_p \tag{1.33}$$

An interesting observation from the previously mentioned expressions for the Joule−Thomson coefficient is that the Joule−Thomson coefficient of an ideal gas is identically equal to zero. However, real fluids take positive or negative Joule−Thomson values.

1.7 NATURAL GAS RESERVES

As natural gas is essentially irreplaceable, it is important to have an idea of how much natural gas is left in the ground to use. Measuring natural gas in the ground involves a great deal of inference and estimation. There is no single way that every industry player uses to quantify estimates of natural gas. Therefore, it is important to delve into the assumptions and methodology behind each study to gain a complete understanding of the estimate itself. With new technologies, these estimates are becoming more and more reliable; however, they are still subject to revision. The Energy Information Administration (referred to as the EIA) estimates world proved[8] natural gas reserves to be around 5210.8 Tcf. The biggest reserves are located in the Middle East with 1836.2 Tcf (or 34% of the world total), and

[8]Proved reserves are those estimated quantities of natural gas that can be commercially recoverable from a given date forward, from known reservoirs, and under current economic conditions.

Europe and the Former U.S.S.R with 2158.7 (or 42% of total world reserves), but very significant reserves exist also in other regions. Note should be made that the most recent data on the world proved natural gas reserves can be found by visiting the EIA website (www.eia.doe.gov).

Natural gas reserves have grown rapidly in recent years. However, the share of natural gas reserves located onshore, easy to produce and close to consumers, is decreasing and the share of reserves located offshore and in hostile environments appears to be increasing. The availability of these reserves for the end-user is therefore hampered by production and transportation costs which can exceed the price at which the gas can be sold. In such cases, innovative technical options are required for reducing the costs and providing new outlets for natural gas.

1.8 NATURAL GAS EXPLORATION AND PRODUCTION

There are four major activities involved when developing a natural gas resource. They are: exploration, drilling, completion, and production. These activities vary, depending on whether the natural gas is "conventional" or "unconventional," and accordingly, the discussion will follow these two broad categories. In the discussion of production, the emphasis will be on the flow characteristics within the reservoir. However, as the gas needs to travel from the bottom of the well to the wellhead, the wellbore's delivery capacity will also be reviewed.

1.8.1 CONVENTIONAL GAS

1.8.1.1 Exploration

Gas is contained in porous rocks at different depths in different locations. So, the first step is to locate where the gas is likely to be found. This involves the two disciplines of geophysics and geology.

A seismic survey (geophysics) is conducted to determine the layering of the different rock strata. This helps to determine where an accumulation of gas (or oil) may occur, and the potential extent of this accumulation. A seismic survey consists of a wave generator (an explosive device or a vibrator) and a series of geophones, all located at the surface. The geophones detect reflections of the wave from the various layers. Geophysicists interpret the seismic data to generate a 2-D or 3-D picture of the layers in the earth (see Fig. 1.4).

The seismic survey only defines the structure of the rock layers. It does not identify what is contained within the rock. However, it indicates where the highs and lows of the structure are, or if there are any faults. Because of buoyancy effects, the hydrocarbons are more likely to be found in the highs of the structure. In combination with the geoscientist, who brings regional experience and knowledge of the hydrocarbon bearing potential of these layers, a potential drilling location is determined. The chances of success vary significantly, depending on the degree of oil and gas development in the region. Where there is little knowledge (wildcat exploration) the chances of a successful well are 15%−30%, but where there has already been a lot of successful drilling (development wells), the chance of success improves to 75%−100%.

1.8.1.2 Drilling

The mechanics of drilling are complex, and are significantly more so for an off-shore well than for one on land. The well depth can vary from 1000 ft to 20,000 feet. The well may encounter several layers of gas, oil or water bearing rocks, but usually, there is one particular layer that is the primary target of

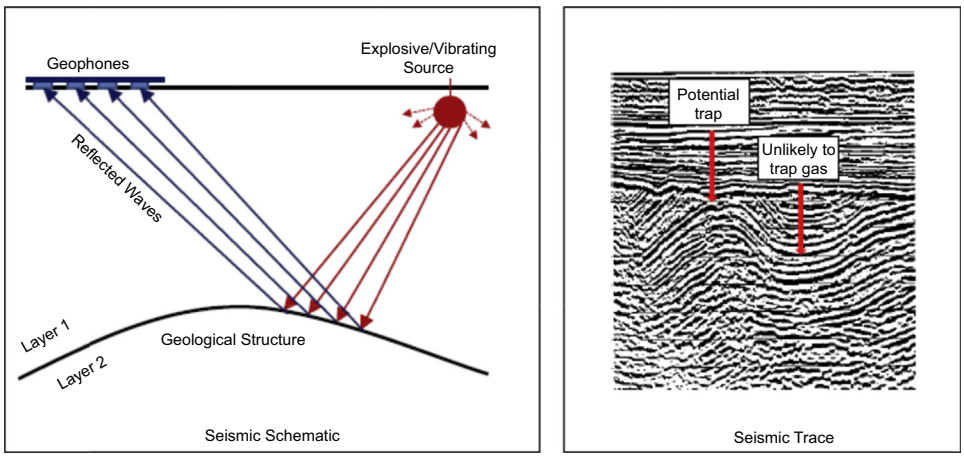

FIGURE 1.4

Seismic survey used in exploration.

interest. While drilling, the wellbore is filled with drilling mud. The hydrostatic pressure of the mud counterbalances the reservoir's pressure and avoids blowouts during drilling.

Once the intended depth is reached, a suite of electric logs is run from the bottom to the top of the well, to determine the porosity, shale content, fluid saturations, and thickness of the rock layers (Fig. 1.5). If a potentially gas-bearing reservoir is indicated, flow tests can be performed to estimate the permeability of the reservoir. If no productive reservoirs are found, the well is abandoned. If one or more productive layers are found, a steel pipe (casing) is placed in the wellbore and cemented. A "wellhead," which is an assembly of control valves, is placed on top of the well to control the flow from the well.

1.8.1.3 Completion

The casing is perforated where the gas reservoir is known to exist. The perforations penetrate both the steel casing and the surrounding cement sheath, thus creating a flow path, allowing the gas to flow from the reservoir into the well (Fig. 1.6). When the reservoir rock has a low permeability, the deliverability of the well can be improved significantly by acidizing or hydraulic fracturing. Acidizing increases the permeability in the vicinity of the well. Fracturing increases the contact area between the well and the reservoir. To fracture a well, a liquid (usually gelled water with a proppant) is injected at high rates and pressures until the rock cracks. After the completion treatment, flow and shut-in tests are conducted to determine the deliverability potential of the well and to estimate the permeability of the reservoir and the effectiveness of the completion.

1.8.1.4 Production

The rate at which a gas well can produce depends, principally, on two fundamental equations, namely Darcy's law and the Material Balance Equation (Dake, 1978). Darcy's law relates the flow rate in a reservoir to the driving force (pressure difference) and the resistance (permeability). Material Balance relates the decrease in the average reservoir pressure to the size of the reservoir and production

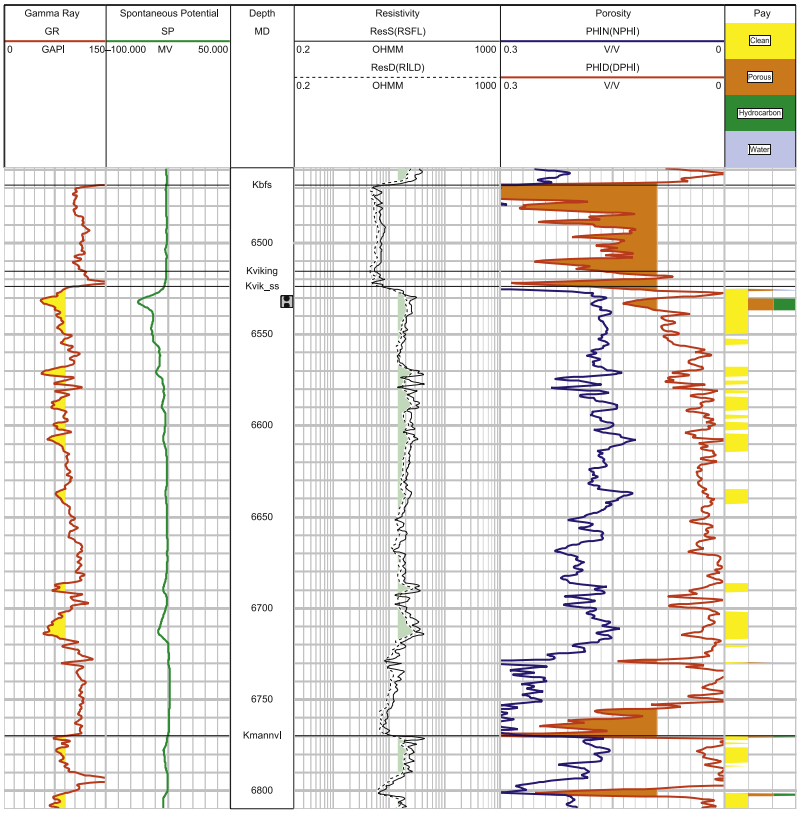

FIGURE 1.5

Electric logs used to determine the presence of hydrocarbons.

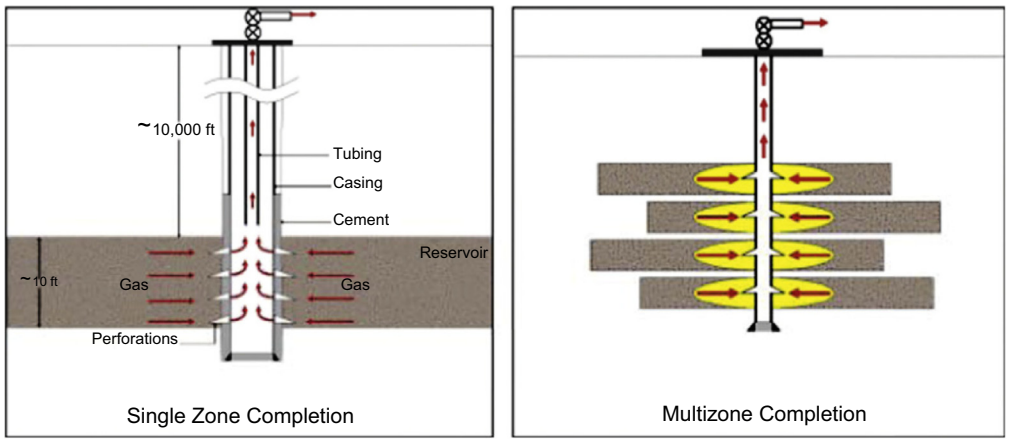

FIGURE 1.6

Different well completions.

volumes (hence to time). The principal factors that determine the deliverability of a well are therefore: reservoir pressure, flowing pressure, permeability, completion effectiveness, original-gas-in-place, and wellbore configuration.

For conventional gas wells, the deliverability equation can, for all practical purposes, be expressed as (ERCB, 1975):

$$q = C(P_{R^2} - P_{WF^2})^n \tag{1.34}$$

where q is the flow rate; C is a constant that encompasses permeability and completion effectiveness and other gas properties such as gravity, viscosity, and temperature; P_R is the reservoir pressure; P_{wf} is the pressure at the well; and n is an exponent (between 0.5 and 1) that accounts for the Darcy and non-Darcy flow in the reservoir (commonly referred to as the laminar and turbulent flow).

The constants C and n are determined from a flow test (often called Absolute Open Flow—AOF). The P_{wf} depends on surface facility restrictions, and usually reflects the pressure at which the gas is to be delivered to the transportation system or to the gas plant.

The material balance equation relates the reservoir pressure to the amount of gas produced:

$$\frac{P_R}{Z} = \frac{P_i}{Z_i}\left(1 - \frac{G_P}{G}\right) \tag{1.35}$$

where Z is the gas deviation factor (compressibility factor); G_p is the gas produced; and G is the Original-Gas-In-Place. The subscript "R" represents the current reservoir pressure, and the subscript "i" represents the initial reservoir pressure.

The previously mentioned two equations appear to be independent of time. However, that is not so. In Eq. (1.35), G_p changes with time. Hence, the reservoir pressure changes with time. This, in turn, causes the flow rate calculated in Eq. (1.35) to decrease as the reservoir depletes.

Combining Eqs. (1.34) and (1.35) and superimposing operating restrictions such as contract rates and facilities limitations (compression/pipeline/processing) result in a forecast of production rate versus time. Production stops when the flow rate becomes uneconomic. The total gas that will have been produced at the time of abandonment is called the Expected Ultimate Recovery (EUR).

The Original-Gas-In-Place (G) is determined from geological estimates of the areal extent and thickness of the reservoir, as well as its porosity and saturation, or from analysis of production data.

The recovery factor is the ratio of the Expected Ultimate Recovery to the Original-Gas-In-Place (EUR/G). It depends primarily on the reservoir pressure at the time of abandonment. The abandonment pressure itself is directly related to the delivery pressure and to the distance of transmission. As a consequence the recovery factor can range from 50% (for remote locations) to 90% for wells adjacent to fully developed transportation systems.

1.8.2 UNCONVENTIONAL GAS

1.8.2.1 Exploration

Unlike conventional gas, the location of unconventional resources is generally known, often as an indirect result of conventional mining or oilfield activity. These unconventional gas resources are generally laterally extensive, and therefore, less exploration is required to locate them.

1.8.2.2 Drilling

Whereas most conventional gas wells are vertical, unconventional gas wells are either horizontal wells or multiple-well pads (Fig. 1.7). There are two principal reasons for this:

1. Either the productivity of the vertical well is too low; this is improved by using a horizontal well (single or multilateral); or
2. The area of the reservoir that is drained by a vertical well is so small that it would require a large number of wells to effectively drain the whole reservoir; this could be very intrusive on the surface land activity and is resolved by drilling multiple directional wells from a single pad, which significantly minimizes the surface footprint.

1.8.2.3 Completion

Typically, the permeability of unconventional gas reservoirs is extremely small. As a consequence, with conventional completions, the deliverability per well can be uneconomic, in spite of the known presence of large quantities of gas. The best way to improve productivity per well is to increase the area of contact between the well and the reservoir. This is what underlies the success of unconventional gas completions. The single most significant contribution to the commercialization of "shale" gas and "tight" gas has been the multiple-stage hydraulic fracturing of horizontal wells to create this increased contact area (Fig. 1.8).

1.8.2.4 Production

The deliverability of gas from unconventional gas wells is governed by a combination of Darcy's law and Material Balance (just as for conventional reservoirs). However, Eqs. (1.34) and (1.35) are not very useful, because they are only applicable after the flow from the reservoir has been stabilized. When a well is first opened to flow, a pressure transient travels through the reservoir (transient flow). It is only when this pressure transient reaches the boundaries of the reservoir (Boundary Dominated Flow) that the flow is considered to be stabilized and Eqs. (1.34) and (1.35) become applicable. The

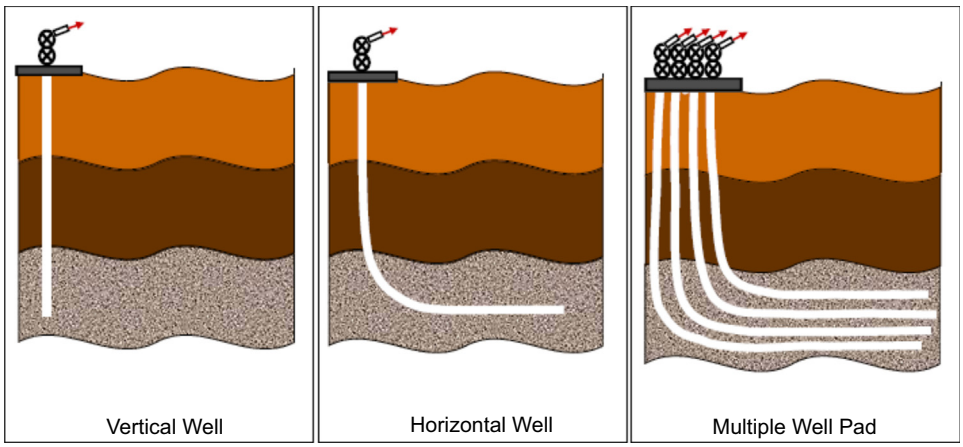

FIGURE 1.7

Different drilling patterns.

FIGURE 1.8

Very large contact area caused by multi-stage hydraulic fracturing.

time to reach stabilization is a function of permeability, and in conventional reservoirs, this time is, for all practical purposes, relatively short (<3 months). However, in unconventional reservoirs, the permeability is so low that it can take many years before Eq. (1.34) becomes applicable. Accordingly, more complex equations applicable during transient flow are needed. Such equations will usually incorporate time explicitly, and typically require computer programs. The form of such an equation is:

$q = f(p_i, p_{wf}$, permeability, well type, completion type, fluid properties, reservoir geometry, and time)

Unconventional gas reservoirs can be extensive, but because of the very low permeability, the effective drainage area per well is very limited. Accordingly the Original-Gas-In-Place is often an "assigned" value, directly linked to the well spacing.

The recovery factor is the ratio of the Expected Ultimate Recovery to the Original-Gas-In-Place (EUR/G). As a consequence the reported recovery factor depends on the spacing of the wells and the assigned drainage area. Accordingly it can range from 20% to 70%.

1.8.3 WELL DELIVERABILITY

The flow of gas from the reservoir into the wellbore, described previously, is often called the Inflow Performance Relationship (IPR). It is usually represented as a graph of flowing bottomhole pressure versus gas rate (see Fig. 1.9a). This graph demonstrates that the flow rate depends on the flowing pressure.

From a production perspective, the flowing pressure is controlled at the surface. The bottom-hole (sand-face) flowing pressure that corresponds to the wellhead flowing pressure depends on the flow rate, pressure level, gas composition, pipe diameter, and depth of the well. For a given wellbore configuration and a specified wellhead pressure, the flowing bottom-hole pressure can be calculated at various arbitrary flow rates. This is shown in Fig. 1.9b, and is called a "Tubing Performance Curve" (TPC).

Since the reservoir and the wellbore must interact, the "operating point" is obtained by overlaying the TPC and the IPR curves (see Fig. 1.9c). The point of intersection is the production rate from the

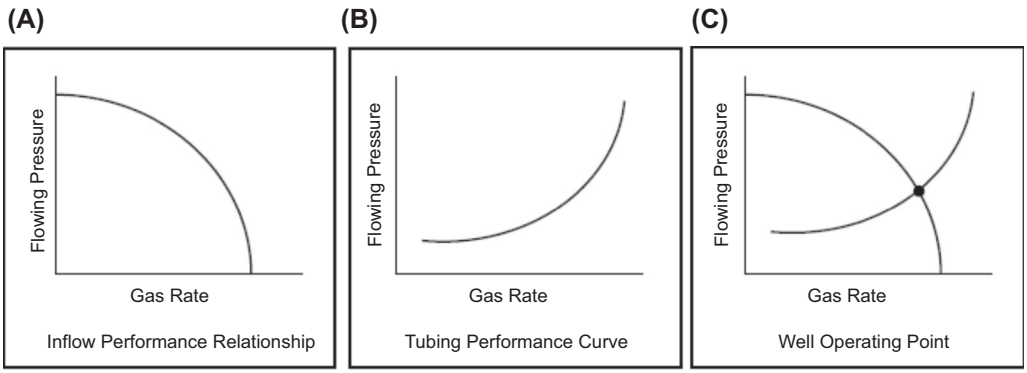

FIGURE 1.9

Well deliverability.

well at the specified conditions. Several TPCs can be generated by varying the specifications of the wellhead conditions or the tubulars. These are overlain on the reservoir's IPR and different operating points will be obtained. The choice of operating conditions is based on the economic factors associated with each TPC.

Calculation of the TPC is based on the friction and hydrostatic pressure drop calculations outlined in Chapter 3. In general, for a single phase flow of gas, the bigger the tubing diameter the larger the operating point flow rate, and the choice of tubing diameter is straightforward and is directly linked to the cost of tubing. However, many gas wells produce gas and liquids (water or condensate). Multiphase calculations are complex and often show that the operating point rate can be increased by "reducing" the tubing diameter.

When a gas well produces liquids, care must be taken to efficiently remove all the liquids, otherwise, they accumulate in the wellbore, and eventually the increasing hydrostatic back pressure "kills" the well. Various mechanisms exist for removing the liquids. These range from "siphon strings" (small diameter tubing) to "plunger lift," to reducing the wellhead pressure, to bottomhole pumps. Many gas wells stop producing (die), even though there is still a lot of gas left in the reservoir. They die simply because it is not economically viable to remove the liquids from the wellbore.

The production rate of a gas well decreases with time, because the reservoir pressure depletes. Eventually, the flow rate becomes uneconomic and the well is abandoned. Typically, to maintain a gas supply contract, additional wells are drilled over time to supplement the decreasing deliverability of the wells.

1.9 NATURAL GAS GATHERING

The gathering of natural gas consists of aggregating raw natural gas produced from various wellheads. Lines from wellheads tend to be small diameter piping that run over relatively short distances compared to transportation pipelines. The gathering piping tends to be larger after field separation

facilities that remove associated oil and water prior to sending natural gas to the processing facility through "trunk lines."

Natural gas gathering systems typically follow one of two basic design styles (radial and axial) in their initial development. In practice, gathering systems often evolve into a combination of these design styles. The main factors in determining the gathering system designs are the wellhead pressures, well spacing pattern, sourness of the raw gas, and richness of the gas composition. However, the selected design of the gathering system must consider other diverse requirements and conditions including geographic considerations, environmental impacts and regulations, field life expectancy, and legal and contractual requirements. Flexibility built into the initial designs can reduce the capital expenditure when an expansion plant is required in the future (Lawlor and Conder, 2013).

1.10 NATURAL GAS TRANSPORTATION

Transportation is an essential aspect of the gas business, since gas reserves are often quite distant from their main markets. For almost a century, natural gas has been transported safely, reliably, and economically via pipelines that are used to bring the gas supply from various production wells to the metropolis. Pipeline system has been providing the stability and long-term security by balancing the supply and demand markets. Now, in the 21st century, the vast majority of the large, conventional natural gas reserves have been already tapped, and attention is shifting to stranded reservoirs that were previously thought too small, too remote, or technically too difficult to develop. The liquefied natural gas (LNG) industry has commercialized many large remote gas fields over the past three decades and developed gas markets commercially unreachable by pipeline.

Over the last two decades, several technologies have been also evaluated and proposed for monetizing hitherto remote gas reserves (see Fig. 1.10). These include: a number of technologies converting natural gas into a range of easily transported and marketed hydrocarbons (grouped under the generic term "gas-to-liquids" or GTL technologies); using gas to produce electricity at the production field and then transporting it by high voltage direct current (HVDC) transmission lines to long distances (generically referred to as "gas-to-wire" technologies); compressed natural gas (CNG) that avoids the cost of gas liquefaction; converting gas, particularly associated gas, into solids or slurries formed of gas hydrates for storage and transportation (generically referred to as "gas-to-solids" technologies). The latter two technologies are still in the research and development stage and, although much work has been done to verify the potential of these options in the past decade, no commercial projects exploiting them have yet been sanctioned (Mokhatab and Wood, 2007).

The following section examines some of these technical methods by which natural gas energy can be converted and transported to the consumers.

1.10.1 PIPELINES

Pipeline transportation has been employed to deliver gas to markets for a long time. However, supply of natural gas to markets via gas pipelines is often faced with technical, economic, and political uncertainties.

Pipelines are a very convenient method of transport but often have limited flexibility. If a pipeline must be shut down, downstream facilities will be shut down. The downstream facilities can continue to operate until the inventory in the gas lines is depleted.

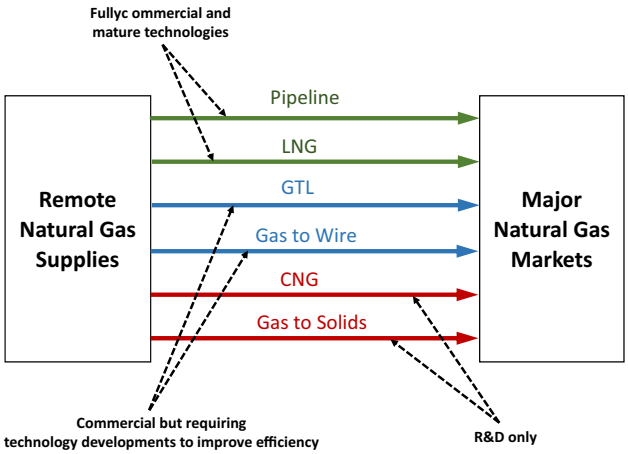

FIGURE 1.10

Technologies available to transport natural gas to long distances (Wood and Mokhatab, 2008).

For onshore and near-shore gas, pipeline is an economical option for transporting natural gas to the consumers. However, as transportation distance increases, particularly in offshore and deepwater exploration, development of these projects is challenging and expensive, and requires a large diameter long distant pipe network. They require both large, high-value markets and substantial proven reserves to be economically viable. On the other hand, gas processing technology has advanced significantly in the past two decades, overcoming challenges of upstream gas conditioning, hydrate control, and subsea pipeline design that makes the gas-transportation economical. Raw (unprocessed) gas transmission by means of pipelines is discussed in detail in Chapter 3.

Intercontinental pipelines usually entail the crossing of several countries and borders, which means that several governments may have jurisdiction over the pipelines, increasing the complexity of the projects. There are many challenges such as unexpected gas supply interruptions, terrorist attack on infrastructure, or pipeline shutdown during political turmoil.

1.10.2 LIQUEFIED NATURAL GAS

Liquefied natural gas (LNG) technology has been proven to be effective over the last 50 years. When natural gas is cooled to approximately $-260°F$ ($-162°C$) at atmospheric pressure, a condensed liquid forms which is termed liquefied natural gas (LNG). The volume reduction is about 1/600th the volume of natural gas at the burner tip. The physical properties of LNG allow for its long-distance transport by ship across oceans to markets and for its local distribution via regasification or by truck transport. Occasionally, liquefaction of natural gas provides the opportunity to store the fuel for use during high consumption periods, as well as in areas where geologic conditions are not suitable for underground gas storage facilities.

The much lower volume of liquefied natural gas (LNG) relative to gaseous natural gas can reduce transportation costs by allowing delivery using cargo ships or transport trucks instead of pipelines. However, the costs of building a liquefied natural gas plant are higher than other project options for a

number of reasons, including high energy consumption, use of expensive cryogenic materials, compliance to strict design and safety standards, design factors to ensure supply security, financial institution requirements, and site remote locations. Plant costs throughout the value chain have been declining through design innovations and cost optimization. Further advances in the LNG technology can be expected in coming years in the areas of liquefaction and shipping, which can lead to lower overall project costs (Cornot-Gandolphe et al., 2003 and Mokhatab et al., 2014). In the recent years, a floating LNG (FLNG) design, where processing and storage facilities are based on a vessel moored offshore in the vicinity of the production fields, has been proven to reduce costs, making development of small and remote gas reserves, offshore gas viable. The FLNG technology can reduce costs by minimizing the offshore platforms and pipelines, eliminating the need for port facilities, minimizing skill labor at the job sites, and reducing the plant delivery date. Vessel construction can be carried out in a low-cost location. However, there are potentially many commercial and technical challenges that need to be resolved during the development phase. The key is to delineate these challenges and provide innovative solutions to solve these problems (Chiu and Quillen, 2006 and Mokhatab et al., 2014).

1.10.3 COMPRESSED NATURAL GAS

Gas can be transported in containers at high pressures, typically 1800 psig for a rich gas (significant amounts of ethane, propane, etc.) to roughly 3600 psig for a lean gas (mainly methane). Gas at these pressures is termed compressed natural gas (CNG). CNG offers proven technology that has the potential to provide an early to market, economic solution for remote offshore gas developments with small to medium reserves or for associated gas reserves in large oil field developments. It could work where subsea pipelines are not viable because of distance, ocean topography, limited reserves, modest demand, or environmental factors, but where LNG is also not economical due to its high cost of liquefaction and regasification facilities, or feasible due to community or safety issues.[9] In addition to being a cost-effective solution for regional gas projects, CNG transport projects also offer several unique and valuable solutions in terms of flexibility and risk mitigation compared to the LNG projects (i.e., easy supply and market access, redeployability, and scalability).

The energy consumed in operating a CNG facility is only about 40% of that of an LNG plant of the same capacity. Thus, the threshold volume of gas reserves needed to support a CNG project is comparatively small, provided the shipping costs can be kept low. However, the containment for CNG is heavier than that for LNG, so the payload per unit weight shipped is smaller. Greater than 85% of a CNG project costs are likely to be associated with the ships, which are based upon conventional bulk carriers with at least four competing certified containment designs (Hatt, 2003): EnerSea (US) VOTRANS carbon steel pressure cells; Trans Ocean Gas (Canada) fiber reinforced plastic (FRP) covering high-density polyethylene cells; TransCanada CPV steel liner cell overwrapped with a glass fiber laminate; and Sea NG (Canada) patented Coselle of coiled X70 high-strength steel pipe wound into a cylindrical storage container. EnerSea's VOTRANS (Volume Optimized Transport and Storage) containment systems is the most cost-effective CNG solution in the marketplace due to greater gas storage/delivery

[9]Safety and security are contentious issues for CNG, but by locating the offloading facilities tens of kilometers offshore it is possible to remove many of the community related safety and environmental issues that have dogged the permitting for LNG receiving terminals located onshore United States in populous areas in recent years.

efficiency. With most of the capital costs invested in the technology in the vessels, it is important to have a large and experienced shipping company such as Teekay at the helm (Wood and Mokhatab, 2008).

1.10.4 GAS-TO-LIQUIDS

In gas-to-liquids (GTL) transport processes, natural gas is converted to a heavier hydrocarbon liquid and transported to the consumers. The technology of converting natural gas to liquids is not new. In the first step, methane is mixed with steam and converted to syngas or synthetic gas (mixtures of carbon monoxide and hydrogen) by one of a number of routes using a suitable catalyst technology (Keshav and Basu, 2007). The syngas is then converted into a liquid using a Fischer-Tropsch (FT) process (in the presence of a catalyst) or an oxygenation method (mixing syngas with oxygen in the presence of a suitable catalyst). The produced liquid can be a liquid fuel, usually a clean burning motor fuel (syncrude), or lubricant, ammonia, methanol, LPG substitute, or some precursors for plastics manufacture, e.g., urea, dimethyl ether (DME), or chemical feedstocks (Knott, 1997; Skrebowski, 1998; and Apanel, 2005). The environmental benefits of clean burning GTL products have been demonstrated to have potential in improving air quality in cities over refinery transportation fuels. However, on a full cycle analysis GTL fuels do not significantly outperform refinery fuels because operation of GTL plants would incur substantial emissions. The problem is primarily with the low energy efficiency of syngas generation and the low carbon efficiencies of the conversion processes such as FT (O'Rear and Goede, 2007). Technology breakthroughs are required to improve capital cost and environmental benefits.

The Fischer-Tropsch GTL (FT-GTL) method is an application of the basic Fischer-Tropsch process, where synthesis gas (or syngas) is reacted in the presence of an iron or cobalt catalyst. End products are determined by the length of the hydrocarbon chain which, in turn, is determined by catalyst selectivity and reaction conditions. FT-GTL is essentially a three stage process (syngas generation, F-T transformation, and product upgrade). Possible end products include kerosene, naphtha, methanol, dimethyl ether, alcohols, waxes, synthetic diesel, and gasoline, with water or carbon dioxide produced as a by-product. FT-GTL has reached a key milestone as an industry in that world-scale capacity plants are in the process of being planned, constructed, and commissioned. However, FT-GTL has a lot left to prove in terms of technical, economic, and environmental efficiency before it can be considered as a rival to LNG on a large scale (Fleisch et al., 2003; Al-Saadoon, 2005; and Apanel, 2005). Modifications, innovations, and patents are being developed for this complex, energy-intensive process. Most recent technical advances are focused on lowering capital expenditures, the economies of scale, and improving operating and energy efficiencies for large-scale FT-GTL plants. Efforts on improving the safe use of oxygen in syngas reforming plants have also received attention. Much research is still ongoing with respect to other GTL processes, but none has yet reached large-scale commercialization although further developments, particularly in methanol to gasoline plants, should be expected in this high-price gasoline market (Wood and Mokhatab, 2008 and Wood et al., 2008).

GTL technology development has reached a stage where its marinization, enabling smaller footprints and more compact plants than other technologies, may be considered for FPSO application. Floating GTL will provide new opportunities for companies to produce, transport, and market gas reserves that would otherwise remain stranded. Also, floating GTL plants could be moved from location to location, enabling access to small fields that would otherwise not justify building a dedicated GTL facility. The GTL FPSO concept, which is still in the development phase, could greatly improve potential project economics (Loenhout et al., 2006).

1.10.5 GAS-TO-SOLID

Gas can be transported as a solid, with the solid being gas hydrate (Børrehaug and Gudmundsson, 1996). Natural gas hydrates (NGHs), which are essentially natural gas in a "frozen" state, form when water and natural gas combine at low temperatures and high pressures. Gas hydrates are clathrates where the guest gas molecules are occluded in a lattice of host water molecules. They are most commonly encountered in the industry as a production problem in pipelines to be avoided as part of flow assurance.

Gas-to-solids (GTS) involve three stages: production, transportation, and regasification. Conceptually, hydrate slurry production is simply mixing chilled water and gas. In practice, processed gas is fed to a hydrate production plant, where a series of reactors convert it into a hydrate slurry. Each reactor further concentrates the hydrate slurry. It is then stored and eventually offloaded onto a transport vessel (insulated to near adiabatic conditions). At the receiving terminal, the hydrate is dissociated and the gas can be used as desired. The water can be used at the destination if there is water shortage, or returned as ballast to the hydrate generator and, since it is saturated with gas, will not take more gas into solution.

Gas storage in hydrate form becomes especially efficient at relatively low pressures where substantially more gas per unit volume is contained in the hydrate than in the free-state or in the compressed state when the pressure has dropped. When compared to the transportation of natural gas by pipeline or as liquefied natural gas, the hydrate concept has lower capital and operating costs for the movement of quantities of natural gas over adverse conditions. NGHs are chemically stable at about $-20°C$ compared with $-162°C$ for LNG, reducing the costs of transportation and storage. One cubic meter of NGH contains approximately 160 m^3 of natural gas, while one cubic meter of LNG contains 600 m^3 of natural gas, thus limiting the quantity of gas that can be transported with the NGH technology. This is a considerable volume penalty (and hence transport cost) if considered in isolation, with the cheaper ships for hydrate transport the process could be economic.

The gas-to-solids option for transporting and storing stranded gas to market has been extensively researched and laboratory tested for more than a decade. BG Group, Marathon, NTNU (Norway), and others have worked on a range of gas-to-solids transportation technologies (Fischer, 2001) and have taken them to small-scale pilot plants. The concepts include storage and transport of gas either as atmospheric hydrates or as a paste in pressurized insulated containers or as frozen hydrates mixed with refrigerated crude oil for atmospheric pressure transport. Even though these studies have proved the concept of storing natural gas in hydrates technically feasible, applications have not progressed beyond the laboratory stage because of complexities of the process, slow hydrate formation rates, and costs. No projects are close to commercialization, but technological advances continue to be made, e.g., forming the hydrates from a surfactant solution (Rogers et al., 2005) that may make this possible in the long-term.

1.10.6 GAS-TO-WIRE

Currently, much of the transported gas destination is fuel for electricity generation. Electricity generation at or near the reservoir source and transportation by cable to the destination(s) (gas-to-wire) are possible. Thus, for instance, offshore or isolated gas could be used to fuel an offshore power plant (may be sited in less hostile waters), which would generate electricity for sale onshore or to other offshore customers.

High voltage direct current (HVDC) transmission lines offer the most technically viable solution to moving large quantities of electric power over large distances (up to about 1500 km) keeping line losses less than 10%. However, HVDC is capital intensive and requires costly converter stations at either end of the transmission line. Additional costs for installing and then operating and maintaining gas turbines at the remote site would be incurred.

While HVDC cables are now being used more widely to transport electricity tens of kilometers no projects to develop remote gas fields in this way have yet been sanctioned. Distance, cost, and efficiency of remote generation make other options currently more attractive. There are other practical considerations to note such as if the gas is an associated gas, then if there is a generator shutdown and no other gas outlet, the whole oil production facility might also have to be shut down, or the gas released to flare. Also, if there are operational problems within the generation plant the generators must be able to shut down quickly (in around 60 s) to keep a small incident from escalating. Additionally, the shutdown system itself must be safe so that any plant that has complicated processes that requires a purge cycle or a cool-down cycle before it can shut down is clearly unsuitable (Ballard, 1965). Finally, if the plant cannot shut down easily and/or be able to start up again quickly (perhaps in an hour), operators will be hesitant to ever shutdown the process, for fear of financial retribution from the power distributors.

1.10.7 COMPARISON BETWEEN VARIOUS METHODS

As discussed previously, there are a number of options of exporting natural gas energy from oil and gas fields to market. However, distance to market and potential production volumes (dependent on the reserves size of the gas resource) influence the technologies that might viably be used to exploit remote gas fields (see Fig. 1.11).

Any gas energy export route requires a huge investment in infrastructure, and long-term "fail proof" contracts, covering perhaps 20 years or more. However, improvements in technology, economies of scale, and synergies will undoubtedly lower capital costs and further improve the project economics over the next few years. Most of these technologies have reached a stage where commercialization on a wide scale is only a few years away. However, their use carries risks in terms of technology, credit worthiness, revenue security, and market competition risks, each of which needs to be appropriately mitigated.

Gas is currently transported to markets primarily via two long-established methods (pipeline and LNG technology). Alternative technologies, which have been refined and developed in recent years, are yet to make serious inroads into the challenges of developing remote gas fields. Fig. 1.12 shows that as the distance over which natural gas must be transported increases, usage of LNG has economic advantages over usage of pipelines. As can be seen, for short distances, pipelines—where feasible—are usually more economical. LNG is more competitive for long-distance routes particularly those crossing oceans or long stretches of water since the overall costs are less affected (Economides and Mokhatab, 2007).

LNG, an effective long-distance delivery method, constitutes only 25% of global gas movement. However, LNG can offer flexibility, diversity, and security of supply advantages over pipeline alternatives. Traditional LNG projects require large investments along with substantial natural gas reserves and are economically viable for transporting natural gas in offshore pipelines for distances of more than 700 miles or in onshore pipelines for distances greater than 2200 miles (Mokhatab and Purewal, 2006). However, lower cost mid-scale LNG technologies have been developed for the smaller natural gas reservoirs, such as the shale gas fields, which will become more prevalent in the coming years.

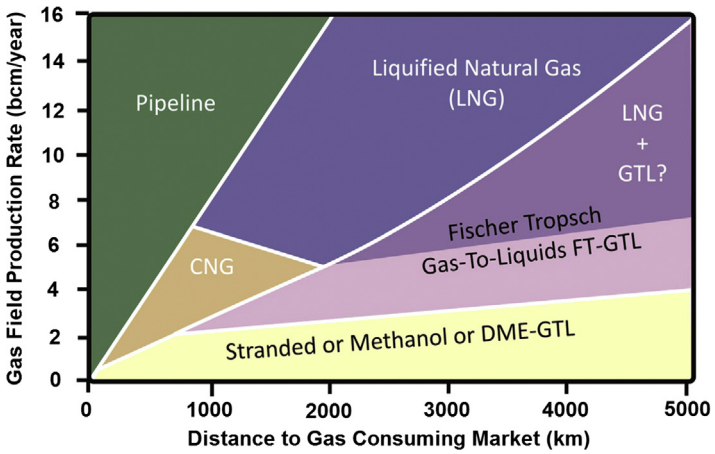

FIGURE 1.11

Production volume versus distance to market framework for gas technologies (Wood and Mokhatab, 2008).

Note, CNG is an economic alternative to monetize stranded gas reserves and creates new market where pipelines and LNG deliveries are not practical. The CNG technology provides an effective way for smaller volumes and shorter-distance transport of gas. The results show that for distances up to 2200 miles, natural gas can be transported as CNG at prices ranging from $0.93 to $2.23 per MMBTU compared to LNG, which can cost anywhere from $1.5 to $2.5 per MMBTU depending on the actual distance. At distances above 2200 miles the cost of delivering gas as CNG becomes higher than the cost for LNG because of the disparity in the volumes of gas transported with the two technologies (Economides et al., 2005). Also, unit gas transportation comparisons for pipeline, LNG, and CNG (see Fig. 1.13) suggest that pipelines will match the CNG costs at transportation volumes of about 750 MMcf/d or greater over intermediate distances. At lower volumes below this, CNG will offer lower unit transportation costs. LNG will match CNG unit transportation costs at larger volumes or longer distances. Therefore, the CNG technology may have the potential to challenge LNG transportation for some niche markets. CNG can start with much smaller initial volumes than either a pipeline or LNG and can grow incrementally to meet demand by simply adding ships. It should be noted that, while pipeline and LNG are proven either as concepts or technologies, CNG is still awaiting its first commercial application. Nevertheless, reflecting on the system's simplicity, the level of engineering efforts invested and developed reliable cost estimates, it is believed that the CNG technology is ready for commercialization (Economides and Mokhatab, 2007).

Further to the CNG technology, there are numerous technology alternatives to the currently commercial pipeline and LNG options for transporting natural gas to markets on a wide range of scales, which have been described previously. Unfortunately, few of them are yet receiving the levels of investment and commitment required to bring them into widespread development. High prevailing oil and gas prices around the world could change this lack of enthusiasm for embracing novel technologies.

The transport options preferred by governments and companies must not only take the economic risks into account but also consider the negative effects of possible terrorist activity, political changes,

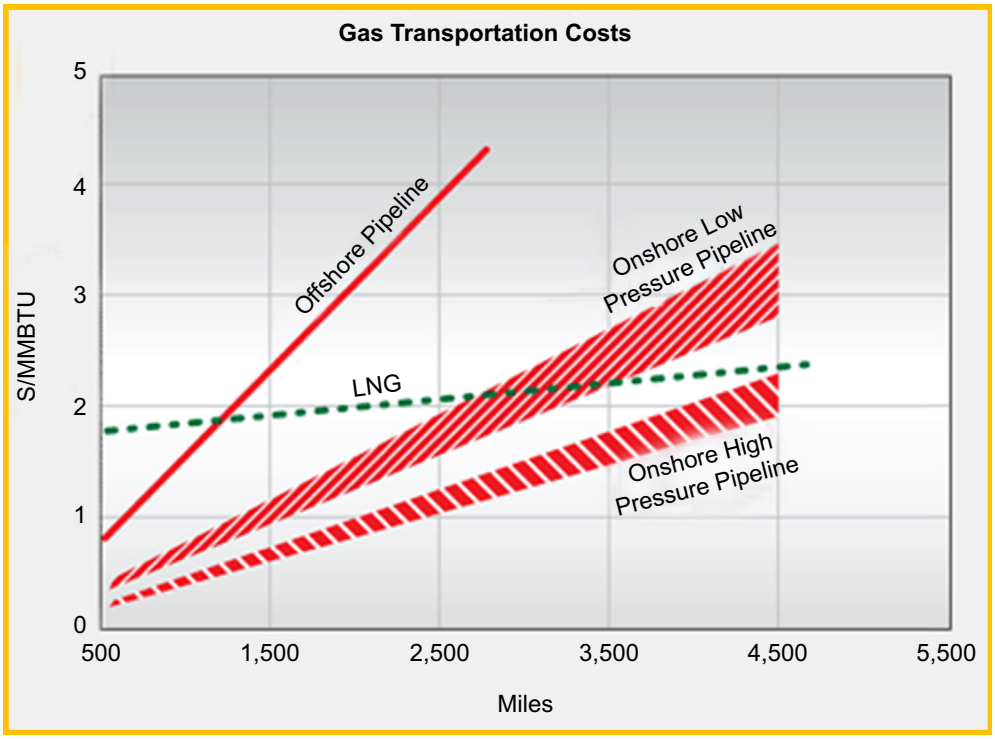

FIGURE 1.12

Comparison of the cost of transporting gas via pipeline and LNG; for 1 tcf/year and including regasification costs (Economides and Mokhatab, 2007).

and trade embargos over long periods of time. Thomas and Dawe (2003) cover many of the essential technical points and broad economic pointers needed to enter the discussion of gas rich states which do not need the gas for domestic use, but wish to monetize their reserves by export.

1.11 NATURAL GAS PROCESSING

As discussed in Section 1.4, natural gas as it leaves the reservoir contains water vapor and all the impurities. Therefore, raw natural gas produced from wells must be processed to meet the quality standards specified by pipeline companies, which must be compatible with the pipeline design and the customer's requirements. Off specification natural gas will cause operational problems associated with corrosion and plugging, which may result in unsafe operation.

If the raw gas contamination levels and acid gas content are low, the gas can be treated and dried at the field processing facility near the wellhead and sent directly to the sales gas pipeline. However, if the contaminant levels are high and the gas is sour then it is typically collected and piped to a gas processing complex where the gas is treated, conditioned, and dried to meet pipeline gas specifications. The design and operation of the different processing units are discussed in the following chapters.

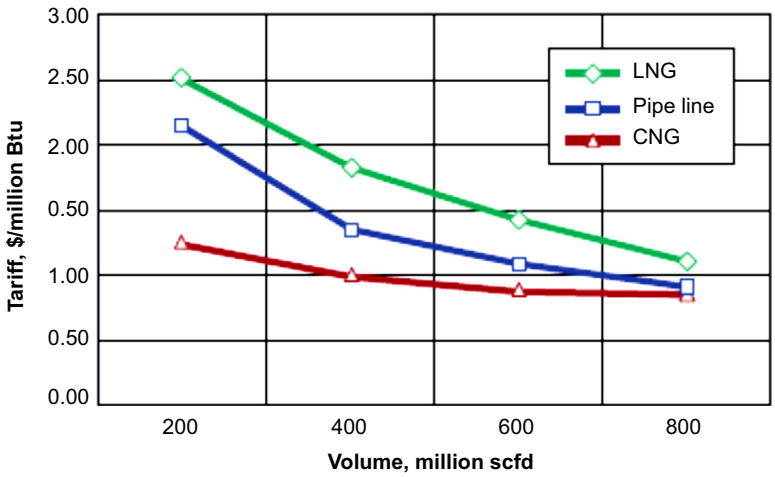

FIGURE 1.13

Transportation tariffs (Economides et al., 2005).

1.12 SALES GAS TRANSMISSION

After the raw gas has been processed to meet pipeline gas specifications, the marketable (sales) gas is transported through pipelines to industrial and residential consumers or to underground storage facilities for later delivery to these consumers as demand dictates. A number of compressor stations (containing one or more compressor units) are located along the pipeline system to maintain the pipeline pressure and overcome the pressure drop in the pipeline. Sales gas transmission will be discussed in detail in Chapter 15.

When the sales gas reaches a local gas utility, it normally passes through a gate station to serve three purposes: (1) reducing the pressure in the line from transmission levels to distribution levels, (2) adding an odorant so that consumers can smell even small quantities of gas, and (3) measuring the flow rate of the gas to determine the amount delivered to the utility. From the gate station, sales gas then moves into distribution lines to supply gas to the end users/customers.

1.13 UNDERGROUND GAS STORAGE

Strategically, underground gas storage provides security of supply in case there are disruptions to production and transmission. This could be due to commercial reasons, such as sales gas price negotiation, political reasons, or an outage. It is a means to balance seasonal variations in consumption; the winter demand is typically greater than the summer usage. It can also enhance the effectiveness of gas transport and production, where it can be stored locally to where it is being used. Commercially, natural gas is a commodity for trading.

There are three principal types of underground storage methods: depleted oil or gas reservoirs, aquifers, and salt cavern formations.

1.13.1 DEPLETED RESERVOIRS

The most common form of underground storage is depleted gas reservoirs. They are formations that have already been exhausted of most of their recoverable oil and natural gas. The empty reservoirs can be used to hold natural gas. Typically, an extensive pipeline network is located close to the reservoir sites for the convenience of the injection and withdrawal operation. Of the three types of underground storage, depleted reservoirs are the cheapest and the quickest to develop, operate, and maintain.

Two of the most important characteristics of an underground storage reservoir are the capability to hold natural gas and the rates at which natural gas inventory can be injected and withdrawn. Note that most of these depleted oil fields had been injected with nitrogen for enhanced oil recovery, and consequently, the nitrogen content in these fields would vary during withdrawal. In some reservoirs the nitrogen content in the reservoir during the withdrawal mode can vary from 3 mol% to 30%. In these facilities, a nitrogen rejection unit must be installed to remove the nitrogen content to meet pipeline specification.

1.13.2 AQUIFERS

In the United States, 16% of storage capacity is in aquifers. Aquifers are underground porous, permeable rock formations that act as natural water reservoirs. An aquifer is suitable for natural gas storage if the water-bearing sedimentary rock formation is overlaid with an impermeable cap rock. While the geology of aquifers is similar to the depleted production fields, they are more expensive to develop for natural gas storage, and consequently, there are limited numbers of aquifer natural gas storage, found only in areas where there are no other alternatives.

1.13.3 SALT CAVERNS

Salt caverns are formed out of existing salt bed deposits. Most of the large salt caverns are located in the salt domes along the Gulf Coast in the US. Salt caverns in Northeastern, Midwestern, and Western States are also available but the applications are limited by the lack of suitable geology.

The cavern is man-made by drilling a well down into the formation, and pumping water through the completed well to dissolve the salt which returns to the surface as brine. The walls of the cavern are very resilient against reservoir degradation.

As the salt cavern is an open vessel, it offers very high deliverability. Flow rates can be high and they can be brought on stream and ramped to full flow quickly. They are best for peak loads and short term trading rather than long term seasonal storage. Peak load can be provided by salt caverns, where the deliverability is higher, turnovers will be higher and facilities are smaller. Salt caverns turnover can be daily or weekly, entirely dictated by commercial trading.

REFERENCES

Al-Saadoon, F.T., April 3–5, 2005. Economics of GTL plant. SPE 94380, Paper Presented at the SPE Hydrogen Economics and Evaluation Symposium, Dallas, TX, USA.

Apanel, G.T., March 12–15, 2005. GTL update. SPE 93580, Paper Presented at the 14th SPE Middle East Oil, Gas Show and Conference, Bahrain.

Ballard, D., 1965. How to operate quick-cycle plants. Hydrocarbon Processing 44 (4), 131.
Børrehaug, A., Gudmundsson, J.S., June 3–5, 1996. Gas transportation in hydrate form. Paper Presented at the EUROGAS 96, Trondheim, Norway.
Chandra, V., 2006. Fundamentals of Natural Gas: An International Perspective. PennWell Books, Tulsa, OK, USA.
Chiu, C.H., Quillen, D., June 5–9, 2006. Commercial and technical considerations in the developments of offshore liquefaction plant. Paper Presented at the 23rd World Gas Conference, Amsterdam, The Netherlands.
Cornot-Gandolphe, S., Appert, O., Dickel, R., Chabrelie, M.F., Rojey, A., June 1–5, 2003. The challenges of further cost reduction for new supply options (pipeline, LNG, GTL). Paper Presented at the 22nd World Gas Conference, Tokyo, Japan.
Dake, L.P., 1978. Fundamentals of Reservoir Engineering. Elsevier Science, Amsterdam, The Netherlands.
Economides, M.J., Mokhatab, S., 2007. Compressed natural gas: another solution to monetize stranded gas. Hydrocarbon Processing 86 (1), 59–64.
Economides, M.J., Sun, K., Subero, G., April 5–7, 2005. Compressed natural gas: an alternative to liquid natural gas. SPE 92047, Paper Presented at the Asia Pacific Oil and Gas Conference and Exhibition, Jakarta, Indonesia.
Elsharkawy, A.M., Hashem, Y.S., Alikhan, A.A., 2001. Compressibility factor for gas condensates. Energy & Fuels 15 (4), 807–816.
ERCB, 1975. Theory and practice of the testing of gas wells. Directive 34, third ed. Energy Resources Conservation Board (ERCB), Calgary, AB, Canada.
Ewan, D.N., Lawrence, J.B., Rambo, C.L., Tonne, R.R., March 10–12, 1975. Why cryogenic processing (investigating the feasibility of a cryogenic turbo-expander plant). Paper Presented at the 54th Annual GPA Convention, Houston, TX, USA.
Fischer, P.A., Nov. 2001. How operators will bring worthless gas to market. Natural Gas, Part 8, Monetizing Stranded Gas, World Oil 222, 11.
Fleisch, T., Sills, R., Briscoe, M., Fteide, J.F., January 2003. GTL-FT in the emerging gas economy, in fundamentals of gas to liquids. Petroleum Economist 39–41.
Gas Processors Association, GPA Standard 2172–2196, 1996. Calculation of Gross Heating Value, Relative Density, and Compressibility of Natural Gas Mixtures from Compositional Analysis. Tulsa, OK, USA.
Hatt, J., December 10, 2003. Newfoundland poised to capture natural gas benefits. Ocean Resources Online.
Heidaryan, E., Salarabadi, A., Moghadasi, J., 2010. A novel correlation approach for prediction of natural gas compressibility factor. Journal of Natural Gas Chemistry 19 (2), 189–192.
Jeje, O., Mattar, L., June 8–10, 2004. Comparison of correlations for viscosity of sour natural gas. Paper Presented at the 5th Canadian International Petroleum Conference, Calgary, AB, Canada.
Kelkar, M., 2008. Natural Gas Production Engineering. PennWell Books, Tulsa, OK, USA.
Keshav, T.R., Basu, S., 2007. Gas-to-Liquid technologies: India's perspective. Fuel Processing Technology 88 (5), 493–500.
Knott, D., June 23, 1997. Gas-to-Liquids projects gaining momentum as process list grows. Oil & Gas Journal 16–21.
Korn, A., February 5, 2010. Prospects for Unconventional Gas in Europe. E.ON Ruhrgas, Essen, Germany.
Lawlor, K.A., Conder, M., 2013. Gathering and processing design options for unconventional gas. Hart Energy 3 (4), 54–58.
Lee, A., Gonzalez, M., Eakin, B., 1966. The viscosity of natural gases. Journal of Petroleum Technology 18, 997–1000.
Loenhout, A.V., Zeelenberg, L., Gerritse, A., Roth, G., Sheehan, E., Jannasch, N., May 1–4, 2006. Commercialization of stranded gas with a combined oil and GTL FPSO. Paper Presented at the 2006 Offshore Technology Conference, Houston, TX, USA.
Mokhatab, S., Purewal, S., 2006. Is LNG a competitive source of natural gas? Petroleum Science and Technology 24 (2), 243–245.

Mokhatab, S., Mak, J.Y., Valappil, J.V., Wood, D., 2014. Handbook of Liquefied Natural Gas. Gulf Professional Publishing, Burlington, MA, USA.

Mokhatab, S., Wood, D., 2007. Why consider exploiting stranded gas? Petroleum Science and Technology 25 (3), 411−413.

O'Rear, D.J., Goede, F., 2007. Concepts for reduction in CO_2 emissions in GTL facilities. Studies in Surface Science and Catalysis 163, 401−409.

Rogers, R.E., Etheridge, J.A., Pearson, L.E., McCown, J., Hogancamp, K., Winter 2005. Gas hydrate storage process for natural gas. Gastips 14−18.

Rojey, A., Jaffret, C., Cornot-Gandolph, S., Durand, B., Jullin, S., Valais, M., 1997. Natural Gas Production, Processing, Transport. Editions Technip, Paris, France.

Skrebowski, C., Jan. 1998. Gas-to-Liquids or LNG? Petroleum Review 38−39.

Speight, J.G., 2013. Shale Gas Production Processes, first ed. Gulf Professional Publishing, Burlington, MA, USA.

Standing, M.B., Katz, D.L., 1942. Density of natural gases. Transactions of the AIME 142, 140−149.

Sutton, R.P., September 22−25, 1985. Compressibility factor for high molecular weight reservoir gases. SPE 14265, Paper Presented at the SPE Annual Technical Conference and Exhibition, Las Vegas, NV, USA.

Thomas, S., Dawe, R.A., 2003. Review of ways to transport natural gas energy from countries which do not need the gas for domestic use. Energy-The International Journal 28, 1461−1477.

Whitson, C.H., Brule, M.R., 2000. Phase behavior. SPE Monograph No. 20, Society of Petroleum Engineers (SPE), Richardson, TX, USA.

Wichert, E., Aziz, K., May 1972. Calculate Z's for sour gases. Hydrocarbon Processing 51, 119−122.

Wood, D., Mokhatab, S., 2008. Gas monetization technologies remain tantalizingly on the brink. World Oil 229 (1), 103−108.

Wood, D., Mokhatab, S., Economides, M.J., March 2−5, 2008. Technology options for securing markets for remote gas. Paper Presented at the 87th Annual GPA Convention, Grapevine, TX, USA.

CHAPTER

PHASE BEHAVIOR OF NATURAL GAS SYSTEMS

2

2.1 INTRODUCTION

Natural gases have so many industrial applications that a major challenge is to develop a thermodynamic model able to predict the phase equilibrium of these mixtures. Such predictions are indeed essential for the processing of natural gases and the design of transportation facilities. As stated by Louli et al. (2012), the most commonly used models for this purpose are cubic equations of state (EoS) and especially the ones issued from the Redlich−Kwong and Peng−Robinson classes. The statistical associating fluid theory (SAFT)-type models are a promising class of EoS emerging since the late 1980s. Although no industrialized version of SAFT EoS really exists nowadays (by industrialized model, it is meant to be a model applicable to a large variety of chemicals and related industrial applications), proof has been given that the Perturbed-Chain SAFT (PC-SAFT) EoS can be successfully used to model natural gas phase envelopes.

As an alternative class of models for natural gases, Kunz and Wagner (2012) developed the Groupe Européen de Recherches Gazières (GERG)-2008, an equation of state expressed in terms of Helmholtz energy applicable to species classically involved in natural gases (methane, nitrogen, carbon dioxide, ethane, propane, n-butane, i-butane, n-pentane, i-pentane, n-hexane, n-heptane, n-octane, n-nonane, n-decane, hydrogen, oxygen, carbon monoxide, water, hydrogen sulfide, helium, and argon) and their related mixtures. Because this model relies on a very large set of adjustable parameters, a good accuracy can be reached explaining why it was adopted as an ISO standard.

The goal of this chapter is to describe and analyze the various EoS models usable for the correlation and prediction of phase equilibrium and energetic properties (enthalpy, heat capacities, and so forth) of natural gases. In the last part of this chapter, some of these models are compared on the basis of the reproduction of experimental phase-envelope data of real or synthetic natural gases (SNGs).

2.2 FUNDAMENTALS OF NATURAL GAS PHASE BEHAVIOR

2.2.1 SINGLE-COMPONENT SYSTEMS

The behavior of a single-phase unary system can be described by any two intensive variables (temperature T, pressure P, molar volume v, molar enthalpy h, and so forth) characterizing the studied phase. Temperature and pressure are certainly the easiest process variables to be measured, explaining why the representation of the information related to the phase behavior of a pure component is frequently reported in a pressure−temperature P-T phase diagram. The 2-phase equilibrium condition

Handbook of Natural Gas Transmission and Processing. https://doi.org/10.1016/B978-0-12-815817-3.00002-2

applied to a pure component i states that its temperature, pressure, and molar Gibbs energy g_i (i.e., its chemical potential) remain the same in each phase:

$$g_{PHASE\,1,\,pure\,i}(T,P) = g_{PHASE\,2,\,pure\,i}(T,P) \tag{2.1}$$

As a direct consequence, the two intensive variables T and P are subject to one constraint equation (the phase-equilibrium condition) so that in a pressure (P)—temperature (T) plane, the locus of the 2-phase equilibrium can be described by a curve $P(T)$.

This result is in agreement with Gibbs's phase rule claiming that the variance (also called number of *degrees of freedom*), denoted *dof*, of a system containing one component is

$$dof = 3 - k \tag{2.2}$$

where k denotes the number of coexisting phases within the a one-component system. Consequently, for a 2-phase equilibrium, the variance is equal to one. The 2-phase system being *monovariant*, the choice of the temperature fixes the equilibrium pressure.

As a consequence, in a P—T plane, the representation of 2-phase equilibrium loci (liquid + vapor or liquid + solid or vapor + solid) requires spaces of dimension 1, i.e., simple curves.

Still according to Gibbs' phase rule, single-phase pure species have a variance equal to 2, whereas 3-phase pure species show a variance equal to zero. Consequently, the graphical representations of such spaces in the P-T plane are area and points as illustrated in Fig. 2.1.

The critical point is defined as the terminal point of the vaporization curve in the P-T plane. At this point, all the intensive properties (density, molar enthalpy …) of the liquid and vapor coexisting phases become strictly identical.

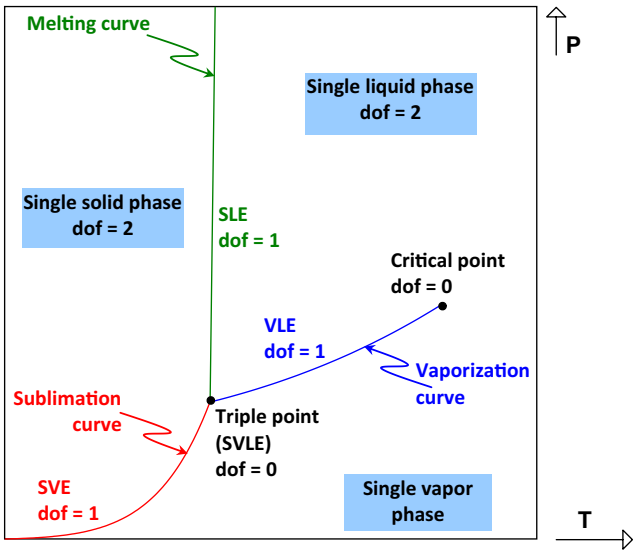

FIGURE 2.1

Representation of pure species states in a P-T plane. *SLE*, solid—liquid equilibrium; *SVE*, solid—vapor equilibrium; *SVLE*, solid—vapor—liquid equilibrium; *VLE*, vapor—liquid equilibrium.

2.2.2 BINARY SYSTEMS

Binary systems are a great help for people elaborating complex models for mixtures (activity coefficient models or EoS) in which the intermolecular interactions are most often supposed to be limited to binary interactions. The thermodynamic phase behavior of real complex mixtures containing N components is seen as the summation of the thermodynamic phase behaviors of the $N(N-1)/2$ pairs of molecules that it is possible to form from N molecules. Binary systems are thus seen as elementary and fundamental systems from which the prediction of the phase behavior of multicomponent mixtures is made possible.

At low pressures and low temperatures, the topology of the (isothermal or isobaric) vapor−liquid phase-equilibrium diagrams exhibited by binary systems appears rather simple because only 6 different configurations exist (Privat and Jaubert, 2013) (by ignoring very rare behaviors such as double azeotropy), according to observations collected by experimentalists. This is illustrated in Fig. 2.2 that shows isothermal *Pxy* phase diagrams of 6 fictitious binary systems. *Pxy* is the abbreviation for the isothermal projection, that is, pressure (P) versus liquid (x) and gas (y) compositions, and similarly, *Txy* will be used for the isobaric projection, that is, temperature (T) versus liquid (x) and gas (y) compositions. Note that by low pressure and low temperature, it is meant that the pressure and the temperature are respectively below the lowest value of the critical temperatures $\left(T_{c,1} \text{ and } T_{c,2}\right)$ and the lowest value of the critical pressures $\left(P_{c,1} \text{ and } P_{c,2}\right)$ of the two components making up the binary system.

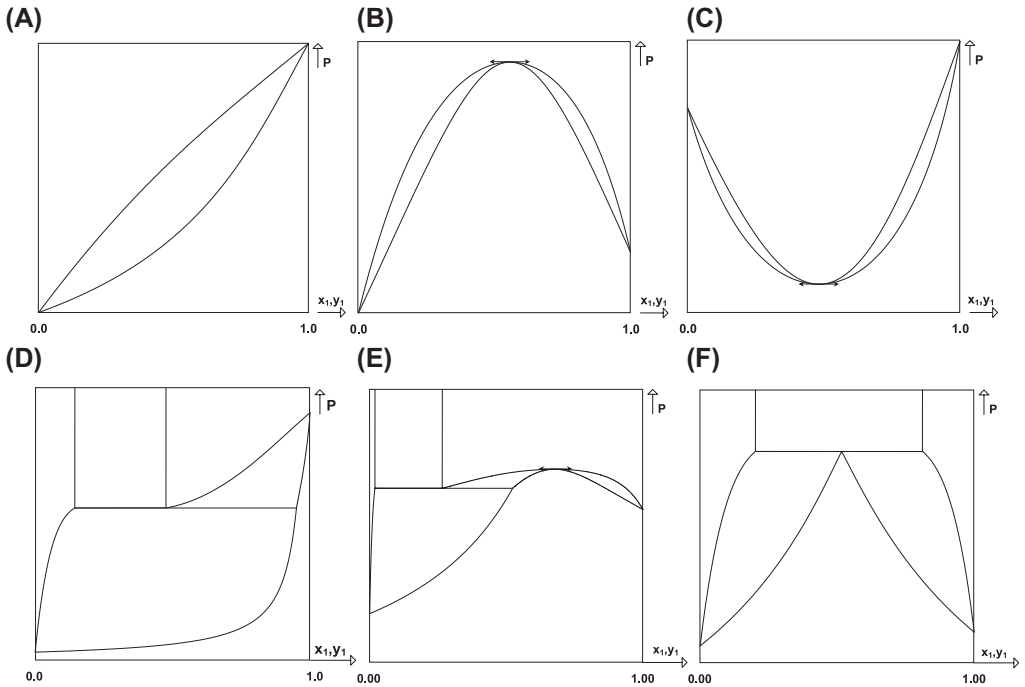

FIGURE 2.2

Sketch of the six possible configurations [(a) to (f)] of isothermal Pxy binary-system fluid-phase equilibrium diagrams can be observed at low temperature ($T < Min\left\{T_{c,1}, T_{c,2}\right\}$). Symmetrically, at low pressure ($P < Min\left\{P_{c,1}, P_{c,2}\right\}$), six configurations would be observed for isobaric *Txy* phase diagrams..

Systems associated with the first three configurations represented in Fig. 2.2A–C only exhibit vapor–liquid equilibrium (VLE) but no liquid–liquid equilibrium (LLE), that is, their liquid phase remains stable at the given temperature, regardless of the composition or pressure considered.

Fig. 2.2A represents the simplest situation in which the bubble and dew curves are monotonically increasing between the two pure-component vapor pressures (i.e., between $x_1 = 0$ and $x_1 = 1$). Fig. 2.2.B and C show systems exhibiting positive and negative azeotropic behaviors, respectively (at an azeotropic point, the isothermal bubble and dew curves pass simultaneously through an extremum in the pressure-composition plane).

Fig. 2.2D–F describe four isothermal phase diagrams for which the liquid phase is not stable over the whole range of composition and pressure; it is then said that the liquid phase unmixes. In each representation, the horizontal straight line materializes the three-phase equilibrium (liquid–liquid–vapor); the pair of vertical lines delimitates the LLE domain.

More particularly, the phase diagram plotted in Fig. 2.2D is obtained by conjugating a simple VLE phase diagram (such as the one shown in Fig. 2.2A) and a liquid–liquid phase split. Similarly, Fig. 2.2E and F are obtained when a system exhibits positive azeotropy and when simultaneously the liquid phase unmixes. Depending on whether the miscibility gap (i.e., the composition range where the liquid phase splits) includes or not the azeotropic composition, Fig. 2.2E and F are observed.

When approaching elevated pressure and temperature domains (i.e., when $T > Min\{T_{c,1}, T_{c,2}\}$ or $P > Min\{P_{c,1}, P_{c,2}\}$), at least one of the two species making up the binary system 1 + 2 reaches a supercritical state at given T or P. Let us now assume that numbers "1" and "2" are affected to the species of a binary system according to the criterion $T_{c,1} < T_{c,2}$. At a given temperature T, such that $T_{c,1} < T < T_{c,2}$, species 1 is supercritical, and it is no longer possible to define its vapor pressure (P_1^{sat}). On the contrary, pure component 2 is still subcritical, and the resulting isothermal *Pxy* projection is illustrated in Fig. 2.3.

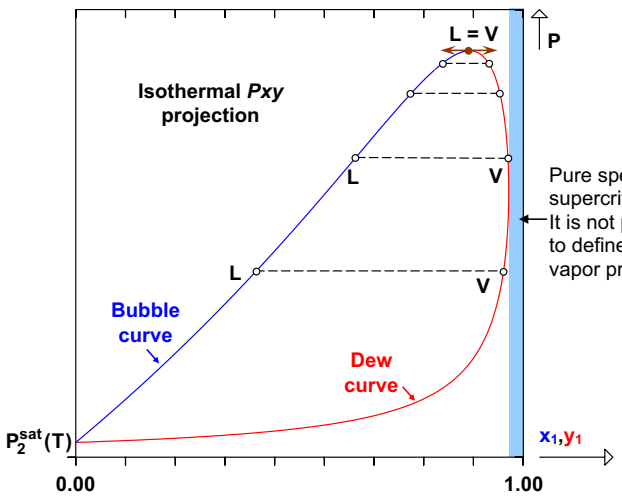

FIGURE 2.3

Schematic isothermal *Pxy* projection of the phase diagram of a binary system 1 + 2 at a given temperature such that pure component 2 is subcritical and pure component 1 is supercritical. L = bubble point; V = dew point; L = V: mixture critical point. *Dashed lines* are tie lines. *Continuous lines* are bubble and dew curves. *Shaded area*: composition range on which the system is single-phase.

The shaded area in Fig. 2.3 specifies the composition range on which the mixture at T is in a 1-phase fluid state, regardless of the pressure value, in other words, by compressing a mixture from very low to very high pressures following an isothermal path, no phase transition is observed; the mixture always remains in a 1-phase state. Similarly, to low-temperature isothermal *Pxy* phase diagrams, vapor−liquid tie lines are horizontal segments joining a bubble point (L) and a dew point (V). At the top of the phase diagram, the bubble and dew points merge in a so-called mixture critical point (denoted by "L = V"). In such a point, the intensive properties of the liquid and gas phase in equilibrium become strictly identical (the two equilibrium phases exhibit the same densities, the same molar enthalpies, the same heat capacities, and so on).

Let us now address a feature of binary system isothermal phase diagrams made up of one sub- and one super-critical compound, which is of particular interest for the study of natural gases, the retrograde condensation phenomenon. This one occurs due to the presence of a composition maximum on the dew curve in the isothermal *Pxy* projection (such a composition is now denoted as $x_{1,\max}$; Fig. 2.4A). To explicate the "retrograde condensation phenomenon," let us consider a gaseous binary mixture, the global composition of which is z_1 at given temperature T.

Upon isothermal compression up to a high-enough pressure, a gaseous binary mixture of fixed composition and temperature is expected to reach a 1-phase liquid state. This phase transition is however possible only if at the fixed composition and temperature, the mixture exhibits both a bubble point and a dew point.

Let us consider now a gaseous binary mixture in an initial state denoted V_1 and represented in Fig. 2.4A. As a noticeable feature, at the temperature T and composition z_1 associated with point V_1, the binary mixture exhibits simultaneously two dew points and does not show any bubble point. Therefore upon isothermal compression from V_1, the binary mixture reaches the first dew point

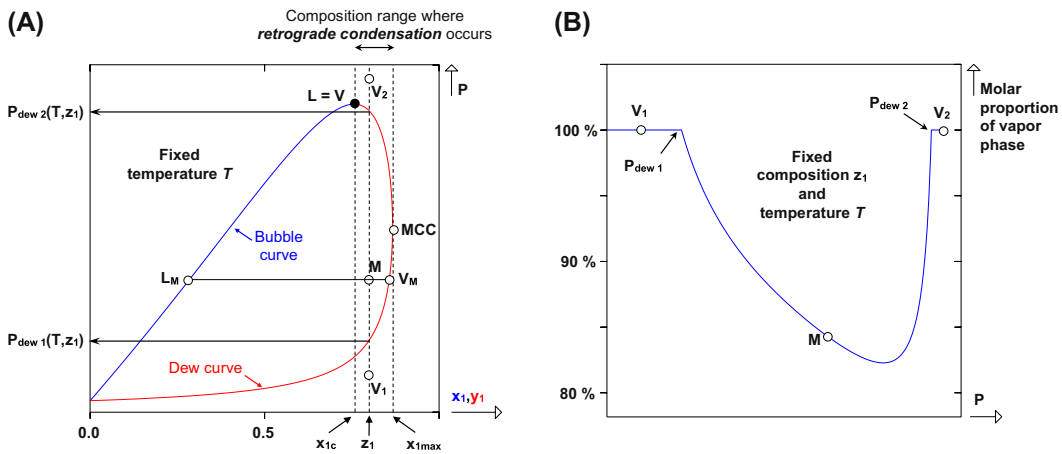

FIGURE 2.4

Illustration of the retrograde condensation phenomenon. (A) Isothermal *Pxy* projection: description of an isothermal compression path from V_1 to V_2 undergone by a binary mixture of fixed composition (z_1); L = V, mixture critical point; x_{1c} = critical composition; *MCC*, MaxCondenComp; $x_{1\max}$ = composition of MCC. (B) Evolution of the gas phase mole proportion along the compression path from V_1 to V_2.

(characterized by pressure $P_{\text{dew }1}$; Fig. 2.4A). At this point, a drop of liquid appears and the gas-phase proportion is equal to 100%. By increasing again the pressure up to, e.g., the one of point M, condensation occurs and an increasing amount of liquid phase appears. Consequently, the mole proportion of the gas phase decreases (Fig. 2.4B). It is recalled that according to the lever rule, the mole proportion of the gas phase, observed at point M, can be graphically determined with the help of Fig. 2.4A by:

$$\begin{cases} \begin{pmatrix} \text{mole proportion} \\ \text{of the gas phase} \end{pmatrix} = 100 \times \dfrac{\text{length of segment } [L_M M]}{\text{length of segment } [L_M V_M]} \\ \begin{pmatrix} \text{mole proportion} \\ \text{of the liquid phase} \end{pmatrix} = 100\% - \begin{pmatrix} \text{mole proportion} \\ \text{of the gas phase} \end{pmatrix} \end{cases} \tag{2.3}$$

Owing to the presence of a composition maximum along the dew curve (called *MaxCondenComp* for "*maximum composition of condensation*," see point MCC in Fig. 2.4A), the vertical line of composition z_1 intersects twice the dew curve so that by increasing the pressure again, the liquid-phase mole proportion is necessarily going to reach a maximum before decreasing because it has to vanish when the dew curve (pressure $P_{\text{dew }2}$) is reached (Fig. 2.4B). This decrease of the mole proportion of the liquid phase upon isothermal compression is called *retrograde condensation* and simply means that the condensation backpedals. To sum up, upon isothermal compression from V_1 to V_2, the binary mixture passes from a gas state to a gas state through vapor−liquid intermediate states.

To understand how isothermal *Pxy* projections of binary systems may evolve from low to high temperatures, let us address the behavior of a fictitious binary system, devoid of singularity (neither azeotropy, nor liquid−liquid phase split) as illustrated in Fig. 2.5. Panel (A) is the P-T projection of the phase diagram. It integrates the vapor-pressure curves of the pure species and the so-called *critical locus*, which is the locus of the mixture critical points connecting the pure-component critical points C_1 and C_2. Along this critical line, the mole fraction of component 1 (x_1) varies between 0 (point C_2) and 1 (point C_1). The vertical dashed lines visible in panel (A) indicate the temperatures of the isothermal *Pxy* projections shown in panel (B). At low temperature T_1, both pure species are subcritical (see panel A), and consequently, the *Pxy* projection at T_1 is connected to the saturation points of the pure components (see panel B). At temperatures such that pure component 1 is supercritical (T_3, T_4, T_5, T_6), saturation points of pure 1 are no longer defined, and consequently, the corresponding isothermal *Pxy* projections are solely connected to the vapor pressure of pure 2. When the temperature reaches $T_7 = T_{c,2} = Max\{T_{c,1}, T_{c,2}\}$, the *Pxy* phase diagram of the binary system reduces to a single point (see panel B).

At this step, it should be mentioned that a great variety of binary-system phase behaviors exist which were classified by Van Konynenburg and Scott 50 years ago following a smart methodology (Van Konynenburg and Scott, 1980). Although the purpose of this chapter does not necessitate going into technical details of their work, it should be mentioned that as an initial approach, their classification is essentially based on the shape of the critical locus in the *P-T* plane. For mixtures containing rather similar molecules in terms of size and interactions, continuous critical loci joining pure component critical points are observed (Fig. 2.6A). For size-asymmetric systems, discontinuous critical loci are observed, as illustrated in Fig. 2.6B and C. In this latter case, critical loci show a nearly vertical branch characterizing extremely high critical pressures.

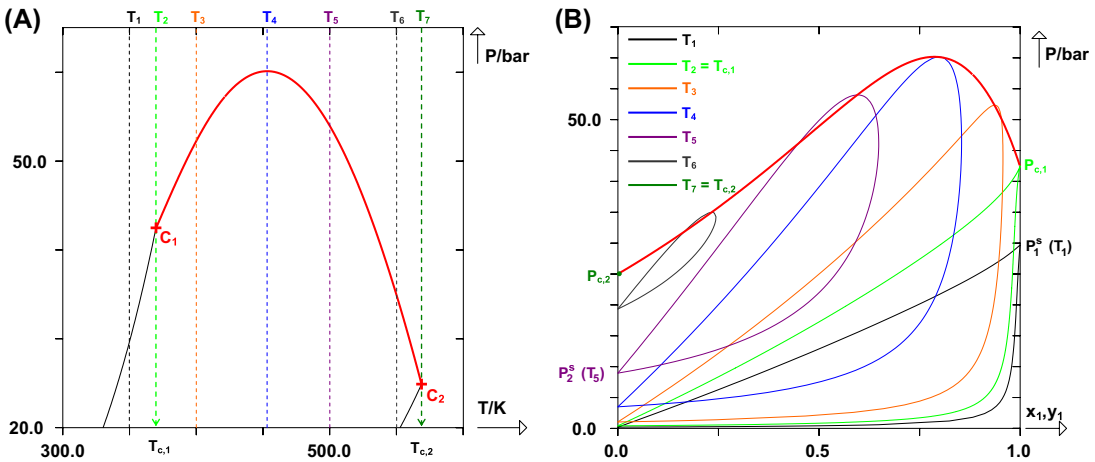

FIGURE 2.5

(A) P-T projection of a binary system 1 + 2: *continuous thin lines* = vapor-pressure curves; *continuous bold line* = critical locus (i.e., locus of mixture critical points); *vertical dashed lines* highlight temperatures T_1 to T_7 of the isothermal *Pxy* projections represented in panel (B); C_1 and C_2 denote the pure-component critical points. (B) Evolution of isothermal *Pxy* projections of the phase diagram of the binary system 1 + 2 from low temperature (T_1) to high temperature (T_7). *Continuous thin line* = isothermal *Pxy* projection; *bold continuous line* = critical locus.

For illustration purpose, let us briefly address the case of the CO_2 + n-octylbenzene system which shows a discontinuous critical locus in the *P-T* plane (Fig. 2.7A). At a temperature well below the temperatures of the vertical branch (e.g., T_1), the *Pxy* projection of the binary system exhibits a high-pressure LLE region connected to the low-pressure VLE region through a horizontal vapor–liquid–liquid (or 3-phase) equilibrium line (see the *Pxy* projection at T_1 in Fig. 2.7B). At higher temperatures, well above the temperatures of the vertical branch (e.g., T_3), the *Pxy* projections turn back to phase diagrams similar to the one presented in Fig. 2.4.

2.2.3 PHASE ENVELOPES (OR ISOPLETHS) OF BINARY SYSTEMS

A phase envelope (or isopleths or *P-T* contour plot) is the *P-T* projection of the phase diagram of a multicomponent system of fixed composition. It is made up of two parts: (1) the bubble curve and (2) the dew curve. These two curves join at a critical point characterized by a critical composition equal to the composition at which the phase envelope is plotted. Fig. 2.8 illustrates the construction of the phase envelope of a binary system of composition $z_1 = 0.5$.

Fig. 2.8A shows a series of isothermal *Pxy* projections from low to high temperatures. At the composition $z_1 = 0.5$ (see the vertical line) and for a selected temperature *T*, it is possible to read in panel (A) the corresponding bubble-point pressure (P_{bubble}, symbol: circles) and dew-point pressure (P_{dew}, symbol: squares). By changing the temperature *T* at the same composition z_1, new values of P_{bubble} and P_{dew} are obtained. By reporting the points, the coordinates of which are (P_{bubble}, *T*) and

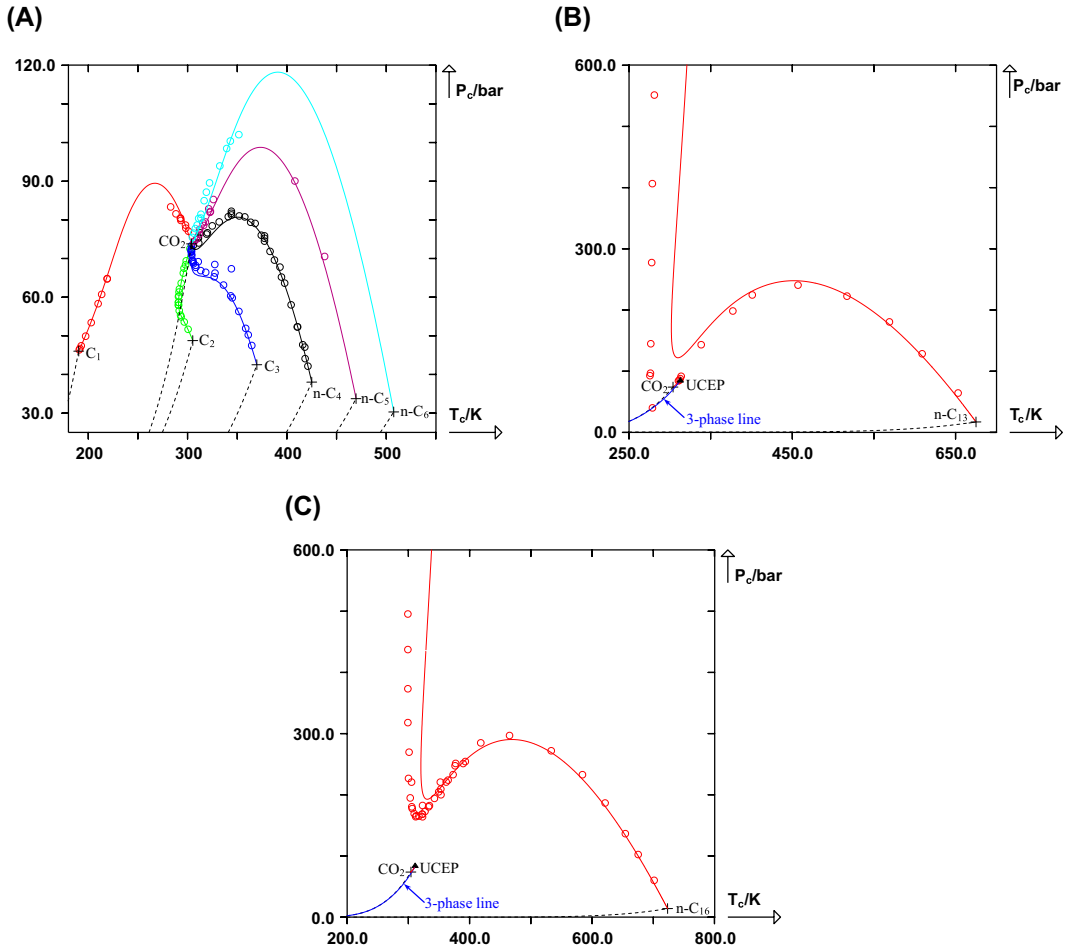

FIGURE 2.6

P-T projections of binary system critical loci. *Circles*: experimental data points. *Continuous line*: prediction from the PPR78 model (Vitu et al., 2008). (A) Continuous critical loci of binary systems containing CO_2 and a light n-alkane. (B) and (C): discontinuous critical loci of binary systems containing CO_2 and a heavy n-alkane. *UCEP*, upper critical end point (for more details, see the paper by Privat and Jaubert (2013)).

(P_{dew}, T) in a P-T plane, one obtains the phase envelope of the binary system at $z_1 = 0.5$ (see panel B) made up of a bubble and a dew curve. The phase envelope of a mixture of known composition has generally a loop shape and is rather simply interpreted as for a temperature and a pressure defining a point inside the loop, the mixture is in a VLE state. Outside the loop, a mixture located above the bubble curve is in a 1-phase liquid state, whereas a mixture located below the dew curve is in a 1-phase gaseous state.

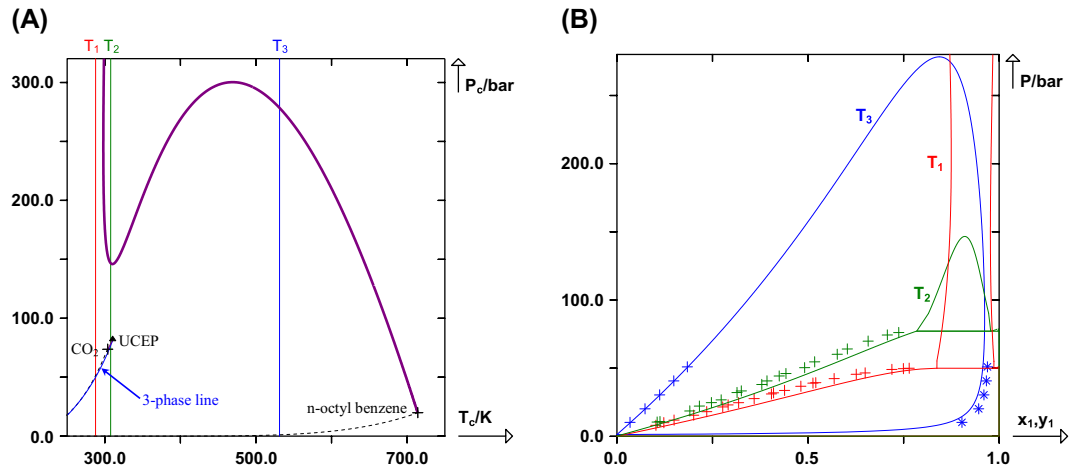

FIGURE 2.7

(A) P-T projection of the CO_2 + n-octylbenzene system; *dashed line* = vaporization curves; *bold line* - = discontinuous critical locus; the *vertical lines* indicate temperatures of the *Pxy* projections shown in panel (B); *UCEP*, upper critical end point. (B) Isothermal *Pxy* phase diagrams at the temperatures selected in panel (A); (+) and (✳): experimental data points; *continuous lines*: prediction from the PPR78 model.

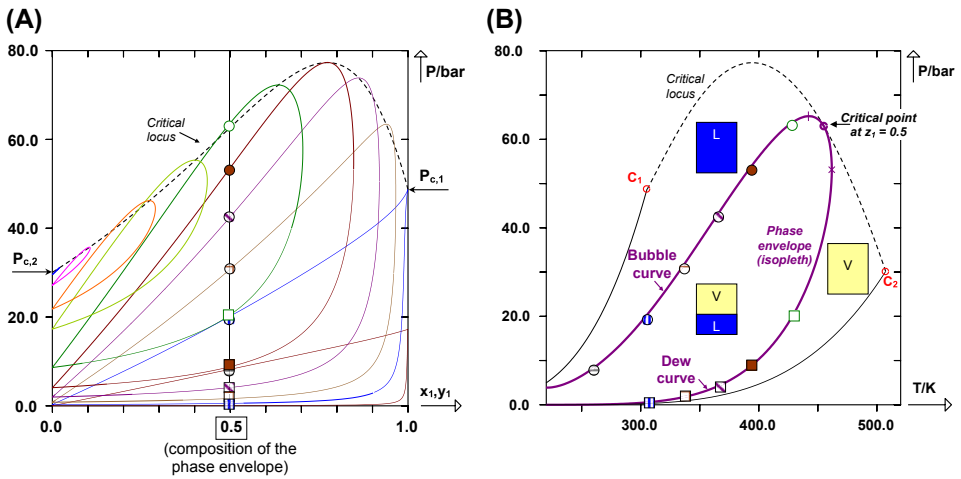

FIGURE 2.8

(A) *Pxy* projections: *continuous lines*, isothermal phase diagrams of a given binary system 1 + 2 from low to high temperatures; *dashed line*, critical locus; *circles*, bubble points; *squares*, dew points. (B) *P-T* projection: *continuous thin lines*, vapor-pressure curves of pure species; *dashed line*, critical locus; *continuous bold line*, phase envelope at $z_1 = 0.5$; C_1 and C_2, pure-component critical points.

Note that the *mixture critical point* can be located anywhere along the phase envelope. Contrary to what is sometimes thought, this point does not lie at the pressure maximum of the phase envelope (Fig. 2.8B). The pressure maximum of the phase envelope is either christened *maxcondenbar* or *cricondenbar* (see symbol "+" in Fig. 2.8B), whereas the temperature maximum is called *maxcondentherm* or *cricondentherm* (see symbol "×" in Fig. 2.8B).

Mainly two types of phase envelopes can be found depending on whether the mixture contains size-symmetric or size-asymmetric compounds, as illustrated in Fig. 2.9.

2.2.4 PHASE ENVELOPES OF PETROLEUM FLUIDS

Crude oils are mixtures containing from light to heavy hydrocarbons that are found in a liquid state in underground geologic formations (mother rock). Natural gases are gaseous mixtures at mother rock temperature and contain essentially methane and some other compounds. Gas condensates can be seen as intermediary fluids in terms of volatility (containing mainly hydrocarbons from C_5 to C_8) that are recovered as liquids in gas-processing plants.

In practice, these three kinds of petroleum fluids are not binary systems but contain from tens to thousands of molecular species. However, similar to binary systems, their phase behavior can be described by phase envelope projections in the *P-T* plane (this type of representation applies actually for any multicomponent mixture of fixed composition).

Fig. 2.10 gives an overview of three schematic phase envelopes for the three aforementioned petroleum fluids (crude oils, gas condensates, and natural gases). For a crude oil, at the temperature of the mother rock, it is possible to define a bubble point (symbol: circle) and a dew point (symbol: square). Consequently, under high pressure, the crude oil is in a liquid state, whereas under low to moderate pressures, the crude oil is in a vapor-liquid state (note that the gas state is generally only found at very low pressure). For a gas condensate, it is possible to define two dew points at the temperature of the mother rock (*retrograde condensation* phenomenon). Hence a gas condensate is in a gaseous state at low or high pressures but exhibits 2-phase equilibria at intermediate pressures. A natural gas is fully gaseous at the mother rock temperature, regardless of the pressure value.

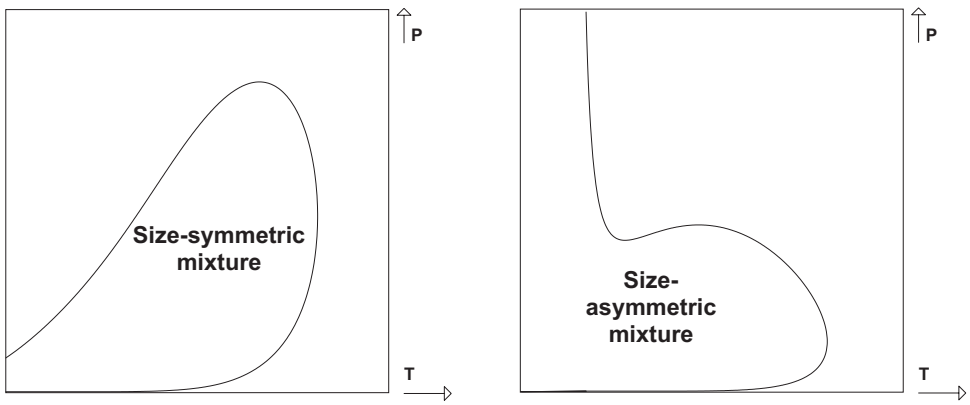

FIGURE 2.9

Schematic representation of the shapes of phase envelopes for size-symmetric and size-asymmetric mixtures.

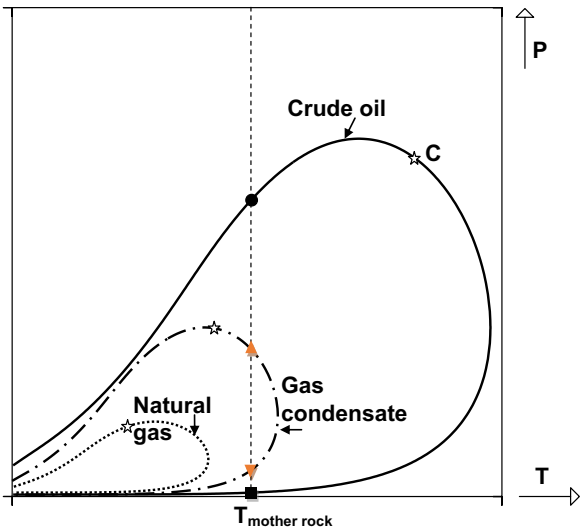

FIGURE 2.10

Schematic phase envelopes of three kinds of petroleum fluids. Symbols: *star* = mixture critical point (also denoted C), *triangles* = upper and lower dew points of a gas condensate, *circle* = crude oil bubble point, *square* = crude oil dew point.

2.2.5 CALCULATION OF VAPOR–LIQUID EQUILIBRIA IN NATURAL GAS SYSTEMS

2.2.5.1 Introduction: Phase Variables Versus Global Variables

The intensive state of any 2-phase equilibrium system can be described by two different sets of intensive variables:

- The intensive phase variables are intensive properties related to a given phase of the 2-phase system, e.g., temperature of the liquid phase, pressure of the gas phase, liquid density, mole fraction y_i of a component i in the gas phase, liquid molar heat capacity …
- The intensive global variables are not specific to a given phase but instead characterize the whole 2-phase system (i.e., the global system). As an example, we can cite the gas-phase molar proportion (defined as the gas-phase mole number divided by the global mole number, i.e., the liquid-phase + the gas-phase mole numbers), the global density (defined as the global mass of the 2-phase system, i.e., $m_{\text{liquid}} + m_{\text{gas}}$, divided by its global volume, i.e., $V_{\text{liquid}} + V_{\text{gas}}$), the global molar enthalpy (defined as the global enthalpy of the 2-phase system divided by its global mole number) …

Extensive variables being additive, extensive global variables are obtained by summing the corresponding total variables of the liquid and gas phases:

$$\underbrace{Q_{2-\text{phase system}}}_{\substack{\text{Extensive global}\\ \text{variable}}} = \underbrace{Q_{\text{liquid phase}}}_{\substack{\text{Extensive total}\\ \text{variable of the}\\ \text{liquid phase}}} + \underbrace{Q_{\text{gas phase}}}_{\substack{\text{Extensive total}\\ \text{variable of the}\\ \text{gas phase}}} \quad \text{with} \quad Q = \begin{cases} \text{n (mole number)} \\ \text{V (volume in m}^3\text{)} \\ \text{H (\textit{enthalpy in} J)} \\ \text{C}_\text{P}\ \text{(heat capacity in J}\cdot\text{K}^{-1}\text{)} \\ \ldots \end{cases} \tag{2.4}$$

As a consequence, the relation between molar phase variables derived from extensive variables ($q_{\text{liquid phase}} = \frac{Q_{\text{liquid phase}}}{n_{\text{liquid}}}$, $q_{\text{gas phase}} = \frac{Q_{\text{gas phase}}}{n_{\text{gas}}}$) and molar global variables $\left(q_{2-\text{phase system}} = \frac{Q_{2-\text{phase system}}}{n_{\text{global}}}\right)$ is given as:

$$n_{\text{global}} \cdot q_{2-\text{phase system}} = n_{\text{liquid}} \cdot q_{\text{liquid phase}} + n_{\text{gas}} \cdot q_{\text{gas phase}} \quad \text{with}$$
$$q = \begin{cases} \text{mole fraction of a given species} \\ \text{h (molar enthalpy)} \\ \text{C}_\text{P}\ \text{(molar heat capacity)} \\ \ldots \end{cases} \tag{2.5}$$

The molar proportions of the phases are now introduced through the equation:

$$\begin{cases} \text{Gas} - \text{phase molar proportion :} & \tau = n_{\text{gas}}/n_{\text{global}} \\ \text{Liquid} - \text{phase molar proportion :} & 1 - \tau = n_{\text{liquid}}/n_{\text{global}} \end{cases} \tag{2.6}$$

By combining Eqs. 2.5 and 2.6, one obtains:

$$q_{2-\text{phase system}} = (1-\tau)\cdot q_{\text{liquid phase}} + \tau \cdot q_{\text{gas phase}} \tag{2.7}$$

This latter equation that connects global and phase molar properties will be of particular importance for *PT* flash calculations, introduced thereafter.

2.2.5.2 The 2-Phase Equilibrium Condition

The 2-phase equilibrium condition is a set of three equations. It imposes the equality of the temperature, pressure, and chemical potential of each component in the two equilibrium phases. It is the central equation for 2-phase equilibrium calculations. For a p-component system in VLE, this condition can be written as:

$$\begin{cases} T_{\text{liquid}} = T_{\text{gas}} (\text{simply denoted T thereafter}) \\ P_{\text{liquid}} = P_{\text{gas}} (\text{simply denoted P thereafter}) \\ \mu^{\text{liquid}}_{\text{component}\,i} = \mu^{\text{gas}}_{\text{component}\,i}, \quad \text{for } i = 1, 2, \ldots, p \end{cases} \tag{2.8}$$

where $\mu_{\text{component } i}$ is the chemical potential of species i in a given phase defined as the molar partial Gibbs energy of species i.

It is, however, well acknowledged that the chemical potential cannot be derived in an absolute manner from EoS or activity-coefficient models classically used to perform VLE calculations.

Consequently the chemical-potential uniformity equation is converted into equations involving quantities derivable from these models, such as the fugacity or the activity:

$$\begin{aligned}\underbrace{\mu^{\text{liquid}}_{\text{component } i} = \mu^{\text{gas}}_{\text{component } i}}_{\text{chemical potentials of i}} &\Leftrightarrow \underbrace{f^{\text{liquid}}_{\text{component } i} = f^{\text{gas}}_{\text{component } i}}_{\text{fugacities of } i} \\ &\Leftrightarrow x_i \cdot \underbrace{\varphi^{\text{liquid}}_{\text{component } i} = \varphi^{\text{gas}}_{\text{component } i}}_{\text{fugacity coefficients of i}} \cdot y_i \\ &\Leftrightarrow \underbrace{a^{\text{liquid}}_{\text{component } i} = a^{\text{gas}}_{\text{component } i}}_{\text{activities of } i}\end{aligned} \tag{2.9}$$

where x_i and y_i are the equilibrium mole fractions of i in the liquid and gas phases, respectively.

As a final remark, note that the 2-phase equilibrium condition only involves *intensive phase variables*.

2.2.5.3 Models for Calculating Vapor–Liquid Equilibria in Natural Gas Systems

Two classes of models could be used potentially to perform phase-equilibrium calculations on natural gases: (1) *pressure-explicit* EoS and (2) activity-coefficient models.

Pressure-explicit EoS are models capable of describing subcritical states, vapor–liquid critical phenomena, and supercritical states. They are thus usable from low to high temperatures and from low to high pressures.

On the contrary, activity-coefficient models do not have the capacity to describe vapor–liquid critical states and supercritical states, and they are thus limited to low-temperature and low-pressure domains.

Natural gases contain generally compounds that are supercritical at temperature and pressure conditions of geological reservoirs or in gas-processing plants. Consequently, only pressure-explicit EoS can be considered for their thermodynamic modeling.

Pressure-explicit EoS for mixtures are models expressing the pressure P of a phase as a function of its temperature T, molar volume v, and composition (vector of component mole fractions z). Fugacity or fugacity coefficient expressions (which are involved in the 2-phase equilibrium condition) can be derived from such a model (Smith et al., 2005; Michelsen and Mollerup, 2007; Sandler, 2017) and expressed with respect to variables (T, v, z).

For instance, cubic EoS, detailed thereafter, are EoS models usable for natural gases. In their general form, they can be written as:

$$\begin{cases} P(T,v,\mathbf{z}) = \dfrac{RT}{v - b_m(\mathbf{z})} - \dfrac{a_m(T,\mathbf{z})}{[v - r_1 b_m(\mathbf{z})][v - r_2 b_m(\mathbf{z})]} \\ \ln \varphi_i(T,v,\mathbf{z}) = \dfrac{1}{v - b_m}\left[\dfrac{d(nb_m)}{dn_i}\right] - \dfrac{1}{RT(r_1 - r_2)b_m}\left[\dfrac{1}{n}\dfrac{d\left(n^2 a_m\right)}{dn_i}\right] \cdot \ln\left(\dfrac{v - r_2 b_m}{v - r_1 b_m}\right) \\ \qquad -\ln\left[1 - \dfrac{a_m(v - b_m)}{RT(v - r_1 b_m)(v - r_2 b_m)}\right] \\ \qquad -\dfrac{a_m}{RTb_m}\left[\dfrac{d(nb_m)}{dn_i}\right]\left[\dfrac{v}{(v - r_1 b_m)(v - r_2 b_m)} - \dfrac{1}{(r_1 - r_2)b_m}\ln\left(\dfrac{v - r_2 b_m}{v - r_1 b_m}\right)\right] \end{cases} \tag{2.10}$$

where (r_1, r_2) are universal constants (i.e., component-independent constants), a_m and b_m are EoS-mixture parameters described in Section 2.3, R is the gas constant, n_i is the mole number of species i in a phase, and $n = \sum_{i=1}^{p} n_i$ is the total amount of matter.

2.2.5.4 Expression of the Equilibrium Condition When Using Pressure-Explicit EoS to Model Fluid Properties

Let us consider a system in 2-phase equilibrium. The molar volume and composition of the liquid phase are denoted as v_{liquid} and $\mathbf{x}$ (vector of component mole fractions); for the gas phase, they are denoted as v_{gas} and $\mathbf{y}$.

When using a pressure-explicit EoS to model a fluid mixture, the VLE condition given by Eqs. 2.8 and 2.9 can be written as:

$$\begin{cases} T_{\text{liquid}} = T_{\text{gas}} \quad (\text{simply denoted } T \text{ thereafter}) \\ P(T_{\text{liquid}}, v_{\text{liquid}}, \mathbf{x}) = P(T_{\text{gas}}, v_{\text{gas}}, \mathbf{y}) \\ x_i \cdot \varphi^{\text{liquid}}_{\text{component } i}(T_{\text{liquid}}, v_{\text{liquid}}, \mathbf{x}) = y_i \cdot \varphi^{\text{gas}}_{\text{component } i}(T_{\text{gas}}, v_{\text{gas}}, \mathbf{y}), \quad \text{for } i = 1, 2, \ldots, p \end{cases} \tag{2.11}$$

or more simply as

$$\begin{cases} P(T, v_{\text{liquid}}, \mathbf{x}) = P(T, v_{\text{gas}}, \mathbf{y}) \\ x_i \bullet \varphi^{\text{liquid}}_{\text{component } i}(T, v_{\text{liquid}}, \mathbf{x}) = y_i \bullet \varphi^{\text{gas}}_{\text{component } i}(T, v_{\text{gas}}, \mathbf{y}), \quad \text{for } i = 1, 2, \ldots, p \end{cases} \tag{2.12}$$

2.2.5.5 Gibbs Phase Rule

Gibbs phase rule provides an expression for the variance (also called number of *degrees of freedom*), denoted *dof*, of a p-component system, containing k phases in equilibrium:

$$dof = p + 2 - k \tag{2.13}$$

This *dof* may be defined as the number of the intensive phase variables of a thermodynamic system that must be specified to fix the intensive state of each phase (or in other words, to fix all the other intensive phase variables of the multiphase system).

It is worth noting that intensive global variables (e.g., molar phase proportions, overall composition …) are not involved in the *dof* definition.

For a VLE ($k = 2$), the Gibbs phase rule leads to:

$$dof = p(\text{system in VLE}) \tag{2.14}$$

This result is basically confirmed by the system of Eq. (2.12):

- System of Eq. (2.12) involves $(p + 1)$ equations.
- A number of independent variables are involved in the system of Eq. (2.12):
  - Vectors $\mathbf{x}$ and $\mathbf{y}$ contain p mole fractions each, but only $(p - 1)$ are independent because of the summation relations such as $\sum_{i=1}^{p} x_i = 1$ and $\sum_{i=1}^{p} y_i = 1$.
  - Three other independent variables are $(T, v_{\text{liquid}}, v_{\text{gas}})$.
  - In total, the system of Eq. (2.12) involves $2(p - 1) + 3 = 2p + 1$ independent variables.

The number of degrees of freedom is thus given as

$$dof = \begin{pmatrix} \text{number of} \\ \text{independent} \\ \text{variables} \end{pmatrix} - \begin{pmatrix} \text{number of} \\ \text{relations between} \\ \text{these variables} \end{pmatrix} = (2p+1) - (p+1) = p \tag{2.15}$$

2.2.5.6 Calculation Principle of a Phase Envelope

A phase envelope is made up of the loci of the bubble and dew points of a mixture of known overall composition z.

A bubble point must be understood here as a 2-phase system of known liquid-phase composition; $\mathbf{x} = \mathbf{z}$ in equilibrium with a bubble of gas, the composition of which is $\mathbf{y}$. A *dew point* is a 2-phase system of known gas-phase composition: $\mathbf{y} = \mathbf{z}$ in equilibrium with a drop of liquid having the composition $\mathbf{x}$.

Specifying the composition of one of the two equilibrium phases is equivalent to specify $(p-1)$ independent variables. Because the *dof* is equal to p, another intensive phase variable must also be specified to make Eq. (2.12) solvable. This can be, e.g., the pressure P or the temperature T.

To sum up, a bubble-point calculation can be performed by specifying the p intensive phase variables:

$$\begin{cases} \mathbf{x} = \mathbf{z} & [(p-1)\text{specified mole fractions}] \\ T = \text{specified value} \end{cases} \tag{2.16}$$

In such a case, the $(p+1)$ unknowns are $\mathbf{y}$ ($p-1$ unknowns), v_{liquid}, and v_{gas}, determined by solving Eq. (2.12). Once done, the bubble pressure is estimated by application of the EoS: $P_{\text{bubble}} = P(T, v_{\text{liquid}}, \mathbf{x})$.

Similarly, a dew point calculation can be performed by specifying:

$$\begin{cases} \mathbf{y} = \mathbf{z} & [(p-1)\text{specified mole fractions}] \\ T = \text{specified value} \end{cases} \tag{2.17}$$

The $(p+1)$unknowns are $(\mathbf{x}, v_{\text{liquid}}, v_{\text{gas}})$. Once determined, the dew pressure is obtained from the equation $P_{\text{dew}} = P(T, v_{\text{gas}}, \mathbf{y})$.

As previously discussed, at a fixed temperature, two dew-point pressures may exist (retrograde condensation phenomenon). In such a case, the system of equations to solve (Eq. 2.12) will exhibit 2 sets of solutions. As another difficulty, at the maxcondentherm, the dew curve exhibits a vertical tangent in the P-T plane (Fig. 2.8B). As a consequence, in this area, a small change in the specified temperature value causes a high variation in the calculated dew point pressure. In such a case, it is advised to specify the pressure instead of the temperature so that the specified variables become:

$$\begin{cases} \mathbf{y} = \mathbf{z} & [(p-1)\text{specified mole fractions}] \\ P = \text{specified value} \end{cases} \tag{2.18}$$

The $(p+2)$ equations to solve are:

$$\begin{cases} P = P(T, v_{\text{gas}}, \mathbf{y}) \\ P(T, v_{\text{liquid}}, \mathbf{x}) = P(T, v_{\text{gas}}, \mathbf{y}) \\ x_i \cdot \varphi^{\text{liquid}}_{\text{component } i}(T, v_{\text{liquid}}, \mathbf{x}) = y_i \cdot \varphi^{\text{gas}}_{\text{component } i}(T, v_{\text{gas}}, \mathbf{y}), \quad \text{for } i = 1, 2, \ldots, p \end{cases} \tag{2.19}$$

with respect to $(p+2)$ unknowns $(T, \mathbf{x}, v_{\text{liquid}}, v_{\text{gas}})$.

Efficient saturation-point calculation algorithms can be found in the reference book by Michelsen and Mollerup (2007).

2.2.5.7 Calculation Principle of a PT Flash

The *PT* flash calculation is certainly the most common kind of phase-equilibrium calculation. For a multicomponent mixture of known overall composition ($\boldsymbol{z}$), at specified temperature and pressure, this algorithm makes it possible to determine whether the system is in a 1-phase or 2-phase state, and in this latter case it provides the compositions of the equilibrium phases ($\boldsymbol{x}$ and $\boldsymbol{y}$) and their relative proportions (Fig. 2.11).

The *PT* flash calculation is sometimes used to perform phase envelope calculation using an indirect way as shown in Fig. 2.12.

Because a *PT* flash calculation problem involves intensive global variables (overall composition of the mixture, gas-phase proportion), Gibbs phase rule cannot be used to determine the degree of freedom of the system.

The equations describing the PT flash problem combine the equilibrium condition and mole-balance equations. Mole-balance equations are deduced from Eq. (2.7) by setting

$$\begin{cases} q_{2-\text{phase system}} = \mathbf{z} \\ q_{\text{liquid phase}} = \mathbf{x} \\ q_{\text{gas phase}} = \mathbf{y} \end{cases}$$

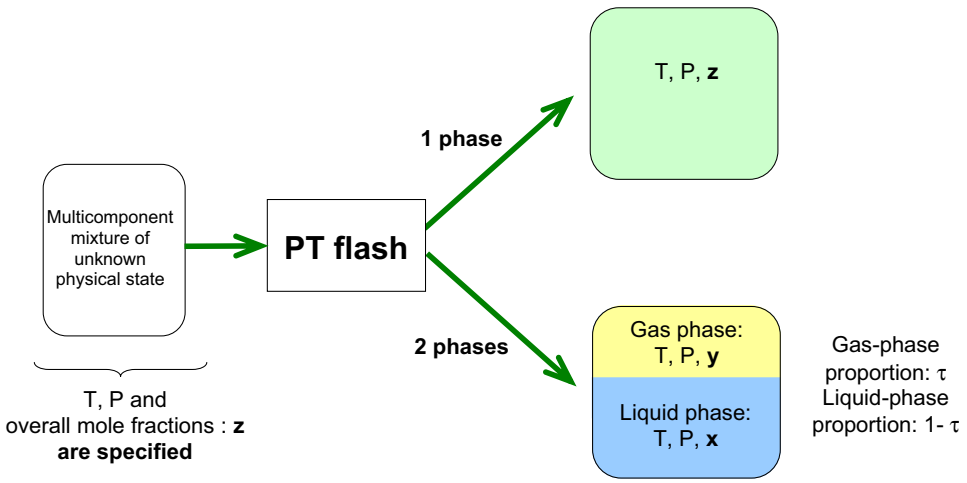

FIGURE 2.11

Schematic principle of a PT flash calculation.

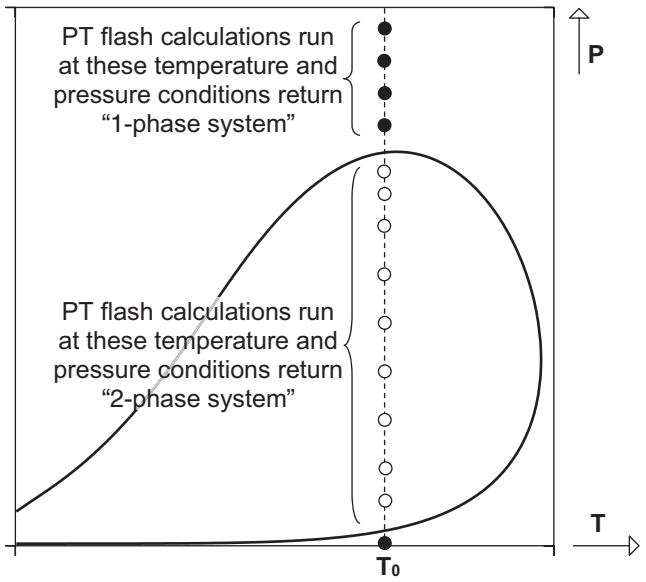

FIGURE 2.12

At given temperature T_0, the saturation pressure (i.e., bubble-point or dew-point pressure) of a phase envelope can be interpreted as the pressure transition between 2-phase state and 1-phase state. *Open circles*: (P, T) coordinates associated with vapor–liquid equilibria. *Full circles*: (P, T) coordinates associated with 1-phase states.

Doing so, the PT-flash problem is thus expressed as:

$$\begin{cases} z_i = (1-\tau)\cdot x_i + \tau \cdot y_i, \quad \text{for } i = 1, 2, \ldots, p-1 \\ P = P(T, v_{\text{gas}}, \mathbf{y}) \\ P(T, v_{\text{liquid}}, \mathbf{x}) = P(T, v_{\text{gas}}, \mathbf{y}) \\ x_i \cdot \varphi^{\text{liquid}}_{\text{component } i}(T, v_{\text{liquid}}, \mathbf{x}) = y_i \cdot \varphi^{\text{gas}}_{\text{component } i}(T, v_{\text{gas}}, \mathbf{y}), \quad \text{for } i = 1, 2, \ldots, p \end{cases} \tag{2.20}$$

Note that only $(p-1)$ mole-balance equations are considered because it is possible to deduce the last one by summing the $(p-1)$ previous ones.

Eq. (2.20) contains $(2p+1)$ equations and involves $(3p+2)$ independent variables:

- 5 variables: $(T, P, v_{\text{liquid}}, v_{\text{gas}}, \tau)$
- $(p-1)$ mole fractions $\mathbf{z}$
- $(p-1)$ mole fractions $\mathbf{x}$
- $(p-1)$ mole fractions $\mathbf{y}$

The *dof* of this problem is thus

$$dof = \begin{pmatrix} \text{number of} \\ \text{independent} \\ \text{variables} \end{pmatrix} - \begin{pmatrix} \text{number of} \\ \text{relations between} \\ \text{these variables} \end{pmatrix} = (3p+2) - (2p+1) = p+1 \qquad (2.21)$$

By specifying **z** (i.e., $(p-1)$ mole fractions), T, and P, the PT-flash problem is thus perfectly determined.

Efficient PT-flash algorithms can be found in the reference book by Michelsen and Mollerup (2007).

2.3 NATURAL GASES PHASE BEHAVIOR MODELING WITH CUBIC EOS

2.3.1 SOME WORDS ABOUT CUBIC EQUATIONS OF STATE HISTORY

Our current industrialized world transports and produces chemicals on an unprecedented scale. Natural gas and oil are today key raw materials from which are derived the gaseous and liquid fuels energizing factories, electric power plants, and most modes of transportation as well. Processes of evaporation and condensation, of mixing and separation, underlie almost any production method in the chemical industry. These processes can be grandly complex, especially when they occur at high pressures. Interest for them has mainly started during the industrial revolution in the 19th century and has unceasingly grown up since then. A huge leap in understanding of the phase behavior of fluids was accomplished during the second half of this century by the scientists Van der Waals and Kamerlingh Onnes and more generally by the Dutch School. It is undisputable that their discoveries were built on many talented anterior works as for instance,

- the successive attempts by Boyle and Mariotte in the 17th century and Gay-Lussac, in the 19th century, to derive the perfect-gas equation,
- the first observation of critical points by Cagniard de la Tour in 1822,
- the experimental determination of critical points of many substances by Faraday and Mendeleev throughout the 19th century,
- the measurement of experimental isotherms by Thomas Andrews showing, at the end of the 19th century, the behavior of a pure fluid around its critical point.

As the major result of the Dutch School, the Van der Waals equation of state (1873)—connecting variables P (pressure), v (molar volume), and T (temperature) of a fluid—was the first mathematical model incorporating both the gas–liquid transition and fluid criticality. In addition, its foundation on, more or less rigorous, molecular concepts (Van der Waals' theory assumes that molecules are subject to attractive and repulsive forces) affirmed the reality of molecules at a crucial time in history. Before Van der Waals, some attempts to model the real behavior of gases were made. The main drawback of the P-v-T relationships presented before was that they did not consider the finite volume occupied by the molecules, similarly, to the perfect-gas equation. Yet the idea of including the volume of the molecules into the repulsive term was suggested by Bernoulli at the end of the 18th century and was then ignored for a long time. Following this idea, Dupré and Hirn (in 1863–64) proposed to replace the molar volume v by $(v-b)$, where b is the molar volume that molecules exclude by their mutual repulsions. This quantity is proportional to the temperature-independent molecular volume v_0 and

named *covolume* by Dupré (sometimes also called *excluded volume*). However, none of these contributions were of general use, and none was able to answer the many questions related to fluid behavior remaining at that time. It was Van der Waals with his celebrated doctoral thesis on "*The Continuity of the Liquid and Gaseous States*" (1873) and his famous equation of state who proposed for the first time a physically coherent description of fluid behavior from low to high pressures. To derive his equation, he considered the perfect-gas law (i.e., $Pv = RT$) and took into account the fact that molecules occupy space by replacing v by $(v - b)$ and the fact that they exert an attraction on each other by replacing P by $P + a/v^2$ (cohesion effect). Therefore owing to mutual repulsion of molecules, the actual molar volume v has to be greater than b while molecular attraction forces are incorporated in the model by the coefficient a. Note also that in Van der Waals' theory the molecules are assumed to have a core in the form of an impenetrable sphere. Physicists and more particularly thermodynamicists rapidly understood that Van der Waals' theory was a revolution-upsetting classical conceptions and modernizing approaches used until then to describe fluids. As a consecration, Van der Waals was awarded the Nobel Prize of physics on December 12, 1910; he can be seen as the father of modern fluid thermodynamics. The equation that Van der Waals proposed in his thesis (Van der Waals, 1873) writes as

$$\left(P + \frac{a}{v^2}\right)(v - b) = R(1 + \alpha t) \tag{2.22}$$

where P and v are the externally measured pressure and molar volume, $R = 8.314472$ J/mol K is the gas constant, and α is a measure of the kinetic energy of the molecule. This equation was rewritten later as follows:

$$P(T, v) = \frac{RT}{v - b} - \frac{a}{v^2} \tag{2.23}$$

It appears that the pressure results from the addition of a repulsive term $P_{\text{rep}} = RT/(v - b)$ and an attractive term $P_{\text{att}} = -a/v^2$. Writing the critical constraints (i.e., that the critical isotherm has a horizontal inflection point at the critical point in the P-v plane), it becomes possible to express the a and b parameters with respect to the experimental values of T_c and P_c, respectively, the critical temperature and pressure:

$$a = \Omega_a \frac{R^2 T_{c,\text{exp}}^2}{P_{c,\text{exp}}} \text{ and } b = \Omega_b \frac{RT_{c,\text{exp}}}{P_{c,\text{exp}}} \text{ with : } \begin{cases} \Omega_a = 27/64 \\ \Omega_b = 1/8 \end{cases} \tag{2.24}$$

The Van der Waals equation is an example of cubic equation. It can be written as a third-degree polynomial in the volume, with coefficients depending on temperature and pressure:

$$v^3 - v^2\left(b + \frac{RT}{P}\right) + \frac{a}{P}v - \frac{ab}{P} = 0 \tag{2.25}$$

The cubic form of the Van der Waals equation has the advantage that three real roots are found at the most for the volume at a given temperature and pressure. EoS including higher powers of the volume comes at the expense of the appearance of multiple roots, thus complicating numerical calculations or leading to nonphysical phenomena. In the numerical calculation of phase equilibrium with cubic equations, one simply discards the middle root, for which the compressibility is negative (this root is associated to an unstable state). Van der Waals' EoS and his ideas on intermolecular forces have

been the subject of many studies and development all through the years. Clausius (1880), proposed an EoS closely similar to the Van der Waals equation in which an additional constant parameter (noted c) was added to the volume in the attractive term, and the attractive term is made temperature dependent. Containing one more adjustable parameter than Van der Waals' equation, Clausius' equation showed a possible way for increasing the model accuracy.

$$\text{Clausius:}\quad P(T,v)=\frac{RT}{v-b}-\frac{a/T}{(v+c)^2} \tag{2.26}$$

In the middle of the 20th century, Redlich and Kwong (1949) published a new model derived from Van der Waals' equation, in which the attractive term was modified to obtain better fluid phase behavior at low and high densities:

$$\text{Redlich-Kwong}:\quad P(T,v)=\frac{RT}{v-b}-\frac{a(T)}{v(v+b)}$$

$$\text{with}\quad \begin{cases} a(T)=a_c\cdot\alpha(T);\ b=\Omega_b RT_{c,\exp}/P_{c,\exp} \\ a_c=\Omega_a R^2T_{c,\exp}^2/P_{c,\exp}\ \text{and}\ \alpha(T)=\sqrt{T_c/T} \\ \Omega_a=1\Big/\left[9\left(\sqrt[3]{2}-1\right)\right]\approx 0.4274 \\ \Omega_b=\left(\sqrt[3]{2}-1\right)\Big/3\approx 0.08664 \end{cases} \tag{2.27}$$

Similarly, to Clausius' equation, a temperature dependency is introduced in the attractive term. The "a" parameter is expressed as the product of the constant coefficient $a_c=a(T_c)$ and $\alpha(T)$ (named alpha function), which is unity at the critical point. Note that only the two pure-component critical parameters T_c and P_c are required to evaluate a and b. The modifications of the attractive term proposed by Redlich and Kwong, although not based on strong theoretical background, showed the way to many contributors on how to improve Van der Waals' equation. For a long time, this model remained one of the most popular cubic equations, performing relatively well for simple fluids with acentric factors close to zero (such as Ar, Kr, or Xe) but representing with much less accuracy complex fluids with nonzero acentric factors. Let us recall that the acentric factor ω_i, defined by Pitzer et al. (1955), as

$$\omega_i=-\log\left[\frac{P_i^{\text{sat}}\left(T=0.7T_{c,i}\right)}{P_{c,i}}\right]-1 \tag{2.28}$$

where P_i^{sat} refers to the vaporization pressure of pure component, i is a measure of the acentricity (i.e., the noncentral nature of the intermolecular forces) of molecule i. The success of the Redlich−Kwong equation has been the impetus for many further empirical improvements. In 1972 the Italian engineer Soave suggested to replace in Eq. (2.27) the α function by a more general temperature-dependent term. Considering the variation in behavior of different fluids at the same reduced pressure (P/P_c) and temperature (T/T_c), he proposed to turn from a two-parameter EoS (the two parameters are T_c and P_c) to a three-parameter EoS by introducing the acentric factor as a third parameter in the definition of $\alpha(T)$. The acentric factor is used to take into account molecular size and shape effects because it varies with the chain length and the spatial arrangement of the molecules (small globular molecules have a

nearly zero acentric factor). The resulting model was named the Soave–Redlich–Kwong (SRK) equation (Soave, 1972) and writes as

$$\text{SRK: } P(T,v) = \frac{RT}{v-b} - \frac{a(T)}{v(v+b)}$$
$$\text{with : } \begin{cases} a(T) = a_c \cdot \alpha(T); \;\; b = \Omega_b R T_{c,\text{exp}} / P_{c,\text{exp}} \\ a_c = \Omega_a R^2 T_{c,\text{exp}}^2 / P_{c,\text{exp}} \;\text{ and }\; \alpha(T) = \left[1 + m\left(1 - \sqrt{T/T_{c,\text{exp}}}\right)\right]^2 \\ m = 0.480 + 1.574\omega - 0.176\omega^2 \\ \Omega_a = 1 \Big/ \left[9\left(\sqrt[3]{2} - 1\right)\right] \approx 0.4274 \\ \Omega_b = \left(\sqrt[3]{2} - 1\right) \Big/ 3 \approx 0.08664 \end{cases} \tag{2.29}$$

The alpha function $\alpha(T)$ used in the SRK equation is often named *Soave's alpha function*. The accuracy of this model was tested by comparing vapor pressures of a number of hydrocarbons calculated with the SRK equation to experimental data. Contrary to the Redlich–Kwong equation, the SRK equation was able to fit well the experimental trend. After Soave's proposal, many modifications were presented in the literature for improving the prediction of one or another property. One of the most popular ones is certainly the modification proposed by Peng and Robinson (1976) (their equation is named PR76 in this chapter). They considered the same alpha function as Soave, but they recalculated coefficients of the m function. In addition, they also modified the volume dependency of the attractive term:

$$\text{PR76 : } P(T,v) = \frac{RT}{v-b} - \frac{a(T)}{v(v+b)+b(v-b)}$$
$$\text{with : } \begin{cases} a(T) = a_c \cdot \alpha(T); \quad b = \Omega_b R T_{c,\text{exp}} / P_{c,\text{exp}} \\ a_c = \Omega_a R^2 T_{c,\text{exp}}^2 / P_{c,\text{exp}} \;\text{ and }\; \alpha(T) = \left[1 + m\left(1 - \sqrt{T/T_{c,\text{exp}}}\right)\right]^2 \\ m = 0.37464 + 1.54226\omega - 0.26992\omega^2 \\ X = \left[1 + \sqrt[3]{4 - 2\sqrt{2}} + \sqrt[3]{4 + 2\sqrt{2}}\right]^{-1} \approx 0.25308 \\ \Omega_a = 8(5X+1)/(49 - 37X) \approx 0.45723 \\ \Omega_b = X/(X+3) \approx 0.077796 \end{cases} \tag{2.30}$$

The accuracy of the PR76 equation is comparable to the one of the SRK equations. Both these models are quite popular in the hydrocarbon industry and offer generally a good representation of the fluid phase behavior of nonassociated molecules (paraffins, naphthenes, aromatics, permanent gases, and so on). Robinson and Peng (1978) proposed to slightly modify the expression of the m function to improve the representation of heavy molecules i such that $\omega_i > \omega_{n-\text{decane}} = 0.491$. This model is named PR78 in this chapter.

$$\text{PR78 : } \begin{cases} m = 0.37464 + 1.54226\,\omega - 0.26992\,\omega^2 & \text{if } \omega \le 0.491 \\ m = 0.379642 + 1.487503\,\omega - 0.164423\,\omega^2 + 0.016666\,\omega^3 & \text{if } \omega > 0.491 \end{cases} \tag{2.31}$$

It is, however, well known that cubic EoS provide inaccurate liquid densities. To fix the ideas, the SRK and PR EoS predict the saturated-liquid volumes with an average deviation of about 16% and 8%, respectively (Le Guennec et al., 2016b). One method to overcome this shortcoming is the so-called volume translation. Indeed, Péneloux et al. (1982) noticed that for a given component, the notable difference between the experimental and the calculated saturated-liquid volume at a given temperature was more or less constant when varying the temperature out of the critical region. Consequently, translating all the calculated molar volumes by a temperature-independent amount c significantly improves the description of the saturated liquid densities. The mathematical expression of the translated EoS can thus be obtained by replacing v by $v + c$ and b by $b + c$ within the untranslated (original) expression. As recently discussed by (Jaubert et al., 2016), such a translation leaves unaffected the calculated vapor pressures, property changes on vaporization, and heat capacities. It is thus possible to keep the same alpha function $\alpha(T)$ for both the translated and untranslated EoS and to determine c to minimize the deviations between experimental and calculated liquid densities. Following the previous work by Péneloux et al. (1982), Le Guennec et al. (2016b) proposed to estimate the volume translation c from the following correlations which involve the Rackett compressibility factor, z_{RA}, defined by Spencer and Danner (1972) when they improved the original Rackett equation (Rackett, 1970):

$$\text{Volume}-\text{translated equations}: \begin{cases} c = \dfrac{RT_c}{P_c}[0.1487 - 0.5052 z_{RA}], & \text{for the SRK equation} \\ c = \dfrac{RT_c}{P_c}[0.1398 - 0.5294 z_{RA}], & \text{for the PR78 equation} \end{cases} \tag{2.32}$$

In a recent paper, Privat et al. (2016) highlighted that the volume-translation concept could be straightforwardly extended to mixtures by using a linear mixing rule. It means that the volume-translation parameter of the mixture $c(T, \mathbf{z})$ is obtained by summing pure-component volume-translation parameters $c_i(T)$ weighted by their corresponding mole fractions:

$$c(T, \mathbf{z}) = \sum_i z_i c_i(T) \tag{2.33}$$

2.3.2 GENERAL PRESENTATION OF CUBIC EQUATIONS OF STATE

All the cubic equations can be written under the following general form:

$$P(T, v) = \frac{RT}{v - b} - \frac{a(T)}{(v - r_1 b)(v - r_2 b)} \tag{2.34}$$

where r_1 and r_2 are two universal constants (i.e., they keep the same value whatever the pure component). As shown with Van der Waals' equation (Eq. 2.25), cubic EoS can be written as third-degree polynomials in v at a fixed temperature T and pressure P:

$$v^3 - v^2\left[b(r_1 + r_2 + 1) + \frac{RT}{P}\right] + v\left[b^2(r_1 r_2 + r_1 + r_2) + \frac{RTb(r_1 + r_2) + a}{P}\right]$$

$$-b\left(r_1 r_2 b^2 + \frac{r_1 r_2 bRT}{P} + \frac{a}{P}\right) = 0 \tag{2.35}$$

As a drawback of cubic equations, the predicted critical molar compressibility factor, $z_c = P_c v_c/(RT_c)$, is found to be a universal constant, whereas, experimentally, it is specific to each pure substance. In a homologous chemical series, the z_c coefficient diminishes as the molecular size increases. For normal substances, z_c is found around 0.27. Table 2.1 provides values of r_1, r_2, and z_c for all the equations presented previously.

Experimental values of T_c and P_c can be used to determine the expressions of $a_c = a(T_c)$, b, and v_c (and thus z_c). Indeed, by application of the classical critical constraints along the critical isotherm at the critical point in a (pressure, molar volume) plane,

$$\begin{cases} \left(\dfrac{\partial P}{\partial v}\right)_T\Big|_{\substack{T=T_{c,\exp}\\ v=v_c}} = 0 \\ \left(\dfrac{\partial^2 P}{\partial v^2}\right)_T\Big|_{\substack{T=T_{c,\exp}\\ v=v_c}} = 0 \\ P_{c,\exp} = P\left(T_{c,\exp}, v_c\right) \end{cases} \tag{2.36}$$

One obtains the following results:

$$\begin{cases} X = \left[1 + \sqrt[3]{(1-r_1)(1-r_2)^2} + \sqrt[3]{(1-r_2)(1-r_1)^2}\right]^{-1} \\ a_c = \Omega_a \dfrac{R^2 T_{c,\exp}^2}{P_{c,\exp}}; \quad b = \Omega_b \dfrac{RT_{c,\exp}}{P_{c,\exp}}; v_c = \dfrac{b}{X}\left(\text{or equivalently} : z_c = \dfrac{\Omega_b}{X}\right) \\ \Omega_a = \dfrac{(1-r_1X)(1-r_2X)[2-(r_1+r_2)X]}{(1-X)[3-X(1+r_1+r_2)]^2} \\ \Omega_b = \dfrac{X}{3-X(1+r_1+r_2)} \quad \text{so that :} \quad z_c = [3-X(1+r_1+r_2)]^{-1} \end{cases} \tag{2.37}$$

Note that a cubic equation of state applied to a given pure component is completely defined by the universal constant values r_1 and r_2, by the critical temperature and pressure of the substance (allowing to calculate b and a_c) but also by the considered alpha function [allowing to evaluate the attractive

Table 2.1 Values of r_1, r_2, and z_c for Some Popular Cubic Equations of State

Equation of State	r_1	r_2	z_c
Van der Waals or Clausius	0	0	$3/8 = 0.375$
Redlich–Kwong or SRK	0	-1	$1/3 \approx 0.333$
PR76 or PR78	$-1-\sqrt{2}$	$-1+\sqrt{2}$	≈ 0.3074

parameter $a(T) = a_c \cdot \alpha(T)$]. The next subsection is dedicated to present some $\alpha(T)$ functions frequently used with cubic equations.

2.3.2.1 Presentation of Some Alpha Functions Usable With Cubic Equations of State

Modifications of the temperature-dependent function $\alpha(T)$ in the attractive term of the SRK and PR equations have been mainly proposed to improve correlations and predictions of vapor pressure for polar fluids. Some of the most used are presented in this section.

- The most popular alpha function is certainly that of (Soave, 1972):

$$\alpha(T) = \left[1 + m\left(1 - \sqrt{T/T_c}\right)\right]^2 \tag{2.38}$$

where m is a function of the acentric factor (expressions of m for the SRK, PR76, and PR78 models are, respectively, given in Eqs. (2.29, 2.30, and 2.31).

- Mathias and Copeman (1983) developed an expression for the alpha function aimed at extending the application range of the PR equation to highly polar components:

$$\begin{cases} \alpha(T) = \left[1 + C_1\left(1 - \sqrt{T/T_c}\right) + C_2\left(1 - \sqrt{T/T_c}\right)^2 + C_3\left(1 - \sqrt{T/T_c}\right)^3\right]^2 & \text{if } T \le T_c \\ \alpha(T) = \left[1 + C_1\left(1 - \sqrt{T/T_c}\right)\right]^2 & \text{if } T > T_c \end{cases} \tag{2.39}$$

Parameters C_1, C_2, and C_3 are specific to each component. They have to be fitted on vapor-pressure data.

- Stryjek and Vera (1986) proposed an alpha function for improving the modeling capacity of the PR equation at low reduced temperatures:

$$\begin{cases} \alpha(T) = \left[1 + m\left(1 - \sqrt{T/T_c}\right)\right]^2 \\ \text{with } m = m_0 + m_1\left(1 + \sqrt{T/T_c}\right)(0.7 - T/T_c) \\ \text{and } m_0 = 0.378893 + 1.4897153\omega - 0.17131848\omega^2 + 0.0196554\omega^3 \end{cases} \tag{2.40}$$

m_1 has to be fitted on experimental vapor-pressure data. Compared to the original PR EoS, this alpha function uses a higher order polynomial function in the acentric factor for the m parameter that allows a better modeling of heavy hydrocarbon phase behavior.

- Twu et al. (1991 and 1995a,b) proposed two different alpha functions. The first one requires, for each pure component, to fit the model parameters (L, M, and N) on experimental pure-component VLE data:

$$\alpha(T) = (T/T_c)^{N(M-1)} \exp\left[L\left[1 - (T/T_c)^{NM}\right]\right] \tag{2.41}$$

The second one is a predictive version of the first one, only requiring the knowledge of the acentric factor. Following Pitzer's corresponding states principle, Twu et al. proposed

$$\alpha(T) = \alpha^0(T) + \omega\left[\alpha^1(T) - \alpha^0(T)\right] \tag{2.42}$$

wherein the expressions of α^0 and α^1 are given by Eq. (2.41). Parameters L, M, and N involved in these two functions are provided in Table 2.2.

A recent study by Le Guennec et al. (2016a, 2017), however, highlighted that α-functions used in cubic equations had to satisfy several constraints. In particular, they have to be positive, monotonically decreasing, convex, and their third derivative with respect to temperature has to be negative. This set of constraints is reported in Eq. (2.43) and establishes what Le Guennec et al. decided to call a "*consistency test for an α-function*." Their papers make it possible to conclude that the nonobservance of one of these constraints may cause the EoS to return inaccurate or unexpected results, especially in the supercritical region.

$$For\ all\ T: \begin{cases} \alpha \geq 0 \ \text{ and } \ \alpha(T) \text{ continuous} \\ \dfrac{d\alpha}{dT_r} \leq 0 \ \text{ and } \ \dfrac{d\alpha}{dT} \text{ continuous} \\ \dfrac{d^2\alpha}{dT^2} \geq 0 \ \text{ and } \ \dfrac{d^2\alpha}{dT^2} \text{ continuous} \\ \dfrac{d^3\alpha}{dT^3} \leq 0 \end{cases} \tag{2.43}$$

To get safe and accurate results, it is thus strongly advised to use in Eq. (2.41) the sets of (L, M, N) parameters recently published by Le Guennec et al. (2016b) for hundreds of pure components and for both the Peng−Robinson and the Redlich−Kwong EoS. Such parameters indeed ensure that the α-function is consistent, i.e., it satisfies all the constraints listed in Eq. (2.43).

Table 2.2 Generalized Parameters of the Predictive Version of the Twu et al. Alpha Function

Alpha Function Parameters	$T \leq T_c$		$T > T_c$	
	α^0	α^1	α^0	α^1
PR				
L	0.125283	0.511614	0.401219	0.024955
M	0.911807	0.784054	4.963070	1.248089
N	1.948150	2.812520	−0.200000	−8.000000
SRK				
L	0.141599	0.500315	0.441411	0.032580
M	0.919422	0.799457	6.500018	1.289098
N	2.496441	3.291790	−0.200000	−8.000000

2.3.3 DISCUSSION ABOUT THE MIXING RULES TO BE USED TO MODEL THE PHASE BEHAVIOR AND ENTHALPIES OF NATURAL GASES WITH CUBIC EQUATIONS OF STATE

The SRK and the PR EoS are the primary choice of models in the gas-processing industries where high-pressure models are required. For a pure component, the three required parameters (T_c, P_c, and ω) were determined from experiments for thousands of pure components. When no experimental data are available, various estimation methods, applicable to any kind of molecule, can be used. Extension to mixtures requires mixing rules for the energy parameter and the covolume. A widely used way to extend the cubic EoS to a mixture containing p components, the mole fractions of which are x_i, is via the so-called Van der Waals one-fluid mixing rules (quadratic composition dependency for both parameters; see Eqs. 2.44 and 2.45) and the classical combining rules, i.e., the geometric mean rule for the cross energy (Eq. 2.46) and the arithmetic mean rule for the cross-covolume parameter (Eq. 2.47):

$$a = \sum_{i=1}^{p} \sum_{j=1}^{p} x_i x_j a_{ij} \tag{2.44}$$

$$b = \sum_{i=1}^{p} \sum_{j=1}^{p} x_i x_j b_{ij} \tag{2.45}$$

$$a_{ij} = \sqrt{a_i a_j}(1 - k_{ij}) \tag{2.46}$$

$$b_{ij} = \frac{1}{2}(b_i + b_j)(1 - l_{ij}) \tag{2.47}$$

Doing so, two new parameters, the so-called binary interaction parameters (k_{ij} and l_{ij}) appear in the combining rules. One of them, namely k_{ij}, is by far the most important one. Indeed, a nonnull l_{ij} is only necessary for complex polar systems and special cases. This is the reason why, dealing with petroleum fluids, phase equilibrium calculations are generally performed with $l_{ij} = 0$, and the mixing rule for the covolume parameter simplifies to

$$b = \sum_{i=1}^{p} x_i b_i \tag{2.48}$$

We know by experience that the k_{ij} value has a huge influence on fluid-phase equilibrium calculation. To illustrate this point, it was decided to plot, using the PR EoS, the isothermal phase diagram for system 2,2,4 trimethyl pentane (1) + toluene (2) at $T = 333.15$ Kgiving to k_{12} different values (Fig. 2.13).

The obtained curves speak for themselves:

- For $k_{12} = -0.07$, the system holds a negative homogeneous azeotrope.
- For $k_{12} = -0.04$, the system still shows negative deviations from ideality, but the azeotrope does not exist any more.
- For $k_{12} = -0.026$, the bubble curve is a straight line, and the liquid phase behaves as an ideal solution.
- For $k_{12} = 0.0$, the system shows positive deviations from ideality.
- For $k_{12} = 0.03$, the system holds a positive homogeneous azeotrope.

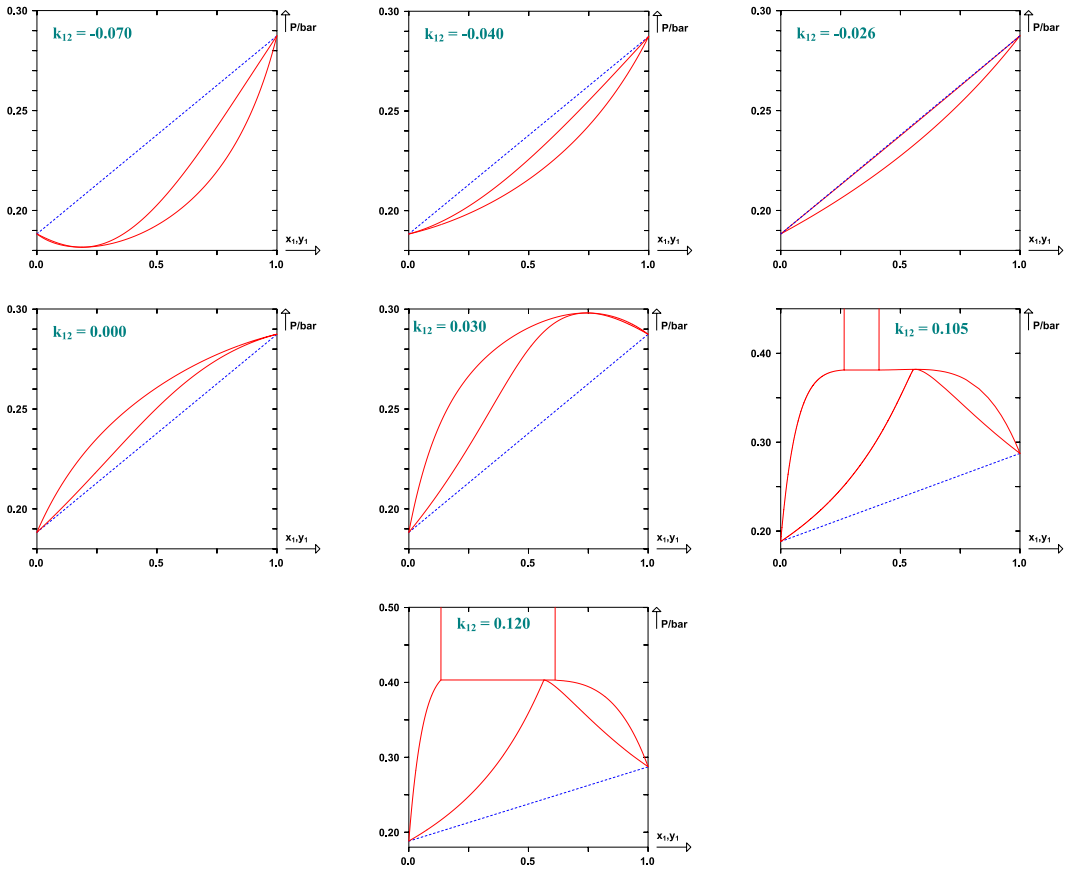

FIGURE 2.13

Influence of k_{12} on the calculated isothermal phase diagram using the PR EoS for system 2,2,4 trimethyl pentane (1) + toluene (2) at $T/\mathrm{K} = 333.15$. The *dashed line* is Raoult's line.

- For $k_{12} = 0.105$, the system simultaneously holds a positive homogeneous azeotrope and a liquid−liquid phase split.
- For $k_{12} = 0.12$, the system holds a heterogeneous azeotrope.

In front of such a big influence, the safest practice is to fit the k_{ij} value to phase equilibrium data. Such an approach, however, requires the knowledge of experimental data for all the binary systems it is possible to define in a multicomponent system. Unfortunately, such data are not always available, inciting many researchers to develop correlations or group contribution methods (GCM) to estimate the k_{ij}.

2.3.3.1 Correlations to Estimate the Binary Interaction Parameters

Most of the proposed correlations are purely empirical and thus often unsuitable for extrapolation. Moreover, they often use additional properties besides those (the critical properties and the acentric factor) required by the cubic EoS itself. They are, however, very useful to clear a phase equilibrium calculation problem.

Following London's theory, Chueh and Prausnitz (1967) proposed a correlation suitable for mixtures of paraffins, which only requires knowledge of the critical volume of the two pure substances i and j (see Eq. (2.49) in Tables 2.2 and 2.3). In 1990 a correlation allowing the estimation of the binary

Table 2.3 Correlations to Estimate the Binary Interaction Parameters

Mathematical Expression of the Correlation	
$k_{ij} = 1 - \left(\frac{2\sqrt{V_{c,i}^{1/3} V_{c,j}^{1/3}}}{V_{c,i}^{1/3} + V_{c,j}^{1/3}}\right)^{n}$	(2.49)
$k_{ij} = k_{ij}^{0} + k_{ij}^{T}[(T/K) - 273.15]$	(2.50)
$1 - k_{ij} = \left(\frac{2\sqrt{T_{c,i} T_{c,j}}}{T_{c,i} + T_{c,j}}\right)^{z_{c,ij}}$ with $z_{c,ij} = \frac{z_{c,i} + z_{c,j}}{2}$	(2.51)
$\begin{cases} k_{ij} = -0,13409\omega + 2,28543\omega^2 - 7,61455\omega^3 + 10,46565\omega^4 - 5,2351\omega^5 \\ k_{ij} = -0,04633 - 0,04367 \ln \omega \end{cases}$	(2.52)
$k_{ij} = A + B\lvert\delta_i - \delta_j\rvert + C\lvert\delta_i - \delta_j\rvert^2$	(2.53)
$k_{ij} = a(T - b)^2 + c$	(2.54)
$k_{ij} = a(\omega_j) + b(\omega_j) \times T_{r,i} + c(\omega_j) \times T_{r,i}^3$	(2.55)
$k_{ij} = A(\omega_j) + B(\omega_j)/T_{r,j}$	(2.56)
$k_{ij} = Q(\omega_j) - \frac{T_{r,i}^2 + A(\omega_j)}{T_{r,i}^3 + C(\omega_j)}$	(2.57)
$1 - k_{ij} = C + D\frac{V_{c,i}}{V_{c,j}} + E\left(\frac{V_{c,i}}{V_{c,j}}\right)^2$ with $\begin{cases} C = c_1 + c_2\lvert\omega_i - \omega_j\rvert \\ D = d_1 + d_2\lvert\omega_i - \omega_j\rvert \end{cases}$	(2.58)

interaction parameters for a modified version of the SRK equation of state was developed by Stryjek (1990). It is applicable to mixtures of n-alkanes and is temperature dependent. The author pointed out that although the temperature dependence of the k_{ij} is moderate for mixtures of paraffins, the use of a temperature-dependent k_{ij} significantly improves the modeling of such systems. The proposed correlation has the form given by Eq. (2.50) in Tables 2.2 and 2.3. Gao et al. (1992) proposed a correlation suitable for mixtures containing various light hydrocarbons (paraffins, naphthenes, aromatics, alkynes). The theoretical approach adopted by these authors is a continuation of that of Chueh and Prausnitz (1967) previously mentioned. It is thus not surprising that their correlation requires the knowledge of critical properties (that are the critical temperature and the compressibility factor). Such a parameter is unfortunately not well known for many hydrocarbons, especially heavy ones. They proposed Eq. (2.51) shown in Tables 2.2 and 2.3. Kordas et al. (1995) developed two mathematical expressions to estimate the k_{ij} in mixtures containing methane and alkanes. The first one is suitable for alkanes lighter than the n-eicosane and the second one for heavy alkanes. In such equations (see Eq. (2.52) in Tables 2.2 and 2.3), ω is the acentric factor of the molecule mixed with methane. Unfortunately, Kordas et al. (1995) failed to generalize their correlations to mixtures containing methane and aromatic molecules. In the open literature, we also can find many correlations to estimate the k_{ij} for systems containing CO_2 and various hydrocarbons. Such equations are of the highest importance because we know by experience that for such systems, the k_{ij} is far from zero. As an example, Graboski and Daubert (1978) proposed a correlation suitable for mixtures containing CO_2 and paraffins. The use of this correlation (see Eq. (2.53) in Tables 2.2 and 2.3), developed for a modified version of the SRK EoS, needs the knowledge of the solubility parameters δ. In Eq. (2.53), subscript i stands for the hydrocarbon and subscript j for CO_2 (or N_2 or H_2S). Another well-known correlation is the one developed by Kato et al. (1981), which has the great advantage to be temperature dependent. It can be applied to the PR EoS and to mixtures containing CO_2 and n-alkanes. It is given in Tables 2.2 and 2.3 (Eq. 2.54). The three coefficients (a, b, and c) only depend on the acentric factor of the n-alkane. A similar approach was followed by Moysan et al. (1986), who developed a correlation in which the temperature-dependent k_{ij} can be estimated knowing the acentric factor of the hydrocarbon mixed with CO_2. A key point of Moysan's work is its applicability to systems containing H_2, N_2, and CO. Another temperature-dependent correlation for systems containing CO_2 and n-alkanes was developed by Kordas et al. (1994). In their approach the k_{ij} depends on the CO_2-reduced temperature ($T_{r,i} = T/T_{c,i}$) and on the alkane acentric factor (ω_j). It can be found in Tables 2.2 and 2.3, Eq. (2.55). Kordas et al. (1994) explain that their correlation can also be used with other hydrocarbons (branched alkanes, aromatics, or naphthenes) under the condition to substitute in Eq. (2.55) the acentric factor (ω_j) of the studied hydrocarbon by an *effective acentric factor*, the value of which has been correlated to the molar weight and to the density at 15°C. The paper by Bartle et al. (1992) also contains a correlation suitable for many systems containing CO_2. Various correlations for nitrogen-containing systems were also developed. Indeed, as shown by Privat et al. (2008b), the phase behavior of such systems is particularly difficult to correlate with a cubic EoS even with temperature-dependent k_{ij}. We can cite the work by Valderrama et al. (1990) who proposed a correlation principally applicable to systems containing nitrogen and light alkanes. The mathematical shape of this correlation was inspired by the previous work of Kordas et al (Eq. 2.55). It is given in Tables 2.2 and 2.3, Eq. (2.56). Such a correlation can be applied to various cubic EoS and to mixtures not only containing alkanes and N_2 but also CO_2 and H_2S. Valderrama et al. (1999) proposed an improved version of their previously published correlation. Although only applicable to the PR EoS, a similar work was conducted in 1994 by

Avlonitis et al. (1994). Once again, the k_{ij} depends on temperature and on the acentric factor (see Eq. (2.57) in Tables 2.2 and 2.3). We cannot close this section before saying a few words about the correlation proposed by Nishiumi et al. (1988). As shown by Eq. (2.58) in Tables 2.2 and 2.3, it is probably the most general correlation never developed because it can be used to predict the k_{ij} of the PR EoS for any mixture containing paraffins, naphthenes, aromatics, alkynes, CO_2, N_2, and H_2S. The positive aspect of this correlation is its possible application to many mixtures. Its negative aspect is the required knowledge of the critical volumes.

Although very useful, these many correlations only apply to specific mixtures (e.g., mixtures containing hydrocarbons and methane, mixtures containing hydrocarbons and nitrogen, mixtures containing hydrocarbons and carbon dioxide, mixtures containing light hydrocarbons, and so on) and to a specific cubic EoS. Moreover they are often empirical and thus unsuitable for extrapolation. In addition, they may need additional properties besides those (the critical properties and the acentric factor) required by the cubic EoS itself. Finally, they do not always lead to temperature-dependent k_{ij}, whereas we know by experience that the temperature has a huge influence on these interaction parameters.

A way to avoid all these drawbacks would be to develop a GCM capable of estimating temperature-dependent k_{ij} and to develop a method allowing switching from a cubic EoS to another one. These issues are discussed in the next subsections.

2.3.3.2 GCMs to Estimate the Binary Interaction Parameters

In any GCM, the basic idea is that whereas there are thousands of chemical compounds of interest in chemical technology, the number of functional groups that constitute these compounds is much smaller. Assuming that a physical property of a fluid is the sum of contributions made by the molecule's functional groups, GCMs allow for correlating the properties of a very large number of fluids using a much smaller number of parameters. These group contribution (GC) parameters characterize the contributions of individual groups in the properties.

2.3.3.2.1 The Abdoul–Rauzy–Péneloux Model

The first GCM designed for estimating the k_{ij} of a cubic EoS was developed by Abdoul et al. (1991) and is sometimes called the Abdoul–Rauzy–Péneloux (ARP; the names of the three creators of the model) model. Even though accurate, such a model has some disadvantages. Indeed, Abdoul et al. (1991) did not use the original PR EoS but instead a nonconventional translated PR-type EoS. Moreover, to estimate the attractive parameter $a(T)$ of their EoS, these authors defined two classes of pure compounds. For components which are likely to be encountered at very low pressure, the Carrier–Rogalski–Péneloux $a(T)$ correlation (Carrier et al., 1988), which requires the knowledge of the normal boiling point, was used. For other compounds, they used a Soave-like expression developed by Rauzy (1982), which is different from the one developed by Soave for the SRK EoS and different from the one developed by Peng and Robinson for their own equation. Moreover the decomposition into groups of the molecules is not straightforward and is sometimes difficult to understand. For example, propane is classically decomposed into two CH_3 groups and one CH_2 group, but 2-methyl propane $\{CH_3–CH(CH_3)–CH_3\}$ is decomposed into four CH groups and not into three CH_3 groups and one CH group. Isopentane is formed by one CH_3 group, half a CH_2 group, and three and a half CH groups. Finally, because this model was developed more than 25 years ago, the experimental database used by Abdoul et al. to fit the parameters of their model (roughly 40,000 experimental data points) is

small in comparison to databases available today. The group parameters obtained from this too small data base may lead to unrealistic phase equilibrium calculations at low or at high temperatures. For all these reasons, this model has never been extensively used and never appeared in commercial process simulators.

2.3.3.2.2 The PPR78 Model

Being aware of the drawbacks of the ARP model, Jaubert et al. (Jaubert and Mutelet, 2004; Jaubert et al., 2005 and 2010; Vitu et al., 2006 and 2008; Privat et al., 2008a,b,c,d; Privat and Jaubert, 2012a; Qian et al., 2013a,b,c,d and 2017; Plee et al., 2015; Xu et al., 2015a,b and 2017a,b) decided to develop the PPR78 model, which is a GC model designed for estimating, as a function of temperature, the k_{ij} for the widely used PR78 EoS. Such an equation of sate was selected because it is used in most of the petroleum companies, but, above all, it is available in any computational package.

2.3.3.2.2.1 Presentation. Following the previous work of Abdoul et al. (1991), $k_{ij}(T)$ is expressed in terms of group contributions, through the following expression:

$$k_{ij}(T) = \frac{-\frac{1}{2}\sum_{k=1}^{N_g}\sum_{l=1}^{N_g}(\alpha_{ik}-\alpha_{jk})(\alpha_{il}-\alpha_{jl})A_{kl}\cdot\left(\frac{298.15}{T}\right)^{\left(\frac{B_{kl}}{A_{kl}}-1\right)} - \left(\frac{\sqrt{a_i(T)}}{b_i}-\frac{\sqrt{a_j(T)}}{b_j}\right)^2}{2\frac{\sqrt{a_i(T)\cdot a_j(T)}}{b_i\cdot b_j}} \quad (2.59)$$

In Eq. 2.59, T is the temperature, a_i and b_i are the attractive parameter and the covolume of pure i, N_g is the number of different groups defined by the method (for the time being, 40 groups are defined so that $N_g = 40$), α_{ik} is the fraction of molecule i occupied by group k (occurrence of group k in molecule i divided by the total number of groups present in molecule i), and $A_{kl} = A_{lk}$ and $B_{kl} = B_{lk}$ (where k and l are two different groups) are constant parameters determined during the development of the model ($A_{kk} = B_{kk} = 0$). As can be seen, to calculate the k_{ij} parameter between two molecules i and j at a selected temperature, it is only necessary to know the critical temperature of both the components ($T_{c,i}$ and $T_{c,j}$), the critical pressure of both the components ($P_{c,i}$ and $P_{c,j}$), the acentric factor of each component (ω_i and ω_j), and the decomposition of each molecule into elementary groups (α_{ik} and α_{jk}). It means that no additional input data besides those required by the EoS itself is necessary. Such a model relies on the Peng–Robinson EoS as published by Peng and Robinson in 1978 (Eqs. 2.30 and 2.31). The addition of a GCM to estimate the temperature-dependent k_{ij} makes it predictive; it was thus decided to call it PPR78 (predictive 1978, Peng–Robinson EoS). The 40 groups which are defined until now are summarized in the following list:

- For alkanes: group 1 = CH_3, group 2 = CH_2, group 3 = CH, group 4 = C, group 5 = CH_4, i.e., methane, group 6 = C_2H_6, i.e., ethane;
- For aromatic compounds: group 7 = CH_{aro}, group 8 = C_{aro}, group 9 = $C_{\text{fused aromatic rings}}$;
- For naphthenic compounds: group 10 = $C_{cyclic}H_2$, group 11 = $C_{cyclic}H = C_{cyclic}$;
- For permanent gases: group 12 = CO_2, group 13 = N_2, group 14 = H_2S, group 21 = H_2, group 28 = CO, group 29 = He, group 30 = Ar, group 31 = SO_2, group 32 = O_2, group 33 = NO, group 34 = COS, group 35 = NH_3, group 36 = NO_2/N_2O_4, group 37 = N_2O;
- For mercaptans: group 15 = −SH;

- For water-containing systems: group 16 = H_2O;
- For alkenes: group 17 = CH_2=CH_2, i.e., ethylene, group 18 = $C_{alkenic}H_2$ = $C_{alkenic}H$, group 19 = $C_{alkenic}$, group 20 = $C_{cycloalkenic}H_2$ = $C_{cycloalkenic}H$;
- For fluorocompounds: group 22 = C_2F_6, i.e., R116, group 23 = CF_3, group 24 = CF_2, group 25 = $C_{alkenic}F_2$ = $C_{alkenic}F$, group 26 = $C_2H_4F_2$, i.e., R152a, group 27 = $C_2H_2F_4$, i.e., R134a;
- For alkynes: group 38 = HC≡CH, i.e., acetylene, group 39 = −C≡CH, group 40 = −C≡C−.

The decomposition into groups of the hydrocarbons (linear, branched, or cyclic) is very easy, that is, as simple as possible. No substitution effects are considered. No exceptions are defined. For these 40 groups, we had to estimate 1560 parameters ($780A_{kl}$ and $780B_{kl}$ values). However, due to a lack of experimental data, some group-interaction parameters could not be determined. The available parameters—determined to minimize the deviations between calculated and experimental VLE data from an extended database containing more than 130,000 experimental data points—are accessible free of charge on the American Chemical Society publications website at http://pubs.acs.org/doi/abs/10.1021/acs.iecr.7b01586. For such experimental data, the PPR78 model makes it possible to predict both the liquid and the gas phase compositions with an average overall deviation of about 8% ($\overline{\Delta x}\% = \overline{\Delta y}\% = 8.0\ \%$). Taking into account the scatter of the experimental data, which inevitably makes increase the deviations, we can assert that the PPR78 model is an accurate thermodynamic model able to cover all the compounds that an engineer of a gas company is likely to encounter. It is today integrated in two well-known process simulators: (1) PRO/II commercialized by Schneider Electrics and (2) ProSimPlus developed by the French company PROSIM. Fig. 2.14 graphically illustrates the accuracy of the PPR78 model.

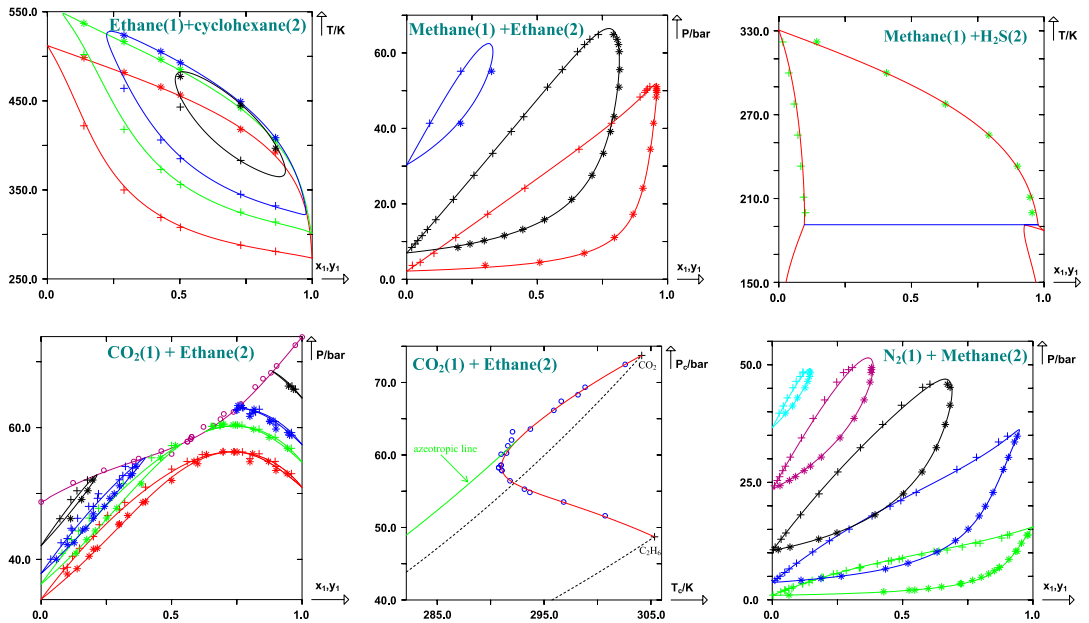

FIGURE 2.14

Illustration of the accuracy of the PPR78 model. The symbols are the experimental data points. The *full lines* are the predictions with the PPR78 model.

2.3.3.2.2.2 On the Temperature Dependence of the k_{ij} Parameter. In mixtures encountered in the gas-processing industries, it is today accepted that the binary interaction parameter k_{ij} depends on temperature. This temperature dependence has been described by a few authors. The paper by Coutinho et al. (1994) gives an interesting review of the different publications dealing with this subject. The same authors give a theoretical explanation for the temperature dependence of the k_{ij} and conclude that this parameter varies quadratically with the inverse temperature ($1/T$). Using Eq. (2.59), it is straightforward to plot k_{ij} versus temperature for a given binary system. As an illustration, Fig. 2.15 presents plots of k_{ij} with respect to the reduced temperature of the heavy n-alkane for three binary systems: (1) methane/propane, (2) methane/n-hexane, and (3) methane/n-decane.

The shapes of the curves are similar to the ones published by Coutinho et al. (1994). At low temperature, k_{ij} is a decreasing function of temperature. With increasing the temperature, the k_{ij} reaches a minimum and then increases again. The minimum is located at a reduced temperature close to 0.55, independent of the binary system. This minimum moves to $T_r = 0.6$ for the system methane/n-C_{30} (results not shown in Fig. 2.15). From Fig. 2.15, we can unambiguously conclude that it is necessary to work with temperature-dependent k_{ij}.

2.3.3.2.3 Soave's GCM

In a recent paper, Soave et al. (2010), also developed a GCM aimed at predicting temperature-dependent k_{ij} for the well-known SRK EoS. Six groups are defined: (1) group 1 = CH_4, group 2 = CO_2, group 3 = N_2, group 4 = H_2S, group 5 = alkyl group, and group 6 = aromatic group. The last two groups are introduced to model alkanes and aromatic compounds. This small number of groups is an advantage because it reduces the number of group parameters to be estimated and it allows a faster estimation of the k_{ij}. Indeed, the calculation of a double sum as the one contained in Eq. (2.59)

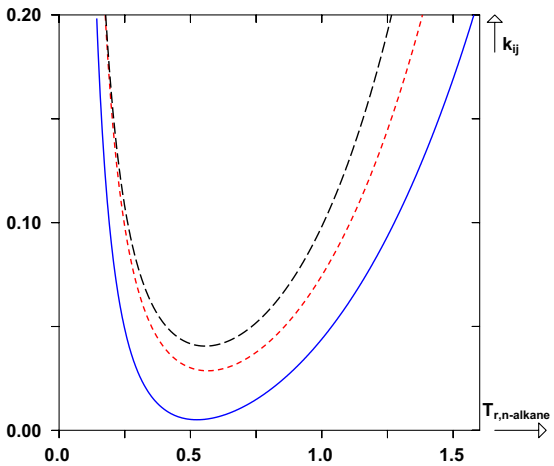

FIGURE 2.15

Temperature dependence of predicted k_{ij} by means of Eq. (2.59). *Solid line*: system methane/propane. *Short dashed line*: system methane/n-hexane. *Long dashed line*: system methane/n-decane. In abscissa, T_r is the reduced temperature of the heavy n-alkane (propane, n-hexane, n-decane).

is time-consuming and strongly affected by the number of groups. Very accurate results are obtained on binary systems. As shown by Jaubert et al. (2011), the accuracy of Soave's GCM, although not tested on many experimental data, is similar to what is observed with the PPR78 model. Whether a naphthenic group was added, this GCM could be applied to predict the phase behavior of natural gases.

2.3.3.3 $k_{ij}(T)$ Values: How to Switch From a Cubic EoS to Another One?

As explained in the previous sections, the key point when using cubic EoS to describe complex mixtures like natural gases is to give appropriate values to the binary interaction parameters (k_{ij}). We, however, know by experience that the k_{ij}, suitable for a given EoS (e.g., the PR EoS), cannot be directly used for another one (e.g., the SRK EoS). Moreover, numerical values of k_{ij} are not only specific to the considered EoS but they also depend on the alpha function (Soave, Twu, Mathias-Copeman, and so on) involved in the mathematical expression of the a_i parameter. This assessment makes it impossible for petroleum engineers to use various EoS and to test different alpha functions. Indeed, they usually have tables containing the numerical values of the k_{ij} only for the most widely used EoS and alpha function in their company. To overcome this limitation, Jaubert and Privat (2010) had the idea to establish a relationship between the k_{ij} of a first EoS (k_{ij}^{EoS1}) and those of a second one (k_{ij}^{EoS2}). As a consequence, knowing the numerical values of the k_{ij} for the first EoS makes it possible to deduce the corresponding values for any other cubic EoS. The obtained relationship is is shown in Eqs. (2.60) and (2.61). To understand the notations, let us consider two cubic EoS (EoS1 and EoS2) deriving from the Van der Waals equation, i.e., having the general form given in Eq. (2.34). At this step, we define the following quantities:

$$\begin{cases} C_{\mathrm{EoS}} = \dfrac{1}{r_1 - r_2} \cdot \ln\left(\dfrac{1 - r_2}{1 - r_1}\right) \text{ if } r_1 \neq r_2 \text{ and } C_{\mathrm{EoS}} = \dfrac{1}{1 - r_1} \text{ if } r_1 = r_2 \\ \xi_{1\to 2} = \dfrac{C_{\mathrm{EoS1}} \cdot \Omega_b^{\mathrm{EoS1}}}{C_{\mathrm{EoS2}} \cdot \Omega_b^{\mathrm{EoS2}}} \\ \delta_i^{\mathrm{EoS}} = \dfrac{\sqrt{a_i^{\mathrm{EoS}}}}{b_i^{\mathrm{EoS}}} \end{cases} \tag{2.60}$$

After some derivation, the obtained relationship is

$$k_{ij}^{\mathrm{EoS2}} = \frac{2\xi_{1\to 2} k_{ij}^{\mathrm{EoS1}} \delta_i^{\mathrm{EoS1}} \delta_j^{\mathrm{EoS1}} + \xi_{1\to 2}\left(\delta_i^{\mathrm{EoS1}} - \delta_j^{\mathrm{EoS1}}\right)^2 - \left(\delta_i^{\mathrm{EoS2}} - \delta_j^{\mathrm{EoS2}}\right)^2}{2\delta_i^{\mathrm{EoS2}} \delta_j^{\mathrm{EoS2}}} \tag{2.61}$$

Eq. (2.61) can also be used if we work with the same EoS (let us say the PR EoS), but if we decide to only change the *alpha* function (e.g., we initially work with a Soave-type $\alpha(T)$ function for which the k_{ij} are known, and we decide to work with a Twu alpha function for which the k_{ij} are unknown). In this latter case, $\xi_{1\to 2} = 1$, but Eq. (2.61) in which the δ parameters depend on the $a(T)$ function will lead to a relationship between the k_{ij} to be used with the first α function and those to be used with the second one.

As previously explained, the PPR78 model is a GCM designed to predict the k_{ij} of the PR EoS. The coupling of this GCM with Eq. (2.61) makes it possible to predict the temperature-dependent k_{ij} of any

desired EoS using the GC concept. Let us indeed consider a cubic EoS (Eq. 2.34), noted EoS1 hereafter, and let us define

$$\xi_{PR\rightarrow \mathrm{EoS1}} = \frac{C_{PR}\cdot \Omega_b^{PR}}{C_{\mathrm{EoS1}}\cdot \Omega_b^{\mathrm{EoS1}}} \tag{2.62}$$

By combining Eqs. (2.59) and (2.61), we can write the following equation:

$$k_{ij}^{\mathrm{EoS1}}(T) = \frac{-\frac{1}{2}\left[\sum_{k=1}^{N_g}\sum_{l=1}^{N_g}(\alpha_{ik}-\alpha_{jk})(\alpha_{il}-\alpha_{jl})\xi_{PR\rightarrow \mathrm{EoS1}}A_{kl}^{PR}\cdot\left(\frac{298.15}{T/K}\right)^{\left(\frac{B_{kl}^{PR}}{A_{kl}^{PR}}-1\right)}\right]-\left(\frac{\sqrt{a_i^{\mathrm{EoS1}}(T)}}{b_i^{\mathrm{EoS1}}}-\frac{\sqrt{a_j^{\mathrm{EoS1}}(T)}}{b_j^{\mathrm{EoS1}}}\right)^2}{2\frac{\sqrt{a_i^{\mathrm{EoS1}}(T)\cdot a_j^{\mathrm{EoS1}}(T)}}{b_i^{\mathrm{EoS1}}\cdot b_j^{\mathrm{EoS1}}}} \tag{2.63}$$

Using Eq. (2.63), it is thus possible to calculate by GC, the temperature-dependent k_{ij} for any desired cubic EoS (EoS1), with any desired $a_i(T)$ function, using the group contribution parameters (A_{kl}^{PR} and B_{kl}^{PR}) that were determined for the PPR78 model. Eq. (2.63) can also be used if we work with the PR EoS but with a different $a_i(T)$ function than the one defined by Eq. (2.31). In this latter case, $\xi_{PR\rightarrow \mathrm{EoS1}} = 1$, but Eq. (2.63) will lead to k_{ij} values different of those obtained from the PPR78 model. Eq. (2.63) was extensively used by Jaubert and Privat (2010) in the particular case in which EoS1 is the SRK EoS. They concluded that the accuracy obtained with the SRK EoS was similar to the one obtained with the PPR78 model. The resulting model, based on the SRK EoS and for which the k_{ij} are estimated from the GCM developed for the PPR78 model, was called PR2SRK. In conclusion, we can claim that the PPR78 model is a *universal* GCM because it can predict the k_{ij} for any desired EoS with any desired $a_i(T)$ function at any temperature for any mixture containing hydrocarbons, permanent gases, and water.

2.3.3.4 Other Mixing Rules

Cubic EoS with Van der Waals one-fluid mixing rules lead to very accurate results at low and high pressures for *simple* mixtures (few polar, hydrocarbons, gases). They also allow the prediction of many more properties than phase equilibria (e.g., excess properties, heat capacities, and so forth). Such mixing rules can, however, not be applied with success to polar mixtures. In return, g^E models (activity coefficient models) are applicable to low pressures and are able to correlate polar mixtures. It thus seems a good idea to combine the strengths of both approaches, i.e., the cubic EoS and the activity coefficient models, and thus to have a single model suitable for phase equilibria of polar and nonpolar mixtures and at both low and high pressures. This combination of EoS and g^E models is possible via the so-called EoS/g^E models which are essentially mixing rules for the energy parameter of cubic EoS. As explained in the recent book by Kontogeorgis and Folas (2010), the starting point for deriving EoS/g^E models is the equality of the excess Gibbs energies from an EoS and from an explicit activity coefficient model at a suitable reference pressure. The activity coefficient model may be chosen among the classical forms of molar excess Gibbs energy functions (Redlich−Kister, Margules, Wilson, Van Laar, NRTL, UNIQUAC, UNIFAC, …). Such models are pressure independent (they only depend on

temperature and composition), but the same quantity from an EoS depends on pressure, temperature, and composition explaining why a reference pressure needs to be selected before equating the two quantities. To avoid confusion, we will write with a special font (G^E) the selected activity coefficient model and with a classical font (g^E) the excess Gibbs energy calculated from an EoS as

$$\frac{g^E}{RT} = \sum_{i=1}^{p} z_i \cdot \ln\left[\frac{\widehat{\varphi}_i(T,P,\mathrm{z})}{\varphi_{\mathrm{pure}\,i}(T,P)}\right] \tag{2.64}$$

where $\widehat{\varphi}_i$ is the fugacity coefficient of component i in the mixture and $\varphi_{\mathrm{pure}\,i}$ is the fugacity coefficient of the pure compound at the same temperature, pressure, and in the same aggregation state as the mixture. The starting equation to derive EoS/g^E models is as follows:

$$\left[g^E/(RT)\right]_P = G^E/(RT) \tag{2.65}$$

where subscript P indicates that a reference pressure has to be chosen.

2.3.3.4.1 The Infinite Pressure Reference

The basic assumption of the method is the use of the infinite pressure as the reference pressure.

2.3.3.4.1.1 The Huron–Vidal Mixing Rules. The first systematic successful effort in developing an EoS/g^E model is that of Huron and Vidal (1979). Starting from Eq. (2.65), they obtained

$$\begin{cases} \dfrac{a(T,\mathbf{x})}{b(\mathbf{x})} = \displaystyle\sum_{i=1}^{p} x_i \frac{a_i(T)}{b_i} - \frac{G^E}{C_{\mathrm{EoS}}} \\ b(\mathbf{x}) = \displaystyle\sum_{i=1}^{p} x_i b_i \end{cases} \tag{2.66}$$

where C_{EoS} is defined by Eq. (2.60). A positive feature of the Huron–Vidal mixing rule includes an excellent correlation of binary systems. A limitation is that it does not permit use of the large collections of interaction parameters of G^E models which are based on low-pressure VLE data (e.g., the UNIFAC tables). Indeed, the excess Gibbs energy at high pressures is, in general, different from the value at low pressures at which the parameters of the G^E models are typically estimated.

2.3.3.4.1.2 The Van der Waals One-Fluid (VdW1f) Mixing Rules. The classical VdW1f mixing rules used in the PPR78 and PR2SRK models are given as

$$a(T,\mathbf{x}) = \sum_{j=1}^{p} x_i x_j \sqrt{a_i a_j}[1 - k_{ij}(T)] \quad \text{and} \quad b(\mathbf{x}) = \sum_{i=1}^{p} x_i b_i \tag{2.67}$$

We want to give proof that such mixing rules are in fact strictly equivalent to the Huron–Vidal mixing rules if a Van-Laar type G^E model is selected in Eq. (2.66). Indeed, by sending Eq. (2.67) in Eq. (2.66), one has

$$\frac{G^E}{C_{\text{EoS}}} = \sum_{i=1}^{p} x_i \frac{a_i(T)}{b_i} - \frac{a(T,\mathbf{x})}{b(\mathbf{x})} = \sum_{i=1}^{p} x_i \cdot \frac{a_i(T)}{b_i} - \frac{\sum_{i=1}^{p}\sum_{j=1}^{p} x_i \cdot x_j \sqrt{a_i \cdot a_j} \cdot [1 - k_{ij}(T)]}{\sum_{j=1}^{p} x_j \cdot b_j}$$
$$= \frac{\sum_{i=1}^{p} x_i \cdot \frac{a_i(T)}{b_i} \times \sum_{j=1}^{p} x_j \cdot b_j - \sum_{i=1}^{p}\sum_{j=1}^{p} x_i \cdot x_j \sqrt{a_i \cdot a_j} \cdot [1 - k_{ij}(T)]}{\sum_{j=1}^{p} x_j \cdot b_j} \tag{2.68}$$

We can write

$$\sum_{i=1}^{p} x_i \cdot \frac{a_i(T)}{b_i} \times \sum_{j=1}^{p} x_j \cdot b_j = \sum_{i=1}^{p}\sum_{j=1}^{p} x_i \cdot x_j \frac{a_i \cdot b_j}{b_i} = \frac{1}{2}\sum_{i=1}^{p}\sum_{j=1}^{p} x_i \cdot x_j \frac{a_i \cdot b_j}{b_i} + \frac{1}{2}\sum_{i=1}^{p}\sum_{j=1}^{p} x_i \cdot x_j \frac{a_j \cdot b_i}{b_j} \tag{2.69}$$

Thus,

$$\frac{G^E}{C_{\text{EoS}}} = \frac{\sum_{i=1}^{p}\sum_{j=1}^{p} x_i \cdot x_j \left[\frac{1}{2}\frac{a_i \cdot b_j}{b_i} + \frac{1}{2}\frac{a_j \cdot b_i}{b_j} - \sqrt{a_i \cdot a_j} \cdot [1 - k_{ij}(T)]\right]}{\sum_{j=1}^{p} x_j \cdot b_j}$$
$$= \frac{\sum_{i=1}^{p}\sum_{j=1}^{p} x_i \cdot x_j \cdot b_i \cdot b_j \left[\frac{1}{2}\frac{a_i}{b_i^2} + \frac{1}{2}\frac{a_j}{b_j^2} - \frac{\sqrt{a_i}}{b_i} \cdot \frac{\sqrt{a_j}}{b_j} \cdot [1 - k_{ij}(T)]\right]}{\sum_{j=1}^{p} x_j \cdot b_j} \tag{2.70}$$

At this step, we introduce for clarity $\delta_i = \sqrt{a_i}/b_i$, which has the Scatchard−Hildebrand solubility parameter feature, and we define the parameter E_{ij} by

$$E_{ij} = \delta_i^2 + \delta_j^2 - 2\delta_i\delta_j[1 - k_{ij}(T)] \tag{2.71}$$

Eq. (2.70) thus writes

$$\frac{G^E}{C_{\text{EoS}}} = \frac{1}{2} \cdot \frac{\sum_{i=1}^{p}\sum_{j=1}^{p} x_i \cdot x_j \cdot b_i \cdot b_j \cdot E_{ij}(T)}{\sum_{j=1}^{p} x_j \cdot b_j} \tag{2.72}$$

Eq. (2.72) is the mathematical expression of a Van Laar−type G^E model. We thus demonstrated that it is rigorously equivalent to use a Van Laar−type G^E model in the Huron−Vidal mixing rules or to

use classical mixing rules with temperature-dependent k_{ij}. From Eq. (2.71) we have the following equation:

$$k_{ij}(T) = \frac{E_{ij}(T) - (\delta_i - \delta_j)^2}{2\delta_i\delta_j} \tag{2.73}$$

Eq. (2.73) thus establishes a connection between E_{ij} of the Van Laar–type G^E model and k_{ij} of the classical mixing rules.

2.3.3.4.1.3 The Wong–Sandler Mixing Rules. It can be demonstrated that the Huron–Vidal mixing rules violate the imposed by statistical thermodynamics quadratic composition dependency of the second virial coefficient:

$$B = \sum_{i=1}^{p}\sum_{j=1}^{p} x_i x_j B_{ij} \tag{2.74}$$

To satisfy Eq. (2.74), Wong and Sandler (1992) decided to revisit the Huron–Vidal mixing rules. Because they made use of the infinite pressure as the reference pressure, like Huron and Vidal, they obtained the following form:

$$a(T,\mathbf{x}) = b(\mathbf{x})\left[\sum_{i=1}^{p} x_i \frac{a_i(T)}{b_i} - \frac{G^E}{C_{\text{EoS}}}\right] \tag{2.75}$$

However, knowing that the second virial coefficient from a cubic EoS is given as

$$B = b - \frac{a}{RT} \tag{2.76}$$

The combination of Eqs. (2.74) and (2.76) gives

$$b(\mathbf{x}) = \frac{a(T,\mathbf{x})}{RT} + \sum_{i=1}^{p}\sum_{j=1}^{p} x_i x_j B_{ij} \tag{2.77}$$

Substituting Eq. (2.75) in Eq. (2.77), we get

$$b(\mathbf{x}) = \frac{\sum_{i=1}^{p}\sum_{j=1}^{p} x_i x_j B_{ij}}{1 + \dfrac{G^E}{RTC_{\text{EoS}}} - \sum_{i=1}^{p} x_i \dfrac{a_i(T)}{RTb_i}} \tag{2.78}$$

The following choice for the cross-virial coefficient is often used:

$$B_{ij} = \frac{1}{2}(B_i + B_j)(1 - k_{ij}) \tag{2.79}$$

Eq. (2.79) makes unfortunately, appear an extra binary interaction parameter (k_{ij}), the value of which can be estimated through various approaches.

Substituting Eq. (2.76) in Eq. (2.79), one has:

$$B_{ij} = \frac{\left(b_i - \dfrac{a_i}{RT}\right) + \left(b_j - \dfrac{a_j}{RT}\right)}{2}(1 - k_{ij}) \tag{2.80}$$

The Wang−Sandler mixing rules thus write:

$$\begin{cases} b(T,\mathbf{x}) = \dfrac{\sum_{i=1}^{p}\sum_{j=1}^{p} x_i x_j \dfrac{\left(b_i - \dfrac{a_i}{RT}\right) + \left(b_j - \dfrac{a_j}{RT}\right)}{2}(1-k_{ij})}{1 + \dfrac{G^E}{RTC_{\text{EoS}}} - \sum_{i=1}^{p} x_i \dfrac{a_i(T)}{RTb_i}} \\ a(T,\mathbf{x}) = b(\mathbf{x})\left[\sum_{i=1}^{p} x_i \dfrac{a_i(T)}{b_i} - \dfrac{G^E}{C_{\text{EoS}}}\right] \end{cases} \tag{2.81}$$

We can thus conclude that the Wong−Sandler mixing rules differ from the Huron−Vidal mixing rules in the way of estimating the covolume. In Eq. 2.81, b has become temperature dependent. Many papers illustrate the key success of the Wong−Sandler mixing rules to predict VLE using existing low-pressure parameters from activity coefficients models. However, parameters for gas-containing systems are not available in activity coefficient models such as UNIFAC, which limits the applicability of these mixing rules to such systems.

2.3.3.4.2 The Zero-Pressure Reference

The zero-pressure reference permits a direct use of G^E interaction parameter tables. Starting from Eq. (2.65) and by setting $P = 0$, one obtains

$$\begin{cases} \dfrac{G^E}{RT} = Q(\alpha) - \sum_{i=1}^{p} x_i \cdot Q(\alpha_i) + \sum_{i=1}^{p} x_i \cdot \ln\left(\dfrac{b_i}{b}\right) \text{ with } \alpha = \dfrac{a}{bRT} \\ Q(\alpha) = -\ln\left(\dfrac{1-\eta_0(\alpha)}{\eta_0(\alpha)}\right) - \dfrac{\alpha}{r_1 - r_2}\ln\left(\dfrac{1-\eta_0(\alpha)\cdot r_2}{1-\eta_0(\alpha)\cdot r_1}\right) \\ \eta_0(\alpha) = \dfrac{r_1 + r_2 + \alpha + \sqrt{(r_1+r_2+\alpha)^2 - 4(r_1 r_2 + \alpha)}}{2(r_1 r_2 + \alpha)} \textit{ submitted to } : \alpha \geq \alpha_{\text{lim}} \\ \alpha_{\text{lim}} = -r_1 - r_2 + 2 + 2\sqrt{1 - r_1 - r_2 + r_1 r_2} \end{cases} \tag{2.82}$$

After selecting a mixing rule for the covolume, Eq. (2.82) becomes an implicit mixing rule for the energy parameter, which means that an iterative procedure is needed for calculating the energy parameter.

2.3.3.4.2.1 The MHV-1 Mixing Rule. To obtain an explicit mixing rule and to address the limitation introduced by the presence of α_{lim}, Michelsen (1990) proposed to define a linear approximation of the Q function by

$$Q(\alpha) = q_0 + q_1 \cdot \alpha \tag{2.83}$$

Doing so, Eq. (2.82) can be written as

$$\alpha = \sum_{i=1}^{p} x_i \cdot \alpha_i + \frac{1}{q_1}\left[\frac{G^E}{RT} - \sum_{i=1}^{p} x_i \cdot \ln\left(\frac{b_i}{b}\right)\right] \tag{2.84}$$

Eq. (2.84) is the so-called MHV-1 (modified Huron−Vidal first order) mixing rule usually used with a linear mixing rule for the covolume parameter. Michelsen advices to use $q_1 = -0.593$ for the SRK EoS, $q_1 = -0.53$ for the PR EoS, and $q_1 = -0.85$ for the VdW EoS.

2.3.3.4.2.2 The PSRK Model. Holderbaum and Gmehling (1991), proposed the PSRK (predictive SRK) model based on the MHV-1 mixing rule. These authors, however, used a slightly different q_1 value than the one proposed by Michelsen. They selected $q_1 = -0.64663$. To make their model predictive, Holderbaum and Gmehling combined the SRK EoS with a predictive G^E model (the original or the modified Dortmund UNIFAC). Moreover, they developed extensive parameter table, including parameters for gas-containing mixtures. The PSRK model may thus be used to model petroleum fluids. No comparison was performed between PSRK and PPR78, but we can expect similar results.

2.3.3.4.2.3 The Universal Mixing Rule of Peng−Robinson and Volume-Translated Peng−Robinson Models. The universal mixing rule by Peng Robinson (UMR-PR) and the volume translated Peng Robinson (VTPR) models, both use the MVH-1 mixing rule. They were respectively developed by Voutsas et al. (2004) and by Ahlers and Gmehling (2001, 2002). In both cases, the same translated form of the PR EoS is used. The Twu $\alpha(T)$ function is, however, used in the VTPR model, whereas the Mathias−Copeman expression is used in the UMR-PR model. Both models incorporate the UNIFAC G^E model in Eq. (2.84). However, to be able to properly correlate asymmetric systems, only the residual part of UNIFAC is used in the VTPR model. These authors indeed assume that the combinatorial part of UNIFAC and $\sum x_i \cdot \ln(b_i/b)$ in Eq. (2.84) cancel each other. In the UMR-PR model the residual part of UNIFAC but also the Staverman−Guggenheim contribution of the combinatorial term is used. These authors also assume that the Flory−Huggins combinatorial part of UNIFAC and $\sum x_i \cdot \ln(b_i/b)$ in Eq. (2.84) cancel each other. A novel aspect of these models is the mixing rule used for the covolume parameter. Both models give better results than PSRK. After noting $\alpha = \frac{a}{bRT}$, the equations to be used are as follows:

VTPR:

$$\alpha = \sum_{i=1}^{p} x_i \cdot \alpha_i + \frac{1}{q_1}\left[\frac{G^{E,\mathrm{UNIFAC}}_{\mathrm{residual}}}{RT}\right]$$
$$b = \sum_{i=1}^{p}\sum_{j=1}^{p} x_i x_j b_{ij} \quad \text{with: } b_{ij} = \left(\frac{b_i^{1/s} + b_j^{1/s}}{2}\right) \quad \text{and} \quad s = \frac{4}{3} \tag{2.85}$$

UMP − PR:

$$\alpha = \sum_{i=1}^{p} x_i \cdot \alpha_i + \frac{1}{q_1}\left[\frac{G^{E,\mathrm{UNIFAC}}_{\mathrm{residual}}}{RT} + \frac{G^{E,\mathrm{UNIFAC}}_{\mathrm{Staverman-Guggenheim\ combinatorial\ contribution}}}{RT}\right]$$
$$b = \sum_{i=1}^{p}\sum_{j=1}^{p} x_i x_j b_{ij} \quad \text{with: } b_{ij} = \left(\frac{b_i^{1/s} + b_j^{1/s}}{2}\right) \quad \text{and} \quad s = 2 \tag{2.86}$$

The mixing rule described by Eq. (2.85) was also applied to the SRK EoS by Chen et al. (2002) to define a new version of the PSRK model. In this latter case the SRK EoS was combined with a Mathias−Copeman alpha function.

2.3.3.4.2.4 The LCVM Model. The LCVM model by Boukouvalas et al. (1994) is based on a mixing rule which is a linear combination of the Vidal and Michelsen (MHV-1) mixing rules:

$$\alpha_{\text{LCVM}} = \lambda \cdot \alpha_{\text{Huron}-\text{Vidal}} + (1-\lambda) \cdot \alpha_{\text{Michelsen}} \tag{2.87}$$

From Eq. (2.66), one has

$$\alpha_{\text{Huron}-\text{Vidal}} = \sum_{i=1}^{p} x_i \cdot \alpha_i - \frac{G^E}{R \cdot T \cdot C_{\text{EoS}}} \tag{2.88}$$

whereas $\alpha_{\text{Michelsen}}$ is given by Eq. (2.84). The LCVM as used today is based on the original UNIFAC G^E model, and the value $\lambda = 0.36$ should be used in all applications. Their authors use a translated form of the PR EoS and obtain accurate results especially for asymmetric systems.

2.3.3.4.2.5 The MHV-2 Mixing Rule. To increase the accuracy of the MHV-1 mixing rule, Dahl and Michelsen (1990) proposed in 1990 a quadratic approximation of the Q function by

$$Q(\alpha) = q_0 + q_1 \cdot \alpha + q_2 \cdot \alpha^2 \tag{2.89}$$

thus defining the MHV-2 model. It is advised to use $q_1 = -0.4783$ and $q_2 = -0.0047$for the SRK EoS and $q_1 = -0.4347$ and $q_2 = -0.003654$ for the PR EoS. Doing so, Eq. (2.82) is written as follows:

$$\frac{G^E}{RT} = q_1 \left(\alpha - \sum_{i=1}^{p} x_i \cdot \alpha_i \right) + q_2 \left(\alpha^2 - \sum_{i=1}^{p} x_i \cdot \alpha_i^2 \right) + \sum_{i=1}^{p} x_i \cdot \ln\left(\frac{b_i}{b}\right) \tag{2.90}$$

Eq. (2.90) does not yield anymore to an explicit mixing rule but instead has to be solved to determine α. For such a mixing rule, parameter tables are available for many gases. As a general rule, MHV-2 provides a better reproduction of the low-pressure VLE data than MHV-1.

2.3.4 ENERGETIC ASPECTS: ESTIMATION OF ENTHALPIES FROM CUBIC EOS

Engineers use principles drawn from thermodynamics to analyze and design industrial processes. The application of the first principle (also named *energy rate balance*) to an open multicomponent system at steady state is written as follows:

$$\dot{W} + \dot{Q} = \sum \dot{n}_{out} h_{out} - \sum \dot{n}_{in} h_{in} \tag{2.91}$$

where $\dot{W}$ and $\dot{Q}$ are the net rates of energy transfer, respectively, by work and by heat; $\dot{n}$ is the molar flow rate and h denotes the molar enthalpy of a stream. Subscripts *in* and *out*, respectively, mean *inlet* and *outlet* streams. Note that kinetic-energy and potential-energy terms are supposed to be zero in Eq. (2.91). According to classical thermodynamics, the molar enthalpy of a p-component homogeneous system at a given temperature T, pressure P, and composition $\boldsymbol{z}$ (mole fraction vector) is

$$\underbrace{h(T,P,\mathbf{z})}_{\substack{\text{molar enthalpy}\\ \text{of an inlet or}\\ \text{an outlet stream}}} = \sum_{i=1}^{p} z_i \left[h_{\text{pure}\,i}(T,P) - h_{\text{pure}\,i}^{\text{ref}} \right] + h^M(T,P,\mathbf{z}) \tag{2.92}$$

wherein $h_{\text{pure}\,i}(T,P)$ is the molar enthalpy of pure component i in its actual aggregation state at the same temperature and pressure as the mixture (Privat and Jaubert, 2012b; Jaubert and Privat, 2014), $h_{\text{pure}\,i}^{\text{ref}}$ is the molar enthalpy of pure component i in its reference state, i.e., at a reference temperature T_{ref}, pressure P_{ref}, and aggregation state. Note that this term is specific to each component i and does not depend on the temperature and pressure of the stream. $h^M(T,P,\mathbf{z})$ is the molar enthalpy change on isothermal and isobaric mixing. This section is dedicated to explain how to calculate these terms when a cubic equation of state (as defined in Eq. 2.34) is used with Soave's alpha function (Eq. 2.38) and classical mixing rules involving a temperature-dependent k_{ij} (Eq. 2.67).

2.3.4.1 Calculation of Pure-Component Enthalpies

At this step, the concept of *residual molar enthalpy* h^{res} needs to be introduced; h^{res} is a difference measure for how a substance deviates from the behavior of a perfect gas having the same temperature T as the real substance. The molar enthalpy of a pure fluid can thus be written as the summation of the molar enthalpy of a perfect gas having the same temperature as the real fluid plus a residual term:

$$h_{\text{pure}\,i}(T,P) = h_{\text{pure}\,i}^{pg}(T) + h_{\text{pure}\,i}^{\text{res}}(T, v_{\text{pure}\,i}(T,P)) \tag{2.93}$$

where the superscript pg stands for *perfect gas*; $v_{\text{pure}\,i}(T,P)$ is the molar volume of the pure fluid i at temperature T and pressure P; it can be calculated by solving the cubic EoS (Eq. 2.35) at given T and P. Because cubic EoS are explicit in pressure (i.e., they give the pressure as an explicit function of variables T and v), the expression of the residual molar enthalpy can be naturally written in variables T and v:

$$h_{\text{pure}\,i}^{\text{res}}(T,v) = \frac{RTb_i}{v-b_i} - \frac{a_i(T)\,v}{(v-r_1 b_i)(v-r_2 b_i)} + \frac{1}{b(r_1-r_2)}\left(a_i - T\frac{da_i}{dT}\right)\cdot \ln\left(\frac{v-r_1 b_i}{v-r_2 b_i}\right) \tag{2.94}$$

If using Soave's alpha function, then

$$\frac{da_i}{dT} = -a_{c,i} m_i \left[1 + m_i\left(1 - \sqrt{T/T_{c,i}}\right)\right] \Big/ \sqrt{T \cdot T_{c,i}} \tag{2.95}$$

Finally, according to Eq. (2.93), the difference of pure-fluid enthalpy terms in Eq. (2.92) is written as

$$\begin{aligned} h_{\text{pure}\,i}(T,P) - h_{\text{pure}\,i}^{\text{ref}} = &\left[h_{\text{pure}\,i}^{pg}(T) - h_{\text{pure}\,i}^{pg}(T_{\text{ref}})\right] + \left[h_{\text{pure}\,i}^{\text{res}}(T, v_{\text{pure}\,i}(T,P))\right. \\ &\left. - h_{\text{pure}\,i}^{\text{res}}(T, v_{\text{pure}\,i}(T_{\text{ref}}, P_{\text{ref}}))\right] \end{aligned} \tag{2.96}$$

wherein the h_i^{res} function is given by Eq. (2.94). Let us recall that

$$\left[h_{\text{pure}\,i}^{pg}(T) - h_{\text{pure}\,i}^{pg}(T_{\text{ref}})\right] = \int_{T_{\text{ref}}}^{T} c_{P,\text{pure}\,i}^{pg}(T)\,dT \tag{2.97}$$

where $c_{P,i}^{pg}(T)$ denotes the molar heat capacity at constant pressure of the pure perfect gas i.

2.3.4.2 Calculation of the Enthalpy Change on Mixing

By definition, the molar enthalpy change on mixing h^M is the difference between the molar enthalpy of a solution and the sum of the molar enthalpies of the components which make it up, all at the same temperature and pressure as the solution, *in their actual state* (Eq. 2.92) weighted by their mole fractions z_i. Consequently to this definition, h^M can be expressed in terms of residual molar enthalpies:

$$h^M(T,P,\mathbf{z}) = h^{\text{res}}(T,v,\mathbf{z}) - \sum_{i=1}^{p} z_i h^{\text{res}}_{\text{pure}\,i}(T, v_{\text{pure}\,i}(T,P)) \tag{2.98}$$

where v is the molar volume of the mixture at T, P, and $\mathbf{z}$. To calculate this molar volume, Eq. (2.35) has to be solved. The residual molar enthalpy of pure component i is given by Eq. (2.94), and the residual molar enthalpy of the mixture is given by Eq. (2.99):

$$\begin{aligned} h^{\text{res}}(T,v,\mathbf{z}) = {} & \frac{RTb(\mathbf{z})}{v-b(\mathbf{z})} - \frac{a(T,\mathbf{z})\ v}{[v-r_1 b(\mathbf{z})][v-r_2 b(\mathbf{z})]} + \frac{1}{b(\mathbf{z})(r_1-r_2)} \\ & \left[a(T,\mathbf{z}) - T\left(\frac{\partial a}{\partial T}\right)_{\mathbf{z}}\right] \cdot \ln\left[\frac{v-r_1 b(\mathbf{z})}{v-r_2 b(\mathbf{z})}\right] \end{aligned} \tag{2.99}$$

If classical mixing rules with temperature-dependent k_{ij} are considered, then

$$\left(\frac{\partial a}{\partial T}\right)_{\mathbf{z}} = \sum_{i=1}^{p}\sum_{j=1}^{p} z_i z_j \left[[1-k_{ij}(T)]\frac{a_j(T)\cdot\frac{da_i}{dT} + a_i(T)\cdot\frac{da_j}{dT}}{2\sqrt{a_i(T)a_j(T)}} - \frac{dk_{ij}}{dT}\sqrt{a_i(T)a_j(T)}\right] \tag{2.100}$$

From Eqs. (2.98)–(2.100), it appears that the use of a temperature-dependent k_{ij} allows a better flexibility of the h^M function (see the term dk_{ij}/dT in Eq. 2.100). As a consequence, a better accuracy on the estimation of the molar enthalpies is expected when temperature-dependent k_{ij} rather than constant k_{ij} are used.

2.3.4.3 Practical Use of Enthalpies of Mixing and Illustration With the PPR78 Model

As previously explained, the molar enthalpy of a multicomponent phase is obtained by adding a pure-component term and a molar enthalpy change on mixing term (Eq. 2.92). When molecules are few polar and few associated (and this is often the case within natural gases), pure-component terms provide an excellent estimation of the molar enthalpy of the mixture. Therefore the enthalpy-of-mixing term can be seen as a correction, just aimed at improving the first estimation given by pure-component ground terms. In other words, with few polar and few associated molecules, h^M terms are generally nearly negligible with respect to pure-component terms in the energy rate balance. Typically, h^M terms are very small in alkane mixtures and are not negligible in natural gases containing CO_2 or H_2O. When parameters involved in k_{ij} correlations are not directly fitted on enthalpy-of-mixing data (and this is, for instance, the case with the PPR78 model), the relative deviations between calculated and experimental h^M data can be very important and reach values sometimes greater than 100%. However, as explained in the introduction part of this section, because h^M quantities are only used to evaluate the molar enthalpies, h_{in} and h_{out}, involved in the energy rate balance, only absolute deviations and their effect on the accuracy of the energy balance are of interest. When experimental and calculated h^M values are very low (typically < 100 J/mol), the energy rate balance is not significantly affected by high relative

deviations. On the contrary, if h^M values are very important (e.g., > 3000 J/mol), important absolute deviations on h^M can have a detrimental impact on the energy rate balance even if the corresponding relative deviation remains low. Note that in such a case, h^M terms can become dominant with respect to pure-component enthalpy terms. As an illustration, the PPR78 model was used to predict isothermal and isobaric curves h^M versus z_1 of two binary mixtures: n-hexane + n-decane and $N_2 + CO_2$ (Fig. 2.16).

One observes that enthalpies of mixing of an alkane mixture (not too much dissymmetric in size) are very low. The PPR78 model predicts h^M with an acceptable order of magnitude (and as a consequence, only pure-component enthalpy terms will govern the energy rate balance). Regarding the binary mixture $N_2 + CO_2$, it clearly appears that the orders of magnitude of h^M are around 10 times bigger than those with the n-hexane + n-heptane system. Deviations between predicted values and experimental data are around 100−150 J/mol at the most, which remains acceptable and should very few affect the energy rate balance. When at the considered temperature and pressure a liquid−vapor phase equilibrium occurs, the corresponding h^M versus z_1 curve is made up of three different parts: (1) a homogeneous liquid part, (2) a liquid−vapor part, and (3) a homogeneous gas part. The liquid−vapor part is a straight line, framed by the two other parts. Fig. 2.17 gives an illustration of the kind of curves observed in such a case. For system exhibiting VLE at given T and P, it is possible to show that the essential part of the enthalpy-of-mixing value is due to the vaporization enthalpies of the pure compounds. As a consequence, a good agreement between experimental and predicted h^M versus z_1 curves of binary systems exhibiting VLE mainly attests the capacity of the EoS to model vaporization enthalpies of pure components rather than its capacity to estimate h^M.

2.4 NATURAL GASES PHASE BEHAVIOR MODELING WITH SAFT-TYPE EOS

Since the late 1980s, the SAFT family of EoS, which has been developed based on the Thermodynamic Perturbation Theory (TPT), has gained considerable popularity in both academia and industry. A large amount of research work has been done over the last almost 3 decades toward the improvement of

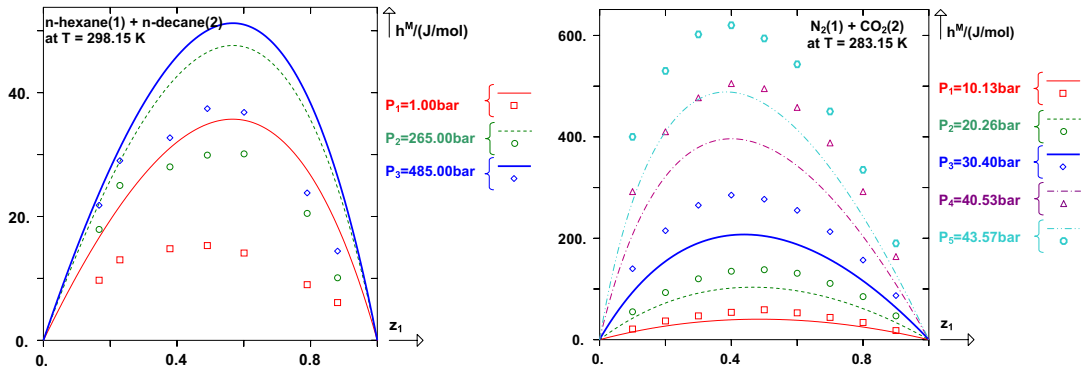

FIGURE 2.16

Representation of molar enthalpy change on isothermal isobaric mixing versus mole fraction z_1. *Symbols:* experimental data. *Full lines:* predicted curves with the PPR78 model.

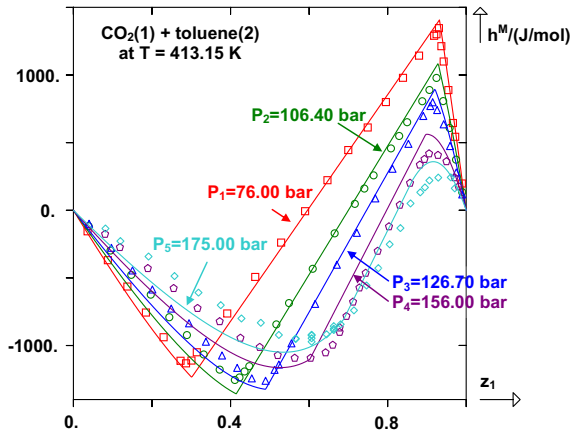

FIGURE 2.17

System $CO_2(1)$ + toluene(2): representation of molar enthalpy change on isothermal isobaric mixing versus mole fraction z_1. *Symbols:* experimental data. *Full lines:* predicted curves with the PPR78 model.

SAFT to become more accurate for different types of systems such as strongly polar mixtures, polymers, and electrolytes, while last years many applications of SAFT in the oil and gas industry have been reported (Ting et al., 2003a,b; Sun et al., 2007; Vargas et al., 2009; Panuganti et al., 2013; Liang et al., 2014 and 2015; Yan et al., 2015; Varzandeh et al., 2017).

By extending Wertheim's (Wertheim, 1984a,b and 1986a,b,c) theory, Chapman et al. (1988, 1990) and Huang and Radosz (1990, 1991) developed the SAFT equation of state. Although SAFT-derived EoS are mathematically complex, the underlying concepts are straightforward. SAFT-based equations are constructed based on summing intramolecular and intermolecular contributions to the Helmholtz energy. The expression for the residual Helmholtz energy (a^{res}) is given by

$$a^{\text{res}} = a^{hs} + a^{\text{chain}} + a^{\text{disp}} + a^{\text{assoc}} \tag{2.101}$$

where a^{hs} is the hard sphere contribution, a^{chain} is the contribution for chain formation, a^{disp} is the contribution from dispersion forces, and a^{assoc} is the contribution coming from association, e.g., hydrogen bonding. Fig. 2.18 shows schematically the procedure followed to form a SAFT model molecule.

Huang and Radosz (1990) were the first to propose an engineering formulation of SAFT EoS and used this equation to correlate vapor–liquid equilibria of over 100 real pure fluids. They demonstrated that SAFT was applicable to small, large, polydisperse, and associating molecules over the whole density range. Furthermore, Huang and Radosz (1991) extended SAFT to mixtures by testing 60 phase equilibrium data sets for both symmetric and asymmetric binary systems, with respect to the size of the molecules, as well as for binary mixtures containing associating compounds. They concluded that the mixing rules for the hard sphere, chain, and association terms were not required when using rigorous statistical mechanical expressions. Only the dispersion term required mixing rules, and only one binary temperature-independent parameter was necessary for the representation of the experimental data.

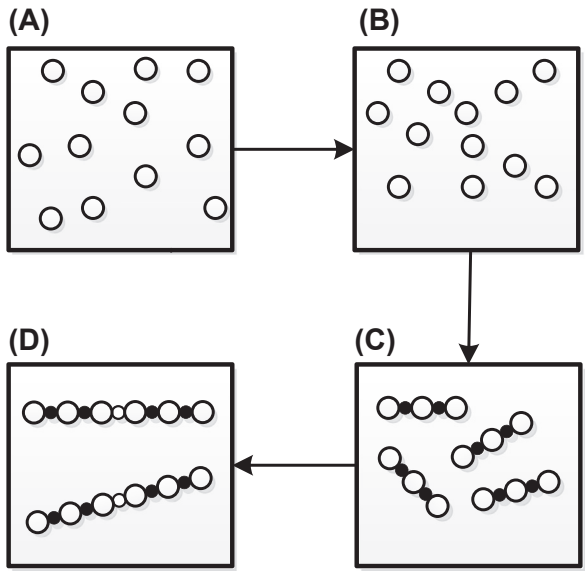

FIGURE 2.18

Schematic representation of the procedure that forms a SAFT model molecule: (A) the reference fluid consists of hard spheres; (B) dispersion forces are added; (C) chain sites are added and chain molecules appear; (D) hydrogen bonding is added and molecules form association complexes through association sites.

2.4.1 THE ORIGINAL SAFT EOS

In the original SAFT (Huang and Radosz, 1990 and 1991) the hard sphere term is calculated as proposed by Carnahan and Starling (1969):

$$\frac{a^{hs}}{RT} = m\frac{4n - 3n^2}{(1-n)^2} \tag{2.102}$$

where m is the number of spherical segments per molecule and n is the reduced density.

The chain and association terms are calculated from the following expressions proposed by Chapman et al. (1990):

$$\frac{a^{\text{chain}}}{RT} = (1-m)\ln\frac{1-0.5n}{(1-n)^3} \tag{2.103}$$

$$\frac{a^{\text{assoc}}}{RT} = \sum_{A=1}^{M}\left(\ln X^A - 0.5X^A\right) + 0.5M \tag{2.104}$$

where M is the number of association sites per molecule and X^A is the mole fraction of molecules not bonded at site A. In Eq. (2.104), the summation is taken over all association sites of the molecule. The quantity X^A is calculated from the following expression:

$$X^A = \left(1 + N_{Av}\sum_B \rho X^B \Delta^{AB}\right)^{-1} \tag{2.105}$$

where the summation is taken over all sites. N_{Av} is Avogadro's number, ρ is the molar density, and Δ^{AB} is the association strength that is calculated from the following equation:

$$\Delta^{AB} = \frac{1 - 0.5n}{(1-n)^3}\left(\exp\frac{\varepsilon^{AB}}{kT} - 1\right)\left(\sigma^3\kappa^{AB}\right) \tag{2.106}$$

where σ is the temperature-independent segment diameter that is calculated by

$$\sigma = \left(\frac{6\tau}{\pi N_{Av}}u^{\infty}\right)^{1/3} \tag{2.107}$$

In Eq. (2.107), u^{∞} is the segment volume and τ is equal to 0.74,048. Also, ε^{AB} and κ^{AB} in Eq. (2.106) are the association energy and volume parameters.

For the dispersion term, a number of different expressions have been proposed in the various SAFT variants. In the original SAFT of Huang and Radosz (1990) the following expression is used:

$$\frac{a^{\text{disp}}}{RT} = m\sum_{i=1}^{4}\sum_{j=1}^{9} D_{ij}\left(\frac{u}{kT}\right)^i\left(\frac{n}{0.74048}\right)^j \tag{2.108}$$

where u is the temperature-dependent dispersion energy of interaction between segments calculated as

$$u = u^o\left(1 + \frac{e}{kT}\right) \tag{2.109}$$

where u^o is the temperature-independent dispersion energy of interaction between segments, and e/k was set equal to 10K for all molecules except a few small molecules.

For pure nonassociating compounds, three pure-component parameters are used in SAFT, namely, m, u^o/k, and u^{∞}, whereas for self-associating compounds, two additional parameters are used, namely, ε^{AB} and κ^{AB}. The three or five pure component parameters are determined by fitting pure compound properties, usually vapor pressures and saturation liquid densities.

For the extension of original SAFT to mixtures, the equation of Mansoori et al. (1971) is used for the hard-sphere mixtures, whereas the chain and the association terms are extended to mixtures rigorously (Carnahan and Starling, 1969). The dispersion term is extended to mixtures by assuming the van der Waals one-fluid theory approximation. Mixing rules are only needed for u/k in the dispersion term, and they are as follows:

$$\frac{u}{k} = \frac{\sum_i\sum_j x_i x_j m_i m_j\left(\frac{u_{ij}}{kT}\right)(u^o)_{ij}}{\sum_i\sum_j x_i x_j m_i m_j (u^o)_{ij}} \tag{2.110}$$

$$(u^o)_{ij} = \left[\frac{(u^o)_j^{1/3} + (u^o)_j^{1/3}}{2}\right]^3 \tag{2.111}$$

$$u_{ij} = (u_{ii}u_{jj})^{1/2}(1 - k_{ij}) \tag{2.112}$$

where k_{ij} is a binary adjustable parameter that is determined by fitting binary phase equilibrium data.

For mixtures containing associating compounds (Huang and Radosz, 1990), the number and type of association sites, i.e., the association scheme of the compound, should be first established. For the association term, only combining rules for the association parameters are needed when two associating species are present in the mixture:

$$\varepsilon_{ij} = (\varepsilon_{ii}\varepsilon_{jj})^{1/2} \tag{2.113}$$

$$k_{ij}^{AB} = \left[\frac{\left(k_{ii}^{AB}\right)^{1/3} + \left(k_{jj}^{AB}\right)^{1/3}}{2}\right]^3 \tag{2.114}$$

2.4.2 MODIFICATIONS OF THE SAFT EQUATION

Since the original development of SAFT, numerous modifications have been proposed. Excellent reviews on the different variations of SAFT are presented by Economou (2002), de Hemptinne et al. (2006), and Kontogeorgis and Folas (2010).

Some of these variations include the following: (1) the simplified-SAFT (Fu and Sandler, 1995) that uses a simplification for the dispersion term; (2) the LJ-SAFT (Kraska and Gubbins, 1996a,b) that accounts explicitly for the repulsive and dispersion interactions using the Lennard−Jones equation as well as for dipole−dipole interactions; (3) the soft-SAFT (Blas and Vega, 1998) that uses a Lennard−Jones reference fluid instead of the hard-sphere fluid in the original SAFT as in LJ-SAFT; and (4) the SAFT-VR (Gil-Villegas et al., 1997) that uses for the dispersion term a square-well potential instead of the hard sphere.

PC-SAFT (Gross and Sadowski, 2001 and 2002) is one of the most successful modifications of the SAFT theory. The main difference between original SAFT and PC-SAFT is on the reference fluid used. Specifically PC-SAFT uses the hard-chain reference fluid to account for the dispersion interactions unlike SAFT that uses the hard-sphere reference fluid. So in Eq. (2.101) the hard-sphere and chain terms are substituted by a hard-chain term (a^{hc}) in PC-SAFT:

$$\frac{a^{hc}}{RT} = \overline{m}\frac{a^{hs}}{RT} - \sum_i x_i(m_i - 1)\ln g_{ii}^{hs}(\sigma_{ii}) \tag{2.115}$$

where m_i is the number of segments in a chain of component i, $\overline{m}$ is the mean segment number in the mixture ($\overline{m} = \sum_i x_i m_i$), and g_{ii}^{hs} is the radial distribution function of the hard sphere fluid:

$$g_{ii}^{hs} = \frac{1}{1-\zeta_3} + \left(\frac{d_i d_j}{d_i + d_j}\right)\frac{3\zeta_2}{(1-\zeta_3)^2} + \left(\frac{d_i d_j}{d_i + d_j}\right)^2 \frac{2{\zeta_2}^2}{(1-\zeta_3)^3} \tag{2.116}$$

$$\zeta_n = \frac{\pi}{6}\rho\sum_i x_i m_i d_i^n \tag{2.117}$$

$$d_i = \sigma_i\left[1 - 0.12\exp\left(-3\frac{\varepsilon_i}{kT}\right)\right] \tag{2.118}$$

where σ_i is the segment diameter and ε_i is the depth of the potential.

Finally, the hard-sphere contribution is given by

$$\frac{a^{hs}}{RT} = \frac{1}{\zeta_0}\left[\frac{3\zeta_1\zeta_2}{1-\zeta_3} + \frac{{\zeta_2}^3}{\zeta_3(1-\zeta_3)^2} + \left(\frac{{\zeta_2}^3}{{\zeta_3}^2} - \zeta_0\right)\ln(1-\zeta_3)\right] \tag{2.119}$$

Similar to original SAFT, PC-SAFT requires three parameters for pure nonassociating compounds: (1) the segment number (m), (2) the segment diameter (σ), and (3) the segment energy parameter (ε/κ). For self-associating compounds, the association energy and volume parameters (ε^{AB} and κ^{AB}) are also required. The three or five parameters are determined as in original SAFT by fitting pure-compound properties such as vapor pressure and saturation liquid densities. For mixtures, an additional binary adjustable interaction parameter is introduced in the dispersion term of the EoS, which is determined by fitting binary phase equilibrium data. Another very promising version of SAFT is the one developed by Polishuk's research group (Polishuk, 2014; Chorążewski et al., 2015a,b; Lubarsky and Polishuk, 2015; Postnikov et al., 2015; Lubarsky et al., 2016a,b; Polishuk et al., 2016 and 2017a,b) and named CP-PC-SAFT for "Critical Point-based Modified PC-SAFT" because the 3 parameters are determined from the mere knowledge of the critical constants (T_c and P_c) and the triple point liquid density. Another key point is that the resulting model appears to be virtually free of several undesired numerical pitfalls characteristic for PC-SAFT (Yelash et al., 2005a,b; Polishuk, 2010; Privat et al., 2010 and 2012; Polishuk and Mulero, 2011; Polishuk et al., 2013).

2.5 NATURAL GASES PHASE BEHAVIOR MODELING WITH THE GERG-2008 EOS

The GERG-2008 model is an equation of state developed for modeling natural gas mixtures containing any of the following pure species:

• Methane	• n-pentane	• Hydrogen
• Nitrogen	• I-pentane	• Oxygen
• Carbon dioxide	• n-hexane	• Carbon monoxide
• Ethane	• n-heptane	• Water
• Propane	• n-octane	• Hydrogen sulfide
• n-butane	• n-nonane	• Helium
• I-butane	• n-decane	• Argon

The GERG-2008 expression is explicit in the Helmholtz free energy a with the independent mixture variables density ρ, temperature T, and the vector of the molar composition $\boldsymbol{x}$. The function $a(\rho, T, \boldsymbol{x})$ is split into a part, a°, which represents the properties of ideal-gas mixtures at given values for ρ, T, and $\boldsymbol{x}$ and a part, a^{r}, which takes into account the residual mixture behavior:

$$a(\rho, T, \mathbf{x}) = a^{\circ}(\rho, T, \mathbf{x}) + a^{r}(\rho, T, \mathbf{x}) \tag{2.120}$$

The use of the Helmholtz free energy in its dimensionless form $\alpha = a/(RT)$ results in the following equation:

$$\alpha(\delta, \tau, \mathbf{x}) = \alpha^{\circ}(\rho, T, \mathbf{x}) + \alpha^{r}(\delta, \tau, \mathbf{x}) \tag{2.121}$$

In Eq. (2.121), δ is the reduced mixture density and τ is the inverse reduced mixture temperature:

$$\delta = \frac{\rho}{\rho_r(\mathbf{x})} \quad \text{and} \quad \tau = \frac{T_r(\mathbf{x})}{T} \tag{2.122}$$

with

$$\begin{cases} \dfrac{1}{\rho_r(\mathbf{x})} = \displaystyle\sum_{i=1}^{N} \frac{x_i^2}{\rho_{c,i}} + \sum_{i=1}^{N-1} \sum_{j=i+1}^{N} 2x_i x_j \, \beta_{v,ij} \, \gamma_{v,ij} \, \frac{x_i + x_j}{\beta_{v,ij}^2 x_i + x_j} \cdot \frac{1}{8} \left(\frac{1}{\rho_{c,i}^{1/3}} + \frac{1}{\rho_{c,j}^{1/3}} \right)^3 \\ T_r(\mathbf{x}) = \displaystyle\sum_{i=1}^{N} x_i^2 T_{c,i} + \sum_{i=1}^{N-1} \sum_{j=i+1}^{N} 2x_i x_j \, \beta_{T,ij} \, \gamma_{T,ij} \, \frac{x_i + x_j}{\beta_{T,ij}^2 x_i + x_j} \cdot \left(T_{c,i} T_{c,j} \right)^{0.5} \end{cases} \tag{2.123}$$

The binary parameters $\beta_{v,ij}$, $\gamma_{v,ij}$, $\beta_{T,ij}$, and $\gamma_{T,ij}$ were fitted to experimental data for binary mixtures. Their values are listed in Table A8 in the paper by Kunz and Wagner (2012). The critical parameters $\rho_{c,i}$ and $T_{c,i}$ of the pure components are given in Table A5 of the same reference.

The dimensionless form of the Helmholtz free energy for the ideal-gas mixture α° is given by

$$\alpha^\circ(\rho, T, \mathbf{x}) = \sum_{i=1}^{N} x_i \left[\alpha_{0i}^\circ(\rho, T) + \ln x_i \right] \tag{2.124}$$

where $\alpha_{0i}^\circ(\rho, T)$ is the dimensionless form of the Helmholtz free energy in the ideal-gas state of component i, in turn given by

$$\begin{aligned} \alpha_{0i}^\circ(\rho, T) = \ln\left(\frac{\rho}{\rho_{c,i}}\right) + \frac{R^*}{R}\left[n_{0i,1}^\circ + n_{0i,2}^\circ \frac{T_{c,i}}{T} + n_{0i,3}^\circ \ln\left(\frac{T_{c,i}}{T}\right) \right] + \sum_{k=4,5,6} n_{0i,k}^\circ \ln\left[\left| \sinh\left(\vartheta_{0i,k}^\circ \frac{T_{c,i}}{T} \right) \right| \right] \\ + \sum_{k=5,6,7} n_{0i,k}^\circ \ln\left[\left| \cosh\left(\vartheta_{0i,k}^\circ \frac{T_{c,i}}{T} \right) \right| \right] \end{aligned} \tag{2.125}$$

the values of the coefficients $n_{0i,k}^\circ$ and the parameters $\vartheta_{0i,k}^\circ$ are listed in Table A1 of Appendix A in the paper by Kunz and Wagner (2012).

The residual part of the reduced Helmholtz free energy of the mixture α^r is given by

$$\alpha^r(\delta, \tau, \mathbf{x}) = \sum_{i=1}^{N} x_i \alpha_{0i}^r(\delta, \tau) + \Delta\alpha^r(\delta, \tau, \mathbf{x}) \tag{2.126}$$

where, $\alpha_{0i}^r(\delta, \tau)$ is the dimensionless form of the residual Helmholtz free energy, in turns given by:

$$\alpha_{0i}^r(\delta, \tau) = \sum_{k=1}^{K_{\text{Pol},i}} n_{0i,k} \delta^{d_{0i,k}} \tau^{t_{0i,k}} + \sum_{k=K_{\text{Pol},i}+1}^{K_{\text{Pol},i}+K_{\text{Exp},i}} n_{0i,k} \delta^{d_{0i,k}} \tau^{t_{0i,k}} \exp(-\delta^{c_{0i,k}}) \tag{2.127}$$

the values of the coefficients $n_{0i,k}$ and the exponents $d_{0i,k}$, $t_{0i,k}$, and $c_{0i,k}$ for all considered components are given in Tables A2 to A4, and the critical parameters are listed in Table A5 in the paper by Kunz and Wagner (2012). In Eq. (2.126), $\Delta\alpha^r$ is a departure function of the dimensionless Helmholtz energy, which is calculated as

$$\Delta\alpha^r(\delta,\tau,\mathbf{x}) = \sum_{i=1}^{N-1}\sum_{j=i+1}^{N} x_i x_j F_{ij}\alpha_{ij}^r(\delta,\tau) \tag{2.128}$$

with

$$\begin{aligned}\alpha_{ij}^r(\delta,\tau) = &\sum_{k=1}^{K_{\mathrm{Pol},ij}} n_{ij,k}\delta^{d_{ij,k}}\tau^{t_{ij,k}} \\ &+ \sum_{k=K_{\mathrm{Pol},ij}+1}^{K_{\mathrm{Pol},ij}+K_{\mathrm{Exp},ij}} n_{ij,k}\delta^{d_{ij,k}}\tau^{t_{ij,k}}\exp\left[-\eta_{ij,k}\left(\delta-\varepsilon_{ij,k}\right)^2-\beta_{ij,k}\left(\delta-\gamma_{ij,k}\right)\right]\end{aligned} \tag{2.129}$$

As explained by Kunz and Wagner, for each binary mixture, the factor F_{ij} is fitted to specific data. The values for the coefficients $n_{ij,k}$ and the exponents $d_{ij,k}$, $t_{ij,k}$, $\eta_{ij,k}$, $\varepsilon_{ij,k}$, $\beta_{ij,k}$, and $\gamma_{ij,k}$ considered in the GERG-2008 equation of state may be found in Table A7 in the paper by Kunz and Wagner (2012).

2.6 DEW POINT PRESSURES PREDICTION OF NATURAL GASES

Accurate prediction of dew point pressures of natural gases is of great importance for the gas industry as it is one of the gas quality specifications used for ensuring safe transport and processing of natural gas. Avoiding hydrocarbon condensation in pipelines is crucial as the presence of liquids increases the pressure drop and introduces operational problems resulting from the two phase flow in pipelines designed for single-phase transportation. In this section the compositions of 10 natural gases, 5 synthetic gases and 5 real gases (i.e., originating from gas fields), for which dew point measurements were performed by several authors (Blanco et al., 2000; Avila et al., 2002; Mørch et al., 2006; Louli et al., 2012; Skylogianni et al., 2016) are summarized in Tables 2.4 and 2.5. The experimental dew point data cover a temperature range from 248 to 297K and a pressure range from 2 to 110 bar. For the five SNGs, the performance of 6 thermodynamic models is evaluated against the experimental data. Four models rely on cubic EoS, such as UMR-PR, PSRK, VTPR, and PPR78, and the two last ones are PC-SAFT and GERG-2008. In return, for the 5 real gases, it was not possible to apply the GERG-2008 model because such natural gases contain cycloalkanes and i-alkanes that cannot be characterized by this EoS.

UMR-PR, PSRK, and VTPR combine the predictive UNIFAC g^E model with either the SRK or the PR EoS through the MHV1 mixing rule. In return, the PPR78 combines the one-parameter Van Laar g^E model with the PR EoS through the Huron−Vidal mixing rule. It is made predictive by the use of a group-contribution method to estimate the binary interaction parameters. These 4 models were thus used in a totally predictive manner meaning that no parameter was fitted on experimental data. The main difference between the UMR-PR, PSRK, and VTPR models from one hand and the PPR78 model on the other hand is the number of parameters per binary systems. Indeed UNIFAC is a 2-parameter g^E model, whereas Van-Laar is a 1-parameter g^E model. The required critical parameters and acentric factors for pure components were taken from the DIPPR data compilation (https://www.aiche.org/dippr/events-products/801-database). The PC-SAFT EoS has also been applied in a predictive manner, i.e., with zero binary interaction parameters. The pure-component parameters (m, σ, and ε) were taken from Gross and Sadowski (2001) and Ting et al. (2010).

Table 2.4 Compositions (mole%) of the 5 SNGs Considered in This Work

Components	SNG1	SNG2	SNG3	SNG4	SNG5
Carbon dioxide					0.5100
Nitrogen					6.9000
Methane	89.0000	94.0850	93.1211	84.1136	88.1882
Ethane	7.0000	4.4680	3.0483	9.9574	2.7200
Propane			0.9936	4.1112	0.8500
i-Butane			1.0323	0.5762	0.1700
n-Butane	4.0000		1.5099	1.0306	0.3200
i-Pentane				0.0028	0.0850
n-Pentane		1.4470		0.0078	0.0940
n-Hexane				0.0050	0.1190
Benzene			0.2948		
n-Heptane				0.1954	0.0258
n-Octane					0.0180

Table 2.5 Compositions (mole%) of the 5 Real Natural Gases (RGs) Considered in This Work

Components	RG1	RG2	RG3	RG4	RG5
Carbon dioxide	1.89224	1.78914	1.67151	2.41947	2.55101
Nitrogen	0.51076	0.50552	0.62276	0.72766	0.71519
Methane	86.62955	85.44976	88.16604	83.01782	82.67253
Ethane	6.19028	7.08992	5.48476	7.79299	7.76674
Propane	2.79406	2.93022	2.31347	3.79525	3.90102
i-Butane	0.46346	0.55347	0.36385	0.52174	0.53663
n-Butane	0.75236	0.84967	0.62520	0.98078	1.06467
2,2-Dimethylpropane	0.01601	0.01730	0.01129	0.02551	0.02681
i-Pentane	0.21094	0.23616	0.18616	0.21128	0.22701
n-Pentane	0.18366	0.21810	0.17430	0.21808	0.23410
2,2-Dimethylbutane	0.00553	0.00883	0.00519	0.00305	0.00324
cyclopentane	0.01644	0.01522	0.01665	0.01310	0.01374
2,3-Dimethylbutane	0.00943	0.01719	0.00896	0.00626	0.00662
2-Methylpentane	0.04019	0.04735	0.04210	0.04106	0.04354
3-Methylpentane	0.02211	0.02498	0.02291	0.02128	0.02245
n-Hexane	0.05026	0.05355	0.05531	0.05400	0.05694
n-Heptane	0.02974	0.03923	0.03304	0.03244	0.03381
Cyclohexane	0.08656	0.09285	0.09323	0.05629	0.05847
Benzene	0.03616	0.00834	0.03993	0.01629	0.01771
n-Octane	0.00394	0.00718	0.00408	0.00566	0.00609
Cycloheptane	0.03171	0.03547	0.03388	0.02422	0.02492
Toluene	0.02088	0.00480	0.02199	0.01023	0.01067
n-Nonane	0.00063	0.00164	0.00051	0.00121	0.00132
Cyclooctane	0.00078	0.00242	0.00075	0.00169	0.00192
m-Xylene	0.00232	0.00117	0.00213	0.00210	0.00223
n-Decane		0.00052		0.00053	0.00061

Figs. 2.19 and 2.20 present graphically the model dew point predictions (UMR-PR, PSRK, VTPR, PPR78, PC-SAFT, and GERG-2008, when possible) along with the experimental data and clearly indicate that the UMR-PR model yields the most accurate dew point curve predictions, especially at high pressures (see Fig. 2.19B or E; for which this phenomenon is unambiguous). The other 5 models lead to similar deviations, and the accuracy may vary from one natural gas to another. As a matter of fact, the PPR78 model often predicts the cricondentherm with the lowest deviation (Fig. 2.20A, D and E), but in return, it underestimates the upper dew pressures. The PC-SAFT model tends to overestimate the cricondentherm but leads to deviations in the same range as those obtained with cubic EoS. The accuracy of the GERG-2008 EoS is in the average of that obtained with other models. Figs. 2.19 and 2.20 highlight a nonintuitive significant difference between the phase envelopes calculated with the UMR-PR and the VTPR models. Such models are indeed very similar and mainly differ through the combining rule used for the covolume. This study thus underlines the strong impact of the covolume when calculations are performed on natural gases.

2.7 EFFECT OF THE HEAVY-END CHARACTERIZATION ON THE HYDROCARBON DEW POINT CURVE CALCULATION

As explained in the previous section, when the gas composition is known, an EoS can be used to generate the complete phase envelope. It is, however, well acknowledged (Elsharkawy, 2002; Moshfeghian et al., 2005; Dustman et al., 2006; Bullin et al., 2011) that results of calculation highly depend on the characterization of the heavy fraction. A natural gas is indeed a complex mixture of hydrocarbons and nonhydrocarbons, the detailed composition of which is often unknown or partially unknown as the number of present components is high. Usually, accurate compositional analysis is available up to normal hexane, whereas the rest of the components consist in an undefined fraction containing hydrocarbons heavier than normal hexane and usually referred to as C_{7+} fraction (Pedersen et al., 2015). As a rule, the composition is obtained by laboratory gas chromatography using a representative sample and performing an offsite analysis. Process chromatographs analyze the C_{7+} fraction in a variety of ways. Some process chromatographs lump all the C_{7+} components into a single plus fraction the molecular weight and density of which are also usually measured. Others analyze the C_{7+} fraction as a series of subfractions through C_9 or higher (i.e., C_7, C_8, C_9, and so forth).

Generally there are two techniques to characterize a hydrocarbon plus fraction: (1) the continuous mixture and (2) the pseudocomponent approaches (Riazi, 2005; Pedersen et al., 2015). In the continuous mixture characterization method, a distribution function is introduced to describe the composition of all the heavies. In the pseudocomponent approach, the C_{7+} is split into a number of subfractions with known mole fraction, boiling point, specific gravity, and molecular weight. For natural gases, it is common to define a paraffinic (P), naphthenic (N), and aromatic (A) tendency for each pseudocomponent (Riazi, 2005). The rule of thumb advises to work with 3 pseudocomponents and to assume either a 60/30/10 $C_6/C_7/C_8$ split or a 47/36/17 $C_6/C_7/C_8$ split. For more accurate results, the method developed by Bullin et al. (2011) is advised. In such a case the mole fractions of pseudocomponents C_6, C_7, C_8, and C_9 can be predicted from the mole fraction of C_5 and C_{6+} in the gas using the following equations:

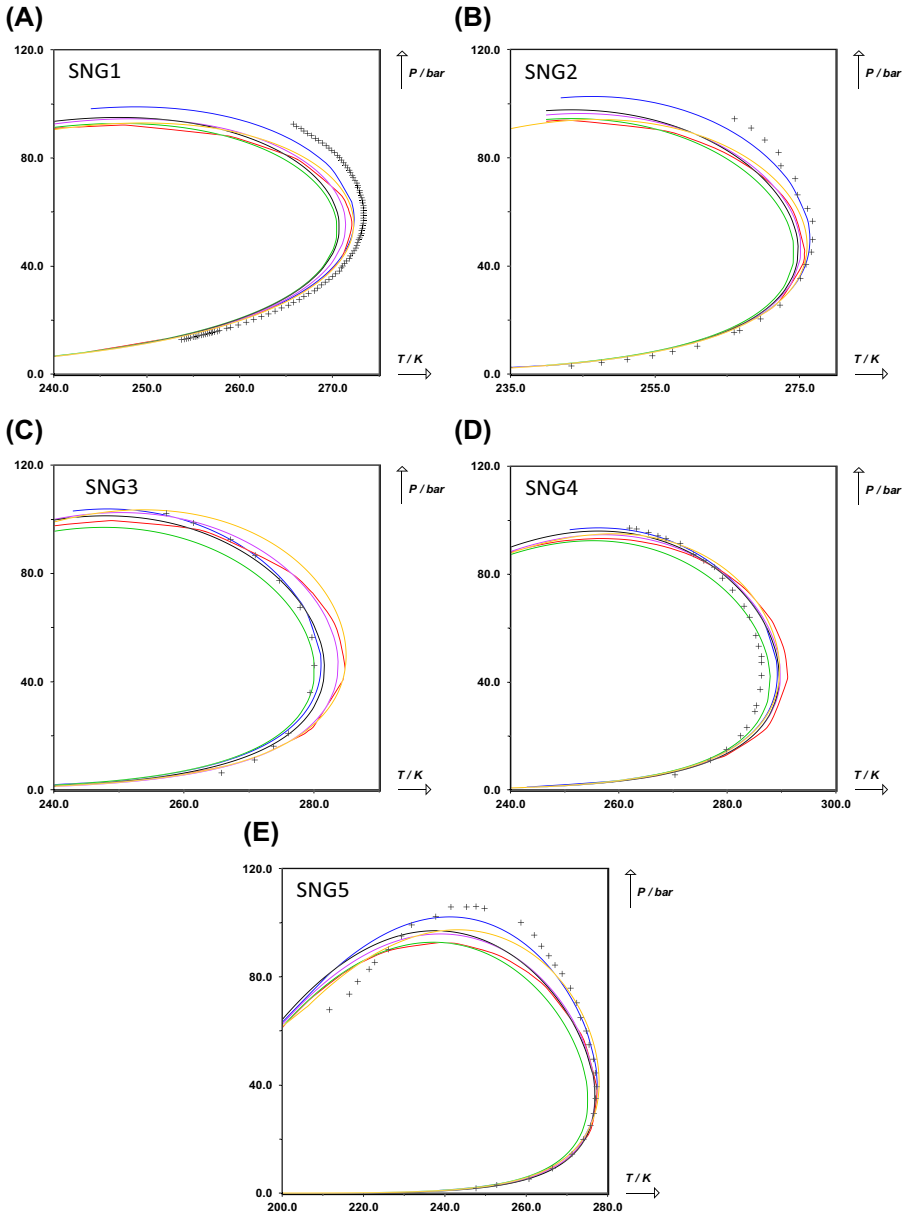

FIGURE 2.19

Predicted dew point curves for (A) SNG1, (B) SNG2, (C) SNG3, (D) SNG4, and (E) SNG5 with the UMR-PR (——), PSRK (——), VTPR (——), PPR78 (——), PC-SAFT (——), and GERG-2008 (——) models.

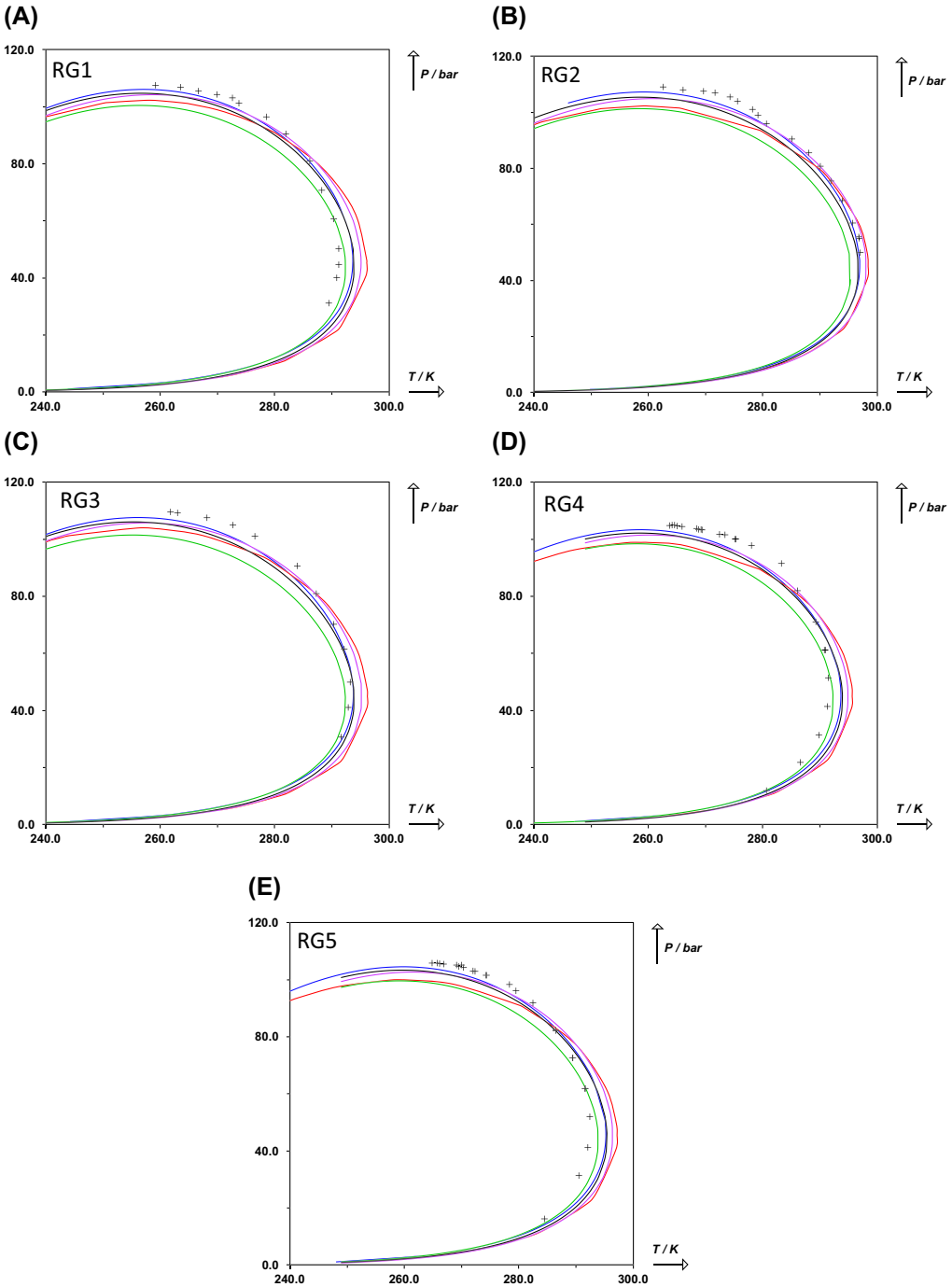

FIGURE 2.20

Predicted dew point curves for (A) RG1, (B) RG2, (C) RG3, (D) RG4, and (E) RG5 with the UMR-PR (——), PSRK (——), VTPR (——), PPR78 (——), and PC-SAFT (——) models.

$$\begin{cases} y_{C_6} = 0.6456\left(y_{C_5}\right)^{0.22}\left(y_{C_{6+}}\right)^{0.7976} \\ y_{C_7} = 0.5044\left(y_{C_5}\right)^{-0.2673}\left(y_{C_{6+}}\right)^{1.3375} \\ y_{C_8} = 0.07014\left(y_{C_5}\right)^{-1.0097}\left(y_{C_{6+}}\right)^{2.04} \\ y_{C_9} = 0.006149\left(y_{C_5}\right)^{-1.5176}\left(y_{C_{6+}}\right)^{2.4312} \end{cases} \tag{2.130}$$

The amount of C_{10} and above is calculated by the relation

$$\log\left(y_{C_{i+1}}\right) = \log\left(y_{C_i}\right) + \log\left(y_{C_9}\right) - \log\left(y_{C_8}\right) \tag{2.131}$$

As previously stated, the heavy fraction characterization affects significantly the dew point predictions calculated by a thermodynamic model. An example is shown in Fig. 2.21 that presents dew point predictions with the Peng–Robinson EoS for a real natural gas (RG), where its C_{7+} fraction has been characterized with three different schemes: (1) with three n-alkanes (n-heptane, n-octane, and n-nonane); (2) with three PNA components in each subfraction, i.e., in the C_7 subfraction all paraffins are represented by n-heptane, all naphthenic compounds by cyclohexane, and all aromatic compounds by benzene. In the C_8 subfraction the representatives are n-octane, cycloheptane, and toluene. In the C_9 subfraction the representatives are n-nonane, cyclooctane, and m-xylene; and (3) with three pseudocomponents of known molecular weight and density, whose critical properties have been estimated by the method of Riazi and Daubert (1987) and the acentric factors from Kesler and Lee (1976).

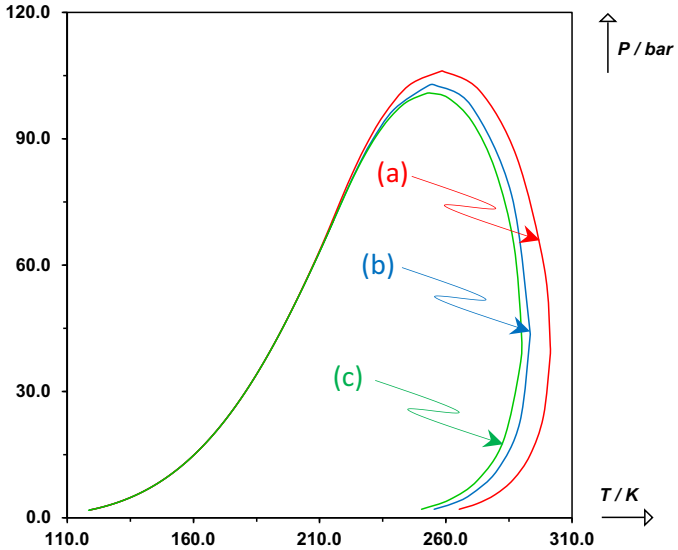

FIGURE 2.21

Effect of the characterization of the C_{7+} fraction of a real natural gas. Calculations were performed with the Peng–Robinson EoS coupled with three different characterization schemes. (a) the C_{7+} fraction is characterized with three n-alkanes. (b) The C_{7+} fraction is characterized with the three fractions C_7, C_8, and C_9 modeled each with PNA components. (c) The C_{7+} fraction is characterized with three pseudocomponents.

Deviations up to 11°C at the cricondentherm temperature and up to 6 bar at the cricondenbar pressure are obtained with the three different schemes.

2.8 CONCLUSION

This chapter highlights that there are no significant differences in the VLE correlation of natural gases with cubic EoS, provided advanced mixing rules involving appropriate activity coefficient model are used. In particular, very accurate results can be obtained with the mixing rules involved in the UMR-PR model.

This is why, in the petroleum industry, only two cubic EoS are generally used, such as the SRK and the PR EoS. Such cubic EoS have many advantages but also shortcomings. The main advantages are

- They are simple and induce fast calculations.
- They can be used to model both liquid and vapor phases.
- They are applicable over wide ranges of pressures and temperatures.
- They allow accurate phase−behavior correlation for nonpolar systems encountered in the gas industry.
- Accurate density prediction is obtained if a volume translation is used.
- They can be made predictive by incorporation in the mixing rules of g^E models in which the binary interaction parameters are calculated through the group contribution concept (UNIFAC or Van Laar).

The following sentence by Tsonopoulos and Heidman (1986) summarizes well the advantages of such models: *cubic EoS are simple, reliable, and allow the direct incorporation of critical conditions. We, in the petroleum industry, continue to find that simple cubic EoS such as RKS and PR are very reliable high-pressure VLE models, and we have not yet found in our work any strong incentive for using non-cubic EoS*.

Among the shortcomings, we can mention

- a poor correlation of associating systems phase behaviors;
- an unsatisfactory correlation of LLE especially for highly immiscible systems (e.g., mixtures of water or glycols with alkanes)

This chapter also highlights that not only SAFT-type but also the GERG-2008 EoS could be used to accurately correlate the phase behavior of natural gases. The GERG-2008, however, suffers of a severe limitation, that is, it cannot be applied to natural gases that contain naphthenic compounds or i-alkanes with more than 5 carbon atoms. The key advantage of SAFT-type EoS is that no binary interaction parameter is needed for such systems and that they can thus be used in a predictive way. Moreover for the compounds encountered in natural gases, the 3 parameters (m, σ, and ε) can be found in the open literature.

To conclude, predictive cubic EoS (PPR78, PSRK, VTPR) and especially UMR-PR make a perfect job to simulate the phase behavior of natural gases. For processes in which water and/or glycol are present (e.g., transportation processes), it is advised to use more complex EoS similar to Cubic Plus Association (Derawi et al., 2003) or models deriving from the SAFT (e.g., PC-SAFT).

REFERENCES

Abdoul, W., Rauzy, E., Péneloux, A., 1991. Group-contribution equation of state for correlating and predicting thermodynamic properties of weakly polar and non-associating mixtures. Fluid Phase Equilibria 68, 47−102.

Ahlers, J., Gmehling, J., 2001. Development of a universal group contribution equation of state. Fluid Phase Equilibria 191 (1−2), 177−188.

Ahlers, J., Gmehling, J., 2002. Development of a universal group contribution equation of state. 2. Prediction of vapor−liquid equilibria for asymmetric systems. Industrial and Engineering Chemistry Research 41 (14), 3489−3498.

Avila, S., Blanco, S.T., Velasco, I., Rauzy, E., Otín, S., 2002. Thermodynamic properties of synthetic natural gases. 1. Dew-point curves of synthetic natural gases and their mixtures with water and methanol. Measurement and correlation. Industrial and Engineering Chemistry Research 41 (15), 3714−3721.

Avlonitis, G., Mourikas, G., Stamataki, S., Tassios, D.A., 1994. Generalized correlation for the interaction coefficients of nitrogen-hydrocarbon binary mixtures. Fluid Phase Equilibria 101, 53−68.

Bartle, K.D., Clifford, A.A., Shilstone, G.F., 1992. Estimation of solubilities in supercritical carbon dioxide: a correlation for the Peng-Robinson interaction parameters. The Journal of Supercritical Fluids 5 (3), 220−225.

Blanco, S.T., Avila, S., Velasco, I., Rauzy, E., Otın, S., 2000. Dew points of ternary methane+ethane+butane and quaternary methane+ethane+butane+water mixtures: measurement and correlation. Fluid Phase Equilibria 171 (1−2), 233−242.

Blas, F.J., Vega, L.F., 1998. Prediction of binary and ternary diagrams using the statistical associating fluid theory (SAFT) equation of state. Industrial and Engineering Chemistry Research 37 (2), 660−674.

Boukouvalas, C., Spiliotis, N., Coutsikos, P., Tzouvaras, N., Tassios, D., 1994. Prediction of vapor-liquid equilibrium with the LCVM model: a linear combination of the Vidal and Michelsen mixing rules coupled with the original UNIFAC and the t-mPR equation of state. Fluid Phase Equilibria 92, 75−106.

Bullin, J.A., Fitz, C.W., Dustman, T., April 3-6, 2011. Practical hydrocarbon dew point specification for natural gas transmission lines. Paper Presented at the 90th Annual GPA Convention, San Antonio, TX, USA.

Carnahan, N.F., Starling, K.E., 1969. Equation of state for nonattracting rigid spheres. The Journal of Chemical Physics 51 (2), 635−636.

Carrier, B., Rogalski, M., Peneloux, A., 1988. Correlation and prediction of physical properties of hydrocarbons with the modified Peng-Robinson equation of state. 1. Low and medium vapor pressures. Industrial and Engineering Chemistry Research 27 (9), 1714−1721.

Chapman, W.G., Jackson, G., Gubbins, K.E., 1988. Phase equilibria of associating fluids: chain molecules with multiple bonding sites. Molecular Physics 65 (5), 1057−1079.

Chapman, W.G., Gubbins, K.E., Jackson, G., Radosz, M., 1990. New reference equation of state for associating liquids. Industrial and Engineering Chemistry Research 29 (8), 1709−1721.

Chen, J., Fischer, K., Gmehling, J., 2002. Modification of PSRK mixing rules and results for vapor−liquid equilibria, enthalpy of mixing and activity coefficients at infinite dilution. Fluid Phase Equilibria 200 (2), 411−429.

Chorążewski, M., Aim, K., Wichterle, I., Jacquemin, J., Polishuk, I., 2015a. High-pressure phase equilibrium in the {carbon dioxide (1) + 1-chloropropane (2)} binary system. Journal of Chemical Thermodynamics 91, 165−171.

Chorążewski, M., Postnikov, E.B., Oster, K., Polishuk, I., 2015b. Thermodynamic properties of 1,2-dichloroethane and 1,2-dibromoethane under elevated pressures: experimental results and predictions of a novel dippr-based version of FT-EoS, PC-SAFT, and CP-PC-SAFT. Industrial and Engineering Chemistry Research 54 (39), 9645−9656.

Chueh, P.L., Prausnitz, J.M., 1967. Vapor-liquid equilibria at high pressures: calculation of partial molar volumes in nonpolar liquid mixtures. AIChE Journal 13 (6), 1099−1107.

Clausius, R., 1880. Ueber Das Verhalten der Kohlensäure in Bezug Auf Druck, volumen Und Temperatur. Annals of Physics 245 (3), 337−357.

Coutinho, J.A.P., Kontogeorgis, G.M., Stenby, E.H., 1994. Binary interaction parameters for nonpolar systems with cubic equations of state: a theoretical approach. 1. CO_2/Hydrocarbons using SRK equation of state. Fluid Phase Equilibria 102 (1), 31−60.

Dahl, S., Michelsen, M.L., 1990. High-pressure vapor-liquid equilibrium with a UNIFAC-based equation of state. AIChE Journal 36 (12), 1829−1836.

de Hemptinne, J.-C., Mougin, P., Barreau, A., Ruffine, L., Tamouza, S., Inchekel, R., 2006. Application to petroleum engineering of statistical thermodynamics−based equations of state. Oil & Gas Science and Technology - Revue d'IFP 61 (3), 363−386.

Derawi, S.O., Kontogeorgis, G.M., Michelsen, M.L., Stenby, E.H., 2003. Extension of the cubic-plus-association equation of state to Glycol−water cross-associating systems. Industrial and Engineering Chemistry Research 42 (7), 1470−1477.

Dustman, T., Drenker, J., Bergman, D.F., Bullin, J.A., March 5−8, 2006. An analysis and prediction of hydrocarbon dew points and liquids in gas transmission lines. Paper Presented at the 85th Annual GPA Convention, Grapevine, TX, USA.

Economou, I.G., 2002. Statistical associating fluid theory: a successful model for the calculation of thermodynamic and phase equilibrium properties of complex fluid mixtures. Industrial and Engineering Chemistry Research 41 (5), 953−962.

Elsharkawy, A.M., 2002. Predicting the dew point pressure for gas condensate reservoirs: empirical models and equations of state. Fluid Phase Equilibria 193 (1−2), 147−165.

Fu, Y.-H., Sandler, S.I., 1995. A simplified SAFT equation of state for associating compounds and mixtures. Industrial and Engineering Chemistry Research 34 (5), 1897−1909.

Gao, G., Daridon, J.-L., Saint-Guirons, H., Xans, P., Montel, F., 1992. A simple correlation to evaluate binary interaction parameters of the Peng-Robinson equation of state: binary light hydrocarbon systems. Fluid Phase Equilibria 74, 85−93.

Gil-Villegas, A., Galindo, A., Whitehead, P.J., Mills, S.J., Jackson, G., Burgess, A.N., 1997. Statistical associating fluid theory for chain molecules with attractive potentials of variable range. The Journal of Chemical Physics 106 (10), 4168−4186.

Graboski, M.S., Daubert, T.E., 1978. A modified Soave equation of state for phase equilibrium calculations. 2. Systems containing CO_2, H_2S, N_2 and CO. Industrial and Engineering Chemistry Process Design and Development 17 (4), 448−454.

Gross, J., Sadowski, G., 2001. Perturbed-chain SAFT: an equation of state based on a perturbation theory for chain molecules. Industrial and Engineering Chemistry Research 40 (4), 1244−1260.

Gross, J., Sadowski, G., 2002. Application of the perturbed-chain SAFT equation of state to associating systems. Industrial and Engineering Chemistry Research 41 (22), 5510−5515.

Holderbaum, T., Gmehling, J., 1991. PSRK: a group contribution equation of state based on UNIFAC. Fluid Phase Equilibria 70 (2−3), 251−265.

Huang, S.H., Radosz, M., 1990. Equation of state for small, large, polydisperse, and associating molecules. Industrial and Engineering Chemistry Research 29 (11), 2284−2294.

Huang, S.H., Radosz, M., 1991. Equation of state for small, large, polydisperse, and associating molecules: extension to fluid mixtures. Industrial and Engineering Chemistry Research 30 (8), 1994−2005.

Huron, M.-J., Vidal, J., 1979. New mixing rules in simple equations of state for representing vapour-liquid equilibria of strongly non-ideal mixtures. Fluid Phase Equilibria 3, 255−271.

Jaubert, J.-N., Mutelet, F., 2004. VLE predictions with the Peng-Robinson equation of state and temperature-dependent k_{ij} calculated through a group contribution method. Fluid Phase Equilibria 224 (2), 285−304.

Jaubert, J.-N., Privat, R., 2010. Relationship between the binary interaction parameters (k_{ij}) of the Peng-Robinson and those of the Soave-Redlich-Kwong equations of state: application to the definition of the PR2SRK model. Fluid Phase Equilibria 295 (1), 26−37.

Jaubert, J.-N., Privat, R., 2014. Application of the double-tangent construction of coexisting phases to any type of phase equilibrium for binary systems modeled with the Gamma-Phi approach. Chemical Engineering Education 48 (1), 42−56.

Jaubert, J.-N., Vitu, S., Mutelet, F., Corriou, J.-P., 2005. Extension of the PPR78 model (predictive 1978, Peng-Robinson EoS with temperature-dependent k_{ij} calculated through a group contribution method) to systems containing aromatic compounds. Fluid Phase Equilibria 237 (1−2), 193−211.

Jaubert, J.-N., Privat, R., Mutelet, F., 2010. Predicting the phase equilibria of synthetic petroleum fluids with the PPR78 approach. AIChE Journal 56 (12), 3225−3235.

Jaubert, J.-N., Privat, R., Qian, J., 2011. Péneloux's mixing rules: 25 Years ago and now. Fluid Phase Equilibria 308 (1−2), 164−167.

Jaubert, J.-N., Privat, R., Le Guennec, Y., Coniglio, L., 2016. Note on the properties altered by application of a Péneloux-type volume translation to an equation of state. Fluid Phase Equilibria 419, 88−95.

Kato, K., Nagahama, K., Hirata, M., 1981. Generalized interaction parameters for the Peng-Robinson equation of state: carbon dioxide n-Paraffin binary systems. Fluid Phase Equilibria 7 (3−4), 219−231.

Kesler, M.G., Lee, B., 1976. Improve prediction of enthalpy of fractions. Hydrocarbon Processing 55 (3), 153−158.

Kontogeorgis, G.M., Folas, G.K., 2010. Thermodynamic Models for Industrial Applications. John Wiley & Sons Ltd., Chichester, UK.

Kordas, A., Tsoutsouras, K., Stamataki, S., Tassios, D., 1994. A generalized correlation for the interaction coefficients of CO_2-hydrocarbon binary mixtures. Fluid Phase Equilibria 93, 141−166.

Kordas, A., Magoulas, K., Stamataki, S., Tassios, D., 1995. Methane hydrocarbon interaction parameters correlation for the Peng-Robinson and the t-mPR equation of state. Fluid Phase Equilibria 112 (1), 33−44.

Kraska, T., Gubbins, K.E., 1996a. Phase equilibria calculations with a modified SAFT equation of state. 1. Pure alkanes, alkanols, and water. Industrial and Engineering Chemistry Research 35 (12), 4727−4737.

Kraska, T., Gubbins, K.E., 1996b. Phase equilibria calculations with a modified SAFT equation of state. 2. Binary mixtures of n-alkanes, 1-alkanols, and water. Industrial and Engineering Chemistry Research 35 (12), 4738−4746.

Kunz, O., Wagner, W., 2012. The GERG-2008 wide-range equation of state for natural gases and other mixtures: an expansion of GERG-2004. Journal of Chemical and Engineering Data 57 (11), 3032−3091.

Le Guennec, Y., Lasala, S., Privat, R., Jaubert, J.-N., 2016a. A consistency test for α-functions of cubic equations of state. Fluid Phase Equilibria 427, 513−538.

Le Guennec, Y., Privat, R., Jaubert, J.-N., 2016b. Development of the translated-consistent tc-PR and tc-RK cubic equations of state for a safe and accurate prediction of volumetric, energetic and saturation properties of pure compounds in the sub- and super-critical domains. Fluid Phase Equilibria 429, 301−312.

Le Guennec, Y., Privat, R., Lasala, S., Jaubert, J.-N., 2017. On the imperative need to use a consistent α-function for the prediction of pure-compound supercritical properties with a cubic equation of state. Fluid Phase Equilibria 445, 45−53.

Liang, X., Yan, W., Thomsen, K., Kontogeorgis, G.M., 2014. On petroleum fluid characterization with the PC-SAFT equation of state. Fluid Phase Equilibria 375, 254−268.

Liang, X., Yan, W., Thomsen, K., Kontogeorgis, G.M., 2015. Modeling the liquid−liquid equilibrium of petroleum fluid and polar compounds containing systems with the PC-SAFT equation of state. Fluid Phase Equilibria 406, 147−155.

Louli, V., Pappa, G., Boukouvalas, C., Skouras, S., Solbraa, E., Christensen, K.O., Voutsas, E., 2012. Measurement and prediction of dew point curves of natural gas mixtures. Fluid Phase Equilibria 334, 1−9.

Lubarsky, H., Polishuk, I., 2015. Implementation of the critical point-based revised PC-SAFT for modelling thermodynamic properties of aromatic and haloaromatic compounds. The Journal of Supercritical Fluids 97, 133−144.

Lubarsky, H., Polishuk, I., NguyenHuynh, D., 2016a. Implementation of GC-PPC-SAFT and CP-PC-SAFT for predicting thermodynamic properties of mixtures of weakly- and non-associated oxygenated compounds. The Journal of Supercritical Fluids 115, 65−78.

Lubarsky, H., Polishuk, I., NguyenHuynh, D., 2016b. The group contribution method (GC) versus the critical point-based approach (CP): predicting thermodynamic properties of weakly- and non-associated oxygenated compounds by GC-PPC-SAFT and CP-PC-SAFT. The Journal of Supercritical Fluids 110, 11−21.

Mansoori, G.A., Carnahan, N.F., Starling, K.E., Leland, T.W., 1971. Equilibrium thermodynamic properties of the mixture of hard spheres. The Journal of Chemical Physics 54 (4), 1523−1525.

Mathias, P.M., Copeman, T.W., 1983. Extension of the Peng-Robinson equation of state to complex mixtures: evaluation of the various forms of the local composition concept. Fluid Phase Equilibria 13, 91−108.

Michelsen, M.L., 1990. A modified Huron-Vidal mixing rule for cubic equations of state. Fluid Phase Equilibria 60 (1−2), 213−219.

Michelsen, M.L., Mollerup, J.M., 2007. Thermodynamic Models: Fundamentals & Computational Aspects, second ed. Tie-Line Publications, Holte, Denmark.

Mørch, ø., Nasrifar, K., Bolland, O., Solbraa, E., Fredheim, A.O., Gjertsen, L.H., 2006. Measurement and modeling of hydrocarbon dew points for five synthetic natural gas mixtures. Fluid Phase Equilibria 239 (2), 138−145.

Moshfeghian, M., Lilly, L.L., Maddox, R.N., Nasrifar, K., 2005. Study compares C6+ characterization methods for natural gas phase envelopes. Oil & Gas Journal 103 (43), 60−65.

Moysan, J.M., Paradowski, H., Vidal, J., 1986. Prediction of phase behaviour of gas-containing systems with cubic equations of state. Chemical Engineering Science 41 (8), 2069−2074.

Nishiumi, H., Arai, T., Takeuchi, K., 1988. Generalization of the binary interaction parameter of the Peng-Robinson equation of state by component family. Fluid Phase Equilibria 42, 43−62.

Panuganti, S.R., Tavakkoli, M., Vargas, F.M., Gonzalez, D.L., Chapman, W.G., 2013. SAFT model for upstream asphaltene applications. Fluid Phase Equilibria 359, 2−16.

Pedersen, K.S., Christensen, P.L., Shaikh, J.A., 2015. Phase Behavior of Petroleum Reservoir Fluids, second ed. CRC Press, Taylor & Francis Group, Boca Raton, FL, USA.

Péneloux, A., Rauzy, E., Freze, R., 1982. A consistent correction for Redlich-Kwong-Soave volumes. Fluid Phase Equilibria 8 (1), 7−23.

Peng, D.-Y., Robinson, D.B., 1976. A new two-constant equation of state. Industrial and Engineering Chemistry Fundamentals 15 (1), 59−64.

Pitzer, K.S., Lippmann, D.Z., Curl, R.F., Huggins, C.M., Petersen, D.E., 1955. The volumetric and thermodynamic properties of fluids. II. Compressibility factor, vapor pressure and entropy of vaporization. Journal of the American Chemical Society 77 (13), 3433−3440.

Plee, V., Jaubert, J.-N., Privat, R., Arpentinier, P., 2015. Extension of the e-PPR78 equation of state to predict fluid phase equilibria of natural gases containing carbon monoxide, Helium-4 and argon. Journal of Petroleum Science and Engineering 133, 744−770.

Polishuk, I., 2010. About the numerical pitfalls characteristic for SAFT EOS models. Fluid Phase Equilibria 298 (1), 67−74.

Polishuk, I., 2014. Standardized critical point-based numerical solution of statistical association fluid theory parameters: the perturbed chain-statistical association fluid theory equation of state revisited. Industrial and Engineering Chemistry Research 53 (36), 14127−14141.

Polishuk, I., Mulero, A., 2011. The numerical challenges of SAFT EoS models. Reviews in Chemical Engineering 27 (5–6), 241–251.

Polishuk, I., Privat, R., Jaubert, J.-N., 2013. Novel methodology for analysis and evaluation of SAFT-type equations of state. Industrial and Engineering Chemistry Research 52 (38), 13875–13885.

Polishuk, I., Nakonechny, F., Brauner, N., 2016. Predicting phase behavior of metallic mercury in liquid and compressed gaseous hydrocarbons. Fuel 174, 197–205.

Polishuk, I., Sidik, Y., NguyenHuynh, D., 2017a. Predicting phase behavior in aqueous systems without fitting binary parameters. I: CP-PC-SAFT EOS, aromatic compounds. AIChE Journal 63 (9), 4124–4135.

Polishuk, I., Lubarsky, H., NguyenHuynh, D., 2017b. Predicting phase behavior in aqueous systems without fitting binary parameters II: gases and non-aromatic hydrocarbons. AIChE Journal 63 (11), 5064–5075.

Postnikov, E.B., Goncharov, A.L., Cohen, N., Polishuk, I., 2015. Estimating the liquid properties of 1-alkanols from C_5 to C_{12} by FT-EoS and CP-PC-SAFT: simplicity versus complexity. The Journal of Supercritical Fluids 104, 193–203.

Privat, R., Jaubert, J.-N., 2012a. Addition of the sulfhydryl group (SH) to the PPR78 model: estimation of missing group-interaction parameters for systems containing mercaptans and carbon dioxide or nitrogen or methane, from newly published data. Fluid Phase Equilibria 334, 197–203.

Privat, R., Jaubert, J.-N., 2012b. Discussion around the paradigm of ideal mixtures with emphasis on the definition of the property changes on mixing. Chemical Engineering Science 82, 319–333.

Privat, R., Jaubert, J.-N., 2013. Classification of global fluid-phase equilibrium behaviors in binary systems. Chemical Engineering Research and Design 91 (10), 1807–1839.

Privat, R., Mutelet, F., Jaubert, J.-N., 2008a. Addition of the hydrogen sulfide group to the PPR78 model (predictive 1978, Peng-Robinson equation of state with temperature-dependent k_{ij} calculated through a group contribution method). Industrial and Engineering Chemistry Research 47 (24), 10041–10052.

Privat, R., Jaubert, J.-N., Mutelet, F., 2008b. Addition of the nitrogen group to the PPR78 model (predictive 1978, Peng-Robinson EoS with temperature-dependent k_{ij} calculated through a group contribution method. Industrial and Engineering Chemistry Research 47 (6), 2033–2048.

Privat, R., Jaubert, J.-N., Mutelet, F., 2008c. Addition of the sulfhydryl group (-SH) to the PPR78 model (predictive 1978, Peng-Robinson EoS with temperature-dependent k_{ij} calculated through a group contribution method). Journal of Chemical Thermodynamics 40 (9), 1331–1341.

Privat, R., Jaubert, J.-N., Mutelet, F., 2008d. Use of the PPR78 model to predict new equilibrium data of binary systems involving hydrocarbons and nitrogen. Comparison with other GCEOS. Industrial and Engineering Chemistry Research 47 (19), 7483–7489.

Privat, R., Gani, R., Jaubert, J.-N., 2010. Are safe results obtained when the PC-SAFT equation of state is applied to ordinary pure chemicals? Fluid Phase Equilibria 295 (1), 76–92.

Privat, R., Conte, E., Jaubert, J.-N., Gani, R., 2012. Are safe results obtained when SAFT equations are applied to ordinary chemicals? Part 2: study of solid-liquid equilibria in binary systems. Fluid Phase Equilibria 318, 61–76.

Privat, R., Jaubert, J.-N., Le Guennec, Y., 2016. Incorporation of a volume translation in an equation of state for fluid mixtures: which combining rule? Which effect on properties of mixing? Fluid Phase Equilibria 427, 414–420.

Qian, J.-W., Privat, R., Jaubert, J.-N., Duchet-Suchaux, P., 2013a. Enthalpy and heat capacity changes on mixing: fundamental aspects and prediction by means of the PPR78 cubic equation of state. Energy & Fuels 27 (11), 7150–7178.

Qian, J.-W., Jaubert, J.-N., Privat, R., 2013b. Phase equilibria in hydrogen-containing binary systems modeled with the Peng-Robinson equation of state and temperature-dependent binary interaction parameters calculated through a group-contribution method. The Journal of Supercritical Fluids 75, 58–71.

Qian, J.-W., Privat, R., Jaubert, J.-N., 2013c. Predicting the phase equilibria, critical phenomena, and mixing enthalpies of binary aqueous systems containing alkanes, cycloalkanes, aromatics, alkenes, and gases (N_2, CO_2, H_2S, H_2) with the PPR78 equation of state. Industrial and Engineering Chemistry Research 52 (46), 16457–16490.

Qian, J.-W., Jaubert, J.-N., Privat, R., 2013d. Prediction of the phase behavior of alkene-containing binary systems with the PPR78 model. Fluid Phase Equilibria 354, 212−235.

Qian, J.-W., Privat, R., Jaubert, J.-N., Coquelet, C., Ramjugernath, D., 2017. Fluid-Phase-Equilibrium Prediction of Fluorocompound-Containing Binary Systems with the Predictive E-PPR78 Model (Prévision En Matière d'équilibre Des Phases de Fluide Des Systèmes Binaires Contenant Des Fluorocomposés Avec Le Modèle Prédictif E-PPR78). International Journal of Refrigeration 73, 65−90.

Rackett, H.G., 1970. Equation of state for saturated liquids. Journal of Chemical and Engineering Data 15 (4), 514−517.

Rauzy, E., 1982. Les Méthodes Simples de Calcul Des Équilibres Liquide-Vapeur Sous Pression (Ph.D. thesis). University of Aix-Marseille II, France.

Redlich, O., Kwong, J.N.S., 1949. On the thermodynamics of solutions. V. An equation of state. Fugacities of gaseous solutions. Chemical Review 44 (1), 233−244.

Riazi, M.R., 2005. Characterization and Properties of Petroleum Fractions. ASTM International, West Conshohocken, PA, USA.

Riazi, M.R., Daubert, T.E., 1987. Characterization parameters for petroleum fractions. Industrial and Engineering Chemistry Research 26 (4), 755−759.

Robinson, D.B., Peng, D.-Y., 1978. The Characterization of the Heptanes and Heavier Fractions for the GPA Peng−Robinson Programs. GPA Research Report-28. Gas Processors Association (GPA), Tulsa, OK, USA.

Sandler, S.I., 2017. Chemical, Biochemical and Engineering Thermodynamics, fifth ed. Wiley, Hoboken, NJ, USA.

Skylogianni, E., Novak, N., Louli, V., Pappa, G., Boukouvalas, C., Skouras, S., Solbraa, E., Voutsas, E., 2016. Measurement and prediction of dew points of six natural gases. Fluid Phase Equilibria 424, 8−15.

Smith, J.M., Van Ness, H.C., Abbott, M.M., 2005. Introduction to Chemical Engineering Thermodynamics, seventh ed. McGraw-Hill, Boston, MA, USA.

Soave, G., 1972. Equilibrium constants from a modified Redlich-Kwong equation of state. Chemical Engineering Science 27 (6), 1197−1203.

Soave, G., Gamba, S., Pellegrini, L.A., 2010. SRK equation of state: predicting binary interaction parameters of hydrocarbons and related compounds. Fluid Phase Equilibria 299 (2), 285−293.

Spencer, C.F., Danner, R.P., 1972. Improved equation for prediction of saturated liquid density. Journal of Chemical and Engineering Data 17 (2), 236−241.

Stryjek, R., 1990. Correlation and prediction of VLE data for n-alkane mixtures. Fluid Phase Equilibria 56, 141−152.

Stryjek, R., Vera, J.H., 1986. PRSV: an improved Peng-Robinson equation of state for pure compounds and mixtures. Canadian Journal of Chemical Engineering 64 (2), 323−333.

Sun, L., Zhao, H., McCabe, C., 2007. Predicting the phase equilibria of petroleum fluids with the SAFT-VR approach. AIChE Journal 53 (3), 720−731.

Ting, P.D., Joyce, P.C., Jog, P.K., Chapman, W.G., Thies, M.C., 2003a. Phase equilibrium modeling of mixtures of long-chain and short-chain alkanes using Peng−Robinson and SAFT. Fluid Phase Equilibria 206 (1−2), 267−286.

Ting, P.D., Joyce, P.C., Jog, P.K., Chapman, W.G., Thies, M.C., 2003b. Corrigendum to ["phase equilibrium modeling of mixtures of long-chain and short-chain alkanes using Peng−Robinson and SAFT". Fluid Phase Equilibria 206 (1-2), 267−286]. Fluid Phase Equilibria 209 (2), 309.

Ting, P.D., Gonzalez, D.L., Hirasaki, G.J., Chapman, W.G., 2010. "Application of the PC-SAFT equation of state to asphaltene phase behavior. In: Asphaltenes, Heavy Oils, and Petroleomics. Springer, New York, NY, USA.

Tsonopoulos, C., Heidman, J.L., 1986. High-pressure vapor-liquid equilibria with cubic equations of state. Fluid Phase Equilibria 29, 391−414.

Twu, C.H., Bluck, D., Cunningham, J.R., Coon, J.E., 1991. A cubic equation of state with a new alpha function and a new mixing rule. Fluid Phase Equilibria 69, 33−50.

Twu, C.H., Coon, J.E., Cunningham, J.R., 1995a. A new generalized alpha function for a cubic equation of state. Part 1: Peng-Robinson equation. Fluid Phase Equilibria 105 (1), 49−59.

Twu, C.H., Coon, J.E., Cunningham, J.R., 1995b. A new generalized alpha function for a cubic equation of state. Part 2: Redlich-Kwong equation. Fluid Phase Equilibria 105 (1), 61−69.

Valderrama, J.O., Ibrahim, A.A., Cisternas, L.A., 1990. Temperature-dependent interaction parameters in cubic equations of state for nitrogen-containing mixtures. Fluid Phase Equilibria 59 (2), 195−205.

Valderrama, J.O., Arce, P.F., Ibrahim, A.A., 1999. Vapour-liquid equilibrium of H_2S-Hydrocarbon mixtures using a generalized cubic equation of state. Canadian Journal of Chemical Engineering 77 (6), 1239−1243.

Van der Waals, J.D., 1873. On the Continuity of the Gaseous and Liquid States (Ph.D. thesis). Leiden University, Leiden, The Netherlands.

Van Konynenburg, P.H., Scott, R.L., 1980. Critical lines and phase equilibria in binary van der Waals mixtures. Philosophical Transactions of the Royal Society A: Mathematical, Physical and Engineering Sciences 298 (1442), 495−540.

Vargas, F.M., Gonzalez, D.L., Hirasaki, G.J., Chapman, W.G., 2009. Modeling asphaltene phase behavior in crude oil systems using the perturbed chain form of the statistical associating fluid theory (PC-SAFT) equation of state. Energy and Fuels 23 (3), 1140−1146.

Varzandeh, F., Stenby, E.H., Yan, W., 2017. General approach to characterizing reservoir fluids for EoS models using a large PVT database. Fluid Phase Equilibria 433, 97−111.

Vitu, S., Jaubert, J.-N., Mutelet, F., 2006. Extension of the PPR78 model (predictive 1978, Peng-Robinson EoS with temperature-dependent k_{ij} calculated through a group contribution method) to systems containing naphtenic compounds. Fluid Phase Equilibria 243 (1−2), 9−28.

Vitu, S., Privat, R., Jaubert, J.-N., Mutelet, F., 2008. Predicting the phase equilibria of CO_2 + hydrocarbon systems with the PPR78 model (PR EoS and k_{ij} calculated through a group contribution method). The Journal of Supercritical Fluids 45 (1), 1−26.

Voutsas, E., Magoulas, K., Tassios, D., 2004. Universal mixing rule for cubic equations of state applicable to symmetric and asymmetric systems: results with the Peng−Robinson equation of state. Industrial and Engineering Chemistry Research 43 (19), 6238−6246.

Wertheim, M.S., 1984a. Fluids with highly directional attractive forces. I. Statistical thermodynamics. Journal of Statistical Physics 35 (1−2), 19−34.

Wertheim, M.S., 1984b. Fluids with highly directional attractive forces. II. Thermodynamic perturbation theory and integral equations. Journal of Statistical Physics 35 (1−2), 35−47.

Wertheim, M.S., 1986a. Fluids of dimerizing hard spheres, and fluid mixtures of hard spheres and dispheres. The Journal of Chemical Physics 85 (5), 2929−2936.

Wertheim, M.S., 1986b. Fluids with highly directional attractive forces. Iii. Multiple attraction sites. Journal of Statistical Physics 42 (3−4), 459−476.

Wertheim, M.S., 1986c. Fluids with highly directional attractive forces. IV. Equilibrium polymerization. Journal of Statistical Physics 42 (3−4), 477−492.

Wong, D.S.H., Sandler, S.I., 1992. A theoretically correct mixing rule for cubic equations of state. AIChE Journal 38, 671−680.

Xu, X., Privat, R., Jaubert, J.-N., 2015a. Addition of the sulfur dioxide group (SO_2), the oxygen group (O_2) and the nitric oxide group (NO) to the e-PPR78 model. Industrial and Engineering Chemistry Research 54 (38), 9494−9504.

Xu, X., Jaubert, J.-N., Privat, R., Duchet-Suchaux, P., Braña-Mulero, F., 2015b. Predicting binary-interaction parameters of cubic equations of state for petroleum fluids containing pseudo-components. Industrial and Engineering Chemistry Research 54 (10), 2816−2824.

Xu, X., Lasala, S., Privat, R., Jaubert, J.-N., 2017a. E-PPR78: a proper cubic EoS for modelling fluids involved in the design and operation of carbon dioxide capture and storage (CCS) processes. International Journal of Greenhouse Gas Control 56, 126−154.

Xu, X., Jaubert, J.-N., Privat, R., Arpentinier, P., 2017b. Prediction of thermodynamic properties of alkyne-containing mixtures with the e-PPR78 model. Industrial and Engineering Chemistry Research 56 (28), 8143−8157.

Yan, W., Varzandeh, F., Stenby, E.H., 2015. PVT modeling of reservoir fluids using PC-SAFT EoS and Soave-BWR EoS. Fluid Phase Equilibria 386, 96−124.

Yelash, L., Müller, M., Paul, W., Binder, K., 2005a. A global investigation of phase equilibria using the perturbed-chain statistical-associating-fluid-theory approach. The Journal of Chemical Physics 123 (1), 014908.

Yelash, L., Müller, M., Paul, W., Binder, K., 2005b. Artificial multiple criticality and phase equilibria: an investigation of the PC-SAFT approach. Physical Chemistry Chemical Physics 7 (21), 3728−3732.

CHAPTER

RAW GAS TRANSMISSION 3

3.1 INTRODUCTION

Natural gas is often found in places where there is no local market, such as in the many offshore fields around the world. For natural gas to be available to the market, it must be gathered, processed, and transported. Quite often, collected natural gas (raw gas) must be transported over a substantial distance in pipelines of different sizes, due to a drive for reduced field processing facilities particularly for offshore fields. These pipelines vary in length between hundreds of feet and hundreds of miles, across an undulating terrain with varying temperature conditions. Liquid condensation in pipelines commonly occurs because of the multicomponent nature of the transmitted natural gas and its associated phase behavior to the inevitable temperature and pressure changes that occur along the pipeline. Condensation subjects the raw gas transmission pipeline to a multiphase, gas−condensate−water, flow transport.

The multiphase transportation technology has become increasingly important for developing marginal fields, where the trend is to economically transport unprocessed well fluids via existing infrastructures, maximizing the rate of return and minimizing both capital expenditure and operational expenditure. In fact, by transporting multiphase well fluid in a single pipeline, separate pipelines and receiving facilities for separate phases, costing both money and space, are eliminated which reduces the capital expenditure. On the other hand, phase separation and reinjection of water and gas save both capital expenditure and operational expenditure, by reducing the size of the fluid transport/handling facilities and the maintenance required for the pipeline operation. Given the savings that can be available to the operators using a multiphase technology, the market for multiphase flow transportation is an expanding one. Hence, it is necessary to predict multiphase flow behavior and other design variables of gas−condensate pipelines as accurately as possible so that pipelines and downstream processing plants may be designed optimally. This chapter covers all the important concepts of multiphase gas−condensate transmission from a fundamental perspective.

3.2 MULTIPHASE FLOW TERMINOLOGY

This section defines the variables commonly used to describe a multiphase flow. Definitions for these variables are described based on Fig. 3.1, which shows an ideal flow of three fluids. It is assumed that water is heavier than oil and flows at the bottom, while oil flows in the middle and the gas flows in the top layer.

Handbook of Natural Gas Transmission and Processing. https://doi.org/10.1016/B978-0-12-815817-3.00003-4

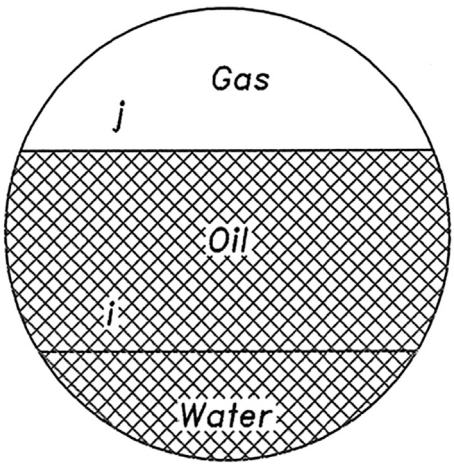

FIGURE 3.1

Three-phase flow pipe cross-section.

3.2.1 SUPERFICIAL VELOCITY

Superficial velocity is the velocity of one phase of a multiphase flow, assuming that the phase occupies the whole cross-section of the pipe by itself. It is defined for each phase as follows:

$$V_{SW} = \frac{Q_W}{A} \tag{3.1}$$

$$V_{SO} = \frac{Q_O}{A} \tag{3.2}$$

$$V_{SG} = \frac{Q_G}{A} \tag{3.3}$$

where

$$A = A_w + A_O + A_G \tag{3.4}$$

The parameter A is the total cross-sectional area of the pipe, Q is the volumetric flow rate, V is the velocity, and the subscript W denotes water, O denotes oil, G denotes gas, and S denotes a superficial term.

3.2.2 MIXTURE VELOCITY

The fluid mixture velocity is defined as the sum of the superficial velocities:

$$V_M = V_{SW} + V_{SO} + V_{SG} \tag{3.5}$$

where V_M is the multiphase mixture velocity.

3.2.3 HOLDUP

Holdup is the cross-sectional area, which is locally occupied by one of the phases of a multiphase flow, relative to the cross-sectional area of the pipe at the same local position.

For the liquid phase:

$$H_L = \frac{A_L}{A} = \frac{A_W + A_O}{A} = H_W + H_O \tag{3.6}$$

For the gas phase:

$$H_G = \frac{A_G}{A} \tag{3.7}$$

where the parameter H is the phase-holdup and the subscript L denotes the liquid and G denotes the gas phase.

Although "holdup" can be defined as the fraction of the pipe volume occupied by a given phase, holdup is usually defined as the in-situ liquid volume fraction, while the term "void fraction" is used for the in-situ gas volume fraction.

3.2.4 PHASE VELOCITY

Phase velocity (in-situ velocity) is the velocity of a phase of a multiphase flow based on the area of the pipe occupied by that phase. It may also be defined for each phase as follows:

$$V_L = \frac{V_{SL}}{H_L} = \frac{V_{SW} + V_{SO}}{H_L} \tag{3.8}$$

$$V_G = \frac{V_{SG}}{H_G} \tag{3.9}$$

3.2.5 SLIP

Slip is the term used to describe the flow condition that exists when the phases have different phase velocities. In most two-phase flow pipelines, gas travels faster than liquid. Under this condition, there is said to be slippage between the phases.

The slip velocity is defined as the difference between the actual gas and liquid velocities, as follows:

$$V_S = V_G - V_L \tag{3.10}$$

If there is no slip between the phases, $V_L = V_G$, and by applying the no-slip assumption to the liquid holdup definition, it can be shown that

$$H_{L,\,\text{no-slip}} = \lambda_L = \frac{V_{SL}}{V_M} \tag{3.11}$$

Investigators have observed that the no-slip assumption is not often applicable. For certain flow patterns in horizontal and upward inclined pipes, gas tends to flow faster than the liquid (positive slip). For some flow regimes in downward flow, liquid can flow faster than the gas (negative slip).

3.2.6 MIXTURE DENSITY

The equations for two-phase gas/liquid density used by various investigators are as follows:

$$\rho_S = \rho_L H_L + \rho_G H_G \tag{3.12}$$

$$\rho_{nS} = \rho_L \lambda_L + \rho_G \lambda_G \tag{3.13}$$

where the subscripts "S" and "nS" represent the slip and the no-slip conditions, respectively.

In these equations, the total liquid density can be determined from the oil and water densities and flow rates if no slippage between these liquid phases is assumed:

$$\rho_L = \rho_O f_O + \rho_W f_W \tag{3.14}$$

where

$$f_O = \frac{Q_O}{Q_O + Q_W} = 1 - f_W \tag{3.15}$$

where the parameter f is the volume fraction of each phase.

3.2.7 MIXTURE VISCOSITY

To determine the mixture viscosity, three approaches have been proposed (Brill and Beggs, 1991):

$$\mu_S = \mu_L H_L + \mu_G H_G \tag{3.16}$$

$$\mu_S = \mu_L^{H_L} \cdot \mu_G^{H_G} \tag{3.17}$$

$$\mu_{nS} = \mu_L \lambda_L + \mu_G \lambda_G \tag{3.18}$$

where μ_L and μ_G are the liquid and gas viscosities, respectively.

The liquid viscosity can be the viscosity of water, oil, or water–oil mixture. Normally, the water–oil mixture viscosity can be calculated as:

$$\mu_L = \mu_O f_O + \mu_W f_W \tag{3.19}$$

Studies have shown that Eq. (3.19) often is not valid for the viscosity of two immiscible liquids, such as oil and water. For some oil/water systems, the emulsion viscosity can be many times higher than the individual phase viscosities. Peak viscosities (over 30 times the oil phase value) typically occur near the inversion point where the emulsion reverts from a water-in-oil dispersion to an oil-in-water dispersion. The inversion point usually prevails at water cuts in the range 20%–50% (Arirachakaran, 1983).

Over the years, quite extensive research has been conducted to develop simplified correlations for the water–oil emulsion viscosity. But since there are so many parameters that affect the emulsion viscosity, none of these correlations can be universally applied to engineering calculations. Instead, the

best way to determine water−oil emulsion viscosity is to perform lab measurements of emulsions of different water cut at elevated pressure and temperature conditions.

3.2.8 MIXTURE PRESSURE DROP

The general pressure drop equation for a multiphase (two- and three-phase) flow is similar to that for a single-phase flow except for that some of the variables are replaced with equivalent variables which consider the effect of a multiphase. The general pressure drop equation for a multiphase flow is as follows (Brill and Beggs, 1991):

$$\left(\frac{dP}{dx}\right)_{tot} = \left(\frac{dP}{dx}\right)_{ele} + \left(\frac{dP}{dx}\right)_{fri} + \left(\frac{dP}{dx}\right)_{acc} \tag{3.20}$$

where

$$\left(\frac{dP}{dx}\right)_{ele} = \rho_{tp}\left(\frac{g}{g_c}\right)\sin\theta \tag{3.20.1}$$

$$\left(\frac{dP}{dx}\right)_{fri} = \frac{\rho_{tp} f_{tp} V_{tp}^2}{2 g_c D} \tag{3.20.2}$$

$$\left(\frac{dP}{dx}\right)_{acc} = \frac{\rho_{tp} f_{tp}}{g_c}\left(\frac{dV_{tp}}{dx}\right) \tag{3.20.3}$$

Where dP/dx is the flow pressure gradient, x is the pipe length, ρ is the flow density, V is the flow velocity, f is the friction coefficient of the flow, D is the internal diameter of pipeline, θ is the inclination angle of pipeline, g is the gravitational acceleration, and g_c is the gravitational constant. The subscript "tot" stands for total, "ele" for elevation, "fri" for friction loss, "acc" for acceleration change terms, and "tp" for two- and/or three-phase flow.

The pressure-drop component caused by acceleration is normally negligible and is considered only for cases of high flow velocities.

Many methods have been developed to predict multiphase flow pressure gradients. They differ in the manner used to calculate the three components of the total pressure gradient. Section 3.4 describes these methods.

3.2.9 MIXTURE ENTHALPY

When performing temperature-change calculations for a multiphase flow in pipelines, it is necessary to predict the enthalpy of the multiphase mixture. If enthalpies of the gas and liquid phases are expressed per unit mass, the enthalpy of a multiphase mixture can be calculated as:

$$h_M = H_L h_L + (1 - H_L) h_G \tag{3.21}$$

3.3 MULTIPHASE FLOW REGIMES

A multiphase flow is characterized by the existence of interfaces between the phases and discontinuities of associated properties. The flow structures are rather classified in "flow regimes" or "flow patterns," whose precise characteristics depend on a number of parameters. Flow regimes vary depending on operating conditions, fluid properties, flow rates, and the orientation and geometry of the pipe through which the fluids flow. The transition between different flow regimes may be a gradual process. Due to the highly nonlinear nature of the forces that rule the flow regime transitions, the prediction is near impossible. In the laboratory, the flow regime may be studied by direct visual observation using a length of transparent piping. However, the most utilized approach is to identify the actual flow regime from signal analysis of sensors whose fluctuations are related to the flow regime structure. This approach is generally based on average cross-sectional quantities, such as pressure drop or cross-sectional liquid holdup.

3.3.1 TWO-PHASE FLOW REGIMES

The description of a two-phase flow can be simplified by classifying types of "flow regimes" or "flow patterns." The distribution of the fluid phases in space and time differs for the various flow regimes and is usually not under the control of the pipeline designer or operator.

Dukler and Hubbard (1966) suggested three basic flow patterns: separated, intermittent, and distributed flow. In separated flow patterns, both phases are continuous and some droplets or bubbles of one phase in the other may or may not exist. In the intermittent flow patterns, at least one phase is discontinuous. In dispersed flow patterns, the liquid phase is continuous, while the gas phase is discontinuous.

Due to multitude of flow patterns and the various interpretations accorded to them by different investigators, the general state of knowledge on flow patterns is unsatisfactory and no uniform procedure exists at present for describing and classifying them. In this section, the basic flow patterns in a gas–liquid flow in horizontal, vertical, and inclined pipes are introduced.

3.3.1.1 Horizontal Flow Regimes

Two-phase, gas-liquid flow regimes for a horizontal flow are shown in Fig. 3.2. These horizontal flow regimes are defined as follows.

3.3.1.1.1 Dispersed Bubble Flow

At high liquid flow rates and for a wide range of gas flow rates, small gas bubbles are dispersed throughout a continuous liquid phase. Due to the effect of buoyancy these bubbles tend to accumulate in the upper part of the pipe.

3.3.1.1.2 Plug (Elongated Bubble) Flow

At relatively low gas flow rates, as the liquid flow rate is reduced, the smaller bubbles of dispersed bubble flow coalesce to form larger bullet shaped bubbles that move along the top of the pipe.

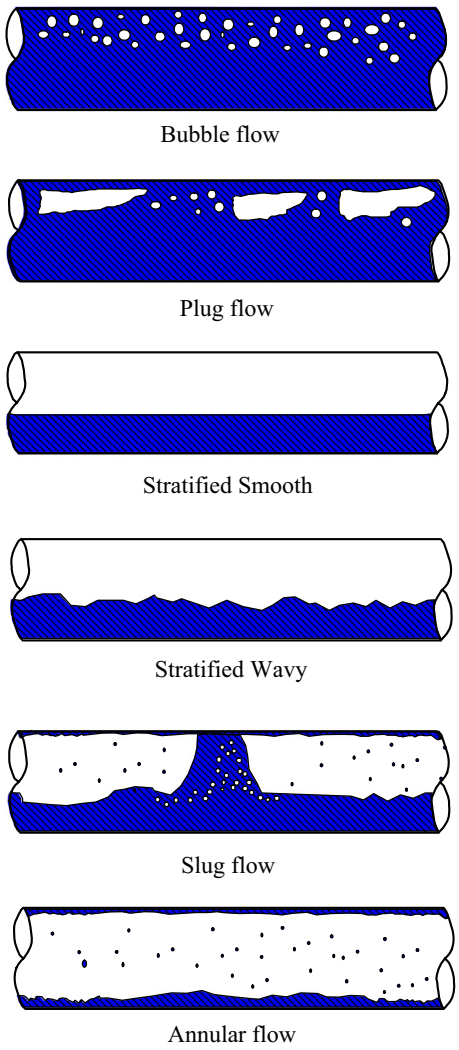

FIGURE 3.2

Horizontal two-phase, gas–liquid flow regimes.

3.3.1.1.3 Stratified (Smooth and Wavy) Flow

At low liquid and gas flow rates gravitational effects cause total separation of the two phases. This results in the liquid flowing along the bottom of the pipe and the gas flowing along the top, where the gas–liquid surface is smooth. As the gas velocity is increased in a stratified smooth flow the interfacial shear forces increase, rippling the liquid surface and producing a wavy interface.

3.3.1.1.4 Slug Flow

As the gas and liquid flow rates are increased further, the stratified liquid level grows and becomes progressively more wavy until eventually the whole cross-section of the pipe is blocked by a wave. The resultant "piston" of liquid is then accelerated by the gas flow, surging along the pipe and scooping up the liquid film in front as it progresses. This "piston" is followed by a region containing an elongated gas bubble moving over a thin liquid film. Hence an intermittent regime develops in which elongated gas bubbles and liquid slugs alternately surge along the pipe. The major difference between an elongated bubble flow and a slug flow is that in an elongated bubble flow there are no entrained gas bubbles in the liquid slugs.

3.3.1.1.5 Annular Flow

When gas flow rates increase, annular (also referred to as annular-mist) flow occurs. During annular flow, the liquid phase flows largely as an annular film on the wall with gas flowing as a central core. Some of the liquid is entrained as droplets in this gas core. The annular liquid film is thicker at the bottom than at the top of the pipe because of the effect of gravity and, except at very low liquid rates, the liquid film is covered with large waves.

3.3.1.2 Vertical Flow Regimes

Flow regimes frequently encountered in an upward vertical two-phase flow are shown in Fig. 3.3. These flow regimes tend to be somewhat more simpler than those in horizontal flow. This results from the symmetry in the flow induced by the gravitational force acting parallel to it. A brief description of the manner in which the fluids are distributed in the pipe for an upward vertical two-phase flow is as follows. It is worth noting that vertical flows are not so common in raw gas systems (i.e., wells normally have some deviation and many risers are also inclined to some extent).

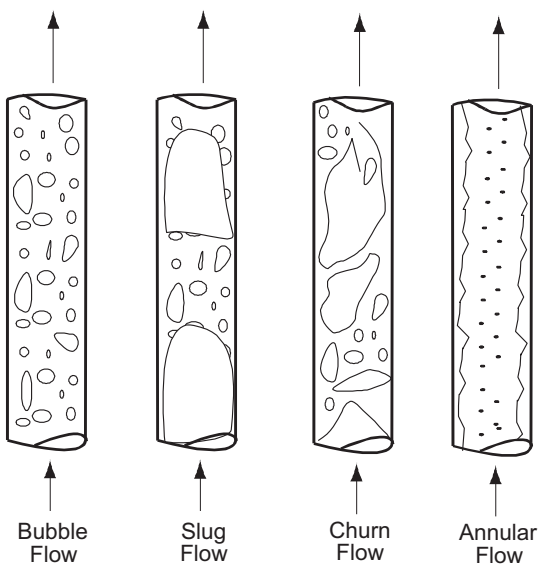

FIGURE 3.3

Upward vertical two-phase flow regimes.

3.3.1.2.1 Bubble Flow

At very low liquid and gas velocities, the liquid phase is continuous and the gas phase travels as dispersed bubbles. This flow regime is called a bubble flow. As the liquid flow rate increases, the bubbles may increase in size via coalescence.

Based on the presence or absence of slippage between the two phases, bubble flow is further classified into bubbly and dispersed bubble flows. In a bubbly flow, relatively fewer and larger bubbles move faster than the liquid phase because of slippage. In a dispersed bubble flow, numerous tiny bubbles are transported by the liquid phase, causing no relative motion between the two phases.

3.3.1.2.2 Slug Flow

As the gas velocity increases, the gas bubbles start coalescing, eventually forming large enough bubbles (Taylor bubbles) which occupy almost the entire cross-sectional area. This flow regime is called slug flow. Taylor bubbles move uniformly upward and are separated by slugs of continuous liquid that bridge the pipe and contain small gas bubbles. Typically, the liquid in the film around the Taylor bubbles may move downward at low velocities although the net flow of liquid can be upward. The gas bubble velocity is greater than that of the liquid.

3.3.1.2.3 Churn (Transition) Flow

If a change from a continuous liquid phase to a continuous gas-phase occurs, the continuity of the liquid in the slug between successive Taylor bubbles is repeatedly destroyed by a high local gas concentration in the slug. This oscillatory flow of the liquid is typical of churn (froth) flow. It may not occur in small diameter pipes. The gas bubbles may join and liquid may be entrained in the bubbles. In this flow regime, the falling film of the liquid surrounding the gas plugs cannot be observed.

3.3.1.2.4 Annular Flow

As the gas velocity increases even further, the transition occurs and the gas phase becomes a continuous phase in the pipe core. The liquid phase moves upward partly as a thin film (adhering to the pipe wall) and partly in the form of dispersed droplets in the gas core. This flow regime is called an annular flow or an annular mist flow.

Although a downward vertical two-phase flow is less common than an upward flow, it does occur in steam injection wells and down comer pipes from offshore production platforms. Hence a general vertical two-phase flow pattern is required that can be applied to all flow situations. Reliable models for downward multiphase flow are currently unavailable and the design codes are deficient in this area.

3.3.1.3 Inclined Flow Regimes

The effect of pipeline inclination on the gas−liquid two-phase flow regimes is of major interest in hilly terrain pipelines that consist almost entirely of uphill and downhill inclined sections. Pipe inclination angles have a very strong influence on flow pattern transitions. Generally, the flow regime in a near horizontal pipe remains segregated for downward inclinations and changes to intermittent flow regime for upward inclinations. An intermittent flow regime remains intermittent when tilted upward and tends to segregated flow pattern when inclined downward. The inclination should not significantly affect the distributed flow regime (Scott et al., 1987).

3.3.1.4 Flow Pattern Maps

In order to obtain optimal design parameters and operating conditions, it is necessary to clearly understand multiphase flow regimes and the boundaries between them, where the hydrodynamics of the flow as well as the flow mechanisms change significantly from one flow regime to another. If an undesirable flow regime is not anticipated in the design, the resulting flow pattern can cause system pressure fluctuation and system vibration, and even mechanical failures of piping components.

Most early attempts to predict the occurrence of the various flow patterns in pipes were based on conducting experimental tests in small-diameter pipes at low pressures with air and water. The results of experimental studies are presented as a flow pattern map. The respective pattern is represented as areas on a plot, the coordinates of which were the dimensional variables (i.e., superficial phase velocities) or dimensionless parameters containing these velocities. For horizontal flows, the classical flow-pattern map is that of Mandhane et al. (1974) as shown in Fig. 3.4. This particular map is based on air−water data at atmospheric pressure in 0.5−6.5 inch pipes.

Fig. 3.5 shows the flow pattern map developed by Aziz et al. (1972) for a vertical upward flow. Eqs. 3.22 and 3.23 define the coordinates.

$$N_x = V_{SG}\left(\frac{\rho_G}{0.0764}\right)^{1/3}\left[\left(\frac{72}{\sigma_L}\right)\left(\frac{\rho_L}{62.4}\right)\right]^{1/4} \tag{3.22}$$

$$N_y = V_{SL}\left[\left(\frac{72}{\sigma_L}\right)\left(\frac{\rho_L}{62.4}\right)\right]^{1/4} \tag{3.23}$$

The bracketed terms in the above equations are attempts to validate the flow pattern map for fluids other than air and water.

Eqs. 3.24−3.26 represent the flow-pattern transitions in Fig. 3.5.

$$N_1 = 0.51(100N_y)^{0.172} \tag{3.24}$$

$$N_2 = 8.6 + 3.8N_y \tag{3.25}$$

$$N_3 = 70(100N_y)^{-0.152} \tag{3.26}$$

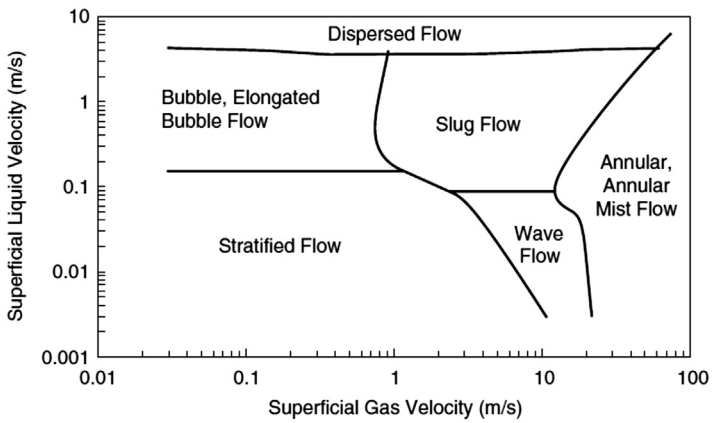

FIGURE 3.4

Mandhane et al. (1974) flow regime map for a horizontal flow.

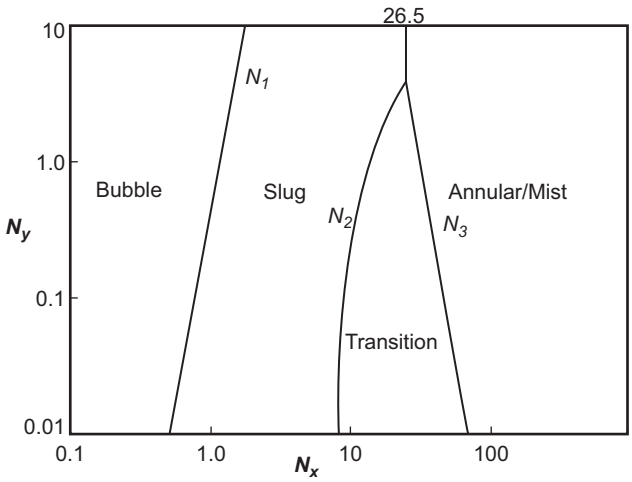

FIGURE 3.5

Aziz et al. (1972) flow pattern map for a vertical upward flow.

where superficial velocities are in feet per second, liquid and gas densities are in pounds per cubic feet, and liquid surface tension[1] (σL) is in dynes per centimeter.

Empirically based flow maps are not particularly accurate for systems where the fluid properties, pipe size, and inclination are different from those for which the flow map was originally produced. In addition, in these flow maps a change in flow rate can lead to a change of flow pattern between the old and new steady states. However, an interesting and important effect that frequently occurs is the existence of temporary flow pattern changes between the respective steady states (Shaha, 1999). A more flexible method, which overcomes this difficulty, is to examine each transition individually and derive a criterion valid for that particular transition. There have been some attempts to evaluate the basic mechanisms of flow pattern transitions and thus to provide a mechanistic flow pattern map for estimating their occurrence (Taitel and Dukler, 1976; Barnea, 1987; Taitel et al., 1980; Petalas and Aziz, 2000). In these transition models, the effects of system parameters are incorporated; hence they can be applied over a range of conditions. However, most of them are somewhat complex and they do require the use of a predetermined sequence to determine the dominant flow pattern.

3.3.2 THREE-PHASE FLOW REGIMES

The main difference between two-phase (gas/liquid) flows and three-phase (gas/liquid/liquid) flows is the behavior of the liquid phases, in three-phase systems the presence of two liquids gives rise to a rich variety of flow patterns (Hall, 1997). Basically, depending on the local conditions, the liquid phases appear in a separated or dispersed form (Brauner and Maron, 1992). In the case of a separated flow, distinct layers of oil and water can be discerned, though there may be some interentrainment of one

[1]Assuming no slippage, the liquid surface tension is calculated from $\sigma_L = \sigma_O f_O + \sigma_W f_W$.

liquid phase into the other. In a dispersed flow, one liquid phase is completely dispersed as droplets in the other, resulting in two possible situations, namely an oil continuous phase and a water continuous phase (Chen and Guo, 1999). The transition from one liquid continuous phase to the other is known as phase inversion. If the liquid phases are interdispersed, then prediction of phase inversion is an important item. For this purpose, Decarre and Fabre (1997) developed a phase inversion model that can be used to determine which of two liquids is continuous.

Due to the many possible transport properties of three-phase fluid mixtures, the quantification of three-phase flow pattern boundaries is a difficult and challenging task. Acikgoz et al. (1992) observed a very complex array of flow patterns and described ten different flow regimes. In their work, the pipe diameter was only 0.748 inch and stratification was seldom achieved. In contrast, the Lee et al. (1993) experiments were carried out in a 4-inch diameter pipe. They observed and classified seven flow patterns, which were similar to those of two-phase flows, (1) smooth stratified, (2) wavy stratified, (3) rolling wave, (4) plug flow, (5) slug flow, (6) pseudo slug, and (7) annular flow. The first three flow patterns can be classified as stratified flow regime and they noted that oil and water are generally segregated, with water flowing as a liquid layer at the bottom of the pipe and oil flowing on top. Even for a plug flow, the water remained at the bottom, because the agitation of the liquids was not sufficient to mix the oil and water phases. Note, turbulence, which naturally exists in a pipeline, can be sufficient to provide adequate mixing of the water and oil phase. However, the minimum natural turbulent energy for adequate mixing depends on the oil and water flow rates, pipe diameter and inclination, water concentration, viscosity, density, and interfacial tension. Dahl et al. (2001) provided more detailed information on the prediction methods that can be used to determine whether a water-in-oil mixture in the pipe is homogeneous or not.

3.3.3 GAS–CONDENSATE FLOW REGIMES

A gas–condensate flow is a multiphase flow phenomenon commonly encountered in raw gas transportation. However, the multiphase flow that takes place in gas–condensate transmission lines differs in certain respects from the general multiphase flow in pipelines. In fact, in gas–condensate flow systems, there is always interphase mass transfer from the gas phase to the liquid phase because of the temperature and pressure variations. This leads to compositional changes and associated fluid property changes (Ayala and Adewumi, 2003). In addition to that, the amount of liquid in such systems is assumed to be small, and the gas flow rate gives a sufficiently high Reynolds number that the fluid flow regime for a nearly horizontal pipe can be expected to be annular-mist flow and/or stratified flow (Asante, 2002). For other inclined cases, even with small quantities of liquids, slug-type regimes may be developed if liquids start accumulating at the pipe lower section.

In water/wet gas–condensate systems it can normally be assumed that the condensate and water phases are well mixed. However, when the water loading is a substantial proportion of the total liquid loading, the water and condensate can separate out at low flow rates leading to the accumulation of stagnant water at low points in the line. The presence of stagnant water can lead to the production of water slugs during normal line operation or flow rate changes.

3.4 DETERMINING MULTIPHASE FLOW DESIGN PARAMETERS

The hydraulic design of a multiphase flow pipeline is a two-step process. The first step is the determination of the multiphase flow regimes, because many pressure drop calculation methods rely on the

type of flow regime present in the pipe. The second step is the calculation of flow parameters, such as pressure drop and liquid holdup, to size pipelines and field processing equipment such as slug catchers.

The analysis of multiphase flow phenomena in pipeline systems is usually classified into steady-state and transient approaches. In steady-state flow, there are no major changes transgressing the pipeline network. In transient or dynamic flows, the flow behavior is changing on a regular and significant basis. Both steady-state and transient analyses shall be performed to study the pipeline system performance under different operating conditions. In preliminary engineering, a design engineer often uses steady-state analysis. However, the dynamic response of the system to startup, shutdown, and flow rate changes must also be considered. For example, liquid slugs are often produced during flow rate increase or line depressurization. The volume of these transient slugs must be determined to ensure that they can be handled by the downstream separation and processing facilities. If there is insufficient capacity, operating procedures can be introduced to limit the rate of change of flow rate and therefore the size of any produced slugs.

3.4.1 STEADY-STATE TWO-PHASE FLOW

The techniques most commonly used in the design of two-phase flow pipeline can be classified into three categories: the single-phase flow approaches, the homogeneous flow approaches, and the mechanistic models. Within each of these groups are subcategories that are based on the general characteristics of the models used to perform design calculations.

3.4.1.1 Single-Phase Flow Approaches

In this method, the two-phase flow is assumed to be a single-phase flow having pseudo-properties arrived at by suitably weighing the properties of the individual phases. These approaches basically rely solely on the well-established design equations for single-phase gas flow in pipes. A two-phase flow is treated as a simple extension by use of a multiplier; a safety factor to account for the higher-pressure drop generally encountered in a two-phase flow. This heuristic approach was widely used and generally resulted in inaccurate pipeline design (Schweikert, 1986).

In the past, single-phase flow approaches were commonly used for the design of wet-gas pipelines. When the amount of the condensed liquid is negligibly small, the use of such methods could at best prevent under design, but more often than not, the quantity of the condensed liquid is significant enough that the single-phase flow approach grossly over predicts the pressure drop. Hence, this method is not covered in depth here but can be reviewed elsewhere (Uhl, 1965).

3.4.1.2 Homogeneous Flow Approaches

The inadequacy of the single-phase flow approaches spurred researchers to develop better design procedures and predictive models for two-phase flow systems. This effort led to the development of homogeneous flow approaches to describe these rather complex flows. The homogenous approach, also known as the friction factor model, is similar to that of the single-phase flow approach except that mixture fluid properties are used in the determination of the friction factor. Therefore, the appropriate definitions of the fluid properties are critical to the accuracy of the model. The mixture properties are expressed empirically as a function of the gas and liquid properties as well as their respective holdups. Many of these correlations are based on flow regime correlations that determine the two-phase (gas/liquid) flow friction factor, which is then used to estimate pressure drop. While some of the

correlations predict pressure-drop reasonably well, their range of applicability is generally limited, making their use as a scale up tool marginal. This limitation is understandable because the database used in developing these correlations is usually limited and based on laboratory-scale experiments. Extrapolation of these data sets to larger lines and hydrocarbon systems is questionable at best (Cindric et al., 1987).

Historically, empirical correlations have been successful in terms of being relatively easy to employ as design tools. Brill and Beggs (1991) and Collier and Thome (1996) provide in-depth comparative analyses of the available correlations. However, two of the better known, more widely applicable correlations are outlined here.

3.4.1.2.1 Lockhart and Martinelli Method

The method was developed by correlating experimental data generated in horizontal isothermal two-phase flow of two-component systems (air−oil and air−water) at low pressures (close to atmospheric) in a 1-inch diameter pipe. Lockhart and Martinelli (1949) separated the data into four sets dependent on whether the phases flowed in a laminar or turbulent flow, if the phases were flowing alone in the same pipe. In this method, a definite portion of the flow area is assigned to each phase and it is assumed that the single-phase pressure drop equations can be used independently for each phase. The two-phase frictional pressure drop is calculated by multiplying by a correction factor for each phase, as follows:

$$\frac{dP}{dx} = \varphi_G^2 \left(\frac{dP}{dx}\right)_G = \varphi_L^2 \left(\frac{dP}{dx}\right)_L \tag{3.27}$$

where

$$\left(\frac{dP}{dx}\right)_G = \left(\frac{f_G \rho_G V_{SG}^2}{2\, g_C D}\right) \tag{3.27.1}$$

$$\left(\frac{dP}{dx}\right)_L = \left(\frac{f_L \rho_L V_{SL}^2}{2\, g_C D}\right) \tag{3.27.2}$$

The friction factors f_G and f_L are determined from Moody (1944) diagram using the following values of the Reynolds number:

$$N_{Re,G} = \frac{\rho_G V_{SG} D}{\mu_G} \tag{3.28}$$

$$N_{Re,L} = \frac{\rho_L V_{SL} D}{\mu_L} \tag{3.29}$$

The two-phase flow correction factors (φ_G and φ_L) are determined from Eqs. 3.30 and 3.31 (Lockhart and Martinelli, 1949; Chisholm and Sutherland, 1969):

$$\varphi_G^2 = 1 + CX + CX^2 \tag{3.30}$$

$$\varphi_L^2 = 1 + \frac{C}{X} + \frac{1}{X^2} \tag{3.31}$$

where

$$X = \left[\frac{\left(\frac{dP}{dx}\right)_L}{\left(\frac{dP}{dx}\right)_G}\right]^{0.5} \tag{3.32}$$

where parameter C is given in Table 3.1.

Note, the laminar flow regime for a phase occurs when the Reynolds number for that phase is less than 1000.

In this method, the correlation between liquid holdup and Martinelli parameter, X, is independent of the flow regime and can be expressed as follows (Collier and Thome, 1996):

$$H_L^{-2} = 1 + \frac{20}{X} + \frac{1}{X^2} \tag{3.33}$$

The fluid acceleration pressure drop was ignored in this method. Although different modifications of this method have been proposed, the original method is believed to be generally the most reliable (Collier and Thome, 1996).

3.4.1.2.2 Beggs and Brill Method

This method was developed from 584 experimental data sets generated on a laboratory scale test facility using an air–water system. The facility consisted of 90 ft of 1 or 1.5 inch diameter acrylic (smooth) pipe, which could be inclined at any angle (Beggs and Brill, 1973). The pipe angle was varied between horizontal to vertical and the liquid holdup and the pressure were measured. For each pipe size in the horizontal position, flow rates of two phases were varied to achieve all flow regimes. Beggs and Brill (1973) developed correlations for the liquid holdup for each of three horizontal flow regimes and then corrected these for the pipe inclination/angle.

The following parameters are used for determination of all horizontal flow regimes (Brill and Beggs, 1991):

$$N_{Fr} = \frac{V_M^2}{gD} \tag{3.34}$$

$$L_1 = 316\lambda_L{}^{0.302} \tag{3.35}$$

$$L_2 = 0.0009252\lambda_L{}^{-2.4684} \tag{3.36}$$

$$L_3 = 0.10\lambda_L{}^{-1.4516} \tag{3.37}$$

Table 3.1 "C" Parameter

Liquid Phase	Gas Phase	C
Turbulent	Turbulent	20
Laminar	Turbulent	12
Turbulent	Laminar	10
Laminar	Laminar	5

$$L_4 = 0.5\lambda_L{}^{-6.738} \tag{3.38}$$

And the flow regime limits are:
segregated,

$$N_{Fr} < L_1 \text{ for } \lambda_L < 0.01$$
$$N_{Fr} < L_2 \text{ for } \lambda_L \geq 0.01$$

transition,

$$L_2 \leq N_{Fr} \leq L_3 \text{ for } \lambda_L \geq 0.01$$

intermittent, and

$$L_3 \leq N_{Fr} \leq L_1 \text{ for } 0.01 < \lambda_L \leq 0.4$$
$$L_3 < N_{Fr} \leq L_4 \text{ for } \lambda_L \geq 0.4$$

distributed

$$N_{Fr} \geq L_1 \text{ for } \lambda_L < 0.4$$
$$N_{Fr} > L_4 \text{ for } \lambda_L \geq 0.4$$

Also, the horizontal liquid holdup, $H_L(0)$, is calculated using the following equation:

$$H_L(0) = \frac{a\,\lambda_L^b}{N_{Fr}^c} \tag{3.39}$$

where parameters a, b, and c are determined for each flow regime and are given in Table 3.2.

With the constraint that $H_L(0) \geq \lambda_L$

When the flow is in the transition region, the liquid holdup is calculated by interpolating between the segregated and intermittent flow regimes as follows:

$$H_L(0)_{transition} = A\,H_L(0)_{segregated} + (1 - A)H_L(0)_{intermittent} \tag{3.40}$$

where

$$A = (L_3 - N_{Fr})/(L_3 - L_2) \tag{3.41}$$

The amount of liquid holdup in an inclined pipe, $H_L(\theta)$, is determined by multiplying an inclination factor (ψ) by the calculated liquid holdup for the horizontal conditions:

$$H_L(\theta) = H_L(0) \times \psi \tag{3.42}$$

Table 3.2 a, b, c Parameters

Flow Regime	a	b	c
Segregated	0.98	0.4846	0.0868
Intermittent	0.845	0.5351	0.0173
Distributed	1.065	0.5824	0.0609

where

$$\psi = 1 + \alpha\left[\sin(1.8\theta) - 0.333\,\sin^3(1.8\theta)\right] \tag{3.42.1}$$

where θ is the pipe angle and α is calculated as follows:

$$\alpha = (1 - \lambda_L)\,\ln\left[d\,\lambda_L^e\,N_{LV}^f N_{Fr}^g\right] \tag{3.42.2}$$

where

$$N_{LV} = V_{SL}\left(\frac{\rho_L}{g\sigma}\right)^{0.25} \tag{3.42.3}$$

The equation parameters are determined from each flow regime using the numbers from Table 3.3. The two-phase pressure gradient due to pipeline elevation can be determined as follows:

$$\left(\frac{dP}{dx}\right)_{ele} = \frac{g}{g_C}\{\rho_L\,H_L(\theta) + \rho_G[1 - H_L(\theta)]\} \tag{3.43}$$

Also, the two-phase frictional pressure drop is calculated as follows:

$$\left(\frac{dP}{dx}\right)_{fri} = \frac{f_{tp}\,\rho_n\,V_M^2}{2\,g_c\,D} \tag{3.44}$$

where

$$f_{tp} = f_n\exp(\beta) \tag{3.44.1}$$

where f_n is the no slip friction factor determined from the smooth pipe curve of the Moody diagram using no slip viscosity and the density in calculating the two-phase flow Reynolds number. In other words:

$$f_n = \frac{1}{\left[2\log\left(\frac{N_{Re,n}}{4.5223\log N_{Re,n} - 3.8215}\right)\right]^2} \tag{3.44.1.1}$$

where

$$N_{Re,n} = \frac{\rho_n V_M D}{\mu_n} = \frac{[(\rho_L\lambda_L + \rho_G(1 - \lambda_L))V_M D]}{[\mu_L\lambda_L + \mu_G(1 - \lambda_L)]} \tag{3.44.1.2}$$

Table 3.3 d, e, f, and g Parameters

Flow Regime	d	e	f	g
Segregated uphill	0.011	−3.768	3.539	−1.614
Intermittent uphill	2.96	0.305	−0.4473	0.0978
Distributed uphill	$\alpha = 0, \psi = 1$			
All flow regimes downhill	4.7	−0.3692	0.1244	−0.5056

The exponent β is given by Eqs. 3.44.2:

$$\beta = [\ln Y] \Big/ \left\{ -0.0523 + 3.182\ln Y - 0.8725(\ln Y)^2 + 0.01853(\ln Y)^4 \right\} \tag{3.44.2}$$

where

$$Y = \frac{\lambda_L}{[H_L(\theta)]^2} \tag{3.44.3}$$

The pressure drop due to acceleration is only significant in gas transmission pipelines at high gas flow rates. However, it can be included for completeness as follows:

$$\left(\frac{dP}{dx}\right)_{acc} = \left[\frac{\rho_S V_M V_{SG}}{g_c P}\right]\left(\frac{dP}{dx}\right)_{tot} \tag{3.45}$$

The Beggs and Brill (1973) method can be used for horizontal and vertical pipelines, although its wide acceptance is mainly due to its usefulness for inclined pipe pressure drop calculation (Brill and Beggs, 1991). However, the proposed approach has limited applications dictated by the database on which the correlations are derived.

Note, the Beggs and Brill (1973) correlation is not usually employed for the design of wet gas pipelines. Specifically the holdup characteristic (holdup vs. flow rate) is not well predicted by this method. This makes design difficult because one is unable to reliably quantify the retention of liquid in the line during turndown conditions.

3.4.1.3 Mechanistic Models

While it is indeed remarkable that some of the present correlations can adequately handle a non-condensing two-phase flow, they give erroneous results for a gas–condensate flow in large diameter lines at high pressures (Battara et al., 1985). This shortcoming of existing methods has led to the development of mechanistic models that are based on fundamental laws and thus can offer more accurate modeling of the pipe geometric and fluid property variations. All of these models firstly predict stable flow pattern under the specified conditions and then use the momentum balance equations to calculate liquid holdup, pressure drop, and other two-phase flow parameters with a greater degree of confidence than that possible by purely empirical correlations (Collier and Thome, 1996; Holt et al., 1999). The mechanistic models presented in the literature are either incomplete in that they only consider flow pattern determination, or are limited in their applicability to only some pipe inclinations or small-diameter, low-pressure two-phase flow lines (Taitel and Dukler, 1976; Barnea, 1987; Xiao et al., 1990; Ansari et al., 1994; Taitel et al., 1995; Wilkens, 1997). However, new mechanistic models presented by Petalas and Aziz (2000) and Zhang et al. (2003) have proven to be more robust than previous models, although further investigations and testing of these models are needed with high quality field and laboratory data in larger diameter, high-pressure systems. Readers are referred to the original references for a detailed treatment of these models.

3.4.2 STEADY-STATE THREE-PHASE FLOW

Compared to numerous investigations on two-phase flows in the literature, there are only limited works on three-phase flows of gas–liquid–liquid mixtures. In fact, the complex nature of such flows makes

prediction very difficult. In an early study, Tek (1961) treated the two immiscible liquid phases as a single fluid with mixture properties, thus a two-phase flow correlation could be used for pressure loss calculations. On the other hand, studies by Pan (1996) have shown that the classical two-phase flow correlations for gas–liquid two-phase flows can be used as the basis in the determination of three-phase flow parameters; however, the generality of such empirical approaches is obviously questionable. Hence, an appropriate model is required to describe the flow of one gas and two liquid phases. One of the most fundamental approaches used to model such systems is the two-fluid model, where the presented approach can be used by combining the two liquid phases as one pseudo-liquid phase and modeling the three-phase flow as a two-phase flow. However, for more accurate results, three-fluid models should be used to account for the effect of liquid–liquid interactions on flow characteristics, especially at low flow rates. Several three fluid models were found in the literature. All of these models are developed from the three-phase momentum equations with few changes from one model to the other. The most obvious model has been developed by Barnea and Taitel (1996), however, such a model introduces much additional complexity and demands much more in computer resources compared with the two-fluid model for a two-phase flow (Bonizzi and Issa, 2003).

3.4.3 TRANSIENT MULTIPHASE FLOW

Steady state operation is the exception rather than the rule in multiphase systems due to a number of factors such as the nature of the flow regimes, interactions with the pipeline profile, and changes in supply or demand. As a result, detailed information of the transient flow behavior is necessary for the designer and the operator of the system to construct and operate the pipeline economically and safely.

A transient multiphase flow is traditionally modeled by one-dimensional averaged conservation laws, yielding a set of partial differential equations. In this section, two models of particular industrial interest are described:

- the two-fluid model (TFM), consisting of a separate momentum equation for each phase, and
- the drift flux model (DFM), consisting of a momentum equation and an algebraic slip relation for the phase velocities.

The two-fluid model is structurally simpler, but involves an extradifferential equation when compared to the drift flux model. They do yield somewhat different transient results, though the differences are often small (Masella et al., 1998).

The following major assumptions have been made in the formulation of the differential equations:

1. Two immiscible liquid phases (oil and water) that are assumed to be a single fluid with mixture properties.
2. Flow is one-dimensional in the axial direction of the pipeline.
3. Flow temperature is constant at wall and no mass transfer occurs between the gas and liquid phase. Note, most commercial codes allow phase change.
4. The physical properties of a multiphase flow are determined at the average temperature and pressure of flow in each segment of the pipeline.

3.4.3.1 Two Fluid Model

The two-fluid model (TFM) is governed by a set of four partial differential equations, the first two of which express mass conservation for gas and liquid phases, respectively:

$$\frac{\partial}{\partial t}[\rho_G H_G] + \frac{\partial}{\partial x}[\rho_G H_G V_G] = 0 \tag{3.46}$$

$$\frac{\partial}{\partial t}[\rho_L H_L] + \frac{\partial}{\partial x}[\rho_L H_L V_L] = 0 \tag{3.47}$$

And the last two equations represent momentum balance for the gas and liquid phases, respectively:

$$\frac{\partial}{\partial t}[\rho_G H_G V_G] + \frac{\partial}{\partial x}\left[\rho_G H_G V_G^2 + H_G \Delta P_G\right] + H_G \frac{\partial P}{\partial x} = \tau_G + \tau_i - \rho_G g \sin\theta \tag{3.48}$$

$$\frac{\partial}{\partial t}[\rho_L H_L V_L] + \frac{\partial}{\partial x}\left[\rho_L H_L V_L^2 + H_L \Delta P_L\right] + H_L \frac{\partial P}{\partial x} = \tau_L - \tau_i - \rho_L g \sin\theta \tag{3.49}$$

In Eqs. 3.48 and 3.49, parameter P denotes the interface pressure, while V_k, ρ_k, and H_k are the velocity, density, and volume fraction of phase $k \in \{G, L\}$, respectively. The variables τ_i and τ_k are the interfacial and wall momentum transfer terms. The quantities ΔP_G and ΔP_L correspond to the static head around the interface (De Henau and Raithby, 1995), defined as follows:

$$\Delta P_G = P_G - P = -\rho_G \left[\frac{1}{2}\cos\left(\frac{\omega}{2}\right) + \frac{1}{3\pi H_G}\sin^3\left(\frac{\omega}{2}\right)\right] gD\cos\theta \tag{3.50}$$

$$\Delta P_L = P_L - P = -\rho_L \left[\frac{1}{2}\cos\left(\frac{\omega}{2}\right) + \frac{1}{3\pi H_L}\sin^3\left(\frac{\omega}{2}\right)\right] gD\cos\theta \tag{3.51}$$

where ω is the wetted angle.

The detailed description of the solution algorithm for the above equations is based on a finite volume method (Masella et al., 1998).

One major limitation of this type of model is the treatment of the interfacial coupling. Whilst this is relatively easy for separated flows (stratified and annular), this treatment is intrinsically flawed for intermittent flows.

3.4.3.2 Drift Flux Model

The drift flux model (DFM) is derived from the two-fluid model by neglecting the static head terms ΔP_G and ΔP_L in Eqs. 3.48 and 3.49 and replacing the two momentum equations by their sum. This leads to a new model that consists of three partial differential equations, i.e., Eqs. 3.46, 3.47, and 3.52.

$$\frac{\partial}{\partial t}[\rho_G H_G V_G + \rho_L H_L V_L] + \frac{\partial}{\partial x}\left[\rho_G H_G V_G^2 + \rho_L H_L V_L^2 + P\right] = \tau_G + \tau_L - (\rho_G H_G + \rho_L H_L)\sin\theta \tag{3.52}$$

The detailed description of the numerical solution for the relevant equations can be found in Faille and Heintze (1999).

The main advantages of this three-equation model are as follows:

- The equations are in conservative form, which makes their solution by the finite volume methods less onerous.
- The interfacial shear term, τ_i, is cancelled out in the momentum equations, although it appears in an additional algebraic relation called the slip law.
- The model is well-posed and does not exhibit complex characteristic.

Note, the drift flux approach is best applied to closely coupled flows such as bubbly flow. Its application to stratified flows is, at best, artificial (Banerjee, 1986).

3.4.4 MULTIPHASE GAS AND CONDENSATE FLOW

In order to achieve an optimal design of gas–condensate pipelines and downstream processing facilities, one needs a description of the relative amount of condensate and the flow regime-taking place along the pipelines, where fluid flowing in pipelines may traverse the fluid phase envelope such that the fluid phase changes from single-phase to two-phase or vice versa. Hence, compositional single-phase/multiphase hydrodynamic modeling, which couples the hydrodynamic model with the natural gas phase behavior model, is necessary to predict fluid dynamic behavior in gas–condensate transmission lines. The hydrodynamic model is required to obtain flow parameters along the pipeline, and the phase behavior model is required for determining the phase condition at any point in the pipe, the mass transfer between the flowing phases, and the fluid properties.

Despite the importance of gas flow with low liquid loading for the operation of gas pipelines, few attempts have been made to study flow parameters in gas–condensate transmission lines. While, the single-phase flow approaches have been previously applied to gas–condensate systems, only a few attempts have been reported for the use of two-fluid model for this purpose. Some of them have attempted to make basic assumptions (e.g., no mass transfer between gas and liquid phases, etc.) in their formulation and others simply assume one flow regime for the entire pipe length. However, a compositional hydrodynamic model that describes the steady-state behavior of multiphase flow in gas–condensate pipelines has been presented by Ayala and Adewumi (2003). The model couples a phase behavior model, based on the Peng and Robinson (1976) equation of state, and a hydrodynamic model, based on the two-fluid model. The proposed model is a numerical approach, which can be used as an appropriate tool for engineering design of multiphase pipelines transporting gas and condensate. However, the complexity of this model precludes further discussion here.

Note, the presence of liquid (condensates), besides reducing deliverability, creates several operational problems in gas–condensate transmission lines. Periodic removal of the liquid from the pipeline is thus desirable. To remove liquid accumulation in the lower portions of pipeline, pigging operations are performed. These operations keep the pipeline free of liquid reducing the overall pressure drop and by the same increase the pipeline flow efficiency. However, the pigging process associates with transient flow behavior in the pipeline. Thus, it is imperative to have a means of predicting transient behavior encountered in multiphase, gas/gas–condensate pipelines. Until recently, most available commercial codes are based on the two-fluid model. However, the model needs many modifications to be suitable for simulating multiphase transient flow in gas/gas–condensate transmission lines. For example, the liquid and gas continuity equations need to be modified to account for the mass transfer between phases. So far, several codes have been reported for this purpose, where three main

commercial transient codes are OLGA (Bendiksen et al., 1991), PROFES (Black et al., 1990), and TACITE (Pauchon et al., 1993). Detailed discussion of these codes is beyond the scope of this book, readers are referred to the original papers for further information.

3.5 PREDICTING TEMPERATURE PROFILE OF A MULTIPHASE PIPELINE

Predicting the flow temperature and pressure changes has become increasingly important for use in both the design and operation of flow transmission pipelines. It is therefore imperative to develop appropriate methods capable of predicting these parameters for multiphase pipelines. A simplified flow chart of a suitable computing algorithm is shown in Fig. 3.6. This algorithm calculates pressure and temperature along the pipeline by iteratively converging on pressure and temperature for each sequential "segment" of the pipeline. The algorithm converges on temperature in the outer loop and pressure in the inner loop because robustness and computational speed are obtained when converging on the least sensitive variable first (Brill and Beggs, 1991).

The pipeline segment length should be chosen such that the fluid properties do not change significantly in the segment. More segments are recommended for accurate calculations for a system where fluid properties can change drastically over short distances. Often, best results are obtained when separate segments (with the maximum segment length less than about 10% of the total line length) are used for up, down, and horizontal segments of the pipeline (Brill and Beggs, 1991).

Prediction of the pipeline temperature profile can be accomplished by coupling the pressure gradient and enthalpy gradient equations as follows (Brill and Beggs, 1991):

$$\Delta h = \frac{-V_M V_{SG} \Delta P}{(778)(32.17)(\overline{P})} + \frac{\Delta Z}{778} - \frac{U\pi D(\overline{T} - T_a)\Delta L}{3600\left(\dot{M}_M\right)} \tag{3.53}$$

where Δh is the enthalpy change in the calculation segment, Btu/lb$_m$; V_M is the velocity of the fluid, ft/sec; V_{SG} is the superficial gas velocity, ft/sec; ΔP is the estimated change in pressure, psi; $\overline{P}$ is the average pressure in the calculation segment, psia; ΔZ is the change in elevation, ft; U is the overall heat transfer coefficient, Btu/hr-ft^2-°F; D is the reference diameter on which U is based, ft; $\overline{T}$ is the estimated average temperature in the calculation segment, °F; T_a is the ambient temperature, °F; ΔL is the change in segment length, ft; and M_M is the gas–liquid mixture mass flow rate, lb$_m$/s.

As can be seen from Eq. (3.53), temperature and pressure are mutually dependent variables so that generating a very precise temperature profile requires numerous iterative calculations. The temperature and pressure of each pipe segment are calculated using a double-nested procedure in which for every downstream pressure iteration, convergence is obtained for the downstream temperature by property values evaluated at the average temperature and pressure of that section of pipe. Experience shows that it is essential to use a good pressure-drop model to assess the predominant parameter, i.e., pressure.

The overall heat transfer coefficient (U) can be determined by combination of several coefficients, which depend on the method of heat transfer and pipe configuration. Fig. 3.7 is a cross-section of a pipe, including each "layer" through which heat must pass to be transferred from the fluid to the surroundings or vice-versa. This series of layers has an overall resistance to heat transfer made up of the resistance of each layer.

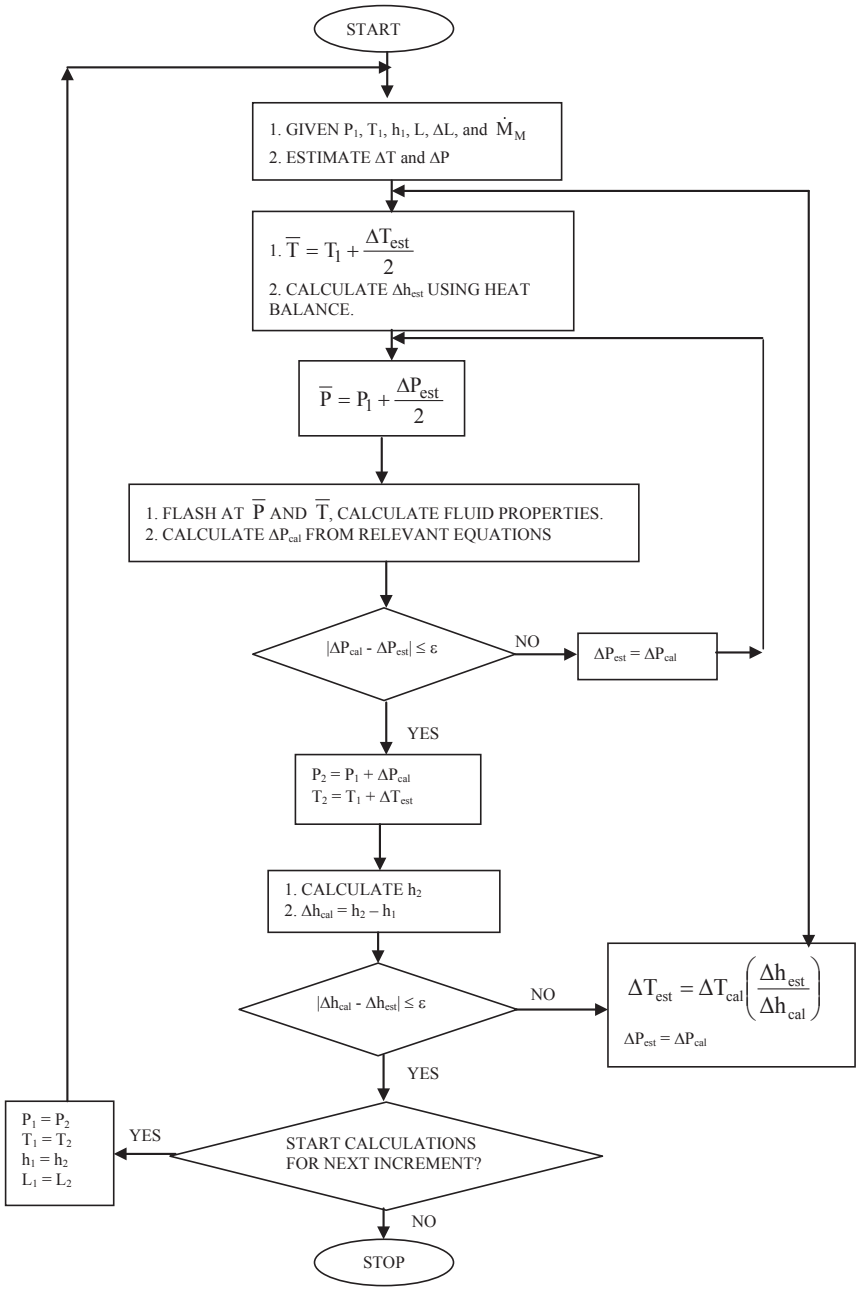

FIGURE 3.6

Pressure and temperature calculation procedure (Brill and Beggs, 1991).

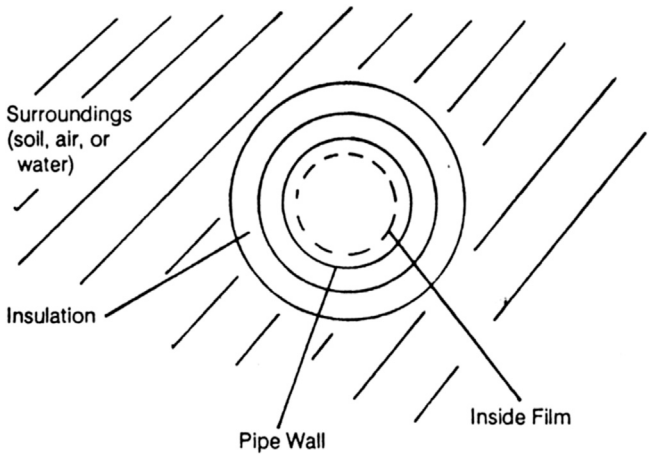

FIGURE 3.7

Cross-section of a pipe showing resistance layers.

Table 3.4 Types of Resistance Layers for a Pipe

Resistance	Due to
$R_{inside,film}$	Boundary layer on the inside of the pipe
R_{pipe}	Material from which the pipe is made
$R_{insulation}$	Insulation (up to five concentric layers)
R_{surr}	Surroundings (soil, air, and water)

In general, the overall heat transfer coefficient for a pipeline is the reciprocal of the sums of the individual resistances to heat transfer, where each resistance definition is given in Table 3.4.

The individual resistances are calculated from the given equations in Table 3.5.

Since fluid properties are key inputs into calculations such as pressure drop and heat transfer, the overall simulation accuracy depends on accurate property predictions of the flowing phases. Most of the required physical and thermodynamic properties of the fluids are derived from the equation of state. However, empirical correlations are used for the calculation of viscosity and surface tension. When the physical properties of the fluids are calculated for a two-phase flow, the physical properties of the gas and liquid mixture can be calculated by taking the mole fraction of these components into account. Similarly, when water is present in the system, the properties of oil and water are combined into those of a pseudo-liquid phase. To produce the phase split for a given composition, pressure, and temperature, an equilibrium flash calculation utilizing an appropriate equation of state must be used.

3.6 VELOCITY CRITERIA FOR SIZING MULTIPHASE PIPELINES

Having selected a line size to meet throughput and pressure drop constraints, it is important to check whether acceptable flowing conditions exist within the pipeline. However, a more useful means of

Table 3.5 Heat Transfer Resistances for Pipes (Hein, 1984; Brill and Beggs, 1991)

$R_{inside,\ film} = D/[0.027\ K_f\ Re^{0.8}\ Pr^{0.33}]$
D = reference diameter on which U is based, inch
K_f = thermal conductivity of the fluid, Btu/hr-ft-°F
Re = Reynolds number

$$= \frac{(\rho_L\lambda_L+\rho_G\lambda_G)(V_{SL}+V_{SG})(D_i)(124.016)}{\lambda_L\mu_L+\lambda_G\mu_G}$$

ρ_L = density of the liquid, lb/ft^3
λ_L = no-slip liquid holdup
ρ_G = density of the gas, lb/ft^3
λ_G = no-slip gas holdup = $1 - \lambda_L$
V_{SL} = liquid superficial velocity, ft/s
V_{SG} = gas superficial velocity, ft/s
D_i = inside diameter of the pipe, inch
μ_L = liquid viscosity, cp
μ_G = gas viscosity, cp
Pr = Prandtl number

$= 2.42\ (\mu_L\lambda_L + \mu_G\lambda_G)\ (C_{pL}\lambda_L + C_{p,G}\ \lambda_G)/K_f$
C_p = specific heat at constant pressure, Btu/lb-°F

$$R_{pipe} = \frac{D\ln(D_o/D_i)}{24k_p}$$

k_p = thermal conductivity of the pipe, Btu/hr-ft-°F
D_o = outside diameter of the pipe, ft
D_i = inside diameter of the pipe, ft

$$R_{insulation} = \frac{D\sum_{j=1}^{n}\frac{1}{k_j}\ln\left(D_j/D_{j-1}\right)}{24}$$

D = reference diameter on which U is based, inch
k_j = conductivity of jth layer of insulation, Btu/hr-ft-°F
D_j = outer diameter of the jth layer, ft
D_{j-1} = inner diameter of the jth layer, ft

For stationary surroundings like soil,

$$R_{surr} = \frac{D\ln\left[\left(2D'+\left(4D'^2-D_t^2\right)^{0.5}\right)/D_t\right]}{24k_{surr}}$$

D = reference diameter on which U is based, inch

k_{surr} = soil thermal conductivity, Btu/hr-ft-°F
D' = depth from the top of soil to the centerline of the pipe, ft
D_t = diameter of the pipe plus insulation, ft

For fluid surroundings like air or water

$$R_{surr} = \frac{D}{12\ k_{surr}10^{\left[0.26694(\log Re_{surr})^{1.3681}\right]}}$$

D = reference diameter on which U is based, inch
k_{surr} = thermal conductivity of the surroundings, Btu/hr-ft-°F
Re_{surr} = Reynolds number for the surroundings
$= 0.0344\ \rho_{surr}V_{surr}D_t/\mu_{surr}$
ρ_{surr} = density of the ambient fluid, lb/ft^3
V_{surr} = velocity of the ambient fluid, ft/h
D_t = total diameter of the pipe plus insulation, inch
μ_{surr} = viscosity of the surrounding fluid, cp

assessing whether flowing conditions are acceptable is to check whether fluid velocities lie within certain limits.

At the low end of the normal throughput range, the actual (not superficial) liquid velocity should ideally be greater than 3 ft/s. This will ensure that sand and water are continuously transported with the liquid phase and not allowed to drop out and accumulate at the bottom of the pipe. However, at the maximum throughput conditions the maximum mixture velocity in the multiphase pipeline must be calculated in order to check that its value does not exceed the erosional velocity limit.

The current industry standard method of determining the erosional velocity limit is through use of the relationship given in API RP 14E (1991):

$$V_e = \frac{C}{(\rho_M)^{0.5}} \tag{3.54}$$

where V_e is the maximum acceptable mixture velocity to avoid excessive erosion, (ft/s); C is the empirical constant; and ρ_M is the no slip mixture density at flowing conditions, lb/ft^3.

Industry experience to date indicates that for solid-free fluids a C-factor of 100 for continuous service and a C-factor of 125 for intermittent service are conservative.

The above simple criterion is specified for clean service (noncorrosive and sand-free), and that the limits should be reduced if sand or corrosive conditions are present. However, no guidelines are provided for these reductions.

If the erosional velocity limit is exceeded either the line diameter must be increased or the production profile constrained to reduce the maximum mixture velocity. Alternatively a higher grade of pipeline material could be used.

In addition to the erosional velocity limit, API RP 14E (1991) also recommends that a line velocity of 60 ft/sec should not be exceeded to ensure that the level of noise emitted by the flow is not excessive. In addition, in some pipeline systems flowing velocities need to be limited by a requirement to avoid removal of corrosion inhibitor film, ensuring a lubricating effect that shifts the erosion velocity limit.

3.7 MULTIPHASE PIPELINE OPERATIONS

After a pipeline is installed, efficient operating procedures must be provided to maintain safe, long-term operation of the pipeline in the face of unexpected upsets, and to improve efficiency and economics of operation. Leak detection, depressurization, and pigging are typically important procedures.

3.7.1 LEAK DETECTION

Leaks in the pipelines originate from a variety of causes, which may include material related damage, physical damage caused by construction in the right-of-way, etc. Because accidental product discharges cannot be entirely eliminated, one of the most effective methods of reducing the impact of spills is to quickly detect the leak and to act quickly to stop the discharge. Methods used to detect product leaks along the pipeline can be divided into two categories, external and internal leak detection systems (API, 1995a). Externally based methods include traditional procedures such as visual inspection, as well as technologies like hydrocarbon sensing using fiber optic or dielectric cables. Internally based methods, also known as computational pipeline monitoring (CPM), use instruments to monitor internal pipeline parameters (i.e., flow, pressure, temperature, and fluid properties), which are continuously input into a computer simulation software linked to a Supervisory Control and Data Acquisition (SCADA) system that mathematically or statistically analyzes the information. Leaks result in unexpected variations or well-defined deviation pattern between simulated and measured values. These patterns can be detected and assessed to determine if a leak is present (API, 1995b). The method of leak detection selected for a pipeline is dependent on a variety of factors including physical pipeline characteristics (length, diameter, thickness, etc.), product characteristics (density, viscosity,

etc.), instrumentation and communication capabilities, and economics (Muhlbauer, 1996). Compared to other leak detection methods, the SCADA-based leak detection methods have the widest range of applicability to pipeline leak detection and are by far the most highly developed of the leak detection methods presented as it can rapidly detect large leaks and, over a period of time, detect smaller leaks as well (Jolly et al., 1992). However, for multiphase flow pipelines, the SCADA-based leak detection methods become much more difficult to apply, and the sensitivity to detecting leaks is reduced because metering multiphase lines is very difficult and inaccurate. Most multiphase meters condition the flow by creating a uniform mist or separating the gas and liquid phases. The big problem in multiphase leak detections is the varying percentage of gas and liquid content and most notably, the formation and expulsion of liquid slugs in the pipeline. Hence, for multiphase SCADA-based leak detection systems, accurate and reliable flow measurement instrumentation and transient flow computer models will need to be developed. Moreover, the capabilities and advantages/disadvantages of new technologies should be analyzed with special consideration given to the possible application in subsea pipelines, for which the remoteness of these pipelines, coupled with a number of complex interactions between the released fluids and the subsea environment, makes detection much more difficult.

3.7.2 PIPELINE DEPRESSURIZATION

Pipeline depressurizing is generally used to refer the controlled and relatively slow evacuation of a pipeline system. Depressurizing is usually performed for process reasons/maintenance requirements. When pipelines transport a gas and liquid mixture a rupture can cause rapid depressurizing and critical flow at the break, additionally, with gas−condensate lines the temperature can drop rapidly due to Joule−Thomson cooling. This can have implications on the brittle fracture of the pipeline and safety valves which may cool significantly before being actuated.

The simulation of depressurizing of a pipeline system is performed in order to determine the minimum temperature experienced, or to calculate the time required to depressurize a system such that the temperature does not drop below the minimum specification value.[2] The transient analysis of pipeline depressurizing can become very complex depending on what is required from the analysis and to what accuracy. OLGA commercial software can simulate the depressurizing of multiphase pipelines and is recommended for most cases.

3.7.3 PIGGING

Pigging is a term used to describe a mechanical method for removing contaminants and deposits within the pipe or to clean accumulated liquids in the lower portions of hilly terrain pipelines, using a mechanized plunger or pigs. Because of the ability of the pig to remove both corrosion products and sludge from the line, it has been found to be a positive factor in the corrosion control of the offshore pipelines. Some specially instrumented pigs, known as “intelligent pigs,” may also be used intermittently for the purpose of pipeline integrity monitoring that includes detecting wall defects (e.g., corrosion, weld defects, and cracks). Pipeline pigs fit the inside diameter of the pipe and scrape the

[2]The time taken to fully depressurize a pipeline to atmospheric pressure will depend on several factors, not least of which will include, the size and type of pipeline inventory, the operating pressure at the time of rupture, the rate of flow escaping and the maximum vent rate at the end section.

pipe walls as they are pushed along the pipeline by the flowing fluid. For offshore platforms the pig is launched from offshore and received in the onshore pig catcher. The receiver is in a direct line with the sealine and can be isolated from it to allow the pigs to be removed. Pigs are available in various shapes (Fig. 3.8) and are made of different materials, depending on the pigging task to be accomplished. Some have spring-loaded steel knives, wire brushes, or abrasive grit surfaces for removal of adhering contaminants. Others are semirigid, nonmetallic spheres.

During pigging operations there are often technical problems due to the lack of the reliable tools for the prediction of the many variables related to the motion of the pig through the pipeline. Hence, the pigging operation requires careful control and coordination. For example, overfrequent pigging causes production downtime or higher operation expenses and infrequent pigging results in less production reduction but increases the risk of pipeline blockages including sticking a pig. The pipeline operator must therefore give serious consideration to whether the pipeline really needs to be pigged and whether it is economical to do so. Since there is no commercially available tool to determine the optimum pigging frequency, operators must choose their pigging frequency using rules of thumb based on their field experience, which often involves a high degree of uncertainty.

In pigging operations where the pipe content is unloaded, the liquid holdup builds up as a slug ahead of the moving pig. The arrival of a slug at production or processing equipment is problematic. It causes both mechanical problems (due to high velocities and momentum) and process problems (increasing liquid levels, causing surges and trips). There are in general several means to reduce slugging in pipelines. In some cases operators can minimize liquid accumulation by managing fields and pipelines in such a way as to create a suitable fluid flow regime (i.e., mist flow regime) under which the gas velocity is high enough to keep liquids continuously dispersed. While it is desirable to design the lines to avoid slugging, in practice this can be difficult while maintaining the ability to turn down the pipeline flow rate. In these cases, consideration should be given to providing suitable process equipment to handle possible slugging (Xiao and Shoup, 1998).

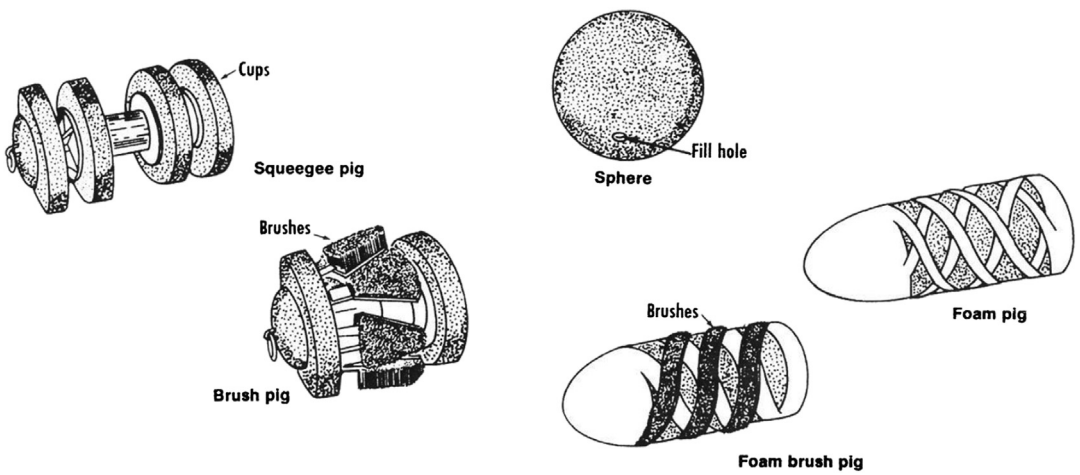

FIGURE 3.8

Typical types of pig (Campbell, 1992).

The pigging operation in multiphase pipelines is a transient operation. Transient flow is observed not only during the pig running time, but also for a long period after the pig exits. This situation occurs even if the inlet gas and liquid flow rates and outlet pressures are kept constant (Minami, 1991). Analysis of such transient flow behavior in a pipeline is necessary not only for designing the downstream processing facilities, but also for establishing safe operating procedures. Hence, there is a definite need to develop reliable and comprehensive pigging models for better understanding of transient behavior of fluids during these operations. A simple model to simulate transient flow behavior in a two-phase flow pipeline under pigging operation has been presented by Minami (1991). In this model, Minami (1991) assumed that the gas phase can be considered to be flowing in a quasi-steady condition, and then coupled it with the Taitel et al. (1989) simplified transient two-fluid model. The model, however, needs significant modifications in order to be used for simulating transient flow in a pipeline-riser system, where the quasi-steady-state approach is not suitable for such systems due to high accumulation of gas upstream of the pig (Yeung and Lima, 2002). For this purpose, a new transient two-fluid model has been developed by Yeung and Lima (2002), which is appropriate for estimating the two-phase flow pigging hydraulics, especially in pipeline-riser systems.

3.8 MULTIPHASE FLOW ASSURANCE

Flow assurance,[3] which is a critical component in the design and operation of multiphase production facilities, refers to ensuring the flow of produced hydrocarbons from the reservoir to the downstream processing facilities. Flow assurance encompasses the thermal-hydraulic design and assessment of multiphase production/transportation systems as well as the prediction, prevention, and remediation of flow problems such as gas hydrate formation, wax and asphaltene deposition on walls, corrosion, erosion, scaling, emulsions, foaming, severe slugging, etc. In all cases, flow assurance designs must consider the capabilities and requirements for all parts of the system throughout the entire production life of the system to reach a successful solution for securing the production operations, minimizing the down times, and reducing the production/transportation costs.

This section addresses the major flow-assurance issues for the raw gas transmission lines and summarizes the commonly used mitigation practices in industry for such purpose. It also provides innovative techniques and practical strategies to design the deepwater pipelines, where traditional approaches are inappropriate for deepwater development systems due to extreme distances, depths, temperature, or economic constraints (Wilkens, 2002).

3.8.1 GAS HYDRATES

A gas hydrate is an ice-like crystalline solid called a clathrate, which occurs when water molecules form a cage-like structure around small guest molecules at certain temperatures and pressures. The most common guest molecules are methane, ethane, propane, isobutane, butane, nitrogen, carbon dioxide, and hydrogen sulfide, of which methane occurs most abundantly in natural hydrates. Several different hydrate structures are known. The two most common are structure I and structure II. Type I forms with smaller gas molecules such as methane, ethane, hydrogen sulfide, and carbon dioxide while

[3]Flow assurance is a term originally coined by Petrobras in the early 1990's. The term in Portuguese was "Garantia de Fluxo," which translates literally to 'Guarantee the Flow."

structure II is a diamond lattice, formed by large molecules like propane and isobutane (Sloan, 2000). However, nitrogen, a relatively small molecule, also forms a Type II hydrate (Carroll, 2003). In addition, in the presence of free water, the temperature and pressure can also govern the type of hydrate structure, where the hydrate structure may change from structure II hydrate at low temperatures and pressures to structure I hydrate at high pressures and temperatures (GPSA, 2004). It should be noted that n-butane does form a hydrate, but is very unstable (Ng and Robinson, 1976; Kumar, 1987). However, it will form a stabilized hydrate in the presence of small "help" gases such as methane or nitrogen (Edmonds et al., 1998). It has been assumed that normal paraffin molecules larger than n-butane are nonhydrate formers (Kumar, 1987). Furthermore, the existence of another hydrate structure, Type H, has been described by Ripmeester et al. (1987). Some isoparaffins and cycloalkanes larger than pentane are known to form structure H hydrates (Mehta and Sloan, 1996). However, little is known about type H structures.

While many factors influence hydrate formation, the two major conditions that promote hydrate formations are (1) the gas being at the appropriate temperature and pressure and (2) the gas being at or below its water dew point (Sloan, 2000). Note, free-water is not necessary for hydrate formation, but it certainly enhances hydrate formation (Carroll, 2003). Other factors that affect but are not necessary for hydrate formation include turbulence, nucleation sites, surface for crystal formation, agglomeration, and the salinity of the system. The exact temperature and pressure at which hydrates form depend on the composition of the gas and the water. For any particular composition of gas at a given pressure, there is a temperature below which hydrates will form and above which hydrates will not form. As the pressure increases, the hydrate formation temperature also increases. As a general rule, when the pressure of the gas stream increases or as the gas becomes colder, the tendency to form hydrates increases (GPSA, 2004). Hence, many gas-handling systems are at significant risk of forming hydrate plugs during shut-in and subsequent startup (Wilkens, 2002).

Although gas hydrates may be of potential benefit both as an important source of hydrocarbon energy and as a means of storing and transmitting natural gas, they represent a severe operational problem as the hydrate crystals may deposit on the pipe wall and accumulate as large plugs that can completely block pipelines, shutting in production (Edmonds et al., 1998; Sloan, 2000). Acceleration of these plugs due to a pressure gradient can also cause considerable damage to production facilities. In addition, the remediation of hydrate blockages can present significant technical difficulties with major cost implications (Mehta et al., 2001). Because of these problems, methods of preventing hydrate solids development in gas production/transportation systems have been of considerable interest for a number of years.

3.8.1.1 Hydrate Locus for Natural Gas Components

The thermodynamic stability of hydrates, with respect to temperature and pressure, may be represented by the hydrate curve. The hydrate curve represents the thermodynamic boundary between hydrate stability and dissociation. Conditions to the left of the curve represent situations in which hydrates are stable and "can" form. Operating under such conditions does not necessarily mean that hydrates will form, only that they are possible. Fig. 3.9 shows the hydrate locus for natural gas components. The extension to mixtures is not obvious from this diagram. The hydrate curve for multicomponent gaseous mixtures may be generated by a series of laboratory experiments, or more commonly, is predicted using thermodynamic software based on the composition of the hydrocarbon and aqueous phases in the system.

The thermodynamic understanding of hydrates indicates the conditions of temperature, pressure, and composition at which hydrates are stable. However, it does not indicate when hydrates will form and, more importantly, whether they will cause blockages in the system.

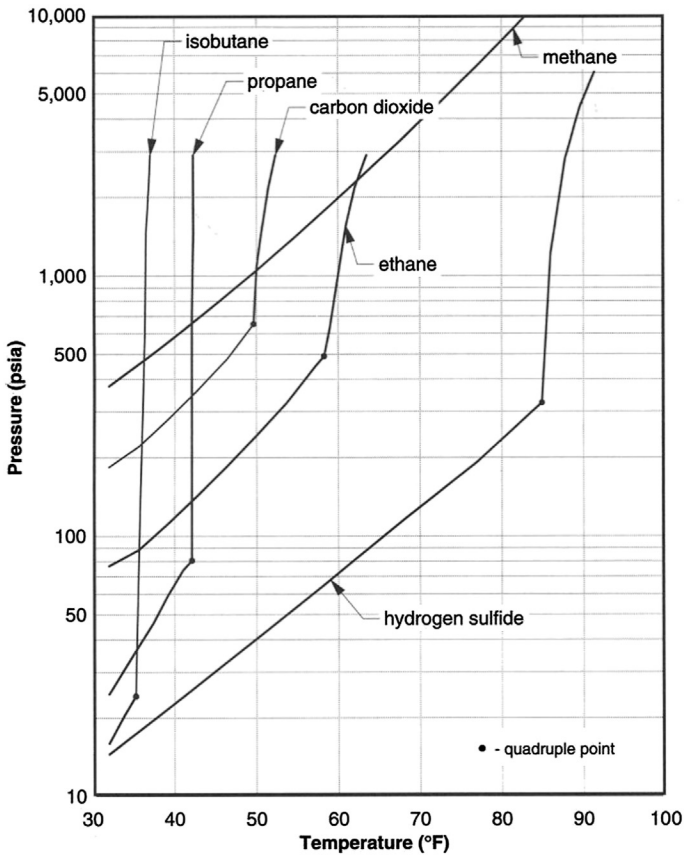

FIGURE 3.9

Hydrate forming conditions for natural gas components (Carroll, 2003).

3.8.1.2 Prediction of Hydrate Formation Conditions

There are numerous methods available for predicting hydrate formation conditions. Three popular methods for rapid estimation of hydrate formation conditions are discussed below. A detailed discussion of other methods that are, perhaps, beyond the scope of the present discussion, can be found in publications by Kumar (1987), Sloan (2000) and Carroll (2003).

3.8.1.2.1 K-Factor Method

This method has been originally developed by Carson and Katz (1942), although additional data and charts have been reproduced since then. In this method, the hydrate temperature can be predicted using vapor–solid (hydrate) equilibrium constants. The basic equation for this prediction is (Carson and Katz, 1942):

$$\sum_{i=1}^{n}\left(\frac{y_i}{K_i}\right) = 1.0 \tag{3.55}$$

where y_i is the mole fraction of component i in gas on a water-free basis, K_i is the vapor–solid equilibrium constant for component i, and n is the number of components.

The calculation is iterative and the incipient solid formation point will determine when the above equation is satisfied. This procedure is akin to a dew point calculation for multicomponent gas mixture.

The vapor–solid equilibrium constant is determined experimentally and is defined as the ratio of the mole fraction of the hydrocarbon component in gas on a water-free basis to the mole fraction of the hydrocarbon component in the solid on a water-free basis (Carson and Katz, 1942):

$$K_i = \left(\frac{y_i}{x_i}\right) \tag{3.56}$$

where x_i is the mole fraction of component i in solid on a water-free basis.

Figs. 3.10–3.14 provide the vapor–solid equilibrium constants at various temperatures and pressures. For nitrogen and components heavier than butane, the equilibrium constant is taken as

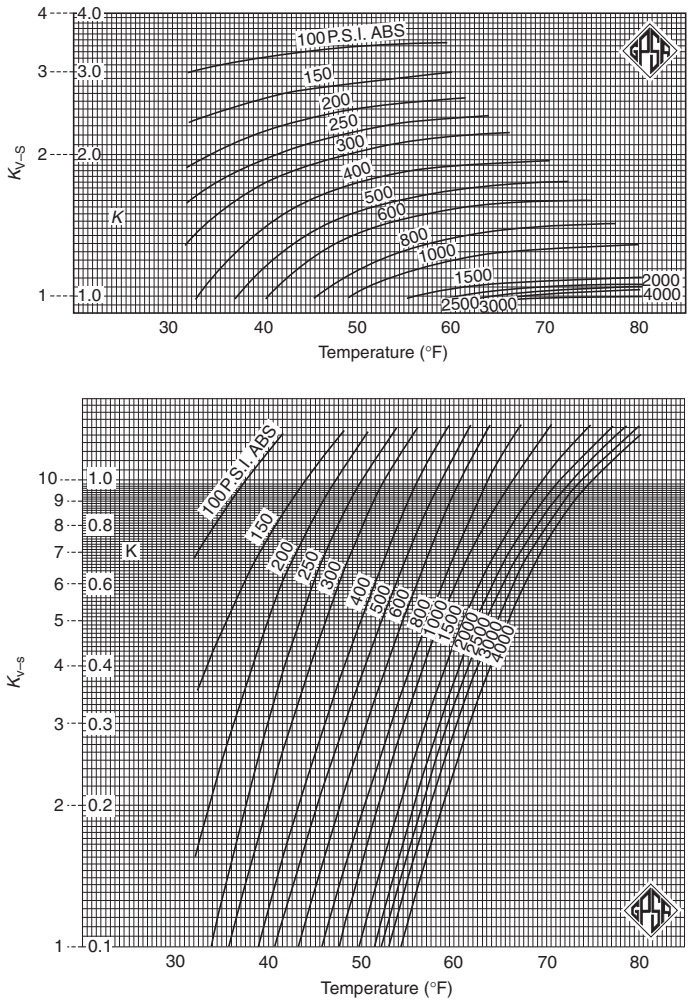

FIGURE 3.10

Vapor–solid equilibrium constants for methane (top) and ethane (bottom) (GPSA, 2004).

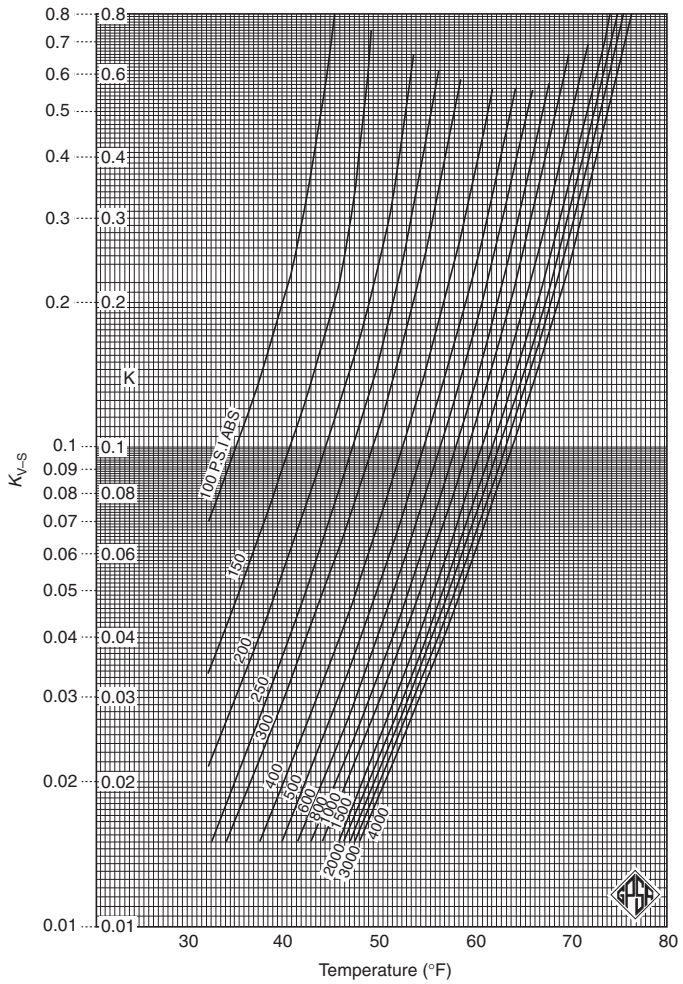

FIGURE 3.11

Vapor–solid equilibrium constants for propane (GPSA, 2004).

infinity. It should be stressed that in the original method of Carson and Katz (1942), it is assumed that nitrogen is a nonhydrate former and that n-butane if present in mole fractions less than 5% has the same equilibrium constant as ethane. Theoretically, this assumption is not correct, but from a practical viewpoint, even using an equilibrium constant equal to infinity for both nitrogen and n-butane provides acceptable engineering results (Campbell, 1992).

The Carson and Katz (1942) method gives reasonable results for sweet natural gases and has been proven to be appropriate up to about 1000 psia (GPSA, 2004). However, Mann et al. (1989) presented

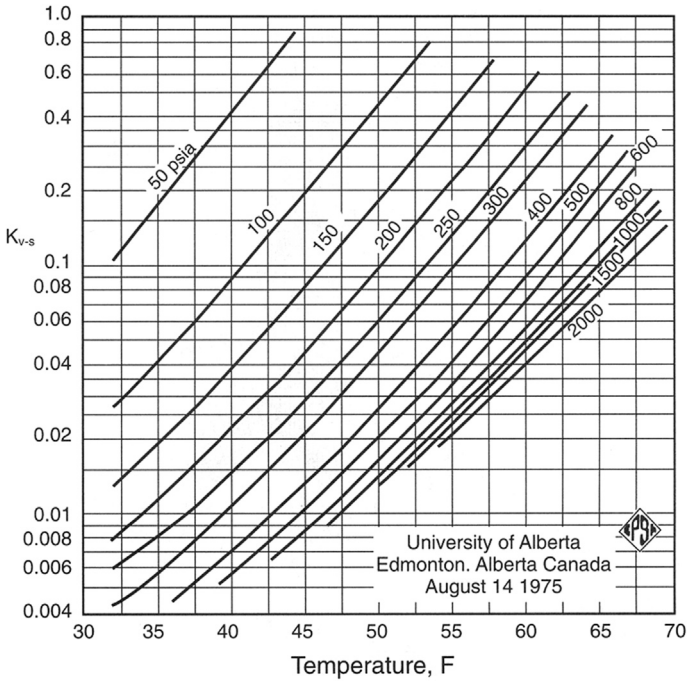

FIGURE 3.12

Vapor–solid equilibrium constants for isobutane (GPSA, 2004).

new K-value charts that cover a wide range of pressures and temperatures. These charts can be an alternate to the Carson and Katz (1942) K-value charts, which are not a function of structure or composition.

Poettmann et al. (1989) also developed vapor–solid equilibrium ratio charts for various natural gas systems using the Colorado School of Mines hydrate program. These charts cover a wide range of pressure, temperature, and composition. Polynomial regression analysis was used to curve fit the computer generated K-values for various systems so that the resulting equations can be programmed and used to predict the hydrate forming conditions for natural gases.

3.8.1.2.2 Baillie and Wichert Method

The method presented by Baillie and Wichert (1987) is a chart method (Fig. 3.15) that permits the estimation of the hydrate formation temperatures at pressure in the range of 100–4000 psia for natural gas containing up to 50% hydrogen sulfide and up to 10% propane (Carroll, 2003). The method may not apply to a sweet gas mixture containing CO_2, but is considered fairly accurate if the CO_2 is less than about 5 mol% (Carroll, 2004).

3.8.1.2.3 Gas Gravity Method

Until now, several other methods have been proposed for predicting hydrate-forming conditions in natural gas systems. The most reliable of these requires a gas analysis. However, if the gas composition

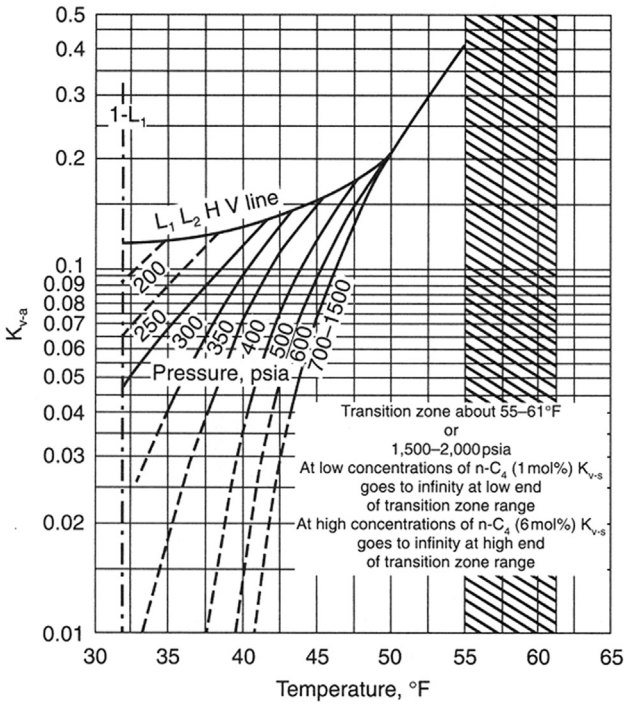

FIGURE 3.13

Vapor–solid equilibrium constants for n-butane (GPSA, 2004).

is not known, even the previous methods cannot be used to predict the hydrate formation conditions and the Katz (1945) gravity chart (Fig. 3.16) can be used to predict the approximate pressure and temperature for hydrate formation, provided hydrates exist in the pressure–temperature region above the appropriate gravity curve. Therefore, as a first step to predict hydrate formation temperature one can develop an appropriate equation representing the Katz (1945) gravity chart. Such a correlation uses two coefficients that correlate temperature, pressure, and specific gravity of gas (Towler and Mokhatab, 2005):

$$T_h = 13.47\ln(P) + 34.27\ln(SG) - 1.675[\ln(P) \times \ln(SG)] - 20.35 \tag{3.57}$$

where T is the gas flow temperature, °F; P is the gas flow pressure, psia; and SG is the specific gravity of gas (air = 1.0).

Note that Eq. (3.57) is based on the GPSA chart but is only accurate up to 65°F. Beyond that it overestimates the temperature slightly.

The Katz (1945) gravity chart was generated from a limited amount of experimental data and a more substantial amount of calculations based on the K-value method. The components used for the construction of this chart are methane, ethane, propane, butane, and pentane, and therefore using this chart for compositions other than those used to derive these curves will produce erroneous results (Sloan, 2000). In fact, this method is an appropriate method of estimating hydrate formation conditions for sweet natural gas mixtures. However, the Baillie and Wichert (1987) method is better than this chart when applied to sweet gas, because of the inclusion of a correction factor for propane (Carroll, 2003).

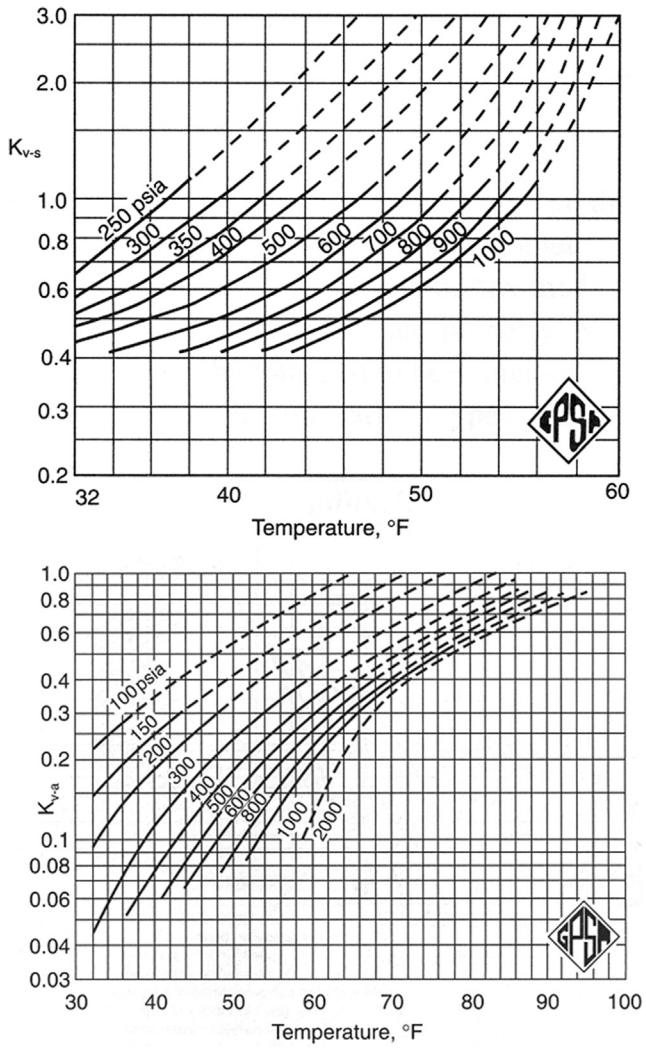

FIGURE 3.14

Vapor–solid equilibrium constants for carbon dioxide (top) and hydrogen sulfide (bottom) (GPSA, 2004).

3.8.1.2.4 Commercial Software Programs

Hydrate formation conditions based on fluid compositions are normally predicted with the commercially available software programs. These programs are generally quite good, and so simple to use, they often require less time than the simplified methods presented. The bases of these computer programs are the statistical thermodynamic models, which use a predictive algorithm with additional experimental data included to modify or "tune" the mathematical predictions. Most commercially available softwares use algorithms developed by D.B. Robinson and Associates (EQUIPHASE), and

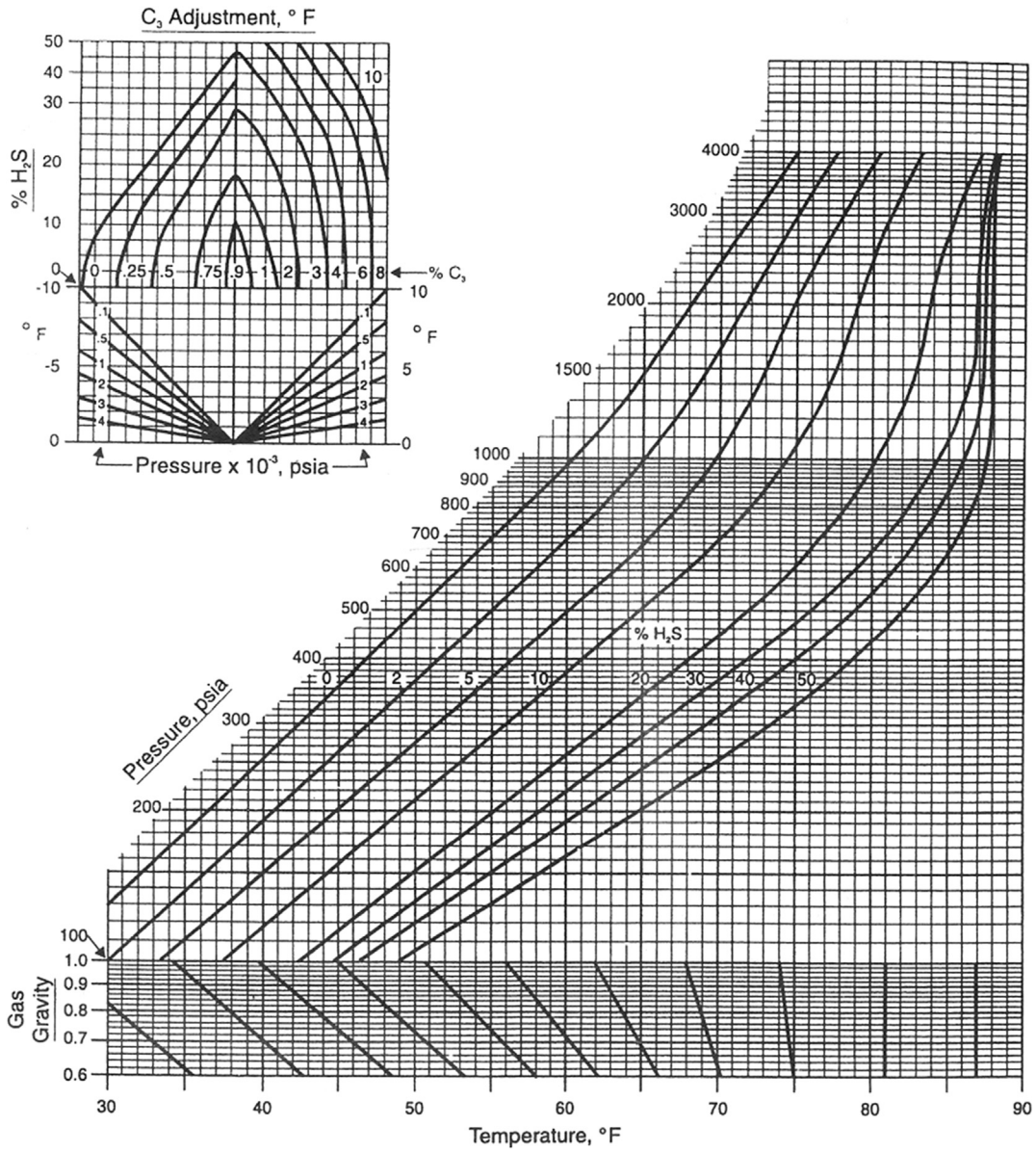

FIGURE 3.15

Baillie and Wichert chart for estimating hydrate formation conditions (GPSA, 2004).

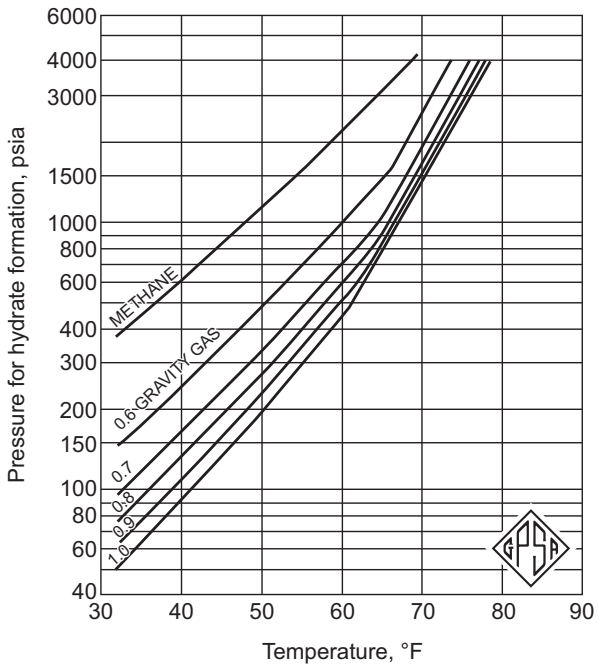

FIGURE 3.16

Katz's gravity chart for predicting hydrate formation conditions (GPSA, 2004).

by Infochem Computer Services Ltd (MULTIFLASH). A detailed discussion of the accuracy of these programs and other hydrate software programs can be found in publications by Sloan (2000) and Carroll (2003).

3.8.1.3 Hydrate Prevention Techniques

The multiphase fluid produced at the wellhead will normally be at a high pressure and a moderate temperature. As the fluid flows through the pipelines, it becomes colder which means such pipelines could experience hydrates at some point in their operating envelope. For this reason, the hydrate formation in gas transmission pipelines should be prevented effectively and economically to guarantee the pipelines operate normally. Control of hydrates relies upon keeping the system conditions out of the region in which hydrates are stable. It may be possible to keep the fluid warmer than the hydrate formation temperature (with the inclusion of a suitable margin for safety) or operate at a pressure less than the hydrate formation pressure.

Although there are several methods to avoid hydrate formation, depending on the possible location of a gas hydrate plug, some of the techniques to remediate onshore hydrates (e.g., installation of line heaters and line depressurization) may not be practical in long and high pressure, subsea gas transmission pipelines (Wilkens, 2002).

There are few methods of preventing hydrate formation in offshore transmission systems. The permanent solution is removal of water prior to pipeline transportation, using a large offshore

dehydration plant that is not often the most cost effective solution. Pipeline system depressurization is also often used to melt the hydrate plug formed in a pipeline. However, the process is fairly slow and can take up to weeks or even months to completely melt a long hydrate plug. In general, at the well site two methods are applicable, namely thermal and chemical. These techniques are discussed in the following sections.

3.8.1.3.1 Thermal Methods

Thermal methods use either the conservation or introduction of heat in order to maintain the flowing mixture outside the hydrate formation range. Heat conservation is a common practice and is accomplished through insulation.[4] By using insulation, it is easy to maintain fluid flowing temperature everywhere along the pipeline above the hydrate formation temperature. But no matter how much insulation is put on the pipeline, after a long pipeline shutdown, the fluid temperature will fall below the hydrate formation temperature and eventually cool down to the ambient temperature. Therefore, thermal insulation itself is not enough for hydrate mitigation for long pipeline shutdowns and other mitigation strategies will be needed (Guo et al., 2005).

A number of different concepts are available for introducing additional heat to a pipeline. The simplest is an external hot-water jacket, either for a pipe-in-pipe system or for a bundle. Other methods use either conductive or inductive heat tracing. There is concern over the reliability of conductive systems. An electrical resistance heating system may be desirable for long offset systems, where available insulation is insufficient, or for shut-in conditions (Langner et al., 1999). The ability to heat during production depends on the specific electrical heating implementation. Such systems provide environmentally friendly fluid temperature control without flaring for pipeline depressurization. The effect is also an increase in production as there is no time lost by unnecessary depressurization, pigging, heating-medium circulation, or removal of hydrate blockage. But still it is difficult to persuade operators to install an acting heating system.

3.8.1.3.2 Chemical Inhibition

An alternative to the thermal processes is chemical inhibition. Chemical inhibitors are injected at the wellhead and prevent the hydrate formation by depressing the hydrate temperature below that of the pipeline operating temperature. Chemical injection systems for subsea lines have a rather high capital expenditure price tag associated with them, in addition to the often high operating cost of chemical treatment (Sloan, 2000). However, hydrate inhibition using chemical inhibitors is still the most widely used method for unprocessed gas streams, and the development of alternative, cost-effective, and environmentally acceptable hydrate inhibitors is a technological challenge for the gas production industry.

3.8.1.3.2.1 Types of Inhibitors. Traditionally, the most common chemical additives used to control hydrates in gas production systems have been methanol, ethylene glycol, or triethylene glycol at a high enough concentration (Sloan, 2000). These chemicals are called "thermodynamic inhibitors" and have the effect of shifting the hydrate curve to the left, which causes the hydrate stability point to be displaced to a lower temperature and/or a higher pressure. Fig. 3.17 shows how the hydrate curve shifts with different amounts of methanol inhibition. Increasing salt content in the produced brine (by injecting electrolyte solutions such as sodium chloride, calcium chloride, and potassium chloride) can

[4]Burying the pipeline alone is not enough for thermal insulation and some extra insulation will be needed.

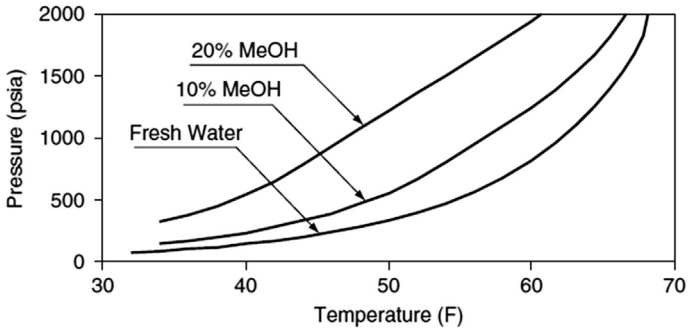

FIGURE 3.17

Hydrate curves with different amounts of methanol inhibition (Guo et al., 2005).

also provide some hydrate temperature suppression[5] (see Fig. 3.18), but normally this alone is not sufficient to avoid hydrates in the subsea gas production systems. In some cases, blended inhibitors of methanol/glycols and electrolyte(s) are preferred for subsea applications (Zuo and Zhang, 1999).

The inhibitor selection process often involves comparison of many factors including capital/operating cost, physical properties, safety, corrosion inhibition, gas dehydration capacity, etc. However, a primary factor in the selection process is whether or not the spent chemical will be recovered, regenerated, and reinjected. Usually methanol is not regenerated because its use is intermittent (i.e., during startup or shutdown). However, when it is injected continuously, as is often observed in gas systems, it is sometimes regenerated. But loses to the vapor phase can be prohibitive, in which case operators select monoethylene glycol (GPSA, 2004). Often when applying this inhibitor, there is a significant expense associated with the cost of "lost" methanol. However, since methanol has lower viscosity and lower surface tension it helps in an effective separation from the gas phase at cryogenic

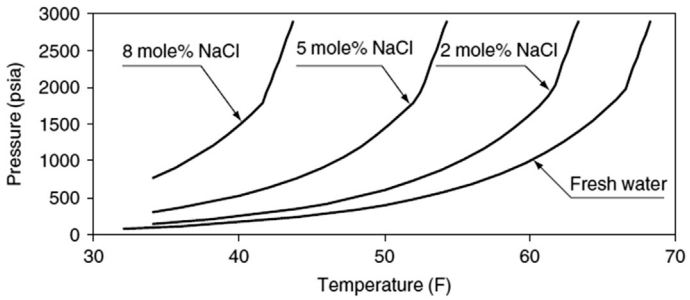

FIGURE 3.18

Impact of NaCl salt on hydrate formation curve (Guo et al., 2005).

[5]Even though salt solution can be used for hydrate inhibition, too much salt can cause salt deposition and scale deposits in the system facilities. Salt solution is also corrosive and can cause corrosion problems to equipment.

conditions (below −13°F), and it is usually preferred (Esteban et al., 2000). In many cases hydrate plug formation is prevented through the addition of glycols (usually ethylene glycol because of its lower cost, lower viscosity and lower solubility in liquid hydrocarbons, and lower vapor pressure giving reduced gas-phase losses) to depress the hydrate formation temperature. In order to be effective, glycols must be added at rates of up to 100% of the weight of water. Since glycols are expensive inhibitors, there is a definite need for extra, costly, and space consuming onshore or offshore plants for their regeneration. Therefore, it would be useful to develop new hydrate depressants, which can be used at much lower concentrations, and therefore much lower cost. Recently, two new types of low-dosage inhibitors have been developed, which will enable the subsea gas transmission pipelines to handle increased gas volumes without additional glycol injection, or extra glycol recovery units (Bloys et al., 1995; Lederhos et al., 1996; and Palermo et al., 2000). These new hydrate inhibitors can lead to very substantial cost savings, not only for their reduced cost but also in the size of the injection, pumping, and storage facilities (Mehta et al., 2002). These new hydrate inhibitors called "Low Dosage Hydrate Inhibitors" (LDHIs) form the basis of a technique that does not operate by changing the thermodynamic conditions of the system. In fact, LDHIs act at the early stages of hydrate formation by modifying the rheological properties of the system (Sinquin et al., 2004). There are two types of LDHIs: the "kinetic hydrate inhibitors" (KHIs), and "antiagglomerants" (AAs). Most commercial kinetic inhibitors are high molecular weight polymeric chemicals (i.e., poly [N-vinyl pyrrolidone] or poly [vinylmethylacetamide/vinylcaprolactam]), which are effective at concentrations typically 10 to 100 times less than thermodynamic inhibitor concentrations. KHIs may prevent crystal nucleation or growth during a sufficient delay compared to the residence time in the pipeline. The deeper a system operates in the hydrate region, the shorter the time during which kinetic hydrate inhibitors can delay hydrate formation. The achievable delays range between weeks if the pipeline operates less than 42°F in the hydrate region and hours if the pipeline operates at 50°F in the hydrate region (Mokhatab et al., 2007b). Kinetic inhibitors are relatively insensitive to the hydrocarbon phase and may therefore turn out to be applicable to a wide range of hydrocarbon systems. However, the industrial application of kinetic inhibitors depends on the repeatability of multiphase pipeline testing results among laboratory, pilot plant, and field, and the transferability among different plants (Kelland et al., 2000).

In contrast to other types of inhibitors, AAs, which are surface active chemicals (i.e., alkyl aromatic sulphonates or alkyl phenyl ethoxylates), do not prevent the formation of hydrate crystals but keep the particles small and well dispersed so that fluid viscosity remains low, allowing the hydrates to be transported along with the produced fluids. AAs performance is relatively independent of time. In addition, AAs appear to be effective at more extreme conditions than KHIs, which makes these products of interest to operators looking for cost effective hydrate control in deepwater fields. These additives are currently applied in the Gulf of Mexico, the North Sea, and West Africa (Mehta et al., 2002; Frostman, 2003). However, they have mainly limitations in terms of water cut, where they require a continuous oil phase and therefore only applicable at lower water cuts. The maximum water cut is expected to be between 40% and 50%. This limitation is caused by the rheological properties of suspensions with high solid fraction and may depend on flow regime conditions (Frostman, 2000; Mehta et al., 2002).

As stated earlier, the choice between inhibitor alternatives must be based on physical limitations as well as economics. However, operating conditions may also limit the number of available choices. For example, in a recent project carried out by Baker Petrolite it was shown that under severe conditions, the required dosage of an antiagglomerator unlike thermodynamic and kinetic inhibitors does not

increase as the degree of subcooling increases. Therefore, this method of treatment would be a cost-effective solution for the control of gas hydrates (Ramachandran et al., 2000).

3.8.1.3.2.2 Prediction of Inhibitor Requirements. The inhibitor must be present in a minimum concentration to avoid hydrate formation. Accurate prediction of this minimum inhibitor concentration is required for cost-effective design and operation of multiphase pipelines. Various empirical methods, charts, and computer programs have been developed for this purpose including the venerable Hammerschmidt's empirical equation (1934), which is a relatively simple method that has been used to calculate the amount of inhibitor required in the water phase to lower the hydrate formation temperature:

$$\Delta T = \frac{K \cdot W}{100(MW) - (MW)W} \tag{3.58}$$

where ΔT is depression of hydrate formation temperature, °F; MW is the molecular weight of inhibitor; W is the weight percent of inhibitor in the final water phase; and K is constant, depending on the type of inhibitor.

Experimentally determined values of K and molecular weights of inhibitors are given in Table 3.6. To use this equation, the hydrate formation temperature in the gas without the inhibitor being present must be known. In fact, Eq. 3.58 only predicts the deviation from the hydrate formation temperature without an inhibitor present.

The Hammerschmidt equation is limited to inhibitor concentrations of about 20–25 wt% for methanol and 60–70 wt% for the glycols (GPSA, 2004). However, for higher methanol concentrations, Nielsen and Bucklin (1983) have recommended the following equation:

$$\Delta T = -129.6 \ln(X_{H_2O}) \tag{3.59}$$

where X_{H_2O} is the mole fraction of water in the aqueous phase.

They claim that this equation is accurate up to 90 wt% methanol, which gives the maximum suppression because methanol freezes at concentrations above 90 wt%. However, recent studies of GPSA (2004) only recommend the Nielsen and Bucklin (1983) equation for methanol concentrations ranging from 25 to 50 wt%. Eq. 3.59 was developed for use with methanol, however, this equation is actually independent of the choice of inhibitor and therefore, theoretically, it can be used for any glycols.

Table 3.6 Physical Constants of Inhibitors (Hammerschmidt, 1934)

Inhibitor	MW	K
Methanol	32.04	2335
Ethanol	46.07	2335
Isopropanol	60.10	2335
Ethylene glycol	62.07	2200
Propylene glycol	76.10	3590
Diethylene glycol	106.10	4370
Triethylene glycol	150.17	5400

Maddox et al. (1991) have described a graphical procedure for estimating the required inhibitor concentration for both methanol and glycol. This method is a trial and error approach, which can be used when the activity coefficients of water in methanol and glycol are available. Although this method provides better accuracy, no recommended applicable range is provided (Esteban et al., 2000).

If the produced water or seawater is in contact with the hydrocarbon fluid, the salinity of the water will itself inhibit hydrate formation. Therefore, it is important to be able to estimate the effect of the brine in the produced water on the hydrate formation temperature. For this purpose, McCain (1990) presented the following equation:

$$\Delta T = AS + BS^2 + CS^3 \tag{3.60}$$

where ΔT is temperature depression, °F; S is water salinity, wt%; and

$$A = 2.20919 - 10.5746\ (SG) + 12.1601\ \left(SG^2\right) \tag{3.60.1}$$

$$B = -0.10605 + 0.72269\ (SG) - 0.85093\ \left(SG^2\right) \tag{3.60.2}$$

$$C = 0.00347 - 0.01655\ (SG) + 0.01976\ \left(SG^2\right) \tag{3.60.3}$$

Eq. 3.60 is limited to salt concentrations of less than 20 wt% and for gas specific gravities (SG) ranging from 0.55 to 0.68.

All of these simple methods predict the depression of the hydrate formation temperature; they do not predict the actual hydrate formation conditions. However, several thermodynamic models have been proposed for predicting the hydrate formation conditions in aqueous solutions containing methanol/glycols and electrolytes (Edmonds et al., 1996; Nasrifar et al., 1998; and Zuo and Zhang, 1999). These rigorous models can also account for the effect of pressure and the type of hydrate that are neglected in the simple mentioned methods. However, available models have limitations that include the types of liquid and compositions of fluids and inhibitors used.

The amount of inhibitor required to treat the water phase, the amount of inhibitor lost to the vapor phase, and the amount that is soluble in the hydrocarbon liquid equals the total amount required. Methanol vaporization loss can be estimated from Fig. 3.19, while glycol vaporization losses are generally very small and typically can be ignored. More details on how to estimate the amount of methanol or glycols lost in vapor and condensate can be found in the study of Sloan (2000).

In addition, prediction of inhibitor losses to the hydrocarbon liquid phase is difficult. However, many of the commercially available software programs include proper calculations to account for the loss of methanol and glycols to the hydrocarbon liquid phase.

3.8.1.3.2.3 Design of Injection Systems. Proper design of an inhibitor injection system is a complex task that involves optimum inhibitor selection, determination of the necessary injection rates, pump sizing, and pipeline diameters. Inhibitors for a subsea gas transmission system are selected before gas production is started on the facility. This makes inhibitor selection difficult as a large number of factors including brine composition, temperature, pressure, etc. that affect the performance of inhibitors are unknown (Ramachandran et al., 2000). Therefore, at this stage, an appropriate multiphase flow simulation package must be used to calculate some of the unknown necessary variables, which are required for injection systems design.

To determine the appropriate injection rate, it is preferable to determine inhibitor requirements by field-testing. The inhibitor dosing requirements are later used to determine the requirements for

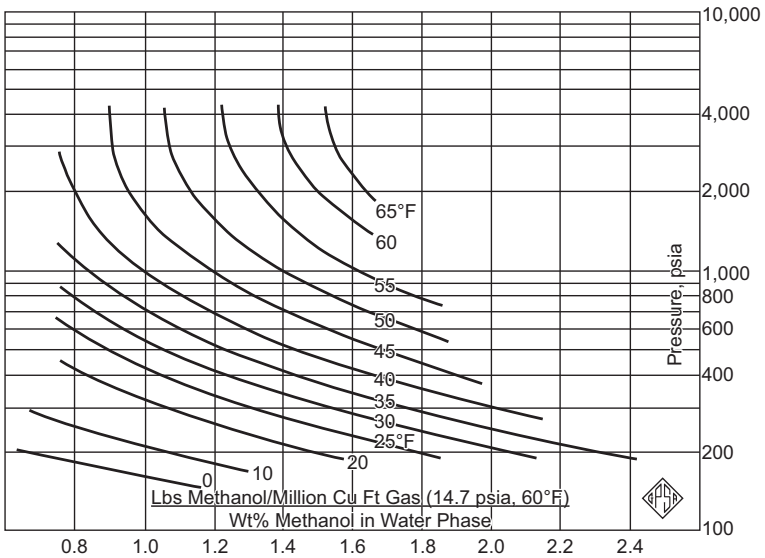

FIGURE 3.19

Prediction of methanol vaporization loss (GPSA, 2004).

inhibitor storage, pumping capacities, and number of inhibitor lines in order to ensure that inhibitor can be delivered at the required rates for treating wells and flow lines during startup and shut-in operations. In addition, points of injection should be chosen to provide maximum benefit in the pipeline system. The most effective position for injection is generally at the center of the pipe in the direction of the product flow. However, the injection rate, and location of injection points will be a function of flow geometry, fluid properties, pressure–temperature relationships, etc., that will be encountered in the actual field application. For instance hydrate inhibitors for a deepwater production system are often pumped through long umbilicals that are ½ inch to ¼ inch in diameter. The injection pump is a positive-displacement metering pump (Kumar, 1987) capable of generating sufficient injection line pressure (normally between 3000 and 4000 psi) to overcome the line operating pressure. Ideally the injection pressure should be 100 psi above the line pressure. However, varied injection rates can be achieved by changing the pressure differential. Ramachandran et al. (2000) provide a discussion on proper design of deepwater injection systems and predicting systems behavior.

3.8.2 CORROSION

One of the common problems in the multiphase flow transmission pipelines is metal corrosion. Corrosion is defined as the deterioration of material, usually a metal, because of its reaction with the environment or handling media. This material degradation leads to the impairment of the intended function of the metal, environment or the integrity of the system. This can be general corrosion (regular loss of metal on the exposed surface) or it can be localized corrosion where only a limited portion of the surface is in contact.

Corrosion can occur in different forms and can be caused by a variety of different reasons. The cause of corrosion can be directly attributed to the impurities found in the produced gas as well as the corrosive components which are by-produced. Because of the nonspecificity of the components produced from a production well, some or all of these components may be active to create a corrosive environment in the pipelines. Corrosion in multiphase systems is a complex phenomenon, including dependency on the partial pressure, temperature, flow regime/velocity, pH, and concentration of corrosive components. Consequently, corrosion prediction requires substantial understanding of the simultaneous interaction of many process variables that govern both the flow and corrosion conditions.

An important aspect of maintaining pipeline performance is adequate control of corrosion[6] both internally—caused by the flow components and their by-products—and externally—because of pipeline exposure to the soil and water (Hartt and Chu, 2004). Pipeline corrosion can be inhibited by several means:

- choice of corrosion-resistant metals,
- injection of corrosion inhibitors,
- cathodic protection, and
- external and/or internal protective coatings

While corrosion control can be achieved by selection of an appropriate corrosion-resistant metal, operating considerations usually dictate that a high-efficiency corrosion control system be used. Protecting pipelines from corrosion is achieved internally by injection of inhibitors to mitigate internal corrosion and externally by the use of cathodic protection and/or combination of coatings and cathodic protection (for buried or subsea pipelines).

3.8.2.1 Choice of Corrosion-Resistant Metals

Corrosion resistance is a basic property related to the ease with which materials react with a given environment. All metals have a tendency to return back to stable conditions. This tendency causes metals to be classified according to rising nobleness that again leads to classification of decreasing activity and increasing potential. When it is observed that the existing material of construction is prone to corrosive attack, generally a decision is made to change the materials of construction and select an alternate material to suit the specific need. For specific recommendations concerning materials selection refer to the ANSI B31.3 and B31.8, API RP 14E (1991), and NACE (1975) MR-01-75. It should be noted that no single material can serve as a cure for all the corrosion evils. Therefore, a detailed study of process and operating conditions has to be carried out before selection of a new material.

Corrosion resistance is not the only property to be considered in the material selection process, and the final selection will generally be the result of several compromises between corrosion resistance and economic factors. Historically, carbon steel has been the most economical material for construction of long-distance, large diameter gas transmission pipelines.[7] However, the inherent lack of corrosion resistance of these materials in subsea application requires a corrosion control system with a high degree of reliability (Hartt and Chu, 2004).

---

[6]Corrosion can result in the loss of millions of dollars if a pipeline is not properly protected.

[7]Corrosion resistant alloy (CRA) is often used to replace carbon steel for corrosive applications. But, CRAs are normally expensive than carbon steel and should be used depending on the overall economics.

3.8.2.2 Corrosion Inhibitors

Sometimes it is necessary to reduce the intensity of corrosive attack of the environment by adding certain chemicals known as "inhibitors" to reduce the aggressiveness of the media. Corrosion inhibition is necessary in gas–condensate pipelines when the required corrosion allowance for an uninhibited pipeline is excessive. If this is the case a corrosion allowance for the inhibited pipeline system can be calculated from the allowance for the uninhibited system and the inhibitor efficiency.[8] If the required corrosion allowance is still excessive a higher grade material must be used for the pipeline.

Corrosion inhibitors are cationic surfactant chemicals such as filming amines, which, when added in a small concentration (between 10 and 1000 ppm), effectively reduce the corrosion rate of a metal.[9] The injected inhibitor forms a protective layer on the internal surface of the pipe and the continuity and the quality of this layer are the controlling factors for effective corrosion protection. Corrosion inhibitors can be applied in batches resulting in a protective film, which may last for weeks or months. Enough inhibitor should be introduced to provide an appropriate wall coating thickness. Frequency of the treatment is governed by the remaining effectiveness of the inhibitor after a specified amount of commodity has been moved through the line. Inhibitors are often continuously injected in low concentrations where a thin film is laid down and maintained over time.

Corrosion inhibitors will only perform at their nominal efficiency if they remain in contact with the pipe wall at the correct concentration (Erickson et al., 1993). However, for some specific flow patterns in multiphase flows such as slug flow, inhibitor stripping can occur due to turbulence and high shear stress (Kang et al., 1996). But the slug can also help by distributing corrosion inhibitor and preventing top-of line corrosion. As gas–condensate pipelines operate primarily in a stratified flow regime, corrosion inhibitor is only deposited on the pipe's top wall if there is a substantial fraction of the liquid entrained as droplets in the gas phase. However, at some locations, corrosion will still occur due to the condensation of water that dilutes the inhibitor concentration.

There are numerous corrosion inhibitor types and compositions. Corrosion inhibitor selection is a complex process that needs to balance a number of competing demands. The inhibitor must both reduce corrosion rates to an acceptable level and be compatible with system materials and other production chemicals such as hydrate inhibitors and biocides. The selected corrosion inhibitor must also not adversely affect hydrocarbon production processes by formation of foams or emulsions. Finally, the selected chemical must meet environmental regulations.

Although inhibitors can be used to a great advantage to suppress the corrosion of metals in many environments, there are certain limitations of this type of corrosion prevention which should be recognized. First, it may not be possible to add inhibitors to all corrosive systems because they may contaminate the environment. Further, inhibitors generally rapidly lose their effectiveness as the concentration and temperature of the environment increase. Finally, many inhibitors are toxic, and their application is limited. Therefore, new inhibitors are continuously being developed to handle more aggressive conditions and comply with more stringent environmental regulations.

---

[8]For smooth pipeline, the efficiency of corrosion inhibitors can be as high as 85%–95%, but can drop if the shear stress increases drastically at locations such as fittings, valves, and bends (Guo et al., 2005).

[9]In a gas–condensate pipeline, adding the thermodynamic hydrate inhibitors can also reduce the corrosion rate. This is because, they absorb free water and make the water phase less corrosive.

3.8.2.3 Cathodic Protection

Cathodic protection is the most successful method for reducing or eliminating corrosion for buried or submerged metallic structures that involves using electric voltage to prevent corrosion (Colson and Moriber, 1997). When two metals are electrically connected to each other in an electrolyte (e.g., seawater), electrons will flow from the more active metal (anode) to the other (cathode) due to the difference in the electrochemical potential. The anode supplies current, and it will gradually dissolve into ions in the electrolyte and at the same time produce electrons that the cathode will receive through the metallic connection with the anode. The result is that the cathode will be negatively polarized and hence be protected against corrosion. The two methods of achieving cathodic protection are (1) the use of sacrificial or reactive anodes with a corrosion potential lower than the metal to be protected and (2) applying a direct current. The use of direct current system is less costly than sacrificial anodes and provides a higher range of possible potential differences, although they may require greater maintenance during the lifetime of the operation (Uhlig and Revie, 1985).

3.8.2.4 Protective Coatings

While cathodic protection has historically been employed as the sole corrosion control methodology for subsea gas production systems, the nature of multiphase pipelines is such that the combined use of protective coatings with cathodic protection is necessary to achieve the effective protection[10] (Samant, 2003). In fact, protective coatings help control pipeline corrosion by providing a barrier against reactants such as oxygen and water. But, because all organic coatings are semipermeable to oxygen and water, coatings alone cannot prevent corrosion and so a combination of cathodic protection is often used (Varughese, 1993).

Pipelines are often internally coated to minimize corrosion when lying in pipeline dumps prior to construction, and to provide a smooth surface that reduces friction when fluids are in transit. It should be noted that the initial period in a production well's life can be its most corrosive time due to the high partial pressure of carbon dioxide. Therefore, it may be more economical to protect the multiphase pipelines from a young field. The coating must be compatible with the commodity and should have suitable resistance to attack by the commodity as well as any contaminants, corrosives, or inhibitor associated with it. Coatings such as epoxies, plastics, or metallic compounds can be used for selected applications. The oldest and still used approach consists of hot-applied bituminous material wrapped with an appropriate covering (Polignano, 1982). External coatings are used to reduce the value of the external current to an economic level by imposing a barrier of high electrical resistance between metal and its environment. Rhodes (1982) reports the use of many such coatings, including polyurethane, phenolic resin, phenolic epoxy, and fusion-bonded epoxy powder.

3.8.2.5 Corrosion Monitoring

Pipelines are susceptible to both internal and external corrosion. Therefore, both internal as well as external monitoring of pipeline is required for a complete assessment, thus providing the direction that will ensure proper utilization of materials and corrosion control methodologies. While traditional inspection and monitoring techniques (such as pigging and corrosion coupons) may represent effective solutions for assessment of the condition and integrity of a pipeline, the sensitivity and accuracy of

[10]For some installations (e.g., deepwater) one might choose continuous inhibition over protective coating due to the implications of a coating failure.

these methods may be inadequate for monitoring inhibitor performance since they do not provide real-time information but rather focus on historical analysis. Therefore, traditional techniques of monitoring must be supplemented with online techniques that provide more appropriate real-time data. This allows operators to be more proactive in preventing corrosion-related pipeline failures.

3.8.3 WAX

Multiphase flow can be severely affected by deposition of organic solids, usually in the form of wax crystals, and their potential to disrupt production due to deposition in the production/transmission systems. The wax crystals reduce the effective cross-sectional area of the pipe and increase the pipeline roughness, which results in an increase in pressure drop. The deposits also cause subsurface and surface equipment plugging and malfunction, especially when oil mixtures are transported across Arctic regions or through cold oceans. Wax deposition leads to more frequent and risky pigging requirements in pipelines. If the wax deposits get too thick, they often reduce the capacity of the pipeline and cause the pigs to get stuck. Wax deposition in well tubings and process equipment may lead to more frequent shutdowns and operational problems.

3.8.3.1 Wax Deposition

Precipitation of wax from petroleum fluids is considered to be a thermodynamic molecular saturation phenomenon. Paraffin wax molecules are initially dissolved in a chaotic molecular state in the fluid. At some thermodynamic state the fluid becomes saturated with the wax molecules, which then begin to precipitate. This thermodynamic state is called the onset of wax precipitation or solidification. It is analogous to the usual dew point or condensation phenomenon, except that in wax precipitation a solid is precipitating from a liquid, whereas in condensation a liquid is precipitating from a vapor. In wax precipitation, resin and asphaltene micelles behave like heavy molecules. When their kinetic energy is sufficiently reduced due to cooling, they precipitate out of solution but they are not destroyed. If kinetic energy in the form of heat is supplied to the system, these micelles will desegregate and go back into stable suspension and Brownian motion.

3.8.3.1.1 Wax Deposition Envelope

Many reservoir fluids at some frequently encountered field conditions precipitate field waxes. It is very important to differentiate field waxes from paraffin waxes. Field waxes usually consist of a mixture of heavy hydrocarbons such as asphaltenes, resins, paraffins (or paraffin waxes), cyclo-paraffins, and heavy aromatics. Wax precipitation primarily depends on fluid temperature and composition and it is dominated by van der Waals or London dispersion type of molecular interactions. Pressure has a smaller effect on wax precipitation. As with asphaltenes, the fact that waxes precipitate at some and not at other thermodynamic states, for a given fluid, indicates that there is a portion of the thermodynamic space that is enclosed by some boundary within which waxes precipitate. This bounded thermodynamic space has been given the name Wax Deposition Envelope, WDE (Leontaritis, 1995). A typical WDE is shown in Fig. 3.20.

The upper WDE boundary can have either a positive slope or a negative slope. In most cases where the WDE has been obtained experimentally the upper WDE boundary was very close to a vertical line.

The intersection of the WDE boundary with the bubble-point line is generally expected to be to the left of the onset of wax crystallization (cloud point) of the stock tank oil. This has been the case with

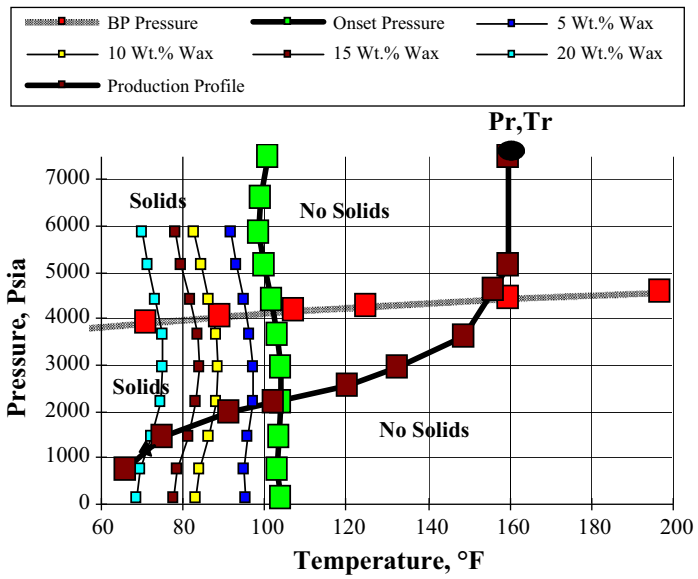

FIGURE 3.20

Typical wax deposition envelope (Leontaritis, 1995).

many reservoir fluids whose WDE has been measured (Leontaritis, 1995). This is due to the fact that light ends, when pressured into oil, usually cause a suppression of the onset of wax crystallization temperature. The actual shape of the lower WDE boundary is primarily a function of the compositions of the intermediates and light ends of the reservoir fluid. The technology for measuring WDEs has been perfected only recently. Because the technology is new and the cost of measurements is relatively high, most companies do not find it economical to obtain the complete WDE of their reservoir fluid through laboratory measurements. Hence, obtaining only a few experimental data points and using them to fine-tune phase behavior models that are then used to calculate the remaining WDE more economically is preferred. It should be noted that most of these models have very little predictive capacity at this time and they are primarily used as combination correlational-predictive type of tools. One of the main reasons for the lack of pure predictive capability is improper or inadequate crude oil characterization (Leontaritis, 1997a).

3.8.3.1.2 Gas–Condensate Wax Deposition Envelope

Some gas condensates, especially rich gas condensates with yields in excess of 50 bbls/MMSCF, are known to contain high carbon number paraffins that sometimes crystallize and deposit in the production facilities. The obvious question is: what is the shape of the thermodynamic envelope (i.e., P and T surface) of these gas condensates within which waxes crystallize? Or, in order to maintain the previous terminology, what is the WDE of gas condensates typically?

The shapes of the WDEs of two gas condensates in the Gulf of Mexico are presented here. The shapes of the above WDEs indicate potential wax deposition in those cases where the gas condensate contains very high carbon number paraffins that precipitate in solid state at reservoir temperature. In

other words, the temperature of the reservoir may not be high enough to keep the precipitating waxes in liquid state. Hence, the gas condensate, which is a supercritical fluid, enters the WDE at the "dew point" pressure. This casts new insight into the conventional explanation that the productivity loss in gas condensate reservoirs, when the pressure near the wellbore reaches the dew point, is only due to relative permeability effects.

Fig. 3.21 shows the Vapor–Liquid envelope (V–L envelope) of what one might call a typical Gulf of Mexico gas condensate. This gas condensate (called Gas Condensate "A" for our purposes here) was analyzed with PARA (Paraffin-Aromatic-Resin-Asphaltene) analysis (Leontaritis, 1997a) and found to contain normal paraffins with carbon numbers exceeding 45. The V–L envelope was simulated using the Peng and Robinson (1976) original equation of state (EOS) that had been fine-tuned to PVT data obtained in a standard gas–condensate PVT study. The first question that was addressed in a wax study involving this fluid was: what happens as the fluid is cooled at some constant supercritical pressure? What actually happened is shown in Fig. 3.22.

Fig. 3.22 shows several onset of wax crystallization data points obtained with the NIR (Near-Infra-Red) equipment (Leontaritis, 1997b) by cooling the Gas Condensate "A" at different constant pressures. It was evident from the NIR data that there was a thermodynamic envelope, similar to the one defined and obtained experimentally for oils, to the left of which (i.e., at lower temperatures) wax crystallization occurred. The complete wax deposition envelope shown in Fig. 3.22 is calculated with a previously tuned wax phase behavior model (Narayanan et al., 1993). Despite the clarity of the WDE obtained for Gas Condensate "A" as shown in Fig. 3.22, more data were needed to confirm the

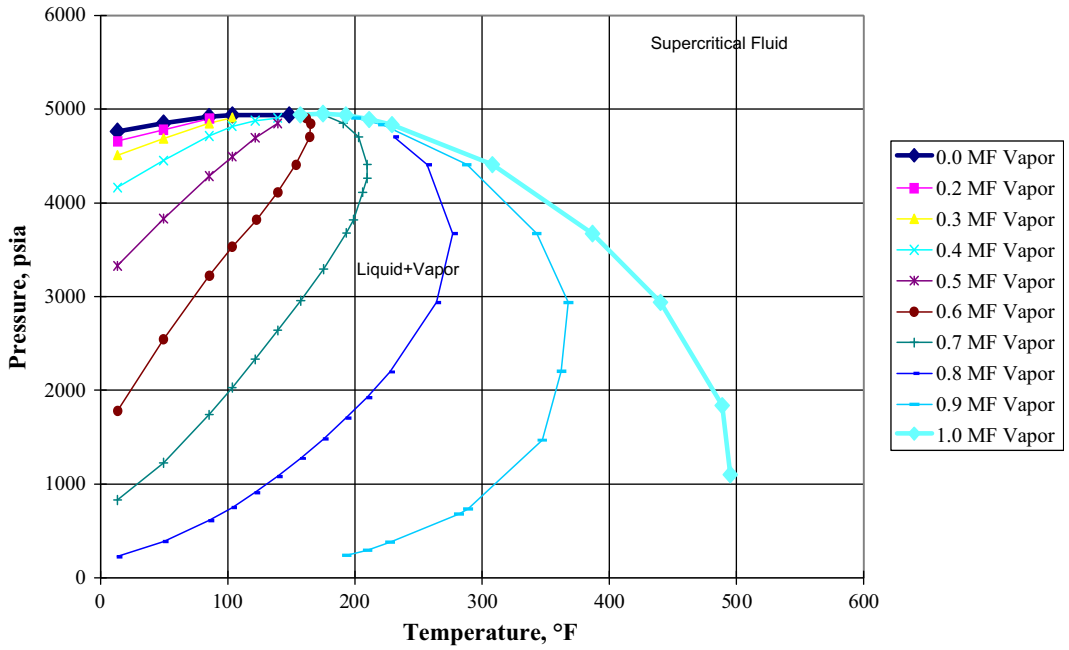

FIGURE 3.21

Vapor–Liquid envelope, Gulf of Mexico Gas–Condensate "A" (Leontaritis, 1998).

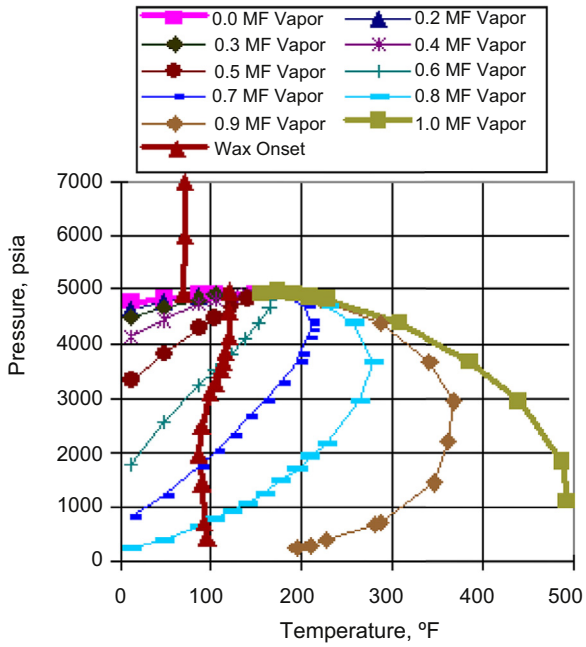

FIGURE 3.22

Wax deposition envelope, Gulf of Mexico Gas–Condensate "A" (Leontaritis, 1998).

presence of WDE in other condensates and establish its existence as a standard thermodynamic diagram.

Fig. 3.23 shows the V–L envelope of another typical Gulf of Mexico condensate. This condensate (called Gas Condensate "B" for our purposes here) also contains paraffins with carbon numbers exceeding 45, although the data show that Gas Condensate "B" is lighter than Gas Condensate "A." The V–L envelope was again simulated using the Peng and Robinson (1976) original EOS after it had been tuned to PVT data obtained in a standard gas condensate PVT study.

Fig. 3.24 shows the NIR onset data superimposed on the V-L envelope. It is evident again from the NIR data that there is a thermodynamic envelope to the left of which (i.e., at lower temperatures) wax crystallization occurs. Once again, the complete wax deposition envelope shown in Fig. 3.24 was calculated with a previously tuned wax phase behavior model (Narayanan et al., 1993).

Data presented here confirm the presence of a WDE in gas condensates that contain high carbon number paraffin waxes ($\geq$45). This WDE is similar to oil WDEs and as a result it should be considered a standard thermodynamic diagram. The shape of the WDE inside the V-L envelope seems to be consistent with existing information regarding the effect of light hydrocarbons on the onset of wax crystallization or wax appearance temperature. That is, as the pressure rises the WDE tilts to the left (negative slope) due to the ability of light hydrocarbons to depress wax crystallization. However, at the pressure where retrograde condensation begins the WDE turns forward thus acquiring a positive slope. This is because the light ends begin to vaporize and the waxes remaining in the liquid phase begin to

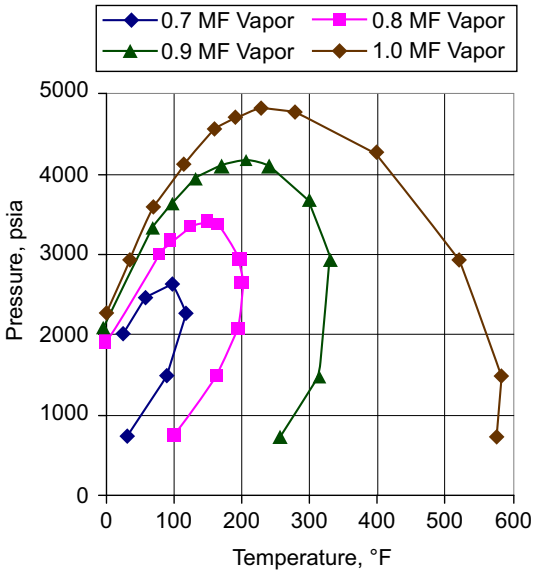

FIGURE 3.23

Vapor–Liquid envelope, Gulf of Mexico Gas–Condensate "B" (Leontaritis, 1998).

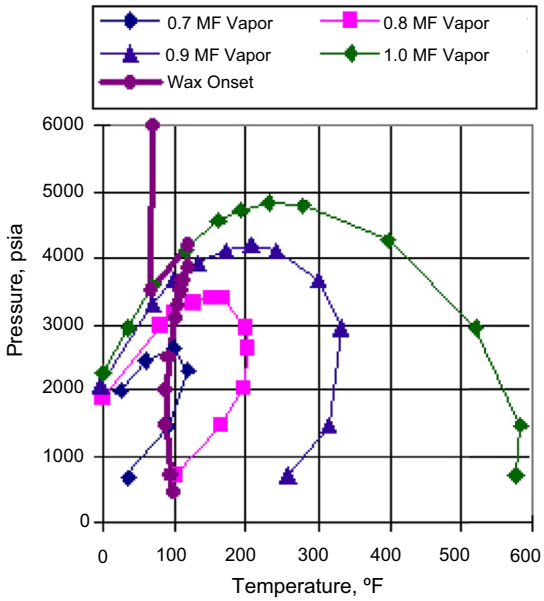

FIGURE 3.24

Wax deposition envelope, Gulf of Mexico Gas Condensate "B" (Leontaritis, 1998).

concentrate. This is simply caused by the change in normal paraffin concentration which in turn is caused by retrograde concentration. In most condensates the V-L envelope is fairly horizontal at the saturation line (dew point or bubble point). Hence, when this general pressure is reached the WDE seems to coincide with the V-L saturation line until the temperature becomes low enough for the waxes to begin crystallizing from the supercritical condensate. This is in agreement with prior observations that indicate a substantial increase in the solvent power of some fluids when they become supercritical (i.e., propane, CO_2, etc.). That is, supercritical hydrocarbon fluids are expected to require cooling to much lower temperatures before paraffin waxes begin to crystallize because of their increased solvent power.

3.8.3.2 Wax Formation in Multiphase Gas–Condensate Pipelines

When the production pressure and temperature profile of a gas condensate cross the WDE and the Hydrate Envelope (HE), waxes and hydrates may form. The formed hydrates can grow in mass and yield strength to the point that they restrict and finally stop the flow. If the waxes form while the liquid is in contact with the wall, some of them should attach to the wall thus resulting in wax deposition. The P-T diagram of a Gulf of Mexico gas–condensate as shown in Fig. 3.25 demonstrates the above situation.

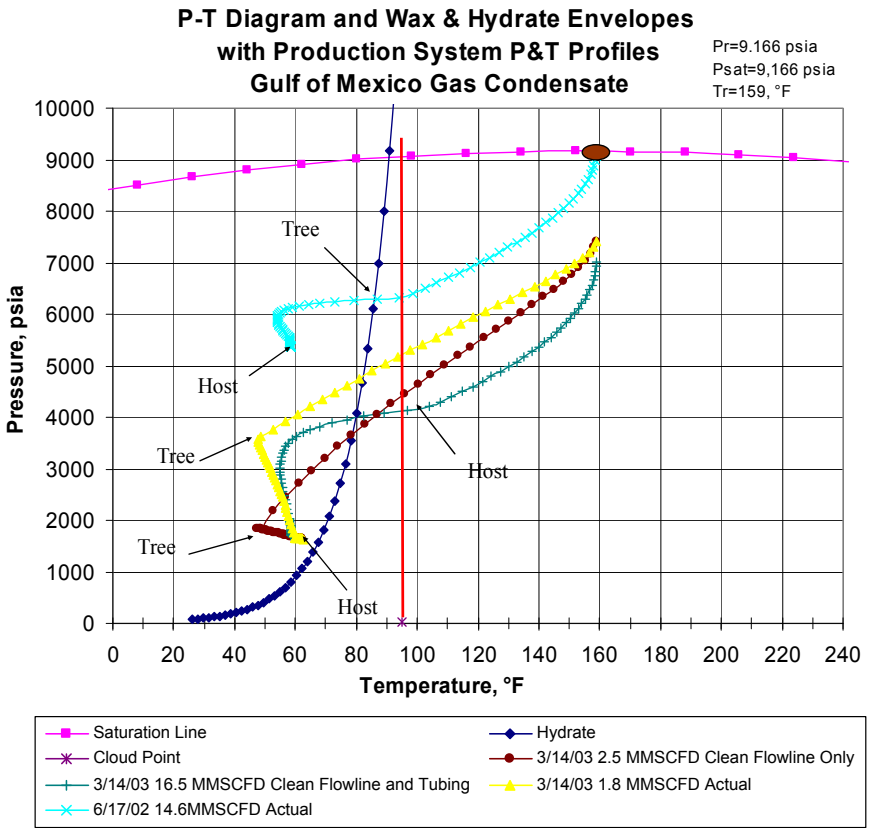

FIGURE 3.25

Gulf of Mexico gas–condensate wax and hydrate deposition envelopes (AsphWax's Flow Assurance course, 2003).

The diagram indicates that there was not any live NIR done with this fluid. The only point on the WDE that was measured was the cloud point of the condensate, shown in the diagram at 95°F at the bottom of the orange vertical line. The clean tubing and flow line of this system would deliver about 14.5 MMSCFD. From the light blue P and T profile line and dark blue hydrate line, it was very clear at the outset that the main flow assurance issues in this system would be hydrate and wax formation and deposition. Hence, because of this illustrative important information, the effort to obtain the above diagram is obviously very worthwhile.

Sometimes oil and gas operators decide to design the facilities such that their operation is to the left of the WDE and HE (such as the example in Fig. 3.25). In these situations, wax and hydrate formation takes place if the fluids are left untreated with chemicals. In the above example, methanol was injected to inhibit successfully the formation of hydrates formed due to the production of reservoir equilibrium water. However, because the operator was not aware of the wax phase behavior of this condensate at startup, no wax chemical was injected. Wax deposition was severe enough to cause the production rate to drop down to 1.8 MMSCFD on March 14, 2003. The estimated maximum production rate via simulation on March 14, 2003was 16.5 MMSCFD. The data in the plot show that the maximum friction loss was in the upper part of the tubing. Indeed, the yellow P and T line shows that the wax deposition and hydrate envelopes were being crossed in the tubing at that time.

3.8.3.2.1 Identification of Wax Deposition Problems

A rather simple chart that allows daily monitoring of wax deposition problems in multiphase gas–condensate pipelines is shown in Fig. 3.26.

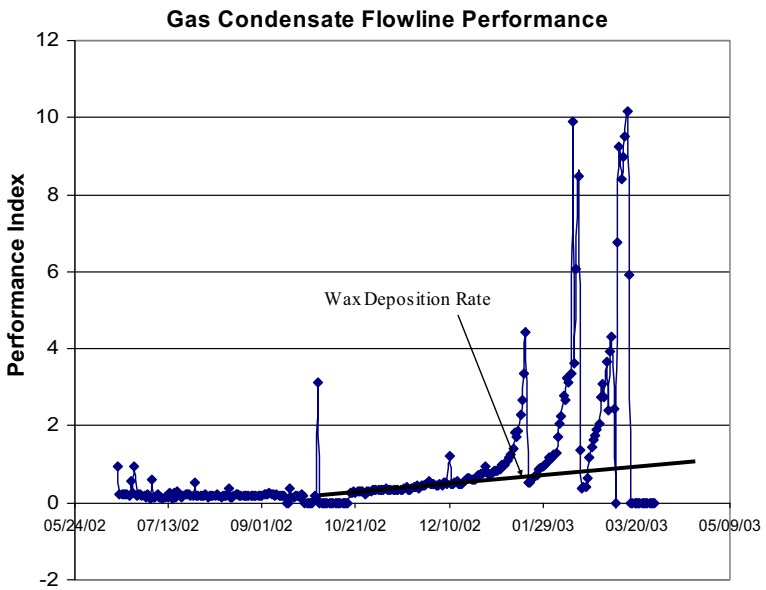

FIGURE 3.26

Gas–condensate flow line performance index (AsphWax's Flow Assurance course, 2003).

The above performance chart is for the gas condensate shown in Fig. 3.25. The above chart was made by plotting the Performance Index (PI) versus time. The PI is calculated from the following equation:

$$PI = \frac{\Delta P^2}{Q^{1/0.54}} \tag{3.61}$$

where ΔP is the pressure drop in the pipeline, psi and Q is the flow rate, MMSCFD.

The performance index (PI) should remain as a horizontal straight line during production if there is no restriction formed in the line. It is evident in Fig. 3.26 that around October 21, 2002 a restriction was being formed in the line. At the beginning of January there was a very sharp loss of hydraulic capacity. This cannot be due to wax deposition because the rate of wax deposition does not change so sharply in a produced fluid. Indeed, the sharp rise in the PI was caused by hydrate formation that occurred on top of wax crystal formation and deposition. Several sharp rises in PI followed caused by hydrates until it was determined that the well started producing free water and required a much higher methanol injection rate. While all of this is happening with the advent of water and hydrate formation the wax deposition rate was increasing steadily, as shown in the chart.

It should be noted that the engineer needs to be very careful in attributing a rise in the PI only to wax and hydrates. One needs to make sure that other culprits such as fines, salts, returning drilling and completion fluids, etc. are not present.

3.8.3.2.2 Wax Deposition Inhibition/Prevention

It is not always clear to the engineer what would be the wax deposition mechanism and what type of chemical treatment would be the most effective in gas condensate situations. In oil flow lines, wax deposition occurs by diffusion of wax molecules and crystals toward and attachment at the wall. Prevention or inhibition of wax deposition is mainly accomplished by injection of a special class of molecules that interact with paraffin molecules at temperatures above the cloud point and influence their crystallization process in a way that diminishes the attraction of the formed crystals toward the wall. The inhibited formed wax crystals are removed from the system by the shear forces caused by the flowing oil.

The above mechanism occurs when the wax crystal forms at the wall. This is the case with most liquid filled bare (uninsulated) lines. The two important requirements are fast heat transfer and fast diffusion of paraffin molecules toward the wall. This is not the case in many situations of flow lines carrying gas condensates. There is fast cooling but the majority of the gas cools down while in the main flow thus forming wax crystals with the main flow that would have a tendency to deposit or sediment by gravity in the liquid holdup. Also, the liquid that forms near the inlet of the bare line that has not reached its cloud point cools with a velocity that is almost standstill compared to the main flow. Slugging in this case would be beneficial in removing wax slush from the line. Additionally, these flow lines are essentially soaked in methanol to prevent hydrate formation. It just so happens that most (if not all) chemicals with wax crystal modification properties, as discussed later, are incompatible with alcohols and glycols. Hence, the inhibited wax crystals accumulate in the flow line in the liquid holdup thus adding to the wax accumulation. This accumulation forms what has been called “wax slush.” This wax slush is viscous but it moves and can flow given enough shear force.

The above theory has been documented several times from field data. In the year 2000 enough production and laboratory data and simulations were available to make the case for one field, but there was no direct evidence of wax slush from the field. During a shutdown caused by a hurricane, the flow line was depressurized at the tree, in an effort to dissolve any existing hydrates. At startup, the well was started very fast to try to initiate movement and flow of any liquids (via an induced slug) and the previously theorized existing "wax slush." The fast flow did mobilize a phase that was loaded with wax. The wax slush flowed into the separators and plugged lines and equipment making them temporarily incapable of operation.

It is appropriate at this time to give a brief description of the main two chemical classes used to treat wax deposition. There are three types of wax crystals: plate crystals, needle crystals, and mal or amorphous crystals.

Paraffinic oils form plate or needle crystals. Asphaltenic oils form primarily mal or amorphous crystals. Asphaltenes act as nucleation sites for wax crystal growth into mal crystals.

Plate crystals look as their name implies like plates under the microscope. Needle crystals look like needles and mal crystals are amorphous and generally like small round spheres. The interaction between crystals and pipe wall increases from mal to needle to plates. Thus, maintaining newly formed wax crystals small and round, i.e., like mal crystals, is desirable.

The behavior and properties, e.g., cloud point and pour point, of paraffin crystals precipitating from a hydrocarbon can be affected in three ways:

1. Crystal size modification: modification of the crystal from larger sizes to smaller sizes.
2. Nucleation inhibition: inhibition of the growth rate of the crystal and its ultimate size.
3. Crystal type or structure modification: that is modification of the crystal from one type to the other. For instance, modify a crystal from needle to mal type.

A wax crystal modifier works primarily to modify the crystal size. The plate crystals of an n-paraffin look much smaller under the microscope when precipitating from hydrocarbons inhibited with a wax crystal modifier. Smaller crystals have lower molecular weights and thus higher solubility in oil. Furthermore, smaller particles have smaller energy of interaction among themselves and the pipe wall. A crystal modifier interrupts the normal crystal growth of the n-paraffins by inserting itself in the crystal and thus stopping its growth.

It is noted that another name for a wax crystal modifier is pour point depressant or PPD. As the name implies, wax crystal modifiers are very effective at suppressing the pour points of crude oils because they suppress the wax crystal growth and thus minimize the strength of their interactions.

A wax dispersant may act to inhibit wax nucleation and change the type of wax crystals from plate or needle to mal or amorphous. Inhibited amorphous crystals are smaller and carried much easier by the hydrodynamic drag of the flowing fluid. The presence of asphaltenes and resins facilitates the effect of the dispersant. The dispersant interacts with the asphaltenes and resins and ties them up thus removing nucleation sites required by wax crystals to grow. A dispersant, when added to the oil at a temperature above the cloud point, has occasionally an additional benefit of suppressing the cloud point by interacting with and tying up the asphaltenes and resins that tend to come out first. A dispersant tends to usually disperse the wax particles at the water−oil interface.

Both wax crystal modifiers and wax dispersants are useful chemicals that have the ability to diminish wax formation and deposition, although through different mechanisms. Wax dispersants are usually much smaller in molecular weight and size than wax crystal modifiers. Hence, their viscosity

and flow properties in general are more favorable in cold applications. Also, some wax dispersants are soluble with alcohols and glycols thus making them compatible for simultaneous injection. The selection of the wax chemical should be made after careful consideration of the produced hydrocarbon and facilities.

3.8.3.2.3 Wax Deposit Remediation

On occasion, if a substantial amount of wax accumulates in the line, as evidenced by the PI chart such as the one shown in Fig. 3.26, a temporary shutdown to do a chemical soak, with a potential modification to the chemical to give it more penetrating power at cold temperatures, and fast startup might be necessary to cause the wax slush cough.

Pigging is an option, but only after very careful consideration of the system's performance to understand the dynamics of the moving pig and continuous removal of the wax cuttings ahead of it. This is a very difficult job. Controlling the bypass of flow around the pig for such a purpose is difficult. Hence, many pigging operations end up in failure with stuck pigs. The pigging analysis and decision must be left to true experts. Starting a pigging program at the beginning of the life of the system has a better chance of success than at any other time. Even then, excellent monitoring of the system's PI is a must. It is recommended that a short shutdown, chemical soak, and fast startup be considered first, because it is the safest option.

3.8.3.2.4 Controlled Production of Wax Deposits

From a technical standpoint, spending enough capital initially to design the facilities to operate outside the wax and hydrate forming conditions or to the right of the WDE and HE is obviously the best solution. However, very often in practice, controlling wax deposits during production is preferred because of the lower facilities cost. Economically marginal fields can only be produced under this scenario. Hence, in these cases, the following three options prevail:

1. pigging only
2. chemical injection only
3. combination of pigging and chemical injection

Whilst frequent pigging of the line clears up any wax deposits, it may be necessary to chemically inhibit wax deposition during times when pigging is unavailable. Pigging often is inadequate or uneconomical, unless used in conjunction with a chemical treatment program. This program is often performed into two stages: (1) removal of wax deposits in the production/transmission lines and (2) continuous chemical injection or periodic treatment (such as batch treatments, etc.) in order to ensure pipeline integrity.

Chemical injection is the safest of the three, if good technical support and testing are available. The approach is discussed as follows:

1. Inject a strong chemical dispersant/inhibitor down hole to keep the formed wax particles small and suspended in the flow line. The majority of them would be carried away with the gas/liquid flow.
2. The chemical dispersant/inhibitor must be compatible and soluble with methanol to prevent precipitation of the chemical itself in the line.

3. Monitor the hydraulics in the flow line and occasionally, if necessary, cause a "slug" or "cough" to cough-up any accumulated wax.
4. On occasion, if a substantial amount of wax accumulates in the line, a temporary shutdown to do a chemical soak, with a modification to the chemical to give it more penetrating power at cold temperatures, and fast startup might be necessary to cause the wax slush cough.

When properly implemented, the above approach should provide the lowest cost wax deposition control in gas–condensate transmission lines.

3.8.4 SLUGGING

Slugging, which refers to varying or irregular flows of gas and liquids (or liquid surges) in pipelines, is a major flow assurance challenge. Slug flow can pose serious problems to the designer and operator of two-phase flow systems. Large and fluctuating rates of gas and liquid can induce severe mechanical vibrations in the pipe, and severely reduce the production and in the worst case shut down or damage downstream equipment like separator vessels and compressors. As a result, prediction of slug characteristics is essential for the optimal, efficient, safe, and economical feasible design and operation of two-phase gas–liquid slug flow systems.

Slugging can take several forms (hydrodynamic slugging, terrain/riser induced slugging, and operationally induced slugging) that will be discussed here.

3.8.4.1 Hydrodynamic Slugging

Hydrodynamic slugs are formed by growing of waves on the gas–liquid interface in the stratified flow under certain flowing conditions, where the amplitude of these waves becomes sufficiently large and they can bridge the pipe. Hydrodynamic (normal) slugs tend to be longer, the pipe can, unfortunately, be thousands of feet long. Brill et al. (1981) noted from field tests at Prudhoe Bay that not all slugs are of the same length and that a log-normal distribution was observed.

When hydrodynamic slugs are numerous, the pipeline is said to be operating in the slug flow regime. Hydrodynamic slugs travel through a pipeline and can cause significant damage to, or operational problems for, downstream equipment. A usual design practice is to find the volume of the large slugs and design a separator or slug catcher able to handle this. There are two main methods that are typically used for slug size prediction: the simple correlation of field data, and transient one-dimensional slug-tracking simulators, which use empirical correlations to compensate for the fact that their one-dimensional models cannot model these mechanisms directly. The simple correlations have been developed by correlating field slugging results to key parameters such as flow line diameter and fluid physical properties. However, these correlations ignore the important effect of line topography, and therefore give misleading results. Slug-tracking simulators give reasonable predictions when they will be tuned to field data. However, their ability to make a priori predictions of slug flow (including slug size and frequency) remains limited. Therefore, good design practice still requires the application of healthy design margins (FEESA, 2003).

3.8.4.2 Terrain Induced Slugging

In pipes across an undulating terrain, a major cause of slugging is the topography. Liquid tends to build up and sit at the lowest points of the pipeline, until it is forced onwards through the rest of the pipe by the pressure of the gas caught behind. Terrain slugging is most likely to occur at low flow rates, with a low pipeline pressure. When terrain-induced slugging is predicted, slugs will only form in upwardly

inclined section of flow line. These slugs are unlikely to persist throughout the length of the line. Instead they will steadily decay and then collapse in horizontal or downwardly inclined sections (Bendiksen et al., 1986).

Terrain induced slugging is highly undesirable due to the long-duration instabilities and the related oscillating momentum which can damage process equipment and necessitate major slug catchers. A mechanistic model or a transient program can provide a more realistic estimate of the terrain slug characteristics (McGuinness and McKibbin, 2002). During production, the length and velocity of a slug can be also estimated by monitoring the pressure variation at the outlet of the pipeline.

3.8.4.3 Riser Induced (Severe) Slugging

Terrain induced slugging at a pipeline-riser system is denoted severe slugging. For this system liquid will accumulate in the riser and the pipeline, blocking the flow passage for gas flow. This results in a compression and pressure build-up in the gas phase that will eventually push the liquid slug up the riser and a large liquid volume will be produced into the separator that might cause possible overflow and shut down of the separator. The severe slugging phenomenon is very undesirable due to pressure and flow rate fluctuations, resulting in unwanted flaring and reducing the operating capacity of the separation and compression units (Schmidt et al., 1980). Figs. 3.27 and 3.28 show example time traces for the riser outlet liquid and gas flow rates during severe slugging, respectively. These figures show the large surges in liquid and gas flow rates accompanying the severe slugging phenomenon. Clearly such large transient variations could present difficulties for topside facilities unless they are designed to accommodate them.

Usually, the operators try not to operate in the severe slugging region. But, the inlet conditions of a production pipeline are linked to the number and the capacity of the producing wells, the availability of wells, and also to some undesirable operation such as shut down or restart. The natural trend when dimensioning a production line is to do whatever is possible to avoid critical flooding of the separator, and therefore to over dimension the separator unit. But in offshore production, over dimensioning the

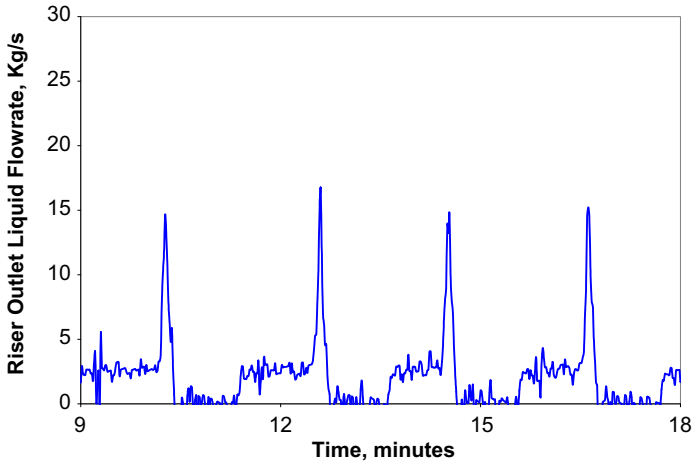

FIGURE 3.27

Example time trace of the riser outlet liquid flow rate during severe slugging (Mokhatab, 2007).

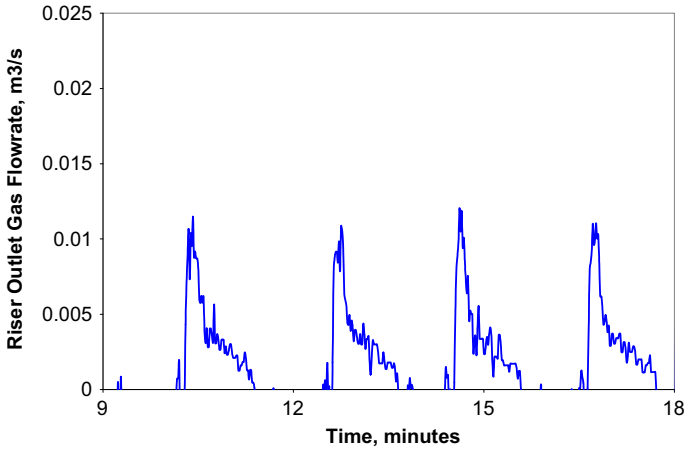

FIGURE 3.28

Example time trace of the riser outlet gas flow rate during severe slugging (Mokhatab, 2007).

installation is very costly and not always possible. So, the design engineers require more accurate dynamic simulations to correctly design and dimension their production schemes (which are more sensitive to transients occurring when slug flow conditions build-up, and require high performance control systems to maintain the plant within the preset operating ranges), and to be able to propose new concepts suitable to every situation they can be faced to (Sagatun, 2004). The prediction of pipeline simulation with respect to slug dynamics will be strongly affected by the specification of boundary conditions. Hence, a tight integration of the hydrodynamic model of pipeline-riser system with the dynamic model of the receiving plant is very important for achieving correct simulation results, especially for studying severe slugging dynamics (Mokhatab and Towler, 2007a).

Given these potential problems of severe slugging in such systems, an understanding of how and when severe slugging will form, as well as providing significant information on the best method to prevent and control this phenomenon is highly necessary.

Although the research community has undertaken a thorough exposition of severe slugging phenomenon in flexible risers, there is a lack of sufficiently wide ranging and openly available transient code testing and full scale data on flexible risers for better understanding of the physics and characteristics of severe slugging and carrying out more vigorous verification (Mokhatab and Towler, 2007b). Unless such a vigorous link with reality is maintained, designers and operators will not have the confidence to expand the use of flexible risers in more critical applications.

3.8.4.3.1 Severe Slugging Mechanism

The process of severe slugging in a pipeline-riser system consists of four steps; (1) slug formation, (2) slug production, (3) bubble penetration, and (4) gas blow down. This phenomenon had been previously identified by Schmidt et al. (1980) as a cyclic flow rate variation, resulting in periods both of no flow and very high flow rates substantially greater than the time average. Fig. 3.29 illustrates the stages of a severe slugging cycle.

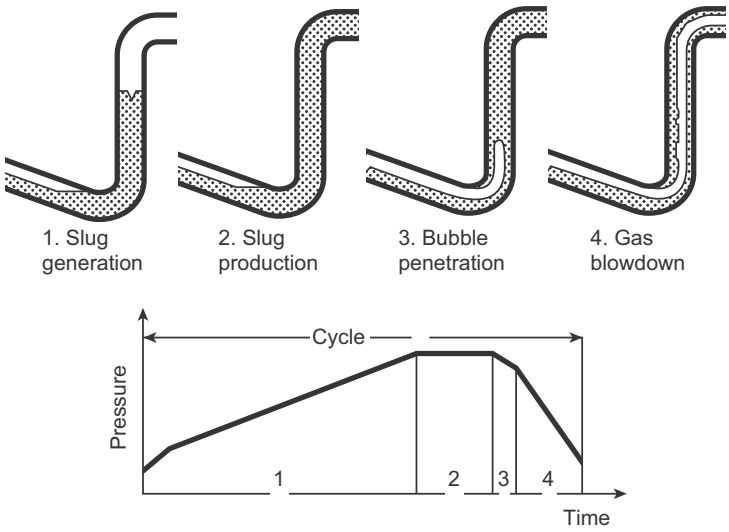

FIGURE 3.29

Description of severe slugging in pipeline/riser systems (Fabre et al., 1990).

The first step, slug formation, corresponds to an increase of the pressure in the bottom of the riser. The liquid level does not reach the top of the riser. During this period, the liquid is no longer supported by the gas and begins to fall, resulting in the riser entrance blockage and the pipeline pressure buildup until the liquid level in the riser reaches to the top. During the second step, slug production, the liquid level reaches the riser outlet, and the liquid slug begins to be produced until the gas reaches the riser base. In third step, bubble penetration, gas is again supplied to the riser, so the hydrostatic pressure decreases. As a result, the gas flow rate increases. The fourth step corresponds to gas blow down. When the gas produced at the riser bottom reaches the top, the pressure is minimal and the liquid is no longer gas-lifted. The liquid level falls and a new cycle begins (Fabre et al., 1990). This cyclic process becomes steady state when the rate of penetration of the gas into the riser is always positive. However, it is also possible that the penetration of the gas into the riser becomes zero. In this case, liquid blocks the bottom of the riser. This is followed by a movement of the liquid interface into the pipeline and blocking of the gas passage into the riser until the liquid interface reaches the bottom of the riser. At this point, penetration of gas into the riser starts and a new cycle begins again.

When liquid penetrates into the pipeline, the gas in the riser propagates to the top until all of the gas in the riser disappears. When the liquid input is very low, the propagation of the gas towards the top of the riser causes accumulation of all the gas at the top as the liquid falls back. This process is termed cyclic process with fallback, while the former case is termed cyclic process without fallback. In summary, three different possibilities that can occur as a result of penetration of gas into a liquid column in a quasi-steady severe slugging process are identified (Jansen et al., 1996):

1. penetration of the gas that leads to oscillation, ending in a stable-steady state flow,
2. penetration of the gas that leads to a cyclic operation without fall back of liquid, and

3. penetration of the gas that leads to a cyclic operation with fall back of liquid.

Severe slugging in a pipeline-riser system can be considered as a special case of flow in low velocity hilly terrain pipelines, which are often encountered in offshore fields. This is a simple case of only one downward inclined section (pipeline), one riser, and constant separator pressure. For this reason, severe slugging has been termed "terrain-induced slugging." This phenomenon has also various names in the industry, including "riser-base slugging" and "riser-induced slugging."

3.8.4.3.2 Stability Analysis

The flow characteristics of a multiphase flow in a pipeline-riser system are divided into two main regions, stable (steady flow) region and unstable (pressure cycling) region, in which the stability line on the flow pattern map separates the two regions. The steady region includes acceptable slugging, annular-mist, and bubble flows, while the pressure cycling region includes the severe slugging and transitional flows. Fig. 3.30 shows a typical flow map for a pipeline-riser system developed by Griffith and Wallis (1961) featuring regions of stable and unstable behavior. In the figure, N_{Fr} and λ_G are the Froude number of two-phase gas/liquid flow and no-slip gas holdup, defined previously. As can be seen from that figure, at low Froude numbers, bubble flow prevails and fluids will flow through riser pipes without slug formation. However, as Froude number increases the slug flow range is entered.

The stability analysis predicts the boundary between stable and unstable regions, where the resultant stability map helps the engineer to design systems that operate well into the stable zone thus offering an adequate margin of safety. The stability analysis seek to model a particular process required for severe slugging and hence predicts the likelihood of severe slugging, as such these stability models are termed criteria for severe slugging. The severe slugging process was first modeled by Schmidt et al. (1980); however, their model formed the basis of much of the early works for the stability of severe slugging. A review of the existing stability criteria for predicting severe slugging in a pipeline-riser system can be found in Mokhatab (2010).

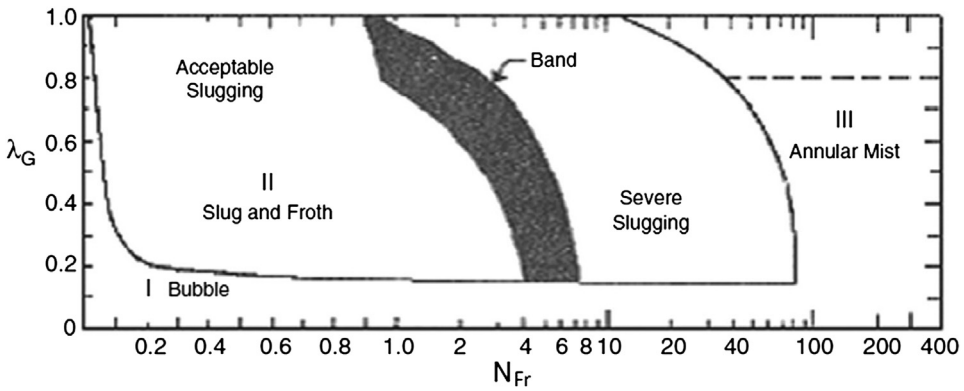

FIGURE 3.30

Griffith and Wallis flow pattern map with Yocum (1973) transition band (Brill and Beggs, 1991).

3.8.4.3.3 Prevention and Control of Severe Slugging

The flow and pressure oscillations due to severe slugging phenomenon have several undesirable effects on the downstream topside facilities unless they are designed to accommodate them. However, designing the topside facilities to accept these transients may dictate large and expensive slug catchers with compression systems equipped with fast responding control systems. This may not be cost-effective and it may be more prudent to design the system to operate in a stable manner (Sarica and Tengesdal, 2000). While lowering production rates (slowing fluid velocity) can minimize severe slugging, operators are investigating alternatives that would allow for maximum production rates without the interruptions caused by slugs (Furlow, 2000). Mokhatab et al. (2007a) provide a combination of industrial experience and information from the literature to compile a list of methods of remediating the problems associated with severe slugging in pipeline-riser systems. In general, the severe slugging prevention and elimination strategies seek three following approaches.

3.8.4.3.3.1 Riser Base Gas Injection. This method provides artificial lift for the liquids, moving them steadily through the riser. This technique can alleviate the problem of severe slugging by changing the flow regime from slug flow to annular or dispersed flow, but does not help with transient slugging in which the liquid column is already formed before it reaches the riser base. It is one of the most frequently used methods for the current applications. However, for deepwater systems increased frictional pressure loss and Joule–Thomson cooling are potential problems resulting from high injection gas flow rates.

The riser base gas injection method was first used to control hydrodynamic slugging in vertical risers. However, Schmidt et al. (1980) dismissed it as not being economically feasible due to the cost of a compressor or pressurizing the gas for injection, and piping required to transport the gas to the base of the riser. Pots et al. (1985) investigated the application of the method to control severe slugging. They concluded that the severity of the cycle was considerably lower for riser injection of about 50% inlet gas flow. Hill (1990) described the riser-base gas injection tests performed in the S.E. Forties field to eliminate severe slugging. The gas injection was shown to reduce the extent of severe slugging.

The riser base gas lift method may cause additional problems due to Joule–Thomson cooling of the injected gas, where the lift gas will cause cooling and make the flow conditions more susceptible for the wax precipitation and hydrate formation. Hence, Johal et al. (1997) proposed an alternative technique "multiphase riser base lift" that requires nearby high capacity multiphase lines diverted to the pipeline-riser system that alleviate the severe slugging problem without exposing the system to other potential problems.

Sarica and Tengesdal (2000) proposed a new technique for sourcing riser base gas lift. The principle of the proposed technique is to connect the riser to the downward inclined segment of the pipeline with a small diameter conduit, where the conduit will transfer the gas from the downward inclined segment to the riser at points above the riser base (multiposition gas injection). The transfer process reduces both the hydrostatic head in the riser and the pressure in the pipeline consequently lessening or eliminating the severe slugging occurrence. This method can be considered as self-gas lifting. Sarica and Tengesdal (2000) claimed that the proposed technique is expected to increase production since it does not impose additional backpressure to the production system. The cost of implementing and operation of the proposed systems in the field application are also expected to be low compared to other elimination methods.

3.8.4.3.3.2 Topside Choking. This method induces bubble flow or normal slug flow in the riser by increasing the effective backpressure at the riser outlet. While, a topside choke can keep liquids from

overwhelming the system, it cannot provide required control of the gas surges that might be difficult for the downstream system to manage. This is a low-cost slug-mitigation option, but its application might be associated with considerable production deferment.

Topside chocking was one of the first methods proposed for the control of severe slugging phenomenon (Yocum, 1973). Yocum observed that increased backpressure could eliminate severe slugging but would severely reduce the flow capacity. Contrary to Yocum's claim, Schmidt et al. (1980) noted that the severe slugging in a pipeline-riser system could be eliminated or minimized by choking at the riser top, causing little or no changes in flow rates and pipeline pressure. Taitel (1986) provided a theoretical explanation for the success of choking to stabilize the flow as described by Schmidt et al. (1980).

Jansen et al. (1996) investigated different elimination methods such as gas lifting, chocking, and gas lifting and chocking combination. They proposed the stability and the quasi-equilibrium models for the analysis of the above elimination methods. They experimentally made three observations; (1) large amounts of injected gas were needed to stabilize the flow with the gas-lifting technique, (2) careful chocking was needed to stabilize the flow with minimal backpressure increase, and (3) gas-lifting and chocking combination were the best elimination method reducing the amount of injected gas and the degree of choking to stabilize the flow.

3.8.4.3.3.3 Control Methods. Control methods (feed forward control, slug choking, and active feedback control) for slug handling are characterized by the use of process and/or pipeline information to adjust available degrees of freedom (pipeline chokes, pressure, and levels) to reduce or eliminate the effect of slugs in the downstream separation and compression unit. Control based strategies are designed based on simulations using rigorous multiphase simulators, process knowledge, and iterative procedures. To design efficient control systems, it is therefore advantageous to have an accurate model of the process (Bjune et al., 2002).

The feed-forwarded control aims to detect the buildup of slugs and, accordingly, prepares the separators to receive them, e.g., via feed-forwarded control to the separator level and pressure control loops. The aim of slug choking is to avoid overloading the process facilities with liquid or gas. This method makes use of a topside pipeline choke by reducing its opening in the presence of a slug, and thereby protecting the downstream equipment (Courbot, 1996). Like slug choking, active feedback control makes use of a topside choke. However, with dynamic feedback control, the approach is to solve the slug problem by stabilizing the multiphase flow. Using feedback control to prevent severe slugging has been proposed by Hedne and Linga (1990), and by other researchers (Molyneux et al., 2000; Havre and Dalsmo, 2001; Bjune et al., 2002). The use of feedback control to stabilize an unstable operating point has several advantages. Most importantly, one is able to operate with even, nonoscillatory flow at a pressure drop that would otherwise give severe slugging. Fig. 3.31 shows a typical application of an active feedback control approach on a production flow line/pipeline system, and illustrates how the system uses pressure and temperature measurements (PT and TT) at the pipeline inlet and outlet to adjust the choke valve. If the pipeline flow measurements (FT) are also available, these can be used to adjust the nominal operating point and tuning parameters of the controller.

Note, the response times of large multiphase chokes are usually too long for such a system to be practical. The slug suppression system (S3) developed by Shell has avoided this problem by separating the fluids into a gas and liquid stream, controlling the liquid level in the separator by throttling the liquid stream and controlling the total volumetric flow rate by throttling the gas stream. Hence, the gas

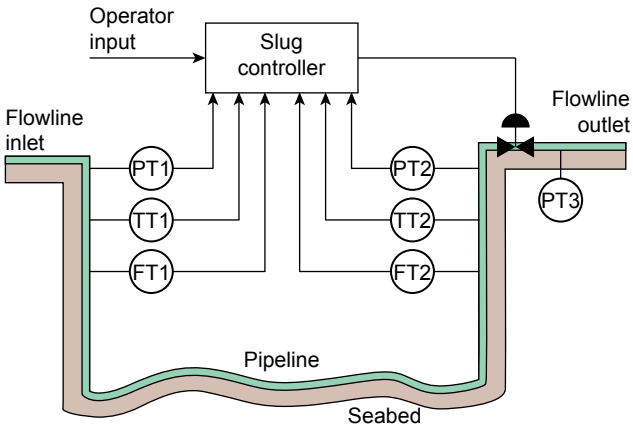

FIGURE 3.31

Typical configuration of a feedback control technique in flow line/riser systems (Bjune et al., 2002).

control valve back pressures the separator to suppress surges and as it is a gas choke, it is smaller and therefore more responsive than a multiphase choke.

The S3 is a small separator with dynamically controlled valves at the gas and liquid outlets, positioned between the pipeline outlet and the production separator. The outlet valves are regulated by the control system using signals calculated from locally measured parameters, including pressure and liquid level in the S3 vessel and gas and liquid flow rates. The objective is to maintain constant total volumetric outflow. The system is designed to suppress severe slugging and decelerate transient slugs so that associated fluids can be produced at controlled rates. In fact, implementation of the S3 results in a stabilized gas and liquid production approximating the ideal production system. Installing S3 is a cost effective modification and has lower capital costs than other slug catchers on production platforms. The slug suppression technology also has two advantages over other slug-mitigation solutions, where unlike a topside choke, the S3 does not cause production deferment and controls gas production, and the S3 controller uses locally measured variables as input variables and is independent of downstream facilities (Kovalev et al., 2003).

The design of stable pipeline-riser systems is particularly important in deepwater fields, since the propensity towards severe slugging is likely to be greater and the associated surges more pronounced at greater water depths. Therefore, system design and methodology used to control or eliminate severe slugging phenomenon become very crucial when considering the safety of the operation and the limited available space on the platform. Currently, there are three basic elimination methods that have been already proposed. However, the applicability of current elimination methods to deepwater systems is very much in question. Anticipating this problem, different techniques should be developed to be suitable for different types of problems and production systems (Mokhatab et al., 2007a).

3.8.4.4 Operationally Induced Slugging

These types of slugging are initiated by pipeline operations, which may result in large production losses. Pigging of a pipeline causes most of the liquid inventory to be pushed from the line as a liquid

slug ahead of the pig. When a pipeline is shut down, the liquid will drain to the low points in the line, and when the pipeline is restarted, the accumulated liquid can exit the pipeline as a slug. Slugs may also form during depressurization due to high gas velocities. In addition to these mechanisms, slugs may be produced as a result of flow rate changes. Increasing or decreasing the flow rate of either gas or liquid leads to a change in liquid holdup. This can come out in the form of a slug, depending on the flow rate.

A transient multiphase flow program must be used to estimate the characteristics of these types of slugs. The volume of these transient slugs must be determined to ensure that they can be handled by the downstream separation and processing facilities. If there is insufficient capacity, operating procedures can be introduced to limit the size of any produced slugs.

3.8.5 FLOW ASSURANCE RISK MANAGEMENT

Flow assurance risk management for a new pipeline project is usually performed during the different project engineering and design phases. The better the flow assurance risks are defined during the project phases, the fewer the operational problems that are likely to be encountered. Similarly, the sooner the flow assurance risks are identified, the earlier their impacts on the project economics and the design of the pipeline system can be established.

Six phases exist for consideration of the flow assurance risk management for pipelines: assessing the risks, defining the mitigation strategies, defining flow operability, finalizing the operating procedures, optimizing system performance, and real time monitoring. A brief description of each of these phases of flow assurance management is given below (Song, 2008).

3.8.5.1 Phase I: Assessing Flow Assurance Risks

At first Phase I flow assurance risks are assessed from the sample analysis of the reservoir fluid, which is one of the most critical phases in flow assurance management. No matter how accurate the laboratory measurements and interpretations are, if the fluids do not represent the real production fluids, erroneous conclusions may be drawn.

From the collected samples, producers then consider which tests are critical to enabling the goal of properly evaluating the flow characteristics of the fluid and designing a pipeline system. Any inaccurate fluid properties that are reported are likely to lead to inappropriate flow assurance mitigation strategies that will not work properly and also lead to the pipeline system risks encountering severe operational impacts.

Water sampling to determine the composition extent is also very critical in establishing flow assurance risks and may be very challenging to perform. Analysis of hydrate risk, corrosion prediction, and scaling tendency are dependent upon an assessment of the salinity and composition of the water produced with oil or gas. However, no water sample may be available because either the exploration wells never reach the aquifer zones or the water samples are contaminated by drilling muds (Guo et al., 2005).

Also many oil fields start production with little associated water initially present, but water content gradually increases over the production life. In such cases, the flow assurance specialist must often be content with estimates of salinity and compositions based upon analogs, such as samples taken from nearby fields or adjacent reservoir zones that have already been put into production. Consequently, all these potential water sampling issues may result in high uncertainty in the development of the flow assurance mitigation strategies (Wilkens, 2002).

3.8.5.2 Phase II: Defining Flow Assurance Mitigation Strategies

How all the flow assurance risks will be mitigated is studied in this Phase II and a high level mitigation strategy is then developed. The flow assurance mitigation strategy is best developed with a good understanding of pipeline operating issues. The mitigation strategy details are also very closely related to the configuration of the pipeline system. The system configuration will dictate how many different ways the flow assurance must be mitigated and, similarly, critical flow assurance mitigation requirements will also drive some specific configurations being developed. For example, different hydrate mitigation strategies must be developed if the system configuration consists of single flow line or dual flow lines. On the other hand, if chemical inhibitors will be required to mitigate the hydrate risks, then a separate, additional service line or a flow line could be required in the pipeline system to deliver the chemicals.

3.8.5.3 Phase III: Defining Flow Operability

Phase III involves defining flow operability. Operability is the set of design provisions and operating strategies that ensure the pipeline system can be started, operated, and shut down under all possible operating conditions (planned and unplanned) throughout the system life-cycle. Operability is intrinsic to the flow assurance/pipeline system design process. In fact, after defining the high-level flow assurance mitigation plans in phase II, good operating procedures (applying dynamic multiphase flow modeling of the system) will be defined that enable the pipeline system to perform with minimal flow assurance risks under a specified range of operating conditions.

3.8.5.4 Phase IV: Finalizing the Pipeline Operating Procedures

During this next Phase IV, the pipeline system components (e.g., flow line connectors, insulation system, flow line joints, and valves) are changed from the original design for various reasons, such as different vendors, different materials, different properties, etc. Due to these changes, the corresponding flow assurance mitigation techniques and operating procedures may need to be modified to reflect the changes. Also, even if the components are not modified, the actual manufactured ones may have different thermal-hydraulic properties from the designed ones based upon performance tests conducted on selected components. At the end of this phase, the flow assurance mitigation procedures and pipeline operating procedures will be finalized and used for system commissioning, startup, and daily operations.

3.8.5.5 Phase V: Optimizing System Performance

In this Phase V, the procedures will be modified based upon the actual recorded performance data from the pipeline system. Analysis of such data may identify some requirements that can be beneficially adjusted to optimize the system performance.

3.8.5.6 Phase VI: Real Time Flow Assurance Monitoring

The last Phase VI describes real time flow assurance monitoring. In most cases flow assurance problems cannot be completely eliminated due to unpredictable system component failures, unsuitability for operating conditions, faulty operational procedures for some situations, or operator failures/human errors that can occur in realtime operations. Significant efforts are therefore necessary to minimize the occurrence and impact of such failures. In this regard, real-time flow assurance monitoring systems can provide optimum asset management. Continuously monitoring the operating

conditions of the pipeline for anomalous readings may indicate possible restrictions leading to potential blockage (i.e., observation of erratic pressure fluctuations is usually indicative of hydrate formation or wax deposition).

In fact, reliable, real-time data provided quickly and continuously throughout the life cycle of the pipeline can be tied to a software simulation program which can enable the data to be analyzed and modeled in a timely fashion. When a process interruption or operational upset occurs, the software can predict where problems are most likely to occur (some can recommend the best corrective action sequence). This feature allows faster detection and diagnosis of problems decreasing the potential additional cost of multiphase production, and substantially reducing the risk of environmental disasters due to the failure of unmonitored pipelines.

Continuous monitoring systems can provide wide bandwidth capability via fiber optic-distributed sensors. Real-time data can pass at optimal transmission rates for analysis, ensuring that the data are moved reliably and appropriately referenced at each interval along the pipeline (Brower et al., 2005). However, for deepwater installations, the need for accurate and advanced distributed sensor systems is more critical. Such systems present greater opportunities for the occurrence of flow assurance problems with potentially significant adverse consequences.

REFERENCES

Acikgoz, M., Franca, F., Lahey Jr., R.T., 1992. An experimental study of three-phase flow regimes. International Journal of Multiphase Flow 18 (3), 327−336.

Ansari, A.M., Sylvester, A.D., Sarica, C., Shoham, O., Brill, J.P., 1994. A comprehensive mechanistic model for upward two-phase flow in wellbores. SPE Production & Facilities 9 (2), 143−151.

API, 1995a. Computational Pipeline Monitoring, vol. 1130. API Publications, American Petroleum Institute (API), Washington, DC, USA.

API, 1995b. Evaluation Methodology for Software Based Leak Detection Systems, vol. 1155. API Publications, American Petroleum Institute (API), Washington, DC, USA.

API RP 14E, 1991. Recommended Practice for Design and Installation of Offshore Production Platform Piping Systems, fifth ed. American Petroleum Institute (API), Washington, DC, USA.

Arirachakaran, S.J., 1983. An Experimental Study of Two-Phase Oil-Water Flow in Horizontal Pipes (M.Sc. thesis). University of Tulsa, Tulsa, OK, USA.

Asante, B., October 23−25, 2002. Two-phase flow: accounting for the presence of liquids in gas pipeline simulation. Paper Presented at 34th PSIG Annual Meeting, Portland, Oregon, USA.

AsphWax's Flow Assurance course, 2003. Fluid Characterization for Flow Assurance. AsphWax Inc., Stafford, TX, USA.

Ayala, F.L., Adewumi, M.A., 2003. Low-liquid loading multiphase flow in natural gas pipelines. Journal of Energy Resources Technology 125 (4), 284−293.

Aziz, K., Govier, G.W., Fogarasi, M., 1972. Pressure drop in wells producing oil and gas. Journal of Canadian Petroleum Technology 11 (3), 38−48.

Baillie, C., Wichert, E., 1987. Chart gives hydrate formation temperature for natural gas. Oil & Gas Journal 85 (4), 37−39.

Banerjee, S., March 17−21, 1986. "Basic Equations", Short Course on Modeling of Two-Phase Flow Systems. ETH Zurich, Switzerland.

Barnea, D., 1987. A unified model for prediction flow pattern transitions for the whole range of pipe inclinations. International Journal of Multiphase Flow 13 (1), 1−12.

Barnea, D., Taitel, Y., 1996. Stratified three-phase flow in pipes-stability and transition. Chemical Engineering Communications 141−142, 443−460.
Battara, V., Gentilini, M., Giacchetta, G., 1985. Condensate-line correlations for calculating holdup, friction compared to field data. Oil & Gas Journal 83 (52), 148−152.
Beggs, H.D., Brill, J.P., 1973. A study of two-phase flow in inclined pipes. Journal of Petroleum Technology 25 (5), 607−617.
Bendiksen, K.H., Brandt, I., Fuchs, P., Linga, H., Malnes, D., Moe, R., August 27−29, 1986. Two-phase flow research at SINTEF and IFE: some experimental results. Paper Presented at the 86th Offshore Northern Seas Conference, Stavanger, Norway.
Bendiksen, K., Malnes, D., Moe, R., Nuland, S., 1991. The dynamic two-fluid model OLGA: theory and application. SPE Production Engineering 6, 171−180.
Bjune, B., Moe, H., Dalsmo, M., September 2002. Upstream control and optimization increases return on investment. World Oil 223 (9), 55−57.
Black, P.S., Daniels, L.C., Hoyle, N.C., Jepson, W.P., 1990. Studying transient multiphase flow using the Pipeline Analysis Code (PLAC). Journal of Energy Resources Technology 112, 25−29.
Bloys, B., Lacey, C., Lynch, P., May 1−4, 1995. Laboratory testing and field trial of a new kinetic hydrate inhibitor. OTC 7772, Paper Presented at the Offshore Technology Conference (OTC), Houston, TX, USA.
Bonizzi, M., Issa, R.I., 2003. On the simulation of three-phase slug flow in nearly horizontal pipes using the multi-fluid model. International Journal of Multiphase Flow 29, 1719−1747.
Brauner, N., Maron, M.D., 1992. Flow pattern transitions in two-phase liquid-liquid flow in horizontal tubes. International Journal of Multiphase Flow 18, 123−140.
Brill, J.P., Beggs, H.D., January 1991. Two-phase Flow in Pipes, sixth ed. Tulsa University Press, Tulsa, OK, USA.
Brill, J.P., Schmidt, Z., Coberly, W.A., Herring, J.D., Moore, D.W., 1981. Analysis of two-phase tests in large diameter Prudhoe Bay flowlines. SPE Journal 21 (3), 363−378.
Brower, D.V., Prescott, C.N., Zhang, J., Howerter, C., Rafferty, D., May 2−5, 2005. Real-time flow assurance monitoring with non-intrusive fiber optic technology. OTC 17376, Paper Presented at the Offshore Technology Conference (OTC), Houston, TX, USA.
Campbell, J.M., 1992. Gas Conditioning and Processing, third ed. Campbell Petroleum Series, Norman, OK, USA.
Carroll, J.J., 2003. Natural Gas Hydrates: A Guide for Engineers. first ed. Gulf Professional Publishing, Amsterdam, The Netherlands.
Carroll, J.J., May 19−21, 2004. An examination of the prediction of hydrate formation conditions in sour natural gas. Paper Presented at the GPA Europe Spring Meeting, Dublin, Ireland.
Carson, D.B., Katz, D.L., 1942. Natural gas hydrates. Petroleum Transactions AIME 146, 150−158.
Chen, X., Guo, L., 1999. Flow patterns and pressure drop in oil-air-water three-phase flow through helically coiled tubes. International Journal of Multiphase Flow 25, 1053−1072.
Chisholm, D., Sutherland, L.A., Sepember 24−25, 1969. Prediction of pressure gradient in pipeline systems during two-phase flow. Paper Presented at Symposium on Fluid Mechanics and Measurements in Two-Phase Flow Systems, Leeds, UK.
Cindric, D.T., Gandhi, S.L., Williams, R.A., 1987. Designing piping systems for two-phase flow. Chemical Engineering Progress 83 (3), 51−59.
Collier, J.G., Thome, J.R., 1996. Convective Boiling and Condensation, third ed. Clarendon Press, Oxford, UK.
Colson, R., Moriber, N.J., 1997. Corrosion control. Civil Engineering 67 (3), 58−59.
Courbot, A., May 6−9, 1996. Prevention of severe slugging in the Dunbar 16" multiphase pipelines. OTC 8196, Paper Presented at the Offshore Technology Conference (OTC), Houston, TX, USA.
Dahl, E., et al., June 2001. Handbook of Water Fraction Metering. Rev. 1, Norwegian Society for Oil and Gas Measurements, Norway.

Decarre, S., Fabre, J., 1997. Etude Sur La prediction de l'Inversion de phase. Revue de l'Institut Français du Petrole 52, 415–424.
De Henau, V., Raithby, G.D., 1995. A transient two-fluid model for the simulation of slug flow in pipelines. 1-Theory. International Journal of Multiphase Flow 21, 335–349.
Dukler, A.E., Hubbard, M.G., 1966. The Characterization of Flow Regimes for Horizontal Two-Phase Flow. Proc. Heat Transfer and Fluid Mechanics Institute, 1, 100–121. Stanford University Press, Stanford, CA, USA.
Edmonds, B., et al., April 16–17, 1996. A practical model for the effect of salinity on gas hydrate formation. Paper Presented at the European Production Operations Conference and Exhibition, Norway.
Edmonds, B., Moorwood, R.A.S., Szczepanski, R., May 14, 1998. Hydrate update. Paper Presented at the GPA Europe Spring Meeting, Darlington, County Durham, UK.
Erickson, D., Buck, E., Kolts, J., 1993. Corrosion inhibitor transport in wet-gas pipelines. Journal of Materials Performance 32 (9), 49–56.
Esteban, A., Hernandez, V., Lunsford, K., March 13–15, 2000. Exploit the benefits of methanol. Paper Presented at the 79th Annual GPA Convention, Atlanta, GA, USA.
Fabre, J., et al., 1990. Severe slugging in pipeline/riser systems. SPE Production Engineering 5 (3), 299–305.
Faille, I., Heintze, E., 1999. A rough finite volume scheme for modeling two-phase flow in a pipeline. Computers & Fluids 28 (2), 213–241.
FEESA, 2003. Hydrodynamic Slug Size in Multiphase Flowlines. Case Study Report. Feesa Ltd., Hampshire, UK.
Frostman, L.M., October 1–4, 2000. Anti-aggolomerant hydrate inhibitors for prevention of hydrate plugs in deepwater systems. Paper Presented at the SPE Annual Technical Conference and Exhibition, Dallas, TX, USA.
Frostman, L.M., November 19–21, 2003. Low dosage hydrate inhibitor (LDHI) experience in deepwater. Paper Presented at the Deep Offshore Technology Conference, Marseille, France.
Furlow, W., October 2000. Suppression system stabilizes long pipeline-riser liquid flows. Offshore, 60 (10), 48+166.
GPSA, 2004. Engineering Data Book, twelfth ed. Gas Processors Suppliers Association (GPSA), Tulsa, OK, USA.
Griffith, P., Wallis, G.B., August 1961. Two-phase slug flow. Journal of Heat Transfer, Transactions of ASME 82, 307–320.
Guo, B., Song, S., Chacko, J., Ghalambor, A., 2005. Offshore Pipelines. Gulf Professional Publishing, Burlington, MA, USA.
Hall, A.R.W., June 18–20, 1997. Flow patterns in three-phase flows of oil, water, and gas. Paper Presented at the 8th BHRG International Conference on Multiphase Production, Cannes, France.
Hammerschmidt, E.G., 1934. formation of gas hydrates in natural gas transmission lines. Industrial and Engineering Chemistry Research 26, 851–855.
Hartt, W.H., Chu, W., 2004. New methods for CP design offered. Oil & Gas Journal 102 (36), 64–70.
Havre, K., Dalsmo, M., September 30–October 3, 2001. Active feedback control as the solution to severe slugging. SPE 71540, Paper Presented at the SPE Annual Technical Conference and Exhibition, New Orleans, Louisiana, USA.
Hedne, P., Linga, H., 1990. Suppression of terrain slugging with automatic and manual riser chocking. Advances in Gas-Liquid Flows 453–469.
Hein, M., 1984. HP41 Pipeline Hydraulics and Heat Transfer Programs. PennWell Books, Tulsa, OK, USA.
Hill, T.H., 1990. Gas injection at riser base solves slugging, flow problems. Oil & Gas Journal 88 (9), 88–92.
Holt, A.J., Azzopardi, B.J., Biddulph, M.W., 1999. Calculation of two-phase pressure drop for vertical up flow in narrow passages by means of a flow pattern specific models. Chemical Engineering Research and Design 77 (1), 7–15.
Jansen, F.E., Shoham, O., Taitel, Y., 1996. The elimination of severe slugging, experiments and modelling. International Journal of Multiphase Flow 22 (6), 1055–1072.

Johal, K.S., et al., September 9−12, 1997. An alternative economic method to riser base gas lift for deepwater subsea oil/gas field developments. Paper Presented at the Offshore Europe Conference, Aberdeen, Scotland.

Jolly, W.D., Morrow, T.B., O'Brien, J.F., Spence, H.F., Svedeman, S.J., April 1992. New Methods for Rapid Leak Detection in Offshore Pipelines. Final Report, SWRI Project No. 04-4558, Southwest Research Institute (SWRI), San Antonio, TX, USA.

Kang, C., Wilkens, R.J., Jepson, W.P., March 24−29, 1996. The effect of slug frequency on corrosion in high-pressure, inclined pipelines. Paper Presented at the NACE International Annual Conference and Exhibition, Denver, CO, USA.

Katz, D.L., 1945. Prediction of conditions for hydrate formation in natural gases. Transactions of AIME 160, 140−149.

Kelland, M.A., Svartaas, T.M., Ovsthus, J., Namba, T., 2000. A new class of kinetic inhibitors. Annals of the New York Academy of Sciences 912, 281−293.

Kovalev, K., Cruickshank, A., Purvis, J., September 2−5, 2003. Slug suppression system in operation. Paper Presented at the Offshore Europe Conference, Aberdeen, UK.

Kumar, S., 1987. Gas Production Engineering. Gulf Publishing Company, Houston, TX, USA.

Langner, et al., May 3−6, 1999. Direct impedance heating of deepwater flowlines. OTC 11037, Paper Presented at the Offshore Technology Conference (OTC), Houston, TX, USA.

Lederhos, J.P., Longs, J.P., Sum, A., Christiansen, R.l., Sloan, E.D., 1996. Effective kinetic inhibitors for natural gas hydrates. Chemical Engineering Science 51 (8), 1221−1229.

Lee, H.A., Sun, J.Y., Jepson, W.P., June 6−11, 1993. Study of flow regime transitions of oil-water-gas mixture in horizontal pipelines. Paper Presented at the 3rd International Offshore and Polar Engng Conference, Singapore.

Leontaritis, K.J., March 19−23, 1995. "The asphaltene and wax deposition envelopes", Paper Presented at the symposium on thermodynamics of heavy oils and asphaltenes, area 16C of fuels and petrochemical division. AIChE Spring National Meeting and Petroleum Exposition, Houston, TX, USA.

Leontaritis, K.J., February 18−21, 1997a. PARA-based (Paraffin-Aromatic-Resin-Asphaltene) reservoir oil characterization. SPE 37252, Paper Presented at the SPE International Symposium on Oilfield Chemistry, Houston, TX, USA.

Leontaritis, K.J., 1997b. Asphaltene destabilization by drilling/completion fluids. World Oil 218 (11), 101−104.

Leontaritis, K.J., May 4−7, 1998. Wax deposition envelope of gas condensates. OTC 8776, Paper Presented at the Offshore Technology Conference (OTC), Houston, TX, USA.

Lockhart, R.W., Martinelli, R.C., 1949. Proposed correlation of data for isothermal two-phase, two-component flow in pipes. Chemical Engineering Progress 45, 39−48.

Maddox, R.N., et al., March 4−6, 1991. Predicting hydrate temperature at high inhibitor concentration. Paper Presented at the 41st Annual Laurance Reid Gas Conditioning Conference, Norman, OK, USA.

Mandhane, J.M., Gregory, G.A., Aziz, K., 1974. A flow pattern map for gas-liquid flow in horizontal pipes. International Journal of Multiphase Flow 1, 537−553.

Mann, S.L., et al., March 13−14, 1989. Vapour-solid equilibrium ratios for structure I and II natural gas hydrates. Paper Presented at the 68th Annual GPA Convention, San Antonio, TX, USA.

Masella, J.M., Tran, Q.H., Ferre, D., Pauchon, C., 1998. Transient simulation of two-phase flows in pipes. Oil & Gas Science and Technology - Revue d'IFP 53 (6), 801−811.

McCain, W.D., 1990. The Properties of Petroleum Fluids, second ed. PennWell Books, Tulsa, OK, USA.

McGuinness, M., McKibbin, R., February 11−15, 2002. Terrain induced slugging. Paper Presented at the 2002 Mathematics-in-Industry Study Group Meeting, University of South Australia, Adelaide, Australia.

Mehta, A.P., Sloan, E.D., March 11−13, 1996. Structure H hydrates: the state-of-the-art. Paper Presented at the 75th Annual GPA Convention, Denver, CO, USA.

Mehta, A., Hudson, J., Peters, D., March 28−29, 2001. Risk of pipeline over-pressurization during hydrate remediation by electrical heating. Paper Presented at the Chevron Deepwater Pipeline and Riser Conference, Houston, TX, USA.

Mehta, A.P., Hebert, P.B., Weatherman, J.P., May 6−9, 2002. "Fulfilling the promise of low dosage hydrate inhibitors: Journey from academic curiosity to successful field implementations", OTC 14057. Paper Presented at the 2002 Offshore Technology Conference (OTC), Houston, TX, USA.

Minami, K., 1991. Transient Flow and Pigging Dynamics in Two-Phase Pipelines (Ph.D. thesis). University of Tulsa, Tulsa, OK, USA.

Mokhatab, S., 2007. Severe slugging in a catenary-shaped riser: experimental and simulation studies. Petroleum Science and Technology 25 (6), 719−740.

Mokhatab, S., 2010. Severe Slugging in Offshore Production Systems. Nova Science Publishers, Inc, New York, NY, USA.

Mokhatab, S., Towler, B.F., 2007a. Dynamic simulation of offshore production plants. Petroleum Science and Technology 25 (6), 741−745.

Mokhatab, S., Towler, B.F., 2007b. Severe slugging in flexible risers: review of experimental investigations and OLGA predictions. Petroleum Science and Technology 25 (7), 867−880.

Mokhatab, S., Towler, B.F., Purewal, S., 2007a. A review of current technologies for severe slugging remediation. Petroleum Science and Technology 25 (10), 1235−1245.

Mokhatab, S., Wilkens, R.J., Leontaritis, K.J., 2007b. A review of strategies for solving gas hydrate problems in subsea pipelines. Energy Sources Part A 29 (1), 39−45.

Molyneux, P., Tait, A., Kinving, J., June 21−23, 2000. Characterization and active control of slugging in a vertical riser. Paper Presented at the 2nd North American Conference on Multiphase Technology, Banff, Canada.

Moody, L.F., Nov.1944. Friction factors for pipe flow. ASME Transactions, 66, 671−684.

Muhlbauer, K.W., 1996. Pipeline Risk Management Manual, second ed. Gulf Publishing Company, Houston, TX, USA.

Narayanan, L., Leontaritis, K.J., Darby, R., March 28−April 1, 1993. A thermodynamic model for predicting wax precipitation from crude oils", Paper Presented at the Symposium of solids deposition, area 16C of fuels and petrochemical division. AIChE Spring National Meeting and Petroleum Exposition, Houston, TX, USA.

Nasrifar, K., Moshfeghian, M., Maddox, R.N., 1998. Prediction of equilibrium conditions for gas hydrate formation in the mixture of both electrolytes and alcohol. Fluid Phase Equilibria 146 (1−2), 1−13.

NACE, 1975. Sulfide stress cracking resistant metallic materials for oil field equipment. NACE Standardd MR 01−75, National Association of Corrosion Engineers (NACE), Houston, TX, USA.

Ng, H.J., Robinson, D.B., 1976. The measurement and prediction of hydrate formation in liquid hydrocarbon-water systems. Industrial and Engineering Chemistry Fundamentals 15 (4), 293−298.

Nielsen, R.B., Bucklin, R.W., 1983. Why not use methanol for hydrate control? Hydrocarbon Processing 62 (4), 71−78.

Palermo, T., Argo, C.B., Goodwin, S.P., Henderson, A., 2000. Flow loop tests on a novel hydrate inhibitor to be deployed in North Sea ETAP field. Annals of the New York Academy of Sciences 912, 355−365.

Pan, L., 1996. High Pressure Three-phase (Gas/Liquid/Liquid) Flow (Ph.D. thesis). Imperial College London, London, UK.

Pauchon, C., Dhulesia, H., Lopez, D., Fabre, J., June 16−18, 1993. TACITE: a comprehensive mechanistic model for two-phase flow. Paper Presented at the 6th BHRG International Conference on Multiphase Production, Cannes, France.

Peng, D., Robinson, D.B., 1976. A new two-constant equation of state. Industrial and Engineering Chemistry Fundamentals 15 (1), 59−64.

Petalas, N., Aziz, K., 2000. A mechanistic model for multiphase flow in pipes. Journal of Canadian Petroleum Technology 39, 43−55.

Poettmann, F.H., Sloan, E.D., Mann, S.L., McClure, L.M., March 13−14, 1989. Vapor-solid equilibrium ratios for structure I and structure II natural gas hydrates. Paper Presented at the 68th Annual GPA Convention, San Antonio, TX, USA.

Polignano, R., 1982. Value of glass-fiber fabrics proven for bituminous coatings. Oil & Gas Journal 80 (41), 156−158, 160.

Pots, B.F.M., et al., March 11−14, 1985. Severe slug flow in offshore flowline/riser systems. SPE 13723, Paper Presented at the SPE Middle East Oil Technical Conference & Exhibition, Bahrain.

Ramachandran, S., Breen, P., Ray, R., 2000. Chemical programs assure flow and prevent corrosion in deepwater facilities and flowlines. InDepth 6, 1.

Rhodes, K.I., 1982. Pipeline protective coatings used in Saudi Arabia. Oil & Gas Journal 80 (31), 123−127.

Ripmeester, J.A., Tse, J.S., Ratcliffe, C.I., Powell, B.M., 1987. A new clathrate hydrate structure. Nature 325, 135−136.

Sagatun, S.I., 2004. Riser slugging: a mathematical model and the practical consequences. SPE Production & Facilities 19 (3), 168−175.

Samant, A.K., February 2003. Corrosion problems in oil industry need more attention. Paper Presented at ONGC Library, Oil and Natural Gas Corporation (ONGC) Ltd, India.

Sarica, C., Tengesdal, J.Q., October 1−4, 2000. A new technique to eliminate severe slugging in pipeline/riser systems. SPE 63185, Paper Presented at the 75th SPE Annual Technical Conference & Exhibition, Dallas, TX, USA.

Schmidt, Z., Brill, J.P., Beggs, D.H., 1980. Experimental study of severe slugging in a two-phase flow pipeline-riser system. SPE Journal 20 (5), 407−414.

Schweikert, L.E., 1986. Tests prove two-phase efficiency for offshore pipeline. Oil & Gas Journal 84 (5), 39−42.

Scott, S.L., Brill, J.P., Kuba, G.E., Shoham, K.A., Tam, W., October 26−27, 1987. Two-phase flow experiments in the Prudhoe Bay field of Alaska. Paper Presented at the Multiphase Flow Technology and Consequences for Field Development Conference, Stavanger, Norway.

Shaha, J., 1999. Phase Interactions in Transient Stratified Flow (Ph.D. thesis). Imperial College London, London, UK.

Sinquin, A., Palermo, T., Peysson, Y., 2004. Rheological and flow properties of gas hydrate suspensions. Oil & Gas Science and Technology − Revue d'IFP 59 (1), 41−57.

Sloan Jr., E.D., 2000. Hydrate Engineering. SPE Monograph, 21, Society of Petroleum Engineers (SPE) Publications, Richardson, TX, USA.

Song, S., May 5−8, 2008. Managing flow assurance and operation risks in subsea tie-back system. OTC 19139, Paper Presented at the Offshore Technology Conference (OTC), Houston, TX, USA.

Taitel, Y., 1986. Stability of severe slugging. International Journal of Multiphase Flow 12 (2), 203−217.

Taitel, Y., Barnea, D., Brill, J.P., 1995. Stratified three-phase flow in pipes. International Journal of Multiphase Flow 21 (1), 53−60.

Taitel, Y., Barnea, D., Dukler, A.E., 1980. Modeling flow pattern transitions for steady upward gas-liquid flow in vertical tubes. AIChE Journal 26 (3), 345−354.

Taitel, Y., Dukler, A.E., 1976. A model for predicting flow regime transitions in horizontal and near horizontal gas-liquid flow. AIChE Journal 22 (1), 47−55.

Taitel, Y., Shoham, O., Brill, J.P., 1989. Simplified transient solution and simulation of two-phase flow in pipelines. Chemical Engineering Science 44 (6), 1353−1359.

Tek, M.R., 1961. Multiphase flow of water, oil, and natural gas through vertical flow strings. Journal of Petroleum Technology 1029−1036.

Towler, B.F., Mokhatab, S., 2005. Quickly estimate hydrate formation conditions in natural gases. Hydrocarbon Processing 84 (4), 61−62.

Uhl, A.E., 1965. Steady Flow in Gas Pipelines. IGT Report No. 10. American Gas Association (AGA), New York, NY, USA.

Uhlig, H.H., Revie, R.W., 1985. Corrosion and Corrosion Control, third ed. John Wiley and Sons, New York, NY, USA.

Varughese, K., 1993. In-situ pipeline rehabilitation techniques, equipment improved. Oil & Gas Journal 91 (25), 54–57.

Wilkens, R.J., 1997. Prediction of the Flow Regime Transitions in High Pressure, Large Diameter, Inclined Multiphase Pipelines (Ph.D. thesis). Ohio University, Athens, OH, USA.

Wilkens, R.J., 2002. Chapter 29: flow assurance. In: Saleh, J. (Ed.), Fluid Flow Handbook. McGraw-Hill Book Company, New York, NY, USA.

Xiao, J.J., Shoham, O., Brill, J.P., September 23–26, 1990. A comprehensive mechanistic model for two-phase flow in pipelines. SPE 20631, Paper Presented at the 65th SPE Annual Technical Conference & Exhibition, New Orleans, LA, USA.

Xiao, J.J., Shoup, G., 1998. Sizing wet-gas pipelines and slug catchers with steady-state multiphase flow simulations. Journal of Energy Resources Technology 120 (2), 106–110.

Yeung, H.C., Lima, P.C.R., 2002. Modeling of pig assisted production methods. Journal of Energy Resources Technology 124 (1), 8–13.

Yocum, B.T., April 2–3, 1973. Offshore riser slug flow avoidance: mathematical model for design and optimization. SPE 4312, Paper Presented at the SPE European Meeting, London, UK.

Zhang, H.-Q., Wang, Q., Sarica, C., Brill, J.P., 2003. Unified model for gas-liquid pipe flow via slug Dynamics-Part 1: model development. Journal of Energy Resources Technology 125 (4), 266–273.

Zuo, J.Y., Zhang, D.D., February 21–24, 1999. Gas hydrate formation in aqueous solutions containing methanol and electrolytes. Paper Presented at the 49th Annual Laurance Reid Gas Conditioning Conference, Norman, OK, USA.

CHAPTER

BASIC CONCEPTS OF NATURAL GAS PROCESSING

4

4.1 INTRODUCTION

Raw natural gas from production wells may contain a full range of hydrocarbons, carbon dioxide, hydrogen sulfide, nitrogen, water, and other impurities. Consumers generally have no use for gas in its raw state, so it may have to undergo several phases of processing before it can be purchased and utilized. The objective of a natural gas processing plant is to produce a treated (product) gas by removing the acid gases, heavy hydrocarbons, nitrogen, water, and other impurities to acceptable levels that are compatible with the pipeline design and the customer's requirements. Off-specification natural gas may cause operational problems associated with pipeline corrosion and/or plugging, which may result in unsafe operation.

This chapter gives an overview of the design and function of the different process units within a natural gas processing plant.

4.2 NATURAL GAS PROCESSING OBJECTIVES

Raw natural gas streams must be treated to comply with emissions, regulations, and pipeline gas specifications. Typical pipeline gas specifications are shown in Table 4.1. The specifications ensure gas quality to provide a clean and safe fuel gas to consumers. The product gas must meet the heating values or Wobbe Index specifications, which are required to ensure optimum operation of gas turbines and combustion equipment to minimize NOx, CO, and soot emissions. Pipeline operators also require the product gas to be interchangeable and similar in properties with existing pipeline gas.

When the gas is high in heavy hydrocarbon content, it may exceed the maximum allowable British thermal unit (Btu) specification. In such cases, at least some of those heavy components must be removed to meet the heating value specification. The removed liquid hydrocarbons can typically command a higher value than natural gas for the same heating value. Propane and butane can be sold as liquefied petroleum gas (LPG). Ethane can be used as a feedstock to petrochemical plants. The C_{5+} components fraction (condensate) can be exported to refineries as a blending stock for gasoline. The characteristics of various types of natural gas liquid (NGL) products can be found in the GPSA (2004) Engineering Data Book.

It is important to recognize the definitions and specifications of the treated gas and product specifications. The product specifications of condensate and NGLs are described in the later chapters.

Handbook of Natural Gas Transmission and Processing. https://doi.org/10.1016/B978-0-12-815817-3.00004-6

Table 4.1 Typical Pipeline Gas Specifications

Characteristics	Specification
Water content	4–7 lbm H_2O/MMscf of gas
Hydrogen sulfide content	0.25–1.0 grain/100 scf
Gross heating value	950–1200 Btu/scf
Hydrocarbon dew point	14–40°F at specified pressure
Mercaptan content	0.25–1.0 grain/100 scf
Total sulfur content	0.5–20 grain/100 scf
Carbon dioxide content	2–4 mol%
Oxygen content	0.01 mol% (max)
Nitrogen content	4–5 mol%
Total inert content ($N_2 + CO_2$)	4–5 mol%
Sand, dust, gums, and free liquid	None
Typical delivery temperature	Ambient
Typical delivery pressure	400 to 1200 psig

Sometimes a slight change in the product specifications may have significant impacts on the treatment and processing options, which will affect the cost and complexity of the gas plant.

4.3 GAS PROCESSING PLANT CONFIGURATIONS

The gas processing plant configuration and complexity depend upon the feed gas composition and the levels of treating and processing required in meeting product specifications and emission limits. Liquid product values can also drive the level of NGL components to be recovered, which can, in turn, affect process complexity. Fig. 4.1 shows two simplified gas processing plant schematics. The first scheme is to remove condensate, sulfur, and the heavier components to meet sales gas specifications. The second scheme is to process the feed gas for recovery of individual NGL components to increase plant revenues. The residue gas may need to be recompressed to the sales gas pipeline pressure, adding cost and complexity. The sales gas may ultimately be used as fuel for power plants, or as a feedstock to petrochemical plants, or even for residential customers. The gas may also be sent to a liquefaction plant for liquefied natural gas (LNG) production, although additional CO_2 may need to be removed to meet a 50 ppm specification.

The gas processing plant must be a "fit-for-purpose" design, meeting the project economics and environmental requirements. While sulfur compounds and other contaminants must be removed to meet emission requirements as shown in both schemes, the extent of processing in the second scheme is project specific. It depends on the commercial agreements between upstream producers and downstream product distributors and buyers. More details on the contractual terms are discussed later in this chapter.

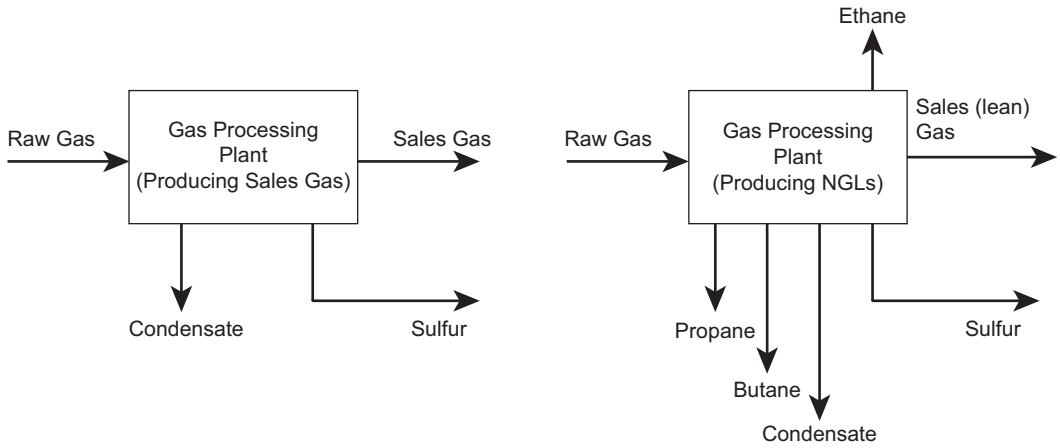

FIGURE 4.1

Two different schemes of natural gas processing plants.

4.3.1 GAS PLANT WITH HYDROCARBON DEW POINT CONTROLLING

Raw gas to a gas processing plant can be relatively lean, that is, containing a small amount of C_{2+} hydrocarbons. This lean gas can be processed by the process units as shown in Fig. 4.2. The main process units consist of acid gas removal, gas dehydration, and hydrocarbon dew point control. There

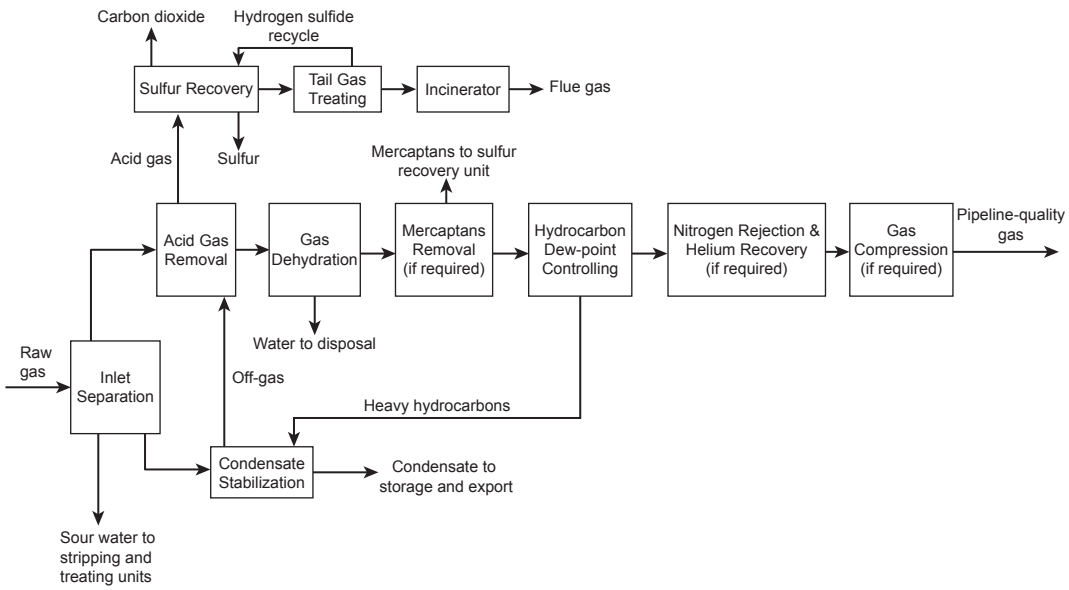

FIGURE 4.2

Process units in a gas processing plant with hydrocarbon dew point controlling.

are other support systems such as sulfur recovery, tail gas treating (TGT), and sulfur forming, which are necessary to meet environmental requirements. If the gas contains liquid condensate, a condensate stabilization unit is required. If the gas contains high levels of nitrogen (greater than around 5 mol%), nitrogen rejection is required. Other units, such as a gas compression unit may also be required.

4.3.1.1 Inlet Separation

Feed gas and liquid from production wells is first separated in the inlet facility, which often includes slug catchers, separation equipment, and a pressure protection system. Typically, a highly reliable safety system is installed at the inlet to protect the gas plant from a block discharged emergency condition.

The slug catcher is designed with adequate surge volume to hold the maximum liquid slug during a pigging operation and to provide to a steady flow of liquid to the stabilization unit.

The slug catcher is usually located at a safe distance from the gas plant, with adequate separation distance for safety reasons. The design is either a "vessel-type" or a "finger-type." A vessel-type slug catcher consists of a phase separator for vapor, liquid, and water and a storage vessel to contain the liquid slug during pigging. The design is suitable to handle feed gas with high gas-to-liquid ratio and a steady flow. It is used where there are space limitations, such as offshore platform installations. The finger-type slug catcher is common in land-based plants where there are no space constraints. It is less costly than the vessel type, especially in high-pressure (HP) services. It consists of multiple long pieces of pipes, which provide the surge volume.

Produced gas from the slug catcher is directed to an HP separator, which protects the gas plant from upstream system upsets. More details about the phase separation facilities are presented in Chapter 5.

The water in the liquids from the slug catcher is separated and sent to a sour water stripper unit, if H_2S is present. The hydrocarbon liquid is processed in a condensate stabilization unit to reduce its vapor pressure for storage and transport. The produced water is typically mixed with monoethylene glycol (MEG), which is used for hydrate control. The MEG is recovered from an MEG regenerator. If salts are present, a slipstream of the MEG is reclaimed in an MEG reclamation unit. Other contaminants, such as corrosion inhibitors, are also removed in the reclaimer.

4.3.1.2 Condensate Stabilization

The condensate contains dissolved light hydrocarbons and H_2S, which must be removed to meet the export condensate specifications. A condensate stabilization unit is designed to produce a condensate with 4 ppm H_2S and Reid vapor pressure specifications, ranging from 8 to 12 psi. The stabilizer overhead vapor is compressed and recycled to the HP separator. There are different design options in configuring the stabilization unit, which are discussed in Chapter 6.

The H_2S content in the condensate from the stabilization unit can typically meet 10 H_2S ppmv specifications. However, it may contain higher levels of organic sulfur compounds such as carbonyl sulfide (COS) and mercaptans (RSH). If condensate is exported as a product, the total sulfur content specification must be met, and a separate unit for removal of the mercaptan content may be necessary. If the condensate is sent to refineries, the condensate can be blended with the refinery feedstock and treated in the refinery units.

4.3.1.3 Acid Gas Removal

The acid gas removal unit (AGRU) is designed to remove the acidic components to meet sales gas sulfur and CO_2 specifications. H_2S must be removed to meet the sales gas specification of 4 ppmv, or ¼ grains per 100 scf of gas. In addition, COS, mercaptans, and other organic sulfur species must be

removed if they exceed the total sulfur specification. Considering today's stringent emission regulations, an AGRU alone may not be sufficient to meet the requirements. Treated gas from the AGRU may need to be further treated with additional units, such as molecular sieves and sulfur scavengers. Design details of the AGRUs are discussed in Chapter 7.

4.3.1.4 Sulfur Recovery and Handling

Acid gas from the amine regenerator contains concentrated H_2S, which cannot be vented for safety reasons or flared due to acid gas pollution. If reinjection wells are available, acid gas can be reinjected into reservoirs for sequestration, which would avoid the investment of a sulfur recovery unit (SRU). In most instances where a reinjection facility is not available, H_2S is processed in an SRU. The SRU can be coupled with a TGT unit to achieve 99.9% sulfur removal to meet today's emission targets. The design of the SRU as well as a brief discussion of acid gas injection is discussed in Chapter 8.

4.3.1.5 Gas Dehydration

Treated gas from the AGRU is fed to the gas dehydration unit to meet the water dew point specification for pipeline transmission, typically 7 lbs water/MMscf. In colder climates, the water dew point specification can be as low as -40°F to avoid hydrate formation in the pipeline. Depending on the plant capacity and extent of drying, different types of dehydration methods are available, including glycol dehydration and solid desiccant (i.e., molecular sieve, silica gel, or activated alumina) dehydration. Different natural gas dehydration systems are discussed in Chapter 9.

4.3.1.6 Mercaptans Removal

Natural gas coming from the wellhead may contain mercaptans (RSH) and other sulfur components. Therefore, removing mercaptans from the feed gas may be required to meet a maximum total sulfur specification in the treated gas or natural gas liquids and to comply with environmental regulations and avoid problems with corrosion and damage to downstream equipment.

There are a number of processes for removing mercaptans from natural gas streams. However, it is the level of mercaptans in the feed gas that will most likely influence the selection of the most appropriate mercaptan removal method (Mokhatab and Northrop, 2017a). While Chapter 9 addresses natural gas dehydration processes, mercaptan removal that can be integrated into the molecular sieve unit is discussed at the end of this chapter.

4.3.1.7 Hydrocarbon Dew Point Controlling

The hydrocarbon dew point temperature must be reduced to a temperature below the coldest ambient temperature during transmission. This is to avoid hydrocarbon liquid condensation in the pipeline, which is a safety hazard. Depending on the phase envelope of the pipeline gas, the hydrocarbon dew point can actually increase when the pressure is lowered, which must be considered in the design of the unit. Details of hydrocarbon dew point processes are discussed in Chapter 11.

4.3.1.8 Nitrogen Rejection and Helium Recovery

Nitrogen content in natural gas varies depending on the gas source. Nitrogen can be naturally occurring in high concentration in some gas fields, such as in the South China Sea where 30%–50% nitrogen content gas can be found. For onshore facilities where nitrogen injection is employed for enhanced oil recovery, nitrogen content can also be very high.

The objective of the nitrogen rejection unit (NRU) is to remove nitrogen from residue gas to produce a treated gas with minimal nitrogen and improved lower heating value specification. Although a less common process in the gas processing industry, nitrogen rejection will become more important as we shift to lower-quality gas feedstock.

The optimal nitrogen rejection process is highly dependent on the nitrogen content in the feed gas stream. When nitrogen is present in high concentrations, it should be removed downstream of the NGL recovery unit. Heavy hydrocarbons (BTEX aromatics) must be recovered in the NGL recovery unit, as these hydrocarbons would solidify in the cryogenic section of the NRU. If the gas is used for LNG production, the nitrogen content must be removed to below 1 mol% to meet LNG specification. Nitrogen is not desirable in an LNG product, as it will lower the liquefaction temperature, which would increase the power consumption. Feed gas concentration up to 2% nitrogen is possible as some of the nitrogen is removed in the end flash process of LNG production (Mokhatab et al., 2014).

Nitrogen removal by cryogenic separation is more efficient than other alternatives (Finn, 2007; Garcel, 2008). Membrane separators and molecular sieves can be used for nitrogen rejection, but their processing capacity is relatively limited. They are suitable for bulk separation and are not economical to meet stringent specifications. The rejected nitrogen would contain a significant amount of hydrocarbons, which may be an environmental issue, so would likely require flaring. More details on nitrogen rejection processes are discussed in Chapter 12.

Natural gas may also contain helium, which is a noble gas that has a wide range of medical and industrial applications, based on its very low boiling temperature, inert and nonflammable nature. Few gas processing plants are dedicated primarily to helium recovery. In fact, helium recovery is uncommon and uneconomical, unless the helium content is above 0.5 vol% (Gottier; Herron, 1991; Kidnay and Parrish, 2006). Helium is a difficult diluent to recover from natural gas unless nitrogen rejection is used. If recoverable quantities of helium exist in the gas stream, helium recovery can be integrated into the NRU. A brief description of helium recovery processes is given in Chapter 12.

4.3.1.9 Sales Gas Compression, Transmission, and Measurement

Feed gas to the gas plant is typically reduced in pressure such that phase separation is feasible. Most often, recompression of the residual (sales) gas to the pipeline pressure is necessary. The sales gas is then transported via a pipeline network to the industrial and residential consumers. Accurate measurement of the sales gas to determine the energy content in the gas, compounds mixed into the gas, water content, and flow rate is very important to the parties who trade in natural gas. Details of the natural gas compression, transmission, and measurement systems are discussed in Chapters 14, 15 and 16, respectively.

4.3.2 GAS PLANT FOR NATURAL GAS LIQUID PRODUCTION

When the feed gas contains a significant amount of liquids (C_{3+} hydrocarbons), there are economic incentives to produce the LPG (and sometimes liquid ethane) as by-products. The liquid recovery facility typically includes storage, pipeline, metering, and custody transfer, and must include safety systems to protect against liquid leakage or spillage. This type of plant is complex and costs more than the simple hydrocarbon dew point controlling plant.

Fig. 4.3 illustrates a block flow diagram of a gas plant for NGL production. The following sections describe the units that are unique to NGL production. The balance of plant is similar to the hydrocarbon dew pointing plant.

4.3.2.1 Deep CO_2 Removal

CO_2 removal is required to meet the sales gas CO_2 specification, typically limited to 2−3 mol%. CO_2 may need to be removed to even a lower level to avoid CO_2 freezing in the cold section of the NGL recovery unit. Typically, in a propane recovery process, 2 mol% of CO_2 can be tolerated, as the NGL column operates at a relatively warm temperature. Deep CO_2 removal may not be required, unless the gas is sent to a liquefaction unit. In that case, CO_2 must be removed down to 50 ppmv.

If the NGL recovery unit is used for ethane recovery, the demethanizer column will operate at a much lower temperature and will be prone to CO_2 freezing. CO_2 freezing may not be a problem if a good portion of the CO_2 condenses with the ethane product. However, the liquid product may not meet the CO_2 specification (typical Y-Grade NGL limits CO_2 content in ethane to 500 ppmv). When ethane recovery is required, the design must ensure that CO_2 in the feed gas is removed sufficiently to avoid CO_2 freezing as well as to meet the CO_2 specification of the ethane product.

4.3.2.2 Deep Dehydration

For NGL recovery, the deethanizer or demethanizer must operate at low temperatures. This would require sufficient water to be removed to avoid hydrate formation in the columns. If only propane recovery is considered, the column will operate at a warmer temperature, at about −60°F. In this case, the use of DRIZO triethylene glycol (TEG) dehydration may be sufficient. TEG unit is more compact

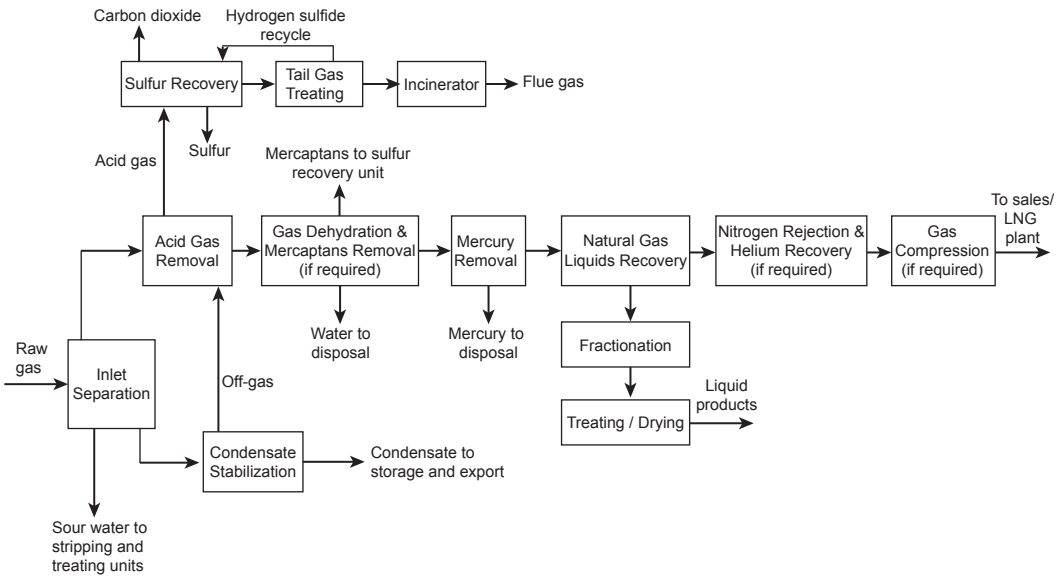

FIGURE 4.3

Process units in a gas processing plant for natural gas liquid production.

and less expensive than a molecular sieve unit and is more suitable for offshore design. If ethane recovery is required, then molecular sieve dehydration is necessary. More details of dehydration system designs are discussed in Chapter 9.

4.3.2.3 Mercury Removal

Mercury is often present in the feed gas at pptw or higher levels. Mercury removal using sulfur-impregnated carbon beds or metal sulfide beds are required to avoid the risks of mercury attack on the brazed aluminum heat exchangers. Brazed aluminum exchangers are commonly used in NGL recovery process to achieve high NGL recovery. Aluminum is reactive with elemental mercury, and can corrode quickly, resulting in failure of the exchangers.

The mercury removal bed is typically designed with mercury removal to below 0.01 μg/Nm^3. The mercury removal step can be positioned upstream of the AGRU or downstream of the dehydration unit. Installing the mercury removal unit upstream can prevent mercury migration to downstream units, ensuring both the sales gas and the liquid products are mercury free. More details of the mercury removal processes are discussed in Chapter 10.

4.3.2.4 Natural Gas Liquid Recovery and Fractionation

There are numerous NGL patents and proprietary technologies for NGL recovery. Unlike an AGRU, the NGL recovery process selection must be evaluated based on meeting the NGL recovery levels, feed gas pressure, temperature, gas compositions, and product specifications, and NGL recovery flexibility. The NGL process must be designed to handle a rich gas case and a lean gas case. If nitrogen injection is considered for enhanced recovery in the same hydrocarbon formation, a higher nitrogen feed gas case must be considered in the design.

Typically, the design of the front section of the NGL recovery unit is controlled by the rich gas case operating in the summer, as the refrigeration duty is highest for that case. However, the lean gas and the high nitrogen gas would control the design of the demethanizer and the residue gas compressor as the gas flow is higher.

The NGL recovery unit can be designed for propane recovery or ethane recovery. For operating flexibility, the NGL process can be designed for ethane recovery but can be operated on ethane rejection when ethane margins are low. Another alternative is to design the unit for propane recovery but can be operated on ethane recovery. More details of the various NGL recovery processes are discussed in Chapter 11.

NGL product compositions depend on the desirable propane and ethane recovery. The NGL product pump and NGL pipeline must be designed for the ethane recovery case as the NGL flow rate and the pipeline pressure are higher. NGL is typically transported to an NGL fractionation center, which produces the final liquid products. The NGL products may need additional treatment and processing to meet the product specifications (see Table 4.2). Details on NGL fractionation and liquid products processing are discussed in Chapter 11.

Table 4.2 Maximum Levels of Major Contaminants of Common Liquid Products

	H_2S (ppmw)	Total Sulfur (ppmw)	CO_2 (ppmw)	H_2O (ppmw)
High-ethane raw streams	50	200	3500	No free
Ethane–propane mixes	Pass copper strip test	143	3000	No free
High-purity ethane	10	70	5000	No free
Commercial propane	Pass copper strip test	185	–	Pass ASTM D2713-91(2001) standard test
Commercial butane	Pass copper strip test	140	–	–
Commercial butane–propane mixes	Pass copper strip test	140	–	–
Propane HD-5	Pass copper strip test	123	–	Pass ASTM D2713-91(2001) standard test

(GPSA, 2004).

4.4 FINDING THE BEST GAS PROCESSING ROUTE

When determining the best processing scheme for a gas processing project meeting the desired economics and environmental requirements, it is important not only to select the proper technology within each processing unit but also to consider interactions between different gas processing units. One may adjust the sequence of the processing steps to optimize the whole operation, thereby increasing operating flexibility within the overall gas processing plant (Mokhatab and Meyer, 2009; Mokhatab, 2010). More details on the different integration schemes of the gas processing steps to determine the optimal processing lineup for producing pipeline-quality gas from a sour feed gas containing mercaptans can be found in Mokhatab and Bloemendal (2017).

There are various technologies, conventional or proprietary, that can be used in the design of the gas processing plant (Mokhatab and Northrop, 2017b). The design must be "fit-for-purpose," meeting the immediate requirements but also considering potential modifications to the process for future gas compositions and NGL recovery requirements. More importantly, the design must be reviewed by the plant operators to obtain their buy-in.

The design of the elements of the front section of the gas plant, such as the slug catcher and condensate stabilization unit, may be conventional. Designs of the gas treating unit and sulfur recovery/handling system are more involved and are dependent on the feed gas' acid gas content. Design of the NGL recovery unit is dependent on the levels of NGL recovery, energy efficiency, and operation flexibility. In the past, most NGL recovery units were designed for very high propane recovery (typically, 99% propane), as NGL was valued significantly higher than natural gas. High-NGL recovery units require the use of a turboexpander, feed gas and residue gas compressors, and propane refrigeration, all of which are more costly than a simple hydrocarbon dew point controlling plant. However, with shale gas, remote gas, and distributed gas playing a vital role in the global energy

economy, there is no longer a shortage of NGL; therefore, the economic driver for maximizing NGL production is generally becoming less attractive.

Today's NGL design trend tends to focus on minimizing capital investment. Ethane demand is driven by incremental demands from new petrochemical plants. Prefabricated modular equipment is frequently used to reduce field construction time and lower capital and operating costs. These modular units can be prefabricated as packaged units in various capacities, typically 60 to 100 MMscfd, but can be as high as 200 MMscfd. This modular design, when properly executed, can generate significant value for gas producers and processors.

In summary, there is no single best design approach for the gas processing plant. NGL recovery unit design continues to evolve around the economics of NGL markets. NGL recovery unit designs that are optimized today may not work well in the future when feed gas compositions changes. An optimized gas plant design must be flexible and be suitable for revamp to meet future requirements and project economics, while preserving the key equipment.

4.5 SUPPORT SYSTEMS

4.5.1 UTILITY AND OFF-SITE

Operating gas plants require support from utility and off-site systems. These typically include power generation, steam generation, heat medium supply, cooling water, instrument and plant air, nitrogen (or inert) gas, fuel gas system, relief and flare, potable water, and wastewater treatment systems.

Small gas plants typically purchase electrical power off the local power grid. Larger gas plants or plants in remote areas tend to generate their own power. For uninterrupted supply, power can be supplied from the power grid as a backup or by using an emergency power generator. A diesel-driven generator is typically required for plant black start. A battery power supply is required for life support during an emergency.

Cogeneration plants are energy efficient and can be attractive options for reducing operating costs, especially where the gas turbine exhaust can be used for heating or steam generation. Most large compressors in gas plants use gas engines or gas turbine drivers, which can be integrated with the steam system. Steam is used in gas plants for solvent regeneration and reboilers in NGL recovery and fractionation units. These units require cooling; and where available, cooling water is the most economical. In desert areas where water supply is not available, air coolers are the only choice for cooling.

A demineralizer unit is required to supply boiler feed water makeup to steam generators and make up water to amine-treating units. Wastewater must be treated in a wastewater treater before it can be discharged from the facility.

A reliable source of instrument air is critical to gas plant operation. Typically, instrument air is supplied at about 100−120 psig and must be dried to meet a −40°F water dew point. The air must be clean and dried to avoid water condensation and corrosion in the instrument air piping. One or multiple backup air compressors are required to ensure plant safety and reliability. Plant air can also be supplied from the same air compressors. Air receivers are sized to dampen out fluctuations in demand and to provide an uninterrupted supply of instrument air.

Nitrogen is required for plant purging during start-up. It is also used for seal gas and for blanketing of storage tanks. Nitrogen consumption is typically very low in gas plant operation. Nitrogen can be

produced by a membrane separator, or liquid nitrogen can be purchased from outside suppliers and stored on site. In small gas plants, nitrogen can be supplied by nitrogen cylinders.

Fuel gas is required to meet the fuel gas demands by steam boilers, hot oil furnaces, and gas turbine drivers. For turbines, the fuel gas must be supplied at higher pressure. Fuel gas must be treated and conditioned to meet the sulfur and heating value specifications.

A brief description of the common utility and off-site systems found in gas processing plants as well as many of the basic design and operation considerations are discussed in Chapter 18.

4.5.2 PROCESS CONTROL

Process control has always played a role in gas plants but has become more important over the years as companies try to reduce labor and operating costs. Most plants use a distributed control system (DCS) for individual units to provide both process control and operation history. Advanced process control (APC) systems, which are integrated with the DCS systems, provide sophisticated plant control for plant optimization. APC system uses multivariable algorithms that are programmed to perform online optimization. Another commonly used process control is supervisory control and data acquisition (SCADA) system. One important use of SCADA is the monitoring of field operations, with the capability of controlling the process unit equipment, flow valves, and compressor stations from the gas plant. Automation requires accurate input data to make the proper control decisions. These temperature, pressure, flow sensors, and gas analyzers require regular maintenance and tuning to ensure accurate data are transmitted to the computer system. Chapter 20 discusses the elements of automating today's gas processing plants including considerations for instrumentation, controls, data collection, operator information, optimization, information management, etc.

4.5.3 SAFETY SYSTEMS

A relief and flare system must be provided to ensure plant safety. Multiple flares are typically installed to allow one flare to be taken off-line for maintenance without shutting down the entire facility. The flare must be designed to protect against feed gas block discharge, as well as full relief loads from power failure and cooling water failure or other major failure modes. Proper sizing of relief valves and rupture disks is critical to ensure that each process unit is protected during an emergency. During normal operations, the gas plant is designed to avoid venting and flaring. If the plant is flaring mostly methane, the flame is bright but smokeless. If heavier hydrocarbons are flared, the flame will smoke and will be more noticeable from a distance. Smoke is undesirable and may create environmental problems. Steam can be injected to the flare system to maintain a smokeless flare. If the fuel has a low Btu content, fuel gas can be added to ensure complete combustion.

4.6 CONTRACTUAL AGREEMENTS

The gas processing industry performs the processing steps required to make the product gas marketable. These functions may include gas gathering, gas compression, and pipeline transmission. The gas must be conditioned to meet the sales gas specification. In addition to gas purification functions, the gas processors may elect to add discretionary processes to recover NGLs, as liquid revenue can sometimes generate higher revenues.

When new ventures are being evaluated, there are contractual agreements, which must be put in place to establish the legal framework that defines the gas plant economics. This establishes a balance between capital expenditures and operating costs. The type of contract is dependent on the risks and potential rewards. There is no straightforward answer to the type of agreements, as different companies may take a different approach, depending on their willingness to take risks. Most facilities may have a combination of agreements to hedge the risks.

There are four major types of agreements, which are discussed below.

4.6.1 KEEP WHOLE CONTRACTS

In "keep whole" contracts, the gas processor agrees to process or condition the producer's gas to meet sales gas specifications and to return to the producer 100% of the Btu value of the raw gas in exchange for retaining ownership of liquids extracted from the gas. The processor usually retains the liability for all processing costs and energy costs. The gas price is usually indexed on a spot gas price or an average of spot gas prices.

One of the variations to the keep whole agreement is to have a Btu cap or crude cap clause. The gas price is capped at a maximum price (Btu cap) or a maximum price relative to the price of crude oil (crude cap).

These contracts are more complex, more favorable to the producer, and more risky to the processor. The producer, in essence, sells the whole hydrocarbon stream, at the price of natural gas on a Btu basis, to the processor. The processor makes or loses money, depending on the price difference between natural gas and the NGL, which the processor sells.

Most contracts contain penalties for variations from contracted liquid content, impurities, and delivery pressure. Contracts may be set to allow for incremental variations from base composition. Contracts are commonly a combination of two or more of the above basic types.

4.6.2 FLAT FEE CONTRACTS

In fee-based contracts, the producer pays the gas processor a flat fee based on the gas produced. The processor may charge fees for additional services, such as gas gathering, gas compression, and pipeline transmission. In these contracts, the processor's income is independent of fluctuation of gas and NGL prices.

The gas processor takes custody of the gas and then bears all of the gas processing risk. The processor has the benefits of liquid uplift, along with the risk on volatility, but has to bear all operating costs, such as fuel, power, and transmission. Some producers/processors include offset terms to mitigate the risks of keep whole contracts or flat fee contracts.

4.6.3 PERCENTAGE OF PROCEEDS CONTRACTS

In percentage of proceeds contracts, the two parties agree to the percentage of the proceeds from the sale of the gas and liquids. Typically, the producer retains more than 70% of the proceeds from the sale of all products. In the case of multiple producers, each has a percentage share of the proceeds, allocated on the contribution to the proceeds.

Allocations can be based on the Btu content of the gas delivered from the wellhead for a producer divided by the sum of the Btu content of the gas from all producers. Both the producers and processors share the effect of gas and NGL price fluctuations, the cost of gathering and production, and the sales price of the gas and liquids production.

4.6.4 PROCESSING FEE CONTRACTS

This is a risk-free agreement from a processor's standpoint. The producer pays a fee based on the gas volume processed, which is generally a flat fee based on the types of gas conditioning and processing requirements. If only gas gathering and compression are required, the fee will be lower than that required to sweeten, dry and recover NGL.

Depending on the processing fees, the liquids may be retained by the producer. In most contracts, the processor will take title to a portion of the liquids. This arrangement is common in small isolated fields where there is limited competition.

In summary, the processing costs are shared between producer and processor for capital projects and the terms depend on the nature of the project and the potential risks. Capital items that benefit both parties may be cost shared. However, maintenance, replacements, and costs of environment and emissions compliance are borne by the processor as a cost of staying in business. Situations arise in which costs are too high for the processor to absorb alone, and producers must decide to either share the costs or cease production.

REFERENCES

Finn, A.J., 2007. Nitrogen rejection strategies. Hydrocarbon Engineering 12 (10), 49–52.

Garcel, J.C., May 14–16, 2008. Liquefaction of non-conventional gases. Paper Presented at the GPA Europe Conference, Ashford, Kent, UK.

Gottier, G.N., Herron, D.M., May 21, 1991. Dephlegmator Process for the Recovery of Helium. US5017204-A.

GPSA, 2004. Engineering Data Book, twelfth ed. Gas Processors Suppliers Association (GPSA), Tulsa, OK, USA.

Kidnay, A.J., Parrish, W., 2006. Fundamentals of Natural Gas Processing, first ed. CRC Press, Taylor & Francis Group, Boca Raton, FL, USA.

Mokhatab, S., 2010. An optimum lineup for sour gas processing. Petroleum Technology Quarterly, Gas, 37–43.

Mokhatab, S., Bloemendal, G., 2017. Optimal processing scheme for producing pipeline quality gas. Petroleum Technology Quarterly, Q1, 71–77.

Mokhatab, S., Mak, J.Y., Valappil, J.V., Wood, D.A., 2014. Handbook of Liquefied Natural Gas. Gulf Professional Publishing, Burlington, MA, USA.

Mokhatab, S., Meyer, P., May 14–15, 2009. Selecting best technology lineup for designing gas processing units. Paper Presented at GPA Europe Sour Gas Processing Conference, Sitges, Barcelona, Spain.

Mokhatab, S., Northrop, S., 2017a. Handling mercaptans in gas processing plants. Hydrocarbon Processing 96 (1), 31–34.

Mokhatab, S., Northrop, S., May–June 2017b. Integrated treatment strategies for gas processing projects. Gas Processing 9–11.

CHAPTER

PHASE SEPARATION

5

5.1 INTRODUCTION

Separation of oil and gas is a critical field processing operation. As producing pressure is increased and lighter condensates are produced, efficient separation has become more critical than ever. Moreover, some of the new concepts in separation technology have been applied to advantage on old lease producing oil at moderate or low pressures. As gas transmission lines raise their standards, separation becomes a part of the overall field processing necessary to condition the gas. Several technologies are available to remove liquids and solids from gases. However, selecting gas–liquid separation technologies requires not only knowledge of the process conditions but also knowledge of the characteristics of the liquid contaminants. Selection should be made based on the droplet size, concentration, and whether the liquid has waxing or fouling tendencies (Brown et al., 1994). Before evaluating specific technologies, it is important to understand the mechanisms used to remove liquids and solids from gases. Three principles used to achieve physical separation of gas and liquids or solids are momentum, gravity settling, and coalescing. Any separator may employ one or more of these principles; however, the fluid phases must be immiscible and have different densities for separation to occur. Momentum force is utilized by changing the direction of flow and is usually employed for bulk separation of the fluid phases. The gravitational force is utilized by reducing velocity so that the liquid droplets can settle out in the space provided. Gravity segregation is the main force that accomplishes the separation, which means the heaviest fluid settles to the bottom and the lightest fluid rises to the top. However, very small droplets such as mist cannot be separated practically by gravity. These droplets can be coalesced to form larger droplets that will settle by gravity.

The purpose of this chapter is to review the principles governing the basic separation process and to describe the commonly used separation facilities in the gas processing industry.

5.2 GRAVITY SEPARATORS

Gravity separators are pressure vessels that separate a mixed-phase stream into gas and liquid phases that are relatively free of each other. In a gravity separator, gravitational forces control separation, and the efficiency of the gas–liquid separation is increased by lowering the gas velocity. Because of the large vessel size required to achieve settling, gravity separators are rarely designed to remove droplets smaller than 250 microns (Talavera, 1990). However, an analysis of this type of separator is given because it is useful to help understand the settling mechanism of other separators.

Handbook of Natural Gas Transmission and Processing. https://doi.org/10.1016/B978-0-12-815817-3.00005-8

Gravity separators are often classified by their geometrical configuration (vertical, horizontal) and by their function (two-phase/three-phase separator). In other words, gravity separators are classified as "two-phase" if they separate gas from the total liquid stream and "three-phase" if they also separate the liquid stream in to its crude oil− and water-rich phases. Additionally, separators can be categorized according to their operating pressure. Low-pressure units handle pressures of 10−180 psi. Medium-pressure separators operate from 230 to 700 psi. High-pressure units handle pressures of 975−1500 psi.

Separators are sometimes called "scrubbers" when the ratio of gas rate to liquid rate is very high. These vessels usually have a small liquid collection section and are recommended only for following items:

- Secondary separation to remove carryover fluids from process equipment such as absorbers and liquid dust scrubbers.
- Gas line separation downstream from a separator and where flow lines are not long.
- Miscellaneous separation where the gas−liquid ratio is extremely high.

In any case, the processing equipment should have the same configuration and are sized in accordance with the same procedure of separators.

5.2.1 GENERAL DESCRIPTION

All gravity separators normally have the following components or features (API Spec 12J, 1989):

- A primary gas−liquid separation section with an inlet divertor to remove the bulk of the liquid from the gas.
- A gravity settling section providing adequate retention time so that proper settling may take place.
- A mist extractor at the gas outlet to capture entrained droplets or those too small to settle by gravity.
- Proper pressure and liquid level controls.

Gravity separators are designed as either horizontal or vertical pressure vessels. Fig. 5.1 is a typical scheme of a three-phase horizontal separator. The fluid enters the separator and hits an inlet diverter. This sudden change in momentum generates the initial bulk separation of liquid and gas. In most

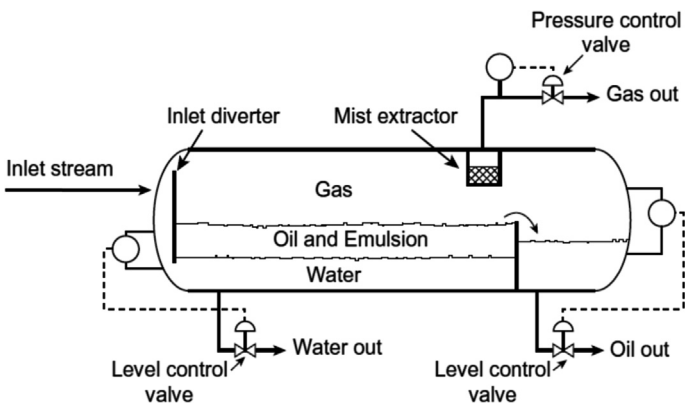

FIGURE 5.1

A typical scheme of horizontal three-phase separator.

designs, the inlet diverter contains a downcomer that directs the liquid flow below the oil−water interface. This forces the inlet mixture of oil and water to mix with the water continuous phase in the bottom of the vessel and rise through the oil−water interface. This process is called "water-washing" and it promotes the coalescence of water droplets that are entrained in the oil continuous phase. The inlet divertor assures that little gas is carried with the liquid, and the water wash assures that the liquid does not fall on top of the gas−oil or oil−water interface, mixing the liquid retained in the vessel and making control of the oil−water interface difficult. The liquid collecting section of the vessel provides sufficient time so that the oil and emulsion form a layer or "oil pad" at the top. The free water settles to the bottom. The produced water flows from a nozzle in the vessel located upstream of the oil weir. An interface level controller senses the height of the oil−water interface. The controller sends a signal to the water dump valve, thus allowing the correct amount of water to leave the vessel so that the oil−water interface is maintained at the design height.

The gas flows horizontally and outs through a mist extractor (normally known as a demisting device) to a pressure control valve that maintains constant vessel pressure. The level of the gas−oil interface can vary from half the diameter to 75% of the diameter depending on the relative importance of liquid−gas separation, and what purpose the separator has. For example, degassers and produced water flash drums have very high liquid−gas interfaces. However, the most common configuration is half full.

Fig. 5.2 shows a typical configuration for a vertical three-phase separator. In the vertical separator, the flow enters the vessel through the side as in the horizontal separator, and the inlet diverter separates the bulk of the gas. The gas moves upward, usually passing through a mist extractor to remove suspended mist, and then the dry gas flows out. A downcomer is required to transmit the liquid collected

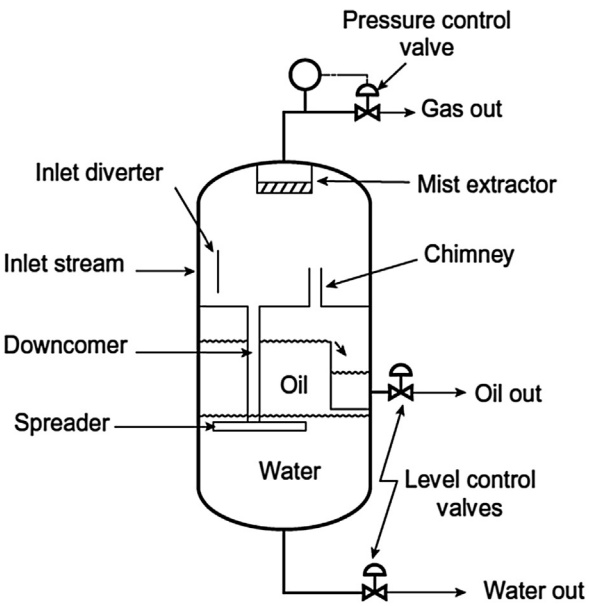

FIGURE 5.2

A typical scheme of vertical three-phase separator.

through the oil–gas interface so as not to disturb the oil skimming action taking place. A chimney is needed to equalize gas pressure between the lower section and the gas section. The spreader or downcomer outlet is located at the oil–water interface. From this point, as the oil rises any free water trapped within the oil phase separates out. The water droplets flow countercurrent to the oil. Similarly, the water flows downward and oil droplets trapped in the water phase tend to rise countercurrent to the water flow. It should be clear that the principles of operation (such as oil–water interface level controlling) of three-phase vertical separators are the same as three-phase horizontal separators those described above. Essentially, the only difference is that horizontal separators have separation acting tangentially to flow, whereas vertical separators have separation acting parallel to flow. In the vertical separator, level control is not also critical, where the liquid level can fluctuate several inches without affecting operating efficiency (GPSA, 2004). However, it can affect the pressure drop for downcomer pipe (from the demister) and can therefore reduce demisting device drainage.

5.2.2 SEPARATORS SELECTION

There are no simple rules for separator selection. Sometimes, both configurations should be evaluated to decide which is more economical. The relative merits and common applications of vertical and horizontal separators are summarized by Manning and Thompson (1995).

5.2.2.1 Horizontal Separators

Horizontal separators are most commonly used in the following conditions:

- Large volumes of gas and/or liquids
- High-to-medium gas–oil ratio (GOR) streams
- Foaming crudes
- Three-phase separation

The advantages and disadvantages of these separators are as follows:
Advantages:

- Require smaller diameter for similar gas capacity as compared with vertical vessels.
- No counter flow (gas flow does not oppose drainage of mist extractor).
- Large liquid surface area for foam dispersion generally reduces turbulence.
- Larger surge volume capacity.

Disadvantages:

- Only part of shell available for passage of gas.
- Occupies more space unless “stack” mounted.
- Liquid-level control is more critical.
- More difficult to clean produced sand, mud, wax, paraffin, etc.

5.2.2.2 Vertical Separators

These separators are used in the following conditions:

- Small flow rates of gas and/or liquids
- Very high GOR streams or when the total gas volumes are low.

- Plot space is limited.
- Ease of level control is desired.

The advantages and disadvantages of these separators are as follow.
Advantages:

- Liquid-level control is not so critical.
- Have good bottom-drain and clean-out facilities.
- Can handle more sand, mud, paraffin, wax without plugging.
- Lower tendency for reentrainment.
- Has full diameter for gas flow at top and oil flow at bottom.
- Occupies smaller plot area.

Disadvantages:

- Require larger diameter for a given gas capacity, therefore, most competitive for very low GOR or very high GOR or scrubber applications.
- It is not recommended when there is a large slug potential.
- More difficult to reach and service top-mounted instruments and safety devices.

5.2.3 GRAVITY SEPARATION THEORY

Vapor–liquid separation is usually accomplished in three stages. The first stage, primary separation, uses an inlet divertor[1] to cause the largest droplets to impinge by momentum and then drop by gravity. The next stage, secondary separation, is gravity separation of smaller droplets as the vapor flows through the disengagement area. Gravity separation can be aided by utilizing distribution baffles that create an even velocity distribution in the fluid, thus allowing enhanced separation. The final stage is mist elimination, where the smallest droplets are coalesced on an impingement device, such as a mist pad or vane pack, followed by gravity settling of the larger formed droplets.

In the gravity settling section of the separators, the liquid drops will settle at a velocity determined by equating the gravity force (F_B) on the drop with the drag force (F_D) caused by its motion relative to the vapor continuous phase. When the drag force is equal to the buoyancy (gravity) force, the droplets acceleration is zero so that it moves at a constant velocity. This velocity is the terminal or free settling velocity, which is determined with respect to the following equations:

$$F_B = \left(\frac{\pi}{6}\right) D_d^3 (\rho_L - \rho_V)\left(\frac{g}{g_C}\right) \tag{5.1}$$

where D_d is drop diameter, ft; ρ_L is liquid density, lbm/ft^3; ρ_V is vapor density, bm/ft^3; g is gravitational constant, 32.174 ft/sec^2; and g_c is conversion factor, 32.174 lbm-ft/sec^2-lbf.

[1]Inlet divertors are very old technology now and are very rarely used. Revamps in the North Sea replace these inlet devices all the time, especially where the asset is producing more throughput than originally expected. If incorrectly sized, inlet devices can cause serious separation issues due to droplet shatter. Schoepentoeters became the popular inlet device for a while, but these were designed for vertical separators and are therefore not always applicable. Cyclonic and distribution baffle inlet devices are more common nowadays.

Also, the drag force on the droplet is given by:

$$F_D = C_D(A_P)\left(\frac{\rho_V V_d^2}{2g_C}\right) \tag{5.2}$$

where C_D is the drag coefficient, dimensionless; A_p is the projected drop area, $ft^2 = (\pi/4)\, D_d^2$, (area of circle, not sphere); V_d, drop velocity, ft/sec.

Therefore, the terminal settling velocity of the liquid droplets (V_t) can be determined by equating Eqs. (5.1) and (5.2) as follows:

$$V_t = \sqrt{(4/3)D_d(\rho_L - \rho_V)g/(C_D\,\rho_V)} \tag{5.3}$$

The drag coefficient can also be calculated as follows (Svrcek and Monnery, 1993):

$$C_D = \frac{5.0074}{\mathrm{Ln}(x)} + \frac{40.927}{\sqrt{X}} + \frac{484.07}{X} \tag{5.4}$$

and

$$X = \frac{0.95 \times 10^8 D_d^3 \rho_V(\rho_L - \rho_V)}{{\mu_V}^2} \tag{5.5}$$

where D_d is in ft, densities are in lb/ft^3, and viscosity is in cP.

The droplet-settling velocity equation considers the escape of a drop from the continuous phase (e.g., the escape of an oil drop from the gas phase). For this purpose, the droplet-settling velocity must be greater than the superficial upward bulk vapor velocity, V_V. Typically, the allowable vapor velocity is set between 0.75 V_t and V_t (Svrcek and Monnery, 1993). Eq. (5.3) can be rearranged as a Souders and Brown (1934) type equation as follows:

$$V_t = K_{SB}\sqrt{(\rho_L - \rho_V)/\rho_V} \tag{5.6}$$

where

$$K_{SB} = \sqrt{\frac{4gD_d}{3C_D}} \tag{5.7}$$

In practice, the Souders and Brown design coefficient (K_{SB}) depends primarily on the type of mist extractor present, separator geometry, flow rates, and fluid properties. Therefore, K_{SB} is usually determined from experiments. A well-known source of empirical K_{SB} factors for mist pads is the GPSA (2004) Engineering Data Book. The GPSA's K_{SB} factors have been curve fitted and are given as:

$$K_{SB} = 0.35 - 0.0001(P - 100) \tag{5.8}$$

where K_{SB} is in ft/sec and P is the separator pressure in psig. Also, the factor K_{SB} should be adjusted as follows:

1. For most vapors under vacuum, $K_{SB} = 0.20$.
2. For glycols and amine solutions, multiply K_{SB} values by 0.6–0.8.
3. For compressor suction scrubbers and expander inlet separators, multiply K_{SB} by 0.7–0.8.

Maximum terminal velocities calculated using the K_{SB} factors are for separators normally having a wire mesh mist extractor and should allow all liquid droplets larger than 10 micron to settle out of the gas. If no mist extractor is present, multiply K_{SB} by 0.5.

It is often necessary to separate two immiscible liquids, the light and heavy phases, and a vapor. A typical example in the petroleum industry is the separation of water, and a hydrocarbon liquid and vapor. For this system, the flow of rising light droplets in the heavy liquid phase or settling heavy droplets in the light liquid phase is considered laminar and is governed by Stokes law (Monnery and Svrcek, 1994):

$$V_t = \frac{K_s(\rho_H - \rho_L)}{\mu} \tag{5.9}$$

$$K_s = 2.06151 \times 10^{-5} D_d^2 \tag{5.10}$$

where, V_t is in inch/min, densities of light and heavy liquid phases (ρ_L, ρ_H) are in lb/ft^3, viscosity is in cP, and D_d is in microns (1 microns = 3.28,084 $\times$ 10^{-6} ft).

As can be seen from Eq. (5.9), the settling velocity of a droplet is inversely proportional to the viscosity of the continuous phase. Hence, it requires more time for the droplets to settle out of the continuous phase with greater viscosity. In practice, V_t is typically limited to 10 in./min.

5.2.4 DESIGN CONSIDERATIONS

The following factors must be determined before beginning separator design:

- Gas and liquid flow rates (minimum, average, and peak).
- Operating and design pressures and temperatures.
- Surging or slugging tendencies of the feed streams.
- Physical properties of the fluids such as density, viscosity, and compressibility.
- Designed degree of separation (e.g., removing 100% of particles greater than 10 microns).

Consideration for the future life of the field should also be included. For example, most North Sea separators were designed for high oil cuts but are now operating on high water cuts, which produce a lot of nozzle problems.

The initial design and calculation of gravity separators are discussed in many books and basic references (Kumar, 1987; Campbell, 1992; Arnold and Stewart, 1998). However, a more accurate and detailed sizing of two- and three-phase separators can be performed by using the design methods developed by Svrcek and Monnery (1993), and Monnery and Svrcek (1994), which have been well received by the industry worldwide. These procedures are a result of a review of literature sources and accepted industrial design guidelines and allow the production facility engineer to choose the detailed sizing parameters of the two- and three-phase separators. However, it is reasonably common nowadays for vessel sizing to be subcontracted out either directly to the vessel supplier or sometimes to the internals supplier.

5.3 MULTISTAGE SEPARATION

To achieve good separation between the gas and liquid phases and maximizing the hydrocarbon liquid recovery, it is necessary to use several separation stages at decreasing pressures in which the well

stream is passed through two or more separators that are arranged in series. The operating pressures are sequentially reduced, hence the highest pressure is found at the first separator and the lowest pressure at the final separator. In practice, the number of stages normally ranges between 2 and 4, which depends on the GOR and the well stream pressure. Two-stage separation is usually used for low GOR and low well stream pressure, three-stage separation is used for medium to high GOR and intermediate inlet pressure, and four-stage separation is used for high GOR and high pressure well stream. Note that three-stage separation usually represents the economic optimum, where it allows 2%−12% higher liquid recovery in comparison with two-stage separation and, in some cases, recoveries up to 25% higher (Rojey et al., 1997). To recover the gases fractions produced in the separators operating at medium pressure and at low pressure, it is necessary to recompress them to the pressure of high-pressure separator. However, for an associated gas, recompression is sometimes considered too costly; hence the gas produced from the low pressure separator may be flared.

It should be noted that the main objective of stage separation is to provide maximum stabilization to the resultant phases (gas and liquid) leaving the final separator, which means the considerable amounts of gas or liquid will not evolve from the final liquid and gas phases, respectively. The quantities of gas and liquid recovered at a given pressure are determined by equilibrium flash calculations using an appropriate equation of state (EOS). This helps to optimize the value of pressure that is set for each separator. The pressures are often staged so that the ratio of the pressures in each stage is constant. Therefore, if the pressure in the first separator (which is normally fixed by specification or economics) and the pressure in the final separator (which will be near the atmospheric pressure) are known, the pressure in each stage can be determined.

5.4 CENTRIFUGAL SEPARATORS

In centrifugal or cyclone separators, centrifugal forces act on a droplet at a force several times greater than gravity, as it enters a cylindrical separator (Fig. 5.3). This centrifugal force can range from 5 times gravity in large, low velocity unit to 2000 times gravity in small, high pressure units. Generally, centrifugal separators are used for removing droplets greater than 100 μm in diameter, and a properly sized centrifugal separator can have a reasonable removal efficiency of droplet sizes as low as 10 μm.

Centrifugal separators are also extremely useful for gas streams with high particulate loading (Talavera, 1990). Such equipment has already been studied; however, a simple, compact, and light-weight gas−liquid cylindrical cyclone (GLCC) separator has been developed by Tulsa University that requires little maintenance and is easy to install and operate. The compact dimensions, smaller footprint, and lower weight of the GLCC have a potential for cost savings to the industry, especially in offshore applications. Also, the GLCC reduces the inventory of hydrocarbons significantly, which is critical to the environmental and safety considerations. The GLCC separator, used mainly for bulk gas−liquid separation, can be designed for various levels of expected performance. Typical performance levels from the GLCC separator are 0.5−2.0 gallons of liquid per MMscf in the gas outlet and 0%−5% gas in the liquid outlet (NATCO, 2002). More information on the design, control system studies, experimental investigations, and field applications of GLCC separators is discussed in greater detail by Gomez et al. (2000), Mohan and Shoham (2003), and Wang et al. (2003).

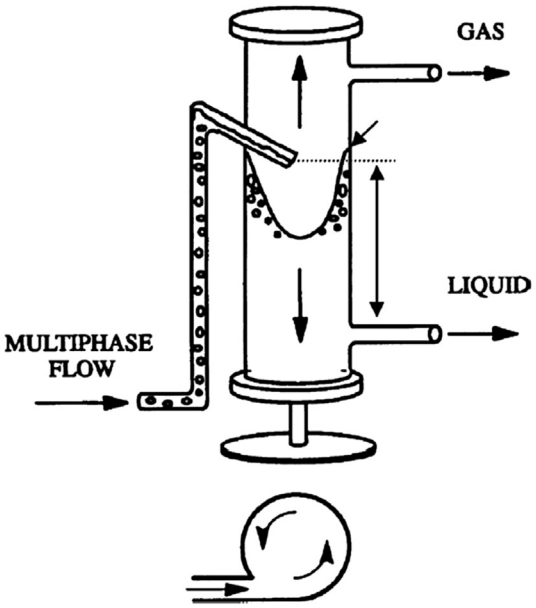

FIGURE 5.3

Gas–liquid cylindrical cyclone configuration (Kouba et al., 1995).

5.5 TWISTER SUPERSONIC SEPARATOR

The Twister supersonic separator is a unique combination of the expansion, cyclonic gas–liquid separation, and recompression process steps in a compact, static, tubular device to condense and separate water and heavy hydrocarbons from natural gas. Significant potential has been identified for future of Twister technology for other gas processing applications including deep LPG extraction, bulk removal of CO_2 and H_2S, mercury removal, and subsea gas processing.

Twister has thermodynamics similar to a turboexpander, which transforms pressure to shaft power. Therefore, Twister achieves a similar temperature drop by transforming pressure to kinetic energy (i.e., supersonic velocity). The tube is the heart of the Twister system that combines adiabatic cooling, in which no heat enters or leaves the system, with cyclonic separation in a single, compact device. Fig. 5.4 details the cross section and key components of the tube design. As can be seen, adiabatic cooling is achieved in a Laval nozzle—an aerodynamically shaped venturi tube—which is used to expand the saturated feed gas to supersonic velocity, resulting in a low temperature and pressure. This results in the formation of a mist of water and hydrocarbon condensation droplets. The fine, dispersed liquids formed during the adiabatic expansion are separated using a cyclonic separator as a result of the centrifugal forces exerted by the strong swirling flow and removed from the dry flow with significantly high separation efficiency. The liquid stream contains slip-gas, which will be removed in a compact liquid degassing vessel and recombined with the dry gas stream (see Fig. 5.5). Twister is a

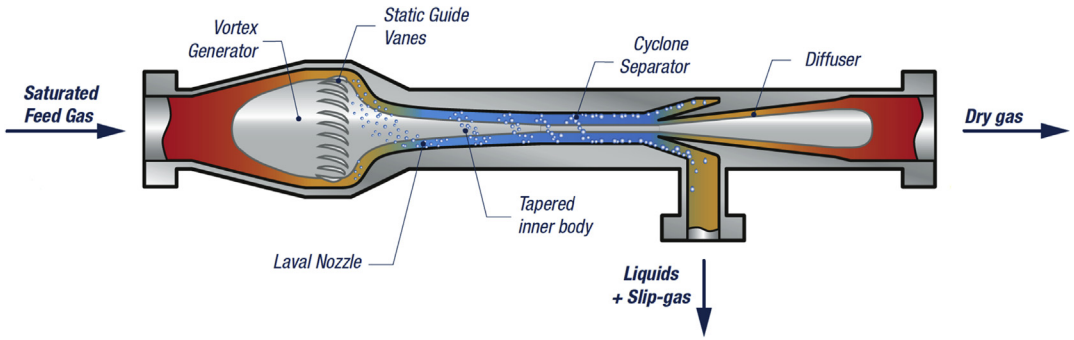

FIGURE 5.4

Cross section of a Twister tube.

Courtesy of Twister BV.

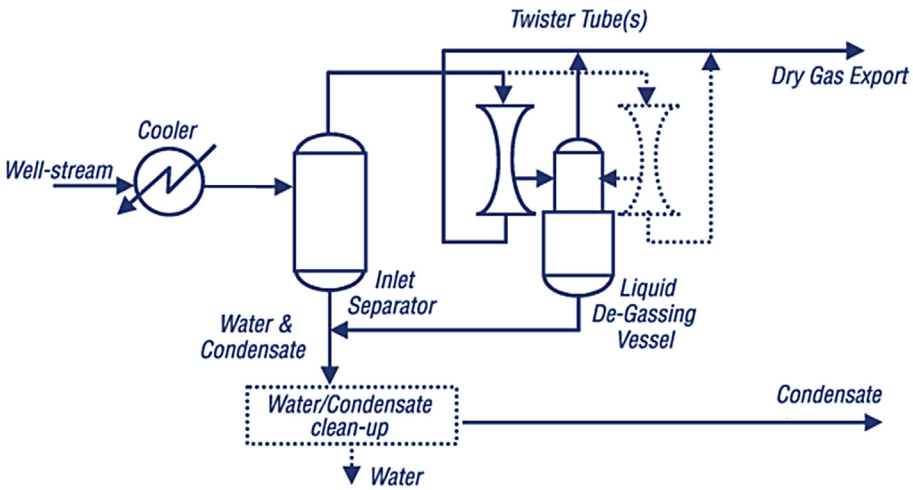

FIGURE 5.5

Process flow diagram for a typical Twister system.

Courtesy of Twister BV.

low-temperature separation process, for which performance can be optimized by inlet cooling. The inlet separator upstream of the Twister tubes is designed to remove produced liquids and prevent carryover of slugs and solids.

The residence time inside the Twister supersonic separator is only milliseconds, allowing hydrates no time to form and avoiding the requirement for hydrate inhibition chemicals. The simplicity and reliability of a static device, with no rotating parts which operates without chemicals, ensures a simple and safe facility with a high availability, suitable for unmanned operation in harsh and/or offshore environments.

Twister technology was developed in 1998 for hydrocarbon dewpoint control for offshore application. Current commercial experience is two Twister separation units installed on the Petronas/Sarawak platform in Malaysia. Recently, Twister BV introduced the Twister SWIRL valve, which claims to have higher separation efficiency. UOP has also joined the development effort, applying their multiple valves switching technology to dampen out gas flow fluctuation required by the Twister separator operation.

5.6 SLUG CATCHERS

Slug catchers are used at the terminus of large gas–condensate transmission pipelines to catch large slugs of liquid in pipelines, to hold these slugs temporarily, and then to allow them to follow into downstream equipment and facilities at a rate at which the liquid can be properly handled. In fact, the slug catcher provides temporary storage for any surges (slugs) in liquid flows and roughly separates the gas from the liquids. The gas then exits the top of the slug catcher and flows to the plant inlet separator via a pressure control valve, which reduces the pressure of the gas, and further condenses water and some of the heavier hydrocarbons.

Slug catchers may be either of the vessel or of the manifold pipe type. A vessel-type slug catcher is essentially a knockout vessel. This type is simple in design and maintenance. A pipe-type slug catcher consists of several long pieces of pipe (fingers), which together form the buffer volume to store the largest slugs expected from the upstream system. Vessel-type slug catchers can only be used if the incoming liquid volume is small. When larger liquid volumes have to be accommodated, say of more than 100 m^3 (3531 ft^3), the pipe-type slug catcher should be used (Shell DEP 31.40.10.12-Gen, 1998). Pipe-type slug catchers are frequently less expensive than vessel-type slug catchers of the same capacity due to thinner wall requirements of smaller pipe diameter. The manifold nature of multiple pipe-type slug catchers also makes possible the later addition of additional capacity by laying more parallel pipes. As the pipe-type slug catcher is defined as a piping configuration rather than a pressure vessel, it is not constrained to the same requirements as a normal vessel. However, due to its large size, it will contain the majority of high-pressure hydrocarbon gas on the site. It is therefore recommended that the slug catcher be automatically depressurized (for prevention of fire) as quickly as possible without imposing unusually high flow rates on the flare system.

A schematic of a pipe-type slug catcher is shown in Fig. 5.6. The general configuration consists of the following parts:

- Fingers with dual slope and three distinct sections: gas–liquid separation, intermediate and storage sections.
- Gas risers connected to each finger at the transition zone between the separation and intermediate sections.
- Gas equalization lines located on each finger. These lines are located within the slug storage section.
- Liquid header collecting liquid from each finger. This header will not be sloped and is configured perpendicular to the fingers.

Note that it has been assumed that all liquids (condensate and water) are collected and sent to an inlet three-phase separator, although it is possible to separate condensate and water at the fingers

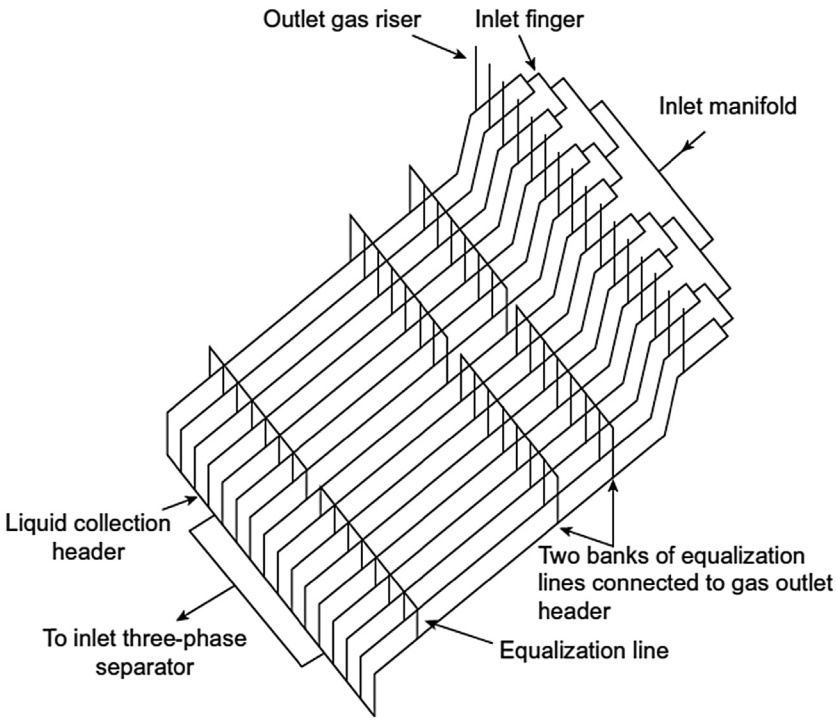

FIGURE 5.6

Three-dimensional rendering of finger-type slug catcher.

directly. When doing condensate—water separation at the slug catcher itself, we have to allow separately for the maximum condensate slug and the maximum water slug to ensure continuous level control.

Separation of gas and liquid phases is achieved in the first section of the fingers. The length of this section will promote a stratified flow pattern and permit primary separation to occur. Ideally liquid droplets, 600 micron and below, will be removed from the gas disengaged into the gas risers, which are located at the end of this section. The length of the intermediate section is minimal such that there is no liquid level beneath the gas riser when the slug catcher is full, i.e., storage section completely full. This section comprises of a change in elevation between the gas risers and the storage section that allows a clear distinction between liquid and gas phases. The length of the storage section ensures that the maximum slug volume can be retained without liquid carryover in the gas outlet. During normal operations, the normal liquid level is kept at around the top of the riser from each finger into the main liquid collection header, which is equivalent to approximately 5 min operation of the condensate stabilization units at maximum capacity.

Because the slug catcher is the first element in the gas processing plant, determining its proper size is vital to the operation of the entire plant. In fact, if more liquid is brought in than the slug catcher can handle, the plant normally shuts down. Therefore, slug sizing results should always be treated with

caution, and slug catchers should be designed with an ample design margin (Burke and Kashou, 1996; Xiao and Shoup, 1998). Shell DEP 31.40.10.12-Gen (1998) specifies requirements and gives recommendations for the design of multiple-pipe slug catchers. However, vendors should be requested to provide detailed design guidelines.

5.7 HIGH-EFFICIENCY LIQUID–GAS COALESCERS

Aerosols in gas streams can often be less than 5 micron in size and require the use of special separation equipment. High-efficiency liquid–gas coalescers have been applied effectively for the removal of fine aerosols in gas production, processing, and transmission. Coalescers are typically constructed as cartridges that use pleated glass fiber media supported by a metal core. The coalescer cartridges are then placed in a housing that controls the inlet–outlet gas velocities to ensure good separation and prevent any reentrainment of liquids. The coalescer media contains a much finer pore structure and larger surface area as compared with traditional separators that often use mesh pads or vane pack internals.

5.7.1 AEROSOLS

Aerosols are formed by three mechanisms: condensation, atomization, and entrainment. The relative sizes produced by these formation mechanisms are given in Fig. 5.7.

Aerosols formed by condensation of a vapor into a liquid are the smallest and most difficult to remove contaminants having a size distribution in the range of 0.2–5 microns. Atomization creates aerosol drops by breaking up larger liquid drops through mechanical shear such as passing through a constriction in a valve under a high velocity. Atomization forms aerosols in the size range of 10–200 microns. Entrainment involves the movement of liquid slugs along pipelines, and here the liquid drop sizes are very large from 500 to 5000 microns. All three types of aerosol liquids are commonly found in gas systems. High-efficiency liquid–gas coalescers can effectively remove the fine aerosols created by the condensation mechanism.

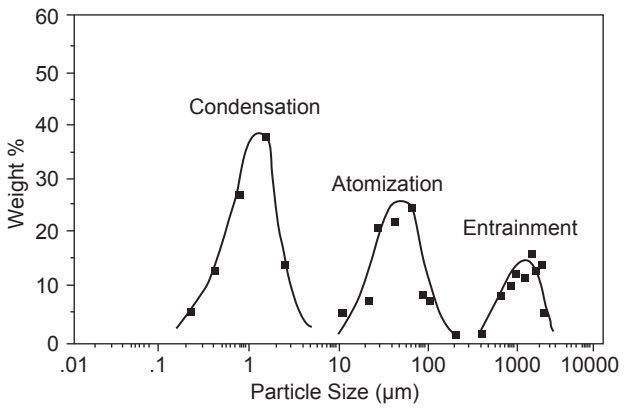

FIGURE 5.7

Aerosol types (Brown et al., 1994).

5.7.2 COALESCER CONSTRUCTION/OPERATION PRINCIPLES

High-efficiency liquid–gas coalescers are generally constructed from glass fibers because this material allows for a fine porous structure with fiber diameters of a few microns. The small pore size is needed to achieve greater capture and separation of these small aerosols. The primary rational for the use of high-efficiency coalescers is that significant aerosol contaminant exists in the plants that are in the submicron and low micron size range (Brown et al., 1994).

This type of liquid–gas coalescer can operate at significantly lower flow rates than the initial design flow rate and therefore can tolerate a high turn down ratio. This is due to the separation mechanisms for coalescing that are primarily diffusion and direct interception unlike vane separators and mesh pads that rely heavily on inertial separation principles. This allows the high-efficiency liquid–gas coalescer systems a greater degree of flexibility, and they can operate at peak performance even for high turndown ratios (reduced flow rates), which can occur during commonly encountered partial plant shutdowns and upset conditions.

The use of a surface treatment (Miller et al., 1988) on high-performance vertical liquid–gas coalescer cartridge systems has been proven to significantly enhance performance by allowing higher flow rates or smaller housing diameters compared with untreated coalescers. The surface treatment alters the properties of the coalescer medium so that it will not wet out with oil or water-based fluids. The treatment has also been found to extend the service of the coalescer by reducing fouling and also to lower the saturated pressure drop. A Pall vertical high-efficiency liquid–gas coalescer system is depicted in Fig. 5.8.

The inlet gas with liquid aerosol contamination first enters at the bottom of the housing into a first-stage knockout section. Here any slugs or larger size droplets (approximately >300 μm) are removed by gravitational settling. The gas then travels upward through a tube sheet and flows radially from the inside of the cartridges through the coalescer medium to the annulus. The inlet aerosol distribution is in the size range of 0.1 −300 μm and after passing through the coalescer medium is transformed to enlarged coalesced droplets in the size range of 0.5–2.2 mm. The advantage of flowing from the inside to outside of the coalescer cartridge is that the gas velocity can be more easily adjusted in the annulus by selecting the optimum housing diameter to prevent reentrainment of coalesced droplets.

As the gas leaves the coalescer cartridge and travels upward in the annulus, it contributes to the total flow, thereby increasing the annular velocity. The annular velocity is modeled as a linear function with vertical distance, and the annular velocity is zero at the bottom of the cartridge and increases to a maximum value at the top of the cartridge.

Once the coalesced droplets are formed, they immediately drain vertically downward in the coalescer medium pack. The surface treatment greatly enhances this drainage, and as a direct consequence of the treatment, the coalesced droplets are shielded from the upward gas flow in the annulus in the upper 2/3 section of the coalescer cartridge. The coalesced droplets are first exposed to the annular gas flow when they appear on the external face of the coalescer medium pack at the bottom third of the coalescer cartridge (see Fig. 5.9). Once the coalesced droplets are released to the annular space they are subjected to the force of the upward flowing gas. The trajectory of the coalesced droplets is modeled on a force balance between gravity settling and the drag force created by the gas flow past the droplets. This analysis leads to the calculation of a critical annular velocity for reentrainment.

Due to the surface treatment, there are minimal coalesced droplets present in the annulus above the drainage point at the bottom third of the coalescer cartridge. For a coalescer cartridge that is not

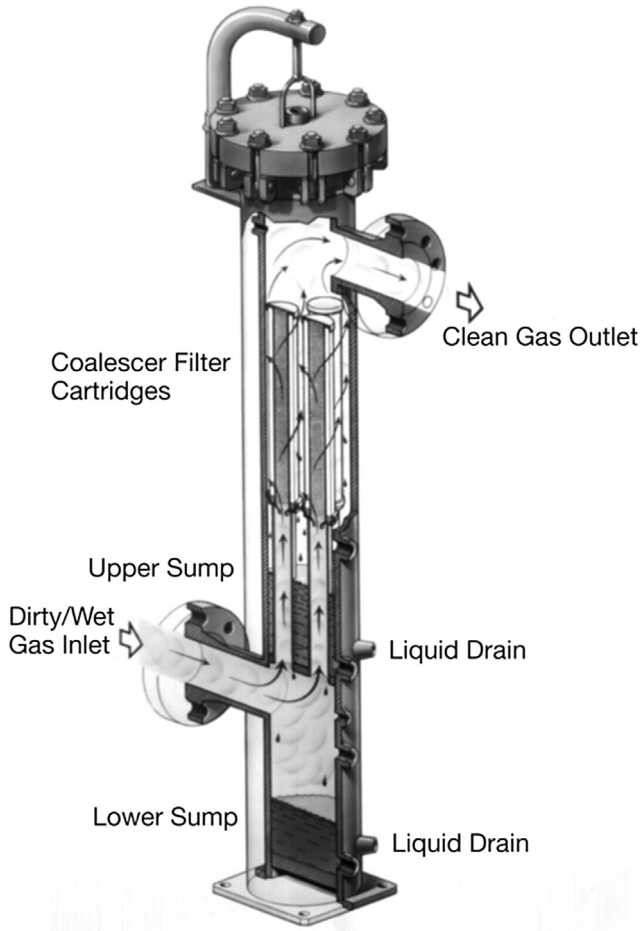

FIGURE 5.8

High-efficiency vertical liquid–gas coalescer system.

Courtesy of Pall Corporation.

specially surface treated, the coalesced liquids are present throughout the length of the coalescer in the annulus space, and the critical annular velocity for reentrainment is given for the top of the element (see Fig. 5.9). For the treated coalescer, it is allowable to have annular velocities greater than the critical value for reentrainment in the portion of the annulus space where there are no liquids present. This allows the maximum annular velocity at the top of the coalescer cartridge to be about three times the critical reentrainment value needed at the vertical position of the lower one-third of the cartridge height where liquids are present.

Therefore, the maximum annular velocity at the top of the coalescer cartridge is found to be about three times greater than the value for an untreated coalescer. The annular area is determined using the maximum allowable annular velocity and designed to be of sufficient size to prevent reentrainment and as small as possible to minimize the housing diameter.

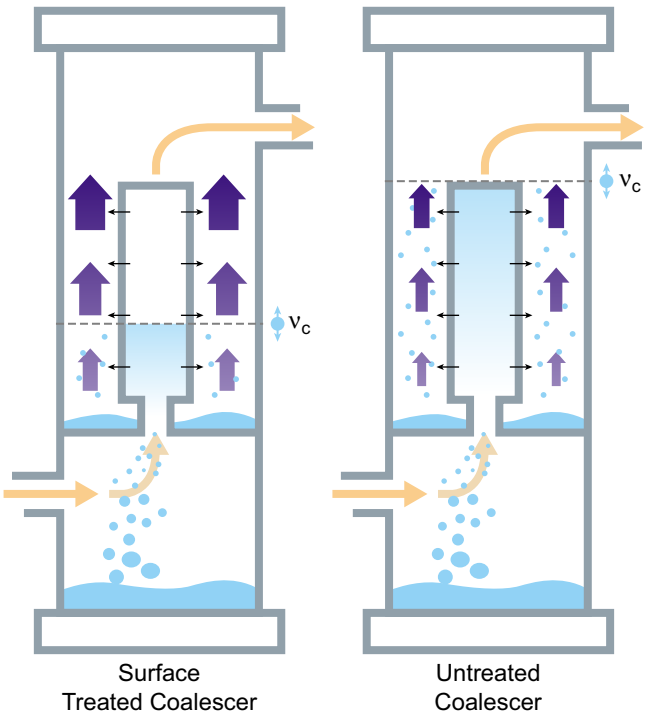

FIGURE 5.9

Effect of surface treatment on coalescer drainage (Wines, 2004).

5.7.3 MODELING THE LIQUID–GAS COALESCER

The modeling of the liquid–gas coalescer system can be divided into two basic aspects for performance: media velocity and annular velocity. The other consideration to be taken into account is pressure drop. The pressure drop for a given system can be decreased by using more coalescer elements.

5.7.3.1 Media Velocity

The media velocity (V_{med}) is defined as the actual flow rate divided by the coalescer filter area (Wines, 2004):

$$V_{med} = \frac{Q_a}{NA_{med}} \tag{5.11}$$

where N is number of coalescers, A_{med} is media area for one coalescer, and Q_a is actual system flow rate at system conditions that is obtained from the standard system flow rate (Q_s) as:

$$Q_a = \frac{Q_S(SG)\rho_{Air,stp}}{\rho_G} \tag{5.12}$$

where SG is gas specific gravity, $\rho_{Air,stp}$ is density of air at standard temperature and pressure, and ρ_G is density of gas at system conditions.

The media velocity is not the actual velocity through the open pores of the media, but rather an average by convention over the combined pore area and solid matrix area in the spatial plane normal to the flow direction. The maximum media velocity for a coalescer construction is related to a number of factors intrinsic to the particular coalescer design and to the physical properties of the system. Four steps have been identified with the mechanism of the formation and removal of droplets in the coalescer medium: capture, coalescing, release, and drainage.

The formation of the coalesced droplets first involves the capture of the small aerosols onto the fibers of the coalescer medium. The actual coalescing or merging of the fine droplets is believed to take place on the fibers and especially at fiber intersections. The coalesced droplets are then released from the fiber due to the drag force of the gas flow exceeding the adsorption energy. This process is repeated through the depth of the coalescer medium until the coalescing process is completed and the largest possible stable droplet size is achieved. During the coalescing stages, the growing droplets are also draining downward inside the media pack due to the force of gravity.

The surface treatment allows the release and drainage process to proceed at a faster rate which in turn frees up more coalescing sites on the fibers and allows the coalescer to process higher inlet liquid aerosol concentrations than the untreated coalescer medium.

5.7.3.2 Effect of System Conditions on Media Velocity

The ability of the coalescer medium to perform effectively will also depend on the system environment. While different coalescer constructions will exhibit quantitative differences, they will follow the same qualitative behavior. The media velocity has been determined to depend on system parameters such as inlet aerosol concentration, aerosol density, gas density, and gas viscosity.

At low aerosol concentrations, the maximum media velocity is constant and is unaffected by aerosol levels. Under these conditions the media is limited by the capture mechanism and is not affected by drainage. At higher levels of aerosol concentration, the coalescer medium becomes limited by drainage and is inversely proportional to the aerosol concentration. The effect of the surface treatment on this process is to enhance the drainage and allow for higher maximum media velocities under the same aerosol loading when limited by drainage.

5.7.3.3 Annular Velocity

The annular velocity (V_{ann}) is defined as the actual flow rate divided by the annulus area (Wines, 2004):

$$V_{ann} = \frac{Q_a}{A_{ann}} \tag{5.13}$$

where, A_{ann} is cross-sectional annular area defined as the cross-sectional area of the housing without coalescers minus the area of the coalescer end caps:

$$A_{ann} = \pi R_h^2 - N\pi R_c^2 \tag{5.14}$$

where R_h is radius of the housing, R_c is radius of coalescer end cap, and N is number of coalescers.

The enlarged droplets leaving the coalescer media pack can be assumed to be as large as possible for the given flow conditions when complete coalescence has occurred. Therefore, the coalesced

droplet diameter will be the same for any specific design of the coalescer cartridge as long as complete coalescence has been achieved. If complete coalescence is not achieved, the calculation of the coalesced droplets must take into account the degree of coalescence.

In most industrial applications, the coalesced droplets will range in size from 0.5 to 2.2 mm and will be mostly influenced by the interfacial tension, which is significantly affected by the liquid density, system temperature, and system pressure. As the pressure is increased, the gas density will increase while the liquid density is only slightly affected. The solubility of the gas in the liquid is enhanced with increasing pressure. This leads to a substantial decrease in interfacial tension with increasing pressure and consequently to significantly smaller coalesced droplets at the higher pressures.

Once the coalesced droplet size has been estimated, the next step is to determine the maximum annular velocity that can be sustained without reentrainment. In general, the coalesced droplets will produce Reynolds numbers (Re) outside of the creeping flow regime (<0.1) and Stokes law. Instead, a force balance is used between the liquid droplets settling by gravity and the drag force of the gas flowing upward in the opposite direction.

5.7.3.4 Determination of Minimum Housing Diameter

The housing diameter is determined from the area of the annulus and the area of the coalescer end caps. The maximum annular velocity at the top of the coalescer cartridges is used to determine the annular area required. The value of the maximum annular velocity ($V_{ann,max}$) at the top of the coalescer cartridges is dependent on the critical annular velocity for reentrainment (V_c) and the vertical location at which the coalesced droplets are present in the free annulus space. This relationship can be described as follows (Wines, 2004):

$$V_{ann,max} = k_a V_c \tag{5.15}$$

where, k_a is the annular velocity enhancement factor due to drainage.

For the untreated coalescer medium, the coalescer cartridge is completely wetted and coalesced droplets are present in the annulus space up to the top of the annulus where the annular velocity is highest. There is no drainage enhancement and $k_a = 1$. The maximum annular velocity to prevent reentrainment is then equal to the critical value for reentrainment:

$$\text{Untreated Coalescer: } V_{ann,max} = V_c \tag{5.16}$$

The effect of the surface treatment is to greatly increase the drainage, and the annular velocity at the top of the coalescer cartridge can now be significantly higher than the critical value because there are no coalesced droplets present in the annulus except in the bottom third of the cartridge. The maximum annular velocity is now determined with $k_a = 3.1$ as follows:

$$\text{Surface Treated Coalescer } V_{ann,max} = 3.1 V_c \tag{5.17}$$

Convincing evidence for the enhanced maximum annular velocity given by Eq. (5.15) has been demonstrated by laboratory tests (Murphy, 1984; Williamson et al., 1988) and is presented in Fig. 5.9. Visual observations during these tests also confirm that liquids are present on the outside of the coalescer pack only at the bottom third for the surface-treated coalescer and are present throughout the length of the wetted untreated coalescer.

5.7.4 COALESCER PERFORMANCE/OPERATIONAL LIMITS

Generally, the high-efficiency liquid–gas coalescers are used for inlet aerosol concentrations of a few thousand ppmw or less and are placed downstream of other bulk removal separators as the final purification stage. Under these conditions, typical service life for liquid–gas coalescers is 1–2 years. Coalescer systems are usually sized for a clean differential pressure (DP) of 2–5 psi, and when this DP reaches 15 psi, they are replaced with new elements. Outlet concentrations for these high-efficiency liquid–gas coalescers are as low as 0.003 ppmw (Murphy, 1984; Williamson et al., 1988).

5.7.5 LIQUID–GAS COALESCER APPLICATIONS

The separation of liquid aerosol contamination with high-performance liquid–gas coalescer cartridge systems has found widespread acceptance in gas plants in recent years for a number of applications such as protection of compressors, turbo equipment, low NOx burner nozzles, amine and glycol contactors, and molecular sieve beds. This has largely been the result of traditional separation approaches including knockout vessels, centrifugal separators, mesh pads, or vane separators not meeting the end user's requirements for aerosol reduction. A brief description of some of the main applications is given by Wines and Mokhatab (2017a).

5.8 HIGH-EFFICIENCY LIQUID–LIQUID COALESCERS

Liquid–liquid separations may require the use of special equipment when the drop sizes are small typically in the range of 1–50 microns in size. These fluid systems are classified as stable emulsions, and often conventional bulk separators with mist pads or plate type internals will not be effective. High-efficiency liquid–liquid coalescers have been developed to break these emulsions and provide improved separation.

5.8.1 EMULSIONS

Emulsions consist of three components: oil (representing hydrocarbon or organic liquids), water (including any aqueous mixtures), and surfactants.[2] Depending on the ratio of these components, oil-in-water emulsions or water-in-oil emulsions can exist. The structure of the oil-in-water or water-in-oil emulsions is well defined with spherical droplets of the dispersed phase surrounded by a bulk continuous phase and surfactant sheathing the droplets. Surfactants contain both hydrophilic (water loving) and hydrophobic (water fearing) portions in the same molecule. This unique structure allows them to associate at water–oil interfaces and helps them to stabilize the droplet shape. A spherical drop shape is formed to minimize the surface area between the oil and water, and this also minimizes the free energy required to make this surface. To make an emulsion, the system must be subjected to shear or mixing to allow the three components to break up into the droplet structure.

Emulsions are inherently unstable and will spontaneously separate out into two bulk phases. This process requires that the small droplets merge together or coalesce repeatedly until they form

[2]Surfactants consist of polar or hydrophilic groups joined to nonpolar or hydrophobic hydrocarbon chains. The ability of surfactants to aid in the emulsification process will depend on the ratio of the polar to nonpolar groups, the charge density and size of the polar group, and the volume occupied by the nonpolar groups (branching and length).

increasing drop sizes that eventually merge with a bulk phase until all of the drops are gone. Depending on the nature of the emulsion, the separation can occur in a matter of seconds or months. Many of the same factors that affect emulsion stability also influence coalescer performance.

5.8.2 COALESCER PRINCIPLES AND MATERIALS OF CONSTRUCTION

Coalescers are typically manufactured as either pads or cartridge filters that have been designed especially to take small droplets in an emulsion and grow them into large drops that are more easily separated. This process is accelerated over natural coalescing by the fibers present in coalescer media that force the contact of small droplets thereby promoting the coalescing process. The pore gradient of coalescer medium is constructed so that the inlet medium has fine pore sizes that increase in size with the flow direction (see Fig. 5.10).

Coalescers have been primarily constructed with glass fiber media until recently when polymer and fluoropolymer materials were adopted. Glass fiber works adequately for emulsions with interfacial tensions >20 dyne/cm. It is known to disarm and lose efficiency in the presence of surfactants (Hughes, 1997). These coalescers are widely used to dewater jet fuel for the aviation industry.

High-efficiency liquid–liquid coalescers are the newest generation of coalescers, incorporating the latest in coalescer technology. They are constructed from polymer and fluoropolymer materials that have been optimized to separate the most difficult emulsions with interfacial tensions as low as 0.5 dyne/cm. This coalescer can be used with a broad range of applications. It can process aggressive chemicals and handle demanding operating conditions while providing the highest level of performance.

5.8.3 COALESCER MECHANISM OF OPERATION

The liquid–liquid coalescing system operates in three stages: separation of solids/preconditioning, coalescence, and separation of coalesced drops.

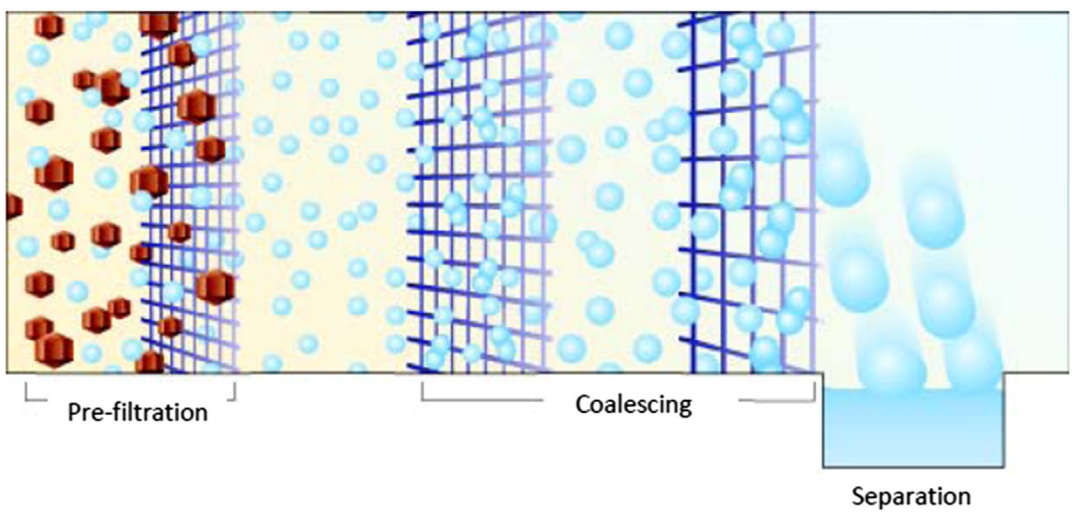

FIGURE 5.10

Coalescing in the media.

Courtesy of Pall Corporation.

5.8.3.1 Separation of Solids/Preconditioning of the Fluid

Solids can increase the stability of an emulsion, and removing solids can make coalescing easier. Generally, this step can be achieved by a separate cartridge filter system or by a regenerable backwash filter system for high levels of solids. In addition, the filtration stage protects the coalescer and increases service life. This step also initiates the coalescence of the hydrocarbon droplets, thereby enhancing the separation capabilities of the system.

5.8.3.2 Coalescence

The next step in the process is the primary coalescence. In this stage, the pore dimensions begin with a very fine structure and then become more open to allow for void space for the coalescing droplets. In the primary coalescence zone, the inlet dispersion containing fine droplets in the size range of 0.2−50 microns is transformed into a suspension of enlarged droplets in the size range of 500−5000 microns.

The coalescence mechanism can be described by the following steps:

1. Droplet adsorption to fiber
2. Translation of droplets to fiber intersections by bulk flow
3. Coalescence of two droplets to form one larger droplet
4. Repeated coalescence of small droplets into larger droplets at fiber intersections
5. Release of droplets from fiber intersections due to increased drag on adsorbed droplets caused by bulk flow
6. Repeat of steps 1−5 with progressively larger droplet sizes and more open media porosity

Based on this mechanism, we can predict that a number of factors will influence the coalescence performance. The specific surface properties of the coalescer fibers are critical in influencing the adsorption of droplets as well as the ultimate release after coalescing. There is a balancing act between increasing the attraction or adsorption characteristics of the fibers against the release mechanism, which strong adsorption would inhibit. The necessary condition that droplet fiber adsorption occur for coalescing has been supported by a number of sources (Jeater et al., 1980; Basu, 1993).

5.8.3.3 Separation of Coalesced Droplets

Once the droplets have been coalesced, they are now as large as possible for the given flow conditions. The separation stage can be achieved in one of two ways:

Horizontal Configuration: The coalescer housing contains a settling zone that relies on the difference in densities between the coalesced droplets and the bulk fluid (see Fig. 5.11). This configuration can be used for both hydrocarbon from water and water from hydrocarbon separation, but the location of the collection sump and outlet nozzle will need to be reversed. For the case of the removal of hydrocarbon from water, a collection sump is located at the top of the housing and the purified water leaves at the bottom outlet nozzle. The sump can be manually drained on a periodic basis or equipped with an automatic level control and drain system. Estimation of the coalesced drop size and required settling zone are best determined through pilot scale tests at field conditions.

Vertical Configuration: Once the droplets have been coalesced they are now as large as possible for the given flow conditions, in the range of 0.5−2 mm in diameter. The separation stage is achieved using hydrophobic separator cartridges that provide an effective barrier to aqueous coalesced drops, but allow hydrocarbon to pass through them. The separator cartridges can be stacked below the coalescers for the most efficient utilization of the separator medium. This configuration only applies to the separation of water or aqueous contaminants from hydrocarbons (see Fig. 5.12).

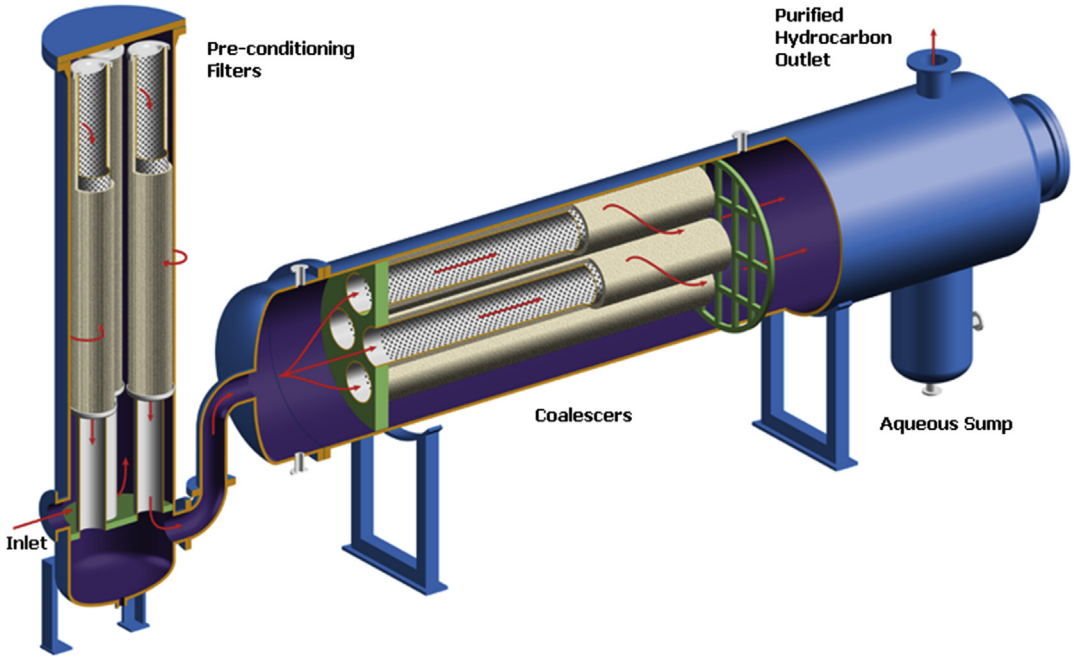

FIGURE 5.11

Horizontal liquid–liquid coalescer configuration.

Courtesy of Pall Corporation.

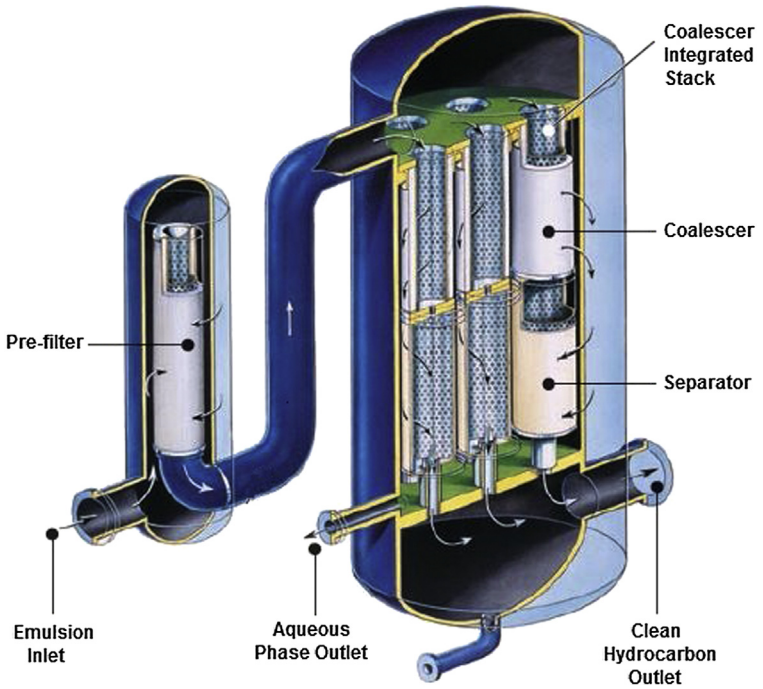

FIGURE 5.12

Vertical liquid–liquid coalescer configuration.

Courtesy of Pall Corporation.

After leaving the coalescing stage, the large aqueous coalesced drops and hydrocarbon then flow axially in a downward direction, and the flow direction is from the outside of the separator to the inside. The large coalesced drops are repelled by the separators and are collected in the bottom sump. The purified hydrocarbon passes through the separators and exits at the bottom of the housing. The aqueous phase in the collection sump can be manually drained on a periodic basis or equipped with an automatic level control and drain system.

5.8.4 LIQUID–LIQUID COALESCER PERFORMANCE

Properly designed and sized high-efficiency coalescer systems can process inlet discontinuous phase concentrations up to 10% and reduce them to ppm levels in the outlet for interfacial tensions as low as 0.5 dyne/cm. For water from hydrocarbon separations, coalescer outlets below 15 ppmv per the AquaGlo (*registered trademark of Gammon Corp.*) method (ASTM D3240, 1991) can be achieved and for hydrocarbons from water, concentrations below 20 ppmw per the oil and grease method have been demonstrated.

The use of polymers and fluoropolymers in the coalescer materials of construction allows for expanded use of coalescers over earlier conventional types so that they can withstand an array of aggressive chemical applications over a wide range of temperatures from −40°F up to 300°F.

5.8.5 LIMITATIONS OF USING COALESCERS

While liquid–liquid coalescers have many benefits in breaking tough emulsions, there are some limitations to consider. Solids can become problematic at higher concentrations and lead to excessive changes out of disposable prefilters. Generally, the solid range that liquid–liquid coalescers can operate economically with disposable filters is less than 10 ppm. Above this level of solids, further pretreatment will be required such as backwash cartridge filters, mixed media packed beds, or hydrocyclones for solids removal.

The operational limits of the coalescer for removal of free liquids must also be understood. If the clarified stream leaving the coalescer is then cooled, condensation of previously dissolved contaminant can occur leading to a hazy fluid at the lower temperature. The coalescer will not be able to remove contaminants that are dissolved in solution and therefore, the location to place the coalescer and any subsequent change in process conditions after the coalescer must be considered carefully.

The coalescers typically will have a service life of 1–2 years when protected adequately by prefiltration. Despite the long life, the coalescers will eventually require disposal and replacement; however, this will be minimal, given the low frequency of replacement.

For liquid–liquid coalescers constructed from glass fiber medium, the problem of surfactant disarming must also be considered, and for low interfacial tension emulsion systems (<20 dyne/cm), they will not operate efficiently for separation. For these conditions, nondisarming fluoropolymer or polymer coalescers should be considered. These types of materials also have wider compatibility for chemical streams and a wider temperature range.

5.8.6 APPLICATIONS

High-efficiency liquid–liquid coalescers are finding increasing applications in industry where problematic emulsions exist. They are used to protect equipment, recover valuable streams, and to meet environmental discharge limits. Some examples are given by Wines and Mokhatab (2017b).

5.9 PRACTICAL DESIGN OF SEPARATION SYSTEMS

Designing a separation system capable of separating oil, water, gas, and any solids traditionally relies upon the application of standard calculation methods using certain values for design criteria (such as inlet momentum, gas K value, and liquid separation residence time) that are based on empirical information and tested configurations. As such, these classic methods do not consider matters such as droplet size distribution and mist fraction in the inlet piping, droplet capture efficiencies, and separation performance of each separation step in the separator. As a result, the carryover rate associated with the separator design and operating conditions is commonly not known at the design stage. Therefore, designs based on these classic criteria—based methods have an inherent risk of malperformance and operating problems upon start-up. Fortunately, recent developments have made advanced separator design and rating softwares available on the market. These softwares include the complex calculations associated with droplet size distributions and internals efficiencies based upon the design and operating conditions, thus providing the designer with a prediction of the separator's performance and carryover. With this key information, the designer can adjust the separator design to suit its required performance in the system. This significantly reduces the risk of operating problems in the field.

The classic design methods also assume that the nature of flow in the separators is uniform, whereas in reality it will be strongly three-dimensional and highly turbulent. Therefore, problems occur frequently when commissioning new separators or existing separators under unusual loading conditions. Modeling the complex three-dimensional flow within the separation equipment (piping, vessels, and internals) can provide a visual indication of the weaknesses in the process design. This will help to optimize the design of new separators and solve operational problems with existing designs. Computational fluid dynamics (CFD) is a key tool for modeling and predicting fluid flow behavior inside the separation equipment under real operating conditions. CFD enables the nature of the flow in the separator to be illustrated so that the interaction between the equipment and the different flow components can be understood. Qualitative comparisons of the performance of different models can then be made to identify the optimal solution. The optimized CFD model can be verified with on-site test capabilities if this is required. The verified model can then be used in fine-tuning designs prior to separator manufacturing, resulting in a significant saving in time and money and allows operational problems to be identified and solved before they even manifest themselves. In conclusion, many practical designs and redesign applications for separators may be performed by CFD modeling and simulations.

CASE STUDY

The following case study demonstrates the power of using CFD to analyze and find the root causes of operational issues in separation facilities. Using this tool would reveal the areas in the separation facilities where special attention is required to mitigate or prevent operating issues. With these insights, the design engineer can address the potential issues at the design stage, which is far less costly than rectifying malperforming designs after they have been built and put into operation.

THE SITUATION

An operator has been experiencing problems with one of their gas scrubbers. Large amounts of carryover were found in equipment downstream of a gas scrubber. To reduce the carryover and associated operational issues, the operator had to reduce the production rate through the scrubber from 100 MMSCFD to less than 70 MMSCFD, resulting in a considerable loss of revenues.

The gas scrubber, with an inside diameter of 1.5 m and a Tan-to-Tan length of 2.6 m, was equipped with a deflector plate at the inlet and a horizontal flow vane pack acting as the demisting device. The operating pressure was 35 barg.

THE OBJECTIVE AND METHODOLOGY

A first-pass analytical analysis showed that the root cause of the issue was most likely within the gas scrubber. To investigate this further, a CFD model of the existing vessel with its internals and the upstream piping was made (Fig. 5.13). The actual operating conditions were imposed on the model.

THE ANALYSIS

The CFD results revealed both analytical and visual insights. In Fig. 5.13, it can be seen that the gas flow in the vessel is far from ideal. The configuration of the deflector and the horizontal flow vane pack causes severe maldistribution and "jetting" inside the vessel. The deflector causes high gas velocities over the liquid surface which may cause liquid reentrainment. Furthermore, the CFD simulation also shows that the deflector baffle will cause significant droplet shattering due to high turbulent dissipation rates. The gas velocity profile on the face of the vane pack shows a nonuniform profile (i.e., maldistribution), with unacceptably high local velocities. The combination of high liquid load and the high local gas velocities through the vane pack will cause the vane pack to fail. All these issues explain the high carryover observed during operation of this gas scrubber.

MODIFIED SITUATION

With the root causes of the malperformance identified, a solution to the problem was developed. The solution comprised a redesign of the vessel internals, the adequacy of which was verified through CFD analysis. At the inlet nozzle, the inlet baffle was replaced with a proper vane-type inlet device. For the

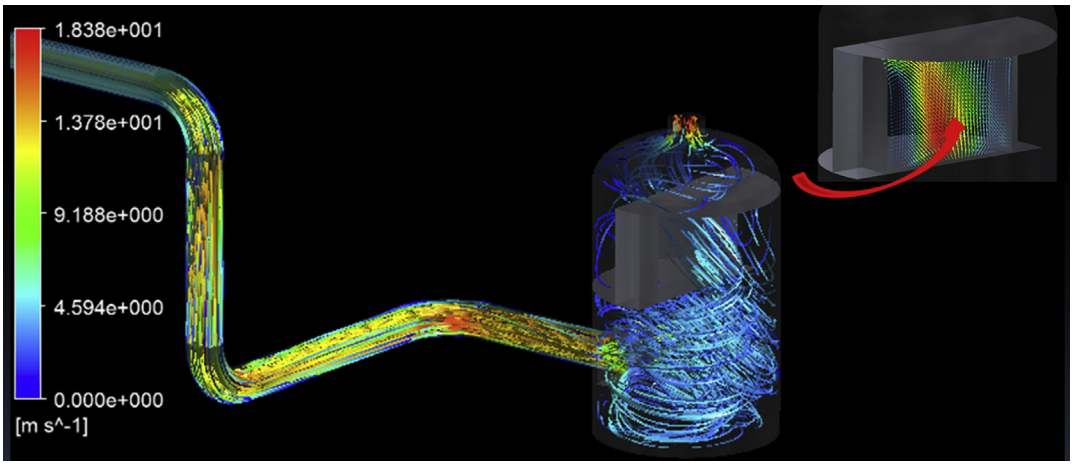

FIGURE 5.13

Gas scrubber—current situation.

Courtesy of Kranji Solutions Pte Ltd.

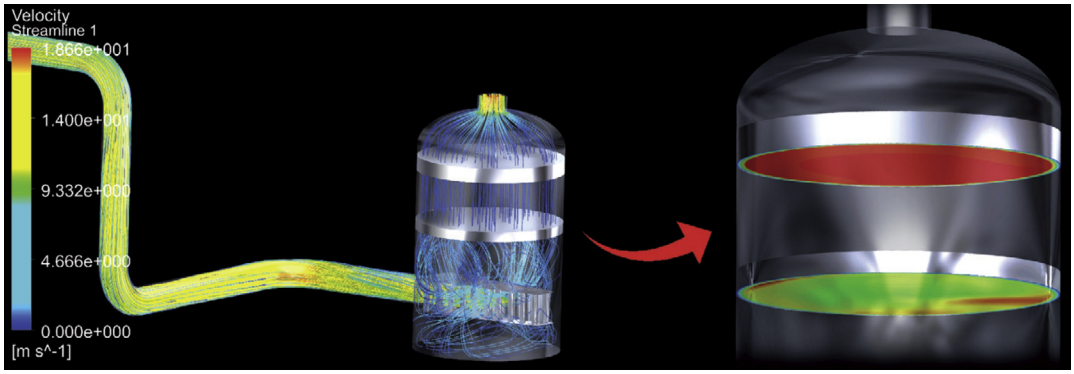

FIGURE 5.14

Gas scrubber—modified situation.

Courtesy of Kranji Solutions Pte Ltd.

demisting section, the vane pack was replaced with a double mesh pad configuration; one acting as a mesh agglomerator and one as a mesh demister. The design and results of the CFD simulation are shown in Fig. 5.14. The CFD simulation of the modified design showed that the gas distribution inside the vessel was improved drastically. The velocity over the liquid level became acceptable, and the velocity profile on the face of the top mesh demister showed a proper uniform velocity profile. With the recommended internals, the operator can suitably operate at the required gas flow of 100 MMSCFD.

REFERENCES

API Spec 12J, 1989. Specification for Oil and Gas Separators, seventh ed. American Petroleum Institute (API), Washington, DC, USA.

ASTM D3240, 1991. Standard Test Method for Undissolved Water in Aviation Turbine Fuels. American Society for Testing and Materials (ASTM). West Conshohocken, PA, USA.

Arnold, K., Stewart, M., 1998. Surface Production Operations, Vol. 1: Design of Oil-handling Systems and Facilities, second ed. Gulf Publishing Company, Houston, TX, USA.

Basu, S., 1993. A study on the effect of wetting on the mechanism of coalescence. Journal of Colloid and Interface Science 159, 68–76.

Brown, R.L., Malbrel, C., Wines, T.H., February 27 – March 2, 1994. Recent developments in liquid/gas separation technology. Paper Presented at the 44th Laurance Reid Gas Conditioning Conference, Norman, OK, USA.

Burke, N.E., Kashou, S.F., 1996. Slug-sizing/slug-volume prediction: state of the art review and simulation. SPE Production & Facilities 11 (3), 166–172.

Campbell, J.M., 1992. Gas Conditioning and Processing, seventh ed. Campbell Petroleum Series, Norman, OK, USA.

Gomez, L.E., Mohan, R.S., Shoham, O., Kouba, G.E., 2000. Enhanced mechanistic model and field application design of gas-liquid cylindrical cyclone separators. SPE Journal 5 (2), 190–198.

GPSA, 2004. Engineering Data Book, twelfth ed. Gas Processors Suppliers Association (GPSA), Tulsa, OK, USA.

Hughes, V.B., April 1–2, 1997. Aviation fuel handling: new mechanism insight into the effect of surfactants on water coalescer performance. Paper Presented at the 2nd International Filtration Conference, San Antonio, TX, USA.

Jeater, P., Rushton, E., Davies, G.A., March/April 1980. Coalescence in fibre beds. Filtration & Separation 129.
Kouba, G.E., Shoham, O., Shirazi, S., June 7−9, 1995. Design and performance of gas liquid cylindrical cyclone separators. Paper Presented at the BHR Group 7th International Conference on Multiphase Flow, Cannes, France.
Kumar, S., 1987. Gas Production Engineering. Gulf Publishing Company, Houston, TX, USA.
Manning, F.S., Thompson, R.E., 1995. Oil Field Processing, Vol. 2: Crude Oil. PennWell Books, Tulsa, OK, USA.
Miller, J.D., Koslow, R.R., Williamson, K.W. U.S. Patent 4, 676, 807 (June 1987); id. U. S. Patent 4, 759, 782 (July 1988).
Mohan, R.S., Shoham, O., June 25, 2003. Design and Development of Gas-liquid Cylindrical Cyclone: Compact Separators for Three-phase Flow. Final Technical Report submitted to the U.S. Department of Energy. University of Tulsa, Tulsa, OK, USA.
Monnery, W.D., Svrcek, W.Y., 1994. Successfully specify three-phase separators. Chemical Engineering Progress 90 (9), 29−40.
Murphy, W.L., Nov. 1984. Practical In-service Simulation Tests for Rating of High Efficiency Aerosol Coalescing Performance. PEDD-FSR-101a. Pall Corporation Equipment Development, New York, NY, USA.
NATCO, July 2002. NATCO Group Products Manual. Gas-liquid Cylindrical Cyclone (GLCC) for Compact Gas-Liquid Separations, vol. 1, 1243−A1/A2.
Rojey, A., Jaffret, C., Cornot-Gandolphe, S., Durand, B., Jullian, S., Valais, M., 1997. Natural Gas Production, Processing, Transport. Editions Technip, Paris, France.
Shell DEP 31.40.10.12-Gen, July 1998. Design Manual of Multiple-pipe Slug Catchers. Design and Engineering Practice (DEP) Publications, Shell Global Solutions International B.V, The Hague, The Netherlands.
Souders, M., Brown, G.G., 1934. Design and fractionating columns. 1. Entrainment and capacity. Journal of Industrial and Engineering Chemistry 26 (1), 98−103.
Svrcek, W.Y., Monnery, W.D., 1993. Design two-phase separators within the right limits. Chemical Engineering Progress 89 (10), 53−60.
Talavera, P.G., 1990. Selecting gas/liquid separators. Hydrocarbon Processing 69 (6), 81−84.
Wang, S., Gomez, L.E., Mohan, R.S., Shoham, O., Kouba, G.E., 2003. Gas-liquid cylindrical cyclone (GLCC) compact separators for wet gas applications. Journal of Energy Resources Technology 125 (1), 43−50.
Williamson, K., Tousi, S., Hashemi, R., March 21−25, 1988. Recent developments in performance rating of gas/liquid coalescers. Paper Presented at the 1st Annual Meeting of the American Filtration Society, Ocean City, MD, USA.
Wines, T.H., 2004. Optimize NOx reductions facility-wide. Hydrocarbon Processing 83 (4), 53−59.
Wines, T.H., Mokhatab, S., 2017a. “High Efficiency Coalescers for Gas Processing Operations”, Petroleum Technology Quarterly, Q4, 51−59.
Wines, T.H., Mokhatab, S., 2017b. “Removing Liquid-phase Contaminants from Hydrocarbon Liquids”, Petroleum Technology Quarterly, Gas, 51−55.
Xiao, J.J., Shoup, G., 1998. Sizing wet-gas pipelines and slug catchers with steady-state multiphase flow simulations. Journal of Energy Resources Technology 120, 106−110.

CHAPTER

CONDENSATE PRODUCTION 6

6.1 INTRODUCTION

Production well fluids entering the inlet reception facility is first separated in the slug catcher. The hydrocarbon liquid stream contains mainly light hydrocarbons (methane and ethane in particular), water, salts, corrosion and hydrate inhibitors, acid gases, mercaptans, and other sulfur compounds. The condensate production unit is designed to separate these contaminants to produce a marketable hydrocarbon liquid (condensate) for export.

Condensate production involves three steps: water washing, condensate stabilization, and condensate treating. Depending upon the associated water quality, the condensate may require a water wash to remove salts and additives. After dewatering step, which requires a careful evaluation of the condensate/water separation technology, the condensate goes to the condensate stabilization unit where remaining lighter hydrocarbons are stripped and recombined with the gas that leaves the inlet reception facility. The process of increasing the amount of intermediate (C_3 to C_5) and heavy (C_{6+}) components in the condensate is called condensate stabilization. This process is performed primarily to reduce the vapor pressure of the condensate so that a vapor phase is not produced upon flashing the liquid to atmospheric storage tanks. Stabilized condensate generally has a vapor pressure specification, typically identified by its Reid vapor pressure (RVP[1]) or true vapor pressure. RVP is set by local emissions authorities to limit hydrocarbon emissions during storage and transport. Typical RVP specification ranges from 4 to 8 psia. For hydrocarbon storage in high elevation, the atmospheric pressure is lower, and consequently a low RVP as low as 4 psia may be necessary, allowing some safety margins. After the stabilization step, condensate must be treated to remove heavy mercaptans and other undesirable contaminants to very low levels to produce a liquid product that has specifications to be sold as "natural gasoline." In addition to the aforementioned RVP specification, other typical specifications of the commercial grade condensate are water content (0.05 volume %), butanes (2 volume %), H_2S (10 ppmw), and total sulfur content as S (50 ppmw). Recent accidents of condensate rail cargoes and condensate trucks in North Dakota and Oklahoma areas prompt the transportation authority and administrators to tighten the safety codes. It is expected that the condensate specifications will be more stringent: lower RVP and lower sulfur content.

[1]Reid vapor pressure (RVP) is related to the vapor pressure of a petroleum product, which measures its inherent tendency to evaporate at 100°F with vapor/liquid ratio of 4/1 (ASTM D323). RVP is a function of the hydrocarbon's composition and is independent of operating temperature and pressure.

Handbook of Natural Gas Transmission and Processing. https://doi.org/10.1016/B978-0-12-815817-3.00006-X

The objective of this chapter is to review some of the basic processes for condensate stabilization and the associated facilities such as condensate storage, condensate hydrotreating, monoethylene glycol (MEG) regeneration and reclaiming, and sour water treatment.

6.2 CONDENSATE STABILIZATION

There are two basic stabilization processes: cascade flash separation and distillation separation. Cascade flash separation consists multiple separators and compressors, is common in offshore gas processing plants due to its simplicity, but its efficiency and condensate yields are lower. The distillation separation type is more complex, and more efficient, which is common in onshore gas processing plants.

6.2.1 STABILIZATION BY CASCADE FLASH SEPARATION

The principle of the cascade flash separation is to remove the lighter components by flashing to lower pressures in several steps. The condensate can also be heated to promote removal of the light components. The process equipment can be very compact, which is advantageous in offshore gas installation where equipment weight and plot space must be minimized. However, the condensate yield is low, particularly when processing a lighter condensate to meet a low RVP requirement. The process is more suitable for processing crude oil or heavier condensate.

A typical cascade flash separation process is shown in Fig. 6.1. The condensate is flashed and separated at three successive pressures at 500, 100, and 15 psig. The flashed vapor can be used as a fuel

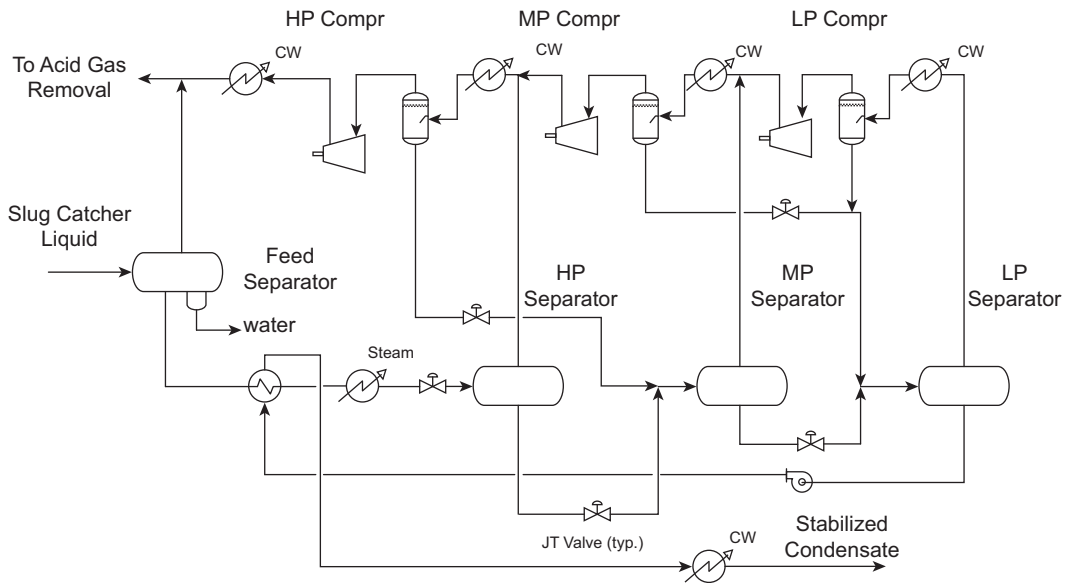

FIGURE 6.1

Condensate stabilization by cascade flash separation. *HP*, high pressure; *MP*, medium pressure; *LP*, low pressure.

gas in the facility or sent to the flare (during early production developments). Typically, the vapors are compressed back to the feed section for recovery. Vapor from compressor discharge is cooled and the condensed liquid is blended with the condensate product, which helps to reduce the condensate losses.

To achieve a low RVP condensate, the feed must be heated to higher temperatures, typically about 150−250°F. In fact, the feed temperature must be sufficiently high to drive off its H_2S content to meet the H_2S specification in the product. Once the H_2S specification has been met, heating can be adjusted as needed to meet the vapor pressure specification.

It is impractical for the flash stabilization process to meet a very low RVP specification. If a low RVP is required, the only solution is the distillation type, which is discussed in the following sections.

6.2.2 STABILIZATION BY DISTILLATION

Distillation process is an efficient method for separating the C_{5+} from the lighter components, instead of using multiple flash stages. The distillation column can be a refluxed type or a nonrefluxed type (simple stripper). A nonrefluxed type is lower in capital cost, as the overhead reflux condenser system is not required. The drawback is the loss of C_{5+} components in the overhead. The C_{5+} components can be partially recovered by recycling the condensate later, which in most cases, can be economically justified.

With the refluxed column, there are two design options. The first option is to produce a condensate product, with the butane and lighter components returned to the acid gas removal unit (AGRU). The second option is to produce a condensate and a liquefied petroleum gas (LPG) fraction. Both configurations are described in the following sections.

6.2.2.1 Condensate Production Only

The process flow schematic of a condensate stabilization unit is shown in Fig. 6.2. The condensate is flashed and separated in an intermediate separator, with flashed vapors compressed and returned to the AGRU. The flashed liquid is preheated with the stabilizer bottom and routed to the stabilizer for separation. The stabilizer typically operates between 150 and 250 psia and contains about 20−25 trays.

The stabilizer column is heated with medium pressure steam to meet the RVP specification. The overhead vapor is partially condensed, by air or cooling water, producing a reflux to the column and a butane and lighter vapor that is compressed to the AGRU. No liquid overhead product is produced in this configuration.

Because the condensate is saturated with water, water will be stripped and condensed in the upper column. Water is collected in the reflux drum as an aqueous phase and may be trapped in the upper section of the stabilizer column. Any free water must be removed from the column or it will build up inside the column, resulting in column flooding. Typically, interface controllers are provided to allow withdraw of water from the reflux drum and the top trays. The draw tray locations can be determined to detect three phase conditions with simulation software.

The advantage of the condensate only design is that it recycles the LPG portion to the gas processing plant. This avoids producing LPG that may not meet the color and water specifications for export. The disadvantage is that the gas plant has to be designed for a higher duty from the recycled LPG.

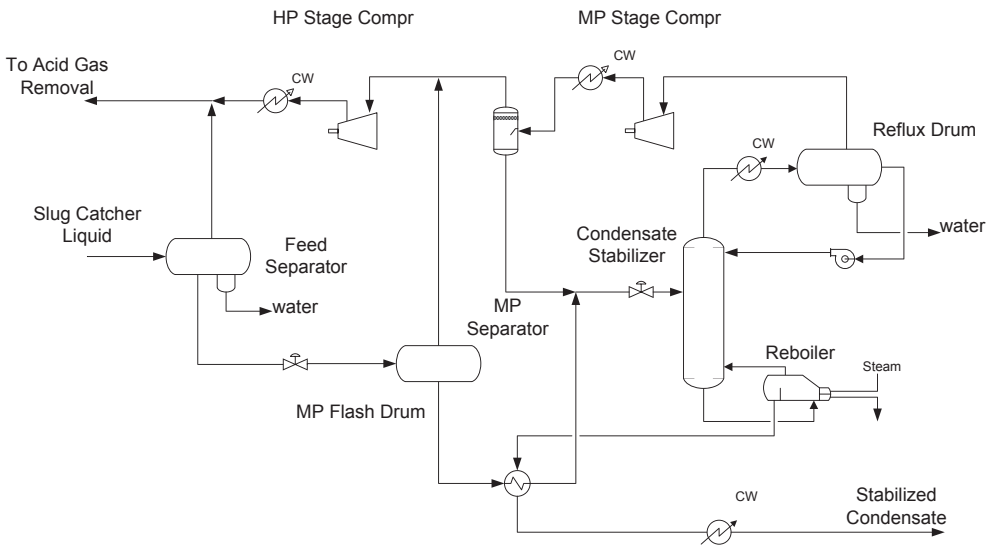

FIGURE 6.2

Condensate stabilization by distillation.

6.2.2.2 Condensate and Liquefied Petroleum Gas Production

The condensate stabilization process can be configured to produce LPG from the stabilizer column. To meet the ethane content in the LPG product, a feed liquid stripper is required upstream of the stabilizer. This stripper is designed to remove all the acid gases and lighter components such that the LPG product from the downstream stabilizer would meet the H_2S and vapor pressure specifications. The process flow schematic for the feed liquid stripper and stabilizer is shown in Fig. 6.3. The feed liquid stripper pressure is typically set at about 200 psia or at slightly higher pressure than the stabilizer such that pumping can be avoided. The advantage of this process is that it avoids recycling the LPG portion and minimizes the size of the gas processing plant. However, the LPG product may contain other contaminants that may not meet specifications for export.

6.2.3 DESIGN CONSIDERATIONS

The condensate stabilization unit shall be designed to meet the process design basis, which must consider the ranges of condensate flow rates and compositions and inlet pressures and temperatures. The design basis must be conservative, as it is difficult to predict the upstream operations. These design parameters will affect the sizing of the separators, stabilizer column, reboiler, heat exchangers, and compression system.

Two important design considerations of the stabilizer column are described in the following sections.

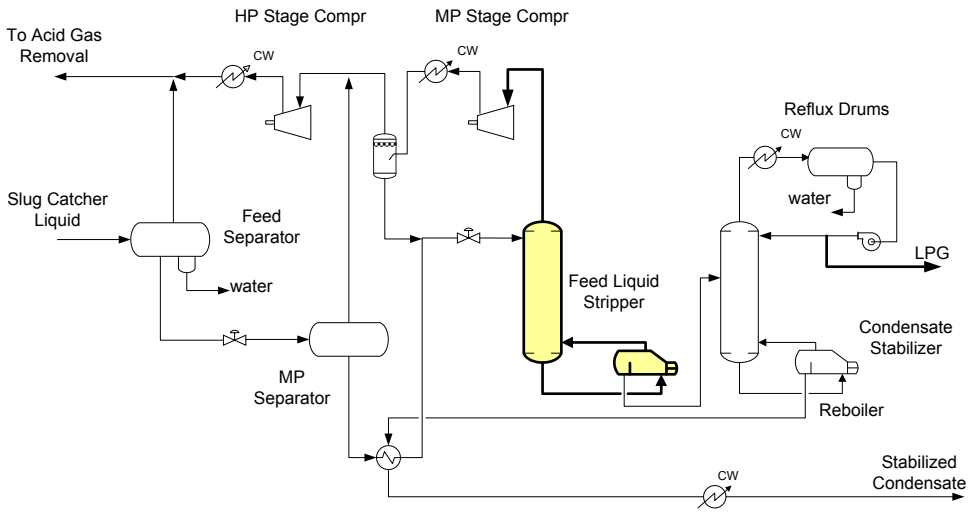

FIGURE 6.3

Condensate and liquefied petroleum gas production.

6.2.3.1 Stabilizer Column Pressure

For a given condensate composition (i.e., 0.1% C_4, 14.6% iC_5, 27.8% nC_5, and 57.5% C_6+), there is a relationship between the stabilizer bottom temperature and the product's vapor pressure, and they vary with operating pressures, as shown in Fig. 6.4.

For a given stabilizer pressure, the bottom temperature decreases with increasing RVP specification. Conversely, the bottom temperature increases when the RVP specification is lowered, as more butane and pentane components are stripped overhead. As can be expected, higher column pressure

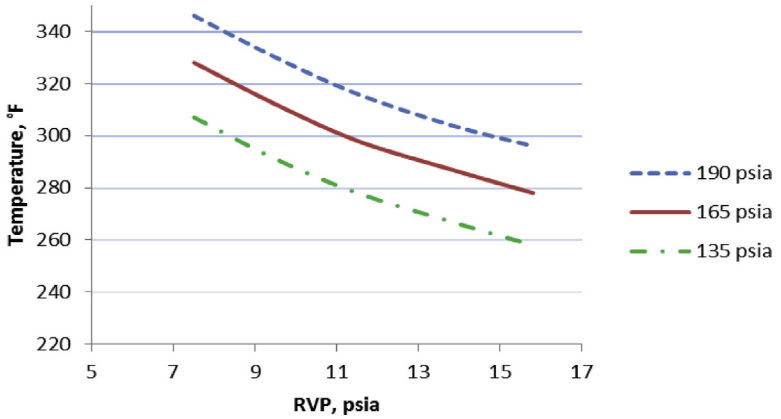

FIGURE 6.4

Stabilizer bottom temperature versus Reid vapor pressure (RVP).

requires more stripping steam and tends to increase the equipment cost. However, this may be offset by the lower compression cost of the column overhead gas.

The column pressure should be selected by considering the operating costs such as utilities consumption (steam, cooling water, and power), capital costs, and incremental revenue from condensate production.

6.2.3.2 Stabilizer System Control

The stabilizer operation is very sensitive to inlet feed gas changes. To maintain a stable column pressure, the slug catcher and the feed separator should be designed conservatively to dampen out flow fluctuation, which the plant will experience during pipeline pigging operation. Predictive methods can also be built into the control system, such as the use of upstream feed conditions, and column tray data to adjust the reboiler steam flow using a feed-forward controller. Dynamic simulation model can be set up to optimize the control variables that can respond to changes in feed composition and flow conditions.

6.2.4 OPERATING PROBLEMS

The common operating problems of the condensate stabilization units are failure to meet product specifications and unstable column operation. These can be contributed by one of the following factors:

- Feed flow rate and conditions are significantly different than design
- Carryover of contaminants and injection chemicals from upstream operation
- High corrosion, resulting in failure of piping and heat exchanger equipment
- Column flooding and unstable operation
- Equipment fouling

Many of these problems can be avoided in the feed stage of the project by defining the ranges of operating conditions.

6.3 CONDENSATE HYDROTREATING

While steam stripping in the stabilizer can be used to remove lighter hydrocarbon and acid gas components, it has minimal effect on the removal of mercaptans. If the condensate contains the lower-molecular-weight mercaptans (methyl mercaptan), it can be treated by conventional liquid-treating technologies, such as caustic wash, UOP's Merox, molecular sieves, and catalyst solid beds.

If the condensate contains the higher-molecular-weight mercaptans, aromatic compounds, and other undesirable sulfur components, it must be processed with a hydrotreater, which is a common process in refinery to desulfurize high sulfur feedstock. The primary function is to use a hydrotreater catalyst to promote the following desulfurization reactions:

$$R - S - H + H_2 = R - H + H_2S \tag{6.1}$$

$$R - S - R' + 2H_2 = R - H + R' - H + H_2S \tag{6.2}$$

where, R and R′ are hydrocarbon and alternate hydrocarbon chains, respectively.

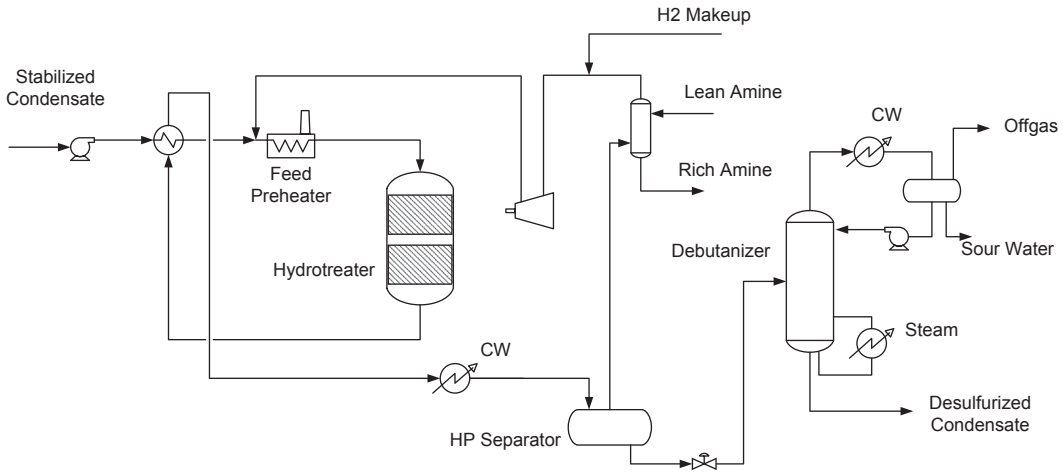

FIGURE 6.5

Condensate hydrotreating.

A typical process flow scheme of a condensate hydrotreating unit is shown in Fig. 6.5. The process consists of a high-pressure reactor loop where sulfur compounds are converted to H_2S, and aromatic hydrocarbons are saturated and converted to paraffinic hydrocarbons. The reactor effluent is cooled; recycle gas and product liquids are separated. The H_2S content in the flashed gas is removed by an amine-treating unit.

The flashed liquid is letdown in pressure and fractionated in a debutanizer, which strips off the H_2S, butane, and light components from the condensate to produce a sulfur-free hydrocarbon liquid. Hydrogen compression is necessary to maintain the hydrogen partial pressure in the hydrotreater reaction loop. A hydrogen generation unit is used to supply high-purity hydrogen to support the hydrotreater reaction.

6.4 EFFLUENT TREATMENT

6.4.1 MONOETHYLENE GLYCOL REGENERATION AND RECLAIMING

The condensate may contain MEG solution, which is used for hydrate control in subsea pipelines. The glycol solution is contaminated with salts, corrosion inhibitors, and pipe scales, which must be removed to avoid fouling in the downstream process equipment.

Separation of condensate from the MEG solution requires special design attention. Phase separation is affected by operating temperatures. Temperatures lower than 40°F will result in poor separation due to high viscosity of glycol and potential emulsion formation. Separation would be improved if the temperature were above 60°F. For this reason, the condensate temperature is typically preheated to above 60°F prior to the feed separator, which is necessary to avoid contamination of the condensate by the MEG solution.

Water separated from the MEG regeneration unit contains H_2S, CO_2, and ammonia, and may contain other undesirable pollutants such as phenols, cyanide and various salts, organic or inorganic

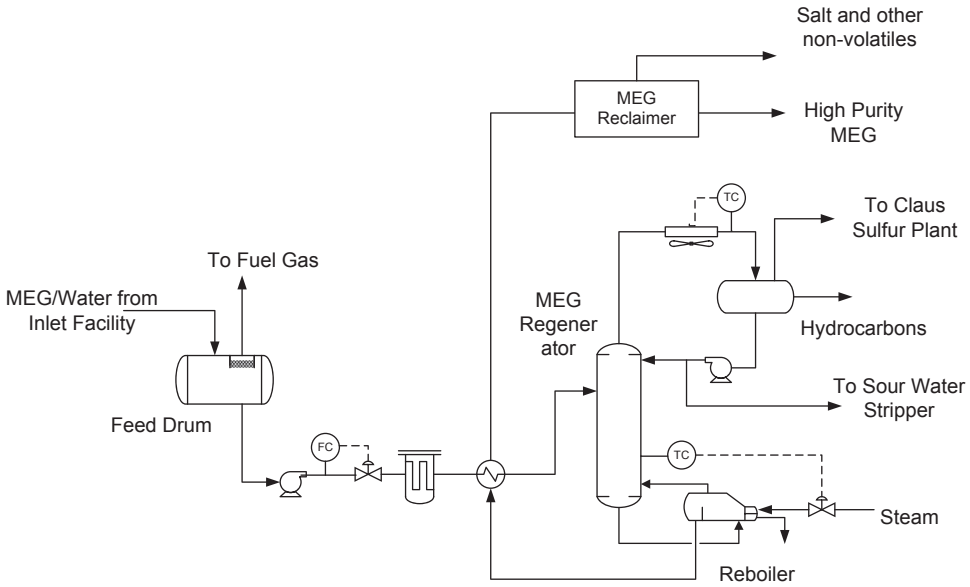

FIGURE 6.6

Monoethylene glycol (MEG) regeneration and reclaiming.

acids. The type and quantity of these pollutants depends on the well properties and the injection chemicals. They must be removed to comply with environmental regulations.

A typical MEG regeneration/reclaiming unit is shown in Fig. 6.6. As can be seen, MEG solution is flashed to a feed drum operating at a lower pressure, which removes the dissolved gas from MEG. The flashed gas is treated and sent to the fuel gas system. The flashed liquid is pumped and filtered, removing most of the solids and pipe scales before entering the regenerator.

The MEG regenerator is stripped by medium pressure steam, producing an acid gas and sour water overhead, and a concentrated MEG solution. The acid gas is sent to the Claus burners in the sulfur-recovery unit, and the water is routed to a sour water stripper. Any entrained hydrocarbon will be skimmed off from the reflux drum.

The MEG regenerator bottom is concentrated in salt and other nonvolatile materials, which is purified before recycling to the upstream facility. MEG can be reclaimed by vacuum stripping to separate MEG from the salty water. There are commercial designs that can be used to reclaim the MEG. Licensed units, from Prosernat or Cameron Process System, are skid-mount units that can remove salts, water, and other solids and produce a high-purity glycol.

6.4.2 SOUR WATER STRIPPING

The main function of a sour water stripping unit, as shown in Fig. 6.7, is to remove H_2S and ammonia from sour water before sending it to a wastewater treatment unit or recycling back to the process units. The overhead gas from the sour water stripper is routed to the acid gas burners in the sulfur recovery

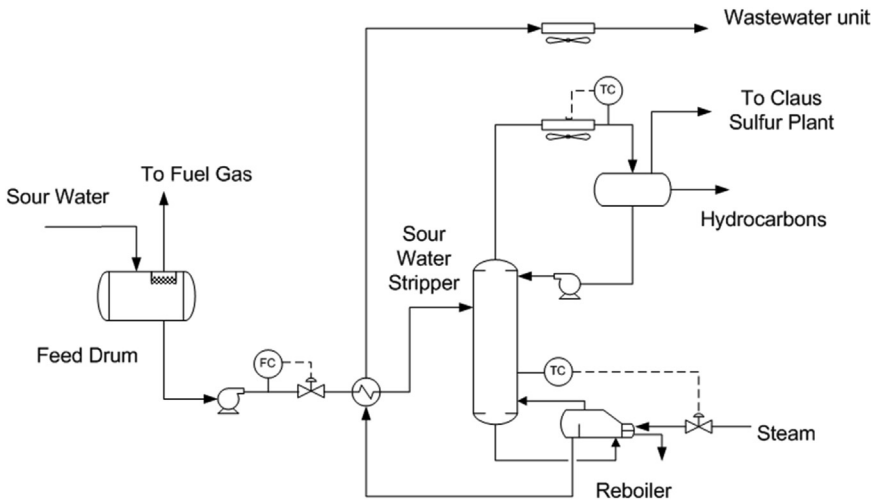

FIGURE 6.7

Sour water stripping process.

unit for destruction. In some designs, to minimize acid gas corrosion, a pump-around system with cooler is used in the top section, instead of the conventional overhead condenser.

Sour water stripper typically contains about 30 trays that are required to meet the ammonia specification of 10 ppmw for emissions compliance. In some installations, there are traces of acidic compounds in the sour water, which would fix the ammonia in solution. In these cases, addition of caustic may be necessary to neutralize the acidic compounds.

Low-pressure steam can be used to supply stripping requirement by the reboiler. The stripper bottom temperature is typically maintained at about 230°F or higher temperatures sufficient to meet the ammonia specification. The overhead temperature is controlled at 180°F or higher to avoid formation of ammonia bisulfide. The formation of the ammonia salt will cause fouling and corrosion in the overhead system. The overhead piping and equipment are constructed with specialty alloy steel and must be electric or steam traced to stay above the bisulfide formation temperature.

6.5 CONDENSATE STORAGE

The stabilized condensate products are stored in condensate storage tanks before they are transported to the refineries for further processing. The storage tanks must be designed to avoid flashing of the condensate under different operations. A vapor recovery system should be used to minimize any hydrocarbon emissions as described in the following sections.

6.5.1 TANK DESIGN CONSIDERATIONS

Condensates are commonly stored in cylindrical steel tanks at atmospheric pressure. The tanks are flat bottomed and are provided with a roof, which is of conical or domed shape.

The storage tank is typically designed to operate at a slightly positive and a slightly negative atmospheric pressure to provide flexibilities during operations. The tank's design temperature should be based on the minimum storage fluid temperature or the lowest ambient air temperature. The exterior of the condensate tanks are typically coated or painted for corrosion protection and designed with a corrosion allowance per code and regulation.

The two standards commonly used for tank design are British Standard BS 14015 "Standards on specification for manufacture of vertical steel welded non-refrigerated storage tanks with butt-welded shells for the petroleum industry," and the American Petroleum Institute Standard API 650 "Venting Atmospheric and Low-Pressure Storage Tanks." API standards provide design guidelines for the determination of venting requirements that may be used under normal tank operations and emergency conditions. Specially designed pressure/vacuum vent valves should be provided to protect the tank against overpressure or vacuum conditions as follows:

Vacuum conditions:

- Withdrawal of product from the tank
- Contraction of vapors caused by a drop in atmospheric temperature

Pressure buildup conditions:

- Vapor generation when condensate is letdown from a high-pressure source
- Vapor displacement by product into the tank, product evaporation, and heat of mixing with dissimilar liquid in the tank
- Expansion and evaporation caused by a rise in atmospheric temperature
- Fire exposure

Tanks should be configured to operate with a nitrogen or fuel gas blanketing system that maintains the tank at positive pressures under all operating conditions.

Tank vent piping should include flame arrestors, which protect the tank against ignition of the vent gases due to lightning strike or a discharge of static electricity at the vent location. Where the vent piping is routed to a flare system, a constant bleed of purge gas into the vent is required in addition to a flame arrestor. More complex flow devices, such as fluidic seals and molecular seals, are available from several manufacturers to minimize the amount of purge gas needed to avoid hazardous conditions occurring in the storage tank.

Direct-acting pressure/vacuum relief valves are special types of relief valves, specifically designed for tank protection. They can be designed for pressure relief only, vacuum only, and combined pressure/vacuum. Pressure and vacuum protection levels are controlled with weighted pallets or springs and can be adjusted to provide the required pressure/vacuum settings. It is common to combine pallet and spring systems in one unit, i.e., pressure settings require a spring section, while the vacuum settings use the pallet method.

6.5.2 TANK EMISSION CONTROL

Emissions of hydrocarbons from condensate storage tanks are sources of greenhouse gas pollutants. The tank emissions can be minimized with a vapor recovery system, as shown in Fig. 6.8.

Storage tank pressure is controlled by at least two sets of pressure-regulating valves within a set pressure range. When the tank pressure drops below the set pressure, such as during unloading of the

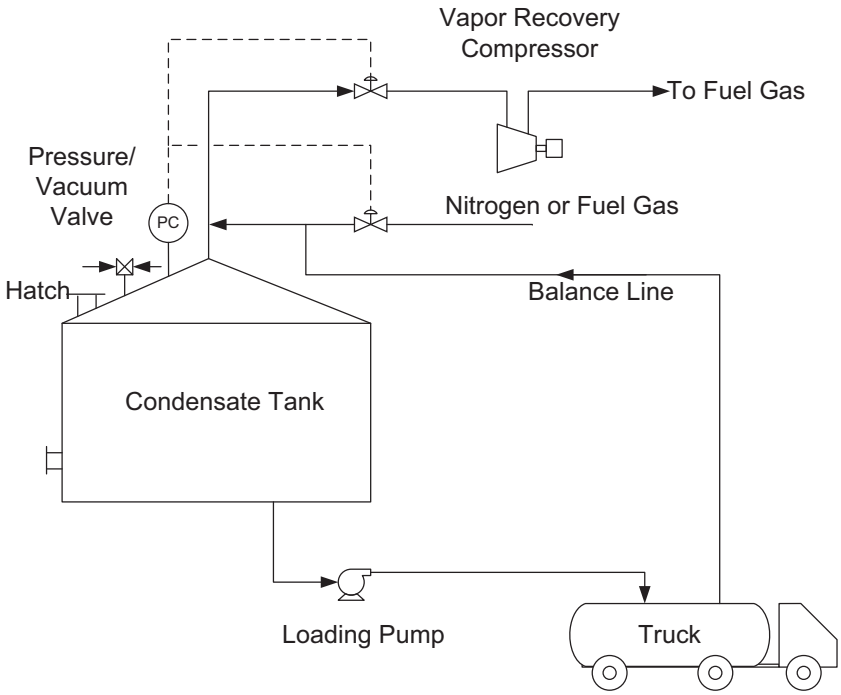

FIGURE 6.8

Schematic of tank emission control system.

condensate, the first pressure control valve is opened, introducing vapor (nitrogen or fuel gas) to the tank. When the tank pressure goes up above the set point, such as introduction of condensate to the tank, the second pressure control valve will open, sending the excess vapor to the vapor recovery system. These two pressure control valves operate using split-range control logic to avoid simultaneous opening of both valves. To handle the displacement vapor during truck unloading, a balance line between the truck and the tank can be used to equalize the pressure.

CHAPTER

NATURAL GAS TREATING 7

7.1 INTRODUCTION

Natural gas, which consists of mainly methane and light hydrocarbons, contains acid gases such as hydrogen sulfide (H_2S) and carbon dioxide (CO_2). In addition to acid gases, natural gas may contain other sulfur contaminants such as mercaptans (R−SH) and carbonyl sulfide (COS) and carbon disulfide (CS_2). Natural gas with H_2S or other sulfur compounds is called *sour gas*, whereas gas with only CO_2 is called *sweet gas*. Sour gas can cause corrosion to natural gas processing equipment and pipelines. Combustion of sulfur compounds produces sulfur oxide air pollutants that must be limited to protect the environment and to prevent health-related problems. Carbon dioxide is an inert gas that does not have any heating value, but it is also the main source of greenhouse gas responsible for climate changes.

The main challenge in today's natural gas treating units is to remove high concentration of CO_2 from sour gas and the sulfur components to meet stringent emission standards. A number of methods are available for the removal of acid gases. Some are suitable for bulk acid gas removal. Some are effective in total acid gas removal but ineffective in the removal of organic sulfur compounds such as mercaptans, disulfides, or carbonyl sulfide. These different methods are discussed in this chapter. The objective of this chapter is to review the basic concepts and discuss some of today's gas treating problems, but is not intended to cover every aspect of gas treating. For more in-depth knowledge, "Gas Purification" book by Kohl and Nielsen (1997) is recommended to be used for reference.

7.2 GAS TREATING SPECIFICATIONS

When natural gas is used by the consumers, the gas must be treated to meet pipeline gas specifications. Detailed specifications are shown in Table 4.1 in Chapter 4.

For natural gas liquid (NGL) recovery plants, CO_2 removal is required to avoid CO_2 from freezing in cold sections of the plants. Natural gas liquefaction plant typically requires CO_2 content to be less than 50 ppmv. For coal gasification plants, carbon capture of 90%−95% of the CO_2 content for sequestration may be necessary to meet the greenhouse gas mandate.

7.3 GAS TREATING PROCESSES

The natural gas treating processes can be grouped in several categories as shown in Fig. 7.1. If the sulfur content is relatively low, direct conversion processes are an option. These processes use an

Handbook of Natural Gas Transmission and Processing. https://doi.org/10.1016/B978-0-12-815817-3.00007-1

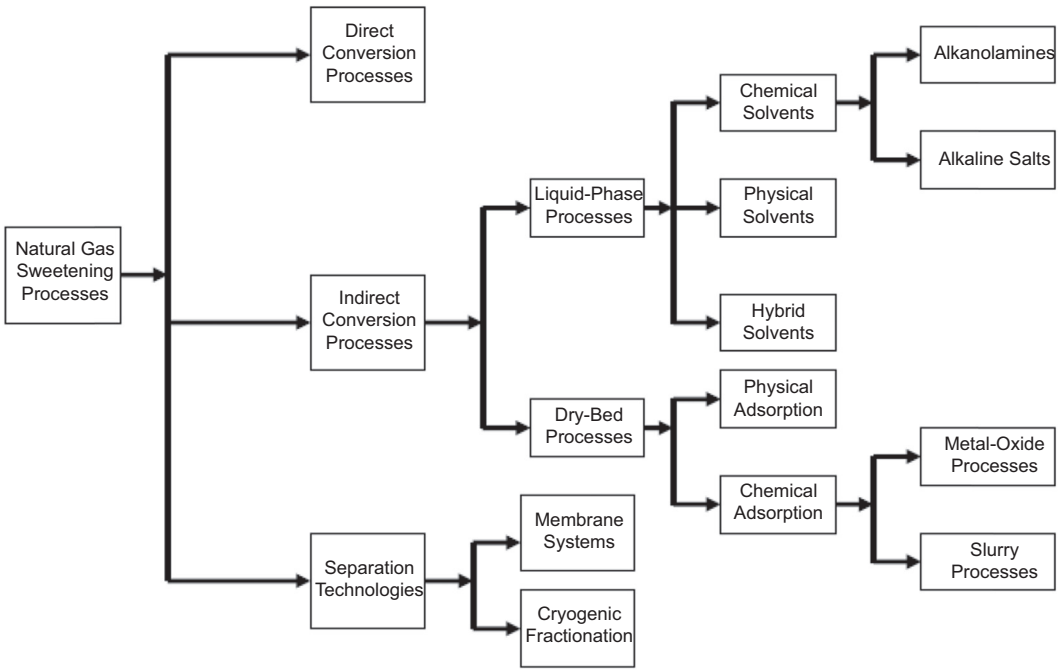

FIGURE 7.1

Alternatives for natural gas treating.

alkaline solution for absorption of H_2S and then a chelate agent and oxidation with air to form elemental sulfur. Details of this process are discussed in Chapter 8.

There are two types of indirect acid gas removal: adsorption and absorption. Adsorption is a physical–chemical phenomenon, in which impurities of the gas is trapped and removed physically or chemically by the surface of a selective solid. Absorption is the removal of acid gases by physical absorption by physical solvent toward acid gases or by chemical reaction with the acid gases using a chemical alkaline solvent.

The dry-bed processes, which use a fixed bed of solid materials to remove acid gases either through ionic bonding or chemical reactions, can be divided into two categories: physical adsorption (i.e., molecular sieve process) and chemical absorption.

The gas treating processes shown in Fig. 7.1 will be discussed in the following sections.

7.4 CHEMICAL SOLVENT PROCESSES

The chemical solvent processes can be broadly classified into two groups:

- Alkanolamine solution
- Potassium carbonate solution

In chemical solvent processes, absorption of the acid gases is achieved mainly by use of alkanolamines or alkaline salts of various weak acids such as sodium and potassium salts of carbonate. Regeneration (desorption) can be brought about by use of reduced pressures and/or high temperatures, whereby the acid gases are stripped from the solvent. Chemical absorption processes chemically absorb the H_2S, CO_2, and to some extent COS. Organic sulfur components do not chemically react with the solvent. Chemical solvents are specifically suitable when contaminants at relatively low partial pressure have to be removed to very low concentrations. Chemical solvents will not remove mercaptans down to low levels due to the low solubility of these components. An advantage, however, is that there is minimum coabsorption of hydrocarbons.

7.4.1 ALKANOLAMINE SOLVENTS

The chemical solvent process using the various alkanolamines is the common gas treating process. Amines are well suited for applications where the acid gas partial pressures are low, and low acid gas contents are required on the treated gas.

The application of alkanolamines as solvents for acid gas removal began in the 1930. In earlier applications, these amines were represented by monoethanolamine (MEA), and diethanolamine (DEA). Later, other amines such as diglycolamine (DGA) and diisopropanolamine (DIPA) gained commercial recognition. In recent years, various methyldiethanolamine (MDEA) and specialty solvent blends were developed which takes the advantage of the low energy characteristics of MDEA.

Amines are compounds formed from ammonia (NH_3) by replacing one or more of the hydrogen atoms with another hydrocarbon group. Amines are categorized as primary, secondary, and tertiary, depending upon the degree of substitution of the hydrogen atoms by organic groups. Replacement of a single hydrogen atom produces a primary amine (MEA, DGA), replacement of two hydrogen atoms produces a secondary amine (DEA, DIPA), and replacement of all three hydrogen atoms produces a tertiary amine (MDEA).

The chemical solvent processes are characterized by a relatively high heat of acid gas absorption. A substantial amount of heat is required for solvent regeneration. Amines are thermally stable, but are sensitive to degradation from oxidation and high temperatures, and may have various side reactions with CO_2, COS, and CS_2. The degraded amine can be recovered thermally or by ion exchange, as specified by the solvent suppliers.

Acid gas loading of amines is not very sensitive to changes in acid gas partial pressure as compared with physical solvents. While acid gas loading of a physical solvent increases with partial pressure of the acid gases, amine acid gas loading stays fairly constant regardless of operating pressure and cannot take advantage of the high operating pressure.

Different amines have different reaction rates with respect to the various acid gases. In addition, different amines vary in their equilibrium absorption characteristics for the various acid gases and have different sensitivities with respect to solvent stability and corrosion characteristics. Some of the specific details for the amine processes are discussed in the following sections.

7.4.1.1 Monoethanolamine

MEA is a primary amine and is the most aggressive amine among the group. MEA is also the lowest cost solvent.

MEA can remove both H_2S and CO_2 from gas streams to meet sales gas specifications. MEA solvent is very corrosive at high acid gas loadings and high solution concentrations. It reacts irreversibly with carbonyl sulfide (COS) and carbon disulfide (CS_2), which can degrade the solvent and form heat-stable salts. MEA has a higher vapor pressure than other amines, and the high equilibrium losses can be a problem. Amine losses can typically be minimized using a water wash section in the upper section of the amine absorber.

7.4.1.2 Diglycolamine

DGA was developed in the late 1960s by Fluor Corporation and Jefferson Chemical Company, a predecessor to Texaco Chemical and later Huntsman Corporation. The advantage of DGA in gas treating is that it can operate with air cooling in hot climate locations and was chosen as the sole treating solvent for the Saudi Aramco gas projects in the 1970s. Fluor patented this technology as the Fluor Econamine process that includes a side cooler on the amine absorber.

As a primary amine, DGA is similar in many respects to MEA except that it exhibits lower vapor pressure, lower solution corrosion tendency and improved solution properties and can operate at higher concentrations than MEA. The higher operating concentration (up to 60 wt%) results in significantly lower circulation rates and energy consumption.

DGA can remove COS, CS_2, and (partially) mercaptans but also forms degradation products which are not reversible at normal amine regenerator temperature. Degradation reactions produce N,N′,bis-(hydroxyethoxyethyl) urea (BHEEU), and N,N′,bis-(hydroxyethoxyethyl)thiourea (BHEETU). To maintain the amine activity, thermal reclaiming of a slipstream of the circulating amine is required.

7.4.1.3 Diethanolamine

DEA is a secondary amine. The amine reactivity and corrosivity are lower than primary amines. Vapor pressure and heat of reaction are also lower. DEA is common amine used for H_2S and CO_2 removal in refineries due to its stabilities with contaminants in the refinery gas streams. DEA can partially remove COS and CS_2. However, the reaction rate of DEA with COS and CS_2 is lower than with MEA. The solution strength of DEA solvent is typically 25 to 30 wt%.

When used for high pressure acid gas removal, the SNPA-DEA process (developed by Societe Nationale des Petroles d'Aquitaine—SNPA of France in the gas field at Lacq) has success in meeting the pipeline specifications (Kohl and Nielsen, 1997).

7.4.1.4 Diisopropanolamine

DIPA is a secondary amine, and its reactivity with acid gases is similar to DEA. DIPA is more widely used in gas processing industries in Europe and Asia. As it also has some steric hindrance, it can be used either selectively to remove H_2S (at low pressures) or to remove both CO_2 and H_2S (at higher pressures). DIPA can be used to partially remove COS and CS_2. The solution strength of DIPA solvent is typically 20 to 40 wt%.

7.4.1.5 Methyldiethanolamine

MDEA, a tertiary amine, is the most widely used gas treating agent today. Unlike primary and secondary amines, MDEA cannot react with CO_2 by the carbamate reaction. It can only absorb CO_2 by the slow bicarbonate formation. This property allows MDEA to selectively remove H_2S when treating a gas stream containing both H_2S and CO_2. The slippage of CO_2 opens up more capacities in

debottlenecking gas treating units. By reducing CO_2 absorption, more solvent is available for H_2S removal. Other advantages of MDEA solvent include low vapor pressure and solution losses, low energy for solvent regeneration, low corrosiveness, and resistance to degradation. However, generic MDEA process would require low absorption temperature to improve the amine-H_2S equilibrium for absorption to meet low H_2S specification. Alternatively, MDEA that is acidified with phosphoric acids, sulfuric acids, or other acids can be regenerated more easily and can be used to produce an ultralow H_2S content lean amine for treating. However, the level of acidification has a certain limit, as there is an impact on the pH value of the amine solution and the equilibrium curve of the acid gas solubility in the solvent (Vorberg et al., 2010).

Generic MDEA has minimal COS and CS_2 removal capability. The solution strength of MDEA solvents is 35−50 wt%.

To meet stringent emission requirements, and to take advantage of the low energy consumption of MDEA, MDEA can be blended with chemical promoters to meet the treating requirements. Promoters work by a shuttle mechanism and affect thermodynamics, but more importantly, they can control the reactivity with CO_2 (Weiland et al., 2003). Varying the concentration of chemical activators such as peperazine offers one of the solutions to meet the acid gas specifications in H_2S and CO_2. With other proprietary additives, they can be used for removal of mercaptans and COS and other contaminants. Some of the proprietary formulated technology suppliers include the following:

- aMDEA (by BASF)
- ADIP X (by Shell)
- AdvAmine (by Prosernat)
- GAS/SPEC (by Ineos)
- Jefftreat (by Huntsman)
- UCARSOL (by Dow Chemical Company)

7.4.1.6 Sterically Hindered Amines

Sterically hindered amines are compounds in which the nitrogen atom of the amine molecule is partially shielded by neighboring groups so that larger molecules cannot easily approach and react with the nitrogen.

Hindered amine concept is based on the reaction rates of the acid gases with different amine molecules. In the case of CO_2 removal, the capacity of the solvent can be greatly enhanced if one of the intermediate reactions, i.e., the carbamate formation reaction can be slowed down by providing steric hindrance to the reacting CO_2. In addition to slowing down the overall reaction, bulkier substitutes give rise to less stable carbamates. By making the amine carbamate unstable, one can theoretically double the capacity of the solvent (Chakma, 1994).

The molecular configuration of hindered amine dictates the amount of CO_2 slippage while maintaining high H_2S removal. Moderately hindered amines are characterized by high rates of CO_2 absorption and high capacities for CO_2. Moderately hindered amine may be used with physical solvents for simultaneous removal of CO_2 and H_2S from synthesis gas and natural gas. A severely hindered amine is characterized by a very low rate of CO_2 absorption and exhibits high solvent capacity, which is typically used in tail gas unit.

ExxonMobil developed the FLEXSORB SE process, which is based on a family of proprietary sterically hindered amines. The FLEXSORB SE process removes H_2S selectively or removes a group

of acidic impurities (H_2S, CO_2, COS, CS_2, and mercaptans) from a variety of gas streams, depending on the selected solvent. One version of the solvent, FLEXSORB SE Plus, is used to selectively remove H_2S as well as organic sulfur impurities commonly found in natural gas. It is claimed that FLEXSORB SE Plus in these services requires lower circulation rate than other amines (Garrison et al., 2002).

7.4.1.7 Amine Processes

The basic flow scheme of amine treating units has remained unchanged throughout the years. Amine unit requires steam for solvent regeneration and is a major steam consumer in a gas plant. In some designs, the amine regenerator is actually used as a heat rejection method to get rid of excess steam in the gas plant. A picture of a DGA unit is shown Fig. 7.2.

A typical process flow diagram of the amine unit is shown in Fig. 7.3. Typically, sour feed gas to the amine unit is filtered and cleaned of entrained liquids and pipe scales using an inlet filter separator. The separator gas is fed to the amine absorber where the acid gas content is removed by an aqueous amine solution, producing a rich amine at the bottom and a H_2S-depleted gas from the top. Depending on the applications, some CO_2 as much as 2 mol% can be left in the treated gas if the gas is used as pipeline gas. If the gas is sent to an NGL recovery unit or an LNG production plant, deeper CO_2 removal is required.

The rich amine is letdown in pressure to the rich amine flash drum. The rich amine flash drum is a three-phase separator designed for hydrocarbon liquids and amine separation. Hydrocarbon liquids are removed from the flash drum using a skimming device to avoid buildup that would cause foaming. The flashed gas containing some H_2S is treated using a small packed section and recovered as fuel gas.

FIGURE 7.2

Diglycolamine unit.

Courtesy of Fluor.

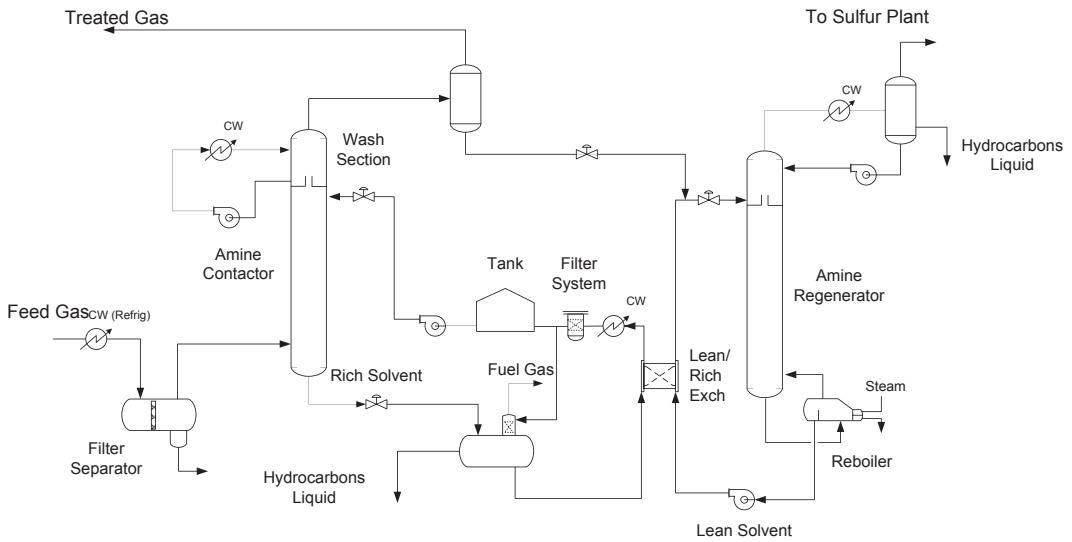

FIGURE 7.3

Typical flow schematic of an amine treating unit.

The flashed amine is preheated in the lean/rich exchanger, typically a plate and frame heat exchanger, to about 200−215°F, before entering the regenerator. The regenerator typically operates at about 10−15 psig producing an acid gas to the sulfur recovery unit. The rich amine is heated in the regenerator and stripped with steam, producing a lean amine. The lean amine is cooled in the lean/rich exchanger, lean amine cooler, and filtered prior to returning to the absorber. The filter system typically includes a particulate filter for removal of corrosion materials and a carbon filter for removal of heavy hydrocarbons. The filtration system is typically installed on the lean amine side which is easier for maintenance as the system is free of H_2S. Alternatively, it can also be installed on the rich amine side which has the advantage of protecting the amine regenerator from fouling. In this design, proper operating procedure must be exercised because of the H_2S content in the rich amine.

The amine storage tank acts as a surge for the amine system which dampens out flow fluctuation, maintaining a constant circulation. The storage tank is typically designed to hold the volume of the entire amine inventory. The amine tank content should be periodically checked for active amine and purity, and should be adjusted by makeup as necessary.

If the feed gas contains ammonia, they will be stripped off in the overhead system, which will combine with acid gases to form ammonia salt, such as ammonia bisulfate. Excessive buildup of ammonia salt will cause severe corrosion, causing hydrogen blistering on piping and exchangers. The ammonia content in the overhead system should be maintained at below 1 wt% by purging the reflux water.

There are variations of the basic flow scheme, which may include lean and semilean solvent circuits, additional flash regeneration stages, multiple absorbers, H_2S concentrator. The complexity depends on the solvent used, the acid gas concentration, operating pressure and temperature, and the product gas specifications. Some of these process variations are discussed in the following sections.

7.4.1.7.1 Two-Stage Absorption Process

The two-stage amine absorption process is applicable to MDEA solvent, which can be partially regenerated by pressure letdown, reducing the overall steam consumption. The two-stage MDEA process has been used in treating high CO_2 content synthesis gas in ammonia plants. Synthesis gas mainly consists of hydrogen, CO and CO_2, and H_2S and does not contain any hydrocarbons. For this reason, there is typically no foaming problem in synthesis gas plants. On the other hand, there are problems with a two-stage MDEA process in natural gas plants. This is typically due to the adequate solvent regeneration which results in buildup of hydrocarbons in the amine circuit, resulting in foaming and failure to meet specifications. For this reason, two-stage amine unit is seldom used in natural gas processing plants.

A typical process configuration of a two-stage process is shown in Fig. 7.4. The amine absorber consists of two absorption sections: a top lean amine section and a lower semilean solvent section. The lean amine is produced by steam stripping and the semilean solvent is produced by flash regeneration. The main purpose of the two-stage pressure is to reduce steam consumption using the semilean amine. The ratio of lean and semilean solvent flow is an important parameter in designing a two-stage MDEA

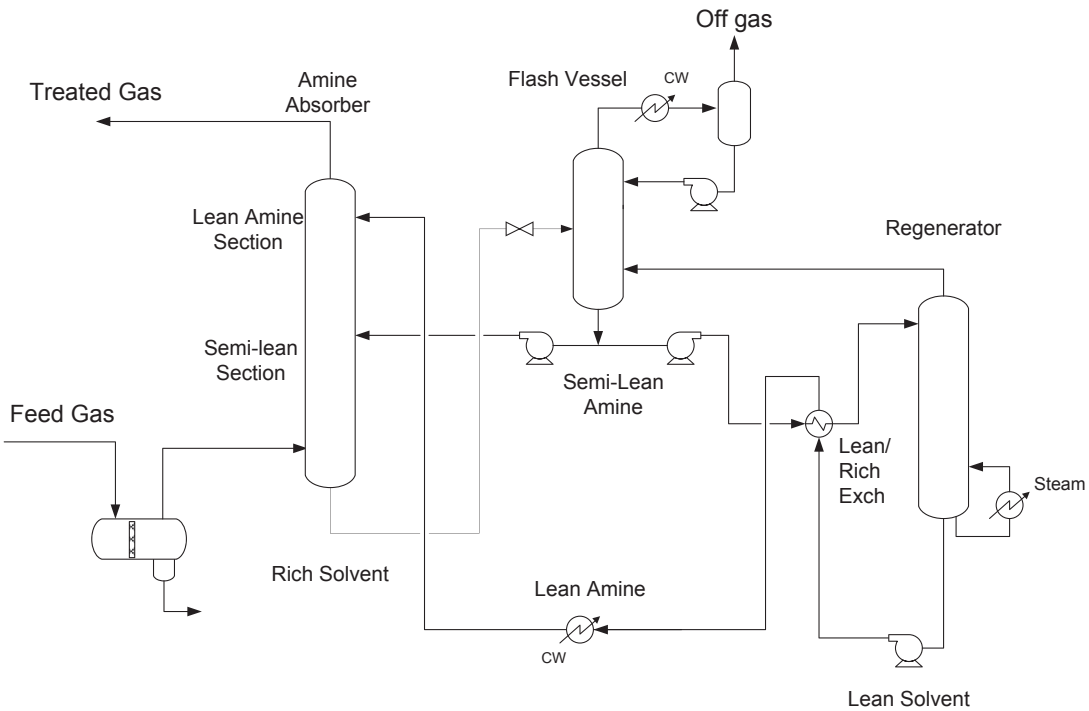

FIGURE 7.4

Flow schematic of two-stage methyldiethanolamine process.

system. Increasing the lean to semi-lean ratio will increase the steam consumption but would enhance stripping of hydrocarbons and can produce a lean amine to meet a more stringent CO_2 specification. Lowering the ratio has the opposite effect. It would lower steam consumption but may risk in inadequate stripping, resulting in foaming and failure to meet specifications. The design must consider the different feed gas conditions and compositions, and contaminant levels. Operating experience is important in the design of a two-stage MDEA unit as the performance is dependent on the reaction kinetics of CO_2 absorption, which is difficult to accurately predict even with a rate based simulator.

The two-stage MDEA process has a higher equipment count than a single-stage MDEA process. The higher equipment cost must be justified by the reduction in operating cost. In summary, the use of a two-stage process may be justified for a feed gas with low hydrocarbon content, and where steam supply is limited.

7.4.1.7.2 Double Absorption Process

The double absorption process is used for enriching the H_2S content in the feed gas to operate a straight-through Claus sulfur recovery unit.

When the gas plant is used to treat a high CO_2 content feed gas, the H_2S content in the acid gas from the amine unit frequently falls below 10%, which makes operating a conventional Claus sulfur recovery unit difficult. The acid gas can be processed an innovative method using a patented double absorption process as shown in Fig. 7.5.

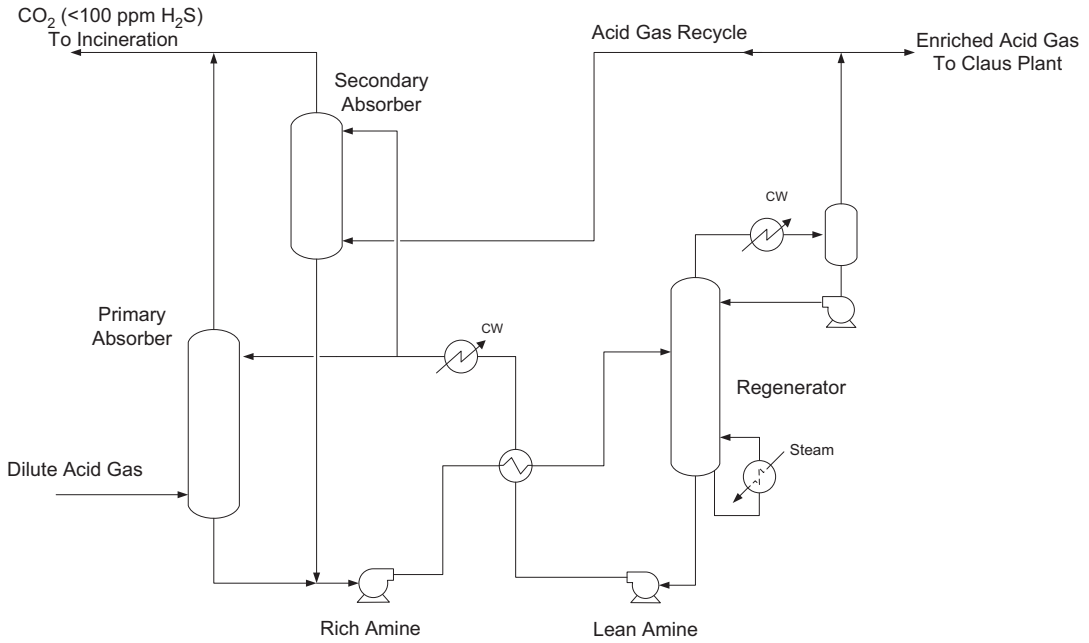

FIGURE 7.5

Flow schematic of double amine absorption process (Mak et al., 2009).

The process uses a selective solvent, such as MDEA, to process a dilute acid gas to produce two gas streams via selective absorption of H_2S. One gas stream predominantly comprises CO_2 that can be sent to a thermal oxidizer or incinerator, prior to being discharged to the atmosphere. The other gas stream is enriched in H_2S, which can be processed in a Claus sulfur recovery unit.

The process uses two absorbers, a primary absorber and a secondary absorber, to separately treat the dilute feed gas and the regenerator overhead recycle gas. The dilute acid gas, typically at slightly above atmosphere pressure, is first contacted with a lean MDEA in the primary absorber which selectively removes H_2S, while rejecting CO_2 to the overhead. The overhead gas can meet 150 ppm H_2S specification, as required to meet sulfur emission requirements. The rich solvent is pumped to a higher pressure to a regenerator operating at 10 to 15 psig.

To enrich the acid gas to the Claus unit, a portion of the regenerator overhead is recycled back to the secondary absorber. Similar to the primary absorber, CO_2 is rejected from the secondary absorber, concentrating the H_2S content in the rich amine, which indirectly increases the H_2S content in the regenerator overhead gas. The H_2S content in overhead gas can be increased by increasing the recycle flow and can reach over 60% as needed for optimum Claus unit operation.

This double absorption process can also be integrated with the tail gas treating unit to achieve over 99.9% sulfur recovery.

7.4.1.8 Special Design Considerations

General equipment design guidelines of an amine treating unit can be found in the GPSA (2004) Engineering Data Book. Followings are the design options that are normally not covered in typical amine unit design.

7.4.1.8.1 Water Wash Trays

When the absorber operates at high ambient temperature, the vaporization loss of amine can be significant. To minimize amine losses, a water wash section can be installed on the upper section of the amine absorber. Typically, a water wash pump and three to four scrubber trays are required. The water wash rate is designed to meet the minimum tray liquid loading hydraulic requirement.

7.4.1.8.2 Feed Gas and Amine Temperatures

To avoid hydrocarbon condensation, lean amine must be controlled at 10−15°F above the feed temperature. However, if the plant is located in desert areas, feed gas temperature can be as high as 140°F, which means the lean amine temperatures must be kept at 150−155°F. The high amine temperature has two undesirable effects. First, there will be an equilibrium pinch at the top of the absorber resulting in the treated gas not meeting the H_2S specification. Second, there will also be a pinch at the absorber bottom due to high operating temperature, which would require a higher solvent circulation to reduce the absorption temperature.

In the hot climate applications, it may be more cost-effective to cool the feed gas first to reduce the inlet temperature and then use a chilled lean amine to avoid the temperature pinches. Typically, a chilled water system is available for process and utility cooling.

7.4.1.8.3 Lean Amine Feed Locations

Multiple lean amine feed points can be installed in the absorber to provide the flexibility for selective CO_2 removal. When producing a pipeline gas, the feed location can be lowered to minimize CO_2

absorption as the pipeline gas specification is only 2 mol% CO_2. This is particularly useful in tail gas treating unit operation which requires maximum slippage of CO_2, and moving the feed location to a lower location will help to concentrate H_2S content in the acid gas to the Claus sulfur recovery unit. However, if stringent sulfur specification must be met, the lean amine must be raised to a higher tray location, which would add more contacting stages but would also reduce the amount of CO_2 slippage.

7.4.1.8.4 Absorber Side Cooler

When amine is used to treat high partial pressure acid gases, especially CO_2, the heat of reaction would be significant, which would raise the temperature of the absorber. The amount of acid gas that can be absorbed by the amine is determined by the rich amine acid gas loading at the bottom, which is a function of operating temperature. In a conventional amine unit design, the absorber bottom temperature is maintained at about 200°F (to minimize corrosion) by increasing amine circulation. Therefore to treat a high CO_2 content feed gas, a high amine circulation is required.

In treating high CO_2 gases, a more efficient design is to install a side cooler in the lower section of the absorber as shown in Fig. 7.6. The hot semi-rich amine is withdrawn using a chimney tray in the absorber, pumped, cooled, and returned to the absorber. With this configuration, the absorber can be maintained at a relatively low temperature without increasing amine circulation.

The temperature profile of the absorber with the side cooler is shown in Fig. 7.7. The side cooler should be located where the peak absorption temperature occurs, typically four trays from the bottom. With the side cooler design, the absorber bottom temperature can be controlled using a bypass on the heat exchanger.

7.4.1.8.5 Design Guidelines

The operating parameters of an amine process vary with the type of the amine as well as the feed gas conditions. The main differences are the amine strengths, which are dependent on the physical–chemical properties and the corrosion characteristics. Table 7.1 summarizes some of the typical design

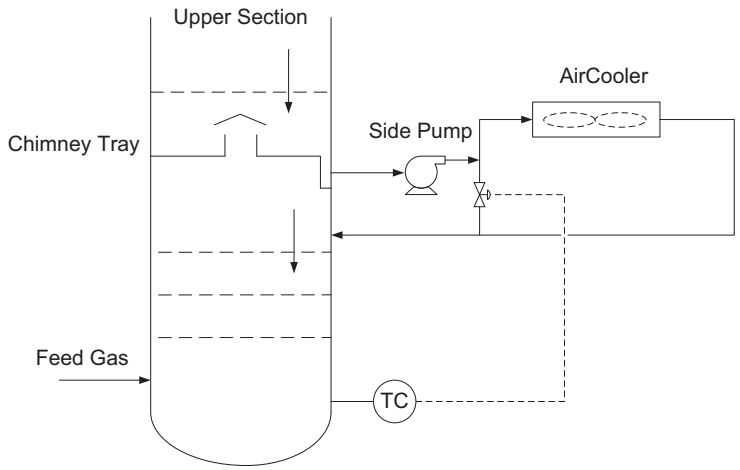

FIGURE 7.6

Absorber side cooler schematic.

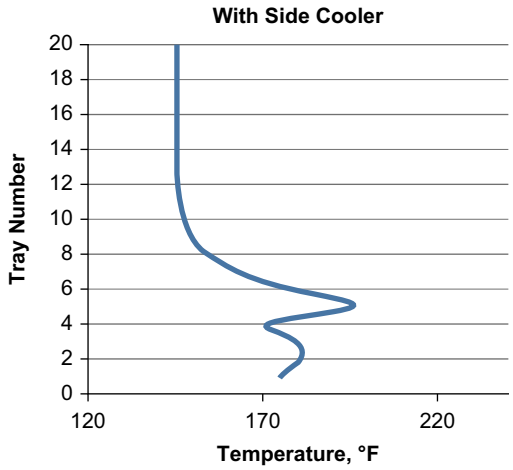

FIGURE 7.7

Absorber temperature profile with side cooler.

parameters for the different amines. Note that this table is intended to be used as a general guide, and the users must also consider other parameters such as operating pressure and temperature, feed gas and product gas specifications.

The amine circulation rate is dependent on the acid gas loading of the rich amine, which, in turn, is a function of the amine−acid gases equilibrium at the absorber bottom condition. A higher acid gas loading means the amine can pick up more acid gases per gallon of solution, requiring a lower amine circulation. Typically, the absorber bottom is designed at no more than 80% approach to equilibrium. The absorber contains at least 20 absorption trays, and more trays may be required to meet the treated gas specifications which must be determined by simulation of the amine unit.

Low-pressure steam must be supplied for solvent regeneration to produce a lean amine suitable for treating. Steam consumption is typically defined as the mole of steam per mole of acid gas (typically 1.0) or pounds of steam per gallon of amine circulation (1−1.2), as shown in Table 7.1. Steam consumption is higher for the primary amines (MEA and DGA) than the tertiary amine (MDEA), which is mainly due to the differences in heat of reaction with acid gases.

Amine concentrations are set by unit operating experience considering the solvent stability, foaming tendency, corrosion rates, and unit performance. Higher concentration can reduce amine circulation but would also increase the absorption temperature and corrosion rate. The typical amine concentrations for the different amines are shown in Table 7.1. For example, DGA can be operated at high concentration as it is proven to be stable, and in fact, the high temperature enhances DGA ability to remove COS.

7.4.1.9 Amine Unit Operating Problems

Amine unit operating problems have been well documented and published. New amine units can typically meet the performance guarantees and have no operating problems in early operation. However, unit performance generally deteriorates over time, mainly due to the buildup of

Table 7.1 Design Parameters of Generic Amines

Solvent	Monoethanolamine	Diglycolamine	Diethanolamine	Diisopropanolamine	Methyldiethanolamine
Typical concentration (wt%)	15−20	45−60	25−30	30−40	35−50
Typical lean loading (mol/mol)	0.1−0.15	0.05−0.1	0.05−0.07	0.02−0.05	0.004−0.01
Typical rich loading (mol/mol)	0.30−0.35	0.35−0.45	0.35−0.40	0.30−0.40	0.45−0.55
Typical steam usage (lb/gal)	1.0−1.2	1.0−1.2	0.9−1.1	0.8−1.1	0.9−1.1
Heat of reaction with CO_2 (Btu/lb)	825	850	653	550	475
Heat of reaction with H_2S (Btu/lb)	820	674	511	475	455

contaminants and impurities, and lack of maintenance. The end results are failure to meet product specifications and reduction in treating capacity.

Absorber and regenerator typically experience foaming problems, resulting in carryover of amine to downstream units. Foaming is caused by hydrocarbon entrainment in the feed gas. Hydrocarbon contamination can be mitigated by maintaining a temperature approach between the lean amine and the feed gas, skimming of hydrocarbons from the rich amine flash drum and reflux drum, and frequent change-out of particulate filters and carbon filters.

Foaming can also be caused by heat-stable salts, which are formed from amine degradation. There are different methods that can be used to control the levels of heat-stable salts, including purging, caustic addition, and reclamation.

Continuous amine reclaiming is considered more effective in solving the heat-stable salt-related problems. Formation of heat-stable salts depends on the feed gas compositions, particularly sulfur contaminants and the H_2S to CO_2 ratio. Most amine units can operate without reclaiming for some time, especially with low H_2S content gases. Most amine suppliers are knowledgeable of the heat-stable salt problems and can provide the reclaiming equipment to maintain the amine purity. For more detail discussion on the operating issues and troubleshooting methods, please refer to technical papers such as by Seagraves et al. (2010) and the LRGCC proceedings.

7.4.2 THE POTASSIUM CARBONATE SOLUTION

The potassium carbonate solution is a vintage treating solvent. In the potassium carbonate process, which is referred to as the "hot pot" process, the process system operates at high temperature (in the range of 230−240°F) and was very popular in CO_2 removal in ammonia plant. Potassium carbonate is known to cause equipment failure from excessive corrosion. All carbon steel must be stress relieved. A variety of corrosion inhibitors are also available to combat corrosion.

Potassium carbonate solvent absorbs CO_2 at a relatively slow rate. The reaction rates are increased through the use of catalytic promoters, such as DEA, arsenic trioxide, selenous acid, and tellurous acid. In applications for the removal of hydrogen sulfide, tripotassium phosphate may be added. These activators are claimed by the licensors to improve the potassium carbonate performance.

There are three potassium carbonate processes using different additive: Catacarb, Vetrocoke, and Benfield.

The Catacarb process uses amine borates additive and vanadium-based inhibitors to mitigate the corrosion, which are toxic materials.

The Vetrocoke process utilizes organic and inorganic additives to activate the solution. One of the common corrosion inhibitors is arsenic trioxide, which, however, is also a toxic material.

The Benfield process, licensed by UOP, uses the less toxic DEA as an activator. A variant of the Benfield process is the DEA-hot carbonate process which consists of bulk CO_2 removal combined with a downstream DEA polishing unit. The UOP Benfield ACT-1 activator is another activator which is claimed to have a better performance. A typical flow scheme for the UOP Benfield process is shown in Fig. 7.8.

Potassium carbonate units are slowly replaced by promoted MDEA units for CO_2 removal. However, there are still many existing potassium carbonate units that may benefit using the less toxic activators.

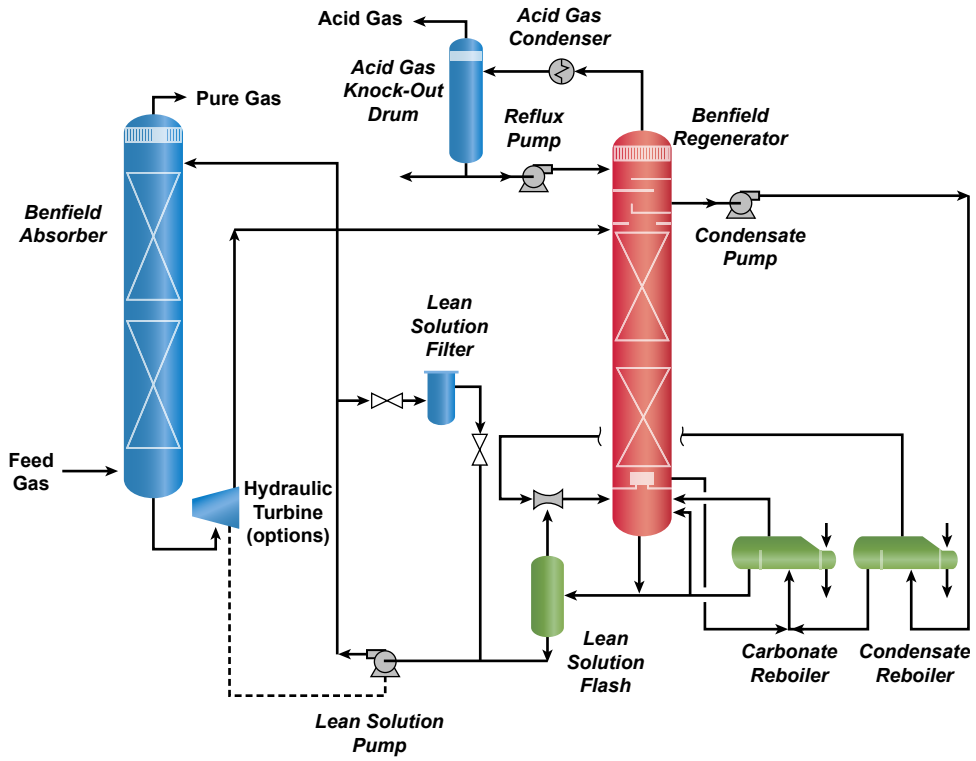

FIGURE 7.8

UOP Benfield process.

7.5 PHYSICAL SOLVENT PROCESSES

Physical solvent processes can remove acid gases and organic sulfur based on physical absorption, and no chemical reaction occurs.

Physical solvents have an advantage over chemical solvents when treating sour feed gas streams with high acid gas content. The physical solvent's acid gas holding capacity increases with the partial pressure of acid gas (Henry's Law). Thus, they are more economical over chemical solvents in treating high pressure high CO_2 content gas.

Unlike chemical solvents, physical solvents operate at ambient to subambient temperatures. They are noncorrosive and do not require stainless steel material to combat corrosion. Unless operating at cryogenic temperatures, only carbon steel is required.

Physical solvents can be regenerated by reduction in solvent pressure. Compared with chemical solvents, physical solvents absorb more hydrocarbons and have high hydrocarbon losses. For this reason, physical solvents are more common in treating synthesis gas which has no hydrocarbons.

When used in natural gas treating applications, flash gas compressor recycle is required to minimize the hydrocarbon losses.

Some of the more common physical solvents used in gas treating include the following:

- Propylene carbonate (PC)
- Dimethyl ether of polyethylene glycol (DEPG)
- Methanol (MeOH)
- N-methyl-2-pyrrolidone (NMP)

These solvents are used to remove CO_2 from high-pressure sour gases. During the absorption processes, they also coabsorb other components. The solubility of the various components in relationship to CO_2 is shown in Table 7.2. To minimize hydrocarbon losses, the solvent that has the lowest solubility with methane and ethane is preferred.

PC and DEPG solvents have been used for both natural gas and syngas treating units. Among all the physical solvents, PC exhibits the lowest hydrocarbon solubility, which means a lower hydrocarbon loss in the CO_2 stream; hence PC is more suitable for treating natural gas streams than other physical solvents.

Table 7.2 Relative Solubility of Components in Physical Solvents (Burr and Lyddon, 2008)

Gas Component	Propylene Carbonate at 25°C	Dimethyl Ether of Polyethylene glycol at 25°C	N-Methyl-2-Pyrrolidone at 25°C	Methanol at −25°C
Carbon dioxide	1.0	1.0	1.0	1.0
Hydrogen sulfide	3.29	8.82	10.2	7.06
Carbonyl sulfide	1.88	2.30	2.72	3.92
Methyl mercaptans	27.2	22.4	34.0	–
Hydrogen	0.0078	0.013	0.0064	0.0054
Nitrogen	0.0084	0.020	–	0.012
Oxygen	0.026	–	0.035	0.020
Carbon monoxide	0.021	0.028	0.021	0.020
Methane	0.038	0.066	0.072	0.051
Ethane	0.17	0.42	0.38	0.42
Ethylene	0.35	0.47	0.55	0.46
Propane	0.51	1.01	1.07	2.35
i-Butane	1.13	1.84	2.21	–
n-Butane	1.75	2.37	3.48	–
i-Pentane	3.50	4.47	–	–
n-Pentane	5.0	5.46	–	–
n-Hexane	13.5	11.0	42.7	–
n-Heptane	29.2	23.7	50.0	–

Methanol and NMP solvents are common in syngas treating units. They are seldom used in natural gas treating units mainly due to their high solubility of hydrocarbons as shown in Table 7.2. They will coabsorb most of the propane and heavier hydrocarbons, resulting in high product losses.

Unlike amine processes, physical solvent process configurations are much more complex. Physical solvent processes require proven design and engineering skill, unit operating data, coupled with accurate thermodynamic data and heat and mass transfer model that are only available from licensors. The process configurations must be customized for specific feed gas compositions, operating temperatures and pressures, and product specifications.

7.5.1 PROPYLENE CARBONATE

Propylene carbonate, $C_4H_6O_3$, is a polar solvent. As discussed in the previous section, PC has the lowest solubility of hydrocarbons compared with other solvents. Among all the solvents, PC has the least H_2S selectivity and is not as effective for H_2S removal. In terms of regeneration, PC requires the lowest regeneration energy, and can be regenerated without the use of heat.

The Fluor Solvent process which uses PC as the solvent was commercialized by Fluor in the early 1960s. The Fluor Solvent process is a refrigerated solvent process, operating at low temperatures (10 to $-20°F$), which has several advantages. At low temperatures, the PC unit can operate with a lower solvent circulation, requiring less power and a lower capital investment than competing processes. The freezing point of PC is $-57°F$, which makes PC an ideal solvent for cold climate operation.

PC is often compared with formulated or promoted MDEA for bulk CO_2 removal. Bulk CO_2 removal is typically required to meet pipeline gas specification, typically 2 mol%. Both processes have been proven suitable in meeting pipeline specifications. However, the unit complexity, process performance, and design characteristics are very different which can be compared in Table 7.3.

As can be seen in the comparison table, when used to treat a lean gas with low H_2S content, PC has a clear advantage over MDEA. It can produce a dry gas and does not require the use of steam or heating. No water makeup is required and no solvent monitoring is necessary. These advantages are important in offshore applications where limited support and operating personnel are available. The use of PC has a competitive advantage over MDEA when the CO_2 partial pressure is greater than 60 psi.

The following sections describe the development of the Fluor Solvent process from the original Fluor Solvent unit to the new innovations that are applicable in today's high CO_2 gas plants.

7.5.1.1 Fluor Solvent Unit

The first Fluor Solvent unit is located in Terrell County, Texas. The PC unit was built in 1960 and has been operating successfully for the past 50 years, using the same equipment, without any operating problems.

The unit was originally designed for 220 MMscfd of feed gas with 53 mol % CO_2 at about 900 psig pressure. Over the years, the feed gas pressure and CO_2 content have declined. The unit is now treating 120 MMscfd of feed gas with about 36 mol % CO_2. The Terrell County process flow schematic is shown in Fig. 7.9. The unit picture is shown in Fig. 7.10.

The unit feed gas is treated in the absorbers with about 3000 gpm of lean PC. The rich solvent from the absorber is cooled by the absorber overhead gas and the CO_2 vent stream. The cooled solvent is

Table 7.3 Comparison of Fluor Solvent to Formulated Methyldiethanolamine (MDEA) Processes (Mak et al., 2003)

Treating Process	Fluor Solvent	Formulated MDEA Gas
Equipment count	Low	High
Operational complexity	Low	High
H_2S removal	Limited	No limit
Suitability for rich gas	No	Yes
Stainless steel materials	No	Yes
Stress relieving of carbon steel	No	Yes
Fired heater/steam required	No	Yes
Produces dry treated gas	Yes	No
Ability to handle higher level of CO_2	Yes	No
Vulnerable to solvent foaming	No	Yes
Winterization required	No	Yes
Solvent concentration monitoring	No	Yes
Hazardous solvent	No	Yes
Water consumption	No	Yes
Recycle gas compressor	Yes	No
Hydrocarbon loss in CO_2	1%	Less than 1%

regenerated by successively letdown in pressure to 445 psig and 175 psig. The flash gas, typically containing about 65% methane, is compressed and recycled back to the absorber for hydrocarbon recovery. The rich solvent is letdown in pressure using the hydraulic turbines, which generate refrigeration for solvent cooling and shaft power to operate the circulation pumps.

To comply with emissions regulations, the flash vapor from the medium pressure stage is treated in a reabsorber, which recovers the hydrocarbons contents in the solvent. The methane content in the CO_2 vent is reduced to about 1 mol % that is required to meet the local methane emission limit. The vacuum pressure in the last flash stage is maintained by a vacuum compressor.

The Fluor Solvent unit produces sales gas with a CO_2 content of about 2 mol %. However, H_2S in the treated gas is 6 ppmv which is slightly higher than the 4 ppmv pipeline specification. Presently, a sulfur scavenger bed (PURASPEC) is installed to treat about 20% of the absorber overhead gas to meet the pipeline specification. The water content of the treated gas is about 1 lb water/MMscf, which meets pipeline specification.

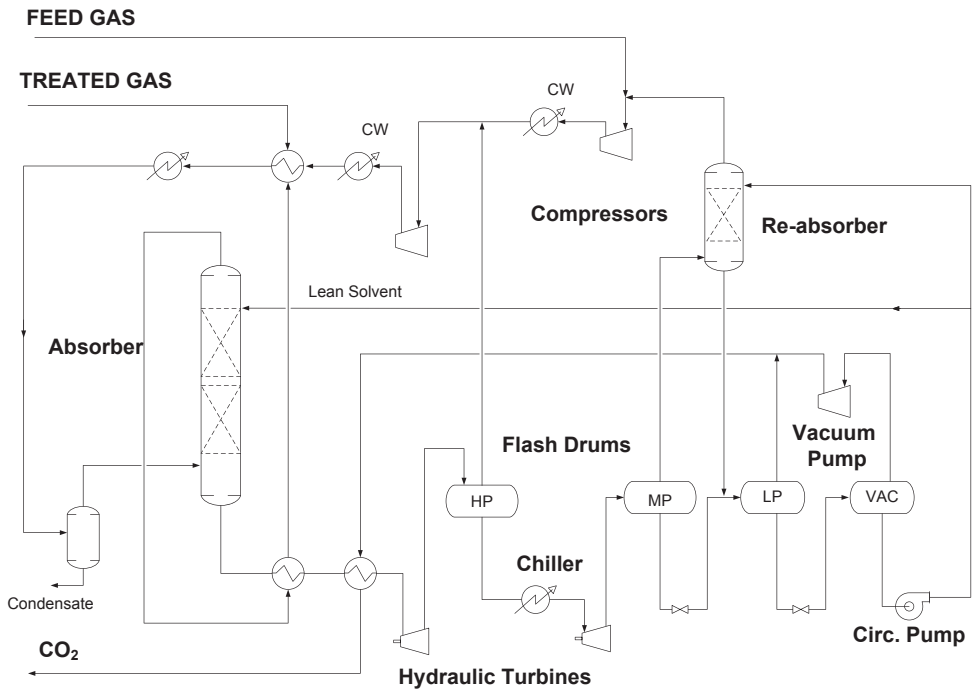

FIGURE 7.9

Fluor Solvent process (Mak et al., 2007).

FIGURE 7.10

Terrell County Fluor Solvent unit (Mak et al., 2007).

7.5.1.2 Innovations in Fluor Solvent Process

Natural gas from unconventional gas, such as coal-bed methane and offshore gas fields, is typically very lean, containing almost no H_2S and has a very high CO_2 content. As an example, offshore gas from South China Sea typically contains 30%−60% CO_2 with almost no H_2S and is available at 1000 psig. These gases are ideal for the Fluor Solvent process.

For other solvents and membrane separation processes, the processing requirement increases with the CO_2 content. If the feed gas CO_2 content increases over time, additional treating units or membrane units must be added. Typically, high CO_2 gas will require more investment.

The patented Fluor Solvent process is designed different than conventional process. High CO_2 content is actually an asset to the process. In the Fluor Solvent process, the potential energy of CO_2 is used to produce power and cooling for the CO_2 absorption process. The development is a result of many years of research and development in the physical solvent process. With advanced modeling and accurate thermodynamic data, the Fluor Solvent unit can operate with almost no power input and refrigeration when used in treating high-pressure high CO_2 content gases. The basic configuration is shown in Fig. 7.11. Main design features of the process are described by Mak et al. (2004), Mak (2007), and Mak et al. (2007).

The innovation is the use of the refrigeration produced by flash regeneration process to cool the absorber. The use of hydraulic turbines produces power that further generates cooling as well as power to operate the circulation pumps. The cooling of the absorber is achieved by a side cooler that cools the semirich solvent withdrawn from the absorber. With such integration, the process can operate without

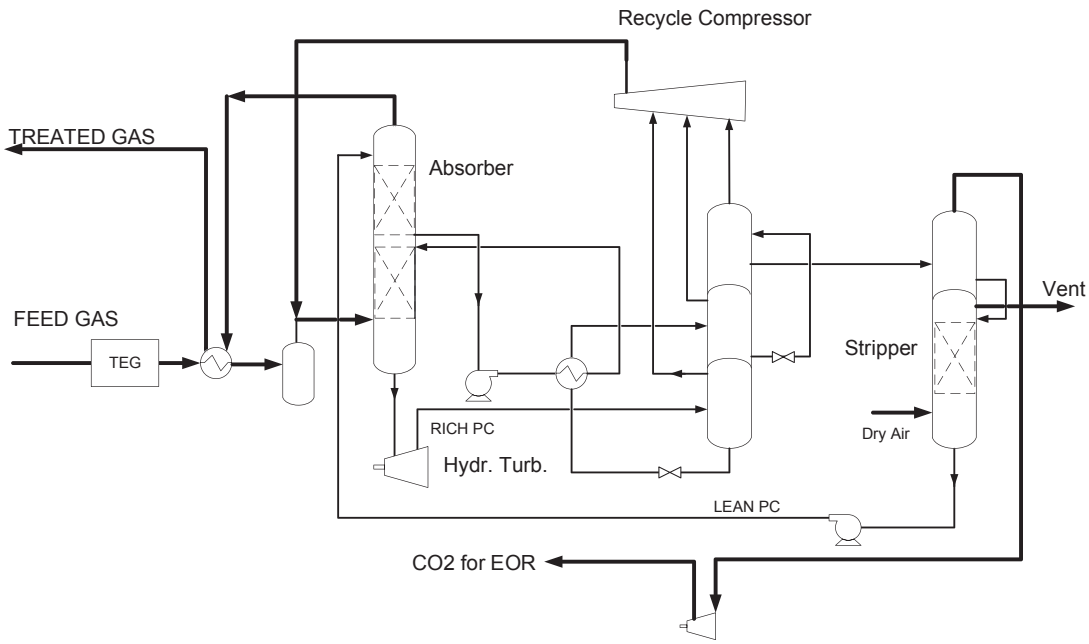

FIGURE 7.11

Fluor process for treating high CO_2 gas (Mak et al., 2004, 2007; Mak, 2007).

the use of external refrigeration as most of the cooling can be achieved by the flashing of CO_2. This typically occurs when the CO_2 content in the feed gas is greater than 30%.

Similar to the original design, the Fluor Solvent process can operate at as low as −20°F, and water in the feed gas should be removed to avoid hydrate formation in the absorber.

The rich solvent is successively flashed to lower pressures, producing vapors which are recycled back to the absorber. The methane content in the flash vapors is recovered in the absorber. The rich solvent is finally flashed at atmospheric pressure, producing a 95% CO_2 stream that can be compressed for reinjection for enhanced oil recovery. With the improved process, hydrocarbon loss in the CO_2 stream can be reduced to less than 1%.

The solvent can be regenerated using a gas stripper, which is very efficient to produce an ultralean solvent. If H_2S has been removed upstream, dried air or nitrogen stripping can be used and can be economical. With this stripping method, the treated gas can meet 500 ppmv or lower CO_2 specification.

7.5.2 DIMETHYL ETHER OF POLYETHYLENE GLYCOL

DEPG is a mixture of dimethyl ethers of polyethylene glycol. Solvents containing DEPG are manufactured by several companies including Coastal Chemical Company, Dow, or Clariant. DEPG is marketed by Dow as the Selexol solvent or by Clariant as the Genosorb solvent. The DEPG solvent process can be licensed from UOP as the Selexol process or from Fluor as the EconoSolv process.

Similar to PC, the DEPG solvent can be regenerated by successive pressure letdown and/or stripping with air or nitrogen for deeper CO_2 removal. DEPG can dehydrate feed gas and remove hydrogen cyanide (HCN), mercaptans, and heavy hydrocarbons from natural gas.

While PC can operate at 10 to −20°F temperature, DEPG is limited to 32°F. The difficulty with DEPG operating at low temperature is the viscosity problem. At lower temperatures, DEPG viscosity will greatly increase, which will impede the heat and mass transfer operation in heat exchangers, separators, and columns, making absorption more difficult.

The other difference between the PC process and the DEPG process is the solvent concentration. PC can operate as a pure component, while the DEPG process requires maintaining 95 wt% concentration. This is necessary to maintain the regenerator bottom temperature about at 300°F to avoid solvent degradation.

Compared with other physical solvents, DEPG requires higher solvent circulation mainly due to the high operating temperature.

The advantage of DEPG is the high H_2S to CO_2 selectivity (see Table 7.2), only second to NMP. The high selectivity means that DEPG can remove H_2S preferentially to CO_2. Vapor pressure of DEPG is very low, and its equilibrium losses are almost negligible. DEPG is a stable solvent and is very resistant to degradation, even with oxygen. For this reason, DEPG is often used in gasification plants for gas cleanup for power generation and in recovery methane in landfill gas plants.

7.5.2.1 Dimethyl Ether of Polyethylene Glycol Process

DEPG has been used in gasification projects to selectively remove CO_2 from the synthesis gas, to produce a clean fuel for integrated gasification combined cycle (IGCC) power plants. In these plants where the syngas feed to the DEPG process is unshifted (without converting CO to CO_2 and hydrogen), a single-stage DEPG unit can be used. A picture of a DEPG unit for IGCC plant is shown in Fig. 7.12.

FIGURE 7.12

Dimethyl ether of polyethylene glycol unit for integrated gasification combined cycle plant (Mak, 2011).

The basic DEPG process flow diagram is shown in Fig. 7.13. The feed gas at about 600 psig pressure is first cooled by heat exchanged with the cold treated gas and enters the absorber where its H_2S content and a portion of the CO_2 content are absorbed by the lean DEPG. For H_2S selective removal, the absorber must contain sufficient trays, and the solvent flow must be minimized to avoid excessive coabsorption of CO_2. The absorber typically requires four or more sections of packing.

The rich solvent from the absorber is letdown in pressure to a flash drum. The flash gas containing the absorbed hydrogen is recycled back to the absorber for recovery. The flashed solvent is then heated in the lean/rich exchanger and then regenerated in a solvent regenerator, similar to the design of an amine unit.

Heavy hydrocarbons and sulfur compounds such as mercaptans are preferentially absorbed by DEPG. These components may be removed in the regenerator by steam stripping and end up in the reflux drum. However, the DEPG regenerator typically operates at 300°F which may not be high enough to boil off the heavier compounds. If this is the case, the heavier compounds will accumulate in the system which may cause foaming problems. Since DEPG is soluble in water, the heavy hydrocarbons can be removed by extraction with water by processing a slipstream of the rich solvent from the process.

7.5.2.2 Dimethyl Ether of Polyethylene Glycol Carbon Capture Process

In meeting today's environmental requirements, the syngas from gasification plant must be shifted to form CO_2 and hydrogen which would allow CO_2 to be captured; consequently, only hydrogen is combusted in the power plant for power production, while CO_2 is reinjected for sequestration, thus eliminating all the greenhouse gas.

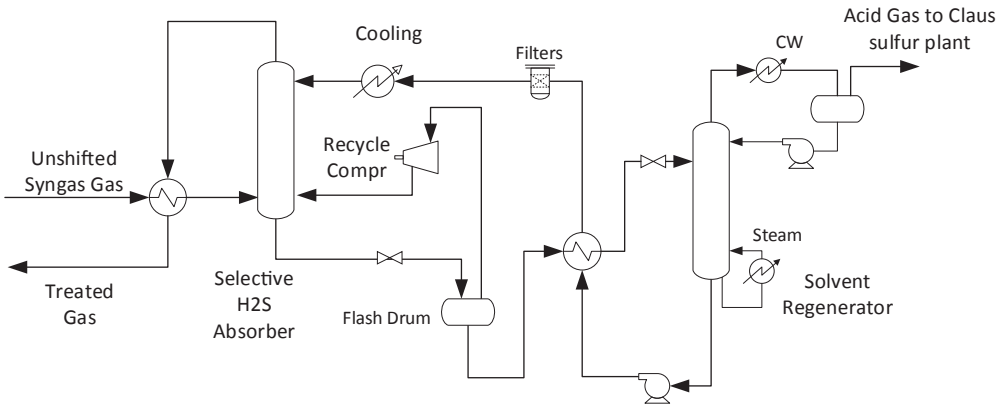

FIGURE 7.13

Single-stage dimethyl ether of polyethylene glycol process.

The DEPG process can be configured for carbon capture using a two-stage absorption process. The first stage is the H_2S absorption stage which is designed to remove essentially all the H_2S from the feed gas and produce an H_2S-enriched acid gas to a Claus sulfur recovery unit. The second stage is the CO_2 absorption stage which removes the CO_2 from the H_2S absorption stage for sequestration.

The coabsorption of CO_2 in the H_2S absorption stage makes the design challenging. The H_2S absorption process must be designed to be H_2S selective for two reasons. First, the Claus sulfur recovery unit requires the H_2S content to be kept at high concentration (see Chapter 8). Second, excessive slippage of CO_2 to the sulfur recovery unit will increase carbon emissions in the tail gas treating unit, defeating the purpose of carbon capture.

To increase the H_2S content in the rich solvent, CO_2 is stripped from the solvent in a CO_2 stripper, and recycled back to the process, as shown in Fig. 7.14. The recycle of CO_2 would require a higher solvent circulation to meet H_2S specification. To avoid reabsorption of the recycled CO_2, CO_2 preloaded solvent from the CO_2 absorption stage is used. With a CO_2 saturated solvent, the amount of CO_2 absorption can be minimized.

Similar to the single-stage absorption process, the rich solvent from the first stage is regenerated using steam, producing a H_2S-free lean solvent. The lean solvent is routed to the CO_2 absorber. In this arrangement, the treated gas from the second stage is sulfur free.

In the CO_2 removal section, the rich solvent is regenerated by successive reduction in pressures. Steam stripping is typically not required in the second stage. The last stage flash can operate at atmospheric pressure or under a slight vacuum, producing a semilean solvent which is adequate for bulk CO_2 removal. The process can be configured to produce high-pressure CO_2, which can be fed to the

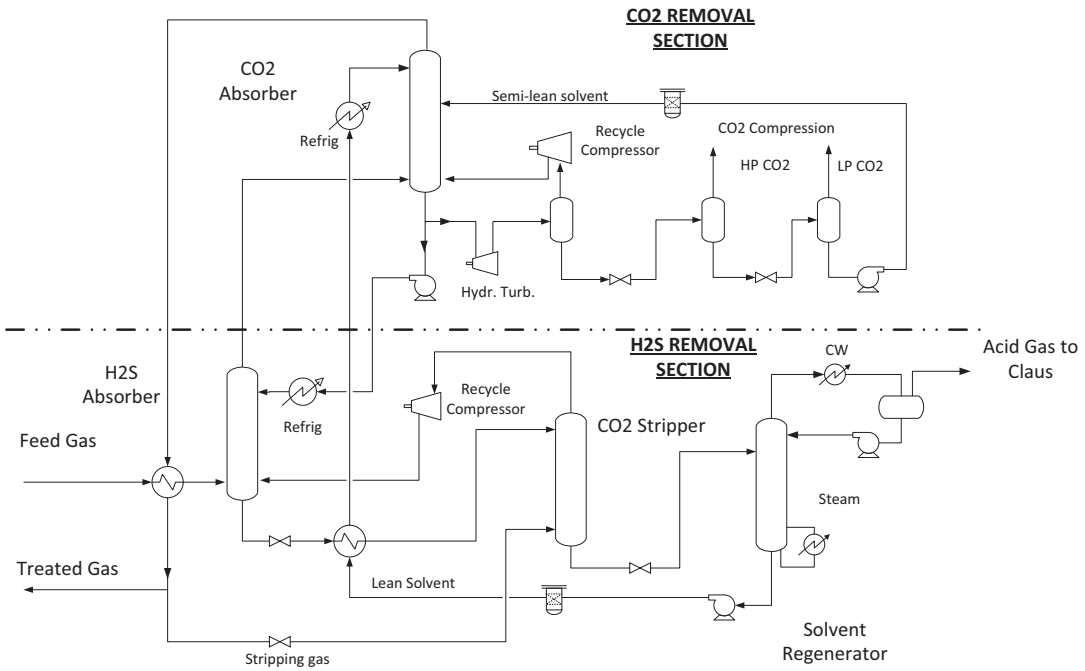

FIGURE 7.14

Two-stage dimethyl ether of polyethylene glycol process (Mak et al., 2009; Mak, 2011).

CO_2 compressors, reducing the power consumption for CO_2 sequestration. The treated gas can be sent to a power plant for power production or used for ammonia or urea production.

This two-stage DEPG system can be used to capture over 95% of the carbon content in today's gasification plants (Mak et al., 2009; Mak, 2011).

7.5.2.3 Mercaptan Removal

As can be seen in Table 7.2, the solubility of methyl mercaptan is 340 times that of methane. When molecular sieves are used for dehydration, the spent regeneration gas from the molecular sieve beds typically contains high levels of mercaptans. The mercaptans content can be removed by the DEPG solvent, producing a sulfur-free treated gas.

7.5.2.4 Landfill Gas

Landfill gas typically contains significant amounts of CO_2, some H_2S, O_2, and other contaminants, such as mercaptans. Depending on the sales gas requirements, it may be necessary to remove some or all of these contaminants. DEPG is proven to be highly oxygen tolerant and has demonstrated its ability to remove heavy metals and hydrocarbons.

7.5.2.5 Hydrocarbon Dew Point Control

Typical hydrocarbon dew point specification for the pipeline gas is 14°F. If a gas stream is near this specification, usually all that is required is removal of a small amount of heavy hydrocarbons. Heavy hydrocarbons are very soluble in DEPG. The use of DEPG to meet the hydrocarbon dew point

specification can be effective and simple. This approach can be used to condition small gas streams that are used in gas turbines or engine drivers.

7.5.3 METHANOL (RECTISOL PROCESS)

Historically, methanol was the first commercial organic physical solvent and has been used for hydrate inhibition, natural gas treating, dehydration, and hydrocarbon liquids recovery. The methanol process is also called the Rectisol process (licensed by Linde AG and Lurgi AG), which uses cold methanol at -40°F to remove acid gases at high pressure, which is very popular in ammonia plants.

Operation of a physical solvent unit favors low temperatures. Physical solvent's acid gas holding capacity increases with low temperatures, which would reduce the solvent circulation requirement. Methanol is an alcohol-based solvent which can operate at cryogenic temperatures without encountering viscosity problems. Low-temperature operation is necessary for the methanol process due to the high vapor pressure of methanol resulting in high methanol losses.

Operation of the Rectisol process is similar to the DEPG process. Methanol's H_2S selectivity is close to DEPG (see Tables 7–2) and can also be used to produce an acid gas with high H_2S content to the sulfur recovery unit and remove CO_2 for sequestration. Similar to the DEPG process, methanol can be regenerated by steam, which accounts for its capability to produce very high-purity products.

For chemical production, such as ammonia and urea, high-purity hydrogen is required, which is the main application for Rectisol process. If the product gas is used as fuel gas for power generation in IGCC plant, the Rectisol process may be an overkill. Because of the extensive use of stainless steel material and the high power requirement of the refrigeration unit, Rectisol process is typically more expensive than competing processes. The use of molecular sieve technology is alternative to Rectisol to produce high-purity hydrogen and can be a lower cost option (Mak et al., 2004).

The process flow diagram of a typical Rectisol unit is depicted in Fig. 7.15, and the basic process is described in the following.

The syngas is scrubbed in the methanol scrubber which consists of an upper section for bulk CO_2 removal and a lower section for H_2S removal. A portion of the CO_2-rich solvent is drawn from the CO_2 removal section and letdown in pressure to the CO_2 flash drum. The H_2S-rich solvent from the H_2S removal section is also letdown in pressure to the H_2S flash drum. The flash gas from both drums is recompressed and recycled to the inlet of the unit for hydrogen recovery.

The rich solvent is letdown in pressure to the CO_2 stripper that produces an overhead tail gas containing methane and light components, and a bottom product containing mainly CO_2 and H_2S. The bottom stream is fractionated in the H_2S concentrator that produces a CO_2 overhead product, and a bottom solvent enriched in H_2S. Inert or treated gas can be used as a stripping gas in the H_2S concentrator. Acid gas is finally regenerated in the methanol regenerator and sent to the sulfur recovery unit. To maintain methanol purity and avoid buildup of water, a small fractionating column can be used to process a slipstream of the circulating solvent.

7.5.4 N-METHYL-2-PYRROLIDONE

NMP is a high boiling liquid with very high solubility for H_2S. The use of NMP (licensed as the Purisol process by Lurgi AG) is particularly suited for purification of high-pressure, high CO_2 content synthesis gas in gasification applications.

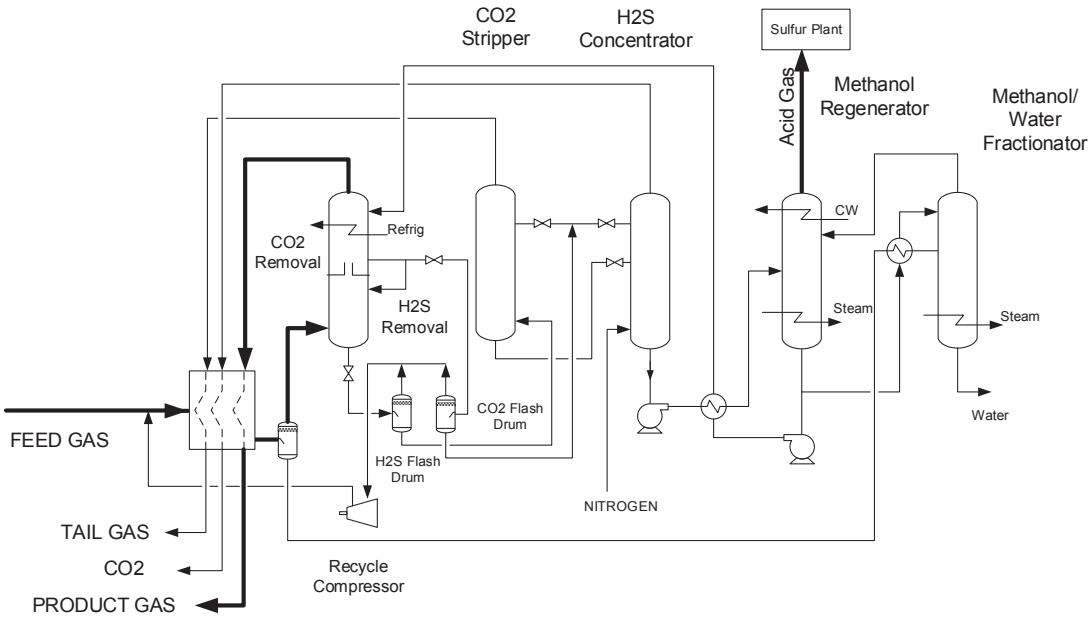

FIGURE 7.15

Typical Rectisol unit process flow scheme (Mak et al., 2004).

The "Purisol" process typically operates at 5°F to minimize solvent losses. NMP has a relatively high vapor pressure compared with DEPG or PC, and low operating temperature would help to minimize solvent losses. NMP cannot significantly remove COS, but COS can be hydrolyzed and then removed by the NMP solvent. The Purisol process is similar to the DEPG process.

7.6 MIXED PHYSICAL AND CHEMICAL SOLVENT PROCESSES

Some chemical manufacturers have developed processes that take advantage of the benefits of physical and chemical solvents. These mixed solvents or "hybrid solvents" have different formulation of the solvent mixtures and are trade marked by the solvent manufacturers. These solvents take advantage of physical solvent properties, such as high acid gas solubility at high pressure, high solubility of mercaptans and organic sulfur. It also has the acid gas reactivity of a chemical solvent to meet tight specifications.

The use of hybrid solvents is more beneficial at high acid−gas partial pressures. By using various amine combinations with the physical solvents, the hybrid solvents can be formulated to allow for complete CO_2 removal, bulk CO_2 removal, or CO_2 slip, while achieving H_2S removal comparable with alkanolamines. In hybrid systems, mercaptans and organic sulfur can be removed by the physical solvent portion. However, the hybrid solvent system also inherits some of the drawbacks of a physical solvent system, such as more absorber stages, high hydrocarbon losses, and ineffective treating at low

pressures. Examples of hybrid solvents include Sulfinol from Shell and UCARSOL from Dow Chemical.

Shell offers the Sulfinol solvent to treat various levels of acid gases and different sulfur contaminants. The solvent contains sulfolane, which can be formulated according to feed gas compositions and product gas specifications. The formulation combines the chemical reaction properties of amines and the physical absorption properties of sulfolane. Three different solvents are available for the Sulfinol process:

- Sulfinol-X consists of sulfolane, MDEA, piperazine, and water
- Sulfinol-M consists of sulfolane, MDEA, and water
- Sulfinol-D consists of sulfolane, DIPA, and water

Dow Chemical also offers similar hybrid solvents, Ucarsol LE-701, 702, and 703.

7.7 SOLID BED ABSORPTION PROCESSES

The solid fixed bed absorption processes remove a small quantity of H_2S from gas stream to meet a tight sulfur specification. The absorption processes rely on reaction of a metal oxide with H_2S to form a metal sulfide compound. The metal oxides can be regenerated with oxygen or air, producing the sulfur waste product. The metal oxides used for the absorption processes are typically iron oxide and zinc oxide.

7.7.1 IRON SPONGE PROCESS

The iron sponge absorption is the earliest sulfur removal process and remains one of the widely used processes today. Iron sponge is very selective for H_2S removal.

In this process, the inlet gas is fed at the top of the fixed-bed reactor filled with hydrated ferric oxide (Fe_2O_3). The basic reaction is:

$$2Fe_2O_3 + 6H_2S \rightarrow 2Fe_2S_3 + 6H_2O \tag{7.1}$$

The reaction requires the presence of slightly alkaline water and a temperature below 110°F. A pH level, in the order of 8−10, should be maintained through the injection of caustic soda with the water.

The bed is regenerated by controlled oxidation as:

$$2Fe_2S_3 + 3O_2 \rightarrow 2Fe_2O_3 + 6S \tag{7.2}$$

For the conversion process, oxygen should be introduced slowly to react with the iron sulfide. If oxygen is introduced quickly, there is a danger of intensive heat of reaction that may ignite the bed.

$$S_2 + 2O_2 \rightarrow 2SO_2 \tag{7.3}$$

Generally, the iron oxide process is suitable for small to moderate quantities of hydrogen sulfide (300 ppm) operating at low to moderate pressures (50−500 psig). Removal of larger amounts of hydrogen sulfide requires a continuous process, such as the ferrox process or the Stretford process. The ferrox process is based on the same chemistry as the iron oxide process except that it is in a liquid state

and the operation is continuous. The Stretford process employs a solution containing vanadium salts and anthraquinone disulfonic acid which are known to be difficult to handle (Maddox, 1982).

7.7.2 ZINC OXIDE PROCESS

The zinc oxide process can also be used for H_2S removal from various gas streams. It uses a solid bed of granular zinc oxide to react with hydrogen sulfide:

$$ZnO + H_2S \rightarrow ZnS + H_2O \tag{7.4}$$

The zinc oxide process can produce a treated gas with H_2S concentration as low as 1 ppm but would require operating temperature as high as 550°F. The use of this process has been decreasing in recent years due to the problems on disposing the zinc sulfide waste product, which is considered a hazardous material.

7.7.3 PURASPEC

PURASPEC technology was originally developed by Johnson Matthey based on their catalytic absorbents for the refining industries. It can be used for natural gas processing plants to remove impurities, such as H_2S, COS, mercury, and chlorides, from liquid and gaseous hydrocarbon streams to extremely low levels. H_2S and COS are removed by irreversible reactions with metal oxides (MO).

$$MO + H_2S \rightarrow MS + H_2O \tag{7.5}$$

$$MO + COS \rightarrow MS + CO_2 \tag{7.6}$$

The absorption beds are typically designed in a lead−lag reactor configuration as shown in Fig. 7.16, which would facilitate the catalyst bed change-out.

The PURASPEC catalysts are proprietary formulation oxides which have higher capacities and selectivity than generic metal oxides. Their costs are also higher and should only be used for polishing to meet stringent emissions specifications (Mak et al., 2012).

The application range of the PURASPEC process is shown in Fig. 7.17.

7.7.4 SLURRY PROCESSES

Slurries of iron oxide have been used to selectively absorb H_2S. Two different slurry processes are described below.

7.7.4.1 Chemsweet Process

The Chemsweet process (developed by NATCO) is a zinc oxide−based process for the removal of H_2S from natural gas. The Chemsweet white powder, which is an aqueous mixture of zinc oxide and zinc acetate, is also a dispersant that keeps the zinc oxide particles in suspension. The process has no impact on CO_2, as the pH of the solution is low enough to prevent any appreciable absorption, even at a high

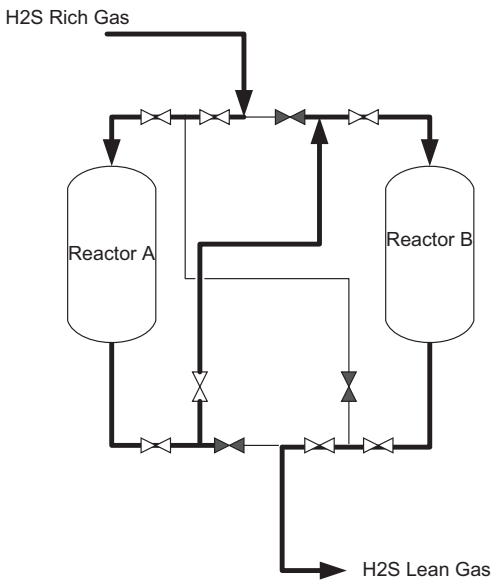

FIGURE 7.16

Typical lead–lag absorption reactors.

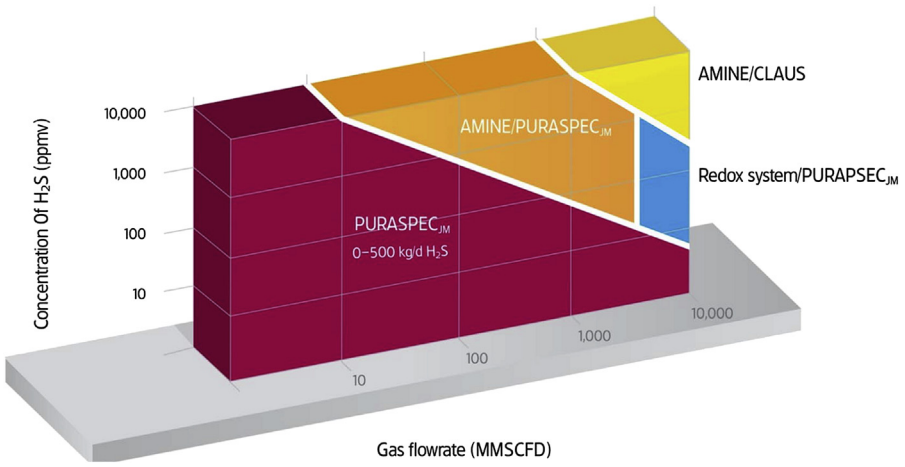

FIGURE 7.17

Selection guide for PURASPEC process (Mak et al., 2012).

CO_2 to H_2S ratio (Manning and Thompson, 1991). The following reactions are performed in this process:

$$\text{Absorption: } ZnAc_2 + H_2S \leftrightarrow ZnS + 2HAc \tag{7.7}$$

$$\text{Regeneration: } ZnO + 2HAc \leftrightarrow ZnAc_2 + H_2O \tag{7.8}$$

$$\text{Overall: } ZnO + H_2S \leftrightarrow ZnS + H_2O \tag{7.9}$$

The Chemsweet process can treat gas streams with high H_2S concentration between pressures of 90 and 1400 psia. The presence of mercaptans in gas streams can be a problem. Some of the mercaptans will react with the zinc oxide forming a sludge composed of zinc mercaptides, Zn(OH)RH, which potentially can cause foaming problems (GPSA, 2004).

7.7.4.2 Sulfa-Check Process

The Sulfa-Check process (marketed by NALCO) selectively removes H_2S from natural gas, in the presence of CO_2 (Dobbs, 1986). This process is accomplished using an aqueous solution of sodium nitrite ($NaNO_2$) which is buffered to stabilize the pH of the solution to above 8.

This process is generally operated at ambient temperature and produces a slurry of sulfur and sodium salts.

$$NaNO_2 + 3H_2S \leftrightarrow NaOH + NH_3 + 3S + H_2O \tag{7.10}$$

CO_2 also reacts with the sodium hydroxide to form sodium carbonate and sodium bicarbonate. Sodium nitrite and sodium hydroxide are consumed in the processes. When the chemicals are completely reacted, the system must be shut down to remove and replenish the chemicals.

7.8 SOLID BED ADSORPTION PROCESS

For physical adsorption, the holding forces of the adsorbate on the adsorbent are weaker than chemical bonding, and the adsorbate can be desorbed by raising the temperature or reducing the partial pressure. When an adsorbed component reacts chemically with the adsorbent, the process is termed chemisorption and desorption by pressure reduction is generally not possible. The main advantage of physical adsorption over chemical is lower energy consumption in regeneration, which can be achieved using a pressure swing or temperature swing cycle.

The most common adsorbents in the natural gas treating industries are molecular sieves, activated alumina, and silica gels. Molecular sieve adsorbents are zeolite-based compounds which are commonly used for removal of CO_2 and H_2S, mercaptans, and other sulfur compounds. This technology is used for treating low concentrations of sulfur components in natural gas stream where deep removal is required.

The typical molecular sieve unit consists of two or more fixed-bed adsorbers and a regeneration system. With two molecular sieve beds, one bed is treating the feed gas while the other bed is being regenerated. Switching between the beds is automated using programmed timer and switching valves. During regeneration, the molecular sieve bed is heated up by a slipstream of the product gas, which desorbs the sour components from the molecular sieves. The hot regeneration gas is cooled and treated by an amine or physical solvent (depending on the mercaptans level), which is later regenerated and sent to the sulfur recovery unit. Details on the molecular sieve unit operation are discussed in Chapter 9.

7.9 MEMBRANE

Membrane systems, which consist of semipermeable elements (polymeric membranes), separate gases by selective permeation of the gas constituents. The gases dissolve in the membrane materials and move across the membrane barrier under a partial pressure gradient, which is established by maintaining a high feed pressure on one side of the membrane while maintaining the low pressure on the permeate side.

Many different types of membranes have been developed for gas separations. For natural gas separation, most common membranes are of the "glassy" type of which the industry's common standard is cellulose acetate. These membranes are of the solution−diffusion type, which consists of a thin layer of cellulose acetate built on top of a thicker layer of a porous support material. The membranes are thin to maximize mass transfer, which requires a supporting layer for mechanical strength (Baker, 2002). Other membrane in natural gas service includes polyimides and more recent a class of membrane using "rubbery" polymers.

Membranes separate by solution and diffusion. The smaller and more soluble components such as H_2O, H_2, He, CO_2, H_2S permeate quicker, leaving behind the less soluble components such as CO, methane, and nitrogen. The driving force is the partial pressure differential of the permeate components. The preferable operating conditions are (1) high feed gas pressure (because it offers a higher acid gas partial pressure for a given component concentration) and (2) low permeate pressure (lower acid gas partial pressure). In most cases, the feed gas pressure is set by available well pressures or by required pipeline pressures. If the feed gas is available at a lower pressure than the pipeline requirement, compression would typically take place prior to membrane separation to take advantage of the higher pressure.

In addition to the component partial pressures, the performance of membrane depends on the permeability and selectivity of the membrane elements for the different compounds. Relative permeation of the different compounds for a typical glassy type, cellulose membrane is illustrated in Fig. 7.18.

The membrane separation is intended for bulk removal, which results in high hydrocarbon losses. More advanced membrane designs and polymers may reduce hydrocarbon losses, although generally at a higher cost due to the need for increased membrane area. Vendors of membrane systems offer CO_2 gas purification solutions using a variety of membrane forming polymers with performances ranging from high productivity/low selectivity (i.e., lower cost but lower purity or hydrocarbon recovery) to low productivity/high selectivity options. With productivity/selectivity trade-offs, vendors provide systems optimized toward project-specific required performance and cost.

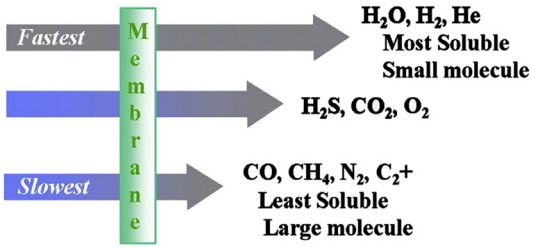

FIGURE 7.18

Relative permeation rates in membrane (Cnop, 2012).

7.9.1 MEMBRANE PROCESS ADVANTAGES

For bulk removal where stringent specifications are not required, membrane process offers several advantages over solvent-treating processes such as:

- Membranes are skid-mounted units. They can be installed in modules, relatively inexpensive to install.
- The membrane module is compact, requiring small plot space for installation, suitable for offshore applications.
- Membranes have no moving parts, requiring minimal operator attention and low operating and maintenance cost.
- Membranes are self-supporting and do not require utilities such as water and instrument air.

7.9.2 MEMBRANE PROCESS DISADVANTAGES

The decision to go with membrane for separation must consider the following shortcomings:

- Losses of hydrocarbon products with the permeate. If the permeate is vented to atmosphere, this may create greenhouse gas impacts. In most applications, it is desirable to minimize hydrocarbon losses as it represents a revenue loss.
- Prone to fouling from contaminants. The elements are prone to degradation from heavy hydrocarbons and aromatics. An upstream pretreatment unit is required to prevent damage to the membranes, and depending on the feedstream, the pretreatment can be limited such as a filter, heater, and carbon bed or elaborate such as regenerable adsorbent beds. The pretreatment unit will increase the installation cost and space requirement, reducing the advantages of a membrane unit.
- Replacement cost of membranes can be expensive which must be factored into the operating costs.
- Limited membrane manufacturer suppliers, making the membrane less competitive.
- There is no economy of scale compared with the solvent treating process. Additional membrane modules must be added to handle higher flow. The number of membrane modules is directly proportional to the feed gas flow rate. Solvent process can accommodate the higher feed gas flow by increasing the solvent circulation.

7.9.3 MEMBRANE PACKAGING

Both spiral wound and hollow-fiber membranes are packaged in elements (also called modules or bundles) that for commercial natural gas applications range from 6 in. in diameter to 12 in. or more. Most commonly, 8- and 12-in. elements are used. The length of the elements can vary, but in most cases are 3–5 feet so that they can be handled by one person. They typically weigh about 50 lbs. The individual elements thus allow vertical or horizontal placement. Horizontal orientation is common, although in Air Liquide's modules operating in condensing mode (where heavy hydrocarbons are drained from the module), a vertical orientation is preferred. A typical hollow-fiber module sketch is shown in Fig. 7.19.

Elements are inserted in a pressure vessel shell and, depending on the size of the plant, the packaging of the membranes ranges from a single element per vessel, two elements in a dual module (inserted from either end of the vessel), up to systems that hold multiple elements with 4–6 being common for larger flow rates. Overall membrane cost of the elements is fixed, but by using multiple elements within a single pressure vessel, the cost of the system can be reduced. This is especially true for offshore applications where footprint reduction greatly lowers the cost. A module with four elements in a single vessel is shown in Fig. 7.20.

7.9.4 MEMBRANE PROCESSES

Membrane processes can be configured as a single membrane unit (Fig. 7.21), which may result in significant hydrocarbon losses (typically over 10% of the feed gas).

Hydrocarbon losses may be reduced by using a two-stage membrane system as shown in Fig. 7.22. However, this arrangement would require the addition of a recycle gas compressor and a second stage of membrane unit. While this may improve the recovery, often to above 95%, the economics of the

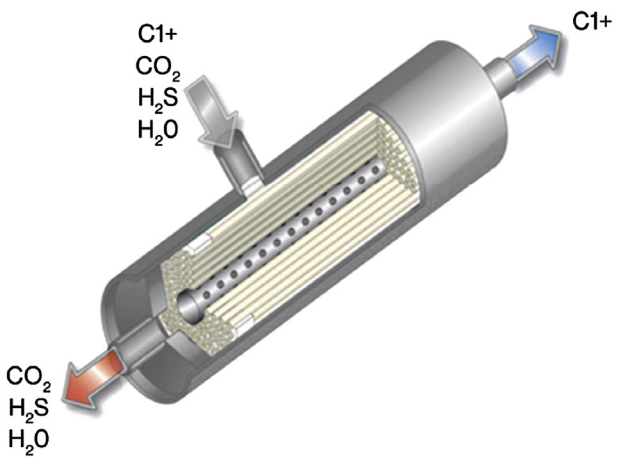

FIGURE 7.19

A sketch of a single acid gas hollow fiber module (Mokhatab and Mitariten, 2018).

Courtesy of Air Liquide.

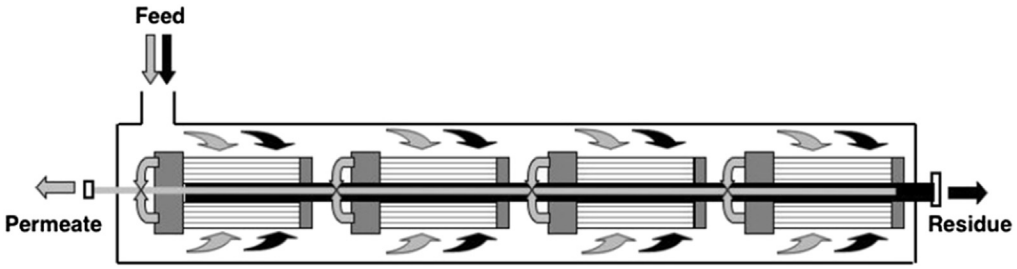

FIGURE 7.20

A sketch of multiple modules arranged in a single pressure vessel (Mokhatab and Mitariten, 2018).

Courtesy of Air Liquide.

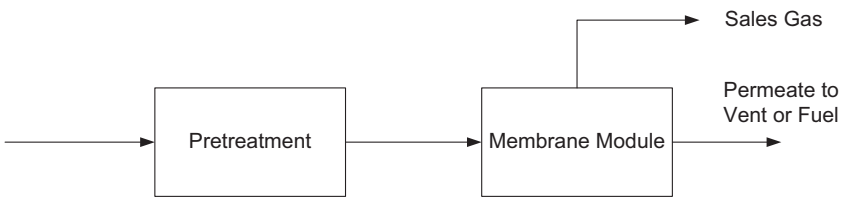

FIGURE 7.21

Single membrane unit.

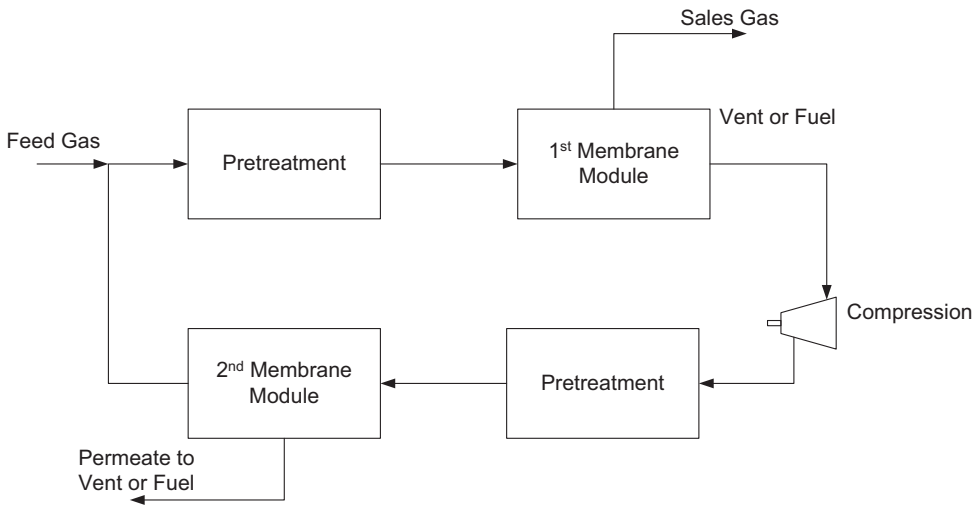

FIGURE 7.22

Two-stage membrane unit.

additional compressor and membrane unit can be difficult to justify, in terms of equipment cost and space requirement.

7.9.5 MEMBRANE PRETREATMENT SYSTEM

To protect the membrane elements and minimizing operating difficulties with heavy hydrocarbons, particulates, and contaminants, a pretreatment system is necessary to ensure a continuous operation and avoid elements degradation. The pretreatment system typically includes the following design provisions:

- Filter coalescer for removal of hydrocarbon liquids; carryover amine, chemicals, and solvents.
- Nonregenerable activated carbon adsorbent beds for removal of heavy hydrocarbons, aromatics, and contaminants that are detrimental to the life of the membrane elements.
- Heavy hydrocarbons can also be removed using a refrigeration unit.
- Particulate filters for removal of particulates and carryover adsorbent dust to avoid plugging of the membranes
- A regeneration system for the adsorbent beds that includes heater, cooler, separator, and blower.
- A heater to maintain superheated feed gas to avoid condensation across the membrane, which is detrimental to the membrane elements.

The pretreatment system can be assembled as a modular unit upstream of the membrane unit, such as UOP's MemGuard system, as shown in Fig. 7.23.

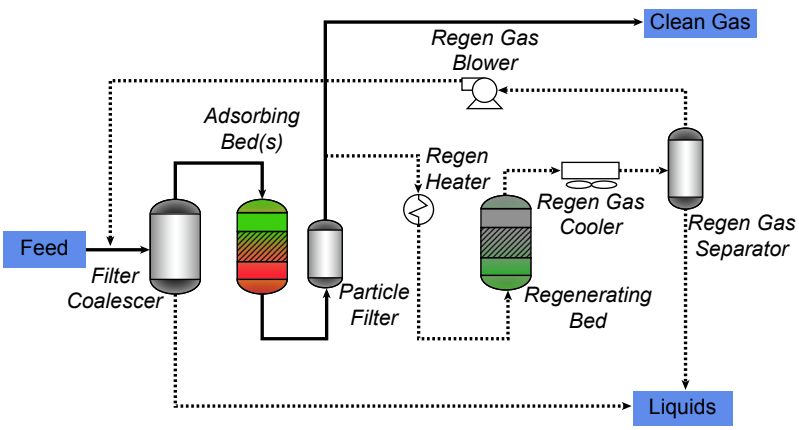

FIGURE 7.23

UOP MemGuard system.

7.10 CRYOGENIC FRACTIONATION

Cryogenic separation involves cooling the acid gases to a very low temperature so that the CO_2 can be liquefied and separated. This technology requires substantial power to operate the refrigeration unit. It also needs pretreatment and dehydration of the feed gas to remove components that would result in hydrate formation and CO_2 freezing in cold section of the fractionation equipment.

For typical natural gas plants, cryogenic fractionation of CO_2, H_2S, and hydrocarbons requires several fractionation steps, which would require extensive refrigeration and heating. The Ryan-Holmes process, which was created for enhanced oil recovery for fractionation of high CO_2 gases, is still the most expensive process for CO_2 separation.

There are other techniques that were developed for cryogenic fractionation with the intent to make it economical and avoid freezing problems. FZ technology, developed at ExxonMobil Upstream Research Company, is a cryogenic distillation process for the single step removal of CO_2 and H_2S from natural gas involving the controlled freezing and remelting of CO_2. This process is conceptual sound but has not been commercially proven (Northrop and Valencia, 2009).

The application for acid gas fractionation that proves to be economical is in the area of helium production and enhanced oil recovery. These plants typically process a very lean gas with high CO_2 content, typically over 70%, and a very low H_2S content. Where CO_2 is used for enhance oil recovery, it is more energy efficient to fractionate CO_2 in a fractionation column and pump the bottom CO_2 liquid to high pressure for reinjection. Pumping CO_2 liquid requires significantly less power than conventional vapor compression.

For helium recovery, a methanol wash column is used to polish the overhead gas from the CO_2 fractionation column to produce an overhead vapor that is recycled to extinction. The clean gas from the methanol wash column can be fractionated in a nitrogen rejection column, producing a bottom stream containing the methane and hydrocarbons, which can be sent to the sales gas pipeline. The nitrogen rejection column overhead, containing nitrogen and helium, is fractionated in a helium recovery unit into the helium overhead product and a nitrogen bottom. More details of the helium recovery process can be found in Chapter 12.

7.11 MICROBIOLOGICAL TREATMENT PROCESSES

Continual search for more economical, safer, and simpler removal methods has led to the development of microbiological solutions for H_2S removal. One of the recent technologies for biological treatment is the THIOPAQ process (codeveloped between Shell Global Solutions and Paques BV), which can potentially be applied to replace the acid gas removal unit, the sulfur recovery unit, and the tail gas unit.

The THIOPAQ process, as shown in Fig. 7.24, removes H_2S by absorption into a mild alkaline solution followed by oxidation of the absorbed sulfide to elemental sulfur under the following reaction equations:

- Absorption and hydrolysis of H_2S: $H_2S + OH^- \rightarrow HS^- + H_2O$
- Biological sulfur formation: $HS^- + ½\ O_2 \rightarrow S + OH^-$

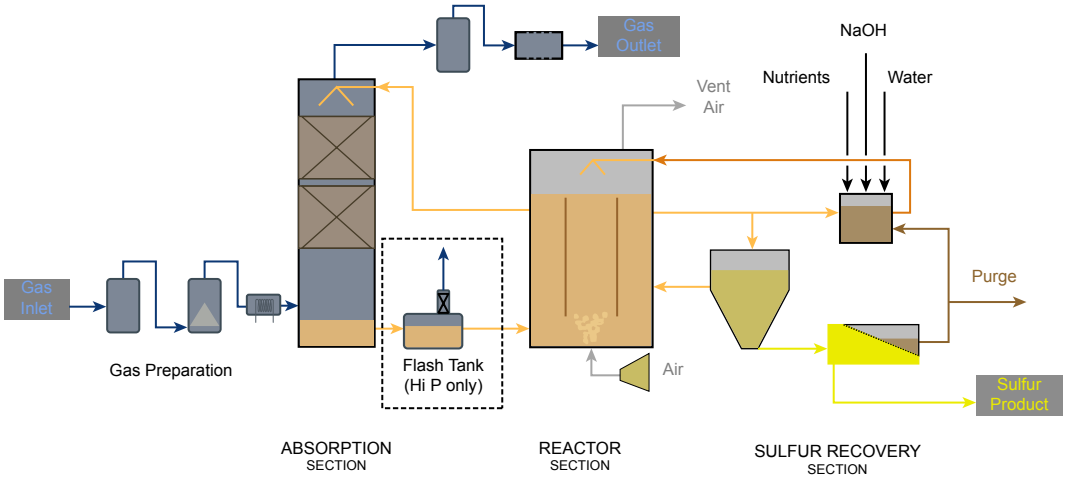

FIGURE 7.24

THIOPAQ process (Lee et al., 2013).

The oxidation reaction requires the use of a consortium of naturally occurring sulfur treating bacteria.

To avoid buildup of the sulfate waste product, a purge stream from the bioreactor is required. For heat and material balance of the process, makeup of water, caustic, and nutrients addition is required. To reduce the sulfate waste, membrane filter can be used to separate the sulfate ions from the other ions, concentrating the sulfate content and reducing the effluent quantity. Recycling of the sulfate effluent to a sulfate reducing reactor can also reduce the sulfate effluent.

The practical processing capacity for the THIOPAQ process is about 50 tons per day of sulfur.

7.12 SELECTING THE GAS TREATING PROCESS

The gas treating process selection should be based on the feed gas compositions, acid gas contents and sulfur compound levels, as well as the treated gas product specifications. If the sulfur compounds are not removed, they will end up in the liquid products which will require further treatment.

A number of variables must be considered and evaluated in the selection process such as:

- Variation in sour gas flow rate and composition, pressure, and temperature.
- Unit capacity, site location, ambient temperatures, and onshore or offshore units.
- Treated gas, acid gas, and liquid products specifications.
- Unit turn-up and turn-down requirements.
- Environmental requirements on air emissions, liquid effluent, and solid waste discharges.
- Capital and operating costs.

Sometimes a high-level screening of the above variables can determine the treating gas technologies. For example:

- Fixed-bed scavengers are applicable when the sulfur capacity is less than 0.1 ton/day. When tight sulfur emissions must be met, scavengers should be considered for polishing the treated gas from the acid gas removal unit.
- When the sulfur capacity is between 15 ton/day and 50 ton/day, direct conversion processes, such as the Redox processes (see Chapter 8) and microbiological treatment processes, are applicable.
- Low partial pressure of acid gases favors amine treating. High partial pressure (greater than 50 psi) and lean gases favor the use of physical solvents, especially for bulk CO_2 removal. Both PC and DEPG are suitable for natural gas treating while PC is more economical due to its lowering operating temperature.
- If selective removal of H_2S and other sulfur contaminants and mercaptans is required, physical solvent or hybrid solvent should be considered.
- If the feed gas contains COS, DGA or formulated MDEA should be considered.
- For tail gas treating, formulated MDEA and Flexsorb can meet the stringent sulfur emissions.
- For LNG production, DGA or activated MDEA can meet the 50 ppm CO_2 specification.

In summary, in treating today's higher CO_2 gases, the traditional amine processes may no longer be adequate. The high acid gas contents will require a different gas treating approach to meet the energy and the emissions targets. The gas treating technologies will require the use of several technologies and will invariably require the use of physical solvent for bulk removal to minimize energy consumption, the use of amine solvents for sulfur removal, and/or sulfur scavenger to meet the sulfur emission requirements.

REFERENCES

Baker, R.W., 2002. Future directions of membrane gas separation technology. Industrial & Engineering Chemistry Research 41, 1393−1411.

Burr, B., Lyddon, L., Mar. 2−5, 2008. A comparison of physical solvents for acid gas removal. Paper Presented at the 87th Annual GPA Convention, Grapevine, TX, USA.

Chakma, A., 1994. Separation of acid gases from power plant flue gas streams by formulated amines. In: Vansant, E.F. (Ed.), Gas Separation. Elsevier Science, Burlington, MA, USA.

Cnop, T., May 23−25, 2012. Membrane technology introduction. Paper Presented at the GPA Europe Annual Conference, Berlin, Germany.

Dobbs, J.B., March 3−5, 1986. One step process. Paper Presented at the 36th Annual Laurance Reid Gas Conditioning Conference, Norman, OK, USA.

Garrison, J., Moore, B.K., Loucks, S., Sheth, P.S., Tanzi, C.S., February 24−27, 2002. Keyspan energy Canada rimbey acid gas enrichment with FLEXSORB SE Plus technology. Paper Presented at the 52nd Annual Laurance Reid Gas Conditioning Conference, Norman, OK, USA.

GPSA, 2004. Engineering Data Book, twelfth ed. Gas Processors Suppliers Association (GPSA), Tulsa, OK, USA.

Kohl, A.L., Nielsen, R.B., 1997. Gas Purification, fifth ed. Gulf Publishing Company, Houston, TX, USA.

Lee, C., Bowerbank, G., Heeringen, G., September 18−20, 2013. THIOPAQ O&G bio-desulfurization: an alternative sulfur recovery technology. Paper Presented at the GPA Europe Annual Conference, Edinburgh, Scotland, UK.

Maddox, R.N., 1982. Gas and Liquid Sweetening, third ed. Campbell Petroleum Series, Norman, OK, USA.

Mak, J., Wierenga, D., Nielsen, D., Graham, C., May 5−8, 2003. New physical solvent treating configurations for offshore high pressure CO_2 removal. Paper Presented at the Offshore Technology Conference, Houston, TX, USA.

Mak, J., Heaven, D., Kubek, D., Sharp, C., October 4−6, 2004. Synthesis gas purification in gasification to ammonia/urea plants. Paper Presented at the Gasification Technologies Conference, Washington, D.C., USA.

Mak, J., March 20, 2007. Configurations and Methods for Improved Gas Removal. US Patent No. 7,192,468.

Mak, J., Nielsen, D., Schulte, D., February 25−28, 2007. An update of the Fluor Solvent™ process. Paper Presented at the 57th Annual Laurance Reid Gas Conditioning Conference, Norman, OK, USA.

Mak, J., Nielsen, D., Chow, T., Morgan, O., Wong, V., December 22, 2009. Configurations and Methods for Acid Gas Enhancement. US Patent No. 7635408.

Mak, J., October 13−14, 2011. Carbon capture present and future − retrofit China CO_2 removal plant and design of a 95% carbon capture IGCC plant. Paper Presented at the 3rd China Energy Chemical International Forum, Coal Clean Processing and Efficient Utilization, Urumqi City, Xinjiang, China.

Mak, J., Atma, V., Varnado, C., April 15−18, 2012. Production of pipeline gas from a raw gas with a high and variable acid gas content. Paper Presented at the 91st Annual GPA Convention, New Orleans, LA, USA.

Manning, F.S., Thompson, R.E., 1991. Oil Field Processing of Petroleum, vol. 1. Natural Gas. PennWell Books, Tulsa, OK, USA.

Mokhatab, S., Mitariten, M., 2018. Efficient acid gas removal using membrane systems. Gas Processing Part 1 (June Issue, 35−37), Part 2 (August Issue, 27−30).

Northrop, P.S., Valencia, J.A., 2009. The CFZ™ process: a cryogenics method for handling high CO_2 and H_2S gas reserves and facilitating geosequestration of CO_2 and acid gases. Energy Procedia 1 (1), 171−177.

Seagraves, J., Quinlan, M., Corley, J., February 21−24, 2010. Fundamentals of gas treating. Paper Presented at the 60th Annual Laurance Reid Gas Conditioning Conference, Norman, OK, USA.

Vorberg, G., Katz, T., Notz, R., Hearn, J., September 22−24, 2010. Capacity increase included: a new generation of promoter for selective H_2S removal. Paper Presented at the 27th GPA Europe Annual Conference, Lisbon, Portugal.

Weiland, R.H., Sivasubramanian, M.S., Dingman, J.C., February 23−26, 2003. Effective amine technology: controlling selectivity, increasing slip, and reducing sulfur. Paper Presented at the 53rd Annual Laurance Reid Gas Conditioning Conference, Norman, OK, USA.

CHAPTER

8 SULFUR RECOVERY AND HANDLING

8.1 INTRODUCTION

Acid gas is a mixture of hydrogen sulfide (H_2S) and carbon dioxide (CO_2), with small amounts of hydrocarbon gases and usually water vapor. It is the by-product of the sweetening of sour gas and can be generated via any number of treating processes. If a nonaqueous solvent is used, then there may be a minimal amount of water in the acid gas stream, which may be advantageous.

In the past, gas producers could flare/incinerate the acid gases; however, with growing environmental concerns from the emission of sulfur dioxide (SO_2), the flaring of even small quantities of acid gas to the surroundings is generally unacceptable. This means that the hydrogen sulfide extracted from the acid gas removal unit must be further processed or must be injected downhole.

Hydrogen sulfide is a flammable gas with a wide limit of flammability and, unlike elemental sulfur, is extremely toxic. Therefore, one option is to convert H_2S to harmless elemental sulfur. Elemental sulfur can be stored, handled, and transported in bulk. Ease of storage is an important advantage as it enables sulfur to be stockpiled in periods of reduced demand. The primary use of sulfur is for the production of sulfuric acid, much of which is used to manufacture phosphate fertilizer. Other minor uses include manufacture of fungicide, pesticide, bactericide in food preservation, and other fine chemicals. However, the demand for elemental sulfur is less than the potential supply from the involuntary production of it due to the large sulfur contents in sour gas and crude oils.

Chemical conversion of H_2S for disposal as solid waste (such as calcium sulfate) is technically feasible but usually uneconomical and impractical. If the total sulfur content of the sour gas is small, it may be more economical to recover the sulfur by some other processes; however, they have drawbacks of their own.

In remote locations, or where there is no market for sulfur, acid gas compression and injection (usually into a nonproducing formation) are alternatives to sulfur recovery. This is environmentally desirable as it eliminates the emission of sulfur compounds and CO_2 to the atmosphere.

This chapter covers all the important aspects of sulfur recovery and handling and briefly describes the acid gas injection (AGI) process.

Handbook of Natural Gas Transmission and Processing. https://doi.org/10.1016/B978-0-12-815817-3.00008-3

8.2 SULFUR PROPERTIES

Elemental sulfur, which usually occurs in the form of eight-member rings, is a relatively nontoxic and chemically inert substance and is insoluble in water and most other liquids. It is solid at ambient temperatures and exists in two crystalline and amorphous forms. The main crystalline types are rhombic and monoclinic. These two forms differ in the way in which the rings are stacked. Rhombic sulfur is the most stable form of the element at room temperature. If rhombic sulfur is heated to about 203°F, it changes into monoclinic crystals. Above 203°F and up to 239°F, monoclinic sulfur becomes the more dominant structural form. Amorphous sulfur is formed when liquid sulfur, which has been heated to elevated temperatures, is allowed to cool rapidly. Amorphous sulfur slowly changes to the rhombic crystalline form at ambient temperatures. During this slow transition, the solid shrinks and cracks, making it rather friable.

When melted, sulfur becomes a brownish-yellow transparent liquid whose molecular structure also consists of eight-member rings. As liquid sulfur is heated to about 320°F, the structure of the liquid undergoes a change (forming long-chain sulfur polymers in conjunction with the eight-member sulfur rings); its color turns dark reddish brown, and its viscosity increases significantly. The effect of temperature on the liquid sulfur viscosity is shown in Fig. 8.1.

Sulfur vapor exists as S_x (where x can have values from 1 through 8), but the principal sulfur species are S_2, S_6, and S_8. The distribution of sulfur-vapor species vary significantly with changes in

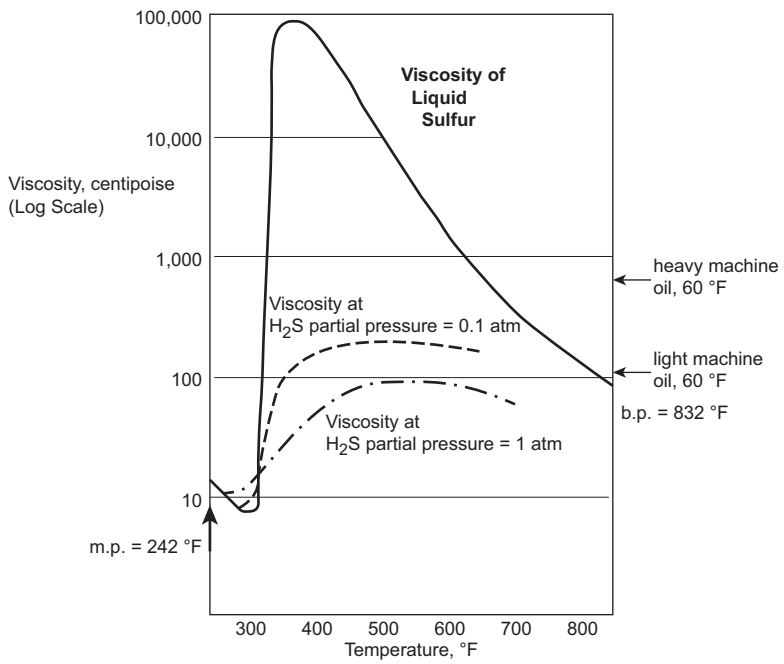

FIGURE 8.1

Viscosity of liquid sulfur versus temperature (Bacon and Fanelli, 1943).

temperature, where at lower temperatures, S_8 dominates, but as the temperature rises, S_8 is converted to S_6, and finally to S_2.

The physical and chemical properties of sulfur are unusual. Therefore, any attempt to understand sulfur handling processes requires an understanding of the behavior of the various sulfur species. The properties of elemental sulfur are well described in the literature (Meyer, 1976; Chao, 1980; Shuai and Meisen, 1995).

8.3 SULFUR RECOVERY

Sulfur recovery refers to the conversion of H_2S to elemental sulfur. The original sulfur recovery process was developed in 1883 by Carl Friedrich Claus, a London chemist, and described in a British patent application as a means to recover sulfur as a by-product in the manufacture of soda (Na_2CO_3).

In the original Claus process, elemental sulfur was produced by the partial oxidation of H_2S in a single step over a preheated catalyst bed, according to the following exothermic reaction:

$$H_2S + 1/2\ O_2 \rightarrow 1/8\ S_8 + H_2O \tag{8.1}$$

However, since the reaction was extremely exothermic, the original process was severely limited by the inability to control the reaction temperature, and consequently sulfur recovery was limited.

In 1938, I.G. Farbenindustrie A.G. in Germany described a modification to the Claus process, in which the oxidation of 1/3 of the hydrogen sulfide to sulfur dioxide was carried out in a boiler, and the remaining 2/3 hydrogen sulfide reacted with the sulfur dioxide over a catalyst. The modified Claus process has become the standard sulfur recovery technology of today.

The following sections cover the conventional Claus process, and its various modifications and extensions, as well as some other lesser-utilized sulfur recovery processes.

8.3.1 MODIFIED CLAUS PROCESS

In the modified Claus sulfur recovery process the overall reaction is carried out in two stages. In the first stage (thermal section), enough air is added to oxidize only one-third of the incoming H_2S to SO_2. This reaction is highly exothermic and is not limited by equilibrium.

$$H_2S + 3/2\ O_2 \rightarrow SO_2 + H_2O \tag{8.2}$$

In the reaction furnace the unburned H_2S in the acid gas reacts with the produced SO_2 to yield elemental sulfur vapor. This reaction is referred to as the Claus reaction and is shown in Eq. (8.3). This reaction is endothermic and is limited by equilibrium.

$$SO_2 + 2H_2S \leftrightarrow 3/2\ S_2 + 2H_2O \tag{8.3}$$

Usually 60%–70% of the total conversion of H_2S to elemental sulfur is achieved in the thermal stage (Gamson and Elkins, 1953; Opekar and Goar, 1966). The theoretical equilibrium percentage of H_2S conversion to sulfur is shown in Fig. 8.2.

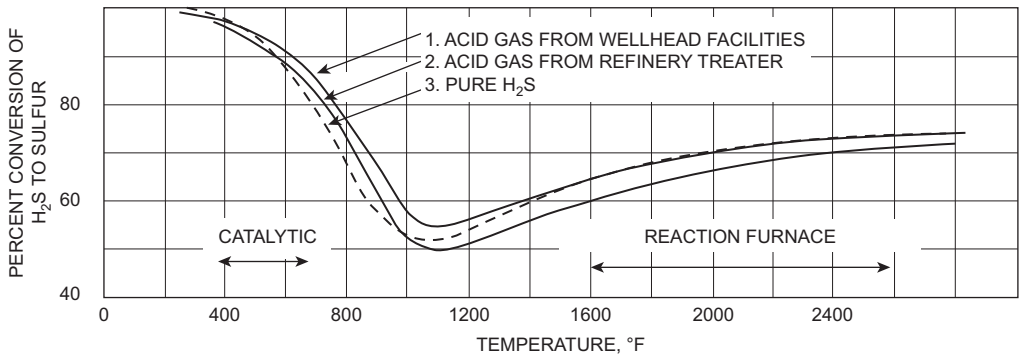

FIGURE 8.2

Theoretical equilibrium % of H_2S conversion to sulfur (Valdes, 1964).

8.3.1.1 Process Description

A typical modified Claus process flow schematic is shown in Fig. 8.3. A photo of a typical sulfur recovery unit (SRU) is shown in Fig. 8.4. In this process the overall reaction is carried out in two stages, thermal and catalytic.

8.3.1.1.1 Thermal Section

The hot combustion products from the reaction furnace flow through the tubes of waste heat boiler (WHB) and are partially cooled to 600−800°F by generating high-pressure (HP) or medium-pressure (MP) steam. As the gases from the reaction furnace are cooled in the WHB, the S_2 sulfur vapor species shift through a number of exothermic reactions to other sulfur species, primarily S_6 and S_8 (Goar and Fenderson, 1996).

The cooled gases from the WHB are further cooled (to 340−375°F typically) in the first sulfur condenser by generating low-pressure or medium-pressure steam, where most of the sulfur vapor formed in the reaction furnace is condensed. The condensed sulfur is separated from the gas and drained from the condenser through a hydraulic seal and rundown line to the sulfur collection pit.

8.3.1.1.2 Catalytic Section

The catalytic section has three processing steps. The first is the reheater step, which raises the temperature of the gas from the sulfur condenser to avoid condensation of sulfur vapor in the pores of the catalyst in the next reactor. Typically, the first reheater is required to increase the temperature to as high as 600°F, which is necessary to promote the destruction of COS and CS_2 to H_2S and CO_2 on the catalyst.

In the second step the hydrogen sulfide and sulfur dioxide are reacted over an activated alumina catalyst in a series of catalytic reactors (1−3). Other catalysts may be used to promote COS and CS_2 destruction, but they are typically more expensive. However, if the COS and CS_2 make it through the Claus reactors, they will have to be handled in the tail gas treating process.

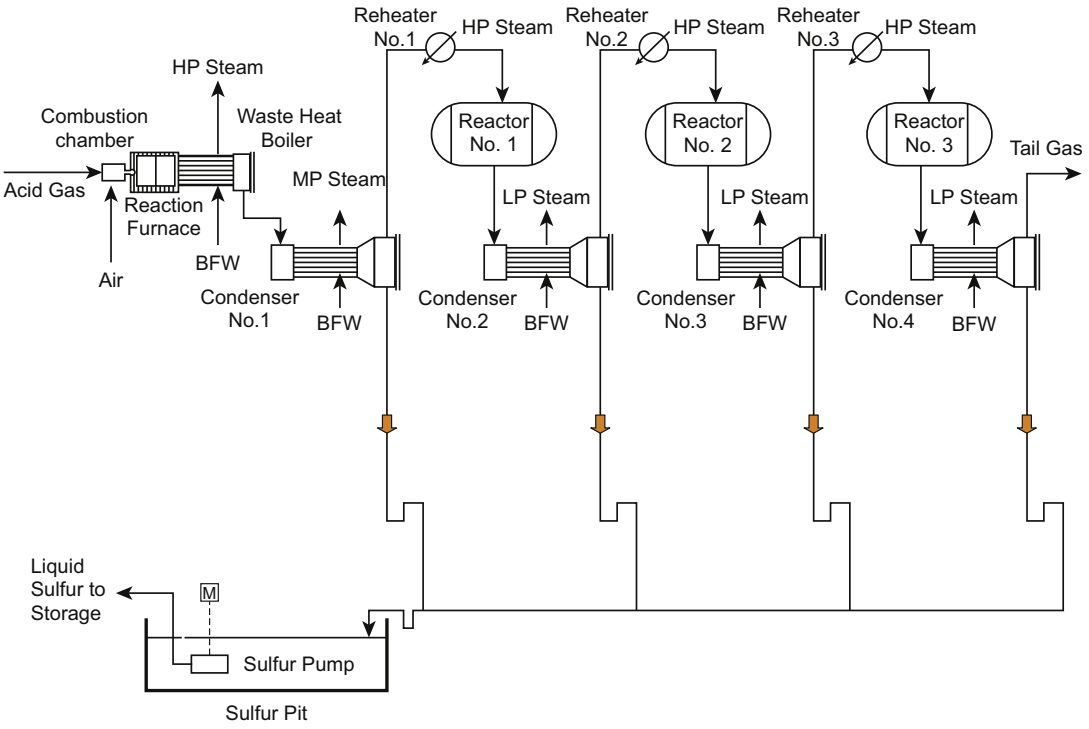

FIGURE 8.3

Typical process flow schematic of a once-through, three-stage Claus sulfur recovery unit. *BFW*, boiler feed water.

The Claus reactions in the catalytic section are slightly different from the thermal section reaction. These reactions are both exothermic and are represented as follows:

$$2H_2S + SO_2 \leftrightarrow 3/6\ S_6 + 2H_2O \tag{8.4}$$

$$2H_2S + SO_2 \leftrightarrow 3/8\ S_8 + 2H_2O \tag{8.5}$$

In the third step the sulfur condenser is used to remove liquid sulfur, the product of reactions Eqs. (8.4) and (8.5). Removing the elemental sulfur shifts the equilibrium so that further reaction may take place in the next catalytic converter (reactor).

The final sulfur condenser is typically at 270°F to minimize sulfur vapor losses in the vent gas (Goar and Fenderson, 1996). The effluent (tail) gas, which still contains appreciable amounts of sulfur compounds and a small amount of sulfur as vapor and entrained liquid, is routed to either a tail gas treating unit (TGTU) for further sulfur recovery to minimizing impacts on the environment. Depending on the jurisdiction, it may be permissible to send the tail gas to a thermal oxidizer to

FIGURE 8.4

Typical Claus sulfur recovery unit.

Courtesy of Fluor.

incinerate all of the sulfur compounds to sulfur dioxide (and concomitant SO_3) before dispersing the effluent to the atmosphere.

The overall sulfur recovery depends on the feed acid gas composition, age of the catalyst, and number of reactor stages. Typical once-through (i.e., no recycle) sulfur recovery efficiencies for standard Claus units are 90%–96% for a two-stage catalytic conversion and 95%–98% for a three-stage catalytic conversion. Because of equilibrium limitations and other sulfur losses, overall sulfur recovery efficiency in a standard, once-through Claus unit is typically limited to 98% (Lagas et al., 1989).

8.3.1.1.3 Claus Burner Performance

The reaction furnace is the critical piece of equipment in the Claus process. For Claus units processing ammonia-laden sour water stripper off-gas, or feeds containing heavy hydrocarbons, BTEX (benzene, toluene, ethylbenzene and xylene), and cyanide, the minimum furnace operating temperature required must be increased above 925°C (1700°F) to ensure destruction of these components. Ammonia, in particular, requires a high combustion temperature, and SRUs operating at inadequate temperatures are prone to shutdowns from plugging due to deposition of ammonia salts. Coke formation from cracking and incomplete reaction of heavy hydrocarbons can cause deactivation of the downstream Claus catalyst.

Fig. 8.5 provides an operating guideline of the theoretical, adiabatic flame temperature as a function of the H_2S content in the acid gas feed. The two horizontal dashed lines provide the operator with the temperature targets, depending on the nature of the hydrocarbons contained in the acid gas feed.

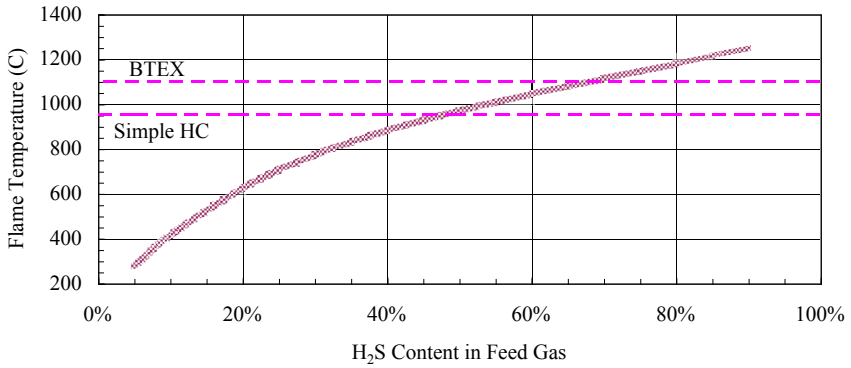

FIGURE 8.5

Flame temperature versus H_2S content (Flood et al., 2011). *BTEX*, benzene, toluene, ethylbenzene and xylene; *HC*, hydrocarbon.

8.3.1.1.4 COS and CS_2 Destruction

Traditional activated alumina Claus catalyst gives high conversion of H_2S but only about 65% hydrolysis of COS and about 30% hydrolysis of CS_2 in the first Claus converter at a typical temperature of 600°F. Conversions are reduced in subsequent Claus stages due to the lower temperatures. For the second stage, activated alumina catalyst gives about 20% hydrolysis of COS and only about 5% hydrolysis of CS_2.

For the catalytic stages, some technology licensors such as Fluor employ titanium oxide (TiO_2) catalyst in one or more of the Claus converters, which greatly improves the ability to hydrolyze COS and CS_2 (Flood et al., 2011). When applied properly, the TiO_2 catalyst is capable of achieving over 90% hydrolysis of COS and CS_2 in the first Claus converter. This increases the overall sulfur recovery efficiency, which may be necessary to meet the sulfur emissions target.

8.3.1.2 Lean Acid Gas Operations

The amount of heat generated in the reaction furnace depends on the amount of H_2S available to the burners. With rich acid gas (60%−100% H_2S), the reaction heat keeps the flame temperature above 2200°F. When the gas is leaner, the flame temperature is reduced, where at 1800°F−1900°F, the flame starts to become unstable. This point is usually reached when the H_2S content is lower than 50%. However, when the H_2S in the acid gas falls below 40%, the reaction furnace may become inoperable and may cause operating problems in the downstream Claus reactors (Goar, 1974). To overcome the problem of processing these "lean" acid gases, there are several design options that can be incorporated into the SRU design. They are discussed in the following sections.

8.3.1.2.1 Feed Preheating

The low furnace temperature problem can be overcome, within limits, by preheating the acid gas and/or air before it enters the burner.

Both the combustion air and the acid gas can be preheated in order to raise the flame temperature. Usually combustion air is the first choice since it is more benign than the acid gas. Furthermore, there are pressure drop considerations. The upstream amine regeneration unit often limits the available acid

gas pressure. The extent of combustion air preheat is an economic choice. Steam at a suitable pressure level is preferred over a fired heater due to ease of operation and lower cost. It is also desirable to use carbon steel material rather than the more exotic and expensive piping and equipment material that may be required for a fired heater.

8.3.1.2.2 Hot Gas Bypassing

The use of hot gas bypass is another solution to raise the furnace temperature, particularly where there is limited access to external heat sources, such as high-pressure steam and power. It is the lowest cost option to process medium acid gas composition since no additional equipment and operating cost is required.

By bypassing part of the feed acid gas around the reaction furnace, the flame will burn nearer to stoichiometric ratio for SO_2 formation. Consequently, the flame temperature is increased. However, the bypass is limited to two-thirds of the total feed because it is undesirable to operate the furnace under oxidizing conditions to a point beyond complete combustion of H_2S to SO_2.

However, the downside of this scheme is the contaminants in the feed gas, particularly heavy hydrocarbons. If present, those hydrocarbons that bypass the reaction furnace will not be destroyed. The detrimental effects will be seen in catalyst deactivation, high corrosion rates, and equipment and line plugging, which will jeopardize the proper operation of the SRU.

8.3.1.2.3 Acid Gas/Natural Gas Fuel Burner

Acid gas fired burners have also been extensively used in many SRUs. Acid gas burners are usually operated far away from stoichiometry to minimize oxygen slippage. When the acid gas is lean in H_2S, the burner is usually designed for firing nearer to stoichiometry to reduce the amount of acid gas. Consequently, only an acid gas with stable composition should be used to avoid oxygen slippage.

Their primary advantage is the ability to achieve the required catalytic reactor inlet temperature. To operate the inline burner, the air/fuel ratio must be closely monitored to avoid oxygen breakthrough and soot formation.

Both the hot gas bypass and the inline burner option have lower sulfur recovery efficiency than the straight-through Claus process. If hydrocarbons and other contaminants are present in the feed gas, they may also cause deactivation of the catalysts.

8.3.1.2.4 Acid Gas Enrichment

The lean acid gas (typically 10%−20%) can be processed in an acid gas enrichment unit (AGEU) to increase its H_2S content to above 50% in order to operate a straight-through Claus Unit.

By using a selective amine, such as proprietary MDEA or the Flexsorb processes, H_2S can be selectively absorbed from the acid gas, producing two acid gas streams. The treated gas from the amine absorber is primarily CO_2, containing perhaps 100 ppmv H_2S, which can be vented, incinerated, or used for enhanced oil recovery. The gas stream leaving the amine regenerator is the acid gas recycled to the SRU, which is now enriched in H_2S to over 50 mol %.

8.3.1.3 Oxygen Enrichment

Oxygen enrichment can be used to sustain a high reaction furnace temperature. It can be used to process lean acid gas, destroy contaminants, and increase the SRU throughput.

With lower nitrogen content in the combustion oxygen, a higher flame temperature can be reached without additional fuel gas firing. However, if the H_2S content drops below 20 mol%, there will not be sufficient heating value in the feed gas, and additional fuel firing may still be necessary (Goar and Fenderson, 1996).

The main advantage of oxygen enrichment is the smaller size of the SRU equipment. Oxygen enrichment is economically attractive for debottlenecking an existing SRU, and it may not need any changes to the existing combustion equipment. For a grass roots installation, the lower SRU cost can be offset by the cost of an air separation unit. In this case, oxygen enrichment can be economical if there is a low-cost oxygen supply.

There are three levels of oxygen enrichment: low (less than 28 vol% oxygen), medium (28–45 vol % oxygen), and high (greater than 45 vol% oxygen). Fig. 8.6 shows the increase in sulfur capacity and furnace flame temperature with various levels of oxygen enrichment.

For an increase in capacity of up to 20%–25%, low-level oxygen enrichment technology is generally adequate. The capital cost for the SRU is mainly in the installation of an oxygen supply system to the reaction furnace burner with no change to the burner being necessary. For a 50% increase in unit capacity, medium-level oxygen enrichment is required. The capital cost is in the installation of an oxygen supply system and a new oxygen combustion burner (with more exotic material). Typically, the cost associated with an oxygen enrichment revamp is 10%–15% of a new air-based SRU (excluding the cost of the oxygen supply).

A challenge for the oxygen-blown Claus process is controlling the high flame temperatures in the front-end furnace (FEF) to avoid overheating and damaging the reaction furnace refractory. There are

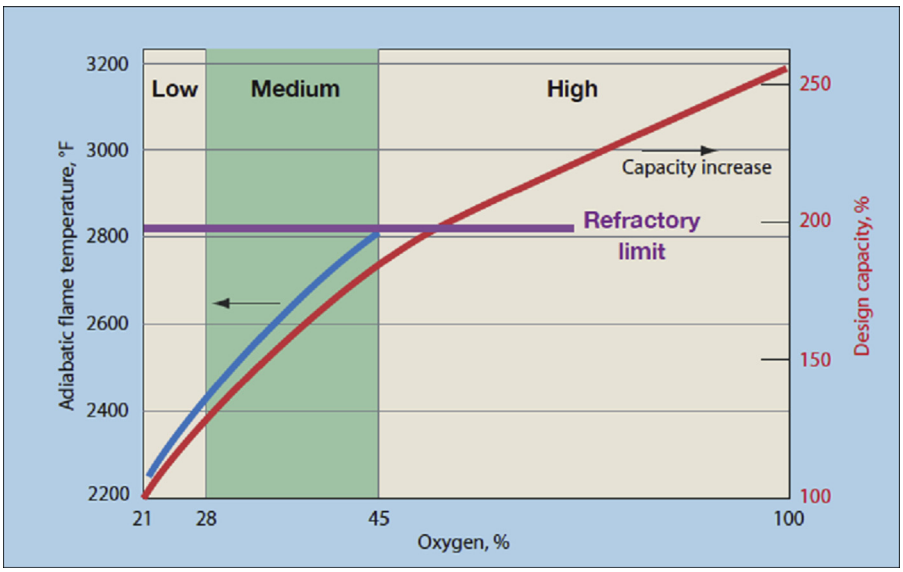

FIGURE 8.6

Effect of oxygen enrichment on the calculated reaction furnace temperature and % Claus unit capacity increase (Gandhi et al., 2010).

FIGURE 8.7

COPE oxygen enrichment unit.

Courtesy of Fluor.

several design and control options to handle this. A common design is to recycle cooled gas to the FEF (Fluor COPE process); a unit picture is shown in Fig. 8.7. Special oxygen burners (developed by Lurgi) or temperature control using a staged combustion process (SURE process developed by British Oxygen Corp. and Parsons Corp.) can also be used.

8.3.2 DIRECT OXIDATION PROCESSES

For lean acid gases that contain 5–30 mol % H_2S, the straight-through Claus process is not workable without additional equipment, fuel gas assist, or AGEU. The alternative is to replace the thermal section of the modified-Claus process by a direct oxidation process. There are several commercially proven processes including UOP's Selectox process and Linde's Clinsulf process, which are described in the following sections.

8.3.2.1 Selectox Process

UOP offers the Selectox process using their proprietary catalysts. Over the catalysts, air oxidizes H_2S to SO_2 that reacts with additional H_2S to produce elemental sulfur, as shown in the following reactions.

Overall sulfur recoveries of 95%–97% are possible with one Selectox followed by a two-stage Claus process (Goar and Fenderson, 1996).

$$H_2S + 3/2O_2 \rightarrow SO_2 + H_2O \tag{8.6}$$

$$2H_2S + SO_2 \rightarrow 3/x\ S_x + 2H_2O \tag{8.7}$$

$$\text{Overall: } 3H_2S + 3/2O_2 \rightarrow 3/x\ S_x + 3H_2O \tag{8.8}$$

Two versions of the process are offered by UOP. If the H_2S content in the acid gas feed is 5 mol% or less, the "once-through" mode can be used for the catalysts. The gas stream from the Selectox converter is cooled, then reheated and treated in one or two additional conventional Claus catalytic stages. If the H_2S content is above 5 mol%, the "recycle mode" Selectox process can be used, where the cooled gas is recycled from the first condenser outlet to maintain the Selectox converter temperature at about 700°F (Gowdy and Bertram, 1998).

The drawback of the catalytic process is the inability to handle contaminants. Contaminants, such as hydrocarbons and aromatics, will react on the Selectox and Claus catalysts, causing hot spots and coke formation (Jones and Bertram, 2001). Thus, the process is not as robust and forgiving as the thermal reactor in the Claus process. The Selectox units are generally smaller in capacities than the Claus units with a maximum of 45 long tons/day (LT/D) of sulfur production.

8.3.2.2 Clinsulf Process

Linde A.G. has developed a nonthermal, direct oxidation process called the Clinsulf process, which is typically applied to syngas operation. In the Clinsulf process, H_2S is directly oxidized to sulfur and H_2O in a reactor filled with a suitable catalyst. In this process the heat of reaction is removed directly from the Claus reactor with a coil-type tubular heat exchanger arranged within the catalyst bed. The internal cooling keeps the reaction temperature close to the sulfur dew point in order to maximize sulfur yield.

A single-stage Clinsulf unit claims to be capable of attaining up to 92% sulfur recovery for very lean acid gases (<5% H_2S) and up to 95% for gases with 10%–20% H_2S content. With the cooling provided by the Linde reactor, it is theoretically possible to control the reaction temperature to below the sulfur dew point, which can further improve the recovery to 99% (Gemmingen and Lahne, 1994; Heisel et al., 1999).

8.3.3 SMALL- AND MEDIUM-SCALE PROCESSES

While the Claus process is still the main process for recovering sulfur from H_2S, several new processes are vying for acceptance for the recovery of sulfur from low-quality acid gas streams (less than 40 mol % H_2S), or if recovery is required for very low mass flow rates of sulfur production.

8.3.3.1 H_2S Scavenger

8.3.3.1.1 Fixed Bed Scavenger

For small amounts of sulfur (less than 0.2 long tons/day), nonregenerable H_2S scavengers such as activated carbon, iron oxide, other metal oxides, and caustic solution are frequently used with good success (Fisher et al., 1999). The details of several nonregenerable fixed bed processes are discussed in Chapter 7.

8.3.3.1.2 Liquid Injection Scavenger

Although fixed bed scavengers are proven commercially, the direct injection method is a lower cost alternative when a suitable pipeline length is available for contact. The direct scavenger injection process consists of a chemical injection pump and injection nozzles for injecting the liquid scavenger in a sour gas pipeline. The pipeline must be of sufficient length for good gas/liquid contact. A separator is located downstream to separate the scavenger agent from the treated gas. The amount of gas/liquid contact time is dependent on the type of contacting device, the gas velocity, and residence time. Because of this, the degree of mixing and efficiency is sensitive to changes in gas flow. Good separation of the scavenger and treated gas is required since some scavengers can cause foaming problems in downstream equipment.

Triazine is a common liquid chemical that is used for instantaneous removal of H_2S from natural gas. Triazine is an H_2S scavenging chemical that will not absorb CO_2. The injection method provides a single stage of contact and is not as efficient as an absorber. Sulfur scavenger injection can produce a treated gas with H_2S content at around 20–40 ppm. Lower content may be achievable if sufficient time, pipe length, and injection agent are provided. The cost of sulfur scavenger is relatively low for treating ppm levels of H_2S; however, the disposal cost of the spent scavenger can be very high.

8.3.3.2 Redox Process

For the mid-size SRUs (producing between 0.2 and 25 long tons/day of elemental sulfur) that are required to process a lean acid gas (with 10% H_2S), the operating cost of the H_2S scavengers is very high, and the use of straight-through Claus unit by itself is not feasible. The niche application can be the "liquid redox" technology. Liquid redox sulfur recovery processes are based on reduction–oxidation (Redox) chemistry to oxidize the H_2S to elemental sulfur in an alkaline solution containing a redox catalyst.

The liquid redox technology was introduced in the beginning of the 18th century and was developed to process coal gas and synthesis gas for the removal of H_2S. There are many versions of the redox processes, but most have limited commercial success due to various operational and environmental problems. Currently, only a few liquid redox technologies are being practiced. This includes the LO-CAT process from Merichem and the SulFerox process from Shell. Both the LO-CAT and the SulFerox processes are essentially the same in principle.

The process flow schematic diagram of a typical redox process is shown in Fig. 8.8. The sour gas stream is fed to the redox absorber, which employs a dilute water solution of ferric iron, held in solution by organic chelating agents, which are proprietary compounds that maintain iron ions in solution and prevent the precipitation of $Fe(OH)_3$ and FeS.

The redox technology represents a single step that can be used to replace the traditional H_2S removal unit, Claus unit, and the TGTU. In principal the redox process is a very versatile process that is suitable to treat different feed gases, not limited to acid gases, to meet very low H_2S specifications.

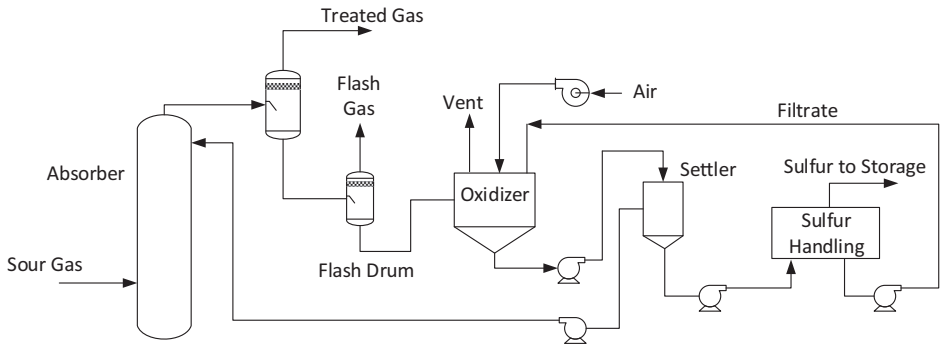

FIGURE 8.8

Typical redox unit.

Unlike traditional acid gas removal solvents, coabsorption of CO_2 and hydrocarbons by the chelated solution is relatively low. The energy consumption is low compared with traditional solvents since regeneration is not done thermally. Liquid redox can achieve 99% sulfur recovery efficiency. The disadvantages of the redox process are as follows: complex operation, high consumption of catalysts and chemicals, and low product sulfur quality.

8.3.3.3 CrystaSulf

The CrystaSulf process is a licensed process from CrystaTech, Inc., which is based on nonaqueous, liquid-phase Claus reaction that combines H_2S with SO_2 to form dissolved elemental sulfur in a single step. Elemental sulfur is soluble in the CrystaSulf solution, which avoids circulating solids in high-pressure equipment. The sulfur is crystallized by cooling and separated from the process with solid handling equipment. This maintains the rest of the process in a solids-free state. It is suitable for the medium-scale sulfur removal market (0.2−25 tons per day). The process can meet H_2S specifications of less than 4 ppmv at pressures above 150 psig, and CO_2 has no negative effect on the CrystaSulf process. The basic flow schematic diagram is shown in Fig. 8.9.

The elemental sulfur crystals are not high in quality and are suitable to be used as a soil amendment for agricultural use, blended with other sulfur streams, or disposed as a nonhazardous waste.

8.3.4 MICROBIOLOGICAL TREATMENT PROCESSES

The Bio-SR process was developed in Japan in 1984 to recover sulfur from sour gas (Satoh et al., 1988). In this process the sour gas is contacted with a solution containing ferric sulfate [$Fe_2(SO_4)_3$] in an absorber, where a chemical reaction occurs between the ferric sulfate and the H_2S, yielding sulfur and ferrous sulfate ($FeSO_4$). The elemental sulfur is conglomerated to a large particle size in the slurry tank. Sulfur is separated from solution through filter and settler. The ferrous sulfate solution is then introduced into the bio-reactor, where *Thiobacillus ferrooxidans* bacteria are employed for the regeneration of the solution. The bacteria oxidize ferrous sulfate into ferric sulfate. The regenerated solution is then recycled to the absorber to repeat the cycle. In this closed-loop system, there is no

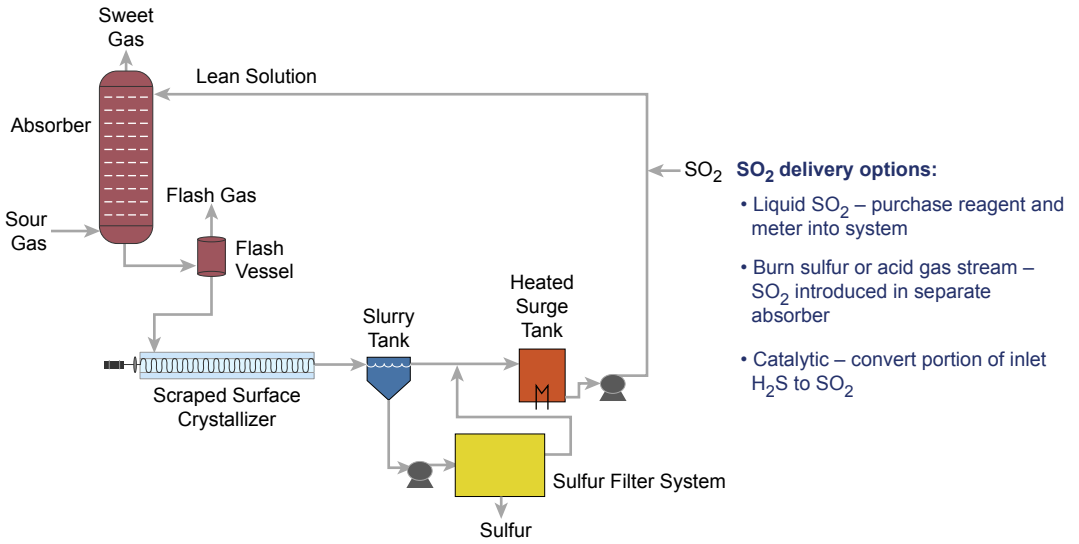

FIGURE 8.9

CrystaSulf process flow schematic.

Courtesy of CrystaTech Inc.

degradation of the solution, no waste is generated, and essentially neither catalyst nor any chemicals need to be added.

The THIOPAQ process (co-developed between Shell Global Solutions and Paques BV) is one of the common technologies for biological treatment of sour gas, which can be used to remove H_2S from sour gas or from acid gas (see Section 7.11 in Chapter 7 for description of the THIOPAQ process).

8.4 TAIL GAS CLEANUP

Tail gas from a Claus unit invariably contains small quantities of sulfur compounds whether it is from the conventional Claus process or its extended version. In earlier SRUs, removal of these trace quantities was not considered necessary since there were no strict regulations that limited sulfur emissions. However, as the air became more polluted, environmental regulations were imposed, and the unconverted sulfur emissions from the Claus unit tail gas became a target of regulation. This led to the development of Claus tail gas cleanup processes in order to remove the residual sulfur species to meet emissions regulations. Tail gas cleanup processes can be categorized into three general groups: reduction, SO_2 scrubbing, and catalytic oxidation.

8.4.1 REDUCTION PROCESSES

Reduction processes, which are commonly used in tail gas treating processes, convert all sulfur compounds (e.g., SO_2) in the tail gas to H2S by hydrogenation. This is followed by H2S scrubbing by

one of the selective amine-type processes so that H2S−rich gas can be recycled to the inlet of the Claus unit for destruction. Therefore, the only sulfur emission is from the CO_2 vent gas. Processes of this type include Shell Claus Off-gas Treating (SCOT) and the Parsons/Unocal's Beavon Sulfur Removal series of processes. The SCOT process was the first to be developed and is the most widespread, with more than 200 units constructed all over the world since 1973.

Two processes involved in the TGTU are described in the following sections.

8.4.1.1 Hydrogenation Section

The hydrogenation section (Fig. 8.10) comprises three steps: Claus tail gas preheat, hydrogenation of SO_2 and other sulfur species to H_2S, and quenching and removal of water from the effluent gas.

The fundamental process would require an in-line fired heater to raise the tail gas to 550−650°F by substoichiometric combustion of natural gas in a reducing gas generator (RGG) for subsequent catalytic reduction of virtually all non-H_2S sulfur components to H_2S, including COS. Conversion of SO_2 and elemental sulfur is by hydrogenation over CoMo catalyst.

Alternatively, "low-temperature" CoMo catalyst can be used. The reactor can be operated at 410°F using steam heating. This option avoids the use of an RGG, saving capital and operating costs while also minimizing the dilution effect from the combustion by-products. However, the use of a steam reheater will limit the ability to compensate for normal catalyst activity loss with age, potentially limiting its useful life.

The CoMo catalyst in the reactor hydrogenates/hydrolyzes essentially all of the sulfur species in the Claus tail gas to H_2S according to the following reactions:

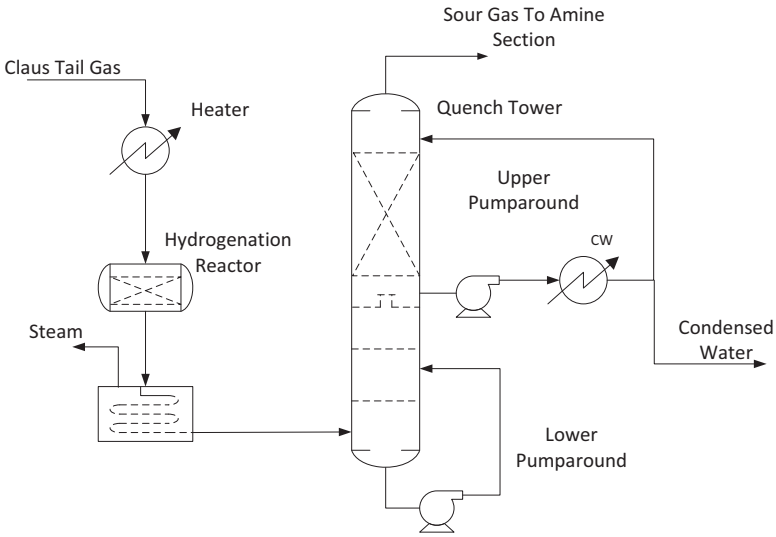

FIGURE 8.10

Typical hydrogenation section of tail gas treating unit.

Hydrogenation reaction:

$$SO_2 + 3\ H_2 \rightarrow 2\ H_2O + H_2S \tag{8.9}$$

$$S_X + x\ H_2 \rightarrow x\ H_2S \tag{8.10}$$

Hydrolysis reaction:

$$COS + H_2O \leftrightarrow CO_2 + H_2S \tag{8.11}$$

$$CS_2 + 2\ H_2O \leftrightarrow CO_2 + 2\ H_2S \tag{8.12}$$

$$CO + H_2O \leftrightarrow H_2 + CO_2 \tag{8.13}$$

CO and H_2 naturally present in the Claus tail gas are sufficient to meet most of the hydrogenation demand, with the balance produced in the RGG, if present.

The hydrogenated tail gas is cooled by generating steam in the effluent cooler. The effluent gas is further cooled in a quench tower to condense the reaction water. The hot gas is directly contacted with circulation water in the quench tower where heat and steam condensate are removed. Caustic solution can be injected to the circulation water to ensure that any SO_2 breakthrough can be eliminated under any operations. This design feature is essential, as it would avoid contamination of the expensive amine solution downstream.

8.4.1.2 Selective H_2S Removal Section

After quench cooling, the hydrogenated tail gas is treated by a selective amine treating unit to remove H_2S (Fig. 8.11). The common selective amines include generic MDEA (40−45 wt%), FlexsorbSE and SE Plus, UCARSOL HS-101 and 103, GAS/SPEC SS and TG-10, and Huntsman MS-300.

The amine is typically designed for a maximum rich loading of 0.1 mol acid gas ($H_2S + CO_2$) per mole amine at these low pressures. Cooling of the lean amine to at least 100°F is critical for favorable H_2S-amine equilibrium that is necessary to reduce the residual H_2S in the CO_2 vent. If necessary, a chilled water system can be used. Specialty TGU amines are essentially pH-modified MDEA to facilitate stripping that is necessary to treat the CO_2 gas to below 10 ppm H_2S, allowing it to be vented to atmosphere, rather than incinerated. Venting avoids fuel costs associated with incineration or thermal oxidizers.

Proprietary solvents, such as ExxonMobil's Flexsorb, which is a sterically hindered amine with a very high selectivity toward H_2S, can meet very low emission requirements. Another advantage is equipment cost savings from the 20%−30% reduction in circulation rate. Flexsorb SE Plus is available for treatment to below 10 ppmv H_2S. Both solvents require a license agreement with ExxonMobil. The Flexsorb solvent is more stable than MDEA, but the main drawback is that the solvent is more expensive.

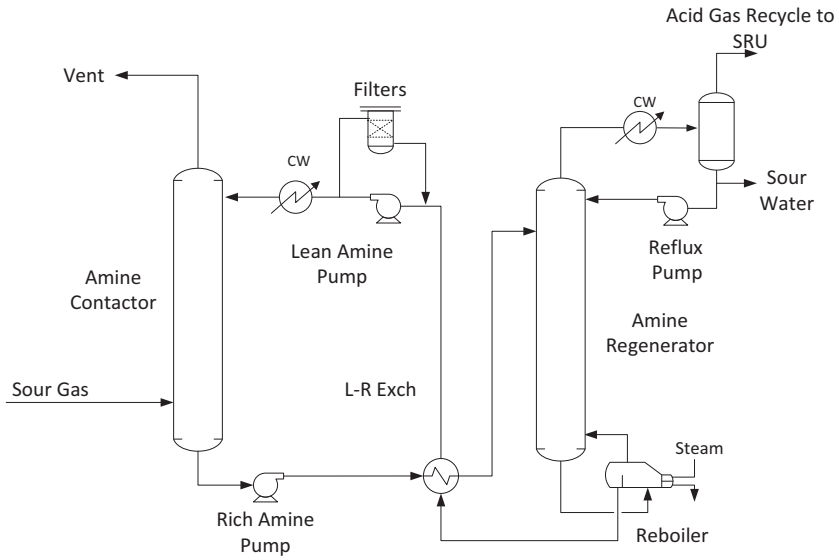

FIGURE 8.11

Typical amine section of tail gas treating unit.

In tail gas applications, FLEXSORB SE solvents can use as little as one-half of the circulation rate and regeneration energy typically required by MDEA-based solvents. CO_2 rejection in TGTU applications is very high, typically greater than 90%, which reduces the size of the amine system and the size of the SRU.

8.4.2 SO_2 SCRUBBING PROCESSES

The basic principle behind these processes lies in the incineration or catalytic oxidation of Claus tail gas streams to convert all sulfur species to SO_2. If the resulting SO_2 concentration is below the emission limit, the gas can be discharged to the atmosphere. If the SO_2 concentration following oxidation is higher than permitted, the gas must be treated to remove the SO_2. The enriched SO_2 stream may be recycled to the Claus unit for conversion to elemental sulfur.

One SO_2 removal process is caustic wash. The spent caustic is nonregenerable, so this process is seldom used because of the cost and the associated waste disposal problem. Regenerative processes such as CanSolv or Clintox that use a proprietary solvent for SO_2 removal can achieve high overall sulfur recovery, up to 99.9%. However, the residual SO_2 content in the vent gas is typically about 80 ppmv, which may require further treatment to meet the 10 ppmv requirement for venting.

8.4.3 CATALYTIC OXIDATION

Sulfur recovery of the conventional Claus unit can be further increased to over 99% by the addition of one or more catalytic stages, such as the SuperClaus process or a sub-dewpoint reaction process. These two processes are described in the following sections.

8.4.3.1 SuperClaus Process

The SuperClaus process was developed by Comprimo B.V. (now Jacobs Comprimo Sulfur Solutions) to increase the overall sulfur recovery of the Claus process by reducing its inherent thermodynamic limitations (Lagas et al., 1994). The SuperClaus process consists of a conventional Claus unit thermal stage, followed by two reactors filled with standard Claus catalyst and a final reactor filled with the SuperClaus catalyst. In the thermal stage, the acid gas is burned with a substoichiometric amount of controlled combustion air such that the tail gas leaving the second reactor contains typically 0.8−1.0 vol% of H_2S. In cases where substoichiometric combustion in the reaction furnace is not possible due to minimum flame temperature requirements, the 0.8−1.0 vol% H_2S concentration is maintained by routing a portion of the acid gas feed downstream of the first condenser. The residual H_2S is oxidized directly to elemental sulfur by the addition of a small amount of air. A total sulfur recovery efficiency of up to 99% can be obtained.

8.4.3.2 Sub-dewpoint Processes

The conventional Claus sulfur recovery process is limited by reaction equilibrium to sulfur recoveries in the range of 94%−97%. When a sub-dewpoint reaction stage is added to the Claus unit, sulfur recovery can be increased to 97.5%−99.5%, depending on the H_2S concentration in the acid gas and the number of catalytic stages.

The sub-dewpoint reactor operates below the sulfur dew point (260−320°F), resulting in a favorable shift in the reaction equilibrium and higher sulfur conversion. The liquid sulfur deposited in the sub-dewpoint catalyst bed is removed cyclically by passing hot gas through the bed to vaporize the adsorbed liquid sulfur, which is then condensed and removed in the sulfur condensers. The catalyst bed is then cooled before returning for adsorption.

Cyclical operation requires two beds: one operating on conversion and the other on regeneration. Owing to the cyclic nature of the sub-dewpoint process, the reactor switching valves are subjected to thermal stress and corrosion from the sulfur vapor service. The sub-dewpoint units have encountered significant operation and maintenance problems in some installations.

Processes of this type include Cold Bed Absorption (Goddin et al., 1974), MCRC (Heigold and Berkeley, 1983), and Sulfreen technology (Willing and Linder, 1994).

8.4.4 OTHER TAIL GAS TREATING CONFIGURATIONS

The TGTU can be integrated with the upstream acid gas removal unit (AGRU) or the AGEU to reduce emissions and equipment count, hence capital cost. However, if there is SO_2 breakthrough in the tail gas unit to the amine, the contaminated amine will be shared with other connected units.

8.4.4.1 Integration with AGRU for Zero Emissions

The tail gas from hydrogenation section can be compressed and recycled back to inlet of the AGRU for selective H_2S removal, as shown in Fig. 8.12. This would eliminate the tail gas amine treating unit and the incinerator. The main advantage is the elimination of an emission source from the typical TGTU, which makes permitting easier. In this configuration the treated gas from the selective AGRU contains all the CO_2 and the residual H_2S (4 ppm), while most of the sulfur species are destroyed in the Claus SRU, achieving a "zero-emissions" status. However, compressing the tail gas from atmospheric pressure to the feed gas pressure requires several compression stages. There are associated capital and operating costs to operate the recycle gas process. Also, compressing wet, sour gas can be a challenge.

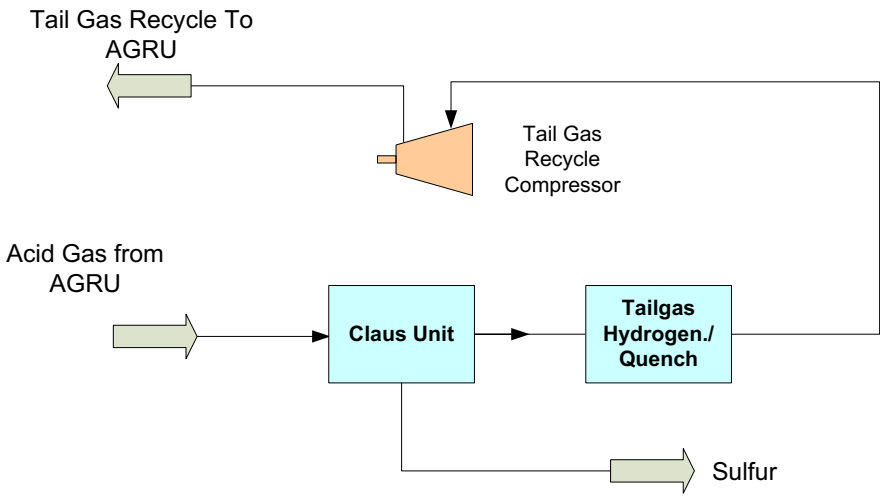

FIGURE 8.12

Zero-emission with tail gas recycle (Flood et al., 2011).

8.4.4.2 Integration With Acid Gas Removal Unit

The TGTU and AGEU can be designed as an integrated unit, as shown in Fig. 8.13. As can be seen, the AGEU absorber can be used to selectively absorb H_2S from the lean acid gas feed, producing an H_2S rich solvent and a CO_2–rich overhead gas. Similarly the H_2S in the tail gas can be removed in the TGTU absorber. A common solvent regenerator can be used to regenerate the rich solvents from both absorbers. The CO_2 gases from the AGEU and TGTU absorbers containing trace amounts of H_2S (as low as 10 ppmv) can be directly vented to the atmosphere.

Note should be made that the acid gas enrichment process can also be integrated to advanced tail gas absorption processes, including the Fluor patented Double Absorption Process (DAP). Details of the DAP process are described in Chapter 7.

8.5 SULFUR DEGASSING

Sulfur pits are used to collect raw liquid sulfur from the sulfur condensers under gravity. Raw liquid sulfur produced from the Claus sulfur condensers typically contains about 300 ppmw of soluble H_2S as hydrogen polysulfide (H_2S_X) and about 20–30 ppmw SO_2. H_2S_X is a weakly bound polymeric sulfur compound formed by the equilibrium reaction between sulfur and H_2S following the below reaction:

$$H_2S + (X-1)\ S \leftrightarrow H_2S_X \tag{8.14}$$

This reaction proceeds to the right with increasing temperature. During storage or transport, H_2S_X will decompose. This results in formation of dissolved H_2S in the liquid sulfur, which will vaporize by physical desorption. H_2S and SO_2 can accumulate to dangerous levels in the storage pits. If liquid sulfur is not degassed, H_2S will be released during storage, handling, loading, and transport. Undegassed sulfur can also create an explosive mixture of H_2S in air and poses a toxicity hazard and a noxious odor when H_2S is released from the liquid sulfur.

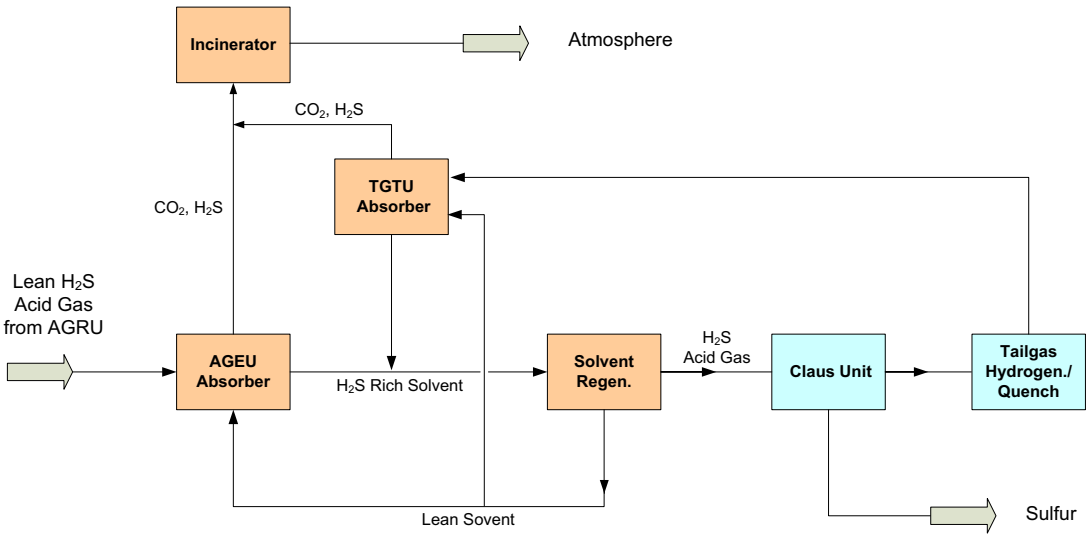

FIGURE 8.13

Integrated tail gas treating scheme and acid gas enrichment (Flood et al., 2011).

The desirable liquid sulfur product should contain a H_2S concentration of 10 ppmwt or less, suitable for transport. To meet the 10 ppmw total H_2S requirement, sulfur degasification processes employ a combination of residence time, agitation, and sometimes catalysts. All degassing processes involve agitation of the liquid sulfur and removal of the evolved H_2S with a sweeping gas. Generally, air is used as the sweep gas since oxygen helps to release the H_2S from the polysulfide molecule. The contaminated degassing off-gas is typically vented to the thermal oxidizer for oxidation to SO_2, or directed to the front-end of the SRU. A properly sized wire mesh mist eliminator is utilized to minimize potential liquid sulfur entrainment in the overhead vapor stream.

The most common degassing processes capable of meeting a 10 ppmw total H_2S specification are the D'GAASS process (licensed from Fluor) and the Aquisulf process (licensed from Lurgi).

8.5.1 D'GAASS PROCESS

The D'GAASS process (developed and commercialized by Goar, Allison, and Associates, later acquired by Fluor) can achieve 10 ppmw residual H_2S/H_2S_X in liquid sulfur without catalyst addition. There are over 80 D'GAASS units worldwide with total capacity of over 40,000 LT/D sulfur. A photo of a typical D'GAASS module is shown in Fig. 8.14.

In this process, degasification is carried out in a pressurized vertical vessel, using instrument air or clean plant air. In fact the key to the D'GAASS process is the elevated operating pressure (typically over 60 psig), using proprietary vessel internals for degassing. Operation at elevated pressure facilitates degassing operation and results in low capital and operating costs. Owing to the elevated operating pressure, the D'GAASS contactor is relatively small. The contactor vessel is typically located outside the pit, which makes it easy to install in a grassroots unit or for retrofitting an existing facility.

FIGURE 8.14

D'GAASS module.

Courtesy of Fluor.

For SRUs with TGTUs that are required to meet 99.9+% sulfur recovery, conventional degassing systems that vent the vapor stream to the incinerator can be a significant emission source. In these cases emission from the degassing systems is the only emission source from the SRU/TGTU. For the D'GAASS process, 90+% of the H_2S/H_2S_X feed and the overhead stream can be recycled back to the SRU, resulting in a zero emission design.

8.5.2 AQUISULF PROCESS

Among these degassing processes, the earliest process is the Aquisulf process (Nougayrede and Voirin, 1989), with more than 80 references from 15 to 1200 LT/D sulfur (single train). This process is based on the two principles: mechanical degassing by agitation and pulverization to promote gas-liquid contact; and chemical degassing by catalyst injection to speed up the decomposition of H_2S_X. The Aquisulf process is available in batch and continuous versions. In the continuous version (see Fig. 8.15) the liquid sulfur pit consists of two or more compartments. The sulfur in the first compartment is pumped and mixed with the catalyst and sprayed back into the compartment. The liquid sulfur overflows from a weir to the second compartment. The liquid sulfur is again pumped and

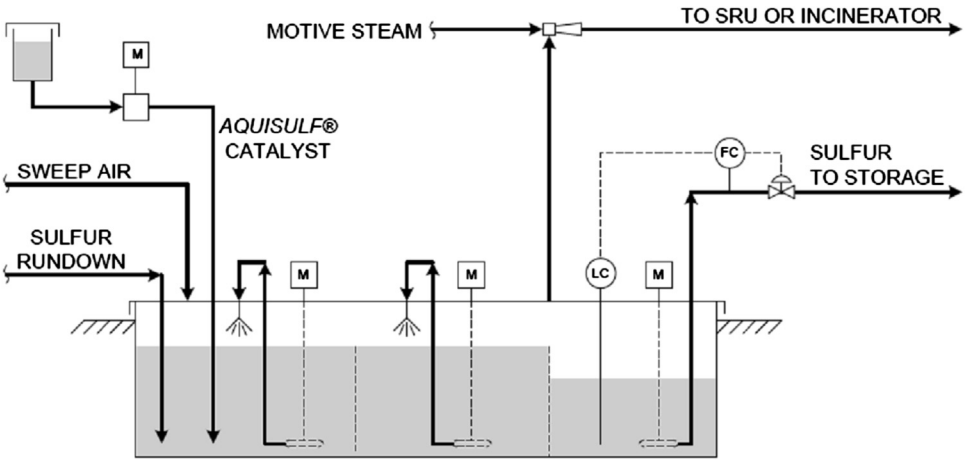

FIGURE 8.15

Continuous Aquisulf scheme (Nougayrede and Voirin, 1989).

sprayed in this tank to provide more agitation. The original catalyst was ammonia. However, problems associated with ammonium salts have resulted in the development of an improved version of the proprietary Aquisulf liquid catalyst.

8.6 SULFUR STORAGE AND HANDLING

Liquid sulfur, degassed to below 10 ppmw H_2S, has a strong equilibrium driving force to react with air (oxygen) to form SO_2 in air-purged storage tanks (Johnson, 2005). The degassed liquid sulfur, containing traces of SO_2, is typically directed to an insulated and heated carbon steel storage tank to provide a buffer between the SRU and the downstream system. Some H_2S will evolve inside the tank, due to the air/sulfur/H_2S equilibrium.

Despite both H_2S and sulfur being flammable in air, the current industry practice is to use an air sweep to the vapor space in the sulfur tank to maintain the H_2S concentration to below the lower explosive limit, which is 3.4% volume at the storage temperature of 330°F (Iyengar et al., 1995).

The stored liquid sulfur can be shipped to the market by tank trucks or by railcars or pipeline. In most cases, it is converted into a solid form for ease of handling and transportation. The liquid sulfur can also be poured to a block for short-term storage during emergency. The sulfur fines reclaimed from the sulfur block can be melted to provide feed for shipments or to sulfur-forming facilities.

8.6.1 MOLTEN SULFUR HANDLING SYSTEM

Molten sulfur transmission pipelines must be maintained within the upper and lower temperature limits that are necessary to prevent high viscosity and solidification, respectively. In fact, to pump sulfur, a minimum temperature (255°F) is needed, but if heated to an excessive temperature (320°F), sulfur degrades and thickens. Therefore, all lines and equipment must be adequately heated to maintain

the sulfur in the appropriate temperature range. A number of heating systems have been successfully employed, including steam, heating medium, glycol, pressurized hot water, and skin effect electrical heat tracing (SEEHT).

It is widely accepted by pipeline operators that SEEHT system, monitored and controlled by fiber optic technology, is cost effective and reliable for long sulfur transmission pipelines (Beres et al., 2004). A SEEHT system is typically designed to maintain the sulfur at an average fluid temperature of 275−284°F. The fiber optics temperature measurement should be accurate to ±1°F, for identification of cold spots throughout the pipelines network (Johnson, 2008).

When the molten sulfur is supplied to a forming facility, it is cooled with air or water to just above its solidification temperature (250°F) and is filtered to avoid plugging up of the sulfur spray nozzles in the forming facility (Johnson, 2009).

8.6.2 SULFUR FORMING

Bulk solid sulfur is produced in many different forms, which vary in their friability and mechanical strength, using different technologies and processes.

Slating was the sulfur industry's first attempt at developing a formed product, which generates less dust than the traditional crushed bulk sulfur method. The slate form of sulfur is produced by pouring and spreading liquid sulfur onto a slow moving belt while simultaneously cooling the belt by air from above and water from below. There is a tendency for slates to break into flake and dust, and therefore, slated sulfur is a less desirable form.

Prilled sulfur is created when sulfur droplets are cooled by a surrounding fluid, which may be air or water. Air-prilled sulfur is created when spraying liquid sulfur from the top of a tower against an upward flow of air. However, the facility is costly and generates sulfur emissions. This method is not common these days.

Wet-prilled sulfur is created when sulfur droplets fall into an agitated water bath, which solidifies the sulfur into uniformly sized prills. The prills are then separated from the water in high-frequency vibrating screens.

Granulated sulfur is created through the gradual buildup of successive layers of sulfur around a central core. The ultimate product size can be controlled. In the granulation process, small particles of sulfur are introduced to a long horizontal rotating drum where the particles are spray-coated with molten sulfur.

8.6.3 CONVEYING FORMED SULFUR

From the forming facility, the bulk sulfur is transported to the storage area. Typically rubber belt conveyors are used in transferring the sulfur from production to storage. Front-end loaders are used to transfer bulk sulfur from a stockpile to a hopper feeding a conveyor.

During the normal course of handling solid sulfur, some sulfur dust will be generated. To keep this fugitive dust from accumulating within the conveyors, the conveyor enclosures are swept with air. This dust laden air system, if vented directly, would be a major source of particulate emissions. Therefore, dust suppression systems must be installed at conveyor transfer points and at load out stations. This system typically uses a combination of water, compressed air, and a surfactant mixed in a proprietary foam generator, where the foam is applied to the formed sulfur at the aforementioned points to help suppress dust (Riegel and Kent, 2003).

8.6.4 STORAGE OF FORMED SULFUR

Sulfur storage has been incorporated into the design of many SRUs to allow for accumulation of sulfur during interruptions in the sulfur shipping system or during periods of low sulfur demand. The sulfur is often stored in the open in huge stockpiles where it is exposed to wind, rain, dust, etc. In some cases, sulfur is stored indoors where some protection from the elements is available. Although this refinement may be expensive, it is the preferred modern method of storing formed sulfur product awaiting delivery to end users. However, if indoor storage cannot be provided, a location shielded from prevailing winds should be selected to reduce the migration of fugitive dust. Also, the capability to collect and dispose of water effluent off the pad will be required.

8.7 SULFUR RECOVERY UNIT DESIGN CONSIDERATIONS

Overall, SRU reliability can be increased through proper design methods and practices. Unit reliability can be significantly improved by attention to details in designing the unit, typically requiring only a modest increase in the initial capital cost. However, many of the features that can be incorporated into a design are difficult and more expensive to implement later on into an existing unit. Therefore, it is extremely important for the designer to design the SRU for optimum reliability at the earliest stage of design. The following identifies some of the key design parameters that need to be considered.

8.7.1 PIPING

Piping design, equipment layout, and plot layout are among the most important aspects of the SRU design. The rules for piping design are relatively simple such as:

- Steam jacket all liquid sulfur lines
- Piping should be free-draining
- Piping runs to be as short as practical
- Utilize crosses at all direction changes in all liquid sulfur lines
- Slope all liquid sulfur lines to promote gravity flow.

Sulfur will solidify at temperatures between 245 and 250°F. It is therefore imperative to maintain the sulfur piping above 250°F using steam-jacketed piping (or SEEHT). The steam supply and condensate piping, and particularly the steam traps, should be properly installed. Steam traps should be provided at frequent intervals to maintain the sulfur temperature.

It is important to avoid liquid sulfur cooling in the piping, as it may result in additional pressure drop through the SRU. This may cause equipment damage, corrosion, and it may even imperil personnel safety and cause equipment damage. The piping design should insure that any liquid is freely drained and pumped back to the process equipment.

Keep the pipe runs short and the process hot. It is easier to keep the process hot if the pipe runs are short. Heat loss from uninsulated flanges and valves promotes condensation, corrosion, and plugging in the piping system. All lines containing ammonia and sulfur vapor should use only steam-jacketed control and block valves to avoid plugging.

It should be noted that most lines will plug at some point during the life of the SRU. To avoid creating a permanent plug, any change in flow direction in liquid sulfur service should be provided

with a cross, which allows the piping to be rodded out to break the plug. In addition, the upstream valves should be steam jacketed to allow rodding.

Liquid sulfur can be a viscous fluid and can become very viscous at certain temperatures. Gravity flow liquid sulfur piping should be designed to run only partially full. All liquid sulfur piping should be sloped at a minimum of 1/8″ per foot to promote free-draining.

8.7.2 ACID GAS FEED DRUMS

The acid gas feed drum will remove entrained liquids from the amine regenerator overhead, during normal operation and upset conditions. Entrained liquids may be sour water, hydrocarbons, and amine. If not removed, entrained liquids can cause problems with the feed metering system, cause plugging in the burners, refractory damage, and eventual failure of the burners and reaction furnace.

The KO drums should be equipped with pumps to remove the collected liquids to the sour water system or waste tanks. The pumps should have a spare and should be operated on a start-stop basis, being activated on high-liquid level.

8.7.3 COMBUSTION AIR BLOWERS

For reliability, combustion air blowers should have spares, either two 100% capacity blowers or three 50% blowers. Multistage centrifugal motor driven blowers are common.

8.7.4 MAIN BURNER AND REACTION FURNACE

The burner must be of high-intensity design with efficient mixing, which is critical to ensure complete reaction. It must perform the function of burning 1/3 of the feed H_2S to SO_2 to satisfy the modified Claus process. The temperature must be high enough to destroy impurities and contaminants in the acid gas (see previous section). The burners must be capable of performing efficiently at normal operation and during turndown.

The feed impurities and contaminants must be destroyed in the reaction furnace or they will cause fouling problems in the downstream equipment. There must be adequate time for the oxidation reactions to reach completion. The reaction furnace is typically designed for a 0.6−1.5 s residence time.

The burner and furnace are typically constructed of carbon steel. The extremely high temperature, reducing atmosphere, and acid gas environment are very corrosive. The furnace refractory lining must be designed with the proper material for the corrosive environment. The furnace is typically equipped with proprietary internal components supplied by a licensor to promote mixing, and the designs are dependent on feed gas compositions, temperature, and the quantity of contaminants.

The burner and furnace system must be equipped with necessary instrumentation for control and monitoring. The other critical burner instruments are the flame scanners. If the flame scanners are unreliable, they can result in nuisance shut downs. The normal arrangement is one out of two voting to keep the SRU on line.

It is necessary to purge each instrument nozzle when the SRU is shutdown. The sulfur content in the process gas will condense and solidify if allowed to enter the instrument leads.

8.7.5 WASTE HEAT BOILER

SRU WHBs are typically of the fire-tube design. They serve the dual purposes of heat recovery by generating steam and cooling the process gas from 2000°F to about 600°F. The steam drum and associated equipment of the SRU WHB's should be designed in accordance with ASME boiler codes.

8.7.6 SULFUR CONDENSERS

Sulfur condensers serve the primary function of cooling and condensing sulfur from the upstream reaction. Sulfur condensers are normally kettle-type shell-and-tube exchangers. The sulfur condensers are designed to condense and separate product sulfur from the process gases. The sulfur condenser design must operate within the range of the design mass velocities, typically ranging from 2 to 6 lb/sec ft^2.

8.7.7 SULFUR PIT

Product sulfur is normally collected below grade, in a concrete pit equipped with steam coils to keep the sulfur molten. The pit does not directly affect the SRU process operation unless the SRU must be shut down because of problems with the pit.

Some common sulfur pit problems are steam coil leakage, sulfur pump failure, internal sulfur fires, and even internal explosions. There are design features that will improve the reliability of the sulfur pit:

- Constructing the pit with sulfate-resistant concrete and limestone-free aggregate.
- Using alloy piping for the steam supply piping and internal components.
- Installing dual steam jacketed sulfur transfer pumps.
- Using a fully steam-jacketed steam eductor to continuously provide sweep air to the pit to prevent accumulation of H_2S.
- Installing steam snuffing connections for extinguishing internal sulfur fires.

8.8 SULFUR RECOVERY UNIT OPERATION PROBLEMS

Problems associated with SRU operation generally relate to misoperation of the furnace and reactor systems, reduced catalyst activity, and throughput limitation due to high pressure drop. The end result is failure to meet the required SRU throughput, sulfur recovery target, or sulfur emission limit. Emissions from the SRUs are continuously monitored. If they do not meet the emission permit requirements for a certain amount of time and remedies fail to resolve the problem, the complete facility has to be shutdown. The following sections summarize these problems and provide guidelines to mitigate the problems.

8.8.1 PROPER AIR RATIO

For optimum conversion, the ratio of H_2S/SO_2 should be 2:1. However, to avoid excess SO_2 formation while the process undergoes normal variations, it is often run at slightly higher ratios of $\sim$2.2:1. This ratio is measured in the tail gas from the final condenser. SRUs are best operated on closed-loop control

based on tail gas analyzer. In practice, other methods can also be used to adjust air to the reaction furnace, such as feed forward control based on inlet flow rate and H_2S concentration. Excessive airflow to the reaction furnace may result in formation of SO_3 and possible sulfation of the catalyst.

Incinerator temperature can be used to adjust the airflow to the reaction furnace. A high incinerator temperature, coupled with low fuel consumption, is a sign of insufficient air to the reaction furnace. Alternately, if a large amount of fuel gas is used to maintain the incinerator temperature, this may also indicate that much air is used in the reaction furnace.

8.8.2 REACTOR ACTIVITY

To verify the reactor activity, the temperature rise across each reactor should be checked. If there is a temperature drift from the design, it may indicate that the effluent from the first stage is not reaching equilibrium. Sulfur formation in the first reactor may have decreased. The overall catalyst effectiveness may have declined. The problem may be due to catalyst deactivation caused by sulfur precipitation. This can be a result of low reactor feed temperatures. Check the operation of the reheat exchanger upstream of the reactor. If the upstream temperature is normal and it has been determined that catalyst activity has been irreversibly lost, the catalyst may need to be changed.

The catalyst performance can be monitored by reading the vertical temperature profile through the first catalyst bed. Typical temperature profiles of fresh catalyst and damaged catalyst are shown in Fig. 8.16. If the catalyst is in good condition, 90% of the heat of reaction is released in the top 6 in. of the bed. If catalyst activity is impaired the reaction is shifted down the bed. The loss of activity can be a result from many factors such as carbon deposits, leaking condenser tubes, damaged reactor support screens or internals, sulfuric acid formation, or operating below the sulfur dew point.

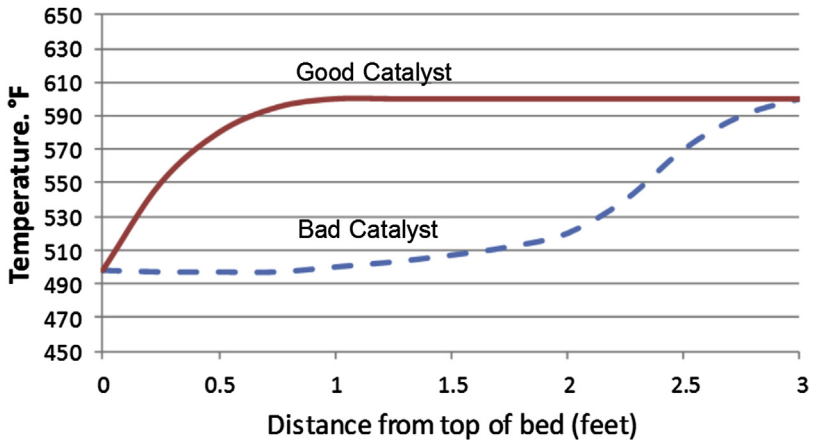

FIGURE 8.16

Vertical temperature profile shows condition of catalyst.

8.8.3 EXCESSIVE COS AND CS_2

The presence of hydrocarbons and CO_2 in the acid gas promotes the formation of COS and CS_2 in the reaction furnace. These compounds can significantly contribute to SO_2 formation in the incinerator. The COS and CS_2 can be eliminated by operating the first reactor at an outlet temperature of 650°F and having titania catalyst in the bottom of the bed. At this temperature these compounds are converted to H_2S and CO_2. An increase in SO_2 emissions, accompanied by a lower than design first reactor inlet temperature, is likely due to the presence of COS and CS_2.

8.8.4 LEAKAGE OF REHEAT EXCHANGER

Some multistage SRUs reheat the third-stage reactor feed with first-stage reactor effluent. The reheat exchangers are prone to leakage due to the corrosive environment, which may contribute to lower conversion. If there is a large increase in the third-stage inlet temperature, there is possibility that the reheat exchanger is leaking.

8.8.5 REACTOR PRESSURE DROP

To properly operate an SRU, it is important that the pressure drop in the unit be monitored. A sudden increase in pressure in the SRU is a warning of equipment being fouled. Pressure drop in an SRU is proportional to the square of the gas flow. If the high pressure drop is not due to higher flow, it may suggest that the catalyst beds are plugged with carbon or some equipment component has failed.

8.8.6 CARBON DEPOSITS

Heavy hydrocarbons and BTEX may be in the feed gas from the production wells. Some of these compounds are absorbed by amines in the amine absorber, so they will end up in the acid gas to the SRU.

Ten times more air is needed to oxidize propane than H_2S. When light hydrocarbon vapors are reacted in the converters, carbon black is formed. A gradual increase in pressure drop is an early warning sign of carbon deposit. When this happens, check for low steam production rates from the high-pressure boiler. If both steam production and reactor outlet temperature are low and the pressure drop is high, it may indicate a tube leakage. The SRU may need to be shutdown for repair.

If sulfur condenses in the catalyst, it may restrict gas flow through the unit. The worst thing that can happen to an SRU is a crash shutdown. When the unit suddenly shuts down, precipitating sulfur could solidify in the catalyst beds if allowed to cool. SRUs may be cleared of sulfur by burning natural gas instead of H_2S before a shutdown.

8.8.7 CATALYST SUPPORT SCREENS

SRU catalyst is supported by thin flexible screens. These screens are lapped and folded over to keep catalyst from leaking through the support grating. Improper installation of screens occurs frequently during catalyst change-out. The catalyst may wash down into a seal leg and result in plugging.

8.8.8 WATER VAPOR AND CARBON DIOXIDE

The capacity of the SRU is negatively impacted by an increase in water and CO_2 vapor in the acid gas. Reducing the water content can be done by more cooling in the regenerator overhead condenser. For example, lowering the overhead temperature from 135°F to 110°F can reduce the water content by about 5%, which can be translated to a 2% increase in SRU throughput.

By lowering the feed location of the lean amine to the amine absorber, more CO_2 can be slipped and rejected to the absorber overhead, which would correspondingly reduce the CO_2 content in the acid gas, opening up more capacity to the SRU. The use of selective amine such as formulated MDEA or Flexsorb would further reduce the CO_2 content to the SRU.

8.8.9 STEAM HEATER

High-pressure steam is the most common source of heat for the SRU reheaters. Steam reheaters are very reliable and easy to operate. However, the maximum reheater outlet temperature is limited to about 460°F when using high-pressure steam. This low temperature can be a problem for the first-stage reactor, particularly if significant quantities of COS and CS_2 are formed in the burner/reaction furnace.

8.8.10 COMBUSTION AIR CONTROL

Control of combustion air feed is the most critical part of the sulfur recovery process to ensure efficient and reliable operation. The combustion air control should be split into two sections, a main airflow loop based on acid gas flow rate (and H_2S concentration) and a trim airflow loop based on the tail gas analyzer.

Air demand is calculated from the acid gas flow and used as a feed forward ratio set point for the main air control loop. The main air loop supplies about 90% of the total air to the burner.

The trim air loop operates on feedback control from the tail gas analyzer. The analyzer measures the relative amount of H_2S and SO_2 in the tail gas. The analyzer controller provides a remote set point signal to the trim air loop based on the relationship $2SO_2 - H_2S = 0$.

When this relationship is satisfied, the optimum amount of combustion air is being supplied to the SRU. If the result is positive, too much air is being fed and the rate should be reduced. Similarly, if the result is negative, too little air is being fed, and the rate should be increased. It is apparent that the tail gas analyzer must work properly to achieve optimum air control. If the air controls are off, inadequate impurity destruction with equipment plugging and/or equipment corrosion may result.

8.9 SELECTING THE SULFUR RECOVERY PROCESS

The large variations in concentration and flow require different methods for H_2S removal and sulfur recovery. For relatively small quantities of H_2S/sulfur, scavenger processes are often used. For sulfur quantities up to 10–20 T/D of sulfur, liquid reduction–oxidation (redox) processes are common, but the sulfur is produced as aqueous slurry. Direct oxidation can sometimes be utilized for low H_2S concentrations to produce high-quality liquid sulfur. The selection criteria based on H_2S concentration in the acid gas is shown in Fig. 8.17.

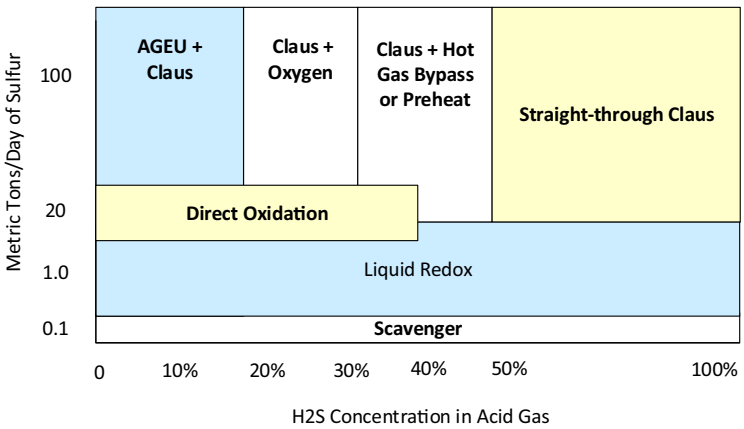

FIGURE 8.17

Selection of sulfur recovery process.

Typical acid gas in a gas processing plant that contains hydrocarbons and BTEX component. Ammonia is frequently present in refinery acid gas. The thermal section of the Claus process is the most robust process stage that can be used to destroy the hydrocarbons and contaminants. When the Claus process is followed by a tail gas selective treating unit, 99.99% sulfur recovery and 10 ppmv H_2S in the vent gas can be achieved if sulfur pit vapor is fed to the Claus. If the acid gas is lean, an AGEU can be installed prior to the Claus SRU.

The use of direct oxidation of H_2S is most likely applicable to syngas due to the absence of hydrocarbons, but it is rarely used in natural gas processing plants.

For new SRUs, most countries today require the best available technologies to minimize sulfur emissions. Some of the key parameters affecting the selection of the sulfur recovery process are as follows:

- Acid gas composition, including H_2S content and hydrocarbons and other contaminants
- Required recovery efficiency
- Concentration of sulfur species in the stack gas
- Turndown requirements
- Ease of operation
- Remote location
- Sulfur product quality
- Capital and operating costs
- Is it a revamp unit?

When required recovery efficiency and concentration of sulfur species in the stack gas are known, the tail gas cleanup process licensor can be evaluated. When concentration of impurities in the acid gas such as COS and CS_2, H_2S content, and the treated gas specifications are established, the type of amine used for a particular application could be selected.

Finally, the selection of similar processes will be based on the ease of operation, robustness, experience, capital and operating cost, and remote location. For revamp units, minimum equipment modifications, and process configuration should be considered as the main key factors.

8.10 SULFUR DISPOSAL BY ACID GAS INJECTION

The acid gas stream, which is the by-product of the acid gas removal process, is normally sent to a SRU. However, if the acid gas contains more than about 60% CO_2, which is often the case with small amounts of H_2S in the sour natural gas, then a modified Claus plant may not be the best choice for small-scale sulfur recovery. Instead, a redox unit could be selected for converting H_2S to sulfur. However, redox processes are limited to small capacity and are relatively expensive in terms of cost per ton of sulfur. It is somewhat difficult to operate, and the resulting sulfur product does not meet sulfur product purity specifications. In such situations, the best solution may be to compress the acid gas stream for disposal into depleted oil and gas reservoirs or into deep saline aquifers (Wichert and Royan, 1997). In addition, injecting the acid gas stream into an underground formation is a viable process for gas processing plants located in remote locations where transport the sulfur product is not easy. This is also the only option if the gas plant is in an environmentally sensitive region, which mandates a zero emissions policy.

Generally, an AGI unit is lower in capital and operating costs than a SRU, if the injection destinations are nearby, and especially if the injection wells can be converted from existing producing wells. An AGI is less complex, making the unit easier to control and more reliable, if critical equipment is spared. AGI systems can also easily handle wide ranges in the acid gas composition. In addition, to providing a cost-effective alternative to sulfur recovery, the deep injection of acid gas may also help to maintain the oil field pressure, which enhances oil recovery and increases revenue. However, there are risks associated with handling hazardous gases at elevated pressures. Furthermore, AGI processes are limited to cases where suitable injection reservoirs are available. If injected into an oil production reservoir, the sour gas will likely be reproduced at some point in the future.

8.10.1 PROCESS DESCRIPTION

In the basic AGI scheme the acid gas mixture is liberated from the AGRU at low pressure and at relatively high temperature. It is typically compressed in three or four stages to sufficient pressure to inject it into a subsurface formation such as an aquifer or a depleted reservoir. High-pressure acid gas flows through the pipeline to the well site, into the wellbore, down the well tubing, and finally into a subsurface formation that is selected based on certain geological criteria. Therefore, the basic unit components are a compressor, a pipeline, an injection well, and an injection reservoir. Water vapor, which is almost always present in the feed acid gas stream, can contribute to corrosion of the compressor and the pipeline if it is allowed to condense. If cold enough, water condensation may facilitate hydrate formation. In many injection schemes, compression and cooling alone is sufficient to dehydrate the gas to a point where neither free water nor hydrates are a problem. However, in some cases additional dehydration (usually with triethylene glycol) may be required (Carroll, 2009a).

While high-pressure subsurface gas injection has been used extensively around the world, it is most commonly used for injection of sweet gas or low flow rates of acid gas (5−10 MMSCFD).

However, the LaBarge facility in Wyoming injects approximately 60 MMCF/D of 65% H_2S (Carroll, 2009b).

There are opportunities for AGI from large gas processing plants, such as the Shah gas plant in Abu Dhabi that has been designed to process about 1 billion standard cubic feet per day (BSCFD) of feed gas containing 25% H_2S and 10% CO_2. Processing 1 BSCFD feed gas would result in over 330 MMscfd acid gas with 10,000 tons of sulfur per day (Schulte et al., 2017). The current plant does not have AGI, due to safety concerns on high concentration of H_2S. However, AGI would eliminate the CO_2 emissions from the acid removal units and avoid the large sulfur storage. These disadvantages of conventional sulfur plants, combined with the low prices of the sulfur products, may make AGI the most viable solution.

8.10.2 DESIGN CONSIDERATIONS

Operating above the critical pressure and temperatures above the water dewpoint (and hydrate point) will prevent condensation of water or liquid acid gas at any point in the injection system. However, the efficient design of an injection system to ensure that the high pressure acid gas is safely contained and disposed of properly requires numerous design considerations. This section covers some of the main design considerations of the compression, pipeline, and injection portions of the facility.

8.10.2.1 Compression

The maximum pressure for compression of the acid gas depends on the reservoir pressure, permeability, and depth. The required compression ratio for the acid gas is frequently over 50, and in some cases, it exceeds 100. Even if this much compression could be achieved using a single compressor, the exiting gas would be at a temperature above the maximum recommended to avoid corrosion, which is generally around 300°F. Therefore, the compression takes place in a multi-stage compressor with interstage cooling and liquid knock-out. The interstage exchangers are typically aerial coolers and are designed to cool the acid gas to 120°F (if ambient temperature permits). At this temperature, a free aqueous phase is likely to form and is removed using interstage knock-out scrubbers. The lower the cooling temperature, the more water is removed.

For most acid gas mixtures, there is a minimum in water-carrying capacity in the pressure range of 700—900 psig. Thus, additional compression above this range increases the water-carrying capacity as the density of acid gas increases substantially. The compressibility of the acid gas also decreases, so the horsepower required to pump dense liquid is much less than that to compress gas. In any case, the temperature must always be kept above both the dew point of the acid gases and the hydrate formation temperature (Fig. 8.18).

It is also very important to select a compressor supplier who has experience with high-pressure acid gas, particularly in the dense-phase region. Note that lower than ambient temperature can be achieved by recycling the compressor discharge and JT to the compressor suction. By operating at lower temperature and removal of sufficient water from the compressor suction drum, hydrate can be prevented and glycol injection may not be necessary.

8.10.2.2 Pipeline

Based on safety considerations, the pipeline is generally kept as short as possible so that the quantity of gas released can be kept to a minimum.

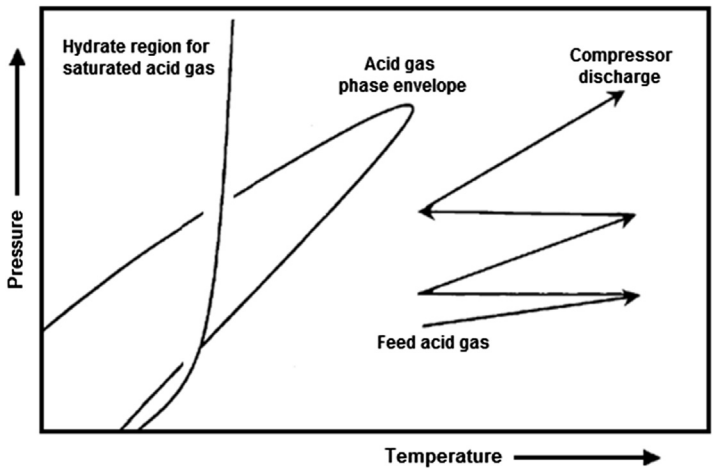

FIGURE 8.18

Acid gas compression in relation to phase behavior and hydrate formation (Clark et al., 1998).

The design of the pipeline carrying a gas, a liquid, or a mixture of both follows the standard procedures for pipeline design. As long as free water is avoided, the pipeline can be fabricated from carbon steel.

8.10.2.3 Injection

In the AGI process, the drilling of an acid gas disposal well is a major expense. Therefore, the first task is to check if an existing well near the sour gas processing plant can be converted to an injector. The acid gas must arrive at the wellhead with sufficient pressure that it can be injected into the formation for disposal while overcoming the hydrostatic head of the liquid acid gas (Carroll, 2010).

The injection zone should be selected where its seal can be maintained to avoid potential gas breakthrough to production wells. Detailed subsurface modeling and analysis will assist with prediction of the reservoir response to the injected fluid. A depleted reservoir zone is a good candidate because the main reservoir parameters (size and original pressure) are known, and the amount of acid gas that can be safely injected will be more accurately estimated. Large aquifers and zones that produce sour fluids are also suitable for injection (Carroll et al., 2010). Later, if the sulfur price increases to profitable levels, the acid gas could be reproduced and the H_2S could be converted to sulfur (Wichert and Royan, 1997).

The injection reservoir is usually separate from the source reservoir. While recycling the acid gas to the source reservoir is possible, this can potentially increase the acid content of the feed gas sent to the AGRU, so this configuration is less common.

REFERENCES

Bacon, R.F., Fanelli, J., 1943. The viscosity of sulfur. Journal of the American Chemical Society 65, 639–648.

Beres, J., Chakkalakal, F., McMechen, W., Sandberg, C., September 13–15, 2004. Controlling skin effect heat traced liquid sulfur pipelines with fiber optics. Paper Presented at the 51st Annual Petroleum and Chemical Industry Conference, San Francisco, CA, USA.

Carroll, J.J., May 13–15, 2009a. Acid gas injection-the next generation. Paper Presented at the GPA Europe Sour Gas Processing Conference, Sitges, Spain.

Carroll, J.J., October 5–6, 2009b. Acid gas injection: past, present, and future. Paper Presented at the International Acid Gas Injection Symposium 2009, Calgary, AB, Canada.

Carroll, J.J., 2010. Acid Gas Injection and Carbon Dioxide Sequestration. Scrivener-Wiley Publishing, Salem, MA, USA.

Chao, J., 1980. Properties of elemental sulfur. Hydrocarbon Processing 59 (11), 217–223.

Clark, M.A., et al., March 16–18, 1998. Designing an optimized injection strategy for acid gas disposal without dehydration. Paper Presented at the 77th Annual GPA Convention, Dallas, TX, USA.

Fisher, K.S., Lundeen, J.E., Leppin, D., October 24–27, 1999. Fundamentals of H_2S scavenging for treatment of natural gas. Paper Presented at the 9th GRI Sulfur Recovery Conference, San Antonio, TX, USA.

Flood, T.M., Wong, V.W., Chow, T., October 10, 2011. The optimal sulfur recovery solution for coal gasification plants in achieving & maintaining a green China. Paper Presented at the 3rd China Energy Chemical International Forum, Urumqi City, Xinjiang, China.

Gamson, B.W., Elkins, R.H., 1953. Sulfur from hydrogen sulfide. Chemical Engineering Progress 49 (4), 203–215.

Gandhi, S., Chung, W., Nangia, K., 2010. Designing for sulfur removal and storage: Part II. Petroleum Technology Quarterly, Q3, 111–117.

Gemmingen, U., Lahne, U., 1994. The Linde Clinsulf® process for sulfur recovery: modeling and simulation. Gas Separation & Purification 8 (4), 241–246.

Goar, B.G., 1974. Impure feeds cause claus plant problems. Hydrocarbon Processing 53 (7), 129–132.

Goar, B.G., Fenderson, S., March 3–6, 1996. Fundamentals of sulfur recovery by the claus process. Paper Presented at the 46th Annual Laurance Reid Gas Conditioning Conference, Norman, OK, USA.

Goddin, C.S., Hunt, E.B., Palm, J.W., 1974. CBA process ups Claus recovery. Hydrocarbon Processing 53 (10), 122–124.

Gowdy, H.W., Bertram, R.V., March 1–4, 1998. UOP's Selectox process improvements in the technology. Paper Presented at the 48th Annual Laurance Reid Gas Conditioning Conference, Norman, OK, USA.

Heigold, R.E., Berkeley, D.E., March 7–9, 1983. The MCRC sub-dewpoint sulfur recovery process. Paper Presented at the 33rd Annual Laurance Reid Gas Conditioning Conference, Norman, OK, USA.

Heisel, M.P., Kunkel, J., Nillson, U., Eriksson, P., 1999. Operating experience of CLINSULF®-SDP for up to 99.85% sulfur recovery. Linde Reports on Science and Technology 61, 12–17. Linde A.G., Munich, Germany.

Iyengar, J.N., Johnson, J.E., O'Neill, M.V., March 13–15, 1995. Sulfur emissions identification and handling for today's SRU/TGU facilities. Paper Presented at the 74th Annual GPA Convention, San Antonio, TX, USA.

Johnson, J.E., November 26–29, 2005. Hazards of molten and solid sulfur storage, forming, and handling. Paper Presented at the 2005 Sour Oil & Gas Advanced Technology Conference, Abu Dhabi, UAE.

Johnson, J.E., April 27–May 1, 2008. Handling sulfur production in weak market conditions: sulfur recovery and block storage versus acid gas injection. Paper Presented at the 2008 Sour Oil & Gas Advanced Technology Conference, Abu Dhabi, UAE.

Johnson, G.J., 2009. Sulfur handling, forming, storage, and shipping. Hydrocarbon World 4 (1), 55–62.

Jones, S.G., Bertram, R.V., February 25–28, 2001. Lisbon plant Selectox Unit 7 Years operating performance. Paper Presented at the 51th Annual Laurance Reid Gas Conditioning Conference, Norman, OK, USA.

Lagas, J.A., Borsboom, J., Heijkoop, G., 1989. Claus process gets extra boost. Hydrocarbon Processing 68 (4), 40.

Lagas, J.A., Borsboom, J., Goar, B.G., February 27–March 2, 1994. SuperClaus: 5 years operating experience. Paper Presented at the 44th Annual Laurance Reid Gas Conditioning Conference, Norman, OK, USA.

Meyer, B., 1976. Elemental sulfur. Chemical Reviews 76, 367–388.

Nougayrede, J., Voirin, R., Jul. 17, 1989. Liquid catalyst efficiently removes H_2S from liquid sulfur. Oil & Gas Journal 65–69.

Opekar, P.C., Goar, B.G., June 1966. This computer program optimizes sulfur plant design and operation. Hydrocarbon Processing 181–185.

Riegel, E.R., Kent, J.A., 2003. Riegel's Handbook of Industrial Chemistry", tenth ed. Kluwer Academic/Plenum Publishers, New York, NY, USA.

Satoh, H., Yoshizawa, J., Kametani, S., 1988. Bacteria help desulfurize gas. Hydrocarbon Processing 67 (5), 76D–76F.

Schulte, D., Wagensveld, S., Graham, C., Lynch, B., April 9–12, 2017. Improved econamine treatment of ultra-sour gas. Paper Presented at the 96th Annual GPA Convention, San Antonio, TX, USA.

Shuai, X., Meisen, A., 1995. New correlations predict physical properties of elemental sulfur. Oil & Gas Journal 93 (42), 50–55.

Valdes, A.R., March 1964. A new look at sulfur plants. Hydrocarbon Processing 43, 104–108.

Wichert, E., Royan, T., 1997. Acid gas injection eliminates sulfur recovery expense. Oil & Gas Journal 9 (17), 67–72.

Willing, W., Linder, T., November 6–9, 1994. Lurgi's TGT processes and new operational results from Sulfreen plants. Paper Presented at the Sulfur 94 International Conference & Exhibition, Tampa, FL, USA.

CHAPTER

NATURAL GAS DEHYDRATION AND MERCAPTANS REMOVAL

9

9.1 INTRODUCTION

Natural gas stream from production wells is saturated with water vapor, which will condense and form gas hydrates if the gas temperature is cooled below its hydrate formation temperature. Gas hydrates are solids which can agglomerate and plug pipelines and equipment, interrupting operations and stopping gas production. This may create an unsafe condition, especially if significant pressure differential occurs across the hydrate plug. Also, water vapor may condense in pipelines, resulting in erosion and corrosion. When accumulated in the pipelines, it might form liquid plug, reducing the pipeline flow capacity. To avoid these potential problems, the gas stream needs to be dried to lower its water dew point.

Pipeline specifications typically call for water content to be no more than 7 lb/MMscf for US pipeline systems, 4 lb/MMscf for Canadian pipeline systems, and even lower 1−2 lb/MMscf for Alaskan environment. These values provide protection against water condensation and hydrate formation during winter. For cryogenic NGL processing and LNG feed pretreatment, the water removal level is even more demanding, down to a few ppm water with a dew point of −150°F and below.

There are several methods for dehydrating natural gas, including absorption, adsorption, and direct cooling of the wet gas. The absorption using liquid (glycol) and adsorption using solid desiccants are the most common, when a low water dew point gas is required for pipeline gas or for NGL recovery. The direct cooling method by expansion or refrigeration, with injection of hydrate inhibitors, is common for less dew point depression in the production of pipeline gas in mild weather regions. Several other advanced dehydration technologies (i.e., membranes and supersonic processes) offer some potential advantages, particularly for offshore applications due to their compact design. However, they have limited commercial experience. There are solvents that can remove both heavy hydrocarbons and water, including DPEG and methanol (see Chapter 7), but water removal by these solvents is considered incidental and typically cannot be customized. The glycol absorption and solid desiccant adsorption methods are discussed in more detail in this chapter.

With the development of more sour gas fields around the world, the removal of mercaptans from natural gas streams is becoming a challenge for today's gas processing plants. The key elements are: meeting environmental regulatory standards, maximizing productivity, and minimizing total lifecycle costs. This chapter addresses natural gas dehydration and discusses mercaptans removal that can be also integrated to the molecular sieves unit.

Handbook of Natural Gas Transmission and Processing. https://doi.org/10.1016/B978-0-12-815817-3.00009-5

9.2 WATER CONTENT DETERMINATION

The first step in evaluating and/or designing a gas dehydration system is to determine the water content of the gas. This is most important when one designs sour-gas dehydration facilities and estimates water production with sour gas in the plant inlet separator.

Determining the saturation water content of a gas is a standard but complex problem in thermodynamics. There are numerous methods available for determining water contents of natural gases. A detailed discussion of those methods that are perhaps beyond the scope of the present discussion can be found in Carroll (2002, 2009). In general, for acid gas concentrations less than about 30%, the existing methods are satisfactory. For higher acid gas concentrations (above 50%), particularly at higher pressures, existing methods can lead to serious errors in estimating water contents. An appropriate method has been introduced by Wichert and Wichert (2003). It is chart based and provides good estimates of the equilibrium water vapor content of sour natural gas for a range of conditions, including H_2S contents of 3−38 mol% with CO_2 contents of 3−43 mol%, pressures from 290 psi to 10,153 psi, and temperatures from 50 to 347°F. The overall average error of this method is less than 1%. However, a few points showed a discrepancy of more than ±10%. In the method developed by Wichert and Wichert (2003), the water content of the sour gas is calculated by multiplication of correction factor and the water content of sweet gas from the McKetta and Wehe (1958) chart, as follows:

1. Determine the equilibrium water vapor content of sweet gas at the operating temperature and pressure conditions using the McKetta and Wehe (1958) chart (see Fig. 9.1).
2. Determine the mole % H_2S equivalent concentration of the sour gas as:

$$\text{Mole \% } H_2S \text{ equivalent} = \text{mole \% } H_2S + 0.7 \times \text{mole \% } CO_2 \tag{9.1}$$

3. From Fig. 9.2 at the bottom left hand temperature scale, move to the right to the mole % H_2S equivalent (interpolate between the lines if necessary).
4. From this point, move to the upper chart, to the pressure of interest. From the pressure point, move to the left, to the ratio scale.
5. Multiply the value from step 4 by the water content determined for sweet gas in step 1. The result is the estimate of the saturated water content of the sour gas at the pressure and temperature of interest.

Commercial process simulation software programs are available with the latest GPSA (2004) data and vapor−liquid equilibrium (VLE) correlations for accurate calculation of water content of sour gas streams. The AQUAlibrium software by Flow Phase Inc, developed based on a rigorous thermodynamic model rather than mere empiricism, is a useful tool for predicting equilibrium water content of pure acid−gas components and acid−gas mixtures, and may produce more accurate results, particularly for high pressure system where no data exist (Carroll, 2009).

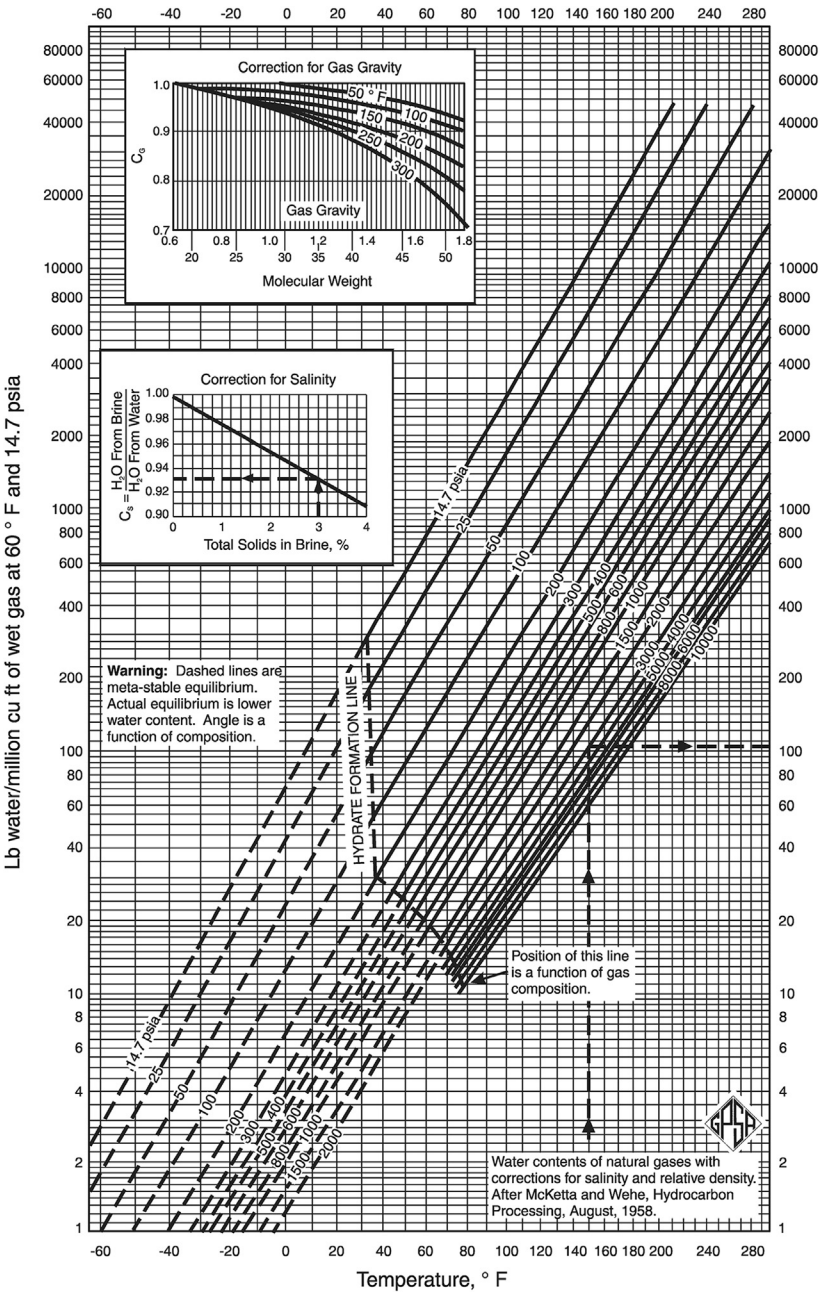

FIGURE 9.1

McKetta and Wehe (1958) chart (GPSA, 2004).

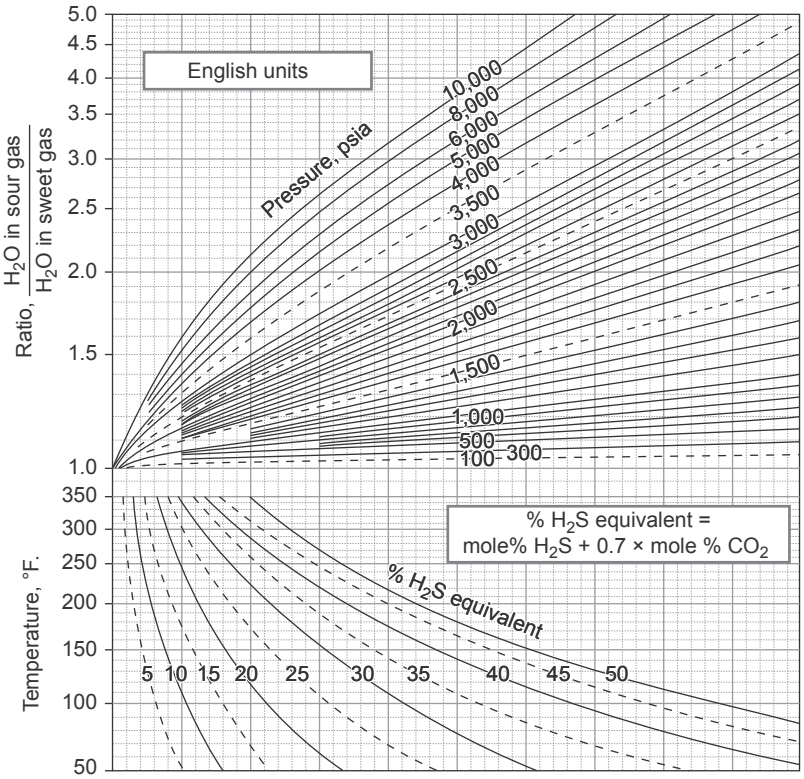

FIGURE 9.2

Water-content ratio chart (Wichert and Wichert, 2003).

9.3 GLYCOL DEHYDRATION

Among the different natural gas dehydration processes, absorption is the most common technique, where the water vapor in the gas stream becomes absorbed in a liquid solvent stream. Although many liquids possess the ability to absorb water from gas, the liquid that is most desirable to use for commercial dehydration purposes should possess the following properties:

1. high absorption efficiency,
2. easy and economic regeneration,
3. noncorrosive and nontoxic,
4. no operational problems, such as high viscosity when used in high concentrations, and
5. minimum absorption of hydrocarbons in the gas and no potential contamination by acid gases.

Glycols are the most widely used absorption liquids as they approximate the properties that meet the commercial application criteria. Several glycols have been found suitable for commercial

application. The properties of commonly available glycols can be found in the manufacturer's website. Their pros and cons can be summarized as follows (Katz et al., 1959):

1. Monoethylene glycol (MEG) - high vapor pressure and seldom used in contactor at ambient temperature due to high losses in the treated gas. Normally, it is used as hydrate inhibitor where it can be recovered from gas by separation at below ambient temperatures. It is used in glycol injection exchanger operating at −20°F to minimize losses.
2. Diethylene glycol (DEG) - high vapor pressure leads to high losses in contactor. Its low decomposition temperature requires a low reconcentrator temperature (315−340°F) and thus glycol purity is not high enough for most applications.
3. Triethylene glycol (TEG) - a relatively low vapor pressure when operating at below 120°F. The glycol can be reconcentrated at 400°F for high purity. Dew point depressions up to 150°F can be achieved with enhanced glycol processes like DRIZO.
4. Tetraethylene glycol (TREG) - more expensive than TEG but less glycol loss at high gas contact temperatures. It reconcentrates at 400−430°F.

TEG is the most common liquid desiccant used in natural gas dehydration.

In process design of the TEG dehydration unit, the upstream unit operation must be considered, as the TEG inlet temperature and water saturation will significantly impact the unit performance. For hot climate regions, the feed gas should be cooled to the lowest possible temperature with cooling water (or chilled water). This is necessary to ensure that the feed gas temperature meets the inlet maximum temperature of the TEG unit.

9.3.1 CONVENTIONAL TEG DEHYDRATION PROCESS

Fig. 9.3 shows the scheme of a typical TEG dehydration unit. As can be seen, wet natural gas is processed in an inlet filter separator to remove liquid hydrocarbons and free water. The separator gas is then fed to the bottom chamber of an absorber where residual liquid is further removed. It should be cautioned that hydrocarbon liquids must be removed as any entrainments will result in fouling of the processing equipment and produce carbon emissions. The separator gas is then contacted counter-currently with TEG, typically in a packed column.

Typically, the liquid loading on the tray (GPM per square foot) is very low, due to the low liquid to gas ratio. To avoid liquid maldistribution, structured packing or bubble cap trays should be used.

TEG will absorb the water content, and the extent depends on the lean glycol concentration and flow rate. TEG will not absorb heavy hydrocarbons to any degrees; however, it will remove a significant portion (up to 20%) of the BTEX (benzene, toluene, ethylbenzene, and xylenes) components. BTEX is considered as VOC (volatile organic compounds), which must be incinerated to comply with emission requirements.

Dry natural gas exiting the absorber passes through a demister, and sometimes through a filter coalescer to minimize TEG losses. Because of the relatively low TEG flow rate, there is not much sensible heat exchange, hence the dried gas temperature is almost the same as the feed gas.

The rich glycol is used to cool the TEG regenerator overhead, minimizing glycol entrainment and losses from the overhead gas. Rich glycol is further heated by the glycol heat exchanger and then flashed to a flash tank. The flash gas can be recovered as fuel gas to the facility.

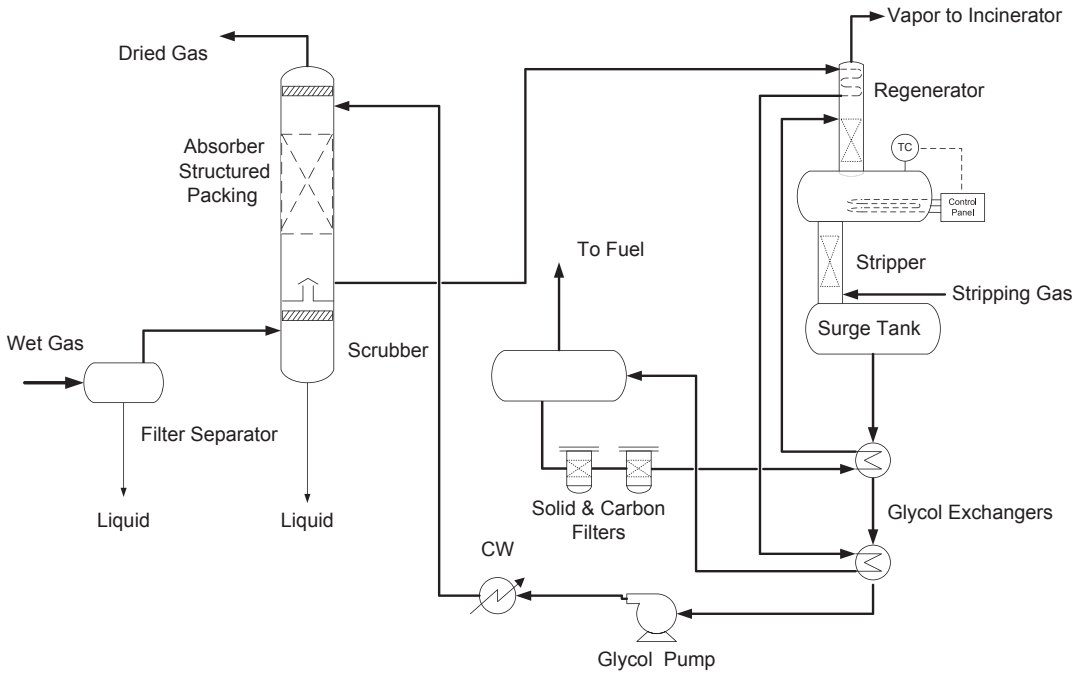

FIGURE 9.3

Typical flow diagram for conventional TEG dehydration system.

The rich TEG is filtered with solid and carbon filters, heated, and fed to the regenerator. The filtration system would prevent pipe scales from plugging the column and hydrocarbons from coking and fouling the reboiler. The water content in the glycol is removed with a reboiler. Heat supply to the reboiler can be by a fire heater or an electrical heater. An electric heater is preferred as it would avoid emission problems, particularly in smaller units. The water vapor and desorbed natural gas are vented from the top of the regenerator.

The dried glycol is then cooled via cross exchange with rich glycol; it is pumped and cooled in the gas/glycol heat exchanger and returned to the top of the absorber.

The glycol regeneration is typically designed as a skid mounted unit that can be prefabricated and shipped to the site. A three-dimensional rendition of the modular TEG dehydration unit is shown in Fig. 9.4.

9.3.2 ENHANCED TEG DEHYDRATION PROCESS

There are improved regeneration techniques that can produce higher glycol concentrations to be used to further lower the water dew point of the treated gas beyond the conventional TEG dehydration process. By injecting dry (stripping) gas into the base of the glycol reboiler to further reduce the partial pressure of water, and provide agitation of the glycol in the reboiler, the TEG concentration can be

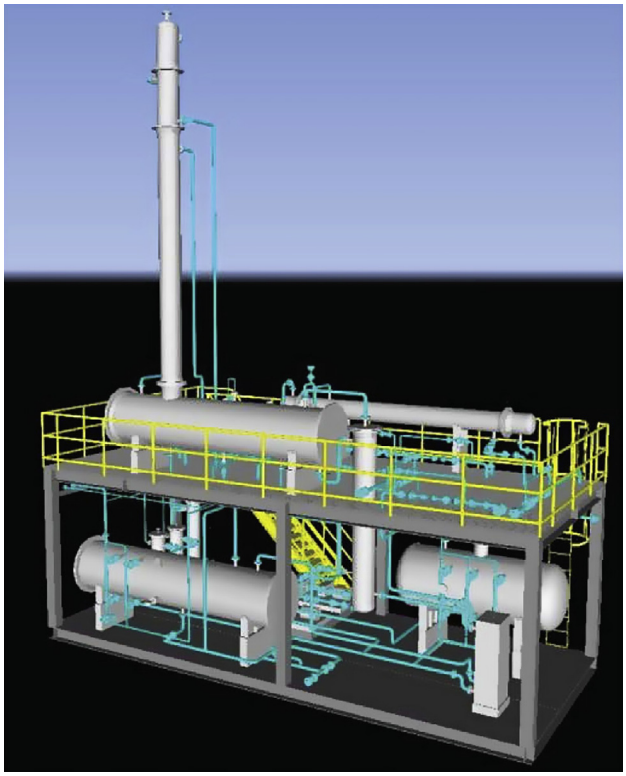

FIGURE 9.4

Three-dimensional rendition of a TEG dehydration unit.

increased from 99.1% to 99.6% by weight. Typically, a packed column located below the reboiler section is used for TEG stripping.

The DRIZO process (under PROSERNAT license) can regenerate TEG to a higher purity than the conventional gas stripping process. Solvent stripping can produce much higher glycol purities than gas stripping and consequently allows the process to achieve a much larger water dew point depression, up to -150°F and even higher in some cases. The solvent required by the DRIZO process is usually obtained from the C_6^+ (BTEX) present in the natural gas itself and in most cases the process will produce some liquid hydrocarbons.

The main advantages of the DRIZO process are that all BTEX compounds are recovered from the regenerator before being sent to atmosphere and no external stripping gas is required. The DRIZO technology may be adapted to existing dehydration units which need to be upgraded to meet requirements for higher glycol purity, or for better emission control of BTEX.

A typical process flow schematic for the DRIZO system is shown in Fig. 9.5. The main difference from the conventional TEG stripping unit is the proprietary separation process in the regenerator overhead where the oil is separated from the aqueous phase. The aqueous phase, containing the entrained glycol, is refluxed to the regenerator. The hydrocarbon phase is removed, heated, filtered,

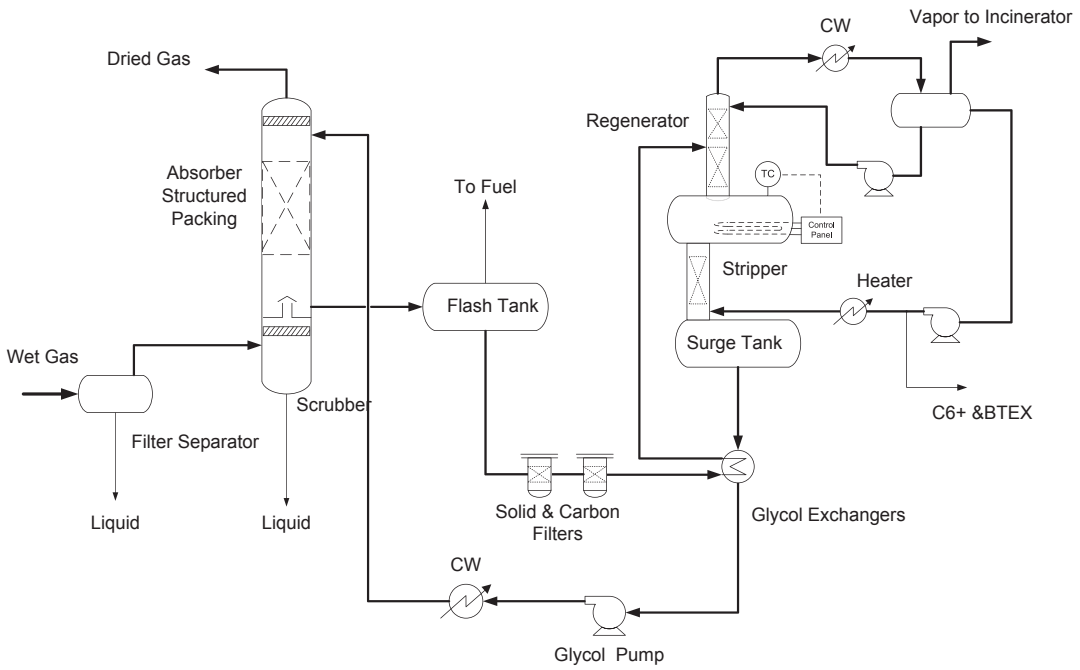

FIGURE 9.5

A typical flow diagram for a DRIZO dehydration system.

and used as the stripping gas for TEG regeneration. Purity of the lean glycol can be controlled by adjusting the amount of stripping gas recycle and the regeneration temperature.

There are other solvent stripping processes that can be used to improve the glycol purity without the use of stripping gas. There are two basic processes that can be used for glycol regeneration. One is the vacuum based process that uses vacuum pressure to reduce the partial pressure of water in the lean glycol. The other one is the "Coldfinger" process which uses a condenser to condense and collect water/hydrocarbons from the reboiler vapor phase and remove them from the reboiler that can be applied to a glycol regeneration system to accomplish the higher glycol purity. The Coldfinger process can achieve a TEG concentration of approximately 99.96 wt%. Table 9.1 compares the water depression performance of these processes.

Table 9.1 Characteristics of Glycol Regeneration Processes (GPSA, 2004)

Regeneration Process	TEG Purity, wt%	Water Dew Point Depression, °F
Vacuum	99.2 to 99.9	100 to 150
Coldfinger	99.96	100 to 150
DRIZO	99.99+	180 to 220
Stripping Gas	99.2 to 99.98	100 to 150

9.3.3 GLYCOL INJECTION PROCESS

Wet gas can be chilled to meet pipeline water as well as hydrocarbon dew point specification using the glycol injection process, which includes propane refrigeration for chilling. Glycol injection is preferred by most pipeline operators because of its simplicity. The process flow schematic for a glycol injection dehydration system is shown in Fig. 9.6.

Glycol injection systems are the lower cost option than TEG dehydration unit or fixed bed dehydration systems. The lowest temperature at which ethylene glycol injection units can be operated is −30°F. Below this temperature, the viscosity of glycol becomes too high for good phase separation. Beyond this temperature, methanol injection or other dehydration techniques should be considered.

Glycol has limited solubility in the gas phase so the glycol must be carefully distributed to each heat exchanger tube to ensure that an adequate amount is present in each tube to prevent hydrate formation. The spray system is critical in the design of heat exchangers with glycol injection. The potential problems include:

- incomplete coverage of all heat exchanger tubes with glycol spray, resulting in hydrate formation and plugging in some tubes,
- inadequate mist formation by the injection system, resulting in uneven glycol distribution, and
- plugging of the spray nozzles.

A well-designed glycol injection dehydration system should provide sufficient glycol delivery pressure from the glycol regeneration unit for an even spray pattern. There is a direct correlation between the glycol flow and the differential pressure across the nozzle. Therefore, both flow and differential pressure indication must be provided for monitoring spray performance. If there is a decrease in flow, this may be an indication that the spray nozzles are plugged. Filters provided upstream of the spray nozzles can avoid plugging of the spray heads.

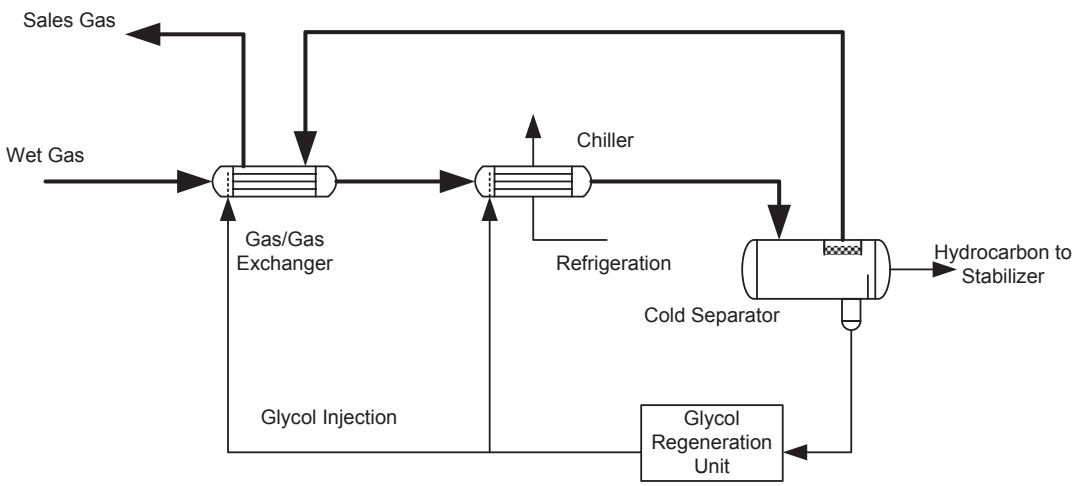

FIGURE 9.6

A typical flow diagram for glycol injection dehydration system.

9.3.4 HEAT EXCHANGER DESIGN FOR GLYCOL INJECTION

The tube side inlet nozzle of the gas−gas exchanger is typically designed with a cone inlet channel designed with a specific angle and oriented in an axial position. A cone inlet channel provides a better distribution of gas compared to a conventional radial nozzle. In addition, a cone inlet channel helps to maintain a uniform gas velocity profile so that the glycol spray pattern is not distorted. This allows for even glycol distribution.

The glycol spray systems are designed to have sufficient pressure drop across the nozzles for good atomization of the injected glycol and even coverage of the exchanger tubes. When glycol is sprayed onto the tube sheet and the glycol solution is cooled, the viscosity of the glycol solution increases. As the hydrocarbon starts condensing, the flow regime of the three-phase mixture changes, which affects heat transfer, pressure drop, and emulsion forming tendencies. These factors must be considered in the detailed design of these heat exchangers. The design techniques for these exchangers are based on empirical data.

Factors that must be considered in the design of these heat exchangers include:

- the effect of glycol on the pressure drop of the heat exchanger,
- he reduction in heat transfer due to the presence of glycol,
- continuous changes in the flow regime across the heat exchanger tubes,
- maximum allowable tube length as a function of tube diameter,
- maximum allowable velocity to prevent emulsion formation, and
- minimum allowable velocity to maintain the glycol in the annular flow regime.

9.3.5 TEG UNIT DESIGN CONSIDERATIONS

General equipment design guidelines of TEG dehydration unit can be found in the GPSA (2004) Engineering Data Book. Followings are some of the key design parameters that the designer should be aware of in the design of the TEG absorber and the regenerator.

9.3.5.1 Glycol Circulate Rate

The amount of water to be removed in a TEG dehydration system is calculated from the gas flow rate, the water content of incoming gas, and the desired water content of outgoing gas. The water removal rate, assuming the inlet gas is water saturated, can be determined as:

$$W_r = \frac{Q_G(W_i - W_o)}{24} \tag{9.2}$$

where W_r is water removed, lb/hr; W_i is the water content of inlet gas, lb/MMscf; W_o is the water content of outlet gas, lb/MMscf; and Q_G is the gas flow rate, MMscfd.

The glycol circulation rate is determined on the basis of the amount of water to be removed, and is usually between 2 and 6 gallons of TEG per pound of water which depends on the number of equilibrium stages in the absorber. For absorber with more than three equilibrium stages (a typical absorber design), 3 gallons TEG/lb water is sufficient.

Higher circulation rates provide little additional dehydration benefit while increasing reboiler heating duty and pumping requirements. The heat required by the reboiler is directly proportional to the glycol circulation rate. Therefore, an increase in circulation rate may decrease the reboiler

temperature, lowering lean glycol concentration, and actually decrease the amount of water that is removed by the glycol. On the other hand, problems can arise if the TEG circulation rate is insufficient; therefore, a certain amount of over design is required to accommodate changes in feed gas conditions. An optimal circulation rate for each dehydration unit typically ranges from 10% to 30% above the minimum glycol circulation rate (EPA430-B-03-013, 2003). The minimum glycol circulation rate can be calculated as:

$$Q_{TEG,min} = G \times W_r \tag{9.3}$$

where $Q_{TEG,min}$ is the minimum TEG circulation rate (gal TEG/hr) and G is the glycol-to-water ratio (gal TEG/lb water removed).

Fig. 9.7 shows the effect of TEG circulation rate on water removal for an absorber with 2.5 equilibrium stages, at various glycol concentration levels. Note that the water removal curves become relatively flat at glycol circulation rates of 3−3.5 gal/lbm water.

9.3.5.2 Glycol Purity

TEG purity can be controlled by the reboiler temperature and pressure in the regenerator. If necessary, the use of a stripping gas can remove the residual water in the lean glycol to produce a very lean glycol.

Fig. 9.8 shows the relationship of regenerator reboiler temperature and glycol purity. The reboiler temperature for the TEG regenerator is typically limited to about 400°F to minimize glycol degradation. Consequently, this temperature limits the lean glycol concentration to between 98.5% and 98.9%. Some operators limit the reboiler temperature to between 370°F and 390°F. If higher purity is required to meet stringent pipeline dew point specification, stripping gas may be necessary.

The effect of stripping gas on glycol purity is shown in Fig. 9.9. As can been seen, when the number of equilibrium stages is greater than three, increasing stripping gas can improve the glycol purity to as high as 99.95%. While stripping gas can be used to meet water specification of the product gas, they should be used only if the TEG dehydration unit fails to meet specifications. The use of stripping gas

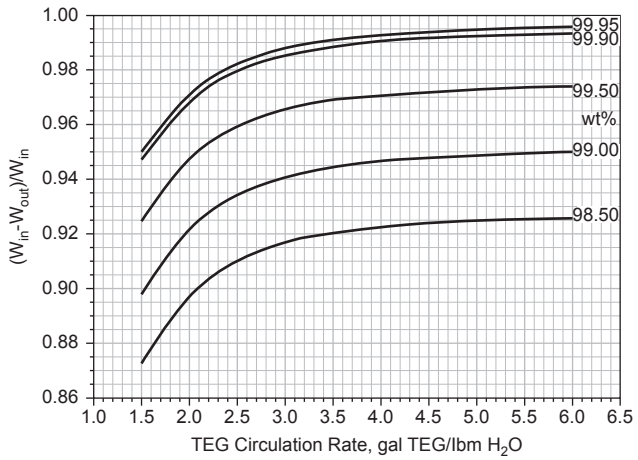

FIGURE 9.7

Effect of TEG concentration and circulation rate on water removal (N = 2.5) (GPSA, 2004).

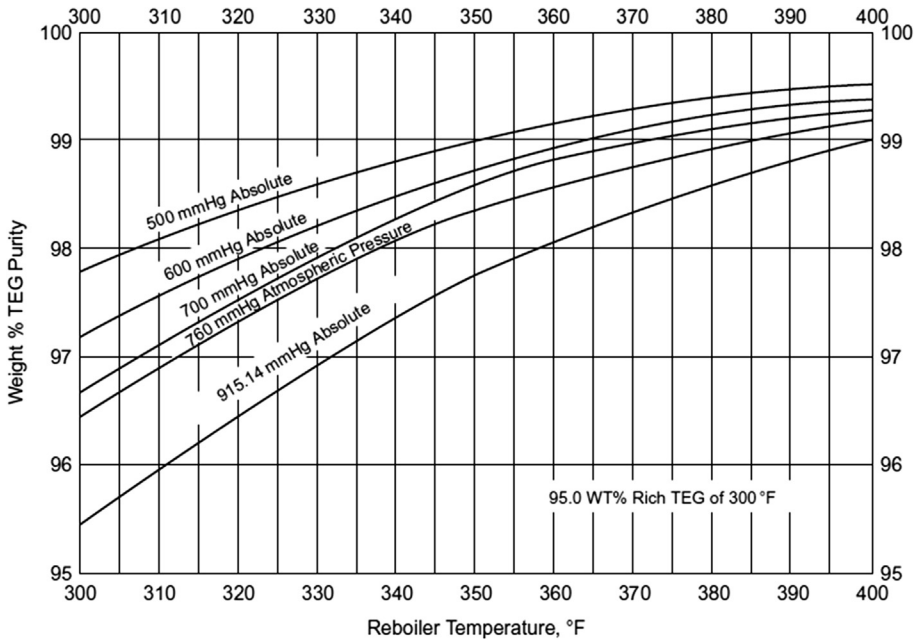

FIGURE 9.8

Glycol purity versus reboiler temperature at different levels of vacuum (GPSA, 2004).

generates another gaseous waste stream. TEG overhead vapor is considered as a source of emissions. The offgas is typically sent to an incinerator to comply with VOC permits or recycled to the front section of the unit.

9.3.6 OPERATIONAL PROBLEMS

The operational problems of a TEG dehydration unit are typically related to the nonperformance of the absorber and regenerator, and summarized in the following sections.

9.3.6.1 Absorber

The main problems with the glycol absorber are described in the following sections.

9.3.6.1.1 High Feed Gas Temperature

Feed gas temperature higher than the design value has two negative impacts. First, the feed gas would contain more water at the higher temperature. Secondly, the absorber will operate at a higher temperature which is unfavorable for the glycol−water equilibrium, reducing the dehydration capacity of glycol. To minimize the water content to the TEG dehydration unit, particularly in hot climate areas, feed gas should be first cooled with a chilled water system. A chilled water system can easily cool the feed gas to about 70°F, at which the bulk of its water content is condensed and can be removed.

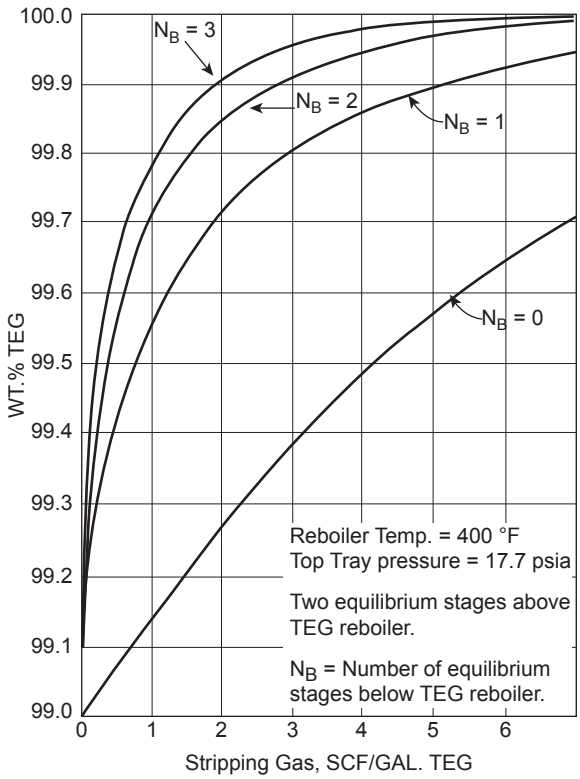

FIGURE 9.9

Effect of stripping gas on TEG concentration.

9.3.6.1.2 Foaming Problems

TEG foaming in contactor (absorber) will result in disruption of downstream operation. It is typically caused by dirty glycol and contaminants such as hydrocarbon condensate, well treating chemicals, salts, and pipe scales. To minimize this problem, the glycol must be maintained clean with filtration. This would require filtering 10% of the circulation flow through a mechanical (solid) filter and a carbon filter. Pressure drop across the filters should be monitored and the filters changed out as needed. The feed gas inlet separator should also be monitored to avoid contaminants from entering the glycol system.

9.3.6.1.3 BTEX Content in Feed Gas

BTEX hydrocarbons are soluble in TEG, which is an environmental problem, as the absorbed gas is released to the atmosphere from the glycol regenerator. To avoid venting BTEX, glycol dehydration unit must send the overhead offgas to an incinerator to destroy the BTEX components. BTEX absorption can be minimized by using more equilibrium stages in the absorber, which would lower the glycol circulation and reduce the BTEX absorption. Alternatively, the absorbed BTEX can be recovered as a liquid byproduct with the DRIZO unit discussed in the previous section.

9.3.6.2 Regenerator

The main problem with the glycol regenerator is high glycol losses, which can be contributed by entrainment and high overhead temperature. The equilibrium glycol in the overhead gas increases significantly at higher temperatures, particularly higher than 250°F. However, low overhead temperatures can also be a problem. Low overhead temperatures, especially during winter operation, may result in excessive water condensation, and may cause column flooding. The water balance of the glycol system must be monitored and excess water must be purged from the overhead.

The glycol regenerator design and heating duty must match the glycol flow. If the glycol circulation exceeds the regeneration duty, it will not help the dehydration process. Overcirculation without the required heating duty will lower the regenerator temperature, making it unable to produce the glycol purity required for drying.

9.3.6.3 Reboiler

The main problems with the glycol reboiler are:

Carryover of Brine Solutions—Contaminants from the field operation can lead to buildup of salts in the glycol reboiler system. Sodium salts (typically sodium chloride, NaCl) are a source of problem in the reboiler. The salt will precipitate from the solution at the reboiler temperatures of 350−400°F, and can deposit on the reboiler tube, reducing the heat exchanger performance and may cause corrosion. The salt content in the glycol reboiler system should be maintained at no more than 1% by removal of some of the glycol content.

Glycol Degradation—Glycol degradation is caused primarily by oxidation or thermal degradation. Glycol readily oxidizes to form corrosive acids. Oxygen can enter the system with incoming gas, from unblanketed storage tanks or sumps, and through packing glands. The oxidation problem can be eliminated by blanketing with fuel gas or inert gas. Thermal degradation can be reduced by proper filtration and maintenance of equipment.

Acid Gas—H_2S and CO_2 are absorbed by glycol to some degrees and may cause corrosion in the reboiler and the regenerator overhead system. Typically, the reboiler and overhead system should be constructed of stainless steel or other suitable materials to resist acid gas corrosion.

9.3.7 FUTURE TECHNOLOGY DEVELOPMENTS

Glycol dehydration will continue to be a workhorse in the gas processing industry due to proven record and relatively low cost. So far, most of the research works are carried on glycol−BTEX equilibrium and design that produce high purity glycol to meet deep water dew pointing requirement. Future developments most likely will be on standardization and modular design that can be prefabricated to meet the accelerating shale gas field development.

9.4 SOLID BED DEHYDRATION

Solid bed dehydration is the process where a solid desiccant (adsorbent) is used for the removal of water vapor from a gas stream to meet water dew points less than −40°F. The desiccant material becomes saturated as moisture is adsorbed onto its surface. A good desiccant should therefore have the greatest surface area available for adsorption.

The mechanisms of adsorption on a desiccant surface are of two types: physical and chemical. In physical adsorption (or physisorption), the bonding between the adsorbed species and the solid-phase hold liquids (condensed water vapors) and solids together give them their structure. In chemical adsorption, involving a chemical reaction that is termed "chemisorption," a much stronger chemical bonding occurs between the surface and the adsorbed molecules. Chemical adsorption processes find very limited application in gas processing. This section considers only physical adsorption, and all references to adsorption mean physical adsorption.

Physical adsorption is an equilibrium process, where for a given vapor-phase concentration (partial pressure) and temperature, an equilibrium concentration exists on the adsorbent surface that is the maximum concentration of the adsorbate on the surface. The measurement of the amount of gaseous compound adsorbed over a range of partial pressures at a single (fixed) temperature results in a graph known as an adsorption isotherm, which can have very different shapes depending on the type of adsorbent, the type of adsorbate, and intermolecular interactions between the adsorbate and the adsorbent surface. In addition to concentration (i.e., partial pressure for gases), two properties of the adsorbate (polarity and size) dictate its concentration on the adsorbent surface (Kidnay and Parrish, 2006).

9.4.1 ADSORPTION CAPACITY

Adsorption capacity (or loading) is the amount of adsorbate taken up by the adsorbent per unit mass (or volume) of the adsorbent.[1] The adsorption capacity of a solid desiccant for water is expressed as the mass of water adsorbed per mass of desiccant. There are three water-adsorption capacity terms used as follows (Campbell, 2000):

- *Static equilibrium capacity*: the water capacity of a new (fresh) solid desiccant (usually expressed in weight percent) as determined in an equilibrium cell at a fixed temperature and 100% relative humidity.
- *Dynamic equilibrium capacity*: the water capacity of solid desiccant as the fluid is flowing through the desiccant at the design flow rate, temperature, and pressure.
- *Useful capacity:* the design capacity that accounts for the loss of solid desiccant capacity with time due to the fact that the total desiccant bed cannot be fully utilized.

The static adsorption capacity is greater than the dynamic adsorption capacity. The dynamic equilibrium loading is generally 50%−70% of the static equilibrium capacity. The static adsorption capacity is the maximum theoretical capacity of the desiccant and can be used for comparison of different desiccants while the dynamic adsorption capacity is used to calculate the required filling amount of adsorbents.

The dynamic moisture adsorption capacity of a desiccant depends on a number of factors, such as the relative humidity of the inlet gas, the gas flow rate, the temperature of the adsorption zone, the mesh size of the adsorbent, and the length of service and degree of desiccant degradation, and not the least on the type of desiccant. Moisture adsorption capacity is not materially affected by variations in pressure except where pressure may affect the other variables previously listed.

[1]Adsorption capacity is of great importance to the capital cost because it dictates the amount of adsorbent required, which also fixes the volume of the adsorber vessels.

9.4.2 ADSORBENT SELECTION

A variety of solid desiccants is available in the market for specific applications. Some are good only for dehydration of natural gas and natural gas liquids (NGLs) while others are capable of performing simultaneous dehydration and desulfurization/hydrocarbon dew point controlling. The selection of proper desiccant depends on the given application and sometimes is a complex problem. For solid desiccants used in gas dehydration, the following properties are desirable (Campbell, 2000; Daiminger and Lind, 2004):

1. High adsorption capacity—this reduces the adsorbent volume, requiring smaller vessels, resulting in lower capital and operating costs.
2. High selectivity—this permits removal of only the undesirable components and reduces operating expenses.
3. Easy regeneration—low regeneration temperature reduces the heating requirement for solid desiccant regeneration.
4. Low pressure drop design—this makes more pressure available for the turboexpander operation in an NGL recovery process.
5. Good mechanical integrity—high crush strength, low attrition, low dust formation, and high stability against aging reduce the frequency of adsorbent change-out and downtime-related losses in production.
6. Environmental friendly properties—the materials should be noncorrosive, nontoxic, and chemically inert to permit safe handling.
7. Reasonable adsorbent price.

The common commercial adsorbents used in solid-bed dehydrators (that possess these characteristics in a satisfactory manner) are molecular sieves, silica gels, and activated alumina, which are described in the following sections.

9.4.2.1 Molecular Sieves

Molecular sieves or zeolites are crystalline alkali metal alumino-silicates with a typical structure of the form $M_{x/n}[(AlO_2)_x(SiO_2)_y]zH_2O$, where n is the valence of the cation and M is the metal ion inside each aluminosilicate cage. The zeolite is a three dimensional tetrahedral structure of silica and alumina. The alumina tetrahedra carry a net negative charge, and need to be balanced by a cation such as Na^+. The tetrahedra build up to form a truncated octahedra, which are either stacked in a cubic structure to make the A type zeolite, or in a tetrahedral structure to make X type zeolite (Fig. 9.10).

In the zeolite structure, the cations determine the pore opening size, and depending on the type of cation, molecular sieves with a specific pore opening can be created (Table 9.2). The benefit of having an adsorbent with a specific pore opening can be seen when observing nominal diameters of typical molecules within a hydrocarbon feed stream. To be efficiently adsorbed, the polar molecules must be small enough to enter the cavities via their pores. Hence, water molecule (with the nominal size of 2.6 Å) can be adsorbed on 3A, 4A, 5A, and 13X molecular sieves.

Molecular sieve is the most versatile adsorbent because it can be manufactured for a specific pore size, depending on the application. Molecular sieves are the only choice for natural gas dehydration to cryogenic processing standards (less than 0.1 ppmv water or −150°F dew point). Molecular sieves can also provide a solution for removal of carbon dioxide and sulfur compounds such as hydrogen sulfide,

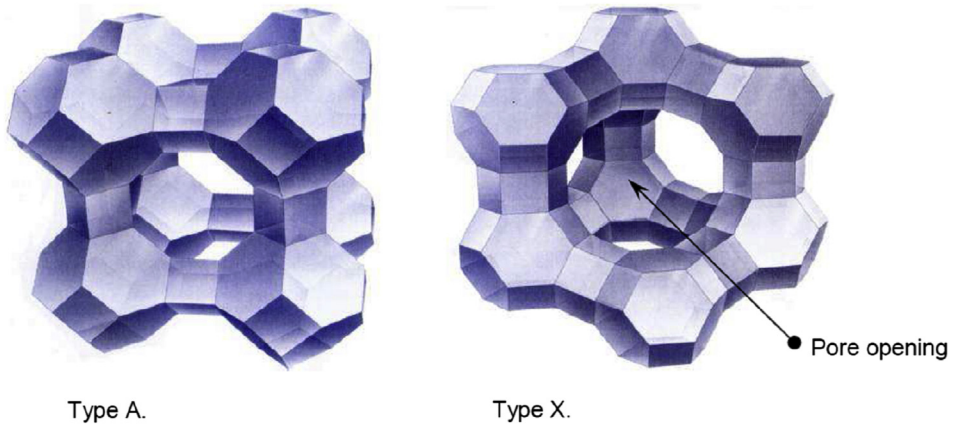

FIGURE 9.10

Molecular sieve types A and X structures (Secker and Zafirakis, 2011).

Table 9.2 Most Common Types of Molecular Sieves (Angstrom = 10^{-10} m)

Zeolite Type	Cation	Nominal Pore Size (Angstrom)	Measured Pore Size (Angstrom)
A	K	3	3.3
	Na	4	3.9
	Ca	5	4.3
X	Na	10	7.4–12.5

mercaptans, carbonyl sulfide,[2] and other sulfides (with the exception of carbon disulfide[3]) from natural gas and NGLs to very low outlet specifications, either as a stand-alone unit or as a polishing unit within a combination of gas treating processes. The applicability of a molecular sieve unit for sweetening purposes will be based on the required outlet specification for the product stream, and the level of contaminants and operating conditions of the feed (see Table 9.3).

The choice of molecular sieve type depends on the type and concentration of contaminants in the feed gas. Depending on the type of feed and species to be removed, the different grades of adsorbents can be selected based on the general guideline shown in Fig. 9.11.

The adsorption characteristics of the different molecular sieve sizes can be summarized as follows:

- In general, type 4A is the most common sieve for dehydration of gases and liquids, but the smaller pore 3A is sometimes preferred to standard 4A for minimizing coadsorption of CO_2 and H_2S. If both oxygen and H_2S are present, 3A reduces the production of elemental sulfur that can block the

[2]Although carbonyl sulfide can be adsorbed on zeolites, its adsorption kinetics is very poor and it will slip very fast through the molecular sieve vessel.

[3]As carbon and sulfur have the same electronegativity, carbon disulfide cannot be polarized and therefore is not adsorbed by molecular sieves.

Table 9.3 Typical Feed and Product Limits of Molecular Sieve Units (Secker and Zafirakis, 2011)

Process	Feed Quality	Product Specification
Gas Drying	0%−100% relative humidity	<0.1 ppmv
Gas Sweetening	<500 ppmv	1 ppmv for each sulfur compound
Liquid Sweetening	<2000 ppmw	Copper Strip 1A
CO_2 Removal	<2% vol	<1 ppmv

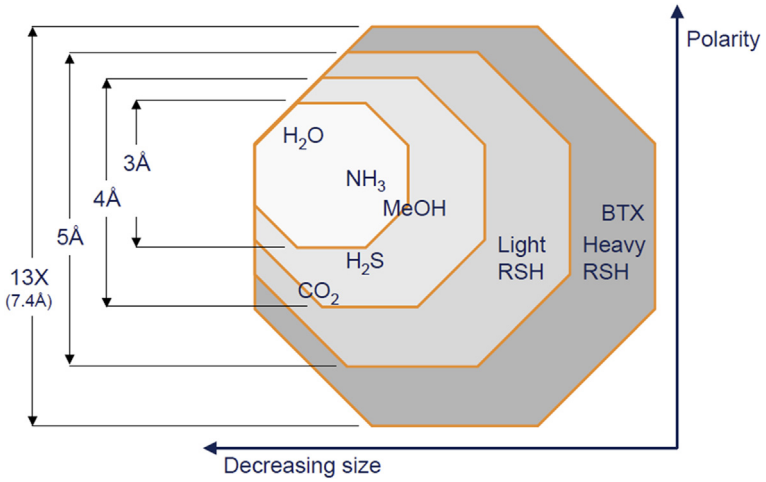

FIGURE 9.11

Molecular sieves selection chart (Meyer, 2011).

adsorbent pores. The 3A form is normally used to treat reactive streams such as olefins since it excludes most molecules except water. It is also widely used for alcohol dehydration since it excludes the highly polar alcohol molecule.

- Molecular sieves 5A and 13X are commonly used for desulfurization (5A for light sulfur while 13X for heavy and branched sulfur species). Type 13X has larger pore openings and therefore has better kinetics than type 5A; however, coadsorption of BTX (benzene, toluene, and xylene) components, which can block pores and deactivate the molecular sieve, may hinder heavy mercaptans removal (Mokhatab and Meyer, 2009).

It is sometimes better to use a compound bed with successive layers of molecular sieves for adsorbing the different impurities. This combination increases the useful capacity of the bed, which is typically the case when water, H_2S, mercaptans, and other sulfur species need to be removed at the same time.

When CO_2 is present in the feed gas, the molecular sieve may promote the hydrolysis reaction of H_2S and CO_2 to form carbonyl sulfide (COS). COS is a main concern as it can be later converted back to H_2S in the presence of water, causing corrosion and emission problems. Molecular sieve manufacturers have developed specific products, which are 3A-based, for minimizing the COS reaction.

9.4.2.2 Silica Gels

Silica gel is a generic name for a gel manufactured by adding aqueous sodium silicate to sulfuric acid. It is an amorphous product similar to alumina. There are different grades of silica gel commercially available for natural gas drying. Silica gels can be used for heavy hydrocarbon and water removal to meet a water dew point of −40°F or lower with specialty grades silica gel.

Silica gel can be used to process sour gases, but not alkaline materials such as caustic or ammonia. Although there is no reaction with H_2S, sulfur can deposit and block their surface pores. The H_2S content in the feed gas should stay below 5%.

Generic grades of silica gel will break up when exposed to liquid water; however, there are specialty grades commercially available that are more liquid water stable. Engelhard (now acquired by BASF) manufactures an improved silica gel called Sorbead, which is supposed to have a higher performance in heavy hydrocarbons and water removal than generic silica gel.

Silica gel is typically used in feed gas pretreatment units for removal of trace components of heavy hydrocarbons and water, such as feed gas to a membrane separation unit, or conditioning flash gas to the fuel gas system. It is not used in drying feed gas to NGL and LNG production plants because of its lower adsorption capacity, and inability to meet low water dew point.

The adsorption capacity of silica gel is typically exhausted in a short time, in the range of dozen of minutes up to 2−3 h,[4] which increases the number of adsorption cycles and reduces the life time of the silica gel (Kane et al., 2004).

9.4.2.3 Activated Alumina

A hydrated form of aluminum oxide ($Al_2O_3 \cdot 3H_2O$), alumina, is the least expensive adsorbent for gas dehydration. Alumina is alkaline which should not be used for drying gas with high concentrations of acid gases (CO_2 and H_2S). Alumina does not have a precise pore opening the way molecular sieves do. Consequently, it is not selective since more molecules have access to the active sites.

There are several types of alumina available for use as a solid desiccant. Activated alumina is a manufactured or naturally occurring form of aluminum oxide that is activated by heating. The structure of the product is amorphous rather than crystalline. Activated alumina holds onto water less strongly than molecular sieves and therefore requires lower regeneration temperature and less regeneration heat duty. Similar to molecular sieves, feed temperature should be kept at below 120°F to avoid overloading the adsorbents.

Activated alumina is typically used to dry a wet lean natural gas to a dew point of −60°F. Activated alumina has a higher equilibrium water capacity than molecular sieves. It can adsorb water of 35%−40% of its own weight. Activated alumina is usually applied as a top layer on the molecular sieves to reduce cost, and to protect the molecular sieves.

9.4.2.4 Comparison of Different Adsorbents

Table 9.4 summarizes some of the key properties of the three solid desiccants mentioned previously. These properties are for comparison purposes and may differ among solid desiccant manufacturers. Note, the selection of these solids desiccants depends on economics. The aluminas have the lowest cost

[4]The adsorption cycle times of the silica gels are very short due to lower useful capacity of the desiccant for hydrocarbons relative to water. Hence, the silica gel units are often called “short cycle” or “quick cycle” units.

Table 9.4 Properties of Solid Desiccants (Campbell, 2000)

Desiccant	Silica Gel	Activated Alumina	Molecular Sieves
Pore diameter, Å	10–90	15	3, 4, 5, 10
Water dew point, °F	−40 to −60	−60 to −90	−150 to −300
Bulk density, lb/ft^3	45	44–48	43–47
Heat capacity, Btu/lb°F	0.22	0.24	0.23
Design capacity, wt%	4–20	11–15	8–16
Regeneration stream temperature, °F	300–500	350–500	425–550
Heat of adsorption, Btu/lb	—	—	1800

per unit of dehydration capacity. The silica gels are next. Molecular sieves are the most expensive and must be justified by their special characteristics.

9.4.3 ADSORPTION TECHNOLOGY

9.4.3.1 Adsorption Principle

There is an equilibrium relationship between the fluid and the solid adsorbents in the mass transfer applications, which can be expressed in the form of isotherms as shown in Fig. 9.12. As the isotherm shows, the concentration of the adsorbate, which in this case would be water, is a function of the concentration of water in the fluid phase and the adsorbing temperature.

The level to which gas is dried is a function of the regeneration conditions. A thoroughly regenerated bed will be in equilibrium with the gas used for regeneration. The concentration of water left on the bed at the end of the regeneration cycle determines the performance of the bed because the outlet gas will be in equilibrium with the last particle of adsorbent. The adsorption process is dynamic as the adsorbent removes the water content from a continuously flowing stream. This process is intrinsically an unsteady state operation.

In commercial practice, adsorption is carried out in a vertical, fixed bed of adsorbent, with the feed gas flowing down through the bed (Fig. 9.13). The feed gas entering the bed from the top and the upper zone becomes saturated first, where equilibrium between the water partial pressure in the gas and the water adsorbed on the desiccant is established and no additional adsorption occurs. This zone is called equilibrium zone (EZ).

With the adsorption going on, the EZ will grow and more and more water will be adsorbed. The length of the adsorber bed across which the concentration of the adsorbate is reduced from inlet to outlet conditions is known as the mass transfer zone (MTZ). This is simply a zone or section of the bed where a component is transferring its mass from the gas stream to the surface of the solid desiccant.

The nonutilized zone (NZ) is the part of the bed that has not encountered water yet because all water molecules were adsorbed in the EZ and MTZ. This zone will only serve for drying when the EZ and MTZ have lost their adsorption capacity.

As the flow of gas continues, the mass transfer zone moves downward through the bed and water displaces the previously adsorbed gases until finally the entire bed is saturated with water vapor. When

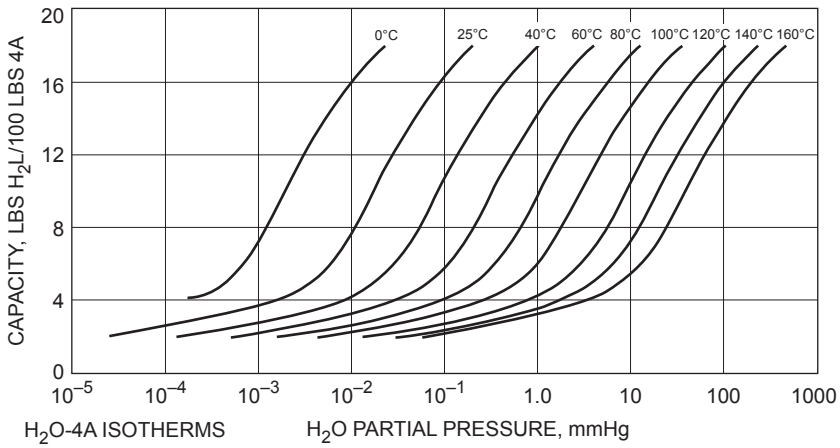

FIGURE 9.12

Typical water adsorption isotherms of a 4A molecular sieve (Trent, 2012).

the leading edge of the MTZ reaches the end of the bed, breakthrough occurs (see Fig. 9.14). At this time, the adsorber vessel should be switched to the regeneration mode.

9.4.3.2 Solid Bed Design Considerations

Optimization of solid desiccant bed size is a key factor in reducing the overall cost of a solid bed dehydration unit. For a given performance, shorter beds mean smaller vessels and lower utility requirements. However, adsorbent requirements must be sufficient to accommodate the equilibrium section as well as the mass-transfer zone length. The MTZ is usually assumed to form quickly in the adsorption bed and to have a constant length as it moves through the bed, unless its particle size or shape is changed. The length of the MTZ is mainly a function of the feed flow rate, but is also influenced by the feed composition and temperature, and the adsorbent type, bulk density, particle size and shape. The length of the MTZ is usually 0.5−6 ft, and the gas is in the zone for 0.5−2 s (Trent, 2004). To maximize bed useful capacity, the MTZ needs to be as small as possible because the water loading in this zone is low when compared to the equilibrium (saturation) zone. Normally, the most efficient adsorbent bed will be a tall, thin bed using the smallest particle size that have a larger surface area and thus improves the adsorption kinetics, resulting in a shorter MTZ. This higher bed efficiency has to be paid for by a higher pressure drop. The total pressure drop across an adsorbent bed should not exceed 8−10 psi. The desired bed length to bed diameter ratio should also fall between 2.5 and 6.

Note should be made that compound desiccant beds, which use more than one desiccant size or desiccant type, increase the useful capacity of the bed by increasing the equilibrium capacity or shortening the MTZ, or both. The most common example of a compound bed is the use of large size desiccant at the top of the bed (which minimizes pressure drop and forces on the bed supports) and small size at the bottom, resulting in longer cycle times and/or shorter bed lengths. Another compound desiccant bed application involves the use of activated alumina at the top of the molecular sieve beds. This application has been used in commercial natural gas dryers for decades.

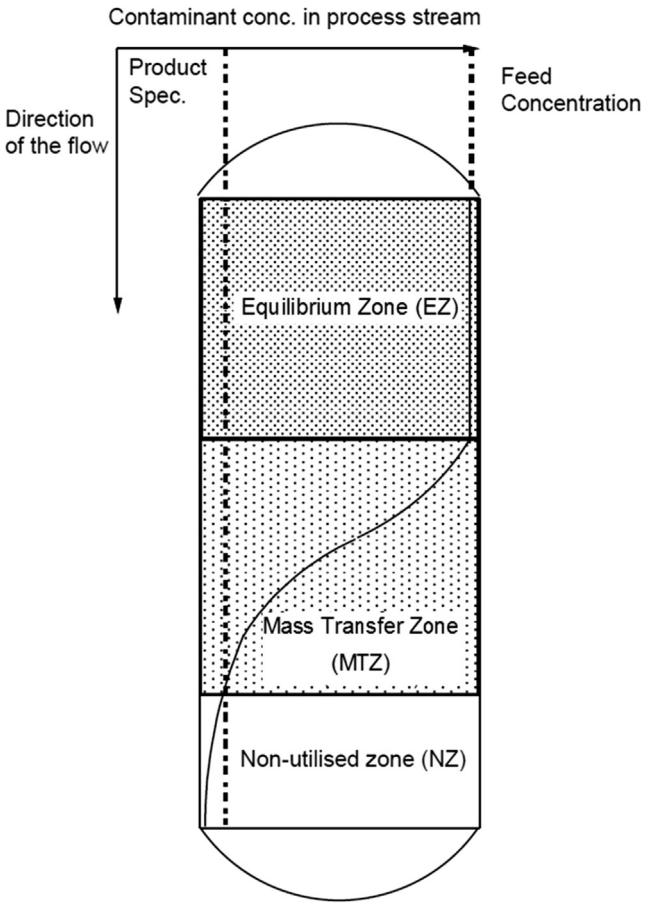

FIGURE 9.13

Schematic of the adsorption zones in an adsorber vessel (Smit et al., 2009).

There are a number of benefits to use an activated alumina/molecular sieve compound bed, including lower overall adsorbent cost and higher resistance to liquid carryover into the bed from upstream separation facilities. Also, activated alumina has a higher static equilibrium capacity for water than molecular sieve when the feed gas is near saturation (as shown by the typical isotherms in Fig. 9.15) as well as a lower heat of adsorption. This results in a higher useful capacity and lower regeneration heating requirements. The higher water capacity of activated alumina also ensures that the mercaptans removal specification will be met by reducing the chance of water breakthrough from a compound bed of activated alumina/different types of molecular sieves (Northrop and Sundaram, 2009).

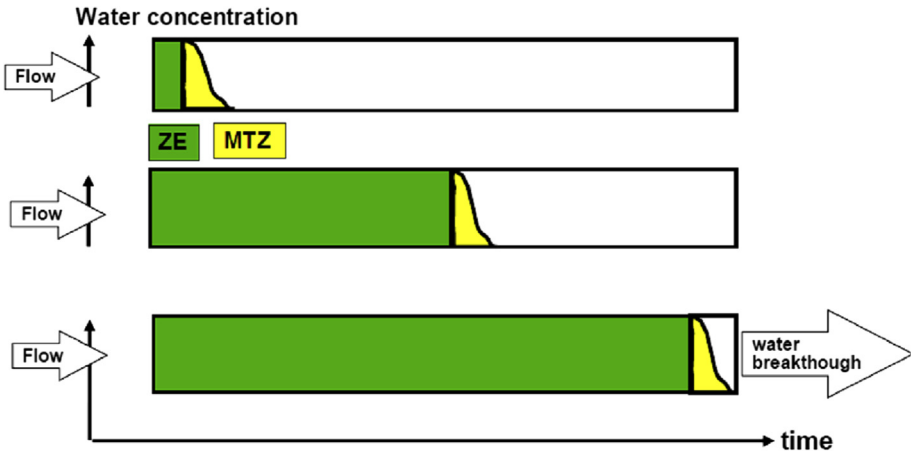

FIGURE 9.14

Variation of adsorption zone front with time (Savary, 2004).

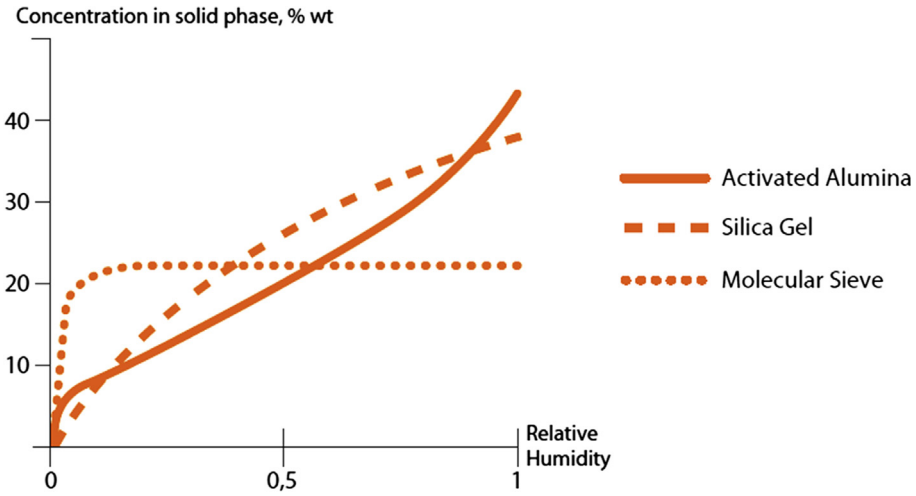

FIGURE 9.15

Typical isotherms of activated alumina, silica gel, and molecular sieve.

9.4.4 OPERATION OF SOLID-BED DEHYDRATOR

Optimizing the performance of the solid-bed dehydration unit requires a detailed understanding of its operation. The process flow schematic of a typical molecular sieve dehydration unit is shown in Fig. 9.16. A picture of the corresponding dehydration unit is shown in Fig. 9.17. The illustrated dehydration system is for a large gas processing plant, which typically consists of four solid-desiccant

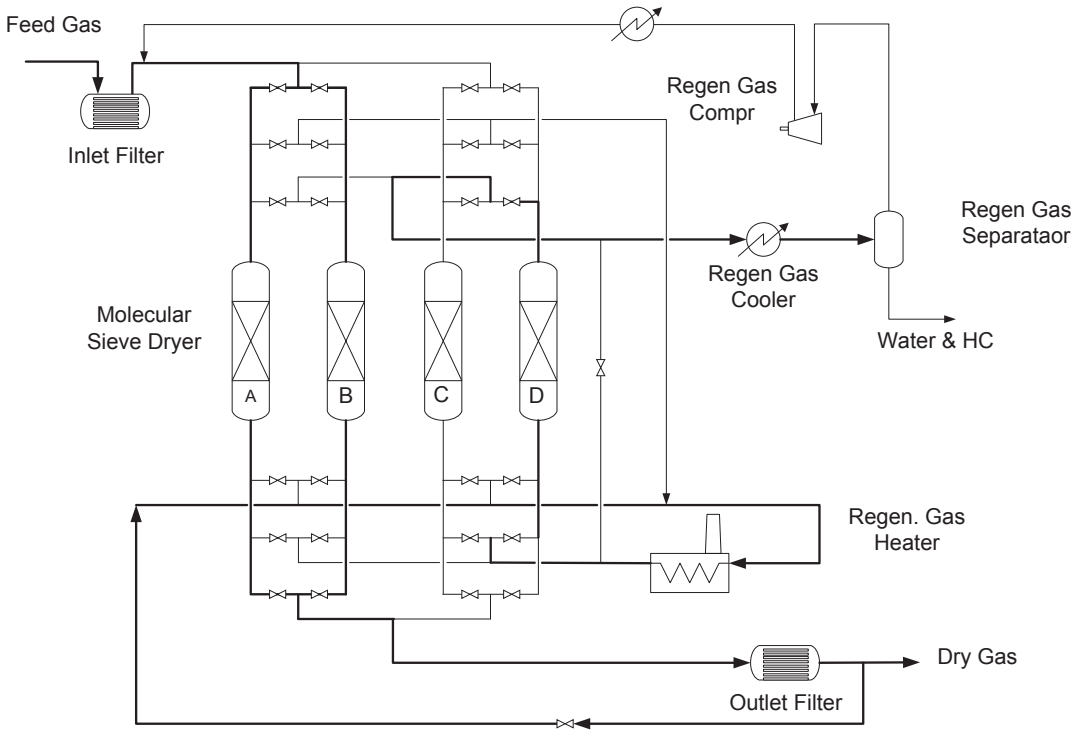

FIGURE 9.16

Process flow schematic of a typical molecular sieve dehydration unit.

beds, packed with molecular sieve and activated alumina. The number of drying beds varies depending on the feed gas flow rate and the mode of operation.

9.4.4.1 3 + 1 Mode of Operation

The dehydrators can operate in a $3 + 1$ mode, i.e., a three parallel beds drying and one bed on regeneration. In fact, three vessels will be on-line removing water vapor from the feed gas while one bed is being regenerated with a slipstream of the dry (product) gas. For example, in processing 600 MMscfd feed gas, three adsorber vessels can be in parallel, handling 200 MMscfd of feed gas each. The advantages of three-bed parallel operation are lower pressure drop and an extended molecular sieve lifetime, due to less frequent regeneration.

The direction of flow for the solid bed gas dehydration system is designed in such a way that the adsorption, depressurizing, and repressurizing steps are downward flow through the bed, and the heating and cooling steps are upward flow. The dehydrator beds are configured to operate under a timed cycle. The control of each step is accomplished using a dedicated programmable logic controller (PLC).

FIGURE 9.17

Four-bed gas dehydration system.

9.4.4.1.1 Adsorption Step

For three-bed parallel operation, the approximate cycle time for adsorption is 18 h followed by a 6 h regeneration cycle. The regeneration is comprised of a 30 min depressurizing step, a 3 h heating step, a 2 h cooling step, and a 30 min repressurizing step. The cycle times are generally set by the molecular sieve vendors and can be adjusted during unit startup. Table 9.5 shows a typical operating sequence of the four-bed dehydration system.

The dry gas leaves the drying beds and enters the outlet filters. The function of these filters is to remove molecular sieve or any other solid particles.

9.4.4.1.2 Depressurization Step

At the completion of the 18 h adsorption cycle, the dehydrator must be depressurized to prepare the environment for the regeneration heating step, which uses dry residue gas at low pressure. The normal depressurization lines for the four dehydrators should have flow restriction orifices to effectively limit the rate of depressurization. In accordance with recommendations from molecular sieve vendors, the depressurization rate should not exceed 75 psi/min to prevent bed movement and fluidization. The gas will flow downward via the restriction orifices in order for the vessel to depressure within the allotted time of 20 min.

Table 9.5 Typical Operating Sequence of the 3 + 1 Bed Dehydration System for a 24 h Cycle

Elapsed time	Bed A	Bed B	Bed C	Bed D
0:20	A	D	A	A
3:15	A	H	A	A
2:05	A	C	A	A
0:20	A	R	A	A
0:20	A	A	D	A
3:15	A	A	H	A
2:05	A	A	C	A
0:20	A	A	R	A
0:20	A	A	A	D
3:15	A	A	A	H
2:05	A	A	A	C
0:20	A	A	A	R
0:20	D	A	A	A
3:15	H	A	A	A
2:05	C	A	A	A
0:20	R	A	A	A

where *A,* adsorption; *C,* cooling; *D,* depressurizing; *H,* heating; *R,* repressurizing.

During the depressurization step, the regeneration gas is compressed in the regeneration compressor and routed through the bypass valve to the regeneration gas cooler where it is cooled. The cooled gas flows to the regeneration gas separator, and returns to the residue gas stream.

9.4.4.1.3 Heating Step

Once the dehydrator has been depressurized, the heating step begins. The residue gas is continuously compressed by the regeneration gas compressors and flows through the bypass valve to the regeneration gas heater. The gas outlet temperature is controlled to 570−600°F. The hot gas flows upwards through the dehydrator being regenerated and heats up the bed to a temperature at which the water content of the molecular sieve is reduced to the required low level.

As a result, the water leaves the surface of the molecular sieve and is removed by the regeneration gas flowing upward through the bed. The heat required to desorb the water from the sieve can be as high as 1800 Btu/lb. The wet regeneration gas is then sent to the regeneration gas cooler. The gas is cooled to ambient temperature to form a two-phase stream; the liquid is the water desorbed from the dehydrator plus liquid hydrocarbons coadsorbed during the drying step. The two-phase stream is then separated in the regeneration gas separator and the vapor is returned to the residue gas line. The condensed water and coadsorbed liquid hydrocarbons are removed from the separator on level control.

9.4.4.1.4 Cooling Step

Following the heating step, the dehydrator is cooled with cold compressed regeneration gas to cool the molecular sieve to the normal adsorption temperature prior to repressurizing and returning it to normal service. The cool gas flows upward through the dehydrator and then to the regeneration gas heater, so that the fired heater can be operated continuously. It is important for the fired heater to operate

Table 9.6 Typical Operating Sequence of a 2 + 2 Bed Dehydration System

Time (hour)	Bed A	Bed B	Bed C	Bed D
6	A	A	C R	D H
12	D H	A	A	C R
18	C R	D H	A	A
24	A	C R	D H	A

continuously to minimize thermal stress on the heating system which would be the case if the heater is completely shutdown during the cooling cycle.

At the beginning of the cooling cycle, the temperature of the gas from the dehydrator outlet to the fired heater is about 540°F. To maintain the minimum fired heater duty required for continuous burner operation, the cold regeneration gas is split, sending about 75% into the dehydrator and 25% to bypass the dehydrator. The two streams combine downstream of the dehydrator before entering the regeneration gas heater. It leaves the heater at about 570−600°F. With these conditions, the burner main fuel valve will remain almost closed most of the time and the burners will be firing near their lower operating point.

9.4.4.1.5 Repressurization Step

After the cooling step, the dehydrator must be pressurized to prepare the vessel to be brought back on-line. The normal repressurization lines for the four dehydrators have flow restriction orifices to effectively limit the rate of repressurization to no more than 75 psi/min downwards.

9.4.4.2 2 + 2 Mode of Operation

The dehydration process can also be arranged in the 2 + 2 mode of operation. In this operating mode, two dehydrators are in the adsorption cycle and two dehydrators are in the regeneration cycle at any given time. In the regeneration cycle, one dehydrator is in the heating cycle and one dehydrator is in the cooling cycle, simultaneously. This allows circulation of the regeneration gas in series, which flows first to the vessel that is being cooled, then to the heater, and finally to the other vessel that is being heated. The flow sequence is shown in Table 9.6.

The regeneration in series reduces the regeneration gas consumption and uses the energy of the dehydrator that is being cooled down. The only drawback is the higher capital cost compared to the 3 + 1 mode, but it provides a more robust operation.

9.4.4.3 Other Modes of Operation

There are other modes of operation, depending on the number of beds and the dehydration unit operating conditions. It can be operated on 2 + 1 mode where two dehydrators are on the adsorption cycle and one dehydrator is on the regeneration and heating cycle. For smaller gas dehydration units, it can be arranged on 1 + 1 mode, with one dehydrator on adsorption cycle and one on regeneration and heating cycle. For smaller solid-bed dehydration units, it may be more economical to use electric heater for sieve regeneration, which would also minimize emissions from the conventional fired heater.

9.4.5 DEHYDRATION UNIT DESIGN CONSIDERATIONS

The capital and operating costs of a solid bed dehydration unit are high, considering the high pressure adsorption beds, the regeneration heater, recycle compressor, and separation system. Some of the design considerations and options are summarized in the following sections.

9.4.5.1 Feed Gas Preconditioning

It is crucial in the operation of a solid-bed dehydration unit to provide an efficient knockout drum to remove any liquid entrainment. Free water can damage the molecular sieves. On the other hand, entrained water droplets can often increase the water load by 200%−300%. The knockout system must also have inlet filter separation equipment to remove solids and pipe scales to the ppm levels.

The water content in the feed gas can be reduced by compression, chilling, and separation. The dehydration unit location in the gas processing plant should be placed at the highest pressure possible, which would reduce the saturated gas water content significantly. If the gas has to be compressed for NGL recovery, the solid-bed dehydrators should be located downstream of the compressors.

9.4.5.2 Feed Gas Chilling

Feed gas to the dehydrators typically comes from the acid gas removal unit and is saturated with water. The treated gas temperature is cooled by lean amine which in turn is cooled by ambient air. In hot climate operation, air temperature in the summer can be very high, consequently impacting the feed gas temperature.

To reduce the water content in the feed gas, the gas to the dehydrators can be cooled with cooling water or a chilled water system. As shown in Fig. 9.1, reducing the feed gas temperature, say by 20°F, can reduce the water content in the gas by 50%. Cooling the feed gas to the lowest possible temperature to about 70°F or before the hydrate point may be the best way to reduce dehydration unit cost. The cooling always helps to remove heavy hydrocarbons and other contaminants that might come in with the feed gas.

The refrigeration step in the feed gas chiller can be by propane refrigeration or can be from the cold residue gas stream from the NGL recovery unit. Potential energy savings by integrating with the other processing units can significantly reduce the cost of the dehydration unit.

9.4.5.3 Pressure Drop

Pressure drop across an adsorber can be a significant cost penalty. It is desirable in an NGL recovery turboexpander unit to provide a high inlet pressure to the NGL distillation column. A high pressure drop in the dehydrator would lower the expansion ratio across the turboexpander and would reduce cooling by the expander, consequently lowering the NGL recovery efficiency. This is the reason of the popularity of the 3 + 1 mode of operation. With three beds operating in parallel rather than two, they result in a lower operating pressure drop. The flow rate to each bed is one third of the total rather than one-half. The pressure drop can be reduced to as low as 3 to 5 psi. The lower flow rate and pressure drop in each bed can also extend the useful life of the adsorbents.

The shape of the molecular sieve can have an impact on pressure drop. The beaded sieve typically has a lower drop than the pellet type, and may reduce up to 20% of the bed pressure drop. However, their performance may not be as predictable as the regular pellet type. The standard pellet shaped molecular sieves are more common due to their proven performance in mass transfer, higher surface area, a shorter diffusion path and mass transfer zone, and consistent physical strength over the other types.

9.4.5.4 Cycle Time

Another obvious area for cost savings is to operate the adsorbers to its water breakthrough point. Molecular sieve deterioration increases with increasing the frequency of molecular sieve regeneration cycle. Each regeneration cycle deposits some carbon due to thermal decomposition of the heavy hydrocarbons from the feed gas. Reducing the number of regeneration cycle by operating the adsorbers to close its water breakthrough point will prolong the life of the molecular sieve. Bed temperatures and moisture analyzers should be used to vary the operation to operate at close to its water breakthrough point.

9.4.5.5 Regeneration Methods

There are two basic ways to regenerate a solid desiccant bed. They are Temperature Swing Adsorption (TSA) and Pressure Swing Adsorption (PSA) in which the change in the adsorption equilibrium is obtained by increasing the temperature and decreasing the pressure, respectively. TSA is generally used for natural gas drying or removal of CO_2 from natural gas streams to meet stringent product specifications. PSA is typically used for drying of air and industrial gases for general use, and not used for natural gas plants where stringent specifications are required.

9.4.5.6 Regeneration Gas Heater

Depending on the mode of operation, the fired heater can be subjected to cyclical operation. A heater is considered cyclical when it is shutoff and then brought back on by reigniting the burners. The three-bed parallel arrangement operates in this manner, since the heater shuts down while the regenerating bed is in the cooling cycle. A heater endures significantly less thermal stress as long as the burners remain on at all times. This is the case for the $2 + 2$ mode of operation where the heater is always kept at its minimum turndown capability. Minimum turndown is defined as the minimum heat release, which can maintain a stable burner flame. The typical heater turndown ratio is 10 to 1.

A cyclical heater has several issues that must be addressed to avoid the thermal stress due to cycling operation. By properly addressing the heater for cyclical operation, the heater can be designed with reliability and durability close to a heater in continuous service.

9.4.5.7 Regeneration Gas Flow Direction

The regeneration gas flow direction for regeneration heating and cooling affects the efficiency of water removal from the molecular sieve bed. For three-bed parallel operation ($3 + 1$ mode of operation), the heating and cooling are in the upflow direction because it results in better overall regeneration than its alternative, heating upflow and cooling downflow. Specifically, upflow cooling ensures good dew point control and prevents the potential leakage of wet feed gas into the cooling gas across a defective switching valve.

For two-bed series operation ($2 + 2$ mode of operation), upflow heating and downflow cooling are typical because the potential leakage of wet feed gas into the cooling gas does not exist for series operation. However, different manufacturers can recommend different flow directions for regeneration heating and cooling to maintain the performance of their molecular sieves.

9.4.5.8 Insulation

Solid desiccant vessels are insulated externally or internally. Internal refractory requires careful installation and curing, usually before the desiccant is installed. It saves energy and can dramatically reduce the required heating and cooling times. This is an important benefit for systems where

regeneration times are limited. However, internal insulation is prone cracking due to thermal stress, which may retain moisture in the cracks during the regeneration cycle, resulting in off-spec product during the absorption cycle.

9.4.5.9 Regeneration Gas Compressor

The pressure ratio across the compressor depends on the required regeneration pressure. The lower pressure improves regeneration but it would also increase the regeneration compressor horsepower. Conversely, increasing the regeneration pressure makes regeneration more difficult and will take longer and higher temperature, but the compression horsepower would be reduced.

The regeneration gas compressor can also be integrated with the upstream facility where there is a recompressor. For example, the stabilizer overhead or stripper overhead in the condensate stabilization unit typically includes an overhead compressor which can be used to recompress the regeneration gas back to the inlet of the acid gas removal unit.

9.4.6 OPERATIONAL PROBLEMS

The molecular sieve design details and operation have been described in the previous sections. Problems associated with molecular sieve operation generally relate to misoperation of the upstream units and improper installation and operation of the molecular sieve beds. The following sections summarize these problems and provide guidelines to mitigate these problems.

9.4.6.1 Inlet Conditions

Often a small change in the inlet temperature can significantly increase the water content in the feed gas, which can impact the solid-bed dehydration system performance (see Fig. 9.1). Also the adsorbents capacity drops as the temperature increases (see Fig. 9.12).

A drop in inlet gas pressure will evaporate more water, increasing its water content. The lower feed pressure will also increase the gas velocity through the bed and will extend mass transfer zone which may result in an earlier breakthrough.

Changes in gas composition should be monitored. If the inlet gas source is changed from lean gas fields to rich gas fields, more liquids can enter the dehydration unit. The slug catcher and inlet separator may not be adequate, allowing more liquid hydrocarbons and water to enter the dehydration unit.

High pressure gas dehydration may reduce the water content in the feed gas, which is advantageous, but may create a different problem. Depending on the feed gas composition, there is a point where hydrocarbon liquid may drop out as the pressure is reduced when transversing the retrograde condensation region. This can result in wetting the adsorbents due to the normal pressure drop gradient throughout the bed. Retrograde condensation is very difficult to predict. A condensate may be detected by a steadily increasing pressure drop during the adsorption cycle due to liquid accumulation on the adsorbent beds. The only solution is to avoid the retrograde region as much as possible by increasing the feed temperature.

9.4.6.2 Contamination

The most frequent cause of solid desiccant bed failure is the incomplete removal of contaminants from the inlet gas. Following is a list of the most common contaminants.

9.4.6.3 Liquid Carryover

Liquid carryover can be due to design deficiency of the feed separator or malfunctioning of the upstream amine treating unit. The cause can also be due to upset of the regeneration gas separator. During system startup or shutdown, the regeneration compressor can surge and can entrain liquid from the regeneration gas separator. In the worst scenario, the liquid (hydrocarbon liquids and water) can flood the dehydrators and pulverize the adsorbents. The sieves can agglomerate and form a paste like substance, as can be seen in Fig. 9.18.

To avoid the liquid carryover, the regenerator gas separator should be designed with an emergency shutdown system with high liquid level alarms that should shut down the compressor and stop the flow to the dehydrator in case of high liquid levels.

As for the adsorbent materials, some manufacturers can provide more robust and liquid tolerant adsorbents that can handle the transient problems and minimize the adsorbent damage.

9.4.6.4 Salt Entrainment

Salt contamination comes from the treating units from salt water bearing formations, or from salt dome storage caverns. Salt will accumulate and block the opening and pores in the sieves. In extreme cases, all the voids between the molecular sieve beads will plug up, resulting in an increase in pressure drop. Eventually, the adsorbent must be replaced.

To minimize the salt content in the feed gas, the design of inlet scrubbers and separators coalescer is extremely important. In some gas plants, water washing of the feed gas coupled with an inlet cooler is used to protect the solid-bed dehydrators.

9.4.6.5 Corrosion Products

Corrosion materials can come from upstream equipment and piping. H_2S in the feed gas can react with carbon steel equipment during regeneration to produce pyrite flakes. These can deposit on the

FIGURE 9.18

Damaged sieve at the bottom of the dehydrator.

molecular sieves surface and can block the bottom outlet screen, which can result in maldistribution among the dehydrators.

The corrosion materials can also deposit on the fire-tube on the regeneration heater which may result in hot spots damaging the heater.

9.4.6.6 Oxygen

If there is any oxygen in the feed gas stream, it may react with H_2S and other sulfur compounds on the molecular sieves surface to form elemental sulfur. In extreme cases, this will not only block macro and micropores but also the spaces between the sieves, resulting in one large "lump" blockage, which is difficult to remove.

Oxygen can also react with heavy hydrocarbons in the feed gas to form coke during the regeneration cycle, causing fouling of the molecular sieves and the regeneration heater.

Oxygen can be present in the feed or enter through the vapor recovery system, or other means. It is a good practice to monitor the oxygen content in the feed gas during daily stream analysis. If trace oxygen is detected initially, the unit can be repaired, and the source can be isolated.

9.4.6.7 Incomplete Regeneration

Insufficient or incomplete regeneration of the adsorbent beds will lead to a sudden loss in adsorption capacity and premature breakthrough. Insufficient adsorbent bed regeneration is a result of one or all of the following factors:

- low regeneration gas flow rate/temperature,
- insufficient regeneration time, and
- change of regeneration gas composition.

To fully regenerate the adsorbents, the inlet and outlet temperatures of the adsorber in the regeneration step should be monitored. In order to make sure the adsorbents are properly regenerated, three points have to be checked:

1. The inlet temperature should reach the temperature required to adequately regenerate the bed (depending on the desiccant type).
2. The outlet temperature should show an almost constant value (during the heating step) for 30−120 min, depending on the vessel size and cycle time (see Fig. 9.19). This is necessary to make sure that the adsorbents near the vessel walls are fully regenerated.
3. The temperature difference between inlet and outlet streams at the end of the heating cycle should not be more than 50−60°F depending on the vessel insulation (see Fig. 9.19).

9.4.6.8 Bed Refluxing

Heating up the adsorber without using a heating ramp or an intermediate heating step may result in a large temperature difference across the bed. During regeneration, as the regeneration gas flows from the bottom to the top, water is desorbed, and readsorbed many times. Often it is carried off at such a rapid rate that it condenses on the cool top head of the vessel and dripped back down onto the bed. This phenomenon is called water refluxing which increases with high pressures and low regeneration flow rates. At some point, the ascending heat zone mixes with the descending water resulting in boiling, which may cause hydrothermal damaging of the molecular sieves. Hydrothermal damaging may alter the binder material and destroy the crystal structure of the zeolite.

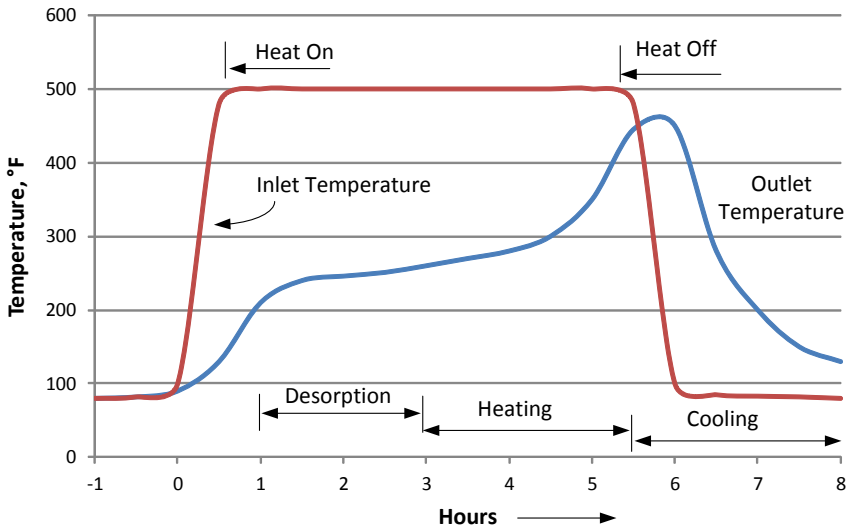

FIGURE 9.19

Typical inlet and outlet temperatures during solid bed regeneration cycle.

In order to prevent hydrothermal damaging of molecular sieves, it is not only important to choose the right formulation of the molecular sieve (binder and zeolite) but the proper regeneration conditions. The adsorbent supplier should be consulted in trouble-shooting the problems. Most suppliers have seen many different misoperations and molecular sieve damages and their experience can save time and money.

9.4.6.9 Improper Bed Loading

The same quantity of each adsorbent grade in each vessel must be used to prevent unequal flow distribution among the different beds to avoid premature breakthrough. For optimum bed loading, the bed may require a mixed bed of large and small particles, typically with the small particles being at the bottom of the bed. If the adsorbents are loaded differently among the beds, the mass transfer zone may be different among beds which may prolong the adsorption time to meet dew point specifications.

9.4.6.10 Unequal Flow Distribution

Sometimes premature breakthrough occurs on only one vessel and this is the case when working with several vessels in adsorption in parallel. If there is a problem with one vessel only it is in general an issue of bed configuration and not of the molecular sieves. Unequal flow distribution due to bed configuration or internal misalignment can be detected by a high pressure drop difference in the vessels during adsorption.

9.4.6.11 Bottom Support

Experience shows that more and more problems of solid bed failure are caused by failure of the support grid. Nevertheless, very often the reason is not the support grid itself but the way how it was installed.

The mechanical design of the support bed must be strong, and the quantity and size of ceramic balls must be according to manufacturer guidelines.

9.4.6.12 Bed Bumping

A rapid depressurization possibly from a sticking valve can lift the bed and even fluidize it. Normally a solid desiccant bed should not be depressurized at a rate greater than 50 psi/minute, and under normal operation the operating pressure must be within 30 psi before the process valves are opened. Bed pumping will crush the molecular sieves making them inoperable. Severe damage may require dumping and replacing the sieves.

9.4.6.13 Switching Valve Leakage

The switching valves on the molecular sieve beds ensure extreme temperature and pressure fluctuation on a daily basis, varying from ambient temperature during the adsorption cycle to 500°F during the regeneration cycle. These cyclic operations impose undue stress on these valves, which may affect the valve performance. If leakage occurs, this may result in off-spec product. The orbit valves are more reliable but they are also expensive. High performance butterfly valves are less costly but more prone to leakage. The switching valves must be monitored and maintained routinely.

9.4.6.14 Moisture Analyzer

To optimize the life of the molecular sieves, reduce energy, and prevent wet gas from contaminating downstream equipment, a highly reliable and rapid-response moisture analyzer is crucial. Some of the recent advances in noncontact laser type detector are now available. The moisture analyzer must be selective so that interferences from other compounds (such as methanol) are eliminated. The response rate of the analyzer must be fast, detecting rapid breakthrough in the molecular sieve beds.

9.4.6.15 Internal Insulation Failure

The internal insulation in the molecular sieve beds also goes through severe thermal stress during the adsorption and regeneration cycles. If the insulation is damaged, moisture may be retained within the insulation, which may be the cause of off-spec products. The insulation should be repaired and replaced as necessary.

9.4.6.16 Molecular Sieve Handling Safety

Many vintage gas processing plants have been operating for many years without any incidents. Typically, the H_2S content of the inlet feed gas has increased over the years. Contractors and staff in these plants must be constantly reminded of the danger and hazards associated with operating a molecular sieve unit.

Typically, during shutdown, molecular sieve units are purged with nitrogen to remove H_2S content from the vessel before entering. However, there are still H_2S that are tightly adsorbed by the molecular sieve. When molecular sieves are changed out, they are usually dumped into water to avoid the pyrophoric reaction. When molecular sieves are in the water, H_2S will be displaced from them, as sieves have higher affinity towards water than H_2S. There were accidents in the past relating to fatality from H_2S poisoning during the change-out operation. The molecule sieve operation program must insist personnel to carry H_2S monitors and escape masks even when the unit feed gas contains low levels of H_2S.

9.5 OTHER GAS DEHYDRATION PROCESSES

Other less frequently used dehydration methods can be applicable to some operations listed in the following.

9.5.1 CALCIUM CHLORIDE

Calcium chloride can be used as a consumable desiccant to dry natural gas. Anhydrous calcium chloride combines with water to form various calcium chloride hydrates. As water absorption continues, calcium chloride is converted to successively higher states of hydration—eventually forming a calcium chloride brine solution. Outlet water contents of 1 lb/MMscf can be achieved with calcium chloride dehydrators.

Calcium chloride dehydrators may offer a viable alternative to glycol units on small feed rate-remote dry gas wells. Calcium chloride must be changed out periodically. Brine disposal is an environmental issue.

9.5.2 METHANOL REFRIGERATION

Dehydration of natural gas to −150°F using methanol as the hydrate inhibitor has been used for ethane recovery in the Empress plant. The condensed water and methanol streams can be decanted in the cryogenic unit and can be separated by distillation. This can be found in a patented process called IFPEX-1.

The difficulty in the methanol refrigeration process is the high methanol losses associated with the high vapor pressure. The process must work with cryogenic temperature refrigeration to minimize losses. The methanol process is more complex in terms of operation than the molecular sieves process, and is seldom used in NGL recovery processes today.

9.5.3 MEMBRANE AND TWISTER

The Membranes and Twister technology can be used to remove water and hydrocarbons from the natural gas to meet water and hydrocarbon dew point specifications of pipeline gas. Please see Chapter 11 for details of the discussions on the membrane separation systems.

9.6 GAS DEHYDRATION PROCESS SELECTION

The natural gas dehydration process is selected based on the water dew point requirements, as shown in Fig. 9.20.

The process selection can be quite straight forward. If dehydration is required only to meet the pipeline specification of 4−7 lb/MMscf, any of the previously mentioned processes can be applicable. Typical glycol dehydration process is suitable for meeting pipeline gas specification as low as −40°F and is more economical than molecular sieves technology. Solid desiccant dehydrators are chosen for deep dehydration to meet a low water dew point for NGL recovery or LNG production. Membrane and Twister processes are suitable for small gas plants and offshore installation where space is limited.

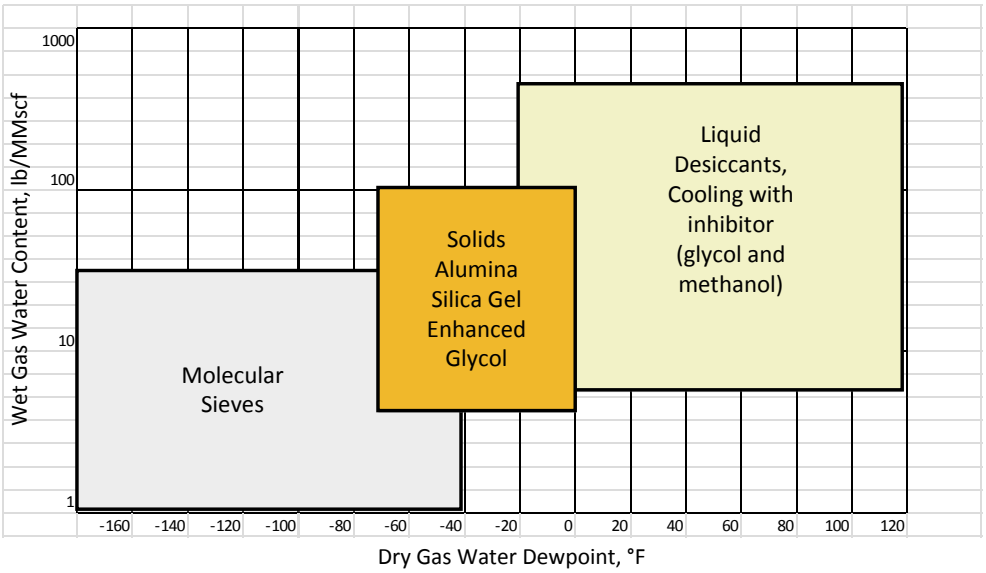

FIGURE 9.20

Gas dehydration technology selection.

If hydrocarbons dew point control is required, cooling with inhibitor, such as the use of ethylene glycol injection with propane chilling or the use of silica gel can be suitable. It can also be accomplished with a TEG dehydration unit followed by propane chilling.

As for the use of silica gel dehydration process, because of its limited short cycle time, it is more suitable for polishing services, such as membrane separator pretreatment, and fuel gas conditioning rather than feed gas to a gas processing plant.

For water dew pointing lower than −40°F and down to −80°F, the enhanced TEG dehydration process, such as DRIZO, is suitable. A TEG dehydration unit is lower in CAPEX and OPEX than the molecular sieve unit, especially for offshore installation where plot space is limited. There are other considerations that may favor the use of molecular sieves. Molecular sieves are selective and do not appreciably adsorb BTEX components hence avoiding the emission problems in conventional TEG dehydration units. However, advances in enhanced glycol dehydration processes, such as the DRIZO system, can solve the problem by production of a BTEX hydrocarbon liquid. Molecular sieves can be designed to remove mercaptans to meet the sulfur specifications. The mercaptans are concentrated in the regeneration gas, and can be selectively removed using a physical solvent process, such as the DEPG process. The mercaptan components can then be converted to sulfur in a Claus sulfur recovery unit to eliminate sulfur emissions.

9.7 MERCAPTANS REMOVAL

Whereas deep removal of carbon dioxide (CO_2) and hydrogen sulfide (H_2S) is now mastered, mercaptans (R−SH) removal from a sour natural gas stream is considered a challenge, depending on the concentrations involved. However, for very sour gas in the Middle East such as that found in the Shah gas processing plant in Abu Dhabi, the new DGA unit has demonstrated some success for treating 30 mol% sour gas contaminated with mercaptans.

The primary motive for removing mercaptans in the gas-processing plant is to meet a maximum total sulfur specification in the treated gas or natural gas liquids. To meet sales gas product specifications, and avoid operating problems with corrosion and damage to downstream equipment, typical total sulfur specifications generally range from 30 to 100 ppmv.

There are several processes for removing mercaptans from natural gas streams. However, it is the acid gas concentrations and the level of mercaptans in the feed gas that will most likely influence the selection of the most appropriate mercaptan removal method (Mokhatab and Northrop, 2017).

9.7.1 GAS TREATING UNIT

In a gas treating line-up, the removal of acid gas and sulfur compounds (H_2S, CO_2, COS, and mercaptans) is required. Removal of these components is commonly carried out by a chemical solvent or physical solvent. The selection of solvent is determined by the richness of the feed gas, the level of treating, and the concentrations of the contaminants. There are other considerations, including the H_2S/CO_2 ratios, organic sulfur content, and heavy hydrocarbons coabsorption, which needs to be assessed when fed to the sulfur recovery units.

Amine can remove some mercaptans via chemical and physical absorption. The removal mechanism varies from system to system and is dependent on the operating conditions and the specific types of mercaptans in the feed gas. From a chemical perspective, mercaptans have acidic properties, like H_2S, but because of the hydrocarbon functional group, they are much weaker acids than H_2S. Mercaptans behave less like acids and more like hydrocarbons as the hydrocarbon chain length increases. Due to their acidic properties, mercaptans chemically react with amines, but these chemical bonds are weak and are readily dissociated by more acidic compounds (e.g., H_2S and CO_2). The solubility of mercaptans in amine solutions increases with increased solvent alkalinity (less absorbed H_2S and/or CO_2), and decreases with increased temperature (Kohl and Nielsen, 1997). Similar to other physical absorption systems, the rate of physical absorption of mercaptans by amine, such as DGA, increases with an increase in the absorber pressure. This is due to the increased partial pressure of mercaptans in the gas (Schulte et al., 2017).

Physical solvents can be used to remove H_2S and CO_2, and are also very effective in removing mercaptans and organic sulfurs. Unlike amine, a physical solvent also absorbs the heavy hydrocarbons, which will generate a hydrocarbon laden acid gas to the sulfur recovery units. For this reason, physical solvent process is seldom used to treat rich gas streams. However, a physical solvent can be blended with an aqueous amine to form a mixed chemical/physical solvent, which will reduce the hydrocarbon pickup capacity. A mixed solvent process is suitable in treating less sour and leaner gases.

9.7.2 MOLECULAR SIEVE UNIT

The Molecular sieve unit (MSU) generally removes water from the gas, but can also be designed to remove trace components such as mercaptans. Molecular sieves (4A, 5A, and 13X) have polar internal surfaces that interact favorably with polar molecules such as water or mercaptans, making it possible to adsorb very low concentrations of mercaptans. During the regeneration cycle, the mercaptans are desorbed which can be removed with the use of a physical solvent and can be sent to the sulfur recovery unit for conversion. Depending on the acid gas contents and the levels of mercaptans, the molecular sieve unit can be used in combination with the gas treating unit for mercaptan removal.

9.7.3 PROCESS OPTIONS

Three gas-treating options for the combination of gas treating and molecular sieves process are considered here.

- Option 1: Removal of H_2S and CO_2 in a promoted MDEA unit and dehydration/mercaptans removal in a molecular sieve unit (Fig. 9.21).

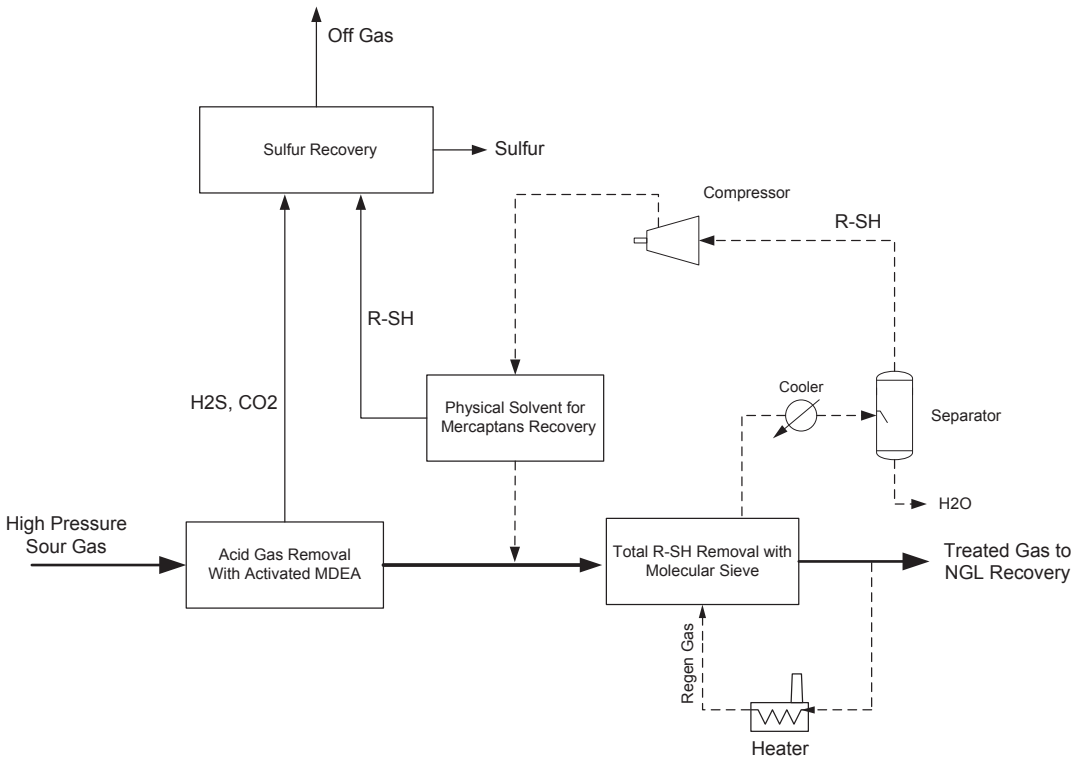

FIGURE 9.21

Removal of all R−SH in a molecular sieve unit.

- Option 2: Removal of H_2S and CO_2 and all mercaptans in Fluor DGA unit and dehydration only in a molecular sieve unit (Fig. 9.22).
- Option 3: Partial removal of R−SH in a hybrid (mixed) solvent unit plus polishing with a molecular sieve unit (Fig. 9.23).

Option 1 (as shown in Fig. 9.21) is the conventional acid gas and mercaptans removal process used in NGL recovery plants. MDEA activated with piperazine is used in the removal of H_2S and CO_2 to a very low level, as required for the downstream units. Amine alone cannot remove any appreciable amounts of mercaptans, consequently, the treated gas would still contain significant amounts of mercaptans going to the molecular sieve unit.

With the selected molecular sieves as described earlier, molecular sieves can adsorb mercaptans and other organic sulfurs. For a larger gas plant which contains significant levels of mercaptans, the sieve volume requirement can be very large, making it uneconomical. When used for mercaptans adsorption, mercaptans will be desorbed during the regeneration cycle. The mercaptans can then be removed with a physical solvent, and sent to the sulfur recovery unit. The advantage of this configuration is that aqueous amine does not absorb significant amounts of heavy hydrocarbons and

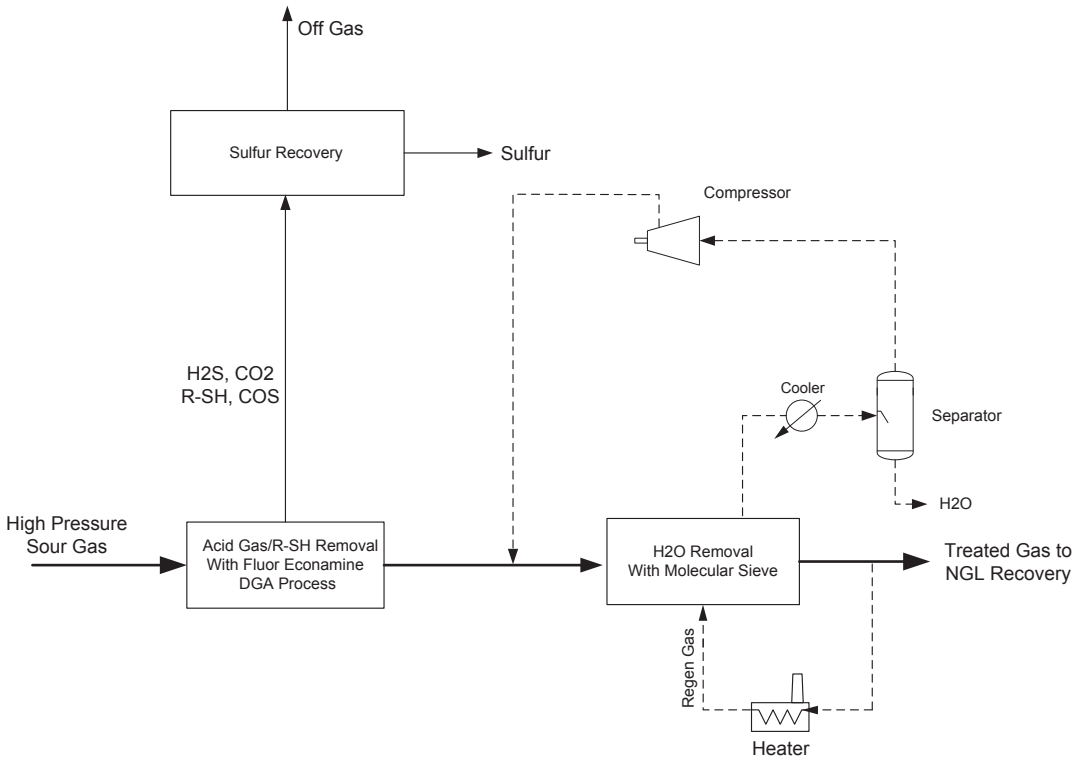

FIGURE 9.22

Total removal of R−SH in a Fluor Econamine DGA unit (Schulte et al., 2017).

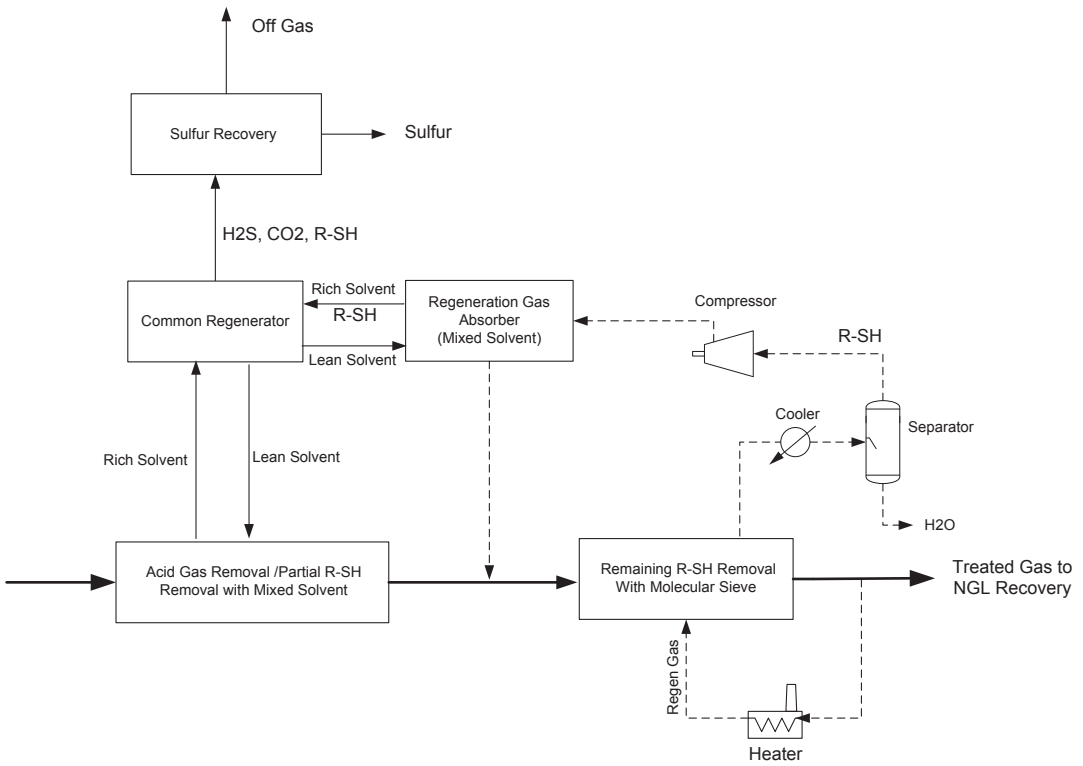

FIGURE 9.23

Partial removal of R−SH in a hybrid solvent unit and polishing with a molecular sieve unit (after Carlsson et al., 2007).

mercaptans, and the acid gas to the sulfur recovery unit can be directly processed without difficulties. The disadvantage is the large molecular sieve beds and the complexity in operating the molecular unit with a physical solvent unit.

In Option 2 (as shown in Fig. 9.22), the Fluor Improved Econamine DGA process that has proven to be very effective at treating large volumes of gas at both high and low absorption pressures is used for total removal of R−SH from the feed natural gas stream.

Recently, a high capacity acid gas removal unit based on Fluor Improved Econamine DGA technology was started up in 2014 for the Shah sour gas processing plant in Abu Dhabi (Schulte et al., 2017). The DGA unit treats 250 MMscfd of sour gas at 990 psig pressure. The sour gas contains 25.1% mol% H_2S, 9.4% CO_2, with 300 ppmv COS and 330 ppmv mercaptans. The Fluor unit uses a highly concentrated DGA solution and a side cooler to remove the heat of acid gas absorption that controls the absorber bottom temperature. The bottom temperature should be maintained to increase the rich solvent acid gas loading, reducing solvent circulate, and reduce the flashed gas from the rich solvent flash drum.

DGA is a primary amine as compared to MDEA, which is a tertiary amine. Hence, DGA is very reactive with acid gas, and can remove H_2S and CO_2 to the low ppm levels. The Fluor Improved Econamine for the Shah gas processing plant in Abu Dhabi uses 6600 GPM circulation with 55 weight % DGA at 140°F. The process, started up in 2014, is effective in removing all acid gases to produce a treated gas with less than 1 ppmv of H_2S and CO_2, demonstrating that DGA is an extremely effective solvent for ultrasour feed gases (Schulte et al., 2017). Plant data also show low concentrations of COS and mercaptans in the sweet gas, indicating that for this system, DGA removes not only majority of COS in the feed, as expected, but the majority of the mercaptans as well. The high efficiency of mercaptan absorption can most likely be attributed to high absorption pressure and the high reactivity of the DGA solvent. In the process, acid gas absorption occurs mostly in the lower section of the absorber, freeing up most of the upper trays for absorption of mercaptans and organic sulfurs. Removal of mercaptans is over 90%.

Another innovative approach is the patent-pending Fluor Two Stage Absorption process, which is developed to take advantage of improved mercaptan removal at higher pressures in a way that maintains the health and safety advantages of the low pressure absorption configuration. In this approach most of the acid gases are removed in the low pressure absorber, the treated gas is compressed to a higher pressure to operate a high pressure absorber which is more effective in mercaptans removal. The improved mercaptan removal process will reduce or, in some scenarios, eliminate the need for downstream mercaptan removal (Schulte et al., 2017).

Option 3 (as shown in Fig. 9.23) uses the combination of amine and physical solvent process and molecular sieve for removal of mercaptans. Mixed solvent processes, such as Sulfinol process, can be used to remove H_2S, CO_2, COS, and mercaptans from gases.

When mercaptan concentrations are low, the combination of mixed solvent and a molecular sieve unit may be considered. When the mixed solvent is used in the acid gas removal unit, a limited fraction of mercaptans can be removed from the gas phase. The remaining mercaptans can subsequently be removed using the molecular sieve unit. The mercaptans in the regeneration can be removed with the same mixed solvent. In this option, a single mixed solvent can be used in the acid gas removal unit and the regeneration gas absorber using a common regenerator unit.

9.7.4 PROCESS SELECTION

Treating mercaptans containing gas is to meet product specification and environmental compliance. There are no operating revenues that can be derived from mercaptan treatment, and as such, the capital cost of the installation should be minimized. The gas treating technology selection is dependent on the gas flow rate, gas composition, temperature, pressure, and the nature of impurities, as well as product specifications. The other factors are low equipment counts, low capital cost, and operating cost, and most importantly, reliability, operability, and flexibility. It is important to understand that a less reliable unit can result in total gas plant shutdown, which would result in significant loss of revenue. For the very sour gas, the Fluor DGA unit can be effectively used for removal of mercaptans, without the need for a physical solvent unit or a molecular sieve unit for mercaptan removal. Selection of the right process is very crucial. Establishing and conducting all the elements together at the same time for the specific conditions are also important.

REFERENCES

Campbell, J.M., 2000. Gas Conditioning and Processing, eighth ed. Campbell Petroleum Series, Norman, OK, USA.

Carlsson, A.F., Last, T., Smit, C.J., March 11−14, 2007. Design and operation of sour gas treating plants for H_2S, CO_2, COS, and mercaptans. Paper Presented at the 86th Annual GPA Convention, San Antonio, TX, USA.

Carroll, J.J., March 11−13, 2002. The water content of acid gases and sour gas from 100 to 220°F and pressures to 10,000 Psia. Paper Presented at the 81st Annual GPA Convention, Dallas, TX, USA.

Carroll, J.J., 2009. Natural Gas Hydrates, a Guide for Engineers, second ed. Gulf Professional Publishing, Burlington, MA, USA.

Daiminger, U., Lind, W., 2004. Adsorption-based processes for purifying natural gas. World Refining 14 (7), 32−37.

EPA430-B-03-013, December 2003. Optimize glycol circulation and install flash tank separators in glycol dehydrators. In: Lessons Learned, Natural Gas Star Program, U.S. Environmental Protection Agency (EPA), Washington, DC, USA.

GPSA, 2004. Engineering Data Book, twelfth ed. Gas Processors Suppliers Association (GPSA), Tulsa, OK, USA.

Kane, A., Shelenko, L., Kauders, P., February 26−27, 2004. Co-adsorption of mercaptans using silica gel in sour gas dewpointing applications. Paper Presented at the GPA Europe Meeting, London, UK.

Katz, D.L., Cornell, R., Kobayashi, R., Poettmann, F.H., Vary, J.A., Elenblass, J.R., Weinaug, C.G., 1959. Handbook of Natural Gas Engineering. McGraw-Hill Book Company, New York, NY, USA.

Kidnay, A.J., Parrish, W., 2006. Fundamentals of Natural Gas Processing, first ed. CRC Press, Taylor & Francis Group, Boca Raton, FL, USA.

Kohl, A.L., Nielsen, R.B., 1997. Gas Purification, fifth ed. Gulf Publishing Company, Houston, TX, USA.

Mcketta, J.J., Wehe, A.H., 1958. Use this chart for water content of natural gases. Petroleum Refiner (Hydrocarbon Processing) 37 (8), 153.

Meyer, P., March 21−24, 2011. Mercaptans removal with molecular sieves − options and reality. Paper Presented at the GPA Europe Conference, Amsterdam, The Netherlands.

Mokhatab, S., Meyer, P., May 13−15, 2009. Selecting best technology lineup for designing gas processing units. Paper Presented at the GPA Europe Sour Gas Processing Conference, Sitges, Spain.

Mokhatab, S., Northrop, P.S., 2017. Handling mercaptans in gas processing plants. Hydrocarbon Processing 96 (1), 31−34.

Northrop, S., Sundaram, N., 2009. Strategies for gas treatment with adsorbents. Petroleum Technology Quarterly, Gas, 7−11.

Savary, L., May 05, 2004. From purification to liquefaction - gas processing with Axens technology. Paper Presented at the 12th GPA GCC Chapter Technical Conference, Kuwait.

Schulte, D., Wagensveld, S., Graham, C., Lynch, B., April 9−12, 2017. Improved econamine treatment of ultra-sour gas. Paper Presented at the 96th Annual GPA Convention, San Antonio, TX, USA.

Secker, H., Zafirakis, V., May 25−27, 2011. Adsorbent solutions for removal of mercaptans and other sulfur compounds. Paper Presented at the GPA Europe Spring Conference, Copenhagen, Denmark.

Smit, C.J., Carlsson, Last, T., September 23−25 2009. Pitfalls in design and operation of molecular sieve units for the removal of water and mercaptans. Paper Presented at the 26th Annual GPA Europe Conference, Venice, Italy.

Trent, R.E., February 28−March 03, 2004. Dehydration with molecular sieves. Paper Presented at the 54th Annual Laurance Reid Gas Conditioning Conference, Norman, OK, USA.

Trent, R.E., February 26−29 2012. Zeochem dehydration with molecular sieves. Paper Presented at the 62nd Annual Laurance Reid Gas Conditioning Conference, Norman, OK, USA.

Wichert, G.C., Wichert, E., 2003. New charts provide accurate estimations for water content of sour natural gas. Oil & Gas Journal 101 (41), 64−66.

CHAPTER

MERCURY REMOVAL 10

10.1 INTRODUCTION

Mercury, which is present in varying concentrations and as a variety of species in many of the world's natural gas fields, has to be removed to near nondetectable levels in any gas processing facility, particularly those involving cryogenic gas processing, to ensure the safety and reliability of the operations. In fact, even low levels of mercury pose a health hazard (because it is toxic) and will damage aluminum heat exchangers, such as those used in cryogenic gas processing plants, which are susceptible to corrosion attack by mercury. This chapter describes distinctive methods to remove mercury and discusses the implications of deposition of mercury in various locations of a gas processing plant.

10.2 MERCURY IN NATURAL GAS STREAM

Mercury (Hg) is a trace element often found in natural gas and natural gas liquid streams. It can be present as organometallic and inorganic compounds, and/or in the elemental form depending on the origin of the gas. While organometallic mercury most typically ends up in the hydrocarbon liquids, the elemental form can be found in both gas and liquid phases (Rios et al., 1998). Because elemental mercury has low solubility in water, the majority of mercury in aqueous streams is mostly present in ionic and suspended forms (i.e., inorganic mercury).

The concentration of mercury in natural gas streams can range from a few ng/Nm^3 to a few hundreds of μg/Nm^3 among different production fields (Fig. 10.1). It is very difficult to predict or measure the concentration of mercury at the low levels present in production reservoirs. Furthermore, elemental mercury needs to saturate tubulars and piping, so it may take some time before the mercury is detected in the facility. This means in the design stage, operators will often have no idea of its steady-state concentration. This can lead to either not including a mercury removal system or installing a system that is underdesigned. Conversely, it may lead to the installation of an unnecessarily large mercury unit for those who design plants conservatively.

In the former case, the operator may be unaware of impending trouble until failure of an equipment item due to mercury-induced corrosion. While detection methods are continuously being improved to more accurately and reliably detect low levels of mercury in feed gas, they still have shortcomings. For the most accurate measurements, sampling should be done at operating conditions over a prolonged collection period. Earlier studies have shown that samples collected in the gas field and brought to the laboratory may show that some of the mercury is adsorbed on the container walls (Rios et al., 1998). This can result in false, low readings. It has also been observed that mercury levels in natural gas may

Handbook of Natural Gas Transmission and Processing. https://doi.org/10.1016/B978-0-12-815817-3.00010-1

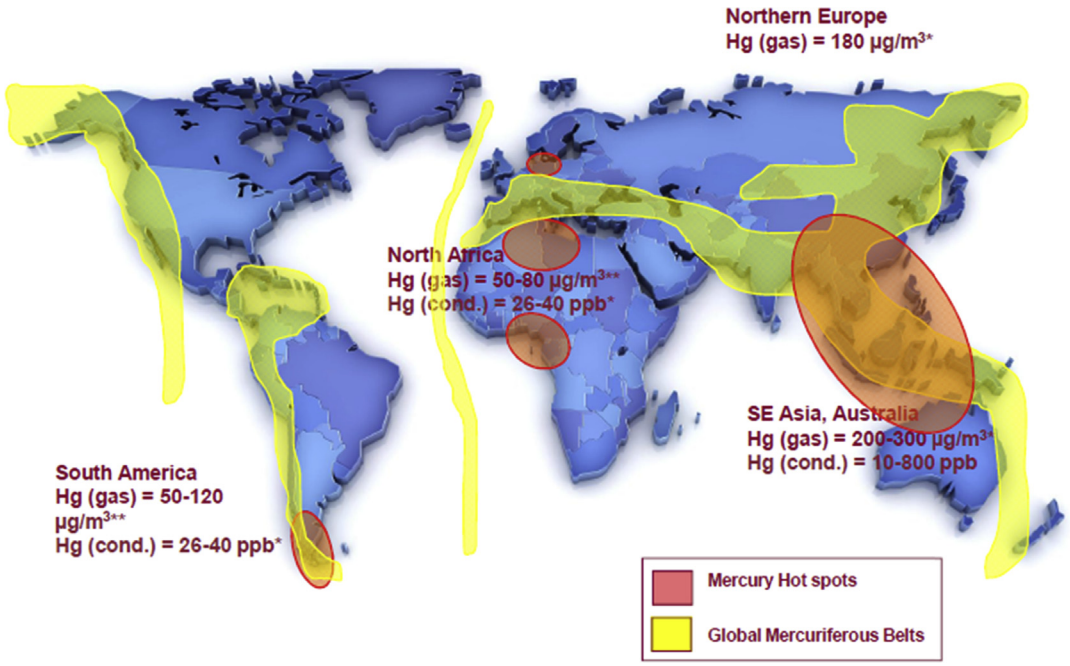

FIGURE 10.1

Mercury belt and global hot spots for mercury (Row, 2012).

fluctuate by a factor of five over periods longer than 8 h (Lewis, 1995; Rios et al., 1998). Methods that involve flowing of a known quantity of gas past a gold foil to accumulate mercury over time can give a good idea of the average mercury content. The difficulty of measuring mercury means that it is challenging for operators to both identify and design for the presence of the hazardous element in their system. This is particularly true for offshore wells, where flow tests are very expensive and limited to short durations. The concern is that there is not enough mercury to saturate the metal pipe in that short time, again leading to false, low measurements.

10.3 MERCURY-RELATED ISSUES

The effect of mercury attack on certain metal alloys is well researched (Coade and Coldham, 2006). The main mode of corrosion attack on aluminum alloys is liquid metal embrittlement (LME) where liquid mercury diffuses along the small defects and grain boundaries of the alloy, reducing its ductility and strength. This can lead to rapid propagation of cracks (Rios et al., 1998) such as that shown in Fig. 10.2. Another mode of attack is amalgam corrosion where the mercury forms a solution with the base metal. This again changes the properties of the alloy, potentially resulting in catastrophic failure because these cryogenic heat exchangers are generally subjected to high pressures.

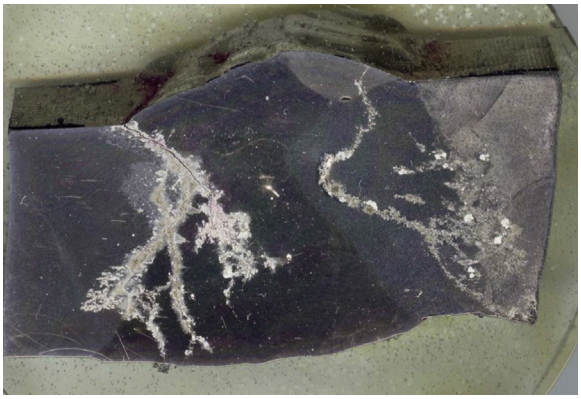

FIGURE 10.2

Liquid metal embrittlement failure on brazed aluminum heat exchanger.

Reproduced courtesy of Chart Energy and Chemicals by Carnell et al. (2007).

Corrosion occurs with any metal which can form an amalgam with mercury. If the oxide layer that protects most metals from corrosion is damaged (e.g., by mechanical cleaning), liquid mercury can quickly attack the metal, resulting in etching and pitting. If water is present, the corrosion can proliferate with only miniscule amounts of free mercury. This is because the amalgam with mercury is regenerated in the presence of water. For the case of aluminum, the following reactions take place:

$$\mathrm{Hg} + \mathrm{Al} \rightarrow \mathrm{Hg(Al)} \ \text{ amalgam} \tag{10.1}$$

$$2\mathrm{Hg(Al)} + 6\mathrm{H_2O} \rightarrow 2\mathrm{Al(OH)_3} + 3\mathrm{H_2} + 2\mathrm{Hg} \tag{10.2}$$

Cold boxes and cryogenic heat exchangers are particularly susceptible when constructed of aluminum alloys. LME will also affect other materials, including some stainless steels.

As mercury is present in trace amounts in natural gas, and brazed aluminum heat exchangers are used in many gas processing facilities (and virtually all LNG facilities), it is essential to address the issue. A number of equipment failures have been attributed to mercury. These led to unscheduled shutdowns and, in extreme cases, loss of containment with potential for subsequent explosion and fire (Lund, 1996; Eckersley, 2010). In theory, both methods of attack can be prevented in operation by maintaining the temperatures at low enough levels so that the reactions do not proceed (mercury freezes at $-39°C$), or by an oxide coating on the surface of the base metal (Rios et al., 1998). The mercury, however, may collect in areas prone to attack. A rise in temperature, or damage to the oxide layer (as might occur in a maintenance scenario), will initiate the attack.

The presence of mercury in feedstocks to petrochemical plants will also cause poisoning of precious metal catalysts (Affrossman et al., 1968; Dunleavy, 2006) with potential for significant financial loss to the operator.

Mercury can also pose significant environmental and safety hazards, as evidenced by the now-recognized disaster that gave its name to the Minamata disease (Tsuda et al., 2009). The

cumulative effect of these hazards has led to a conservative approach to the design of mercury removal units in gas processing plants, with specifications set at the traditional lowest level of detection. Currently, this means reducing the mercury to below 0.01 μg/Nm^3 (Stiltner, 2002).

In addition, mercury is generally harmful to human health, and numerous regulations have been issued to control and limit its emission from anthropogenic sources into the environment. Suitable personal protective equipment is required during maintenance work in areas where mercury is suspected. The European Union Scientific Committee on Occupational Exposure Limits proposes 0.02 mg/m^3 as the limit for elemental mercury in inhaled air during 8-h time-weighted average and 0.01 mg/L in blood as the biological limit (Pirrone and Mahaffey, 2005; Jubin and Ducreux, 2014).

10.4 MERCURY DISTRIBUTION IN GAS PROCESSING PLANTS

Mercury that enters a gas processing plant will distribute itself across the different process and waste streams. Mercury distribution will depend on its concentration in the raw natural gas and on the conditions existing in the processing facility. Fig. 10.3 shows the approximate mercury distribution through a typical gas processing scheme producing Y-grade natural gas liquids, based on an average from analytical tests from a number of facilities. It was observed that solutions used for acid gas and moisture removal have a relatively strong affinity for mercury (Row and Humphrys, 2011). This leads to mercury absorption in these solvents, ultimately lessening the amount of mercury flowing to the cryogenic section. Mercury removed from the main process stream by an acid gas removal unit (AGRU) utilizing an amine-based solvent will subsequently be released during amine regeneration. This mercury can end up in the carbon dioxide waste vent stream or (where applicable) in the product sulfur. Mercury removed from the main process stream in dehydration units utilizing molecular sieve or glycol-based solvent technologies will be released during regeneration and will end up either in the regeneration gas stream or the waste water. Mercury remaining in the sales gas will be released at the point of use of the gas (Row and Humphrys, 2011).

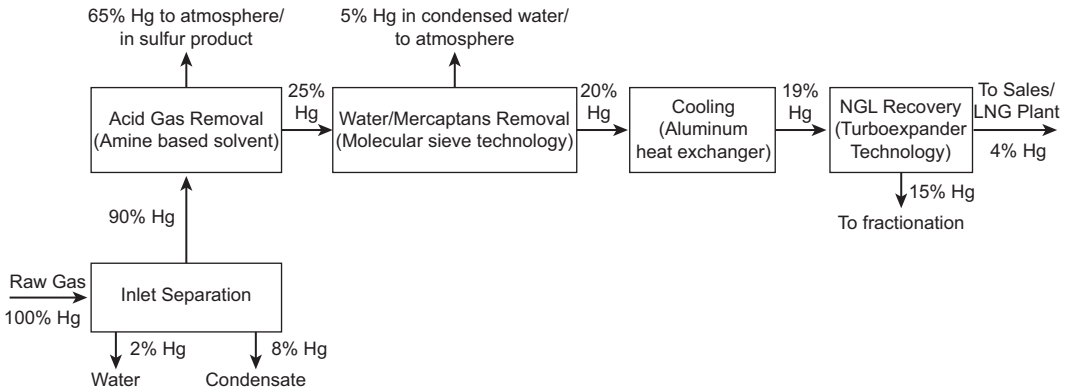

FIGURE 10.3

Typical mercury distribution on a gas processing plant (Row and Humphrys, 2011).

Note that the proportions of mercury removed at various processing steps and entering the finished gas and liquid products vary from plant to plant. Therefore, mercury distribution in cryogenic gas processing plants must be properly studied to determine the areas most in danger of mercury attack, and which streams have the highest concentration (Mokhatab et al., 2017).

10.5 MERCURY REMOVAL TECHNIQUES

Any mercury removal process must be effective at very low concentrations of mercury due to the low vapor pressure of elemental mercury and its low solubility in water and liquid hydrocarbon. The majority of currently used methods for removing mercury from natural gas and hydrocarbon liquids employ fixed-bed technologies (Markovs and Clark, 2005). The main process stream flows through a fixed bed in which mercury undergoes a physical or chemical interaction with the reagent in the mercury removal vessel, producing a mercury-free product.

Mercury can be removed using either regenerative adsorbents or nonregenerative sorbents.

10.5.1 REGENERATIVE MERCURY ADSORBENTS

Regenerative mercury removal processes utilize the high affinity of mercury for precious metals such as gold and silver. The relatively high cost of gold has resulted in silver being the metal of choice for the duty. An example of its use in practice is silver deposited on the surface of molecular sieve material (UOP HgSIV). The silver-coated zeolite is installed as a layer within the molecular sieve unit utilized for natural gas dehydration, saving the cost of an additional vessel and adsorbent, as well as reducing the overall pressure drop. In operation, the unit is used to remove both moisture and mercury from the main process stream. As per normal molecular sieve operation, the mercury- and moisture- saturated unit is then regenerated by hot regeneration gas (typically at temperatures around 290°C), then cooling to process temperature prior to returning the sieve to service. The cycle is usually repeated on a preset timeline depending on the sorbents' capacities for the respective contaminants.

The mercury is removed from the main process stream by the silver-coated sorbent and is concentrated in the regeneration stream. Depending on the fate of this stream, further processing may be required. This can include nonregenerative technologies that chemically react and remove the mercury from the regeneration stream or physical separation methods such as condensing and separating it within the aqueous stream (Markovs and Clark, 2005). The requirement for further processing of the regeneration stream to completely remove trace amounts of mercury leads to the molecular sieve method rarely being applied as a stand-alone system for mercury removal (Mokhatab et al., 2017).

10.5.2 NONREGENERATIVE MERCURY SORBENTS

Nonregenerative mercury removal processes utilize the chemical reaction between mercury and sulfur (or metal sulfides) which forms cinnabar (HgS), the most stable form of mercury in nature. A number of different mercury removal sorbents are available with various tolerances to operating temperature, liquid hydrocarbons, and water (Markovs and Clark, 2005).

The most common nonregenerative mercury removal processes are sulfur-impregnated activated carbon and mixed metal sulfides.

10.5.3 SULFUR-IMPREGNATED ACTIVATED CARBON

Although plain activated carbon is a fair adsorbent for mercury removal, its capacity is significantly increased by impregnation with a material such as sulfur that chemically reacts with and binds the mercury. Sulfur-impregnated activated carbon is a proven commercial process for effectively removing the mercury from natural gas. In this process, a thin layer of sulfur covers the internal surface of the activated carbon. The reaction between mercury and sulfur forms nontoxic, stable mercury sulfide (HgS), which is then retained in the pores of the carbon bed.

$$\mathrm{Hg} + \mathrm{S} \rightarrow \mathrm{HgS} \tag{10.3}$$

Activated carbon typically has a very large surface area and relatively small pore size. Both factors contribute to a higher potential for capillary condensation, leading to a free liquid phase within the system. Free liquids will have a detrimental effect on the material not only as a diffusion barrier but also potentially washing away the active phase, as it is held onto the carbon support by physical rather than chemical bonds. Although there have been recent improvements in this area, this still limits the use of sulfur-impregnated activated carbon to lean and dry gas streams (Reddy et al., 2015). The pore size may also restrict the access of mercury to the sulfur sites and therefore increase the length of the reaction zone. An additional limitation is that at higher temperatures, sublimation of sulfur may cause loss of the active component. This would reduce mercury removal capacity. Furthermore, it is often difficult to dispose of the spent mercury-laden carbon material (Abbott and Oppenshaw, 2002).

10.5.4 MIXED METAL SULFIDES

Recognition of the drawbacks of mercury removal by sulfur-impregnated activated carbon led to examining alternative technologies. The result has been the development of a range of nonregenerable absorbents utilizing transition metal oxides and sulfides. The mercury removal reaction using mixed metal sulfides (i.e., copper and zinc sulfides) is as follows:

$$\mathrm{MS_x} + \mathrm{Hg} \rightarrow \mathrm{MS_{x-1}} + \mathrm{HgS} \tag{10.4}$$

Improvements include the safer handling of discharged absorbents. In these systems, the reactive metal is incorporated in an inorganic support, and the absorbent is supplied with reactive sulfide component by either ex situ or in situ sulfiding (Carnell et al., 2007). The active component can be impregnated onto the support. However, potential retrograde condensation will have a similar effect to the sulfur-impregnated activated carbon, i.e., loss of the active component to the free liquid phase.

Mixed metal sulfides are not affected by the presence of water or hydrocarbons accompanying the mercury in the gas. Therefore, the mercury removal unit may be installed upstream or downstream of dehydration/heavy hydrocarbon removal units. Any oxygen present in the feed gas will react with the mixed metal sulfides and reduce the capacity of the mercury removal bed. If oxygen is present, then the bed should be placed downstream of the AGRU. Some of the oxygen will be absorbed in the AGRU solvent, thus minimizing the detrimental effect of oxygen on the mercury adsorbent capacity.

Johnson Matthey has taken the concept of utilizing mixed-transition metal absorbents further and supply an established range of absorbents marketed under the $\mathrm{PURASPEC_{JM}}$ brand. The $\mathrm{PURASPEC_{JM}}$ materials consist of mixed metal sulfides, which can operate in both wet and dry gas environments (Row and Humphrys, 2011). Fig. 10.4 shows the results of mercury content measurements in a natural gas stream over a specified period of time after the installation of a mercury guard bed

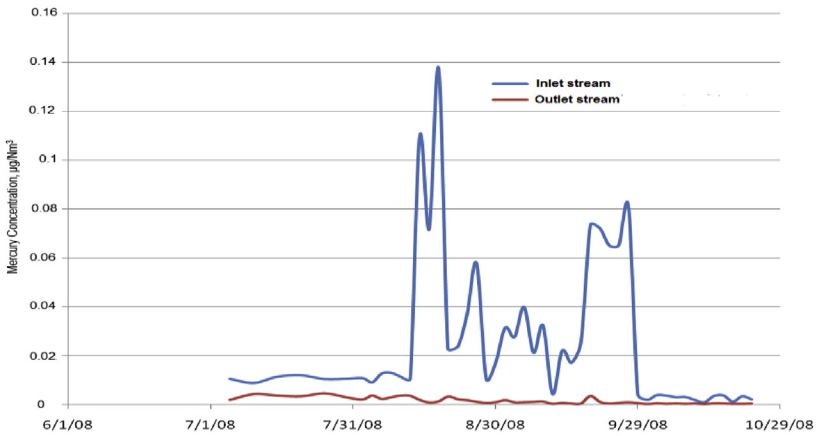

FIGURE 10.4

Mercury content measurements after installing PURASPEC$_{JM}$ guard bed (Baageel, 2009).

utilizing PURASPEC$_{JM}$ absorbent. This material can be designed into systems that can achieve less than 0.01 μg/Nm^3 from inlet gas with levels that exceed 1000 μg/Nm^3 (Mokhatab et al., 2017).

Note that the nonregenerative methods require simpler systems both in construction and in operation because no regeneration equipment or special valving is required. At the end of life of the material, disposal of the spent sorbent can be challenging as it will contain the trapped mercury and be considered a hazardous waste.

10.6 MERCURY REMOVAL FROM NATURAL GAS

While many methods have been investigated for preventing or remediating attack once the equipment has been contaminated by mercury, the best approach is preventing the contamination by removing the mercury from the feed gas. There are four possible options for mercury removal from the feed gas, as described below:

Option 1: Installing a mercury removal unit utilizing a nonregenerative sorbent at the plant inlet, upstream of the AGRU (Fig. 10.5). This option removes all the mercury and ensures no contamination in any downstream processing units (Edmonds et al., 1996). The system is simple both in construction and operation. Although potentially larger volumes of sorbent are required due to the large volumetric flow of feed gas (including acid gases), this does not affect in any way the process or the absorbent and the overall plant performance. However, in this case the absorbent technology employed must consider the feed gas composition, operating conditions, and any potential upset scenarios.

Option 2: Installing a mercury removal unit utilizing a nonregenerative sorbent downstream of the AGRU and upstream of the molecular sieve unit. This option reduces the size of the beds to some extent (as the stream being treated does not include the acid gases). It does not, however,

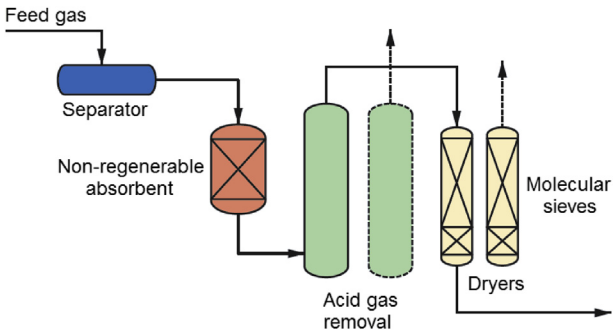

FIGURE 10.5

Installing nonregenerative mercury removal sorbents before the amine unit (Barthel, 2010; Eckersley, 2010).

eliminate the risks of mercury contamination in the AGRU solvent. In addition, some mercury may be displaced to the regeneration stream, so further processing of that stream may be required.
Option 3: Installing an additional layer of a special, regenerable silver-impregnated mercury sieve section to the molecular sieve beds (Fig. 10.6). This option can operate to remove water and mercury at the same time without a separate mercury bed. It does, however, present problems with a high mercury content in the regeneration stream and the condensed water that would pose operating hazards, unless treated by another mercury removal step (Hudson, 2010). Other considerations would be the regeneration system and the additional size requirement for the molecular sieve bed, which potentially pose additional capital costs.
Option 4: Installing a mercury removal unit utilizing a nonregenerative sorbent after the molecular sieve unit (Fig. 10.7). This option yields good mercury removal performance (less impact of retrograde condensation and no caking due to water condensation), as the feed gas has been dried and cleaned, and operation can be well controlled. Because the feed gas is a dry gas, mercury removal is effective. However, in this case, mercury contamination in the AGRU and other upstream units (i.e., dehydration unit including spent regeneration gas facilities and any associated effluent treatment facilities) can still occur and may pose operating hazards (Row and Humphrys, 2011).

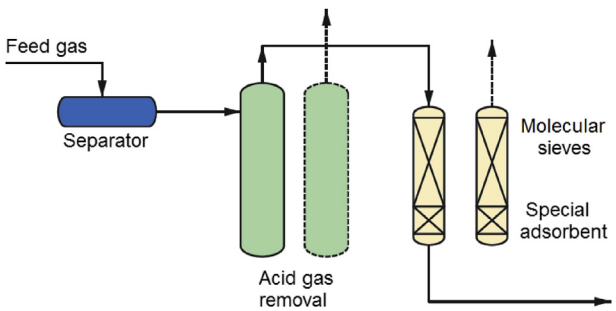

FIGURE 10.6

Adding a silver-impregnated mercury sieve section to the molecular sieve beds (Barthel, 2010; Eckersley, 2010).

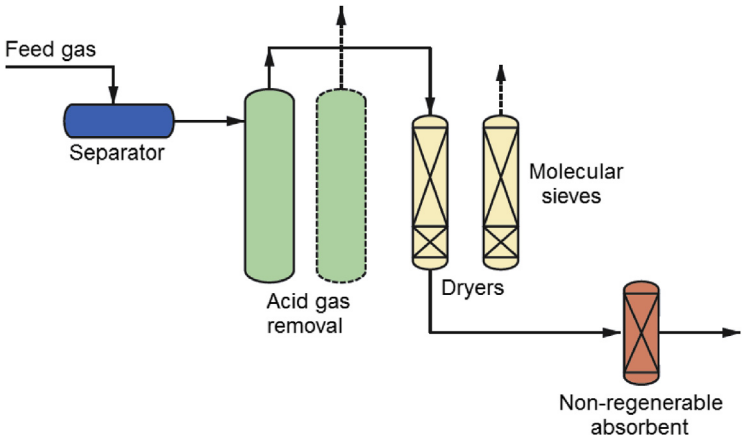

FIGURE 10.7

Installing a nonregenerative mercury removal bed after the molecular sieve unit (Barthel, 2010; Eckersley, 2010).

Mercury levels, volumetric flow rates to be treated, life cycle costs, sorbent disposal methods, environmental limits, operating hazards, and plant operator procedures must be evaluated in the selection of a suitable mercury removal system. The optimum mercury removal method may also be a combination of nonregenerative and regenerative mercury removal systems.

10.7 DISPOSAL OF MERCURY-CONTAMINATED WASTE

Mercury-laden waste of this type can contain up to 15 wt% mercury and its safe, so responsible disposal can prove a challenge. Hazardous landfill sites were developed in the short-term interest of operators, but many are now considered environmentally unsound. The Minamata Convention on Mercury (2013) was recently formulated in an attempt to control the use of mercury owing to its recognized toxicity. With a large number of countries ratifying the agreement, while also being signatories to the Basel Convention (1992) that limits the transport of hazardous waste, disposal of mercury-laden waste is becoming tightly controlled. Mercury remediation is thus required and can be done only by companies specialized in the area, found only in a small number of locations around the globe. Shipment of mercury-containing waste to a central processing site thus may have to be considered, as mobile treatment units are not designed to process large quantities of waste (Rios et al., 1998). This is an operation that must follow strict protocols (Mokhatab et al., 2017). The Johnson Matthey PURACARE$_{JM}$ program offers disposal of spent mercury absorbents in an environmentally proper manner, utilizing a route in which the chemically absorbed mercury is removed in the nearest suitable treatment facility. While disposal of mercury-laden carbon requires expensive thermal processing and leaves unwanted residue, the spent PURASPEC$_{JM}$ material can be reprocessed for metal recovery and can be used as a secondary raw material that can offset part of the remediation cost

(Carnell et al., 2007). Both the transporter and the reprocessor must be appropriately certified and regularly audited. The PURACARE$_{JM}$ service therefore simplifies and potentially recovers some cost from an otherwise costly and complicated exercise.

REFERENCES

Abbott, J., Oppenshaw, P., March 11−13, 2002. Mercury removal technology and its applications. Paper Presented at the 81st Annual GPA Convention, Dallas, TX, USA.

Affrossman, S., Erskine, W.G., Paton, J., 1968. Investigation of the poisoning of platinum group catalyst by thermal desorption − part 1: mercury poisoning of benzene hydrogenation on platinum. Transactions of the Faraday Society 64, 2856−2863.

Baageel, O.M., May 06, 2009. Mercury removal unit process, operation and bed replacement experience. Paper Presented at the 17th Annual GPA GCC Chapter, Abu Dhabi, UAE.

Barthel, R., May 24−26, 2010. Advanced mercury removal technologies. Presented at the XIX International Gas Convention (AVPG 2010), Caracas, Venezuela.

Basel Convention, May 5, 1992. Basel Convention on the Control of Transboundary Movements of Hazardous Wastes and Their Disposal. International Environment House, Chatelaine, Switzerland.

Carnell, P.J.H., Row, V.A., McKenna, R., April 24−27, 2007. A rethink of the mercury removal problem for LNG plants. Paper Presented at the 15th International Conference & Exhibition on Liquefied Natural Gas (LNG 15), Barcelona, Spain.

Coade, R., Coldham, D., 2006. The interaction of mercury and aluminium in heat exchangers in a natural gas plants. International Journal of Pressure Vessels and Piping 83, 336−342.

Dunleavy, J.K., July 2006. Mercury as a catalyst poison. Platinum Metals Review 50 (3), 156.

Eckersley, N., 2010. Advanced mercury removal technologies. Hydrocarbon Processing 89 (1), 29−35.

Edmonds, B., Moorwood, R.A.S., Szcepanski, R., March 21, 1996. Mercury partitioning in natural gases and condensates. Paper Presented at the GPA Europe Conference, London, UK.

Hudson, C., April 18−21, 2010. Implications of mercury removal bed material changeout: brownfield versus greenfield. Poster Presented at the 16th International Conference & Exhibition on Liquefied Natural Gas (LNG 16), Oran, Algeria.

Jubin, C., Ducreux, O., September 17−19, 2014. Operation of mercury removal units on wet gas. Paper Presented at the Annual GPA Europe Conference, Madrid, Spain.

Lewis, L., March 13−15, 1995. Measurement of mercury in natural gas streams. Paper Presented at the 74th Annual GPA Convention, San Antonio, TX, USA.

Lund, D.L., March 11−13, 1996. Causes and remedies for mercury exposure to aluminium coldboxes. Paper Presented at the 75th Annual GPA Convention, Denver, CO, USA.

Markovs, J., Clark, K., March 13−16, 2005. Optimized mercury removal in gas plants. Paper Presented at the 84th Annual GPA Convention, San Antonio, TX, USA.

Minamata Convention on Mercury, October 2013. United Nations Environment Program. Kenya, Nairobi.

Mokhatab, S., Theophanous, P., Shanableh, A., 2017. Handling mercury in gas processing plants. Petroleum Technology Quarterly, Q2, 31−37.

Pirrone, N., Mahaffey, K.R., 2005. Dynamics of Mercury Pollution on Regional and Global Scales: Atmospheric Processes and Human Exposures Around the World. Springer, New York, NY, USA.

Reddy, K.S.K., Al Shoaibi, A., Srinivasakannan, C., 2015. Sulfur leaching facts from sulfur impregnated porous carbons in mercury removal process. Energy and Fuels 29 (7), 4488−4491.

Rios, J.A., Coyle, D.A., Durr, C.A., Frankie, B.M., March 16–18, 1998. Removal of trace mercury contaminants from gas and liquid streams in the LNG and gas processing industry. Paper Presented at the 77th Annual GPA Convention, Dallas, TX, USA.

Row, V.A., October 9, 2012. Desulphurization and mercury removal from natural gases. Presentation at the GasTech Centre of Technical Excellence, London, UK.

Row, V.A., Humphrys, M., May 25–27, 2011. The impact of mercury on gas processing plant assets and its removal. Paper Presented at the GPA Europe Spring Conference, Copenhagen, Denmark.

Stiltner, J., March 11–13, 2002. Mercury removal from natural gas and liquid streams. Paper Presented at the 81st Annual GPA Convention, Dallas, TX, USA.

Tsuda, T., Yorifuji, T., Takao, S., Miyai, M., Babazono, A., 2009. Minamata disease: catastrophic poisoning due to a failed public health response. Journal of Public Health Policy 30 (1), 54–67.

CHAPTER

NATURAL GAS LIQUIDS RECOVERY

11

11.1 INTRODUCTION

Most natural gas sources contain hydrocarbon liquids that must be removed to meet the hydrocarbon dew point and heating value specifications for safe transmission by pipelines supplying consumers. The hydrocarbon liquids can be grouped into natural gas liquids (C_2 to C_4) and natural gas condensate (C_{5+}). Usually, there is a commercial benefit to recovering these hydrocarbon liquids in greater amounts than required for pipeline specifications due to a premium price over natural gas for the equivalent heating value. The majority of the C_{5+} condensate is separated in the condensate stabilization unit that has been discussed in Chapter 6. The C_3 to C_4 liquids are valued as a liquid fuel for domestic uses or as petrochemical feedstocks. The C_2 component can also be separated and is very desirable for ethylene and other petrochemical production. Separation processes for the natural gas liquids (NGL) are discussed in this chapter.

The richness of the NGL components can be expressed by the term "GPM", that is, gallons of C_{2+} liquids per 1000 standard cubic feet of gas. The liquid value "gallons per lb mole" and the higher heating value "HHV, Btu/scf" for the respective components are shown in Table 11.1.

Table 11.1 Recoverable Hydrocarbons and Heating Values of NGL

	Recoverable Hydrocarbons, Gallons per lb mole	HHV, Btu/scf
C_1	–	1010.0
C_2	10.126	1769.6
C_3	10.433	2516.1
iC_4	12.386	3251.9
nC_4	11.937	3262.3
iC_5	13.860	4000.9
nC_5	13.713	4008.9
nC_6	15.566	4755.9
nC_7	17.468	5502.6
nC_8	19.385	6248.9

Handbook of Natural Gas Transmission and Processing. https://doi.org/10.1016/B978-0-12-815817-3.00011-3

Table 11.2 Typical Y-Grade NGL Specifications

Characteristics	Product Specifications
Composition	
Methane, maximum	Not to exceed either 0.5 vol% of total stream or 1.5 vol% of ethane content
Aromatics, maximum	1 wt% in total stream or 10 vol% in contained natural gasoline
Olefins, maximum	1 vol%
Carbon dioxide	500 ppmv or 0.35 LV% of ethane
Vapor pressure at 100°F	600 psi maximum
Corrosiveness	Copper strip at 100°F−1 A/1B pass
Total sulfur	150 ppm wt
H_2S copper strip	Pass
Distillation: end point at 14.7 psia	375°F maximum
Free water	None at 35°F
Product temperature	60−120°F

The C_{2+} NGL mixture recovered from an NGL recovery unit is sometimes referred to as "Y-grade NGL" or "raw NGL mix". The Y-grade NGL is typically transported to a centralized facility for fractionation where the mixed NGLs are separated into discrete NGL products: ethane, ethane−propane mix, propane, normal butane, iso-butane, and natural gasoline. The Y-grade NGL typically must meet the specifications given in Table 11.2.

The Y-grade liquids must be free from sand, dust, gums, gum-producing substances, oil, glycol, inhibitor, amine, caustics, chlorides, oxygenates, heavy metals, and any other contaminants or additives used to meet specifications.

This chapter covers the production of NGL from the conventional dew point controlling unit to technologies that can achieve higher recovery of propane and ethane, NGL fractionation, and liquid products treating.

11.2 REFRIGERATION PROCESSES

Refrigeration units are designed to meet the process cooling temperature requirements. In NGL recovery or a natural gas liquefaction plant, a two or three-stage propane compressor is common, typically designed to meet the process chilling temperature of about −20 to −30°F. If lower temperatures are required, ethane refrigeration or mixed refrigeration system can be used. Alternatively, gas expander or Joule−Thomson (J−T) cooling can also produce deeper refrigeration using feed gas as the working fluid.

11.2.1 PROPANE REFRIGERATION

Propane is a common refrigerant and has a lower environmental impact compared to the fluorocarbon refrigerant alternatives. Propane is a flammable refrigerant while fluorocarbon refrigerants are

nonflammable. Design and operation of a propane refrigeration system must comply with safety guidelines and proper training on safety requirements.

A refrigeration system operates on a vapor-compression refrigeration cycle principle. Fig. 11.1 plots the horsepower required per MM Btu/hr of cooling duty against the propane evaporating temperature for various propane condensing temperatures. In a gas processing plant, propane refrigerant is typically condensed by cooling water or ambient air. For a fixed condensation temperature, the

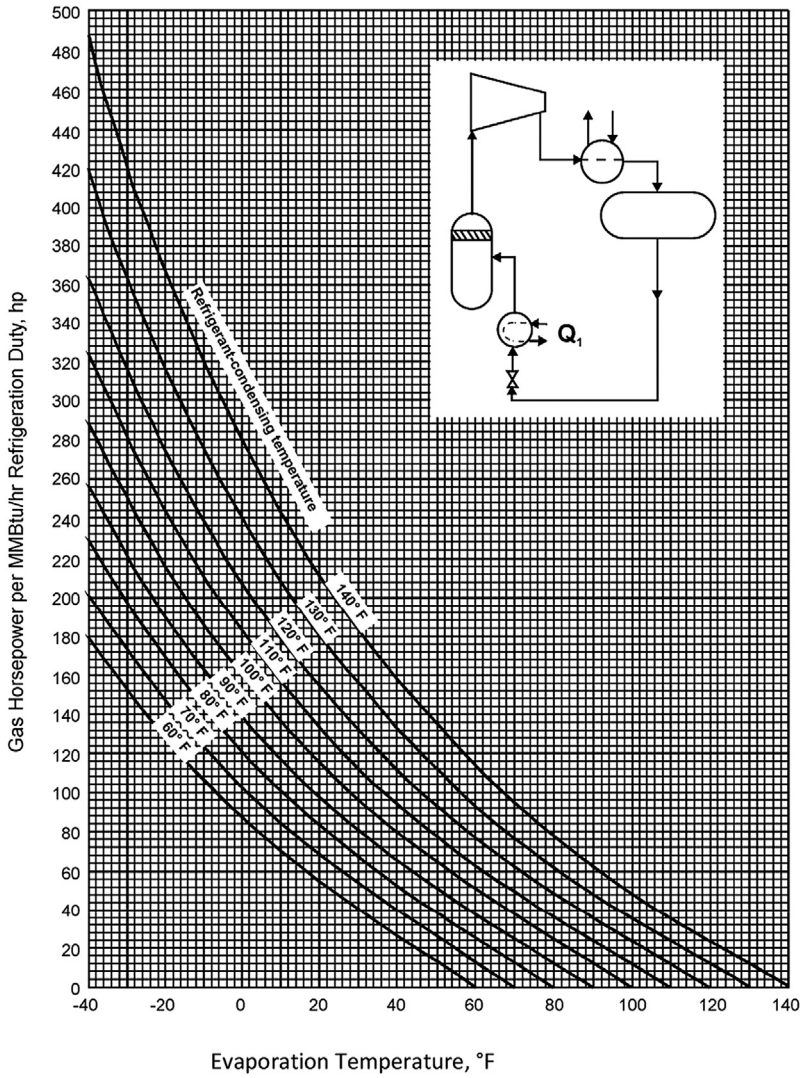

FIGURE 11.1

Refrigeration horsepower versus evaporation temperature (GPSA, 2004).

compression horsepower increases with lower refrigerant evaporating temperatures. This is mainly because a lower evaporating temperature also requires a lower evaporating pressure, which requires a higher compression ratio. Conversely, refrigeration horsepower is lower with a higher evaporating temperature. A refrigeration unit, which is typically designed for the summer operation, would have more cooling capacity during winter.

Propane refrigeration can provide coolant at −40°F at atmospheric pressure. Lower chilling temperatures could be achieved with a fourth stage compression operating under vacuum pressure. However, most gas plants would avoid the use of vacuum pressure because of the potential fire hazards from air ingress into the system.

The more efficient gas plants typically use a three-stage propane compression system as shown in Fig. 11.2. Centrifugal compressors are used since they typically have a higher efficiency than screw or rotary compressors. However, for smaller plants, two-stage refrigeration systems using screw type or reciprocating type machines are more common.

For a three-stage compression system, the feed gas cooling system typically consists of two chillers operating in series. The first chiller uses the refrigerant from the MP drum while the second chiller uses the atmospheric drum liquid. Cooling in two stages improves the thermodynamic efficiency, lowering the power consumption.

The chillers are typically kettle-type exchangers with propane evaporating on the shell side. The evaporated propane from the first stage chiller is sent to the second stage compressor suction, and the vapor from the second stage chiller is sent to the first stage compressor suction. The propane compressor also has a third stage that receives vapor from the HP suction drum.

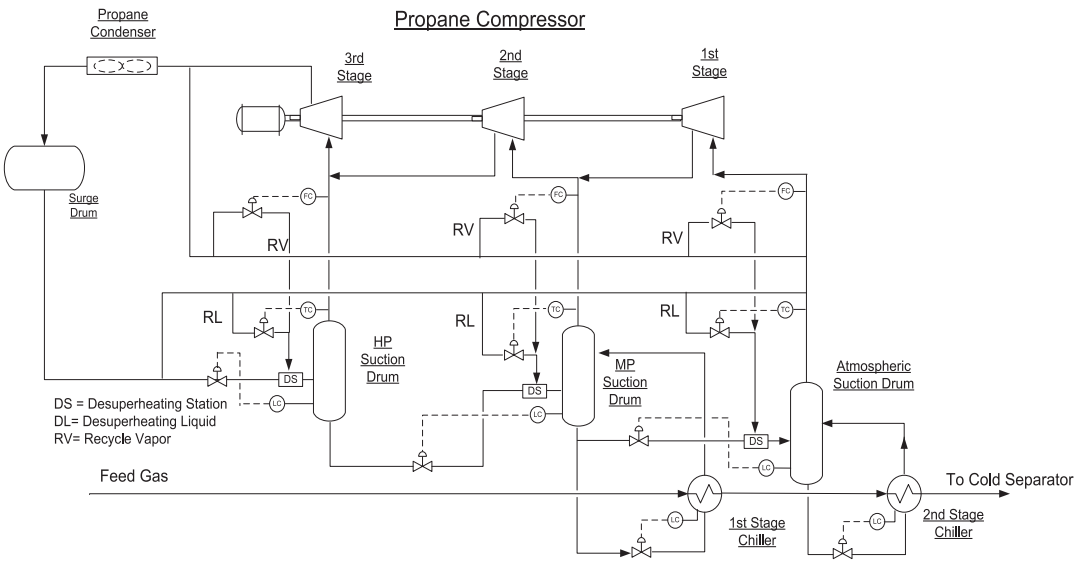

FIGURE 11.2

Process flow schematic of a three-stage propane refrigeration system.

The aerodynamic of a centrifugal compressor typically requires the compressor flow to stay above 60% of the design flow. Below this point, the compressor will be in a "surge" condition and become unstable. Gas recycle (RV) is required for compressor protection, when the gas plant is operating under turndown conditions, during plant startup or shutdown. Desuperheating station (DS) must be installed which cools the compressor recycle gas by injecting propane liquid (DL) to maintain the design suction temperatures. The propane compressor control and the propane desuperheating schematic are shown in Fig. 11.2.

11.2.2 CASCADE REFRIGERATION

Propane refrigeration can produce refrigeration at −40°F, which is adequate for the hydrocarbon dew point controlling operation for pipeline gas applications. However, for rich gas, such as shale gas, with a higher ethane content, a lower refrigerant temperature is required to meet the pipeline gas heating value specifications. Alternatively, when ethane and propane recoveries are attractive, lower temperature cooling is also necessary. Cascade refrigeration can be an option to generate a low temperature refrigerant. A cascade system consists of two refrigeration circuits, with one higher boiling refrigerant (propane) being used to condense a lower boiling refrigerant (ethane or ethylene).

A typical cascade refrigeration schematic is shown in Fig. 11.3. The feed gas is first cooled in the first stage chiller and second stage chiller in the propane refrigeration circuit, and then in the first stage chiller and second stage chiller in the ethane refrigeration circuit. The propane condenser is cooled by ambient air or cooling water and the ethane condenser is cooled by evaporating propane at −40°F. With such an arrangement, an ethane refrigerant at −120°F can be produced for cooling in the demethanizer in a gas plant.

Because of the high equipment counts, high capital costs, and complexity in operation, cascade refrigeration system is seldom used in NGL recovery.

11.2.3 MIXED REFRIGERANTS

An alternative to the multistage cascade refrigeration is to use a single mixed refrigerant. A multiple component refrigeration system in combination with a propane precooling system is common in liquefaction of natural gas. The mixed refrigerant composition must be varied such that the evaporating heat curve of the mixed refrigerant matches closely with the gas cooling and condensing heat curve. Although the equipment count is lower than the cascade refrigeration, mixed refrigeration system is also seldom used in NGL recovery due to operation complexity.

However, when feed gas pressure is low, such as 300 to 400 psig, refrigeration generated by a J−T valve or turboexpander is limited, mixed refrigerant is an alternate solution to generate cold temperature refrigeration, such as the IPOR process offered by Randall Gas Technologies (Huebel and Malsam, 2011). The refrigeration process can be configured with propane refrigeration and mixed refrigeration, with the mixed refrigerant imported or extracted from the fractionation column.

11.3 LIQUID RECOVERY PROCESSES

There are various processes in natural gas liquids recovery, depending on the feed gas compositions, the recovery levels, and the product target specifications. It can vary from the simple hydrocarbon dew

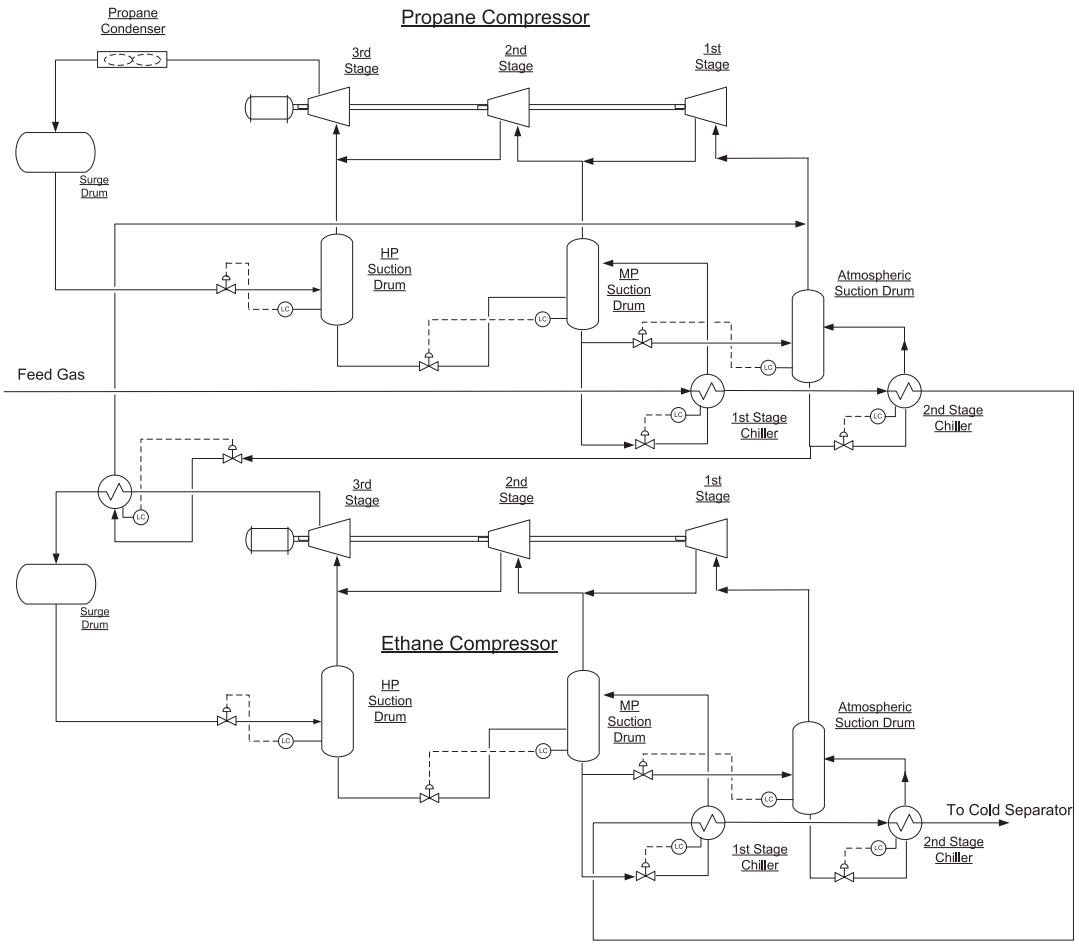

FIGURE 11.3

Process flow schematic of a cascade refrigeration system.

point controlling unit to the more complex cryogenic turboexpander units. While some designs can be standardized, the variations in feed gas composition and recovery targets require some modifications of the standard units.

11.3.1 HYDROCARBON DEW POINT CONTROLLING WITH JOULE–THOMSON COOLING

When the feed gas is available at high pressure, the gas high pressure can be used to generate cooling by isenthalpic expansion or Joule–Thomson cooling. The gas cooling effect will cause heavy hydrocarbons to drop out. Removal of the heavy hydrocarbons can then meet the hydrocarbon dew point

specification. However, even if the hydrocarbon dew point were met, the product gas still may not meet the specifications on heating value and Wobbe Index, if the ethane content is high, such as the shale gas.

For smaller plants, the glycol injection unit is a standard unit which can be used to control the water dew point and hydrocarbon dew point of the gas, which is discussed in Chapter 9. Alternatively, feed gas can be separately dried using TEG dehydration or the molecular sieve unit followed by hydrocarbon removal as shown in Fig. 11.4. In this process, dried gas is cooled by the cold separator vapor in a gas/gas shell and tube exchanger. The chilled gas is reduced in pressure using a Joule−Thomson (J−T) valve. The J−T letdown operation cools the gas further, producing a liquid condensate in the cold separator.

The cold separator pressure operates at the feed gas pressure, such as 600 to 700 psig. A high separator pressure would lower the recompression requirement of the residue gas. However, high pressure also reduces the relative volatility between components, making removal of the desirable products difficult.

Liquid from the cold separator is fractionated in a stabilizer or stripper, which removes the methane and lighter components. For Y-grade NGL production, the stabilizer operates as a demethanizer, heated with steam or a heat medium.

Where NGL export pipeline does not exist, the stabilizer can be operated at a lower pressure, to produce a condensate product, typically with 10 psia vapor pressure. When the NGL contains excessive amounts of pentane, the pentane hydrocarbons must be removed as a side-draw from the stabilizer column, in order to meet the product's vapor pressure specification.

The conventional dew pointing unit is designed to recover condensate hydrocarbons and can only recover a moderate level of the propane (C_3^+) product. If high propane recovery is required, a deep hydrocarbon dew pointing process (Fluor Process) can be used which can recover over 95% propane (see Section 11.3.3).

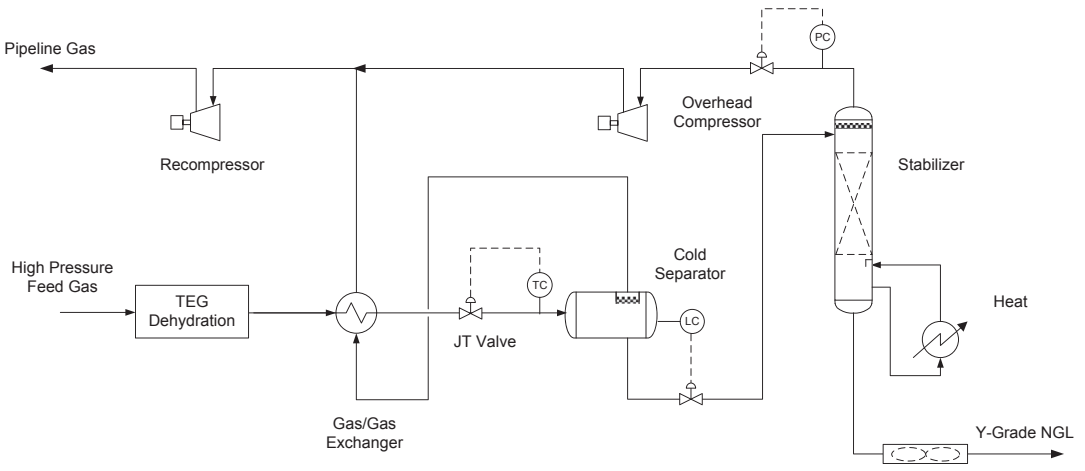

FIGURE 11.4

Hydrocarbon dew point controlling using the J−T process.

11.3.2 HYDROCARBON DEW POINT CONTROLLING WITH A MECHANICAL REFRIGERATION UNIT

When feed gas is supplied at low pressures, there will not be sufficient pressure differential to operate the J−T process. In this situation, the feed gas can be chilled at pressure using a Mechanical Refrigeration Unit (MRU). The basic process is shown in Fig. 11.5, where the J−T valve is replaced by the propane refrigeration chiller. The chiller is a kettle-type exchanger with propane evaporating on the shell side. The propane level can be varied to control the separator temperature, or the hydrocarbon dew point temperature.

When feed gas is supplied at low pressures, the J−T operation can be replaced by mechanical refrigeration. Typically, rich gas would require higher refrigeration duty which can be supplied by a mechanical refrigeration system.

When the feed gas pressure is high, mechanical refrigeration can be used in combination with J−T operation to provide a lower separator temperature, to further lower the hydrocarbon dew point temperature.

11.3.3 DEEP HYDROCARBON DEW POINTING UNIT (DDP)

The J−T units and the mechanical refrigeration units have been used to meet the hydrocarbon dew point specification of the sales gas. Typically, with a lean gas with low ethane content, the heating value specification can be met. However, with a higher ethane content feed, the heating value of the product gas may exceed specification. Particularly, in Western US and Europe, a very lean gas with low Btu content is required. The California pipeline typically operates with heating values as low as 970 Btu/scf (Mak et al., 2004b).

To meet the heating value specifications for these markets, most of the propane and butane components must be removed. The conventional J−T process or the refrigeration process in the

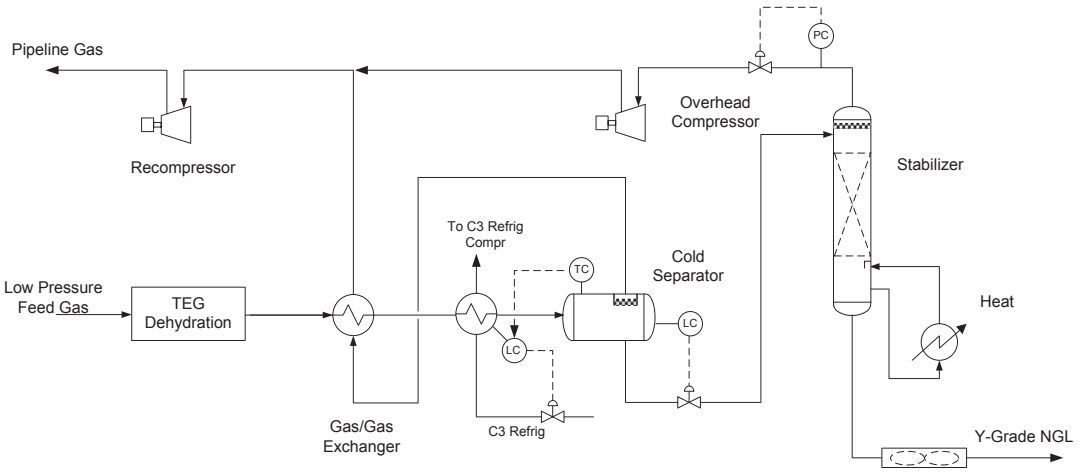

FIGURE 11.5

Hydrocarbon dew point controlling using propane refrigeration.

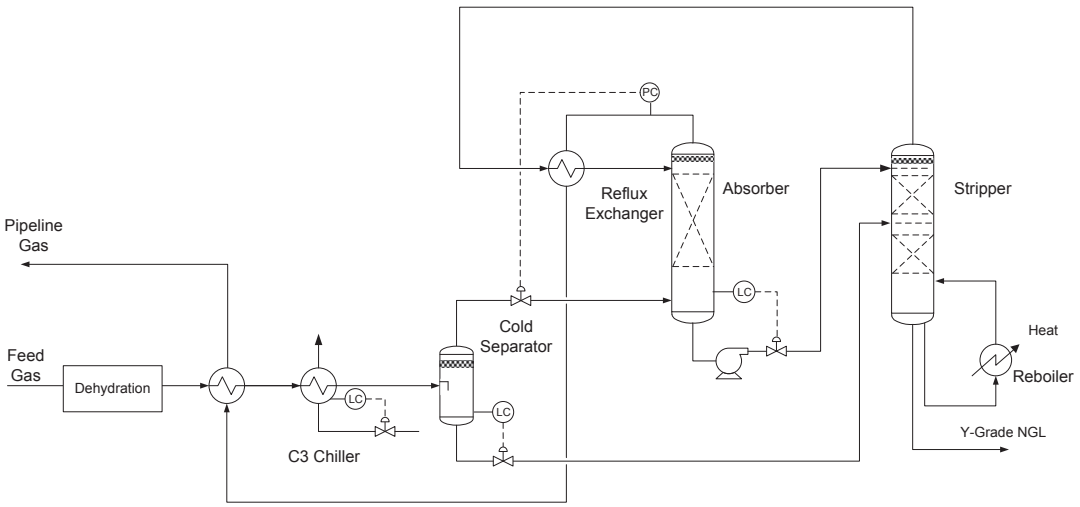

FIGURE 11.6

Deep hydrocarbon dew point controlling process.

previous would not meet the specifications. Fluor patented a deep hydrocarbon dew pointing process (DDP) that can achieve over 95% propane recovery. The process schematic is shown in Fig. 11.6. The process uses propane refrigeration and J−T expansion. This deep hydrocarbon dew pointing unit requires two columns: an absorber and a demethanizer. The absorber operates at cryogenic temperature while the deethanizer operates at −30°F and higher temperature.

The feed gas must be dried with a molecular sieve unit to avoid hydrate formation on the top of the absorber. As seen in the process, the absorber overhead vapor is used to cool and condense the stripper overhead vapor, which forms a cold two-phase reflux stream to the absorber. The stripper reflux recycles the C_2+ components to the absorber, which condenses the $C_3{}^+$ component from the feed gas. With propane refrigeration and J−T cooling, the process can recover or remove most of the propane and heavier components.

The main advantage of the deep hydrocarbon dew point unit is the flexibility to produce NGL with varying ethane content. The ethane content can be lowered to 1 vol% as needed to meet specification of the propane product. Alternatively, the ethane content can be increased to meet the Y-grade NGL specifications if there is an ethane demand.

The other advantage is the turndown flexibility. The unit can be turned down to below 25%, which is necessary in operation when the initial feed gas rate is lower than expected. This is a significant advantage over a conventional turboexpander plant which is limited to 50% turndown.

11.3.4 TURBOEXPANDER NGL RECOVERY PROCESSES

The term "turboexpander" is referred to an expander/compressor machine as a single unit. It consists of two primary components: the radial inflow expansion turbine and a centrifugal compressor

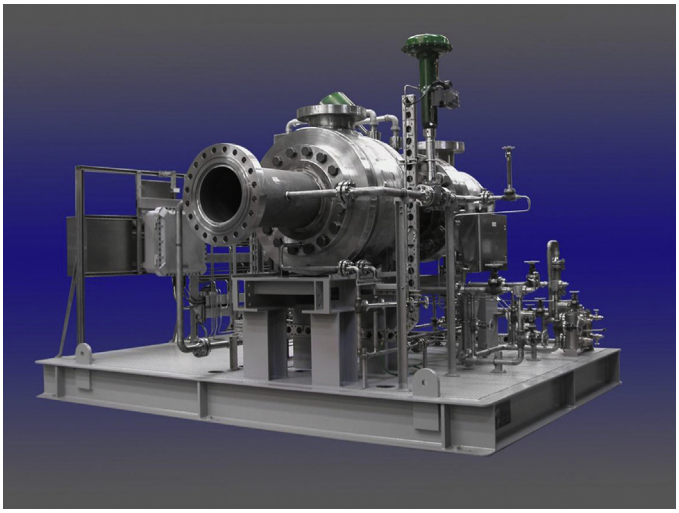

FIGURE 11.7

Typical expander–compressor setup (Mather and Ershaghi, 2012).

Courtesy of Atlas Copco.

integrated as a single assembly (see Fig. 11.7). The expansion turbine is the power unit and the compressor is the driven unit.

In cryogenic NGL recovery processes, the turboexpander achieves two different but complementary functions. The main function is to generate refrigeration to cool the gas stream. This is done by the expansion turbine end that expands the gas isentropically by extracting the enthalpy from the gas stream, causing it to cool. The other function is the use of the extracted energy to rotate the shaft to drive the compressor end of the turboexpander, which recompresses the residue gas stream.

The first turboexpander unit was built in 1964 for NGL recovery in the city of San Antonio, Texas. The gas is supplied at 700 psig pressure and is letdown in pressure to about 300 psig to the demethanizer. Methanol injection was used for hydrate inhibition. Until this time, LPG recovery was mainly achieved with refrigerated lean oil, which is described in the later section.

The first turboexpander process patent was issued to Bucklin (Fluor) in 1966. The flow schematic is shown in Fig. 11.8. The concept was to use turboexpander, which is a more efficient method of cooling, to generate cooling instead of the J–T valve. The feed gas is cooled by the cold demethanizer overhead and separated in the HP cold separator. The separator vapor is letdown in pressure using the turboexpander and fed to the top of the demethanizer as a reflux. The HP cold separator liquid is letdown in pressure to the LP cold separator. The separator liquid is further letdown and used to cool the feed gas before it is fed to the lower part of the demethanizer. The demethanizer bottom product is heated with steam that controls the methane content (see Table 11.2).

Earlier NGL recovery units did not have the benefits of the compact the brazed aluminum heat exchanger and would require multiple shell and tube heat exchangers to achieve the chilling requirements. Even with an extensive heat integrated scheme as shown in Fig. 11.9, high NGL recovery could not be achieved. The other limitation of earlier expander designs is the low expansion ratio,

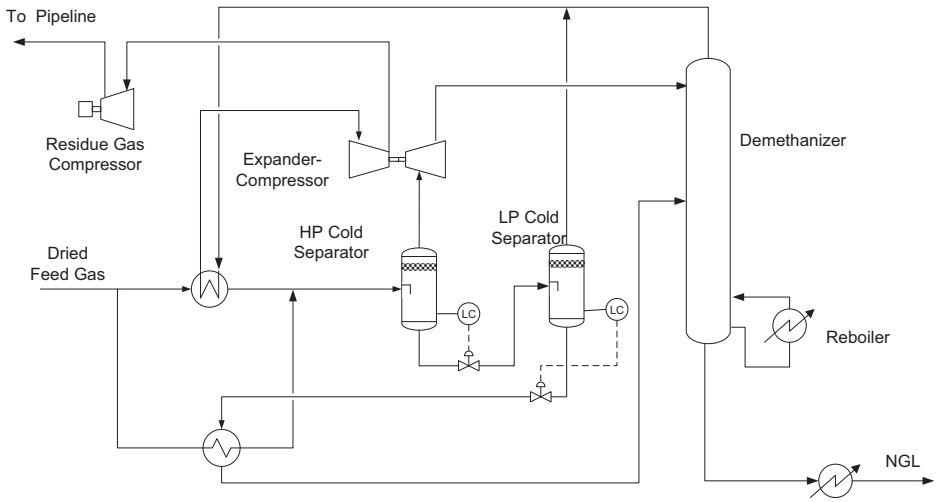

FIGURE 11.8

Process flow schematic of the first turboexpander NGL recovery process (Bucklin, 1966).

which required two expanders operating in series to achieve a high expansion ratio. A higher expansion ratio would generate more cooling that is necessary for a high NGL recovery.

The process flow schematic of a turboexpander plant built in the 1970's is shown in Fig. 11.9. The process uses two expander–compressor sets operating in series and several separators to produce various liquid streams that are fed to different locations in the demethanizer. The process also requires propane refrigeration for feed gas cooling. The NGL recovery process could achieve about 70% ethane recovery and was typically based on a relatively rich feed at about 950 psig pressure. Most of these

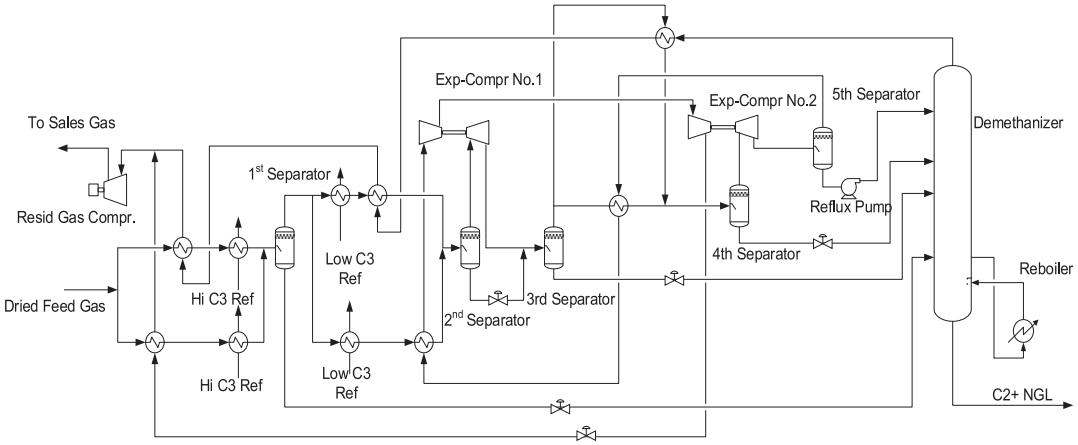

FIGURE 11.9

Process flow schematic of an earlier turboexpander NGL recovery unit.

FIGURE 11.10

An earlier turboexpander NGL recovery unit.

Courtesy of Fluor.

NGL recovery plants are still operating today, but they are processing much leaner gases as the reservoirs are depleted. Unless these plants were revamped for the new feed conditions, ethane recovery would drop to about 55%. A picture of the earlier NGL recovery unit is shown in Fig. 11.10.

The main contributors to the success of today's NGL recovery plants are the turboexpanders and the brazed aluminum exchangers. The application of turbo-expanders to the natural gas industry began in the early 1960, which was followed by the development of brazed aluminum heat exchangers.

11.3.4.1 Turboexpander

Today's turboexpander designs can yield very high adiabatic efficiencies (over 85%). However, there are aerodynamic limitations for both the expander and compressor. Machinery efficiencies will drop if the gas composition or flow rate were different than the design points. In most instances, when the changes are temporary, they can be managed by the expander bypass J−T valves. During the expander bypass operation, the recompressor will also be bypassed, resulting in a lower pressure to the residue gas compressor. Consequently, the NGL plant temperature profile will increase, and liquid recovery and plant capacity will be reduced. If the flow conditions are expected to continue, rewheeling of the expander and compressor is required.

11.3.4.2 Brazed Aluminum Heat Exchanger

The application of a Brazed Aluminum Heat Exchanger (BAHX) to the gas processing industry is another important advance. The BAHX can significantly reduce the size of heat exchangers while achieving a close temperature approach on the heat exchanger. The exchanger is compact, requiring about 20% the size of a shell and tube exchanger of comparable performance. Furthermore, the

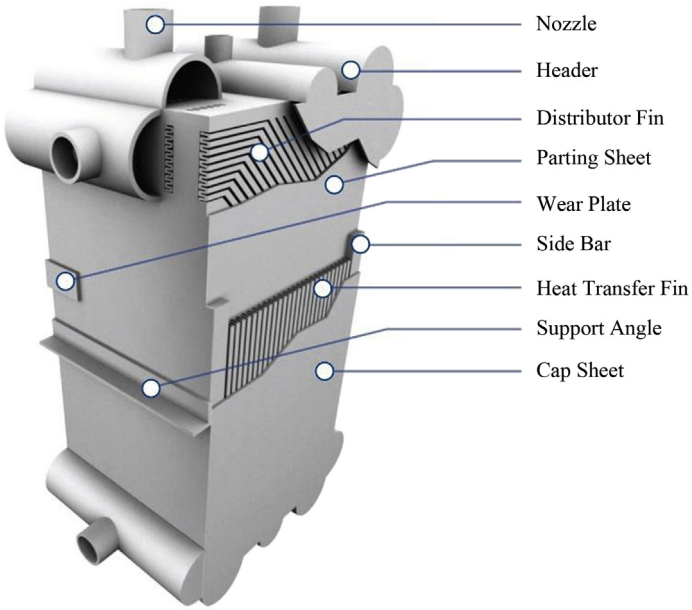

FIGURE 11.11

Brazed aluminum heat exchanger.

Courtesy of Chart.

alternating plate fin construction offers multiple stream capability and can replace multiple shell and tube heat exchangers, significantly reducing the space requirement and simplifying installation. A typical brazed aluminum heat exchanger is shown in Fig. 11.11.

BAHX are constructed of aluminum material and are light in weight. The relatively high conductance of aluminum and the fin configuration can produce very close temperature approaches among different passes, which contributes to the lower power consumption and higher NGL recovery. The disadvantages are that they are prone to fouling from hydrates or other foreign matters and they are susceptible to aluminum corrosion by mercury contaminants. They require feed gas filtration and pretreatment with mercury removal beds. Aluminum is also a weaker material than stainless steel and is prone to thermal stress. The maximum operating is limited to 150°F and the temperature differentials among exchanger passes must be kept below 50°F.

When all these design limits are circumvented, BAHX can be effectively used to produce a highly efficient NGL recovery design. The exchanger designs are well known and are available from several manufacturers in different countries.

11.3.5 LEAN OIL ABSORPTION

The lean oil absorption process was developed in the early 1910s which was used exclusively until the 1970s. The absorption unit uses a lean oil to absorb the C_3^+ components followed by a deethanizer, and a rich oil still to regenerate the rich oil. Propane and butane products can be produced. A typical refrigerated lean oil absorption process is shown in Fig. 11.12.

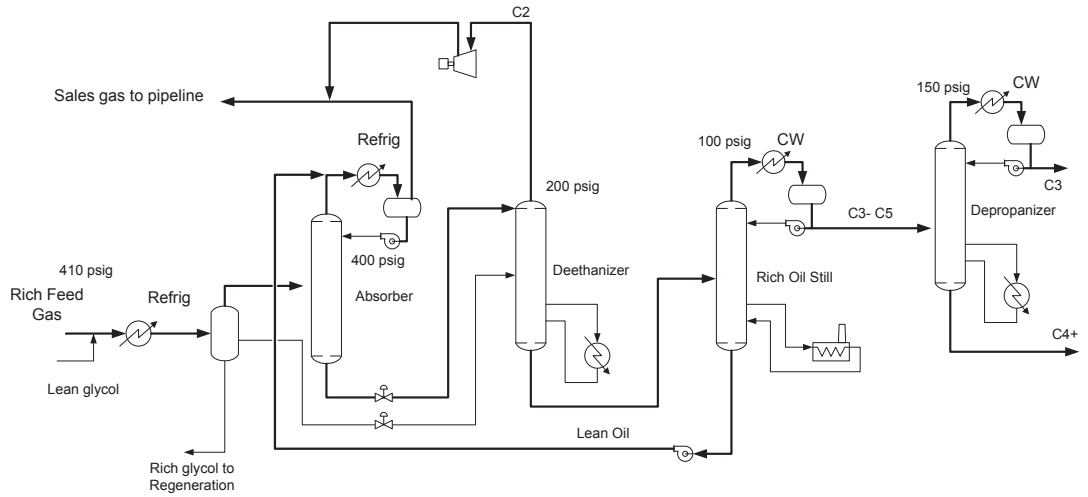

FIGURE 11.12

A typical lean oil absorption process.

To allow the unit to operate at low temperatures, the feed gas must be injected with ethylene glycol solution to avoid hydrate formation in the heat exchangers. The feed gas is cooled by propane refrigeration and separated in a cold separator, typically at about 0°F. The separator liquid is sent to the deethanizer while the separator vapor is routed to the absorber operating at 400 psig. Refrigerated lean oil is used to absorb the C_3^+ content from the feed gas, producing a lean gas and a propane rich bottom which is sent to the deethanizer. The deethanizer operates at a lower pressure, typically at 200 psig, producing an ethane rich gas and a rich oil bottom containing the C_3^+ components.

The deethanizer overhead is compressed to the sales gas pipeline or used as fuel gas. The bottom product is further processed in a rich oil still which regenerates a lean oil to be recycled back to the absorber and an overhead distillate containing the C_3^+ components. The C_3^+ stream can be fractionated in a depropanizer, which produces the propane and butane product. Because of the high boiling material of the lean oil, a fired heater is used in the rich oil still. If necessary, the lean oil composition can be controlled using a lean oil still (not shown) to remove the heavy tails of the lean oil from the process.

A typical refrigerated lean oil process can achieve 50%−60% propane recovery, depending on the feed gas composition. Because of the high equipment counts and the process complexity, lean oil absorption processes are not cost competitive to expander plants and are seldom used today.

11.3.6 MODERN NGL RECOVERY PROCESSES

Modern NGL recovery processes are turboexpanders based using various reflux configurations. There are many patented processes that can be used to improve NGL recovery, either for propane recovery or ethane recovery. In addition, some of ethane recovery units can operate on ethane rejection mode with

minimum loss in propane. Similarly, some of the propane recovery units can also be operated on ethane recovery. These processes are discussed in detail in the following sections.

11.3.6.1 Dual Column Reflux Process

The dual column process was quite common among NGL recovery units. Typically, the first column acts as an absorber recovering the bulk of the NGL components and the second column serves as deethanizer during propane recovery and demethanizer during ethane recovery. Adding refluxes to the dual column design process was originally configured for high propane recovery. The process is very efficient and can achieve over 99% propane recovery. The process flow schematic of the dual column reflux process is shown in Fig. 11.13.

Feed gas, typically supplied at about 1000 psig, is first dried using molecular sieve dryers, and then cooled in a feed exchanger (BAHX). The feed gas is chilled with the absorber overhead vapor, cold separator liquid, and the absorber bottoms. Refrigeration is generated using a turboexpander by expanding the separator gas to the absorber typically operating at 450 psig. When processing a rich feed gas, propane refrigeration is often used to supplement the cooling requirement.

The absorber bottom liquid is pumped by the bottom pump to the deethanizer which operates at a slightly higher pressure than the absorber. The deethanizer overhead is cooled using propane refrigeration, producing a C_2 rich liquid that is used as reflux to the deethanizer and the absorber. The absorber overhead is used to cool and condense the absorber reflux stream, which further lowers the reflux temperature for the separation process. With the dual reflux process, a very high propane recovery can be achieved with very low energy consumption.

Fig. 11.14 shows a picture of a dual column reflux processing plant. The absorber requires less number of trays, located in front of the deethanizer.

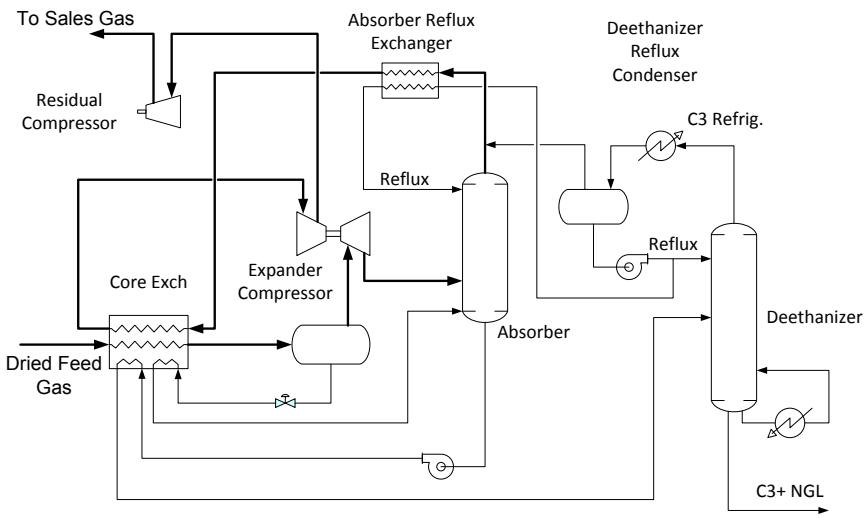

FIGURE 11.13

Dual column reflux process (Mak, 2005).

FIGURE 11.14

Dual column reflux unit.

Courtesy of Fluor.

11.3.6.2 Gas Subcooled Process (GSP)

The Gas Subcooled Process (GSP) is a common ethane recovery in the gas processing industry. The process was invented by Ortloff in the late 1970. The schematic of a typical GSP process is shown in Fig. 11.15. The unique feature of the GSP process is the split flow arrangement using a portion of cold

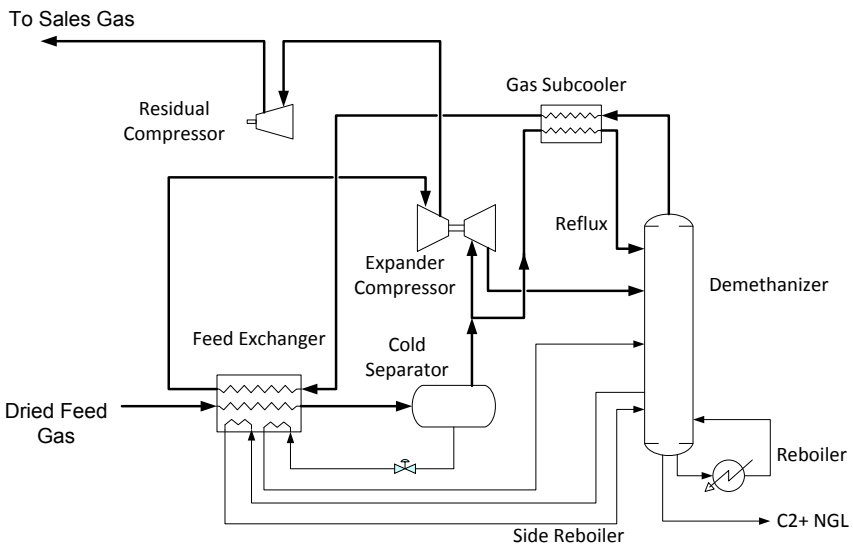

FIGURE 11.15

Schematic of a gas subcooled process (Pitman et al., 1998).

separator vapor (about 30%) to form a lean reflux stream to the demethanizer. The refrigeration content of the residue gas from the demethanizer is used in subcooling the reflux stream in the gas subcooler. The remaining portion is expanded in a turboexpander, generating the low temperature refrigeration for the demethanizer. One- or two-side reboiler on the demethanizer is typically used to reduce the refrigeration requirement.

The demethanizer reboiler is used to produce an ethane rich liquid which must meet methane and CO_2 specifications (see Table 11.2). The column typically operates between 350 and 450 psig, depending on the feed gas inlet pressure, the feed gas composition, and the ethane recovery level. The Gas Subcooled Process typically recovers 70%–80% of the ethane content.

11.3.6.3 Ortloff SCORE

The SCORE (single column overhead recycle process) licensed by Ortloff Engineers Ltd. is based on the same reflux principle as the Dual Column Reflux Process. The SCORE process is designed to recover over 99% propane from the feed gas in a single column configuration.

This process recovers the C_3^+ hydrocarbons from the feed gas and produces a lean residual gas for sales. Alternatively, the residue gas can be sent to the natural gas liquefaction plant. It has been used in natural gas liquefaction unit to accomplish the function of the scrub column for the removal of C_{5+} hydrocarbons. The recovered NGL can be exported or used for blending with LNG if a higher heating value LNG is required. Fig. 11.16 shows a simplified process schematic of a typical SCORE process (Thompson et al., 2004).

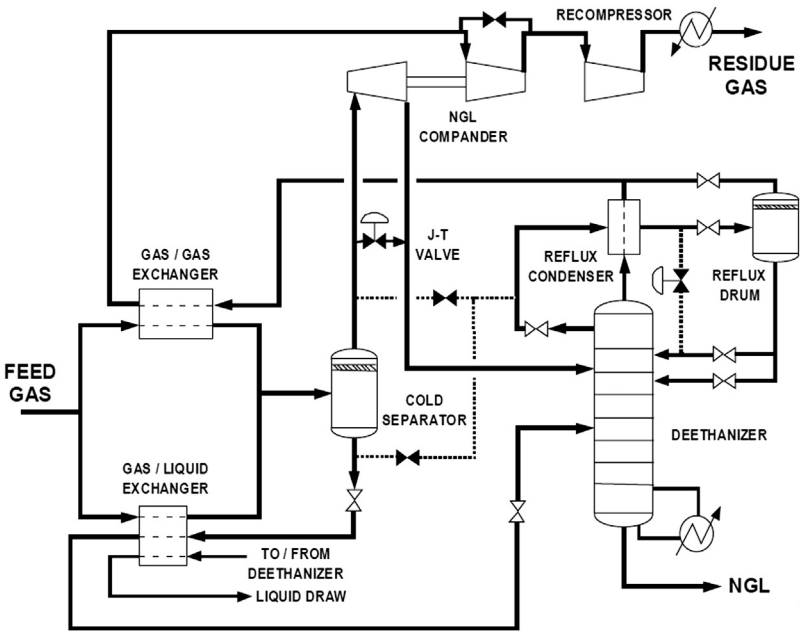

FIGURE 11.16

Ortloff SCORE process (Thompson et al., 2004).

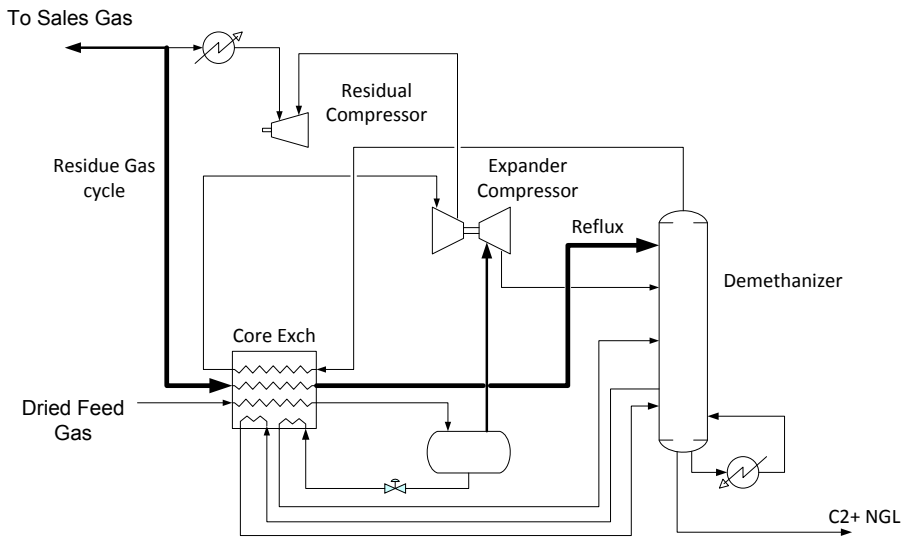

FIGURE 11.17

Residue gas recycle for high ethane recovery.

11.3.6.4 Residue Gas Recycle

When high ethane recovery is required, additional cooling is required by lowering the demethanizer pressure or by recycling a portion of the residue gas as reflux to the absorber. If low residue gas pressure is acceptable, lowering the column pressure would lower the reflux temperature, and is more efficient than recycling residue gas. In any cases, the CO_2 in the feed gas must be lowered to 500 ppmv to avoid CO_2 freezing. The process flow schematic of a residual gas recycle process is shown in Fig. 11.17. With this configuration, C_2 recovery as high as 98% can be achieved.

Optimum C_2 recovery levels should be evaluated based on the project economics. Typically, C_2 recovery level greater than 95% would require a significant increase in capital and operating cost.

11.3.6.5 Fluor TCHAP

When the sales gas must be compressed to the pipeline pressure, it is desirable to operate the demethanizer at as high a pressure as possible. However, this may not be feasible in conventional demethanizer designs, such as that shown in Fig. 11.15.

Conventional demethanizer is a single column design, which operates between 350 and 450 psig. The operating pressure should stay way below the critical pressure. More importantly, the critical region of the demethanizer column is the column bottom which has the highest temperature. Increasing the column pressure will increase the bottom temperature, further moving the operating point closer to the critical region, which makes fractionation of methane from ethane difficult. For this reason, most of the demethanizers typically operate between 350 and 450 psig, with 500 psig as the upper limit.

To overcome the fractionation difficulty, Fluor has developed the TCHAP (Twin Column High Absorption Process) using a dual column approach. The first column operates as an absorber at 600

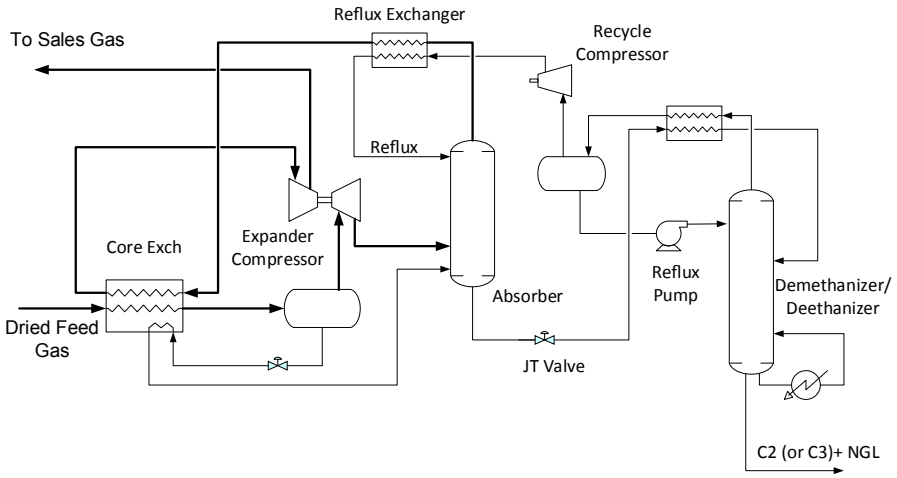

FIGURE 11.18

Fluor TCHAP process (Mak et al., 2003).

psig or higher pressure and is designed for bulk absorption. The second column operates at a lower pressure at about 450 psig, which operates as a demethanizer or deethanizer. To improve NGL recovery, the overhead vapor from the second column is recycled using a small overhead compressor. The recycle gas is chilled using the absorber overhead vapor and used as a cold reflux to the absorber.

The process schematic of the TCHAP process is shown in Fig. 11.18. This NGL process may eliminate residue gas compression which can significantly reduce the overall power consumption of the facility. The TCHAP process can achieve over 80% ethane and 99% propane recovery.

It should be recognized that when residue gas is used as feed gas to an LNG liquefaction plant, the high residue pressure has the benefit of reducing the refrigeration power consumption in the LNG liquefaction process.

11.3.6.6 Fluor TRAP

NGL recovery units are frequently required to operate in ethane rejection mode when the profit margin of ethane product is low. In today's open markets, the ethane price is lower than natural gas price on a Btu basis. Unless ethane production is tied to a contractual requirement, total or partial ethane rejection is required. During the ethane rejection operation, the NGL recovery units are required to reject their ethane content to the sales gas pipeline. Ethane recovery processes, such as the GSP (Gas Subcooled Process), can typically recover about 70%−80% of ethane content and about 98% of propane content. When operated in ethane rejection, propane recovery will drop to 85%−90%, resulting in a loss in liquid revenue.

To circumvent this problem, Fluor has developed the TRAP (Twin Reflux Absorption Process). The process can be operated in ethane recovery and can also be operated in ethane rejection while maintaining high propane recovery (Mak et al., 2004a). The process flow schematic is shown in Fig. 11.19.

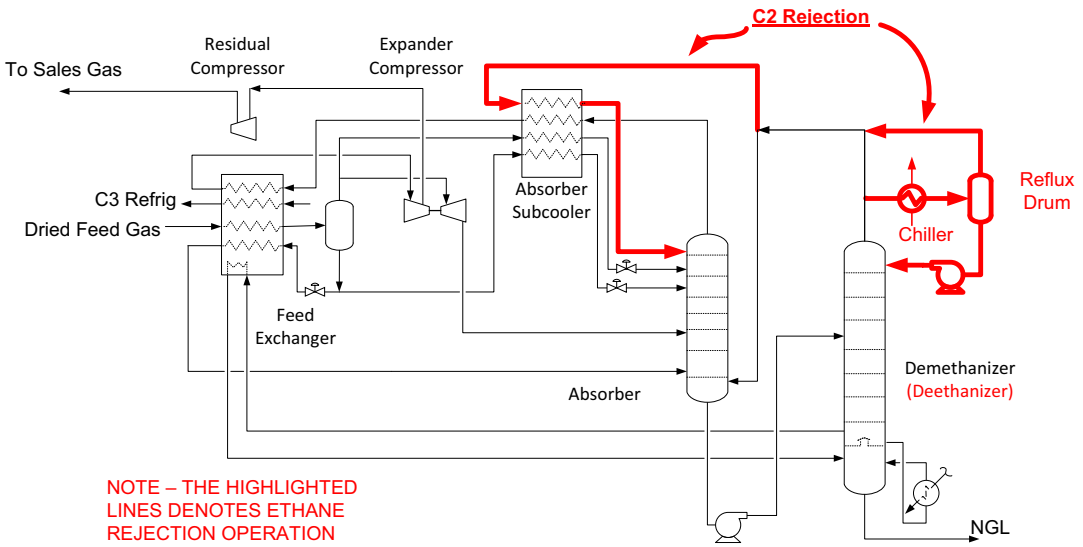

FIGURE 11.19

Fluor TRAP process (Mak et al., 2004a).

The process is a dual column design, with the second column acting as a demethanizer during ethane recovery and as a deethanizer during ethane rejection. During ethane recovery operation, feed gas is chilled using the cold residue gas and propane refrigeration and separated in the cold separator. About 30% of the expander drum vapor is subcooled in the absorber subcooler forming a subcooled reflux stream to the absorber. The remaining is expanded across a turboexpander producing the refrigeration.

The absorber produces a bottom liquid enriched in the C_2+ liquids, which are routed to the second column. During ethane recovery, the second column operates as a demethanizer, stripping the methane content to meet the Y-grade specification. The demethanizer overhead vapor is routed to the bottom of the absorber where the ethane content is reabsorbed. During this operation, the demethanizer reflux system is bypassed.

During ethane rejection, the second column operates as a deethanizer. The deethanizer overhead vapor, which is an ethane rich stream, is routed to the absorber subcooler, forming an absorber reflux stream. The ethane rich stream absorbs the propane content from the feed gas and is recycled back to the deethanizer. During ethane rejection, the TRAP process can recover over 98% propane.

11.3.7 OTHER HYDROCARBONS REMOVAL PROCESSES

For removal of small quantities of heavy hydrocarbons, such as in fuel gas conditioning, there are other simpler processes that can be used, instead of the traditional NGL recovery processes. Some of these processes are briefly described in the following sections.

11.3.7.1 Solid Bed Adsorption

Solid bed adsorption process can be designed to selectively remove specific hydrocarbons. The adsorbent can be silica gel (i.e., Sorbead) that can be designed to remove most of the C_6^+ hydrocarbons. A typical two-bed adsorption process is shown in Fig. 11.20. Regeneration is accomplished by passing heated recycle gas through the bed. The heavy hydrocarbon is recovered from the regeneration gas by cooling, condensation, and separation.

The solid bed adsorption process can be used to adsorb hydrocarbons at high pressure. This process has an advantage over the refrigeration process which depends on low pressure for phase separation (Parsons and Templeman, 1990). The disadvantage is the high pressure vessels which can be expensive. Details of the design and operation of a solid bed adsorption system can be found in Chapter 9.

11.3.7.2 Membrane Separation

The membrane-based process is a compact design, widely used onshore and particularly suitable for offshore installation due to small footprints and low weight. The process is simple and is suitable for remote-controlled operation.

In the membrane process a high pressure stream is passed over a polymeric fiber or sheet, while low pressure is maintained on the opposite side of the membrane. The more permeable gas passes through the membrane. Due to the high permeability of CO_2 (and H_2S) most applications in natural gas are used for acid gas removal but other applications exist. Rubbery membranes that are more permeable to heavy hydrocarbons over methane have been used commercially. The hydrocarbon permeation membranes are typically made with vitreous polymers that exhibit high permeability with respect to heavy hydrocarbons (C_6^+). New membrane materials are continuously being developed. Both Air

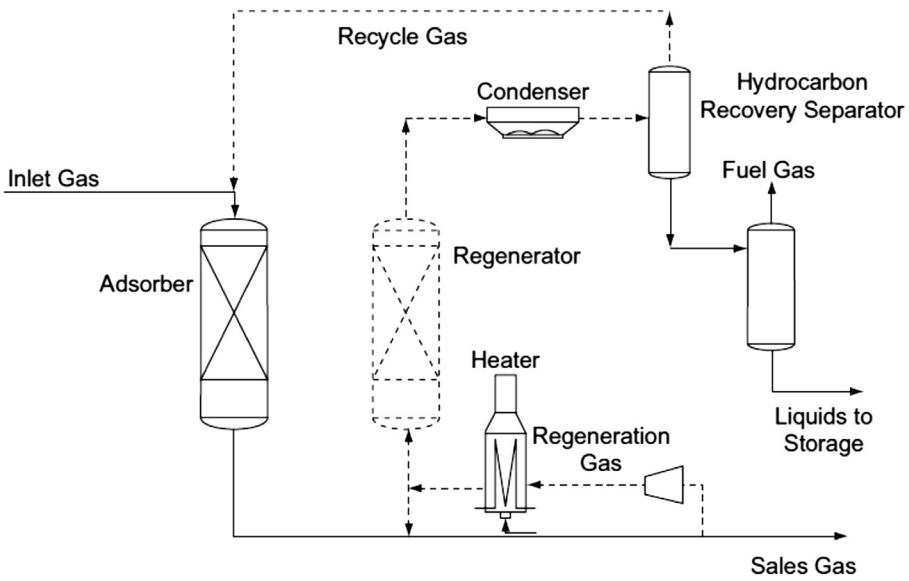

FIGURE 11.20

Schematic of a solid bed adsorption process.

Liquide (PoroGen) and Membrane Technology & Research Inc. (MTR) have commercialized and offer systems using these new membranes that permeate heavy hydrocarbons.

The two major applications for rubbery membranes that are used for heavy hydrocarbon removal are the production of a lean fuel gas and hydrocarbon dew point control for pipeline specification (Mokhatab et al., 2017).

Fig. 11.21 shows the flow scheme of a membrane system used to produce a lean fuel gas for the engine of the pipeline compressor. In this process, a slip stream of the pipeline gas is processed in the membrane module which removes the heavy hydrocarbons, producing a lean gas as gas engine fuel. The benefit of lean fuel is improved operation and reduced maintenance of the gas fueled driver. This application is attractive since the removed heavy hydrocarbons can be recycled back to the compressor suction and recompressed back to the pipeline system, thus there is no loss of hydrocarbons. Alternatively, the hydrocarbon contents can be recovered by condensation and chilling to produce a liquid byproduct.

The application for compressor station is one use for the heavy hydrocarbon permeating membrane. Other applications have also been considered. These include dedicated fuel gas conditioning for gensets, most commonly for offshore platforms where quality fuel may not exist. Another process of recent interest is the treatment of flare gas for the conditioning of the gas at stranded sites with treated gas used as local fuel and with recovery of heavy hydrocarbons.

Recent developments in dew point control include membrane designs that can operate in condensing mode as well as membranes that allow the simultaneous removal of water and heavier hydrocarbons from natural gas. The most common application for such membranes is for fuel gas conditioning where water and heavy hydrocarbons permeate from high pressure to low pressure, leaving a lean fuel stream at high pressure. As with all membrane systems disposition of the low pressure permeate stream must be considered, in this case a stream rich in heavy hydrocarbons and water. Overall dozens of systems operate in this service, and industry acceptance is slowly growing.

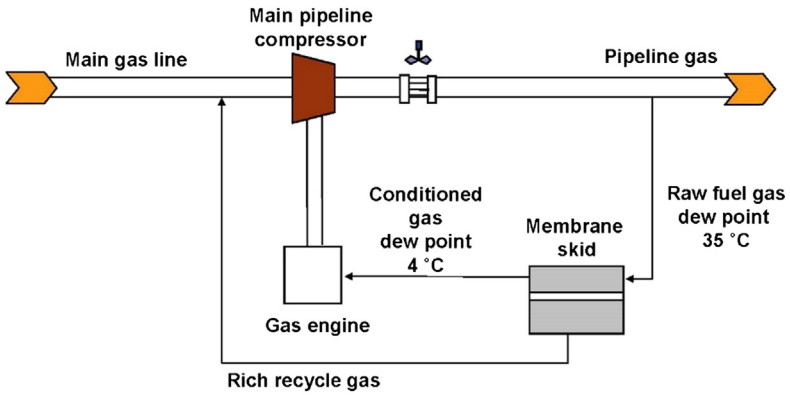

FIGURE 11.21

Process schematic of the membrane separation process.

11.3.7.3 Twister Supersonic Separation

The Twister separation technology is based on a supersonic mechanism (a combination of aerodynamics, thermodynamics, and fluid dynamics) to condense and remove water and heavy hydrocarbons from natural gas. It is based on the concept that condensation and separation at supersonic velocity reduce the residence time to milliseconds, allowing no time to form hydrates.

The Twister supersonic separation technology can potentially offer significant costs and environmental benefits for offshore operation. A more detailed discussion of the Twister technology can be found in Chapter 5.

11.4 SELECTION OF THE NGL RECOVERY PROCESS

The NGL recovery process must be selected based on the feed gas composition (GPM), feed gas inlet pressure, and residue gas delivery pressure. The ethane content in the feed gas is important as it will determine the design that meets the sales gas heating value specification. The amount of ethane recovered or removed with the selected process must meet the sales gas heating specification, typically 1200 Btu/scf.

If the NGL unit is designed for ethane recovery, the unit must be able to operate in ethane rejection mode without propane losses. Ethane rejection operation is necessary when ethane price is lower than natural gas price, on a Btu basis. Ethane recovery may become profitable if there is a high demand for ethane. The NGL unit must be able to operate between these two recovery modes.

Lean oil absorption is not used due to its low efficiency, process complexity, and high maintenance cost. Cascade refrigeration or mixed refrigeration systems are used only if there are no obvious alternatives.

When the gas plant is in a remote area and is remote-controlled, simplicity in operation and maintenance is particularly important. The use of a deep dew pointing unit using J−T cooling avoids the complexity associated with operating a turboexpander. The deep dew pointing unit can achieve high propane recovery although the power consumption is higher than an expander plant. However, with the low energy cost, the slightly lower efficiency may be justified.

Typically, the cost of an NGL recovery unit is a minor contributor to the total plant cost, and in most cases, moderate to high level of recovery can be justified. Other supporting facilities, such as inlet gas compression, gas treating, dehydration, product treating, product storage, and liquid handling and transportation systems must be evaluated. High recovery will require an increase in storage, transportation, and liquid handling facility.

11.5 NGL RECOVERY TECHNOLOGY DEVELOPMENT

The NGL recovery technology is continuously evolving. Today's NGL processes are using the high efficiency expanders and compressors and optimized compact heat exchangers to reduce capital and operating costs.

There are many proprietary NGL technologies available. They typically use multiple refluxes, column design, and heat exchanger configuration closely integrated to reduce cost. While these innovations may be more efficient and increase recoveries, they may prove to be difficult to operate under off-design conditions. Most gas plants prefer operation simplicity and low maintenance. In

addition, very high recovery efficiency may not be economically justified. Typically, high propane recovery is attractive as propane liquid always commands a premium price over natural gas. Ethane price depends on the market demands, and in most cases, lower than natural gas price, on a Btu basis.

Another development is on modularization. Most of the midstream developers expect a high return of their investments. They also desire that the NGL recovery units can be standardized and mobilized quickly. Modular units minimize site work and reduce installation costs. They can be designed to be a truckable unit such that they can be deployed in other sites when the current resource is depleted.

11.6 NGL RECOVERY UNIT DESIGN CONSIDERATIONS

The process performance of an NGL recovery unit is sensitive to feed gas compositions and feed gas inlet pressure. As the unit matures, the feed gas will contain less of the heavy hydrocarbons. When nitrogen injection is used for enhanced oil recovery, the nitrogen content in the feed gas will increase. These changes will negatively affect the NGL recovery unit performance.

Another design consideration, as mentioned in the earlier sections, is the requirement to operate on lower levels of ethane recovery to meet ethane demands. The unit must be designed to operate on feed gas with varying "GPM". The ability to operate on ethane rejection without a loss in propane recovery, such as the TRAP process, is desirable.

11.7 NGL RECOVERY UNIT OPERATING PROBLEMS

The operating problems in an NGL recovery unit are unstable operation and failure to meet NGL recovery targets and product specifications. The following checklists can be used to identify the root cause of the problems.

- If a high pressure drop occurs in the unit, check the CO_2 content in the feed gas. This may be due to CO_2 freezing in the demethanizer. Check the performance of the amine unit.
- Check the moisture content in the dried gas from the molecular sieve unit. The water content should register below 1 ppmv to avoid hydrate formation. Formation of hydrate will plug heat exchange equipment, resulting in high pressure drop. Methanol injection can be started to temporarily relieve the problems.
- If the unit fails to achieve the design capacity, check the feed gas compositions. If the feed gas is leaner and contains more nitrogen, vapor loading on the demethanizer will increase, reducing the capacity of the unit.
- Check the temperature and pressure profile of the NGL unit. If the deethanizer operates at high temperature, propane recovery will be reduced. If the column pressure is too high, separation may become difficult, resulting in lower recovery.
- To debottleneck the demethanizer, check the tray design and conduct a column scan. Follow some of the procedures discussed in the fractionation handbook by Kister (2006).
- If the exchanger fails to achieve design performance, check the temperature profile of the NGL unit to determine if there is a temperature pinch on heat exchangers.
- Verify the expander compressor performance. Is the bypass valve around the expander opened?
- Check the refrigeration system performance. Check the contaminant levels in the propane refrigeration system. Sometimes, leakage of lube oil into the propane system can be a problem.

11.8 NGL FRACTIONATION

The NGL stream exiting an NGL recovery unit consists of a combination of components that must be separated into marketable products. This separation process occurs in a series of fractionators, which can include deethanizers, depropanizers, debutanizers, and butane splitters.

Fractionation may occur at either the gas processing plant itself, or at a third party facility. A simplified NGL fractionation flow schematic is shown in Fig. 11.22. A picture of a fractionation center is shown in Fig. 11.23.

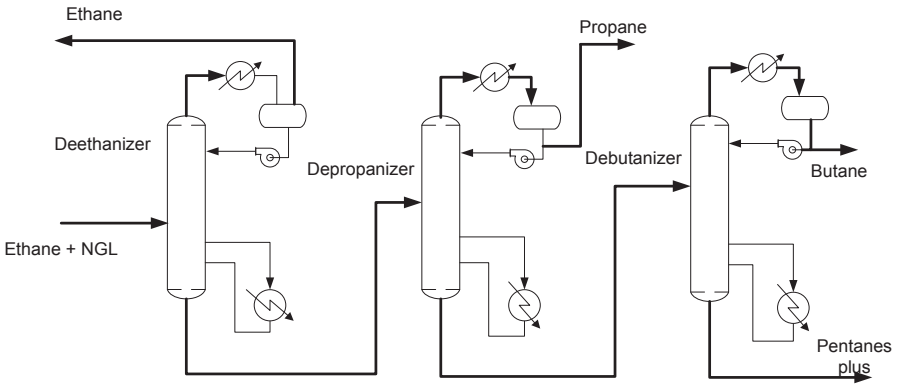

FIGURE 11.22

Typical NGL fractionation flow schematic.

FIGURE 11.23

Typical fractionation center.

Courtesy of Fluor.

Fractionation takes advantage of the differing boiling points of the various NGL components. As the NGL feed stream is heated, the lightest (lowest boiling point) NGL component boils off first and gets separated. The overhead vapor is condensed and a portion is used as reflux and the remaining portion is routed to product storage. The heavier liquid mixture at the bottom of the first column is routed to the second column where the process is repeated and a different NGL component is separated as the product. This process is repeated until the NGL is separated into their individual components.

In some cases, where isobutane is desired, the mixed butane stream can be further separated with a deisobutanizer or butanes splitter to produce the required product for refinery consumption. There are many options in configuring the NGL fractionation train and the optimum arrangement may vary depending on the NGL compositions, and the product specifications.

11.8.1 FRACTIONATION COLUMNS DESIGN AND OPERATION

Fluctuation in feed conditions and compositions, which may happen on a daily basis, has significant impacts on the NGL fractionation unit operation. The impacts on the design can be evaluated on the process simulators and the optimum operating variables can be assessed. The simulation software can now be integrated to the DCS system allowing real-time optimization.

The books on distillation published by Kister (1989, 1992, and 2006) can be used as references and guidelines in the design and operation of distillation columns. These books provide design parameters for equipment, discuss limitations of the design methods, and suggest solutions in trouble-shooting columns. They also contain process calculations on column hydraulic and tower performance, tray and packing design details, and the methods to maximize column operating efficiency.

11.9 LIQUID PRODUCTS PROCESSING

The liquid products from the NGL fractionation unit contain residual contaminants from the upstream NGL recovery units. The contaminants will concentrate in the fractionation unit products, which will require further processing. For example, ethane product may contain residual CO_2 that may not meet customer's specification and would require further treating. Condensate product may contain mercaptans that cannot be removed in the upstream unit and must be further treated by mercaptans removal processes to meet total sulfur specifications. There are other contaminants, such as COS, that would require catalytic conversion to meet sulfur specifications. When the product is treated with amine, it will be saturated with water, and additional drying is required to meet water specifications of the products.

The following sections discuss some of the processing methods to produce marketable liquid products.

11.9.1 NGL CONTAMINANTS TREATING

The distribution of the contaminants for the various NGL products can be summarized in Table 11.3. H_2S will show up in the deethanizer overheads, whilst most COS is concentrated in the propane fraction. The mercaptans tend to split between the various NGL fractions, depending on their molecular weight, with most of the heavy molecular weight mercaptans ending up in the condensate. These contaminants not only lead to odor problems but also form sulfur oxides on combustion. They

Table 11.3 NGL Contaminants Distribution

	Ethane	Propane	Butane	Condensate
H_2O	X	X	X	X
CO_2	X	X		
H_2S	X	X		
COS	X	X		
CH_3SH	X	X	X	
C_2H_5SH	X	X	X	X
C_3H_7SH+		X	X	X
CS_2			X	X
DMS			X	X
Others				X

Modified after John M. Campbell & Co. (2003).

can cause corrosion of equipment unless the liquid is adequately dehydrated. The presence of significant quantities of CO_2 can increase vapor pressure and lower the heating value of the hydrocarbon liquids. Carbonyl sulfide (COS) and carbon disulfide (CS_2), although not corrosive in LPG, will hydrolyze slowly to H_2S, resulting in off-spec products (Nielsen et al., 1997).

Both the quantity of each contaminant present in the untreated hydrocarbon liquid stream and the product specifications determine the treating technology selection. The successful experience of the selected technology for similar application is the key consideration. For comparable performance among the different treating processes, the selection is generally based on capital and operating costs, and the preference of the owners and operators. Where several contaminants are present, hybrid processes, or a combination of different technologies may be required. The following section shows a typical technology for the different applications.

11.9.1.1 Caustic Processes

The hydrocarbon processing industry has historically used caustic solutions to extract or treat acidic impurities (mainly RSH) in hydrocarbon liquid streams. When quantities of acid gas contaminants are small (e.g., less than 200 ppmwt), a simple caustic wash is effective and economical. However, as the quantity of acid gas contaminants rises, once-through caustic washing processes can be expensive due to high chemical consumption and disposal costs of nonregenerable byproducts, making this approach impractical (Nielsen et al., 1997; Matthews et al., 2015).

Several caustic processes, both "regenerative" and "nonregenerative", can be used to remove sulfur compounds from hydrocarbon liquids. The method or combination of methods that can be used depends on the mercaptan characteristics and the product specification that must be met (Fischer et al., 1993).

Nonregenerative caustic treatment processes are applicable if the concentrations of the contaminants are low (Speight, 2014). The use of a nonregenerative solid potassium hydroxide (KOH) bed is effective for removal of H_2S but not for other sulfur compounds. However, this type of treatment

process produces a waste spent caustic stream that must be further processed and disposed (Engel et al., 2016). Since the caustic is consumed and requires continuous makeup, there is an associated operating cost.

One of the common processes for treating hydrocarbon liquids is the use of regenerative caustic wash with sodium hydroxide (NaOH), also known as caustic soda. The pH is so high that it reacts with the weakly acidic mercaptans to form mercaptide salts. Mercaptides can be converted to disulfides by oxidation. These disulfides will remain in the sweetened hydrocarbon product. The overall sulfur content, therefore, remains unchanged. However, the sulfur leaves as disulfide (no odor) rather than mercaptans that are quite malodorous even at ppm levels (Mokhatab et al., 2018).

The UOP Merox process, developed and commercialized over 50 years ago, is one of the most widely used regenerative caustic washing processes for treating product streams by rendering any mercaptan (limited to methyl and ethyl mercaptans) sulfur compounds inactive. This process is used for treating LPG, gasoline, and heavier fractions. The method of treatment is the extraction reaction of the sour feedstock containing mercaptans (RSH) with caustic soda (NaOH) in an extraction column (typically packed with raschig rings), which generates a "spent" or so called "rich caustic" solution that is saturated with mercaptide. The extraction reaction is shown by the following equation:

$$RSH + NaOH \leftrightarrow NaSR + H_2O \tag{11.1}$$

After extraction, the extracted mercaptans in the form of sodium mercaptides (NaSR) are catalytically oxidized (by Merox WS catalyst which is dispersed in the aqueous caustic solution) to water insoluble disulfide oils (RSSR), as shown in the following equation:

$$4NaSR + O_2 + 2H_2O \rightarrow 2RSSR + 4NaOH \tag{11.2}$$

The disulfide oil (DSO) byproduct, which can be a challenge for disposal in a gas processing plant, is decanted and sent to further processing in a hydrotreater in a refinery where the disulfides are hydrogenated to form H_2S and hydrocarbons, and where H_2S is subsequently absorbed in an amine unit and further processed in the sulfur recovery unit (Mokhatab et al., 2018). The regenerated (lean) caustic is then recirculated to the extraction column. Typically, a further polishing process such as solvent washing is required to reduce the amount of unconverted mercaptans and residual DSO in the regenerated caustic stream to prevent formation of disulfides in downstream equipment (Zhang, 2009).

The caustic wash treating process reduces the sulfur content of the extracted hydrocarbon liquid, in which typical product the merthyl mercaptan levels can be controlled to less than 10 ppmwt (UOP, 2003).

A typical flow schematic of the UOP's Merox process is shown in Fig. 11.24. However, in some versions of this process, an optional vessel is used as a caustic settler to minimize the potential for caustic carryover. However, problems occur when there is poor separation in the settling drum where caustic carries over into the liquid product. As such, a specially formulated polymeric coalescer, which is compatible with caustic, can be used to remove carried over caustic (Wines and Mokhatab, 2017a). An optional sand filter coalescer downstream of the extractor can improve the quality of the treated product. Also, if H_2S or CO_2 is present in substantial amounts, the extractor column can be preceded by a caustic (or amine) prewash for acid gas removal, which can minimize caustic consumption. There are other enhancements that can be incorporated into the design, such as single/multistage extraction column, high efficiency trays, and flow configurations that can improve capital and operating costs of the unit.

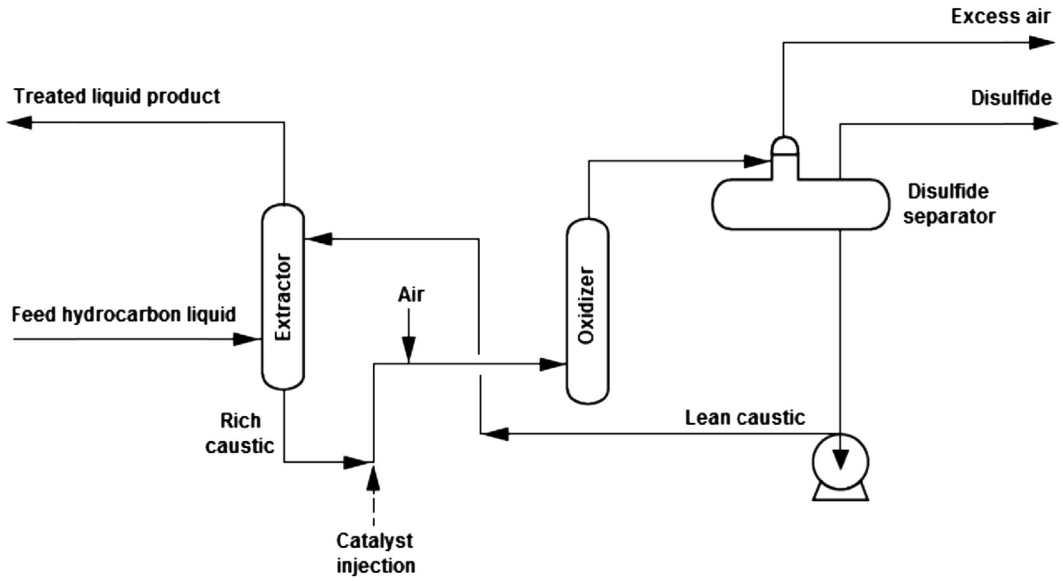

FIGURE 11.24

Typical regenerative caustic mercaptan-removal process (Upson and Schnaith, 1997).

Similar caustic washing processes have been developed by IFP/Axens (the Sulfrex process) and Merichem, where each licensor uses a proprietary catalyst.

11.9.1.2 Molecular Sieve Technology

Molecular sieve technology is commonly used for treating natural gas liquids to extremely low contaminant levels. Molecular sieves can be used for removal of sulfur compounds (H_2S, COS, and mercaptans) either in the gas or liquid phase. There are specificities for either option. The adsorber efficiency is higher in the gas phase since the mass transfer rate of sulfur compounds is much faster in the gas phase. However, the size and number of adsorbers are smaller for the liquid phase as the liquid rate tends to be significantly lower than the gas rate.

The molecular sieve process can be attractive when the amount of sulfur contaminants is low in a feed stream (usually 500 ppmwt for H_2S, less than 100 ppmwt for mercaptans, and less than 50 ppmwt for COS), and the regeneration gas can be sent to the sulfur recovery unit or incineration for proper disposal (Jain, 2018; Mokhatab et al., 2018).

Molecular sieves can dry the feed stream while simultaneously removing sulfur contaminants. Their drawbacks are high capital and operating costs. The formation of COS is another concern if both H_2S and CO_2 are present. COS formation has to be minimized, as it will be converted to H_2S in the presence of water, resulting in an off-spec product and corrosion. Molecular sieve manufacturers can supply customized sieves to minimize COS formation.

For typical liquid-phase treating with molecular sieves, the adsorption flow tends to be upwards, and the regeneration flow downwards. Molecular sieve regeneration is similar to that for gas-phase

application. However, the beds must be designed to ensure that the maximum velocities are not exceeded under the extreme flow conditions, to avoid bed lifting (or fluidizing) and attrition of molecular sieves. More details on the design and operation of molecular sieve units can be found in Herold and Mokhatab (2017). Note that the spent regeneration gas from a molecular sieve treating unit contains the contaminants that must be removed by another solvent unit or converted to usable products. In most cases, they can be destroyed in a sulfur recovery unit or an incinerator, as long as the emissions are within the regulatory limits.

11.9.1.3 Amine Processes

Amine-based treating is usually the most cost-effective option for hydrocarbon liquid treating when significant amounts of acid gases are present. This process is an attractive alternative, especially when an amine gas treating unit is already onsite. In such cases, the liquid treating unit can often be operated using a slipstream of lean amine from the main amine regeneration unit (Nielsen et al., 1997).

Amine treating is often used upstream of caustic treaters to minimize caustic consumption caused by irreversible reactions with CO_2. In this process, H_2S and CO_2 from the sour liquid feed are absorbed by liquid−liquid contacting the sour liquid with the lean amine solvent. The amine unit design should consider the suitable amine solution and the type of contacting device. A variety of amines may be used depending on the contaminants to be removed (Hati, 2012; Matthews et al., 2015). In most cases, generic amines (including DGA and DIPA, and the MDEA based specialty solvents) will perform satisfactorily. The liquid−liquid contacting devices include packed towers, trayed towers, jet eductor-mixers, and static mixers. Most installations use random-packed columns as they are less expensive and avoid the potential back mixing problems with tray columns.

A typical LPG treating unit utilizing amine solvent is shown in Fig. 11.25. As can be seen, raw LPG enters the bottom of a packed absorber and lean amine enters the top of the absorber. Treated LPG leaves the absorber from the top and rich amine leaves the absorber from the bottom. The treated LPG is washed using a recirculating water-wash system to recover the entrained amine and protect downstream caustic treaters. The treated LPG and the wash water are mixed in the water-wash static mixer, which is then coalesced into two liquid phases and separated in the water-wash separator. Makeup water is added to the circulating water-wash circuit to maintain the concentration of the amine system. In some LPG treating units, a knockout drum is located downstream of the contactor tower overhead to recover any carried over amine. However, problems occur when there is poor separation in the knockout drum where amine carries over into the LPG product. In this case, a high efficiency liquid/liquid coalescer system such as Pall's PhaseSep liquid/liquid coalesce, which does not contain glass coalescing media, can provide high efficiency filtration and liquid contaminants separation from the LPG product with the lowest capital and operational costs (Wines and Mokhatab, 2017a,b).

Carbonyl sulfide (COS) is a stable, unreactive compound that cannot be removed to 1 ppm level using conventional amine and molecular sieve designs. The Shell ADIP process is a regenerative amine process to selectively reduce COS to very low levels (5 ppmwt as sulfur) in light hydrocarbon liquids such as LPG. Numerous nonregenerative metallic oxide processes are also available to remove COS from liquid products to meet the most demanding specifications (ppb range). Some of these processes remove the COS directly. Other processes require water to hydrolyze the COS to H_2S before it is reacted, thereby adding a requirement for a downstream dehydration for the liquid product stream (Maddox, 1982).

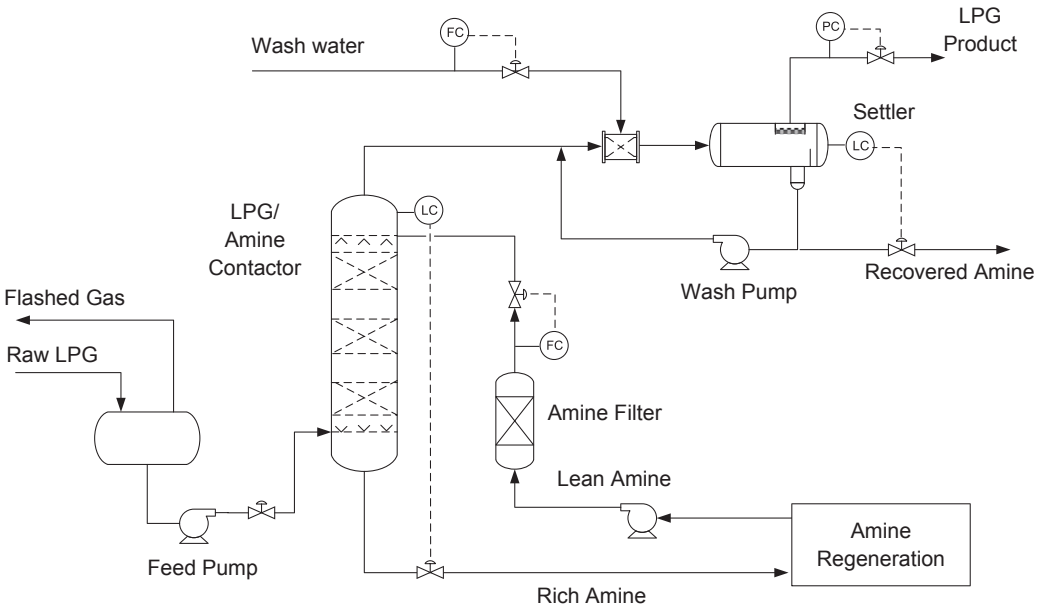

FIGURE 11.25

Process schematic for LPG treating with amine solvent.

Since mercaptans are weak acids, amine solutions are generally not effective for mercaptan removal from hydrocarbon liquids. Amines will absorb light (methyl and ethyl) mercaptans to a limited extent. Heavy mercaptans can be removed by physical solvents that unfortunately also exhibit high hydrocarbon coabsorption. As an alternate, hybrid solvents, such as Shell's Sulfinol process, that take advantage of the effects of a mixture of MDEA, DIPA, and sulfolane can be used for removing mercaptans and acid gases to low levels.

11.9.2 DEHYDRATION

Natural gas liquids must be dehydrated to prevent potential formation of ice and solid hydrates, and to meet requirements of the consumer. The acceptable water content in light hydrocarbon liquid streams varies from no free water present to "very low levels of moisture" in liquid products (GPSA, 2004). For example, most liquid sale specifications require the LPG to yield a negative result to the cobalt bromide test, which is equivalent to a water content of 15−30 ppm (GPA Standard 2140-88, 1988). For hydrocarbon liquids that are further processing in cryogenic temperature, such as LNG liquefaction, practically all of water must be removed.

Various methods have been suggested for drying hydrocarbon liquid streams (Mokhatab et al., 2018). The common operation of liquid drying is the use of calcium chloride salt used as a desiccant. The process can achieve an out-water content of 1 lb/MMscf. Other methods may include stripping with natural gas or steam, which is limited to condensate liquid application.

Glycol dehydration units can be used for dehydration of hydrocarbon liquids, but seldom used due to the process complexity and higher costs. In addition, glycols can form a stable emulsion with the hydrocarbon liquids that makes phase separation difficult and may result in foaming (Mokhatab et al., 2018).

In most cases, regenerative solid adsorbents are used for dehydration of hydrocarbon liquids where they are capable of removing water to low levels. Molecular sieve is an efficient adsorbent if a tight water specification in ppmv levels is required or if simultaneous drying and treating is necessary. In most cases for the liquid product, the very low ppm level specification is not required.

REFERENCES

Bucklin, R., December 20, 1966. Method and Equipment for Treating Hydrocarbon Gases for Pressure Reduction and Condensate Recovery. U.S Patent No. 3,292,380.

Engel, D., Burns, H., Williams, S., March/April 2016. "Remove Mercaptans from Hydrocarbon Condensates and NGL Streams. Gas Processing, 23-28.

Fischer, E., Goel, R., Saunders, D., March 15−17, 1993. Preliminary Process Selection for Natural Gas Liquid (NGL) Treating. Paper presented at the 72nd Annual GPA Convention, San Antonio, TX, USA.

GPA Standard 2140-88, 1988. Liquefied Petroleum Gas Specifications and Test Methods. Gas Processors Association (GPA), Tulsa, OK, USA.

GPSA, 2004. Engineering Data Book, twelfth ed. Gas Processors Suppliers Association (GPSA), Tulsa, OK, USA.

Hati, A.S., February 26−29, 2012. Sour LPG Treating. Paper presented at the 62nd Annual Laurance Reid Gas Conditioning Conference, Norman, OK, USA.

Herold, R.H.M., Mokhatab, S., 2017. Optimal Design and Operation of Molecular Sieve Gas Dehydration Units. Gas Processing, Part 1 (July/Aug): 25−30, Part 2 (Sept/Oct): 33-36.

Huebel, R.R., Malsam, M.G., September 21−23, 2011. New NGL Recovery Process Provides Viable Alternative. Paper presented at the GPA Europe Annual Conference, Prague, Czech Republic.

Jain, S., 2018. Private Communication. Molecular Sieve Department, Arkema, Colombes, France.

John M. Campbell & Co, September 2003. Technical Assistance Service for the Design, Operation, and Maintenance of Gas Plants. Course materials presented at the BP Exploration Company Columbia Ltd, Columbia.

Kister, H.Z., 1989. Distillation Operation. McGraw-Hill, New York, NY, USA.

Kister, H.Z., 1992. Distillation Design. McGraw-Hill, New York, NY, USA.

Kister, H.Z., 2006. Distillation Troubleshooting. John Wiley & Sons Inc, Hoboken, NJ, USA.

Maddox, R.N., 1982. Gas and Liquid Sweetening, third ed. Campbell Petroleum Series, Norman, OK, USA.

Mak, J.Y., January 4, 2005. High Propane Recovery Process and Configurations. U.S. Patent No. 6,837,070.

Mak, J.Y., Deng, E., Nielsen, R., August 5, 2003. Methods and Apparatus for High Propane Recovery. U.S. Patent No. 6,601,406.

Mak, J.Y., Chung, W., Graham, C., Wierenga, D., March 14−17, 2004a. Retrofit of a NGL Process for High Propane and Ethane Recovery. Paper presented at the 83rd Annual GPA Convention, New Orleans, LA, USA.

Mak, J.Y., Nielsen, D., Graham, C., Schulte, D., March 14−17, 2004b. A New and Flexible LNG Regasification Plant. Paper presented at the 83rd Annual GPA Convention, New Orleans, LA, USA.

Mather, I., Ershaghi, B., February 22−24, 2012. LNG Production and Transportation Demands Lead to Development of Larger Frame Sized Turboexpanders. Paper presented at the GPA Europe Conference, Antwerp, Belgium.

Matthews, J., Nichols, J., Johnson, J.E., February 22−25, 2015. The Impacts of Trace Components on the Design and Operation of Gas Treating and Processing Plants. Paper presented at the 65th Annual Laurance Reid Gas Conditioning Conference, Norman, OK, USA.

Mokhatab, S., Northrop, S., Mitariten, M., 2017. Controlling the Hydrocarbon Dew Point of Pipeline Gas. Petroleum Technology Quarterly, Q3, 109-116.

Mokhatab, S., Northrop, S., Echt, W.I., February 25−28, 2018. Dealing with Sour Natural Gas Liquids in Gas Processing Plants. Paper presented at the 68th Annual Laurance Reid Gas Conditioning Conference, Norman, OK, USA.

Nielsen, R.B., Rogers, J., Bullin, J.A., Duewall, K.J., 1997. Treat LPGs with amines. Hydrocarbon Processing 76 (9), 49−59.

Parsons, P.J., Templeman, J.J., 1990. Models performance leads to adsorption-unit modifications. Oil & Gas Journal 88 (26), 40−44.

Pitman, R.N., Hudson, H.M., Wilkinson, J.D., Cuellar, K.T., March 16−18, 1998. Next Generation Processes for NGL/LPG Recovery. Paper presented at the 77th Annual GPA Convention, Dallas, TX, USA.

Speight, J.G., 2014. The Chemistry and Technology of Petroleum, fifth ed. CRC Press, Taylor & Francis Group, Boca Raton, FL, USA.

Thompson, G.R., Adams, J.B., Hammadi, A.A., Sibal, P.W., March 21−24, 2004. Qatargas II: Full Supply Chain Overview. Paper presented at the 14th International Conference and Exhibition on Liquefied Natural Gas (LNG 14) Conference, Doha, Qatar.

UOP, 2003. Merox™ Process for Mercaptan Extraction. UOP 4223−3 Process Technology and Equipment Manual. UOP LLC, Des Plaines, IL, USA.

Upson, L.L., Schnaith, M.W., 1997. Low sulfur specifications cause refiners to look at hydrotreating options. Oil & Gas Journal 95 (49), 47−51.

Wines, T.H., Mokhatab, S., 2017a. Removing Liquid-phase Contaminants from Hydrocarbon Liquids. Petroleum Technology Quarterly, Gas, 51-55.

Wines, T.H., Mokhatab, S., 2017b. High Efficiency Coalescers for Gas Processing Operations. Petroleum Technology Quarterly, Q4, 51-59.

Zhang, T., March 12, 2009. Removal of Residual Sulfur Compounds from a Caustic Stream. US Patent # 2009/0065434 A1.

CHAPTER

NITROGEN REJECTION AND HELIUM RECOVERY

12

12.1 INTRODUCTION

Nitrogen (N_2) may naturally occur in high concentration in certain gas production fields, such as in the US Midwest, North Sea, Eastern Europe, and South East Asia. Approximately, 15% of the nonassociated gas reserves in the world are high in nitrogen content and would not meet the specification for normal pipeline quality gas (typically 3–4 mol%). Nitrogen, being an inert gas, will not support combustion. So, when a gas with too much nitrogen is burned, it may lead to unstable combustion. When high nitrogen gas is processed in a gas plant, recovery of NGL content will be reduced as nitrogen will act as a stripping gas. Additional nitrogen content will increase the compression equipment and size of the transmission pipeline. In an LNG plant, high nitrogen is not desirable as it lowers the LNG temperature, increasing the power for natural gas liquefaction, in addition to increasing the quantity of boil-off gas from the LNG storage tanks.

In production areas where nitrogen injection is used for enhanced oil recovery, nitrogen content in the produced gas will gradually increase over time as nitrogen breaks through from the injection wells to the producing wells. During early production, the production gas can be blended with low nitrogen sources to meet pipeline specification. However, if the nitrogen content continues to increase, with limited low nitrogen content natural gas sources, gas blending may no longer be an option; and the nitrogen content must be removed in a nitrogen rejection unit (NRU).

In some cases, natural gas rich in nitrogen contains a relatively high concentration of helium (He), which may improve the gas plant economics by adding a helium recovery unit (HeRU). Helium is a unique gas and is in high demand, commanding high values in the gas market. This chapter reviews the current state-of-the-art nitrogen rejection technologies and briefly discusses helium recovery that can be also integrated to the nitrogen rejection unit.

12.2 NITROGEN REJECTION OPTIONS

Nitrogen rejection methods can be classified into cryogenic and noncryogenic processes.

12.2.1 CRYOGENIC PROCESSES

Cryogenic nitrogen rejection technology, which is the most common method of removing nitrogen from natural gas, uses the difference of boiling points between nitrogen and methane for separation. Cryogenic processes use Joule–Thomson (JT) cooling of the high-pressure gas and separation in a

Handbook of Natural Gas Transmission and Processing. https://doi.org/10.1016/B978-0-12-815817-3.00012-5

distillation column to produce a nitrogen overhead product and a methane-rich bottom. The nitrogen product contains 1 mole% or lower methane content, which minimizes the greenhouse gas impact, and can be discharged to the atmosphere. The methane rich bottom can contain 1 to 3 mole% nitrogen that can meet the typical natural gas pipeline specifications.

Cryogenic processes are proven processes to process natural gas containing more than 5 to 10 mole% nitrogen with gas flow rates ranging from 30 MMscfd up to 900 MMscfd.

12.2.2 NONCRYOGENIC PROCESSES

Noncryogenic nitrogen separation processes include mainly pressure swing adsorption (PSA) and membrane separation.

PSA uses a zeolite adsorbent to selectively separate nitrogen from methane in a cyclic process. The process includes adsorption of methane at high pressure, during which nitrogen is separated at pressure. Natural gas with low nitrogen content is produced at low pressure. The adsorbent can be regenerated with a combination of pressure and thermal changes. PSA technology is limited in capacity and can typically handle 2 to 15 MMscfd gas flow rate. The drawback of this process is that natural gas is produced at low pressure requiring recompression to pipeline pressure. Also, the hydrocarbon content in the rejected nitrogen is significant which represents a production loss, and will contribute to significant carbon emissions if vented to atmosphere. The losses can be somewhat reduced by recompression to the feed section, which is seldom justified because of the high compression cost. For coal-bed methane applications where there are few impurities, the Molecular Gate adsorption-based technology (developed by Engelhard) can be used to handle small gas flow of 0.5 MMscfd. The Molecular Gate technology traps nitrogen in a unique adsorbent material while letting methane flow through. The Molecular Gate adsorbent is a titanium silicate molecular sieve designed with a 3.7-Å pore size. Because nitrogen has a smaller molecular diameter (3.6 Å) than methane (3.8 Å), nitrogen can enter the pore and be adsorbed while methane passes through the fixed bed of adsorbent with minimal pressure losses.

In membrane process, the feed gas is compressed and passed across the surface of the membrane elements. It separates the hydrocarbon permeate which is compressed back to the pipeline pressure, while the nonpermeate, nitrogen-rich waste gas can be used as fuel. Membrane can handle small flow rates varying from 0.5 to 25 MMscfd. The membrane units are compact and can be supplied in modules, suitable for offshore installation. However, membrane separation systems would require feed gas pretreatment such as aromatics removal and dew point depression to remove impurities that may cause damage to the membrane. Membrane has the same drawback as PSA process, that is, the hydrocarbon losses in the nitrogen waste stream is relatively high, and will contribute to greenhouse gas emissions if vented to atmosphere.

PSA and membrane separation methods are limited in commercial applications and have not found acceptance, especially for larger NRUs.

12.3 NITROGEN REJECTION INTEGRATION WITH NGL RECOVERY

Since NRU operates at cryogenic temperatures, the feed gas pretreatments as shown in Figure 12-1 are required. Pretreatment generally consists of an amine scrubbing unit to remove carbon dioxide (CO_2)

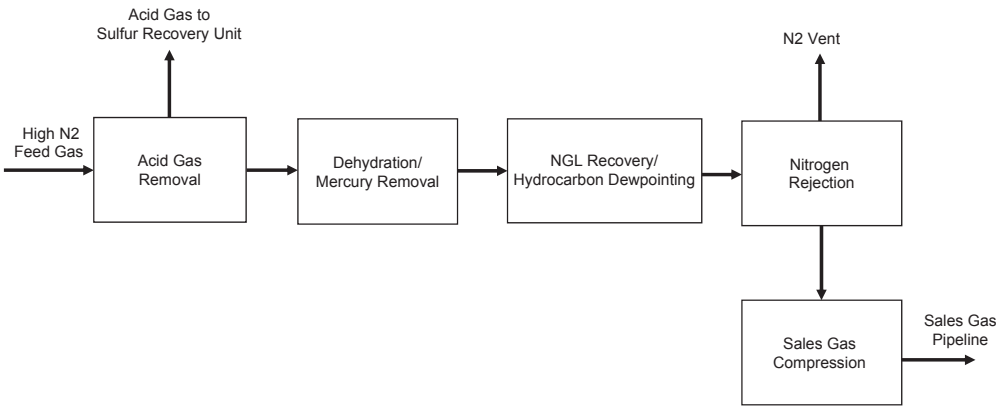

FIGURE 12.1

Nitrogen rejection integration with NGL recovery.

and hydrogen sulfide (H_2S), and a molecular sieve unit for removal of water, mercaptans and undesirable contaminants. Mercury removal bed may also be necessary if the gas shows presence of mercury.

The feed gas to a nitrogen rejection unit must be depleted of the heavy hydrocarbons, typically C_{4^+} hydrocarbons, as the presence of the heavier components will result in freezing in the column overhead that operates at cryogenic temperature.

For rich gas streams, an NGL recovery unit is located downstream of the dehydration unit, as shown in Fig. 12.1. This unit ensures removal of most of the C_{3^+} hydrocarbons, producing a lean gas depleted of heavier hydrocarbons. For lean pipeline gas sources with low C_{4^+} contents, a hydrocarbon dewpointing unit can be used. The residual C_{4^+} hydrocarbons, benzene, toluene, ethylbenzene and xylene (BTEX) and heavier components can be removed in the feed chilling exchanger of the NRU.

Complete CO_2 removal is necessary when the NGL recovery unit operates at high ethane recovery mode that requires cryogenic operating temperatures. For propane recovery operation, deep CO_2 removal may not be necessary as the NGL unit operates at higher temperatures. In the nitrogen rejection unit, the inclusion of a feed separator, will condense most of CO_2 and heavier hydrocarbons, bypassing the fractionation column. This design will avoid heavy hydrocarbons from reaching the NRU column.

For conventional feed gas, the NRU unit is more efficient when integrated with an NGL recovery unit as the lean gas requires less compression and produces a nitrogen reject stream low in hydrocarbons content, which would minimize carbon emissions. For a lean gas, a deep hydrocarbon dewpointing unit may also be used, provided a downstream separator integrated in the cold box, to remove these components, avoiding heavy hydrocarbon losses in the nitrogen vent gas.

12.4 CRYOGENIC NITROGEN REJECTION

Several cryogenic distillation schemes are known to reject nitrogen from natural gas stream. The state of the art of cryogenic nitrogen rejection processes are single-column process, double-column process,

and two-column process. These processes vary in complexity and efficiency and are discussed individually in the following sections.

12.4.1 CLASSICAL SINGLE-COLUMN DESIGN

The classical single-column nitrogen rejection process uses a heat pump to provide the reflux duty and reboiler duty of the fractionation column, as shown in Fig. 12.2. The single column typically operates between 300 and 400 psig. Methane can be used as the working fluid that is compressed to supply the reboiler heating duty, condensed and then evaporated at low pressure providing the condensation duty. Brazed aluminum heat exchangers (BAHXs) are used to achieve a close temperature approach required by the process.

Feed gas is typically supplied at 800 to 1000 psig. The gas is chilled by several effluent streams and then letdown in pressure to the high pressure (HP) column in a JT valve, JT1. The column produces a nitrogen overhead vapor, and a bottom methane-rich liquid. The column bottom is letdown in pressure using valve JT2, providing further chilling to heat exchanger E-1. The low pressure (LP) gas is then compressed to the sales gas pressure.

Due to the large boiling point difference between nitrogen and methane, sharp separation of nitrogen from methane is feasible. Typically, the single-column design can produce a nitrogen overhead product with less than 1% methane and a methane bottom product with less than 1 mol%

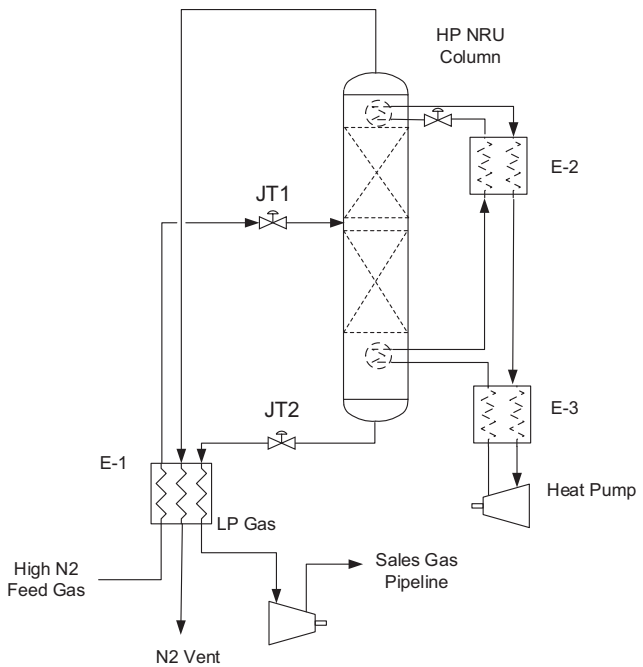

FIGURE 12.2

Single-column nitrogen rejection process.

nitrogen. The single-column process can be used to process variable nitrogen content gas ranging from 3 mol% to as high as 30 mol%. The disadvantage of this process is the high power consumption required by the heat pump and the LP gas compressor. In addition, internal reflux exchanger works best when feed gas composition does not vary. It lacks the controllability to react to varying feed gas changes, particularly its hydrocarbon and nitrogen content which is common in pipeline operation. If the hydrocarbon content increases, it will increase the condensation temperature, which will in turn increase the hydrocarbon losses in the nitrogen vent.

12.4.2 MODIFIED SINGLE-COLUMN DESIGN

To circumvent some of the difficulties in the classical single-column nitrogen rejection process, and reduce the power consumption, the single-column design can be modified for natural gas pipeline operation, as shown in Fig. 12.3.

In the modified version, the high pressure feed gas is chilled to an intermediate temperature, typically −60°F. The condensate, consisting mainly CO_2 and heavy hydrocarbons (BTEX), is separated in cold separator V-1 and removed, bypassing the HP NRU Column. Removal of the CO_2 content also makes the fractionation column more resistant to CO_2 freezing. Refrigeration is provided by the nitrogen vent, HP gas and LP gas, and the reboiler.

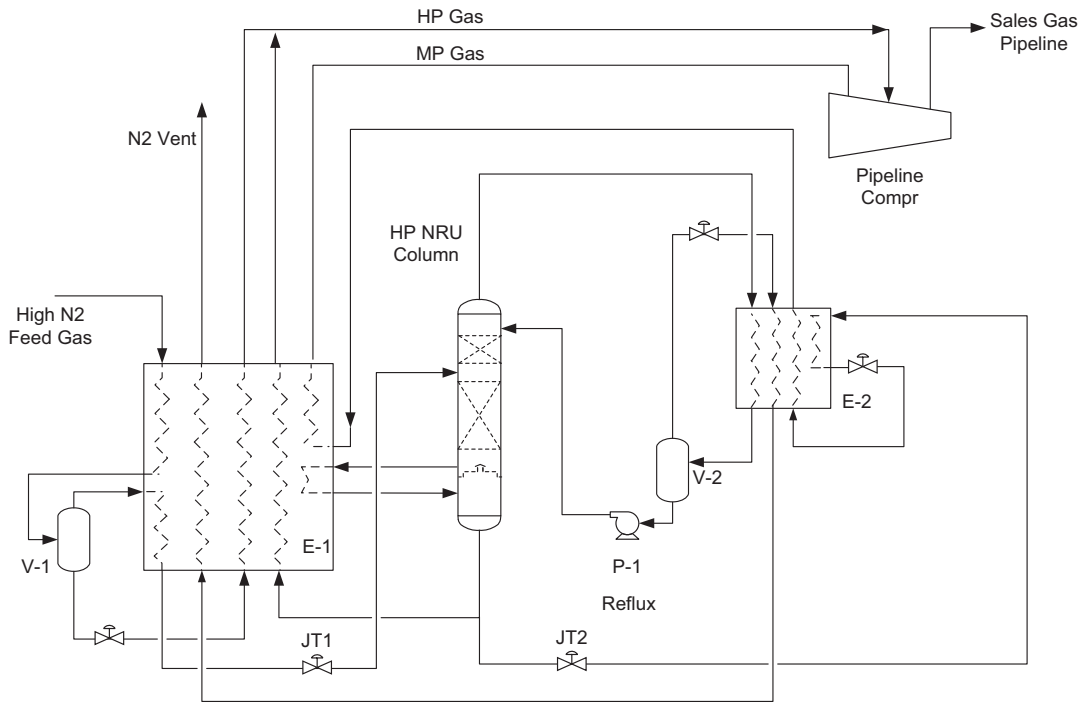

FIGURE 12.3

Modified single-column nitrogen rejection process.

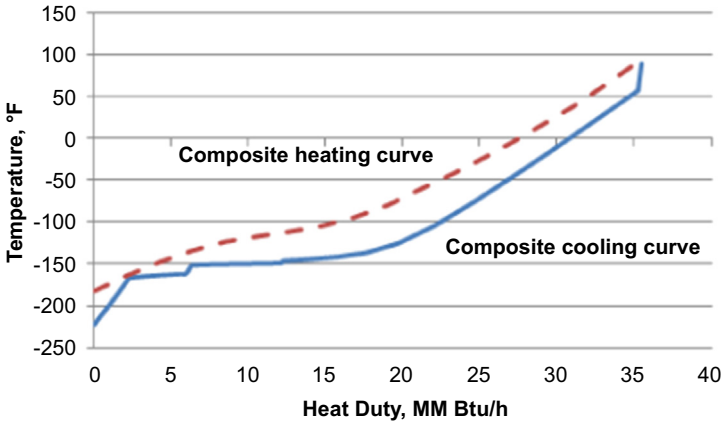

FIGURE 12.4

Heat composite curves for exchanger E-1 in modified single-column nitrogen rejection.

The chilled feed gas is letdown in pressure to 300 psig and 400 psig to the NRU column using valve, JT1. The over-flash vapor is condensed by the reflux condenser E-2. The main refrigeration duty is provided by the letdown of a portion of the HP column bottom liquid in a second valve, JT2.

The modified single-column design uses the pipeline compressor to generate cooling, instead of a dedicated methane compressor. This is thermodynamically more efficient as the heat composite curves can be closely matched, minimizing thermodynamic losses. The heat composite curves of the feed gas and the multistream (low pressure gas, medium pressure gas, nitrogen, and reboiler) are shown in Fig. 12.4. Because of the close approaches of the heat composite curves, power consumption by the pipeline compressor is significantly less than the earlier single-column design.

12.4.3 DOUBLE-COLUMN DESIGN

The double-column nitrogen rejection process was developed in the late 1970. The process is used for air separation plant and can be modified for fractionation of nitrogen from hydrocarbon streams. In this process, nitrogen is separated at low pressure at cryogenic temperature, typically −310°F, which requires the feed gas to contain no more than 40 ppmv CO_2, to avoid CO_2 freezing in the cryogenic column. This scheme takes advantage of the high nitrogen content in the feed gas to produce refrigeration by the JT effect for refluxing the cryogenic column. It has the advantage of low power consumption and a simple configuration that is inherited from the air separation plant design. When adapting the air separation plant design concepts to natural gas plants, the design must be modified to ensure that a low hydrocarbon level in the nitrogen vent to minimize greenhouse gas emissions.

The double-column process, as shown in Fig. 12.5, uses two columns stacked together operating at different pressures, where the reboiler of the LP column is thermally linked to the condenser of the HP column. The hydrocarbon liquid from the LP column is pumped by pump P-1 to an intermediate pressure, and vaporized in the exchangers E-2 and E-1, supplying cooling to the inlet gas and the reflux streams. The pump discharge pressure must be controlled to avoid the temperature pinch on the heat

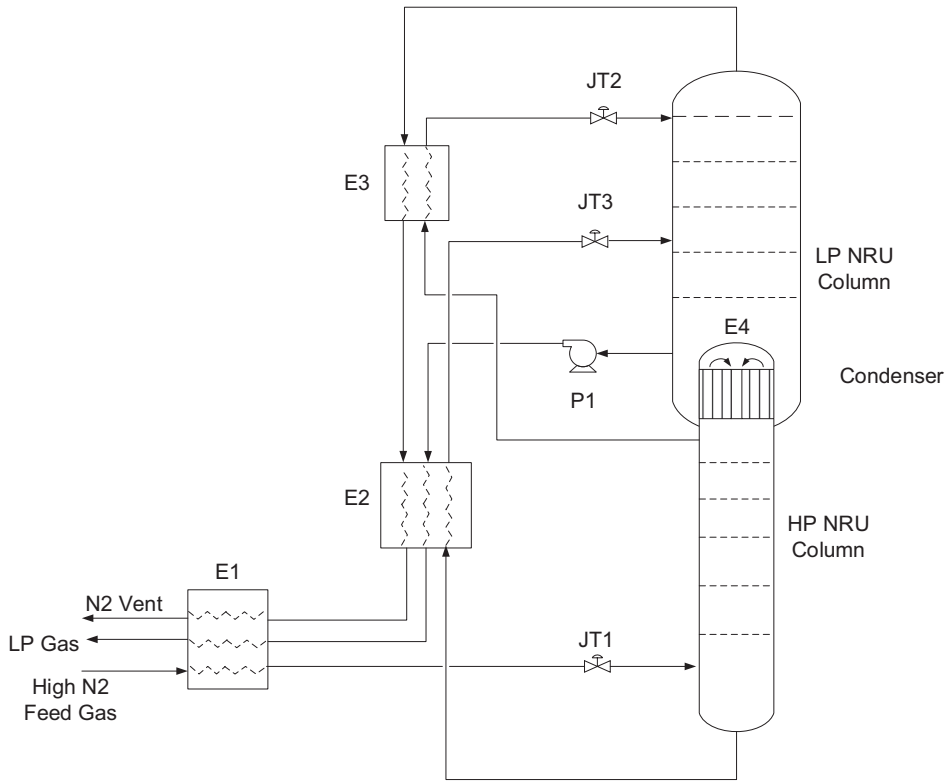

FIGURE 12.5

Typical double-column nitrogen rejection process.

exchangers. Higher pump discharge pressure can reduce compression horsepower, but may result in a temperature cross on the heat curves. In most designs, the optimum discharge pressure is somewhere between 60 and 100 psig.

Nitrogen vent stream from the LP column overhead is used to provide cooling for the feed gas and reflux streams in exchangers. The feed gas is cooled in these exchangers, condensed, and letdown in pressure in valve JT1 to the HP column, typically operating at 300 to 400 psi. The HP column is designed to produce an overhead stream, typically about 50−60 mol% nitrogen, which contains sufficient refrigeration for fractionation in the LP column. The HP column produces a bottom product containing methane and nitrogen, is subcooled in heat exchanger E-2 and then fed to the LP column at close to atmospheric pressure. The LP column fractionates the gas into methane and nitrogen products.

The overhead product from HP column, relatively pure nitrogen, is condensed in E-4, which is internally built-in to the column. This condenser also serves as a reboiler for the LP column. A portion of this liquid nitrogen is used as reflux to the HP column while the remainder is subcooled in heat exchanger E-3, letdown in pressure in valve JT2, and used as reflux to the LP column. The HP column

bottom is subcooled in heat exchanger E2 and letdown in pressure in valve JT3 and fed to the lower section of the LP column.

In principle, when the nitrogen content in the feed gas is high, all the refrigeration requirement can be provided by the JT valves via pressure letdown of the feed gas and products. No external refrigeration should be required. However, when nitrogen content in the feed gas is low, JT cooling is limited, which may not be enough for fractionation purposes, resulting in lower recoveries.

12.4.4 TWO-COLUMN DESIGN

The two column process is an adaptation of the double column process where the two columns are not thermally linked. This configuration, as shown in Fig. 12.6, uses two separate columns, which provide flexibility for heat recovery and integration among different streams, improving the efficiency of the process. The HP column can be considered as a preseparation column as this column removes most of the heavy hydrocarbons and CO_2.

The HP column is a nonrefluxed stripper, operating between 300 and 400 psig. It produces a bottom liquid composed mostly of C_{2+} hydrocarbons and an overhead nitrogen-rich vapor, typically consisting of 60 mol% nitrogen and 40 mol% methane. The refrigerant content in the HP bottom liquid is recovered by cooling the feed gas before it is fed to the HP stage of the pipeline gas compressor. The overhead vapor is chilled in exchanger E-2, letdown in pressure to about 100 psig, and separated. The

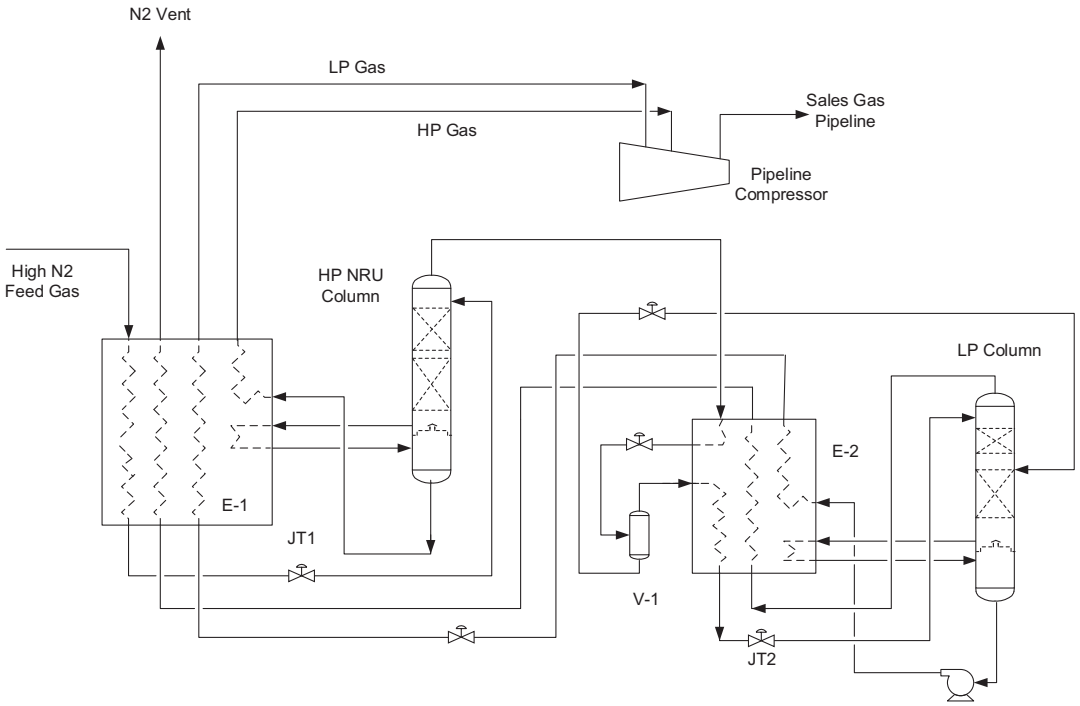

FIGURE 12.6

Two-column nitrogen rejection process.

separator produces a reflux to the LP column and a vapor stream that is further cooled and letdown in pressure to the LP column using valve JT2. The overhead gas is fractionated into an overhead nitrogen stream and a methane bottom stream. The separation can be very sharp, minimizing the methane losses in the nitrogen vent gas.

Although the two-column design is more efficient than the classical double-column process, the process design still has the same limitation. When processing low-nitrogen gas, there is not sufficient nitrogen in the HP overhead vapor, and as a result, there is not enough chilling from the JT operation; and consequently, the methane content in the nitrogen stream is higher than desirable. This process is more suitable to process feed gas with nitrogen content higher than 25 mol%.

12.4.5 PROCESS SELECTION

Process selection for the NRU should be based on the life cycle costs on capital expenditure (CAPEX) and operating expenditure (OPEX). The more important criterion today is the methane content in the nitrogen vent, which is responsible for the greenhouse gas emissions.

The two process configurations that can be considered are the single-column design and the two-column design. The methane content in the nitrogen vent gas for these two designs can be compared in Fig. 12.7. The single-column design can achieve less than 1% methane content in the nitrogen vent for a feed gas with a variable nitrogen content up to 60 mol%. However, for the two-column design, only when the nitrogen content is higher than 25 mol%, the methane content can be kept at below 1 mol%. When operating at lower than 25 mol% nitrogen, the methane content in the nitrogen vent increases significantly.

The power consumption for these two designs is shown in Fig. 12.8. The power consumption is based on processing 70 MMscfd feed gas with variable nitrogen content at 800 psig, and the residue

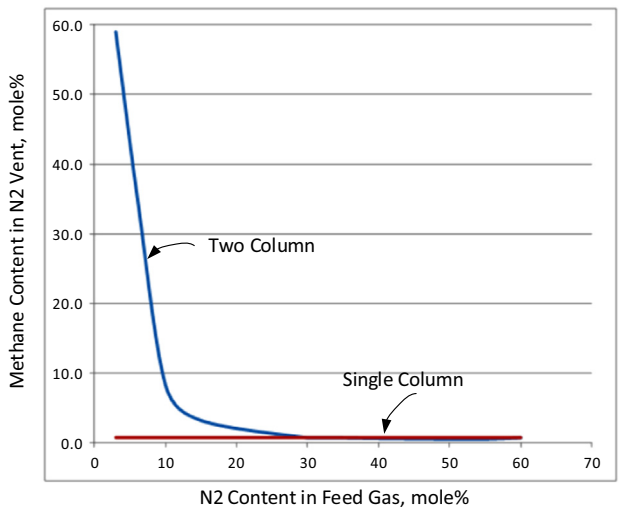

FIGURE 12.7

Methane content in nitrogen vent gas.

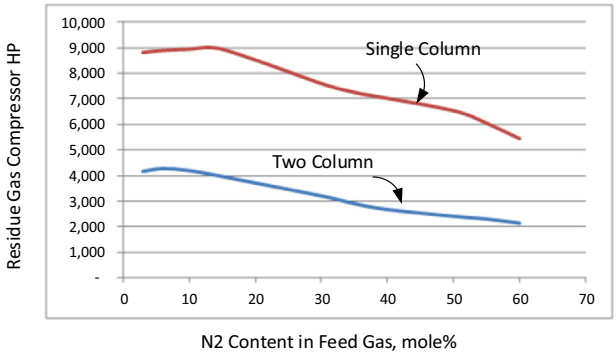

FIGURE 12.8

Comparison of compressor horsepower.

gas is recompressed back to the pipeline. As shown in Fig. 12.8, the two-column design requires about 50% of the power required by the single-column design.

In terms of power consumption, when the feed gas contains higher than 25 mole%, the two column design is lower in energy consumption. When the nitrogen content is lower than 25 mole%, the single column, despite the higher energy consumption, has a much lower carbon emission of less than 1 mole%. In terms of equipment count and operating complexity, and meeting carbon emissions on variable hydrocarbon and nitrogen content, the single column is a more robust design, particularly for smaller units.

12.5 NITROGEN REJECTION UNIT DESIGN CONSIDERATIONS

The following describes some of the cryogenic NRU design issues.

12.5.1 FEED GAS CHARACTERISTICS

The NRU operation is sensitive to changes in feed gas compositions, nitrogen content and inlet temperature and pressure. The upstream NGL recovery unit or hydrocarbon dewpoint unit must be monitored as feed gas composition changes will impact the NRU column condenser and reboiler temperatures. Higher condensation temperature will result in higher hydrocarbon losses in the nitrogen vent gas. Higher nitrogen content will require higher reflux condensation duty. If the feed gas is expected to process a variable nitrogen content gas, the feed gas compositions must be evaluated in the fractionation column and heat exchange system.

Higher feed gas pressure would generate more cooling when feed pressure is letdown to the NRU column. Lower feed gas temperature would reduce refrigeration requirement but may require a higher reboiler duty. An external heater may be required to ensure sufficient reboiler duty especially during startup.

The BAHX heat exchanger must be rerated for the various conditions to ensure there is no temperature pinches among the different passes.

12.5.2 REFLUX AND REBOILER DUTIES

Methane content in the nitrogen vent stream must meet environmental emissions requirements. The nitrogen content in the natural gas bottom stream must meet the nitrogen content in the sales gas specification. If the sales gas is fed to an LNG plant, the nitrogen should be kept as low as possible. The reflux system is typically controlled by the high nitrogen case, while the reboiler design is controlled by the low nitrogen case. For a robust design, the BAHX must be rerated for the extreme conditions to ensure there is no heat curve temperature pinches among passes. The NRU column and the compression requirements must also be checked.

12.5.3 TEMPERATURE AND PRESSURE CONTROL

The NRU column shall be equipped with temperature indicators for monitoring startup, shutdown and normal operation. The BAHX should be provided with temperature indicators that can be used to avoid temperature excursion during startup or upset conditions. The NRU column pressure must be equipped with advanced control system to control the reflux and reboiler duties, as the fractionator temperature is sensitive to a change in column pressure.

Pressure differential across the BAHX, column pressure and feed strainers shall be continuously monitored to detect hydrate formation or blockage by foreign materials.

12.5.4 INSULATION

Cold conservation is critical in an autorefrigerated system. While a design margin can be applied to a mechanically refrigerated system to compensate for external heat leak, an autorefrigerated system relies on efficient insulation to limit heat gain from the environment.

The equipment can be mechanically insulated with advanced efficient insulation materials, or they can be enclosed in a cold box filled with perlite. For a cold box design, an internal, dry nitrogen atmosphere must be maintained to ensure insulation integrity and safety. Leakage of hydrocarbons must be monitored to avoid hydrocarbon accumulation within the cold box.

12.5.5 REBOILER HYDRAULICS

Sufficient heat must be provided to the NRU bottom to meet product specifications. Because of the expansion loops in the reboiler piping, excessive pressure drop can slow down the reboiler flow. A hydraulic study of the reboiler system, especially the inlet and outlet lines, must be carried out for the various operations, particularly during start-up, to ensure adequate heating is provided to the NRU column.

12.6 NITROGEN REJECTION UNIT OPERATING PROBLEMS

The following describes some of the common operation problems encountered in operating the nitrogen rejection unit.

12.6.1 FEED CONTAMINANTS

Feed gas to NRU can contain impurities such as water, BTEX, pipe scales, and other contaminants, resulting from poor performance of the upstream units that will cause blockage of the BAHX. Feed strainers must be provided to avoid fouling of the BAHX. They should be removed for cleaning on-line when high-pressure differentials are detected.

12.6.2 FOAMING

Foaming is an unlikely event. However, if the NRU column pressure drop is higher than design, the column should be shut down for inspection.

12.6.3 HIGH METHANE CONTENT IN NITROGEN VENT

If the methane content in the nitrogen vent gas is high, it is most likely caused by insufficient reflux, which may be due to the limitation of the compression cooling equipment. The other cause could be due to reflux pump capacity limitation, lower fractionation efficiency, and maldistribution in the column that may be caused by hydrates.

12.6.4 HYDRATE FORMATION

During NRU start-up, the system may not be completely dried. Therefore, methanol injection should be used to remove any hydrate.

12.6.5 NITROGEN SAFETY

During plant upset, the nitrogen vent gas can drop to very low temperature, which may cause a safety hazard. Nitrogen vent must be routed to a safe location, away from the operating plant. Nitrogen must not be allowed to accumulate in confined spaces, which may cause accidental asphyxiation.

12.6.6 BRAZED ALUMINUM HEAT EXCHANGER FAILURE

BAHX is known to fail from severe temperature excursion during plant start-up. As such, monitoring of these exchangers is critical, particularly the rate of temperature change. Avoid the “the cold death spiral” on the exchanger. The manufacturer’s guideline on cooling down rate and derimming must be strictly followed.

12.7 HELIUM RECOVERY

Helium is found in natural gas, typically in concentrations from a few parts-per-million up to a few percent in certain fields such as the Hugoton basin and occasionally as high as 7% as seen in a small gas field in San Juan County, New Mexico. The helium is the result of radioactive decay of thorium and uranium in granite near the reservoir. While most helium generated in the earth’s crust escapes through porous rock and through the atmosphere, some helium is found trapped with other natural gases by

impermeable rock. Only a few natural gas fields world-wide have high enough helium content that can be considered to be economical viable for extraction.

When the feed gas contains higher than 0.5 vol% helium content, it may be economical to justify helium recovery. Depending on the applications, helium recovery product purity specification can vary; from low purity about 50% to 99.99+% purity. The design of the helium recovery unit is dependent on the feed gas composition, pressure and temperature, product specification and recovery levels. If helium product purity is in the 50% range, 98% recovery is generally economical. To produce the higher purity helium, helium recovery will be lower due to losses in the rejected nitrogen. The capital and operating costs of the helium recovery unit will increase with purity and recovery levels.

12.7.1 HELIUM RECOVERY PROCESS CONFIGURATION FOR HIGH CO_2 LEAN GAS

Helium can be found in natural gas streams that are high in nitrogen and CO_2. When the feed gas contains a high CO_2 content, such as 20 volume %, the removed CO_2 must be sequestrated to the reservoir formation to avoid carbon emissions. The process configuration of processing such gas for helium recovery is shown in Fig. 12.9.

The feed gas which contains methane, nitrogen and CO_2 is first dried in a molecular sieve dehydration unit to remove its water content, to avoid freezing in the downstream units. The dried gas is fed to a CO_2 fractionation unit which consists a series of chillers and a fractionation column, producing a CO_2 bottom stream and an overhead gas rich in methane, nitrogen and helium. The CO_2 fractionation column is designed for removing about 95 to 98% of the CO_2 in the inlet gas. For this reason, the treated gas from the CO_2 fractionation column contains a significant amount of CO_2 that would not meet the helium product specification. The treated gas is further processed in a methanol wash unit for removal of the residual CO_2. The removed CO_2 from the methanol wash unit is recycled back to the inlet for further processing. The final treated gas is fed to the nitrogen rejection unit that produces the methane sales gas and the nitrogen-rich feed stream to the helium recovery unit.

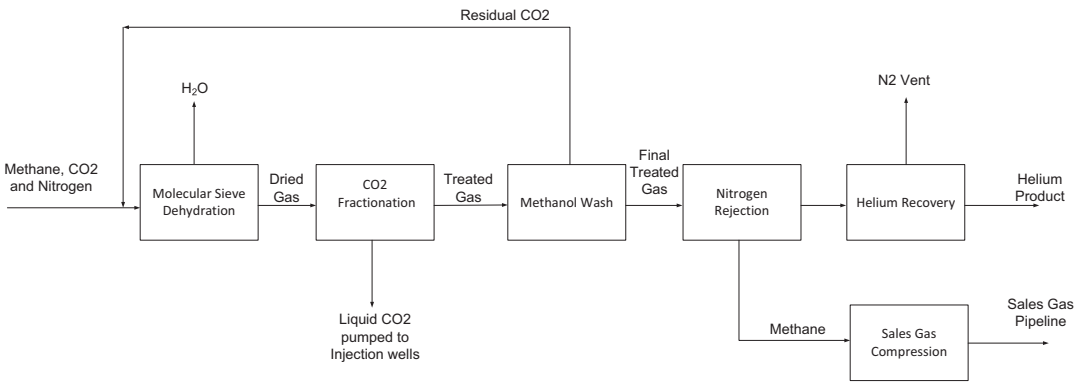

FIGURE 12.9

Nitrogen rejection with helium production.

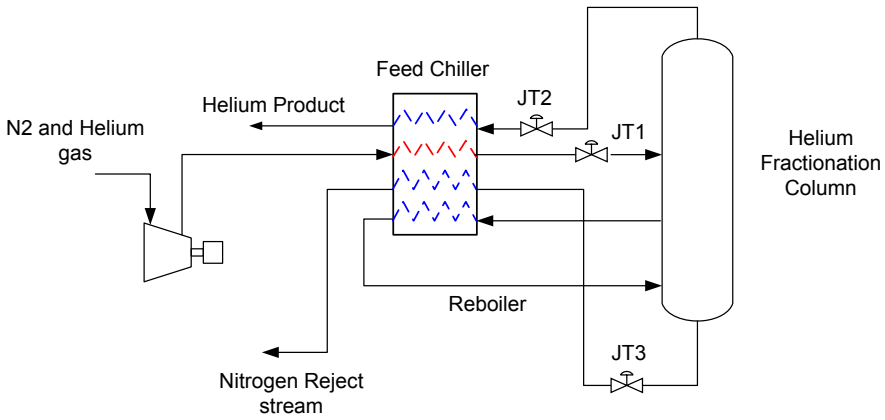

FIGURE 12.10

Helium recovery unit.

12.7.2 HELIUM RECOVERY UNIT

A typical helium recovery unit is shown in Fig. 12.10. Feed gas is compressed to a higher pressure and chilled in the feed chiller exchanger to the cryogenic temperature. The feed chiller is a brazed aluminum exchanger or equivalent exchanger which can achieve a close temperature approach, such as 2°F. A very close temperature design is required due to the cryogenic operating temperatures operation. The chilled gas is letdown in pressure in valve JT-1 and is chilled.

The chilled gas is fractionated in the helium fractionation column, which uses the feed gas for reboiling. The refrigeration process is provided by JT expansion of the bottom stream via valve JT3, and overhead vapor stream via valve JT2, in addition to the reboiler.

There are other separation processes that can be considered, such as PSA or membrane system. The selection depends on the feed gas capacity, recovery levels, purity requirement ad more importantly the sales value of the helium product. PSA and membrane are bulk removal system, and the recovery levels in a single pass operation can be 50 to 80%, depending on the feed gas composition. To improve recovery and purity, multiple units operating in series are required. This will require compression and recycling of the reject stream. There are other innovative schemes, such as hybrid membrane and cryogenic system.

Process selection mainly depends on the feed compositions, which can be a high nitrogen, high CO_2 lean gas, or a rich gas that would require NGL recovery. All these parameters must be considered as they will impact the capital and operating costs, and the justification of a helium recovery unit.

CHAPTER

UNCONVENTIONAL GAS PROCESSING

13

13.1 INTRODUCTION

As conventional natural gas resources are being depleted, the next exploration is to recover natural gas from unconventional sources, such as the rich shale gas, high-nitrogen natural gas, and very sour gases. When compared with gases from conventional plants, these gases, in terms of gas composition, feed locations, and feed conditions, are significantly different. Gas developers also had to consider the fluctuations in natural liquid and natural gas prices, the environmental issues, and public concerns while developing these unconventional gases.

Shale gas: Shale gas exploration in the United States is becoming an alternate source of natural gas. Led by new applications of hydraulic fracturing technology and horizontal drilling, recovery of shale gas has offset decline in production from conventional gas reservoirs and currently has led to major increase in natural gas reserves in the United States.

The characteristics of the shale gas are different from those of conventional gas such that the processing methods are different. These gases are richer in hydrocarbon contents, containing higher levels of C_2+ hydrocarbons. The shale gas can contain ethane and heavier hydrocarbons as high as 12 GPM (gallons of liquids recoverable per 1000 standard cubic feet of gas) C_2+, such as those found in the Bakken fields. On the other hand, conventional gas plant technologies are based on leaner gases, with ethane and heavier content of 2 GPM or lower.

Intuitively, the abundance of C_2+ can add revenues to the processing plants and is potentially attractive. However, with the oversupply and the low ethane price, the gas plants are now operating in ethane-rejection mode. This low ethane price also encourages construction of petrochemical plants and ethane export terminals. In today's design, the shale gas processors would require the gas plants to operate in ethane-rejection mode, which must also be operated for ethane recovery when the ethane prices become attractive. The dual recovery operation creates a challenge to the conventional "standardized" process.

High-nitrogen gas processing: There are some high-nitrogen natural gas fields in the United States, but their capacities are limited. When nitrogen injection is used for enhanced oil recovery (EOR), the produced gas will be contaminated with nitrogen, and its nitrogen content will grow rapidly if EOR continues. Earlier gas plants are typically not designed for natural gas with more than 1 mol% nitrogen. When processing high-nitrogen gases, nitrogen will generate cooling in the letdown process in natural gas liquid (NGL) recovery unit, but it also acts as a stripping gas in the fractionation process, reducing NGL production.

Handbook of Natural Gas Transmission and Processing. https://doi.org/10.1016/B978-0-12-815817-3.00013-7

Nitrogen rejection with helium recovery: Nitrogen-rejection unit (NRU) can be used to recover the nitrogen content from the high-nitrogen gas fields, but the NRU's capital cost is deemed expensive and not justified. However, some of these gases may contain over 0.5 volume% helium, which improves the returns of the project. An integrated NRU plant that can produce NGLs, helium, and sales gas potentially can be attractive.

Offshore gas treating: Offshore gas projects, such as in South China Sea and the pre-salt regions, encounter some very sour gas and gases with high CO_2 content, which creates difficulties with conventional acid gas removal unit (AGRU) processes. Treating sour gas in an offshore environment can be cost prohibitive with conventional treating processes. Offshore treating design must also address safety concerns, space limitation, carbon emissions, and limited manpower.

The objective of this chapter is to disclose some of the new technologies that have been developed to process the different unconventional gases as described previously, as existing technology may find difficulties and may not be the optimum solution in processing these gases.

13.2 UNCONVENTIONAL GAS

Shale gas has become an increasingly important source of natural gas in the United States. The Energy Information Administration predicts that by 2035, 46% of the United States' natural gas supply will come from shale gas (Fig. 13.1). Although Marcellus–Utica will likely continue to be a major producer, much of the shale gas growth will come from other richer basins such as Permian and Bakken (Fig. 13.2).

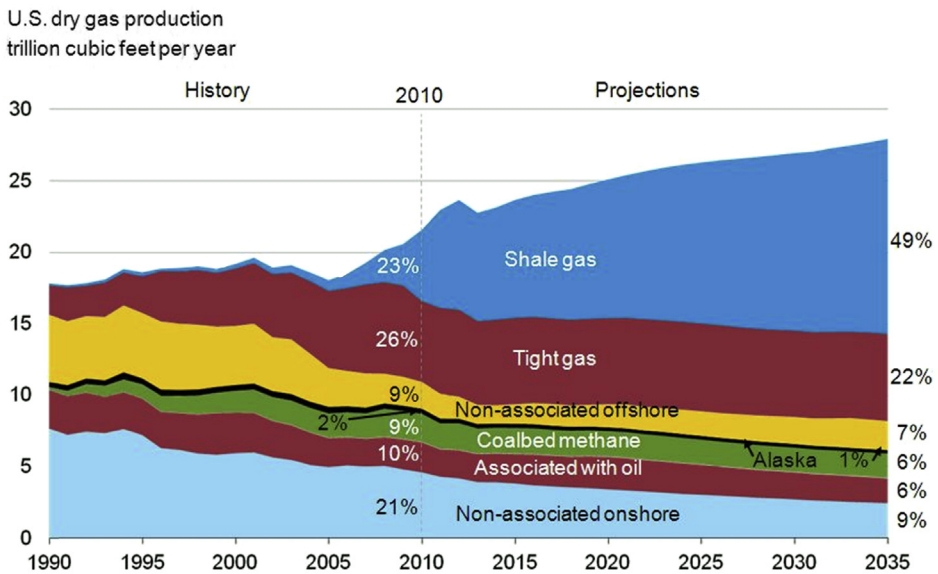

FIGURE 13.1

US dry gas production.

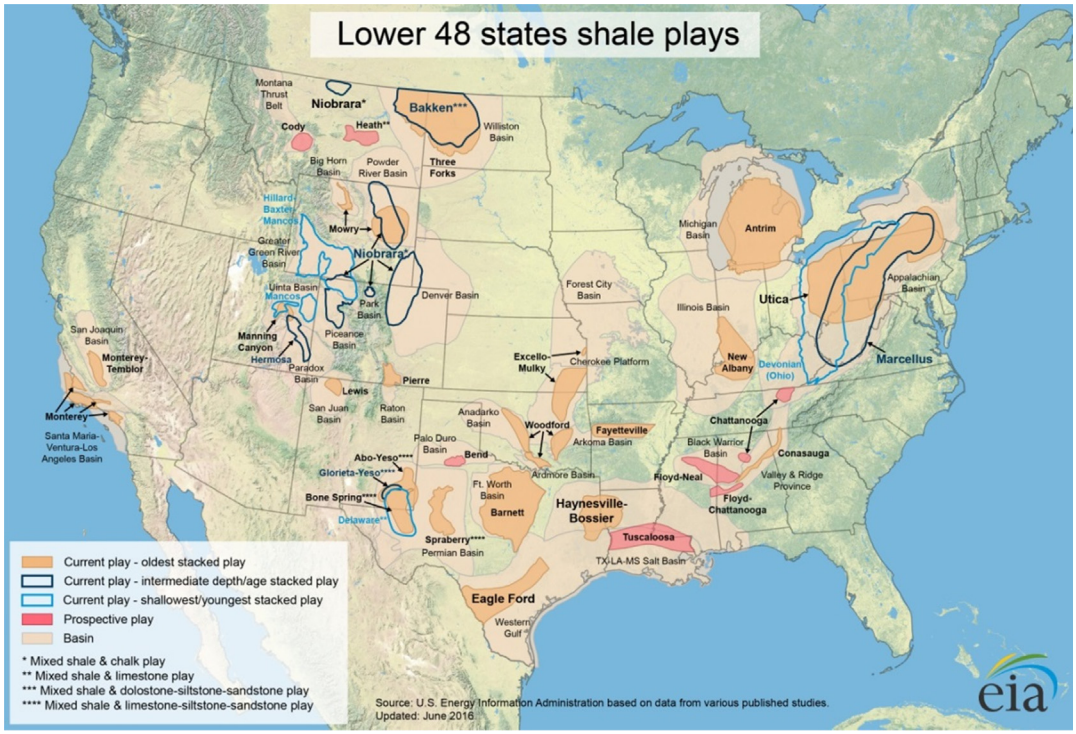

FIGURE 13.2

Lower 48 states shale play.

13.3 SHALE GAS VERSUS CONVENTIONAL GAS

Conventional gas is a leaner gas with lower ethane content and less hydrocarbon contents. Conventional gas is produced from larger fields, either from associated or nonssociated oil gas fields. Liquid recovery processes are mostly based on these leaner gases with the standardized 200 MMscfd cryogenic plant or the customized larger plant, such as the 1500 MMscfd Canadian Empress gas plant.

Shale gas reservoirs are smaller and can be short in the production cycle. Typical shale gas compositions in different regions in the United States are shown in Table 13.1 (Mak et al., 2015). Shale gas typically contains high-level of ethane, up to 20%, with the ethane plus liquids as high as 12 GPM, which are unusual in conventional gas plants.

The pie chart in Fig. 13.3 compares the average shale gas composition to the conventional gas. It illustrates the differences in methane, ethane, and heavier hydrocarbons contents, which obviously would require different processing methods.

Table 13.1 US Shale Gas Compositions (Mak et al., 2015)

Composition (in Mole Fraction)	Location									
	North Dakota Lean	North Dakota Rich	Wyoming Lean	Wyoming Rich	West Texas Lean	West Texas Rich	Colorado	Utica	Rockies	Bakken
Nitrogen	0.012	0.019	0.015	0.021	0.013	0.008	0.01	0.009	0.011	0.028
CO_2	0.011	0.006	0.016	0.008	0.026	0.027	0.016	0.002	0.006	0.006
Methane	0.707	0.613	0.734	0.581	0.71	0.613	0.689	0.803	0.73	0.519
Ethane	0.118	0.227	0.126	0.218	0.106	0.142	0.139	0.115	0.137	0.241
Propane	0.102	0.101	0.075	0.115	0.086	0.134	0.09	0.044	0.065	0.139
i-Butane	0.01	0.008	0.008	0.011	0.008	0.012	0.013	0.007	0.006	0.013
n-Butane	0.029	0.021	0.018	0.031	0.029	0.042	0.026	0.012	0.023	0.039
i-Pentane	0.004	0.002	0.003	0.005	0.006	0.007	0.007	0.003	0.005	0.005
n-Pentane	0.005	0.002	0.003	0.007	0.007	0.008	0.006	0.003	0.009	0.007
n-Hexane+	0.002	0.001	0.001	0.003	0.009	0.006	0.005	0.001	0.009	0.002
C_2+ GPM	7.59	9.93	6.55	10.89	7.19	10	8.08	5.15	7.23	12.43
C_3+ GPM	4.31	3.76	3.08	4.91	4.21	6.04	4.21	2	3.46	5.83

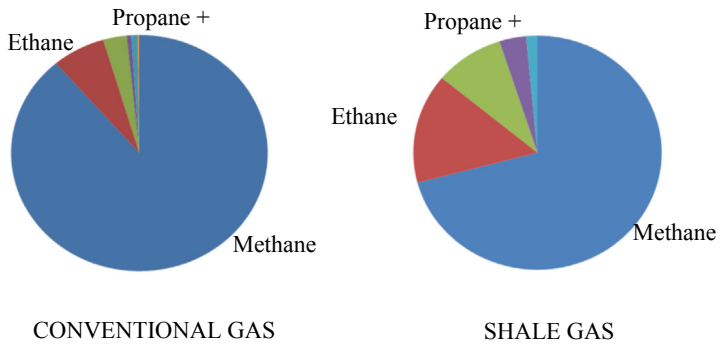

FIGURE 13.3

Conventional versus shale gas compositions.

13.4 SHALE GAS DEVELOPMENT

13.4.1 MODULARIZATION CONSIDERATION

The shale gas production capacity may fluctuate. The plant feed rate may vary over the development period. In some regions, plants that are built for a smaller capacity are quickly found out to run out of capacity. In another region, plants that were built for a higher capacity may experience difficulties in operating the plant at a lower rate during turndown. Operating at lowering capacity typically encounters operation instability and efficiency losses.

One of the solutions is to use a modular design. The modular design can improve labor productivity, reduce cost and schedule, and improve safety and quality. In addition to reducing total installed cost, plant modules can be added as needed to handle the increase in gas production. For example, a 30-MMscfd plant module can be installed in the initial phase, and identical modules can be added to handle the additional flow. Considering the short life span of some of these reservoirs, the modules can be designed as relocatable modules that can be disconnected and relocated to different sites when well capacity is depleted.

13.4.2 ETHANE PRODUCTION

Ethane, a key feedstock for petrochemical manufacturing, is traditionally produced by recovering the ethane content from natural gas as the Y-grade NGL. Currently, there is an oversupply of ethane that has kept the ethane price relatively low, hovering at or below the price of natural gas. In this scenario, gas producers would operate the gas plants in the ethane-rejection mode by mixing the ethane content with the residue gas for pipeline transmission. This is acceptable if there is a sufficient lean gas available to mix with the rich shale gas to meet the pipeline heating value specification.

The inexpensive ethane from shale gas has encouraged construction of new petrochemical plants and ethane export terminals. These investments would provide an outlet for ethane and increase takeaway capacity for ethane from the shale gas production. However, these facilities will take several years to build when growth of shale gas production may still outpace the demand markets. Ethane

prices are expected to fluctuate in the future and can be lower than natural gas prices. Today's US midstream gas processors would reject ethane due to the low prices but would like the process to produce ethane when the ethane markets are attractive.

13.5 CONVENTIONAL NGL RECOVERY PROCESSES

There are different recovery levels of NGL recovery. It can vary from the simple hydrocarbon dewpointing unit to the more complex cryogenic turboexpander units. Within each category, there are many designs that can be applied to meet the product specifications. These processes are described in detail in Chapter 11. These gas plant designs were based on processing a relatively lean gas and can be called "standardized" gas plants. These standardized designs are applicable for most of the lean gases found in the United States and other parts of the world.

13.5.1 HYDROCARBON DEWPOINTING

The hydrocarbon dewpointing unit is mainly designed to dry the gas and to remove the C_5+ content to meet the sales gas specifications. Removal of water can avoid corrosion in the pipeline, and removal of C_5+ content can avoid liquid dropout and condensation in the pipeline. The extracted liquid is a stabilized C_5+ condensate that can be further processed in a refinery. The process configuration of a typical hydrocarbon dewpointing unit is shown in Fig. 13.4.

The hydrocarbon dewpointing unit is typically dried using glycol or molecular sieve and cooled by heat exchange with the residue gas and refrigeration. The chilled gas is letdown in pressure to about 600 psig and further chilled, forming a two-phase stream which is separated in the cold separator. The separator vapor is the residue gas, and the liquid is fed to a stabilizer column to produce a C_5+ condensate. The butane and lighter hydrocarbons are rejected from the stabilizer as the overhead vapor that is compressed in the gas pipeline.

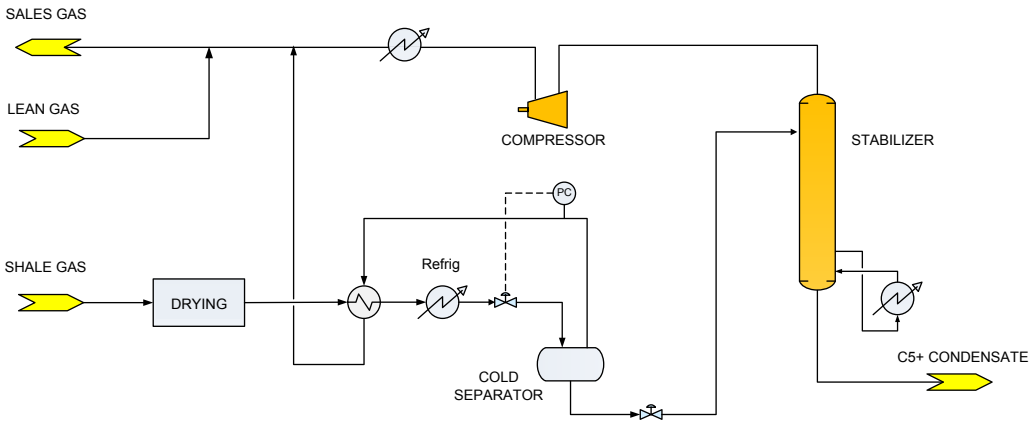

FIGURE 13.4

Hydrocarbon dewpointing unit.

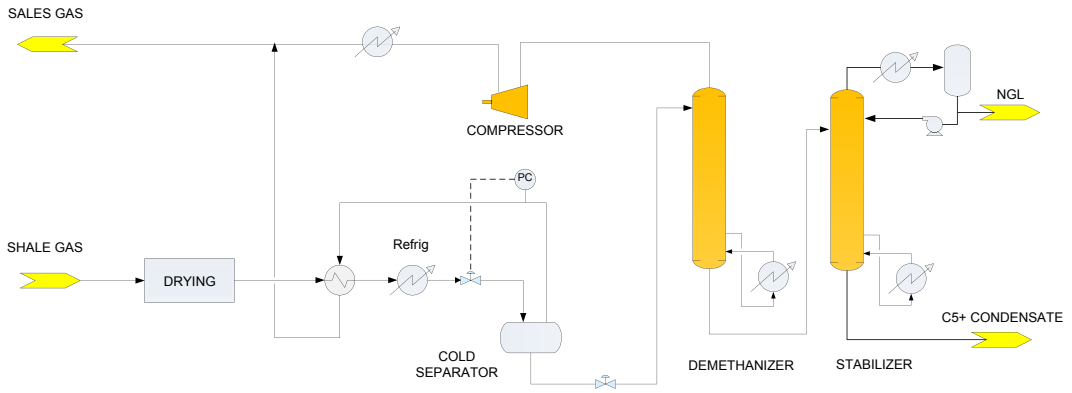

FIGURE 13.5

Modified hydrocarbon dewpointing unit.

The C_5+ condensate production is typically small that it would not change the heating value of the feed gas. When processing a rich gas, the heating value of the residue gas would still be high, which means production of this rich gas would require blending with a lean gas from other sources.

However, when a lean gas is not available for mixing, the solution is to remove the NGL content to lower the heating value. This approach will require additional processing equipment, as shown in Fig. 13.5. The modified dewpointing unit consists of a demethanizer and a stabilizer. The demethanizer operates to remove some of the NGL components, which are then fractionated in the stabilizer, producing the C_5+ condensate and an overhead NGL product. The amount of NGL hydrocarbons production can be varied with the demethanizer operation as necessary to meet the heating value specification of the pipeline gas.

The disadvantage of the dewpointing unit is the low recovery of the NGL hydrocarbons. If liquid production produces the main revenues, the more expensive cryogenic plants would be the better option.

13.5.2 RELATIVE COST OF NGL RECOVERY LEVELS

While NGL recoveries with a dewpointing plant are lower than the cryogenic plant, the capital cost for a dewpointing plant is significantly lower. On the positive side, the dewpointing unit is recognized to be easy to maintain and operate and can be turndown to below 25%. Such flexibilities favor the dewpointing plants.

While recoveries with the cryogenic plant are much higher, the capital cost is also higher. They can only be justified if there is a market for the ethane product and the revenue can pay off the additional investment. If ethane prices are not stabilized and attractive, it may be easy to recover only the propane components. Cost of ethane recovery can be delayed when NGL prices become attractive, as in the past.

A typical cost versus NGL recovery is illustrated in Fig. 13.6. The higher cost associated with the cryogenic unit is due to process complexity, higher refrigeration duty, and larger heat exchanger and column sizes.

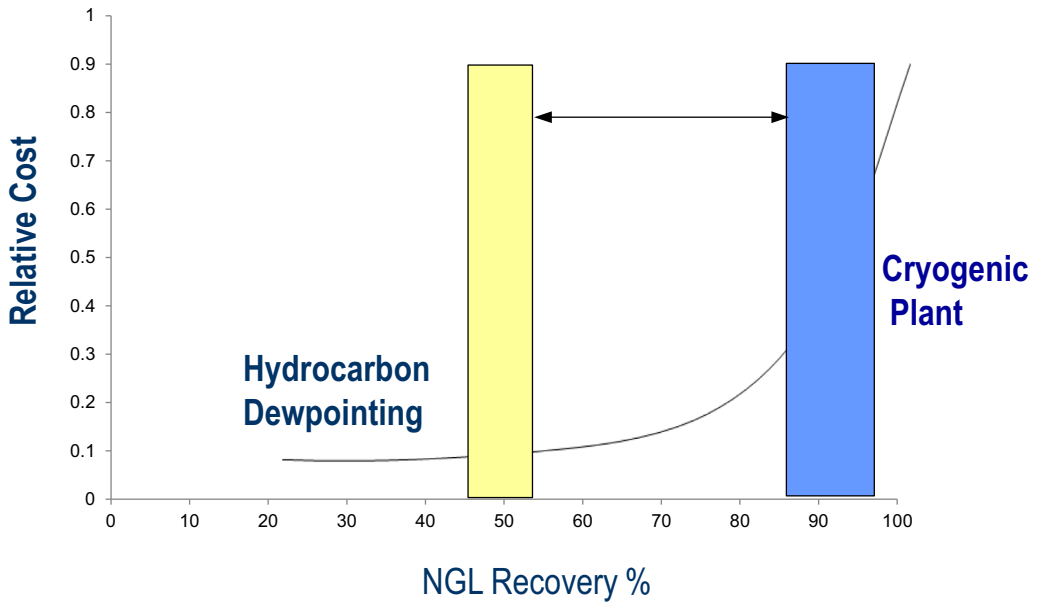

FIGURE 13.6

Relative cost of NGL recovery levels.

The questions often come from the gas processors to the designer, "can you find a process that can fit between these two extremes?" "Our target is to find a moderately cost design with a slightly higher cost than the dewpointing unit, but significantly lower cost than the cryogenic unit, while achieving a moderate level of recoveries."

13.5.3 CRYOGENIC TURBOEXPANDER PLANTS

Cryogenic turboexpander processes such as the Gas Subcooled Process and the Residue Gas Recycle process are configured to meet the high ethane and propane recovery targets, as described in Chapter 11. These processes are not best for lower ethane recovery (ethane rejection), such as 5 % ethane recovery. The disadvantage of these processes is that when ethane market is low, ethane must be rejected to the sales gas, which would result in losing a portion of the valuable propane component, and subsequent loss of plant revenue (Mak, 2017a).

13.5.4 OPERATING CRYOGENIC TURBOEXPANDER PLANT ON SHALE GAS

Turboexpander is an efficient machine that produces low-temperature refrigeration via the isentropic expansion process while generating power to operate a compressor. Turboexpansion of a lean gas is efficient, as it can generate significant power and refrigeration. However, when processing a rich gas, such as the shale gas, bulk of the C_2+ hydrocarbons will be condensed, and the residual methane in the feed gas is significantly reduced. With the C_2+ liquids removed, the flash gas going to the expander is

lower, consequently producing less power and refrigeration. For a rich gas operation, additional propane refrigeration is required to condense the C_2+ hydrocarbons, and to compensate for the lower refrigeration generation from turboexpansion.

Turboexpander plant has limited turndown capability. Expander efficiency would drop during plant turndown. Expander must be bypassed when operating below 50% of the design point. Expander plant is best to operate at close to the design point to maintain high efficiency.

13.6 UNCONVENTIONAL NGL RECOVERY PROCESS

13.6.1 DEEP DEWPOINTING PROCESS

Fluor's deep dewpointing process (DDP) (Mak et al., 2015, 2017a; Mak, 2016a) is an ethane-rejection process to process the rich shale gas, without the use of turboexpander. The process can also be used for propane recovery, producing the truckable-grade propane NGL.

The DDP process uses a two-column design, using an absorber and a stripper. In principle the DDP process uses the overhead vapor from the stripper which is rich in ethane to reflux the absorber. This process has been demonstrated to be very efficient in the recovery of propane. This can be compared with the conventional cryogenic processes, where reflux is produced by the lean feed gas (in the GSP), which is a methane-rich gas. Because of the difference in reflux compositions, the DDP process operates at a higher temperature, requiring lower internal reflux and less refrigeration.

The process configuration is shown in Fig. 13.7. Dry feed gas, typically supplied at 900 psig, is initially chilled in the main exchanger to about −20°F. The DDP process uses a multipass brazed

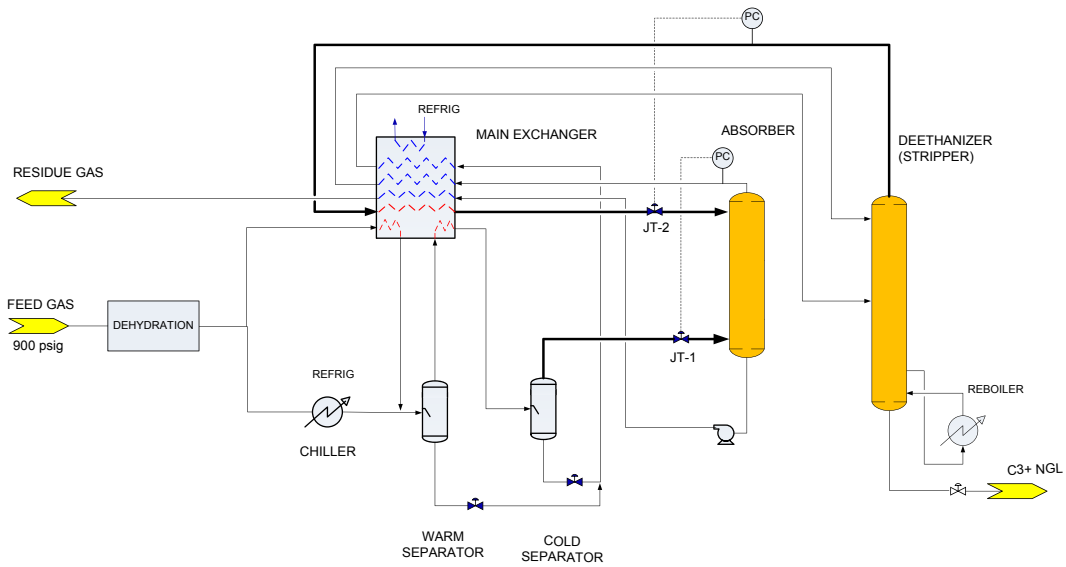

FIGURE 13.7

DDP ethane rejection.

aluminum plate fin exchanger (BAHX) where the refrigerant content in the residue gas, the cold separator liquid, and absorber bottoms are recovered, supplemented by propane refrigeration.

The DDP process operates in the same fashion as the conventional dewpointing unit. With the use of JT valve, instead of turboexpander, the process has avoided the difficulties in the turndown operation. Unlike turboexpander, JT valves are not sensitive to changes in feed gas compositions and feed rates. This process is most advantageous in processing the shale gas fields, when gas compositions and capacities are not fully defined during the project development (Mak et al., 2015). With the use of the DDP process, the unit can be turndown to as low as 25%, limited only by the fractionation column, and not controlled by the operation of the turboexpander.

Fractionation of the C_3+ hydrocarbon is achieved in two steps. An absorber uses the recycled ethane from the stripper to absorb the C_3+ hydrocarbons. The absorber produces an ethane-rich bottom that is refractionated in the stripper to produce an ethane-rich overhead that is recycled back to the absorber as a two-phase reflux. The stripper is a nonreflux column reboiled by steam or hot oil to produce a deethanizer bottoms product that meets the C_3 product specification.

To enhance the absorption process, a second JT valve (JT-2) is used to let down the stripper overhead stream to the absorber pressure, providing a second level of chilling. The DDP process typically can achieve 98%+ propane recoveries in full ethane rejection with the following performance:

- ethane recovery of 2.0%
- propane recovery of 98.0%
- butane recovery of 99.0%
- C_5+ recovery of 99.5%

The DDP unit can also be operated for incidental ethane recovery by reducing the bottom temperature of the stripper. When lowering the bottom temperature, the methane content can be monitored to ensure the NGL product meet the Y-grade specification. Typically, with this operation, 40%−45% of the ethane from the feed gas can be recovered.

13.6.2 HIGH ETHANE RECOVERY CONVERSION

When high ethane recovery over 90% is required, deeper level of refrigeration is required. This would require replacing the J-T valve with a turboexpander. Fig. 13.8 shows the changes required to the DDP process to meet the requirement of high ethane recovery. The changes are summarized in the following:

- The feed gas cooling section operates at slightly lower temperatures than the ethane-rejection mode.
- A turboexpander is used to replace the Joule Thomson valve JT-1.
- The high-pressure vapor from the cold separator, about 50%−60%, is sent to the expander to help cooling. The remaining flow is cooled in the main exchanger to form a reflux to the absorber.
- The stripper overhead vapor is routed to the bottom of the absorber.
- Absorber bottoms liquid is pumped directly to the stripper.
- Stripper reboiler is used to cool a portion of the feed gas.
- The stripper is operating as a demethanizer producing the Y-grade NGL.

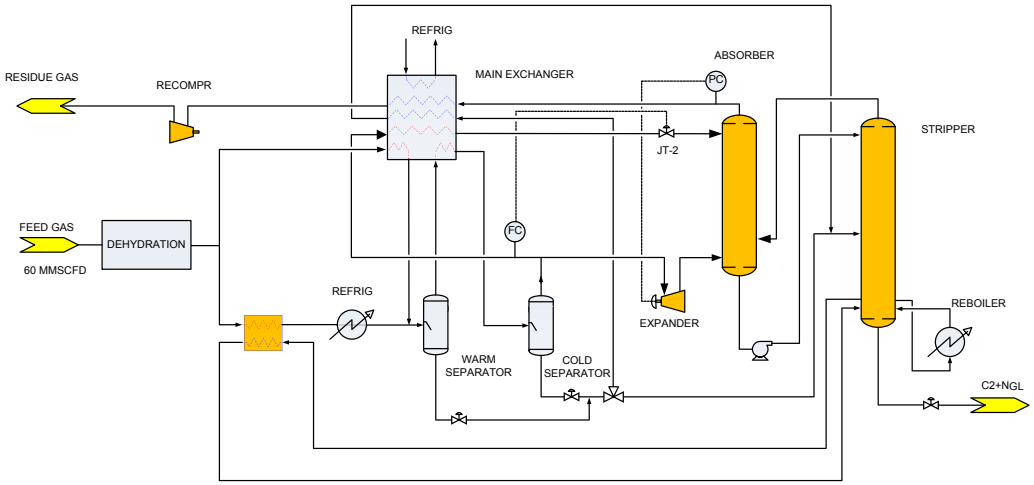

FIGURE 13.8

DDP ethane recovery.

This process change can achieve the following recoveries:

- ethane recovery of 95.0%,
- propane recovery of 98.0%,
- butane recovery of 99.0%,
- C_5+ recovery of 99.5% minimum.

13.6.3 BOLT-ON UNIT FOR HIGH ETHANE RECOVERY

Typically, in conventional gas plant, cryogenic process can recover 75%−85% of the ethane content in the feed gas. When higher ethane recovery is required, additional processing step is necessary to increase the recovery. One of the methods is illustrated in Chapter 11, by using a methane-rich residue gas stream as reflux to the absorber.

However, in most instances, the existing gas plant may not have additional compression or absorption capacity. This can be supplemented with additional equipment as shown in Fig. 13.9. The bolt-on unit includes an absorber, brazed aluminum exchangers, a reflux pump, and a recycle gas compressor. The overhead vapor from the demethanizer is sent to the bolt-on unit, where the vapor is scrubbed by a subcooled liquid from the recycle compressor in the absorber. The ethane-rich liquid from the absorber is pumped by the reflux pump to feed the demethanizer.

The absorber overhead vapor is heated in two stages in the brazed aluminum exchanger. The vapor is heated to an intermediate temperature in the first-stage lean reflux exchanger and is then split into two portions. One portion is returned to the existing reflux exchanger, while the other portion is routed to the second-stage lean reflux exchanger.

The bolt-on unit when integrated with the existing plant can recover up to 99% of the ethane content. For the rich gas, supplementary propane refrigeration is required.

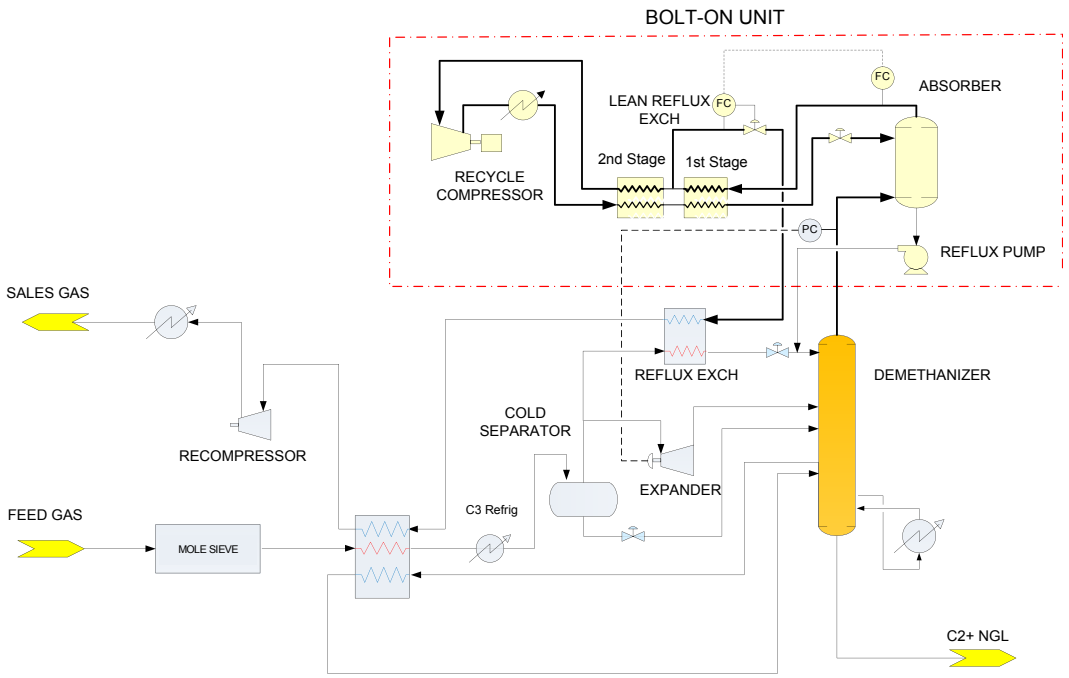

FIGURE 13.9

Bolt-on ethane recovery.

13.7 HIGH-NITROGEN FEED GAS

One of the most cost effective ways to increase oil reservoir pressure is by injecting nitrogen. Nitrogen gas is injected into an oil reservoir to increase the oil recovery factor by oil swelling and viscosity reduction. The continuous nitrogen injection will also increase the nitrogen content of the associated gas from oil production. Over time, the nitrogen content in the reservoirs will steadily increase, as nitrogen injection continues.

For gas plant operation, nitrogen injection will have a significant impact on the NGL recovery operation. The higher nitrogen content will result in colder separator temperatures due to the leaner feed gas (due to the JT effect). Equipment that is designed for warmer temperature may experience temperature colder than the design temperature. To stay above the minimum design temperature, process temperatures must be increased by bypassing some of the exchangers. This will change the NGL plant operation, significantly reducing NGL recovery.

13.7.1 FLUOR PROPANE RECOVERY PLANT

The propane recovery unit for the initial operation is shown in Fig. 13.10. It is a dual column expander plant designed and configured to recover propane for export. It consists of an absorber with stainless steel material and a deethanizer with carbon steel design. The process is configured to maintain a warmer temperature in the deethanizer to avoid the use of the more expensive stainless steel material.

FIGURE 13.10

Fluor propane recovery unit.

The propane recovery plant was designed with 5−6 GPM C_2+ liquid in the feed gas, with less than 0.5% nitrogen as shown in Table 13.2. Owing to the increase in nitrogen-injection activity, the nitrogen content in the feed gas is predicted to gradually increase from the current 4.7 mol% to 54 mol% (Mak et al., 2017b).

In the initial process as shown in Fig. 13.11, feed gas at about 950 psig is treated and dried and then fed to the NGL recovery process. Feed gas is cooled in the feed gas exchanger, a multipass brazed

Table 13.2 Feed Gas Nitrogen Content

Feed Gas Composition, Mole %	Initial Design	Nitrogen Operating Range		
		Low	Medium	High
Nitrogen	0.49	4.77	25.91	53.75
Carbon dioxide	0.02	0.20	0.21	0.37
Methane	71.15	72.52	56.38	33.56
Ethane	16.07	12.90	10.03	6.09
Propane	8.18	5.86	4.56	3.00
i-Butane	0.87	0.75	0.58	0.13
n-Butane	2.13	1.84	1.43	1.31
i-Pentane	0.39	0.39	0.30	0.30
n-Pentane	0.45	0.48	0.37	1.18
n-Hexane+	0.13	0.29	0.23	0.31

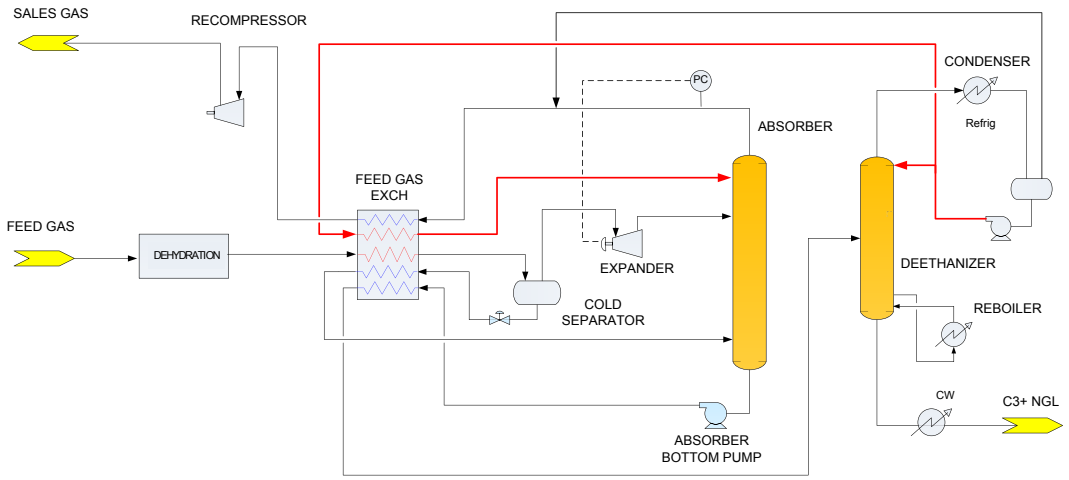

FIGURE 13.11

Fluor propane recovery process.

aluminum heat exchanger, where it countercurrently exchanged with the cold residue gas, absorber bottoms, and cold separator bottoms. The chilled feed gas is separated in the cold separator. The cold separator vapor is expanded with an expander where it is let down to the absorber operating at about 400 psig.

The cold separator liquid is let down in pressure via a cross-control valve and heated in the feed gas exchanger, and it returns to the bottom of the absorber. The absorber bottoms are pumped by the absorber pumps, heated in the feed gas exchanger, and then enters the deethanizer. The deethanizer removes the ethane and lighter hydrocarbons using steam, producing the propane product with less than 1 volume% C_2 content.

C_2 and lighter components in the deethanizer overhead partially condenses in the condensers by propane refrigeration and separated in the deethanizer reflux drum. Part of the C_2-rich deethanizer reflux drum liquids is pumped to the deethanizer as reflux. The other portion is pumped to the feed exchanger to be cooled and fed to the top of the absorber as reflux. The absorber reflux absorbs almost all the C_3+ components in the absorber, resulting in over 99% propane recovery. The deethanizer accumulator vapor combines with the absorber overhead, forming the cold residue gas and is heated in the feed exchanger against the incoming feed gas. The warm residue gas is compressed by the recompressor and sent to the sales gas pipeline.

13.7.2 FLUOR ETHANE RECOVERY REVAMP

Owing to the increasing nitrogen-injection activities, the nitrogen content in the feed gas is gradually increasing. As shown in Table 13.2, the nitrogen content is predicted to increase from the current 4.8 mol% to 25.9 mol% and then to 53.7 mol%.

With the higher nitrogen content, the feed gas generates greater J-T cooling resulting in lower temperatures in the process equipment. Since the cold separator and deethanizer are constructed of

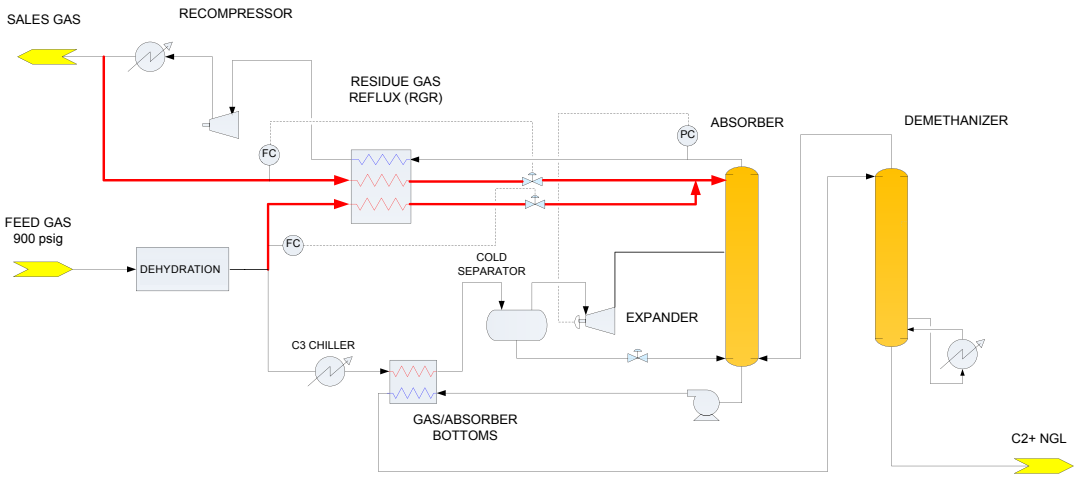

FIGURE 13.12

Fluor ethane recovery process.

carbon steel material, some of the exchangers were bypassed to avoid excessive cooling. Subsequently, the gas plant was revamped to recover 90%+ C_2. The revamp method minimizes changes to the original equipment by reusing the existing turboexpanders, propane refrigeration compressors, residue gas compressors, and existing absorber and deethanizer (or demethanizer). The process flow diagram for the revamp process is shown in Fig. 13.12 (Mak et al., 2017b).

In the revamped unit, about 30% of the feed gas is routed to the residue gas reflux (RGR) exchanger where it is cooled and condensed by the residue gas. The feed gas condensate is flashed across a J-T valve to the absorber operating at about 360 psig of pressure. In addition, about 10% of the high-pressure residue gas is cooled and condensed and is also used as reflux to the absorber.

The remaining 70% of the feed gas is routed to the propane chiller, cooled in the gas/absorber bottom exchanger and then flashed to the cold separator. The cold separator liquid is flashed to the bottom absorber. The cold separator vapor is expanded via the existing expander to the midsection of the absorber. The absorber bottoms is pumped and heated by the feed gas to approximately −35°F before feeding the demethanizer (the deethanizer in the original design). With this temperature, the carbon steel deethanizer can be reused as the demethanizer.

The demethanizer produces the Y-grade NGL product, which is pumped to the NGL pipeline. The cold residue gas from the absorber is heat exchanged in the RGR exchanger before recompression to the sales gas pressure. About 10% of the high-pressure residue gas is recycled back to the RGR exchanger to reflux the absorber.

13.8 NITROGEN- AND HELIUM-RICH GAS

There are significant amounts of high-nitrogen gas fields in the United States, which remains undeveloped. These marginal fields can be upgraded using the nitrogen-rejection system, which seldom can be justified in today's market. With the abundance of shale gas, developing these gas fields for sales

becomes even more difficult. Typical nitrogen-rejection system includes cryogenic processing, pressure swing adsorption, and membrane system, which have been discussed in Chapter 12.

When the nitrogen gas contains some helium component, say 0.5 mol%, recovery of helium in combination of a NRU can be justified. The usage of helium has been increasing, and there is recent shortage of this commodity. Helium now sells for some 30 times the natural gas price, which means even a small quantity can be profitable.

13.8.1 NITROGEN-REJECTION AND HELIUM-RECOVERY BLOCK FLOW DIAGRAM

The integrated NRU and helium block diagram is shown in Fig. 13.13. To prevent freezing in the cryogenic units, H_2S and CO_2 are removed in the AGRU. The treated gas is dried with the molecular sieve, and mercury is removed to a very low level to avoid mercury corrosion. The NGL extraction unit produces the Y-grade NGL and a residue gas that is fed to the NRU. Different methods of NGL recovery process are described in the earlier sections and in Chapter 11.

The NRU is designed to produce a sales gas with 2 mol% nitrogen and an overhead containing low level of methane. The overhead stream is fed to the helium-recovery unit, which is designed to produce a helium product with the following specifications:

- 70 volume % for helium (minimum),
- 3 volume % methane (maximum),
- 2.5 volume % hydrogen (maximum),
- 200 ppmv CO_2 (maximum).

13.8.2 NITROGEN-REJECTION AND HELIUM GAS–RECOVERY PROCESS

The nitrogen-rejection and helium-recovery integrated system is shown in Fig. 13.14. Feed gas to the NRU is the residue gas from the NGL recovery unit. It contains about 23% nitrogen and 0.5% helium. Refer to Table 13.3 for the component balance of the NRU and helium-recovery unit.

The residue gas is supplied at 650 psig and 120°F and is first cooled in the NRU exchanger to about −180°F. The NRU exchanger is a seven-pass BAHX, using refrigeration generated from letdown of process streams. Refrigeration is provided by the letdown of the feed gas from 650 psig to about

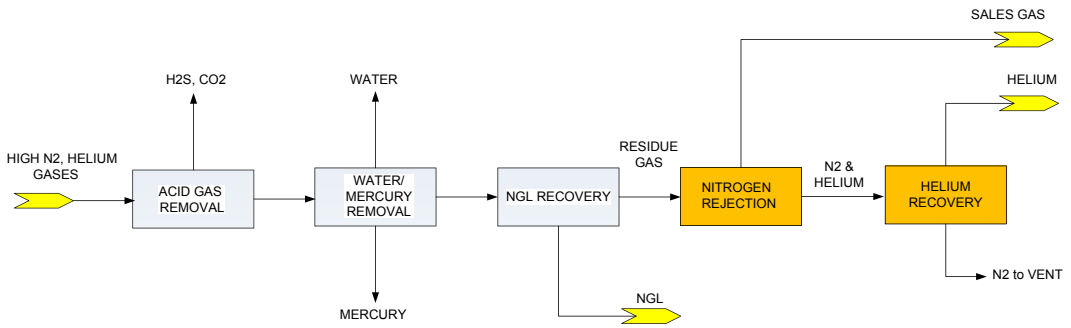

FIGURE 13.13

Nitrogen-rejection and helium-recovery block diagram.

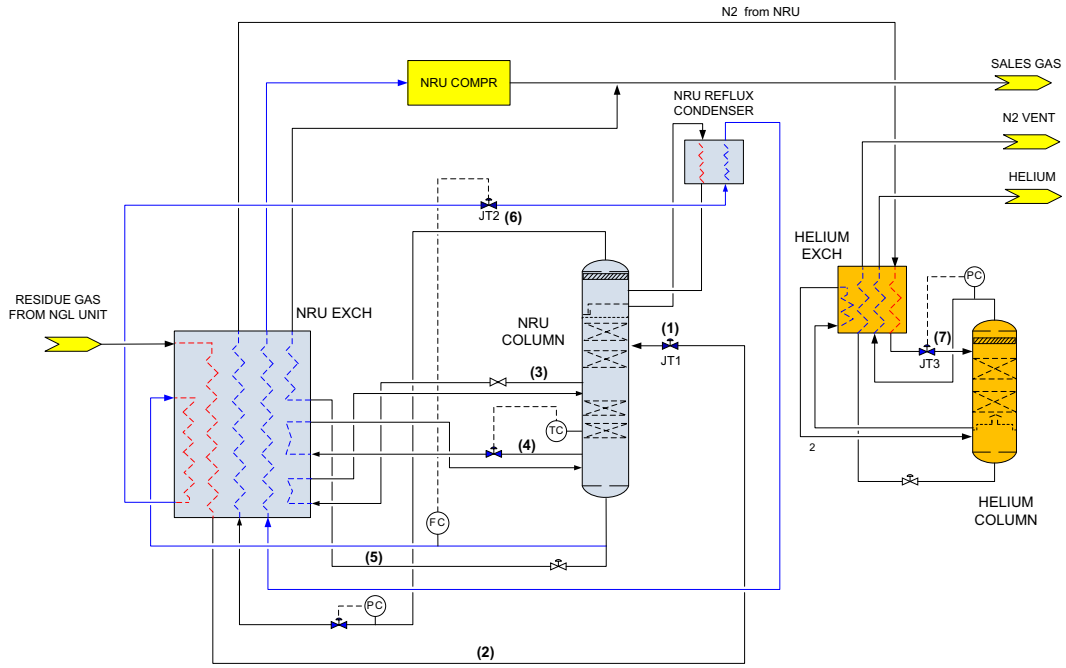

FIGURE 13.14

Nitrogen-rejection and helium-recovery process flow diagram.

Table 13.3 Mass Balance of Nitrogen Rejection and Helium Recovery

Stream Name	Residue Gas	N_2 and Helium	Sales Gas	Helium	N_2 Vent
Helium, mole %	0.55	2.48	0.00	85.85	0.03
Hydrogen, mole %	0.02	0.09	0.00	2.08	0.03
Nitrogen, mole %	22.96	96.43	2.00	12.07	98.91
Methane, mole %	76.09	1.00	97.51	0.01	1.03
Ethane, mole %	0.35	0.00	0.45	0.00	0.00
Propane, mole %	0.01	0.00	0.01	0.00	0.00
Flow, MMscfd	40.0	8.9	31.1	0.3	8.6
Pressure, psig	600	346	346	225	15

350 psig via letdown valve JT1 (1), refrigerant content from nitrogen (2), the reboiler duties from the side exchanger (3) and the bottom reboiler (4), the NRU column bottom liquid (5), and the letdown valve JT2 (6).

The over-flash vapor from the JT1 (1) flows up to the NRU reflux condenser, where the cooling is provided by JT cooling from JT2 (2). The high-pressure gas is let down to about 5−10 psig, as needed, to meet the temperature required for condensation in the reflux condenser (see composite curve in

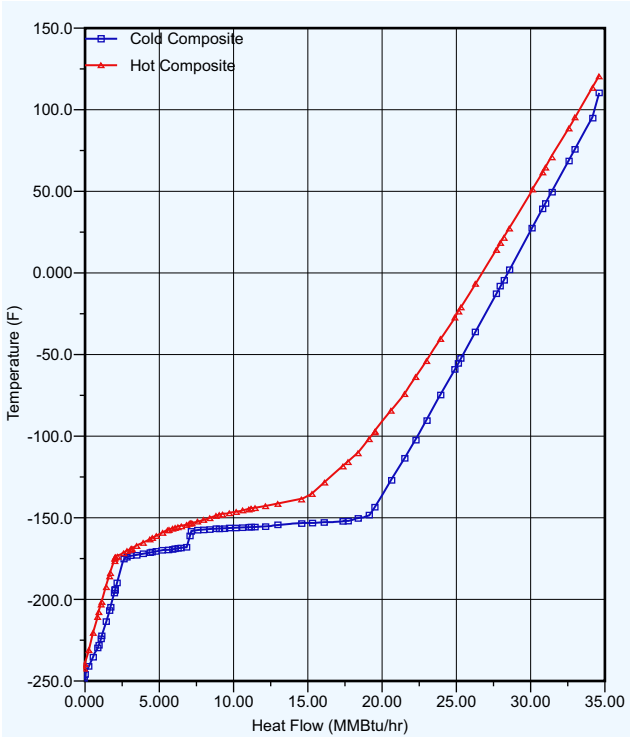

FIGURE 13.15

Heat composite curves for nitrogen rejection.

Fig. 13.15). The low-pressure vapor is compressed by the NRU compressor and combined with the NRU overhead vapor to the sales gas pipeline.

The methane content in the overhead nitrogen stream is controlled by the reflux condenser duty in the rectification section. The methane content in the nitrogen stream can be reduced by increasing the reflux duty by introducing more flow from JT2. Conversely, the nitrogen content in the sales gas product can be reduced by increasing the reboiler duty. Typically, the NRU column operates at 350 psig at −245°F overhead and −160°F at the bottom. The heat exchanger system is closely integrated as shown in the composite heat curves in Fig. 13.15. The NRU column produces a bottom liquid, which is the sales gas with less than 2 mol% nitrogen, and an overhead intermediate nitrogen stream containing nitrogen, helium, and about 1-mol% methane.

The overhead nitrogen stream is fed to the helium-recovery unit and is chilled to −315°F where it condenses in a four-pass BAHX. The chilled liquid is fed to the helium stripping column, which produces a helium-rich stream overhead and a nitrogen-rich bottom. Refrigeration is produced from the JT valve JT3 (7) by letdown of the cold condensate to about 210 psig. The refrigerant content from the reboiler duty, column bottom, and overhead vapor are, in turns, used to cool the feed gas. The heat composite heat curves of the heating and cooling streams are shown in Fig. 13.16.

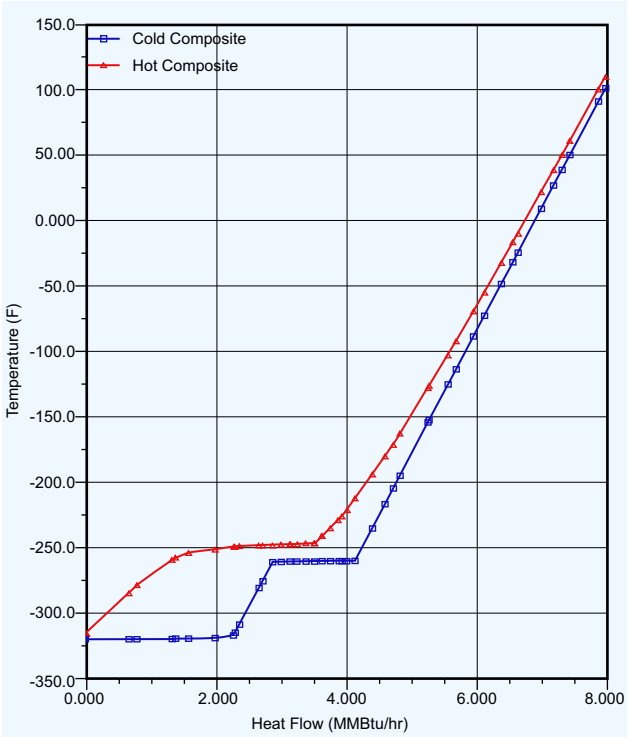

FIGURE 13.16

Heat composite curves for helium recovery.

The helium column produces an overhead helium stream with 85 mol% purity, with recovery level of 99% (Mak, 2016b; Mak, 2017b,c).

13.9 OFFSHORE CARBON DIOXIDE REMOVAL DESIGN CONSIDERATIONS

Removal of CO_2 from feed gases with high CO_2 content using conventional process is an energy-intensive process (Mak and Graham, 2015). For high−CO_2 content gases, traditional amine processes require high solvent circulation and heating and cooling duties, which are not practical in an offshore environment. CO_2 can also be removed using membrane separation, but the application is limited to smaller flow, and hydrocarbon recovery from membrane is low.

From a design and operation standpoint, an offshore gas-treating facility is different from an onshore facility. There is height limitation in offshore platform design. In some cases, equipment height cannot exceed 50 feet, which places a limit on the absorber column size. The motion experienced offshore facility requires special considerations to ensure proper vapor liquid distribution in column and heat exchanger equipment. Offshore facilities have limited staffing, which makes monitoring and controlling a complex process.

Operationally, offshore design needs to emphasize on safety, simplicity, and reliability. Other offshore considerations are eliminating fired equipment, reducing equipment separation, utility requirement, environmental compliance, and operational flexibility.

13.9.1 FLUOR SOLVENT OFFSHORE PROCESS

The Fluor solvent process, which uses PC as the solvent, was commercialized by Fluor in the early 1960s. The Fluor solvent process has been improved in recent years and proven distinctive advantages over competing processes. At low temperatures, the PC unit can operate with a low solvent circulation, recovering more hydrocarbons, and is a lower cost option when used to process high-CO_2 gases. Refrigeration can be generated by letdown of the rich solvent using hydraulic turbine, eliminating external refrigeration requirement. Please refer to Chapter 7 for the background and more details of the Fluor solvent process.

This section describes the application that is customized for offshore operation. The process flow diagram for the offshore application is shown in Fig. 13.17. The feed gas is first dried in a drying unit using glycol injection or molecular sieves dehydrators. The dried gas is combined with recycle gas and is sequentially cooled by the treated gas and the flash solvent. If the feed gas contains a significant amount of C_5+ hydrocarbon, liquid will drop out in the separator and should be removed. Removal of the condensate would reduce hydrocarbon losses in the CO_2 stream.

CO_2 absorption is accomplished in a two-stage absorber system. The absorption system consists of a semilean absorber and a lean absorber. The absorber column height is designed with height limited by the platform design. Feed gas is first scrubbed in the semilean absorber using the semilean solvent from the lean absorber. The semilean solvent from the lean absorber is cooled by the flashed solvent

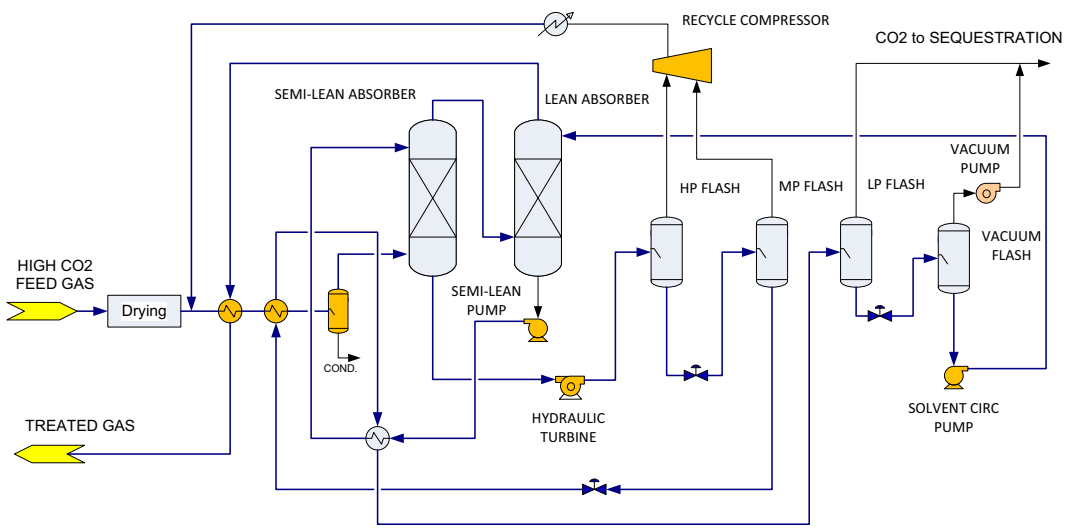

FIGURE 13.17

Fluor solvent offshore process.

and is reused in the lean absorber. This method also allows rich solvent to be heated up for regeneration while recovering the refrigeration content for absorption.

The residual CO_2 in the overhead gas from the semilean absorber is scrubbed with the lean solvent. Lean solvent at $-20^{\circ}F$ is used to meet the sales gas specification of 2-mol% CO_2. The absorbers contain efficient packing that is used for heat and mass transfer for the solvent absorption process.

The rich solvent from the semilean absorber is let down in pressure in the hydraulic turbine, which cools the solvent by removing the flashed vapor. Hydraulic turbine is an energy-efficient device as it produces shaft work to operate the solvent pump while producing cooling. The flashed solvent from the hydraulic turbine is separated in the HP drum, which produces a methane-rich vapor that is recycled back to the absorber. The flashed liquid is let down to the MP drum and cooled, producing a second flashed vapor, which is also recycled back to the absorber. With this recycle scheme, hydrocarbon losses are reduced to less than 1%.

Flashed liquid from the MP drum is heated in the feed exchanger, which assists solvent regeneration, while at the same time, it cools the feed gas and the semilean solvent. This innovation significantly improves the operating efficiency of the Fluor solvent process.

The heated solvent is further let down in the LP drum at close to atmospheric pressure, producing a CO_2 stream with 97%–98% purity. The LP flashed solvent is further let down and flashed to vacuum pressure. The CO_2 streams can be further compressed for CO_2 sequestration.

13.9.1.1 Utility Consumption

For a feed gas rate of 100 MMscfd with 32-mol% CO_2, supplied at 1100 psig, the Fluor solvent process can meet the specification of 2 mol% CO_2 specification and 1% hydrocarbon losses from the CO_2 sequestration stream.

Utility consumption is mainly a power requirement of 2300 kW. About 60% of the power consumed is used in the recycle gas compressor, which is required to reduce hydrocarbon losses to 1 mol%. There is no heating requirement, thus eliminating CO_2 emission sources. There is no water makeup requirement as the solvent operates in an anhydrous state.

A 3D rendition of the Fluor solvent process and the offshore plot plan are shown in Fig. 13.18. The layout of the Fluor solvent is compact. The main processing equipment consists of two short absorbers and four flash drums and heat exchangers. The hydraulic turbines, pumps, and compressors are small, which can be fitted to the plot as shown.

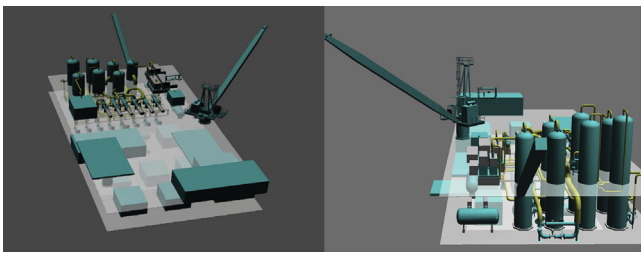

FIGURE 13.18

Fluor solvent offshore plant 3D model.

13.9.2 ACID GAS FRACTIONATION WITH METHANOL SYSTEM

The high acid gas stream can also be removed using a refrigerated fractionation configuration as shown in Fig. 13.19. The heat and material balance is shown in Table 13.4. The high acid gas stream is shown as stream 1, containing about 70% CO_2. The high CO_2 is first dried in a molecular sieve unit for the removal of the water content. There are some cross-exchanged through the process for heat recovery. The dry gas is then mixed with the recycle gas stream 2, forming stream 3, which is sent to the CO_2

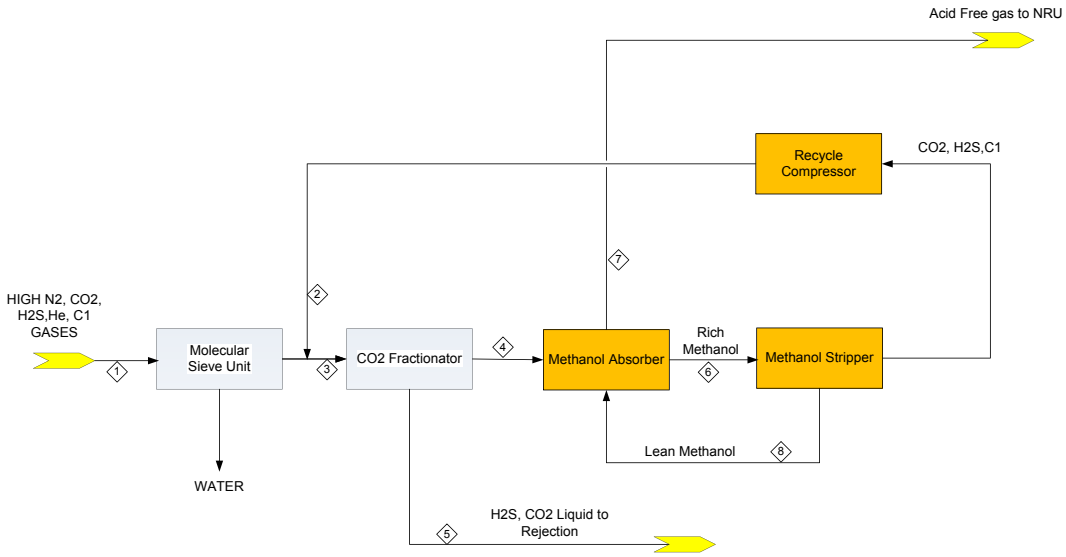

FIGURE 13.19

Acid gas liquefaction block flow diagram.

Table 13.4 Heat and Material Balance for Acid Gas Liquefaction

Stream Name	1	2	3	4	5	6	7	8
Nitrogen, mole %	7.01	1.42	6.32	17.66	0.00	0.16	26.52	0.00
Helium, mole %	0.05	0.01	0.04	0.13	0.00	0.00	0.19	0.00
CO_2, mole %	69.29	82.64	71.20	29.25	94.58	9.02	0.00	0.00
H_2S, mole %	3.67	3.58	3.67	1.27	5.01	0.41	0.01	0.02
Methane, mole %	19.51	12.04	18.62	51.52	0.29	1.31	73.03	0.00
Ethane, mole %	0.01	0.01	0.01	0.01	0.01	0.00	0.01	0.00
Methanol, mole %	–	0.28	0.04	0.00	0.05	89.10	0.01	99.98
Water, mole %	0.36	–	–	–	–	–	–	–
Flow, lbmol/hr	22,035	3185	25,140	8997	16,143	29,175	5822	26,000
Pressure, psig	1335	1325	1325	644	3000	237	235	665

fractionator. The CO_2 fractionator operates at about 644 psig, producing a bottom liquid stream 5 containing the CO_2 and H_2S components, which is pumped to high pressure for reinjection.

The CO_2 fractionator overhead stream 4, containing methane and lighter components, along with remaining acid gas flows to a refrigerated methanol absorber where the residual acid gas is absorbed. The absorber produces a rich methanol bottom, stream 6, containing the acid gases that are sent to the methanol stripper. The stripper separates the acid gas from the rich solvent, producing a lean methanol stream 8, which is free of acid gases. The lean methanol is pumped and recycled to the methanol absorber. The stripper overhead, containing the acid gases and hydrocarbons, is compressed and recycled back to the front section of the process, as stream 2.

After removal of the acid gas content, the nitrogen content in the absorber overhead gas is concentrated to 26 mol%, as seen in stream 7, which is required to be further processed in a NRU to meet pipeline specification.

This configuration will require compressing about 15% of the feed gas from the stripper pressure (typically 5 psig) to 1350 psig, which require a large recycle compressor. The high power consumption is a significant operating expense and must be evaluated.

REFERENCES

Mak, J.Y., August 23, 2016a. Flexible NGL Recovery Methods and Configurations. US Patent 9,423,175.

Mak, J.Y., November 8, 2016b. Configurations and Methods for Nitrogen Rejection, LNG and NGL Production from High Nitrogen Feed Gases. US Patent 9,487,458.

Mak, J.Y., January 31, 2017a. Ethane Recovery and Ethane Rejection Methods and Configurations. US Patent 9,557,103.

Mak, J.Y., February 23-24, 2017b. LNG production from unconventional gas. Paper Presented at the 1st Annual LNG USA Summit, Houston, TX, USA.

Mak, J.Y., June 6, 2017c. Integration Methods of Gas Processing Plant and Nitrogen Rejection Unit for High Nitrogen Gases. US Patent 9,671,162.

Mak, J.Y., Graham, C., July/August 2015. A New Treating Process for LNG Production from High CO_2 Gas Fields. LNG Industry, 39–44.

Mak, J.Y., Devone, S., Shih, J., September 16-18, 2015. New NGL recovery process for unconventional gas applications. Paper Presented at the 2015 Annual GPA Europe Conference, Florence, Italy.

Mak, J.Y., Devone, S., Shih, J., April 9-12, 2017a. Flexible NGL recovery process for shale gas production. Paper Presented at the 96th Annual GPA Convention, San Antonio, TX, USA.

Mak, J.Y., Jung, B., Graham, C., Ramirez, A., September 13-15, 2017b. Revamp of a propane recovery plant to 90% ethane recovery from design to start-up. Paper Presented at the 2017 Annual GPA Europe Conference, Budapest, Hungary.

CHAPTER

NATURAL GAS COMPRESSION 14

14.1 INTRODUCTION

"Compression" is used in all aspects of the natural gas industry including gas lift, reinjection of gas for pressure maintenance, gas gathering, gas processing operations (gas loading and discharge), transmission and distribution systems, and boil-off system (gas storage in tankers for vapor control and to avoid releasing gas into the atmosphere). In recent years there has been a trend toward increasing pipeline-operating pressures. The benefits of operating at higher pressures include the ability to transmit larger volumes of gas (referred at base conditions) through a given size of pipeline, lower transmission losses due to friction, and the capability to transmit gas over long distances without requiring or even reducing additional compressor stations. In gas transmission, two basic types of compressors are used: (1) reciprocating and (2) centrifugal compressors. Reciprocating compressors are usually driven by either electric motors or gas engines, whereas centrifugal compressors use gas turbines or electric motors as drivers. The key variables for equipment selections are life cycle cost; capital cost; maintenance costs including overhaul and spare parts; and fuel or energy costs. The unit's level of utilization, as well as demand fluctuations, plays an important role. Both gas engines and gas turbines can use pipeline gas as a fuel, but electric motor has to rely on the availability of electric power. Owing to the number of variables involved, the task of choosing the optimum driver can be quite involved and a comparison between the different types of drivers should be performed before a final selection is made (Lubomirsky et al., 2010). An economic feasibility study is of fundamental importance to determine the best selection for the economic life of a project. Furthermore, it must be decided whether the compression task should be divided into multiple compressor trains, operating in series or in parallel (Santos, 1997, 2004).

This chapter presents a brief overview of the two major types of compressors, a procedure for calculation of the required compression power, and additional and useful considerations for the design of compressor stations. All performance calculations should be based on compressor suction and discharge flanges conditions. For reciprocating compressors, pressure losses at the cylinder valves and the pressure losses in pulsation dampeners have to be included in the calculation. Additional losses for process equipment such as suction scrubbers, intercoolers, and aftercoolers have to be accounted to define compressor design conditions.

Handbook of Natural Gas Transmission and Processing. https://doi.org/10.1016/B978-0-12-815817-3.00014-9

14.2 RECIPROCATING COMPRESSORS

A reciprocating compressor is a positive displacement machine in which the compressing and displacing element is a piston moving linearly within a cylinder. The reciprocating compressor uses automatic spring-loaded valves that open when the proper differential pressure exists across the valve. Fig. 14.1 describes the action of a reciprocating compressor using a theoretical pressure−volume (PV) diagram. In position A, the suction valve is open and gas will flow into the cylinder (from point 1 to point 2 on the PV diagram) until the end of the reverse stroke at point 2, which is the start of

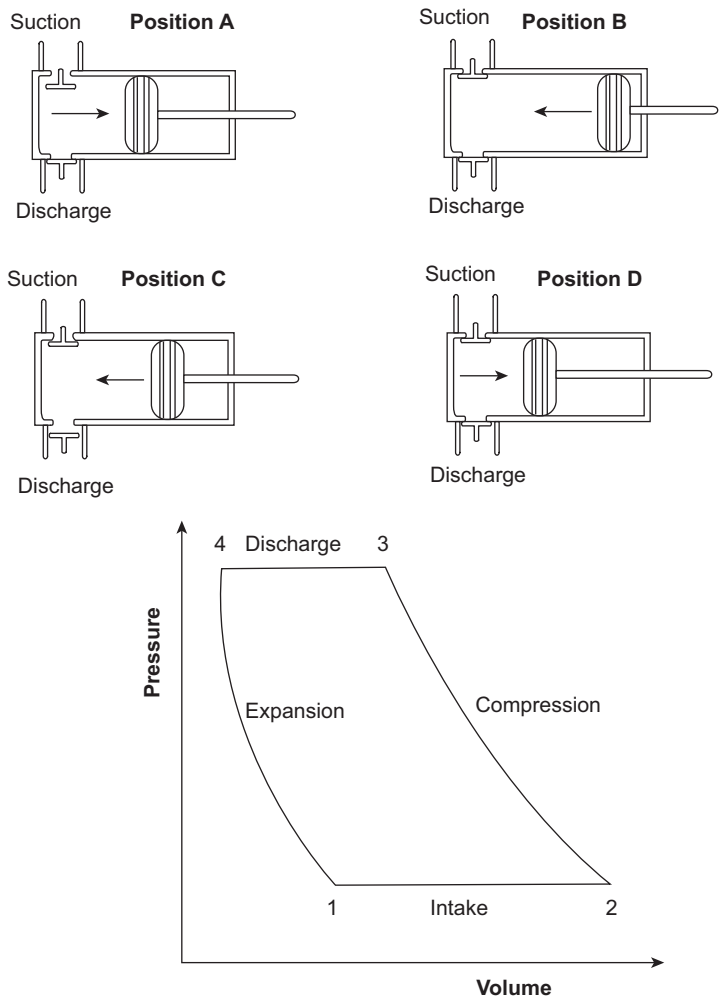

FIGURE 14.1

Reciprocating compressor compression cycle.

compression. At position B, the piston has traveled the full stroke within the cylinder, and the cylinder is full of gas at suction pressure. Valves remain closed. The piston begins to move to the left, closing the suction valve. In moving from position B to position C, the piston moves toward the cylinder head, reducing the volume of gas with an accompanying rise in pressure. The PV diagram shows compression from point 2 to point 3. The piston continues to move to the end of the stroke (near the cylinder head) until the cylinder pressure is equal to the discharge pressure, and the discharge valve opens (just beyond point 3). After the piston reaches point 4, the discharge valve will close, leaving the clearance space filled with gas at discharge pressure (moving from position C to position D). As the piston reverses its travel, the gas remaining within the cylinder expands (from point 4 to point 1) until it equals suction pressure, and the piston is again in position A.

The flow to and from reciprocating compressors is subject to significant pressure fluctuations due to the reciprocating compression process. Therefore pulsation dampeners have to be installed upstream and downstream of the compressor to avoid damages to other equipment. The pressure losses (several percent of the static flow pressure) in these dampeners have to be accounted for in the station design (Botros, 2013).

Reciprocating compressors are widely used in the gas-processing industries because they are flexible in throughput and discharge pressure range. Reciprocating compressors are classified as either "high speed" or "slow speed." Typically, high-speed compressors operate at speeds of 900−1200 rpm and slow-speed units at speeds of 200−600 rpm. High-speed units are normally "separable." That is, the compressor frame and driver are separated by a coupling or gearbox. For an "integral" unit, power cylinders are mounted on the same frame as the compressor cylinders and the power pistons are attached to the same drive shaft as the compressor cylinders. Low-speed units are typically integral in design.

14.3 CENTRIFUGAL COMPRESSORS

A centrifugal compressor achieves the compression task by converting the mechanical energy from the driver to kinetic energy in the gas, using the forces that moving and stationary airfoils exert on this gas. We want to introduce now the essential components of a centrifugal compressor that accomplish the tasks specified previously (Fig. 14.2). The gas entering the inlet nozzle of the compressor is guided to the inlet of the impeller. An impeller consists of a number of rotating vanes that impart the mechanical energy to the gas. The gas will leave the impeller with an increased velocity and increased static pressure. In the diffuser, part of the velocity is converted into static pressure. Diffusers can be vaned, vaneless, or volute type. If the compressor has more than one impeller, the gas will be again brought in front of the next impeller through the return channel and return vanes. If the compressor has only one impeller, or after the diffuser of the last impeller in a multistage compressor, the gas enters the discharge system. The discharge system can either make use of a volute, which can further convert velocity into static pressure, or a simple cavity that collects the gas before it exits the compressor through the discharge flange.

The rotating part of the compressor consists of all the impellers. It runs on two radial bearings (on all modern compressors, these are hydrodynamic tilt pad bearings), while the axial thrust generated by the impellers is balanced by a balance piston, and the residual force is balanced by a hydrodynamic tilt pad thrust bearing. To keep the gas from escaping at the shaft ends, dry gas seals are used. The entire assembly is contained in a casing (usually barrel type).

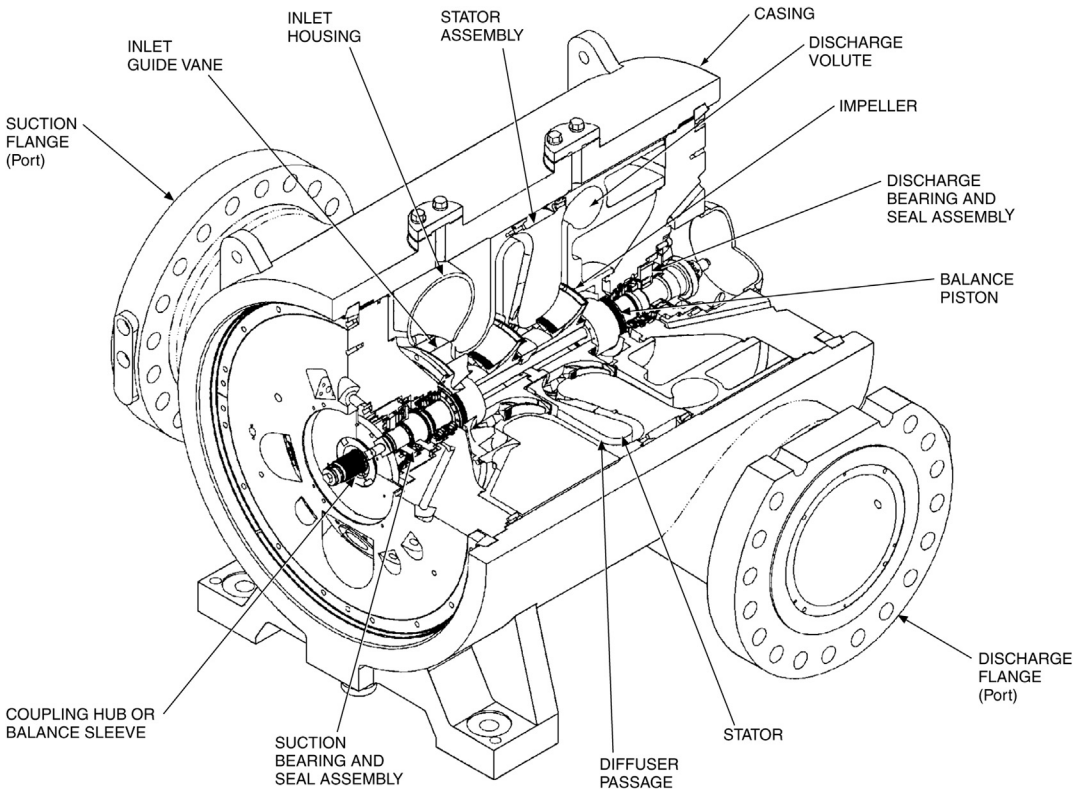

FIGURE 14.2

Typical centrifugal compressor cutaway (GPSA, 2004).

A compressor stage is defined as one impeller, with the subsequent diffuser and (if applicable) return channel. A compressor body may hold one or several (up to 8 or 10) stages. A compressor train may consist of one or multiple compressor bodies. It sometimes also includes a gearbox. Pipeline compressors are typically single-body trains with one or two stages.

The different working principles cause differences in the operating characteristics of the centrifugal compressors compared with those of the reciprocating unit. Centrifugal compressors are used in a wide variety of applications in chemical plants, refineries, onshore and offshore gas lift and gas injection applications, gas gathering, and in the transmission and storage of natural gas. Centrifugal compressors can be used for outlet pressures as high as 10,000 psia, thus overlapping with reciprocating compressors over a portion of the flow-rate/pressure domain. Centrifugal compressors are usually either turbine or electric motor driven. Typical operating speeds for centrifugal compressors in gas transmission applications are about 14,000 rpm for 5000 hp units and 8000 rpm for 20,000 hp[1] units.

[1]HP or hp stands for horsepower, a unit of power.

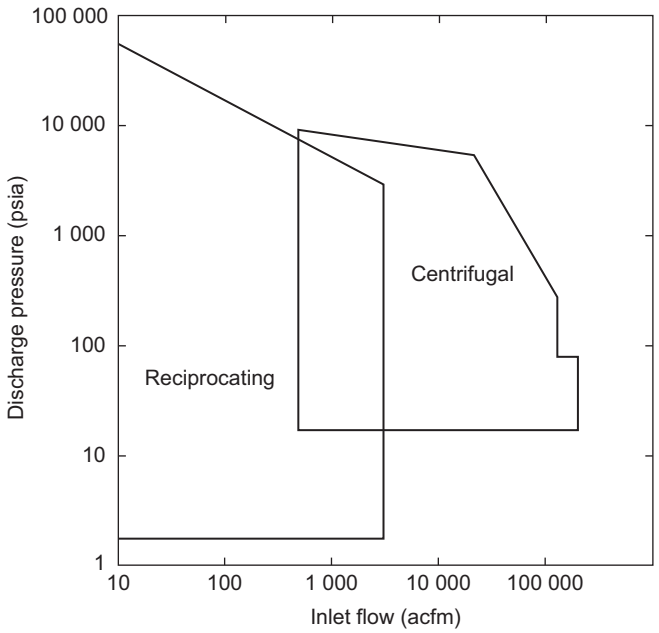

FIGURE 14.3

Coverage chart for reciprocating and centrifugal compressors (Carroll, 2010). *acfm*, actual cubic feet per minute.

14.4 COMPARISON BETWEEN COMPRESSORS

Fig. 14.3 illustrates the approximate application ranges of reciprocating and centrifugal compressors in terms of actual inlet flow and compressor discharge pressure. Although there is a significant overlap, some of the secondary considerations, such as reliability, availability of maintenance, reputation of vendor, price, and so forth, will allow one to choose one of the acceptable compressors. Note should be made that in Fig. 14.3, the actual gas flow rate[2] at suction conditions can be calculated using Eq. (14.1):

$$Q_G = 0.0283 \frac{Z_1 T_1}{p_1} Q_{G,SC} \tag{14.1}$$

where Q_G is an actual cubic feet per minute flow rate of gas; T_1 is the suction temperature in °R; p_1 is suction pressure in psia; Z_1 is the gas compressibility factor at inlet temperature and pressure, dimensionless; and $Q_{G,SC}$ is the standard volumetric flow rate of gas in MMSCFD.

The advantages of a reciprocating compressor over a centrifugal machine include:

- ideal for low volume flow and high pressure ratios
- high efficiency at high pressure ratios

[2]While the sizing of the compressor is driven by the actual volumetric flow rate (Q_G), the flow in many applications is often defined as standard flow. Standard flow is volumetric flow at certain defined conditions of temperature and pressure (60°F or 519.7°R and 14.696 psia) that are usually not the pressures and temperatures of the gas as it enters the compressor.

- relatively low capital cost in small units (less than 3000 hp)
- less sensitive to changes in composition and density

The advantages of a centrifugal compressor over a reciprocating machine include:

- ideal for high volume flow and low head
- simple construction with only one moving part
- high efficiency over normal operating range
- low maintenance cost and high availability
- greater volume capacity per unit of plot area
- no vibrations and pulsations generated

14.5 COMPRESSOR SELECTION

The design philosophy for choosing a compressor should include the considerations:

- good efficiency over a wide range of operating conditions
- maximum flexibility of configuration
- low maintenance cost
- low life cycle cost
- acceptable capital cost
- high availability and reliability

However, additional requirements and features will depend on each project and on specific experiences of the pipeline operator. In many cases, the decision whether to use a reciprocating compressor or a centrifugal compressor, as well as the type of driver, will be made based on operator strategy, emissions restrictions, general life cycle cost assumptions, and so forth. However, a hydraulic analysis should be made for each compressor selection to insure the best choice. In fact, compressor selection can be made for an operating point that will be the most likely or most frequent operating point of the machine. Selections based on a single operating point have to be carefully evaluated to provide sufficient speed margin (typically at 3%−10%) and surge margin to cover other potentially important operating conditions. For reciprocating compressors, operational restrictions, for example, due to rod load limits, or pulsations have to be considered. In general, centrifugal machines have continuous head−flow map coverage, whereas reciprocating machines often have maps with areas where the machine cannot operate. A compressor performance map (head vs. flow map) can be generated based on the selection and is used to evaluate the compressor for other operating conditions, by determining the head and flow required for those other operating conditions. In many applications, multiple operating points are available based on hydraulic pipeline studies or reservoir studies. Some of these points may be frequent operating points while some may occur during upset conditions. With this knowledge, the selection can be optimized for a desired target, such as lowest fuel consumption.

Selections can also be made based on a “rated” point, which happens to be the most onerous operating conditions (highest volumetric flow rate, lowest molecular weight, highest head or pressure ratio, highest inlet temperature). In this situation, however, the result may be an oversized machine that does not perform well at the usual operating conditions.

Once a selection is made, the manufacturer is able to provide parameters such as efficiency, speed, and power requirements, and based on these and the knowledge of the ambient conditions (prevailing summer and winter temperatures and site elevation), one can size the drivers. At this point, the casing arrangement, the number of required units based on desirable flexibility, growth scenarios, and sparing considerations will play an important role in this decision.

14.6 THERMODYNAMICS OF GAS COMPRESSION

The task of gas compression is to bring gas from a certain suction pressure to a higher discharge pressure by means of mechanical work. The actual compression process is often compared to one of two ideal processes: isothermal and isentropic compression.

Isothermal compression occurs when the temperature is kept constant during the compression process. It is not adiabatic because the heat generated in the compression process has to be removed from the system.

The compression process is isentropic (or adiabatic reversible) if no heat is added to or removed from the gas during compression, and the process is frictionless. With these assumptions, the entropy of the gas does not change during the compression process.

The actual or polytropic compression is similar to isentropic compression, but it is not adiabatic. It can be described as an infinite number of isentropic steps, each interrupted by isobaric heat transfer. This heat addition allows the process to yield the same discharge temperature as the actual compression process.

Fig. 14.4 shows the PV diagram for three types of compressions. As can be seen, when the gas compression process is assumed to be isentropic, the calculated work (horsepower) is the maximum, whereas under the assumption of isothermal condition, the required work is less than that for other types of compression. Therefore the actual work required to compress a given gas to obtain the same final pressure is between these maximum and minimum values.

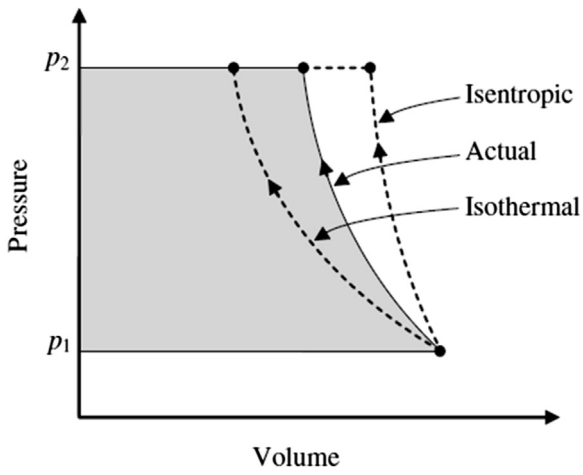

FIGURE 14.4

Pressure-volume diagrams for three types of compression.

14.6.1 BASIC RELATIONS

The design of a compressor begins with the first law of thermodynamics, the conservation of energy. It is written for the steady state gas flow through the compressor as follows:

$$\left(h_2 + \frac{u_2^2}{2} + gz_2\right) - \left(h_1 + \frac{u_1^2}{2} + gz_1\right) = q_{12} + W_{t,12} \tag{14.2}$$

where h is enthalpy, u is velocity, g is gravitational acceleration, z is elevation coordinate, q is heat, and W_t is work done by the compressor on the gas. For gas compressors, the subscripts 1 and 2 refer to the inlet into and the discharge from the compressor.

Neglecting the changes in potential energy (because the contribution due to changes in elevation is not significant for gas compressors), the energy balance equation for adiabatic processes ($q_{12} = 0$) can be written as:

$$\left(h_2 + \frac{u_2^2}{2}\right) - \left(h_1 + \frac{u_1^2}{2}\right) = W_{t,12} \tag{14.3}$$

$W_{t,12}$ is the amount of work[3] that we have to apply to change the enthalpy in the gas. The work $W_{t,12}$ is related to the required power, P, by multiplying it with the mass flow.

$$P = \dot{m} W_{t,12} \tag{14.4}$$

Combining enthalpy and velocity into a total enthalpy $\left(h_t = h + \frac{u^2}{2}\right)$, power and total enthalpy difference are thus related by the equation:

$$P = \dot{m}\left(h_{t,2} - h_{t,1}\right) \tag{14.5}$$

The total enthalpy difference (head) can be expressed as:

$$\Delta h = h(p_2, T_2) - h(p_1, T_1) \tag{14.6}$$

Use of Eq. (14.6) requires that the inlet pressure and temperature and the outlet pressure and temperature be known to evaluate the change in enthalpy. However, in design work, only the first three of these items are known, and the outlet temperature cannot be arbitrarily specified. Hence a compression model is needed.

If we can find a relationship that combines enthalpy with the pressure and temperature of a gas, we have found the necessary tools to describe the gas compression process. For an ideal gas, with constant heat capacity, the relationship between enthalpy, pressures, and temperatures is given as:

$$\Delta h = C_p(T_2 - T_1) \tag{14.7}$$

where T_1 is suction temperature, T_2 is discharge temperature, and C_p is heat capacity at constant pressure.

[3]Physically, there is no difference between work, head, and change in enthalpy. In systems with consistent units (such as the SI system), work, head, and enthalpy differences have the same unit (e.g., kJ/kg in SI units). Only in inconsistent systems (such as US customary units), we need to consider that the enthalpy difference (e.g., in BTU/lb_m) is related to head and work (e.g., in ft lb_f/lb_m) by the mechanical equivalent of heat (e.g., in ft lb_f/BTU).

14.6.2 ISENTROPIC MODEL

For an isentropic compression, the discharge temperature is determined by the pressure ratio as:

$$\frac{T_2}{T_1} = \left(\frac{p_2}{p_1}\right)^{\frac{k-1}{k}} \tag{14.8}$$

where k (isentropic exponent) is ratio of the heat capacities of gas at constant pressure and temperature ($k = C_p/C_v$), p_1 is suction pressure, and p_2 is discharge pressure.

Note that the heat capacities of real gases are a function of the pressure and temperature; however, they are functions of temperature only for ideal gases and can be related together with $C_P - C_V = R$, where R is universal gas constant. The isentropic exponent (k) for ideal gas mixtures can therefore be determined as:

$$k = \frac{\sum y_i C_{Pi}}{[\sum y_i C_{Pi}] - R} \tag{14.9}$$

where C_{Pi} is the molar heat capacity of the individual component at constant pressure, and y_i is the molar concentration of the component. Because the temperature of the gas increases as it passes from suction to discharge in the compressor, common practice is to determine the heat capacities of gas at the average of suction and discharge temperatures.

If the gas composition is not known and the gas is made up of pure hydrocarbons (methane, ethane, propane, and butane), the following simple correlation can be used for determining the isentropic exponent of ideal gases (Moshfeghian, 2013):

$$k = \left(1.6 - 0.44\gamma + 0.097\gamma^2\right)(1 + 0.0385\gamma - 0.000159T) \tag{14.10}$$

where γ is the gas specific gravity, and T is gas temperature in °R. This correlation covers gas specific gravities in the range of 0.55−2.0 and temperatures up to 302°F.

Combining Eqs. (14.7) and (14.8), the isentropic head (Δh_s) for the isentropic compression of an ideal gas can thus be determined as:

$$\Delta h_s = C_p T_1 \left[\left(\frac{p_2}{p_1}\right)^{\frac{k-1}{k}} - 1\right] \tag{14.11}$$

For real gases (where k, and C_p in the aforementioned equation become functions of temperature and pressure), the enthalpy of a gas, h, is calculated in a more complicated way using equations of state.

The isentropic head can also be determined by the equation:

$$\Delta h_s = h(p_2, s_1) - h(p_1, T_1) \tag{14.12}$$

Where entropy[4] of the gas at suction condition (s_1) is given as:

$$s_1 = s(p_1, T_1) \tag{14.13}$$

The relationships described previously can be easily seen in a Mollier diagram (Fig. 14.5).

[4]Entropy is a quantitative measure of the disorder in a system.

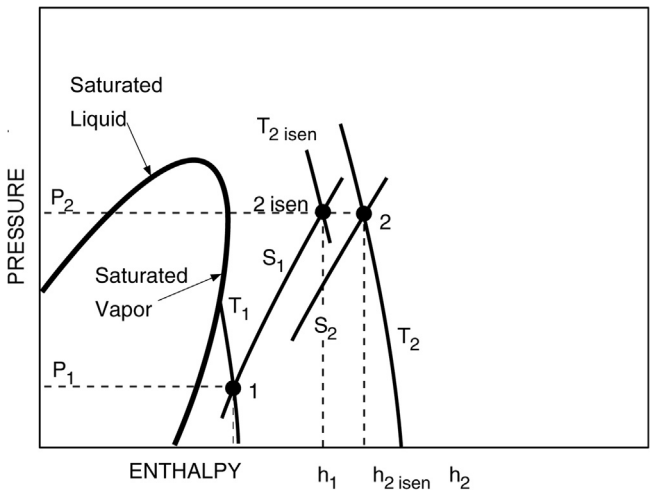

FIGURE 14.5

Compression process in a Mollier (pressure–enthalpy) diagram with lines of constant temperature and constant entropy.

Courtesy of Solar Turbines Inc.

The performance of a compressor can be assessed by comparing the actual head (which directly relates to the amount of required compression power) with the calculated head for an ideal, isentropic compression. This defines the isentropic efficiency (η_s) as:

$$\eta_s = \frac{\Delta h_s}{\Delta h} \tag{14.14}$$

For ideal gases, the actual head can be calculated from the equation:

$$\Delta h = \frac{1}{\eta_s} C_p T_1 \left[\left(\frac{p_2}{p_1} \right)^{\frac{k-1}{k}} - 1 \right] \tag{14.15}$$

and further, the actual discharge temperature (T_2) becomes:

$$T_2 = \frac{T_1}{\eta_s} \left[\left(\frac{p_2}{p_1} \right)^{\frac{k-1}{k}} - 1 \right] + T_1 \tag{14.16}$$

The second law of thermodynamics tells us:

$$\dot{m}(s_2 - s_1) = \int_1^2 \frac{dq}{T} + s_{irr} \tag{14.17}$$

where q is heat added to the process, T is temperature of the process, and s_{irr} is the entropy of the irreversible process.[5]

[5]The second law of thermodynamics states that all natural processes are irreversible.

For adiabatic flows, where no heat enters or leaves ($dq/T = 0$), the change in entropy simply describes the losses generated in the compression process. These losses come from the friction of gas with internal surfaces and the mixing of gas of different energy levels. The isentropic (adiabatic reversible) compression process therefore does not change the entropy of the system.

Eq. (14.6) for calculating the actual head implicitly includes the entropy rise Δs because:

$$\Delta h = h(p_2, T_2) - h(p_1, T_1) = h(p_2, s_1 + \Delta s) - h(p_1, s_1) \tag{14.18}$$

If cooling is applied during the compression process (for example with intercoolers between two compressors in series), then the increase in entropy is smaller than an uncooled process. A gas cooler therefore allows removing some of the entropy generated by the compression from the system. Therefore the power requirement will be reduced.

14.6.3 POLYTROPIC MODEL

Because polytropic compression is similar to adiabatic compression, we can easily calculate the discharge gas temperature in polytropic compression by substituting polytropic exponent (n) for "k" in Eq. (14.8).

$$\frac{T_2}{T_1} = \left(\frac{p_2}{p_1}\right)^{\frac{n-1}{n}} \tag{14.19}$$

However, compressor manufacturers do not supply values for n; instead, they provide a polytropic efficiency. The polytropic efficiency (η_p) is constant for any infinitesimally small compression step, which then allows us to write:

$$\eta_p = \frac{dT_s}{dT} \tag{14.20}$$

where dT_s is elemental temperature rise for isentropic compression, and dT is elemental temperature rise for actual compression.

Integration of Eq. (14.20) and use of Eq. (14.8) yields:

$$\frac{T_2}{T_1} = \left(\frac{p_2}{p_1}\right)^{\frac{k-1}{k\eta_p}} \tag{14.21}$$

Comparison of Eqs. (14.19) and (14.21) shows:

$$\frac{n-1}{n} = \frac{k-1}{k\eta_p} \tag{14.22}$$

The polytropic head (Δh_p) can be calculated from the equation:

$$\Delta h_p = Z_{ave} R T_1 \frac{n}{n-1}\left[\left(\frac{p_2}{p_1}\right)^{\frac{n-1}{n}} - 1\right] \tag{14.23}$$

In the aforementioned equation, Z_{ave} is the average compressibility factor for the gas.

Then the actual head of compression is given as:

$$\Delta h = \frac{\Delta h_p}{\eta_p} \tag{14.24}$$

Finally, comparing Eqs. (14.14) and (14.24), the isentropic and polytropic efficiencies are related by:

$$\eta_s = \eta_p \left[(p_2/p_1)^{(k-1)/k} - 1 \right] \Big/ \left[(p_2/p_1)^{(n-1)/n} - 1 \right] \tag{14.25}$$

For compressor designers, the polytropic efficiency has an important advantage. If a compressor has five stages, and each stage has the same isentropic efficiency η_s, then the overall isentropic compressor efficiency will be lower than η_s. If, for the same example, we assume that each stage has the same polytropic efficiency η_p, then the polytropic efficiency of the entire machine is also η_p. As far as power calculations are concerned, either the approach using a polytropic head and efficiency or using isentropic head and efficiency will lead to the same result:

$$P = \dot{m} \cdot \Delta h = \dot{m} \left(\frac{\Delta h_s}{\eta_s} \right) = \dot{m} \left(\frac{\Delta h_p}{\eta_p} \right) \tag{14.26}$$

14.6.4 REAL GAS BEHAVIOR

Understanding gas compression requires an understanding of the relationship between pressure, temperature, and density of a gas. An ideal gas exhibits the following behavior:

$$\frac{p}{\rho} = RT \tag{14.27}$$

where ρ is density of gas, and R is gas constant (as long as the gas composition remains unchanged). Any gas at very low pressures ($p \to 0$) and high temperatures (ambient and higher) can be described by this equation.

For the elevated pressures we see in natural gas compression, Eq. (14.27) becomes inaccurate, and an additional variable, the gas compressibility factor (Z), has to be added:

$$\frac{p}{\rho} = ZRT \tag{14.28}$$

Consequently, the gas compressibility factor itself is a function of pressure, temperature, and gas composition.

A similar situation arises when the enthalpy has to be calculated. For an ideal gas, we find:

$$\Delta h = \int_{T_1}^{T_2} C_p(T)\, dT \tag{14.29}$$

where C_p is only a function of temperature. This is a better approximation of the reality than the assumption of an ideal gas used in Eq. (14.7).

In a real gas, we get additional terms for the deviation between real gas behavior and ideal gas behavior (Poling et al., 2001):

$$\Delta h = \left(h^0 - h(p_1) \right)_{T_1} + \int_{T_1}^{T_2} C_p dT - \left(h^0 - h(p_2) \right)_{T_2} \tag{14.30}$$

The terms $(H^0-H(p_1))_{T1}$ and $(H^0-H(p_2))_{T2}$ are called departure functions because they describe the deviation of the real gas behavior from the ideal gas behavior. They relate the enthalpy at some pressure and temperature to a reference state at low pressure but at the same temperature. The departure functions can be calculated solely from an equation of state, whereas the term $\int C_p dT$ is evaluated in the ideal gas state. For gas compression applications, the most frequently used equations of state are Redlich–Kwong, Soave–Redlich–Kwong, Benedict–Webb–Rubin, Benedict–Webb–Rubin–Starling, and Lee–Kessler–Ploecker. Kumar et al. (1999) have compared these equations of state regarding their accuracy for compression applications. In general, all these equations provide accurate results for typical applications in pipelines, i.e., for gases with a high methane content and at pressures below 3500 psia.

Modern compressors often operate at pressures higher than the critical pressure of the gas. This is often referred to as "dense phase." All procedures discussed previously are not affected by this.

14.7 COMPRESSION RATIO

Compression ratio (CR) is the ratio of absolute discharge pressure to the absolute suction pressure. Mathematically this can be shown as:

$$CR = \frac{p_2}{p_1} \tag{14.31}$$

By definition, the compression ratio is always greater than one. If there are "n" stages of compression and the compression ratio is equal on each stage, then the compression ratio per stage is given by the equation:

$$CR_{stage} = \left(\frac{p_2}{p_1}\right)^{1/n} \tag{14.32}$$

If the compression ratio is not equal on each stage, then Eq. (14.31) should be applied to each stage.

The term compression ratio can be applied to a single stage of compression and multistage compression. When applied to a single compressor or a single stage of compression, it is defined as the stage or unit compression ratio; when applied to a multistage compressor, it is defined as the overall compression ratio. The compression ratio for typical gas pipeline compressors is rather low (usually below 2). Low pressure ratios can be covered in a single compression stage for reciprocating compressor and in a single body (with 1 or 2 impellers) in a centrifugal compressor.

While the pressure ratio is a valuable indicator for reciprocating compressors, the pressure ratio that a given centrifugal compressor can achieve depends primarily on gas composition and gas temperature. The centrifugal compressor is better characterized by its capability to achieve a certain amount of head (and a certain amount of head per stage). For natural gas (with specific gravity in the range of 0.58–0.70), a single centrifugal stage can provide a pressure ratio of 1.4. The same stage would yield a pressure ratio of about 1.6 if it would compress air. The pressure ratio per stage is usually lower than the aforementioned values for multistage machines. A multistage centrifugal compressor (i.e., a machine with multiple stages) can achieve, with natural gas, a pressure ratio of about 4–5, which equates to about 70,000–90,000 ft lb/lb of head. The temperature rise resulting from this amount of head is usually a limiting factor.

For reciprocating compressors, the pressure ratio per compressor is usually limited by mechanical considerations (rod load) and temperature limitations. Reciprocating compressors can achieve cylinder pressure ratios of 3−6. The actual flange-to-flange ratio will be lower (due to the losses in valves and bottles). For lighter gases (i.e., natural gas), the temperature limit will often limit the pressure ratio before the mechanical limits do. Centrifugal compressors are also limited by mechanical considerations (rotordynamics, maximum speed) and temperature limits. Whenever any limitation is involved, it becomes necessary to use multiple compression stages in series and intercooling. Furthermore, multistage compression may be required from a purely optimization standpoint. For example, with increasing compression ratio, compression efficiency decreases, and mechanical stress and temperature problems become more severe. For reference, if we assume natural gas at 100°F suction temperature, a pressure ratio of 3 will, depending on the compressor efficiency, lead to about 275°F discharge temperature.

For pressure ratios higher than 3, it may be advantageous to install intercoolers between the compressors. Intercoolers are generally used between the stages to reduce the power requirements as well as to lower the gas temperature that may become undesirably high[6]. Theoretically, minimum power requirement is obtained with ideal intercooling and no pressure loss between stages by making the ratio of compression the same in all stages. However, intercoolers invariably cause pressure losses (typically between 5 and 15 psi), which is a function of the cooler design. For preliminary design considerations, a value of 10 psi can be used (coolers, especially gas-to-air coolers for lower pressure drop, tend to become expensive).

Note that an actual compressor with an infinite number of compression stages and intercoolers would approach isothermal conditions (where the power requirement of compression cycle is the absolute minimum power necessary to compress the gas) if the gas were cooled to the initial temperature in the intercoolers.

Interstage cooling is usually achieved using gas-to-air coolers. The gas outlet temperature depends on the ambient air temperature. The intercooler exit temperature is determined by the cooling media. If ambient air is used, the cooler exit temperature, and thus the suction temperature to the second stage, will be about 20−30°F above ambient dry-bulb temperature. Water coolers can achieve exit temperatures of about 20°F above the water supply temperature but require a constant supply of cooling water. Cooling towers can provide water supply temperatures of about wet-bulb temperature plus 25°F.

For applications where the compressor discharge temperature is above some temperature limit of downstream equipment (a typical example are pipe coatings that limit gas temperatures to about 125−140°F) or has to be limited for other reasons (for example, to not disrupt or damage the permafrost), an aftercooler has to be installed.

If we trace the compression process in a Mollier diagram (Fig. 14.5), the compression process will always move away from the two-phase dome of the gas. However, if the gas is cooled after compression, the gas can enter the two-phase region, and liquids can form. It is important that the liquids are removed (for example, by a separator or coalescer) before the gas is fed into the next compressor downstream.

[6]After the cooling, liquids may form. These liquids are removed in interstage scrubbers or knockout drums.

14.8 COMPRESSOR DESIGN

Compressor design involves several steps including selection of the correct type of compressor as well as the number of compression stages required. Depending on the capacity, there is also a need to determine the horsepower required to compress the gas.

14.8.1 DETERMINING NUMBER OF COMPRESSION STAGES

For reciprocating compressors, the number of compression stages[7] is determined from the overall compression ratio as follows (Arnold and Stewart, 1999):

1. Calculate the overall compression ratio. If the compression ratio is under 4, consider using one stage. If it is not, select an initial number of stages so that CR < 4. For initial calculations, it can be assumed that the compression ratio per stage is equal for each stage. Compression ratios of 6 can be achieved for low-pressure applications, however, at the cost of higher mechanical stress levels and lower volumetric efficiency.
2. Calculate the discharge gas temperature for the first stage. If the discharge temperature is too high (more than 300°F), we will either have to increase the number of stages or reduce the suction temperature through precooling. It is recommended that the compressors be sized so that the discharge temperatures for all stages of compression be below 300°F. It is also suggested that the aerial gas coolers be designed to have a maximum of 20°F approach to ambient, provided the design reduces the suction temperature for the second stage, conserving horsepower and reducing power demand. If the suction gas temperature to each stage cannot be decreased, increase the number of stages by one and recalculate the discharge temperature.

For centrifugal compressors, the number of compressor bodies is determined in similar fashion:

1. Calculate the overall isentropic head using Eq. (14.11) or Eq. (14.12). Typically a centrifugal compressor casing can provide about 70,000 ft lb/lb[8] of head due to limitations in speed, number of impellers, and discharge temperature (although 100,000 ft lb/lb might be possible in some cases).
2. If the overall head exceeds 70,000 ft lb/lb, take the square root of the overall pressure ratio (using Eq. 14.32), and calculate the isentropic head for the new pressure ratio. The compression train will consist of two compressors.
3. If the required isentropic head still exceeds 70,000 ft lb/lb, take the cube root of the overall pressure ratio, and calculate the isentropic head for the new pressure ratio. The compression train will consist of three compressors. More than three compressors per train are usually not practical, so if the required head per compressor still exceeds 70,000 ft lb/lb, a second train may have to be considered.
4. For cases 2 and 3, i.e., multiple compressors per train, the head requirement for the second or third body must be recalculated, considering about 20°F approach to ambient for gas-air-coolers and

[7]A stage for a reciprocating compressor is usually a cylinder. For centrifugal compressor, a stage is one impeller with its inlet and diffuser. A compressor body can contain multiple stages (up to 10).
[8]70,000 ft lb/lb is equivalent to a pressure ratio of about 4 for pipeline-quality natural gas.

about 10-psi pressure drop. Unless the gas has a very high inlet temperature or the compressor is low, the 70,000 ft lb/lb limit will keep discharge temperatures at an acceptable level below 350°F. In any case the discharge temperature should be checked using Eq. (14.16).

The 300°F temperature limit is used for reciprocating compressors because the packing life gets shortened above about 250°F, and the lube oil, being directly involved in the compression process, will degrade faster at higher temperatures. The 350°F temperature limit pertains to centrifugals and is really a limit for the seals (although special seals can go to 400–450°F) or the pressure rating of casings and flanges. Because the lube oil in a centrifugal compressor does not come into direct contact with the process gas, lube oil degradation is not a factor.

If oxygen is present in the process gas in the amount that it can support combustion (i.e., the gas-to-oxygen ratio is above the lower explosive limit), much lower gas temperatures than mentioned previously are required. In reciprocating machines, oil-free compression may be required (no lube oil can come into contact with the process gas). This requires special piston designs that can run dry. Also, special precaution has to be taken to avoid hot spots generated by local friction.

14.8.2 COMPRESSION POWER CALCULATION

Once we have an idea about the type of compressor we will select, we also need to know the power requirements so that an appropriate prime mover can be designed for the job. After the gas horsepower (GHP) has been determined by either method, horsepower losses due to friction in bearings, seals, and speed-increasing gears must be added. Bearings and seal losses can be estimated from Scheel's equation (GPSA, 2004). For reciprocating compressors, the mechanical and internal friction losses can range from about 3% to 8% of the design gas horsepower. For centrifugal compressors, a good estimate is to use 1%–2% of the design GHP as mechanical loss.

To calculate brake horsepower (BHP), the following equation can be used:

$$\text{BHP} = \text{GHP} + \text{Mechanical losses} \tag{14.33}$$

The detailed calculation of brake horsepower depends on the choice of type of compressor and number of stages. The brake horsepower per stage can be determined from Eq. (14.34) (GPSA, 2004):

$$\text{BHP} = 0.0854 \cdot Z_{\text{ave}} \left[\frac{(Q_{G,SC})(T_1)}{E \cdot \eta} \right] \left[\frac{k}{k-1} \right] \left[\left(\frac{p_2}{p_1} \right)^{\frac{k-1}{k}} - 1 \right] \tag{14.34}$$

where BHP is brake horsepower per stage; Z_{ave} is average compressibility factor; $Q_{G,SC}$ is standard volumetric flow rate of gas, MMSCFD; T_1 is suction temperature, °R; p_1 and p_2 are pressure at suction and discharge flanges, respectively, psia; E is parasitic efficiency (for high-speed reciprocating units, use 0.72–0.82; for low-speed reciprocating units, use 0.72–0.85; and for centrifugal units, use 0.99); and η is compression efficiency (1.0 for reciprocating and 0.80–0.87 for centrifugal units).

In Eq. (14.34), the parasitic efficiency (E) accounts for mechanical losses and the pressure losses incurred in the valves and pulsation dampeners of reciprocating compressors (the lower efficiencies are

usually associated with low pressure ratio applications typical for pipeline compression)[9]. Hence suction and discharge pressures may have to be adjusted for the pressure losses incurred in the pulsation dampeners for reciprocation compressors. The compression efficiency accounts for the actual compression process. For centrifugal compressors, the lower efficiency is usually associated with pressure ratios of 3 and higher. Very low−flow compressors (below 1000 acfm) may have lower efficiencies.

The total horsepower for the compressor is the sum of the horsepower required for each stage. Reciprocating compressors require an allowance for interstage pressure losses. It can be assumed that there is a 3% loss of pressure in going through the cooler, scrubbers, piping, and so forth, between the actual discharge of the cylinder and the actual suction of the next cylinder. For a centrifugal compressor, any losses incurred between the stages are already included in the stage efficiency. However, the exit temperature from the previous stage becomes the inlet temperature in the next stage. If multiple bodies are used, the losses for coolers and piping have to be included as described previously.

14.9 COMPRESSOR CONTROL

To a large extent, the compressor operating point will be the result of the pressure conditions imposed by the system. However, the pressures imposed by the system may in turn be dependent on the flow. Only if the conditions fall outside the operating limits of the compressor (e.g., frame loads, discharge temperature, available driver power, surge, choke, and speed), control mechanisms have to be in place. On the other hand, the compressor output may have to be controlled to match the system demand. The type of application often determines the system behavior. In a pipeline application, suction and discharge pressure are connected with the flow by the fact that the more the flow is pushed through a pipeline, the more pressure ratio is required at the compressor station to compensate for the pipeline pressure losses. In process-related applications, the suction pressure may be fixed by a back pressure−controlled production separator. In boost applications, the discharge pressure is determined by the pressure level of the pipeline the compressor feeds into, whereas the suction pressure is fixed by the process. In oil and gas field applications, the suction pressure may be depending on the flow because the more the gas is moved out of the gas reservoir, the lower the suction pressure has to be. The operation may require constant flow despite changes in suction or discharge pressure. Compressor flow, pressure, or speed may have to be controlled. The type of control also depends on the compressor driver. Both reciprocating compressors and centrifugal compressors can be controlled by suction throttling or recirculating of gas. However, either method is very inefficient for process control (but may be used to protect the compressor) because the reduction in flow or head is not accompanied by a significant reduction in the power requirement.

[9]Many calculation procedures for reciprocating compressors use numbers for E that are higher than the ones refereed here. These calculations require, however, that the flange-to-flange pressure ratio (which is used in Eq. 14.33) is increased by the pressure losses in the compressor suction and discharge valves and pulsation dampeners. These pressure losses are significant, especially for low-head high-flow applications.

14.9.1 RECIPROCATING COMPRESSORS

The following control mechanisms may be used to control the capacity of reciprocating compressors: (1) suction pressure, (2) variation of clearance, (3) speed, (4) valve unloading, and (5) recycle. Reciprocating compressors tend to have a rather steep head versus flow characteristic. This means that changes in pressure ratio have a very small effect on the actual flow through the machine.

Reciprocating compressors generate flow pulsations in the suction and discharge lines that have to be controlled to prevent overloading and underloading of the compressors, avoid vibration problems in the piping or other machinery at the station, and provide a smooth flow of gas. The flow pulsations can be greatly reduced by properly sized pulsation bottles or pulsation dampeners in the suction and discharge lines.

Controlling the flow through the compressor can be accomplished by varying the operating speed of the compressor. This method can be used if the compressor is driven by an internal combustion engine or a variable speed electric motor. Especially internal combustion engines, but also variable speed electric motors, produce less power if they operate at a speed different from their optimum speed. Internal combustion engines allow for speed control in the range of 70%−100% of maximum speed. Because reciprocating compressors generate pulsations in the piping system, pulsation dampeners have to be installed. Because these have to be optimized based on the frequencies of the pulsations, which are speed dependent, the allowable speed range may be limited.

If the driver is a constant speed electric motor, the capacity control consists of either inlet valve unloaders or clearance unloaders. Inlet valve unloaders can hold the inlet valve into the compressor open and thereby prevent compression. Clearance unloaders consist of pockets that are opened when unloading is desired. The gas is compressed into them at the compression stroke and expands back into the cylinder on the return stroke, thus reducing the intake of additional gas and subsequently the compressor capacity. Additional flexibility is achieved by using several steps of clearance control and combinations of clearance control and inlet valve control. Fig. 14.6 shows the control characteristic of such a compressor.

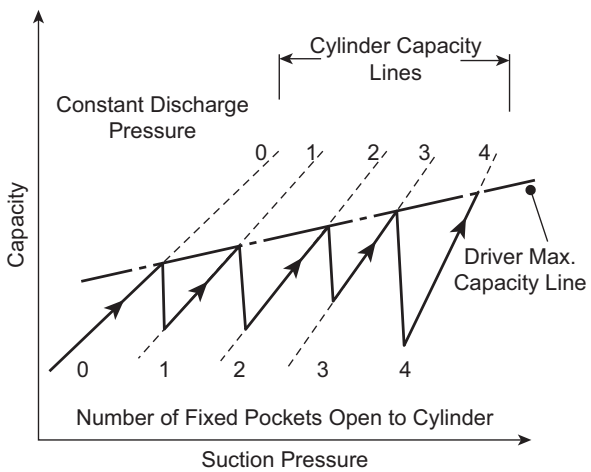

FIGURE 14.6

Control characteristic of a reciprocating compressor with constant speed driver and pockets (GPSA, 2004).

14.9.2 CENTRIFUGAL COMPRESSORS

As with reciprocating compressors, the compressor output must be controlled to match the system demand. The operation may require constant flow despite changes in suction or discharge pressure. Compressor flow, pressure, or speed may have to be controlled. The type of control also depends on the compressor driver. Centrifugal compressors tend to have a rather flat head versus flow characteristic. This means that changes in pressure ratio have significant effect on the actual flow through the machine.

Compressor control is usually accomplished by speed control, variable guide vanes, suction throttling, and recycling of gas. Only in rare cases, adjustable diffuser vanes are used. To protect the compressor from surge, recycling is used. Controlling the flow through the compressor can be accomplished by varying the operating speed of the compressor. This is the preferred method of controlling centrifugal compressors. Two-shaft gas turbines and variable speed electric motors allow for speed variations over a wide range (usually from 50% to 100% of maximum speed or more). Virtually any centrifugal compressor installed in the past 15 years in pipeline service is driven by variable speed drivers, usually a two-shaft gas turbine or a variable speed electric motor. Older installations and installations in other pipeline services sometimes use a single-shaft gas turbines (which allow a speed variation from about 90% to 100% speed) and constant speed electric motors. In these installations, suction throttling or variable inlet guide vanes are used to provide means of control.

The operating envelope of a centrifugal compressor (typically shown in Fig. 14.7) is limited by the maximum allowable speed, the minimum allowable speed, the minimum flow (surge flow), and the maximum flow (choke or stonewall). Another limiting factor may be the available driver power. Only the minimum flow requires special attention because it is defined by an aerodynamic stability limit of the compressor. Operating the compressor at lower flows than defined by the surge line will lead to surge. Surge, which is the flow reversal within the compressor, accompanied by high fluctuating load on the compressor bearings, has to be avoided to protect the compressor. Modern control systems can

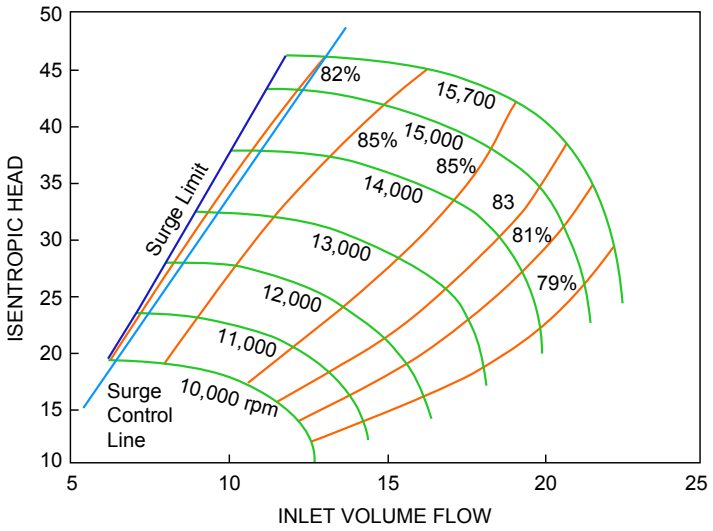

FIGURE 14.7

Typical performance map for a centrifugal compressor (Kurz and Brun, 2001).

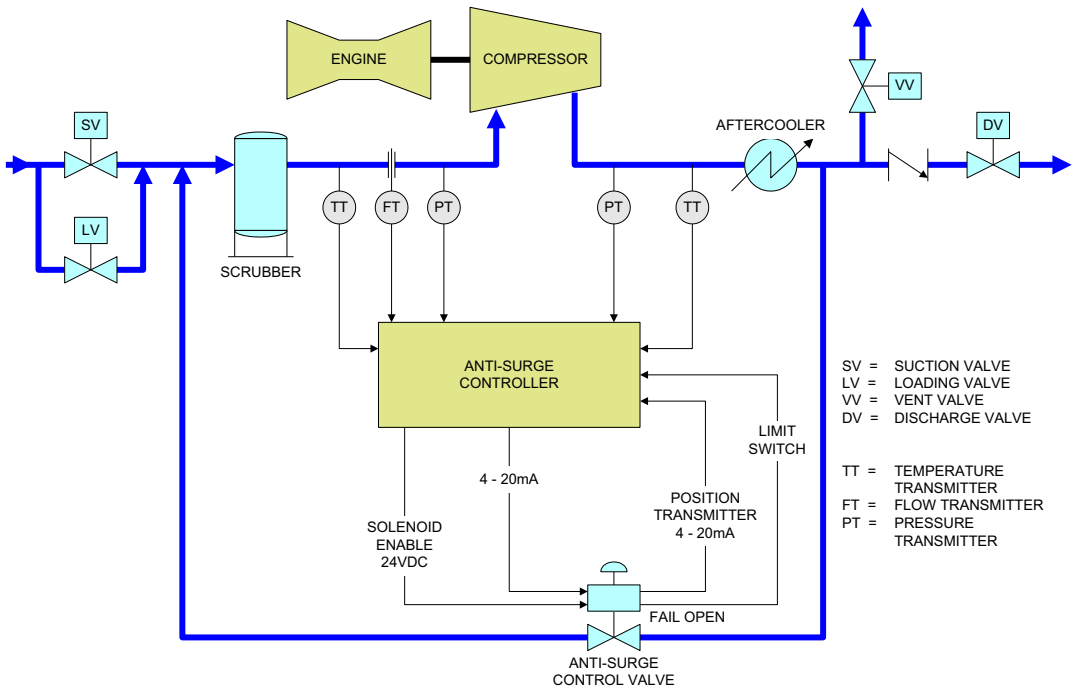

FIGURE 14.8

Antisurge and recycle system.

detect this situation and shut the machine down or prevent it entirely by automatically opening a recycle valve. For this reason, virtually all modern compressor installations use a recycle line (Fig. 14.8) with a control valve that allows the flow to increase through the compressor if it comes near the stability limit. Modern control systems constantly monitor the operating point of the compressor in relation to its surge line, and automatically open or close the recycle valve if necessary. The control system is designed to compare the measured operating point of the compressor with the position of the surge line (Fig. 14.7). To that end, flow, suction pressure, discharge pressure, and suction temperature, as well as compressor speed, have to be measured (Kurz et al., 2013).

Typical control systems use suction and discharge pressures and temperatures, together with the flow through the compressor, to calculate the relative distance (turndown) of the present operating point to the predicted or measured surge line of the compressor. The turndown is defined by Eq. (14.35):

$$\text{Turndown} = \frac{Q_{op} - Q_{surge}}{Q_{op}} | H_s = \text{const} \tag{14.35}$$

If the turndown reaches a preset value (often 10% turndown), the antisurge valve starts to open, thereby reducing the pressure ratio of the compressor and increasing the flow through the compressor. The situation is complicated by the fact that the surge valve also has to be capable of precisely

controlling flow. In addition, some manufacturers place limits on how far into choke (or overload) they allow their compressors to operate.

As part of the control system, the antisurge system has to fulfill three tasks:

- Task 1: Allow the starting and stopping of the compressor
- Task 2: Keep the compressor out of surge during changes in process
- Task 3: Keep the compressor out of surge during emergency shutdowns (ESDs)

Putting it differently, the surge-control system has to protect the compressor and the process. Therefore it has to do its tasks without causing fluctuations or disruptions of the process. Task 2 requires a valve that can be precisely controlled, so that neither opening the valve nor closing the valve upsets the process. In a well-designed system, the compressor can operate from maximum flow all the way down to no station flow at all. This also requires a well-designed control algorithm.

The design of the antisurge and recycle system also impacts the start of operations of the station (Task 1). Particular attention has to be given to the capability to start up the station without having to abort the start due to conditions during which allowable operating conditions are exceeded. Problems may arise from the fact that the compressor may spend a certain amount of time recycling gas until sufficient discharge pressure is produced to open the discharge-check valve (Fig. 14.8), and gas is flowing into the pipeline.

Virtually all the mechanical energy absorbed by the compressor is converted into heat in the discharged gas. In an uncooled recycle system (Fig. 14.9), this heat is recycled into the compressor suction and then more energy added to it. Low pressure ratio compressors often do not require aftercoolers. There are three primary strategies that can be used to avoid overheating the uncooled compressor during the start: (1) accelerate quickly, (2) delay hot gas reentering the compressor, and (3) throttled recycle.

If aftercoolers are used (Fig. 14.9), the heat from recycling can be removed effectively. However, a cooler in the recycle loop increases the volume of the system, and, as we will see, impacts the dynamic behavior of the system, for example, during emergency shutdowns.

A very critical situation arises upon emergency shutdown, Task 3. Here the fuel supply to the gas turbine driver, or the electric current to an electric motor drive, is cut off instantly, thus eliminating the power to the driven compressor.[10] The inertia of compressor, coupling, and power turbine or motor balances the compressor-absorbed power, causing a rapid deceleration. Because the head-making capability of the compressor is reduced by the square of its running speed, while the pressure ratio across the machine is imposed by the upstream and downstream piping system, the compressor will surge if the surge valve cannot provide fast relief of the pressure, and the discharge-check valve closes fast enough. The deceleration of the compressor as a result of inertia and dissipation are decisive factors. The speed at which the pressure can be relieved not only depends on the reaction time of the valve but also on the time constants imposed by the piping system. The transient behavior of the piping system depends largely on the volumes of gas enclosed by the various components of the piping system, which may include, besides the piping itself, various scrubbers, knockout drums, and coolers. With the initiation of a shutdown, the compressor can be expected to decelerate by approximately 30% in the first second. With a 30% loss in speed, the head that the compressor can develop at its surge limit

[10]Some installations maintain fuel flow to the turbine for 1−2 s while the recycle valve opens. However, this can generate a safety hazard.

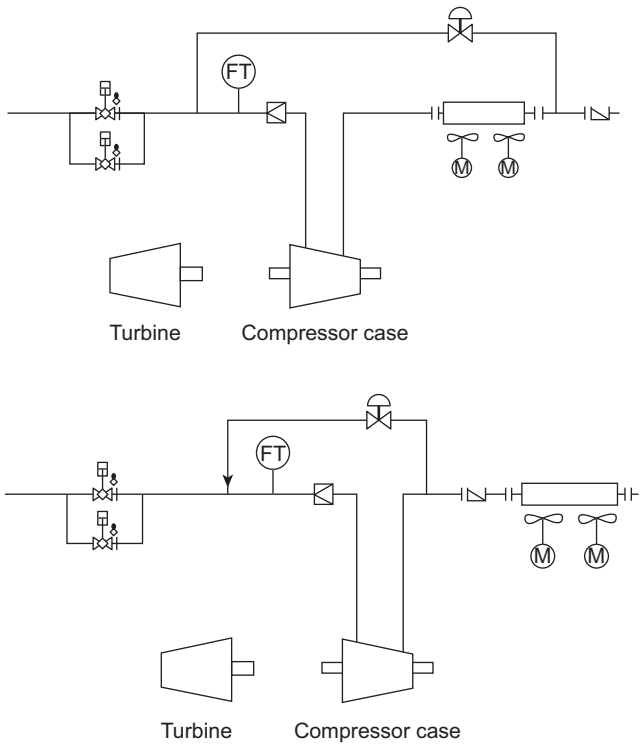

FIGURE 14.9

Recycle system layout for centrifugal compressors: cooled (top) and hot (Bottom) recycle lines.

Courtesy of Solar Turbines Inc.

will drop by approximately 50%. The recycle control valve must, therefore, reduce the pressure ratio across the compressor by one-half in that first second to avoid surge.

Surge-control valves must be sized to meet two diverse objectives. During steady state recycling, the required capacity of the recycle valve can be directly derived from the compressor map (Fig. 14.10), the smaller the valve, the smoother the control. During transient conditions, the required capacity increases due to the volumes on either side of the compressor. Therefore to avoid surge during a shutdown, a bigger valve is preferred; the bigger the valve, the better. To facilitate both smooth throttling at partial recycle and the need to reduce the pressure differential (DP) across the compressor quickly during a shutdown, control valves with an equal percentage characteristic are recommended. With an equal percentage characteristic, the more the valve is opened, the greater the increase will be in flow for the same travel. We recommend two types of valves for surge control: (1) globe valves and (2) noise-attenuating ball valves.

Surge-control valves are primarily sized to fit the compressor (Task 2). In other words, the valve characteristic, that is the flow through the valve for a given pressure ratio over the valve and a given

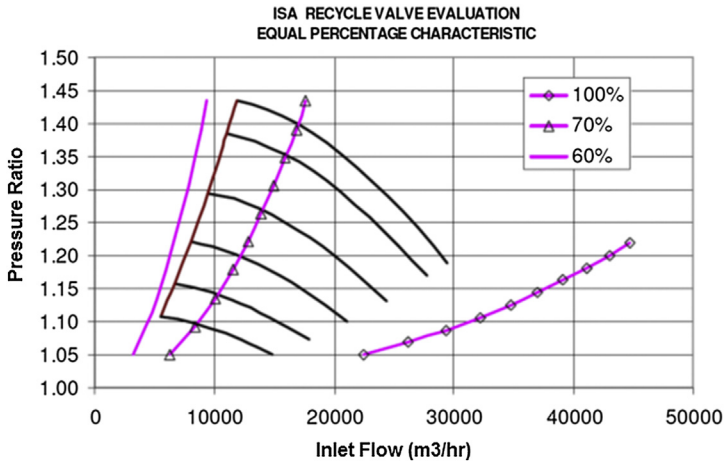

FIGURE 14.10

Matching of valve and compressor. The valve characteristic for a number of opening positions (60%, 70%, and 100%) is superimposed to the compressor performance map (Kurz et al., 2013).

valve position, has to be matched with the compressor map (Fig. 14.10). To handle transient conditions, the required capacity must be greater to allow for the volumes on either side of the compressor.

In some cases a solution using a single valve will not allow to combine the objectives of a smooth process control and the protection of the compressor during emergency shutdowns. In this case, it may be necessary to separate the tasks by installing a valve to handle emergency shutdowns (hot bypass valve) and a separate valve for process control (recycle valve). The recycle valve ideally would include the aftercooler (where available) into the recycle loop, therefore allowing extended recycle without the risk of exceeding allowable gas temperatures. The hot bypass line would seek the shortest connection between compressor discharge and compressor suction. This valve is only activated for emergency shutdown. Other options involve two valves in parallel. The aforementioned recommendations pertain to single-compressor bodies. Compressor trains with multiple compressor bodies or compressor sections, involving intercooling or multiple services, require a more detailed analysis.

Although the valve sizing for Task 2 essentially requires to match the valve with the steady state compressor map, the evaluation of the system behavior in an emergency shutdown (Task 3) requires an assessment of the dynamic behavior of the system. Although it is possible to perform a computational fluid dynamics (CFD) simulation for the compressor with all associated pipes, valves, and coolers, simpler methods are available.

14.10 COMPRESSOR PERFORMANCE MAPS

14.10.1 RECIPROCATING COMPRESSORS

Because the operating limitations of a reciprocating compressor are often defined by mechanical limits (especially maximum rod load), and the pressure ratio of the machine is very insensitive to changes in suction conditions and gas composition, we usually find maps depicting suction and discharge pressures and actual flow. Maps account for the effect of opening or closing pockets and for variations in speed.

14.10.2 CENTRIFUGAL COMPRESSORS

For a centrifugal compressor, the isentropic or polytropic head (rather than the pressure ratio) is relatively invariant with the change in suction conditions and gas composition. As with the reciprocating compressor, the flow that determines the operating point is the actual flow as opposed to mass flow or standard flow. Head versus actual flow maps are therefore the usual way to describe the operating range of a centrifugal compressor. These maps change very little even if the inlet conditions or the gas composition changes. They depict the effect of changing the operating speed and define the operating limits of the compressor, such as surge limit, maximum and minimum speed, and maximum flow at choke conditions. Every set of operating conditions, given as suction pressure, discharge pressure, suction temperature, flow, and gas composition, can be converted into isentropic head and actual flow using the relationships described previously. Once the operating point is located on a head–flow map, the efficiency of the compressor, the required operating speed, as well as the surge margin can be determined.

14.11 EXAMPLE FOR OPERATING A COMPRESSOR IN A PIPELINE SYSTEM

To illustrate how the considerations regarding operating characteristics, system behavior, and control work together, we can look into the operation of a typical compressor station in a pipeline (Kurz et al., 2010).

For a situation during which a compressor operates in a system with pipe of the length L_u upstream and a pipe of the length L_d downstream and further where the pressure at the beginning of the upstream pipe p_u and the end of the downstream pipe p_e are known and constant, we have a simple model of a compressor station operating in a pipeline system (Fig. 14.11).

For a given constant flow capacity Q_{std}, the pipeline will then impose a pressure p_s at the suction and p_d at the discharge side of the compressor. For a given pipeline, the head (H_s)–flow (Q) relationship at the compressor station can be approximated by:

$$H_s = C_p T_s \left[\left(\sqrt{\frac{1}{1 - \dfrac{C_3 + C_4 \cdot Q^2}{p_d^2}}} \right)^{\frac{k-1}{k}} - 1 \right] \tag{14.36}$$

where C_3 and C_4 are constants (for a given pipeline geometry) describing the pressure at either ends of the pipeline and the friction losses, respectively.

Among other issues, this means that for a compressor station within a pipeline system, the head for a required flow is prescribed by the pipeline system (Fig. 14.12). In particular, this characteristic requires the capability for the compressors to allow a reduction in head with reduced flow, and vice versa, in a prescribed fashion. The pipeline will therefore not require a change in flow at constant head (or pressure ratio).

In transient situations (for example, during line packing), the operating conditions follow initially a constant power distribution, i.e., the head–flow relationship follows Eq. (14.37) and will

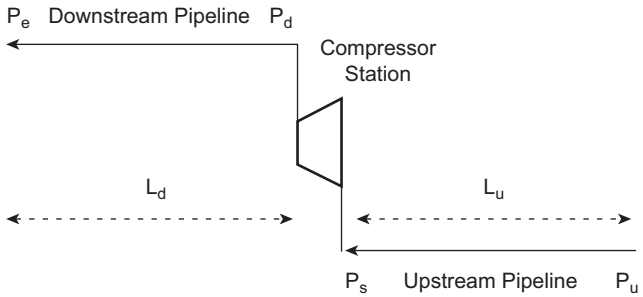

FIGURE 14.11

Conceptual model of a pipeline segment.

asymptotically approach the steady state relationship. This is universally valid for speed-controlled centrifugal compressors. For reciprocating compressors, there might be additional constraints due to rod load and rod load reversal concerns, limitations in clearance control and others.

$$P = \dot{m} \cdot \frac{H_s}{\eta_s} = \text{const}$$
$$H_s = \frac{\eta_s \cdot \text{const}}{\rho} \frac{1}{Q} \tag{14.37}$$

Based on the requirements mentioned previously, the compressor output must be controlled to match the system demand. This system demand is characterized by a strong relationship between system flow and system head or pressure ratio (Fig. 14.12). Given the large variations in operating conditions experienced by pipeline compressors, important questions are how to adjust the compressor to the varying conditions, and, in particular, how does this influence the efficiency.

Centrifugal compressors tend to have rather flat head versus flow characteristic. This means that changes in pressure ratio have a significant effect on the actual flow through the machine. For a centrifugal compressor operating at a constant speed, the head or pressure ratio is reduced with increasing flow. Controlling the flow through the compressor can be accomplished by varying the operating speed of the compressor. This is the preferred method of controlling centrifugal compressors. Two-shaft gas turbines and variable speed electric motors allow for speed variations over a wide range (usually from 40% or 50%−100% of maximum speed or more). It should be noted that the controlled value is usually not speed, but the speed is indirectly the result of balancing the power generated by the power turbine (which is controlled by the fuel flow into the gas turbine) and the absorbed power of the compressor.

Assuming the pipeline characteristic derived in Eq. (14.36), the compressor impellers will be selected to operate at or near their best efficiency for the entire range of head and flow conditions imposed by the pipeline. This is possible with a speed-controlled compressor because the best efficiency points of a compressor are connected by a relationship that requires approximation (Fan law).

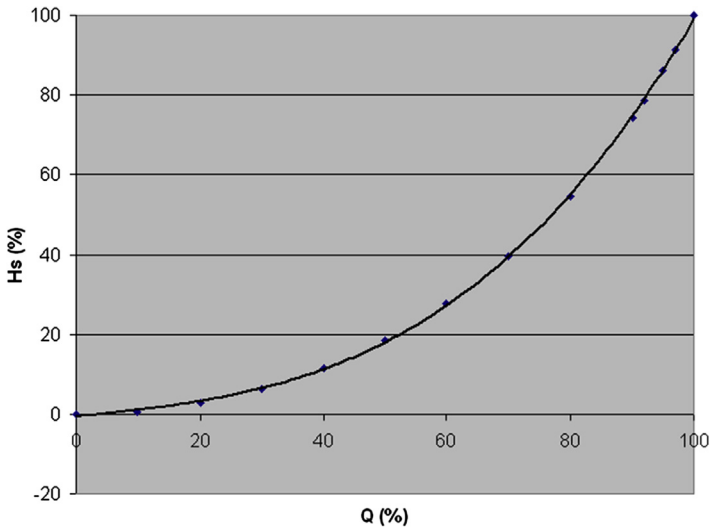

FIGURE 14.12

Station head–flow relationship based on Eq. (14.36).

$$H_s/N^2 = C_5 \quad Q/N = C_6$$
$$H_s = Q^2 \cdot \frac{C_5}{C_6^2} \tag{14.38}$$

For operating points that meet the aforementioned relationship, the absorbed gas power P_g is given as (due to the fact that the efficiency stays approximately constant):

$$P_g = C_7 \cdot H_s \cdot Q = C_7 \cdot \frac{C_5}{C_6^2} \cdot Q^3 = C_5 \cdot C_6 \cdot C_7 \cdot N^3 \tag{14.39}$$

As it is, this power–speed relationship allows the power turbine to operate at, or very close to its, optimum speed for the entire range. The typical operating scenarios in pipelines therefore allow the compressor and the power turbine to operate at their best efficiency for most of the time. The gas producer of the gas turbine will, how"ever, lose some thermal efficiency when operated in part load. Fig. 14.13 shows a typical example based on an existing pipeline, in which pipeline-operating points for different flow requirements are plotted into the performance map of the speed-controlled centrifugal compressor used in the compressor station.

Reciprocating compressors will automatically comply with the system pressure ratio demands, as long as no mechanical limits (rod load, power) are exceeded. Changes in system suction or discharge pressure will simply cause the valves to open earlier or later. The head is lowered automatically because the valves see lower pipeline pressures on the discharge side and/or higher pipeline pressures on the suction side. Therefore, without additional measures, the flow would stay roughly the same, except for the impact of changed volumetric efficiency which would increase, thus increasing the flow with reduced pressure ratio. The control challenge lies in the adjustment of the flow to the

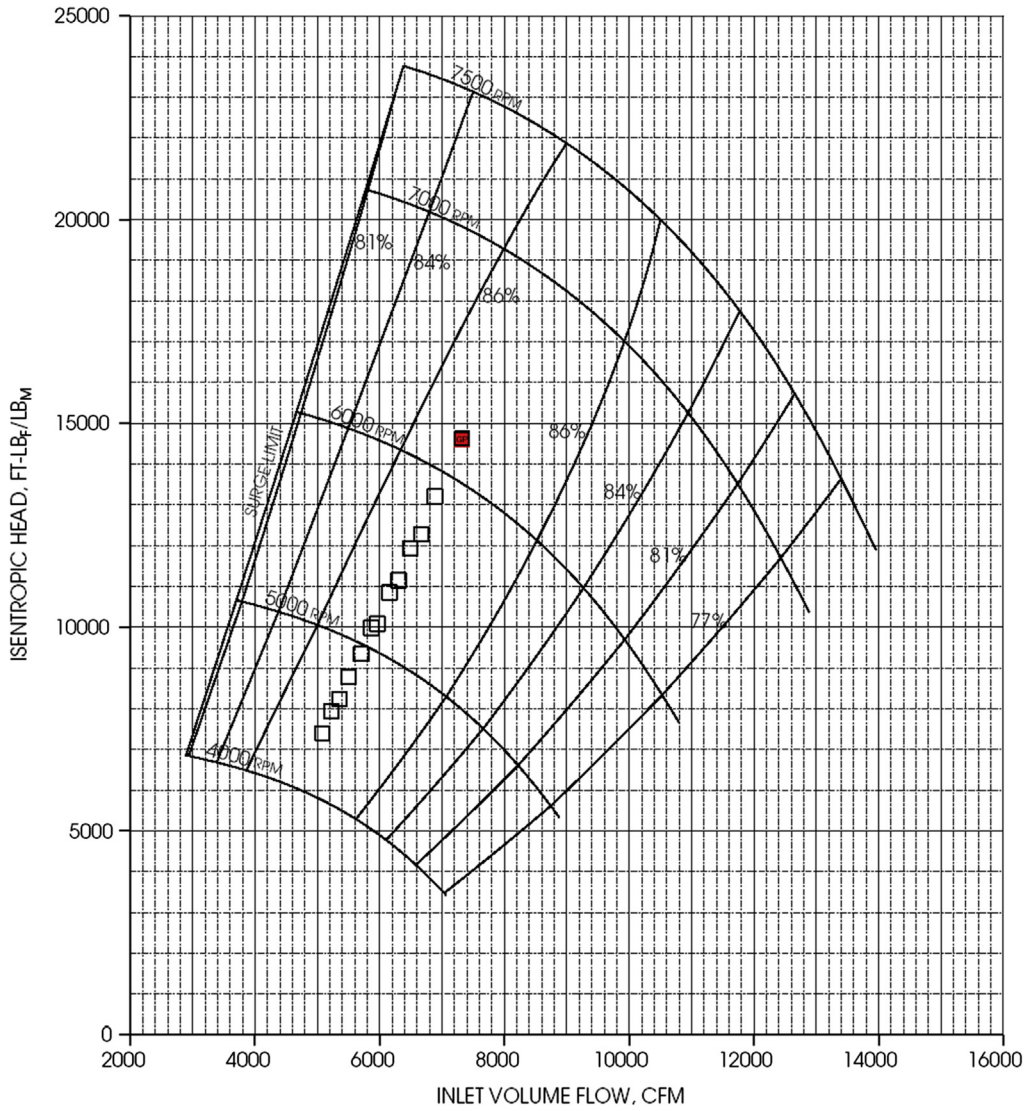

FIGURE 14.13

Typical pipeline-operating points plotted into a typical centrifugal compressor performance map.

system demands. Without additional adjustments, the flow throughput of the compressor changes very little with changed pressure ratio. Historically, pipelines installed many small compressors and adjusted flow rate by changing the number of machines activated. This capacity and load could be fine-tuned by speed or by a number of small adjustments (load steps) made in the cylinder clearance of a single unit. As compressors have grown, the burden for capacity control has shifted to the individual compressors.

Load control is a critical component to compressor operation. From a pipeline operation perspective, variation in station flow is required to meet pipeline delivery commitments, as well as to implement company strategies for optimal operation (i.e., line packing, load anticipation). From a unit perspective, load control involves reducing unit flow (through unloaders or speed) to operate as close as possible to the design torque limit without overloading the compressor or driver. Critical limits on any load map curve are rod load limits and horsepower (HP)/torque limits for any given station suction and discharge pressure. Gas control generally will establish the units within a station that must be operated to achieve pipeline flow targets. Local unit control will establish load step or speed requirements to limit rod loads or achieve torque control.

The common methods of changing flow rate are to change speed, change clearance, or deactivate a cylinder end (hold the suction valve open). Another method is an infinite-step unloader, which delays suction valve closure to reduce volumetric efficiency. Furthermore, part of the flow can be recycled or the suction pressure can be throttled, thus reducing the mass flow while keeping the volumetric flow into the compressor approximately constant.

Control strategies for compressors should allow automation and be adjusted easily during the operation of the compressor. In particular, strategies that require design modifications to the compressor (i.e., rewheeling of a centrifugal compressor, changing cylinder bore, or adding fixed clearances for a reciprocating compressor) are not considered here. It should be noted that with reciprocating compressors, a key control requirement is to not overload the driver or to exceed mechanical limits.

As mentioned previously, we are describing the situation for a pipeline operating at or near steady state conditions. For conditions where the compressor operates at low load in steady state and the power supply is increased instantly, the compressor operating point will move to an increased flow, without initially seeing a change in pressure ratio (because the gas volume in the pipeline has to be increased first). Then the pressure ratio dictated by the pipeline will cause the compressor operating point to drift back to the steady state line, after a line of more or less constant absorbed power (Eq. 14.37).

REFERENCES

Arnold, K., Stewart, M., 1999. Surface Production Operations, vol. 2: Design of Gas-Handling Systems and Facilities, second ed. Gulf Publishing Company, Houston, TX, USA.

Botros, K., October 6–9, 2013. Predicting the power loss in reciprocating compressor manifolds. Paper Presented at the GMRC Gas Machinery Conference, Albuquerque, NM, USA.

Carroll, J.J., 2010. Acid Gas Injection and Carbon Dioxide Sequestration. Scrivener Publishing LLC, Salem, MA, USA.

GPSA, 2004. Engineering Data Book, twelfth ed. Gas Processors Suppliers Association (GPSA), Tulsa, OK, USA.

Kumar, S., Kurz, R., O'Connell, J.P., June 7–10, 1999. Equations of state for compressor design and testing. ASME Paper 99-GT-12, Paper Presented at the ASME Turbo Expo 99 Conference, Indianapolis, IN, USA.

Kurz, R., Brun, K., 2001. Degradation in gas turbine systems. Journal of Engineering for Gas Turbines and Power 123 (1), 70–77.

Kurz, R., Winkelmann, B., Mokhatab, S., 2010. Efficiency and operating characteristics of centrifugal and reciprocating compressors. Pipeline & Gas Journal 237 (10), 42–46.

Kurz, R., White, R.C., Mokhatab, S., June 2013. Surge prevention in centrifugal compressor systems. Pipeline & Gas Journal 240 (6), 77, 78, 86.

Lubomirsky, M., Kurz, R., Klimov, P., Mokhatab, S., January/February 2010. Station configuration impacts availability, fuel consumption and pipeline capacity. Pipeline & Gas Journal. Part 1: 48−56, Part 2: 38−44.

Moshfeghian, M., May 2013. Variation of Ideal Gas Heat Capacity Ratio with Temperature and Relative Density. Tip of the Month, John M. Campbell & Co., Norman, OK, USA.

Poling, B.E., Prausnitz, J.M., O'Connell, J.P., 2001. The Properties of Gases and Liquids. McGraw-Hill Book Company, New York, NY, USA.

Santos, S.P., October 15−17, 1997. Transient analysis − a must in gas pipeline design. Paper Presented at the 29th PSIG Annual Meeting, Tucson, AZ, USA.

Santos, S.P., October 20−22, 2004. Series or parallel arrangement for a compressor station? - a recurring question that needs a convincing answer. Paper Presented at the 36th PSIG Annual Meeting, Palm Springs, CA, USA.

CHAPTER

SALES GAS TRANSMISSION 15

15.1 INTRODUCTION

Natural gas continues to play a great role as a worldwide energy supply. In fact, major projects are being planned to move massive amounts of high-pressure sales gas from processing plants to distribution systems and large industrial users through large-diameter buried pipelines. These pipelines utilize a series of compressor stations along the pipeline to move the gas over long distances. In addition, gas coolers are used downstream of the compressor stations to maintain a specified temperature of the compressed gas for pipeline pressure drop reduction and to protect gas pipeline internal and external coating against deterioration due to high temperatures. This chapter covers all the important concepts of sales gas transmission from a fundamental perspective.

15.2 GAS FLOW FUNDAMENTALS

Optimum design of a gas transmission pipeline requires accurate methods for predicting pressure drop for a given flow rate or predicting flow rate for a specified pressure drop in conjunction with installed compression power and energy requirements, e.g. fuel gas, as part of a technical and economic evaluation. In other words, there is a need for using analytical methods to relate the flow of gas through a pipeline to the properties of both the pipeline and gas, and to the operating conditions such as pressure and temperature. Isothermal steady-state pressure drop or flow rate calculation methods for single-phase dry gas pipelines are the most widely used and the most basic relationships in the engineering of gas delivery systems (Beggs, 1984; Smith, 1990; Aziz and Ouyang, 1995). Close attention should be given while designing a new gas pipeline project because with the technology now available nonisothermal and transient analysis may be used providing better results and lowering economic risks to the gas pipeline project (Santos, 1997). When enough information is not available for modeling a gas pipeline for transient analysis, designers can make appropriate assumption of future expected operation conditions or make use of load (or swing) factor that will increase design capacity for steady-state calculation of a pipeline diameter.

Handbook of Natural Gas Transmission and Processing. https://doi.org/10.1016/B978-0-12-815817-3.00015-0

15.2.1 GENERAL FLOW EQUATION

Based on the assumptions that there is no elevation change in the pipeline and that the condition of flow is isothermal, the integrated Bernoulli's equation is expressed by Eq. (15.1) (Uhl, 1965; Schroeder, 2001):

$$Q_{sc} = C\left(\frac{T_b}{P_b}\right)D^{2.5}\left(\frac{P_1^2 - P_2^2}{f\,\gamma_G T_a Z_a L}\right)^{0.5} E \tag{15.1}$$

where Q_{sc} is the standard gas flow rate measured at base temperature and pressure, ft^3/day; T_b is the gas temperature at base condition, 519.6°R; P_b is the gas pressure at base condition, 14.7 psia; P_1 is the inlet gas pressure, psia; P_2 is the outlet gas pressure, psia; D is the inside diameter of pipe, inches; f is the Moody friction factor; E is the flow efficiency factor; γ_G is the gas specific gravity; T_a is the average absolute temperature of pipeline, °R; Z_a is the average compressibility factor; L is the pipe length, miles; and C is the constant for the specific units used (77.54).

Although the assumptions used to develop Eq. (15.1) are usually satisfactory for a long pipeline, the equation contains an efficiency factor, E, to correct for these assumptions. Most experts recommend using efficiency factor values close to unity when dry gas flows through a new pipeline. However, as the pipeline ages and is subjected to varying degrees of corrosion, this factor will decrease (Campbell et al., 1992). In practice, and even for single-phase gas flow, some water or condensate may be present if the necessary drying procedure for gas pipeline commissioning is not adopted or scrubbers are not installed. This puts compression equipment at risk of damage and also allowing localized corrosion due to water spots (wetting of the pipe surface). The presence of liquid products in the gas transmission lines can also cause drastic reduction in the flow efficiency factor. Typically, efficiency factors may vary between 0.6 and 0.92 depending on the pipeline liquid contents (Ikoku, 1984). As the amount of liquid content in the gas phase increases, the pipeline efficiency factor can no longer account for the two-phase flow behavior, and two-phase flow equations must be used (Brill and Beggs, 1991; Asante, 2002).

Pipelines are usually not horizontal; however, as long as the slope is not too great, a correction for the static head of fluid (H_c) may be incorporated into Eq. (15.1) as follows (Schroeder, 2001):

$$Q_{sc} = C\left(\frac{T_b}{P_b}\right)D^{2.5}\left(\frac{P_1^2 - P_2^2 - H_c}{L\,\gamma_G T_a Z_a f}\right)^{0.5} E \tag{15.2}$$

where

$$H_c = \frac{0.0375g\,(H_2 - H_1)\,P_a^2}{Z_a T_a} \tag{15.3}$$

and H_1 is the inlet elevation, ft; H_2 is the outlet elevation, ft; and g is the gravitational constant, ft/s^2.

The average compressibility factor, Z_a, is determined from the average pressure (P_a) and average temperature (T_a), where P_a is calculated from Eq. (15.4) (Campbell et al., 1992):

$$P_a = \frac{2}{3}\left[(P_1 + P_2) - \left(\frac{P_1 P_2}{P_1 + P_2}\right)\right] \tag{15.4}$$

where P_1 and P_2 are the upstream and downstream absolute pressures, respectively. The average temperature is determined by Eq. (15.5):

$$T_a = \left[\frac{T_1 - T_2}{\ln\left(\frac{T_1 - T_S}{T_2 - T_S}\right)}\right] + T_S \tag{15.5}$$

In the above equation, parameter T_S is the soil temperature, and T_1 and T_2 are the upstream and downstream temperatures, respectively.

Having obtained P_a and T_a for the gas, the average compressibility factor can be obtained using Kay's rule and gas compressibility factor charts (Campbell et al., 1992).

15.2.2 FRICTION FACTOR CORRELATIONS

The fundamental flow equation for calculating pressure drop requires a numerical value for the friction factor. However, because the friction factor, f, is a function of flow rate, the whole flow equation becomes implicit. To determine the friction factor, the fluid flow is characterized by a dimensionless value known as the Reynolds number, Eq. (15.6):

$$N_{Re} = \frac{\rho V D}{\mu} \tag{15.6}$$

where N_{Re} is the Reynolds number, dimensionless; D is the pipe diameter, ft; V is the fluid velocity, ft/s; ρ is the fluid density, lb_m/ft^3; and μ is the fluid viscosity, $lb_m/ft\ s$.

For Reynolds numbers less than 2000 the flow is considered laminar. When the Reynolds number exceeds 2000, the flow is characterized as turbulent. Note that in high-pressure gas transmission pipelines with moderate to high flow rates, only two types of flow regimes are observed: partially turbulent flow (smooth pipe flow) and fully turbulent flow (rough pipe flow). For gases, the Reynolds number is given by Eq. (15.7) (Kennedy, 1993):

$$N_{Re} = \frac{0.7105\ P_b \gamma_G Q_{sc}}{T_b \mu_G D} \tag{15.7}$$

where D is the pipe diameter, inches; Q_{sc} is the gas flow rate, standard ft^3/day; μ_G is the gas viscosity, cp; P_b is the base pressure, psia; T_b is the base temperature, °R; and γ_G is the gas specific gravity, dimensionless.

For the gas industry, Eq. (15.7) is a more convenient way to express the Reynolds number because it displays the value proportionally in terms of the gas flow rate.

The other parameter in the friction factor correlation is pipe roughness (ε), which is often correlated as a function of the Reynolds number and the pipe relative roughness (absolute roughness divided by inside diameter). Pipe roughness varies considerably from pipe to pipe. Table 15.1 shows the roughness for various types of new (clean) pipes. These values should be increased by a factor ranging between two and four to account for age and use.

The Moody (1944) friction factor, f, in Eq. (15.1) is determined from the Moody diagram. The Moody correlation is shown in Fig. 15.1. The Moody diagram consists of four zones: laminar, transition, partially turbulent, and fully turbulent zones.

Table 15.1 Pipe Roughness Value (Norsok Standard, 1996)

Type of Pipe (New, Clean Condition)	ε (inches)
Carbon steel, corroded	0.019685
Carbon steel, noncorroded	0.001968
Glass fiber reinforced pipe	0.0007874
Steel internally coated with epoxy	0.00018−0.00035

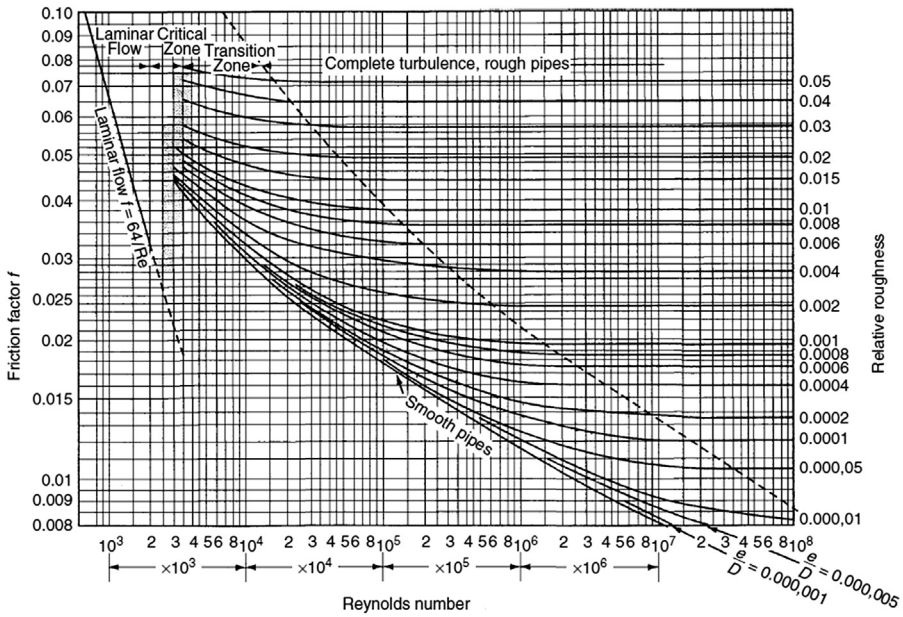

FIGURE 15.1

Moody friction factor diagram (Streeter and Wylie, 1979).

The laminar zone, the left side, is the zone of extremely low flow rate in which the fluid flows strictly in one direction and the friction factor shows a sharp dependency on flow rate. The friction factor in the laminar regime is defined by the Hagen−Poiseuille equation (Streeter and Wylie, 1979):

$$f = \frac{64}{N_{Re}} \tag{15.8}$$

The fully turbulent zone, the right side, describes fluid flow that is completely turbulent (back mixing) laterally as well as in the primary direction. The turbulent friction factor shows no dependency on flow rate and is only a function of pipe roughness, as an ideally smooth pipe never really exists in this zone. The friction factor to use is given by the rough pipe law of Nikuradse (1933), Eq. (15.9):

$$\frac{1}{\sqrt{f}} = 2\ \mathrm{Log}\frac{D}{\varepsilon} + 1.14 \tag{15.9}$$

The above equation shows that if the roughness of the pipeline is increased, the friction factor increases and results in higher pressure drops. Conversely, by decreasing the pipe roughness, lower friction factor or lower pressure drops are obtained. Note that most pipes cannot be considered ideally smooth at high Reynolds numbers (Schlichting, 1979); therefore, the investigations of Nikuradse (1933) on flow through rough pipes has been of significant interest to engineers.

The partially turbulent (transition) zone is the zone of moderately high flow rate in which the fluid flows laterally within the pipe as well as in the primary direction, although some laminar boundary layer outside the zone of roughness still exists. Partially turbulent flow is governed by the smooth pipe law of Karman and Prandtl (Uhl, 1965), Eq. (15.10):

$$\frac{1}{\sqrt{f}} = 2\ \mathrm{Log}\left(N_{Re}\sqrt{f}\right) - 0.8 \tag{15.10}$$

The above correlation has received wide acceptance as a true representation of experimental results. However, a recent study by Zagarola (1996) on the flow at high Reynolds numbers in smooth pipes showed that the relevant correlation was not accurate for high Reynolds numbers, where the correlation was shown to predict very low values of the friction factor.

Consensus on how the friction factor varies across the transition region from an ideal smooth pipe to a rough pipe has not been reached. However, Colebrook (1939) presented additional experimental results and developed a correlation for the friction factor valid in the transition region between smooth and rough flow. The correlation is as follows:

$$\frac{1}{\sqrt{f}} = -2\ \mathrm{Log}\left(\frac{\varepsilon/D}{3.7} + \frac{2.51}{N_{Re}\sqrt{f}}\right) \tag{15.11}$$

The above equation is universally accepted as standard for computing friction factor of rough pipes and incorporated in most thermohydraulic simulation softwares available at the market. Moody (1944) concluded that the Colebrook (1939) equation was adequate for friction factor calculations for any Reynolds number greater than 2000. Certainly the accuracy of the equation was well within the experimental error (about ±5% for smooth pipes and ±10% for rough pipes).

The friction factor is sometimes expressed in terms of the Fanning friction factor, which is one-fourth of the Moody friction factor. Care should be taken to avoid inadvertent use of the wrong friction factor.

15.2.3 SIMPLIFIED FLOW EQUATIONS

The Moody friction factor, f, is an integral part of the general gas flow equation. Because it is a highly nonlinear function, it must be either read from a chart or determined iteratively from a nonlinear equation. Approximations to the Moody friction factor have been widely used because they allow the gas flow equation to be solved directly instead of iteratively. The four most widely published friction factor approximations are Weymouth, Panhandle A, Panhandle B, and IGT[1] (Beggs, 1984; Ikoku, 1984). The Weymouth equation approximates the Moody friction factor by Eq. (15.12), and the remaining three equations approximate the friction factor by Eq. (15.13), where “m” and “n” are constants. These constants are given in Table 15.2.

[1]The IGT equation proposed by the Institute of Gas Technology (IGT) is also known as the IGT distribution equation.

Table 15.2 Constants in Eqs. (15.12) and (15.13)

Equation	m	n
Weymouth	0.032	0.333
Panhandle A	0.085	0.147
Panhandle B	0.015	0.039
IGT	0.187	0.200

$$f = m(D)^{-n} \tag{15.12}$$

$$f = m(N_{Re})^{-n} \tag{15.13}$$

The Reynolds number, N_{Re}, can be approximated by Eq. (15.7). In addition to the Reynolds number, the pipe roughness also affects the friction factor for turbulent flow in rough pipes. Hence, the efficiency factor is chosen to correctly account for pipe roughness (Ouyang and Aziz, 1996).

These approximations can then be substituted into the flow equation for f, and the resulting equation is given by Eq. (15.14) (Kennedy, 1993; Towler and Pope, 1994):

$$Q_{sc} = \frac{a_1 \left(\frac{T_b}{P_b}\right) E \left(P_1^2 - P_2^2\right)^{0.5} D^{a_2}}{(\gamma_G)^{a_3} (T_a Z_a L)^{a_4} (\mu_G)^{a_5}} \tag{15.14}$$

In Eq. (15.14), the values for a_1 through a_5 are constants that are functions of the friction factor approximations and the gas flow equation. These constants are given in Table 15.3.

Inspection of Table 15.3 shows that the gas flow rate is not a strong function of the gas viscosity at high Reynolds numbers because viscosity is of importance in laminar flow, and gas pipelines are normally operated in the partially/fully turbulent flow region. However, under normal conditions, the viscosity term has little effect because a 30% change in absolute value of the viscosity will result in only approximately a 2.7% change in the computed quantity of gas flowing. Thus, once the gas viscosity is determined for an operating pipeline, small variations from the conditions under which it was determined will have little effect on the flow predicted by Eq. (15.14) (Huntington, 1950).

Note that all of the equations noted above have been developed from the fundamental gas flow equation; however, each has a special approximation of the friction factor to allow for an analytical solution. For instance, the Weymouth (1912) equation uses a straight line for f, and thus its approximation has been shown to be a poor estimation for the friction factor for most flow conditions

Table 15.3 Constants in Eq. (15.14)

Equation	a_1	a_2	a_3	a_4	a_5
Weymouth	433.46	2.667	0.5000	0.5000	0.0000
Panhandle A	403.09	2.619	0.4603	0.5397	0.0793
Panhandle B	715.35	2.530	0.4900	0.5100	0.0200
IGT	307.26	2.667	0.4444	0.5556	0.1111

(Kennedy, 1993). This equation tends to over predict the pressure drop and thus provides a poor estimate relative to the other gas flow equations. The Weymouth equation, however, is of use in designing gas distribution systems in that there is an inherent safety in over predicting pressure drop (Maddox and Erbar, 1982). In practice, the Panhandle equations are commonly used for large-diameter, long pipelines where the Reynolds number is on the flat portion of the Moody diagram. The Panhandle "A" equation is most applicable for medium to relatively large-diameter pipelines (12″−60″ diameter) with moderate gas flow rate, operating under medium to high pressure (800−1500 psia). The Panhandle "B" equation is normally appropriate for high flow rate, large-diameter (>36″), and high-pressure (>1000 psi) transmission pipelines (Maddox and Erbar, 1982; Kennedy, 1993). The IGT equation is particularly suitable for high pressure, high flow rates through steel or plastic/polyethylene pipes for most distribution design situations.

Since friction factors vary over a wide range of Reynolds number and pipe roughness, none of the gas flow equations is universally applicable. However, in most cases, pipeline operators customize the flow equations to their particular pipelines by taking measurements of flow, pressure, and temperature and back calculating pipeline efficiency or an effective pipe roughness.

15.3 PREDICTING GAS TEMPERATURE PROFILE

Predicting the pipeline temperature profile has become increasingly important in both the design and operation of pipelines and related facilities. Flowing gas temperature at any point in a pipeline may be calculated from known data to determine (1) location of line heaters for hydrate prevention (Towler and Mokhatab, 2004), (2) inlet gas temperature at each compressor station, and (3) minimum gas flow rate required to maintain a specific gas temperature at a downstream point. To predict the temperature profile and to accurately calculate pressure drop, it is necessary to divide the pipeline into smaller segments. The temperature change calculations are iterative because the temperature (and pressure) at each point must be known to calculate the energy balance. Similarly, the pressure loss calculations are iterative because the pressure (and temperature) at each point along the pipeline must be known to determine the phase physical properties from which the pressure drop is calculated. Thus, generating a useable temperature profile requires a series of complex, interactive type calculations for which even the amount of data available in most cases is insufficient. Additionally, the pipeline outer environment properties such as soil data and temperatures vary along the pipeline route and therefore play a very important role and require a consistent modeling to provide a reliable temperature profile evaluation. A simple and reasonable approach is to divide the pipeline into sections with defined soil characteristics and prevailing soil temperatures for summer and winter time and then to calculate the overall heat transfer that will be highly influenced by the outer conditions. The complexity of this method has led to the development of approximate analytical methods for prediction of temperature profile, which in most situations are satisfactory for engineering applications.

Basic relationships needed for these calculation methods are thermal and mechanical energy balances, and mass balance for the gas flow in pipelines. The general or thermal energy balance can be written as follows (Buthod et al., 1971):

$$C_P\left(\frac{dT}{dx}\right) - \eta C_P\left(\frac{dP}{dx}\right) + \left(\frac{VdV}{g_C}\right)\left(\frac{dV}{dx}\right) + \left(\frac{g}{g_C}\right)\left(\frac{dH}{dx}\right) = -\frac{dq}{dx} \tag{15.15}$$

where T is the gas temperature; P is the absolute pressure of gas; V is the gas linear velocity in pipeline; q is the heat loss per unit mass of flowing fluid; C_p is the constant pressure specific heat; η is the Joule–Thomson coefficient; H is the height above datum; x is the distance along pipeline; g_c is the conversion factor; and g is the gravitational acceleration.

The major assumption in the development of Eq. (15.15) is that the work term is zero between the compressor stations.

To calculate the heat transfer from the pipe to the ground (soil), per unit of pipeline length, the Kennelly equation, Eq. (15.16), is used (Neher, 1949):

$$\frac{dq}{dx} = [2\pi K(T - T_S)] \Big/ m_G \, \mathrm{Ln}\left[\left(2H' + \sqrt{4H'^2 - D_0^2}\right) \Big/ D_0\right] \tag{15.16}$$

where K is the thermal conductivity of soil; T_S is the undisturbed soil temperature at pipe centerline depth; m_G is the mass flow rate of gas; H′ is the depth of burial of pipe (to centerline); and D_0 is the outside diameter of pipe.

A basic assumption in Eq. (15.16) is that the temperature of the gas is the same as the temperature of the pipe wall (the resistances to heat transfer in the fluid film and pipe wall are negligible).

The mechanical energy balance is given by Eq. (15.17) (Streeter and Wylie, 1979):

$$\frac{1}{\rho}\frac{dP}{dx} + \frac{V dV}{g_c dx} + \frac{2\ f\ V^2}{g_c D_i} = 0 \tag{15.17}$$

where ρ is the density of gas; f is the Fanning friction factor; and D_i is the inside diameter of pipe.

The continuity equation, Eq. (15.18), relates velocity to the pressure and temperature (Buthod et al., 1971):

$$\frac{dV}{dx} = \frac{-m_G}{\rho^2 A}\left[\frac{\rho}{P} - \frac{\rho}{Z}\left(\frac{\partial Z}{\partial P}\right)_T\right]\frac{dP}{dx} - \left[\frac{\rho}{T} + \frac{\rho}{Z}\left(\frac{\partial Z}{\partial T}\right)_P\right]\frac{dT}{dx} \tag{15.18}$$

where A is the inside cross-sectional area of pipe and Z is the gas compressibility factor.

Eqs. (15.15)–(15.18) are the basic equations that must be solved simultaneously for the calculation of the gas temperature and pressure profiles in pipelines. Details for solving this set of equations can be found in textbooks on numerical analysis, such as Constantinides and Mostoufi (1999).

The typical equations used to determine pipeline temperature loss are the integrated form of the general equations. However, assumptions and simplifications must be made to obtain the integrated equations, even though the effects of these assumptions or simplifications are not always known. A major advantage of numerical integration of the differential equation is that fewer assumptions are necessary. Considering this fact, Coulter and Bardon (1979) have presented an integrated equation as follows:

$$T_x = \left\{T_1 - \left[T_S + \left(\frac{\eta}{a}\right)\left(\frac{dP}{dx}\right)\right]\right\}e^{-ax} + \left[T_S + \left(\frac{\eta}{a}\right)\frac{dP}{dx}\right] \tag{15.19}$$

where T_1 is the inlet gas temperature and the term "a" is defined as below:

$$a = \frac{2\pi RU}{m_G C_P} \tag{15.20}$$

where R is pipe radius and U is the overall heat transfer coefficient.

Eq. (15.19) can be used to determine the temperature distribution along the pipeline, neglecting kinetic and potential energies and assuming that heat capacity at constant pressure, C_P, and Joule–Thomson coefficient remain constants along the pipeline. For most practical purposes, these assumptions are close to reality and generally do give quite good results. Moreover, for a long gas transmission pipeline with a moderate to small pressure drop, the temperature drop due to expansion is small (Buthod et al., 1971) and Eq. (15.19) simplifies to Eq. (15.21):

$$T_x = T_S + (T_1 - T_S)\ \mathrm{Exp}(-ax) \tag{15.21}$$

Eq. (15.21) does not account for the Joule–Thomson effect, which describes the cooling of an expanding gas in a transmission pipeline. Hence, it is expected that the fluid in the pipeline will reach soil temperature later than that predicted by Eq. (15.19).

While there has been extensive effort in the development of equations for predicting pipeline temperature profile, little attention has been paid to the fact that the Joule–Thomson coefficient and heat capacity at constant pressure are not constants. However, a new analytical technique for the prediction of temperature profile of buried gas pipelines has been developed by Edalat and Mansoori (1988) while considering the fact that η and C_P are functions of both temperature and pressure. Readers are referred to the original reference for a detailed treatment of this method.

15.4 TRANSIENT FLOW IN GAS TRANSMISSION PIPELINES

Transients occur in natural gas pipelines during filling and line pressurization, emergency shutdown, gas blowdown, and line depressurization processes. Transient flow can also occur in the gas pipeline during normal operation due to variations in demand, inlet and outlet flow changes, compressor start and stop, pipe leak, and/or rupture.

There are some reasons for applying transient analysis during design phase of gas transmission pipelines. The first reason is related to the large investment required by such projects, which includes pipeline and compression stations. The designed system must be able to operate under predicted different scenarios; otherwise the transmission company would face penalties for not delivering the contracted gas volumes and will probably have to make additional unpredicted capital investment on the system, dramatically affecting its cash flow. The second reason is related to the operation behavior of some end user such as gas-fired power plant with different gas demand profile that may interrupt gas consumption up to zero for a certain period of time on a weekly basis. These scenarios must be taken into account because they directly affect pipeline capacity management and transmission costs and also affect the assembling schedule of compression stations and compressor units causing cyclic operation, shutting units on and off. Transient analysis is used to help selecting turbo compressors that best fit system requirements arranged in series (few units and bigger machines) or parallel (more units and smaller machines). It is also necessary to run failure analysis for a single compressor unit or even for a complete station and predict system response in terms of remaining capacity versus time. Transient analysis is important to establish maintenance strategy and define whether standby unit will be installed to enhance system availability. Transient analysis will also be very useful along the negotiation process of ship-or-pay contracts that normally starts well before the design phase. Additional uses of transient analysis are related to the operation of the pipeline in control rooms, training operation personnel, and commercial planning (Santos, 1997; Santos and Mokhatab, 2008).

Accurate predictions of the gas flow rate, temperature, and pressure profiles along the pipelines under transient conditions, which are vital to the adequate operation of gas transmission pipelines, indicate the need for appropriate mathematical models to do a detailed analysis. When modeling pipelines, however, it is sometimes convenient to make the simplifying assumption that flow is isothermal and steady state as long as we incorporate a load or swing factor contingent to a latter transient design checking to prevent inadequate pipeline sizing with potential detrimental impact on the feasibility of pipeline projects (Santos, 1997). Steady-state models are widely used to design pipelines and to estimate flow and line pack. However, there are many situations where an assumption of steady state flow and its attendant ramifications produce unacceptable engineering results. Note should be made that the flowing gas temperature in transmission pipeline does not remain constant over the length of the pipeline. Therefore, complete temperature profiles along pipeline length are required to adequately design the pipeline for operation under varying environmental conditions.

The unsteady nonisothermal flow of gas in transmission pipelines can be described by a one-dimensional approach and by using an equation of state and a set of partial differential equations expressing mass, momentum, and energy conservation laws (Osiadacz and Chaczykowski, 2010). In practice, the form of the mathematical relationships depends on the assumptions made based on the operating conditions of the pipelines. For the case of slow transient flows due to fluctuations in demand, it is assumed that the gas in the line has sufficient time to reach thermal equilibrium with its constant-temperature surroundings. Similarly, for the case of rapid transient flows, it is assumed that the pressure changes occur instantaneously, allowing no time for heat transfer between the gas in the pipeline and the surroundings. However, for this case, heat conduction effects cannot be neglected.

15.5 COMPRESSOR STATIONS

A principal component of any gas transmission system is the compressor station. As natural gas flows through a pipeline, it loses pressure due to friction against the inside of the pipe. Therefore, compressor stations are installed along the pipeline to boost the gas pressure in the pipeline to maintain required delivery pressure and flow (Fig. 15.2). A given gas transmission system may have anywhere from a few stations up to well over 50 depending on feasibility studies.

Compressor stations comprise one or more compressor units (designed with enough horsepower and throughput capacity to meet contractual requirements levied on the system), each of which will include a compressor and driver together with valves, control systems, exhaust ducts, and noise attenuation systems. Most compressors are powered by natural gas taken directly from the pipeline, but electric powered compressors are becoming more common. Fig. 15.3 shows a typical compressor station with three gas turbine—driven centrifugal compressors.

A typical single-stage compressor station design, as shown in Fig. 15.4, may consist of an inlet scrubber to collect entrained liquids (i.e. water, corrosion inhibitors, hydrocarbon liquids that may have formed in the gas transmission pipeline) followed by a coalescing filter[2] to remove fine solids (i.e. pipe scale) and hydrocarbon mist from the gas that could otherwise contribute to compressor failure. From the scrubber, the gas is taken to the compressor unit(s) where it is compressed. At the compressor station discharge or between compressor units in case of series arrangement the gas is cooled down,

[2]A coalescing filter also cleans the gas in each fuel supply to the turbines and gas engines.

FIGURE 15.2

Top view of a gas pipeline compressor station (Mokhatab et al., 2007).

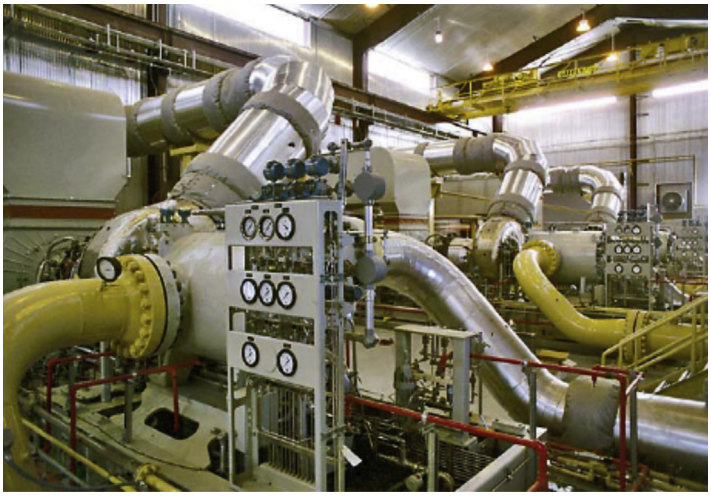

FIGURE 15.3

Typical compressor station with three compression units (Kurz and Mokhatab, 2007).

typically with an air cooler, and then it passes through a scrubber allowing drainage of any formed liquid. In case of reciprocating compressor being used in the compressor station, a coalescing filter shall be used after the scrubber to remove lube oil mist prior to the gas being introduced back into the pipeline.

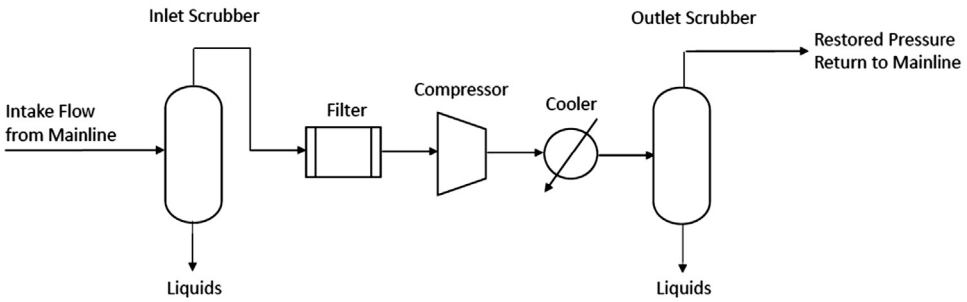

FIGURE 15.4

Schematic process diagram of single-stage gas compressor station.

15.5.1 STATION FACILITIES

Each compressor station will be built up from the same functional blocks of equipment. Each functional element plays a part in the work of the station, and the design and sizing of each is essential to the efficient and safe operation of the plant.

The functional elements include gas scrubbing and liquid removal, compressor and driver units, aftercoolers, pipes, and valves. Controls, including supervisory control and data acquisition (SCADA) system, monitoring and data recording, alarms, and shutdown procedures, both routine and emergency, are integral parts of the station. Provision also has to be made for venting, the compressor, and driver housing and buildings, complete with ventilation and fire protection and safety equipment.

15.5.1.1 Scrubbers

Individual scrubbers (with or without standby unit) may be installed for each stage of compression for each compressor unit. A common scrubber should be considered for multiple units on a common suction line. Scrubbers at compressor inlets and after gas coolers can take several forms, inertial with or without demister pads or the horizontal cyclonic type. The latter are commonly used on mainline transmission stations.

Efficient and safe handling of the liquids collected from the scrubbers in a compressor station is one of the keys to a good design. The liquids removed from the gas flow to a hydrocarbon storage tank to be separated by gravity and then be transported by truck as saleable hydrocarbon liquid or as disposed waste product. There are three main concerns that should be addressed in the liquid handling design for any compressor station: safety, environmental impacts, and economics. An additional point of consideration should be operability, which includes issues such as hydrate formation (when water is present in the gas composition), failure consequences, etc.

15.5.1.2 Compressors

In gas transmission, two basic types of compressors (reciprocating and centrifugal) are used. Reciprocating compressors are usually driven by either electric motors or gas engines, whereas centrifugal compressors use gas turbines or electric motors as drivers.

Compressor selection is based on detailed analysis of the operating conditions in terms of flow and pressure ratio needed by the pipeline hydraulics. Frequently, these conditions will vary over time and

the compressor selection will have to have flexibility, by restaging, if necessary, to accommodate all the expected conditions. From transient analysis based on predicted ramp-up gas demand and flow profiles a set of values are defined that will be used to preselect compressor units depending on the installation layout whether series or parallel (Santos, 1997, 2004).

Typically the conditions for most mainline stations will require compressors with one or two stages, and the compressor design may be of the overhung rotor or barrel design. The determination of operating conditions and hence the development of the compressor characteristics will have to take into account the gas characteristics, suction and discharge pressure, and suction temperatures, usually involving equations of state for the particular gas composition, and the process environment (i.e., climate, altitude, location, etc.).

Pipeline and station designer will make sure that the equipment selection and arrangement including maintenance strategy and level of availability will be subject to a feasibility study (Santos, 2004).

15.5.1.3 Compressor Drivers

Choices for drivers can be gas turbines, or electric motors. The selection is usually based on considerations of cost, both capital and maintenance, fuel or energy cost, availability of power supply, reliability, and availability. Gas turbines are high-speed machines and can be directly coupled to the compressor. Electric motors can be of several types with both fixed and variable speed options. In recent times the high-speed variable speed electric motor operating at super synchronous conditions has become available at powers of more than 25 MW, which makes this option competitive with larger gas turbines (Cleveland and Mokhatab, 2005). The variable speed planetary gear (VSPG) from VOITH, which provides another economic alternative to be used with fixed speed electric motor, is also available in the market.

Capital costs for gas turbines and electric motors are generally similar; electric drives generally have lower maintenance and operating costs than gas turbines. The decision to use gas turbine or electric motor drivers comes from the feasibility analysis for the alternatives available for the project and site logistics, capital expenditure (CAPEX) and operating expenditure (OPEX), availability and reliability for the compressor units and for the energy source, which are key items. Important items in favor of electric driven compressor station that should be considered in the feasibility analysis is that the fuel gas used for gas turbine−driven compressor station will be transformed into capacity increase for the electric driven compressor station and therefore will add revenue to this alternative and also the overhaul cost for the gas turbines that are expressive and will occur after completing around 40,000 running hours, accounted in the OPEX costs (Kurz and Ohanian, 2003). There will always be gas in the pipeline, so the question of reliability and availability of the energy source for the gas turbine does not enter into the question. For the electric drive, there has to be a reliable electric grid within a reasonable distance from the compressor station, transmission lines costs need to be considered in the evaluation. When there is a reliable source of electric energy available, it would be worth to evaluate both alternatives (gas or electric drivers) supported by failure statistics for the electric grid such as loss of load frequency, loss of load duration, and loss of load probability that will allow to define the reliability of the electric grid. Given that these conditions are satisfied, the decision then comes from the economic evaluation of all the alternatives and selecting the one that will give the best economic result. The life cycle cost must examine and test the results for sensitivity to cost escalation in power prices and gas

price taking into account the correlation between these two commodities. A long-term power supply agreement would be required to mitigate risk. The question of using a diesel engine as power source has not been considered as it offers no advantages over a similar gas engine and introduces another fuel, which invokes additional costs for transportation and storage.

Selection of the appropriate units has to consider all aspects of interest including operating cost, reliability, and availability as well as capital cost. The process of selection should be formalized so as to remove as far as possible subjective elements and ensure the decisions are objectively based (Kurz et al., 2003).

15.5.1.4 Piping and Valves

The compressor station will be connected to the gas pipeline via a set of block valves with a bypass. These will be typically ball valves with a block and bleed capability. The piping should be designed to minimize pressure loss as pressure loss represents inefficiency. The supports and anchors for the piping shall be designed to allow for expansion following compression and to keep the forces and moments on the compressor flanges within the limits set by the compressor manufacturer. For centrifugal compressors there will be a surge valve and recycle line for surge protection, this recycle line will connect the discharge line to the suction line adjacent to the compressor and typically can go through the aftercooler. The sizing of this line and the valve is critical and should be done in consultation with the compressor supplier and with knowledge of the compressor characteristics. Each compressor on the station will have its own set of isolation and block valves with a bypass.

15.5.1.5 Shutdown and Venting Systems

For most compressor stations, there are two cases for shutdown and venting. The first can be stated as routine, in which a unit or a station has to be shut down for repair or maintenance and the second is in the case of a failure or emergency when the gas in the station needs to be evacuated safely and as quickly as possible. Most stations are now designed such that the compressors will remain pressurized when idle and routine venting will only be required when work has to be done on the units.

15.5.1.6 Emergency Shutdown System

The compressor station shall be provided with an emergency shutdown system by means of which the station will be isolated from the pipeline and gas flow through the station will be stopped. A blowdown system will release the gas from station piping to the atmosphere. Operation of the emergency shutdown system also shall cause the shutdown of all gas compressing equipment and shall de-energize the electrical facilities located in the vicinity of gas headers and in the compressor room except those that provide emergency lighting for personnel protection and those that are necessary for protection of equipment. The emergency shutdown system shall be operable from any one of the two locations outside the gas area of the station, preferably near exit gates in the station fence, but not more than 150 m (500 ft) from the limits of the station. Blowdown piping shall extend to a location where the discharge of gas is not likely to create a hazard to the compressor station.

15.5.1.7 Pressure Relief Systems

Pressure relief or other suitable protective devices of sufficient capacity and sensitivity shall be installed and maintained to assure that maximum allowable operating pressure (MAOP) of the station piping and equipment is not exceed by more than 5%.

15.5.1.8 Flare System

Flare lines shall be provided to exhaust the gas from the pressure relief and vent valves to atmosphere and shall be extended to a location where the gas may be discharged without hazard. Flare lines shall be sized to provide sufficient capacity so that they will not interfere with the performance of the relief and went valves.

15.5.2 COMPRESSOR ARRANGEMENTS

Because gas pipeline projects demand high amounts of capital expenditure and therefore are involved with investment risks, project sponsors will try to maximize capacity usage and minimize investment so as to have a competitive transportation rate to offer to the market. At the same time, it will avoid the pipeline to operate with spare capacity.

The decision on the compressor arrangement whether series or parallel is mostly based on economics and on simulation of failure analysis (Santos, 2000). While series arrangement may present some advantages when standby compressor units are not required, parallel arrangement provides better results when standby units are required and also provides more operating flexibility under failure scenario analysis. Pipeline designer should evaluate different configuration and compressor unit size and perform technical and economical feasibility study to identify which configuration presents a better overall economic result. The decision process has to take into account issues such as capacity ramp-up, further expansion, back-up strategies, operational strategy, and transient analysis.

For any given pipeline compressor station, two units in series will yield a higher specific speed than two units in parallel. Thus, once the driver size (and thus the power turbine speed) and the desired head and flow through the station are known, one can conceptually decide whether the series or the parallel approach would lead to better aerodynamic performance. With modern compressors and stages with a wide operating range, it is usually possible to have identical stages for both the low-pressure and the high-pressure compressor in a series application. Intercooling is usually not necessary, nor does it typically yield significant savings in power demand (Kurz et al., 2003; Santos, 2004).

15.5.3 STATION CONTROL

Control functions are typically based on personnel safety, the operating parameters of the station, and the types and number of compressor units installed at the station.

Compressor station controls can be divided into two sections, unit control and station control. Digital technology is now used throughout both systems, the unit control utilizes a microprocessor which will control the turbine compressor unit to run to set points under the direction of the operator or the station control system, the set points can be flow or pressure. Commonly, a flow or suction pressure will be the control parameter with discharge pressure and/or suction pressure as overrides. The control protocol will include limits to ensure safe operation. These limits will include pressure and temperatures on discharge and suction on the compressor as well as speed and flow and pressure ratio in relation to surge.

The unit control will monitor the compressor operation to ensure that it will not run into surge. If the operation of the compressor nears the surge line, the unit control will instruct the recycle valve to open and so maintains safe operation. Should the recycle condition continue for a time and if coolers are not provided in the recycle line or compressor discharge, the unit will be shut down on high discharge temperature.

In addition to control and safety, the unit control will monitor key operating parameters and provide video output on demand and printout on a routine basis to provide a continuous record of operation. These readouts and records can be used for trouble shooting and maintenance. The station control system will oversee the unit operation and in addition provide the interface between the operators and the plant. It will also provide video and print data recording of all key station parameters. It has become a practice to operate stations and units remotely from central dispatch stations, and the station control systems will report to the central station via a SCADA link (Cleveland and Mokhatab, 2005).

The overall control of a major gas pipeline transportation system typically originates from a central "Gas Control" office that is remote from all of the compressor stations. Gas Control monitors flow measurement for the total station throughput as well as each compressor's throughput and fuel consumption. The programmable logic controller (PLC) in each compressor unit's control panel communicates to gas control the operating parameters for that compressor and the positions of the valves controlling the gas flow through that compressor. This example station uses redundant communication using microwave, satellite, or conventional leased telephone systems. This station is designed for the option of completely unmanned operation by Gas Control. The PLC compressor on/off operation, performance set points, and all station-critical valves may be remotely controlled. Gas Control may monitor all station alarms and shutdowns.

Gas turbine—driven centrifugal compressor unit panels typically include unit protective functions, local and remote starting, automatic unit valve operation, and equipment and process monitoring instrumentation. If a multiunit station is involved, a separate station panel may be used to automatically control station operation (Mokhatab et al., 2008).

15.5.4 ACOUSTICAL TREATMENT

Noise is a significant environmental pollutant and the reduction of noise is an essential part of the design of a compressor station. The technology of noise reduction has reached the level that for most practical purposes a compressor station can be designed to contribute less than 3 dB to the preexisting background noise level. Local requirements should be taken into account for a proper design. The design of the unit enclosures, buildings, exhaust and inlet silencers are subject to stringent specifications. Double wall enclosures are frequently used to control unit noise emissions as afore mentioned.

Normally an acoustic simulation study is done. If an acoustic simulation study has not been made, the following requirements for the piping system should be made:

- The use of elbows in the piping should be minimized to the minimum number possible.
- Elbows eliminated between compressor cylinders and pulsation suppression devices.

Exhaust emission from the gas turbines now have to meet the environmental limits of the location, and modern gas turbines are designed with low-emission combustion systems to meet these requirements These systems may be dry or wet low NOx and are now becoming the standard equipment for all gas turbines.

Silencing equipment incorporated into the engine air intake ducting and filters, engine exhaust systems, vent and blowdown exits, equipment enclosures, and piping insulation accomplish noise control for the surrounding community and station employees. Liners and baffles of noise reduction material are used inside the engine air intake ducting and filters, engine exhaust, and vent and blowdown exits. Acoustical lining on the internal walls and silenced ventilation systems reduce noise from the compressor buildings.

As much station gas piping as possible is installed below grade to provide additional noise reduction. Above grade station gas piping is acoustically insulated. Internal noise reduction modifications are required in flow control valves. Fan tip speed limitations and low-noise fan drive designs are required for gas and oil coolers. Station noise control provides a day–night average sound level (Ldn) of less than 55 dB per the "A" rating (dBA) of human response to noise at the nearest noise sensitive area. This complies with current US Federal Energy Regulatory Commission regulations. Noise levels within a 3-ft distance from equipment for the employee's average time of exposure is less than 85 dBA. This complies with current US Occupational Safety and Health Administration requirements.

15.5.5 RELIABILITY AND AVAILABILITY

Compressor station reliability and availability are paramount to overall gas pipeline delivery dependability. Reliability considerations are incorporated into many areas of the facility.

- The total amount of installed compression (operating and standby units) must be more than the normal design requirement to allow for scheduled and unscheduled maintenance.
- Spacing between compressors or compressor groups aims at preventing fire damage to one compressor from harming others and to ease maintenance work.
- Using redundant and parallel filter coalescers prevents unexpected large amounts of contaminants from impeding the gas flow and allows filtration cartridge replacement without interrupting compressor operation.
- Monitoring and trending of vibration, bearing temperatures, and other critical operational parameters by the compressor PLC identify service needs to prevent catastrophic equipment failures.
- Maintenance systems should be developed to manage all aspects of maintenance prior to station start-up.
- All belowground steel pipe, conduit, and structures are coated with a corrosion-protective and electrically insulating coating. Additionally, steel pipe installed belowground is protected from external corrosion using cathodic protection as part of the protection system.
- Sufficient operational and capital spare part inventories should be available based on reliability–availability–maintenance (RAM) analysis and life cycle cost considerations.
- Equipment should be preferably standardized as feasible to minimize spare part requirements.

Good human factor practices should be used in evaluating access to and viewing of operating data, manipulation of controls, installation of isolation devices, and removal and replacement of equipment (e.g. equipment and personnel access and egress, lifting points, pull clearances, materials movement, etc.).

15.6 REDUCTION AND METERING STATIONS

In addition to compressor stations, there may be gas injection and delivery points along the line where the pressure and flow will have to be monitored and controlled. Each of these locations will include pressure control facilities and flow measurement.

Each reduction and metering station branches off the pipeline and is used to reduce pressure and meter the gas to the various users. For the reduction and metering stations the main equipment includes

filters, heaters, pressure reduction and regulators, and flow metering skids. In addition, each station is generally equipped with drains collection and disposal, instrument gas system, and storage tanks.

15.6.1 FILTERS

Natural gas filter units are installed at each station to remove any entrained liquids and solids from the gas stream. The filters may comprise cyclonic elements to centrifuge particles and liquids to the sides of the enclosing pressure vessel. These particles and liquids will then drop down for collection in a sump, which can be drained periodically.

15.6.2 HEATERS

Natural gas heaters are installed to avoid the formation of hydrates, liquid hydrocarbons and water as a result of pressure reduction. The gas heater is designed to raise the temperature of the gas such that after pressure reduction, the temperature of the gas will be above the dew point temperature at operating conditions and maximum flow. The heater is a water bath natural circulation type maintained at a temperature between 158 and 176°F. Where gas cost is high, an alternative is to use high efficiency or condensing furnaces for the purpose of preheating the gas rather than the water bath heater.

15.6.3 PRESSURE REDUCTION AND REGULATION SYSTEM

Pressure reduction system controls the supply pressure to the gas users at a regulated value. Each system consists of at least two trains of pressure reduction, one operating, and the other standby. Each train will normally comprise two valves in series, one being the "active valve," the other the "monitor valve." Each valve will be equipped with a controller to operate the valve to maintain the preset discharge pressure.

15.6.4 METERING SYSTEM

The flow rate of the gas has to be measured at a number of locations for the purpose of monitoring the performance of the pipeline system and more particularly at places where "custody transfer" takes place that is where gas is received from the supply source and gas is sold to the customer for distribution. Depending on the purpose for metering, whether for performance monitoring or for sales, the measuring techniques used may vary according to the accuracy demanded. Typically, a custody transfer metering station will comprise one or two runs of pipe with a calibrated metering orifice in each run.

15.7 DESIGN CONSIDERATIONS OF SALES GAS PIPELINES

The typical design of a gas transmission pipeline involves a compromise between the pipe diameter, compressor station spacing, fuel usage, and maximum operating pressure. Each of these variables influences the overall construction and operating cost to some degree, hence an optimized design improves the economics of the construction and operation of the system, and the competitiveness of the project.

15.7.1 LINE SIZING CRITERIA

The pipe size generally is based on the acceptable pressure drop, compression ratio, and allowable gas velocities. Acceptable pressure drop in gas transmission pipelines must be one that minimizes the size of the required facilities and operating expenses such as the pipe itself, the installed compression power, the size and number of compressors, and fuel consumption. In fact, a large pressure drop between stations will result in a large compression ratio and might introduce poor compressor station performance. Experience has shown that the most cost-effective pipeline should have a pressure drop in the range between 3.50 and 5.83 psi/mile (Hughes, 1993). However, for those pipelines (short ones) in which pressure drop is of secondary importance, the pipe could be sized based on fluid velocity only. The flow velocity must be kept below maximum allowable velocity to prevent pipe erosion, noise, or vibration problems, especially for gases that may have a velocity exceeding 70 ft/s. In systems with CO_2 fractions of as low as 1%−2%, field experiences indicate that the flow velocity should be limited to less than 50 ft/s because it is difficult to inhibit CO_2 corrosion at higher gas velocities (Kumar, 1987; Arnold and Stewart, 1999).

The recommended value for the gas velocity in the transmission pipelines is normally 40%−50% of the erosional velocity[3] (Mohitpour et al., 2002). As a rule of thumb, pipe erosion begins to occur when the velocity of flow exceeds the value given by Eq. (15.22) (Beggs, 1984):

$$V_e = \frac{C}{\rho_G^{0.5}} \tag{15.22}$$

where V_e is the erosional flow velocity, ft/s; ρ_G is the density of the gas, lb/ft^3; and C is the empirical constant. In most cases, C is taken to be 100. However, API RP 14E (1984) suggested a value of $C = 100$ for a continuous service and 125 for a noncontinuous service. In addition, it suggests that values of C from 150 to 200 may be used for continuous, noncorrosive or corrosion controlled services, if no solid particles are present.

After selecting the appropriate inside diameter for a pipe, it is necessary to determine the pipe outside diameter (wall thickness), which would result in the minimum possible fabrication cost while maintaining pipeline integrity.

15.7.2 COMPRESSOR STATION SPACING

In long-distance gas transmission systems with a number of operating compressors, there is a definite need to optimize the spacing between compressor stations. Compressor station spacing is fundamentally a matter of balancing capital and operating costs at conditions, which represent the planned operating conditions of the transmission system. The process can become somewhat involved and, particularly lengthy as the selection of spacing needs to be designed in such a way to address a capacity ramp-up scenario that will cover not only the initial condition but also the future years associated to the economics of the pipeline. In case of unexpected growth opportunities we can also rely on loop lines that may be a better additional choice to increase capacity even more.

[3]It is recommended that a minimum gas velocity of 10−15 ft/s in the pipeline be maintained so as to minimize surging and to transport sand and other solids.

For a given pipe diameter, the distance between compressor stations may be computed from the gas flow equation, assuming a value of pipeline operating pressure (station discharge pressure) and a next compressor station suction pressure limited to the maximum compression ratio adopted for the project. Ideally, the pipeline should operate as close to MAOP as possible, as high density in the line of the flowing gas gives best efficiency. This would point to the selection of close compressor station spacing but this approach would not be the best economical decision. A decision based on the pipeline economics is the recommended one. Based on the required gas flow, an initial diameter is assumed that results in a reasonable compression ratio (usually around 1.25−1.6 for transmission lines) and gas velocity, and the compressor station spacing is established by setting the maximum discharge pressure at the MAOP. Other diameters are tested and compressor station spacing calculations are performed again. The optimum diameter is determined based on minimizing capital cost and operating cost resulting in a chart (the so-called J curves, because of their shape) that will plot present value of total project cost per transmission capacity, US$/CFD or transportation rate (tarrif) in US$/MMBTU against transmission capacity, MMCFD, based on predefined economic assumptions and risks (Santos and Saliby, 2003). Such assumptions include the economic life of the facility, the required rate of return or discount rate on capital employed and on annual operating expenses incurred over time to a present value.

Fig. 15.5 illustrates J curves for a 1127-mile gas pipeline with MAOP of 1422.34 psig and compression ratio of 1.4. As can be seen, diameter 36″ produces lower cost indexes, US$/CFD, from 1000 to 1200 MMSFD transmission capacity. Markers represent quantity of compressor stations starting with one (that produces the highest cost index) and adding one more as capacity increases dropping cost index up to minimum and then going up again.

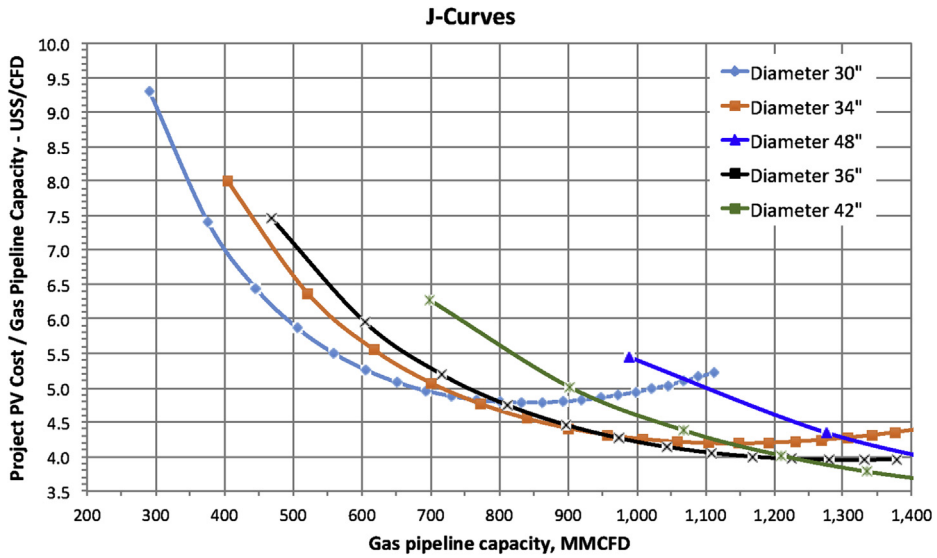

FIGURE 15.5

Typical J curves for a gas pipeline project.

Courtesy of At Work Rio Engineering and Consulting Ltd.

After selecting the best configuration for the project (nominal diameter and compressor stations quantity) next step is to define the capacity buildup. Designer can start from the configuration with maximum capacity with compressor stations already located along the length of the pipeline and then remove gradually compressor stations (e.g. from 14 to 7 then to 4 then to 2 then to 1) keeping compressor spacing equals so as to avoid undesirable bottleneck. This approach will allow a better design and helps defining equipments that would equal. This also allows defining the installation schedule for the compressor stations and compressor units as well.

Gas pipeline feasibility study with its resultant J curves requires detailed technical, economical and operational cost data to be accomplished. Capital expenditures (CAPEX) include costs such as pipe, valves, fittings, compressors, turbines (or electric motors), control and construction and assembly costs. Operating expenditures (OPEX) include all maintenance and supervision, and fuel or energy cost. CAPEX can be derived from past experience and databases. OPEX has to be estimated based on the specific project and past experience. The most significant part of operating costs is fuel or energy and equipment overhaul. Fuel cost is directly related to compressor horsepower. To illustrate how compressor station spacing influences the economics of pipeline operation, a simple model can be set up. This hypothetical pipeline model is based on a system 1000 miles long, operating at a maximum pressure of 1000 psig and flowing 1000 MMscfd. Assuming a uniform pressure loss per unit length of the pipe, and station spacing, the inlet pressure at the first station downstream can be calculated and the horsepower needed to bring the pressure up to the discharge pressure set point. The process is repeated and the total power needed is the sum of all the stations. Fig. 15.6 shows the manner in which total power required increases with spacing of stations. Fig. 15.7 based on the some data shows horsepower in relation to number of stations. We need to keep in mind that even if we have an increase in required power for a pipeline with less compressor stations the overall cost tends to be lower than many compressor stations with lower horsepower requirements. The installed cost per horsepower will be lower for larger compressor units, and thermodynamic performance will be much better pointing to the

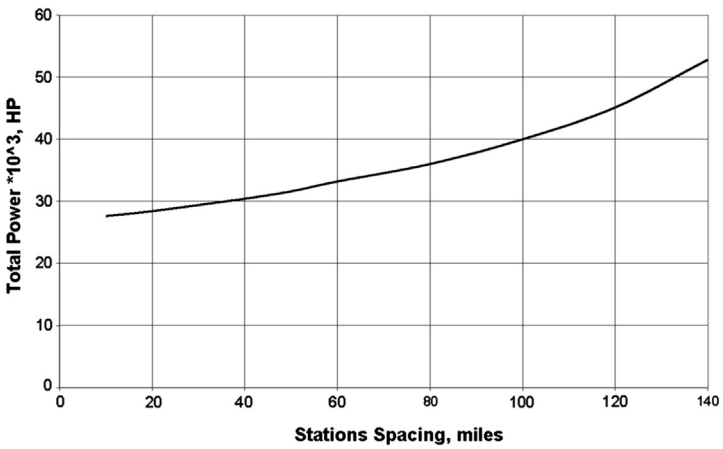

FIGURE 15.6

Effect of the compressor station spacing on total power (Cleveland and Mokhatab, 2005).

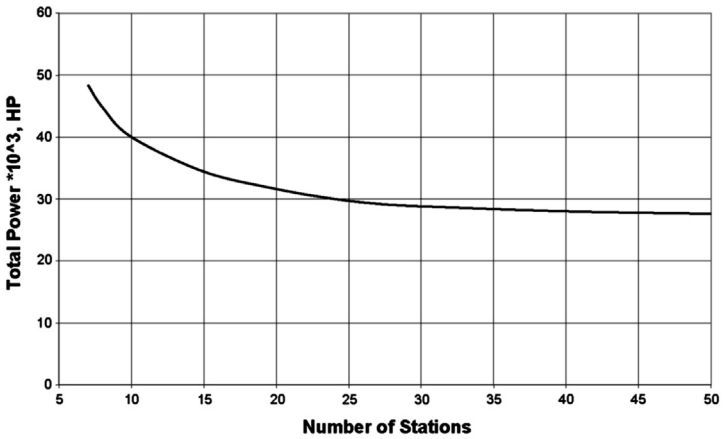

FIGURE 15.7

Effect of the number of compressor stations on total power (Cleveland and Mokhatab, 2005).

direction of having fewer compressor stations with larger compressor units. This explains why an economic evaluation has to be done for each project configuration, taking into consideration all related information in terms of CAPEX and OPEX.

Because fuel use is related to horsepower, minimum operating cost is associated with close compressor station spacing, which is logical because maximum transmission efficiency is obtained at the highest mean line pressure, although the pipeline will have larger diameter requiring higher CAPEX. However, the optimum is influenced by two factors, the first that small turbine compressor units are less efficient than large ones (have a higher specific fuel consumption), although this effect is small and almost negligible at unit powers above 20,000 horsepower. A much greater impact although lies in the cost of the stations and it is this capital cost, which declines as the number of stations is reduced (not linear since large stations are proportionately more costly than small ones). This tends to move the optimum spacing away from the minimum distance shown on Fig. 15.6.

Every project has to be considered individually because of specific factors and the relationship between CAPEX and OPEX that will differ, but the general conclusion that close spacing results in greater transmission efficiency although may not be the best economic selection.

Experience shows that large units (compressor stations) are more efficient than smaller ones because larger centrifugal compressors and gas turbines have better efficiency. However, the impact of unit outage or failure must be simulated under a transient analysis (Santos, 1997) so that we can define the remaining capacity and therefore establish a maintenance criterion in terms of having standby units or spare equipment to allow quick replacing without affecting the contractual obligation in terms of transportation capacity.

When the preferred solution is found it must be tested for robustness not only over the range of throughput anticipated but also for all credible upset conditions. Having developed the optimum solution the result should then be applied to the practical case with elevation changes and other local factors, including the availability of sites, all of which may result in adjustments and minor changes.

15.7.3 COMPRESSION POWER

The next step in the design of a pipeline system is to calculate the maximum power required at the stations and set the design point(s). Typically, a new pipeline system will grow from a low flow condition to the maximum over a period of several years and the decisions on compressors and drivers have to take these changing conditions into account. Growth of flow can be accommodated in several ways. Initially, compressors may only be installed at alternate stations and the intermediate stations built as the growth of flow dictates. Another option is to install one unit at each station location and then add units at the stations as flow increases. On the design phase the capacity ramp-up will determine the installation schedule for the compressor station and also the additional units that will be necessary at the stations. Hydraulic simulators both in steady and transient states will help making an accurate design and will guarantee that the project will have a good performance along the operating years without any unexpected situation. A preselection of the compressor units can also be performed while at the design phase (Santos, 1997). Another important job that can be checked in transient analysis is the pipeline operating points inside the performance maps of the compressors on an early basis so as to allow a proper selection of impellers and number of compressor units as the capacity increases yearly. Different compressor manufacturers can be modeled to check performance and fuel usage. Operations close to surge line or operations that would require recycling would also be identified during transient analysis underlying the importance of doing this kind of simulation on the design phase of a pipeline.

When the compressor design point is decided, the power required from the driver can be calculated using Eq. (11.34).

15.8 PIPELINE OPERATIONS

In the industry supply chain, pipeline operation is an integral part of the transportation between the "upstream end" that precedes it and distribution or the "downstream end" that follows it. Pipeline operation evolved from being prescriptive (i.e., defined by mandatory requirements) to its current stance of being performance based is driven by risk management principles.

These trends stemmed from competitive forces that decrease operating costs; they also have evolved because of the experience gained from several decades of pipeline operations along with the technologies and applications that developed along the way. These evolutions have given pipeline operators the tools they need to survive under these conditions. The pipeline facilities are mature to the point that many of them have exceeded their originally intended design life of approximately 25 years at the time of conception. Today, most of these facilities continue to operate, partly for economic reasons as they are too costly to replace and also partly because these facilities still remain worthy of continued use (i.e., they are still deemed to be safe). Recognizing this, operating companies continue to extract value from these facilities, but under tremendous scrutiny and heightened awareness of their existence and vulnerabilities.

Current pipeline operation activities have taken on a new dimension of performance. While the basic activities continue, such as, mechanical operations and maintenance of the facilities including line pipe, valves, valve actuators, etc., corrosion prevention and control, pipeline monitoring as well as the focus on safety, today optimization of resources is being considered while still achieving safety, reliability, and efficiency. These challenges become more daunting given the fact that these pipeline

systems have expanded and merged, often acquiring systems built by others under different design, construction, and operating philosophies. Further, staff reorganization and attrition saw much of the corporate knowledge and information misfiled or discarded. Some companies remained as free-standing, whereas many became a part of a larger corporate entity. To overcome these developments, pipeline operators now strive for standardization in their procedures and compare their performance with industry benchmarks to gauge their performance and identify areas for improvement.

Certain time-dependent defects such as corrosion and environmental concerns started to manifest themselves in unplanned incidents. Development of other infrastructure at or near pipeline right-of-way saw an increase in third-party incidents and close calls. Pipeline regulators too evolved over these times and increased their vigil over the industry but allowed them to formulate their own facility management programs. Industry-sponsored research programs were founded to better understand the consequential effects of pipeline incidents for risk evaluation.

Consequently, pipeline operation has been transformed toward the following areas of focus:

1. Making effective choices among risk-reduction measures
2. Supporting specific operating and maintenance practices for pipeline subject to integrity threats
3. Assigning priorities among inspection, monitoring, detection, and maintenance activities
4. Supporting decisions associated with modifications to pipelines, such as rehabilitation or changes in service

These focus points require that pipeline operations activities include the following elements (Mokhatab and Santos, 2005):

1. Baseline assessment and hazard identification
2. Integrity assessment by:
   a. In-line inspection
   b. Hydrostatic testing
   c. Direct assessment
   d. Defect management and fitness-for-service
   e. Information management and data integration
   f. Risk management
3. Integrity management programs
4. Operator qualification and training
5. Operating procedures including handling abnormal operating conditions
6. Change management
7. Operating excellence

These elements constitute a broad makeup of pipeline operations. Operators must not only be aware of them but also be well versed in their application, continuously improve them, and incorporate them into a comprehensive and systematic integrity management plan. Combined, these elements form the basis for directing a prevention, detection, and mitigation strategy for their system.

Pipeline operations will be the longest phase of the life cycle of a pipeline when cost management becomes a high priority. This priority will see pipeline operators performing many scenarios of life extension of the existing assets for enhancing value to its stakeholders.

REFERENCES

API RP 14E, April 1984. Design and Installation of Offshore Production Platform Piping Systems, fourth ed. American Petroleum Institute (API), Washington, DC, USA.

Arnold, K., Stewart, M., 1999. Surface production operations, vol. 1: Design of Oil-handling Systems and Facilities, second ed. Gulf Publishing Company, Houston, TX, USA.

Asante, B., October 23–25, 2002. Two-phase flow: accounting for the presence of liquids in gas pipeline simulation. Paper Presented at 34th PSIG Annual Meeting, Portland, OR, USA.

Aziz, K., Ouyang, L.B., 1995. Simplified equation predicts gas flow rate, pressure drop. Oil & Gas Journal 93 (19), 70–71.

Beggs, H.D., 1984. Gas Production Operations. OGCI Publications, Oil & Gas Consultants International Inc, Tulsa, OK, USA.

Brill, J.P., Beggs, H.D., 1991. Two-Phase Flow in Pipes, sixth ed. Tulsa University Press, Tulsa, OK, USA.

Buthod, A.P., Castillo, G., Thompson, R.E., 1971. How to use computers to calculated heat, pressure in buried pipelines. Oil & Gas Journal 69 (10), 57–59.

Campbell, J.M., Hubbard, R.A., Maddox, R.N., 1992. Gas Conditioning and Processing, third ed. Campbell Petroleum Series, Norman, OK, USA.

Cleveland, T., Mokhatab, S., 2005. Practical design of compressor stations in natural gas transmission lines. Hydrocarbon Engineering 10 (12), 41–46.

Colebrook, C.F., 1939. Turbulent flow in pipes with particular reference to the transition region between the smooth and rough pipe laws. Journal of the Institution of Civil Engineers 11, 133–156.

Constantinides, A., Mostoufi, N., 1999. Numerical Methods for Chemical Engineers With MATLAB Applications. Prentice-Hall Inc, New Jersey, NJ, USA.

Edalat, M., Mansoori, G.A., 1988. Buried gas transmission pipelines: temperature profile prediction through the corresponding states principle. Energy Sources 10, 247–252.

Goulter, D., Bardon, M., 1979. Revised equation improves flowing gas temperature prediction. Oil & Gas Journal 77 (9), 107–108.

Hughes, T., 1993. Optimum Pressure Drop Project. Facilities Planning Department Internal Reports, Nova Gas Transmission Limited, Calgary, AB, Canada.

Huntington, R.L., 1950. Natural Gas and Natural Gasoline. McGraw-Hill Book Company, New York, NY, USA.

Ikoku, C.U., 1984. Natural Gas Production Engineering. John Wiley & Sons, Inc., New York, NY, USA.

Kennedy, J.L., 1993. Oil and Gas Pipeline Fundamentals, second ed. PennWell Books, Tulsa, OK, USA.

Kumar, S., 1987. Gas Production Engineering. Gulf Publishing Company, Houston, TX, USA.

Kurz, R., Mokhatab, S., 2007. Considerations on compressor station layout. Pipeline & Gas Journal 234 (9), 22–28.

Kurz, R., Ohanian, S., October 15–17, 2003. Modeling turbomachinery in pipeline simulation. Paper Presented at the 35th PSIG Annual Meeting, Bern, Switzerland.

Kurz, R., Ohanian, S., Lubomirsky, M., June 16–19, 2003. On compressor station layout. ASME Paper GT2003–38019, Paper Presented at the ASME Turbo Expo 2003 Conference, Atlanta, GA, USA.

Maddox, R.N., Erbar, J.H., 1982. Gas Conditioning and Processing: Advanced Techniques and Applications. Campbell Petroleum Series, Norman, OK, USA.

Mohitpour, M., Golshan, H., Murray, A., 2002. Pipeline Design & Construction: A Practical Approach. ASME Press, American Society of Mechanical Engineers (ASME), New York, NY, USA.

Mokhatab, S., Santos, S.P., 2005. Fundamental principles of the pipeline integrity-a critical review. Journal of Pipeline Integrity 4 (4), 227–232.

Mokhatab, S., Santos, S.P., Cleveland, T., 2007. Compressor station design criteria. Pipeline & Gas Journal 234 (6), 26−32.
Mokhatab, S., Lamberson, G., Santos, S.P., 2008. Basic guide to pipeline compressor stations. Pipeline & Gas Journal 235 (6), 60−62.
Moody, L.F., November 1944. Friction factors for pipe flow. ASME Transactions 66, 671−684.
Neher, J.H., 1949. The temperature rise of buried cables and pipes. Transactions of the AIEE 68 (1), 9.
Norsok Standard, September 1996. Common Requirements: Process Design. P-CR-001, Rev. 2. Norwegian Petroleum Industry, Norway.
Nikuradse, J., July/August 1933. Stromungsgesetze in rauhen rohren. Forschungsheft, Vol. B. VDI Verlag, Berlin, Germany.
Osiadacz, A.J., Chaczykowski, M., May 12−14, 2010. Verification of transient gas flow simulation model. Paper Presented at the 41st PSIG Annual Meeting, Bonita Springs, FL, USA.
Ouyang, L.-B., Aziz, K., 1996. Steady state gas flow in pipes. Journal of Petroleum Science and Engineering 14, 137−158.
Santos, S.P., October 15−17, 1997. Transient analysis − a must in gas pipeline design. Paper Presented at 29th PSIG Annual Meeting, Tucson, AZ, USA.
Santos, S.P., October 28−30, 2000. Series or parallel − tailor made design or a general rule for a compressor station arrangement?. Paper Presented at 32nd PSIG Annual Meeting, Savannah, GA, USA.
Santos, S.P., October 20−22, 2004. Series or parallel arrangement for a compressor Station? - a recurring question that needs a convincing answer. Paper Presented at the 36th PSIG Annual Meeting, Palm Springs, CA, USA.
Santos, S.P., Mokhatab, S., 2008. Transient simulation during gas pipeline design saves on later costs. Pipeline & Gas Journal 235 (1), 28−32.
Santos, S.P., Saliby, E., October 15−17, 2003. Compression service contract − when is it worth?. Paper Presented at the 35th PSIG Annual Meeting, Berne, Switzerland.
Schlichting, H., 1979. Boundary Layer Theory, seventh ed. McGraw-Hill Book Company, New York, NY, USA.
Schroeder, D.W., October 17−19, 2001. A tutorial on pipe flow equations. Paper Presented at 33rd PSIG Annual Meeting, Salt Lake City, UT, USA.
Smith, R.V., 1990. Practical Natural Gas Engineering, second ed. PennWell Books, Tulsa, OK, USA.
Streeter, V.L., Wylie, E.B., 1979. Fluid Mechanics. McGraw-Hill Book Company, New York, NY, USA.
Towler, B.F., Pope, T.L., 1994. New equation for friction factor approximation developed. Oil & Gas Journal 92 (14), 55−58.
Towler, B.F., Mokhatab, S., 2004. New method developed for siting line heaters on gas pipelines. Oil & Gas Journal 102 (11), 56−59.
Uhl, A.E., 1965. Steady Flow in Gas Pipelines. IGT Report No. 10. Institute of Gas Technology (IGT), Chicago, IL, USA.
Weymouth, T.R., 1912. Problems in natural gas engineering. Transactions of the ASME 34. Reference No. 1349.
Zagarola, M.V., 1996. Mean Flow Scaling of Turbulent Pipe Flow (Ph.D. thesis). Princeton University, Princeton, NJ, USA.

CHAPTER

NATURAL GAS MEASUREMENT 16

16.1 INTRODUCTION

The purposes of measurement in the natural gas transportation and processing industry include the following: custody transfer, production allocation, revenue generation, operational cost recovery, inventory measurement, process control, and regulatory reporting (Mohitpour et al., 2010). Flow measurement is required throughout the supply chain and the appropriate instruments to make those measurements vary (Hackett, 2016).

Fiscal measurements may be required for allocation purposes where the transfer is not under a contract or for custody transfer where there is a contractual obligation. Custody transfer contracts may require adherence to performance standards. Typical standards include the American Gas Association (AGA), American Petroleum Institute (API), International Organization for Standardization (ISO), and others. A small percentage of inaccuracy can mean millions of dollars in value.

Natural gas is usually measured by volume and expressed in standard cubic feet or normal cubic meters. A standard cubic foot of gas is the amount of gas needed to fill a volume of one cubic foot under standard conditions of 1 atm pressure and 60 degrees Fahrenheit. To measure larger amounts of natural gas, a "therm" is used to denote 100 cubic feet, and "mcf" is used to denote 1000 cubic feet.

To provide greater accuracy in comparing fuels, energy content is measured in terms of "British Thermal Units (BTUs)." A BTU is the amount of heat required to raise one pound of water (approximately a pint) 1°Fahrenheit.

Natural gas energy flow measurement is a count of combustible molecular bonds that pass a given location in time. Such a direct approach, however, is not the traditional approach, nor necessarily the most feasible approach. Energy flow rate may also be represented as the product of flow rate (mass or volume per unit time) and heating value (combustible value per unit mass or volume) (Behring et al., 1999).

The purpose of this chapter is to introduce common measurement technologies for natural gas and natural gas liquids. Methods for energy measurement and the advantages of mass-based energy flow are discussed. Different approaches to volumetric flow rates are presented in addition to flow meter performance metrics, meter proving objectives and flow meter management. Determination of heating value and Wobbe Index is reviewed. Compositional measurements are also briefly discussed.

Handbook of Natural Gas Transmission and Processing. https://doi.org/10.1016/B978-0-12-815817-3.00016-2

16.2 ENERGY MEASUREMENT

The natural gas industry has historically measured the value of gas for custody transfer by referencing flow rate (Q_v) and heating value (H_v) to arbitrary standard volume flow conditions (for example, 14.73 psia and 60°F). When energy flow rate (Q_{energy}) is computed, this arbitrary reference condition cancels, leaving the product of mass-based flow rate (Q_m) and mass-based heating value (H_m) (Behring et al., 1999):

$$Q_{energy} = Q_{v,std} * H_{v,std} = \frac{Q_m}{\rho_{std}} * \rho_{std} H_m = Q_m * H_m \tag{16.1}$$

The standard gas density (density calculated at a standard reference pressure and temperature), ρ_{std}, is a function of the flowing gas composition only and is not a thermodynamic property. Mass flow rate through a volume-based meter is the product of measured volume flow rate and gas density (Behring et al., 1999):

$$Q_{energy,volume-based} = Q_m * H_m = \rho \ \ Qv * H_m \tag{16.2}$$

If a differential pressure producer such as an orifice meter is used, then mass flow rate is nominally proportional to the square root of gas density (Behring et al., 1999):

$$Q_{energy,differential-based} = Q_m * H_m = C\sqrt{\rho} * H_m \tag{16.3}$$

where C is the factor that includes the dependence of all other orifice measurement variables (pressure drop, orifice bore diameter, meter tube diameter, isentropic exponent, and viscosity.

If a mass-based meter such as a Coriolis meter is used, then mass flow rate is determined without reference to gas density:

$$Q_{energy,mass-based} = Q_m * H_m \tag{16.4}$$

16.2.1 ADVANTAGES OF MASS-BASED ENERGY FLOW

Gas composition is traditionally measured through the collection of gas samples (using either spot, online or composite sampling techniques) that are analyzed by gas chromatography (GC). Composition uncertainty through gas density makes volume-based meters more sensitive to composition measurement errors because mass flow rate through a volume-based meter is proportional to density.

Mass-based meters are least sensitive to composition errors because no thermodynamic properties must be measured to determine energy flow rate. Mass-based meters only require knowledge of the mass-based heating value, which depends only on gas composition and is a weak function of hydrocarbon composition.

The mass-based heating value, H_m [Btu/lbm], is a weak function of hydrocarbon composition because the energy released per unit mass is nearly equivalent to the energy released per unit molecular bond for normal paraffins. Energy released by combustion of a carbon−hydrogen bond from methane (C_1) is similar to that of a carbon−hydrogen bond from n-decane (C_{10}), so there is little variation in heating value of natural gas hydrocarbons on a mass basis. This point is demonstrated by two vastly different gas mixture compositions shown in Table 16.1.

Table 16.1 Composition Dependence of Mass-Based Heating Value (Behring et al., 1999)

Gas Component	Gas Mixture#1 [Mole%]	Gas Mixture#2 [Mole%]
Methane	95.58	65.97
Ethane	2.037	10.16
Propane	0.381	8.32
i-butane	0.0728	2.21
n-butane	0.0652	6.53
i-pentane	0.0343	1.90
n-pentane	0.0265	2.32
n-hexane	0.0216	0.534
n-heptane	0.0153	0.190
n-octane	0.0112	0.084
n-nonane	0.0051	0.021
n-decane	0.000	0.011
Carbon dioxide	0.750	0.750
Nitrogen	1.00	1.00
Total	100.00	100.00
$H_{v,std}$ [Btu/scf][a]	1025	1566 (+53%)
ρ_{std} [lbm/scf][a]	0.04474	0.07130
H_m [Btu/lbm]	22,910	21,960 (−4%)

[a]*Standard temperature and pressure are taken to be 60°F and 14.73 psia.*

As seen in Table 16.1, even though the standard volumetric heating values of the mixtures differ by 53% (1566 Btu/scf compared with 1025 Btu/scf), the mass-based heating value varies by only 4% (21,960 Btu/lbm compared with 22,910 Btu/lbm). In this particular example the mass-based heating value is much less sensitive than the standard volumetric heating value to the variations in hydrocarbon composition.

The diluent concentrations (carbon dioxide and nitrogen) are kept constant in the example of Table 16.1, while the hydrocarbon concentrations were varied. This is important because the diluents contribute mass to the mixture but provide no heating value. If the diluent concentrations had varied, greater differences might have been seen. Whereas diluent gases dilute $H_{v,std}$ directly, and their impact on H_m varies, depending on their proximity to the mixture molecular weight. For example, a natural gas mixture with 1 mol% helium has a higher heating value, per unit mass, than a gas mixture with 1 mol% nitrogen; the mixture containing helium has a smaller mass fraction of diluents. So if the diluents remain constant, as in Table 16.1, the heating value per unit mass changes very little, even when the hydrocarbon composition varies significantly (Behring et al., 1999).

If a mass-based flow meter is used to measure energy flow rate, then the only remaining measurement requirement would be H_m, which is principally a function of the diluent concentration of the natural gas. As long as the diluent concentration remained relatively constant, then H_m could likely be measured very infrequently, using a spot sampling and analysis approach. Greater confidence could be

gained if the diluent concentrations were measured online or were inferred by measurement of some other property. A full composition assay would likely be unnecessary since H_m is a weak function of hydrocarbon composition. If any other flow meter (orifice, ultrasonic, turbine, rotary, diaphragm, etc.) is used to measure energy flow rate, then thermodynamic property measurement (principally gas density) becomes a critical issue.

16.3 VOLUME MEASUREMENT

Fluid meters measure either quantity by positive displacement or rate of flow by inference. All fluid meters, regardless of type, consist of a primary element, which is in contact with the fluid, and a secondary element that translates the interaction between the fluid and primary element into a signal that can be converted into volume, weights or rates of flow (Daniel Measurement and Control Inc, 2017).

Selection of the particular measurement device should consider the following (Kumar, 1987):

- Flowing fluid characteristics
- Maximum and minimum range of flow rate
- Range of flow temperature and pressure
- Purpose of measurement (control or fiscal)
- Accuracy
- Reliability
- Installation requirements
- Maintenance requirements
- Life cycle operating cost

16.3.1 QUANTITY METERS

Quantity meters are also classified as positive displacement. Some of the more common positive displacement meters are as follows: reciprocating piston, rotating piston, nutating disk, sliding and rotating vanes, gear and lobed impeller, and the meter most commonly used to sell small quantities of gas at relatively low flow rates, the bellows meter (Daniel Measurement and Control Inc, 2017).

In the reciprocating or rotating piston meter as shown in Fig. 16.1 the fluid enters through an inlet port. The port leads to a precisely measured gap created by a piston in a round chamber. As the piston oscillates around the chamber by mechanical or magnetic means, each stroke displaces an exact volume of fluid.

A nutating disc flow meter as shown in Fig. 16.2 has a round disc mounted on a spindle in a cylindrical chamber. The disk is oscillated around the axis of the cylinder by the fluid flow, and each rotation represents a finite amount of fluid transferred. By tracking the movements of the spindle, the flow meter determines the number of times the chamber traps and empties fluid. This information is used to determine flow rate.

A rotary or sliding vane meter as shown in Fig. 16.3 contains a circular rotor mounted inside a round compartment that holds a number of sliding vanes. The vanes isolate fixed volumes of fluid between the rotor and the wall of the compartment. The center of the rotor is offset from that of the

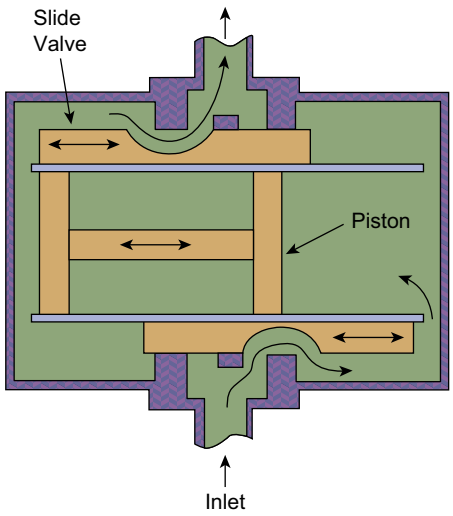

FIGURE 16.1

Reciprocating piston meter.

Source: Omega Engineering.

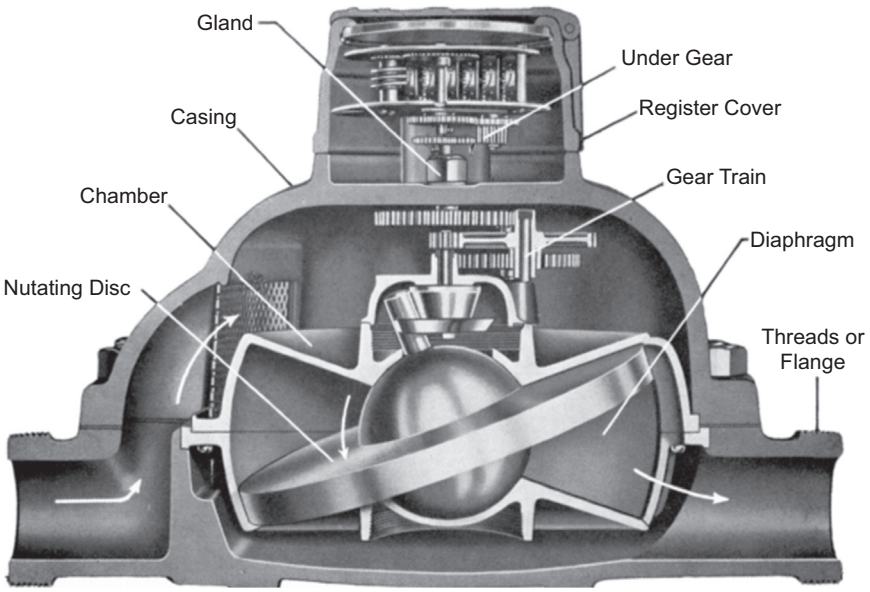

FIGURE 16.2

Nutating disc flow meter.

Source: Protorit.

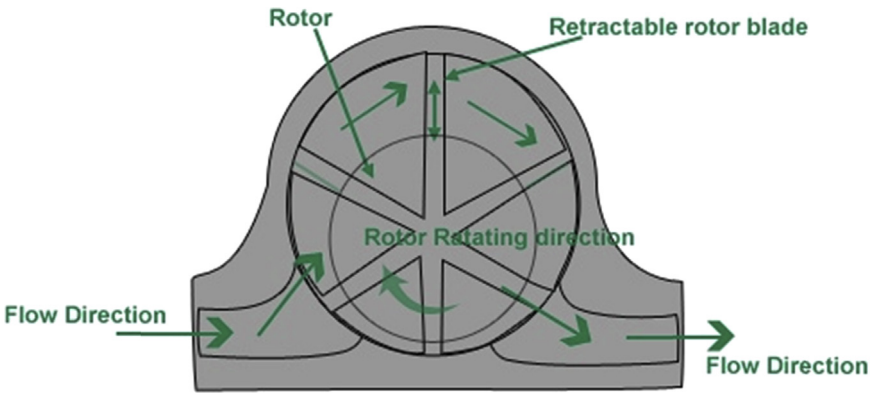

FIGURE 16.3

Rotary vane meter.

Source: Chipkin Automation Systems.

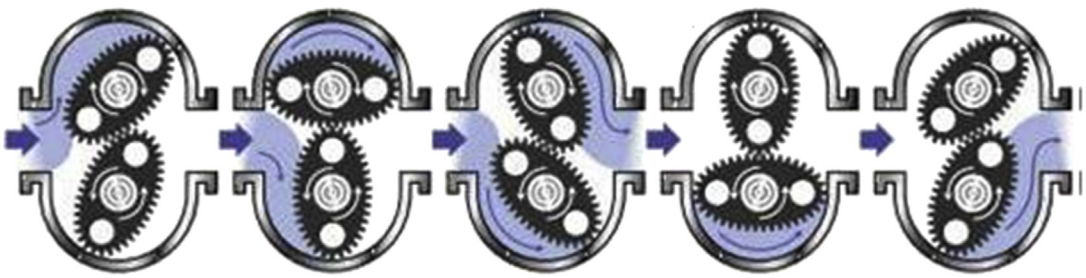

FIGURE 16.4

Oval gear meter.

Source: Badger Meter, Inc.

compartment to keep the rotor in constant contact with the wall of the compartment opposite to that of the pockets to prevent backwashing.

Lobed or gear impeller flow meters, as shown in Fig. 16.4, consist of two impellers rotating in opposite directions due to the forces exerted by the measured gas flow. The placement of the impellers prevents contact while the gap between them remains the same. A gear drive synchronizes the impellers. The number of rotations is proportional to the flow.

Bellows are the most common type of gas meters, seen in almost all residential and small commercial installations (Fig. 16.5). Within the meter, there are two or more chambers formed by movable diaphragms (refer to Fig. 16.6). The gas flow is directed by internal valves to alternately fill the chambers and expel gas producing a near continuous flow through the meter. As the diaphragms expand and contract, levers connected to cranks convert the linear motion of the diaphragms into rotary motion of a crank shaft that serves as the primary flow element. This shaft can drive an odometer-like counter mechanism, or it can produce electrical pulses for a flow computer.

FIGURE 16.5

Residential gas meter.

Source: American Meter Company.

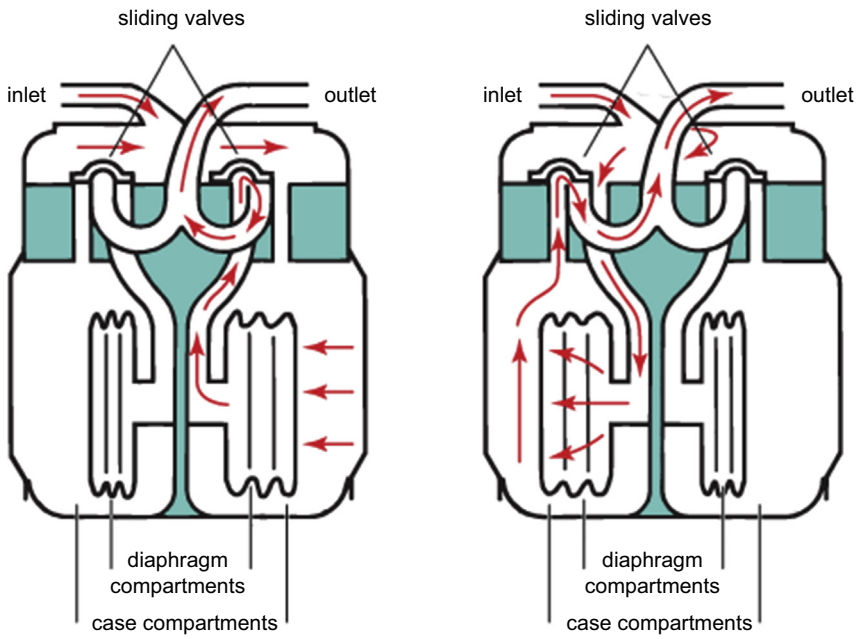

FIGURE 16.6

Bellows meter operations.

Source: American Meter Company.

16.3.2 RATE OF FLOW METERS

Rate of flow (inferential) meters include the following: orifice plates, flow nozzles, venturi tubes, pitot tubes, turbine meters, mass flow meters, ultrasonic flow meters, swirl meters, vortex shedding meters, and rotameters.

Thin, concentric orifice plates are the most commonly used rate of flow meter. Flow nozzles and venturi tubes are primary rate devices that will handle about 60% more flow than an orifice plate for the same bore under the same conditions. If a differential limit is chosen, then a smaller bore nozzle or venturi may be used to measure the same flow. They are more expensive to install and do not lend themselves to as easy size change or inspection as orifice plates.

16.3.2.1 Turbine Meters

For a turbine meter as shown in Fig. 16.7, the primary element is kept in rotation by the linear velocity of the stream in which it is immersed. As the fluid passes over the diffuser section, it is accelerated onto a multi-blade hydrodynamically balanced turbine rotor. The rotor speed is proportional to the volumetric flow rate. As the rotor turns, a mechanical or electronic device mounted on the meter senses the passage of each blade tip and in turn generates a sine wave output with frequency directly proportional to the flow rate (API, 2000a).

Turbine meters are well suited to delivery points due to their accuracy over a wide range. The meter can be damaged form a slug of liquid. They must be calibrated for custody transfer applications and must be proved.

16.3.2.2 Mass Flow Meters

A mass flow meter measures mass flow rate of a fluid traveling through a tube past a fixed point per unit time. Volumetric flow rate is the mass flow rate divided by the fluid density. Actual density can be

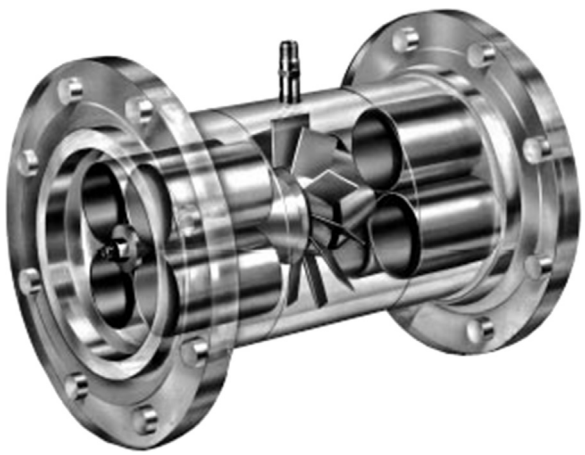

FIGURE 16.7

Turbine meter.

Source: GlobalSpec.

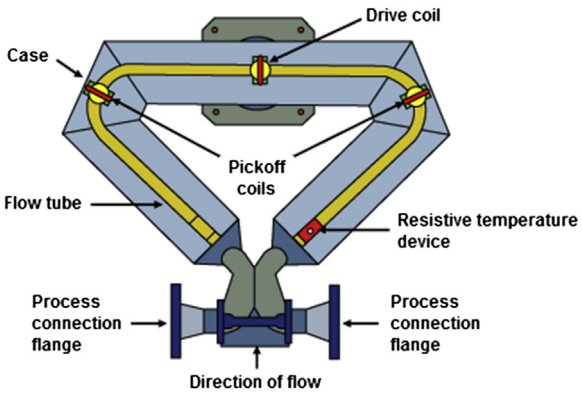

FIGURE 16.8

Coriolis meter.

Source: Emerson Micro Motion.

determined due to dependency of sound velocity on the controlled liquid concentration. Coriolis is the predominate form of mass flow meter.

Coriolis mass flow meters as shown in Fig. 16.8 measure the force resulting from the acceleration or inertia caused by mass moving in relation to a center of rotation. The amount of twist generated by a vibrating tube in which the fluid flows is proportional to its mass flow rate. Sensors are used to measure the twist, and a transmitter generates a linear flow signal.

The cost is high, especially for line sizes above four inches. Pressure drop can be a consideration for "U" shaped tube designs and high viscosity fluids. If the pressure drop is acceptable, operate a Coriolis mass flow meter in the upper part of its flow range because operation at low flow rates can degrade accuracy. For liquid flows, make sure that the flow meter is completely full of liquid. Pay special attention to installation because pipe vibration can cause operational problems.

The mass flow (Q_m) of a u-shaped Coriolis flow meter is given as:

$$Q_m = \left(\left(K_u - I_u\omega^2\right)/2K_d^2\right) * \tau \tag{16.5}$$

where K_u is the temperature-dependent stiffness of the tube, K the shape-dependent factor, d the width, τ the time lag, ω the vibration frequency, and I_u the inertia of the tube. As the inertia of the tube depends on its contents, knowledge of the fluid density is needed for the calculation of an accurate mass flow rate.

If the density changes too often for manual calibration to be sufficient, the Coriolis flow meter can be adapted to measure the density as well. The natural vibration frequency of the flow tubes depend on the combined mass of the tube and the fluid contained in it. By setting the tube in motion and measuring the natural frequency, the mass of the fluid contained in the tube can be deduced. Dividing the mass on the known volume of the tube gives us the density of the fluid.

An instantaneous density measurement allows the calculation of flow in volume per time by dividing mass flow with density.

16.3.2.3 Orifice Meters

Either a volumetric or mass flow rate may be inferred with an orifice meter depending on the calculation associated with the orifice plate. It uses Bernoulli's principle which states that there is a relationship between the pressure of the fluid and the velocity of the fluid. When the velocity increases, the pressure decreases and vice versa. The pressure drop is measured using a differential pressure sensor, and when calibrated, this pressure drop becomes a measure of flow rate.

An orifice meter is an easy method to measure single-phase, continuous flow rates in large pipes and is relatively inexpensive. It has predictable characteristics and occupies a relatively small space (see Fig. 16.9).

An orifice only works well when supplied with a pseudo-fully developed flow profile. This is achieved by an upstream straight pipe length of 20–40 pipe diameters, depending on Reynolds number, or the use of a flow conditioner to eliminate swirl and nonsymmetry.

Orifice plates are small and inexpensive but have higher pressure loss than a venturi. Venturis require much less straight pipe upstream. A venturi meter is usually more expensive and less accurate than an orifice plate.

Some other limitations and considerations include the following:

- The vena contracta length depends on the roughness of the inner wall of the pipe and sharpness of the orifice plate.
- Overall pressure loss varies from 40% to 90% of the differential pressure.
- Flow conditioners or straightening vanes may be required upstream to obtain laminar flow conditions.
- Suspended fluids can clog the orifice.
- Corrosion of the orifice plate may cause inaccuracy.
- The orifice plate has low physical strength.

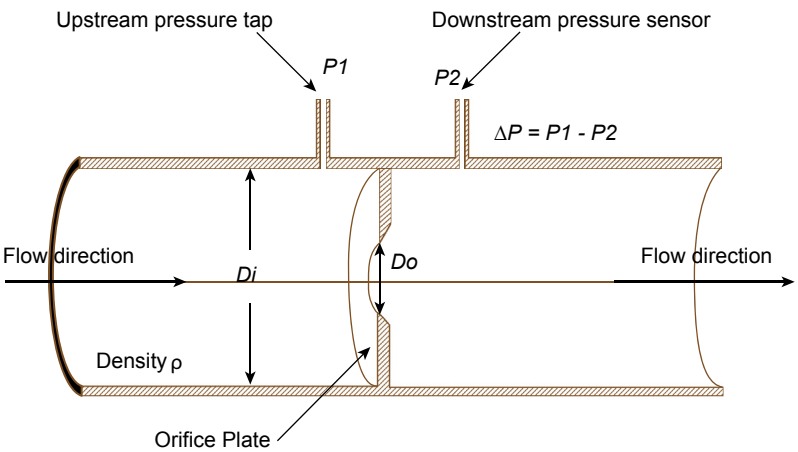

FIGURE 16.9

Orifice meter.

Source: eFunda.

The main parts of an orifice flow meter are as follows:

- A stainless steel orifice plate which is held between flanges of a pipe carrying the fluid.
- It should be noted that for a certain distance before and after the orifice plate, the pipe should be straight in order to maintain laminar flow conditions.
- Openings are provided at two places for attaching a differential pressure sensor.

The fluid having uniform cross section of flow converges upstream of the orifice plate's opening. When the fluid exits the orifice plate's opening, its cross section is minimum and uniform for a particular distance and then the cross section of the fluid starts diverging.

At the upstream of the orifice, before the converging of the fluid takes place, the pressure of the fluid is maximum. As the fluid starts converging to enter the orifice opening, its pressure drops. When the fluid exits the orifice opening, its pressure is minimum, and this minimum pressure remains constant in the minimum cross section area of fluid flow at the downstream. This minimum cross sectional area of the fluid obtained at downstream from the orifice edge is called vena contracta. The differential pressure sensor records the pressure difference which becomes an indication of the flow rate of the fluid through the pipe.

Plates are commonly made with sharp-edged (also referred to as square-edged) circular orifices. The edges may be rounded or conical, the plate may have an orifice the same size as the pipe except for a segment at top or bottom which is obstructed, the orifice may be installed eccentric to the pipe, and the pressure tappings may be at other positions. Each combination gives rise to different coefficients of discharge which can be predicted so long as various conditions are met, conditions which differ from one type to another (Miller, 1996).

Flow rates through an orifice plate can be calculated without specifically calibrating the individual flow meter so long as the construction and installation of the device complies with the stipulations of the relevant standard or handbook. The calculation takes account of the fluid and fluid conditions, the pipe size, the orifice size, and the measured differential pressure; it also takes account of the coefficient of discharge of the orifice plate, which depends upon the orifice type and the positions of the pressure tappings. With local pressure tappings, sharp-edged orifices have coefficients around 0.6 to 0.63 (Bean, 1983), while the coefficients for conical entrance plates are in the range 0.73−0.734 and for quarter-circle plates 0.77 to 0.85 (Miller, 1996). The coefficients of sharp-edged orifices vary more with fluids and flow rates than the coefficients of conical entrance and quarter-circle plates, especially at low flows and high viscosities.

The volumetric flow rate for an incompressible fluid is given by:

$$\mathrm{Q_v} = C_d * A_2 \Big/ \sqrt{\left(1 - ((A_2)/(A_1))^2\right) * \sqrt{2 * \frac{(P_1 - P_2)}{\rho}}} \tag{16.6}$$

where $\mathrm{Q_v}$ is the volumetric flow rate, C_d is the discharge coefficient, A_1 is the cross sectional area of pipe, A_2 is the cross sectional area of orifice, P_1 is the upstream pressure, P_2 is the downstream pressure, and ρ is the fluid density.

The mass flow rate for an incompressible fluid is:

$$\mathrm{Q_m} = \mathrm{Q_v} * \rho = \mathrm{Q_v} = C_d * A_2 \Big/ \sqrt{1 - ((A_2)/(A_1))^2} * \sqrt{2\rho * (P_1 - P_2)} \tag{16.7}$$

For compressible fluids such as gases or steam, an expansion factor (Y) is also calculated. The expansion factor corrects for the density change between the measured tap density and the density at the plane of the orifice face. This factor is primarily a function of the ratio of the measured differential pressure to the fluid pressure and can vary significantly as the flow rate varies, especially at high differential pressures and low static pressures.

$$Q_v = C_d * Y * A_2 \Big/ \sqrt{\left(1 - ((A_2)/(A_1))^2\right)} * \sqrt{2 * \frac{(P_1 - P_2)}{\rho}} \tag{16.8}$$

$$Q_m = C_d * Y * A_2 \Big/ \sqrt{\left(1 - ((A_2)/(A_1))^2\right)} * \sqrt{2\rho * (P_1 - P_2)} \tag{16.9}$$

The coefficient of discharge has been empirically determined for flange-tapped orifice meters. To accurately use these coefficients, the orifice meter must be manufactured to the specifications of the API (API, 2000b). Basically the coefficient of discharge depends on the Reynolds number, sensing tap location, meter tube diameter and orifice diameter with some other smaller influences.

Once the orifice plate is designed and installed, the flow rate can often be measured with high certainty simply by taking the square root of the differential pressure across the orifice's pressure tappings and applying an appropriate constant. Even compressible flows of gases that vary in pressure and temperature may be measured with acceptable certainty by merely taking the square roots of the absolute pressure and/or temperature, depending on the purpose of the measurement and the costs of ancillary instrumentation.

The overall pressure loss caused by an orifice plate is less than the differential pressure measured across tappings near the plate. For sharp-edged plates, it can be approximated by the below equation:

$$\text{Overall pressure loss} = (1 - d/D) * \Delta P \tag{16.10}$$

where d is the orifice diameter, D is the pipe diameter, and ΔP is the pressure drop across orifice.

16.3.2.4 Venturi Meters

Venturi meters consist of a short length of pipe shaped similar to a vena contracta, which fits into a normal pipe line (Fig. 16.10). The obstruction caused to the flow of liquid at the throat of the venturi produces a local pressure drop in the region that is proportional to the rate of discharge. This phenomenon, using Bernoulli's equation, is used to calculate the rate of flow.

Venturi meters have the following characteristics:

- Theoretically there is no restriction to the flow down the pipe.
- They can be manufactured to fit any required pipe size.
- The temperature and pressure within the pipe do not affect the meter's accuracy.
- There are no moving parts.
- The accurate shape required makes them relatively expensive to manufacture.

For the above arrangement shown in Fig. 16.10, the quantity flowing is given by:

$$Q = K\sqrt{h_1 - h_2} \tag{16.11}$$

where the constant K is specific to a particular meter and will include an allowance for a coefficient of discharge.

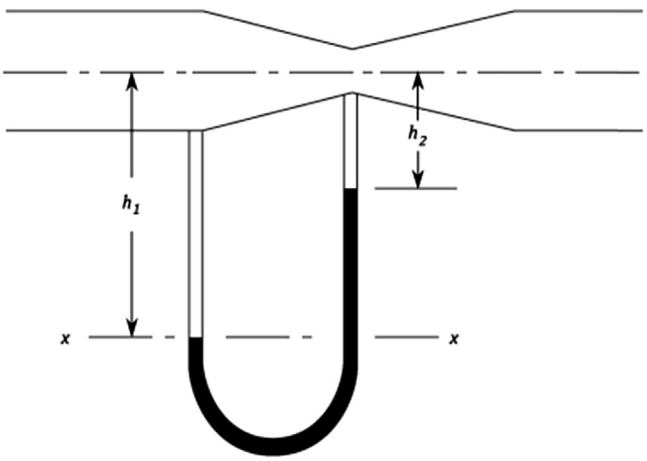

FIGURE 16.10

Venturi meter.

Source: CodeCogs.

Because of fluid resistance, the actual flow is less than that predicted by Eq. (16.11). A coefficient of discharge is therefore introduced, which is usually between 0.96 and 0.99.

16.3.2.5 Ultrasonic Meters

An ultrasonic flow meter as shown in Fig. 16.11 measures the velocity of a fluid to calculate volume flow. The flow meter can measure the average velocity along the path of an emitted beam of ultrasound by averaging the difference in measured transit time between the pulses of ultrasound propagating into and against the direction of the flow or by measuring the frequency shift from the Doppler effect. Ultrasonic flow meters are affected by the acoustic properties of the fluid and can be impacted by

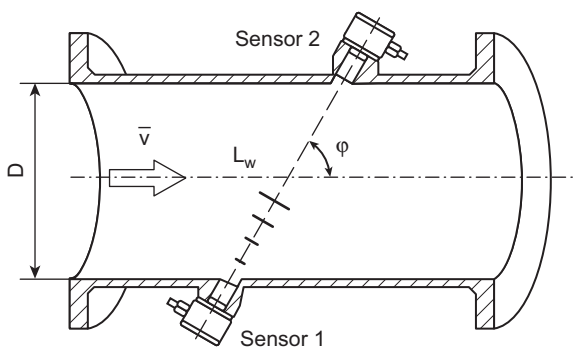

FIGURE 16.11

Ultrasonic flow meter.

Source: Krohne.

temperature, density, viscosity and suspended particulates. They are often inexpensive to use and maintain because they do not use moving parts, unlike mechanical flow meters.

Ultrasonic flow meters measure the difference of the transit time of ultrasonic pulses propagating in and against flow direction. This time difference is a measure for the average velocity of the fluid along the path of the ultrasonic beam. By using the absolute transit times, both the averaged fluid velocity and the speed of sound can be calculated. The average velocity, v, can be calculated using the upstream transit time, τ_1, downstream transit time, τ_2, the diameter of the pipe, D, and the inclination angle, φ, with the following equation (Hofman, 2000):

$$v = D/\sin(2\varphi) * (\tau_1 - \tau_2)/(\tau_1 * \tau_2) \tag{16.12}$$

Flow rate, Q, is determined from the mean flow velocity. In a pipeline with circular cross-section the following applies:

$$Q = \pi D^3/4\sin(2\varphi) * (\tau_1 - \tau_2)/(\tau_1 * \tau_2) \tag{16.13}$$

16.3.2.6 Other Meters

A pitot or impact tube uses the difference between the static and kinetic pressures at a single point. A similar device which is in effect a multiple pitot tube, averages the flow profile. Swirl meters, vortex shedding meters, and rotameters are seldom used.

16.3.3 GAS METERING SYSTEMS

The equipment components of a gas metering system include the following:

- Meters
- Temperature measurement devices to measure the flowing gas temperature
- Pressure measurement devices to measure the flowing gas pressure
- Gas analyzers to determine the chemical composition of the gas and calculate its properties, such as its calorific value and specific gravity
- Conversion devices to perform the flow calculations
- Regulators to reduce the pipeline pressure to a metering pressure
- Filters to remove contaminants from the gas stream
- Flow conditioning devices to remove any swirl in the gas stream caused by upstream pipework configurations that could otherwise affect the accuracy of the meter
- Flow restrictors to prevent excess flow through the meter
- Isolation valves to allow for meter removal
- Indexes and gauges to allow instruments and conversion devices to display measurements and indicate the quantity of gas measured

16.3.4 FLOW METER PERFORMANCE

All meters and metering systems are subject to inaccuracy and uncertainty. Accuracy is the measure of how close to true or actual flow the meter indication may be. It is expressed as a percent of true volume

for a specific flow range. Uncertainty is related to repeatability and is an estimate of the limits where the true value is expected to lie for a given confidence level.

Manufacturers typically state performance characteristics for flow meters based on a factory calibration utilizing water or other stable fluid. In addition to accuracy, the following performance metrics are usually indicated (Yon et al., 2007):

- Linearity
- Repeatability
- Resolution
- Turndown

Linearity is the percentage deviation of measurement from the meter's minimum flow rate specification to the maximum flow rate specification. Repeatability is the meter's ability to indicate the same reading under the same flow conditions. For custody transfer applications, a meter's repeatability is usually specified to be at least 0.05%. Resolution is a measure of the smallest increment of total flow that can be individually recognized by the meter. Turndown is the meter's flow range capability. The flow range of the meter is the ratio of maximum flow to minimum flow over which the specified accuracy or linearity is maintained. A meter should operate optimally around the midpoint of its rated flow range.

16.3.5 METER PROVING

Each gas or liquid flow meter can be calibrated against a master meter onsite, or in liquid metering applications, by a stationary or portable prover. For pipe sizes below 42″ diameter (1.07 m), on-site provers can be used. Flow meters in larger pipe sizes must be shipped to a calibration facility capable of handling larger meters, unless another means of volumetric calibration can be found.

In master meter proving applications, one flow meter is designated as the flow prover. It must have an accuracy that is about four times better than the meter to be tested. The master meter must also have been calibrated against a primary standard within the past 12 months.

To prove a flow meter, the tested meter is valved in series with the master meter prover. The error between the meter under test and the prover or master meter is used to produce a correction factor. This correction factor is programmed into the flow computing system connected to the meter under test. In a multi-run metering system, each flow meter must be proved in turn. Proving of the meters is done as often as necessary depending on the particular application and contractual obligations.

16.4 FLOW METER MANAGEMENT

Traditionally, most operators perform meter calibrations on a time-based calibration schedule and incur recurring maintenance expense. However, other approaches may be more effective. Risk- and condition-based calibrations are other proven options (Gas Processing News, 2018).

Time-based calibration is device calibration on a specified time interval. Factors such as instrument type, operating conditions, measurement application and manufacturer recommendations are considered when selecting a calibration interval. Risk-based calibration is determined by the degree of financial exposure caused by measurement drift over time weighed against the cost of maintaining the

device. Condition-based calibration uses diagnostic data acquired from the device or measurement system. With increased digitization and the availability of analytical tools, condition-based calibration can be adopted with confidence.

The time-based calibration approach does not consider whether the meter actually requires calibration and may not address severe measurement drift that occurs between calibration intervals. In some cases, there may be no need to calibrate as frequently as the schedule demands. It is likely that the calibration schedule is either too frequent and incurs excessive cost or too infrequent that financial exposure associated with the mismeasurement exceeds the cost of more frequent calibration.

Risk- and condition-based approaches are increasingly used for calibration scheduling. In fiscal metering applications, where the measured fluid has a relatively high value, mismeasurements can be costly. Financial exposure results from the uncertainty that is inherent in all measurement systems. If the flow rate and fluid value are taken into consideration, then the financial exposure is the potential cost associated with the possible mismeasurement of that flow stream. The magnitude of the financial exposure within a system corresponds to the level of drift of the meter.

With the risk-based approach, the optimal time to calibrate a meter is the point at which the financial exposure equals the maintenance cost. With every calibration or verification for a given device, data become available that allows the magnitude and rate of drift to be evaluated. Using this data, drift characteristics for each device are determined.

The alternative approach to risk-based calibration scheduling is the condition-based method. With current automation systems significant amounts of data can be captured and analyzed beyond the basic information pertaining to the flow measurement itself. This is particularly true of modern flow meters, which rely on advanced electronics. Data output from flow meters can be postprocessed to provide insight into the performance of the meter.

An example of this postprocessing method is the ability of most ultrasonic meters to return the speed of sound in addition to the axial velocity of the flow. With this information, deviations in fluid composition, which may affect the estimated flow rate can be determined. Other diagnostics include the following (Gas Processing News, 2018):

- Profile factor
- Profile symmetry
- Swirl
- Crossflow
- Turbulence
- Speed of sound
- Automatic gain
- Signals percentage
- Signal to noise ratio

Differential pressure meters work in wet gas flow conditions, where correlations based on experimental research can allow the gas volume fraction to be established from differential pressure ratios measured at different points within the device. Many meters self-diagnose internal mechanical or electronic issues and can provide substantial insight into the operation of the flow meter. These diagnostics can also provide confidence that the meter is functioning correctly. Therefore, when a meter begins to underperform or deviate from its standard performance, it is possible to recognize and evaluate the nature of the problem.

C00ondition monitoring mitigates potential problems proactively. Nevertheless, diagnostics alone are not enough to ensure flow meter accuracy over long-term use, and calibration remains an essential part of flow measurement system maintenance.

16.5 HEATING VALUE DETERMINATION

GC and calorimetry are the most popular methods for determining heating value of natural gas. Calorimetry is a traditional energy measurement alternative to GC. Unfortunately, the traditional calorimeter makes no effort towards the measurement of gas density, an essential requirement of energy measurement. Additional equipment, such as a densitometer or GC, is also required to provide energy flow rate measurement. GCs have the advantage over calorimeters because a composition assay may be used to compute both heating value and density with the addition of pressure and temperature measurements.

16.5.1 GAS CHROMATOGRAPHY

Gas chromatographs measure composition by first separating a natural gas into its pure gas components and then detecting the concentration of those pure gas components. A gas sample is first collected from a pipe and injected into one or more columns. The columns are constructed from tubing that is packed or coated with adsorbent material. A carrier gas such as helium transports the natural gas sample through the columns, a fixed material adsorbs gas components, then desorbs gas components at different rates. The rate of desorption depends on the molecular structure of the pure gas components. The result is that the gas mixture is separated such that the various pure components are eluted from the columns with different residence times. Once the columns separate the gas mixture, the magnitudes of pure gas component concentrations are sensed at detectors. Field GCs typically use thermal conductivity detectors, whereas laboratory units may also use flame ionization detectors due to their increased sensitivity to hydrocarbons in low concentration.

A trend in the GC market is towards smaller columns and detectors to reduce analysis time and instrument size. A detailed extended natural gas analysis (through C_{10}) may require 45 min to complete. Instruments have been developed that can determine hydrocarbon concentrations through C_{9+} in 3−5 min, although many isomers elute from the columns unseparated. This is not a critical issue in energy flow rate measurement, however, because industry standards for calculating density (AGA, 1994) and heating value (GPA, 1994; GPA, 2014a) are designed for groupings of C_6 isomers, C_7 isomers, etc.

Gas Processors Association (GPA) standards also address similar gaseous mixtures to natural gas (GPA, 2013a). Technical Paper TP-31 published by the GPA (2014b) addresses precision statements calculation for the methods described in GPA Standard 2261 (GPA, 2013a) and GPA Standard 2177 (GPA, 2013b).

Most field GCs measure separated hydrocarbon and diluent concentrations through C_5, then flush C_6 and heavier hydrocarbons to the detector as a single C_{6+} concentration. It is then left to the user to characterize the concentration distribution of the C_{6+}'s. Most field units require electrical power, containment structures for hazardous environments, and the use of specially prepared gas composition standards to calibrate detectors for each targeted pure gas component. In the field, calibration gas

standards may require temperature control equipment if ambient temperatures can fall below the hydrocarbon dew point of the gas mixture.

GCs with modern micro-packed columns provide faster analysis times but are not nearly as instantaneous as calorimeters. A properly calibrated and operated online GC can obtain a repeatability of ±1 Btu/scf for a natural gas with a nominal heating value of 1000 Btu/scf (Kizer, 1998).

16.5.2 CALORIMETRY

A calorimeter provides a very direct way to measure heating value because it burns a gas sample and measures the heat generated. GC along with temperature and pressure or densitometry must complement calorimetry because gas density is needed for energy measurement. Calorimeters measure standard volumetric heating value at low-pressure conditions. If a calorimeter could measure actual volumetric heating value at flowing temperature and pressure or mass heating value then the additional density measurement would be unnecessary for volume-based meters.

An inferential calorimeter also burns a sample of gas in air, but instead of measuring the heat released by combustion, it infers heating value from stoichiometric combustion properties. Because heating value is inferred from online combustion properties, this approach is faster than a GC. Inferential calorimeters also measure standard volumetric heating value (Btu/scf) and require the additional use of a densitometer to determine energy flow rate at a volume-based meter. They may also be suited to measure the mass-based heating value (Btu/lbm) since it is an even less sensitive property of the fuel composition.

One popular inferential calorimeter design fixes the air flow rate delivered to the burner, then correlates sample flow rate to heating value at the stoichiometric condition. A flame temperature sensor is used to provide feedback to regulate fuel flow rate to the flame. Since the stoichiometric condition occurs near a peak flame temperature condition, the fuel flow rate is varied until a peak flame temperature is reached. A high heating value gas will require a lower flow rate than a lower heating value gas to reach the stoichiometric condition. The instrument is calibrated periodically with pure methane gas having a known heating value.

Another popular design maintains the exhaust gas temperature at a fixed level by regulating the air supply to the flame, which is then correlated to heating value. Still another design fixes the air flow rate and infers heating value from exhaust gas temperature.

The accuracy of the inferential calorimeter is about 0.15% and that the reproducibility is approximately ±3.2 Btu/scf (Stern, 1984).

16.6 WOBBE INDEX

The Wobbe number, or Wobbe Index, of a fuel gas is found by dividing the high heating value of the gas in Btu per standard cubic foot by the square root of its specific gravity with respect to air. The higher a gases' Wobbe number, the greater the heating value of the quantity of gas that will flow through a hole of a given size in a given amount of time. It is customary to give a Wobbe number without units even though it has the dimensions Btu per scf, because to do so would lead to confusion with the volumetric heating value of the gas.

In almost all gas appliances, the flow of gas is regulated by making it pass through a hole or orifice. The usefulness of the Wobbe number is that for any given orifice, all gas mixtures that have the same

Wobbe number will deliver the same amount of heat. Pure methane has a Wobbe number of 1363; natural gas as piped to homes in the United States typically has a Wobbe number between 1310 and 1390 (AGA, 2002).

16.7 OTHER COMPOSITIONAL MEASUREMENTS

Other common analyses include the following:

- Inert composition of natural gas such as helium, nitrogen, and carbon dioxide.
- Acid gas composition of natural gas including hydrogen sulfide and carbon dioxide.
- Moisture content of natural gas and natural gas liquids.
- Methane, carbon dioxide, methanol, hydrogen sulfide, aromatics, olefins, volatile sulfur, carbonyl sulfide, sodium, lead, mercury, silicon, arsenic, antimony, phosphorous, and halides content of liquid hydrocarbons.
- Reid vapor pressure of liquids products.

16.8 FLOW COMPUTERS

For custody transfer of natural gas streams, flow computers are usually required to meet contractual obligations. These computers measure, monitor, and may provide control of gas flow for all types of meters. In volumetric flow measurement the different types of meters will read different gas characteristics; the flow computer will receive a signal from the meter plus gas temperature and pressure. Since gas is compressible and affected by temperature, the gas temperature and pressure must also be monitored and compared with a specified standard temperature and pressure within an algorithm that converts the reading into a standard flow rate.

Mass flow is based upon the density of the gas, so computation of the density based on composition is necessary. Based on accurate mass flow calculations, the energy content of each gas component will be used to calculate energy flow. Energy flow metering is the ultimate goal, since natural gas is purchased based on heating value. Also, the reserves may be taxed based upon energy content.

In addition to providing volumetric, mass, and energy flow data, the gas flow computer also provides date and time, instantaneous, hourly, and daily data. The gas flow computer typically stores date/time stamped volume records and uploads to a historian for record keeping.

REFERENCES

AGA, July 1994. Compressibility Factors of Natural Gas and Other Related Hydrocarbon Gases. Transmission Measurement Committee Report No. 8, Second Printing, second ed. American Gas Association (AGA), Washington, DC, USA.

AGA, 2002. Interchangeability of Other Fuel Gases with Natural Gases. Research Bulletin 36. American Gas Association (AGA), Washington, DC, USA.

API, 2000a. Chapter 5 — Measurement of Liquid Hydrocarbons by Turbine Meters, fourth ed. Manual of Petroleum Measurement Standards, American Petroleum Institute (API), Washington, DC, USA.

API, 2000b. Chapter 14-Natural Gas Fluids Measurement: Section 3- Concentric, Square-edged Orifice Meters, Part 2: Specifications and Installation Requirements. Manual of Petroleum Measurement Standards, American Petroleum Institute (API), Washington, DC, USA.

Bean, H.S., April 1983. Fluid Meters: Their Theory and Application, 2nd Printing with Editorial Changes of 6th Edition, Report of ASME Research Committee on Fluid Meters. American Society of Mechanical Engineers (ASME), New York, NY, USA.

Behring, K., Kelner, E., Minachi, A., Sparks, C., Morrow, T., Svedeman, S., 1999. A Technology Assessment and Feasibility Evaluation of Natural Gas Energy Flow Measurement Alternatives. Southwest Research Institute, San Antonio, TX, USA.

Daniel Measurement, Control Inc, February 2017. Fundamentals of Orifice Meter Measurement. White Paper, Houston, TX, USA.

GPA, 1994. Table of Physical Constants of Paraffin Hydrocarbons and Other Components of Natural Gas. Standard 2145−2194. Gas Processors Association (GPA), Tulsa, OK, USA.

GPA, 2013a. Analysis for Natural Gas and Similar Gaseous Mixtures by Gas Chromatography. Standard 2261−13. Gas Processors Association (GPA), Tulsa, OK, USA.

GPA, 2013b. Analysis of Natural Gas Liquid Mixtures Containing Nitrogen and Carbon Dioxide by Gas Chromatography. Standard 2177−13. Gas Processors Association (GPA), Tulsa, OK, USA.

GPA, 2014a. Calculation of Gross Heating Value, Relative Density, Compressibility and Theoretical Hydrocarbon Liquid Content for Natural Gas Mixtures for Custody Transfer. Standard 2172−14. Gas Processors Association (GPA), Tulsa, OK, USA.

GPA, 2014b. GPA 2261 and GPA 2177 Methods Precision Statements Calculation. Technical Bulletin TP-31. Gas Processors Association (GPA), Tulsa, OK, USA.

Gas Processing News, February 2018. Optimize Flowmeter Management for Accuracy and Cost Savings. Gulf Publishing Company, Houston, TX, USA.

Hackett, D., June 2016. Selecting flowmeters for natural gas. Applied Automation, A10-A14.

Hofmann, F., 2000. Fundamentals of Ultrasonic Flow Measurement for Industrial Applications. KROHNE Messtechnik GmbH & Co. KG, Duisburg, Germany.

Kizer, P.E., May 19−21, 1998. Energy measurement using on-line chromatographs. Paper Presented at the International School of Hydrocarbon Measurement, Norman, OK, USA.

Kumar, S., 1987. Gas Production Engineering. Gulf Publishing Company, Houston, TX, USA.

Miller, R.W., 1996. Flow Measurement Engineering Handbook. McGraw-Hill, New York, NY, USA.

Mohitpour, M., Van Hardeveld, T., Peterson, W., Szabo, J., 2010. Pipeline Operation & Maintenance − a Practical Approach, second ed. American Society of Mechanical Engineers (ASME), New York, NY, USA.

Stern, R.E., April 10−12, 1984. Determination of calorific values of natural gas by combustion instruments. Paper Presented at the International School of Hydrocarbon Measurement, Norman, OK, USA.

Yon, M., Warner, K.L., Mooney, T., 2007. Liquid and gas measurement. In: Petroleum Engineering Handbook. Facilities and Construction Engineering, vol. 3. Society of Petroleum Engineers, Richardson, TX, USA.

CHAPTER

GAS PROCESSING PLANT OPERATIONS

17

17.1 INTRODUCTION

A well-designed gas processing plant is not successful until it is operating safely and profitably. This requires a smooth start-up as well as a productive and safe environment for the operations. In order to sustain the operation, good maintenance practices are required. Troubleshooting is invariably required to detect and fix issues that occur when the performance of engineered equipment degrades.

An exhaustive coverage of gas plant operation topics would require an entire book. Therefore, the objective of this chapter is to provide an introduction into commissioning and start-up, control room management, maintenance, and troubleshooting techniques applicable to gas processing plants. Commissioning and start-up activities covered include mechanical completion and precommissioning, control systems testing, initial start-up procedures, process commissioning, and performance testing. Control room management topics focus on areas addressed by the United States Department of Labor Occupational Safety and Health Administration and Department of Transportation. These specific areas include roles and responsibilities, process safety management (PSM) focusing on hazards and operability reviews, fatigue mitigation, alarm management, and training for operational excellence.

17.2 COMMISSIONING AND START-UP

17.2.1 MECHANICAL COMPLETION AND PRECOMMISSIONING

Mechanical completion is the stage of a project between equipment installation and process commissioning. Components of the plant are proven to be mechanically ready for their process duty (Horsley, 1997). This stage of plant commissioning may include some specific performance tests on individual components of the plant. Precommissioning is the stage where process materials are introduced to the plant and any preliminary issues are resolved.

The object of mechanical completion is to prove that each installed component is ready for commissioning. This stage includes:

- checking that equipment is installed correctly,
- proving that equipment operates acceptably for commissioning, and
- demonstrating that instruments, controls, and safety system work.

Much of the work to start the checkout of equipment can be completed at the factory before delivery to the site, and the completion of this work should be encouraged as it has the potential to save

Handbook of Natural Gas Transmission and Processing. https://doi.org/10.1016/B978-0-12-815817-3.00017-4

cost and time if vendor equipment does not perform initially. Activities performed at the factory acceptance test can include leak tests, initial operational runs, control system checkout, cleanliness checks, and test fitting of internals.

Inspection of the equipment is carried out before testing and may require specialists depending on the type of equipment. This inspection assures that the equipment meets the specifications as installed and is complete. Also, assurance is made that the drawings pertaining to this equipment is in as-built status.

Safety and operability checks are keys at this stage including adequacy of access, handrails, drains, vents, etc. Orientation of valves, safety devices, and fire protection equipment are critically inspected. Tests of the component parts are witnessed as acceptable in meeting specifications.

All electrical grounding is checked. Wiring is checked for continuity and insulation resistance. Motors are inspected for correct direction of rotation.

Before pipes and equipment are placed in service, it is important that good cleaning procedures be conducted to help ensure a successful and trouble-free start-up. Often initial plant commissioning is marred by foreign materials that have been left inside pipe work and then find their way to pumps and other equipment, causing significant damage and schedule delay as a result of rectification work. The following methods of cleaning are common to fulfill this task: cleaning by blowing (air or nitrogen), steam blowing, cleaning via flushing (water), chemical cleaning, use of a pipeline integrity gauge (pig), mechanical cleaning, and visual inspection.

Hydrostatic tests are conducted to prove pipe integrity; however, many potential leak path points will still exist in an untested state. The object of a full system leak test is to test all leak potential suitably and practically before the introduction of process and hazardous chemicals.

The necessary laboratory facilities should be verified and laboratory personnel trained to carry out the planned tests. Laboratory testing is critical for plant start-up to monitor raw materials and assure that products meet specifications before delivery to customers.

Sampling points and analyzer equipment must be ready once the plant is in operation.

All required raw materials and chemicals need to be on-site in adequate quantities to satisfy the commissioning and initial start-up time frame.

Finally plant operators should have completed all training to assure that they understand the plant systems, start-up procedures, and response to abnormal situations.

17.2.2 CONTROL SYSTEMS TESTING

Control systems testing, as with all commissioning activities, requires careful planning and coordination. Electrical, instrumentation, process control, process engineering, and computer specialists are required and must work closely together.

Precommissioning of field instruments and factory acceptance testing of the distributed control system (DCS), programmable logic controllers (PLCs), and other computer-based equipment are independent activities. This fact makes it even more critical for a comprehensive site acceptance test of the control systems.

Operator screens, databases, configuration, applications, and communications between computer components can be checked during the factory acceptance test. DCS simulators are available that can generate a wide range of representations of the process for testing, validation, and training purposes. Simple models can be built through the use of transfer functions or physical flow networks. The control

system configuration can be tested in an off-line simulation environment before or after the system has been installed in the field. Special attention should be paid to emergency shutdown and equipment protection logic.

All issues found during factory acceptance testing must be corrected and retested before final acceptance.

Motor control systems, switchgear, and other electrical equipment are often installed in a different location from the DCS.

Inspecting the installation of instruments is critical. Power and air supplies, mounting as well as associated piping, tubing, and wiring should be checked thoroughly. The flow lines should be pressure tested for leakage especially at fittings. Primary sensors must be consistent with the type and range of transmitters. Control and solenoid valves must fail safe and positioners must operate correctly.

Instrumentation is often calibrated by the manufacturer, but needs to checked and recalibrated as necessary on-site. When recalibrating it is important to:

- calibrate over the entire range and set any bias correctly according to specifications,
- use the correct process medium when calibrating analyzers, and
- check all configurable settings.

Full loop tests of communication with field devices to the final actuator will be checked during site acceptance testing.

Documentation of the instrumentation and control systems must reflect as-built conditions. Typical documents include:

- process and instrumentation diagrams,
- loop diagrams,
- interconnection schematics,
- database tables,
- sequential flow diagrams,
- wiring diagrams,
- termination rack layouts,
- tag number reference lists, and
- system and operation manuals.

17.2.3 INITIAL START-UP PROCEDURES

When possible, "safe" chemicals are introduced water, steam, and air to simulate closely the unit in actual operation and to provide an indication of how the plant will perform when the process chemicals are introduced before the main commissioning and start-up event takes place. During commissioning execution, all safety-related systems are checked rigorously, including confirmation of alarm activation points by means of manipulation of the actual process variables; confirmation of the operation of all control system software trip logic by various means, including variability of the process conditions both manually and via the control system; confirmation of all hardwired emergency shutdown systems by various documented operational means; and confirmation of the operation and control of all DCS sequences, including full testing of all failure monitoring. All operating modes are tested, including starting up, scheduled and emergency shutdown, and the actions required after a loss of site services, including power and instrument air. The emergency power generation system must be fully tested.

17.2.4 PROCESS COMMISSIONING

Process commissioning can begin after precommissioning tests are complete and all identified issues are corrected. Plant equipment is placed into normal operation during this phase.

Process commissioning should not commence until the final checklist is reviewed and verified. This list will include:

- all safety equipment are in place and functional,
- emergency procedures are known,
- medical and first aid considerations have been arranged,
- all inspection equipment have been removed,
- test orifices and blanks are removed,
- vents and overflows are not obstructed,
- strainers are cleaned and replaced,
- methanol injection system for hydrate control,
- liquid seals are at correct levels,
- emergency and normal lighting systems are functional,
- rotating equipment guards are in place,
- source of ignition has been removed,
- access for emergency vehicles is clear, and
- all operations documentation are in place.

The typical sequence of commissioning will include:

1. Utilities including:
   a. electrical service,
   b. water and water treatment,
   c. compressed air,
   d. nitrogen,
   e. flare system,
   f. backup fuel gas,
   g. fire water system, and
   h. steam system.
2. Storage tanks for raw materials
3. Catalysts and chemicals
4. Process equipment
5. Product storage
6. Emergency power generator
7. Any ancillary equipment

A system for recording times and stages of the process where samples are taken along with their results will accelerate start-up. Many more analyses than during normal operation are required and the laboratory should be staffed accordingly or third party laboratories contracted. The laboratory results will provide information for initial troubleshooting of equipment and instrumentation.

It is very important that scrubbers, separators, and filters are working satisfactorily before introducing material into the main plant equipment.

Raw materials may be consuming faster than normal during initial commissioning due to charging the system and any process issues encountered. The purchasing department should be advised and ready to schedule delivery for additional raw materials.

Often during start-up, material form the process may not meet product specifications. Considerations should be in place for recycling, disposal, or arrangements with buyers for off-specification material. Also, any environmental impacts should be discussed with the regulatory agencies prior to encountering these issues.

The main objective of process commissioning is to achieve stable and reliable operating conditions while meeting product specifications. Most efficient or higher throughput operating conditions will be explored later.

Often a decision must be made to shut down and correct a problem or whether to continue running and work through or around an issue. This decision must be made carefully taking into account safety and hazards. Most process accidents occur during shutdown and start-up than during normal, continuous operation. However, a specific issue's consequences on safety and hazards may outweigh start-up and shutdown safety concerns.

A list of items to resolve before commissioning is complete will be compiled and handled by the construction contractor. Commissioning is complete once the plant can achieve its intended purpose and can be taken over by operations. The intended purpose and conditions of commissioning completion will be stated in the construction contract. Other items that would improve the operability of the plant that were not included in the construction scope should be documented as future enhancements to the plant.

Following commissioning, the start-up and shutdown procedures should be reviewed and modified based on learnings from the commissioning process. For NGL recovery plants, the cooldown procedure must be strictly followed to avoid thermal stress in the processing equipment, such as the brazed aluminum exchangers.

17.2.5 PERFORMANCE TESTING

Performance tests are carried out with the plant as close to design conditions as possible. If the plant or process has been licensed, the licensor usually guarantees the process. Guarantee tests are witnessed by the licensor or engineering contractor as well as plant operations and engineering personnel.

Raw material and other conditions are generally outlined in the contract and efforts are made to replicate these conditions as closely as possible. Duration of the tests, performance criteria, conditions causing postponements and interruptions, methods of measurement and analysis, and allowable tolerances will usually be stipulated.

Performance criteria may include:

- plant capacity,
- quality of products,
- yields,
- utilities consumption, and
- quantity of emissions.

It is important that a mass and energy balance can be calculated or reconciled within a reasonable tolerance before the performance tests are conducted. All data required to calculate the metrics

dictated by the performance criteria should be accurately captured by the plant historian or otherwise recorded at an acceptable frequency. After collection and processing of the data, some corrections may need to be made for off-design conditions such as feed gas composition, feed temperature and pressure, ambient temperature, etc.

There are often contractual consequences for not meeting the performance criteria including resolution, monetary penalties, and liquidated damages. In cases where performance criteria are not part of the construction contract such as the plant is designed by the operating company, performance tests are usually conducted to document the plant capabilities.

17.3 CONTROL ROOM MANAGEMENT

The activities conducted in control rooms must assure compliance with all federal, state, and local regulations. The most important regulations apply to personnel and process safety as this affects the well-being of plant employees and the public. Two federal regulations that have the great applicability to the safety of natural gas transportation and processing operations are 49 *Code of Federal Regulations* (*CFR*) Parts 192 and 195, Pipeline Safety: Control Room Management/Human Factors as well as 29 CFR Part 1910.119, Process Safety Management of Highly Hazardous Chemicals—Compliance Guidelines and Enforcement Procedures.

The US Department of Transportation Pipeline and Hazardous Materials Safety Administration sponsored 49 CFR Parts 192 and 195. This regulation has been adopted by natural gas processing facilities in the United States as well as other parts of the world. This regulation addresses human factors and other aspects of control room management for pipelines where operators use supervisory control and data acquisition (SCADA) systems. Under the final rule, affected pipeline operators must define the roles and responsibilities of operators and provide operators with the necessary information, training, and processes to fulfill these responsibilities. Operators must also implement methods to prevent operator fatigue. The final rule further requires operators to manage SCADA alarms, assure control room considerations are taken into account when changing pipeline equipment or configurations, and review reportable incidents or accidents to determine whether control room actions contributed to the event (US DOT, 2009).

The United States Department of Labor Occupational Safety and Health Administration (OSHA) first issued 29 CFR Part 1910.119 in 1992. Even prior to the official release major oil and gas companies began compliance with the intent of the regulation. The methods used to comply with this regulation are now well established.

17.3.1 ROLES AND RESPONSIBILITIES

According to 49 CFR, each operating company must define the roles and responsibilities of an operator during normal, abnormal, and emergency conditions. To provide for an operator's prompt and appropriate response to operating conditions, an operating company must define each of the following:

- An operator's authority and responsibility to make decisions and take actions during normal operations;
- An operator's role when an abnormal operating condition is detected, even if the operator is not the first to detect the condition, including the operator's responsibility to take specific actions and to communicate with others;

- An operator's role during an emergency, even if the operator is not the first to detect the emergency, including the operator's responsibility to take specific actions and to communicate with others; and
- A method of recording operator shift changes and any handover of responsibility between operators.

17.3.2 PROCESS SAFETY MANAGEMENT

In each industry, PSM applies to those companies that deal with any of more than 130 specific toxic and reactive chemicals in listed quantities; it also includes flammable liquids and gases in quantities of 10,000 pounds (4535.9 kg) or more (US DOL, 2000).

Subject to the rules and procedures set forth in OSHA's Hazard Communication Standard (29 *CFR* 1910.1200(i)(1) through 1910.1200(i)(12)), employees and their designated representatives must be given access to trade secret information contained within the process hazard analysis (PHA) and other documents required to be developed by the PSM standard.

The key provision of PSM is PHA—a careful review of what could go wrong and what safeguards must be implemented to prevent release of hazardous chemicals. Covered employers must identify those processes that pose the greatest risks and begin evaluating those first.

Methodologies allowed are:

- What-if;
- Checklist;
- What-if/checklist;
- Hazard and Operability Study (HAZOP);
- Failure Mode and Effects Analysis;
- Fault Tree Analysis (FTA); or
- An appropriate equivalent methodology.

The PHA shall address:

- The hazards of the process;
- The identification of any previous incident which had a likely potential for catastrophic consequences in the workplace;
- Engineering and administrative controls applicable to the hazards and their interrelationships such as appropriate application of detection methodologies to provide early warning of releases (Acceptable detection methods might include process monitoring and control instrumentation with alarms, and detection hardware such as hydrocarbon sensors.);
- Consequences of failure of engineering and administrative controls;
- Facility siting;
- Human factors; and
- A qualitative evaluation of a range of the possible safety and health effects of failure of controls on employees in the workplace.

The PHA shall be performed by a team with expertise in engineering and process operations, and the team shall include at least one employee who has experience and knowledge specific to the process being evaluated. Also, one member of the team must be knowledgeable in the specific PHA

methodology being used. At least every 5 years after the completion of the initial PHA, the PHA shall be updated and revalidated by a team meeting these requirements to assure that the PHA is consistent with the current process.

The employer shall establish a system to promptly address the team's findings and recommendations; assure that the recommendations are resolved in a timely manner and that the resolution is documented; document what actions are to be taken; complete actions as soon as possible; develop a written schedule of when these actions are to be completed; communicate the actions to operating, maintenance, and other employees whose work assignments are in the process and who may be affected by the recommendations or actions. Employers shall retain process hazards analyses and updates or revalidations for each process covered by this section, as well as the documented resolution of recommendations for the life of the process.

17.3.3 HAZARD AND OPERABILITY STUDY

A HAZOP study is the predominate methodology used to comply with OSHA's PSM requirements.

The HAZOP analysis technique uses a systematic process to (1) identify possible deviations from normal operations and (2) ensure that appropriate safeguards are in place to help prevent accidents. The HAZOP technique uses special adjectives (such as "more," "less," "no," etc.) combined with process conditions (such as speed, flow, pressure, etc.) to systematically consider all credible deviations from normal conditions. The adjectives, called guide words, are a unique feature of HAZOP analysis.

The characteristics of HAZOP include the following:

- A systematic, highly structured assessment relying on guide words and team brainstorming to generate a comprehensive review and ensure that appropriate safeguards against accidents are in place
- Typically performed by a multidisciplinary team
- Applicable to any system or procedure
- Used most as a system-level risk assessment technique
- Generates primarily qualitative results, although some basic quantification is possible

The most common uses of HAZOP include identifying safety hazards and operability problems of continuous process systems, especially fluid and thermal systems, and reviewing procedures and sequential operations.

There are some limitations of this technique as follows:

1. HAZOP requires a well-defined system or activity. The HAZOP process is a rigorous analysis tool that systematically reviews each part of a system or activity. To apply the HAZOP guide words effectively and to address the potential accidents that can result from the guide word deviations, the analysis team must have access to detailed design and operational information. The process systematically identifies specific engineered safeguards (e.g., instrumentation, alarms, and interlocks) that are defined on detailed engineering drawings.
2. HAZOP is time consuming. The HAZOP process systematically reviews credible deviations, identifies potential accidents that can result from the deviations, investigates engineering and administrative controls to protect against the deviations, and generates recommendations for

system improvements. This detailed analysis process requires a substantial commitment of time from the facilitator and other subject matter experts, such as crew members, engineering personnel, equipment vendors, etc.

3. HAZOP focuses on one-event causes of deviations. The HAZOP process focuses on identifying single failures that can result in accidents. If the objective of the analysis is to identify all combinations of events that can lead to accidents of interest, more detailed techniques should be used such as FTA.

The procedure for performing a HAZOP analysis consists of the following five steps:

1. Define the system or activity. Specify and clearly define the boundaries for which hazard and operability information is needed.
2. Define the problems of interest for the analysis. These may include health and safety issues, environmental concerns, etc.
3. Subdivide the system or activity and develop deviations that will be individually analyzed. Once subdivisions are defined, then apply the HAZOP guide words that are appropriate for the specific type of equipment in each section.
4. Conduct HAZOP reviews. Systematically evaluate each deviation for each section of the system or activity. Document recommendations and other information collected during the team meetings and assign responsibility for resolving team recommendations.
5. Use the results in decision-making. Evaluate the recommendations from the analysis and the benefits they are intended to achieve. The benefits may include improved safety and environmental performance or cost savings. Determine implementation criteria and plans.

17.3.4 LAYER OF PROTECTION ANALYSIS

Layer of protection analysis (LOPA) is a methodology for hazard evaluation and risk assessment. On a sliding scale of sophistication and rigor, LOPA lies between the qualitative end of the scale (characterized by methods such as HAZOP and what-if) and the quantitative end (characterized by methods using fault trees and event trees).

LOPA helps the analyst make consistent decisions on the adequacy of the existing or proposed layers of protection against an accident scenario (see Fig. 17.1). LOPA results support:

- Assigning priorities to recommendations and
- Developing safety requirement specifications for safety instrumented systems (SISs), which is a necessary step in complying with ANSI/ISA-84.00.01 (2004).

This decision-making process is ideally suited for coupling with a company's risk-decision criteria, such as those displayed in a risk matrix. LOPA is a recognized technique for selecting the appropriate safety integrity level of your SIS according to the requirements of standards such as ANSI/ISA-84.00.01.

LOPA is a semiquantitative methodology that can be used to identify safeguards that meet the independent protection layer (IPL) criteria. While IPLs are extrinsic safety systems, they can be active or passive systems, as long as the following criteria are met (Summers, 2002):

- Specificity: The IPL is capable of detecting and preventing or mitigating the consequences of specified, potentially hazardous event(s), such as a runaway reaction, loss of containment, or an explosion.

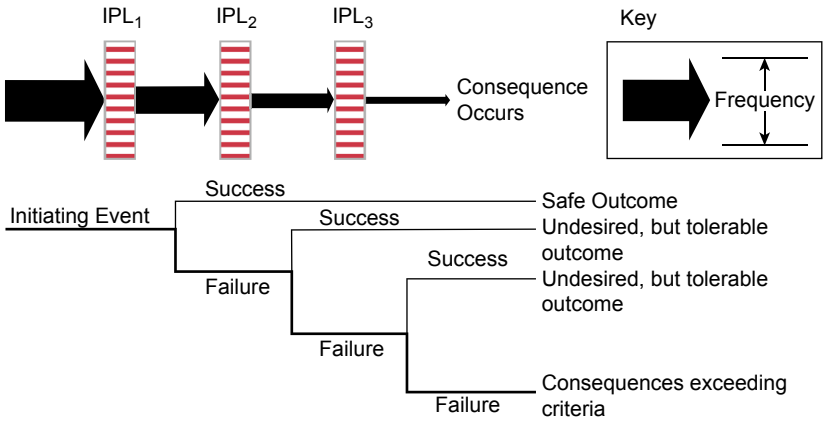

FIGURE 17.1

Layer of protection analysis process diagram. *IPL*, independent protection layer.

Source: ABS Consulting Inc.

- Independence: An IPL is independent of all the other protection layers associated with the identified potentially hazardous event. Independence requires that the performance is not affected by the failure of another protection layer or by the conditions that caused another protection layer to fail. Most importantly, the protection layer is independent of the initiating cause.
- Dependability: The protection provided by the IPL reduces the identified risk by a known and specified amount.
- Auditability: The IPL is designed to permit regular periodic validation of the protective function.

Examples of IPLs are:

- Standard operating procedures,
- Basic process control systems,
- Alarms with defined operator response,
- SIS,
- Pressure relief devices,
- Blast walls and dikes,
- Fire and gas systems, and
- Deluge systems.

LOPA should start from the point where the hazards have been identified, and it is thus complementary to HAZOP. This use of LOPA often results in a second, in-depth analysis of a hazard scenario by a different team of people, which may challenge the HAZOP team's understanding of failure events and safeguards (Brennan, 2012).

17.3.5 OPERATING PROCEDURES

There are several types of operating procedures (Sutton, 2014) as follows:

- Steady-state operations
- Start-up
- Shutdown

Steady-state procedures cover those actions carried out during normal operations. During steady-state operations, the facility is under the immediate control of the instrument systems, so the role of the operator is to monitor the overall operation and to respond to alarms. Therefore, the operating procedures are like checklists rather than statements of actions required. The inside or board operator checks the instrumentation to make sure that operating targets are being met; the outside operator conducts routine rounds to check that equipment is performing correctly.

Steady-state procedures that require routine operator intervention can be either event or time based. Event-based procedures are usually performed in response to a system change or condition; for example, adding chemicals to cooling water. Time-based procedures are those that are to take place at a specified time interval.

Start-ups are often a hazardous time because the facility is in a dynamic state with quite varying conditions and because operations may not have much experience, if any, with these conditions. The improvements in system reliability brought about by risk management programs and extended times between turnarounds means that many personnel, even with significant experience, may never have been through a full start-up because the facility can run for years without a shutdown.

Procedures for planned shutdowns have the same features as start-up instructions, except that they are carried out in the reverse order. The starting point is with the facility in full operating mode with an objective of facility shutdown and equipment evacuation so that maintenance work can proceed. In many cases, shutdowns are only partial. For example, when a compressor or pump fails, then only that piece of equipment will be isolated. The facility may be put in a standby condition in which temperatures and pressures are maintained, and only the section to do with that piece of equipment is actually shut down.

An important difference between shutdown and start-up is if something is not right during a start-up, it is possible to stop further action and correct the problem. The system is probably in a safe condition at that point.

The potential hazards associated with shutdowns are more serious. Once the procedure is started, there may not be an opportunity to delay or abort.

17.3.6 MANAGEMENT OF CHANGE

Most revisions to operating procedures will be approved through the Management of Change process. Often, someone will desire either a change of operating conditions or modifications to equipment or instrumentation. Most Management of Change processes require update of the operating procedures.

After a change has been approved, it is important to conduct an operational readiness or pre-start-up safety review immediately prior to implementing the change. An important part of any pre-start-up safety review is to ensure that the operating and maintenance procedures have been updated and that the affected technicians have been trained (Sutton, 2014).

17.3.7 FATIGUE MITIGATION

Each operating company must implement the following methods to reduce the risk associated with operator fatigue that could inhibit an operator's ability to carry out the roles and responsibilities the operator has defined:

- Establish shift lengths and schedule rotations that provide operators off-duty time sufficient to achieve 8 h of continuous sleep;
- Educate operators and supervisors in fatigue mitigation strategies and how off-duty activities contribute to fatigue;
- Train operators and supervisors to recognize the effects of fatigue; and
- Establish a maximum limit on operator hours of service, which may provide for an emergency deviation from the maximum limit if necessary for the safe operation of a pipeline facility.

As a result of the US Chemical Safety and Hazard Investigation Board (CSB) investigation of the 2005 BP Texas City incident, the CSB issued several recommendations including the development of an American National Standards Institute (ANSI) standard that develops fatigue prevention guidelines for the refining and petrochemical industries that, at a minimum, limit hours and days of work and address shift work.

ANSI RP 755 provides guidance to all stakeholders (e.g., employees, managers, supervisors) on understanding, recognizing, and managing fatigue in the workplace. Owners and operators should establish policies and procedures to meet the purpose of recommended practice (ANSI/API RP-755, 2010).

This document was developed for refineries, petrochemical and chemical operations, natural gas liquefaction plants, and other facilities such as those covered by the OSHA Process Safety Management Standard, 29 CFR 1910.119. This document is intended to apply to a workforce who is commuting daily to a job location.

It has been well documented that excess workplace fatigue can be a risk to safe operations. In the past, it was thought that simply placing limits on the hours of service would adequately address the risk of fatigue. However, over the last several years, a broad international consensus has emerged that the better way manage fatigue risk is through a comprehensive fatigue risk management system (FRMS) that is integrated with other safety management systems as necessary. ANSI/API RP 755 is based on the FRMS approach.

The FRMS should be based on sound science and recognize operational issues and includes consultation with key stakeholders in the development and implementation of the local application of the FRMS. The FRMS should also include a process to review and enhance the FRMS, as needed, with a goal of continuous improvement.

The development of the FRMS should address the following subjects which are discussed in the document:

- Positions in a facility covered by the FRMS
- Roles and responsibilities of those covered by the FRMS
- Staff—workload balance assessments
- Safety Promotion: training, education, and communication
- Work environment
- Individual risk assessment and mitigation

- Incident/near miss investigations
- Hours of service guidelines
- Callouts
- Exception process
- Periodic review of the FRMS to achieve continuous improvement

ANSI/API RP 755 provides guidance on the number of consecutive days that can be worked before a minimum amount of time off is required. The guidance applies to 8, 10, and 12 h shifts and addresses normal operations, outages, and extended shifts.

17.3.8 ALARM MANAGEMENT

According to 49 CFR Parts 192 and 195, each operating company using an SCADA system must have a written alarm management plan to provide for effective operator response to alarms. An operating company's plan must include provisions to (ANSI/ISA−18.2, 2009):

- Review SCADA safety-related alarm operations using a process that ensures alarms are accurate and support safe pipeline operations;
- Identify at least once each calendar month points affecting safety that have been taken off scan in the SCADA host, have had alarms inhibited, generated false alarms, or that have had forced or manual values for periods of time exceeding that required for associated maintenance or operating activities;
- Verify the correct safety-related alarm set-point values and alarm descriptions at least once each calendar year, but at intervals not to exceed 15 months;
- Review the alarm management plan required by this paragraph at least once each calendar year, but at intervals not exceeding 15 months, to determine the effectiveness of the plan;
- Monitor the content and volume of general activity being directed to and required of each operator at least once each calendar year, but at intervals not exceeding 15 months, that will assure controllers have sufficient time to analyze and react to incoming alarms; and
- Address deficiencies identified through the implementation.

ANSI/ISA−18.2 (2009) addresses the development, design, installation, and management of alarm systems in the process industries. Alarm system management includes multiple work processes throughout the alarm system life cycle. This standard defines the terminology and models to develop an alarm system, and it defines the work processes recommended to effectively maintain the alarm system throughout the life cycle.

The stages of the alarm management life cycle are:

a. Alarm philosophy
b. Identification
c. Rationalization
d. Detailed design
e. Implementation
f. Operation
g. Maintenance

h. Monitoring and assessment
i. Management of change
j. Audit

17.3.8.1 Alarm Philosophy

Basic planning is necessary prior to designing a new alarm system or modifying an existing system. Generally, the first step is the development of an alarm philosophy that documents the objectives of the alarm system and the processes to meet those objectives. For new systems, the alarm philosophy serves as the basis for the alarm system requirements specification document.

The philosophy starts with the basic definitions and extends them to operational definitions. The definition of alarm priorities, classes, performance metrics, performance limits, and reporting requirements are determined based on the objectives, definitions, and principles. The schemes for presentation of alarm indications in the human-machine interface (HMI), including use of priorities, are also set in the alarm philosophy, which should be consistent with the overall HMI design.

The philosophy specifies the processes used for each of the life cycle stages, such as the threshold for the management of change process and the specific requirements for change, and is maintained to ensure consistent alarm management throughout the life cycle of the alarm system.

The development of the alarm system requirements specification is included in the philosophy stage of the life cycle. Most of the specification is system independent and can be the basis for determining which systems most closely meet the requirements. The specification typically goes into more detail than the alarm philosophy and may provide specific guidance for system design.

17.3.8.2 Identification

The identification stage is a collection point for potential alarms proposed by any one of several methods for determining that an alarm may be necessary. These methods are defined outside of this standard so the identification stage is represented as a predefined process in the life cycle. The methods can be formal such as PHA, safety requirements specifications, recommendations from an incident investigation, good manufacturing practice, environmental permits, piping and instrumentation diagram (P&ID) development or operating procedure reviews. Process modifications and operating tests may also generate the need for alarms or modifications. Some alarm changes will be identified from the routine monitoring of alarm system performance. At this stage the need for an alarm has been identified and it is ready to be rationalized.

17.3.8.3 Rationalization

The rationalization stage reconciles the identified need for an alarm or alarm system change with the principles in the alarm philosophy. The steps can be completed in one process or sequentially. The product of rationalization is clear documentation of the alarm, including any advanced alarm techniques, which can be used to complete the design.

Rationalization is the process of applying the requirements for an alarm and generating the supporting documentation such as the basis for the alarm set point, the consequence, and corrective action that can be taken by the operator.

Rationalization includes the prioritization of an alarm based on the method defined in the alarm philosophy. Often priority is based on the consequences of the alarm and the allowable response time.

Rationalization also includes the activity of classification during which an alarm is assigned to one or more classes to designate requirements (e.g., design, testing, training, or reporting requirements). The type of consequences of a rationalized alarm, or other criteria, can be used to separate the alarms into classes as defined in the alarm philosophy.

The rationalization results are documented, typically in the master alarm database (i.e., an approved document or file), which is maintained for the life of the alarm system.

17.3.8.4 Detailed Design

In the design stage, the alarm attributes are specified and designed based on the requirements determined by rationalization. There are three areas of design: basic alarm design, HMI design, and design of advanced alarming techniques.

The basic design for each alarm follows guidance based on the type of alarm and the specific control system.

The HMI design includes display and annunciation for the alarms, including the indications of alarm priority.

Advanced alarming techniques are additional functions that improve the effectiveness of the alarm system beyond the basic alarm and HMI design. These methods include state-based alarming and dynamic prioritization.

17.3.8.5 Implementation

In the implementation stage, the activities necessary to install an alarm or alarm system and bring it to operational status are completed. Implementation of a new alarm or a new alarm system includes the physical and logical installation and functional verification of the system.

Since operators are an essential part of the alarm system, operator training is an important activity during implementation. Testing of new alarms is often an implementation requirement.

The documentation for training, testing, and commissioning may vary with classification as defined in the alarm philosophy.

17.3.8.6 Operation

In the operation stage, the alarm or alarm system is active and it performs its intended function. Refresher training on both the alarm philosophy and the purpose of each alarm is included in this stage.

17.3.8.7 Maintenance

In the maintenance stage, the alarm or alarm system is not operational but is being tested or repaired. Periodic maintenance (e.g., testing of instruments) is necessary to ensure the alarm system functions as designed.

17.3.8.8 Monitoring and Assessment

In the monitoring and assessment stage, the overall performance of the alarm system and individual alarms are continuously monitored against the performance goals stated in the alarm philosophy. Monitoring and assessment of the data from the operation stage may trigger maintenance work or identify the need for changes to the alarm system or operating procedures. Monitoring and assessment of the data from the maintenance stage provides an indication of the maintenance efficiency. The overall performance of the alarm system is also monitored and assessed against the goals in the alarm philosophy. Without monitoring an alarm system is likely to degrade.

17.3.8.9 Management of Change

In the management of change stage, modifications to the alarm system are proposed and approved. The change process should follow each of the life cycle stages from identification to implementation.

17.3.8.10 Audit

In the audit stage, periodic reviews are conducted to maintain the integrity of the alarm system and alarm management processes. Audits of system performance may reveal gaps not apparent from routine monitoring. Execution against the alarm philosophy is audited to identify system improvements, such as modifications to the alarm philosophy. Audits may also identify the need to increase the discipline of the organization to follow the alarm philosophy.

17.3.9 TRAINING

The objective of training should be achievement of operational excellence by developing and implementing a plan that addresses the reliable operations (see Fig. 17.2). Training should close the gap between human performance and system complexity.

Operator training should address the following four key components:

- Human by reducing the probability of error
- Equipment by eliminating or reducing deterioration and failure and extending the mean time between failure

FIGURE 17.2

Operational excellence key components. *MTBF*, mean time between failure; *MTTR*, mean time to repair.

Source: GP Strategies Corporation.

- Design by minimizing equipment maintenance, increasing mean time to repair, and ensuring equipment performance objectives and standards are achieved
- Process by developing tools to reduce variability in plant output

Isolated attempts to improve performance in any one of these components will provide benefits, but best results are obtained when all components work well together.

An operating company's program must provide for training each operator to carry out the roles and responsibilities defined by the operating company. In addition, the training program must include the following elements:

- Responding to abnormal operating conditions likely to occur simultaneously or in sequence;
- Use of a computerized simulator or noncomputerized (tabletop) method for training operators to recognize abnormal operating conditions;
- Training controllers on their responsibilities for communication under the operator's emergency response procedures;
- Training that will provide a controller a working knowledge of the system, especially during the development of abnormal operating conditions; and
- For operating setups that are periodically, but infrequently used, providing an opportunity for operators to review relevant procedures in advance of their application.

17.3.10 SHIFT CHANGE

Many accidents occur due to inadequate communication during shift change. Therefore, it is very important to develop and follow handover procedures. Nimmo (2006) suggests organizing the handover information according to the following topics:

- Safety
- Environment
- Quality
- Production
- Reliability

Other topics to be reviewed include maintenance and upcoming work. A routine rounds procedure should be followed by the outside operator at the start and end of each shift.

17.4 MAINTENANCE

"Maintenance" is a term generally used to define the routine activities to sustain standards of performance throughout the in-service, or operational, part of the asset life cycle. In doing this, the maintenance policy designer needs to take account of a range of factors. These include the complexities of operating environment, the available resources for performing maintenance, and the ability of the asset to meet its current performance standards.

Cost-effectively maximizing the overall equipment effectiveness (OEE) should be the objective of any plant maintenance program. Availability, performance rate (also often described as utilization), and quality rate all factor into OEE. Maximum availability is achieved by reducing planned downtime, setup downtime, and unplanned downtime for each piece of equipment. Maximum performance rate is

experienced by minimizing slowdowns and reductions below maximum capacity. Quality rate is maximized when off-specification product is eliminated at maximum yield.

The design and installation of equipment as well as how it is operated and maintained affect the OEE. It measures both efficiency (doing things right) and effectiveness (doing the right things) with the equipment (Mather, 2005).

$$\text{OEE} = \text{A} \times \text{PE} \times \text{Q} \tag{17.1}$$

where A is availability of the machine, PE is performance efficiency, and Q is the quality rate or yield.

Availability is the proportion of time the machine is actually available out of time it should be available.

$$\text{Availability} = \frac{(\text{Planned production time} - \text{unscheduled downtime})}{\text{Planned production time}} \tag{17.2}$$

$$\text{Planned production time} = \text{Gross available production time} - \text{Planned downtime} \tag{17.3}$$

Gross available hours for production include 365 days per year, 24 h per day, 7 days per week. Planned downtime includes vacation, holidays, and insufficient raw materials. Availability losses include equipment failures and changeovers indicating situations when the line is not running although it is expected to run.

$$\text{Performance Efficiency} = \frac{(\text{Amount of products actually produced})}{\text{Planned production}} \tag{17.4}$$

$$\text{Quality (Yield)} = \frac{(\text{Amount of product processed} - \text{Amount of product not recovered})}{\text{Amount of product processed}} \tag{17.5}$$

For availability of 95%, performance efficiency of 90%, and quality of 99%, the result is an OEE rating of 85%.

A good maintenance program will focus on the root cause of equipment failure. Otherwise, the maintenance department is spending its time reacting to the symptoms of the problems.

Often before equipment failure we observe poor performance. Prior to poor performance there are signals that the equipment has deteriorated.

Safety and environmental compliance play their part in creating the drive for maintenance activities, particularly given the changing legal and regulatory frameworks around these two areas; in some industries they are even the principal drivers. However, for most businesses the goal remains that of maximum value from their investment. This means getting the maximum performance possible from the assets, for the least amount spent.

17.4.1 TYPES OF MAINTENANCE

17.4.1.1 Breakdown Maintenance

In this type of maintenance, no care is taken for the machine, until equipment fails. Repair is then undertaken. This type of maintenance could be used when the equipment failure does not significantly affect the operation or production or generate any significant loss other than repair cost. However, an important aspect is that the failure of a component from a big machine may be injurious to the operator. Hence breakdown maintenance should be avoided.

17.4.1.2 Preventive Maintenance

Preventive maintenance is performed periodically (cleaning, inspection, oiling, and retightening). This method retains the healthy condition of equipment and prevents failure by delaying deterioration through inspection or equipment condition diagnosis. It is further divided into periodic maintenance and predictive maintenance.

Condition monitoring plays a dual role in the maintenance process for regulating preventive maintenance applications and, as stress increases, alerting to impending failure.

17.4.1.3 Periodic or Time-Based Maintenance

Periodic maintenance consists of inspecting, servicing, cleaning, and replacing parts to prevent sudden failure and process problems on a predetermined frequency.

17.4.1.4 Corrective Maintenance

Corrective maintenance improves equipment and its components so that preventive maintenance can be carried out reliably. Equipment with design weaknesses must be redesigned to improve reliability or maintainability. This happens at the equipment user level.

17.4.1.5 Predictive Maintenance

Predictive maintenance is a method in which the service life of important parts is predicted based on inspection or diagnosis in order to use the parts to the limit of their service life. Compared to periodic maintenance, predictive maintenance is condition-based maintenance. It manages trend values, by measuring and analyzing data about deterioration and employs a surveillance system, designed to monitor conditions through an on-line system.

Most recently, predictive maintenance (also known as condition monitoring) has been leading the way to additional savings over preventive maintenance. The use of real time or portable instruments such as vibration monitors, thermography, ferrography, etc, has been effective at recognizing the symptoms of impending machine failure. The major benefit is the availability of an earlier warning, from a few hours to a few days, which reduces the number of breakdown "catastrophic" failures.

Predictive maintenance is usually implemented concurrently with preventive maintenance and targets both the warning signs of impending failure and the recognition of small failures that begin the chain reaction that leads to big failures (i.e., damage control).

Predictive maintenance tasks are established to try to detect the warning signs that indicate the onset of failure, thus allowing for actions to be taken to avoid the failure.

17.4.1.6 Proactive "Life Extension" Maintenance

Proactive maintenance has now received worldwide attention as the single most important means of achieving savings unsurpassed by conventional maintenance techniques. The approach supplants the maintenance philosophy of "failure reactive" with "failure proactive" by avoiding the underlying conditions that lead to machine faults and degradation. Unlike predictive/preventive maintenance, proactive maintenance commissions corrective actions aimed at failure root causes, not just symptoms. Its central theme is to extend the life of mechanical machinery as opposed to (1) making repairs when often nothing is broken, (2) accommodating failure as routine and normal, or (3) preempting crises failure maintenance in favor of scheduled failure maintenance.

17.4.2 ENTERPRISE ASSET MANAGEMENT SYSTEMS

Enterprise asset management (EAM) systems provide the ability to capture, manipulate, and analyze historical failure data. The benefits are the ability to highlight the causes for poor performing assets, provide the volume and quality of information for determining how best to manage the assets, and informing decisions regarding end-of-life and other investment points.

The implementation of these products, when bought for these reasons, often focuses on optimizing processes to capture the dynamic data on asset failures, which is then used throughout the system. Maintain, repair, and operate style inventory management algorithms, for example, use this information as one of the key inputs to determine minimum stocking levels, reorder points, and the corresponding reorder quantities.

As a result, analysts often find themselves recommending and analyzing activities of not only maintenance but also other areas of asset management, namely those of asset modification and operations.

17.4.3 RELIABILITY CENTERED MAINTENANCE

If an asset management program is aimed at maximum cost-effectiveness over an asset's life, then it must look at the management of critical failures. By definition, this approach is centered on the reliability of the asset or reliability centered.

The role of the maintenance manager can be defined as formulating cost-effective asset management programs, routine activities, and procedures to maintain standards of performance through reducing the likelihood of critical failures to an acceptable level, or eliminating them.

Many EAM implementations are of limited value because even with well-controlled and precise business processes for capturing data, some of the critical failures that will need to be managed may not yet have occurred. Reliability centered maintenance (RCM) facilitates the creation of maintenance programs by analyzing the four fundamental causes of critical failures of assets, namely:

- poor asset selection,
- asset degradation over time,
- poor asset operation, and
- human errors.

The RCM analyst needs to analyze all of the reasonably likely failure modes in these four areas, to an adequate level of detail. Determining the potential causes for failures in these areas, for a given operating environment, is in part informed by data, but the vast majority of the information will come from other sources.

Sources such as operators' logs are strong sources for potential signs of failure, as well as for failures often not found in the corporate EAM. Equipment manufacturers' guides are also powerful sources for gleaning information regarding failure causes and failure rates.

The factors that decide the lengths that an RCM analyst should go to collect empirical data is driven by a combination of the perceived risk and limitations set on maintenance policy design by commercial pressures. Even when all barriers are removed from the path of the RCM analyst, they are often confronted faced with an absence of real operational data on critical failures.

One of the areas where EAM systems provide substantial benefits is through driving out inefficiencies in business processes. Through the capture, storage, manipulation, and display of historical

transactional data, companies can take great leaps forward in the level of efficiency with which they execute maintenance programs.

This is where RCM style methodologies contribute to the EAM or computerized maintenance management system. By providing the content that the system needs to manage, they are ensuring that the right job is being executed in the right way.

17.5 TROUBLESHOOTING

Troubleshooting is a method of finding the cause of a problem and correcting it. The ultimate goal of troubleshooting is to get the equipment back into operation. This is a very important job because the entire production operation may depend on the troubleshooter's ability to solve the problem quickly and economically, thus returning the equipment to service. Although the actual steps the troubleshooter uses to achieve the ultimate goal may vary, there are a few general guidelines that should be followed. There are often cases where a familiar piece of equipment or system breaks down.

The general guidelines for a good troubleshooter to follow are as follows:

- Use a clear and logical approach
- Work quickly
- Work efficiently
- Work economically
- Work safely and exercise safety precautions

The secret to success in troubleshooting is gathering as much information as possible about a process operation. The largest source of this information is the daily observations made by the shift operators (Lieberman, 1991). To identify a malfunction by process equipment, the technician must first understand the normal function of that equipment (Lieberman, 2011).

17.5.1 TROUBLESHOOTING STEPS

A general troubleshooting process consists of the following:

- Verify that a problem actually exists.
- Isolate the cause of the problem.
- Correct the cause of the problem.
- Verify that the problem has been corrected.
- Follow up to prevent future problems.

17.5.1.1 Verify that Something Is Actually Wrong

A problem usually is indicated by a change in equipment performance or product quality. Verification of the problem will either provide indications of the cause if a problem actually exists or prevent the troubleshooter from wasting time and effort on nonproblems caused by the operator's lack of equipment understanding. It should not be accepted that something is wrong without personally verifying the failure. Some steps to take at this stage include the following:

- Be as specific and defining as possible in stating the problem that is occurring.
- Always check to ensure equipment is lined up for normal operation.

- Analyze the performance of the equipment to make sure it actually has a failure and is not simply reacting to an external condition.
- Determine if the failure is total or if the equipment is operating with degraded performance.

To verify that there actually is a problem, the troubleshooter must use all available means of information. This includes the equipment operator, equipment indications and controls, and technical documentation about the equipment or system. Contacting the equipment operator should be the first action taken. The operator usually can supply many of the details concerning the failure incident. To get the most information, the troubleshooter should ask probing questions. Some examples are as follows:

- What are the operators' indications of the trouble?
- How did the operator discover the trouble?
- What were the conditions at the time the trouble first occurred?
- Is the trouble constant or intermittent?

17.5.1.2 Identify and Locate the Cause of the Trouble

Trouble is often caused by a change in the system. A thorough understanding of the system, its modes of operation, and how the modes of operation are designed to work, the easier it will be to find the cause of the trouble. This knowledge allows the troubleshooter to compare normal conditions to actual conditions. Some recommendations to consider are as follows:

- Start the troubleshooting log with as much background information as possible and document each adjustment and its results.
- Note how readings are affected by all modes of operation and switch lineups.
- Be sure to observe all gages, meters, and other indicators as to how they are responding due to the problem.
- Always note if an adjustment has no effect on the symptom; this will help eliminate possible causes later on.
- Determine if the trouble has slowly developed (i.e., drift) or if it is a sudden failure.
- Perform control manipulation with care since detrimental effects can occur to associated equipment or components within the failed equipment.

Troubleshooting should be a series of small logical steps, each one chosen to show a result leading to discovery of the problem or problems. Always use the functional block diagram to ensure all the possible functions are checked. Include functions such as detectors, switches, cables, meters, wiring, connectors, piping, filters, and regulators. Check all pressures, flows, inputs, and outputs associated with the areas of probable faulty functions. If an abnormal reading is obtained, the equipment setup used to obtain the reading and the reading itself should be rechecked.

Some examples of useful graphic documentation are as follows:

- Panel graphics
- Loop diagrams
- P&IDs
- Block diagrams
- Wiring diagrams
- Schematic diagrams

17.5.1.3 Correct the Problem

It is very important to correct the cause of the problem, not just the effect or the symptom. This often involves replacing or repairing a part or making adjustments. Never adjust a process or piece of equipment to compensate for a problem and consider the job finished; correct the problem!

17.5.1.4 Verify that the Problem has Been Corrected

Repeating the same check that originally indicated the problem can often do this. If the fault has been corrected, the system should operate properly.

Check all the functions that have been affected by the failure. Although the equipment has been repaired and is now functioning, all operations must be checked and verified. The information obtained in this step can also aid in troubleshooting next time by providing some baseline information.

17.5.1.5 Follow Up to Prevent Further Trouble

Determine the underlying cause of the trouble. Suggest a plan to a supervisor that will prevent a future recurrence of this problem.

17.5.2 TROUBLESHOOTING DOCUMENTATION

The troubleshooting log provides a valuable source of information from which the troubleshooter can draw on the experience of past troubleshooting efforts to quickly restore the equipment to service. Problems, symptoms, corrective actions, modifications, and preventive maintenance actions all should have entries that can be referenced at a later date. Many companies require their maintenance personnel or engineering staff to maintain historical data on equipment used within their facilities. It can lead the troubleshooter to the solution to a problem that has not occurred in years and causes troubleshooting efforts to move slowly as the troubleshooter checks every possibility. Additionally, documentation of recurring problems can provide the horsepower needed to get the right part or the engineering solution necessary to not only fix the problem but also correct it.

The equipment history/troubleshooting log is an ideal place to keep the records necessary to establish and maintain a common problems list. The purpose of the common problems list is to provide the troubleshooter with a ready reference of past problems and their corrective actions. It is from this list that quick fixes can be taken.

If a problem occurs on a regular or routine basis, it should be put on the common problems list. This can be referred to at the beginning of a troubleshooting problem so the quick fixes can be tried. This can save the troubleshooter valuable time when troubleshooting. Troubleshooters or technicians need to be careful of what is placed on the common problems list. If something occurs once, it is not necessarily a common problem. The problem should be listed in the history section and should not be put on the common problems list until it occurs again. This is because the tools used for troubleshooting are only as good as their application. If the common problems list is too long and cumbersome, it cannot be used effectively.

17.5.3 INSTRUMENTATION

Instrument and automation technicians are constantly challenged to keep instrumentation loops and I/O working at peak efficiency while using the least possible time to do it (Dewey, 2001).

The first indication of a control loop problem often comes from the operator.

The first step is to measure the 4−20 mA signal, either by breaking the loop connecting in series with a digital multimeter (DMM), or by using a mA clamp meter and verifying the loop current value. If the loop current measured is not as expected, there are three likely causes: broken/disconnected/shorted wires, a bad loop power supply, or faulty instrumentation.

If no problem is found in the wires, use a DMM to check the loop power supply. If the power supply shows no output, use the 24-V loop power function of the meter to substitute for it; if the loop then works properly, the source of the problem is obvious.

If the wiring and the power supply both check out, it is time to check the transmitter. If you have a loop calibrator, process calibrator or multifunction clamp-on meter, use its mA simulate mode to substitute for the transmitter. If the loop performs as requested, the problem lies with the transmitter; if not, it is elsewhere.

If a final control element (valve positioner, etc.) is suspected, use the mA source/simulate mode on a DMM to feed a signal into it while watching the local indicator for a response.

If the problem is not a dead loop but an inaccurate one, likely possibilities include a bad I/O card on the PLC or DCS, or a bad final control element (I/P on a valve positioner, etc.). It is usually best to start by doing a field check of the transmitter, local or remote indicator, or final control element.

For a final control element, use a clamp-on meter to measure loop current and compare the value to the local position indicator on the valve or other final control element. Relay that information to the operator to verify findings.

In the case of a measurement loop, use the clamp meter to measure loop current, then check with the operator to see how well the value indicated on the control panel agrees with the actual loop current. This will give a quick check on the PLC or DCS I/O card that handles that particular loop. It is also possible to use the meter's mA source/simulate mode to send a known signal to the control room. As before, compare the value as read by the operator to the actual current in the loop.

Some loops show random fluctuations or intermittent faults that tend not to happen while a technician is watching. The solution here is to use a clamp meter with a scaled mA output. In this mode, the meter measures the current in the loop without breaking the circuit and produces an identical and isolated mA output. Feed that output to a DMM with a logging function; by allowing the DMM to record over time, any disturbance will be recorded.

The mA process clamp meter can be used as an accurate signal source to check the operation of input/output cards on PLCs and DCSs. For 4−20 mA input cards, disconnect the process loop and use the meter's mA source mode to feed in a known signal value (4.0 mA for zero, 12 mA for 50%—using the meter's 25% step function, and 20.0 mA for 100%) and compare it to the value shown on the operator's readout. Voltage input cards (1−5 V or 0−10 V) are checked in a similar way, using the meter's voltage source function.

Milliamp clamp meters can be used for periodic in-field checks of electronic valve positioners as part of preventive maintenance programs. The general method is to set the meter to the 4−20 mA source/simulate mode and connect it to the input terminals of the valve positioner. Set the meter to output 4 mA and wait for the positioner to settle, then vary the current in small increments between 4.0 mA and approximately 3.9 mA while feeling the valve stem with your free hand to check for any sign of movement. Adjust for zero movement between these two current settings by using the zero adjustment on the positioner.

Next, increase and decrease current from 4 mA to approximately 4.1 mA. Insure that the valve stem just begins movement above the ~4.1 mA setting and fully closed at 4 mA. Span can be checked similarly by setting the meter at 20, ~19.9, and ~20.1 mA, and linearity can be checked by using the meter's 25% step function.

To check a loop isolator, apply an mA input signal to the device and measure its 4–20 mA output using the clamp-on current measuring function.

Variable frequency drives are used to power motors, blowers and fans in process applications as well as conveyor systems and machine tools. Control inputs are generally voltage (1–5 V or 0–10 V) or current (4–20 mA). An mA process clamp meter can feed in a signal to simulate a normal input while the technician observes the result.

While not classified as loop calibrators, today's mA process clamp meters boast accuracies of 0.2% and can be used for quick calibration checks, while cutting down on the number of instruments needed.

For example, checking a process transmitter on the bench normally requires (aside from a pump and separate pressure standard) a loop power supply and an instrument for reading the transmitter's 4–20 mA output. But with today's mA process clamp meters, it is possible to both power the transmitter and read the output.

17.5.4 PROCESS TROUBLESHOOTING

Process troubleshooting includes (Lynch and Pittman, 2000; Lieberman, 2008) the following:

- modeling the original plant design,
- simulating the expected plant performance for the current inlet conditions and pressure profile,
- collecting and reconciling field data,
- developing a model matching the reconciled field data,
- analyze any process equipment problems, and
- make changes in the plant to achieve acceptable plant performance and verify the performance change with the models.

The most effective method to resolving inconsistencies in the data is to close the heat and material balance across each piece of equipment. Data reconciliation methods will consider redundant data, gross errors in the data, and expected accuracy of each measurement.

17.6 TURNAROUNDS

Plant turnarounds are an important aspect of operating a gas plant. A turnaround is a scheduled period when the plant is shut down. These efforts should be well planned to determine the duration, cost, and expected benefits in improving plant reliability, efficiency, and safety. Ideally, a turnaround should result in the plant returning to peak performance levels when it comes back online and should allow it to function efficiently until the next shutdown.

Typical operations cease during a turnaround and the focus of plant personnel shifts to repairs, maintenance, cleaning, and inspection. Plant personnel are usually supplemented by many outside contractors working around the clock.

Detailed planning and coordinated execution are the most critical elements of executing a successful turnaround. While speed is extremely important, safety as always is the highest priority. Many

resources used by outside contractors may be inexperienced with the hazards found in a gas plant. Specific safety training and safety monitoring is essential to assure a turnaround with no accidents. Owing to the extended working hours, worker fatigue should be monitored as part of the safety program.

Maintenance activities during a planned turnaround might include (Sahoo, 2014) the following:

- Routine inspections for corrosion, equipment integrity or wear, deposit formation, integrity of electrical and piping systems
- Special inspections of vessels, heat exchanges, or rotating equipment to investigate the effects of abnormal situations
- Installation of replacement equipment or instruments that have worn out
- Replacement of catalysts or process materials that have been depleted during operations

Improvement activities could include the following:

- Installation of upgraded equipment or technology to improve the processing efficiency
- Installation of new equipment or systems that may significantly alter the processing capacity or products recovered

Some equipment repair issues cannot be resolved because they cannot be addressed while the plant is operational. When these issues affect the overall asset utilization, then a turnaround is warranted to fix the equipment or preclude a more serious safety or efficiency issue. Other maintenance issues often best addressed during a turnaround are overhauls, process piping modifications, process equipment internals, molecular sieve replacement, sulfur reactor catalyst, among others. Sometimes safety regulations or warranty requirements might dictate a turnaround.

Turnarounds are extremely expensive, especially in the upstream oil and gas industry. In addition to the expenses of executing the maintenance activities, there is a loss of production and the profits from the sale of the plant's products during the period. Supplies, rentals, and overtime are some expenses incurred in addition to the contractors' fees. Often turnarounds will be planned when production demands may be seasonally low and preferred contractor crews are available to limit production impacts as well as assure safe and effective execution.

Typically, a turnaround manager will be assigned and all of the plant personnel will participate by contributing their expertise of administration, operations, maintenance, engineering, quality assurance as well as health, safety, and environment.

Regardless of the short-term expense, a safe and effective turnaround will prove very beneficial in the long term.

REFERENCES

ANSI/API RP-755, 2010. Fatigue Prevention for the Refining and Petrochemical Industries, first ed. American Petroleum Institute (API), Washington, DC, USA.

ANSI/ISA-84.00.01, 2004. Functional Safety: Safety Instrumented Systems for the Process Industries. Instrumentation, Systems, and Automation (ISA), Research Triangle Park, NC, USA.

ANSI/ISA−18.2, 2009. Management of Alarm Systems for the Process Industries. Instrumentation, Systems, and Automation (ISA), Research Triangle Park, NC, USA.

Brennan, G., May 23–25, 2012. LOPA sets new requirements for HAZOP. Paper Presented at the GPA Europe Annual Conference, Berlin, Germany.
Dewey, R.G., 2001. Instrument Troubleshooting Handbook. Glen Enterprises, Deer Park, TX, USA.
Horsley, D.M.C., 1997. Process Plant Commissioning – A User Guide, second ed. IChemE Press, Rugby, UK.
Lieberman, N.P., 1991. Troubleshooting Process Operations, third ed. PennWell Books, Tulsa, OK, USA.
Lieberman, N.P., 2008. Troubleshooting Natural Gas Processing: Wellhead to Transmission. Lieberman Books, Tulsa, OK, USA.
Lieberman, N.P., 2011. Process Equipment Malfunctions: Techniques to Identify and Correct Plant Problems, first ed. McGraw-Hill Education, Columbus, OH, USA.
Lynch, J., Pittman, R., March 13–15, 2000. Practical troubleshooting techniques for cryogenic gas plants. Paper Presented at the 79th Annual GPA Convention, Atlanta, GA, USA.
Mather, D., 2005. The Maintenance Scorecard, first ed. Industrial Press, New York, NY, USA.
Nimmo, I., 2006. Effective shift handover is no accident. Chemical Processing 69 (6), 30–33.
Sahoo, T., 2014. Process Plants Shutdown and Turnaround Management. CRC Press, Taylor & Francis Group, Boca Raton, FL, USA.
Summers, A., October 29–30, 2002. Introduction to layer of protection analysis. Paper Presented at the Mary Kay O'Conner Process Safety Center 2002 Annual Symposium. Texas A&M University, TX, USA.
Sutton, I., 2014. Process Risk and Reliability Management, second ed. Gulf Professional Publishing, Oxford, UK.
US DOL, 2000. Occupational Health and Safety Administration, Process Safety Management. OSHA 3132, US Department of Labor (DOL), Washington, DC, USA.
US DOT, 2009. Pipeline and Hazardous Materials Safety Administration, 49 CFR Parts 192 and 195. US Department of Transportation (DOT), Washington, DC, USA.

CHAPTER

UTILITY AND OFFSITE SYSTEMS IN GAS PROCESSING PLANTS 18

18.1 INTRODUCTION

Natural gas processing plants employ several types of utility systems. The most common utilities are described with the acronym WAGES for water, air, gas, electricity and steam. Other utilities include refrigeration systems and nitrogen for purging and inert gas blanketing. Most plants use water for process cooling, equipment cooling, and as feedwater for boilers. However, some plants elect not to use water for process cooling or steam for process heating. All plants probably use air as a utility. Air may be used for cooling as well as a pneumatic medium for instruments. Gas is a common fuel in most industries and especially in the natural gas processing industry. For example, this fuel is used for engines, combustion turbines, boilers, and heaters. Electricity is used by all processing plants. It may be generated on-site, purchased from an electric power supplier, or a combination of both. Steam is used by most plants; however, some facilities decide to employ hot oil systems instead of process heating. When steam is available it may be a power source for turbines as well as process heat.

Many so called "off-sites" systems are required for safe and environmentally friendly plant operations. A variety of these systems are found in most natural gas processing plants. Gas detection and fire water systems are installed to prevent potential loss of lives and assets. Flare systems allow safe emittance of gases with flare recovery systems, contributing to the minimization of these releases. Liquid wastes must be drained in a safe manner and often treated before leaving the site. Facilities are needed to store some raw materials and consumables as well as product and waste streams.

The objective of this chapter is to provide a brief description of the common utility systems and offsite facilities found in gas processing plants. Many of the basic design and operation considerations are discussed. Further details can be found in most of the references provided.

18.2 WATER

Water is used for process cooling either with closed systems using cooling towers or once-through systems. Closed systems are most common and especially when river or sea water is not available. A water source is also required for some cleaning operations and fire water supply.

Industrial cooling towers may use river water, seawater, or well water as their source of fresh cooling water. Mechanical induced draft or forced draft cooling towers in industrial plants continuously circulate cooling water through heat exchangers and other equipment where the water absorbs heat. That heat is then rejected to the atmosphere by the partial evaporation of the water in cooling towers where air is contacted with the circulating downflow of water in a countercurrent fashion. The

Handbook of Natural Gas Transmission and Processing. https://doi.org/10.1016/B978-0-12-815817-3.00018-6

loss of evaporated water into the air exhausted to the atmosphere is replaced by "makeup" fresh water. Since the evaporation of pure water is replaced by makeup water containing carbonates and other dissolved salts, a portion of the circulating water is also continuously discarded as "blowdown" water to prevent the excessive buildup of salts in the circulating water (Beychok, 1967).

On very large rivers and coastal, once-through systems are often used. These plants do not use cooling towers and the atmosphere as a heat sink, but put the waste heat to the river or coastal water instead. Such facilities are often built with intake structures designed to pump in large volumes of water at a high rate of flow. These structures tend to also pull in large numbers of fish and other aquatic organisms on the intake screens (US EPA, 2014).

18.2.1 WATER CHEMISTRY

Water contains varying amounts of impurities from contact with the atmosphere, soil, and containers. Water treatments add other chemicals attempting to maintain satisfactory heat exchange.

Total dissolved solids (TDSs) are measured as the mass of residue remaining when a measured volume of filtered water is evaporated. Probability of scale formation increases with increasing TDSs. Solids commonly associated with scale formation are calcium and magnesium carbonate and sulfate (Franson, 1975).

Salinity measures water density or conductivity changes caused by dissolved materials.

Water ionizes into hydronium (H_3O^+) cations and hydroxide (OH^-) anions. The concentration of ionized hydrogen (as protonated water) is expressed as pH. Low pH values increase rate of corrosion, while high pH values encourage scale formation. Amphoterism (molecules that react as an acid as well as a base) is uncommon among metals used in water cooling systems, but aluminum corrosion rates increase with pH values above 9. Galvanic corrosion may be severe in water systems with copper and aluminum components. Acid may be added to cooling water systems to prevent scale formation if the pH decrease will offset increased salinity and dissolved solids (GE Power and Water, 2012).

Some groundwater contains very little oxygen when pumped from wells, but most natural water supplies include dissolved oxygen. Dissolved oxygen approaches saturation levels in cooling towers and is desirable in blowdown or once-through systems where water is returned to natural aquatic environments.

Manufactured metals tend to revert to ores via electrochemical reactions of corrosion. Water can accelerate corrosion as both an electrical conductor and solvent for metal ions and oxygen. Corrosion reactions proceed more rapidly as temperature increases and with increasing oxygen concentrations. Corrosion rates also initially increase with salinity in response to increasing electrical conductivity, but then decrease after reaching a peak at higher levels of salinity decrease dissolved oxygen levels (GE Power and Water, 2012).

Preservation of piping and machinery in the presence of hot water has been improved by addition of chemicals, including zinc, chromates, and phosphates. Concentrations of polyphosphates or phosphonates with zinc and chromates or similar compounds have been maintained in cooling systems to keep heat exchange surfaces clean, so a film of gamma iron oxide and zinc phosphate may inhibit corrosion by passivating anodic and cathodic reaction points (GE Power and Water, 2012).

Zinc and chromates have toxicity concerns (Kemmer, 1979), while phosphates have been associated with hypertrophication (the depletion of oxygen in a water body) (Goldman and Horne, 1983).

Bio-organisms in water sources may cause fouling of heat exchange surfaces that can reduce heat transfer rates of the cooling system; and of cooling towers that can alter flow distribution to reduce evaporative cooling rates. Biofouling may also create differential oxygen concentrations increasing corrosion rates. Once-through systems are most susceptible to biofouling. Biocides have been commonly used to control biofouling, where sustained facility operation is required (GE Power and Water, 2012). However, biocides may have adverse environmental consequences. Nonoxidizing biocides may be more difficult to detoxify prior to release of blowdown or once-through cooling water to natural aquatic environments.

Chromates reduce biofouling in addition to effective corrosion inhibition, but residual toxicity in blowdown or once-through systems has encouraged reduced chromate concentrations and use of less flexible corrosion inhibitors (Kemmer, 1979). Blowdown may also contain chromium leached from cooling towers constructed of wood preserved with chromated copper arsenate.

Chlorine may be added in the form of hypochlorite to decrease biofouling but is later reduced to chloride to minimize toxicity of blowdown or once-through water returned to natural aquatic environments. Hypochlorite is destructive to wooden cooling towers as pH increases. Chlorinated phenols have been used as biocides or leached from preserved wood in cooling towers. Both hypochlorite and pentachlorophenol have reduced effectiveness at pH values greater than 8 (GE Power and Water, 2012).

Residual concentrations of biocides and corrosion inhibitors are of potential concern for once-through systems and blowdown from open recirculating systems. Closed recirculating systems require periodic cooling water treatment or replacement raising similar concern about ultimate disposal of cooling water containing chemicals used with environmental safety assumptions of a closed system (GE Power and Water, 2012).

18.2.2 COOLING TOWERS

A cooling tower is a heat rejection device that extracts waste heat to the atmosphere though the cooling of a water stream to a lower temperature. The heat from the water stream transferred to the air stream raises the air's temperature and its relative humidity to 100%, and this air is discharged to the atmosphere.

Water, which has been heated by the process, is pumped to the cooling tower through pipes. The water sprays through nozzles onto banks of material called "fill", which slows the flow of water through the cooling tower and exposes as much water surface area as possible for maximum air—water contact. As the water flows through the cooling tower, it is exposed to air, which is being pulled through the tower by an induced draft fan or pushed by a forced draft fan. The cooled water is then pumped back to the process equipment, where it absorbs heat. It will then be pumped back to the cooling tower to be cooled once again (Hensley, 2009).

Not all towers are suitable for all applications. Cooling towers are designed and manufactured in several types, with various sizes available. Understanding the types, along with their advantages and limitations, is important when determining the correct tower.

Fig. 18.1 illustrates the different components of a cooling tower structure.

First, the water is distributed evenly across the top of the cooling tower structure. Tower distribution decks can be a series of spray nozzles oriented up or down to uniformly distribute the water over the tower structure. In some cases the distribution deck may just be a series of holes through which the

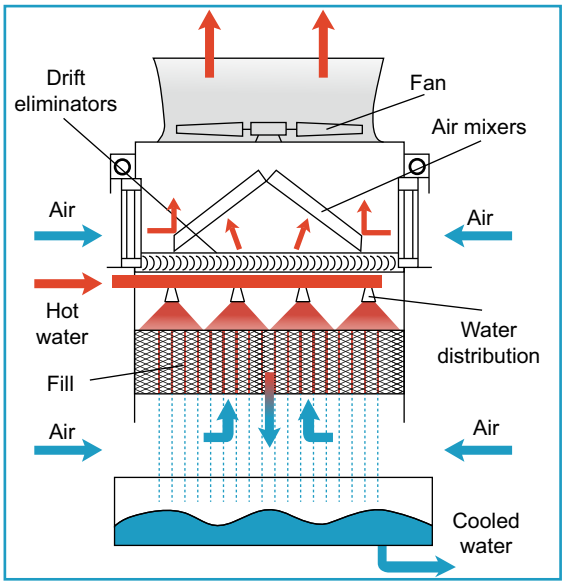

FIGURE 18.1

Cooling tower structure (US DOE, 2011).

water falls onto the tower structure. Regardless the distribution deck must uniformly apportion the recirculating water across the tower structure. Broken nozzles or plugged orifices will impede uniform distribution across the tower structure, negatively affecting the overall heat exchange capacity of the system.

As the water falls from the distribution deck, the surface area is further expanded in the fill section. Older tower systems may feature splash bars made of plastic, fiberglass, or wood that serve to break the falling water into tiny droplets. In recent years, many different forms of labyrinth-like packing or film fill have been incorporated. The closely packed nature of film fill causes the water to travel through this portion of the tower in thin streams, improving thermal efficiency and the evaporation rate, thereby increasing heat rejection (see Fig. 18.2).

There are several variations of film fill geometries commercially available, and though they do greatly increase the heat rejection rate over splash-type fills, they are also much more susceptible to fouling, scaling, and microbiological growth. Development of any of these problems greatly reduces the cooling efficiency and in severe cases can collapse portions of the tower fill or tower structure. To avoid this, film fill should be inspected routinely to ensure it is clean and free of debris, scale, and biological activity.

To minimize losses due to drift and help direct airflow into the tower, louvers and drift eliminators are commonly used. Louvers are most often seen along the sides of the tower structure, while drift eliminators reside in the top section of the tower to capture entrained water droplets that may otherwise leave through the stack. Damaged or incorrectly oriented louvers along with damaged drift eliminators will lead to excessive losses due to drift from the tower structure. Therefore, louvers and drift eliminator sections should be routinely inspected and repaired to ensure optimal water usage.

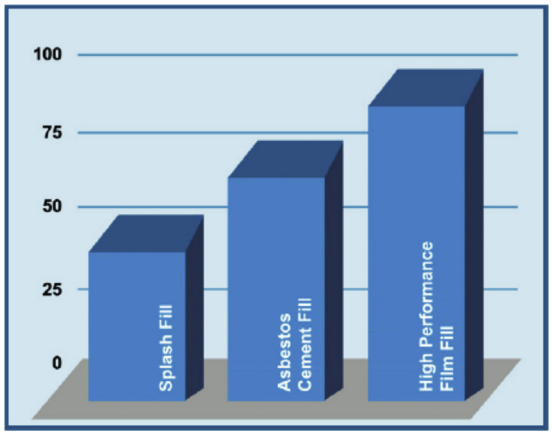

FIGURE 18.2

Fill thermal performance (US DOE, 2011).

After the water passes through the fill it cascades down to a collection basin at the base of the tower structure. From the basin, the cold water can be pumped back into the system to extract process or comfort cooling needs and begin the cycle all over again.

By design, cooling towers consume large volumes of water through the evaporation process to maintain process cooling needs, although they use significantly less water than similar capacity once-through cooling systems.

Because the evaporative loss is water containing little to no dissolved solids, the water remaining in the cooling tower becomes concentrated with dissolved solids, which can lead to scaling and corrosive conditions. To combat these problems, water with high TDS content must be drained from the system via "blowdown". The associated losses caused by blowdown, evaporation, drift, and system leaks must be accounted for by system makeup requirements (US DOE, 2011).

18.2.2.1 Crossflow Cooling Towers

In crossflow towers (Fig. 18.3) the water flows vertically through the fill, while the air flows horizontally, across the flow of the falling water. Because of this, air does not pass through the distribution system, permitting the use of gravity flow hot water distribution basins mounted at the top of the unit above the fill. These basins are applied on all crossflow towers.

18.2.2.2 Counterflow Cooling Towers

Counterflow towers (Fig. 18.4) are designed so that air flows vertically upward, counter to the flow of falling water in the fill. Because of this vertical airflow, it is not possible to use the open, gravity flow basins typical in crossflow designs. Instead, counterflow towers use pressurized, pipe-type spray systems to spray water onto the top of the fill. Since air must be able to pass through the spray system, the pipes and nozzles must be farther apart so as not to restrict airflow.

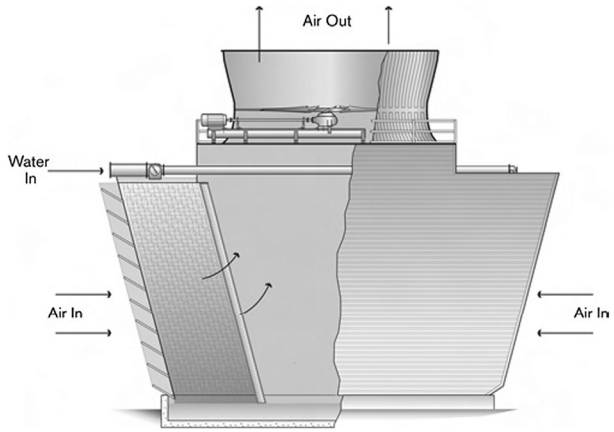

FIGURE 18.3

Crossflow tower (Hensley, 2009).

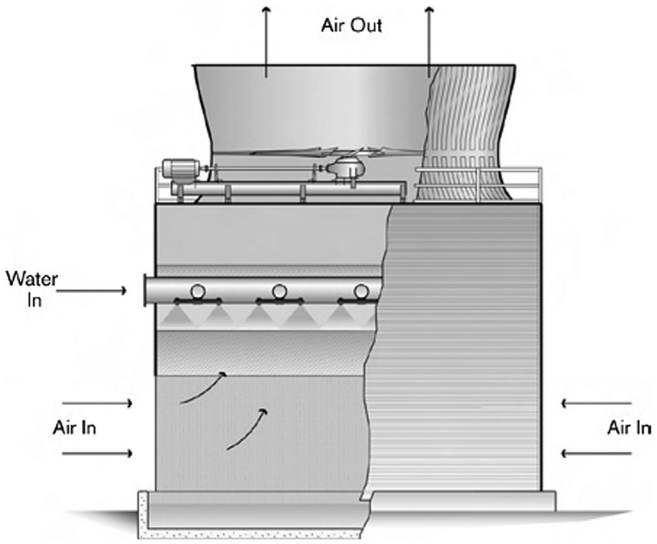

FIGURE 18.4

Counterflow tower (Hensley, 2009).

18.2.2.3 Induced Draft Versus Forced Draft

Induced draft cooling towers have fans that are typically mounted on top of the unit and pull air through the fill media. Conversely, air is pushed by blowers located at the base of the air inlet face on forced draft towers.

18.2.2.4 Factory-Assembled Versus Field-Erected Towers

Factory-assembled towers are rebuilt and shipped in as few sections as the mode of transportation will permit. A relatively small tower will ship essentially intact. A larger, multicell cooling tower is manufactured as modules at the factory and shipped ready for final assembly. Factory-assembled towers are also known as "packaged". Factory-assembled cooling towers can be crossflow or counterflow, induced draft or forced draft, depending on the application.

Field-erected towers are primarily constructed at the site of ultimate use. All large cooling towers, and many of the smaller towers, are prefabricated, piece-marked, and shipped to the site for final assembly. The manufacturer usually provides labor and supervision for final assembly. Field-erected towers can be crossflow or counterflow, depending on the application. Field-erected towers can be customized to meet exact specifications for performance, structure, drift and plume abatement.

18.2.2.5 Performance Considerations

Using a total system approach, every cooling tower component is designed and engineered to work together as an integrated system for efficient performance and long life. The following describe the performance considerations for cooling tower systems.

18.2.2.5.1 Drift

Drift is the term for water droplets that are carried out of the cooling tower with the exhaust air. Drift droplets have the same concentration of impurities as the water entering the tower. The drift rate is typically reduced by employing baffle-like devices, called drift eliminators, through which the air must travel after leaving the fill and spray zones of the tower. Drift eliminators remove water droplets from the discharged air and reduce loss of process water by causing sudden changes in direction. This forces the drops of water to be separated from the air and deposited back into the tower.

18.2.2.5.2 Cycles of Concentration

The mass flow relationship between the amount of system feedwater and the amount of blowdown sent down the drain. Cycles of concentration (COC) correlates with the effective use of water in your system to provide cooling needs. High COC are directly related to low levels of water loss from the system.

18.2.2.5.3 Dissolved Solids

The amount of dissolved minerals present in the water.

18.2.2.5.4 Blowout

Water droplets blown out of the cooling tower by wind, generally at the air inlet openings, are characterized as blowout. Water may also be lost, in the absence of wind, through splashing, or misting. Devices such as wind screens, louvers, splash deflectors, and water diverters are used to limit these losses.

18.2.2.5.5 Plume

A plume is the stream of saturated exhaust air leaving the cooling tower. The plume is visible when water vapor it contains condenses in contact with cooler ambient air. Under certain conditions, a cooling tower plume may present fogging or icing hazards to its surroundings. Water evaporated in the

cooling process is "pure" water, in contrast to the very small percentage of drift droplets or water blown out of the air inlets.

18.2.2.5.6 Blowdown

Blowdown is the portion of the circulating water flow that is removed in order to maintain the amount of dissolved solids and other impurities at an acceptable level.

18.2.2.5.7 Makeup

Water supply needed to replace all losses due to evaporation, leaks, or discharge in cooling systems.

18.2.2.5.8 Leaching

The loss of wood preservative chemicals by the washing action of the water flowing through a wood structure cooling tower is termed leaching.

18.2.2.5.9 Noise

Sound energy emitted by a cooling tower and heard at a given distance and direction may generated by the impact of falling water, by the movement of air by fans, the fan blades moving in the structure, and the motors, gearboxes, or drive belts.

18.2.2.5.10 Variable Flow

There may be significant energy savings opportunities if the cooling tower can be operated under variable flow in off-peak conditions. Variable flow maximizes the effectiveness of the installed tower capacity for the process flow.

18.2.2.5.11 Fill

A very important component of a cooling tower is the fill. The efficiency of the cooling tower is determined by the contact surface area and the contact time between air and water. The two basic fill classifications are splash-type fill (breaks up the water) and film-type fill (spreads the water into a thin layer).

18.2.2.5.12 Nozzles

Crossflow configurations permit the use of a gravity flow distribution system with a nozzle. With this system, the supply water is elevated to hot water distribution basins above the fill and then flows over the fill by gravity through nozzles located in the distribution basin floor. Counterflow configurations necessitate the use of a pressure-type system of closed pipe and spray nozzles.

18.2.2.5.13 Fans

Cooling tower fans must move large volumes of air efficiently and with minimum vibration. The materials of manufacture must withstand the corrosive effects of the environment in which the fans are required to operate. The fans may also be designed for low decibels.

18.2.2.5.14 Driveshafts

Driveshafts transmit power from the output shaft of the motor to the input shaft of the reducing gear. Because the driveshaft operates within the tower, it must be highly corrosion resistant. Turning at full motor speed, it must be well balanced and capable of being rebalanced.

18.2.2.6 Cooling Tower Efficiency Calculations

The calculation of cooling tower efficiency involves the range and approach of the cooling tower (see Fig. 18.5). Cooling tower efficiency is limited by the ambient wet bulb temperature. In an ideal case the cold water temperature will be equal to the wet bulb temperature. This would require a very large tower and yield huge evaporation and drift loss resulting in an impractical solution. In practice the cooling tower efficiency will be between 70% and 75% (Chemical Engineering Site, 2018). In summer the ambient air wet bulb temperature is higher than winter thus decreasing the cooling tower efficiency.

$$\text{Cooling Tower Efficiency} = (\text{Hot Water Temperature} - \text{Cold Water Temperature}) \times 100/ \times (\text{Hot Water Temperature} - \text{Wet bulb temperature}) \quad (18.1)$$

The difference between the Cold Water Temperature (Cooling Tower Outlet) and ambient Wet Bulb Temperature is called Cooling Tower Approach.

$$\text{Approach} = \text{Cold Water Temperature} - \text{Wet Bulb Temperature} \quad (18.2)$$

The difference between the Hot Water (Cooling Tower Inlet) Temperature and Cold water (Cooling Tower Outlet) temperature is called Cooling Tower Range.

$$\text{Range} = \text{Hot Water Temperature} - \text{Cold Water Temperature} \quad (18.3)$$

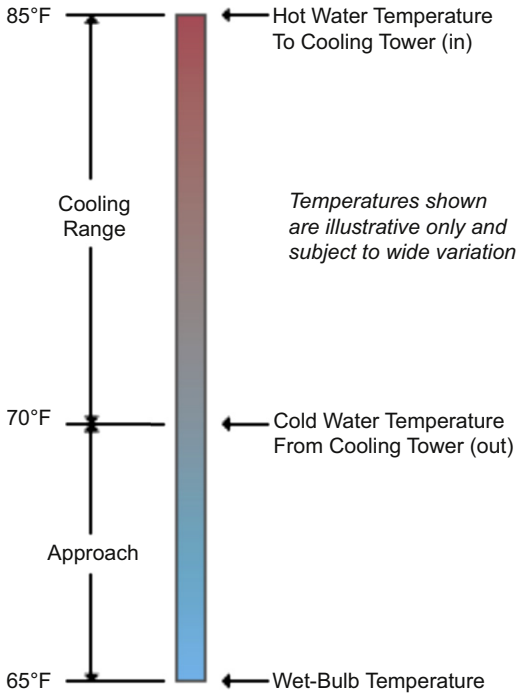

FIGURE 18.5

Relationship between cooling tower approach and range (Chemical Engineering Site, 2018).

So:

$$\text{Cooling Tower Efficiency} = \text{Range}/(\text{Range} + \text{Approach}) \times 100 \tag{18.4}$$

COC is a dimensionless number.

$$\text{COC} = \text{Dissolved Solids in Cooling Water}/\text{Dissolved Solids in Makeup Water} \tag{18.5}$$

The COC normally vary from 3.0 to 7.0 depending on the process design (Chemical Engineering Site, 2018). It is advisable to keep the COC as high as possible to reduce the makeup water requirement of the cooling tower. At the same time, higher cycle of concentration increases the dissolved solids concentration in circulating cooling water, which results in scaling and fouling of process heat transfer equipment.

As the cooling water circulates the cooling tower, part of water evaporates thereby increasing the TDSs in the remaining water. Blow down is a function of COC. Blow down can be calculated from the following equation:

$$B = E/(\text{COC} - 1) \tag{18.6}$$

where B is the Blow Down (gallons per minute or cubic meters per hour), E is the Evaporation Loss (gallons per minute or cubic meters per hour), and COC is the Cycles of Concentration.

Evaporation loss in cooling towers is calculated by the following empirical equation (Green and Perry, 2007):

$$E = 0.00085 \times R \times C \tag{18.7}$$

where E is the Evaporation Loss (gallons per minute or cubic meters per hour), R is the Range in °F, and C is the Circulating Cooling Water (gallons per minute or cubic meters per hour).

Alternatively, the evaporation loss can be calculated from the heat balance across the cooling tower.

$$E = C \times R \times C_p/HV \tag{18.8}$$

where E is the Evaporation Loss in gallons per minute, C is the Cycles of Concentration, R is the Range in °F, C_p is the Specific Heat (1.0 British Thermal Unit [BTU]/lb-°F), and H_V is the Latent heat of vaporization (970 BTU/lb).

Drift loss (D) of the cooling tower is normally provided by the cooling tower manufacturer based on the process design. If it is not available, it may be assumed as follows:

$$\text{For Natural Draft Cooling Tower} = 0.3 \text{ to } 1.0 \times C/100 \tag{18.9}$$

$$\text{For Induced Draft Cooling Tower} = 0.1 \text{ to } 0.3 \times C/100 \tag{18.10}$$

$$\text{For Cooling Tower with Drift Eliminator} = 0.01 \times C/100 \tag{18.11}$$

The cooling tower mass balance gives an idea about makeup water requirement. Cooling tower makeup substitutes the water losses resulting from Evaporation, Drift and Blow down.

$$M = E + D + B \tag{18.12}$$

where M is the makeup water requirement in gallons per minute or cubic meters per hour, E is the Evaporation Loss in gallons per minute or cubic meters per hour, D is the Drift Loss in gallons per minute or cubic meters per hour, and B is the Blow Down in gallons per minute or cubic meters per hour.

18.3 AIR

The main uses of air in a plant, exclusive of process air, are compressed air for tools and vehicles as well as pneumatic purposes for conveyance of instruments.

18.3.1 COMPRESSED AIR SYSTEM DESIGN

Six basic elements, including demand, compressed air quality, supply, storage, distribution, and control/management, must be considered when designing a compressed air system. All six elements must work together for the system to reach top performance levels.

Determining the true demand on a compressed air system is a critical first step. Air demand often fluctuates significantly; however, if actual flow demand at any given time is known, storage and distribution systems can be designed to meet demand without installing additional compressors.

The most accurate method of establishing demand over time in an existing system is to monitor the air flow using a flow meter. Flow meters can be installed at various points in the system but are typically installed in the main headers. Recorded data, such as air flow and pressure, can be evaluated to determine the flow pattern. It is especially important to note the peaks and valleys in demand and their duration. Data historians offer an effective means to track compressor activity over time and the system dynamics.

For smaller, less complex systems, the ratio between loaded and unloaded compressor running time (online/offline or start/stop times) can indicate average demand over a long period of time. When establishing compressed air demand for a new system, the operating pressure requirements must be considered as well as the duty cycle of individual equipment.

Equipment using compressed air is rated by the manufacturer for optimum performance at a certain pressure and air flow. To design a compressed air system that delivers uniform pressure, it is necessary to ensure that all tools and equipment work efficiently within a narrow pressure range. If this is not possible, then there is the option of operating the entire system at the highest pressure and regulating pressure down as required, adding a booster compressor to increase pressure for a particular application, or installing two independent air systems working at different pressures.

Leakage and artificial demand often represent a significant portion of the overall demand. All systems have leaks. Leakage can be measured in several ways while no pneumatic equipment is running: measuring the loaded running time of a compressor, timing the pressure drop of the receiver tank while all compressors are stopped, or measuring leakage at the point of use. The existing compressed air demand will also include artificial demand caused by excess system pressure that does not increase productivity. Artificial demand can be reduced significantly by installing a regulator at the point of use or a flow controller at the beginning of the distribution network.

Compressed air supply is provided by air compressors that must meet compressed air demand. If supply, storage, and distribution are not compatible, then excessive pressure fluctuation will occur, resulting in increased operating cost and reduced productivity.

Most compressors are controlled by line pressure. Typically, a drop in pressure signals an increase in demand, which is corrected by increased compressor output. Rising pressure, indicating a drop in demand, causes a reduction in compressor output.

Compressors use various capacity control systems to monitor these changes in pressure and adapt the air supply to the changing air demand. One of the more efficient one is the load/no load control that runs the compressor at full load or idle, accommodating the demand variations.

Total plant supply can be provided by either a single compressor or a multiple compressor installation which can be centralized or decentralized. Single compressor installations are best suited to smaller systems or systems that operate almost exclusively at full output.

Multiple compressor installations offer numerous advantages, including application flexibility (the ability to efficiently adjust to shift demand variations); maintenance flexibility; the option of centralized or decentralized operation; floor space flexibility; and backup capability.

A compressed air storage system consists of all the compressed air containing vessels in the system. Sufficient storage is critical and represents available energy that can be released or replenished at any time as required.

The air receiver tank typically makes up the bulk of total storage capacity. Because some compressor controls (start/stop and online/offline) depend on storage to limit maximum cycling frequency at demands less than 100% of supply, a properly sized receiver tank prevents excessive cycling.

A properly sized receiver tank also provides sufficient storage capacity for any peaks in demands. During peak demand periods, a poorly designed system will experience a drop in pressure as air in excess of system capacity is taken from the system.

Because not all compressors in a multiple compressor system remain online at all times, the actual air supply at any given time can be less than the total system capacity. During the time required to bring additional compressor capacity online, stored compressed air can be used to prevent any pressure drop in the system. The amount of storage capacity needed depends on the amount of excess demand in cubic feet, available pressure differential between the compressor station and point of use, compressor start-up time, and the time available to replenish stored compressed air.

Flow controllers are also extremely important. Installation of a flow controller after the receiver tank is essential for providing additional compressed air when needed without downstream pressure fluctuations. The flow controller basically works similar to a precision regulator, increasing or reducing flow to maintain constant line pressure. It also provides the necessary pressure differential between the receiver tank and the system to create storage without changing system pressure downstream.

The compressed air distribution piping is your means for transporting compressed air and represents the link between supply, storage, and demand. The ideal distribution system provides a sufficient supply of compressed air at the required pressure to all locations where compressed air is needed. A network of pipelines is used to supply different locations with compressed air.

The flow of compressed air in pipelines, however, creates friction and results in pressure drop. Pressure drop in the pipelines should, ideally, be no more than 1 to 2 psi (Kaeser Compressors, 2007).

The following steps can be taken to reduce pressure drop:

- reduce the distance the air must be transported
- reduce the friction through the pipes by increasing pipe size and eliminating unnecessary elbows, valves, and other flow restrictions
- reduce the flow rate of air through the system
- select smooth bore piping
- minimize the drop in pressure across the system components
- eliminate leaks

Friction loss is higher in longer pipes and in pipes with a smaller diameter. An effective way to reduce pressure drop is to use a loop system that provides bidirectional flow at any point in the system, cutting the flow in each pipe path in half and reducing compressed air velocity.

Even more important than pressure drop caused by friction, however, is that resulting from the system components themselves. This drop typically ranges from 5 to 25 psi (Kaeser Compressors, 2007) and can be controlled, through careful equipment selection and proper maintenance.

The exact layout of the compressed air system will depend on the interplay of the system elements. Important installation considerations are as follows: adequate ventilation, foundation requirements, compressor room requirements, and piping materials.

There are five basic methods of ventilation: natural ventilation; forced ventilation with an exhaust fan; ducted ventilation to the outside without a damper for air recirculation (suitable for ambient temperatures above 32°F); ducted ventilation with circulating air damper for winter operation, mixing warm air with cold intake air (suitable for intake temperatures below 32°F), or an exhaust air duct vented to the outside during summer, and space heating during winter.

Each compressor should have a separate intake air opening. To determine the size of the intake opening, add up the drive power of all the compressors and determine the cooling air flow and the required intake air opening for the total drive power. Divide the area of this opening into smaller intakes, proportional to the relative size of the compressors. No intake ducting is required.

Foundation requirements depend on the size and type of air compressor. Packaged rotary and small reciprocating compressors can be installed without any special foundation. For larger reciprocating compressors, extensive foundations are required. Special foundations are not required for base mounted rotary screw compressors as long as the compressor features vibration insolation mounts.

Compressors, especially medium or large compressors, should be installed in a special room that is clean, dust-free, dry, and cool. All heat-dissipating pipes and machinery should be well insulated. To avoid frost and corrosion from condensate accumulation, the temperature in the room should not fall below 40°F (Kaeser Compressors, 2007).

Compressor units should be easily accessible, and lighting should be adequate for maintenance and inspections. Because air-cooled compressors require sufficient cooling air flow, the temperature in these rooms should not exceed 95°F. For compressors with drives up to 25 hp, natural ventilation is generally sufficient, but larger compressors and smaller compressor rooms will require forced ventilation (Kaeser Compressors, 2007).

Dryers should be properly placed, and cooling ducts or fans may be required for good operation and long service life.

Piping is critical to a compressed air system's reliability and efficiency. Before laying the pipes, material choice, dimensions, layout, conditions on-site, and future needs must all be considered. Piping must be rugged enough for the existing work conditions, provide minimum possible pressure loss and leakage, and be easy to maintain.

Compressed air lines can be black piping, galvanized, copper, or stainless steel. Each has advantages and disadvantages, which should be carefully evaluated.

The best option for installing compressed air lines is above the ground with supports and suspensions. This relatively low-cost option can present construction obstacles. For outdoor installations, pipe freezing can only be avoided if the compressed air has been dried to a dew point below the lowest outside temperature.

18.3.2 INSTRUMENT AIR SYSTEM CONSIDERATIONS

The primary motive force for the actuation of most control valves used in plants is compressed air. The quality of the compressed air quality is much more important for instrument and control use than for general use. The quality of a compressed air system is of vital importance to the efficient operation of plant controls and in minimizing energy costs. Air that contains condensed oils can build up in actuator mechanisms and lead to a sluggish or interrupted response. Water vapor causes corrosion. Particulate contaminants can build up in actuator internals and clog ports (Rattenbury, 2001).

Particulate and oil filters should be replaced periodically and never bypassed. Leaks should always be fixed.

Dew point, which is the measure of the moisture content in air, is the temperature at which the water vapor in air condenses into liquid. In the case of compressed air, dew point is referenced to line pressure, while common psychrometric charts are based on atmospheric pressure.

According to ANSI/ISA-S7.3, Air Quality Standards for Pneumatic Instruments published by American National Standards Institute (ANSI) and International Society of Automation (ISA), where the instrument air system is exposed to exterior temperatures, "the dew point, at line pressure, shall be at least 18°F below the minimum local recorded ambient temperature at the plant site".

If the instrument air system is indoors, "the dew point, at line pressure, shall be at least 18°F below the minimum temperature to which any part of the air system is exposed to at any season of the year. In no case should the dew point at line pressure exceed 39°F″.

The purpose of this dew point specification is to prevent the condensation of moisture and formation of rust or scale in the instrument air system. For interior systems, a refrigerated dryer is usually adequate since it can provide a dew point of about 35−37°F (Rattenbury, 2001).

If any part of an instrument air distribution system is exposed to exterior ambient temperatures, a desiccant-type air dryer must be used to maintain a low enough dew point. A standard heatless desiccant dryer can provide a dew point as low as −100°F, but the expense of purge air is usually not justified (Rattenbury, 2001). Desiccant dryers with dew point monitoring systems can save energy.

Heat-of-compression (HOC) dryers are the most efficient means of drying compressed air. Heatless dryers consume an average of 15% of process air to purge the desiccant media (Rattenbury, 2001). HOC dryers use hot compressed air directly from the last compression stage to regenerate a portion of a desiccant wheel. The air is then routed through a cooler to remove moisture and then directed to the dryer with the rest of the process air.

The only energy required is a low wattage motor to turn the desiccant wheel. While an HOC dryer does not deliver a consistent dew point level, most instrument air systems only need a dew point low enough to avoid condensation. An HOC dryer can provide −20 to −40°F dew points, depending on ambient air conditions and the mode of cooling.

According to ISA, "the maximum particle size in the airstream at the instrument shall be 3 microns". Proper particle filtration is easily established by a simple dust filtration element located before other treatment components. A quality, general purpose prefilter removes particles down to 1 micron. High efficiency after-filters can remove particles down to 0.01 micron (Rattenbury, 2001).

Particle filters, carbon filters, or dryers should be piped in parallel with isolation valves to allow for filter replacement or dryer downtime without interrupting system operation and to provide for a degree of redundancy when one component fails prematurely. A differential pressure gauge should be

installed with an alarm to alert when filters become partially clogged. Keep replacement filters on hand to ensure substitution as quickly as possible. Dirty filters are inefficient and reduce air quality and pressure.

ISA recommends that "the maximum total oil or hydrocarbon content, exclusive of noncondensables, shall be as close to 0 ppm by weight or volume as possible; and under no circumstances shall it exceed 1 ppm under normal operating conditions". Oil-lubricated compressors can have an oil carryover of 5 ppm or more. If lubricated compressors are used, a coalescing filter and activated carbon filter should be installed after the receiver and particulate prefilter. A clean activated carbon filter with appropriate prefiltration removes oil vapor down to a concentration of less than 0.003 ppm at 70°F (Rattenbury, 2001).

Oil removal is particularly important if desiccant dryers are installed for moisture removal. Oil removal must occur before the dryers to protect the desiccant media. Installing two activated carbon filters in series, if the pressure drop is not too great, in a "working/polishing" arrangement helps capture oil carryover when the upstream filter becomes overloaded.

A complete filter system should consist of a particulate prefilter, water/oil coalescing filter, aerosol filter, activated carbon filter, and another activated carbon filter followed by a dryer and after-filter. Install oil coalescing filters after a refrigerated dryer. The dryer removes much of the oil through condensation and extends the life of the coalescing filter.

Compressed air is sometimes described as oil free because filters are used, but filters have limitations. An oil-free compressor is the only way to guarantee compressed air delivery with oil content as close to zero as possible. Oil-free compressors use oil to lubricate bearings and gears, but mechanical seals isolate the compression chamber from any oil. Compressors below the 25–30 horsepower range, usually have no lubricating oil of any kind. They use sealed bearings and teflon-coated mating parts (Rattenbury, 2001).

Since there is no oil in the compression chamber of an oil-free compressor, condensate from the intercooler, after-cooler, separator, receiver, and coalescing prefilters is free of oily waste. Because the compressed air output has no oil carryover, aerosol and activated carbon filters are not needed, which minimizes energy losses through filter pressure drop.

Leaks waste energy and repairing air leaks should be part of any energy savings initiatives. Also, variable speed compressor drives save energy. Traditional, positive displacement air compressors regulate pressure in the air system by loading and unloading. Such a control scheme places the compressor drive under 100% power during 100% loading and around 20%–25% power while unloaded, with the drive motor running at constant speed (Rattenbury, 2001). A variable speed drive (VSD) compressor delivers only the mass of air the system requires. This type of control allows the compressor to consume the minimum amount of power required to deliver the required air with reduced unload power consumption.

18.4 FUEL GAS

Pipeline quality gas is the most common source of fuel for natural gas processing plants. Typically, the fuel for the plant is taken at a sufficient pressure below sales pipeline pressure and usually before the final stages of compression. Gas turbines, engines, boilers, and heaters are the main users of fuel gas.

Table 18.1 Fuel Gas Contaminants

Contaminant	Example	Effect
Solid	Rust, mill scale, sand	Erosion and deposit in the hot section
Liquid	Water, condensed gas, heavy hydrocarbon, lube oil from upstream reciprocating compressor.	Hot spot in combustor. Higher emissions. Deposit on injector.
Gas	Siloxane, hydrogen sulfide	Deposit and corrosion of hot section

Source: EML Manufacturing.

Quality of the fuel is critical for equipment performance and longevity, so conditioning and treatment are often required. In certain cases, treatment is required to meet the fuel requirement and warranty of the gas turbine.

The fuel treatment system for a combustion turbine should remove contaminants and provide the necessary superheating of the fuel gas. The contaminants in the fuel exist in gas, solid, and liquid forms. A few common contaminants that are removed by fuel treatment for gas turbines may include those listed in Table 18.1.

An effective fuel gas conditioning system will remove solid and liquid contaminants using ultra-efficient coalescing filter elements. Fig. 18.6 shows a typical block diagram of a fuel gas conditioning system. After gas contaminant removal, the fuel gas supply is superheated with an electric heater or other heating method. Preheater H-100 may be required to prevent the formation of hydrate due to pressure and temperature drop across pressure regulator PCV-110. The formation of hydrate depends on the presence of free water, gas composition, and amount of pressure drop across PCV-110. Pressure regulator PCV-110 decreases the pressure of the gas when the supply pressure exceeds the requirement of the fuel system. Once the gas is at the correct pressure, it passes through one of the two high efficiency filter coalescers, F-200A/B. Each filter coalescer is rated for full flow, so that a filter may be changed without disrupting the fuel supply to the gas turbine. At this point the gas is completely free of liquid (Source: EML Manufacturing).

In certain applications, it may be desirable to heat the fuel gas to a higher temperature across super heater H-300 to enhance the efficiency of a gas turbine. This is also known as a fuel gas preheater. Typically, these are shell and tube exchangers that utilize the waste heat from the gas turbine to warm the fuel gas.

Occasionally the fuel gas supply pressure is lower than the required fuel gas pressure at the gas turbine. In this instance a fuel gas compressor is required to boost the fuel gas pressure to the required.

There are many choices for the gas compressor. However, an oil-free centrifugal compressor offers an advantage in fuel gas application. All lubricated compressors will have lube oil carry over unless there are filters to ensure 100% of the lube oil removal. Lube oil carry over even at ppm levels will eventually accumulate at low points of the downstream piping, equipment and manifolds. Eventually the oil will enter the combustion chamber and cause costly damage.

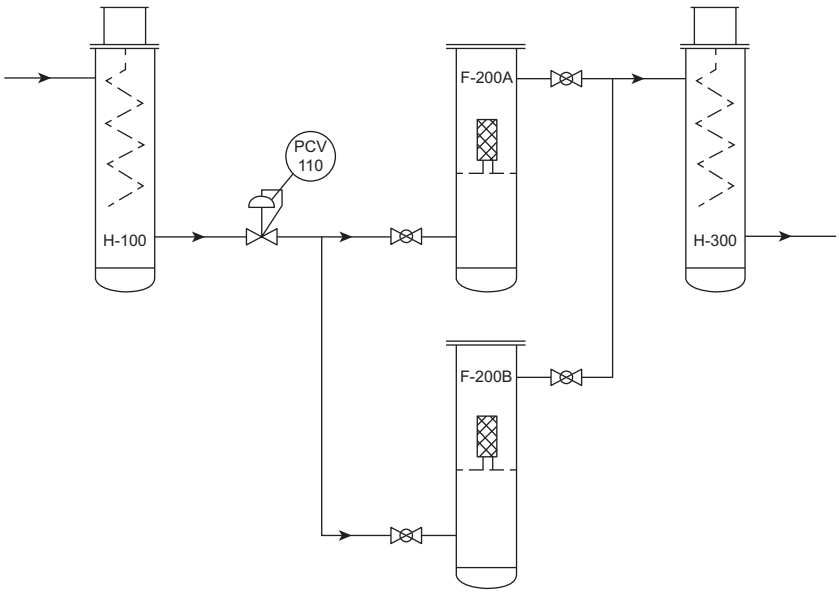

FIGURE 18.6

Typical fuel gas conditioning system.

Source: EML Manufacturing.

In some instances, the fuel gas source is too rich for internal combustion engines and requires the heavier hydrocarbon to be removed before the engine can consume the gas. Some manufacturer may specify the maximum lower heating value of the fuel gas.

18.5 NITROGEN SYSTEM

Nitrogen is normally used as an inert gas for purging seals in rotating equipment, purging air from equipment and components, and for other uses such as tank blanketing. Some gas processing facilities benefit from having an on-site source of nitrogen. It is often economical to have a nitrogen tank on site, which is refilled by a third-party nitrogen supplier or purchase by the tanker.

In industrial areas, nitrogen may be purchased from one of the industrial gas companies via pipeline or a dedicated plant operated by an industrial gas company (Towler and Sinnott, 2013).

In remote facilities or in facilities that require larger volumes, on-site generation is often necessary. Nitrogen can be generated from pressure swing adsorption, membranes separation, or cryogenic separation (Mokhatab and Corso, 2016). Selection of the process is dependent on the purity of nitrogen required, the expected usage rate, and the variability of the nitrogen needs (GPSA, 2016).

18.6 ELECTRICAL SYSTEMS

All plants require electrical power either purchased from a power grid or internally generated. In any case the basic electrical system requirements are similar. Design and maintenance of electrical systems covers a wide range of practices with most of the requirements focused on personnel safety and protection of equipment.

18.6.1 ELECTRICAL SYSTEM DESIGN

The study of a proposed electrical installation requires an adequate understanding of all governing rules and regulations. Any possible extensions or modifications during the whole life of the electrical installation are to be considered. Such a review should estimate the current flowing in each circuit of the installation and the power supplies needed (Schneider Electric, 2015).

The total current or power demand can be calculated from the data relative to the location and power of each load, together with the knowledge of the operating modes (steady state demand, starting conditions, nonsimultaneous operation, etc.). Estimation of the maximum power demand may use various factors depending on the type of application; type of equipment; and type of circuits used within the electrical installation.

From these data, the power required from the supply source and the number of sources necessary for an adequate supply to the installation are readily obtained. Local information regarding tariff structures is also required to allow the best choice of connection arrangement to the power supply network, e.g., at medium voltage (MV) or low voltage (LV) level.

Service connections can be made at a medium or LV level. For MV, a consumer type substation will then have to be studied, built, and equipped. This substation may be an outdoor or indoor installation conforming to relevant standards and regulations (the LV section may be studied separately if necessary). Metering at MV or LV is possible in this case. LV installations will be connected to the local power network and will be metered according to LV tariffs.

The whole installation distribution network is studied as a complete system. Neutral grounding arrangements are chosen according to local regulations, constraints related to the power supply, and to the type of loads. The distribution equipment (panelboards, switchgear, circuit connections, etc.) are determined from the location and grouping of loads. The grounding system having been previously determined, then the appropriate protective devices must be implemented to achieve protection against electric stocks by direct or indirect contact.

Each circuit is then studied in detail. From the rated currents of the loads, the level of short circuit current, and the type of protective device, the cross-sectional area of circuit conductors can be determined, taking into account the nature of the cableways and their influence on the current rating of conductors.

Before adopting the conductor, size indicated from the evaluation, the following requirements must be satisfied:

- The voltage drop complies with the relevant standard
- Motor starting is satisfactory
- Protection against electric shock is assured

Conductors are usually installed in cable trays.

The short circuit current (I_{sc}) is then determined, and the thermal and electrodynamic withstand capability of the circuit is checked. These calculations may indicate that it is necessary to use a conductor size larger than the size originally chosen.

The performance required by the switchgear will determine its type and characteristics. The use of cascading techniques and the discriminative operation of fuses and tripping of circuit breakers are examined.

Direct or indirect lightning strokes can damage electrical equipment at several kilometers. Operating voltage surges, transient and industrial frequency over-voltage can also produce the same consequences. The effects are examined and solutions are proposed.

Before any negotiations or discussions can be initiated with the supply authorities, the following basic elements must be established:

- Maximum anticipated power (kVA) demand
- The utilization factor (ku)
- The simultaneity factor (ks)
- Degree of supply continuity required
- The consumer must estimate the consequences of a supply failure in terms of its duration:
- Loss of production
- Safety of personnel and equipment

All individual loads are not necessarily operating at full rated nominal power or necessarily at the same time. Factors k_u and k_s allow the determination of the maximum power and apparent power demands actually required to dimension the installation.

In normal operating conditions, the power consumption of a load is sometimes less than that indicated as its nominal power rating, a common occurrence that justifies the application of a utilization factor (k_u) in the estimation of realistic values. This factor must be applied to each individual load, with attention to electric motors, which are very rarely operated at full load. In an industrial installation, this factor may be estimated on an average at 0.75 for motors.

It is a matter of common experience that the simultaneous operation of all installed loads of a given installation never occurs in practice, i.e., there is always some degree of diversity, and this fact is considered for estimating purposes using a factor (k_s).

This factor is defined in IEC 60050—International Electrotechnical Vocabulary, as follows:

- Coincidence factor: the ratio, expressed as a numerical value or as a percentage, of the simultaneous maximum demand of a group of electrical appliances or consumers within a specified period, to the sum of their individual maximum demands within the same period. As per this definition, the value is always less than 1 and can be expressed as a percentage.
- Diversity factor: the reciprocal of the coincidence factor. It means it will always be greater than 1.

18.6.2 POWER FACTOR CORRECTION

Alternating current systems supply two forms of energy:

- Active energy measured in kW hours (kWh) which is converted into mechanical work, heat, light, etc.

- Reactive energy, which again takes two forms:
  - Reactive energy required by inductive circuits (transformers, motors, etc.),
  - Reactive energy supplied by capacitive circuits (cable capacitance, power capacitors, etc)

Implementation of measuring devices with an adequate communication system within the electrical installation can produce high benefits for the user or owner: reduced power consumption, reduced cost of energy, and better use of electrical equipment.

An improvement of the power factor of an installation presents several technical and economic advantages, notably, in the reduction of electricity bills. The power factor correction within electrical installations is carried out locally, globally, or as a combination of both methods. Power factor improvement allows the use of smaller transformers, switchgear and cables, etc. as well as reducing power losses and voltage drop in an installation.

Improving the power factor of an installation requires a bank of capacitors that acts as a source of reactive energy. This arrangement provides reactive energy compensation. Compensation is more commonly affected by means of an automatically controlled stepped bank of capacitors. Automatically regulated banks of capacitors allow an immediate adaptation of compensation to match the level of load. Individual compensation should be considered when the power of motor is significant with respect to power of the installation.

In the case of certain (common) types of tariff, an examination of several bills covering the most heavily loaded period of the year allows determination of the kilovolt-amps reactive (kvar) level of compensation required to avoid reactive energy charges. The payback period of a bank of power factor correction capacitors and associated equipment is generally about 18 months.

The installation of a capacitor bank can avoid the need to change a transformer in the event of a load increase. Where metering is carried out at the MV side of a transformer, the reactive energy losses in the transformer may need to be compensated (depending on the tariff). The reactive power absorbed by a transformer cannot be neglected, and can amount to about 5% of the transformer rating when supplying its full load. Compensation can be provided by a bank of capacitors. In transformers, reactive power is absorbed by both shunt (magnetizing) and series (leakage flux) reactances. Complete compensation can be provided by a bank of shunt connected LV capacitors.

18.6.3 HARMONICS MANAGEMENT

Harmonics caused by the nonlinear magnetizing impedances of transformers, reactors, fluorescent lamp ballasts, etc. In addition, power electronic devices have become abundant today because of their capabilities for precise process control and energy savings benefits. However, they also bring drawbacks to electrical distribution systems: harmonics.

Harmonic currents caused by nonlinear loads connected to the distribution system flow through the system impedances, and in turn distorts the supply voltage. Examples include the following:

- Industrial equipment (welders, induction furnaces, battery chargers, direct current (DC) power supplies)
- VSDs for alternating current (AC) and DC motors
- Uninterruptible power supplies (UPSs)
- Office equipment (PCs, printers, servers, displays, etc.)
- Appliances (TVs, microwave ovens, fluorescent and LED lighting, washing machines and dryers, light dimmers)

Harmonic currents increase the root mean square current in electrical systems and deteriorate the supply voltage quality. They stress the electrical network and potentially damage equipment. They may disrupt normal operation of devices and increase operating costs.

Symptoms of problematic harmonic levels include overheating of transformers, motors and cables, thermal tripping of protective devices, and logic faults of digital devices. In addition, the life span of many devices is reduced by elevated operating temperatures.

Capacitors are especially sensitive to harmonic components of the supply voltage because capacitive reactance decreases as the frequency increases. In practice, this means that a relatively small percentage of harmonic voltage can cause a significant current to flow in the capacitor circuit. Harmonics are taken into account mainly by oversizing capacitors and including harmonic suppression reactors in series with them.

18.6.4 ELECTROMAGNETIC COMPATIBILITY

Some basic rules must be followed in order to ensure electromagnetic compatibility. Nonobservance of these rules may have serious consequences in the operation of the electrical installation: disturbance of communication systems, nuisance tripping of protection devices, and even destruction of sensitive devices.

18.6.5 LOADS

The examination of actual values of apparent power required by each load enables the establishment of the following:

- A declared power demand that determines the contract for the supply of energy
- The rating of the MV/LV transformer, where applicable (allowing for expected increased load)
- Levels of load current at each distribution board

The full-load current I_a supplied to the motor is given by the following formulae (Schneider Electric, 2015):

$$\text{3-phase motor: } I_a = P_n \times 1000 \Big/ \left(\sqrt{3} \times U \times \eta \times \cos\varphi\right) \tag{18.13}$$

$$\text{1-phase motor: } I_a = P_n \times 1000/(U \times \eta \times \cos\varphi) \tag{18.14}$$

Where I_a is the current demand (in amps), P_n is the nominal power (in kW), U is the voltage between phases for 3-phase motors and voltage between the terminals for single phase motors, η is the per unit efficiency (i.e., output kW/input kW), and cos φ is the power factor (i.e., kW input/kVA input).

Most electrical appliances and equipment are marked to indicate their nominal power rating (P_n). The installed power is the sum of the nominal powers of all power-consuming devices in the installation. This is not the power to be supplied in practice. This is the case for electric motors, where the power rating refers to the output power at its driving shaft. The input power consumption will evidently be greater than the output power.

The power demand (kW) is necessary to choose the rated power of a generating set or battery, and where the requirements of a prime mover have to be considered. For a power supply from an LV public supply network, or through an MV/LV transformer, the significant quantity is the apparent power in kVA.

The installed apparent power is commonly assumed to be the arithmetical sum of the kVA of individual loads. The maximum estimated kVA to be supplied, however, is not equal to the total installed kVA.

The apparent power demand of a load is obtained from its nominal power rating (corrected if necessary, as noted above for motors, etc.) and the application of the per unit efficiency and the power factor coefficients, where the apparent power kVA demand of the load can be determined as follows: (Schneider Electric, 2015):

$$P_a = P_n/(\eta \times \cos \varphi) \tag{18.15}$$

From this value, the full load current I_a taken by the load will be:

$$I_a = P_a \times 10^3/V;\ \text{for single phase-to-neutral connected load} \tag{18.16}$$

$$I_a = P_a \times 10^3 \times U;\ \text{for three phase balanced load} \tag{18.17}$$

where V is the phase-to-neutral voltage, and U is the phase-to-phase voltage (volts).

It may be noted that, strictly speaking, the total kVA of apparent power is not the arithmetical sum of the calculated kVA ratings of individual loads (unless all loads are at the same power factor).

It is common practice, however, to make a simple arithmetical summation, the result of which will give a kVA value that exceeds the true value by an acceptable "design margin".

18.6.6 POWER SUPPLY AND SWITCHGEAR

The main features that characterize a power supply system include the following:

- The nominal voltage and related insulation levels
- The short circuit current
- The rated normal current of items of plant and equipment
- The grounding system

The national standards of any country are normally rationalized to include one or two levels only of voltage, current, and fault levels, etc.

A circuit breaker (or fuse switch, over a limited voltage range) is the only form of switchgear capable of safely breaking all kinds of fault currents occurring on a power system.

Ground faults on MV systems can produce dangerous voltage levels on LV installations. LV consumers (and substation operating personnel) can be safeguarded against this danger by the following:

- Restricting the magnitude of MV ground fault currents
- Reducing the substation grounding resistance to the lowest possible value
- Creating equipotential conditions at the substation and at the consumer's installation

Centralized remote control, based on SCADA (Supervisory Control and Data Acquisition) systems and recent developments in Information Technology techniques, is becoming more and more common in countries in which the complexity of highly interconnected systems justifies the expenditure.

Protection against electric shocks and over-voltages is closely related to the achievement of efficient (low resistance) grounding and effective application of the principles of equipotential

environments. Following a preliminary analysis of the power requirements of the installation, a study of cabling and its electrical protection is undertaken, starting at the origin of the installation, through the intermediate stages to the final circuits.

The cabling and its protection at each level must satisfy several conditions at the same time to ensure a safe and reliable installation, e.g., it must:

- Carry the permanent full-load current and normal short-term overcurrents
- Not cause voltage drops likely to result in an inferior performance of certain loads, for example, an excessively long acceleration period when starting a motor, etc.

Moreover, the protective devices (circuit breakers or fuses) must:

- Protect the cabling and busbars for all levels of overcurrent, up to and including short circuit currents
- Ensure protection of persons against indirect contact hazards where the length of circuits may limit the magnitude of short circuit currents, thereby delaying automatic disconnection.

The role of switchgear is electrical protection, safe isolation from live parts, and local or remote switching.

Electrical protection assures (1) protection of circuit elements against the thermal and mechanical stresses of short circuit currents, (2) protection of persons in the event of insulation failure, and (3) protection of appliances and apparatus being supplied (e.g., motors, etc.).

A state of isolation clearly indicated by an approved "fail proof" indicator, or the visible separation of contacts, are both deemed to satisfy the national standards of many countries. Switchgear control functions allow system operating personnel to modify a loaded system at any moment, according to requirements, and include the following: functional control (routine switching, etc.), emergency switching, and maintenance operations on the power system.

The choice of a range of circuit breakers is determined by the following: the electrical characteristics of the installation, the environment, the loads and a need for remote control, together with the type of telecommunications system envisaged. The installation of an LV circuit breaker requires a short circuit breaking capacity greater than or equal to or the calculated prospective short circuit current at its point of installation.

18.6.7 LOSS OF POWER

There are several considerations for loss or curtailment of power events. The first is an UPS for short-term power loss to equipment that can run on DC.

Standby generation usually with diesel-driven engines can serve longer term power loss events. These generators can provide power to the larger motor-driven equipment that usually runs on AC. Load shedding schemes should be designed to turn off lower priority services during power outages.

18.7 PROCESS HEATING

Steam or thermal fluids (also called hot oil) normally provide process heating. Thermal fluids, such as mineral oils, may be used where high temperatures (up to 400°C) are required. Thermal fluids are expensive and need replacing every few years, so they are normally restricted to smaller systems. They

Table 18.2 Comparison of Steam and Thermal Fluids (Spirax Sarco, 2018)

Steam	Thermal Fluids
High heat content—latent heat approximately 1000 BTU/lb	Low heat content—specific heat typical 0.5 to 0.75 Btu/lb°F
Inexpensive—some water treatment costs	Expensive
Good heat transfer coefficients	Poor heat transfer coefficients
High pressure required for high temperatures	Low-pressure requirements
No circulating pumps, small pipes	Circulating pumps required, larger pipes
Temperature breakdown is easy through reducing valve	Temperature breakdown more difficult
Steam traps required	No steam trap requirement
Condensate handling	No condensate handling
Flash steam available	No flash stem
Boiler blowdown required	No heater blowdown
Water treatment required to prevent corrosion	Negligible corrosion
Minimal piping requirements	Welded or flanged joints required
No fire risk	Fire risk
System flexible—various temperature levels easily available, can drive steam turbines	System inflexible

are also prone to leakage, and high-quality connections and joints are essential to avoid leakage. Steam is relatively inexpensive but requires treatment for boiler feedwater (BFW) and corrosion protection. Steam systems also require freeze protection.

Steam and thermal fluids are compared in Table 18.2. The final choice of heating medium depends on achieving a balance between technical, practical, and financial factors, which will be different for each user. Broadly speaking, steam remains the most practical and economic choice.

18.7.1 BOILERS

A modern steam boiler will generally operate at an efficiency of between 80% and 85% (Spirax Sarco, 2018). Some distribution losses will be incurred in the pipework between the boiler and the process plant equipment, but for a system insulated to current standards, this loss should not exceed 5% of the total heat content of the steam (Spirax Sarco, 2018). Heat can be recovered from blowdown, flash steam can be used for low-pressure applications, and condensate is returned to the boiler feed tank. If an economizer is fitted in the boiler flue, the overall efficiency of a centralized steam plant will be around 87% (Spirax Sarco, 2018).

Components within the steam plant are also highly efficient. For example, steam traps only allow condensate to drain from the plant, retaining valuable steam for the process. Flash steam from the condensate can be utilized for lower-pressure processes with the assistance of a flash vessel.

The boiler is the heart of the steam system. Gas burners provide heat for the boiler. Steam boilers are operated under pressure, so that more steam at higher temperature can be produced by a smaller

boiler and transferred to the point of use using small bore pipework. When required, the steam pressure is reduced at the point of use.

If the amount of steam produced in the boiler is as great as that leaving the boiler, the boiler will remain pressurized. The burner will operate to maintain the correct pressure. This also maintains the correct steam temperature, because the pressure and temperature of saturated steam are directly related.

The boiler has many controls to ensure that it operates safely, economically, efficiently, and at a consistent pressure.

The quality of water supplied into the boiler is important. Ordinary untreated potable water is not suitable for boilers and can cause scaling. Scaling affects the boiler efficiency and reduces the life of boiler tubes. Feedwater must be treated with chemicals to reduce impurities and heated to avoid thermal shock to the boiler as well as improve efficiency. Both feedwater treatment and heating take place in the feed tank, which is usually situated high above the boiler. The feed pump will add water to the boiler as required. Heating the water in the feed tank also reduces the amount of dissolved oxygen. This is important, as oxygenated water is corrosive.

Impurities remain in the boiler water after treatment in the form of dissolved solids. Their concentration will increase as the boiler produces steam and consequently the boiler needs to be regularly purged of some of its contents to reduce the concentration. This is called control of TDSs. This process can be carried out by an automatic system that uses either a probe inside the boiler or a small sensor chamber containing a sample of boiler water to measure the TDS level in the boiler. Once the TDS content reaches a set point, a controller signals a blowdown valve to open for a set period. The lost water is replaced by feedwater with a lower TDS concentration and consequently the overall boiler TDS is reduced.

If the water level inside the boiler is not carefully controlled, the consequences could be catastrophic. If the water level drops too low, and the boiler tubes are exposed, the tubes could overheat and fail, causing an explosion. If the water level becomes too high, water could enter the steam system and upset the process. For this reason, automatic level controls are used. To comply with legislation, level control systems also incorporate alarm functions that will shut down the boiler. A common method of level control is to use probes that sense the level of water in the boiler. At a certain level, a controller will send a signal to the feed pump to restore the water level and switching off when a predetermined level is achieved. The signal from the probe will cause activation of the pump as well as low- or high-level alarms are activated. Alternative systems use floats.

18.7.2 STEAM CIRCUIT

When steam condenses, its volume and pressure are dramatically reduced. This pressure drop through the system creates the flow of steam through the pipes.

The steam generated in the boiler must be conveyed through the pipework to the point where its heat energy is required. Initially there will be one or more main headers that carry steam from the boiler in the general direction of the steam using plant. Smaller branch pipes can then distribute the steam to the individual pieces of equipment.

It is important to ensure that the steam leaving the boiler is delivered to the process in the right condition. The plant normally incorporates strainers, separators, and steam traps to maintain a satisfactory condition.

A strainer is a form of sieve in the line. It contains a mesh through which the steam must pass. Any passing debris will be retained by the mesh. A strainer should regularly be cleaned to avoid blockage.

The steam should be as dry as possible to ensure it is carrying heat effectively. A separator is a body in the line that contains a series of plates or baffles which interrupt the path of the steam. The steam hits the plates and any drops of moisture in the steam collect on them before draining from the bottom of the separator.

The air surrounding the pipes is cooler than the steam, so the steam will begin to lose heat to the air. Insulation fitted around the pipe will reduce this heat loss considerably.

When steam from the distribution system enters the equipment using the steam, energy will be given up to warm the equipment and transfer heat to the process. As steam loses heat, it turns back into water. Unless superheated the steam begins to condense as soon as it leaves the boiler. The water that forms is known as condensate, which tends to run to the bottom of the pipe and is carried along with the steam flow. This must be removed from the lowest points in the distribution pipework for several reasons:

- Condensate does not transmit heat effectively. A film of condensate will reduce the efficiency with which heat is transferred.
- When air dissolves into condensate, it becomes corrosive.
- Accumulated condensate can cause noisy and damaging water hammer.
- Inadequate drainage leads to leaking joints.

A device known as a steam trap is used to release condensate from the lines while preventing the steam from escaping from the system. There are several types of steam traps (Spirax Sarco, 2018):

- A float trap uses the difference in density between steam and condensate to operate a valve. As condensate enters the trap, a float is raised, and the float lever mechanism opens the main valve to allow condensate to drain. When the condensate flow reduces the float falls and closes the main valve, thus preventing the escape of steam.
- Thermodynamic traps contain a disc that opens to condensate and closes to steam.
- In bimetallic thermostatic traps, a bimetallic element uses the difference in temperature between steam and condensate to operate the main valve.
- In balanced pressure thermostatic traps, a small liquid-filled capsule that is sensitive to heat operates the valve.

Once the steam has been used in the process, the resulting condensate needs to be drained from the plant and returned to the boiler house. Often the condensate will drain easily out of the plant through a steam trap. The condensate enters the condensate drainage system. If it is contaminated, it will probably be sent to drain. If not, the valuable heat energy it contains can be retained by returning it to the boiler feed tank. This also saves on water and water treatment costs.

Sometimes a vacuum may form. This hinders condensate drainage, but proper drainage from the steam space maintains the effectiveness of the plant. The condensate may then require pumping. Mechanical (steam powered) pumps are often used for this purpose. These, or electric powered pumps, are used to lift the condensate back to the boiler feed tank.

Steam flowmeters are used to monitor the consumption of steam and used to allocate costs to individual departments or equipment.

18.8 PROCESS COOLING

Selecting the appropriate cooling medium is an important step in the design of the gas processing plant.

Air and water cooling are the two predominant types of cooling mediums employed in gas processing plants. Refrigeration systems are also used often but are cooled by either air or water. Water cooling can usually achieve lower temperatures than air cooling and is thus a more efficient means of cooling a gas plant. However, when water temperature approaches air temperature, there is less benefit due to the pumping power required for water cooling. Air cooling tends to have a much lower capital expense and environmental impact, especially since low noise fans may be used. Also, the availability of water may be an issue for many inland natural gas processing plants.

18.8.1 AIR COOLING

Air-cooled heat exchangers also known as fin fan heat exchangers are typically used in applications where water is not available or the desired process outlet temperature can be achieved given the maximum ambient temperatures. Ambient air is used as the cooling media to cool hot fluids flowing through finned tubes. Air-cooled equipment can be a simpler solution than that cooled by water because there is no need for pumping the coolant with the piping that accompanies.

Air-cooled heat exchangers are used in a wide variety of applications. They can be used as process fluid coolers, lube oil coolers, water and glycol coolers, inter/aftercoolers on compressors, jacket water cooler, closed loop cooling systems, and condensers.

Air-cooled heat exchangers consist of the following components:

- One or more finned tube bundles of heat transfer surface
- Except in natural draft applications, an axial flow fan and drive system
- A plenum between the bundle or bundles and the axial flow fan
- If grade mounted, a support structure high enough to allow air to enter beneath the air-cooled heat exchanger at a reasonable rate
- Optional header and fan maintenance walkways with ladders to grade
- Optional louvers for process outlet temperature control
- Optional recirculation ducts and chambers for protection against freezing or solidification of high pour point fluids in cold weather
- Hail guards
- Optional variable pitch fan hub for temperature control and power savings

18.8.1.1 Tube Bundles

A tube bundle is an assembly of tubes, headers, side frames, and tube supports. Usually the tube surface exposed to the passage of air has extended surface in the form of fins to compensate for the low heat transfer rate of air at atmospheric pressure and at a low enough velocity for reasonable fan power consumption.

The base tube is usually round and of any metal suitable for the process, due consideration being given to corrosion, pressure, and temperature limitations. Fins are helical or plate type and are usually of aluminum for reasons of good thermal conductivity and economy of fabrication. Steel fins are used for very high-temperature applications.

Fins are attached to the tubes by several methods:

- by an extrusion process in which the fins are extruded from the wall of an aluminum tube that is integrally bonded to the base tube for the full length.
- by helically wrapping a strip of aluminum to embed it in a precut helical groove and then peening back the edges of the groove against the base of the fin to tightly secure it, or
- by wrapping on an aluminum strip that is footed at the base as it is wrapped on the tube.

Sometimes serrations are cut in the fins. This causes an interruption of the air boundary layer, which increases turbulence and the air-side heat transfer coefficient with a modest increase in the airside pressure drop and the fan horsepower.

The choice of fin types is critical. This choice is influenced by cost, operating temperatures, and the atmospheric conditions. Each type has different heat transfer and pressure drop characteristics. The extruded finned tube affords the best protection of the liner tube from atmospheric corrosion as well as consistent heat transfer from the initial installation and throughout the life of the cooler. This is the preferred tube for operating temperatures up to 600°F (Hudson Products Corporation, 2007).

The embedded fin also affords a predictable heat transfer and should be used for all coolers operating above 600°F and below 750°F. The wrap-on footed fin tube can be used below 250°F; however, the bond between the fin and the tube will loosen in time, and the heat transfer is not predictable with certainty over the life of the cooler. It is advisable to derate the effectiveness of the wrap-on tube to allow for this probability (Hudson Products Corporation, 2007).

There are many configurations of finned tubes, but manufacturers find it economically practical to limit production to a few standard designs. Tubes are manufactured in lengths from 6 to 60 feet, and in diameters ranging from 5/8 inch to 6 inches, the most common being 1 inch. Fins are commonly helical, 7 to 11 fins per inch, 5/16 to 1 inch high, and 0.010−0.035 inch thick. The ratio of extended to base surface varies from 7:1 to 25:1. Bundles are rectangular and typically consist of 2−10 rows of finned tubes arranged on triangular pitch. Bundles may be stacked in depths of up to 30 rows to suit unusual services. The tube pitch is usually between 2 and 2.5 tube diameters. Net free area for air flow through bundles is about 50% of face area. Tubes are rolled or welded into the tube sheets of a pair of box headers (Hudson Products Corporation, 2007).

The box header consists of tube sheet, top, bottom, and end plates, and a cover plate that may be welded or bolted on. If the cover is welded on, holes must be drilled and threaded opposite each tube for maintenance of the tubes. A plug is screwed into each hole, and the cover is called the plug sheet. Bolted removable cover plates are used for improved access to headers in severe fouling services. Partitions are welded in the headers to establish the tube-side flow pattern, which generates suitable velocities in as near countercurrent flow as possible for maximum mean temperature difference. Partitions and stiffeners (partitions with flow openings) also act as structural stays. Horizontally split headers may be required to accommodate differential tube expansion in services having high fluid temperature differences per pass.

Bundles are usually arranged horizontally with the air entering below and discharging vertically. Occasionally bundles are arranged vertically with the air passing across horizontally, such as in a

natural draft tower where the bundles are arranged vertically at the periphery of the tower base. Bundles can also be arranged in an "A" or "V" configuration, the principle advantage of this being a saving of plot area. The disadvantages are higher horsepower requirements for a given capacity and decreased performance when winds on exposed sides inhibit air flow.

With practical limits, the longer the tubes and the greater the number of rows, the less the heat transfer surface costs per square foot. One or more bundles of the same or differing service may be combined in one unit (bay) with one set of fans. All bundles combined in a single unit will have the same air-side static pressure loss. Consequently, combined bundles having different numbers of rows must be designed for different velocities.

18.8.1.2 Axial Flow Fans

An axial flow, propeller-type fan forces the air across the bundles (forced draft) or pulls it across (induced draft). To provide redundancy when a mechanical unit fails and to provide the basic control achievable by running one fan or two, a bundle or set of bundles is usually provided with two fans.

Even distribution of the air across the tube bundle is critical for predictable, uniform heat transfer. This is achieved by adequate fan coverage and static pressure loss across the bundle. Good practice is to keep the fan projected area to a minimum of 40% of the projected face area of the tube bundle and the bundle static pressure loss at least 3.5 times the velocity pressure loss through the fan ring. For a two-fan unit this is generally assured if the ratio of tube length to bundle width is in the range of 3—3.5, and the number of tube rows is held to 4 rows minimum with the net free area for air flow at about 50% of the face area of the bundle (Hudson Products Corporation, 2007).

Fans can vary in size from 3 to 60 feet in diameter and can have from 2 to 20 blades. Blades can be made of wood, steel, aluminum, or fiberglass-reinforced plastic, and can be solid or hollow. Blades can have straight sides or be contoured. The more efficient type has a wide chord near the center and tapers to a narrow chord at the tip, with a slight twist. The twist and taper compensate for the slower velocity of the blade nearer the center to produce a uniform, efficient air velocity profile.

Fans may have fixed or adjustable pitch blades. Except for small diameters (less than 5 feet), most air-cooled heat exchangers have adjustable pitch blades (Hudson Products Corporation, 2007). Adjustable pitch fans are manufactured in two types. One is manually adjustable (with the fans off), and the other is automatically adjustable (while running). Most automatically adjustable pitch fans change their pitch by means of pneumatically actuated diaphragm working against large springs inside the hub.

18.8.1.3 Plenum

The air plenum is an enclosure that provides for the smooth flow of air between the fan and bundle. Plenums can be box type or slope sided type. The slope sided type gives the best distribution of air over the bundles but is almost exclusively used with induced draft because hanging a machinery mount from a slope sided forced draft plenum presents structural difficulties.

18.8.1.4 Mechanical Equipment

Fans may be driven by electric motors, steam turbines, gas or gasoline engines, or hydraulic motors. The overwhelming choice is the electric motor. Hydraulic motors are sometimes used when power from an electric utility is unavailable. Hydraulic motors also provide variable speed control but have low efficiencies.

The most popular speed reducer is the high-torque positive-type belt drive, which uses sprockets that mesh with the timing belt cogs. They are used with motors up to 50 or 60 horsepower and with fans up to about 18 feet in diameter. Banded V-belts are still often used in small to medium sized fans, and gear drives are used with very large motors and fan diameters. Fan speed is set by using a proper combination of sprocket or sheave sizes with timing belts or V-belts and by selecting a proper reduction ratio with gears. Fan tip speed should not be above 12,000 feet per minute (Hudson Products Corporation, 2007) for mechanical reasons and may be reduced to obtain lower noise levels. Motor and fan speed is sometimes controlled with variable frequency drives.

18.8.1.5 Structure

The structure consists of columns, braces, and cross beams that support the exchanger at a sufficient elevation above grade to allow the necessary volume of air to enter below at an approach velocity low enough to allow unimpeded fan performance and to prevent unwanted recirculation of hot air. To conserve ground space, air-cooled heat exchangers are usually mounted above, and supported by, pipe racks with other equipment occupying the space underneath the pipe rack.

18.8.1.6 Induced Draft

Advantages of induced draft include (Hudson Products Corporation, 2007):

- Better distribution of air across the bundle.
- Less possibility of hot effluent air recirculating into the intake. The hot air is discharged upward at approximately 2.5 times the intake velocity or about 1500 feet per minute.
- Better process control and stability because the plenum covers 60% of the bundle face area, reducing the effects of sun, rain, and hail.
- Increased capacity in the fan-off or fan failure condition since the natural draft stack effect is much greater.

Disadvantages and limitations include (Hudson Products Corporation, 2007):

- Possibly higher horsepower requirements if the effluent air is very hot.
- Effluent air temperature should be limited to 220°F to prevent damage to fan blades, bearings, or other mechanical equipment in the hot air stream.
- When the process inlet temperature exceeds 350°F, forced draft designs should be considered because high effluent air temperatures may occur during fan-off or low air flow operation.
- Fans are less accessible for maintenance, and maintenance may have to be done in the hot air generated by natural convection.
- Plenums must be removed to replace bundles.

In most cases, the advantages of induced draft design outweigh the disadvantages.

18.8.1.7 Forced Draft

Advantages of induced draft include the following:

- Possibly lower horsepower requirements if the effluent air is very hot (horsepower varies inversely with the absolute temperature)
- Better accessibility of fans and upper bearings for maintenance.
- Better accessibility of bundles for replacement.
- Accommodates higher process inlet temperatures.

Disadvantages and limitations include:

- Less uniform distribution of air over the bundle.
- Increased possibility of hot air recirculation, resulting from low discharge velocity from the bundles, high intake velocity to the fan ring, and no stack.
- Low natural draft capability of fan failure.
- Complete exposure of the finned tubes to sun, rain, and hail, which results in poor process control and stability.

18.8.1.8 Thermal Design

There are more parameters to be considered in the thermal design of air-cooled heat exchangers than for shell and tube exchangers. Air-cooled heat exchangers are subject to wide variety of constantly changing climatic conditions which pose problems of control not encountered with shell and tube exchangers. Designers must achieve an economic balance between the cost of electrical power for the fans and the initial capital expenditure for the equipment. A decision must be made as to what ambient air temperature should be used for design. Air flow rate and exhaust temperature are initially unknown and can be varied in the design stage by varying the number of tube rows and thus varying the face area.

Because the number of tube rows, the face area, the air face velocity, and the geometry of the surface can all be varied, it is possible to generate many solutions to a given thermal problem. However, there is obviously an optimum solution in terms of capital and operating costs.

The basic heat transfer relationships that apply to shell and tube exchangers also apply to air-cooled heat exchangers.

The fundamental relation is the Fourier equation:

$$Q = UA(T - t)_{mean} \tag{18.18}$$

where: U = overall heat transfer coefficient, A = total exchanger bare tube heat transfer surface, T = hot fluid temperature, t = air temperature

$$(T - t)_{mean} = CMTD = LMTD \times F \tag{18.19}$$

where CMTD is the corrected mean temperature difference, and LMTD is the log mean temperature difference. F is a factor that corrects the LMTD for any deviation from true counter-current flow. In air-cooled heat exchangers, the air flows substantially unmixed upward across the bundles, and the process fluid can flow back and forth and downward as directed by the pass arrangement. With four or more downward passes, the flow is considered counter-current; and, so the factor "F" is 1.0. The correction factors for one, two, and three passes are calculated from the effectiveness values developed by Stevens et al. (1957) for the appropriate counter-cross flow arrays.

The traditional approach in the design entailed an iterative trial and error procedure both on the CMTD and the transfer rate until the area satisfied both. However, the Number of Transfer Units (Ntu) Method described by Kays and London (1984) in their Compact Heat Exchangers book, may be applied to air-cooled heat exchangers.

The following are definitions based on Compact Heat Exchangers design:

$$\text{Hot fluid heat capacity rate} = C_h = C_{tube} = (Mc_p)_{tube} = Q/(T_1 - T_2) \tag{18.20}$$

$$\text{Cold fluid heat capacity rate} = C_c = C_{air} = (Mc_p)\text{air} = Q/(t_2 - t_1) \tag{18.21}$$

$$\text{Number of heat transfer units} = \text{Ntu} = A \cdot U/C_{min} \tag{18.22}$$

$$\text{Heat capacity rate ratio} = R = C_{min}/C_{max} \tag{18.23}$$

$$\text{Heat transfer effectiveness} = E \tag{18.24}$$

$$E = C_h(T_1 - T_2)/C_{min}(T_1 - t_1) = Cc(t_2 - t_1)/C_{min}(T_1 - t_1) \tag{18.25}$$

where M is the mass flow rate, c_p is the specific heat, C_{min} is the minimum heat capacity rate, and C_{max} is the maximum heat capacity rate.

18.8.1.9 Fan Selection—Horsepower Requirements

The fan diameter must assure that the area occupied by the fan is at least 40% of the bundle face area. The fan diameter must be 6 inches less than the bundle width. Fan performance curves are used to select the optimum number of blades and pitch angle as well as the horsepower.

To calculate the required horsepower for the fan driver (Hudson Products Corporation, 2007):

$$\text{Motor Shaft Horsepower} = \text{Actual ft}^3/\text{min (at fan)} \times \text{Total Pressure Loss (inches water)}/[6356 \times \text{Fan (System) Efficiency} \times \text{Speed Reducer Efficiency}] \tag{18.26}$$

The actual volume at the fan is calculated by multiplying the standard volume of air by the density of air (0.075 lb/ft^3) at standard conditions divided by the density of the air at the fan. From this relationship, the ratio of the fan horsepower required for a forced draft unit to that required for an induced draft unit is approximately equal to the ratio of the exit air density to the inlet air density, which is in turn equal to the ratio of absolute air temperatures $(t_1 + 460)/(t_2 + 460)$. The total pressure difference across the fan is equal to the sum of the velocity pressure for the selected fan diameter, the static pressure loss through the bundle, (which is determined from the equipment manufacturer's test data for a given fin type and tube spacing), and other losses in the aerodynamic system. Fan diameters are selected to give good air distribution and usually result in velocity pressures of approximately 0.1 inch of water.

The design of the fan, the air plenum chamber, and the fan housing, (in particular fan tip clearance), can materially affect system efficiency, which is always lower than on fan curves based on idealized wind tunnel tests. Well-designed axial flow fans have efficiencies of approximately 75%, based on total pressure. Poorly designed fans may have system efficiencies as low as 40%. Speed reducers usually have about 95% mechanical efficiency (Hudson Products Corporation, 2007). The value of driver output horsepower from the equation above must be divided by the motor efficiency to determine input power.

18.8.1.10 Performance Control

In addition to the fact that the process flow rate, composition, and inlet temperature of the fluid may vary from the design conditions, the ambient air temperature varies throughout the day and from day to

day. Since air coolers are designed for maximum conditions, some form of control is necessary when overcooling of the process fluid is detrimental, or when saving fan power is desired. Although control could be accomplished using bypassing of process fluid, this is rarely done, and the usual method is air flow control.

18.8.1.10.1 Varying Air Flow

Varying air flow can be accomplished by the following:

- Adjustable louvers on top of bundles.
- Two-speed fan motors.
- Fan shut-off in sequence for multi-fan units.
- Variable pitch fans.
- Variable frequency for fan motor control.

Louvers operate by creating an adjustable restriction to air flow and therefore do not save energy when air flow is reduced. In fact, louvers impose a permanent energy loss, even in the open position.

Two-speed motors, variable pitch fans, and variable frequency fan motor control save power when air flow is reduced. In low-temperate climates, as much as 67% of the design power (Hudson Products Corporation, 2007) may be saved over the course of a year with variable pitch fans.

Both louvers and variable pitch fans may be operated automatically through an instrument that senses temperature or pressure in the outlet header. For extreme cases of temperature control, such as prevention of freezing in cold climates, more sophisticated designs may be needed.

Extreme case controls include the following:

- Internal recirculation
  By using one fixed-pitch fan blowing upward and one variable pitch fan, which is capable of negative pitch and thus of blowing air downward, it is possible to temper the air to the coldest portion of the tubes and thus prevent freezing. Normally forced draft units have the negative pitch fan at the outlet end, while induced draft units have the positive pitch fan at the outlet end. In hot weather, both fans can blow upward.
- External recirculation
  This is a more positive way of tempering coolant air but is practical only with forced draft units. Hot exhaust air exits the bundle and enters a top plenum covered by a louver. When no circulation is required, the top louver is wide open, and the heated air exits through it. When the top louver is partially closed, some of the hot air is diverted to a duct, through which it flows downward and back into the fan intake, mixing with some cold ambient air. An averaging air temperature sensor below the bundle controls the amount of recirculated air and thus the average air intake temperature, by varying the louver opening.
- Auxiliary heating coils—steam or glycol
  Heating coils are placed directly under bundles. Closing a louver on top of a bundle will allow the heating coil to warm the bundle or keep it warm in freezing weather, so that on start-up or shut-down the material in the bundle will not freeze or solidify. Heating coils are also occasionally used to temper very cold air to the bundles while the fan is operating and the exhaust louver is open.

18.8.1.11 Noise Control

Air-cooled heat exchanger noise is mostly generated by fan blade vortex shedding and air turbulence. Other contributors are the speed reducer (high torque drives or gears) and the motor. The noise is generally broad band, except for occasional narrow band noise produced by the motor or speed reducer, or by interaction between these sources and the structure.

For efficient fans at moderate fan tip speeds, this noise is proportional to the third power of the fan blade tip speed and to the first power of the consumed fan horsepower. It is quite practical and usually economical to reduce the sound pressure level at 3 feet below an air-cooled heat exchanger to 85 dB(A); but, below 80 dB(A), noise from the drives predominates and special measures must be taken (Hudson Products Corporation, 2007).

18.8.2 REFRIGERATION SYSTEMS

When process temperatures are required that cannot be economically obtained with cooling water, refrigeration systems are employed. For small duties and temperatures above −22°F, chilled water can achieve temperatures to around 30°F. For temperatures, down to about −22°F, sodium chloride or calcium chloride are sometimes used to distribute the cooling from a central refrigeration system. Large refrigeration duties or temperatures below about °F are usually supplied by a standalone refrigeration system (Towler and Sinnott, 2013). Process refrigeration systems have already been described in detail in Chapter 11.

18.9 FLARE SYSTEMS

A flare system collects and discharges gas from pressurized process components to the atmosphere at a safe location for release during abnormal conditions and emergency relief. Flare systems generally have a pilot or ignition device to promote of the gas exiting the system because the discharge may be either continuous or intermittent. A flare system from a pressurized source may include a control valve, collection piping, flashback protection, and a gas outlet. A scrubbing vessel should be provided to remove any liquid droplets that carry over with the gas relief sent to the flare.

A plant relief system often has multiple flares to treat the various sources for waste gases. One common split is between hot and cold flares. The hot flare is normally constructed of carbon steel and the cold fare of stainless steel (Thomas, 2011). The actual configuration of the flare or vent system depends on the hazards assessment for the specific installation. Considerations for the cold fare may include the Joules-Thompson cooling effect when a gas or liquid is depressured.

American Petroleum Institute (API) Recommended Practice (RP) 520, Part 1, Section 8 (API, 2000) and RP 521, Sections 4 and 5 (API, 1999) cover disposal and depressuring system design. RP 521, Appendix C, provides sample calculations for sizing a flare stack. RP 521, Appendix D, shows typical details for flare-stack seal drum, quench drum, and typical flare installation.

When flaring occurs during a plant emergency, a very large flow of gases must be destroyed for safety considerations. The maximum flow that can be handled by a flare is referred to as its hydraulic capacity. The second level of flaring is the treatment of waste gases generated during normal operation, including planned decommissioning of equipment. During normal or controlled operations, safety is still imperative, but emissions are also important. The actual gas flow rate and composition may vary significantly during normal operation (Peterson et al., 2007).

There are three important performance parameters for most flares (Schwartz et al., 2001):

- Smokeless capacity: This is the maximum flow of waste gases that can be sent to the flare without producing significant levels of opacity. A flare is typically sized so that the smokeless capacity is at least as much as the maximum waste gas flow rate expected during normal operation.
- Thermal radiation: This is generated by the flare as a function of the waste gas flow rate and composition. The radiation levels at ground level are typically limited to avoid injuring personnel and damaging equipment. After choosing the most practical flare location, the height of the flare stack is determined so that the acceptable radiation levels are not exceeded at ground level (Hong et al., 2006).
- Noise: Excessive noise can injure personnel inside and outside the plant.

While the primary function of flares is to protect the facility, employees, and the surrounding environment, flaring creates emissions such as nitrogen oxides, sulfur oxides, greenhouse gases, and volatile organic compounds. These components, in combination with any unburned hydrocarbons, contribute to the total facility emissions.

The size of flare flames and elevation above the ground make it very difficult to use a hood to collect exhaust gases and measure emissions. Other very challenging problems are weather conditions, the waste-gas flow rate, and composition that is highly variable and not generally controllable. Wind also plays a very significant role in the performance of a flare (Gogolek and Hayden, 2004).

Predictions of flare emissions are under development based on the composition of gases in the stack prior to burning, but these calculations can underestimate the emissions. One reason is that the calculations do not consider wind. Wind effects can reduce flare destruction efficiency, so the emissions may be much higher under windy conditions.

Another effect is steam injection. Many flares use steam as an assist medium to increase air entrainment into the flame to increase the smokeless capacity. However, over-steaming a flare can reduce the destruction efficiency. The cooling effect of excessive steam may inhibit dispersion of flared gases. In the extreme case, over-steaming can extinguish the flame and allow waste gases to escape into the atmosphere unburned.

There is concern that many flares are over-steamed to minimize smoking over a wide range of waste gas flow rates. In most steam-assisted flares, the steam flow rate is manually controlled and sometimes set for the maximum expected waste gas flow during normal operation. However, this means the flare could be severely over-steamed during periods when the waste gas flow is much lower than maximum.

18.9.1 FLARE GAS RECOVERY SYSTEMS

Flare gas recovery can virtually eliminate normal flaring, limiting flare operation to emergency releases and scheduled maintenance. Captured flare gas can then be reused as fuel or feedstock to provide a return on investment while minimizing emissions.

Flare Gas Recovery System (FGRS) perform the following processes:

- Isolating the flare header with a proprietary-design liquid seal or staging valve
- Recovering normally flared gases and delivering them back into the facility so they can be processed and reused as fuel gas

- Removing liquids
- Compressing gases up to a defined pressure level
- Cooling recovered gases (if required)

Compressors and pumps with liquid rings are typically used in these services.

The FGRS reduces the continuous flare operation, which subsequently reduces the associated smoke, thermal radiation, noise, and pollutant emissions associated with flaring. Capturing waste gases may reduce odor levels. Reduced flaring also reduces steam consumption for steam-assisted flares and can extend the service life of the flare tips.

When the recovered flare gas is to be utilized as a fuel and the flow is less than or equal to the capacity of the FGRS, the flare gas will be recovered and directed to the fuel gas header. During these periods, there will be little or no visible flame at the flare, although the flare pilot may be visible. When the flare gas flow rate is greater than the capacity of the FGRS, the excess flare gas will flow through the liquid seal drum and to the flare tip where it will be combusted. From flaring rates just above the FGRS capacity to a maximum flaring episode, the liquid seal drum will promote smooth, safe operation of the flare tip. The FGRS is operated at a slight positive pressure to prevent air infiltration into the system that could create a flammable mixture.

When a liquid-ring compressor is used, then separating recovered vapor phase from a mixed liquid is accomplished with a horizontal separator vessel. As flare gas flows into the header, an established hydrostatic head in the liquid seal drum will prevent flare gas from flowing to the flare. This causes a slight increase of pressure in the flare gas header but not enough to significantly affect the capacity of the over-pressure protection devices in the plant.

When the flare gas header pressure reaches the gas recovery initialization setpoint, the compression system will begin to compress the flare gas. Additional parallel compressors can be automatically staged on or off to augment the capacity of the base load compressor as needed. Based on the inlet pressure of the flare gas header, adjustment of FGRS capacity control is by the spillback (recycle) of recovered gas from the service liquid separator back to the suction.

Discharge of the liquid-ring compressors will flow into the service liquid separator vessel where the gas and service liquid are disengaged and the compressed recovered flare gas is delivered to the fuel gas scrubbing and distribution system. The compressor service liquid, usually water, is used in the compressor as a seal between the rotor and the compressor case. The service liquid is separated from the recovered gas stream, cooled and recirculated to the gas compressor train for reuse.

The gas processing capacity of the FGRS adjusts to maintain a positive pressure on the flare header upstream from the existing liquid seal drum. This positive pressure will ensure that air will not be drawn into either the flare system or the FGRS.

If the volume of flare gas that is relieved into the flare system exceeds the capacity of the FGRS, the pressure in the flare header will increase until it exceeds the back-pressure exerted on the header by the liquid seal. In this event, excess gas volume will pass through the liquid seal drum and on to the flare where it will be burned. This will be the case when there is a rapid increase in flare gas flow due to an emergency release.

Since the liquid seal serves as a backpressure control device for the FGRS, a properly designed deep-liquid seal is critical to the stable operation of the FGRS and flare. A deep-liquid seal, typically 30-in.W.C minimum, is required to permit a suitable control range for the capacity control of the FGRS (Peterson et al., 2007). As the flow transitions to the flare, this must be done with a very stable

liquid level or else unstable flare header pressure could result, affecting FGRS control and proper flare operation.

If the volume of flare gas relieved into the flare header is less than the total capacity of the FGRS, the capacity of the FGRS adjusts to a turndown condition. This is accomplished by turning off compressors and/or by diverting discharged gas back to the turning off suction header through a recycle control valve (Peterson et al., 2007).

18.10 STORAGE FACILITIES

Gas plant liquid products may be stored in pressurized vessels above ground or below ground in caverns. A horizontal, cylindrical vessel or "bullet" is commonly used as shown in Fig. 18.7. Another option for pressurized fluids is a spherical vessel or Horton sphere as shown in Fig. 18.8.

Spherical construction has several advantages. The main advantage of the spherical construction is that the stress concentration in a spherical shape will be minimal while storing pressurized liquids. The stress resistance will be uniform. The wall thickness of a spherical shell will be about half the wall thickness needed for a cylindrical shell for containing the same pressure. So, in a spherical container, a thinner shell means lesser cost and weight.

The area that a sphere occupies will be lesser compared with a cylindrical container of the same volume. The reduced surface area to volume ratio minimizes the amount transferred to the contents. Also, the footprint is smaller for a spherical tank containing the equivalent volume of a cylindrical tank.

The main drawback of a spherical storage tank is the amount of time required for fabrication. Owing to transportation limitations, these vessels must be fabricated in sections off-site and then completed in the field. The process requires significant time and coordination to ensure proper staging, sequence of assembly, and welding with continual on-site testing throughout the on-site construction process.

FIGURE 18.7

Cylindrical storage vessels.

FIGURE 18.8

Spherical storage vessels.

Chemicals, produced water, diesel fuel, and other low vapor pressure fluids may be stored in vertical cylindrical vessels with flat or dished bottoms and sloped or domed roofs. Bolted tanks may be used for near atmospheric pressure, and welded construction is typically used for pressures above 2.5 psig (Lyons, 2010). Vessels above 15 psig must be constructed per ASME Code (Lyons, 2010). Refrigerated tanks may be used to store higher vapor pressure products at low pressures.

Venting is required for all tanks for normal vacuum relief, normal pressure relief, and emergency pressure relief. Normal venting is accomplished by a pressure relief valve, a vacuum relief valve, a pressure vacuum valve, or an open vent with or without a flame arresting device. Emergency venting is accomplished with additional valves or open vents.

18.11 WASTEWATER TREATMENT

Natural gas processing plants can generate a significant amount of wastewater that has been in contact with hydrocarbons. Wastewater can also include water rejected from BFW pretreatment processes (or generated during regenerations). Wastewater can also refer to cooling tower blowdown stream or even once-through cooling water that leaves the plant.

Once-through cooling water typically does not receive any treatment before discharge. Cooling tower blowdown water and wastewater from raw water treating may or may not receive treatment at the wastewater treatment plant before discharge. Contaminated wastewater is typically sent to either a wastewater treatment plant that is located at the facility, or it can be pretreated and sent to the local publicly owned treatment works or third-party treatment facility for further treatment.

18.11.1 SOUR WATER

Steam is used in many processes as a stripping medium in distillation and as a diluent to reduce the hydrocarbon partial pressure. The steam is condensed as an aqueous phase (called steam condensate) and is removed as sour water. Since this steam condenses in the presence of hydrocarbons, which contain hydrogen sulfide (H_2S) and ammonia (NH_3), these compounds are absorbed into the water at levels that typically require treatment.

The typical treatment for sour water is to send it to a stripper for removal of H_2S and NH_3. Steam is used to inject heat into the strippers. High-performance strippers can achieve <1 ppm H_2S and <30 ppm NH_3 in the stripped sour water (IPIECA, 2010). With these levels, the stripped sour water is an ideal candidate for recycle/reuse. Strippers that use direct steam injection as the stripping medium create more wastewater compared with strippers that use reboilers to inject heat into the strippers.

18.11.2 CONDENSATE BLOWDOWN

Condensate losses are as follows: blowdown from the plant boiler system; blowdown from the various steam generators that are in the process units; and unrecovered condensate from steam traps, steam tracing etc.

A portion (usually up to 5%) of the BFW and condensate that enters the boilers is purged from the system to maintain the dissolved solids level in the system at an acceptable level. This level could be different depending on the pressure level of the steam being produced.

Energy savings are realized when condensate is recovered as it:

- reduces the quantity of BFW makeup required
- any condensate lost to the sewer increases the temperature of the wastewater and thus imposes a heat load at wastewater treatment.

Some of the condensate from steam traps and heat tracing are lost to the atmosphere and/or sewer. Often these traps are discharged directly to the sewer and the hot discharge can ultimately cause deterioration of the sewers.

18.12 DRAINS

Drains design is based on the following segregated systems:

- The open nonhazardous drainage system, providing drainage for locations that are designated nonhazardous.
  This system is segregated from all other open or closed drain (CD) systems. Nonhazardous areas generally include storage vessel areas for utility materials such as lubricating oil, diesel fuel, rain water, or washdown water contaminated with oil. The drain system from these areas typically handles fluids collected from open drip pans, tundishes, and floors in nonhazardous areas. The system discharges to open galleys for the floor drains and a tundish-type system for equipment maintenance drains. The disposal stream is often routed to an API separator. The hydrocarbons settling out in the separator/skimmer will usually be pumped to a burn pit for final disposal.

- The Open Hazardous Drainage (OHD) System, providing drainage for areas that are designated hazardous.
  All process areas and locations where hydrocarbons are present in significant quantities generally fall in this category. The drain system from these areas handles fluids collected from open drip pans, tundishes and floors in hazardous areas. The open drain system should be based on the largest flow of peak rainfall. The OHD streams are collected and often routed to an API separator by a separate channel. Collected hydrocarbons are usually pumped to a burn pit for final disposal. Water is disposed via an oily water pump.
- The CD System that collects hydrocarbon liquids, degases the liquid and safely disposes of the liquids.
  The CD handles hazardous fluids from process vessels while keeping them out of contact with the atmosphere. The CD should be designed to receive and degas the maximum expected production of raw condensate and oil from the various sources and should consist of a CD flash drum with pumps. The drum is designed with sufficient volume to receive the drained fluids and to permit vapor disengagement. A safety margin is applied to cover additional volumes, which may be drained. The drum minimum design pressure should be set to eliminate the risk of rupture in the event of a deflagration. The vent is sized to discharge the highest vapor flow that could enter the drum if gas blow by should occur. The sizing requirement for the pumps is the removal of all liquids between high-level and low-level limits. Heavy liquids (normally water) should underflow and light liquids (normally water) overflow to individual compartments.

18.13 WASTE DISPOSAL

Gas processing plants produce associated wastes, which consist of scrubber liquids and sludge, glycol compounds and used filter media, and miscellaneous other waste streams. Most gas processing plant wastes are disposed by injection, and the remaining is disposed at commercial waste facilities and industrial or municipal disposal facilities.

18.14 FIREWATER SYSTEM

There are many flammable fluids and gases present or generated in a natural gas processing plant. To contain a fire and ensure personnel safety as well as limit damage to the facility, a fire protection system including a firewater system is installed.

Water is used for fire extinguishment, fire control, cooling of equipment, and protection of equipment as well as personnel from heat radiation. Among the different forms of firewater systems are straight jet, water fog, water curtain, water spray, and deluge/sprinkler, for foam making. Fire water system should consist of fire water storage, fire water pumps, and distribution piping network along with hydrants and monitors (OISD, 2007).

18.15 FIRE AND GAS SYSTEM

A fire and gas (F&G) safety system continuously monitors for fire, combustible and toxic gas releases and provides early warning and mitigation actions to prevent the incident or escalation of the incident.

A typical F&G safety system comprises detection, logic control, alarm, and mitigation functions. A logic controller receives alarm and status or analog signals from field monitoring devices required for fire and gas detection. The controller handles the required actions to initiate alarms and mitigate the hazard (Honeywell, 2009).

A good F&G system combines fire and gas detectors, conventional and analog addressable fire panels, clean agent and inert gas fire suppression systems, and a safety integrity level 3—certified fire and gas logic solver. An integrated system provides an operating interface and networking.

F&G systems include detectors for early warnings of explosive and health hazards, including combustible and toxic gas releases, thermal radiation from fires, and minute traces of smoke in sensitive equipment enclosures. They also provide audible and visual alarm indications helping to ensure operators, and personnel are informed of potentially hazardous situations. The F&G system automatically initiates executive actions minimizing escalation of safety incidents and protecting personnel, property, and the environment.

Integration at the controller level provides plant-wide safety instrumented system point data, diagnostics and system information, as well as alarms and events, operator displays and sequence of event information to any station. This minimizes intervention and shutdowns, reduces hardware costs, and allows plants to recover more easily from process upsets.

The safety system includes a secure communication network, transfer alarm signals, fault signals, and system diagnostics. Information from all related systems can be transferred, gathered and handled at the same location, and an additional layer can be achieved to monitor the status and operability of the total F&G detection and control system.

REFERENCES

API, 1999. Guide for Pressure-Relieving and Depressuring Systems. Recommended Practice 521, fourth ed. American Petroleum Institute (API), Washington, DC, USA.

API, 2000. Design and Installation of Pressure Relieving Systems in Refineries. Recommended Practice 520, Part I, seventh ed. American Petroleum Institute (API), Washington, DC, USA.

Beychok, M.R., 1967. Aqueous Wastes from Petroleum and Petrochemical Plants, first ed. John Wiley and Sons, New York, NY, USA.

Chemical Engineering Site, April 8, 2018. Cooling Tower Efficiency Calculations. http://chemicalengineeringsite.in/cooling-tower-efficiency-calculations.

EML Manufacturing. Houston, TX, USA. http://emlmanufacturing.com/Fuel_Gas_Conditioning.htm.

Franson, M.A., 1975. Standard Methods for the Examination of Water and Wastewater, fourteenth ed. American Public Health Association, Washington, DC, USA.

GE Power and Water, 2012. Handbook of Industrial Water Treatment. Water and Process Technologies, General Electric (GE) Company, Atlanta, GA, USA.

Gogolek, P.E., Hayden, A.C., 2004. Performance of flare flames in a crosswind with nitrogen dilution. Journal of Canadian Petroleum Technology 43 (8), 43—47.

Goldman, C.R., Horne, A.J., 1983. Limnology. McGraw-Hill Book Company, New York, NY, USA.

GPSA, 2016. Engineering Data Book, fourteenth ed. Gas Processors Suppliers Association (GPSA), Tulsa, OK, USA.

Green, D.W., Perry, R.H., 2007. Perry's Chemical Engineer's Handbook, eighth ed. McGraw-Hill Book Company, New York, NY, USA.

Hensley, J.C., 2009. Cooling Tower Fundamentals, second ed. SPX Cooling Technologies, Inc, Overland Park, KS, USA.
Honeywell, April 2009. Integrated Fire and Gas Solution Improves Plant Safety and Business Performance. White Paper. Honeywell, Phoenix, AZ, USA.
Hong, J., White, J., Baukal, C., 2006. Accurately predict radiation from flare stacks. Hydrocarbon Processing 85 (6), 79−81.
Hudson Products Corporation, 2007. The Basics of Air-cooled Heat Exchangers. Beasley, TX, USA.
IPIECA, Oct. 2010. Petroleum Refining Water/Wastewater Use and Management. International Petroleum Industry Environmental Conservation Association (IPIECA), London, UK.
Kaeser Compressors, Inc, 2007. Compressed Air System Guide: Designing Your Compressed Air System. Fredicksburg, VA, USA.
Kays, W.M., London, A.L., 1984. Compact Heat Exchangers, third ed. McGraw-Hill Book Company, New York, NY, USA.
Kemmer, F.N., 1979. The NALCO Water Handbook. McGraw-Hill Book Company, New York, NY, USA.
Lyons, W.C., 2010. Working Guide to Petroleum and Natural Gas Production Engineering, first ed. Gulf Professional Publishing, Burlington, MA, USA.
Mokhatab, S., Corso, S., 2016. Onsite nitrogen generation via PSA Technology. Chemical Engineering 123 (7), 48−51.
OISD, August 2007. Fire Protection Facilities for Petroleum Refineries and Oil/Gas Processing Plants. OISD-STANDARD − 116, second ed. Oil Industry Safety Directorate (OISD), New Delhi, India.
Peterson, J., Tuttle, N., Cooper, H., Baukal, C., 2007. Minimize facility flaring. Hydrocarbon Processing 86 (6), 111−115.
Rattenbury, J.M., February 1, 2001. How to optimize an instrument air system. Plant Engineering 55, 1.
Schneider Electric, 2015. Electrical Installation Guide. Rueil-Malmaison, France.
Schwartz, R., White, J., Bussman, W., 2001. In: Baukal, C. (Ed.), "Flares", Chapter 20, John Zink Combustion Handbook. CRC Press, Boca Raton, FL, USA.
Spirax Sarco Limited, 2018. Steam Engineering Tutorials. Cheltenham, Gloucestershire, UK.
Stevens, R.A., Fernandez, J., Wolf, J.R., 1957. Mean temperature difference in one, two and three-pass crossflow heat exchangers. Transactions ASME 79, 287−297.
Thomas, C.E., 2011. Process Technology Equipment and Systems, third ed. Cengage Learning, Clifton Park, NY, USA.
Towler, G., Sinnott, R., 2013. Chemical Engineering Design: Principles, Practice and Economics of Plant and Process Design, second ed. Butterworth-Heinemann, Elsevier, Waltham, MA, USA.
US DOE, February 2011. Cooling Towers: Understanding Key Components of Cooling Towers and How to Improve Water Efficiency. Federal Energy Management Program, DOE/PNNL-SA-75820, US Department of Energy (DOE), Washington, DC, USA.
US EPA, 2014. Cooling Water Intakes. US Environmental Protection Agency (EPA), Washington, DC, USA.

CHAPTER

19 PROCESS MODELING AND SIMULATION OF GAS PROCESSING PLANTS

19.1 INTRODUCTION

At the most abstract and simple level, a process simulation model is a representation of a process plant to facilitate design, rating, monitoring, or other types of analysis of the behavior of that plant. Most of the time, this refers to creating a mathematical representation using a computer software. All simulation models share several basic elements:

- A model of the thermodynamic behavior of fluids handled in the plant
- Models for each equipment present in the process plant
- Representation of chemical reactions
- Connections between equipment to represent the flow of material

The nature and the level of detail of each of these can vary greatly, and the user of the simulation model must make a choice such that the model results and accuracy satisfy the needs of the task at hand. An important element is a selection between steady-state and dynamic modeling. A model should always be fit for purpose. It means that excessive detail should be avoided, but also care should be taken not to oversimplify the model and in that way, overlook possible issues in design or operation.

The benefits of simulation are not unique for gas processing plants. They apply to any process plant. Simulation models bring value throughout the complete lifecycle of a process. At the very early conceptual design phase of the process, the emphasis will be more on relatively simple heat and material balances. As the definition of the plant becomes more detailed, so will the model.

During the conceptual phase, the results of the simulation will be used to determine approximate equipment sizes, power, and utility consumption. Multiple concepts will be analyzed. For each concept an estimate of the investment required for the plant and of the operating costs can then be made. The combination of these numbers with the cost of raw material and the expected market prices of the products will determine the economic viability of each concept and ultimately of the project.

During the front-end engineering design phase, the simulation model will provide sufficient information for a detailed design of each equipment item, the piping that will connect them, and the instrumentation. Dynamic simulation models will also provide insight into the controllability of the proposed design.

In the detailed engineering phase and through the start-up of the plant, dynamic simulation models will uncover design flaws, provide information on the tuning of the process control system, on the validity of the proposed start-up scenarios, and may help the training of the engineers and operators on the operation of the plant. Another very important aspect is the use of models to define safety

Handbook of Natural Gas Transmission and Processing. https://doi.org/10.1016/B978-0-12-815817-3.00019-8

equipment and to ensure that the safety system is designed to protect the plant and the people operating the plant under all incident scenarios.

Finally, simulation models are invaluable during the operation of the plant for monitoring the condition of the equipment, trouble shooting, and for optimizing the performance as a function of current feed product quality, market prices, and environmental factors.

Another use of simulation is when analyzing if an existing plant can be reused or adapted to treat another feedstock or an additional feedstock. Very often the result of dynamic modeling of safety systems can be a deciding factor in the viability of such a project.

This chapter aims to provide guidance in selecting the model nature and level of detail such that it is fit for purpose but can also be reused if more demanding tasks arise in the future. Both steady-state and dynamic models will be discussed. A second part of this chapter introduces modeling best practices. These practices are aimed at faster model development of robust models with the required accuracy.

19.2 THERMODYNAMICS

At the heart of any model is the description of the behavior of the fluids that are to be processed when subject to a wide range of temperatures and pressures. The accuracy of the chosen thermodynamic model is key to the accuracy of the complete model. The selection of a thermodynamic model will depend on the nature of the components to be represented and the range of temperatures and pressures that are to be considered. Hydrocarbon molecules behave in a relatively ideal fashion at low pressure and near ambient temperature. However, most gas processing will involve high-pressure operations and sometimes cryogenic temperatures. To properly model the behavior at high pressure, an equation of state (EOS) should be used. The most popular equations of state for gas processing are Peng-Robinson (PR) and Soave-Redlich-Kwong (SRK).

High-accuracy equations of state exist for hydrocarbon mixtures. The RefProp model from the National Institute of Standards and Technology is an example of such an EOS. This model is seldom used to model a complete flowsheet. The two reasons are that the model consumes much more central processing unit power than an EOS such as PR, and the model is less robust. The reduced robustness may lead to convergence issues when the operating conditions for which the calculations need to be performed fall outside of the normally expected conditions. Therefore it is best to limit the use of complex thermodynamic models to parts of the simulation model that require that specific model to produce meaningful results. Care should be taken to avoid including these calculations in loops with many iterations.

For example, the mass density of the gas may be calculated more accurately with a complex EOS. However, the gain in accuracy will often only be a few percent. For the engineering design calculations, this will not make a meaningful difference. But, when determining the export rate of the gas, a 1% error in mass density means a 1% impact on revenue, and this translates into a considerable amount of money. However, even in this case, it is only important to calculate an accurate mass density at the export point and not throughout the whole process.

In gas processing, not all units are limited to just hydrocarbons. Water is almost always present, and specific chemicals such as triethylene glycol (TEG), monoethylene glycol (MEG), or methanol are used. When these are present, special attention is required to the selected thermodynamics. The Cubic-Plus-Association (CPA) EOS is becoming an important tool in this area. The treatment of liquid water streams in general may also require special attention. More specific information can be found in the case studies section.

An important element that needs to be kept in mind when selecting a thermodynamic model is that the thermodynamic model itself is only a framework represented through a set of equations. These equations require component-specific parameters and also parameters that describe the interaction between components. If those parameters are not known, even the best thermodynamic model is worthless! So be sure to check if your simulator has all the information, especially for more complex equations of state.

When choosing a thermodynamic model, the complexity of the model should be considered. As the thermodynamic routines are called virtually all the time in a simulation model, a complex thermodynamic model will slow down the model execution. Keep in mind that a simulation model will most likely contain iteration loops and possibly optimization routines that mean a single equipment item is calculated many times. If a once through calculation takes 2 s instead of 0.2 s, that is irrelevant. But if that equipment gets calculated a 1000 times, it means 3 or 33 min.

19.3 STEADY-STATE VERSUS DYNAMIC MODELS

Once the thermodynamic model has been selected, the next choice to be made when embarking on a modeling project is whether the task at hand requires a steady-state or a dynamic simulation model. The difference between these two types of models is that a steady-state model assumes the plant is operating in a perfectly stable manner. Variation with respect to time is assumed to be zero. The use of steady-state models is universally accepted in all stages of the design and operation of gas processing plants. The reason for this popularity is that the assumption of a zero derivative with respect to time simplifies the modeling of all equipment enormously. This has a significant impact on model solution time and on modeling complexity. Dynamic simulation has been used for a long time, but rigorous first principles dynamic simulation has been confined to use by specialists. Control engineers were using models based on transfer functions that were incapable of representing the nonlinearity in systems and the discontinuities in start-up cases for example. Only since the late nineteen nineties has dynamic simulation become a more generally accepted tool to be used by process engineers and control engineers alike. But even today, there remains a big barrier for process engineers to use dynamic modeling.

Steady-state modeling allows for more flexibility in the specification of the model. It is very easy to define the model as a task to be accomplished in relatively abstract terms. For example, the process may require the pressure and temperature to be changed. A steady-state model can usually do this with a single-unit operation. Although it is possible to create a similar abstract dynamic model, if the actual equipment function and geometry is not known, the dynamics of the model are arbitrary and may even lead to wrong conclusions.

A dynamic simulation is typically aimed at a more realistic and more detailed model of the behavior of the process, and it includes how the process behaves over time. If we consider a simple vapor-liquid separation vessel, then in a steady-state simulation, the nature of the model and the inlet and outlet connections are all that is required to define the simulation. The volume in the vessel or the liquid level has no impact on the results. In a dynamic simulation the volume and liquid level are key elements of the simulation. The aim of the simulation could for example be to study the level control of the vessel or the pressure transients in the vessel.

For any modeling effort that is aimed at main equipment design, the initial modeling choice will always be a steady-state model. A dynamic model may be used at a later stage to validate the process

behavior given the design choices resulting from the steady-state model combined with specific circumstances. If the aim of a simulation is related to process control or to safety, a dynamic simulation is almost always required as the phenomena to be studied are related to variations in time.

The software available today enables process engineers with some process control knowledge and control engineers with some process knowledge to build dynamic models easily. The constraint to using dynamic simulation is no longer that dynamic simulation is difficult to employ, but foremost to find engineers that have this cross-boundary knowledge between process engineering and process control. Another constraint is that the implementation time for a dynamic model is in the order of 2–4 times as long as the time needed to implement a steady-state model. Frequently a consultant is employed to develop the model and one or more engineers of an operating company or engineering company would use the model to run the needed studies.

19.4 SIMULATION OBJECTIVES VERSUS MODELING EFFORT

19.4.1 SHORTCUT VERSUS RIGOROUS MODELS

Shortcut models tend to describe the process in more abstract terms; the unit operations used do not necessarily directly represent actual plant equipment but sometimes a combination of several equipment items. Rigorous models will model each equipment item individually.

There is no single definition of rigorous. Rigor can be introduced by increasing the number of unit operations used to model the system, and it can also be introduced by changing the methods used inside of a unit operations model to represent the function of the equipment.

As an illustration consider a small part of the plant that has a pump to increase the pressure of a liquid and a heat exchanger that reduces the temperature of the liquid. A shortcut model could represent this as a single-unit operation. The model would provide limited information for the design of the pump or the heat exchanger, but it does bring the liquid to the expected state to feed it in the next unit operation. A first step toward a more rigorous model would be to model this as a pump and a cooler. A next step would be to use a heat exchanger model that also represents the cooling fluid. The model could be further detailed by including geometry information for the heat exchanger or pump performance curves.

For a dynamic model, some of the control valves should be added such that the behavior of controllers can be checked. The model detail can be extended even more by also including the spare pump that will be installed, the block valves that will be included, the minimum flow line on the pump, and the bypass circuit on the exchanger. Additional details such as the inertia of the pump can be added for studying the start-up of the pump.

The choice of the level of detail depends on the purpose of the model. Clearly, the shortcut model will not be of any help investigating the behavior of the system when it switches to the spare pump in case of failure of the normally operating pump. But, if the currently required information is pump power and utilities consumption, a model slightly more rigorous than the shortcut model is sufficient, and additional modeling of the spares and bypasses would be a waste of effort.

Another typical example would be the case where a larger plant includes a TEG dehydration unit, and it is already known that this will be subcontracted to a specialist vendor. The main model can represent the whole TEG dehydration unit as a single simplified block that produces a dehydrated gas with the water content specification demanded from the specialist vendor.

19.4.2 LUMPED PARAMETER VERSUS DISTRIBUTED MODELS

Lumped parameter and distributed models come into play when considering rigorous equipment models. It is a continuation of the sort of choices that are made when choosing between shortcut and rigorous models at the level of a single equipment item. A lumped parameter model will consider the content of one equipment to be homogeneous; it will not consider radial or axial gradients in the fluid properties. A fully distributed model will consider the variation of fluid properties and interaction with its neighboring elements in all three dimensions and over time. Computational fluid dynamics is an example of a method that can be a fully distributed model.

As with shortcut and rigorous process models, there is a continuum of variations between the two extremes. This can also best be illustrated with some examples. A totally lumped model could be a phase separation vessel model that only predicts phase separation and a uniform heat input from the environment. This would be a zero-dimensional model.

A first (small) step toward a distributed model is to calculate the heat input for the part of the vessel that contains the vapor phase and the part that contains the liquid phase separately. A next step could be to drop the assumption of phase equilibrium and to calculate phase compositions and temperatures using the rate of exchange of material and heat between the phases. A practical example of this is the selection of the model used for determining the result of depressuring a vessel over time. If the calculated temperatures approach the limit where a different material of construction needs to be used, it would be prudent to increase the rigor of the model and hence to move to a more distributed model.

Next, we could consider the problem of the behavior of a large liquefied natural gas (LNG) storage tank. A known phenomenon is roll over. The model that may have been satisfactory to describe vessel depressuring would not capture the roll over phenomenon. The model would also need to consider that in the liquid phase, there can be multiple layers with different compositions and properties. This would lead to a 1-dimensional model. If the effect of the pitch and roll of the ship are lumped together in a single parameter, our previous 1-dimensional model would be expanded to be a 2-dimensional model. If the effects of pitch and roll are quantified separately, then the resulting model would be a 3-dimensional model.

The type of model selected should always depend on the purpose of the model and ultimately it will be the economics or safety that determines the choice. If it takes a one-million-dollar study to quantify the additional effect of the sun heating a vessel in a nonuniform way and the potential gain from the results of the study is 25,000 dollars per year, it is highly unlikely that such a study would be done.

19.4.3 STEADY-STATE PERFORMANCE MODELS VERSUS DESIGN MODELS

Steady-state models used for process design are not suited for determining the performance of a process. In many instances the inputs in a design model are the output for a performance and vice-versa. An example is a model of a compressor. In a design model the efficiency of the compressor will be assumed and will be an input to the model, the compressor outlet temperature will be calculated. In a performance model the compressor outlet temperature and pressure will be input values, and the efficiency of the compressor will be calculated. A performance model can also be made such that it predicts the behavior of the plant using measured feed data, controller set points, and simulation models that use the equipment geometry to predict the effect of that operation. An example here is modeling a compressor by including the compressor performance map in the model. This model will

use the feed conditions, the compressor speed, and the performance map to predict the compressor outlet conditions and compressor efficiency.

The two approaches described previously can be used in parallel to provide more valuable results. The first approach will yield the actual current efficiency of the compressor, and the second approach will yield the expected efficiency. The deviation between these two numbers is a measure of the degradation or fouling of the compressor.

A steady-state model that predicts the plant behavior using equipment geometry or performance maps will be more complex to solve. The reason is that such equipment models typically require fully defined inlet stream streams and the equipment geometry. In many cases this will lead to a need for additional recycle and adjust operations. A heat exchanger in a plant with a lot of heat integration will often have one feed that comes from the equipment downstream of itself. In a design model the outlet temperature can be set, and the details of the exchanger can be calculated once the downstream part is calculated. With a rating model, both inlets need to be known before the calculation can proceed, and this is only possible by introducing a recycle in the calculations. Another element that can make the model more complex is the absence of measurements. A heat exchanger may have a bypass that is used to control the outlet temperature. The flow rate of the bypass stream may not be measured and, the model will need to iterate on the bypass flow to match the measured outlet temperature.

The addition of recycle and adjust operations will increase the solution time of the model significantly. The addition of these iterations will also make the model less robust. If the performance model is to be used in an online system, the solution time and solution robustness are important elements in creating a useful online performance monitoring system.

19.4.4 COMMERCIAL MODELS VERSUS BESPOKE MODELS

As a bespoke model will typically be more expensive than an off-the-shelf model, a bespoke model would only be selected if off-the-shelf models cannot provide the required functionality or accuracy. An intermediate solution should also be investigated. Rather than creating a bespoke model from scratch, it may be more economical to use an off-the-shelf tool and construct the required model from elements provided by the off-the-shelf tool. Another element may come into play here. If the new model will likely be useful for several applications, then the added cost may be offset by the cost one would otherwise incur by reimplementing a solution repeatedly in an off-the-shelf tool. Another important factor may be that once the bespoke model has been validated, it does not require revalidation for the next applications.

An element to consider as well is if other operating or engineering companies may have the same needs. In that case, one could try to convince the provider of the off-the-shelf tool to develop the model or if a more rapid response is required, use a third party to develop the bespoke model and make it available to all model users.

19.5 PROCESS SIMULATION APPROACHES

For both steady-state and dynamic models, the approach can be split into two categories: modular models and equation solver type models. As nothing is black and white in this world, there is also scope for approaches that are hybrid between the two.

19.5.1 MODULAR APPROACH FOR STEADY-STATE MODELS

A modular approach is by far the most used approach for steady-state process modeling. Most commercial simulators fall into this category or have this capability in the offering. Every equipment item or combination thereof is modeled as a separate block. Inside each block, different approaches can be used, but the key distinguishing factor is that a block will only attempt to solve if sufficient information has been made available through user input and from upstream or downstream blocks. If a block can use information from both upstream and downstream blocks, the simulator is said to be nonsequential. This capability can be used to create computationally more efficient models.

We can go back to the example application of a pump followed by a generic cooling device. With a sequential modular approach, the feed stream of the pump needs to be completely known. This typically means composition, pressure, temperature, and flow are known. The pump then needs some information that allows it to determine the discharge pressure and a pump efficiency to solve. The generic cooling device needs the results from the pump and information to determine the cooling duty and the outlet pressure. Besides the feed definition, the user input could for example be pump discharge pressure, pump efficiency, cooler pressure drop, and cooler outlet temperature. If the user has as information the pump efficiency, cooler pressure drop, cooler outlet pressure, and outlet temperature, an iterative procedure is required to find the solution to this small problem. With a nonsequential modular solver, the cooler would be able to partially solve the cooler and determine the inlet pressure from the outlet pressure and the pressure drop. This would enable the pump to solve completely and subsequently the cooler would be able to solve for the remaining unknowns.

The modular approach has the advantage of being very robust. The robustness however, comes at the price of speed of solution, if the model involves recycle streams or includes some sort of iterative instruction that varies a parameter to reach a specified target or if the goal is to perform an optimization of the modeled plant.

19.5.2 EQUATION SOLVER APPROACH FOR STEADY-STATE MODELS

In the equation solver approach for steady-state models, all the calculations required for each of the blocks are expressed as equations. The connections between the blocks are also expressed as equations. The solution algorithm is a mathematical equation solver for the combination of these equations. One advantage of this approach is that the user input does not need to be such that at least part of a block can be solved to solve the complete flowsheet.

Going back to the example of the pump and the cooling device, even the nonsequential modular solver is not able to solve the problem if the information available to the user is the cooler outlet temperature, outlet pressure and duty. The cooler can determine the inlet molar enthalpy, but the pump model is not set up to derive the discharge pressure from the molar enthalpy. An equation solver would not require such a specific setup. The equations that govern the pump behavior will either directly or indirectly link the pump outlet molar enthalpy to the pump outlet pressure and be able to solve for it. At the same time, this example illustrates however, the reduced robustness of this solution technique. As the molar enthalpy of the pump outlet is rather insensitive to the pressure, it is very easy to specify a combination of inputs that will be infeasible.

The big advantage of the equation solver approach is speed. The solution of problems with recycles or targets or optimizations does not take substantially longer than the solution of a flowsheet that does

not have this type of added complexity. Because of this combination of advantages and disadvantages, the main area of use of this type of flowsheet solvers is in applications where optimization is a requirement. Online optimization applications are the main applications of this type of simulators.

19.5.3 A COMBINED APPROACH IN STEADY-STATE MODELS

Although most commercial steady-state simulators are said to be modular, they frequently have some specific equation solver type solutions inside them. The main example found in virtually all steady-state simulators is the modeling of the distillation column. A distillation model consists of a stacked series of phase separation stages that are highly interlinked. If this model were to be solved in a strictly modular fashion, a model with N separation stages would require (N-1) recycle or tear streams. The solution time would be very long and quite often no solution would be found. So, for this part of the model, a specific equation solver is used. As the functionality is limited to certain types of equipment, the solver can be optimized to not only be fast but also robust. Despite this, the modeling of a distillation column is often one of the more challenging parts of creating a flowsheet.

19.5.4 MODULAR APPROACH FOR DYNAMIC MODELS

A modular approach is not very often used for dynamic models, at least, not for gas processing applications. The main reason is that most of the time dynamic models also need to capture the hydraulic behavior of a plant. The hydraulics of a plant are determined by the combination of pressures, flows, holdups, and flow resistances of a series of equipment. A change of pressure at one end of the plant can affect the pressures and flows of large parts of the plant, and this happens quasi instantaneously. A modular solution technique is not suitable at all for this type of problem.

In a pharmaceutical plant, the main dynamics of interest are the behavior of liquid holdups and reactors, and a modular approach is appropriate here. In a gas processing plant the hydraulic behavior of fluids is very important and hence no dynamic simulator for gas processing applications uses a purely modular approach.

19.5.5 EQUATION SOLVER APPROACH FOR DYNAMIC MODELS

The equation solver approach for dynamic simulation is very comparable to the equation solver approach for steady-state simulators. However, the disadvantage in robustness is combined with reduced performance when compared with the hybrid approach described below. The biggest CPU power consumers in any process simulation model, be it steady state or dynamic, are the flash and thermodynamic calculations. With an equation solver approach for dynamic modeling, these time-consuming calculations are performed simultaneously and at the same frequency of all other calculations. This usually results in a comparatively poor overall performance. The equation solver approach is used for dynamic modeling if high accuracy is the primary concern.

19.5.6 HYBRID APPROACH FOR DYNAMIC MODELS

The hybrid approach combines an equation solver approach for the hydraulic calculations with a modular approach for all other calculations. This combination yields models that can be very fast, even

for large models and yet have sufficient accuracy. The accuracy of the model can be increased by using smaller time steps in the model but that comes at the price of speed. A common optimized approach is to run the hydraulic calculations at a smaller time step than the modular calculations. The justification is that changes in composition and equilibrium constants happen much slower than changes in pressures and flows. In this way the most time-consuming calculations are executed less frequently, and this benefits the overall speed of the model. Most commercial dynamic simulators use some form of this hybrid approach.

19.6 BEST PRACTICES FOR STEADY-STATE MODELING

This section will describe best practices for steady-state simulations, although some of the best practices apply equally well to dynamic models. A separate section is dedicated to dynamic modeling later in this chapter. The key message is not to blindly start modeling but to consider first what needs to be modeled and what the purpose of the model is.

19.6.1 CHEMICAL COMPONENTS AND THERMODYNAMIC MODELS

19.6.1.1 Component Lists

The first task is to select the components to model the system, and the goal should be to select as few components as possible as more components mean a slower model.

The information at hand for creating a simulation may contain a definition of the feed composition with a list of 30 components. Yet, 15 of those may have a mole fraction in the feed that is negligible. One needs to consider if any of the components seemingly present in negligible amounts will accumulate somewhere in the process in a more concentrated form.

As an example, the feed to a natural gas liquefaction plant is often pretreated using a distillation process to remove the heavier compounds. The amount of isopentane in the original feed may be less than a 10th of a percent, but in the bottom product of that distillation column, there is over 5% of that compound. However, if the scope of the model does not include this distillation, it is quite likely that the isopentane can be removed from the component list. Another obvious reason to keep a trace component in the component list is that one of the objectives of the study is the behavior of that trace component in the plant.

Components to be modeled in gas processing plants are mostly pure chemical compounds. However, the feed to the plant may contain heavier hydrocarbons represented as hypothetical or pseudo components. In most cases, all these heavier compounds can be lumped into a single pseudo component or hypothetical component.

Considering the feed components alone is often not sufficient. Consider the whole process to be modeled and add components that may not appear in the main process feed but are added elsewhere in the system. Water or ethylene glycol is likely candidates for this in a gas processing plant. Blanketing gas or air may also be required as part of the main component suite.

Components exclusively used in utility systems should be placed in a different component list. A typical example could be to have a component list with only water for use in modeling cooling water and steam systems.

19.6.1.2 Thermodynamic Model Selection

In general, for any process with pressures above 10 bar (145 psig), the gas phase should be nonideal, and an EOS should be used to model the gas phase. In gas processing this is almost always the case. If the fluids to be modeled contain significant amounts of polar compounds, then the liquid phase should be modeled using an activity model or another specific thermodynamic model (for example, electrolytes). In gas processing, the main process seldom has a lot of polar compounds and hence the main process fluid is usually modeled entirely using an EOS such as PR or SRK. Small amounts of water (a polar compound) are usually handled with sufficient accuracy in these equations of state, at least the way these are implemented in commercial simulation packages.

The densities of liquids are usually not well modeled with equations of state; most commercial simulators will use a different liquid density method by default to overcome this.

Especially for the sections of the plant that work at cryogenic conditions, it is best to use Lee–Kesler enthalpies rather than the EOS enthalpies. This is not a default option in commercial simulators and the responsibility of the user.

In gas processing there are typically two units that require a specific thermodynamic model. The removal of water using TEG or other solvents requires the use of a different model to accurately model the equilibrium between the solvent and water and of contaminants such as benzene, toluene, and xylene. The removal of CO_2 and sulfur compounds also requires a specific model, often combined with specific equipment models.

19.6.2 THE SIMULATION MODEL

As discussed in previous paragraphs, the level of detail of the model in each equipment item should fit the purpose of the model. This selection has a large impact on the solution speed. Before applying any of the below suggestions, give some thought to the purpose of the model! It could be a one off that will only be used for a couple of calculations, if so, it does not pay to spend an hour improving the model. Balance the optimizations with the expected use of the model.

If all simulations were such that each equipment item is only solved a single time, the considerations around number of components, model detail etc. to ensure sufficient model speed would probably be irrelevant. But there are two factors in modeling that result in each equipment block being calculated many times over: recycles and iterative procedures to reach a specification. These iterative procedures include adjusts, controllers, design specifications, or something else depending on the modeling software you use.

19.6.2.1 Model Speed and Iterations

The presence of physical recycles in a plant requires an iterative solution. In a modular simulator these iterations are introduced through recycle operations. These recycles mean that in a typical modular solution of the model, there are streams that must start with an estimated state. This estimation must then be updated until the estimated state matches within a user-defined tolerance with the calculated state. The number of required iterations required varies but is typically in the order of five iterations. Multiple recycles can be nested, and if an equipment is inside three of these loops, then that one block may need to be calculated a 100 and 25 times before the final convergence of the model. If that block is very simple and is solved in one hundredth of a second, the impact on the total solution time is limited. If that block is complex and requires 1 s to solve, the solution of that block alone will take 2 min. So, it

is important to minimize the number of recycles and to put the tear streams or recycle blocks in locations that will ensure the fastest solution.

Some commercial software provides an automated way to determine these tear streams. These automatically determined tear streams are not necessarily the best choices. The algorithm will normally find the minimum number of tear streams, but the selected location may not be optimum for stability. For nonsequential modular solvers, there usually is not an algorithm that can determine the number of recycle blocks nor the best location. The user must make an analysis which depends on model topology, and the way the model constraints have been specified. The advantage here is that some recycles can be avoided.

The second factor that induces iterations in a model is the presence of control or adjust blocks. These blocks vary a temperature, flow, pressure, or other specification in the model to obtain the desired value of some property that cannot be specified directly in the model. Anytime such a block seems necessary, check and double check if it is really required. The block may not be needed because a direct specification is in fact possible, albeit with some effort. The block may not be needed because obtaining the specification may not be crucial for the model. An often-observed example is the use of an iterative block to obtain a volumetric flow in terms of actual volume flow. Most simulators do not accept this as a specification, but a calculator block or spreadsheet can easily be used to obtain a fluid density and to calculate the required mass flow from this density and the desired volume flow.

Once the iterative procedure has been optimized, it may make sense to look at the nature of the calculations of each object in the iterative calculations. If a block makes a lot of complex calculations, it pays to check if the results of those complex calculations are really needed in each iteration.

The calculation of a heat exchanger can serve as an example. Assume that in the model the exchanger outlet temperature and pressure are fixed, but that a rigorous exchanger model is used to determine the allowable amount of fouling. That allowable amount of fouling may be calculated hundreds of times, and yet it is only the very last calculation that is useful. In this case, it may make sense to replace the rigorous calculation of the exchanger with a simple calculation and to have a parallel block that calculates the fouling that only executes once after everything else has been solved. All simulators have that sort of capability; you just need to find how it is done.

19.6.2.2 Solution Order

Once a model becomes complex with several recycles and adjusts or controllers, the order of solution becomes important. In many scenarios the wrong order of solution may result in nonconvergence. An obvious case could be the steady-state solution of a compressor with antisurge loop. Consider that the compressor is solved using a performance map, it operates at fixed speed, and the net feed is such that the compressor would operate below the minimum allowable feed flow. The amount of recycled material needs to be adjusted until the volumetric feed to the compressor equals the flow that matches the control line of that compressor.

In an initial case, assume that the recycle block or tear stream is located between the location where the recycled amount is specified and the compressor block as you follow the flow (see Fig. 19.1 below). If the solution sequence is set up such that the adjusting iteration executes before the recycling, there is a problem. The result of the modification of the amount recycled will not propagate to the feed of the compressor as long as the recycle is not solved. So, to the adjusting block it will look as if changes to the amount recycled have no impact on the compressor feed flow.

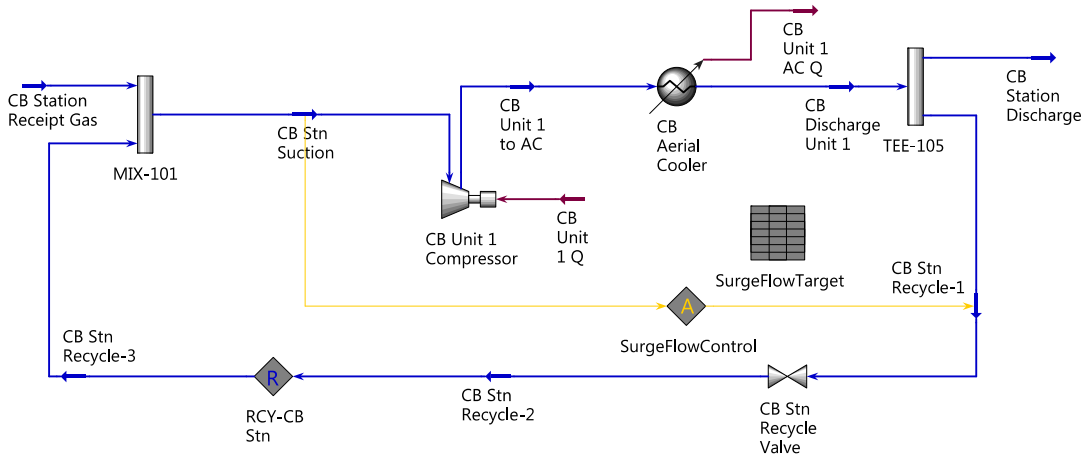

FIGURE 19.1

Compressor antisurge process flow diagram, adjusted value downstream of recycle.

In the second case the recycle is upstream of the location where the amount recycled is specified (see Fig. 19.2 below). In this case, even though the order of solution will not prevent convergence, it may still influence the number of iterations required.

19.6.2.3 Model Robustness

No model will only be used to look at the results of just one set of problem specifications, but often a model seems to be made only for that initial set of specifications. When one or more of those specifications change value, the model may not solve anymore.

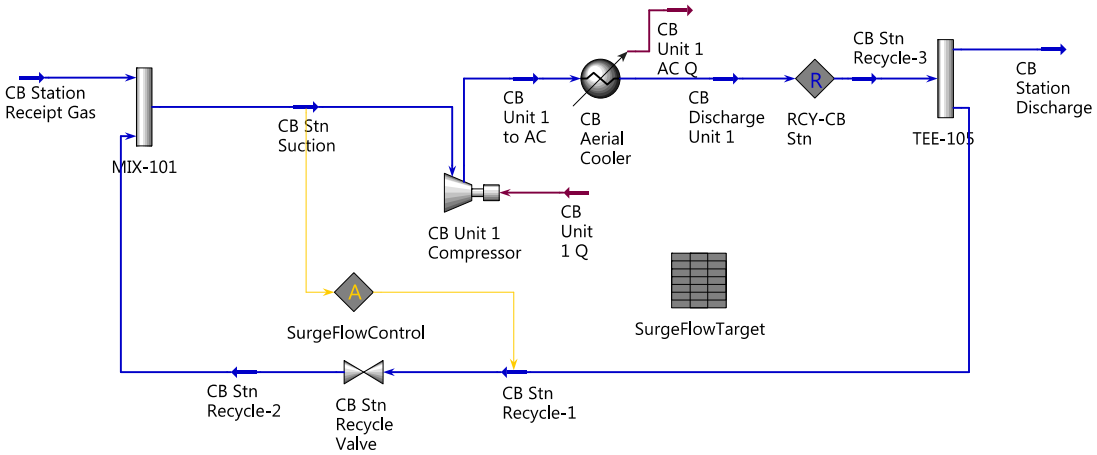

FIGURE 19.2

Compressor process flow diagram, adjusted value downstream of recycle.

A simple example is a model of a distillation column where the specification is the desired flow rate of the overhead vapor. If the feed rate to the model is increased the column will most likely still converge, but if the feed rate is reduced to 50% of the original rate, it is quite likely that the column will no longer converge. It may still be possible to achieve convergence, but some of the initial estimates would require adjustment, and the operating model of the column may be radically different from the initial operating mode. This obviously begs the question if that new operating mode is the intention or not. It is far more likely that the intended operation of the column would see the specified overhead flow reduced to 50% as well when the feed is reduced. So, a specification of the overhead flow as a fraction of the feed flow would probably be a better and more robust specification.

Another example is a model of a burner that takes some fuel source and has air or another oxygen source added to it. The mixer is then modeled in a reactor model to reproduce the effects of the combustion. A typical adjustment or control in the model is a variation of the flow of the oxygen source to achieve a concentration of oxygen in the flue gas. A properly configured control or adjust block would have limits to the flow that can be used. If the fuel flow is changed by a factor 10 or so, it is quite likely that the limits in the adjust block will no longer be valid. Even if they are, it is quite possible that the convergence will take a long time because the air flow will have to be changed by a factor of 10 as well. A more robust solution would be to create a linear relationship between the fuel flow and the oxygen source flow and then adjust the multiplier in that relationship to reach the target oxygen content in the flue gas. With this setup, changes in fuel flow rate will require very few or possibly no iteration at all. If the nature of the fuel or the oxygen source is changed, more iterations will be required, but only the first time after that change.

In general it is a good idea to use your understanding of the process to add feedforward control type calculations to facilitate convergence of the model.

19.7 CASE STUDIES

19.7.1 GAS DEHYDRATION WITH TEG

A gas dehydration plant with TEG typically consists of an absorber column where lean TEG is fed at the top of the column, and the wet gas feeds into the bottom of the column. The TEG that has absorbed the water is then called the rich TEG. This rich TEG is let down in pressure, heated, and regenerated to lean TEG in a distillation column. The regeneration has several variants that can be used depending on the desired water content of the lean TEG.

19.7.1.1 Thermodynamic Model Selection

At the very least, the selected model needs to properly model the vapor–liquid equilibrium of the main components considered: methane, water, and TEG. The EOS models that are typically used to model hydrocarbon systems cannot model this system accurately as both water and TEG are polar molecules with a more complex interaction. Most commonly used simulators make available a model that is specifically tuned for this application. It is best to be aware of the developments for such systems. For example, years ago, the recommended thermodynamic model for TEG dehydration was the PR EOS. The model was adequate because modifications under the hood forced the behavior of the system to properly represent this equilibrium. When the focus of the industry also included the distribution of BTEX (benzene, toluene, ethyl-benzene, xylene) in the process, this EOS model was no longer

adequate. A new specific TEG dehydration package was developed to properly model the distribution of the BTEX and better model other aspects such as the solubility of TEG in high-pressure methane.

19.7.1.2 Modeling the TEG Dehydration System

The main points of attention are the modeling of the columns and the modeling of the TEG recycling.

The absorber column typically does not pose many issues for convergence. The main task is to choose the number of stages that is sufficient to dehydrate the gas. This will mainly depend on the initial water content of the gas and the desired final water content and lean TEG purity. The regenerator column mostly has a very low number of stages (one or two). Despite its relative simplicity, it is more difficult to converge the column because of the large temperature difference between the top of the column and the bottom. The key is to choose the correct specifications for the column. Usually the top of the column has a temperature specification or a reflux ratio specification. The bottom of the column quite often also has a temperature specification. The reason for the latter choice is that TEG starts degrading at temperatures above 400°F and hence 400°F is a typical bottom temperature specification. If a higher purity TEG is required, other solutions such as stripping gas are used rather than a higher bottoms temperature.

When modeling the TEG recycling, it is important to make the model robust against TEG losses. Although the TEG losses in the overhead of both columns are minimal, there are many "opportunities" for losses while running a simulation model. A temporary use of an alternative specification on the regenerator column might result in significant losses of TEG in the overhead. If the recycling system is not set up to cope with this, the model may not converge. The typical solution to this is to include a TEG make up stream with a flow that is calculated to be just enough to maintain a specified circulation rate of the TEG. The specified circulation rate may be a fixed number, or in a design case it may be better to use a number calculated based on the amount of water that needs to be removed from the gas stream.

A dynamic model of this process would not pose special challenges once a steady-state model is available. With a dynamic model, the column solution typically poses less issues as specifications are replaced by the actions of controllers on the condenser and reboiler duty. The time span over which a dynamic model is run is typically at most a couple of hours, the loss of TEG over that time span is very small and hence the model does not really need to represent the TEG make up.

19.7.2 SOUR GAS SWEETENING WITH AMINES

A sour gas sweetening process looks very much similar to dehydration with TEG. It also consists of an absorber column where lean amine is fed at the top of the column, and the sour gas feeds into the bottom of the column. The amine that has absorbed the sour components is then called the rich amine. This rich amine is let down in pressure, heated, and regenerated to lean amine in a distillation column. Sour gas sweetening is a more challenging simulation problem because the interaction between the amine and the sour components is a chemical reaction, and the amine solution can be cataloged as an electrolytic fluid.

Given the complexity of this system, it is a good idea to consider if you need a rigorous model for your purpose or if a simple component splitter block will be good enough.

19.7.2.1 Thermodynamic Model Selection

The model selected needs to account for the electrolytic nature of the amine solution. It also needs to account for the chemical reactions that take place between the CO_2 and H_2S and the amine. Depending on the amine type used, the reaction rates may also come into play to model the system accurately. Select a thermodynamic package that is specific for gas sweetening and make sure it can handle the amine or amine mixture that you want to model. An additional problem is that there exist myriad licensor processes that use amine mixtures or amines combined with activator components of which the exact nature is unknown.

19.7.2.2 Modeling the Absorption and Regeneration

The classic distillation unit operation in a simulator assumes vapor–liquid equilibrium on each stage, and sometimes an efficiency is applied. In a gas sweetening application, equilibrium is seldom reached, and the approach to equilibrium is different for different components. The rigorous method to calculate the column is to use a rate-based approach. This approach calculates the rate of transfer of a component from one phase to the other based on convection, diffusion, and equilibrium. This requires the addition of the rate of reaction between the amine and the dissolved CO_2 and H_2S.

Several specialized packages exist for this purpose. Some of these are simulators specific for gas sweetening, and some of them are included in the more widely used process simulation packages. Given the complexity of the phenomena that are modeled, you should expect to spend considerably more time to model these columns than for modeling a TEG dehydration column or a condensate stabilizer column for example.

When trying to replicate the mass and energy balance of a licensor process, be aware that the reboiler duty of the regenerator column is extremely sensitive to the requested residual content of CO_2 or H_2S in the lean amine. It is typically better to impose the duty received from the licensor and to compare the sour component concentration than to impose the concentration. You may end up with a reboiler duty that is a multiple of the duty reported by the licensor if you specify the residual CO_2 concentration. When you specify the duty, the error on the CO_2 concentration may well be less than 5%.

When setting up the recycle of the amine, more care is needed than with a TEG dehydration. Water and amines are lost at different rates, in a steady-state simulation it is best to calculate make-up rates for each that are such that the total desired circulation rate is maintained, and the desired amine concentration is maintained. In a dynamic model the control scheme of the make-up flows needs to replicate the real-life control scheme.

19.7.3 TURBOEXPANDER NGL RECOVERY

A turboexpander plant has a high degree of heat integration. The same type of heat integration is commonly found in all processing units that operate at subambient temperatures. The high-pressure feed gas is typically cooled in a multistream heat exchanger before being fed into an expander unit. The near isentropic expansion reduces the temperature enough to condense the heavier hydrocarbons in the gas. This condensate is removed in a knock out drum, and the power generated by the expander is used to recompress the gas. This combination is called a turboexpander. A second compressor is needed to bring the gas back to the feed pressure, and one or more columns are used to produce natural gas liquid (NGL) products to the desired specification.

19.7.3.1 Thermodynamic Model Selection

An EOS such as PR or SRK is most often used to model this process. As the heat integration and compressor and expander power calculation is important here, the EOS enthalpy method is very often replaced with the Lee−Kesler method. A problem that may need addressing is the behavior of trace amounts of mercury in the process. The multistream heat exchangers are usually constructed in aluminum, and this metal is very sensitive to the presence of mercury. Equations of state do not properly represent the behavior of mercury out of the box, so you need to check if the implementation in your simulator has made special provisions for this.

19.7.3.2 Modeling the Multistream Exchanger

A dedicated multistream exchanger is usually available in the simulator. It is important to keep in mind a key design strategy used in multistream exchangers. The physical exchanger normally operates such that all the cold streams share the same temperature at a given location along the length of the exchanger and similarly, for the hot streams. The multistream exchanger model typically includes this assumption in the way the calculations are done.

Consider the model in Fig. 19.3. Stream "Column OVHD" is warmer than stream "Expander KO Out." The multistream model typically assumes that "Column OVHD" enters the exchanger in the middle at a location where the exchanger internal cold pass temperature matches the temperature of the stream. Similarly, it is assumed that if a cold stream has an outlet temperature different from the highest cold stream outlet, it exits the exchanger at the location that matches the specified outlet temperature.

A multistream exchanger can have multiple inlets and outlets to optimize the heat recovery. The resulting representation using a single-block multistream exchanger (Fig. 19.4) can become difficult to understand. It is often useful to split the multistream exchanger into multiple blocks (Fig. 19.5) such that the process flow diagram view matches the physical reality of where streams enter and leave the exchanger.

Splitting one exchanger block into three separate blocks introduces additional degrees of freedom. These degrees of freedom should first be consumed by specifications that impose the design strategy of having a common cold temperature and a common hot temperature everywhere in the exchanger. In the aforementioned process flow diagram for the split block exchanger, the bottom and middle block should each have two specifications that set the temperature of an outgoing hot stream identical to one of the other outgoing hot streams, and the top block should have one such specification.

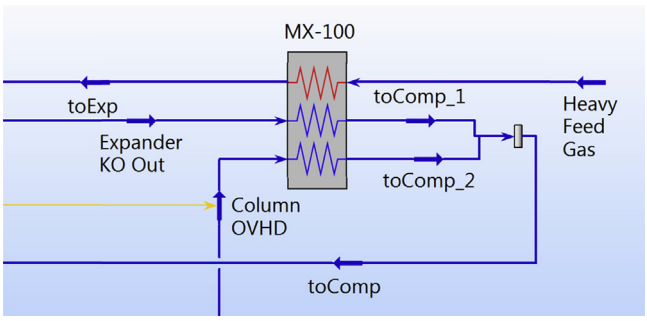

FIGURE 19.3

Multistream exchanger.

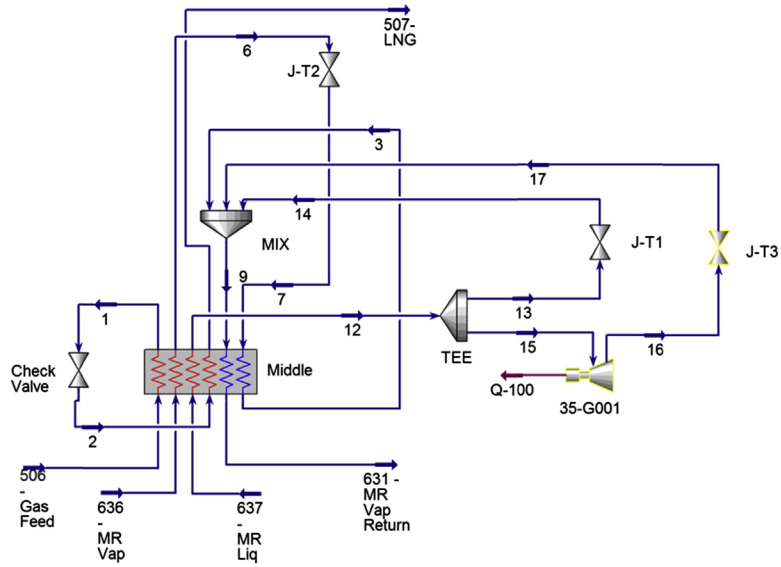

FIGURE 19.4

Single block multistream exchanger.

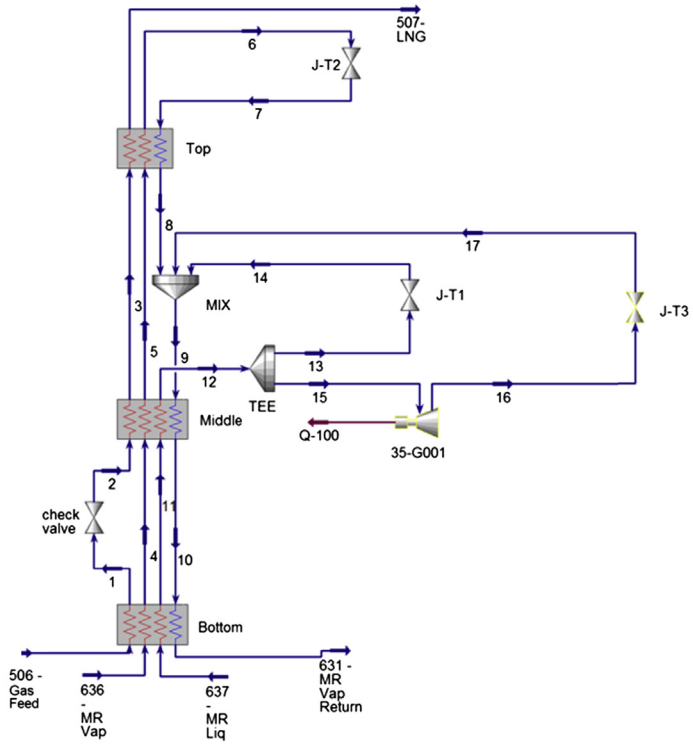

FIGURE 19.5

Split block multistream exchanger.

19.7.3.3 Modeling the Turboexpander

For a pure design type model, all simulators provide models for expanders and compressors and the power generated by the expander can in one way or another be transferred to the compressor. However, when it comes to modeling an existing plant, the modeling of the expander in rating mode is a lot more difficult using the standard available unit operations. The key problem is that an expander is more restricted in the feed flow rate it can accept. In a real plant this is accomplished with a combination of actions on the inlet guide vanes and by using a bypass valve. In addition, the inlet pressure can be allowed to float to accommodate additional throughput. The performance characteristic of the expander is also often implemented as an inverted compressor curve where the true performance characteristic is quite different. The speed of the expander and the compressor are linked, and a power balance needs to be done to determine the speed of the unit. Commercial add-on modules are available to model turboexpanders considering these limitations (see Fig. 19.6).

19.7.3.4 NGL Fractionation Train

The fractionation train is composed of up to four distillation columns. The number of columns present depends on what market exists for ethane, propane, and butane. If a sufficient market exists for ethane or if the plant is close enough to an ethylene plant, the first column will be a demethanizer.

The goal of the demethanizer column is to prevent having too much methane in the ethane product in the second column. There is no commercial purity specification on the methane, but one does want to limit the loss of ethane with the methane. The overhead product of the column returns to the produced natural gas. For this reason, this column usually has a reboiler, but no condenser. The simulation specification on this column is dependent on the required purity of the ethane. If the

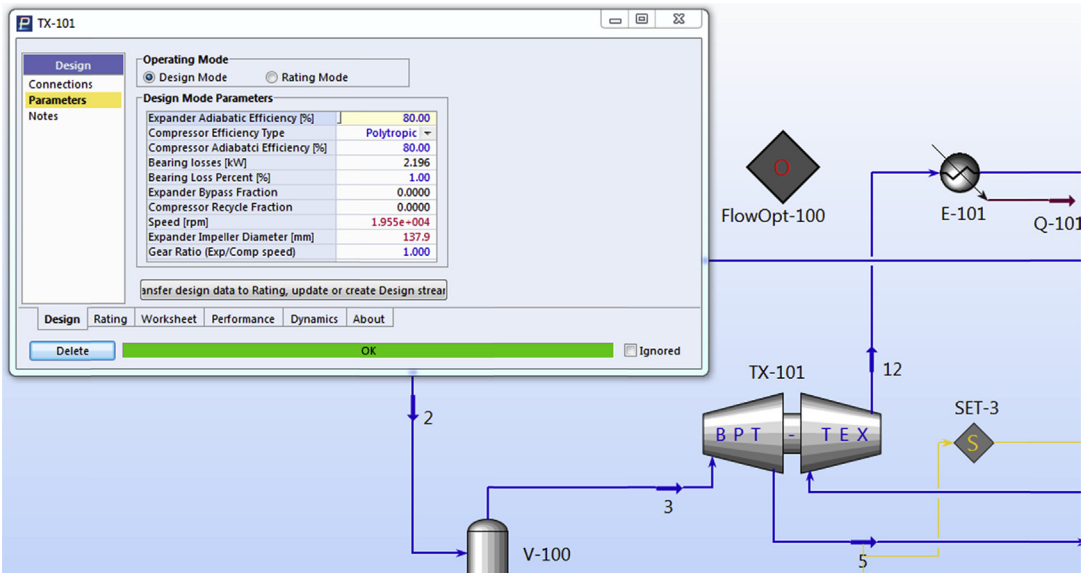

FIGURE 19.6

Commercial add-on to model a turboexpander.

methane content in the ethane needs to be strictly controlled, a specification on the methane remaining in the bottom of the deethanizer or a methane/ethane ratio could be used as a specification. If the emphasis is more on loss of ethane, a specification of ethane in the top product may be more appropriate.

The deethanizer column overhead product is also produced as a gas. However, as the ethane product does have purity requirements, it does require a reboiler and a reflux condenser. The two typical specifications here are an ethane purity specification and a specification on the ethane content in the bottoms. The amount of ethane in the bottom is often expressed as ethane/propane ratio specification as this also has an impact on the purity of the propane and propylene product.

The depropanizer column usually has a liquid overhead product as it is often fed to a propane splitter. Specifications on the butanes content in the overhead product and propane in the bottoms product are common.

If a sufficient market exists, a fourth column may be present to separate the butanes from the pentanes and heavier products. Also, sometimes butane splitter may be desirable to separate the iso and normal butanes.

The columns of an NGL fractionation train are not particularly difficult to solve as the fluids behave in a relatively ideal way. However, when modeling the complete separation train, one needs to keep in mind that the bottom specification of the upstream column sets an upper limit for the purity of the overhead product. In some simulation tools, it is possible to model all columns in a single equation−based simulation. This facilitates taking this interaction into account, but it does not prevent you from making the wrong specification! For example, if the methane/ethane ratio in the demethanizer bottoms is 0.01, it will be impossible to obtain an ethane product with a purity of above 99% in the deethanizer. This specification in the demethanizer column may also be more indirect. A specification of the recovery of ethane in the bottoms may lead to a methane content in the bottom product that makes it impossible to obtain 99% ethane in the deethanizer.

19.7.4 MEG REGENERATION

Ethylene glycol is one of the main products used to protect gas pipelines against hydrate formation. At the arrival facilities of a gas pipeline protected with MEG, there should be a unit to regenerate the rich MEG to lean MEG. The regeneration consists of a partial or total evaporation process. The partial evaporation only aims at removing the absorbed water from the MEG. However, in many cases, the MEG picks up more than only water. Salts may be present in the water coming from various sources: salty formation water, corrosion inhibitor by-products, and corrosion products. These salts accumulate in the MEG, and if the amount of salts is too high, the MEG must either be replaced or undergo a more thorough regeneration. The regeneration evaporates both water and MEG that are then separated in a distillation column.

19.7.4.1 Thermodynamic Model Selection

The challenges posed here are similar to the ones for TEG dehydration. However, for the simulator user, they are not so easy to solve as not all simulators have a special package to handle the equilibrium between MEG, water, and various hydrocarbons. The CPA model can handle this mixture but you need to make sure that the CPA model in your simulator also has the necessary parameters to do this accurately. Also watch out for solution speed, as advanced thermodynamic models can be very slow.

The salts add another level of difficulty to this; there are a few special thermodynamic packages or modeling tools that can handle this.

19.7.4.2 Modeling the Process

The process itself does not pose problems. One issue you may encounter is that the process is said to be covered by patents, and vendors may be secretive about the actual operating conditions. Some of the equipment such as the separation of salts from concentrated MEG may not have a rigorous model; a simple component splitter type model may be the only available option.

19.8 BEST PRACTICES FOR DYNAMIC SIMULATION

This section highlights the areas of application of dynamic process modeling best practices for building suitable models. The use of dynamic models in specific gas processing units will be analyzed. Some case studies will be presented to illustrate the use and impact of dynamic simulation on the design and operation of gas processing and transmission plants.

19.8.1 AREAS OF APPLICATION OF DYNAMIC SIMULATION

The areas of application have been divided in two large groups. The plant design group highlights applications that are most frequently used by engineering companies whereas the plant operation group is mostly used by operating companies.

19.8.1.1 Plant Design

Dynamic models have several applications in plant design, although it is often difficult to quantify the benefits associated with dynamic simulation. It is important to realize that a dynamic model can be reused and evolved for various applications in the design of a plant and in later stages of the project. The most detailed and rigorous model will be used close to plant commissioning and beyond (Brown and Hyde, 2001).

19.8.1.1.1 Controllability and Operability

Decisions taken very early in the design phase of a new plant or a revamp of a plant can have a significant impact on the controllability or operability of that plant. If the design calculations only use steady-state process simulation, the decision to employ a novel design is often a trade-off between the advantages of the novel design and the potential controllability and operability issues. A dynamic model will shed more light on the problems that can be expected and allows control engineers to devise adapted control strategies to mitigate or remove controllability problems. The use of dynamic simulation will increase the adoption of novel designs and ultimately the efficiency of new or revamped plants.

As these issues need to be analyzed in the early development of a process, the models will necessarily be simpler than the models used when the design has been completed. At this stage, concepts are tested and one would not expect quantitative answers from a dynamic model but rather indications of process stability or control feasibility.

19.8.1.1.2 Safety Analysis

A lot of effort goes into ensuring a plant will be safe for the operators and the people living near the plant. Huge liabilities are associated with the safety of a plant. For applications such as depressuring dynamic models are standard practice, but surprisingly in other areas the use of dynamic models is still limited.

For virtually any plant operating at high pressure, depressuring studies will be a standard part of the detailed engineering phase. The depressuring study defines the flaring capacity that is needed, and the results may also impact the choice of materials of vessels. Typically, if the pressure let-down of a vessel results in too low temperatures, carbon steel must be replaced with stainless steel to prevent the metal becoming too brittle. The other class of depressuring studies is related to the consequences of a fire in the area where a vessel is located. The main goal here is to determine the minimum vent rate that is need to keep the vessel pressure under control and to bring down the vessel pressure to prevent a failure of the vessel wall as temperature rises.

All plants have emergency shutdown (ESD) systems. The design of a system to safely stop the operation of part of or a complete plant can be very complex, and it is often difficult to foresee all the consequences of everything that happens during a shutdown. A dynamic simulation model of the plant is an invaluable tool to properly set up an ESD system. Far too often a dynamic model is used after an incident has taken place to analyze the exact causes of it. The use of such a model during the design phase might have prevented the occurrence of the incident.

19.8.1.1.3 Start-Up Procedure Definition

The use of a dynamic model to verify the start-up procedures of a plant can reduce the commissioning time by weeks. This exercise consists of adding the start-up logic to the model and to run this logic while observing the behavior of the plant model. When problems occur, the model can be stopped, and the start-up logic can be reviewed, amended, and rerun. Not only does the start-up procedure become streamlined, the engineers that have worked on it acquire a detailed understanding of the behavior of the plant which allows them to make better decisions during plant commissioning and subsequent operation of the plant.

19.8.1.1.4 DCS Check-Out

Distributed control system (DCS) check-out alone will not warrant the construction of a dynamic model of a plant. But if a model is available, the modifications required for running a DCS check-out are relatively small. The purpose of the DCS check-out is to verify that all the cabling connecting the DCS to the plant and the DCS internal TAG allocations are hooked up properly. Obviously, a dynamic model will not be able to help with checking the physical cabling, but the signals from a dynamic model can replace the plant signals. This will help tremendously in verifying the logical connections inside the DCS. If a wrong measurement is routed to a controller, this will be seen quite readily as the dynamic model provides realistic numbers for these. It is much easier to discern an erroneous number among realistic numbers than to match quasi-random numbers.

19.8.1.1.5 Operator Training

In most new projects an operator training system is a standard requirement, and it is yet another driver to start using dynamic simulation early in plant design as part of the earlier work can be reused in an operator training system.

19.8.1.1.6 Advanced Process Control

Advanced process control (APC) and multivariable predictive control (MPC) normally require access to plant data and step test results from the operating plant. Hence MPC is usually only implemented once the plant has been commissioned. With a dynamic model available, this is no longer a limitation, and the necessary information can be obtained from the step tests on that model. This part will be covered in more detail in the plant operation part.

19.8.1.2 Plant Operation

In operation, it is quite often easier to quantify the benefits that will be gained from the use of a dynamic model. Often a problem is impacting production or product quality, and dynamic modeling may be the most cost-effective way to solve the issue.

19.8.1.2.1 Troubleshooting

Issues in the control or operability of the plant can be resolved easier, safer, and with no loss of production using a dynamic model. A dynamic model can be manipulated at will where the engineer has very little freedom to test things on the real plant. Maintaining production on spec will almost always override the need for testing to solve a problem. The solution imagined by the plant engineer is not necessarily the right one and implementing an untested solution may lead to unsafe operation. With a dynamic model, the worst that can happen is that the model fails. The engineer can test a large range of operating conditions to ensure that the implemented solution will hold up in abnormal conditions for example.

19.8.1.2.2 Plant Performance Enhancement

Most plant engineers will accept that many of the controllers in a plant are operated in manual. This is frequently a source of added operating cost for the plant. A typical example would be the reflux rate of a distillation column that is set to a fixed relatively high value to ensure that the product is always meeting the specifications. Most of the time the reflux could be run significantly lower, and only during less than 5% of the time the fixed reflux is needed to maintain product quality. It is easy to compute the financial benefit associated with keeping the controller in automatic.

The reason that controllers are put in manual is often related to the confidence operators have in controllers. There are generally two possible reasons for distrust. Either the operator does not understand properly how the controller will cope with upsets, or the controller has shown in the past that it is incapable of dealing with those upsets. Even without a full operator training system, a dynamic model can be used to show the operators how a series of typical upsets will be handled by the control system. Some of the responses may appear illogical at first. This can help to instil more confidence in the automated control and let it run in automatic mode.

Of course, the distrust of the operator may be well founded, but in this case the dynamic model can be used as described previously to improve the controller behavior and subsequently illustrate to the operators that the problem has been solved to restore trust.

19.8.1.2.3 Incident Analysis

Although this is not the best use of a dynamic model, it is all too often the first step toward using dynamic simulation. After an incident, there is always the need to know why it happened. If the incident resulted in damages, there will be legal requirements to determine the root cause of the

incident. A dynamic simulation model will often be used in this analysis to determine the sequence of events that led to the incident and the adequacy of the ESD procedures to mitigate the consequences of the incident.

19.8.1.2.4 Operator Decision Support

Operator decision support is an emerging use of dynamic simulation models. In this type of application the dynamic simulation model is run in real time, and it is receiving the same input signals as the real plant. It is impossible to cover the entire plant with instrumentation to provide all the information one would like to obtain. The real-time model provides the operators and engineers with simulated measurements throughout the entire plant to better appreciate current operation. Typical parts of a plant that do not have all the instrumentation one would like are long pipelines and high temperature outlets of reactors or furnaces. A second use of the online model is its predictive capability.

Assuming the dynamic simulation model is fast enough, it can be used to predict events minutes or even hours ahead of the actual event. This information can be used to improve the handling of the event and to keep the plant operating within specifications.

19.8.1.2.5 Operator Training

It is important for the operators to keep their knowledge of the plant operation up to date. Especially with highly automated plants, it is important that operators are confronted with abnormal situations using the simulator. New operators will also benefit from the use of an operator training system.

If is therefore very important to keep the operator training system that was installed as part of the plant commissioning up to date. This means that any change to the process itself and to the DCS screens and systems must also be made to the operator training system.

19.8.1.2.6 Advanced Process Control

The implementation of an APC system requires a significant investment and such a decision is not taken lightly. A dynamic simulation model can assist in determining the relevance of an APC implementation, and it can help to streamline the implementation itself. The dynamic simulation must have a sufficiently high fidelity to capture all elements that will influence process control, including imperfections in response of control valve for example.

It is straightforward to run the necessary step tests for the implementation of an MPC on a dynamic process simulation. The results can be used to design the MPC and to run the MPC on the dynamic model. A comparison of the plant performance using the existing control system and with the MPC can provide the necessary information to decide if an MPC implementation is an attractive investment. Running step tests on a model has several advantages over step tests on the real plant:

- No disturbance of the plant operation
- Step tests can use a broader range of conditions
- Step tests do not depend on the availability of plant personnel, plant incidents, and other events that are not compatible with step tests on the plant
- The dynamic model does not suffer from valves that get stuck and other incidents that make life difficult when performing step tests
- The dynamic model can be run faster than real time and hence step test that would otherwise take days can be run in an hour or less

When the final MPC controller has been designed, and implemented, it can first be put online using the dynamic simulation model. This set up can be used to discover a significant part of the practical problems that would otherwise only surface during the commissioning of the MPC on the real plant.

19.8.2 MODELING BEST PRACTICES

19.8.2.1 Level of Detail in the Model

The level of detail required for a dynamic simulation model is very dependent on the application. Most of the time a model will contain some components that are modeled in detail (high fidelity), while other components only capture the overall dynamic behavior. A typical example is the modeling of a gas compressor.

An initial application is for the analysis of the behavior of the antisurge control logic. In this case, it will be important to properly model all the gas volumes in the main gas lines and in the antisurge system. The control logic used in the model will be an exact replication of the commercial system that will be installed. As compressor surge is a very fast phenomenon, these controllers have sampling times on the order of 50 ms, and the model will need to run using a time step that can capture these phenomena and hence have a time step that is even smaller than 50 ms. Therefore, the model may run slower than real time. But, as in this case the time span of interest is a few minutes at the most, the slower model performance is not really a problem.

A second application for this dynamic model may be for operator training. It is not relevant to model events that happen so fast it is impossible for an operator to respond to during the event. So, the step size and hence the speed of the model can be increased. However, it will be important to include manually operated purge valves in the dynamic model to allow the operator to perform all actions he deems necessary. This is a bit of detail that is of no use for the initial application.

So the level of detail required should be assessed based on the objectives for the model. This assessment is not a global assessment for the complete model, but the assessment should consider the objectives for each section of the plant down to each piece of equipment.

19.8.2.2 Model Speed

The speed of a model is most frequently expressed as the real-time factor of the model. This is the ratio of the simulated time divided by the real time. The speed requirements vary depending on the application. For an operator training simulator, the model at least needs to run in real time (real time factor $= 1$). Quite often the real-time factor should be higher, up to 10 times real time. This allows the operator to fast-forward through periods of stabilization of the process for example.

For an engineering study, the important factor is the total amount of time it takes to study an event. Ideally, that time would be 10 min or less. This means that 3 h events should have a real-time factor of 18 or higher. If the event to be studied only lasts for 1 min, then a real-time factor of 0.1 is acceptable. The model speed is mainly affected by the following factors:

- Time step of the integrator
- Complexity of the model
- Thermodynamics: number of components used and complexity

As the same factors will also affect the accuracy of the model, a balance must be found between speed and accuracy. In seeking the balance between accuracy and speed the so-called

Courant–Friedrichs–Lewy (CFL) condition comes into play. This condition is well known in pipeline modeling applications, but it is also relevant in process modeling. The Courant number is the ratio of the time step and the residence time of the fluids in equipment volume. This ratio should not exceed a maximum value which depends on the mathematical model used. For an explicit integration scheme the maximum value is one (1.0). Note that this criterion is only guaranteeing convergence or a stable solution, not the accuracy. To obtain an accurate solution, the maximum value will be smaller than one.

19.8.2.3 Equipment Specific Considerations

The sections below will recommend the information to consider when modeling various equipment items. Depending on the available modeling tool, the recommended level of detail may differ. Recommendations only apply to the main aspects of the model. A general warning is to beware of default values. Although these are very convenient to get a model running quickly, it is easy to overlook totally inappropriate values. A very often overlooked value here is the default volume of certain equipment items. It is quite common to see equipment with a holdup of 0.1 m^3 with a flow rate through that equipment of 1.0 m^3/s and using the default time step of 0.5 s. The Courant number for that equipment is 0.5 s/(0.1 m^3/1.0 m^3/s) = 5.0 compared with the maximum allowable of 1.0!

19.8.2.3.1 Valves

The minimum requirement to model a valve properly is to use the correct Cv value and the type of valve characteristic. For some studies, it is important to capture the dynamic behavior of the valve. For example, an ESD valve needs a certain time to close. For safety studies, it is important to consider the time taken to close. Most plants will have one or more check valves. It is important to include these valves in the model, in particular when the model will be used to run scenarios far away from normal operation.

19.8.2.3.2 Rotating Equipment

For pumps, compressors, and expanders, it is best to always use the performance curves of the equipment. If this information is not available it is relatively simple to create a generic performance curve starting from the normal operating point of the equipment. This information is then complemented with either the speed or with the absorbed power. For most motor-driven equipment, a speed specification will be the best option except when studying start-up and shutdown phenomena. For equipment driven by a gas turbine a specification of the absorbed power is usually a better choice.

If the study concerns the start-up or shutdown of the equipment, it will be necessary to include details such as the rotor inertia, the friction losses, and the dynamics of the driver (e.g., an electrical motor) in the model.

19.8.2.3.3 Piping Equipment

The level of detail required for modeling the piping depends a lot on the application. For process piping, it is quite often sufficient to model the pressure loss. Most of the time the volume of the piping is negligible compared with the volume of the process equipment. A notable exception is the modeling of compressor antisurge systems. An accurate representation of the system volume is crucial to obtain correct results.

For transport pipelines the model should usually be more detailed as the expected results may include information such as the time lag of a product in the pipeline, the evolution of the temperature,

and the multiphase behavior of the fluid. The required information includes the pipeline elevation profile, the pipeline diameter, pipe schedule, insulation, and environment. The Courant number is often applied as a smaller grid or mesh on the pipeline topology means using smaller volumes and this means a smaller residence time. To keep satisfying the CFL conditions, the time step will need to be decreased simultaneously, and this may lead to a very slow model.

19.8.2.3.4 Columns

Distillation models should reflect the hold-up volumes of both the liquid and the vapor phase properly. A significant difference between tray columns and packed columns is that the much smaller liquid hold-up of packed columns will reduce the response time of the column compositional perturbations for example. For columns, the Courant number is also an important factor, if the duration of composition transients is important. A low liquid holdup in a column section means that for a given liquid flow, the residence time is small and as in pipelines, the time step needs to be reduced. An inappropriate selection of the time step may lead to results indicating a transient that takes twice as long as it does in the real column.

It is customary to use a reduced number of theoretical stages to model distillation columns in steady-state simulations. If the same approach is used in a dynamic simulation, the tray or packing characteristics will need to be modified to use the correct hold-up volumes for liquid and vapor. Another approach is to use tray efficiencies and keep the number of trays used equal to the number of real trays in the column. Keep in mind that the tray efficiency and the column overall efficiency are not the same.

19.8.2.3.5 Heat Exchangers

The level of detail for a heat exchanger will strongly depend on the role of the heat exchanger and the phenomena to be studied. For example, if the exchanger serves to cool down a condensate stream before it proceeds to storage and the focus of the study is on the equipment upstream of this exchanger, then it may be enough to use a model that simply assumes the exchanger is always cooling the fluid down to the required temperature. At the opposite side of the spectrum would be the case of a plate fin heat exchanger in a natural gas liquefaction plant. In this case the exchanger is the heart of the plant, and the model needs to accurately represent the construction of the exchanger and consider elements such as the heat capacity of the metal and the dynamics of the metal temperature. The model will need to provide information such as the temperature and pressure profiles inside the exchanger.

19.8.2.3.6 Control Systems

Contrary to steady-state simulation, the modeling of the control equipment is crucial to the success of a dynamic simulation model. Quite often the control strategy and controller tuning are the final objectives of the dynamic simulation, but even if this is not the case, without proper configuration of the control system, the model will quickly end up in totally abnormal operating conditions.

For regular proportional-integral-derivative (PID) controllers, the main points to consider are as follows: correct direction of the action taken (reverse or direct), realistic tuning constants, and proper range of the instrumentation. Once the simulation model has reached relatively stable conditions, attention can focus on a high-fidelity representation of the control systems.

The high-fidelity representation can come in various forms. For an operator training system, most of the DCS vendors will be able to provide software that emulates the DCS system. The model itself is then

only used to represent the noncontrol equipment. The DCS emulation will receive the plant measurements from the model such as the real DCS would receive the measurements from the plant, and the DCS will send signals to the valve positioners according to the control algorithms defined in the DCS.

The verification of a surge controller for a compressor is also an area where a high-fidelity representation of the controller is crucial. The representation can be built by combining blocks that are part of the dynamic simulator, by writing a custom model for the controller, by linking the model to an emulation program, or even linking the model to the controller hardware.

19.8.3 CONTROL OF EQUIPMENT AND PROCESS SYSTEMS

This section enumerates some typical applications of dynamic simulation in the various processes that are employed in gas treatment and transportation. The application is usually governed by the equipment used in the process.

19.8.3.1 Gas Gathering and Transportation

The key equipment in gas gathering and transportation are pipelines, valves, and compressors. The range of applications in this area is very wide.

- Assess the risk of condensate accumulation and associated slug sizes
- Line packing capacity studies
- Safety studies on pipeline shutdowns
- Pipeline depressuring studies
- Compressor station antisurge control studies

19.8.3.2 Gas Treating

The main equipment used for the absorption of CO_2 and H_2S are absorption and regeneration columns using amine solutions to absorb the acid gas components. A dynamic model will prove useful if the quality of the feed gas can fluctuate significantly. In such a case the product gas quality will be affected directly by the amount of amine solution that is circulated and by the quality of the lean amine solution, which is indirectly influenced by the amount of acid gas in the feed.

19.8.3.3 Sulfur Recovery

The performance of a sulfur recovery unit is mainly governed by the operation of the various reactors in the process. A key factor in the reactor performance is the correct air−gas ratio of the reactor feed. If the acid gas feed is unstable, dynamic modeling can be used to select the best control strategy to cope with these fluctuations and to improve the controller tuning (Young et al., 2001).

19.8.3.4 Gas Dehydration

The glycol gas dehydration process is very similar to the acid gas removal process. Fluctuations in water content of the feed gas and gas flow rate affect the product gas quality. The control strategy insures quality of the product by selecting the appropriate glycol flow rate and by maintaining the quality of the lean glycol.

For dehydration processes using mole sieve beds, the application of dynamic simulation is similar to an application for plant start-up. The model would include the logic that is driving the bed switching and regeneration cycles. Once implemented in the model, the logic can be tested by running it on the model and by tracking critical operating parameters of the mole sieve unit.

19.8.3.5 Liquids Recovery, Natural Gas Liquefaction

A cold box is a key equipment item in these processes. The fluids that exchange heat in the cold box exchanger create a multitude of thermal loops in the process, which make it more difficult to control. A detailed dynamic model of the overall process including a detailed model of the cold box will help to understand the severity of the interactions created by these thermal loops. A control strategy designed to cope with these interactions can be tested thoroughly (Valappil et al., 2005).

From the perspective of pressures and flows, the operation of turboexpanders or turboexpanders coupled to compressors is important. The efficiency of a turboexpander drops quickly as one deviates from the design conditions, and the impact of a temporary deviation of the operating conditions on the process dynamics is difficult to understand without help. A dynamic model will aid in understanding the behavior and in selecting the correct control structure and controller tuning to cope with a transient deviation from design conditions.

19.8.3.6 NGL Fractionation

NGL fractionation comprises a series of distillation columns. As the purity specs on the columns are severe on both the top and bottom products, the control of the columns is not straightforward. A dynamic model will provide the capability to select the best control strategy given the column operation and specifications and given the expected disturbances in the feeds.

19.9 CASE STUDIES

19.9.1 DESIGN OF THE SAFETY SYSTEM OF AN LNG REGASIFICATION PLANT

The following case study reviews a dynamic simulation study conducted to help in the design of the ESD system of an LNG regasification plant. Planta de Regasification de Sagunto, S.A (SAGGAS) decided to construct a new LNG receiving facility in Sagunto, 50 km north of Valencia (Spain), with a capacity of 3 million tons of LNG annually to be supplied from Egypt through a project promoted by Union Fenosa. On February 2003, Saggas awarded the engineering, procurement and construction (EPC) contract to a consortium consisting of five European and Japanese companies; ACS, SENER, DYWIDAG, TKK, and OGE. The design of the ESD system was within the scope of work awarded to SENER (Contreras and Ferrer, 2005).

The process of an LNG Import Terminal is relatively simple. The LNG from the ship is unloaded into LNG storage tanks. Boil-off gas (BOG) is used to equilibrate the gas atmosphere in the ship; the remaining gas is condensed in a recondenser unit. The recondenser also acts as a surge vessel for the primary LNG export pumps. The secondary LNG export pumps send the LNG to the vaporizers, where the LNG is heated and vaporized to a temperature above 0°C. Two kinds of vaporizers are in use, the Open Rack Vaporizer (ORV), which uses seawater to heat the LNG, and the Submerged Combustion Vaporizer (SCV), which burns a portion of the gas to heat a water tank, which heats the LNG. The gas coming from the vaporizers is directed, through a common collector, to the systems of regulation, measurement, and odorization. The gas is then injected in the general network. Fig. 19.7 gives an overview of the process.

The first phase of the plant has two LNG storage tanks, and the plant's capacity is 600,000 Nm^3/h with a peak flow of 750,000 Nm^3/h. In the second phase, with a third LNG storage tank, the capacity will be 1,000,000 Nm^3/h with a peak flow of 1,300,000 Nm^3/h.

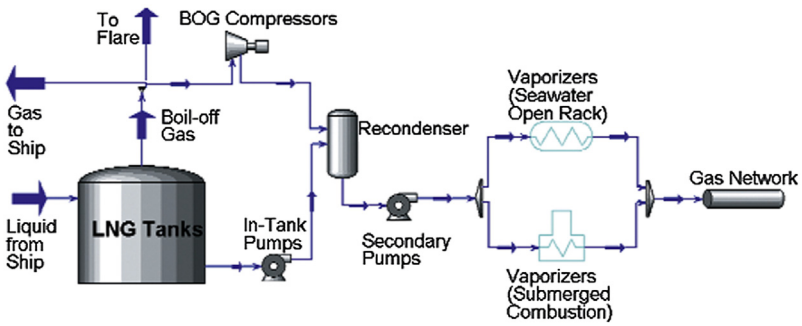

FIGURE 19.7

Overview of the Sagunto LNG regasification plant model (Contreras and Ferrer, 2005).

Safety has always been an important factor in the design of process plants. Stricter regulations regarding hazardous spills and waste generation, and the ever-increasing fines that result from infractions, have placed an even greater emphasis on fault-tree and plant safety design.

One of the most critical systems of a plant is the ESD system, and the most common way to define the logic of the ESD system is through a Cause and Effect Matrix (CEM). This matrix contains rows that are the inputs (or causes), which are based on critical instrumentation signals of the plant. The columns are the outputs (or effects), which close or open certain valves (ESD Valves) or shutdown equipment to stop the plant safely. A thorough analysis of the response of the process to the actions taken through the CEM in case of emergencies is needed. These responses are tied to the process and are inherently dynamic. Specialized expertise is necessary to design these systems with confidence, and dynamic simulation is a valuable tool in the effort. The availability of a CEM module in the simulator facilitates the modeling. Besides its use in safety system design, the dynamic model is particularly useful in the hazard identification techniques: HAZard and Operability studies, or Failure Modes and Effects Analysis. These methodologies analyze failure modes and safety system robustness. The dynamic model offers the review committee the luxury of asking and answering many more questions than are practical given the normal time limitations.

The following scenarios have been studied by SENER:

1. Pumps start-up/shutdown (primary/secondary): Provoke the tripping conditions to shutdown primary and secondary pumps, and the restart transients. The sizing of the valves was confirmed during this part of the study as well as closing time and minimum flow assurance to keep line temperatures inside acceptable limits.
2. Gas export cutoff and shutdown of the vaporizers: In such a shutdown, the export gas valve is closed, and the plant is isolated from the gas network. The secondary pumps and the SCV vaporizers are stopped, but the ORV vaporizers are still using the sea water, and they vaporize all the liquid. The study showed that this gas can be accumulated in the export collector, a 30″ pipeline of 250 m, without the need to resort to flaring. The ORV vaporizers and export collector work at 85 bar, and the PSVs are set to 130 bar. So there is a 45 bar margin and a large buffer volume in the export collector line to avoid the opening of the relief valves. Without this

confirmation, the vent and flare system would have had to be redesigned, and this would have doubled its size.

3. General or partial shutdown: The total gas flow to flare was calculated under general or partial shutdown conditions. This confirmed the calculated sizing of the venting system.
4. Failure in the BOG compressor: During the unloading of a ship, one BOG compressor is stopped. This case allowed the analysis of the pressure transients and the time it would take before the relief valves would open. It also allowed exploring different procedures to reach normal conditions.

19.9.2 ONLINE DYNAMIC MODEL OF A TRUNK PIPELINE

The 235-mile NOGAT trunk line is in the Dutch part of the North Sea, and it connects eight offshore platforms to onshore gas processing facilities near Den Helder, the Netherlands. The pipeline operates inside the two-phase region; each platform delivers both gas and condensate to the line. Two of the platforms sit on oil fields, and the off gas from the oil stabilization units is compressed and delivered to the pipeline. The current total capacity of the gas transportation system is about 22 million m^3/day, associated with 750 m^3 of condensate/day (La Riviére and Rodriguez, 2005).

The onshore facilities include a 1000 m^3 slug catcher, condensate stabilization units that remove volatile components from the trunk line produced liquids, and a series of low-temperature separation units to dry the sales gas prior to delivery to the distribution network. Fig. 19.8 shows a representation of the system.

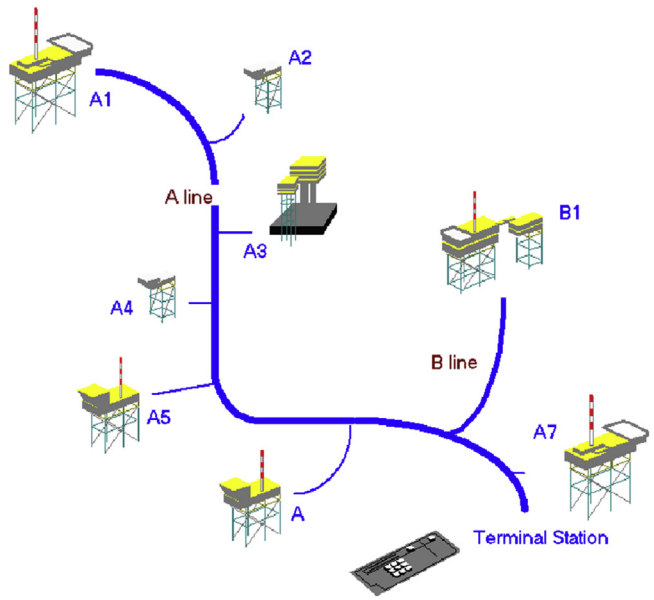

FIGURE 19.8

NOGAT trunk line system (La Riviére and Rodriguez, 2005).

There are two major challenges to operating the system:

1. Controlling the sales gas quality in terms of its Wobbe Index. The different platforms produce different gas qualities and quantities that are fed into the line at different locations. Therefore, the quality of the gas that travels through the trunk line varies along its length with time. Despite this, the sales gas quality must always stay within the contractual limits (i.e., Wobbe Index values between 49 and 54).
2. Controlling the condensate inventory of the trunk line. The amount of condensate retained inside the line builds up during periods of low gas demand, particularly in trunk line depressions. The available slug catchers and condensate stabilization unit capacities limit the production ramp-up speed and force the scheduling of periodical clean-up cycles to keep the trunk line liquids hold-up below certain critical limits.

Neither the Wobbe Index nor the condensate hold-up profiles along the length of the trunk line are directly measurable through field instrumentation.

A system has been constructed around an executive application that uses dynamic models as the main simulation engine and data historians to access the current operating conditions. The executive application handles the necessary data transfer between historical databases and simulation models. Two dynamic models are integrated in the application. These are the so-called "online model" to monitor the present time conditions in the trunk line, and the "predictive model" to perform what-if analyses and determine the consequences of programmed or unexpected variations in operating conditions (typically gas supply flow rates).

Gas and condensate sources are modeled by means of standard process streams. While gas flow rates are automatically retrieved from data historians, condensate flow rates are calculated using average condensate/gas ratio (CGR) values for each platform. Gas and condensate compositions are set as fixed parameters. The multiphase pipelines are modeled using a Shell in-house model that operates as a unit operation inside the dynamic simulator. The trunk line inside temperature profile was assumed to be equal to the ambient temperature profile (simulation runs revealed the adequacy of such assumption). Ambient temperature profiles were obtained from a North Sea temperature map that considers depth and date.

The physical properties of the gas condensate mixtures are calculated using the Shell SMIRK proprietary correlations and PEPPER databases. Although the available chromatographic analysis provided information for up to 49 chemical species, the components slate was simplified by lumping the hexanes and heavier components into a smaller slate to achieve the desired model calculation speed.

Even on today's powerful desktop computers, calculation speed is still a limiting factor for dynamic two-phase flow combined with rigorous physical property calculations. It is therefore necessary to choose a balanced solution between accuracy and speed of calculation by optimizing the number of trunk line cells, time step size, and number of chemical components. Dedicated simulation runs were performed to select the most suitable values for these parameters. The online trunk line model was given a mathematical grid of 84 cells, and it could run as fast as 40 times real time in a Pentium IV mathematical processor. The predictive model is a copy of the online model, which uses a grid containing fewer cells than the online model and performs its calculations 250 times faster than real time (La Riviére and Rodriguez, 2005).

While the predictive model to some extent sacrifices accuracy, predictions are found always to be influenced more by the estimates and forecasts of future platform flows provided by the user as simulation inputs than by model inaccuracies.

Platform discharge pressures and gas delivery flow are computed by the simulation models and stored by executive application back into the data historian. Space discrete information, such as pressure, temperature, flow rates, velocities, and holdup profiles are archived in a dedicated database. A user interface for the system shows actual conditions versus model calculated data. Predictive what-if or look-ahead studies are triggered from the system graphical interfaces. The predictive model retains the process and trunk line internal conditions to serve as an initial state for simulations. The user is given the option to edit individual platform flows and onshore landing pressure or flow. The time horizon of the prediction is also an input value.

Simulation results provided by the online and predictive parts of the tool are available to the operators by means of graphical user interfaces (GUIs). Predictive results are shown as a series of tables and charts that track the evolution of line conditions (i.e., Wobbe index, compositions, condensate holdup, velocities, flows, and pressure) along the trunk line distance and versus time. Fig. 19.9 shows a comparison between the observed and the simulated Wobbe Index of the gas at the terminal station.

Connecting the process engineering models to online measurement data stored in historians has been successful for the support of operational decisions. The described computer program has been installed in the control room of the onshore processing facilities since March 2003, and the operators successfully utilize the system for predicting and managing the gas quality. The calibrated models developed for the online system are now also used by process engineers for offline analysis of, for example, the clean-out cycles for managing the large amount of condensate which develops inside the trunk line. Potential slug catcher overflow was prevented by a correct adjustment of platform flows. The model-centric approach of the system and the clear split between application components and

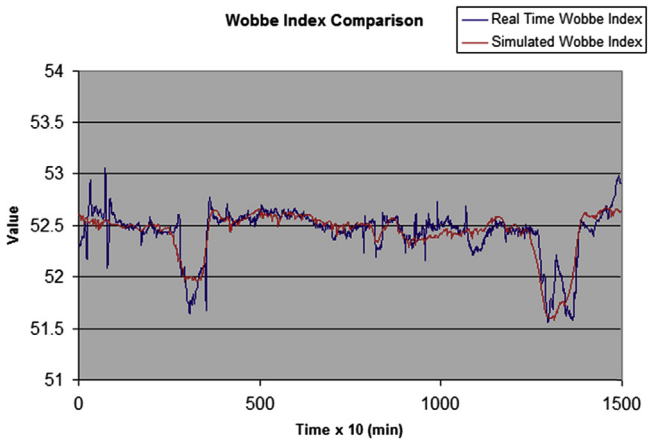

FIGURE 19.9

Comparison between the real and the simulated Wobbe Index (La Riviére and Rodriguez, 2005).

simulation model also facilitate model maintenance and upgrades. The speed of calculation is more than sufficient to keep the online model synchronized with real-time events. Similarly, the predictive case's time response is satisfactory for the end users. The accuracy of the calculated results for gas quality is more than sufficient to support the necessary operational decisions. Although the accuracy of the results regarding liquid inventories is not clear at present, the availability of these data is already a major improvement with respect to the previous situation when information on this aspect of the process was completely missing.

19.9.3 TURBOEXPANDER NGL RECOVERY PLANT

A turboexpander plant presents two specific challenges for dynamic modeling. The multistream heat exchanger and the turboexpander. The challenge for the multistream exchanger is in assembling all the information about the construction of the exchanger and implementing this information correctly and efficiently in a dynamic simulation model. For the turboexpander, the challenge is more that the operation of an expander is not well modeled in most dynamic simulators.

19.9.3.1 Multistream Exchanger

The multistream exchanger is usually a brazed aluminum plate fin exchanger that consists of many layers. Hot and cold layers alternate in the exchanger, and there can be multiple hot and cold fluids. The model needs to take this into account.

A single multistream exchanger easily has 200 layers, and it would be very cumbersome to configure an exchanger with the exact pattern of all layers. Fortunately, there often is a repeating pattern that is limited to 10 or 20 layers. The simulation model can be set up with this limited pattern and be instructed to repeat this pattern the required number of times. Fig. 19.10 shows a very simple model with only four layers that are repeated 38 times.

The temperature profile along the length of the exchanger (parallel with the flow) can also be complex, especially if one or more fluids pass from single phase to multi phase or vice versa. To capture this behavior, the exchanger needs to be split lengthwise in multiple zones. In Fig. 19.10, 10 zones were specified. As the simulation model allows the possibility to split or merge layers from one zone to the next or to leave or enter the exchanger at an arbitrary point in the exchanger, the user must specify the connectivity of the layers and zones. For trivial patterns, an automatic routine is usually provided to do this. The presence of cross-flow layers can also be accounted for. Fig. 19.11 shows the resulting temperature profile in the exchanger.

Even though the model of the multistream exchanger is complex, the heat transfer coefficient model is usually simple. This may lead to inaccuracies and temperature cross. Most simulators have options to help prevent this. Reducing the time step also helps, but obviously slows down the model.

19.9.3.2 Turboexpander

The main challenge here is that the expander part in most simulators is modeled as if this is a compressor in reverse. In a steady-state model this often does not pose a problem, but in a dynamic model, a rating model is required, and the expander behaves quite differently compared with a compressor (Fig. 19.12). The flow through the expander is controlled by the inlet guide vanes. These act as an orifice with a variable orifice surface area. Most expanders are designed such that the flow through the orifice is sonic. So, the flow through the expander only depends on the conditions and

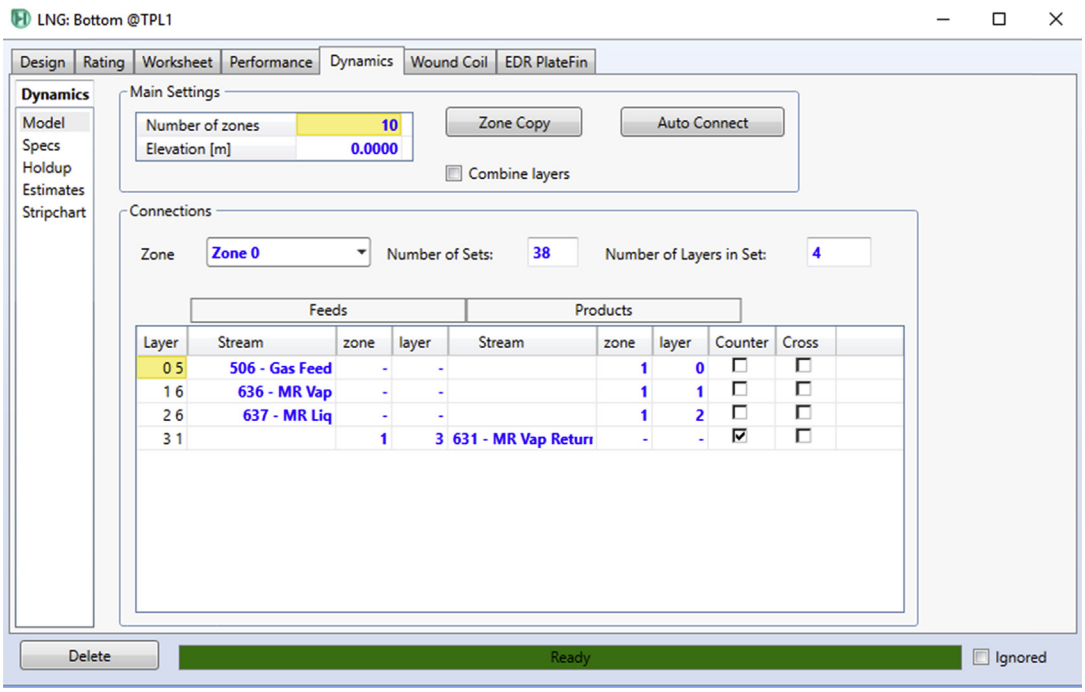

FIGURE 19.10

Multistream exchanger layer and zone setup.

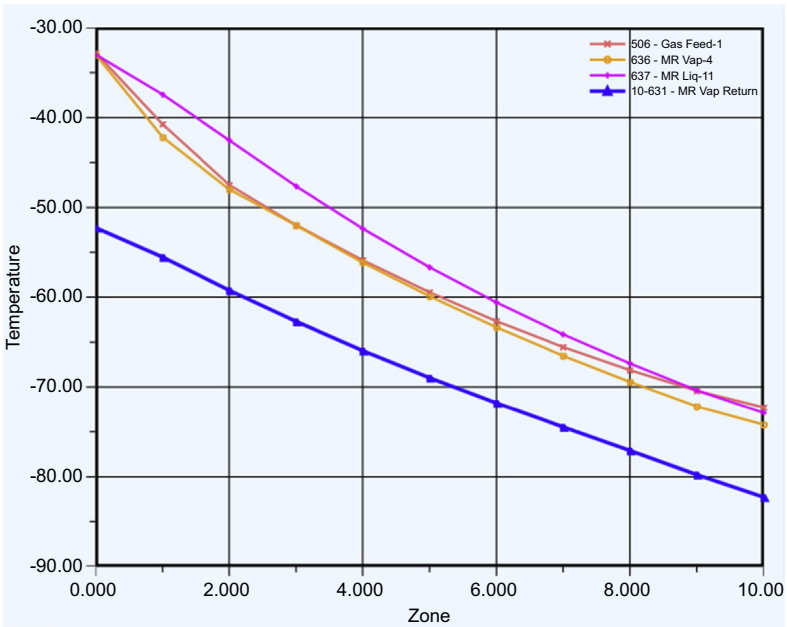

FIGURE 19.11

Multistream exchanger temperature profile.

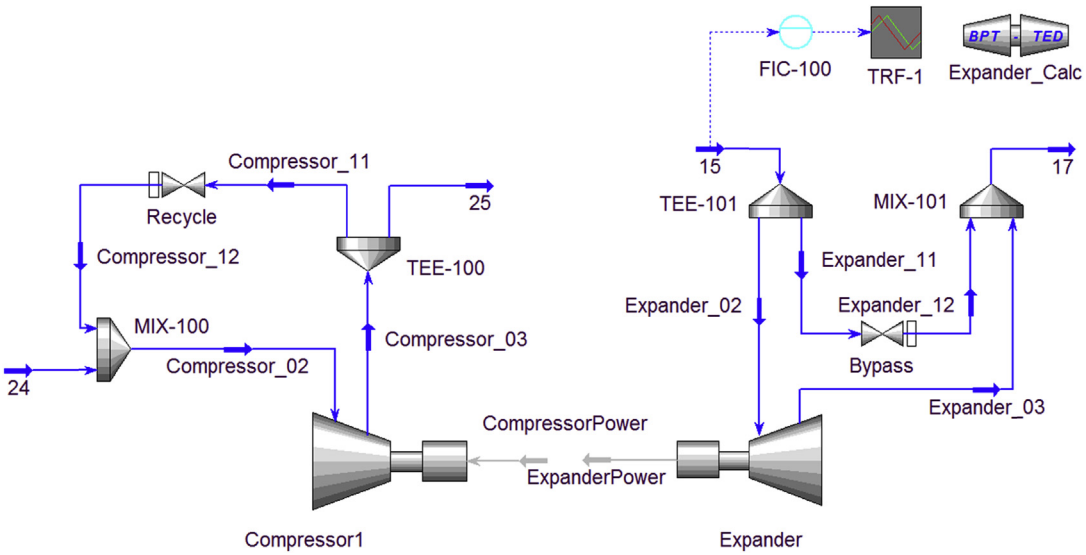

FIGURE 19.12

Turboexpander model using external model for expander performance and flow.

properties of the fluid upstream of the expander. Under normal operation, the downstream conditions have no impact on the flow. The efficiency of conversion of the energy to mechanical energy does depend on upstream and downstream fluid conditions and on the geometry and speed of the expander wheel. This efficiency could be cast in a performance map that is typically available in dynamic process simulators, but the pressure flow dependency is quite different.

For an accurate representation of the expander, it should be modeled in the simulator with a fixed efficiency and capacity and then an external calculation of the current capacity and efficiency that depends on the operating conditions and geometry needs to be added.

REFERENCES

Brown, C., Hyde, A., September 25–27, 2001. Dynamic simulation on the Shell Malampaya onshore gas plant project. Paper Presented at the GPA Europe Annual Conference, Rome, Italy.

Contreras, J., Ferrer, J.M., 2005. Dynamic simulation: a case study. Hydrocarbon Engineering 10 (5), 103–107.

La Riviére, R., Rodriguez, J.-C., 2005. Program tracks wet-gas feedstocks through two-phase offshore trunk line. Oil & Gas Journal 103 (14), 54–59.

Valappil, J., Messersmith, D., Mehrotra, V., 2005. LNG lifecycle simulation. Hydrocarbon Engineering 10 (10), 27–34.

Young, B., Baker, J., Monnery, W., Svrcek, W.Y., 2001. Dynamic simulation improves gas plant SRU control-scheme selection. Oil & Gas Journal 99 (22), 54–57.

FURTHER READING

James, G., Reeves, J., September 23–27, 2001. Dynamic simulation across project and facility lifecycles. Paper Presented at the 6th World Congress of Chemical Engineering, Melbourne, Australia.

Muravyev, A., Kelahan, R., Kowallis, P., Torgesen, G., October 21–23, 2003. Dynamic modeling of the plant gas system: process control and design applications. Paper Presented at the ISA Expo 2003 Conference, Houston, TX, USA.

CHAPTER

GAS PROCESSING PLANT AUTOMATION

20

20.1 INTRODUCTION

Automation has become an increasingly important aspect of gas processing. The amount of specific types of automation is a major decision now in the construction of new plants. With many existing plants having debottlenecked and improved process efficiency through mechanical means, automation is now a focus for further improvements. Automation provides the means for fully using the mechanical capabilities of the equipment at all times and to run the process at its most efficient points in a stable and reliable fashion. A good automation platform can be leveraged to provide the right information at the right time to the right personnel to make the right decisions in a timely manner. Historical data can be collected in virtually any time frame and analyzed statistically. With these historical data, upset situations can be reconstructed, and production reports can be automatically generated, just to name a couple of the numerous uses for these data. Many processors have upgraded their plants to higher level control systems such as distributed control systems (DCS). Some of these processors ask, "Where are the benefits?" The correct questions to ask are "'How do I best leverage by automation equipment to maximize benefits?" and "What are the best methods for measuring these benefits?"

This chapter discusses the elements of automating today's gas processing plants, including considerations for instrumentation, controls, data collection, operator information, optimization, information management, and so forth. The advantages and disadvantages of various automation and control approaches are analyzed in this chapter. Also strategies for identifying and quantifying the benefits of automation are discussed.

20.2 EARLY METHODS OF GAS PLANT AUTOMATION

The earliest gas processing plants were typically controlled manually by opening, pinching, and closing valves to meet their operating requirements. Pneumatic control systems were quickly adopted. These pneumatic control systems allowed the use of proportional, integral, and derivative (PID) controllers to send analog outputs to control valves to change their opening. As long as a sensor is available as a process variable for the controller, then a set point given by the operator can be targeted automatically. Discrete control could also be accomplished with pneumatic control systems by using devices to fail with or without an air signal. In most cases, compressed air is used as the pneumatic conveyor; however, natural gas is used in some remote operations, and hydraulic oils are also used.

A reliable source of clean, oil-free air is quite important in the operation of pneumatic air systems.

Handbook of Natural Gas Transmission and Processing. https://doi.org/10.1016/B978-0-12-815817-3.00020-4

As electronic controls were developed, these systems became the standard, although some elements of the pneumatic control systems are still in use. Most control valves today are still pneumatically operated for new and existing plants even though electronic control valves have been on the market for decades. Electronic controllers were accepted because of their lower price and greater reliability. These controllers included fewer moving parts to maintain. For new installations, wire was now run instead of pneumatic tubing with electronic to pneumatic (I/P for current to pressure) transducers added at the control valves. Process sensors such as temperature, pressure, level, and flow indicators were converted to electronic types as available and justified. Electronics also brought widespread use of safety systems such as vibration sensors, burner management, and emergency shutdown systems. Other special controllers such as dedicated surge controllers for rotating equipment and triple modular redundant shutdown devices were developed.

20.3 MICROPROCESSOR-BASED AUTOMATION

20.3.1 PROGRAMMABLE LOGIC CONTROLLERS

Programmable logic controllers (PLCs) use programming of a microprocessor to mimic electronic relays. As PLCs gained wider acceptance, the functionality expanded to include PID control and other nondiscrete capabilities. PLCs are still quite effective for batch-type operations in the gas processing industry, such as solid bed gas dehydration and start-up as well as shutdown sequencing for rotating equipment. This automation platform is often used for smaller new facilities and smaller scope retrofits of existing facilities. A human—machine interface (HMI) is highly recommended to monitor the activities of the PLC.

20.3.2 DISTRIBUTED CONTROL SYSTEMS

The definition of a Distributed Control System (DCS) varies somewhat, but a rather simple definition is a control system method that is spread, or distributed, among several different unit processes on a common computer platform. These systems are typically hardwired and exist within finite boundaries, although wireless means are becoming accepted, as data-security issues are resolved. DCS offers the advantage of centralized control while retaining the capability of local control. True distributed control systems use localized control, which is in turn controlled by the operator located at a central location. A DCS consists of the following:

- remote control panel or device
- communications medium
- central control panel or facility
- control, interface, and database software

A DCS may be as simple as one PLC remotely connected to a computer located in a field office. Larger systems may be PLC based, but they will most likely consist of specially designed cabinets containing all the equipment necessary to provide input—output (I/O) and communication. One point to consider during the design and specification of a control system is the level of autonomy each node will have in the event of a network or system failure. A true distributed system will allow most remote nodes to operate independently of the central control facility should the facility go off-line or lose communication capability. Each remote node should be able to store the minimum process data

required to operate in the event of such a failure. In this manner, costly and potentially disastrous process upsets can be avoided. If the system is both monitoring and controlling process or facility, it is referred to as a Supervisory Control and Data Acquisition (SCADA) system. Most systems will transfer data and commands using communication protocols such as Ethernet, or some other open standard, depending upon the DCS vendor (Capano, 2002).

20.3.2.1 Remote Control Panel

The remote panel for a DCS or SCADA is typically referred to as a Remote Transmission Unit (RTU). A typical RTU contains terminal blocks, I/O modules (both analog and digital), a computer or proprietary processor, and a communications interface. An RTU, depending upon where it is located in the world, can both monitor and control a given process or processes.

20.3.2.2 Communications Medium

The communication medium is a cable or wireless link that serves to connect the RTU to the central control facility. There are several methods of doing this; typically a cable, either a coaxial or twisted pair, is connected between the central control computer and the remote unit or RTU. It is considered prudent to run two cables, on different routes, between the two to increase the reliability of the system. A network operates by taking data from the sending station, or node, and packaging and routing the information to the proper receiving station. The possibility of electrical noise, physical abuse, and software bugs should be considered when implementing a DCS.

20.3.2.3 Central Control

The control room is the center of activity and provides the means for effectively monitoring and controlling the process or facility. The control room contains the HMI, a computer that runs specialized software designed for that purpose. There may be multiple consoles, with varying degrees of access to data. In most cases, each operator or manager is given specific rights to allow more or less access and control of the system. The plant superintendent, for instance, may have complete control over his facility, whereas a technician may only have access to specific data on a particular process. This is done to avoid accidents and process upsets. This scheme also affords a degree of security, ensuring that only properly trained and authorized personnel can operate the various parts of the facility. The HMI presents the operator with a graphical version of the remote process. Depending on the skill of the operator and the level of sophistication of the interface, the process may be represented by anything from simple static graphics and displays to animation and voice alerts. Most packages afford the operator wide latitude on the design of the interface. The common thread to each system is the I/O database.

The database contains all the I/O defined for that DCS. This does not mean that all process data will be monitored and controlled; it means that only the data defined by the designers to be monitored and controlled will be available to the DCS. This database is a product of detailed evaluation of the process by the designer who typically has the responsibility, with operator input, to design the most effective control schemes for a particular facility. The database is the reference the control software uses to correctly address each remote I/O point. Each database entry corresponds to an entity on the system, whether it is a physical point or an internal or "soft" point such as an alarm, timer, or screen entity. A disadvantage of the early generations of PLC and DCS was the proprietary communication protocols used. Some protocols such as MODBUS were adopted as a de facto standard but had limitations as communication complexity increased.

20.3.3 STANDARDS AND PROTOCOLS

More recently, control systems have standardized on protocols made popular through the wide use of personal computers. Ethernet and Object Linking and Embedding (OLE) for Process Control (OPC) are two examples of highly accepted protocols. Ethernet is used mainly for device-to-device communications, whereas OPC is used primarily for application-to-application communications. Various versions of field buses have been developed to further standardize device-to-device communications. Early DCS was also based on legacy computing platforms such as Virtual Memory System (VMS) and the many different UNIX versions (Poe and Harris, 2005). Today, Microsoft's Windows platform is used for virtually all DCS.

20.4 INSTRUMENTATION

There are two main types of measuring instruments: (1) analog and (2) digital. Analog instruments are mechanical devices that indicate the magnitude of the quantity in the form of the pointer movement, and the value is read according to markings on a scale. The readings may not always be entirely correct because some human error is always involved in interpretation. These types of instruments have almost entirely been replaced by digital instruments.

Digital measuring instruments indicate the values of the quantity in numbers, which can be read easily. Because there is no human error involved in reading these instruments, they are more accurate than the analog instruments. Some digital measuring instruments can also carry out calculations including highly complex equations.

The main advantages of digital instruments are (Poe and Mokhatab, 2016):

- They are very easy to read.
- They are usually more accurate than the analog instruments because there are very few moving parts in the electronic instruments.
- The electronic items tend to be less expensive than the mechanical items.
- The output can be transmitted to a computer and can be recorded for future reference.
- The output of the digital devices can be obtained in the computer.

There are also come disadvantages of the digital instruments, namely:

- Sometimes they tend to indicate erratic values due to faulty electronics or damaged displays.
- In case of high humidity and corrosive atmospheres the internal parts may become damaged and indicate faulty values.
- Sometimes these instruments show a reading even though there is no applied measurable parameter.

The advantages of digital instruments tend to outweigh the disadvantages, which is why they have become highly popular.

Some typical, basic measured variables are flow, temperature, pressure, level, speed, and vibration (Poe and Mokhatab, 2016). These are described in more detail in the following sections.

20.4.1 FLOW RATE

Flow measurement determines the amount of material purchased and sold, and in these applications, very accurate flow measurement is required. In addition, flows throughout the process should be

regulated near their desired values with small variability; in these applications, good reproducibility is usually sufficient.

Flowing systems require energy, typically provided by pumps and compressors, to produce a pressure difference as the driving force. Flow sensors should introduce a small flow resistance, minimizing the additional process energy consumption. Most flow sensors require straight sections of piping before and after the sensor; this requirement places restrictions on acceptable process designs, which can be partially compensated by straightening vanes placed in the piping.

Several sensors rely on the pressure drop or head as fluid flows by a resistance. In these cases the relationship between flow rate and pressure difference is determined by the Bernoulli equation, ignoring changes in elevation, work, and heat transfer.

Some typical head meters are described in the following sections.

20.4.1.1 Orifice

The orifice plate is the most commonly used flow sensor, but it creates a rather large nonrecoverable pressure due to the turbulence around the plate, leading to high energy consumption. An orifice plate has an opening that is smaller than the pipe diameter. The typical orifice plate has a concentric, sharp-edged opening. Because of the smaller area, the fluid velocity increases to cause a corresponding decrease in pressure. The flow rate can be calculated from the measured pressure drop across the orifice plate.

20.4.1.2 Venturi Tube

The venturi tube is similar to an orifice meter, but it is designed to form drag by nearly eliminating boundary layer separation. The change in cross-sectional area in the venturi tube causes a pressure change between the convergent section and the throat, and the flow rate can be determined from this pressure drop. Although more expensive than an orifice plate, the venturi tube introduces substantially lower nonrecoverable pressure drops.

20.4.1.3 Pitot Tube and Annubar

The pitot tube measures the static and dynamic pressures of the fluid at one point in the pipe. The flow rate can be determined from the difference between the static and dynamic pressures, which is the velocity head of the fluid flow.

An annubar consists of several pitot tubes placed across a pipe to provide an approximation of the velocity profile. The total flow can be determined based on the multiple measurements. Both the pitot tube and annubar contribute very small pressure drops, but they are not physically strong and should be used only with clean fluids.

The following flow sensors are based on physical principles other than head.

20.4.1.4 Turbine Meters

A turbine rotates as fluid flows through the turbine. The angular velocity is proportional to the fluid flow rate. The frequency of rotation can be measured and used to determine flow. This sensor should not be used for slurries or systems experiencing large rapid flow or pressure variation.

20.4.1.5 Vortex Shedding

Fluid vortices are formed against the body introduced in the pipe. These vortices are produced from the downstream face in an oscillatory manner. The shedding is sensed using a thermistor, and the frequency of shedding is proportional to volumetric flow rate.

20.4.1.6 Positive Displacement

The fluid is separated into individual volumetric elements, and the number of elements per unit time is measured with these sensors. High accuracy over a large range is possible with these meters. Provers for custody transfer meters are usually positive displacement.

Inertial meters such as a Coriolis can directly measure mass flow rate.

20.4.2 TEMPERATURE

Resistance temperature detectors (RTDs) and thermocouples are the most common devices used for measuring temperature.

20.4.2.1 Resistance Temperature Detectors

An RTD is a passive circuit element whose resistance is greater at higher temperature in a predictable manner. The traditional RTD element is constructed of a small coil of platinum, copper, or nickel wire wound to a precise resistance value around a ceramic or glass bobbin. The winding is generally of helix style for industrial use.

The most common RTD element material is platinum, as it is more accurate, reliable, chemically resistant, and stable material, making it less susceptible to environmental contamination and corrosion than other metals. It is also easy to manufacture and widely standardized with readily available platinum wire available in very pure form with excellent reproducibility of its electrical characteristics. Platinum also has a higher melting point, giving it a wide operating temperature range. For an RTD sensor, it is the wires, which connect to the sensing element and the wire insulation, which generally limit the maximum application temperature of the sensor.

Measuring the temperature requires accurate resistance measurement. To measure the resistance, it is necessary to convert resistance to a voltage, and use the voltage to drive a differential input amplifier. The use of a differential input amplifier is important as it will reject the common mode noise on the leads of the RTD and provide the greatest voltage sensitivity.

The RTD signal is generally measured by connecting the RTD element in one leg of a Wheatstone bridge excited either by a constant reference voltage or by running it in series with a precision current reference and measuring the corresponding intensity resistance (IR) voltage drop. The latter method is generally preferred as it has less dependence on the reference resistance of the RTD element.

20.4.2.2 Thermocouples

A thermocouple is comprised of at least two metals joined together to form two junctions. One junction is connected to the body whose temperature is to be measured, and the other junction is connected to a body of known temperature and is the reference junction. Therefore the thermocouple measures unknown temperature of the body with reference to the known temperature of the other body.

The working principle of thermocouple is based on three effects, discovered by Seebeck, Peltier, and Thomson. They are as follows:

1. **Seebeck effect:** When two different or unlike metals are joined together at two junctions, an electromotive force (emf) is generated at the two junctions. The amount of emf generated is different for different combinations of the metals.

2. **Peltier effect:** When two dissimilar metals are joined to form two junctions, emf is generated within the circuit due to the different temperatures of the junctions of the circuit.
3. **Thomson effect:** When two unlike metals are joined to form junctions, the potential exists within the circuit due to temperature gradient along the entire length of the conductors within the circuit.

In most cases the emf suggested by the Thomson effect is very small and can be neglected by proper selection of the metals. The Peltier effect plays a prominent role in the working principle of the thermocouple.

The general circuit for a thermocouple comprises two dissimilar metals. These metals are joined to form two junctions, which are maintained at different temperatures. Because the two junctions are maintained at different temperatures, the Peltier emf is generated within the circuit and is a function of the temperatures of the two junctions.

If the temperature of both the junctions is the same, then equal and opposite emf will be generated at both the junctions, and the net current flowing through the junction is zero. If the junctions are maintained at different temperatures, the emf will not become zero, and there will be a net current flowing through the circuit.

The device for measuring the current is connected within the circuit of the thermocouple. The output obtained from the thermocouple circuit is calibrated directly against the unknown temperature. Thus the voltage or current output obtained from the circuit gives the value of the unknown temperature directly.

The amount of emf developed within the thermocouple circuit is very small, usually in millivolts. Highly sensitive instruments should be used for measuring the emf generated in the thermocouple circuit. A balancing potentiometer is used most often.

20.4.3 PRESSURE

The following pressure sensors are based on deformation caused by force:

- bourdon tube
- bellows
- diaphragm

A bourdon tube is a curved, hollow tube with the process pressure applied to the fluid in the tube. The pressure in the tube causes the tube to deform or uncoil. The pressure can be determined from the mechanical displacement of the pointer connected to the bourdon tube. Typical shapes for the tube are "C," spiral, and helical.

A bellows is a closed vessel with sides that can expand and contract. The bellows itself or a spring can determine the position of the bellows without pressure. The pressure is applied to the face of the bellows, and its deformation and position depend on the pressure.

A diaphragm is typically constructed of two flexible disks, and when a pressure is applied to one face of the diaphragm, the position of the disk face changes due to deformation. The position can be related to pressure.

The following pressure sensors are based on electrical principles:

- capacitive or inductance
- resistive strain gauge
- piezoelectric

The movement associated with one of the mechanical sensors can be used to influence an electrical property, such as capacitance, affecting a measured signal. Deflection of the diaphragm due to the applied pressure causes strain in the wire, and the electrical resistance can be measured and related to pressure. A piezoelectric material, such as quartz, generates a voltage output when pressure is applied on it. Process pressure applies a force by the diaphragm to a quartz crystal disk that is deflected.

20.4.4 LIQUID LEVEL

Level is usually reported as percent of span, rather than in height. Sensors are installed in the vessel holding the liquid or in an external "leg" that acts as a manometer. When in the vessel, float and displacement sensors are usually placed in a "stilling chamber," which reduces the effects of flows in the vessel.

Some typical types of level measurement are float, displacement, differential pressure, and capacitance.

A float follows the movement of the liquid level. The material of construction of a float of material must be lighter than the fluid in the vessel. The position of the float, usually attached to a rod, can be determined to measure the level.

A body immersed in a liquid is buoyed by a force equal to the weight of the liquid displaced by the body. Thus a body that is denser than the liquid can be placed in the vessel, and the amount of liquid displaced by the body, measured by the weight of the body when in the liquid, can be used to determine the level.

The difference in pressures between two points in a vessel depends on the fluid between these two points. If the difference in densities between the fluids is significant, the difference in pressure can be used to determine the interface level between the fluids. Usually, a seal liquid is used in the two connecting pipes (legs) to prevent plugging at the sensing points.

A capacitance probe can be immersed in the liquid of the tank, and the capacitance between the probe and the vessel wall depends on the level. By measuring the capacitance of the liquid, the level of the tank can be determined.

20.4.5 SPEED

Magnetic pickups (MPUs) are commonly used because of simplicity, reliability, and low cost. Passive MPUs require no active signal conditioning electronics in the probe. Passive probes have variable signal outputs that depend on many factors and can be difficult to apply. Sensors with integrated active signal conditioning usually have more consistent signal output because of the integrated electronics but with the associated increase in complexity.

Passive probes cause a magnetic flux to be generated in the probe, which is converted to an electrical signal by a coil inside the probe. The amplitude of this signal is proportional to:

- amount of magnetic flux generated by the passing tooth
- number of turns in the coil
- loading on the coil due to the sensing circuit

The amount of magnetic flux generated is a function of the probe pole face dimensions, the speed tooth dimensions, tooth speed, magnetic properties, and the gap between the probe and the gear tooth.

The flux change results from a change in the magnetic coupling as the tooth edge passes the pole face. The amount of flux in the magnetic circuit is also dependent on the material properties of the MPU core and the tooth. The tooth must be a ferromagnetic material such as annealed iron and not a paramagnetic material such as aluminum or stainless steel.

20.4.6 VIBRATION

Sensors used to measure vibration come in three basic types: (1) displacement, (2) velocity, and (3) acceleration.

Displacement sensors measure changes in distance between a machine's rotating element and its stationary housing. Displacement sensors consist of a probe tapped in the machine's frame, just above the surface of a rotating shaft. Velocity and acceleration sensors measure the velocity or acceleration of the element attached to the sensor.

Some displacement sensor designs use magnetic eddy current technology to sense the distance between the probe tip and the rotating machine shaft. The closer the shaft moves toward the sensor tip, the tighter the magnetic coupling between the shaft and the sensor coil and the stronger the eddy currents.

The oscillator circuit providing sensor coil excitation is called a proximitor. The proximitor module is powered by an external DC power source and drives the sensor coil through a coaxial cable. Proximity to the metal shaft is represented by a DC voltage output from the proximitor module. Because the proximitor's output voltage is a direct representation of distance between the probe's tip and the shaft's surface, a "quiet" signal (no vibration) will be a pure DC voltage. Any vibration of the shaft will cause the proximitor's output voltage to vary in precise step. The shaft vibration in cycles per second will cause the proximitor output signal to be the same waveform in hertz superimposed on the DC bias voltage set by the initial probe to shaft gap. An oscilloscope connected to this output signal will show a direct representation of shaft vibration, as measured in the axis of the probe.

It is also common to see one phase reference probe installed on the machine shaft, positioned so that it detects the periodic passing of a keyway or other irregular feature on the shaft. The "Keyphasor" signal will consist of one large pulse per revolution.

The Keyphasor signal provides a reference point in the machine's rotation to correlate other vibration signals and a simple means of measuring shaft speed. The location in time of the pulse represents shaft position, whereas the frequency of that pulse signal represents shaft speed.

20.5 ANALYZERS

Some important chemical compositions in natural gas processing operations include:

- hydrocarbons
- hydrogen sulfide
- carbon dioxide
- nitrogen
- helium
- water

- mercury
- oxygen
- mercaptans

Gas chromatographs are probably the most widely used on-line analytical instruments in natural gas processing plants. These analyzers are effective for measuring a wide range of hydrocarbons, helium, oxygen, nitrogen, carbon dioxide, and hydrogen sulfide. Liquid streams are analyzed by vaporizing the sample.

The main disadvantages of gas chromatographs are that the measurement is not instantaneous, they are not effective for trace components, and they are maintenance intensive. If the analysis of specific components is required continuously or at very low concentrations, then other methods may be preferred.

Tunable Diode Laser Absorption Spectroscopy (TDLAS) is gaining popularity for a wide variety of analyses. However, TDLAS is not very effective for mixtures of hydrocarbons.

The following summarizes typical techniques for on-line measurement of nonhydrocarbon components.

For low concentrations or more frequent measurement of carbon dioxide, infrared techniques are often used, whereas ultraviolet absorption spectroscopy and TDLAS are sometimes used depending on the application.

Colorimetric principles were the first techniques used for measuring hydrogen sulfide in process streams. The advantages are:

- interference free (selective to hydrogen sulfide only),
- detection limit <1 ppb,
- no zero drift,
- five seconds response on breakthrough,
- linear response, and
- no other utilities than power supply required for ranges up to 100 ppm.

In cases for which other sulfur species, in addition to hydrogen sulfide, are measured, ultraviolet absorption spectroscopy is often used. For atmospheric hydrogen sulfide detection, electrochemical and solid-state sensors are used.

Advantages of using an electrochemical sensor include allowing sensors to be specific to a particular gas in the parts per million range, low power requirements, high accuracy, and lower cost than other gas-detection technologies. However, electrochemical sensors are sensitive to temperature, subject to interference from other gases, and have a shorter lifespan depending on how greater the exposure is to the targeted gas.

Solid-state sensors can detect both low ppm levels of gases, as well as high combustible levels. However, they are not very specific to a particular gas and could potentially provide false alarms. Solid-state sensors may be affected by fugitive volatile organic compounds (VOCs) and must be in areas without these gases present.

Mercury detection in process streams is important when aluminum-brazed heat exchangers are used. Atomic fluorescence allows absolute detection levels of below 0.1 pg.

Moisture content is important in dehydrated gas streams. Quartz crystal analyzers are often used in this service.

Oxygen measurement is desirable in various services with flue gases the most common. Zirconium oxide cells are the most popular with TDLAS sometimes used.

Combustibles measurement is important in flue gas streams and for detection in enclosed spaces. Infrared and catalytic gas detectors are the most popular methods used to measure combustibles. Infrared is often used for flue gas streams and catalytic gas detectors in atmospheric conditions where hydrogen may be detected as well.

Online calorimeters are used to quickly and accurately measure the calorific value of gas streams. These analyzers use a combustion chamber or measure thermal conductivity and various temperatures. In combustion chamber devices, either the exhaust temperature can be controlled or the residual oxygen measured. These analyzers typically include the capability to measure specific gravity and therefore calculate the Wobbe Index.

Sampling systems for ex situ analyzers and placement of in situ systems is extremely important for accurate and reliable results regardless of analyzer.

20.6 CONTROL OF EQUIPMENT AND PROCESS SYSTEMS

20.6.1 GAS GATHERING

Gas gathering systems are typically controlled through pressure control. Because most gathering systems use primarily reciprocating compressors (using a piston or screw), the discussion will focus on control of this type of compression. Rod loadings, maximum discharge temperature, liquid entry, as well as minimum and maximum speeds must be considered when operating these machines. It is quite important to prevent liquids from entering the compressor. An adequately sized upstream scrubber with mesh pad should be installed. A level controller to automatically dump liquids is required. The basic purpose of the gas gathering compressors is to keep the wellhead pressures down and the pressure to the downstream facilities, whether gas conditioning systems, liquids recovery facilities, or transmission pipelines, up to a minimum pressure. The speed of the reciprocating machine is the main manipulation to control the suction pressure, whereas the discharge pressure is dictated by flow rate and downstream resistance. Speed range is rather limited for these compressors but can be manipulated from about 90% to 100% of maximum speed. Other forms of capacity control include pockets and valve unloaders. These may be manual or automated. Rod loading, which is a function of the pressure differential across the compressor (discharge pressure minus suction pressure), must not be exceeded or damage will result. Beccause there is no direct way to limit discharge pressure, a recycle line is installed to allow gas to recycle to the suction and raise the suction pressure. This line is often controlled by a minimum flow controller but is more effective from an efficiency perspective when controlled off a differential pressure or even a rod load calculation where the control platform can be configured accordingly. The recycle line should be routed after the discharge cooler and discharge scrubber to increase its effectiveness. The temperature rise across the compressor is dictated by the ratio of discharge pressure to suction pressure. High temperatures can warp piping and destroy packings. Discharge temperature should be monitored and the speed reduced or recycle rate increased to keep the temperature below the maximum allowable. The primary medium for provision of cooling the gas discharged from gas gathering systems is air. The following typically controls these coolers:

- louvers
- on−off fans
- multispeed fans

- variable-pitch fans
- variable-speed fans or gas recirculation

In most cases, lower temperatures of gas exiting the cooler are preferred for downstream processes. However, temperatures below the hydrate or freezing point are not desired. In these cases a temperature controller manipulating any of the abovementioned can maintain the desired temperature. Logic may be used to determine when fans are turned on, off, or selected to run in a discrete speed.

20.6.2 GAS TREATING

The primary method of gas treating is by using chemical absorbents. This process is analogous to gas dehydration with absorbents but with some differences:

1. The objective is acid gas removal and therefore the contactor outlet gas should be analyzed for H_2S and/or CO_2.
2. Reflux temperature is set lower to maximize the retention of water.
3. In some cases, selective treating of H_2S versus CO_2 is desired, and the contactor outlet analyzer can drive a stripper overhead temperature set point, which in turn drives the ratio of heat medium used for the reboiler to absorbent flow.

Physical absorption is sometimes used that utilizes a series of flash tanks, which yield better absorbent regeneration at lower temperatures. Vacuum is often pulled on the final stage of flash. In this case the vacuum driver may need to be on speed control or eductor on flow control to prevent implosion of the vessel. Hydraulic turbines that use the energy of depressuring to drive recirculation pumps are quite effective. A "helper" pump is always required to make up the horsepower deficiency.

20.6.3 SULFUR RECOVERY

The most common sulfur recovery process is the Claus process where one-third of the H_2S must be converted to SO_2 for proper stoichiometry. The theoretical sulfur recovery efficiency drops sharply when the stoichiometry differs from the desired 2 mol of H_2S to 1 mol of SO_2. A proper amount of oxygen, typically in the form of air, must be introduced to the reaction furnace. A tail gas analyzer is installed after the final reaction stage and before incineration. Two parallel valves, a main valve and a trim valve, are usually available on the discharge of the combustion air blower. Ideally the main combustion air is manipulated on a feed forward basis as acid gas feed rate, and H_2S percentage varies. Feedback from the tail gas analyzer will control the trim valve. Because the time delay between the air introduction and tail gas analysis may be significant, a model predictive scheme may improve the ability to maintain proper stoichiometry.

Reaction furnace temperature must be maintained between a minimum and maximum temperature. Infrared measurements are quite effective in this service. Air preheat can be increased or decreased to raise or lower the reaction furnace temperature. Otherwise air input requires adjustment. Conversion in the reactors is a trade-off between equilibrium favored at lower temperatures and kinetics favored at higher temperatures. Equilibrium usually dictates when catalyst is fresh, whereas kinetics typically dictates when catalyst is near the end of life. Another factor when the temperatures are low is that the converter outlet temperature must be maintained above the sulfur dewpoint. Converter outlet

temperature is controlled primarily by the reheat, which directly controls the converter inlet temperature. Reheat can be classified as direct or indirect. Direct reheat is when hot gas bypasses the waste heat boiler at the outlet of the reaction furnace and is injected at the inlet of each converter. Lowering the converted inlet temperature when kinetics allow causes less gas to bypass and gives more shots at additional stages of conversion. Indirect reheat is with a heat medium such as steam or hot oil. Control of the reheat is straightforward with the indirect methods. Condensers are air cooled or water cooled and operated at their lowest temperature to achieve minimum dewpoint.

20.6.4 GAS DEHYDRATION

This section will cover two types of gas dehydration typically used in gas processing operations. The first is absorption, typically with a glycol, and the second is fixed-bed absorption, typically with molecular sieve.

20.6.4.1 Absorption

Dehydration by absorption includes several aspects that require control:

- lean absorbent flow rate and temperature
- contactor pressure
- flash tank pressure (where applicable)
- stripper pressure
- stripper reboiling
- stripper reflux

Because the objective of gas dehydration is removal of water from the gas stream, the outlet gas stream should be monitored continuously with a moisture indicator. This indication should be monitored to adjust the flow of lean absorbent and the heat input to the stripper reboiler. The flow of absorbent should be based on a ratio of the gas flow that is corrected based on the moisture indicator reading. This adjustment should take precedence when the moisture is lower than required because sensible heat will be saved in the stripper in addition to latent heat. The flow of heating medium to the stripper should be on ratio control and corrected based on the moisture indicator reading. This adjustment should take precedence when the moisture is higher than required because the ability to dry to driven largely by the water content of the lean absorbent. If the lean absorbent is increased without increasing the ratio of heat to flow, then the lean absorbent's moisture content may not be reduced. Bottom temperature is not a good control basis as it will only indicate the boiling temperature of water at the pressure encountered at the bottom of the stripper. A better indication is a pressure-compensated top tray (or above the packing height) temperature. This has direct correlation with the water content of the lean absorbent. A low absorbent temperature improves its ability to hold water. However, too low temperature may lead to condensation of hydrocarbons into the absorbent causing foaming. An ideal strategy is to control the temperature of the absorbent at about 5−10°F above the temperature of the inlet gas.

Feed forward strategies that take into account the water content, flow rate, and temperature of the inlet gas to the absorber can also be used. Model predictive strategies can account for the relative effects of lean absorbent temperature, flow, and stripper heat. A high pressure on the contactor is desirable to increase the contactor capacity and enhance the absorption of water. A back pressure

controller should be used to maintain a high pressure without causing the relief valve to function. The pressure should be maintained as low as possible when a flash tank exists between the contactor and stripper. A minimum pressure is required to "push" liquids into the contactor while decreasing the demand for stripper reboiler duty. One strategy will raise or lower the flash tank pressure when the liquid level exceeds a desired deadband around the set point. If the liquid rises above the deadband, the pressure is increased. Once the liquid falls within the deadband, the pressure can be slowly decreased. This strategy works best with nonlinear level control, which is always recommended for flash or feed tanks.

The stripper pressure should also be maintained as low as possible to lower the boiling point of the water stripped and allow the flash tank, if installed, to run at a lower pressure. Differential pressure measurements should be installed to indicate the onset of column flooding. When the differential pressure approaches the set point, the stripper pressure should be raised to alleviate flooding. The reflux condenser should be set at a temperature to attain maximum recovery of entrained glycol without condensing excessive water unless required by environmental considerations.

20.6.4.2 Adsorbents

Because drying with fixed bed adsorbents is a multibed process, the main control is cycle and bed switching. The dryer modes include drying, regenerating, cooling, and standby. Typically each cycle is set for a fixed time, and the beds are cycled through the use of switching valves as per this timer.

20.6.5 LIQUIDS RECOVERY

20.6.5.1 Condensate Stabilization

Condensate is stabilized by stripping light hydrocarbon components in a fractionation tower. Nonlinear level control is recommended for the upstream flash or feed tank to provide a steady feed rate. Owing to the nature of the condensate, online analysis is very difficult. Typically a bottom temperature, preferably pressure compensated, is used to control the input of heat to the reboiler. A laboratory analysis is required to verify the adequacy of the bottom temperature set point. An inferential property predictor can be added to drive the temperature set point in between laboratory updates. The reflux temperature, when used, should be controlled by a sensitive tray above the feed tray. Tower pressure should be driven as low as possible to enhance separation subject to constraints on an overhead compressor.

20.6.5.2 Refrigeration

Refrigeration is used to achieve the bulk condensation of natural gas liquids. Propane refrigerant is the primary medium used in gas processing. The main control aspects are compression, compression driver, refrigerant condenser, economizers, and chillers. Both centrifugal and reciprocating compressors are commonly used in this service with turbine, electric motor, or gas engine drivers.

Lower temperatures are achieved at lower compressor suction pressures subject to surge conditions on centrifugal compressors and rod loading of reciprocating compressors. The suction pressure directly affects the pressure on the chillers.

Level control of the chillers is cascaded to the flow of refrigerant to the chiller. This control is critical to assure that the chiller tubes are covered without carryover of liquids. A scrubber or economizer before each compression stage is necessary to dump liquids whenever encountered.

Economizers should be used on multistage systems. The economizer pressure should be set to accommodate the compressor load and minimize kickback of high-stage vapor to lower stages. Refer to the sections in this chapter for compressor and driver control considerations.

20.6.5.3 Cryogenic Recovery (Turboexpander Processes)

Expansion with turboexpanders is now the main process used for recovering natural gas liquids. Turboexpanders can be controlled for various objectives, among which inlet pressure, demethanizer pressure, and residue pressure are the most common. Guide vanes are manipulated to control the speed of the expander. A Joules—Thompson (JT) valve is always included to allow rapid unloading of the expander. One split-range controller typically operates the guide vanes and JT valve so that the JT valve will open when the manipulation of the guide vanes has been exhausted. The compressor driven by the turboexpander in either inlet compression or residue compression mode requires a recycle valve to maintain a minimum flow for surge protection. Depending on the exact cryogenic recovery processing scheme, additional controls may be required for heat exchanger circuit flow splits, chillers, separator levels, and pressure profiles. Heat exchanger flow splits are typically configured as flow ratios. This ratio may be overridden to prevent "cold spins" or prevent temperatures below the critical temperature in the cold separator upstream of the turboexpander.

20.6.5.4 Demethanizer

The demethanizer is integral to the turboexpansion process. The various feeds to the column are created at multiple points in the process. Side reboil heat sources and sometimes the bottom reboiler heat are integral to the heat exchanger circuit. Seldom are the side reboiler temperatures controlled. Manipulating the heat to the bottom reboiler controls a bottom temperature, preferably pressure compensated. An on-line chromatograph monitors the methane and/or carbon dioxide content.

Ideally this output would reset the bottom temperature. Demethanizers are good candidates for model predictive control because of the disturbances caused by the side reboilers, inlet flow rates, and inlet compositions. Minimizing the pressure of the demethanizer based on turboexpander constraints and residue compression constraints is a major opportunity for increasing liquids recoveries.

20.6.5.5 NGL Fractionation

Natural gas liquid (NGL) fractionation consists of deethanization, depropanization, debutanization, and butane splitting (or deisobutanization). The control schemes for each are analogous. The major control points for these fractionators are reboiling heat, reflux, and pressure. Again nonlinear level control is recommended for feed tanks and bottom surge levels. Reboiling heat is manipulated to control the bottom composition. The composition is cascaded to a sensitive temperature below the feed tray. Preferably the temperature is pressure compensated.

Reflux flow is manipulated to control the bottom composition. The composition is cascaded to a sensitive temperature above the feed tray. Preferably the temperature is pressure compensated. Minimum reflux schemes are used to assure that reboiling load is not increased due to excessive reflux and, conversely, excessive reboiling leading to greater reflux rates for a given separation. Internal reflux calculations and multivariable control schemes can achieve minimum energy consumption for a given separation.

Pressure should be minimized on these towers subject to constraints such as flooding, condenser temperature, and bottom hydraulics. Flooding is indicated by delta pressure measurements across the

tower. Reflux is more difficult at lower temperatures as the available duty of the condenser may be limited. There must be sufficient head on the bottom of the tower to allow the liquids to feed downstream towers or satisfy minimum head requirements for pumps. Again, multivariable control schemes handle the pressure minimization issue elegantly.

20.6.5.6 Centrifugal Compressors

Centrifugal compressors (using an impeller to increase the kinetic energy of a vapor) are gaining wider acceptance in a variety of gas processing services including feed, residue, and refrigeration compression. These compressors are typically driven by gas turbines or electric motors but can sometimes be steam turbines. There are several control considerations for this unit operation. Upstream liquids removal, surge prevention, suction pressure, discharge pressure, and driver speed control are the primary issues. Upstream liquid removal is accomplished with vessels upstream of the compressor that remove any entrained liquids and automatically dump liquids based on a liquid level. A simple on−off level control scheme is adequate for this purpose.

Surge is caused by excessive head requirements for a given suction pressure. The horsepower delivered by the compressor driver can be reduced to prevent surge, or gas can be recirculated from a higher stage of compression. Slowing the compressor driver is usually the most energy-efficient means. However, some drivers are limited in their speed range. There are many schemes that use antisurge or kick-back valves to quickly increase the suction pressure by recirculating gas. The most sophisticated will take gas density and head curve characteristics into account for a wide variety of operating conditions. The simplest schemes assure a minimum flow or minimum suction pressure for the compressor. These simpler schemes yield horsepower inefficiencies due to a more conservative approach. Kick-back schemes that use cooler gases and minimize the number of stages that gas is recycled are also the most energy efficient.

Suction and discharge pressures can be controlled by adjusting the driver speed, recycling gas, or with throttling valves. Driver speed adjustments are the most energy efficient. Gas turbines will typically have a wide speed range. Steam turbines have a moderate speed range. Electric motors may be of constant speed; however, variable speed and variable frequency drives are becoming more popular.

20.6.5.7 Centrifugal Pumps

Centrifugal pumps are analogous to centrifugal compressors but are seldom driven by a gas turbine. The same control considerations exist except, of course, the requirement to remove liquids upstream is replaced by a need to remove entrained vapors upstream. The net positive suction head dictates the surge point. Therefore the level and density of the liquid at the suction of the pump is important.

20.6.5.8 Reciprocating Pumps

Reciprocating pumps are typically driven by electric motors, but some applications use gas engines or steam turbines. These pumps are rather forgiving in their operation and require minimal control. The most common control required is capacity control because these are positive displacement machines. Variable speed and liquid recycle based on minimum flow or upstream level considerations are the main forms of capacity control.

20.6.6 UTILITIES

The most common utilities found in gas processing plants for process purposes are refrigeration systems, heating (hot oil or steam) systems, and cooling water systems. Refrigeration systems have been covered previously. Hot oil systems use heaters, mixing tanks, and headers. It is not uncommon for a plant to use at least two levels of hot oil temperatures. The various temperatures are distributed through separate header systems. Some processes, such as amines and glycols, will degrade when high skin temperatures are encountered. Lower temperature heat medium minimizes reboiler skin temperatures. A common hot oil temperature scheme is to accumulate all heat medium returning from the process in a surge tank. A portion of the hot oil is routed through the heater to the temperature target for the high-temperature header. Enough of the liquid in the surge tank bypasses the heater and is mixed with the right amount of heated oil to achieve the low-temperature header target. Steam systems also typically use several levels of temperature (or pressure). Boilers produce sufficient steam to satisfy a high-pressure header. Steam users, heat exchangers, and steam turbines discharge the exhausted steam into a lower pressure header to be reused or into the condensing system for collection and reuse. Steam turbines that exhaust steam into a lower pressure header for reuse at a lower temperature are called topping turbines. Otherwise, the steam turbines are total condensing turbines.

To satisfy the balance for the entire steam system for all the temperature (or pressure) levels required, let down valves are used to route higher pressure steam into lower pressure headers based on pressure control. Exhausted system is collected in the lowest pressure header, typically at atmospheric pressure, deaerated, replenished with make-up boiler feedwater to replace losses and boiled again. Process temperature control is usually achieved by simply regulating the flow of heat medium to the heat exchanger.

20.7 AUTOMATION APPLICATIONS

A central control room using electronic means to transmit data prompted the advent of applications to reside on the automation platform. These applications are focused on collecting information and using it to operate more profitably (Poe and Harris, 2005).

20.7.1 DATA HISTORIANS

The ability to collect and store a large amount of data on a disk is a key advantage of the microprocessor-based automation platforms. Even so, several vendors have specialized in developing historians to more efficiently and effectively store and analyze the data. Data compression techniques are used to store a maximum amount of information in the minimum space while maintaining resolution of the data. These historian packages come with tools to assist in mining the data, graphing, tabulating, and analyzing statistically. The historical database can be manipulated to automatically generate reports as well.

20.7.2 ASSET AND PERFORMANCE MANAGEMENT

Asset and performance management software has been developed to also tap into the wealth of information that is now available with microprocessor-based automation systems. These solutions include:

- computerized maintenance management
- work order generation
- predictive maintenance
- control loop performance and tuning
- on-line equipment health monitoring
- process performance monitoring

Asset management focuses on maintaining the plant equipment. Inventory management, work order generation, predictive maintenance programs, and turnaround planning can be accomplished with these tools. Many of these packages include hooks into enterprise planning systems. Control loop performance monitoring and tuning packages are available. These applications can determine whether a control loop is experiencing problems with a valve, positioned, or controller tuning for example. Other applications trend the vibration, temperatures, and other key parameters for rotating equipment to determine when a failure is expected to occur.

Process models can be run online to determine how well a plant is performing compared to an expected performance. Heat exchanger fouling, expander and compressor efficiencies, as well as tower efficiencies can be calculated and monitored. These packages include data reconciliation features to overcome the problem of how to adjust process models for inconsistent, missing, or bad data.

The opportunities for application of the process performance audit initiative for increased plant profitability in the gas processing and NGL fractionation industries can be defined by analysis of the individual facilities to pinpoint the control loops that are the economic drivers of each facility. The following is a list of applications that require minimum control variability and tight adherence to hard spec limits to maximize economic performance (Kean, 2000):

20.7.2.1 Distillation Towers

- feed and reflux flow control loops
- reflux temperature control loop
- reboiler temperature control loop
- reboiler-level control loop
- pressure control loop

20.7.2.2 Gas Compressors

- flow and pressure control loops
- surge control loops
- station recycle control loops
- gas temperature control loops

20.7.2.3 Acid Gas Treating Systems

- stripper reboiler temperature control loop
- stripper overhead temperature control loop
- stripper reflux flow control loop
- contactor and flash drum—level control loops
- hot oil heater fuel and air flow control loops

20.7.2.4 Steam Boiler Systems

- steam drum—level/feedwater flow-control loops
- steam pressure and fuel flow control loops
- feedwater heater train control loops
- combustion air/O_2 control loops

20.7.2.5 Plant Utility Systems

- cooling water flow control loops
- fired heater fuel and air flow control loops
- refrigeration chiller level control loops

Control loop optimization through the use of a formal process performance audit by skilled process consultants and control engineers can be an effective route to increased plant profitability. This economic improvement initiative could make the difference between a plant being economically viable or one that is considered for temporary shutdown or asset disposition (Kean, 2000).

As discussed previously, the basic control loop greatly affects plant performance due to the following facts:

- Process optimization requires optimization of the entire process, both hardware and software (Rinehart, 1997).
- The final control loop plays a significant role in process optimization (Rinehart, 1997).
- Control loop optimization reduces process variability and also increases process reliability.
- Optimization of the control loop is an essential step for successful application of advanced control.
- Large economic returns result from proper sizing, selection, and maintenance of the process control equipment.
- Continuous, online monitoring of both loop equipment and loop performance is a key element for achieving the lowest cost of production while minimizing the life cycle cost of the processing facility.

20.7.3 STATISTICAL PROCESS CONTROL

Data from the automation system can be interfaced to statistical process control packages. This software is used to generate run charts, process capability analyses, process characterization, experimental design, and cause and effect diagrams. This type of information is quite valuable to determine the causes of plant instability and off-specification products. It is also an excellent tool when

baselining the plant performance and determining the benefits of improved control. Statistical process control concepts form a foundation for many of the Six Sigma and other quality initiatives when applied to continuous processes.

20.7.4 ADVANCED REGULATORY CONTROL

Advanced regulatory control was made much easier with the advent of microprocessor-based controllers. This control methodology basically turns single-input−single-output control into multiple-input−single-output control through the use of cascading controllers, selectors, feed forwards, ratios, and so forth. Shinskey (1996) discusses the variety of control strategies that can be used in this way. Although not impossible with single-loop pneumatic and electronic controllers, the software configuration approach with microprocessor-based controllers superseded the tubing runs, wiring, and other devices necessary to accomplish these strategies with earlier controller forms.

20.7.5 MULTIVARIABLE PREDICTIVE CONTROL

A more elegant and robust form of control is multivariable predictive control. This form of control has been used in the petroleum refining industry since the 1970s and provides true multiple-input−multiple-output control. Multivariable predictive process control provides a structured approach to managing process constraints, such as limits on valves and rates of change of temperature and pressures. A model for long-range prediction is used to ensure that the constraints upon these variables are not violated. This enables the maintenance of an operating envelope within which the process is constrained. Recently introduced technology that enhances capability in this area includes constrained quadratic programming. To determine the optimal set points and constraint values for the controller, an outer optimization can be performed. This optimization can be described as a linear programming technique, which is combined with a steady state model and a cost function, determining the optimum operating point to be derived from a strategy based on minimum energy usage, maximum throughput, or a balance between these or other objectives.

Fig. 20.1 shows a multivariable control strategy for a typical cryogenic demethanizer. A multivariable controller takes advantage of the interactive nature of the process. Key controlled variables are modeled dynamically as a function of key manipulated and disturbance variables. Flows depend on the pressure profile, the compression horsepower available, and the efficiency of the turboexpander. When more horsepower is available such as at night and in cooler weather, then the flow can be increased or the pressure on the demethanizer can be lowered to increase NGL recovery for a given flow demand. Control of the NGL quality, typically for methane or carbon dioxide in ethane, becomes more difficult as tower pressure is adjusted. The multivariable controller can determine the correct heat input as tower pressure is adjusted to maintain maximum recovery and product quality. Pressure-compensated temperature is a key element of this strategy.

Other controlled variables can be minimum and maximum flows, pressures, temperatures, levels, speeds, and so forth. Demethanizer pressure, flow splits, reboiler flow, and plant inlet pressure are some manipulated variables, whereas disturbances such as residue pipeline pressure, inlet flow, and inlet composition are considered.

In the aforementioned manner, a “team” of key controllers are pushing the plant to its optimum operating point at all times. Controllers are effectively decoupled, thereby making adjustments similar

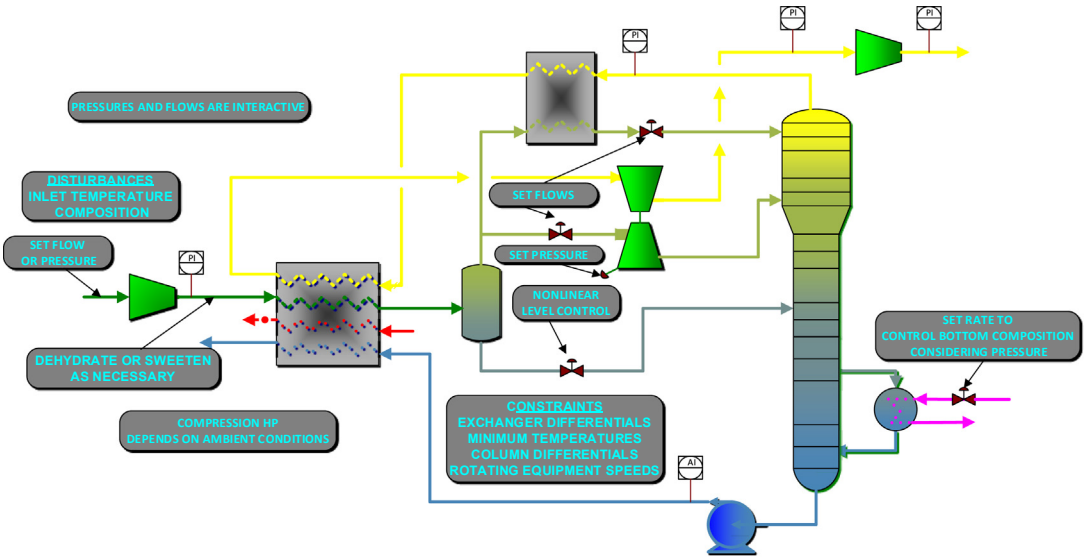

FIGURE 20.1

Multivariable control on a typical cryogenic demethanizer.

to an automobile on cruise control. In many regards the objectives of statistical process control are achieved.

Fig. 20.2 shows the beneficial effects of advanced controls. First the variability of the process is reduced by the ability to control closer to set points with the model predictive capability. Once variability is reduced, then the process can be pushed closer to the operating constraints where maximum profitability is attained. This is an area where operators hesitate to operate due to the

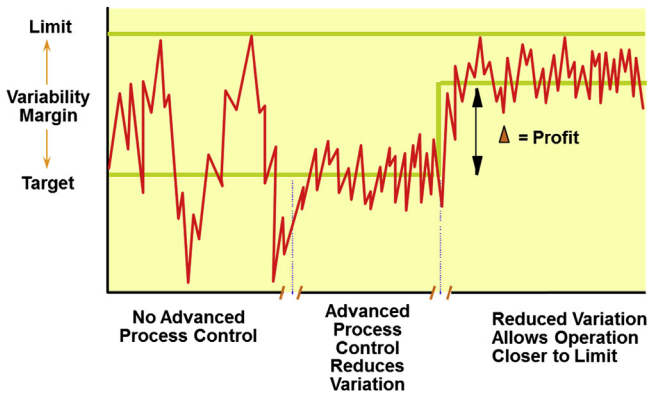

FIGURE 20.2

Impact of advanced controls.

possibility of exceeding a constraint. With advanced process control, set points can be put closer to these constraints without the fear of exceeding the constraints.

Examples of the benefits from the application of model predictive have been widely documented (Alexander et al., 2007).

20.7.6 OPTIMIZATION

The next level of automation is optimization. For simpler optimization problems, linear programming (LP) techniques can be used. Nonlinear techniques may be warranted for more complex optimization opportunities where linear methods would miss significant benefits. With the advances in computing power and optimization mathematics, on-line, rigorous optimization has become a reality. Again, petroleum refining is leading the way, but several gas processing applications have been developed. Optimization systems must rely on a multivariable predictive control system. As the robustness of the multivariable predictive control system improves, so does the effectiveness of the optimization system. With the business focus that optimization brings, multivariable predictive control developments should address the requirements of operations management. Table 20.1 details recent technology developments that have improved operations management and the benefits of multivariable predictive control applications. These advancements have enhanced basic process operations. This enables staff to be redeployed and provide more valuable operations functions that provide increased efficiency, reliability, reduced cost, improved quality, ideal staffing, and responsiveness to changing business requirements.

Networking and Web capabilities continue to impact advanced applications. Some companies have central support centers or have contracted application service providers. Automated testing can be easily monitored remotely. Performance monitoring technologies and tools provide clear benchmarks of expected performance. Updates and improvements can be applied remotely. These capabilities reduce project and support costs and further improve the economics of multivariable predictive control initiatives. Mixed integer programming and enhanced state-space methods are now used to improve models and decrease the impacts of unmeasured disturbances. New developments in sensor technology supply new valuable, low-cost process information. Methods for property estimation and predicting

Table 20.1 Recent Developments in Multivariable Predictive Control Technology (Canney, 2004)

Development	Technology
Nonlinear controllers	Neural nets and other empirical modeling techniques
Automated process testing	Multistep, random frequency testing
Performance monitoring	Metrics for model adequacy
Remote implementation and support	Web-enabled applications
Adaptivity	Background testing and model identification
Control system embedded	Powerful processors coupled with programming efficiencies

the behavior of multiphase and complex reaction systems are also improving. Multivariate statistical methods continue to progress. Visualization technology may be a key to making the models transparent to the end user.

20.7.7 LEVERAGING AUTOMATION

To get the most benefit, the automation platform should be leveraged to its maximum capability. The platform itself is about 80% of the cost for about 20% of the potential benefits. A multitude of additional benefits are there for a fraction of the platform cost by adding applications as shown in Fig. 20.3. Include adequate instrumentation upfront for grassroot plants and during retrofits of existing plants to support the advanced applications. It is much more cost-effective to add instrumentation during construction rather than adding it later. Use control system consultants rather than relying solely on equipment manufacturers. Many equipment manufacturers are penalized for including more instrumentation than their competitors. For control system upgrades, do not just replace in kind, replace and enhance. A DCS gives limited additional value when used simply as a panel board replacement (Poe and Harris, 2005).

20.7.7.1 Automation Upgrade Master Plans

Many gas processors have developed automation upgrade master plans for existing facilities where the relative benefits of each unit and the value of enhancements are estimated. In this way the area with the most benefits can bear the majority of the initial cost of the platform. Additions to the platform, once the infrastructure is in place, typically cost less per I/O than the initial installation. Master plans are quite effective when the gas processor teams with an automation consultant. The consultants can share their past experience and advise of future developments that should be considered.

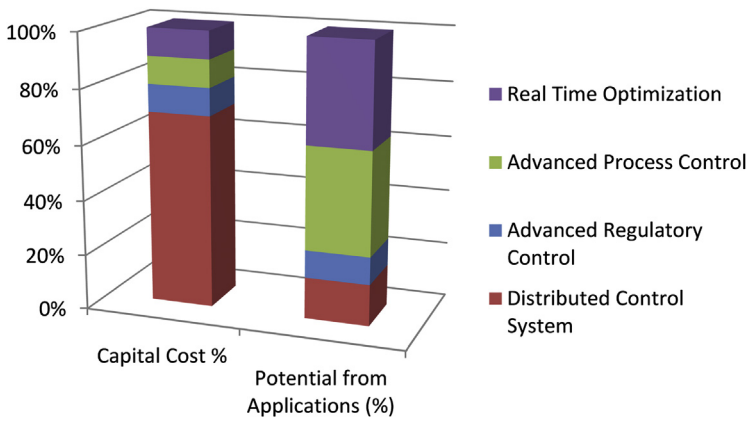

FIGURE 20.3

Relative values of automation stages.

20.7.7.2 Determining the Benefits

The benefits of a fully leveraged automation system are numerous and include:

- control room consolidation (reduced manpower)
- plant reliability (uptime)
- plant stability (better efficiency due to fewer process upsets)
- maintenance management (reduced inventories)
- product quality (fewer off-specification penalties or give-away of over processed product)
- continuous constraint pushing (increased throughput and recoveries as well as energy savings)
- optimization (energy savings and increased recoveries)

When approached appropriately, these benefits are easily quantified. The key is measuring through baselining and monitoring the results through proper metrics.

20.7.7.2.1 Baselining

A good baseline is a crucial element of determining benefits. Historical data are necessary to derive a good baseline. The historical data should include the primary measurement as well as any factors that should be used to normalize the result. For instance, ethane recovery should be normalized for inlet gas flow and composition, as well as for ambient temperature. Data during upset periods and outliers should be discarded. True process variability is measured best with frequent data capture on the order of every minute. High-quality baselining requires an excellent understanding of the operation in addition to statistical analysis. In addition to measuring mean performance of a process, baselining will reveal the amount of variability in the process and the source of the variability. Reducing variability is one of the main benefits of automation. With reduced variability, the process has freedom to shift to a more beneficial operating point.

20.7.7.2.2 Statistical Analysis

Statistical analysis is crucial in determining the benefits of automation. A good statistical analysis will give the most accurate assessment of process performance under changing conditions. Mean or average performance is always the final measure between before and after performance. Again the mean should be evaluated on a normalized basis so that the performance is assessed on a fair or equivalent basis. Total liquids or even total ethane recovered is not a normalized evaluation. Barrels per MMCF of inlet are a better metric but do not take into account changes in inlet composition. Recovery levels take into account inlet composition, but not process capability under variable inlet rates or ambient conditions that provide more mechanical horsepower availability. Standard deviation gives a measure of the amount of variability for a normal (bell-shaped) response curve. Depending on the process and the sources of variability anywhere from one-half to two, standard deviation improvement is reasonably expected. One way to check this is to compare best performance or process capability (entitlement) to the mean performance. This difference can be compared to the standard deviation to give an idea that the maximum standard deviation improvement is possible. Because standard deviation gives an absolute number and is difficult to compare to the mean, coefficient of variation, which is the standard deviation divided by the mean gives a relative measure of standard deviation. In other words the coefficient of variation gives a percentage improvement potential. All responses are not normal or bell-shaped. Kurtosis is a measure of the skewness of the response curve and should be considered when evaluating standard deviation. A common example of an abnormal response is when

a process runs close to its physical limits to the upside or downside and far from its physical limits to the opposite side. Elimination of upset conditions can sometimes shift a response curve close to normality. Multivariable control packages also include the capability to further identify the dynamic performance of a process with tools such as autocorrelation, power spectrum, and Fourier transforms. Determining financial benefits in the face of uncertainty is always a challenge. Even though we may have a good gauge on process improvement potential from the standpoint of increased product, the value of these improvements is dependent on economic conditions such as pricing, feedstock availability, and product demand. Risk management tools, such as Monte Carlo simulations, can be used to establish the range and certainty within these ranges of financial benefits over the variety of conditions anticipated.

20.7.7.2.3 Performance Improvement Initiatives

Many companies are adopting Six Sigma and other statistically founded performance improvement initiatives. Automation can greatly enhance the effectiveness of Six Sigma and other performance improvement initiatives. Conversely, the rigor of these performance improvement methodologies is useful in documenting the benefits of automation. Take Six Sigma as an example of how performance improvement methodologies and automation complement each other. The four phases of Six Sigma include measure, analyze, improvement, and control (Breyfogle, 1999).

Measurement can sometimes be difficult and painful without automation. With automation and data historians, the measurement and analysis task becomes much easier. After the data are collected, the process capability assessment, run charts, cause and effect matrices, and so forth can be developed to assess the performance improvement opportunity and where to focus the effort. The many elements of automation can be the enabling technology for the implementation and control phases of Six Sigma. Stabilizing the process is always a key element of performance improvement and is enabled by automation, especially advanced controls. The control phase pretty well speaks for itself.

20.8 CONDENSATE STABILIZER CASE STUDY

The following case study reviews an application of some of the advanced control features and the benefits. This case study is for an actual condensate stabilization process. The main reason for advanced process control on this unit was for quality purposes. Condensate product must meet a Reid vapor pressure (RVP) specification as defined by the customer. The previous method of production relied on laboratory sampling to verify the RVP, which was infrequent. Online analyzers are available but can be expensive. Instead of an online analyzer, the important quality measurement was derived through inferential means. The advanced process control (APC) solution provided a stable plant and reduced the RVP variation.

BG Tunisia implemented multivariable predictive control on their gas condensate production system at the Hannibal plant in Sfax, Tunisia. The aims of the project were to maximize condensate yields, improve the stability of the condensate stabilization process, and ensure quality limits for the product are adhered to at all times. BG Tunisia's Hannibal terminal processes gas at 5.4 MMSCM/D with the condensate column operating at a typical rate of 550 L/m controlling RVP to a maximum limit of 12 psia. Condensate can be sold as crude oil and is therefore more valuable than the alternative natural gas liquids products (Hotblack, 2004).

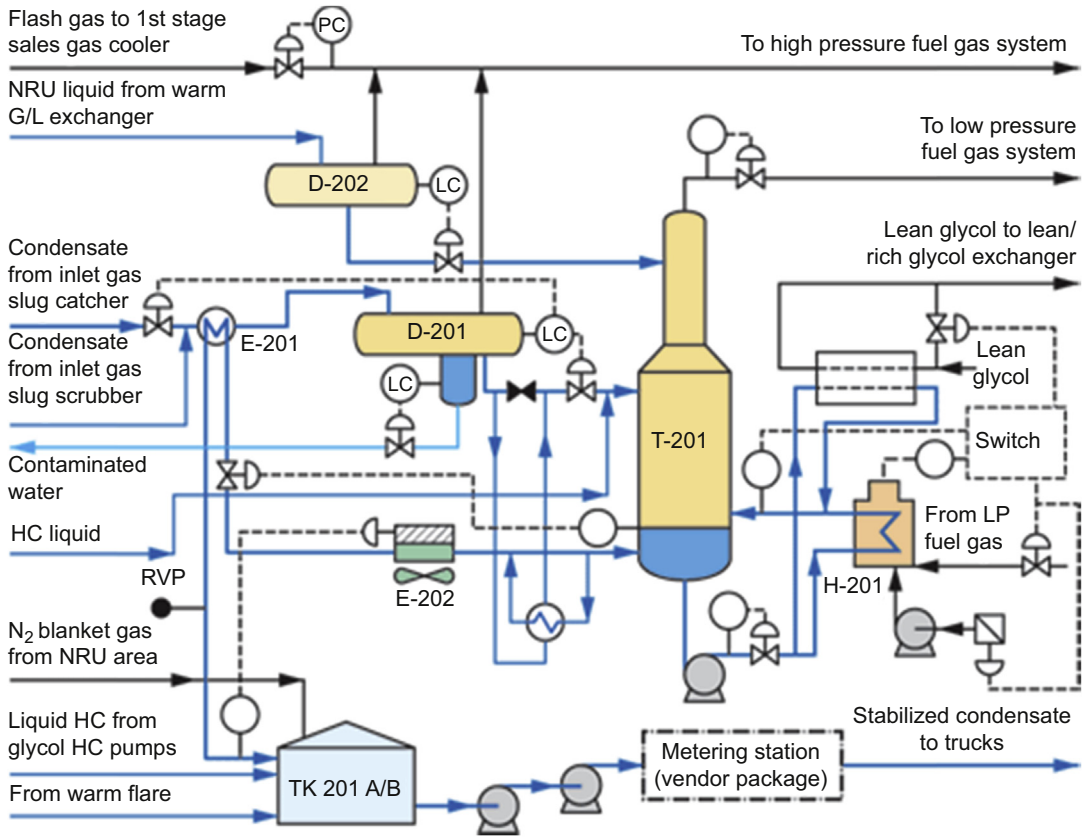

FIGURE 20.4

Schematic for BG Tunisia's Hannibal terminal condensate process (Hotblack, 2004).

Fig. 20.4 shows a detailed schematic for the condensate process. The liquid hydrocarbon condensate is brought into the plant from the slug catcher and preheated in the stabilizer feed/bottoms exchanger E−201. The preheated feed is flashed in the stabilizer feed drum D-201. Liquid from the feed drum is further preheated through the feed/bottoms exchanger and fed to the stabilizer T-201 on local flow control. The feed drum level controller maintains level by manipulating the feed to the drum. The flashed vapor is sent to the high-pressure fuel gas system. A boot is provided on the feed drum to separate any entrained water, which is sent to the warm flare drum under level control. Condensed hydrocarbon liquid from the warm separator in the Nitrogen Rejection Unit (NRU) is fed to the NRU liquids flash drum D-202 under level control via the warm gas/liquid exchanger in the NRU. The flashed vapor is sent to the high-pressure fuel gas system, and liquid from the drum is fed to the stabilizer.

The condensate stabilizer T-201 reduces the vapor pressure of the condensate by removing the lighter components. It is a stripper column with 24 trays. Liquid from the stabilizer feed drum is fed at

the midpoint on tray 9, and liquid from the NRU liquids flash drum is fed to the top tray. Overhead vapor from the stabilizer is sent to the low-pressure fuel gas system through a back-pressure control valve that maintains the tower pressure to set point under the action of pressure controller.

The bottom part of the tower is divided into two sections by a baffle—the baffle does not extend to the very bottom of the tower, so there is some mixing between the two sections. Liquid from the bottom tray flows into the section that is preferentially pumped through the fired stabilizer reboiler H-201. The two-phase stream from the reboiler is returned to the other compartment where the liquid is separated as stabilized product, and the vapor flows up the tower to provide stripping action. The glycol/condensate exchanger provides additional heat duty if required.

Stabilized condensate leaving the stabilizer is cooled in the condensate cooler E−202 and by exchange with cold inlet feed condensate in the exchanger E−201, and it is sent to the condensate storage tanks TK-201 A/B.

The main objectives of the condensate stabilizer connoisseur controller are:

- control RVP to an operator-specified target value
- enforce any specified unit operating constraints at all times
- stabilize the unit operation

The controller uses a real-time online estimate (inferential) of RVP. By controlling more tightly to the target value, excessively high RVP and the associated increased flashing of stabilized condensate in the storage tanks and during tanker transfer can be minimized, thus reducing losses. The product specification for RVP is 10−12 psia. Fig. 20.5 shows the before and after trends of key process variable. The baseline assessment before APC was a mean RVP of 12.25 psia with one standard deviation of 0.43. After APC was installed, the standard deviation dropped to 0.26, enabling control to 11.5 psia with 95% confidence on the 12-psia limit (Hotblack, 2004).

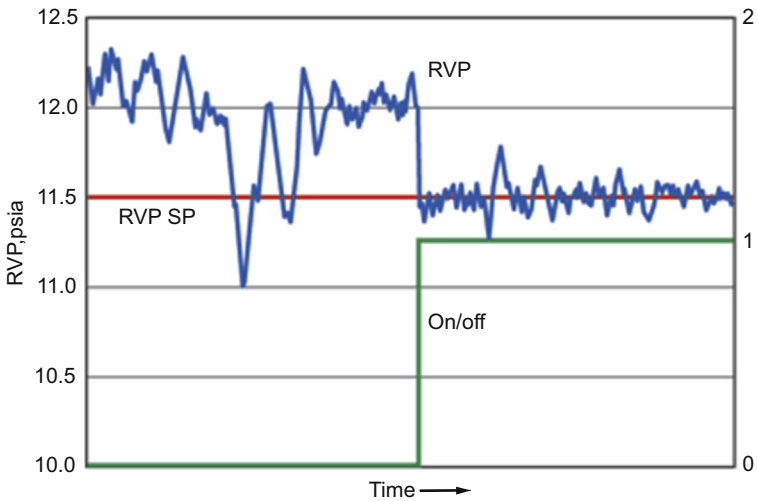

FIGURE 20.5

Reid vapor pressure (RVP) at BG Tunisia's plant, before and after trends of key process variable (Hotblack, 2004).

Constrained optimization drives the process to an optimum without violating process constraints such as the RVP limit imposed by the condensate purchaser.

A hybrid RVP sensor using both first principle and neural network technology provides a continuous measurement for control. Laboratory samples taken on a periodic basis are integrated into the control scheme improving accuracy and ensuring product quality is maintained.

The inferential estimate is implemented directly within the controller as a hybrid of a first principles model based on the Antoine vapor pressure equation and a radial basis function neural network. Both the first principles model and the neural network require the stabilization column base temperature and top vapor pressure. Compensation for process drift and process measurement error is via feedback from the laboratory analysis. A weekly laboratory sample is inserted as a minimum for this purpose.

REFERENCES

Alexander, B., Harris, S., Poe, W., Toillion, M., Whatley, L., March 11−14, 2007. Maximizing helium and NGL recovery at DCP midstream's panhandle region gas plants with model predictive control. Paper Presented at the 86th Annual GPA Convention, San Antonio, TX, USA.

Breyfogle, F.W., 1999. Implementing Six Sigma. John Wiley & Sons Inc., New York, NY, USA.

Canney, W., 2004. Advanced process control powers developments in operations management. Oil & Gas Journal 102 (42), 50−53.

Capano, D., 2002. Distributed Control Systems Primer. DTS, Inc.

Hotblack, C., 2004. BG Tunisia's advanced process control improves condensate product stability. World Oil 225 (9), 40−43.

Kean, J., March 13−15, 2000. Maximize plant profitability through control loop optimization. Paper Presented at the 79th Annual GPA Convention, Atlanta, GA, USA.

Poe, W.A., Harris, S., March 13−16, 2005. Gas processing plant automation A-Z. Paper Presented at the 84th Annual GPA Convention, San Antonio, TX, USA.

Poe, W.A., Mokhatab, S., 2016. Modeling, Control, and Optimization of Natural Gas Processing Plants. Gulf Professional Publishing, Burlington, MA, USA.

Rinehart, N.F., October15, 1997. The impact of control loop performance on process profitability. Paper Presented at the AspenWorld-97, Boston, MA, USA.

Shinskey, F.G., 1996. Process Control Systems-Application, Design and Tuning, fourth ed. McGraw-Hill Book Company, New York, NY, USA.

CHAPTER

REAL-TIME OPTIMIZATION OF GAS PROCESSING PLANTS 21

21.1 INTRODUCTION

Gas processing operations constantly experience changing conditions due to varying contracts, feed rates, feed compositions, and pricing. To capture the maximum entitlement measured in profits, these operations are prime candidates for real-time optimization (RTO) (Bullin and Hall, 2000). RTO allows operating facilities the ability to respond efficiently and effectively to the constantly changing conditions of feed rates and composition, equipment, and dynamic processing economics. In fact, world-class gas processing operations have learned how to optimize in real time to return maximum value to their stakeholders. Applications of RTO of gas processing facilities have recently been adopted. Advances in computer power, robust modeling approaches and the availability of real-time pricing have enabled this technology. An online optimization model also provides a continuously current model for accurate simulations required for off-line evaluations and studies. Equipment conditions including fouling factors for heat exchangers and deviation from efficiencies predicted by head curves for rotating equipment are tracked over time. The impact of additional streams under different contractual terms can be evaluated with the most up-to-date process model available.

The objective of this chapter is to introduce the concepts of RTO and describe the considerations for successful application in the gas processing industry.

21.2 REAL-TIME OPTIMIZATION

RTO refers to the online economic optimization of a process plant or a section of a process plant. An opportunity for implementing RTO exists when the following criteria are met:

- Adjustable optimization variables (degrees of freedom) exist after higher priority safety, product quality, and production rate objectives have been achieved.
- The profit changes significantly as values of the optimization variables are changed.
- Disturbances occur frequently enough for real-time adjustments to be required.
- Determining the proper values for the optimization variables is too complex to be achieved by selecting from several standard operating procedures.

Real-time online adaptive control of processing systems is possible when the control algorithms include the ability to build multidimensional response surfaces that represent the process being controlled. These response surfaces, or knowledge capes, change constantly as processing conditions,

Handbook of Natural Gas Transmission and Processing. https://doi.org/10.1016/B978-0-12-815817-3.00021-6

process inputs, and system parameters change, providing a real-time basis for process control and optimization.

RTO applications have continued to develop in their formative years with 100 or so worldwide large-scale processing applications. RTO systems are frequently layered on top of an Advanced Process Control (APC) system as shown in Fig. 21.1, producing economic benefits using highly detailed thermodynamic, kinetic, and process models, as well as nonlinear optimization. Whereas an APC system typically pushes material and energy balances to increase feed and preferred products with some elements of linear optimization, RTO systems can trade yield, recovery, and efficiency among disparate pieces of equipment.

Processors frequently use real-time optimization (RTO) applications for off-line studies because they provide a valuable resource for debottlenecking and evaluating changes in feed, catalyst,

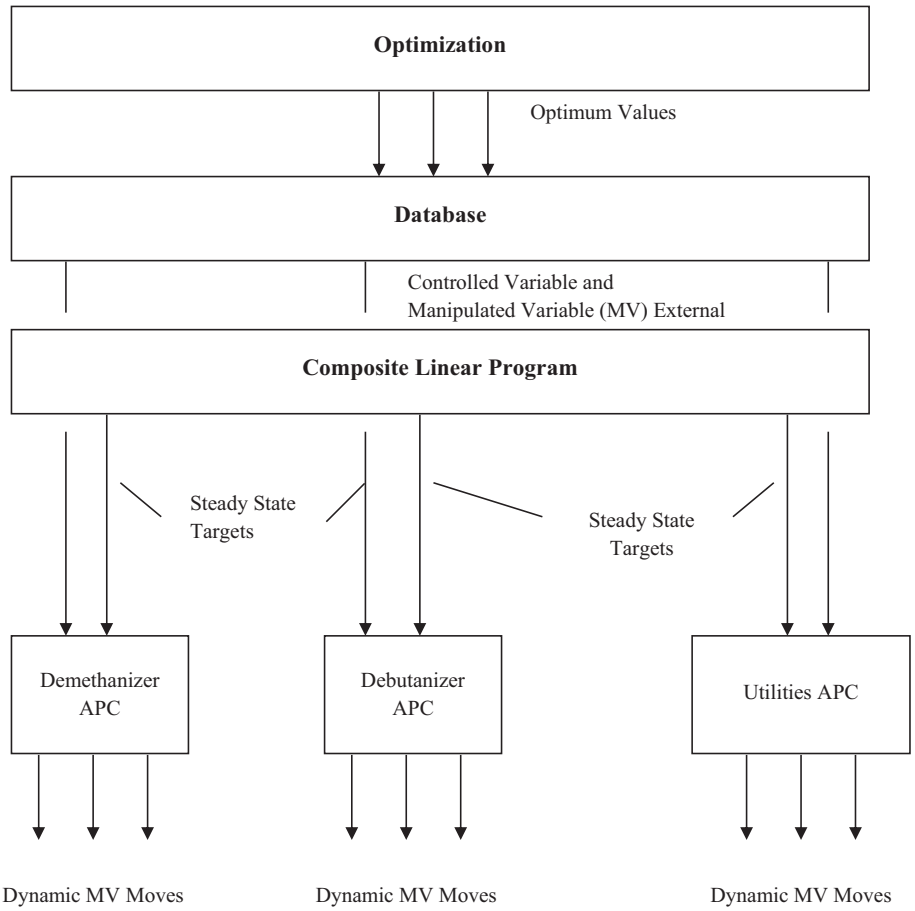

FIGURE 21.1

Advanced Process Control (APC) with optimization solution architecture.

equipment configuration, operating modes, and chemical costs. Processing RTO has been hampered by the lack of reactor models for major processing units, property estimation techniques for hydrocarbon streams, and the availability of equipment models. Continued technology advancement has removed many of these hurdles, however, and the number of reported RTO successes continues to grow.

RTO systems perform the following main functions:

- **Steady-state detection**—Monitor the plant's operation and determine if the plant is sufficiently steady for optimization using steady-state models.
- **Reconciliation/parameter estimation**—Collect operating conditions and reconcile the plant-wide model determining the value of the parameters that represent the current state of the plant.
- **Optimization**—Collect the present operating limits (constraints) imposed and solve the optimization problem to find the set of operating conditions that result in the most profitable operation.
- **Update set points**—Implement the results by downloading the optimized set points to the historian for use by the control system.

A good RTO system utilizes the best process engineering technology and operates on a continuous basis. The system constantly solves the appropriate optimization problem for the plant in its present state of performance and as presently constrained.

A typical system consists of an efficient (fast) equation solver/optimizer "engine," coupled with robust, detailed, mechanistic (not correlation based) equipment models, and a complete graphical interface that contains a real-time scheduling (RTS) system and an external data interface (EDI) to the process computer. Three primary components of a fully integrated graphical interface are shown in Figs. 21.2–21.4.

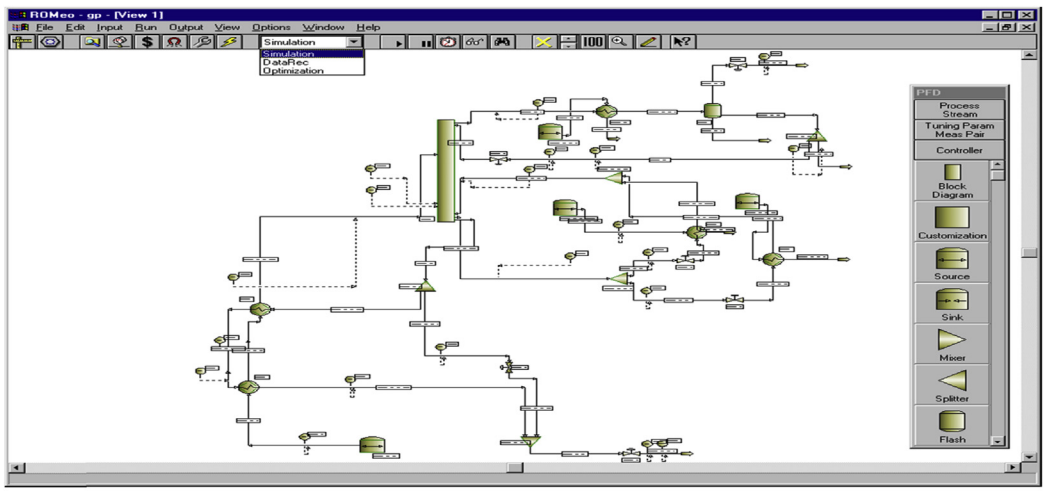

FIGURE 21.2

Real-time optimization model interface.

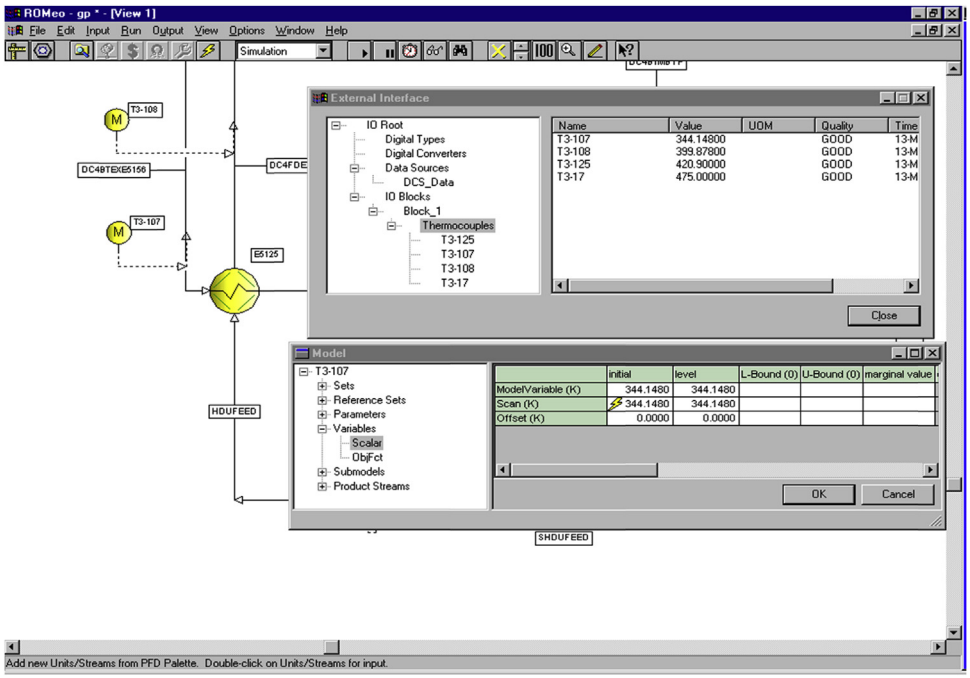

FIGURE 21.3

Real-time optimization external data interface interface.

The RTO model is composed of separate models for each major piece of equipment. These separate models are integrated and are solved simultaneously. The simultaneous solution (rather than sequential) approach allows for solution of large-scale, highly integrated problems that would be difficult or impossible to solve using sequential techniques offered by many flow sheet vendors.

An RTO system will determine the plant optimum operation in terms of a set of optimized set points. These will then be implemented via the control system.

21.2.1 PHYSICAL PROPERTIES

All of the process models for a rigorous RTO system use mixture physical properties, such as enthalpy, K-values, compressibility, vapor pressure, and entropy. Equations of state, such as Soave–Redlich–Kwong or Peng–Robinson, are used for fugacities, enthalpy, entropy, and compressibility of the hydrocarbon streams. The enthalpy datum is based on methods such as the enthalpy of formation from the elements at absolute zero temperature. This allows the enthalpy routines to calculate heats of reaction as well as sensible heat changes. Steam and water properties are calculated using routines based on standards such as the National Institute of Standards and Technology.

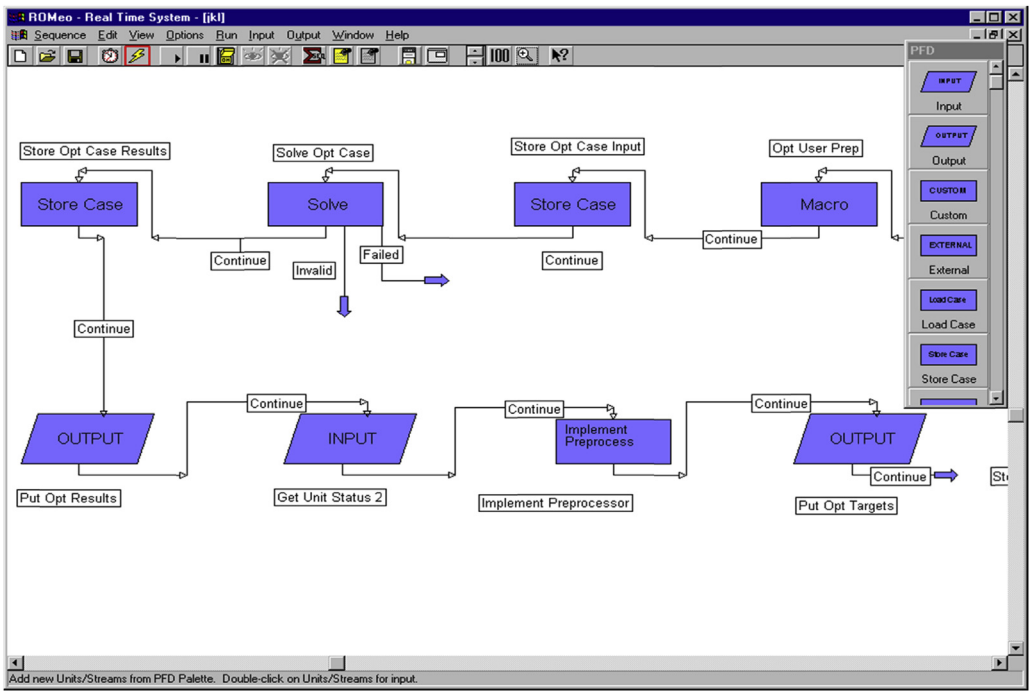

FIGURE 21.4

Real-time optimization real-time scheduling interface.

21.2.2 OPTIMIZATION MODELS

Models used in the optimization system must be robust, easily specified (in an automated manner) to represent changing plant situations, and solve efficiently. These models must be able to fit observed operating conditions, have sufficient fidelity to predict the interactions among independent and dependent variables, and represent operating limits or constraints. State-of-the-art models meet these requirements by using residual format ($0 = f(x)$), open equations, fundamental, mechanistic relationships and by incorporating meaningful parameters within the models. These state-of-the-art systems provide the highly efficient equation solver/optimizer and the interface functionality that automates sensing the plant's operating conditions and situations, and automate posing and solving the appropriate parameter and optimization cases.

Most plant models are standard models. Sometimes custom models are created specifically for the equipment of a unit. All the models use thermodynamic property routines for enthalpy, vapor–liquid equilibrium, and entropy information.

Rotating equipment models such as compressor, pump, engine, gas turbine, and steam turbine models contain, along with all the thermodynamic relationships, the expected performance relationships for the specific equipment modeled.

21.2.2.1 Optimization Objective Function

The objective function maximized by a high-level optimization system is the net plant profit. This is calculated as product values minus feed costs minus utility costs, i.e., the P−F−U form. When appropriately constrained, this objective function solves either the "maximize profit" or "minimize operating cost" optimization problem. Economic values are required for each of the products, feeds, and utilities. The value of each stream is derived from the composition-weighted sum of its components. Economic values for feeds, products, and utilities in the optimization system are reset on a regular basis for best performance.

21.2.2.2 Custom Models

Often custom models must be incorporated into a standard optimization package to predict proprietary processes and solvents. The custom model may be incorporated with special properties packages or integrated into the system in a semiopen approach where the iteration criterion is handled by the optimization system but the actual kinetics or thermodynamic equations remain the same as the off-line custom model. Proprietary gas sweetening solvent formulations may be the most common example of a custom model in the natural gas industry.

21.2.2.3 Fractionators

Fractionators are modeled using tray-to-tray distillation. Heating and cooling effects as well as product qualities are considered. Column pressure is typically a key optimization parameter. Temperature measurements are used to determine heat transfer coefficients for condensers and reboilers.

21.2.2.4 Absorbers and Strippers

These units will be modeled using tray-to-tray distillation, if required. Component splitters may be used to simplify the flow sheet where acceptable when these units have little effect on the optimum.

21.2.2.5 Compression Model

The main optimization set point variables for the compressors are typically suction or discharge pressures. Important capacity constraints are maximum and minimum speed for the driver; maximum current for electric motors and maximum power for steam turbines, gas turbines, and engines. Sometimes maximum torque will be considered for engines.

A multistage compressor model consists of models for a series of compressor stages, interstage coolers, and adiabatic flashes. Drivers are included for each compressor machine. For each single-compressor stage, the inlet charge gas conditions (pressure, temperature, flow rate, and composition) and the discharge pressure specification are used with the manufacturer's compressor performance curves to predict the outlet temperature and compressor speed. The power required for the compression is calculated from the inlet and outlet conditions.

The first step in the development of the compression model is to fit the manufacturer's performance curves for polytropic head and efficiency to polynomials in suction volume and speed. The equations for each compressor stage (or wheel, if wheel information is available) take the form:

$$E_p = A * N^2 + B * N + C * N * V_s + D * V_s + E * V_s{}^2 + F \tag{21.1}$$

$$W_p = a * N^2 + b * N + c * N * V_s + d * V_s + e * V_s{}^2 + f \tag{21.2}$$

where V_s is the suction volume flow rate, N is the compressor speed, E_p is the stage or wheel polytropic efficiency, W_p is the stage or wheel polytropic head, and "A" through "F" and "a" through "f" are correlation constants.

The polytropic head change across the stage or wheel can also be calculated from the integral of VdP from suction pressure to discharge pressure. This integration can be performed by substituting $V = Z*R*T/P$ and integrating by finite difference approximation:

$$W_p = R * \ln(P_d/P_s) * ((Z_s * T_s) + (Z_d * T_s))/2 \quad (21.3)$$

where R is the gas constant, P_d is the discharge pressure, P_s is the suction pressure, Z_s is the compressibility at suction conditions, T_s is the absolute suction temperature, Z_d is the compressibility at discharge conditions, and T_d is the absolute discharge temperature.

For simplicity, the above equations are formulated in terms of a single integration step between suction and discharge, but in the actual implementation, each stage or wheel is to be divided into at least five sections to describe the true profile. The enthalpy change across the stage or wheel can be calculated from the inlet and outlet conditions, the polytropic head change, and the polytropic efficiency.

This analysis results in three simultaneous equations and three unknowns for each integration step. The unknowns are the discharge temperature, discharge pressure, and enthalpy change for each step except the last. The known discharge pressure for the last step is related to the speed of the machine. In state-of-the-art approaches, all of the integration steps are solved simultaneously.

Measured discharge pressures, speeds, and temperatures are used in the parameter estimation run to update the intercept terms in the polynomials used to represent the manufacturer's polytropic head and efficiency curves. These parameters represent the differences between the actual performance and expected/design performance. As compressors foul, these parameters show increasing deviation from expected performance. It is this difference that has significant meaning since an absolute calculation of efficiency at any moment in time can vary with feed rate and several other factors, which dilute the meaning of the value. By showing a difference from design, we get a true measure of the equipment performance and how it degrades over time.

The discharge flow from each stage is sent through a heat exchanger model coupled with an adiabatic flash. The heat transfer coefficient for each exchanger is based on the measured suction temperature to the next stage, corrected for addition of any recycle streams. Suction and/or discharge flows are measured to fit heat loss terms in the interstage flash drums.

21.2.2.6 Expander Model

The actual work produced and actual efficiency are the key values to determine for the expander. The amount of work produced is simply the difference in enthalpy between inlet and outlet conditions multiplied by the mass flow rate. Enthalpies are determined from the observed stream composition, temperature, and pressure.

The ideal enthalpy at outlet conditions is required to determine the actual efficiency. Since the turboexpander process is an isentropic process at 100% efficiency, stream entropy at inlet conditions is required for the efficiency calculation. Referring to Fig. 21.5, the steps to determine actual efficiency include (Simms, 2009) the following:

1. Calculate the stream entropy and enthalpy at inlet conditions.
2. Calculate the ideal outlet temperature by determining the temperature at the observed outlet pressure for the stream entropy at inlet conditions.

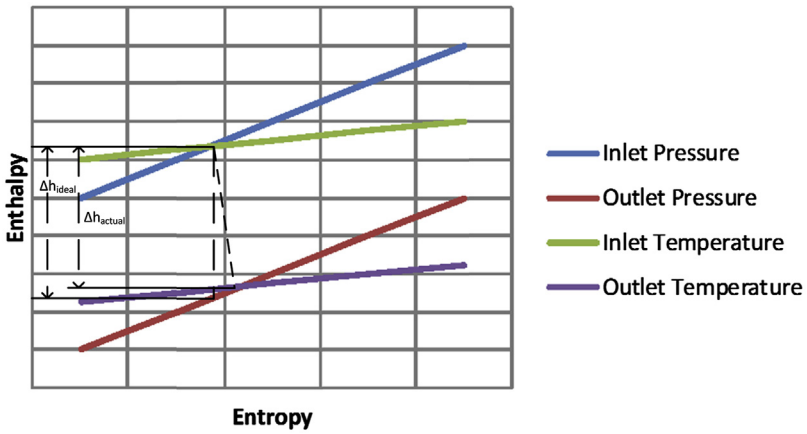

FIGURE 21.5

Expander thermodynamics (Simms, 2009).

3. Calculate the ideal enthalpy for the stream at ideal outlet temperature and observed outlet pressure.
4. Calculate the ideal enthalpy change from the difference between ideal enthalpy and inlet enthalpy (Δh_{ideal}), which is also defined as isentropic enthalpy change.
5. Calculate the actual enthalpy at outlet conditions from the stream composition and observed outlet temperature and pressure.
6. Calculate the actual enthalpy change from the difference between actual inlet and outlet enthalpy (Δh_{actual}).
7. Calculate the ratio of actual enthalpy change to ideal enthalpy change to determine the actual efficiency.

The deviation from the performance curve for the current expander performance can be used to estimate the work produced at different outlet pressures.

Expander performance curves are typically given as efficiency versus velocity ratio and efficiency versus velocity ratio (Jumonville, 2010). These performance curves can be regressed similar to Eq. (21.1) for the compressor model for the velocity ratio defined as expander wheel tip speed (U) divided by isentropic spouting velocity (C_o) as well as specific speed (N_s).

$$U = D * N/229 \tag{21.4}$$

where D is expander wheel diameter, inches and N is speed of expander wheel, rpm.

$$C_o = 223.8 * \sqrt{\Delta h_{ideal}} \tag{21.5}$$

Specific speed is defined as:

$$N_s = N * \sqrt{V_0} \Big/ \Delta h_{ideal}^{0.75} \tag{21.6}$$

where V_0 is actual volumetric flow at outlet conditions, cubic feet per second.

The deviation from the head curve for each of these performance factors can be used to predict the performance at other conditions to determine optimum usage of the turboexpander. Finally, compare compressor work with expander work to determine bearing losses.

To determine the expander speed to achieve a desired outlet pressure for given inlet conditions (pressure, temperature, volume, and stream composition) and expander wheel diameter, use the following procedure:

1. Calculate mass flow rate from inlet volume and stream composition.
2. Determine inlet entropy from given inlet conditions.
3. Determine inlet enthalpy from given inlet conditions.
4. Determine outlet temperature at constant entropy found in step 2.
5. Calculate change in enthalpy at constant entropy (Δh_{ideal}).
6. Calculate isentropic spouting velocity from Eq. (21.5).
7. Assume speed.
8. Calculate expander wheel tip speed from Eq. (21.4).
9. Calculate velocity ratio from isentropic spouting velocity found in step 6 and expander wheel tip speed found in step 8.
10. Determine expander efficiency according to biased performance curve at velocity ratio found in step 9.
11. Calculate actual change in enthalpy from Δh_{ideal} found in step 5 and expander efficiency found in step 10.
12. Calculate outlet enthalpy from inlet enthalpy found in step 4 and actual change in enthalpy found in step 11.
13. Calculate actual outlet temperature from outlet enthalpy found in step 12, desired outlet pressure, and stream composition.
14. Calculate actual volumetric flow at outlet conditions.
15. Calculate specific speed from Eq. (21.6).
16. Determine expander efficiency according to biased performance curve at specific speed found in step 15.
17. If efficiency determined from velocity ratio from step 10 and efficiency determined from specific speed found in step 15 is equal (within desired tolerance), then calculate expander work from mass flow rate and actual change in enthalpy.
18. If efficiency determined from velocity ratio from step 10 and efficiency determined from specific speed found in step 15 is the not equal (outside desired tolerance), then return to step 7.

With the above procedure, the expander outlet pressure can be optimized considering the other processing equipment.

21.2.2.7 Distillation Calculations

Standard tray-to-tray distillation models are used for distillation calculations in an optimization system. The "actual" number of trays is used wherever possible and performance is adjusted via

efficiency. This allows the model to more accurately represent the plant in a way that is understandable to a plant operator.

All distillation models predict column-loading constraints accurately as targets are changed. Condenser and reboiler duties are also calculated for predicting utility requirements and exchanger limitations.

21.2.2.7.1 Tray-to-Tray Distillation Method

An equation-based tray-to-tray distillation method is based on mass, heat, and vapor liquid equilibrium balances on each physical tray. Fig. 21.6 depicts a typical distillation column tray.

Component mole balances for each component i on tray j are:

$$F_i Z_{ij} + L_{i+1} X_{(i+1)j} + V_{(i-1)} Y_{(i-1)j} - (L_i + LP_i) X_{ij} - (V_i + VP_i) Y_{ij} = 0 \tag{21.7}$$

The overall mole balance is:

$$F_i + L_{i+1} + V_{i-1} - (L_i + LP_i) - (V_i - VP_i) = 0 \tag{21.8}$$

The vapor–liquid equilibrium definition is written in terms of the liquid mole fractions and K-values:

$$Y_{ij} = K_{ij}(X_{ij}, T_{jl}, P_i) * X_{ij}, \tag{21.9}$$

where T_{jl} is the liquid temperature on tray j.

The requirement that the mole fractions balance is expressed as:

$$\sum [X_{ij}] - \Sigma [K_{ij}(X_{ij}, T_{jl}, P_i) * X_{ij}] = 0 \tag{21.10}$$

The Murphree vapor tray efficiency, which accounts for differences between the equilibrium vapor composition $[K_{ij}(X_{ij}, T_{jl}, P_i) * X_{ij}]$ and the actual mixed vapor composition $[Y_{ij}]$ leaving the tray is an important adjustable parameter. It is defined as:

$$E_{ij} = (Y_{ij} - Y_{ij-1}) / \left(K_{ij}\left(X_{ij}, T_{jl}, P_i\right) * X_{ij} - Y_{ij-1}\right) \tag{21.11}$$

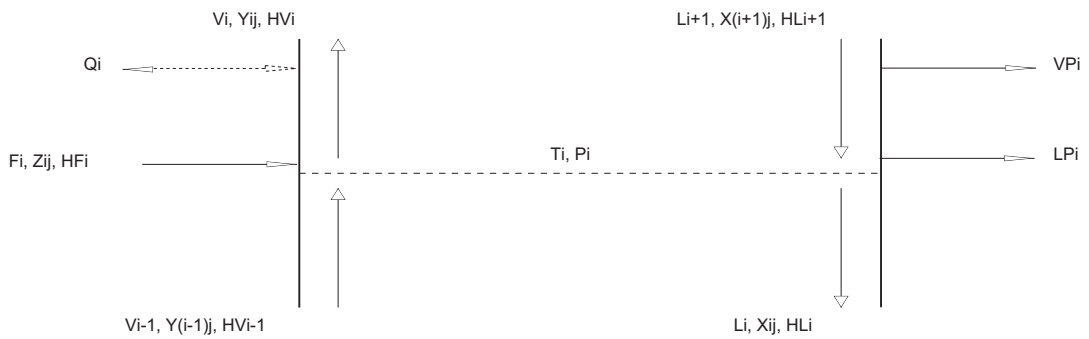

FIGURE 21.6

Mass transfer operations in a tray distillation column.

The vapor and liquid enthalpies are defined as:

$$HV_i - HV(Y_{ij}, T_{jv}, P_j) = 0 \tag{21.12}$$

$$HL_i - HL(X_{ij}, T_{jl}, P_j) = 0 \tag{21.13}$$

where T_{jv} is the vapor temperature on tray j.

The overall tray heat balance is:

$$F_i HF_i + L_{i+1} H_{i+1} + V_{i-1} HV_{i-1} - (L_i + LP_i) HL_i - (V_i + VP_i) HV_i + Q_i = 0 \tag{21.14}$$

The liquid and vapor flow rates on the capacity limiting trays are used in conjunction with tray loading calculations to predict column pressure drops. The vapor area factor in the loading correlation is parameterized to enable matching calculated column differential pressure against the measured differential pressure. Upper limits are placed on this calculated differential pressure during the optimization case to ensure avoidance of flooding.

Condenser and reboiler limitations are handled by placing constraints on the minimum approach temperature in these exchangers or on the maximum heat transfer area in the case of variable level exchangers. Heat transfer coefficients are calculated for the exchangers in the parameter case.

21.2.2.7.2 Demethanizer

Set point variables for a cryogenic demethanizer are typically the bottoms methane or carbon dioxide content and the overhead pressure. Constraint variables include overhead condensing capability and minimum column temperatures. The expansion impacts on the demethanizer and the overhead ethane losses are key profit variables.

The demethanizer is modeled with a tray-to-tray distillation model. Rigorous K-values for the demethanizer column are recommended due to nonlinear vapor–liquid equilibrium relationships. Overall heat transfer coefficients for the reboilers and feed chillers are calculated from temperature and flow data.

21.2.2.7.3 Deethanizer

The set point variables in the deethanizer are the overhead pressure, the overhead propane content, and the bottoms ethane content. Any cooling medium (such as refrigeration, cooling water, or air) and heat medium (such as steam or hot oil) requirements of the deethanizer and the propane loss in the overhead are the major profit considerations.

The deethanizer is modeled with a tray-to-tray distillation model. Parameters include column pressure, column pressure drop, propane content in the deethanizer overhead, reflux flows, deethanizer bottoms ethane content, and bottoms draw rate. Overall heat transfer coefficients are calculated for the exchangers.

21.2.2.7.4 Depropanizer

The set point variables for the depropanizer are the overhead butane content and column pressure. Key constraint variables are the propane in the debutanizer overhead, the overhead exchanger capacities, and column pressure drop (flooding). Any cooling and heat medium usage requirements of the depropanizer are the major profit considerations.

The depropanizer is modeled with tray-to-tray distillation models. Parameters considered include column feed temperature, column pressure, column pressure drop, butane content in the tops, reflux

flow, bottoms propane content, and bottoms draw rate. Overall heat transfer coefficients are calculated for the reboiler and condenser. A column capacity factor is also parameterized.

21.2.2.7.5 Debutanizer

The set point variables for the debutanizer are the overhead pentanes and heavier content as well as column pressure. Key constraint variables are the propane in the debutanizer overhead, the overhead exchanger capacities, and column pressure drop (flooding). Any heating and cooling medium usage requirements of the debutanizer are the major profit considerations.

The debutanizer is modeled with a tray-to-tray distillation model. Parameter considered include column feed temperature, column pressure, column pressure drop, pentanes and heavier content in the overhead, reflux flow, bottoms butanes content, and bottoms draw rate. Overall heat transfer coefficients are calculated for the reboiler and condenser. A column capacity factor is also parameterized.

21.2.2.7.6 Butanes Splitter

The set point variables for the butanes splitter is the column pressure, normal butane in overhead, and isobutane in the bottoms. The constraint variables of interest are reboiler and condenser loading and product specifications. The profit variables of interest are the isobutane losses in the bottoms normal butane stream.

The butanes splitter is modeled with a tray-to-tray distillation model. The parameters considered include column pressure, column differential pressure, normal butane in the isobutane product, bottoms isobutane concentration, reflux flow rate, bottoms flow rate, product draws, bottom reboiler flow rate. Heat transfer coefficients for the exchangers are calculated.

21.2.2.7.7 Refrigeration Models

The main set point variable for refrigeration machines is the first-stage suction pressure. Refrigeration system models relate refrigeration heat loads to compressor power. The compressor portions of the refrigeration models use the same basic equations as compressor models discussed above. Refrigeration systems should use the appropriate composition and will have a component mixture for any make-up gas.

The measured compressor suction flows and the heat exchange duties calculated by the individual unit models are used to determine the total refrigeration loads. The refrigerant vapor flows generated by these loads are calculated based on the enthalpy difference between each refrigerant level. Exchanger models of the refrigerant condensers are used to predict compressor discharge pressures.

21.2.2.7.8 Demethanizer Feed Chilling Models

The demethanizer feed chilling system is modeled as a network of heat exchangers and flash drums. These models are used to predict the flow rates and compositions of the demethanizer feeds. The effects of changing demethanizer system pressures and flow rates are predicted.

The demethanizer feed drum temperatures and feed flow rates are measured to fit the fractions of heat removed from the feed gas by each exchanger section. Flow and temperature measurements on the cold stream side allow the fraction of feed gas heat rejected to each stream to be estimated. The two sides of the feed exchangers are coupled through an overall heat balance. The inlet and outlet temperatures from the refrigerant and other process exchangers are used to fit overall heat transfer factors in the parameter case. A pressure drop model for the feed gas path is also included.

21.2.2.8 Steam and Cooling Water System Models

Heat and material balance models of the steam system are developed. These models include detailed representations of the boilers.

The cooling water system will be modeled with heat exchangers, mixers, and splitters to allow for constraining the cooling water temperature and its effects on the operation of distillation columns and compressors.

21.2.2.9 Turbines

A turbine model, as shown in Fig. 21.7, is used for steam turbines (back pressure, condensing, or extraction/condensing) or any expander in which the performance relationship can be expressed using the following equation:

$$\text{Design Power} = \text{A} + \text{B} \times (\text{Mass Flow}) + \text{C} \times (\text{Mass Flow})^2 + \text{D} \times (\text{Mass Flow})^3 \tag{21.15}$$

Back pressure and condensing turbine expected performances are usually presented as essentially linear relationships between power and steam flow. Extracting/condensing turbine expected performance relationships are typically presented as power versus throttle steam flow, at various extraction steam flows. This kind of performance "map" can be separated into two relationships of the form above, one representing the extraction section, and the other the condensing section. An extraction/condensing turbine can be thought of as two turbines in series, with part of the extraction section flow going to the condensing section.

Design power refers to expected power from performance "maps" that are at specific design inlet pressure, inlet temperature, and exhaust pressure. Expected power is the power expected from a turbine operating at other than design conditions. The design power is adjusted by the "power factor," as illustrated:

$$\text{Expected Power} = \text{Design Power} \times \text{Power Factor} \tag{21.16}$$

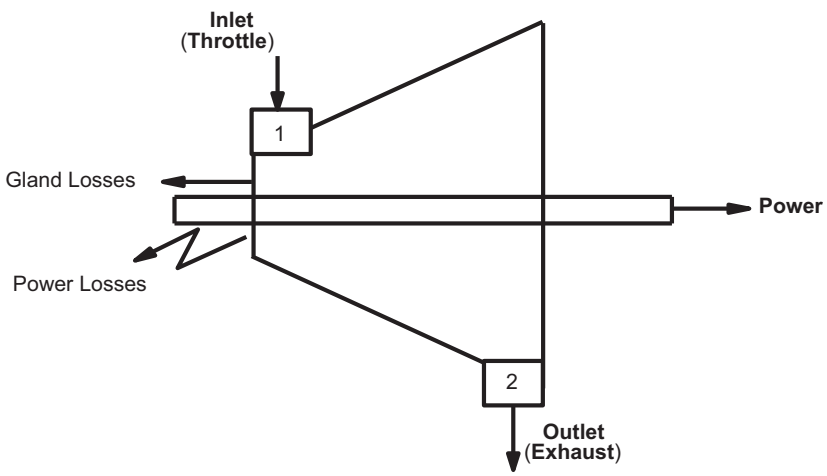

FIGURE 21.7

Schematic of turbine model.

$$\text{Power Factor} = \frac{\Delta \text{ Isentropic Enthalpy at actual conditions}}{\Delta \text{ Isentropic Enthalpy at design conditions}} \tag{21.17}$$

$$\text{Brake (shaft) Power} = \text{Expected Power} + \text{Power Bias} \tag{21.18}$$

Design power and expected power are equal if actual expanding fluid (i.e., steam) conditions are the same as design conditions. The power bias can be parameterized using the exhaust temperature for back-pressure turbines or the extraction section of an extraction/condensing turbine. In both of these cases the exhaust steam is superheated (single phase). For condensing turbines or the condensing section of an extraction/condensing turbine, the measured steam flow is calculated since the temperature of the two-phase exhaust cannot be used. The fraction vapor of the two-phase exhaust is determined by energy balance. The total energy demand can be determined from the compressor (or other driven power consumer). The power extracted from the extraction section can be determined from the throttle steam flow and the inlet and outlet (single phase) conditions. The power extracted from the condensing section is just the difference between the total demand and the extraction section power.

The power loss is taken from the steam and affects its outlet conditions but is not transferred to the shaft or brake power.

To calculate the change of enthalpies needed for the power factor and for the energy balance, fluid conditions are calculated for each turbine section at the inlet (throttle), outlet (exhaust), and at inlet entropy and outlet pressure for both actual and design conditions. The nomenclature associated with the exhaust fluid conditions required for the enthalpy change calculations is:

Exh IDM = Exhaust **I**sentropic at **D**esign inlet conditions for vapor/liquid **M**ixture
Exh IDV = Exhaust **I**sentropic at **D**esign inlet conditions for **V**apor
Exh IDL = Exhaust **I**sentropic at **D**esign inlet conditions for **L**iquid
Exh IAM = Exhaust **I**sentropic at **A**ctual inlet conditions for vapor/liquid **M**ixture
Exh IAV = Exhaust **I**sentropic at **A**ctual inlet conditions for **V**apor
Exh IAL = Exhaust **I**sentropic at **A**ctual inlet conditions for **L**iquid

For condensing turbines or the condensing section of extraction/condensing turbines the exhaust pressure is used to specify the model. The parameter that this measurement updates is the condenser heat transfer coefficient. The exhaust pressure is free to move in the optimization cases, since the actual pressure moves as the condenser calculates the pressure required to condense the steam sent to the condensing turbine or condensing section.

The maximum mass flow at reference (usually design) conditions is used to predict the maximum mass flow at actual conditions as an additional constraint on the turbine performance. Sonic flow relationships are used for this prediction. This is the maximum flow through the inlet nozzles when the inlet steam chest valves are wide open. The nozzle area is not needed if the maximum flow at a set of reference conditions is known. Vendors usually list the maximum flow and not the nozzle area.

The model also includes the gland steam flow which is used to counterbalance the axial thrust on the turbine shaft and which is lost through labyrinth seals. The gland steam does not contribute to the shaft power.

Typically, turbine performance is not considered to be a function of speed. Consequently, speed is a variable that has no effect on the solution. However, turbine performance is typically a very weak function of speed over a wide range, and its effect on performance is not typically presented on the expected performance "maps." The possibility of adding the weak effect of speed on performance will be considered when the model is being built.

21.2.3 PLANT MODEL INTEGRATION

After the plant section models have been developed, they are integrated into the overall plant model. All of the interconnecting streams are specified and checked and a consistent set of variable specifications developed. At this stage, the overall validity of the plant model is checked using off-line plant data.

Reconciliation/parameter and optimization cases are run and the results are checked for accuracy and reasonableness. A material balance model is included in the plant model integration work to confirm an absolute model material balance closure. This material balance will include a furnace area balance, a recovery area balance, and an overall balance. In addition, the plant integration allows the objective function to be tested and validated with connections to all feed, product, and utility variables.

It is important to have the engineers who will be responsible for commissioning the optimization system involved in the project during plant model integration. A thorough understanding of the plant model is imperative for a smooth implementation of the online system.

21.2.3.1 Model Fidelity and Measurement Errors

In an optimization system as described here, neither the models nor the measurements need to be absolutely perfect for the system to work well and to deliver significant improvement in profitability. An online optimization system continuously receives feedback from real-time measurements. The model parameters are updated prior to each optimization so that the models fit the plant and the optimum set points calculated are valid and can be confidently implemented. Without this constant feedback of plant measurements and regular updating of the plant model, the optimization solution might not be feasible. The fidelity of the models and the accuracy of the measurements are reflected in trends of the parameters. During commissioning of the optimization system, the best available measurements are identified by analyzing many parameter cases, running with real-time data and prior to closing the loop.

If, for example, significant heat balance discrepancies exist between process side and fuel/flue gas side measurements in a furnace, that discrepancy can be handled by determining the bias required on the fuel gas flow measurement(s) to satisfy the heat balance. That bias could be a parameter that is updated prior to each optimization. The variation of the bias over time (its trend) would be monitored. If this parameter varies significantly, the furnace model and other measurements used by it would be investigated thoroughly. Alternate measurements used to "drive" the parameter case solution would be investigated as well. The outcome of this analysis is that the best available measurements are selected and the model relationships are thoroughly investigated to ensure that all significant relationships are included. This analysis is a standard and required step in building the optimization system.

Validity checking is an integral part and is built into an online optimization system. It is used to screen out gross errors. If alternate measurements are available, the validity checkers can use these when primary measurements are unavailable or bad. Generic validity checkering takes care of common errors, while custom validity checking can respond to site-specific situations. Measurements can be designated as critical, so if they are unavailable, the optimization cycle will be directed to monitor for steady state and will only complete its cycle when the measurement becomes available. Validity checking has several features designed to keep the online service factor of the optimization system high in the face of imperfect measurements. Another feature of the online system is that the

measurements used to drive the solution of the parameter case are averages over a specified time window (usually 1 h) so that measurement noise is suppressed.

The better the measurements and the better the models, the better a RTO can fully exploit the process equipment, and consequently, the more potential profit is realized.

Processing RTO in the future will likely include wider applications driven by demonstrated benefits, reduced implementation costs, and acceptance as a best practice. RTO applications are also becoming tightly intertwined with economic planning systems, where real-time pricing and contractual considerations are available.

Evolving technologies changing the value proposition for refining RTO include:

- Detailed kinetic models for all major processing units and configurations, proven by reported applications.
- Optimization technology improvements that incorporate robust solvers, integer variables, and the capability to handle increasing problem sizes. Today's technology can handle applications with several hundred 1000 equations; a typical refining application has 100 measurements, more than 100,000 variables and 25 outputs.
- Greater integration with higher-level systems including shared models and reconciled measurement data.
- Multiunit optimization that leverages shared resources between process units and continues to lead toward rigorous refinery-wide optimization.
- Computing technology improvements, which have already shifted RTO from minicomputers to personal computers, and that will allow more solutions/day and more complex formulations. Solver and computing improvements will eventually lead to true dynamic optimization.
- Application and model building tools, operating graphical user interfaces, and sustained performance technologies that will lower cost, improve benefits, and remove other hurdles.

21.3 REAL-TIME OPTIMIZATION PROJECT CONSIDERATIONS

The steps of a real-time project implementation include:

- Front-end engineering design
- Flow sheet development
- Model testing and tuning
- Online open loop testing
- Online closed loop testing
- Application sustainment

During front-end design, the project objectives should be clearly defined including:

- Process envelope—The system boundaries shall be determined including the process equipment included within the boundary. Various equipment line-ups that will be considered for optimization are identified. Also, the modeling methodology decisions occur at this stage.
- Economic parameters and objective function—The profit function requires definition including the specific economic parameters that contribute to the profit function.

- Source of process and economic information—Process and economic information will be available from various sources. Process information is typically acquired from a process historian while economic information will come from various commercial sources. Care should be taken to determine a source that is current and updated frequently.
- Set points to be generated from the optimizer—Process set points are critical for effective optimization. These set points must be selected where process control action will be attained accurately. APC strategies are usually best for implementing set points from a real-time analyzer.
- Metrics required for success—Metrics to track optimizer online time as well as optimizer effectiveness should be determined. An owner of these metrics should be identified to take responsibility for the success and sustainability of the optimizer.

Flow sheet development is obviously a critical step in the implementation of a RTO project. The flow sheet should be developed by subsections of the plant and imported into the main application flow sheet as block diagrams. Redundant streams and equipment used in the initialization phase are removed from the flow sheet, and the sections of the plant are connected together at the block boundaries to fully integrate the subsections into a single flow sheet. Unit and flow sheet customizations are then added to improve the model's representation of the process.

Model testing and tuning includes reconciling the imported data in off-line mode and testing the real-time sequencing. The standard data reconciliation report is used to identify the measurements with the worst mismatch, and corrective action is taken. The model is then tested by importing multiple sets of data via the electronic data interface before placing the model online. Optimization cases are run and verified. Steady-state detection is fine-tuned. Initial online runs are observed to verify transfer of optimal set points to the advanced control and distributed control systems.

Sustainment of the application is critical to the long-term success. An engineer should be assigned responsibility for maintaining the application and working with operations to resolve any concerns immediately. Metrics should be tracked and reported to measure the success. These metrics may include the following:

- The time on optimization as a percentage of time on control, averaged over all optimizable controllers.
- The time the optimizable controllers had optimization set points rejected as a percentage of the time on-control.
- The time the optimizable controllers ran at expired optimization set points as a percentage of the time on-control.

Optimization set points should expire after a predetermined amount of time, reflecting the nominal period for which a single optimization solution is valid. A standard stream-factor tracking program will calculate and report these statistics.

21.4 EXAMPLE OF REAL-TIME OPTIMIZATION

The Gassled joint venture operated by Gassco and supported by Statoil has applied RTO at their Kårstø gas processing plant in Norway (Kovach et al., 2010). The model is called the Plant Production Performance Model or 3PM.

Kårstø is the largest natural gas liquids (NGLs) recovery plant in Europe. The Gassled owners have first rights to book capacity. Spare capacity is available for any other qualified shipper and subject to published tariffs for transporting and processing gas.

Gassled has a flexible gathering network connecting the respective producers and processing terminals allowing gas streams from several fields to be routed to different destinations. Mixing of gas streams provides sales gas quality with respect to gross calorific value (GCV), Wobbe index (WI), and CO_2.

Rich gas processing capacity at the Kårstø plant depends on several variables and constraints. One of the most significant variables is the feed gas composition. Simulations demonstrate that the rich gas processing capacity may be significantly lower than the nominal design capacity if the feed has a high NGL content.

New expansion to increase the capacity of the Kårstø facilities has increased the complexity of the Kårstø facilities. The need for an online model to determine plant capacity was recognized to enable the plant to operate with a high degree of capacity utilization, realizing that production regularity is an inherent property of the throughput obligations. Underutilization of capacity sacrifices processing fees. The RTO model allows precise and reliable capacity predictions while reducing the work required to determine the capacity. Operating set points required to reach the predicted capacity are generated as well as information for maintenance planning and infrastructure development.

21.4.1 PROCESS DESCRIPTION

Fig. 21.8 shows a simplified process diagram of the Kårstø gas processing plant. As can be seen, rich gas enters the plant and is preconditioned by removal of H_2S and mercury. The gas is then preheated prior to dehydration, and NGL is extracted from the rich gas. The fractionation facilities produce raw ethane, stabilized condensate, propane, n-butane, i-butane, and naphtha. CO_2-rich ethane extracted from each train is routed for purification of ethane.

The processing facilities include 26 distillation columns. Steam is used as the heating medium for the reboilers on the distillation columns and to power turbines. Steam boilers and waste heat recovery systems on gas turbines generate the steam. Three levels of steam are employed. Additional utilities used are seawater for cooling and propane for refrigeration.

Sales gas is exported to two high-pressure subsea pipelines operated at pressures up to 189 barg. The export compression facilities include four compressor manifolds operated at different suction and discharge pressures. The compressors are driven by both gas turbines and electric motors.

In the Kårstø plant, the extraction trains may be bypassed. This allows more gas to be produced and processed. However, the bypass quantities are limited to provide sales gas quality to comply with the GCV, WI, and CO_2 specifications.

21.4.2 PLANT OPERATION

Effective field production and development of new offshore fields requires high capacity utilization of the Kårstø plant. By squeezing the throughput margins, the plant performance becomes increasingly sensitive to variations in feed gas composition and the plant constraints become more evident. Operating toward the plant limits challenges plant regularity. A conceptual illustration of the intrinsic relation between these two characteristic parameters is shown in Fig. 21.9.

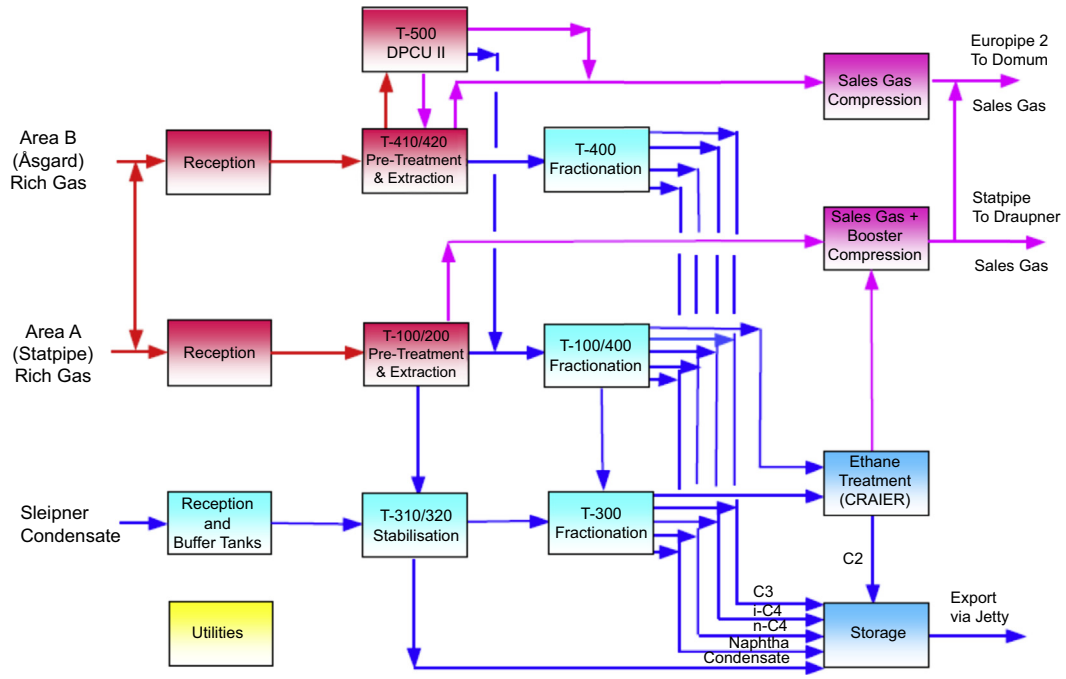

FIGURE 21.8

Process flow overview of Kårstø gas processing plant.

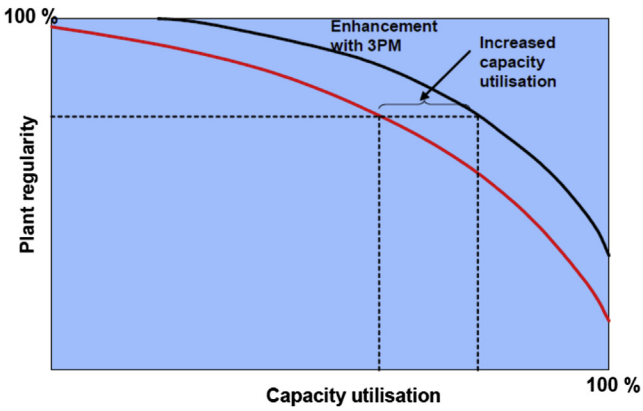

FIGURE 21.9

Trade-off between plant regularity and capacity utilization (Kovach et al., 2010).

Several parameters impact the rich gas capacity at Kårstø plant. Some of the most important parameters are rich gas composition, NGL recovery, product purity, and CO_2 recovery. Production rates and the fluid composition determine the rich gas composition to the Kårstø plant. Significant and sometimes rapid changes in the feed composition must be handled continuously. Changes in feed composition may move the capacity constraint from one facility to another. For example, a richer composition of the feed gas may cause the plant to reach a constraint in the NGL fractionation. A leaner gas could hit a constraint in the extraction facilities. Crossover piping allows several combinations of routing of the gas streams.

The NGL extraction trains at Kårstø plant are designed to provide about 90% recovery of NGL. However, recovery of NGL products may be limited for some feed compositions by the fractionation capacity. When the production objective is to maximize rich gas throughput, the NGL recovery can be decreased to process more gas until reaching a constraint in the extraction facilities, compression, preconditioning, or other parts of the plant. Specifications for the liquid products, defined in the transportation and processing agreements, require a minimum purity.

The carbon dioxide concentration of the sales gas is a contractual constraint with a limit of 2.5% mole. The CO_2 removal capacity of the plant is not fixed. Feedstock composition and gas rate are the major factors that affect CO_2 removal capacity. Optimum CO_2 removal can be affected by the routing of gas and liquids through the plant as well. Rich gas can be split between two treating systems or bypassed and delivered to two export pipelines. Also the GCV is controlled between an upper and lower constraint. Routing rich gas through one of the bypass connections may be employed to increase plant throughput, but this rate is then limited by the upper GCV constraint. To avoid breaching the lower GCV constraint, extracted ethane can be reinjected in the sales gas. Furthermore, the sales gas streams can be mixed at the compressor manifolds by utilizing the downstream crossover. In addition to increased capacity utilization, the crossover pipelines allow enhanced flexibility of the operations with respect to handling of feedstock variations. It is possible to mix the various feed streams to optimize NGL recovery, CO_2 extraction, and quality of the products.

21.4.3 PRODUCTION OBJECTIVES

The primary production objective is typically plant throughput and to deliver sales gas and products within the specifications. However, the production objectives include maximum daily throughput, high annual capacity utilization, optimum NGL production, and optimum fuel gas consumption.

Most shippers request high production at Kårstø throughout the year, taking into account the seasonal swing in gas demand. This means there is high demand for processing capacity at Kårstø throughout the year.

The operator is responsible for coordination of the yearly maintenance planning of all the installations connected to the gas transport infrastructure. A primary objective is to obtain a total plan where the availability of gas for deliveries to the market is maximized. Depending on the extent of yearly maintenance at Kårstø as well as at the upstream fields, this could put restrictions on production from certain fields, or allow accelerated production of more natural gas liquid—rich or CO_2-rich gas from other fields. Maximizing CO_2 production from CO_2-rich fields could imply postponed or reduced investments in future CO_2-removal capacity, to meet sales specifications.

In periods when processing demand is below the plant capacity (when Kårstø has no bottleneck effect on the offshore production), the primary operational objective is to maximize NGL recovery to

provide for increased value creation for the shippers. For the NGL products, this means achieving the minimum product purity.

The Kårstø plant is a large energy consumer, and optimizing energy consumption is an important objective. However, optimizing energy consumption should not compromise the primary production objectives, related to the value creation at Kårstø.

21.4.4 PROJECT DRIVERS

Value generated by RTO for the Kårstø plant operations comes from the following:

- Increased utilization of the plant capacity, by introducing RTO
- Improved quality of the capacity figures issued for booking
- Reduced time needed to prepare for the booking process
- Improved position in the business development process.

On a daily basis the feed stream compositions will vary. Processing feeds of variable composition requires the plant control system to give fast and accurate responses to maintain production targets. Skilled operators have a basic understanding of the plant operational characteristics and learn how to respond to feed disturbances. However, in transition periods the plant capacity will not be fully utilized. Also, the operator may not push the plant to its full capacity, or they may choose a suboptimal routing of the gas through the processing facilities. On a regular basis, the RTO determines optimized set points for the advanced control system, thereby ensuring a rapid and smooth transition period to new optimal plant conditions.

An illustration of the possible benefits with the 3PM employed for RTO to handle feed composition variations is shown in Fig. 21.10. In this example, the primary operational objective is to achieve maximum plant throughput. The upper curve illustrates achieved production over a day when the operator employs the 3PM. The lower curve illustrates production with no 3PM implemented.

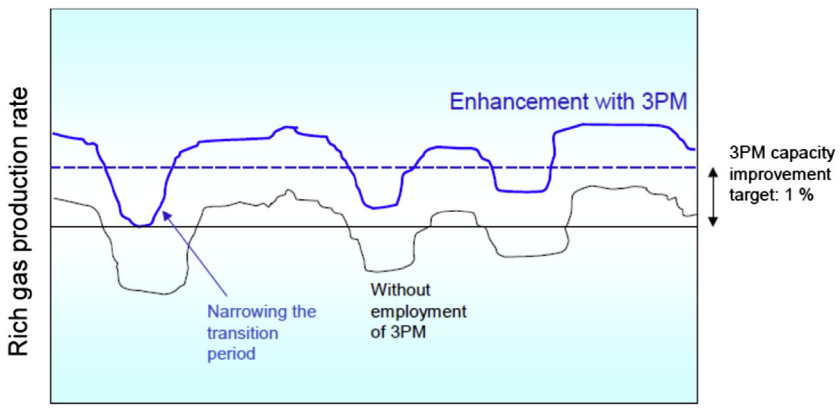

FIGURE 21.10

Illustration of enhanced processing capabilities.

It should be recognized that the upper curve assumes a shorter transition period following changes in the feed conditions. The 3PM model enables an increase of the plant throughput by 1%.

Plant regularity has a very high focus, and a regularity target of at least 98.5% is set for the Kårstø plant. However, when failure occurs, emphasis is put on maintaining the highest possible service degree to limit upstream consequences to oil production and minimize the consequences for the gas customers. In situations where equipment exhibit underperformance like fouling in heat exchangers or degrading of compressors, this is revealed by the optimization model and appropriate actions to correct the problem could be executed. If equipment fails to work or is temporarily out of service the optimization model automatically computes new set points of the APC to minimize the consequences.

The operator of the plant is responsible for issuing capacity figures for the booking processes. Often there are requests for processing capacity beyond current capacity at the plant. This puts pressure on the capacity margins of the plant. With the optimization model, which closely mimics the real operation performance, Gassco can provide enhanced confidence to reduce the uncertainty margins.

Extraction of NGL from the rich gas and subsequent fractionation into commercial products adds value to the shippers. Some shippers limit their gas deliveries based on their booked fractionation capacity, while shippers with leaner gas are limited by their booked extraction capacity. Any free processing capacity is identified and can be available to the shippers, allowing them to optimize their petroleum portfolio. This allows accelerated production of NGL-rich gas to maximize revenue for the shippers.

Boosting processing capacity within the limits of the facilities is the primary objective. The online model improves planning with a higher accuracy than the current process simulation models. Improved quality and accuracy of the planning tool results in a higher confidence in the calculation of the maximum plant capacity, denoted available technical capacity. The capacity committable on a long-term basis is denoted maximum available capacity (MAC). This allows for an operational margin for daily operations as shown in Fig. 21.11.

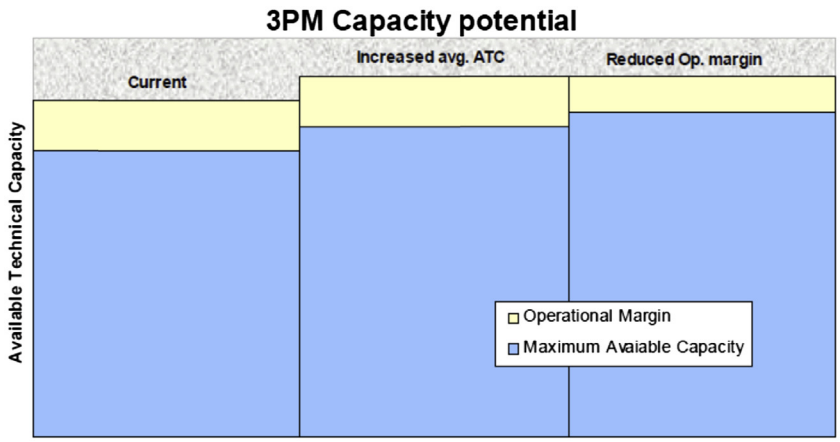

FIGURE 21.11

Increased available technical capacity and maximum available capacity.

Reduced uncertainty due to the capability of the optimization model may narrow the operational margin and thereby increase the MAC. The biannual capacity estimation process is demanding and time consuming. Performance of existing equipment and systems that limit capacity utilization of the plant require evaluation. The optimization model allows this estimation process to be run more efficiently.

21.4.5 FEATURES OF THE OPTIMIZATION MODEL

A single model that is applied for various purposes minimizes the inconsistency between various simulation results and the actual operation of the plant. A high degree of confidence in the planning scenarios and simulation results is achieved as the same model is applied for optimization of the plant in real time. With the increased complexity of the plant, and thereby the increase in number of opportunities for routing/processing the gas at Kårstø, a model of this type provides a means of improving the plant performance by optimizing the operation by use of a mathematical model to compute the optimum operation point and routing.

21.4.5.1 Implementation and Usage of the Model

The model is built in a commercially available equation-based modeling tool developed specifically for real-time online optimization in the hydrocarbon and chemical industry. The model is a single model, used for all purposes of the 3PM project, i.e., RTO, simulation, and planning. The setup of the system is described briefly here. The online model reads automatically plant measurement tags, and based upon these readings, a steady state test is performed. With the steady plant, a data reconciliation with the actual plant data is performed. Afterward the reconciled model is subject to optimization with a given objective function.

The online system is located at the Kårstø gas processing facility. The offline system is located at both Kårstø and the Gassco. The model includes the four gas separation trains (serving the Åsgard and Statpipe rich gas pipelines), the Sleipner condensate train, and simplified representations of the utility (steam and refrigeration) systems. This results in the following unit counts:

- Distillation columns—26
- Single compressors—18
- Paired expander compressors—13
- Process measurements—1600
- Controllers (regulatory and advanced control, 175 and 110 variables, respectively)
- Associated heat exchangers, drums, motors, furnaces, pumps, pipes, and valves

The output of the optimization is a set of set points to the advanced control system. The online model is anticipated to run in intervals of 2−4 h, depending on solution time, performance, and actual implementation and usage in the daily routines.

The planning interface is a simplified representation of the plant in an external graphical user interface (GUI), where one has the opportunity to generate new feeds by mixing different field flows and compositions to test out the performance in simulation as well as optimization mode. The simplified representation of the plant consists in principle of a block diagram, where the blocks represent sections of the plant. The planner then has the option to switch off one or more blocks and check the capacity (performance) of the plant with this very simplified model user interface. The fact that the planner has a

simplified overall GUI for the model of the plant, with a number of sections representing logical groups of unit operations in the plant, makes it easy to do scenario analysis for both new fields (new compositions) and for shutdown and maintenance. In each case, it becomes easier for the planning department to give a precise answer to the capacity of any feed with a given layout of the plant.

Simulation is done in the core model GUI, which is also used in the RTO mode. Further, new plant developments may be simulated with the model to get a better prediction of throughput capacity than a conventional simulation would give.

The online model is located on a computer in the plant control room. It is running in a fully automated fashion, on a given interval basis. The model immediately sends the solution to a central storage computer. From here the model can then be accessed by planners and offline simulation engineers, who copy the solved models to their own computers, respectively. This facilitates a common arena for operations as well as the planning and engineering departments.

The online model produces results to various types of end users. In addition to generating the actual set points to the advanced control system (and the operators), the model generates a set of reports with different types of information every time it is solved. The type of information to be generated is mass and energy balances, production figures, economical performance, utility consumption, capacity utilization of each unit, shadow prices, and equipment monitoring.

21.4.5.2 Modeling and Optimization Strategy

The model for the Kårstø plant is a plant-wide model, comprising all processing facilities, as well as the steam boilers and other utilities. The model is a single plant model, based on open equations. The individual unit operations are modeled by use of standard library models. In the cases of rotating equipment and important valves, Statoil and original vendor performance curves are used. The plant instruments that the model reads and applies are carefully chosen, to ensure that sufficient and trustworthy signals form the basis of the data reconciliation, and subsequently the optimization. All alternative operation scenarios in terms of equipment failure, maintenance, etc. are dealt with by lineups defined by a set of macros.

The various crossovers that are normally in use, in the plant are treated as continuous variables to avoid integer variables in the optimization problem. Only equipment that plays an active role in the plant are modeled, and the set of compounds used are as comprehensive as necessary to achieve representative results. This is to maintain a fairly reasonable size (and solution time) of the model.

The model (and the planning facility) comprises a set of objective functions from which one can be applied according to the desired operation mode. The objective functions for the optimizer reflect operation modes that are, or may be, relevant to operation of the Kårstø plant. The objective functions are predefined and can be chosen arbitrarily by the system administrator. Typical examples of objective functions are to maximize sales gas production or to maximize liquid NGL production. For all cases, the general product qualities are modeled as constraints together with the relevant operational limitations.

There are over 100 flags to indicate the routings and equipment status in the plant. While the physical realities prevent this from being a true combinatorial problem, in practice there are easily over a 100 possible plant configurations. This poses challenges in both making sure that the appropriate equipment is on or off in the model, but more importantly, in creating a good starting point for the equation-based solver.

In addition, the CO_2 removal and ethane recovery unit can operate near the CO_2/C_2 azeotrope and some portions of the unit approach the critical point of the mixture. As with most modern gas plants, it is heavily heat integrated with many heat-pumped columns, cold boxes, and paired expander compressors.

21.4.5.3 Online Usage

The online system follows the sequence of detecting steady state, checking data consistency, reconciling the data, calculating the optimal set points, and sending the optimized set points to the controllers.

21.4.5.4 Quantifying Measurement Errors

The 3PM model imports over 1600 process measurements, which are used in data reconciliation. Of these, several hundreds were identified as key process variables and have results from the data reconciliation runs written back to the database. The data exported for these points consist of the sample value used in the data reconciliation, the reconciled value, and the measurement offset.

Some nonmeasured variables such as compressor efficiencies are also saved. The scan and reconciled values are accessible on operator process displays. The same operator displays have links to preconfigured trends of the measurement offsets. This gives operations a quick way of evaluating the accuracy of their process measurements and seeing inferred values (e.g., efficiencies and unmeasured temperatures) in a familiar format.

Data reconciliation detects and runs when the plant is steady and puts the data in a readable format that supports scanning the data over long time periods. Any trended offset which is not distributed around zero and which has a consistent bias may be in error.

A suspected point can be immediately checked. Quantifying measurement errors can also help improve the accuracy of other off-line simulation tools. Any process variable that is used as a specification in a process simulator needs to be accurate. Detecting a bias can significantly improve the accuracy of the simulation results.

In addition to highlighting possible measurement errors, an understanding of the behavior of unmeasured variables such as intermediate temperatures or efficiencies can have a positive impact on operations. Data reconciliation results have highlighted differences in efficiencies between parallel compressor trains and furnaces.

21.4.5.5 Off-line Usage

The off-line system consists of a web-based interface, an SQL data repository for storing cases, and rigorously validated models from the online system. The interface is designed to facilitate queued simulation and optimization runs of the most common plant configurations using various combinations of flows from the 30+ fields which feed the plant. Planning personnel have the option to run the model either through the standard web-based simulation interface or through the more detailed model builder interface. The latter is used to explore special situations which are not supported by the web-based interface. This requires a more detailed knowledge of the model and the simulation software. The model is only run in this mode to conduct special studies with high value.

21.4.5.6 Use for Planners

The user of the planning system can use two strategies to create a starting point. In the first, the user starts with an online model taken from the fully operational plant, then specifying the sections that are to be turned off and the feed rates. In the second, they begin with an online model which very closely resembles the plant configuration they wish to model.

For general studies, the first method is simpler and will generate acceptable results. For very specific conditions such as modeling CO_2 constraints, the second method will generate the most

accurate results because the model tuning parameters will have been reconciled for the exact conditions of interest.

The second method is feasible because the online system archives valid models to a separate directory. In this way a library of models for all process operating modes is created automatically.

To locate the time of the desired operating mode, the user can either look at trends of the appropriate equipment flags or use the operator display to identify the time and date that the appropriate model was created. Once the date is determined, the user can then copy the model from the library and move it into the planning system for further study.

REFERENCES

Bullin, K.A., Hall, K.R., March 13−15, 2000. Optimization of Natural Gas Processing Plants Including Business Aspects. Paper presented at the 79th Annual GPA Convention, Atlanta, GA, USA.

Jumonville, J., October 4−7, 2010. Tutorial on Cryogenic Turboexpanders. Paper presented at the 39th Turbomachinery Symposium, Houston, TX, USA.

Kovach, J.W., Meyer, K., Nielson, S.-A., Pedersen, B., Thaule, S.B., March 21−24, 2010. The Role of Online Models in Planning and Optimization of Gas Processing Facilities: Challenges and Benefits. Paper presented at the 89th Annual GPA Convention, Austin, TX, USA.

Simms, J., March 23, 2009. “Fundamentals of Turboexpanders”, Simms Machinery International. Santa Maria, CA, USA.

CHAPTER

22 ENERGY AND EXERGY ANALYSES OF NATURAL GAS PROCESSING PLANTS

22.1 INTRODUCTION

With the increasing awareness of the impacts of large energy consumptions, it is crucial to understand and analyze the systems where resources and energy are consumed and depleted to plan improvements. Gas processing plants require a large amount of energy to separate impurities from raw inlet gas to produce a treated methane-rich (product) gas. Generally the performance of such plants is evaluated through energetic performance criteria based on the first law of thermodynamics. Recently, the exergetic performance based on the second law of thermodynamics has been considered as a useful method in the design, evaluation, optimization, and improvement of processing plants. By performing the energy and exergy analyses together, it is possible to determine the steps toward improvement.

This chapter deals with useful methods to carry out energy analyses and calculate performance indices of process configurations and procedures to optimize the use of energy inside a natural gas processing plant. Also, the exergy concept is introduced together with the exergy analysis, which represents a suitable method for guiding efforts to reduce the inefficiencies in existing systems and developing strategies for more effective fuel use. In the last part of this chapter, all the concepts previously discussed are illustrated by means of examples and case studies taken from the open literature.

22.2 FUNDAMENTALS OF ENERGY ANALYSES

Although everyone has a feeling of what energy is, it is difficult to give a precise definition for it (Cengel and Boles, 2006). Energy is usually defined as the capacity to do work (Perry and Green, 2008) or can be viewed as the ability to cause changes (Cengel and Boles, 2006).

All aspects of energy and energy transformations are the subject of *thermodynamics*. Although the principles of thermodynamics have always been in existence, thermodynamics was established as a science with the construction of the first successful atmospheric steam engines in England by Thomas Savery in 1697 and by Thomas Newcomen in 1712. In the 1850s, the first and second laws of

Handbook of Natural Gas Transmission and Processing. https://doi.org/10.1016/B978-0-12-815817-3.00022-8

thermodynamics emerged as a result of the works of William Rankine, Rudolph Clausius, and Lord Kelvin. Indeed, the word "thermodynamics" first appeared in 1849 in a publication by Lord Kelvin, and the first textbook on it was written 10 years later by William Rankine.

Thermodynamics is commonly encountered in many aspects of life as well as in many engineering systems. A system is a part of the universe set aside for study, which must have enclosing boundaries, outside of which are the surroundings (Ikoku, 1992).

One of the most fundamental laws of nature is the *conservation of energy principle* (an expression of the first law of thermodynamics): according to it, during an interaction, energy can change from one form to another one, but its total amount remains constant. That is, energy cannot be created nor destroyed.

Energy exists in numerous forms, such as thermal (heat), mechanical, electrical, chemical, and nuclear, and their sum constitutes the total energy, E, of a system. Thermodynamics provides no information about the absolute value of the total energy but only deals with its change: typically a system is assigned a value of zero total energy ($E = 0$) at some convenient reference point and the change is independent of it. In thermodynamic analyses, it is helpful to classify the various forms of energy that make up the total energy of a system into two groups: *macroscopic* and *microscopic*.

The macroscopic forms of energy are those that a system possesses as a whole, with respect to some outside reference frame: they include *kinetic energy* (*KE*) and *potential energy* (*PE*). Kinetic and potential energies are also the familiar forms of *mechanical energy*, which is defined as the form of energy that can be converted to mechanical work by a mechanical device (e.g., a turbine or a pump).

The microscopic forms of energy are those related to the molecular structure of a system and the degree of molecular activity, which are independent of outside reference frames. The sum of these forms was called *internal energy* by Rudolph Clausius and William Rankine, who also introduced its symbol U in the second half of the 19th century. This form of energy can be also viewed as the sum of the kinetic and potential energies of the molecules the system is composed of.

In the absence of magnetic, electric, and surface tension effects, the total energy of a system consists of the kinetic, potential, and internal energies (Eq. 22.1).

$$E = KE + PE + U = m\frac{v^2}{2} + mgz + U \tag{22.1}$$

The forms of energy already defined can be contained or stored in a system and can be, thus, seen as the static forms of energy. On the contrary, the forms of energy which are not stored in a system can be conceived as the dynamic forms of energy or as energy interactions: they represent the energy gained or lost by a system during a process through its boundary (i.e., the real or imaginary surface that separates the system from its surroundings). For a closed system (i.e., a system consisting of a fixed amount of mass with no mass that can cross its boundary), energy can be transferred to and from the system by means of *work* and *heat*. For an open system (i.e., a system for which both mass and energy can cross the boundary), often called control volume, energy can be also exchanged via mass transfer since any time mass is transferred into or out of it, the energy content of the mass is also transferred with it.

- Work: It refers to the energy transfer associated with macroscopic forces and displacements at the system boundary. This is often called "shaft work" and does not include work lost because of friction. The work done during a process between two states (1 and 2) is denoted by W_{12}, or simply W. The work done per unit time is called power and is denoted by $\dot{W}$.
- Heat: Heat is the form of energy that is transferred between two systems (or a system and its surroundings) due to a temperature difference and in the direction of decreasing temperatures. The amount of heat transferred during the process between two states (1 and 2) is denoted by Q_{12}, or just Q. Sometimes, it is desirable to know the rate of heat transfer, denoted by $\dot{Q}$.

Heat and work are directional quantities and, thus, the complete description of a heat or work interaction requires the specification of both the magnitude and direction. In this respect, a sign convention is adopted (Moran and Shapiro, 2006). It is a common practice to use the classical thermodynamics formal sign convention for heat and work interactions, according to which heat to be transferred into the system (heat input) and work to be done by the system (work output) are taken as positive quantities, whereas heat transfer from a system and work done on a system are negative. Alternatively, the subscripts "in" and "out" can be used to indicate the direction for the transfer. When the direction of a heat/work interaction is not known, it is possible to simply assume a direction for the interaction and solve for it: a positive result indicates the assumed direction is right and a negative sign indicates the opposite. Many similarities exist between heat and work: for example, both are path functions, since their magnitudes depend on the path followed during a process as well as the end states. As such, they have inexact differentials, designated by the symbol δ (δQ and δW, respectively). A distinction is typically made for heat and work because, even if they are not different from the first-law point of view, they differ from the second-law point of view (as discussed in later sections).

The different forms of energy can be related to each other during a process. The *first law of thermodynamics* provides a sound basis for studying the relationships among the various forms of energy and energy interactions. In the following, the first and second laws of thermodynamics are introduced, which are functional to later deal with the exergy analysis that takes them into use (Voldsund, 2014).

22.2.1 FIRST AND SECOND PRINCIPLES OF THERMODYNAMICS

The *first law of thermodynamics* is simply an expression of the conservation of energy principle, and it states that energy is a thermodynamic property.

Based on experimental observations, the first law of thermodynamics states that *energy can be neither created nor destroyed during a process; it can only change forms.* A typical example concerns an object that falls: in its initial state at some elevation it possesses some potential energy and part of it is converted to kinetic energy as it falls. In particular, the decrease in potential energy exactly equals the increase in kinetic energy when the air resistance is negligible.

The first law cannot be proven mathematically, but no process in nature is known to have violated it and this is taken as sufficient proof.

In mathematical terms, the first law can be written in the following form, which involves the principle of conservation of energy:

$$\Delta E = Q - W \tag{22.2}$$

The first law of thermodynamics places no restrictions on the direction of a process, but in common practice we experienced that processes proceed in a certain direction and not in the reverse direction. For example, a cup of hot coffee left in a cooler room eventually cools off, but the opposite process (consisting in the hot cup getting even hotter because of heat transfer from the room air) never takes place. Even if both processes satisfy the first law (since in the first case the amount of energy lost by the coffee is equal to the amount gained by the surrounding air, and in the opposite case the amount of energy lost by the air is equal to the amount of energy gained by the coffee), only one of them actually occurs. To overcome this inadequacy of the first law, another general principle was introduced: the *second law of thermodynamics*.

The second law of thermodynamics was first enunciated by Clausius (1864) and Kelvin and Thomson (1882), based on the work made by Carnot (1978) 25 years later. As reported by Cápek and Sheehan (2005), once it established, many formulations came out, reflecting its many facets and applications. The two most cited versions are the *Clausius statement* and the *Kelvin–Planck statement*.

The Clausius statement can be expressed as follows: it is impossible to construct a device that operates in a cycle and produces no effect other than the transfer of heat from a body at lower temperature to a body at a higher temperature. In other words, no process is possible for which the sole effect is that heat flows from a reservoir at a given temperature to a reservoir at a higher temperature (i.e., heat flows from hot to cold). This does not imply that it is not possible to construct a cyclic device that transfers heat from a cold medium to a warmer one. It simply states that such a device cannot operate unless the net effect on the surroundings involves the consumption of some energy in the form of work, in addition to the transfer of heat from a colder body to a warmer one. The Clausius statement is related to refrigerators and heat pumps.

The Kelvin–Planck statement can be expressed as follows: no device, operating in a cycle, can produce the sole effect of extraction of a quantity of heat from a heat reservoir and the performance of an equal quantity of work. This implies that such a device must exchange heat with a low-temperature sink as well as a high-temperature source to keep operating.

The two formulations are equivalent in their consequences: any device that violates the Clausius statement also violates the Kelvin–Planck statement and vice versa.

Both the Clausius statement and the Kelvin–Planck statement of the second law are negative statements and cannot be proven. Thus, the second law of thermodynamics is based on experimental observations, as any other physical law, and it has not been contradicted so far.

The second law leads to expressions that involve inequalities; one of them is the Clausius inequality, Eq. (22.3), which states that the cyclic integral of $\delta Q/T$ (denoted by the integral symbol with a circle in the middle) is always less than or equal to zero.

$$\oint \frac{\delta Q}{T} \leq 0 \tag{22.3}$$

This inequality is valid for all thermodynamic cycles, either reversible (i.e., that can be reversed without leaving any trace on the surrounding) or irreversible. In particular, the equality in the Clausius inequality holds for totally or just internally reversible cycles and the inequality for irreversible ones. In 1865, Clausius realized he had discovered a new thermodynamic property which helps to quantify

the effects of the second law. Clausius chose to name it *entropy*. It is designated by S and is defined according to:

$$dS = \left(\frac{\delta Q}{T}\right)_{\text{int rev}} \quad (kJ/K) \tag{22.4}$$

The entropy change of a system during a process can be determined by integrating the above equation between the initial and the final states:

$$\Delta S = S_2 - S_1 = \int_1^2 \left(\frac{\delta Q}{T}\right)_{\text{int rev}} \quad (kJ/K) \tag{22.5}$$

The entropy value of a substance at any state can be determined by choosing state 1 to be the reference state, to which a zero value can be assigned, and by letting state 2 be the state at which entropy is to be determined. It is important to point out that the integral of $\delta Q/T$ gives the value of entropy change only if the integration is carried out along an internally reversible path between the two states. On the contrary, the integral along an irreversible path is not a property and for irreversible processes the entropy change should be determined by carrying out the integration in Eq. (22.5) along some convenient imaginary internally reversible path between the specified states.

Consider now a cycle that is made up of two processes: an arbitrary process 1−2 (that can be either reversible or irreversible) and an internally reversible process 2−1. The Clausius inequality in Eq. (22.3) implies that:

$$\int_1^2 \left(\frac{\delta Q}{T}\right) + \int_2^1 \left(\frac{\delta Q}{T}\right)_{\text{int rev}} \leq 0 \tag{22.6}$$

$$\int_1^2 \left(\frac{\delta Q}{T}\right) + S_1 - S_2 \leq 0 \tag{22.7}$$

$$S_2 - S_1 \geq \int_1^2 \left(\frac{\delta Q}{T}\right) \tag{22.8}$$

Eq. (22.10) can be also written in the differential form:

$$dS \geq \frac{\delta Q}{T} \tag{22.9}$$

The inequality sign in Eq. (22.8) reminds that the entropy change of a closed system during an irreversible process is always greater than the entropy transfer with heat, given by $\int_1^2 \delta Q/T$. That is, some entropy is generated during an irreversible process due to the presence of irreversibilities. The entropy generated during a process, S_{gen}, is called *entropy generation* and is the difference between the entropy change of a closed system and the entropy transfer. Thus, Eq. (22.8) can be rewritten as an equality as:

$$\Delta S_{\text{system}} = S_2 - S_1 = \int_1^2 \left(\frac{\delta Q}{T}\right) + S_{\text{gen}} \tag{22.10}$$

Eq. (22.10) has important implications in thermodynamics. For an isolated system or an adiabatic closed system the heat transfer is zero and Eq. (22.10) reduces to:

$$\Delta S_{\text{isolated}} \geq 0 \tag{22.11}$$

This is known as the *increase of entropy principle*, according to which the entropy of an isolated system during a process always increases or, in the limiting case of a reversible process, remains constant (isentropic process). According to Eq. (22.11), in the absence of any heat transfer, entropy change is due to irreversibilities only and their effect is always to increase entropy.

It is, thus, possible to conclude that:

- a process must proceed in the direction that complies with the increase of entropy principle;
- entropy is a nonconserved property since it is conserved in idealized reversible processes and increases during all actual processes;
- the performance of engineering systems is affected by the presence of irreversibilities and entropy generation is a measure of the magnitudes of the irreversibilities present during that process.

22.2.2 ENERGY BALANCE

The energy balance is an important consideration in making engineering calculations (Ikoku, 1992).

The first law of thermodynamics accounts for the net change in the total energy that a system experiences during a process (ΔE), which is equal to the difference between the total energy entering the system (E_{in}) and the total energy leaving it (E_{out}) during that process. This can be expressed by means of an equation, Eq. (22.12), that is often referred to as the *general energy balance*.

$$E_{\text{in}} - E_{\text{out}} = \Delta E \quad (J) \tag{22.12}$$

Eq. (22.12) is applicable to any kind of system undergoing any kind of process and can be used to solve engineering problems, provided that the various forms of energy are understood and the forms of energy transfer are recognized.

The energy balance can be also written in the rate form, Eq. (22.13), or on a per unit mass basis, Eq. (22.14), which is obtained by dividing all the quantities in Eq. (22.12) by the mass m of the system.

$$\frac{dE}{dt} = \dot{E}_{\text{in}} - \dot{E}_{\text{out}} \quad (W) \tag{22.13}$$

$$e_{in} - e_{out} = \Delta e \tag{22.14}$$

The energy-balance analysis can be performed for closed systems (control-mass analysis) or for control volumes (control-volume analysis) (Ikoku, 1992).

22.2.3 CLOSED SYSTEMS

The general energy balance, or the first law of thermodynamics, for closed systems can be expressed in accordance to Eq. (22.2) or in differential form as:

$$dE = \delta Q - \delta W \tag{22.15}$$

For a closed system undergoing a cycle, the initial and final states are identical and, thus, the net energy change is zero, Eq. (22.16).

$$\Delta E = E_2 - E_1 = 0 \text{ or } E_{\text{in}} = E_{\text{out}} \tag{22.16}$$

22.2.4 OPEN SYSTEMS

Unlike closed systems, control volumes involve mass flow across their boundaries, and some work is required to push the mass into or out of the control volume (CV). This work is known as *flow work or flow energy*, and it is necessary for maintaining a continuous flow through a control volume. A relation can be obtained for it, considering a fluid element of volume V (Fig. 22.1).

The fluid immediately upstream forces this fluid element to enter the control volume and can be regarded as an imaginary piston. The fluid element can be chosen to be sufficiently small so that it has uniform properties throughout. If the fluid pressure is P and the cross-sectional area of the fluid element is A (Fig. 22.1), the force applied on the fluid element by the imaginary piston is:

$$F = P \cdot A \tag{22.17}$$

To push the entire fluid element into the control volume, this force must act through a distance L. Thus, the work done in pushing the fluid element across the boundary (i.e., the flow work) is:

$$W_{\text{flow}} = F \cdot L = P \cdot A \cdot L = P \cdot V \quad [J] \tag{22.18}$$

Eq. (22.18), which is the same whether the fluid is pushed into or out of the control volume, can be also written per unit mass by dividing both sides of this equation by the mass of the fluid element:

$$w_{\text{flow}} = P \cdot v \quad [J/kg] \tag{22.19}$$

The work flow must be taken into account when considering the total energy of a flowing fluid, which consists of kinetic, potential, internal, and flow energies, Eq. (22.20).

$$e = ke + pe + u + P \cdot v \quad [J/kg] \tag{22.20}$$

The combination of the last two terms in Eq. (22.20) is defined as the *enthalpy*, Eq. (22.21); by using it, the energy associated with pushing the fluid into or out of the control volume is automatically taken into account and there is no need to be concerned about the flow work.

$$h = u + P \cdot v \quad [J/kg] \tag{22.21}$$

Thus, the total energy of a flowing fluid of mass m is simply:

$$E = m\left(h + \frac{v^2}{2} + gz\right) \quad [J] \tag{22.22}$$

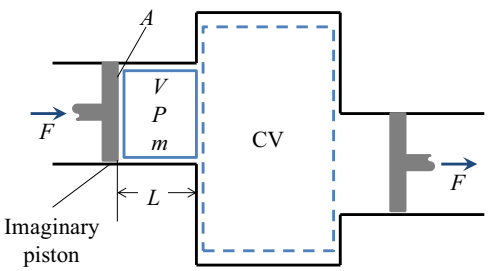

FIGURE 22.1

Schematic for flow work. *CV*, control volume.

Similarly, when a fluid stream with uniform properties is flowing at a mass flow rate of $\dot{m}$, the rate of energy flowing with that stream is:

$$\dot{E} = \dot{m}\left(h + \frac{v^2}{2} + gz\right) \quad [W] \tag{22.23}$$

When the kinetic and potential energies of a fluid stream are negligible, Eqs. (22.22) and (22.23) simplify.

Under steady-state conditions, the total energy content of a control volume remains constant and, thus, the change in the total energy of the control volume is zero. Therefore, the amount of energy entering a control volume in all forms (by heat, work, and mass) must be equal to the amount of energy leaving it. As a result, the rate form of the general energy balance reduces to:

$$\dot{E}_{\text{in}} - \dot{E}_{\text{out}} = \frac{dE_{\text{system}}}{dt} = 0 \quad (W) \tag{22.24}$$

Since the energy can be transferred by heat, work, and mass only, the energy balance in Eq. (22.24) can also be written in a more explicit form as:

$$\dot{Q}_{\text{in}} + \dot{W}_{\text{in}} + \sum_{\text{in}} \underbrace{\dot{m}\left(h + \frac{v^2}{2} + gz\right)}_{\text{for each inlet stream}} = \dot{Q}_{\text{out}} + \dot{W}_{\text{out}} + \sum_{\text{out}} \underbrace{\dot{m}\left(h + \frac{v^2}{2} + gz\right)}_{\text{for each outlet stream}} \tag{22.25}$$

As previously stated, when solving a problem that involves an unknown heat or work interaction, it is a common practice to assume a direction for them. In such cases, it is a common practice to assume heat to be transferred into the system at a rate of $\dot{Q}$, and work produced by the system at a rate of $\dot{W}$, and to write the energy balance relation as:

$$\dot{Q} - \dot{W} = \sum_{\text{out}} \underbrace{\dot{m}\left(h + \frac{v^2}{2} + gz\right)}_{\text{for each outlet stream}} - \sum_{\text{in}} \underbrace{\dot{m}\left(h + \frac{v^2}{2} + gz\right)}_{\text{for each inlet stream}} \tag{22.26}$$

If a negative quantity results from calculations for $\dot{Q}$ or $\dot{W}$, this would suggest that the assumed direction is wrong and it should be reversed.

22.3 THE DIFFERENT ENERGY CONTRIBUTIONS

Several energy contributions are involved in gas processing.

Thermal energy is used to provide heat and cold duties to different process units. This can be accomplished via several utility levels (e.g., steam levels, refrigeration levels, hot oil circuit, furnace flue gas, *etc.*), while always trying to save energy and operating costs. A way to optimize the use of thermal energy is *pinch technology*. This is used, for example, to determine appropriate modifications (e.g., reflux improvement, feed preheating or cooling, side condensing, and reboiling) of stand-alone distillation columns (widely used in the gas processing industry, although they are energy expensive) and their integration with the remaining process.

Another kind of energy consumed in natural gas processing plants is the *mechanical energy* required for fluid transport, which is consumed mainly by compressors and pumps.

A third kind of energy is the *electric energy* that is required for instrumentation and control as well as to drive motors related to pumps and compressors.

In the following, pinch technology will be outlined with reference to a simple case, and the requirement of mechanical and electric energy in natural gas processing plants will be discussed.

22.3.1 PINCH TECHNOLOGY

Pinch technology provides a systematic methodology based on thermodynamic principles for energy saving in processes (Linnhoff, 1998). Once the heat and material balances are available, as well as thermal data, all streams are divided into "hot streams" and "cold streams": the former ones need cooling (i.e., they represent heat sources), whereas the latter ones need heating (i.e., they represent heat sinks). Also the supply temperature (T_s) and the target temperature (T_t) must be known, together with the heat capacity flow rate ($\dot{m} \cdot c_P$). Starting from these data, the energy targets are obtained using a tool called the *composite curve*. Composite curves consist of temperature−enthalpy ($T-H$) profiles which show the heat availability in the process (the "hot composite curve") and the heat demands in the process (the "cold composite curve"). To better explain how their construction is carried out, a simple case is taken as reference in the following. Table 22.1 shows the thermal data needed for pinch analysis. A *minimum temperature difference* must be assumed during the analysis: it is considered to be 20°C in the following example.

Fig. 22.2 illustrates the construction of the "hot composite curve" for the example process, which has two hot streams (stream number 1 and 2, see Table 22.1). Their $T-H$ representation is shown in Fig. 22.2A and their composite representation is shown in Fig. 22.2B. Stream 1 has a heat capacity flow rate of 40 kW/°C and is cooled from 180 to 40°C, releasing 5600 kW of heat. Stream 2 is cooled from 150 to 60°C with a heat capacity flow rate of 30 kW/°C and loses 2700 kW.

The construction of the hot composite curve (as shown in Fig. 22.2B) simply involves the addition of the enthalpy changes of the streams in the respective temperature intervals. In the temperature interval 180 to 150°C, only stream 1 is present. Therefore the heat capacity flow rate of the composite curve equals that of stream 1 (i.e., 40 kW/°C). In the temperature interval 150 to 60°C, both streams 1 and 2 are present, therefore the heat capacity flow rate of the hot composite equals the sum of those of the two streams (i.e., 40 + 30 = 70 kW/°C). In the temperature interval 60 to 40°C only stream 1 is present, thus the heat capacity flow rate of the composite curve is 40 kW/°C. The construction of the

Table 22.1 Thermal Data Required for Pinch Analysis

Stream No.	Stream Type	T_s [°C]	T_t [°C]	Heat Capacity Flow Rate [kW/°C]
1	Hot	180	40	40
2	Hot	150	60	30
3	Cold	30	180	60
4	Cold	80	160	20

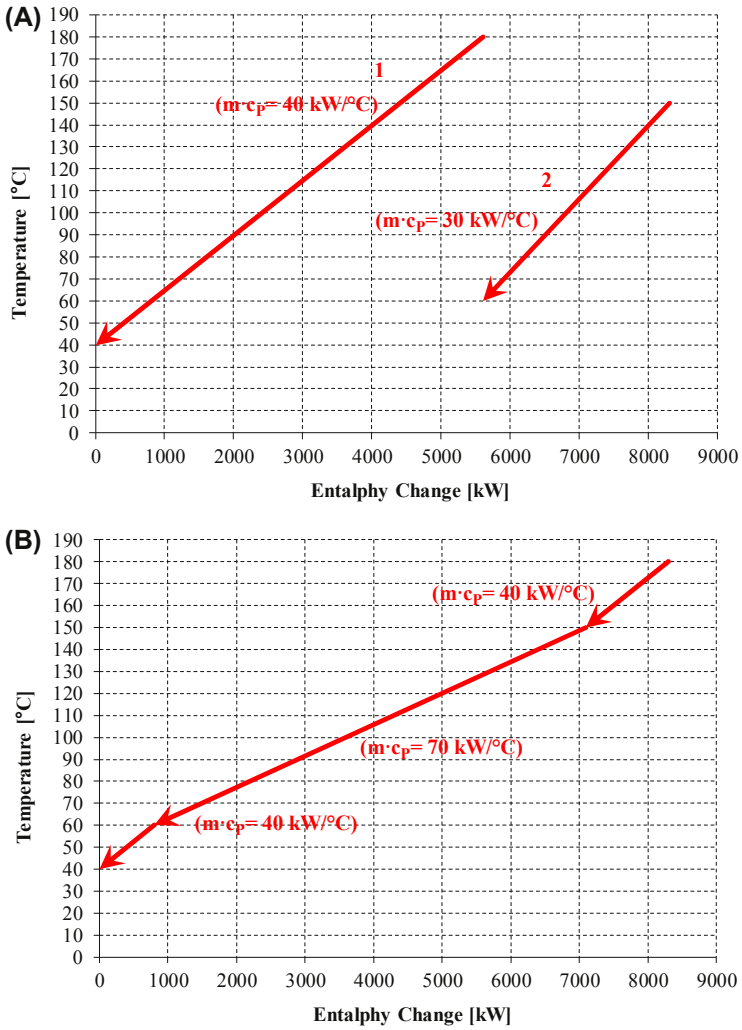

FIGURE 22.2

Construction of the hot composite curve (B) from combination of hot stream curves (A).

cold composite curve (Fig. 22.3) is similar to that of the hot composite curve involving the combination of the cold stream $T-H$ curves for the process.

The composite curves provide a countercurrent picture of heat transfer and can be used to indicate the minimum energy target for the process. This is achieved by overlapping the hot and cold composite curves, as shown in Fig. 22.4, separating them by the minimum temperature difference $\Delta T_{\min}$ (20°C for this example). This overlap shows the maximum process heat recovery possible, indicating that the remaining heating and cooling needs are the minimum hot utility requirement ($Q_{H\min}$) and the

minimum cold utility requirement ($Q_{C\min}$) of the process for the chosen $\Delta T_{\min}$ (2900 and 600 kW, respectively).

The point where $\Delta T_{\min}$ is observed is known as the "pinch": once it has been identified, it is possible to consider the process as two separate systems, one above and one below the pinch, as shown in Fig. 22.5. The system above the pinch requires a heat input and is, therefore, a net heat sink. Below the pinch, the system rejects heat and so is a net heat source.

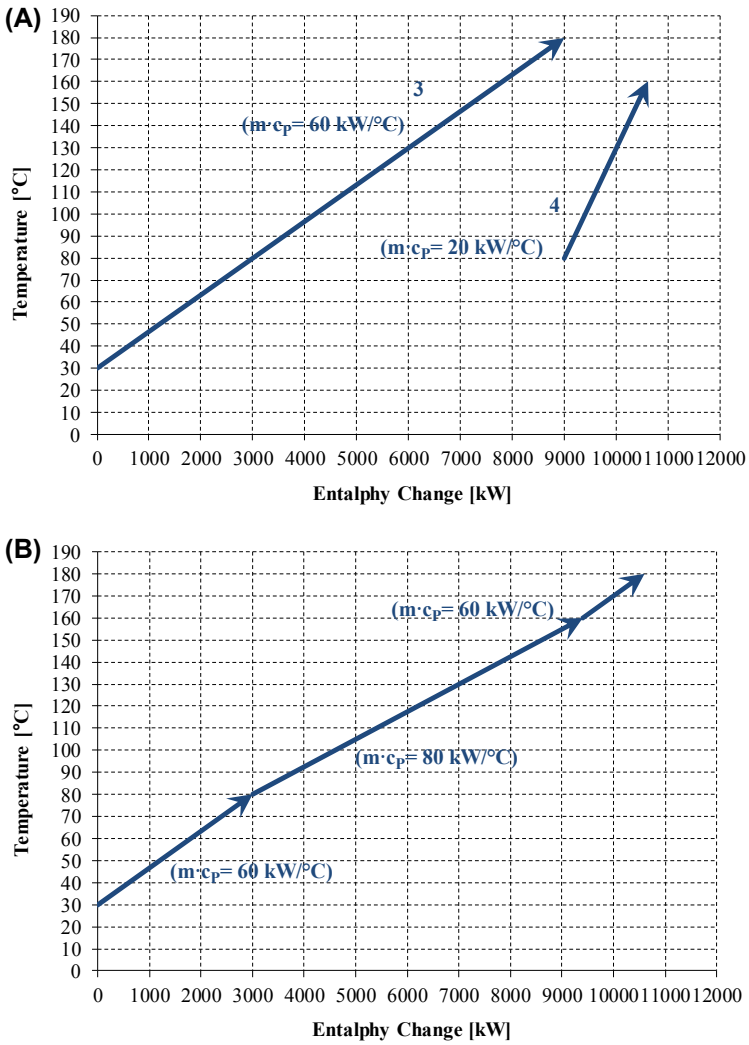

FIGURE 22.3

Construction of the cold composite curve (B) from combination of cold stream curves (A).

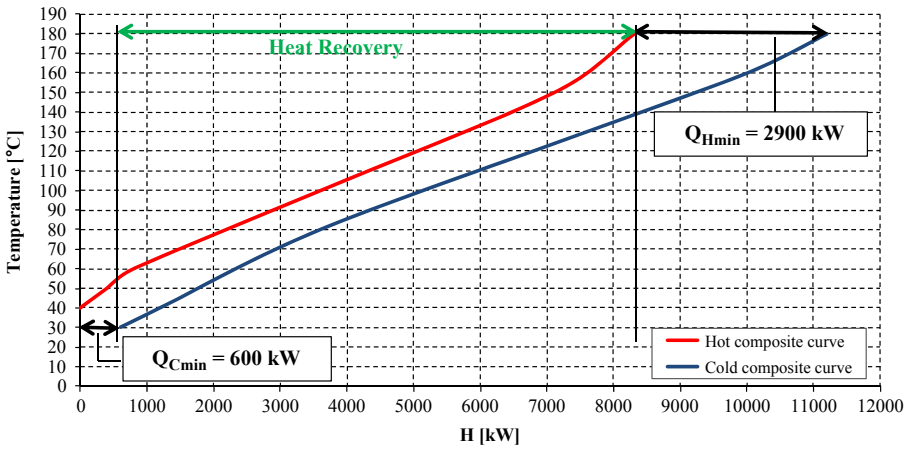

FIGURE 22.4

Use of the hot and cold composite curves to determine the energy targets.

The understanding of the pinch gives three rules that must be obeyed to achieve the minimum energy targets for a process:

- heat must not be transferred across the pinch;
- there must be no external cooling above the pinch;
- there must be no external heating below the pinch.

Violating any of these rules will lead to *cross-pinch heat transfer* resulting in an increase in the energy requirement beyond the target. The abovementioned rules form the basis for the heat exchanger network (HEN) design procedure, which ensures that there is no cross-pinch heat transfer.

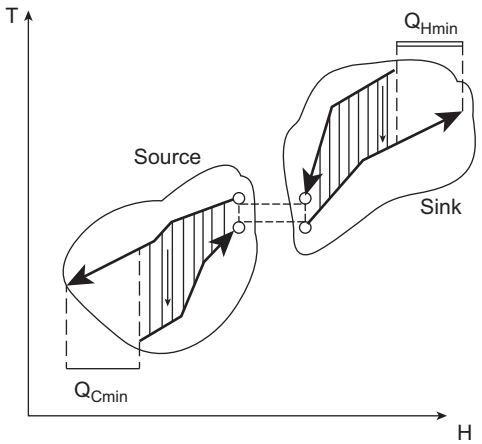

FIGURE 22.5

The *Pinch Principle*: the pinch point divides the problem into a hit source and a heat sink (Linnhoff, 1998).

The composite curves provide overall energy targets but do not clearly indicate how much energy needs to be supplied by different utility levels. For this purpose, the *Grand Composite Curve* is used. Its construction starts with the composite curves, making adjustments in their temperatures. This involves increasing the cold composite temperature by ½ ΔT_{min} and decreasing the hot composite temperature by ½ ΔT_{min}. As a result of this temperature shift, the composite curves (now called "shifted composite curves") touch each other at the pinch (Fig. 22.6).

The Grand Composite Curve is then constructed from the enthalpy (horizontal) differences between the shifted composite curves at different temperatures (Fig. 22.7).

The Grand Composite Curve provides a convenient tool for selection of appropriate utility levels and for setting the targets for the multiple utility levels. Of course, the best design for an energy-efficient heat exchange network will often result in a trade-off between the equipment and operating costs. This is dependent on the choice of the ΔT_{min} for the process, since the lower the ΔT_{min}, the lower the energy costs, but conversely the higher the heat exchanger capital costs (lower temperature driving forces in the network will result in the need for a greater surface). On the other hand, a large ΔT_{min} will mean increased energy costs as there will be less overall heat recovery, but the required capital costs will be less. The trade-off is further complicated in a retrofit situation, where a capital investment has already been made.

The next step in the pinch analysis is to explore various options for process improvement, such as energy recovery, process modifications, and utility system integration. Then, the key improvement options need to be implemented in design. In doing that, the designer should keep in mind the rule according to which, for the temperature feasibility of the stream matches close to the pinch:

- above the pinch the $(\dot{m} \cdot c_P)$ of the stream going *out* of the pinch needs to be *greater* than the $(\dot{m} \cdot c_P)$ of the stream coming *into* the pinch
- below the pinch the $(\dot{m} \cdot c_P)$ of the stream going *out* of the pinch needs to be *greater* than the $(\dot{m} \cdot c_P)$ of the stream going *into* the pinch.

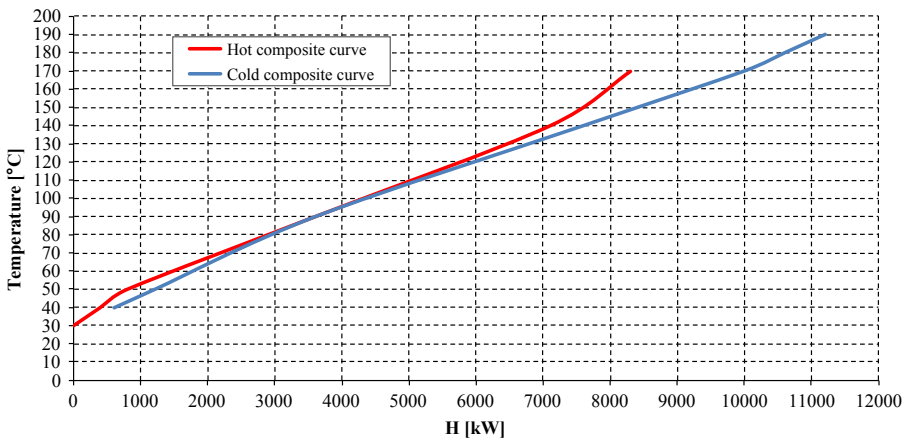

FIGURE 22.6

The shifted composite curves.

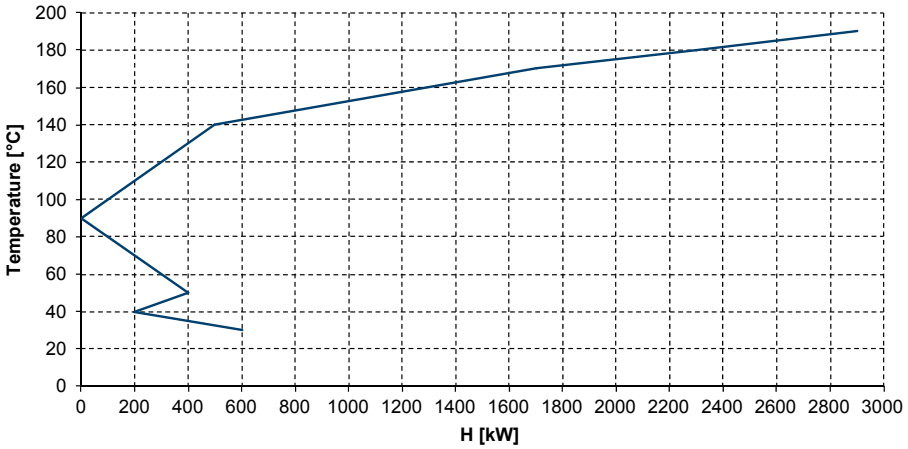

FIGURE 22.7

The Grand Composite Curve.

22.3.2 MECHANICAL ENERGY

In addition to thermal energy, also mechanical energy is required in natural gas processing plants for fluid transport, which is consumed mainly by compressors and pumps.

22.3.2.1 Compressors

Compression is used in all aspects of the natural gas industry. A brief overview of the major types of compressors in the natural gas processing and transmission industry as well as a procedure for calculation of the required compression power has already been presented in Chapter 14.

22.3.2.2 Pumps

The energy conservation equation for pump or hydraulic turbine systems comes from Bernoulli's theorem. This is a special form of the mechanical energy balance, which applies to a particular set of assumptions: a control volume with fixed solid boundaries, except for those producing a shaft work $(\dot{W}_s)$, steady-state conditions, and mass flow rate at a rate $\dot{m}$ through a single planar entrance and a single planar exit to which the velocity vectors are perpendicular (Perry and Green, 2008). Under these assumptions the mechanical energy equation is reduced to:

$$\frac{v_1^2}{2g} + z_1 + \frac{\dot{W}_s}{\dot{m}} = \frac{v_2^2}{2g} + z_2 + \int_{P_1}^{P_2} \frac{dP}{\gamma} + \frac{\dot{E}_v}{\dot{m}} \tag{22.27}$$

In Eq. (22.27), γ denotes the specific gravity and $\dot{E}_v$ the energy dissipation due to frictional losses. For an incompressible flow, Eq. (22.27) becomes:

$$\frac{P_1}{\gamma} + \frac{v_1^2}{2g} + z_1 + \frac{\dot{W}_s}{\dot{m}} = \frac{P_2}{\gamma} + \frac{v_2^2}{2g} + z_2 + \frac{\dot{E}_v}{\dot{m}} \tag{22.28}$$

The above equation can be used to relate the total head in two points of any suction-and-discharge-system, the friction losses between these points and the equipment total head. Elevations are measured from the equipment datum.

The equipment total head, H, is the outlet nozzle total head (h_{out}) minus the inlet nozzle total head (h_{in}):

$$H = h_{out} - h_{in} = z_{out} - z_{in} + \frac{(P_{out} - P_{in})}{\gamma} + \frac{\left(v_{out}^2 - v_{in}^2\right)}{2g} + h_{fout} + h_{fin} \tag{22.29}$$

In Eq. (22.29), subscripts "in" and "out" are used for variables at pumps inlet and outlet nozzles, respectively. Moreover, h_{fin} and h_{fout} are the inlet system friction head and the outlet system friction head, respectively.

When the elevation and size of inlet and outlet nozzles are the same, from Eq. (22.29), it follows that the equipment total head equals the difference of pressure heads plus the system friction head. The equipment total head is positive for pumps and negative for hydraulic power recovery turbines.

22.3.3 ELECTRIC ENERGY

A third kind of energy involved in natural gas processing plants is the electric energy that is required for power distribution, illumination, space heating, heat tracing of water and product lines, communication, automation, signal transmission for process control, data logging, cathodic protection, grounding, and others (GPSA, 2004).

Most gas plants purchase electrical power, but some generate at least part of their power on site (Kidnay and Parrish, 2006). Cogeneration plants are becoming more attractive options for reduction of operating costs, especially when gas turbines are used for driving compressors.

In gas plants where the usage of each motor is generally known, making a load list is the best way to determine the system requirements in terms of the operating load (GPSA, 2004). The load list should list the horsepower rating of each motor as well as its operating horsepower (brake hp), and whether the motor will run continuously, intermittently, or is a standby for other motors. When the above list is completed, the kilowatts of each motor should be calculated. This total load is the *minimum* value to use in sizing the supply capacity (GPSA, 2004). This does not leave any spare capacity for future additions. Other issues should also be considered. If one motor is large in relationship to the total load, or if two or more motors must be started at the same time, it will generally be necessary to increase the supply capacity to provide the starting current which is approximately 5.5 times normal running current.

22.4 THE NET EQUIVALENT METHANE APPROACH: THE ACTUAL ENERGY PERFORMANCES IN NATURAL GAS PROCESSING PLANTS

As discussed in the previous sections of this chapter, natural gas processing plants require different kinds of energy for different operations performed inside process units to process feed gas to meet commercial specifications as pipeline-grade or liquefied natural gas (LNG)-grade natural gas. A question that can arise when evaluating the best process solution, among different ones, to perform a precise task inside a process unit is how much is the effective energy efficiency of the considered

process? To answer this question a method to compare energy streams having different qualities is needed to make comparisons on a common basis. Basically, the natural gas processing plant takes a raw natural gas stream containing several impurities as feed and processes it to produce a final product with a higher energetic value (a higher heating value). The different types of energy used to perform this task impact on the effective energy output of the plant, since each kind of energy has its own "cost" that can be different depending on its nature. To perform an energy analysis focused on estimating the impact of the energy input (utilities) on the effective energy output (produced methane) of the plant, a simple method to harmonize the different qualities of the consumed energy is the estimation of the amount of methane (product) that is needed to produce each energy stream assuming to use certain technologies for energy conversion: methane-fired steam boilers, combined cycles, refrigeration cycles, *etc*. In practice, it is possible to consider methane as fuel for energy production plants and estimate the amount of produced methane that has to be burned to supply energy, in its different forms, to the natural gas processing plant in order to meet its requirements. In this way, it is possible to estimate the effective net methane output of a natural gas production process comparing all the different kinds of energy involved on a common basis.

Moreover, this parameter can be used to compare different process technologies that can be potential candidates to perform specific tasks and, thus, to choose the best one that allows to reduce the methane consumptions to support the production.

In this section, the method of the *net equivalent methane* to account for the actual energy performance of a natural gas processing plant is described together with a critical discussion of its advantages and its limitations.

The method has been developed and used in the work by Pellegrini and coworkers for the comparison between low-temperature and classical amine scrubbing natural gas treating technologies (Pellegrini et al., 2015; Baccanelli et al., 2016; Pellegrini et al., 2017 and 2018) and for the selection of the proper complete natural gas processing sequence considering classical technologies (amine scrubbing for acid gas removal, glycol dehydration, and demethanizer unit for NGL recovery), low-temperature processes (dual pressure low-temperature distillation and extractive distillation for the separation of the ethane−carbon dioxide azeotrope), carbon dioxide compression, and dehydration for the purpose of carbon capture and storage (CCS) or enhanced oil recovery (EOR) and combinations of these process units for the definition of the natural gas processing plant layout (Langé and Pellegrini, 2016). Moreover, it has been proven that the results obtained with this method are in good agreement with the ones obtained by means of a more detailed exergy analysis (Baccanelli et al., 2016), thus showing the benefit of disposing of a simple performance index easy to be used to compare process technologies on a common basis.

22.4.1 BASIC ASSUMPTIONS

To harmonize all the different energy consumptions on a common basis, some assumptions are made on the technology used to produce the energy stream:

- *Heat duties* provided to the process units are accounted for in terms of steam produced by means of a methane-fired boiler;

- *Cooling duties* for refrigeration are produced considering a vapor-compression refrigeration cycle, where compressors are driven by means of electric engines;
- *Mechanical power* for rotating equipment is provided by means of electric engines;
- The *electric energy* supplied to engines to drive rotating equipment (including compressors of refrigeration cycles) is produced by means of a methane-fired combined cycle power plant.

In the analysis, the energy terms that can be considered recoverable inside the process (e.g., power produced by means of turboexpanders, waste heat at high temperatures, and cold at low temperatures) can be accounted as "methane production," decreasing the effective amount of methane needed to supply energy to the process. While for mechanical power the recovery can be considered, in general, without problems; in the case of thermal energy, caution should be taken to account for the thermal power recovery as methane savings because they may be overestimated if no pinch analysis is carried out. A good practice is to perform the analysis before the energy integration has been optimized or, in order to be conservative, to exclude from the analysis all the terms of energy savings or just the ones associated to thermal energy recovery.

The net equivalent methane can be estimated, considering the general case, as:

$$CH_4^{\mathrm{NET}} = \sum_{i=1}^{NC} CH_{4,i}^{\mathrm{eq}} - \sum_{j=1}^{NS} CH_{4,j}^{\mathrm{eq}} \tag{22.30}$$

where CH_4^{NET} is the net equivalent methane, $CH_{4,\,i}^{\mathrm{eq}}$ is the methane equivalent to the *ith* energy consumption of the *NC* ones of the process, and $CH_{4,\,j}^{\mathrm{eq}}$ is the methane equivalent to the *jth* energy saving of the *NS* ones of the process. The amount of methane that has to be burned to provide energy to the plant is then given by Eq. (22.31), or, equivalently, the effective methane output (or efficiency) of the natural gas processing plant can be defined according to Eq. (22.32):

$$CH_4^{\mathrm{Burned}}\% = \frac{CH_4^{\mathrm{NET}}}{CH_4^{\mathrm{Prod}}} \cdot 100 \tag{22.31}$$

$$\eta_{CH_4} = \frac{CH_4^{\mathrm{Prod}} - CH_4^{\mathrm{NET}}}{CH_4^{\mathrm{Prod}}} = 1 - CH_4^{\mathrm{Burned}} \tag{22.32}$$

In the following, the methods used to calculate the equivalent methane associated with the production of each energy stream are outlined together with the definition of the parameters used for calculations.

22.4.1.1 Thermal Energy Estimation

Thermal energy at temperatures above the ambient one (298.15 K) is supplied in terms of steam produced by means of a methane-fired boiler. Knowing the thermal power that has to be converted in terms of net equivalent methane, it is possible to apply the following equation:

$$\dot{m}_{CH_4} = \frac{\dot{Q}}{\eta_B LHV_{CH_4}} \tag{22.33}$$

where $\dot{m}_{CH_4}$ is the amount of methane that has to be burned in the boiler to produce the thermal power $\dot{Q}$, η_B is the boiler thermal efficiency, and LHV_{CH_4} is the lower heating value of methane. Eq. (22.33)

derives from the definition of the energy efficiency of a steam boiler, as the ratio between the required thermal energy and the available energy produced during the combustion of methane. Typically, the boiler thermal efficiency (fuel-to-steam) varies between 0.7 and 0.9 (CleaverBrooks, 2011). For the net equivalent methane analysis, the average value of 0.8 can be considered. The lower heating value of methane is about 50 MJ/kg (Demirel, 2012).

22.4.1.2 Cooling Duty Estimation

Cooling duties useful to cool down a process stream below the ambient temperature are produced by means of vapor-compression refrigeration cycles. The mechanical energy needed to drive compressors for the refrigeration cycle is produced by means of a methane-fired natural gas combined cycle. To derive the expression useful to estimate the equivalent methane for cooling duties, it is necessary to introduce the definition of the coefficient of performance for a refrigeration cycle (COP_R) in both ideal and real terms. The real coefficient of performance expresses the ratio between the cooling power produced by the cycle ($\dot{Q}$) and the mechanical work used by compressors to drive the cycle ($\dot{W}_C$):

$$COP_R = \frac{\dot{Q}}{\dot{W}_c} \tag{22.34}$$

The direct use of a real value for the COP_R requires the definition of a precise technology for refrigeration. If this value is known a priori the related COP_R can be used directly for calculations. On the contrary, if no specific information about the refrigeration technology is known, the real COP_R can be calculated starting from the ideal one $COP_{R,id}$, corrected considering a second law efficiency (η_{II}) equal to 0.6 (Baccanelli et al., 2016):

$$COP_R = \eta_{II} \cdot COP_{R,id} \tag{22.35}$$

The ideal value of the COP can be calculated knowing the temperature of both the hot and the cold sinks, according to Eq. (22.36), where T_0 is the hot sink temperature (considered equal to the ambient temperature) and T is the temperature of the working fluid in the evaporator of the refrigeration cycle, that can be set equal to the outlet temperature of the process stream to be cooled down (as obtained from simulations/calculations).

$$COP_{R,id} = \frac{1}{\frac{T_0}{T} - 1} \tag{22.36}$$

The compression work is the term that is effectively converted into the amount of methane that has to be burned inside the combined cycle to produce mechanical power:

$$\dot{m}_{CH_4} = \frac{\dot{W}_c}{\eta_{CC} \cdot LHV_{CH_4}} \tag{22.37}$$

The efficiency of the combined cycle (η_{CC}) is considered equal to 0.55 (Kehlhofer et al., 2009).

By substituting Eq. (22.34) into Eq. (22.37), it is then possible to derive the expression for the equivalent methane related to the production of cooling duties:

$$\dot{m}_{CH_4} = \frac{\dot{Q}}{COP_R \cdot \eta_{CC} \cdot LHV_{CH_4}} \tag{22.38}$$

22.4.1.3 Mechanical Work Estimation

Mechanical work, as mentioned before, is converted into the net equivalent methane through Eq. (22.37), considering burning methane to produce mechanical energy by means of a combined cycle.

22.4.2 PROS AND CONS OF THE METHOD

The proposed method is simple, and once the energy consumptions are known from process calculations/simulations, their conversion in terms of equivalent methane is straightforward. This method is defined to perform energy analysis that impacts mostly on the operating costs related to the natural gas processing plant. However, despite its simplicity, the method is based on several assumptions, particularly concerning the type of energy production technologies and their efficiency. Moreover, it is suggested to apply this methodology once the plant layout, including the details of process sequences, has been defined considering also its energy integration. In fact, the net equivalent methane method does not take into account pinch limitations, hence attention should be paid in considering energy savings associated to the recovery of thermal power from process streams at any temperature level. Without pinch analysis, the assumption that there exists a proper way to entirely reuse the recovered thermal energy (cold or heat from stream temperature to the ambient one) inside the process may lead to a severe overestimation of the energy performances.

22.5 EXERGY ANALYSIS: THE QUALITY OF ENERGY IN NATURAL GAS PROCESSING PLANTS

The energy conservation idea alone is inadequate for depicting some important aspects of resource utilization. This led to introduce the concept of exergy.

Exergy has become a quantity extensively used nowadays for the analysis of process systems, particularly, attention has been devoted to the use of exergy for the optimization of processes to improve the proper use of energy, reducing not only the operating costs associated to energy but also the impact of energy on the surrounding environment. Moreover, the concept of exergy to analyze a process can show where the inefficiencies are located, thus defining the direction and the efforts that should be taken to optimize the process to improve the energy management.

In this section, the application of exergy analysis to natural gas processing plants is discussed, introducing the definition of exergy balance and describing the terms that compose this balance equation. The definition of the properties of the environment useful to calculate exergy terms will be provided prior to define the different exergy contributions.

22.5.1 EXERGY CONCEPT AND EXERGY BALANCES

The concept of exergy dates back to the 19th century: Important milestones were Carnot's work published in 1824 (Carnot et al., 1897) on heat engines, as well as Gibb's work in 1873, where an equation for available work was given that is in correspondence with the present definition of exergy.

According to Szargut (1980), "Exergy is the amount of work obtainable when some matter is brought to a state of thermodynamic equilibrium with the common components of the natural surroundings by means of reversible processes, involving interaction only with the abovementioned components of nature." From this, it follows that high-temperature thermal energy is rated higher than low-temperature energy because it provides a higher potential to perform work. In addition to this, internal losses due to irreversibilities are accounted for, and the locations of these process inefficiencies can be found.

Since there are many forms in which energy flow presents itself in nature, there are several corresponding forms of exergy. The most commonly used are summarized by Sciubba and Wall (2007) and are reported in Table 22.2.

According to the "equivalence table" (Table 22.2), the specific exergy is the same as the specific energy for kinetic, potential, mechanical, and electrical energy forms because in all these cases the energy can be entirely converted into other forms. However, this is not the case for chemical energy since the maximum work that we can extract from a system composed of a single pure substance depends not only on the chemical enthalpy of formation of that substance but also on the difference between its concentration in the system and in the reference environment. As for heat, it is the "least available" form of energy flow: the portion that can be converted into work depends on both the system (T) and the reference (T_0) temperatures.

Before evaluating exergy, it is important to introduce the concepts of the *reference environment* and of the *dead state*.

Table 22.2 Specific Exergy Contents of Different Energy Flows (Sciubba and Wall, 2007)

Type of Energy Flow	Specific Energy	Specific Exergy	Source	Notes
Kinetic	$v^2/2$	$v^2/2$	/	J/kg; follows from definition
Potential	$g\Delta z$	$g\Delta z$	/	J/kg; follows from definition
Heat	q	$q\left(1-\frac{T_0}{T}\right)$	/	J/kg; follows from definition
Mechanical	w	w	/	J/kg; follows from definition
Electrical[a]	$\mathrm{It}\Delta\mathrm{V}$	$\mathrm{It}\Delta\mathrm{V}$	/	J; follows from definition
Chemical, pure substance	Δg_G	$\mu-\mu_0+RT_0\ln\left(\frac{c}{c_0}\right)$	(Wall, 1977)	$\mu-\mu_o=\Delta g_G=g_G-g_{G,o}$
Radiation[b]	IR	$\sigma\left(T^4-\frac{4T^3T_0}{3}+\frac{T_0^4}{3}\right)$	(Petela, 1964)	W/m^2; from black body radiation

[a] I *denotes the electric current,* t *the time, and* ΔV *the electric potential.*
[b] IR *denotes the radiative energy flux,* σ *the Stephan–Boltzmann constant.*

The *reference environment* is typically considered as the portion of the system's surroundings at a distance where intensive properties are not affected by any process involving the systems and its immediate surroundings. Thus, the reference environment is regarded to be large in extent, free of irreversibilities and uniform in temperature, T_0, and pressure, P_0, which are normally taken as typical environmental conditions: the ambient temperature and pressure are, respectively, 298.15 K and 1 atm, while the environment composition is defined in terms of molar fractions. The environment is made mostly by nitrogen (75.67%), oxygen (20.35%), water (3.12%), carbon dioxide (0.03%), and "other species" (0.83%). This last term is used to lump all the other possible chemical species that are typically present in traces in the air and do not impact significantly on mixture properties.

The *dead state* can be defined considering a system that is in a state different from that of the environment, which offers an opportunity for developing work. Such an opportunity diminishes as the system changes state toward that of the environment and ceases to exist when the two are in equilibrium. This state of the system is called "dead state": at it, both the system and the environment possess energy, but the value of exergy is zero because there is no possibility of a spontaneous change within the system or the environment, nor can there be an interaction between them (Moran and Shapiro, 2006). Thus, as shown in the following, exergy is a measure of the departure of the state of a system from that of the environment, and can be viewed as an attribute of the combined system consisting of the system and the environment together. However, once the environment is specified, a value can be assigned to exergy in terms of property values for the system only. Therefore, exergy can be regarded as a property of the system.

Neglecting the electrical energy, for an open system identified by the thermodynamic parameters T_1, P_1, μ_1, V_1, z_1 that can interact only with a reference environment at T_0, P_0, μ_0, V_0, z_0, and in which the concentration of substance 1 is c_0, the specific exergy content, in J/kg, is a state function given by:

$$e_1 = h_1 - h_0 + \frac{V_1^2 - V_0^2}{2} + g(z_1 - z_0) + \Delta g_{1,0} + RT_0 \ln\left(\frac{c_1}{c_{1,0}}\right) - T_0(s_1 - s_0) \tag{22.39}$$

Some observations can be made with reference to Eq. (22.39) (Sciubba and Wall, 2007).

- If the system is in state "0" (i.e., the dead state, where all of its relevant parameters take the same value as those of the reference environment), its exergy is equal to zero.
- If the system proceeds from state 1 to state 2, its exergy variation in the transformation $1 \rightarrow 2$ is also a function of state:

$$e_1 - e_2 = h_1 - h_2 + \frac{V_1^2 - V_2^2}{2} + g(z_1 - z_2) + \Delta g_{1,0} - \Delta g_{2,0} + RT_0 \ln\left(\frac{c_1}{c_2}\right) - T_0(s_1 - s_2) \tag{22.40}$$

- If in the transformation $1 \rightarrow 2$ some heat Q flows into the system, the exergy of the state 2 is smaller than that of state 1 augmented of the quantity of energy Q, since exergy has been destroyed in the transfer of heat from higher to lower temperatures.
- Any irreversibility in the process is reflected in a further decrease of exergy between the initial and the final state. Denoting by $\Delta s_{\text{gen},1\rightarrow 2}$ the irreversible entropy generation, we have:

$$\Delta e_{1\rightarrow 2} = T_0 \cdot \Delta s_{\text{gen},1\rightarrow 2} \tag{22.41}$$

- The reference state (T_0, P_0, μ_0, V_0, z_0) is necessary to the definition of exergy and for an isolated homogeneous system, which cannot exchange either mass or energy with any other system, exergy is not defined.
- If we consider processes that take place in finite times (always maintaining the assumption that they can be represented by a proper succession of quasi-equilibrium states), Eqs. (22.39)–(22.41) maintain their significance if all the terms therein are substituted by their derivatives.
- If a system evolves in the presence of a varying environment, its exergy level (and, thus, the maximum work we can extract from the system) varies accordingly, even if its state does not.
- Exergy is typically referred to as the *maximum* theoretical amount of work obtainable from the combined system composed of the system and the environment as the system passes from a given state to the dead state while interacting with the environment only. Alternatively, it can be regarded as the magnitude of the *minimum* theoretical work input required to bring the system from the dead state to a given state.

The exergy analysis, frequently also named "availability analysis," is a method particularly suited to pursue the goal of a more efficient resource use (Moran and Shapiro, 2006). Indeed, it enables the locations, types, and magnitudes of waste and loss to be determined.

22.5.1.1 Closed Systems

The exergy balance for a closed system is developed by combining the closed system energy and entropy balances:

$$E_2 - E_1 = \int_1^2 \delta Q - W \tag{22.42}$$

$$S_2 - S_1 = \int_1^2 \left(\frac{\delta Q}{T}\right)_b + S_{\text{gen}} \tag{22.43}$$

In Eqs. (22.42) and (22.43), W and Q represent, respectively, work and heat transfers between the system and its surroundings. In the entropy balance, Eq. (22.43), T_b denotes the temperature on the system boundary where δQ is received and the term S_{gen} accounts for entropy produced by internal irreversibilities.

To derive the exergy balance, multiply the entropy balance by the temperature T_0 and subtract the resulting expression from the energy balance:

$$E_2 - E_1 - T_0(S_2 - S_1) = \int_1^2 \delta Q - T_0 \int_1^2 \left(\frac{\delta Q}{T}\right)_b - W - T_0 S_{\text{gen}} \tag{22.44}$$

Since:

$$Ex_2 - Ex_1 = (E_2 - E_1) + P_0(V_2 - V_1) - T_0(S_2 - S_1) \tag{22.45}$$

Eq. (22.44) can be rearranged as follows:

$$Ex_2 - Ex_1 - P_0(V_2 - V_1) = \int_1^2 \left(1 - \frac{T_0}{T_b}\right)\delta Q - W - T_0 S_{\text{gen}} \tag{22.46}$$

Thus, the *exergy balance for a closed system* results in:

$$\underbrace{Ex_2 - Ex_1}_{\text{Exergy change}} = \underbrace{\int_1^2 \left(1 - \frac{T_0}{T_b}\right)\delta Q - [W - P_0(V_2 - V_1)]}_{\text{Exergy transfers}} - \underbrace{T_0 S_{\text{gen}}}_{\text{Exergy destruction}} \tag{22.47}$$

Since Eq. (22.47) is obtained by combining the energy and entropy balances, it is not an independent result, but it can be used in place of the entropy balance as an expression of the second law of thermodynamics. According to Eq. (22.47), the change in exergy of a closed system can be accounted for in terms of exergy transfers (the first underlined term on the right-hand side, composed of the exergy transfer accompanying heat and the exergy transfer accompanying work) and of the destruction of exergy (the second underlined term on the right-hand side) due to irreversibilities within the system. In accordance with the second law of thermodynamics, the exergy destruction (Ex_d) is positive when irreversibilities are present within the system during the process, and it vanishes in the limiting case where there are no irreversibilities. Like other properties, the change in exergy (Ex_2-Ex_1) can be positive, negative, or zero.

For a closed system the exergy balance can be also written in the rate form:

$$\frac{dEx}{dt} = \sum_j \left(1 - \frac{T_0}{T_j}\right)\dot{Q}_j - \left(\dot{W} - P_0 \frac{dV}{dt}\right) - \dot{E}x_d \tag{22.48}$$

22.5.1.2 Open Systems

The exergy balance can be also extended to a form applicable to control volumes. Let us consider a generic control volume (Fig. 22.8), representing a generic system, process operation, or process equipment, able to exchange heat and work with the external environment and crossed by inlet and outlet mass flows.

The exergy balance, for a generic control volume, can be derived from the coupling of energy and entropy balances (Bejan, 2002):

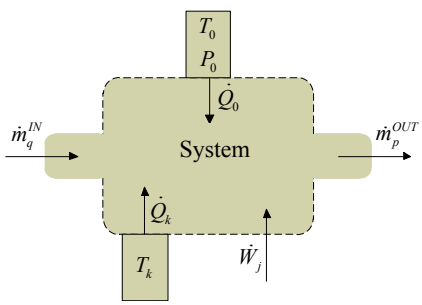

FIGURE 22.8

Schematic representation of the generic control volume.

$$\begin{cases} \dfrac{dE}{dt} = \sum_j \dot{W}_j + \dot{Q}_0 + \sum_k \dot{Q}_k + \sum_q \dot{m}_q^{\mathrm{IN}} \left(gz + \dfrac{v^2}{2} + h \right)_q^{\mathrm{IN}} - \sum_p \dot{m}_p^{\mathrm{OUT}} \left(gz + \dfrac{v^2}{2} + h \right)_p^{\mathrm{OUT}} \\ \dfrac{dS}{dt} = \dfrac{\dot{Q}_0}{T_0} + \sum_k \dfrac{\dot{Q}_k}{T_k} + \sum_q \dot{m}_q^{\mathrm{IN}} s_q^{\mathrm{IN}} - \sum_p \dot{m}_p^{\mathrm{OUT}} s_p^{\mathrm{OUT}} + \dot{S}_{\mathrm{gen}} \end{cases} \tag{22.49}$$

In Eq. (22.49), E is the system energy, t is the time, $\dot{W}_j$ is the jth mechanical power entering or leaving the system, $\dot{Q}_0$ is the thermal power exchanged between the system and the environment at its temperature T_0, $\dot{Q}_k$ is the *kth* thermal power exchanged between the system and an external source at a temperature T_k different from the ambient one, $\dot{m}_q^{\mathrm{IN}}$ is the *qth* mass flow entering the system, gz is the potential energy of the fluid, $\frac{v^2}{2}$ is the kinetic energy of the fluid, h is the specific enthalpy of the fluid, $\dot{m}_p^{\mathrm{OUT}}$ is the *pth* mass flow leaving the system, S is the system entropy, s is the specific entropy of the fluid, and $\dot{S}_{\mathrm{gen}}$ is the generated entropy flow.

By multiplying the entropy balance per T_0 and subtracting it from the energy balance, the following equation, representing the exergy balance, is obtained:

$$\begin{aligned} \frac{dEx}{dt} = {} & \sum_j \dot{W}_j + \sum_k \dot{Q}_k \left(1 - \frac{T_0}{T_k} \right) + \sum_q \dot{m}_q^{\mathrm{IN}} \left(gz + \frac{v^2}{2} + h - T_0 s \right)_q^{\mathrm{IN}} \\ & - \sum_p \dot{m}_p^{\mathrm{OUT}} \left(gz + \frac{v^2}{2} + h - T_0 s \right)_p^{\mathrm{OUT}} - \dot{S}_{\mathrm{gen}} T_0 \end{aligned} \tag{22.50}$$

where Ex is the exergy of the control volume.

Eq. (22.50) can be rewritten in a more compact way as:

$$\frac{dEx}{dt} = \sum_j \dot{E}x_j^{W} + \sum_k \dot{E}x_k^{Q} + \sum_q \dot{E}x_q^{\dot{m}^{\mathrm{IN}}} - \sum_p \dot{E}x_q^{\dot{m}_{\mathrm{OUT}}} - \dot{E}x_D \tag{22.51}$$

where $\dot{E}x^{W}$ and $\dot{E}x^{Q}$ are the exergy flows related to work and heat exchange with the environment, $\dot{E}x^{\dot{m}_{\mathrm{IN}}}$ and $\dot{E}x^{\dot{m}^{\mathrm{OUT}}}$ are the exergy flows related to the inlet and outlet streams passing the control volume, and $\dot{E}x_D$ is the destroyed exergy flow related to irreversible processes.

In the next section, each term of the exergy balance will be defined together with the relative calculation methods. The aim is to provide the reader with a practical guideline useful to perform exergy analyses for natural gas processing plants.

22.5.2 EXERGY ASSOCIATED TO MECHANICAL WORK

Exergy associated to work derives only from the energy balance (Eq. 22.49). According to the definition of exergy as the maximum work potential, the analogy between energy related to work and exergy follows (Querol et al., 2012):

$$\sum_j \dot{E}x_j^{W} = \sum_j \dot{W}_j \tag{22.52}$$

In the case that the control volume has not rigid walls, but its volume can vary, this contribution has to be taken into account:

$$\sum_j \dot{E}x_j^W = \sum_j \dot{W}_j + P\frac{dV}{dt} \tag{22.53}$$

The term $P\frac{dV}{dt}$ represents the work related to a volume change. The direction and the magnitude of mechanical work and exergy related to work is the same.

22.5.3 EXERGY ASSOCIATED TO HEAT

Exergy related to heat depends not only on the amount of heat flowing through the control volume but also on the temperature level at which the heat exchange occurs. The temperature is the one of the external source that exchanges heat with the system. It has to be pointed out that the magnitude and the direction of heat exchanged and exergy related to heat are not necessarily the same. The expression is:

$$\sum_k \dot{E}x_k^Q = \sum_k \dot{Q}_k \tau_k \tag{22.54}$$

The heat flow is positive when entering the system and negative when leaving the system. The term τ_k is the Carnot factor, or the dimensional exergetic temperature (Kotas, 1985), related to the *kth* thermal duty exchanged between the system and the external source, defined as:

$$\tau_k = \left(1 - \frac{T_0}{T_k}\right) \tag{22.55}$$

The Carnot factor accounts for the thermal level at which the heat exchange occurs: $\frac{T_0}{T_k}$ is the ratio between the reference ambient temperature (298.15 K) and the average temperature of the heat source (utility side). If this temperature is lower than the reference ambient one (cooling processes), the Carnot factor is negative and, so, the direction of the exergy flow is opposite to the one of the heat flow. By contrary, if the average source temperature is greater than the ambient reference one (heating process), the Carnot factor is positive and the exergy flow has the same direction of the heat flow. In this way, for cooling processes, the lowest the temperature level, the highest the exergy output, and, by consequence, the exergy leakages. This is particularly true for cryogenic processes, such as LNG production and NGL recovery, or low-temperature natural gas purification processes.

22.5.4 EXERGY ASSOCIATED TO MASS FLOWS

The exergy related to mass flows is composed of different contributions: a physical term (ex_{ph}), a chemical term (ex_{ch}), a kinetic term (ex_{kin}), and a potential term (ex_{pot}) (Kotas, 1985). Generally, the last two terms are neglected since their effect is minimum respect to the physical and chemical terms (Querol et al., 2012). The exergy associated to a mass flow is the maximum work potential obtainable by means of processes between the mass flow and the environment, assuming to take the mass stream from its generic state to the dead state (Kotas, 1985):

$$\sum_r \dot{E}x_r^{\dot{m}} = \sum_r \dot{m}_r \left(ex_{\text{ph}} + ex_{\text{ch}} + ex_{\text{kin}} + ex_{\text{pot}}\right)_r \tag{22.56}$$

Before defining the different terms in Eq. (22.56), it is useful to define the generic state and the ambient state. The generic state of a mass flow is defined by its temperature (T), pressure (P), and composition (y). The ambient state of a mass flow is defined by the ambient temperature (T_0) and pressure (P_0) at the same composition of the generic state. The dead state, previously introduced, is defined by ambient temperature (T_0), ambient pressure (P_0), and ambient composition (y_0). These three states are of paramount importance to calculate the exergy contributions: the mass flow is taken from the generic state to the ambient state (physical contribution) and, then, from the ambient state to the dead state where composition changes (chemical contribution). These processes are represented in Fig. 22.9.

It is possible now to provide the definition of the exergy contributions to the total exergy of a mass flow.

- *Physical exergy* is defined as the maximum work potential obtainable by taking the mass stream at thermal and mechanical equilibrium with the environment (Querol et al., 2012). To calculate the specific physical exergy of a material stream, it is necessary to know the specific enthalpy and entropy of each compound i of the mass flow at both the generic and the ambient states temperature and pressure. Then, the specific exergy of the mixture is calculated as the molar average:

$$ex_{\mathrm{ph},i} = \left(h_i - h_{0,i}\right) - T_0\left(s_i - s_{0,i}\right) \tag{22.57}$$

$$ex_{\mathrm{ph,MIX}} = \sum_i y_i ex_{\mathrm{ph},i} \tag{22.58}$$

- *Chemical exergy* is defined as the maximum work potential obtainable by taking the mass flow from the ambient state to the dead state. This process implies a change in the system composition at constant temperature and pressure, equal to the ones of the ambient state. This means that not only thermal and mechanical equilibrium conditions are needed but also the chemical equilibrium of the system should be reached. The driving force of this process is the difference of composition

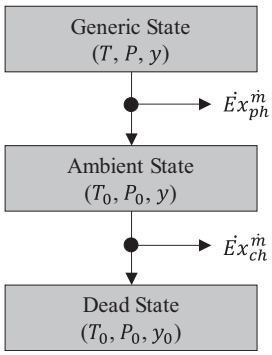

FIGURE 22.9

Schematic representation of the procedure to calculate contributions to the exergy related to mass flows.

between the mass stream and the environment. The calculation can be performed by means of the following equation:

$$ex_{\mathrm{ch,MIX}} = \sum_i \left(y_i ex_{\mathrm{ch},i}\right) + T_0 R \sum_i \left[y_i \ln\left(y_i \gamma_i\right)\right] \tag{22.59}$$

where R is the ideal gas constant and γ_i is the activity coefficient of the *ith* compound. Eq. (22.59) can be used for both gaseous and liquid streams. The term $ex_{\mathrm{ch},i}$ is the specific chemical exergy of the *ith* compound, and its calculation varies according to the chemical species considered. It is clear that Eq. (22.59) is made of two terms: the molar average of the specific chemical exergy of mixture compounds and the exergy destroyed by mixing effects. The activity coefficient is equal to one if the mixture is assumed ideal, while it assumes values different from unity if the mixture is considered nonideal. Typically, the exergy destroyed by mixing effects is negative (the argument of the logarithm is generally smaller than one) and, so, the chemical exergy of the mixture is lower than the chemical exergy of pure compounds. The specific chemical exergy of pure compounds can be calculated using a direct methodology for compounds that are present in the reference ambient (nitrogen, oxygen, carbon dioxide, and water), while for other compounds (fuels) it is necessary to adopt a different method, called the *Van't Hoff box*. Similar to the specific physical exergy, the specific chemical exergy for compounds can be calculated starting from their specific enthalpy and entropy at ambient conditions as pure compounds, assuming the existence of an ideal separation that can split the different compounds into different streams comprising each single pure compound:

$$ex_{\mathrm{ch},i} = \left(h_{*,i} - h_{0,i}\right) - T_0\left(s_{*,i} - s_{0,i}\right) \tag{22.60}$$

where the subscript $*$ refers to the pure compound (molar fraction equal to one) stream at ambient conditions. If the compound is already present in the ambient, Eq. (22.60) becomes:

$$ex_{\mathrm{ch},i} = T_0 R \ln\left(\frac{P_*}{P_{0,i}}\right) = T_0 R \ln\left(\frac{P_0}{P_0 y_{0,i}}\right) = T_0 R \ln\left(\frac{1}{y_{0,i}}\right) \tag{22.61}$$

Otherwise, if the compound of the mixture is not present in the ambient (typically the other compounds are hydrocarbons), its transformation by means of a chemical reaction (combustion) is considered (Van't Hoff box): the specific chemical exergy for this "fuel" is the maximum work potential obtainable by means of its stoichiometric combustion, where both reactants and products are in the dead-state conditions. This reaction is:

$$\mathrm{C_aH_b} + \left(\mathrm{a} + \frac{\mathrm{b}}{4}\right)\mathrm{O_2} \rightarrow \mathrm{aCO_2} + \frac{\mathrm{b}}{2}\,\mathrm{H_2O} \tag{22.62}$$

It is possible to notice that in the reaction not all the compounds are present in the dead state at the composition of the dead state, but the hydrocarbon reactant is in the ambient state. It is necessary, then, to harmonize the different states of the species involved in the chemical reaction: this procedure is explained graphically in Fig. 22.10.

The combustion of the hydrocarbon is performed using oxygen taken at its partial pressure in the dead state and compressed as pure oxygen at the ambient pressure. Inside the box the combustion reaction takes place and products are formed. The products are split as pure compounds at ambient pressure and expanded back to their partial pressures in the dead state. From this process, it is evident

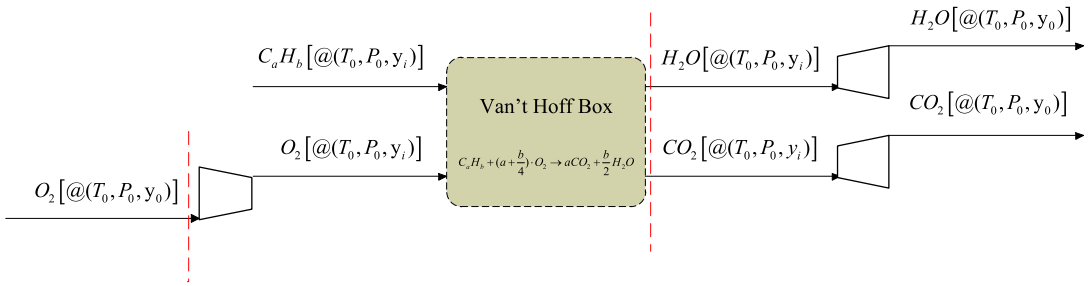

FIGURE 22.10

Schematic representation of the Van't Hoff box for the calculation of the specific chemical exergy of hydrocarbons (*red [light gray in print version] dashed lines* indicate the ideal separation useful to obtain each compound as pure compound from the starting mixture).

that for hydrocarbon compounds the specific chemical exergy is composed of three different terms: the compression, the reaction, and the expansion (Eq. 22.63):

$$ex_{\mathrm{ch},i} = w_{\mathrm{compression}} + w_{\mathrm{reaction}} + w_{\mathrm{expansion}} \tag{22.63}$$

In Eq. (22.63), $w_{\mathrm{compression}}$ is the maximum work theoretically needed to compress the oxygen from the dead state to the ambient state:

$$w_{\mathrm{compression}} = T_0 R \nu_{O_2} \ln\left(\frac{P_0 y_{0,O_2}}{P_{*,O_2}}\right) = T_0 R \nu_{O_2} \ln\left(\frac{P_0 y_{0,O_2}}{P_0}\right) = T_0 R \nu_{O_2} \ln\left(y_{0,O_2}\right) \tag{22.64}$$

where ν_{O_2} is the stoichiometric coefficient of oxygen.

The term w_{reaction} is the maximum work obtainable from the combustion reaction inside the Van't Hoff box:

$$\begin{aligned} w_{\mathrm{reaction}} &= \left[\sum_{i=1}^{R}\left(\nu_i h_{f,i}^0\right) - \sum_{j=1}^{P}\left(\nu_j h_{f,j}^0\right)\right] - T_0\left[\sum_{i=1}^{R}\left(\nu_i s_{f,i}^0\right) - \sum_{j=1}^{P}\left(\nu_j s_{f,j}^0\right)\right] = -\Delta H_R^0 - T_0\left(-\Delta S_R^0\right) \\ &= -\Delta G_R^0 \end{aligned} \tag{22.65}$$

where ν are the stoichiometric coefficients, h_f^0 are the specific enthalpies of formation at ambient conditions, s_f^0 are the specific entropies of formation at ambient conditions, ΔH_R^0 is the reaction heat at ambient conditions, ΔS_R^0 is the reaction entropy at ambient conditions, and ΔG_R^0 is the Gibbs free energy of the reaction at ambient conditions. The Van't Hoff box is assumed to exchange heat only with the ambient at T_0; both reactants and products are considered as pure compounds at ambient state conditions and the produced water is considered as ideal gas.

The term $w_{\mathrm{expansion}}$ is the maximum work potential obtainable from taking the reaction products (carbon dioxide and water) from the ambient state to the dead state:

$$w_{\mathrm{expansion}} = T_0 R \sum_{j=1}^{P}\left(\nu_j \ln\left(\frac{P_*}{P_{0,j}}\right)\right) = T_0 R \sum_{j=1}^{P}\left(\nu_j \ln\left(\frac{P_0}{P_0 y_{0,j}}\right)\right) = T_0 R \sum_{j=1}^{P}\left(\nu_j \ln\left(\frac{1}{y_{0,j}}\right)\right) \tag{22.66}$$

By combining the different terms (Eqs. 22.69–22.66), it is possible to derive the expression for the specific chemical exergy of hydrocarbons species:

$$ex_{\mathrm{ch},i} = T_0 R \nu_{O_2} \ln\left(y_{0,O_2}\right) - \Delta G_R^0 + T_0 R \sum_{j=1}^{P} \left(\nu_j \ln\left(\frac{1}{y_{0,j}}\right)\right) \tag{22.67}$$

Considering the chemical reaction (Eq. 22.62), the expression becomes:

$$ex_{\mathrm{ch},C_aH_b} = \left(\Delta g_{f,C_aH_b}^0 + \left(a + \frac{b}{4}\right)\Delta g_{f,O_2}^0 - a\Delta g_{f,CO_2}^0 - \frac{b}{2}\Delta g_{f,H_2O}^0\right) + T_0 R \ln\left(\frac{y_{0,O_2}^{\left(a+\frac{b}{4}\right)}}{y_{0,CO_2}^a y_{0,H_2O}^{\frac{b}{2}}}\right) \tag{22.68}$$

By combining the different terms, it is then possible to calculate the exergy related to a mass flow.

22.5.5 THE DESTROYED EXERGY

The destroyed exergy $\dot{E}x_D$ is the exergy loss caused by irreversible processes in the control volume: they account for a loss of work potentially recoverable from the system during its evolution to reach the equilibrium with the external environment. This term allows to close the exergy balance, that otherwise will not close to zero by itself and, so, it is a virtual term and is not associated with a physical exergy flow. The estimation of the destroyed exergy is made using the Gouy–Stodola theorem (Kotas, 1985) as the difference between the work potentially recoverable from the system (by means of reversible and irreversible processes) and the effective work recoverable by means of reversible processes. The lower the destroyed exergy, the more efficient is a system:

$$\dot{E}\mathrm{x}_D = \dot{W} - \dot{W}_{\mathrm{rev}} = T_0 \dot{S}_{\mathrm{gen}} \tag{22.69}$$

This term is always positive independently of the fact that the system consumes or produces work and it assumes zero value only in the case that the considered process inside the control volume is totally reversible. The destroyed exergy is a key parameter for the analysis and the optimization of processes with the aim to minimize the exergy loss.

22.5.6 DEFINITION OF THE EXERGY EFFICIENCY

As for the energy evaluation of processes, also for the exergy analysis of systems it is possible to define the exergy efficiency. Unlike energy, which is conserved in a process, exergy is destroyed due to internal and external losses caused by irreversible processes. Internal losses are caused by the exergy destruction (heat transfer at high temperatures, chemical reactions, mixing, *etc.*) and external losses are caused by the exergy contents of the streams leaving the system that contain exergy that is not used (exhaust gases, wastes, purge streams, cooling water, *etc.*). A good approach to properly calculate the exergy efficiency is to calculate the total exergy output and to divide it by the exergy input to the system:

$$\eta_{Ex} = \frac{\sum_{\mathrm{out}} \dot{E}x_{\mathrm{out}}}{\sum_{\mathrm{in}} \dot{E}x_{\mathrm{in}}} \tag{22.70}$$

The exergy efficiency assumes the highest value when exergy losses are the lowest. This parameter provides a performance index useful to compare different process solutions, as for the case of the net equivalent methane, but with no assumptions on the technology adopted to produce the energy streams for the process and accounting for the quality of the energy and its proper use inside the process.

22.5.7 EXAMPLES AND CASE STUDIES

In this section, the application of the concepts this chapter deals with are better highlighted by means of examples and case studies taken from the open literature.

22.5.8 THE NET EQUIVALENT METHANE APPROACH FOR THE COMPARISON OF LOW-TEMPERATURE PURIFICATION PROCESSES WITH AMINE SCRUBBING

In this case study, taken from the works by Pellegrini et al. (2015, 2017), the application of the net equivalent methane approach is shown for the comparison between low-temperature natural gas purification processes and classical amine scrubbing for the purification of a raw gas stream with the aim to produce LNG and capture CO_2 for further uses, such as CCS or EOR. The considered low-temperature purification processes are the Ryan–Holmes process (Holmes and Ryan, 1982a,b; Holmes et al., 1983) and the dual pressure low-temperature distillation process (Pellegrini, 2015). Low-temperature purification processes have started to gain attention in the last decades for the valorization of natural gas reserves having high CO_2 contents since in these cases classical chemical absorption processes require huge amounts of heat to regenerate the solvent. Useful heat is required not only to strip the dissolved acidic gases from the solvent but also to break chemical bonds formed due to the chemical reaction between the dissolved acidic species and the solvent itself. Hence, the highest the content of carbon dioxide in the raw feed gas to be treated, the highest the heat requirement for solvent regeneration, which accounts for about 80% of the total operating costs of a chemical scrubbing unit (Chakma, 1997). Low-temperature natural gas purification processes have shown potential benefits, in terms of costs and energy savings, when used to treat raw natural gas streams having high CO_2 contents (Northrop and Valencia, 2009), particularly higher than about 10 mol% (Langè et al., 2015). In low-temperature natural gas purification processes, attention has to be paid to handle the formation of dry ice inside process unit operations since these processes are typically operated at temperatures below the triple point of CO_2. Several technologies have been proposed to handle the problem of CO_2 freeze-out. In this example, two low-temperature processes have been considered. The Ryan–Holmes process performs the removal of carbon dioxide by means of an extractive distillation: a hydrocarbon with a higher boiling point than methane, typically n-butane, is fed to a pressurized distillation column operated at low temperatures to shift the CO_2 freezing conditions to lower temperatures and pressures and to enhance the solubility of carbon dioxide in the liquid phase. The dual pressure low-temperature distillation process is based on a proper thermodynamic cycle that allows to bypass the maximum of the freezing line of CO_2 in mixture with methane by operating a distillation unit at two different pressure levels: a pressure higher than the maximum one of the CO_2–CH_4 solid–liquid–vapor locus for a bulk removal and a

pressure below the critical pressure of pure methane for a final purification operated away from freezing conditions.

Since all the process streams entering and leaving the process must be at the same conditions (temperature, pressure, composition) so that the difference between processes is exactly the energy consumption needed to transform the inlet raw material in the final product, discharging the same "waste," the same feed stream has been considered for all the analyzed process schemes. The feed gas is a binary CH_4−CO_2 mixture with 40 mol% of carbon dioxide. The pressure of the inlet gas stream is 50 bar and its temperature is 35°C. The molar flow rate of the feed gas has been fixed at 5000 kmol/h. The desired final product in all the considered case studies is LNG at 1 atm. The target purity for the produced gas has been fixed at 50 ppm of CO_2, as recommended for LNG production to avoid freezing problems in liquefaction process equipment. For the CO_2 product stream, the mole fraction of CH_4 has been set at 0.0001 to enhance the CH_4 recovery and to maintain the same standards applied to the design of the dual pressure low-temperature distillation process. Regarding the final conditions for the CO_2-rich stream, the goal is to obtain it as a liquid under pressure, which makes it suitable for further uses such as EOR, transport, and reinjection. Process specifications have been determined to obtain the same outlet stream characteristics to perform the energy analysis based only on differences related to mechanical works, cooling, and heating duties. Both for low-temperature technologies and methyl-diethanolamine (MDEA) purification units, no dehydration steps have been considered since for the low-temperature processes, the feed gas stream is dehydrated before the purification section, while for MDEA scrubbing units, water is removed after the purification section. Moreover, this assumption has been tested in the work by Pellegrini et al. (2018), showing that it has a low impact on the final results of the analysis.

In all the process configurations, the LNG production train has been assumed to be the same, consisting of a turbine followed by a cooler. It is important to highlight that the chosen sequence of operations for liquefaction is not intended to represent the best process configuration, but only a thermodynamic cycle to bring pressure and temperature levels to the LNG storage ones. The top product stream from the purification section is a pure and pressurized methane in the gas phase. This stream is further expanded to atmospheric pressure, recovering power. The use of a flashing liquid expander instead of a Joule−Thomson valve can favor the LNG production since lower cooling duties are needed: an expansion turbine works at isentropic conditions and the enthalpy of the expander outlet stream is lower, while an expansion valve operates at isenthalpic conditions. The complete liquefaction of the expander outlet stream is achieved by means of a heat exchanger having a pressure drop of 0.1 bar.

When low-temperature purification processes are considered, the feed gas has to be cooled and processed to meet the inlet conditions required by each distillation operation.

The final carbon dioxide produced stream has to be properly treated to be the same in all the three process layouts.

In the first analyzed process scheme, the Ryan−Holmes process is considered for natural gas purification (Fig. 22.11). For a detailed description of the process, the reader can refer to the work by Pellegrini et al. (2015, 2017). This process is considered as a low-temperature one because of the temperature profile in column T-100: at the reboiler the temperature is 13.06°C, but at the condenser it is −87.3°C. The regeneration column (T-101) operates at higher temperature levels: the condenser temperature is close to −5.5°C and the bottom one is 137°C. According to these considerations, the

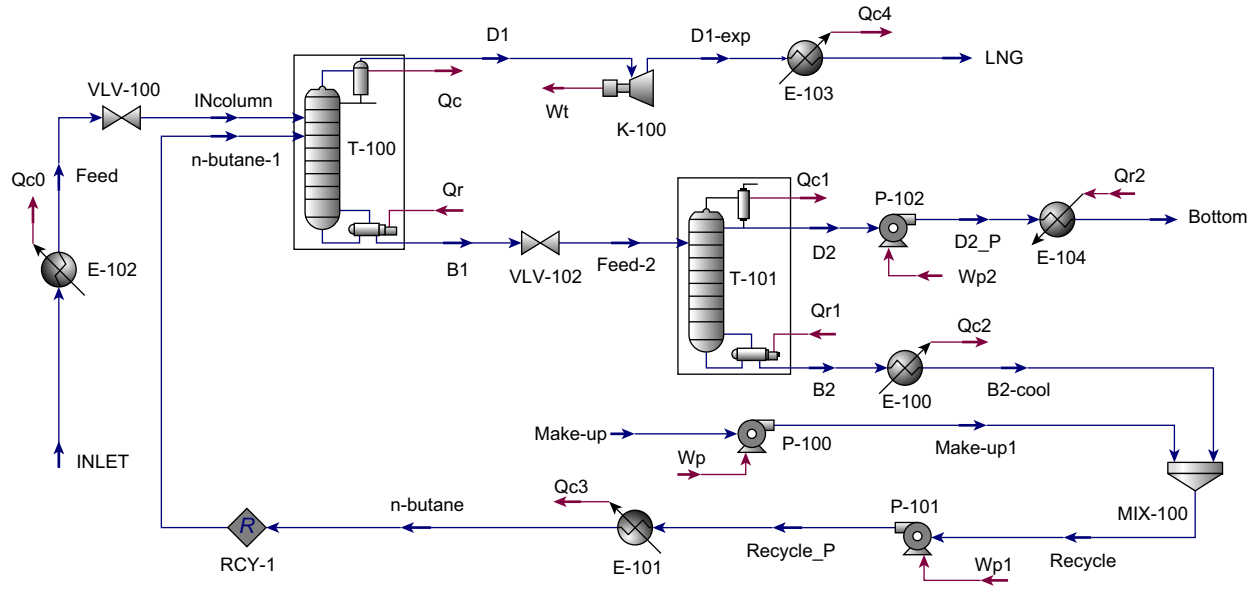

FIGURE 22.11

Ryan–Holmes process for acid gas removal from natural gas in liquefied natural gas production (Pellegrini et al., 2015).

energy demand of column T-100 is mainly determined by the condenser duty, while the reboiler duty plays the most important role for column T-101.

In the second process scheme considered, the dual pressure low-temperature distillation process is used for the purification of natural gas (Fig. 22.12). For a detailed description of the process the reader can refer to the patent by Pellegrini (2015) and to the works by Pellegrini et al. (2015, 2017).

The third considered process solution for the LNG production uses a more traditional MDEA scrubbing unit for gas sweetening. The flow sheet (Fig. 22.13) is just a qualitative scheme of the real process since the real simulation of the MDEA unit requires the detailed design of both the absorption and the regeneration columns. This is because CO_2 absorption is controlled by chemical reaction kinetics and equipment geometry plays a significant role on process performances, including energy estimations. On the other hand, the adoption of rules of thumb simplifies the analysis without compromising the validity of the obtained results.

Typically, MDEA can be used in concentrations up to 60 wt% (Chakma, 1997) due to its lower volatility in respect to other amines. In this example, a 40 wt% amine solution has been assumed.

The rich loading (*RL*) has been selected to be 0.45 (moles of CO_2 per moles of MDEA)—typically it can reach a maximum value of 0.5 on a molar basis (Chakma, 1997).

The lean solvent is regenerated to obtain an acid loading (*LL*) equal to 0.0045 (1/100 of the rich loading).

Heat to the reboiler of the regeneration column is supplied using low-pressure steam at 3.5 bar.

In the literature, several useful correlations to estimate energy consumptions, particularly regarding process heat supplied to the reboiler of the regeneration column (Q_{reb}), are available (Maddox, 1974; Addington and Ness, 2009; Langè et al., 2015). Compared to the other studied process solutions, this last scheme typically operates at ambient or higher temperatures. In this way, the higher costs are related to the regeneration column (T-101).

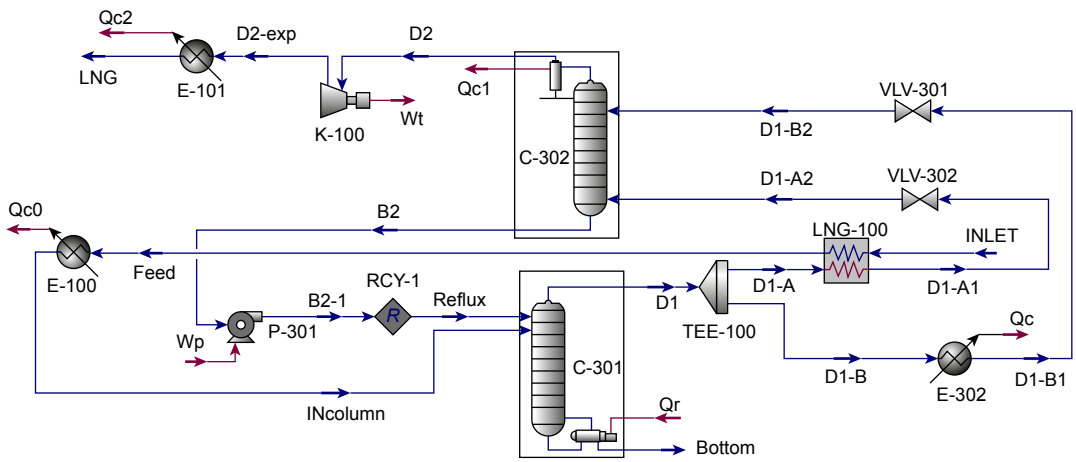

FIGURE 22.12

Dual pressure low-temperature distillation process for acid gas removal from natural gas in liquefied natural gas production (Pellegrini et al., 2015).

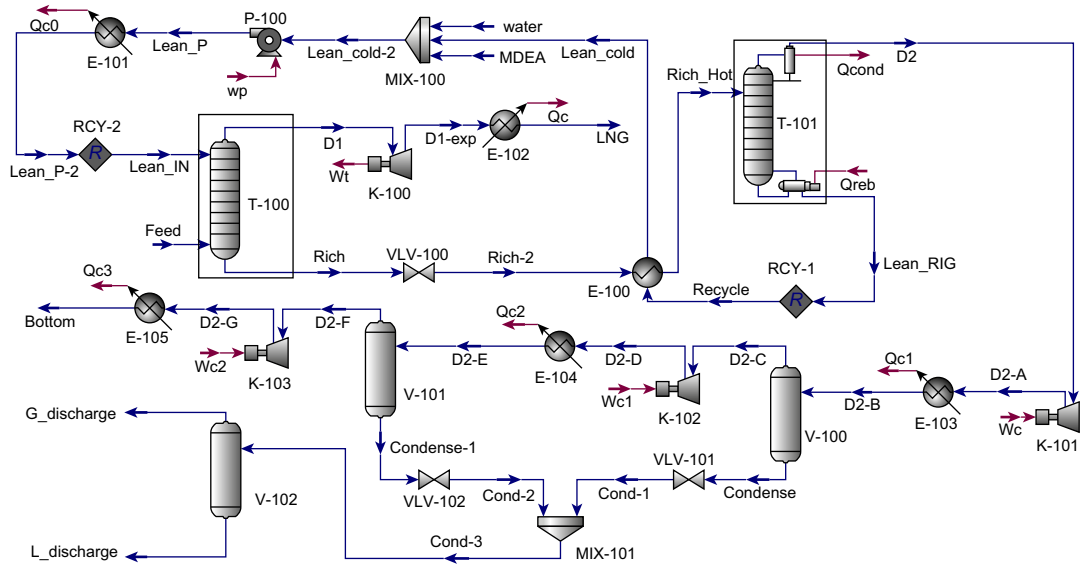

FIGURE 22.13

Methyldiethanolamine chemical absorption process for acid gas removal from natural gas in liquefied natural gas production (Pellegrini et al., 2015).

Generally, according to rules of thumb, linear relations between steam consumptions (and, thus, thermal power) and the circulating solvent volumetric flow rate (that takes into account the effect of the inlet CO_2 content of the raw gas) can be used for the estimation of the reboiler duty. For the two methodologies (Maddox, 1974; Langè et al., 2015) used in this work, the coefficients implemented for the calculation of the steam flow rate are different.

As for the steam ratio (in terms of kg of LP steam per liter of lean circulating solution), which can be varied up to 0.18 kg/L (Addington and Ness, 2009), in the former method (Maddox, 1974) a value of 0.12 kg/L has been adopted, whereas a value of 0.14 kg/L has been used in the second approach (Langè et al., 2015).

To determine the lean amine flow rate, it is necessary to calculate the amount of the absorbed acid gas (CO_2) to treat the raw natural gas stream to the required specifications. Knowing the raw gas flow rate and composition, it is possible to compute the molar flow of the absorbed acidic compound from:

$$\mathrm{mol}_{\mathrm{CO_2}}^{\mathrm{ABSORBED}} = \mathrm{mol}_{\mathrm{CO_2}}^{\mathrm{IN}} - \frac{\mathrm{mol}_{\mathrm{CH_4}}^{\mathrm{OUT}}\left(x_{\mathrm{CO_2}}^{\mathrm{SPEC}}\right)}{1 - x_{\mathrm{CO_2}}^{\mathrm{SPEC}}} \tag{22.71}$$

where $x_{\mathrm{CO_2}}^{\mathrm{SPEC}}$ is the commercial specification for CO_2 in the purified gas at the absorber outlet.

The MDEA aqueous solvent flow rate can be determined knowing the total molar flow of the absorbed acid gas, the rich loading of 0.45, and the lean loading of 0.0045. In this way, the difference between the rich and the lean loadings is the ratio between the absorbed CO_2 and the moles of amine in

the solvent. It is possible to calculate the molar flow of MDEA in the aqueous solution, Eq. (22.72) and, therefore, the molar flow rate of the solvent.

$$\mathrm{mol}_{\mathrm{MDEA}} = \frac{\mathrm{mol}_{\mathrm{CO_2}}^{\mathrm{ABSORBED}}}{\mathrm{RL} - \mathrm{LL}} \tag{22.72}$$

To calculate the steam consumption at the reboiler, it is necessary to determine the volumetric flow rate of the circulating lean solvent. The molar concentration (C_{MDEA}) of the solvent (37.81 kmol/m at 30°C and 50 bar) is calculated using the Amine Package available in Aspen HYSYS, which uses the Kent−Eisenberg (Kent and Eisenberg, 1976) thermodynamic model for aqueous amine solutions:

$$\mathrm{Volume}_{\mathrm{Solvent}} = \frac{\mathrm{mol}_{\mathrm{Solvent}}}{\mathrm{C}_{\mathrm{MDEA}}} \tag{22.73}$$

Using the assumptions for the two different methods, it is possible to determine both steam consumption and duty at the regeneration column reboiler:

$$\mathrm{Steam} = \mathrm{Volume}_{\mathrm{Solvent}} K \tag{22.74}$$

$$\mathrm{Duty} = \mathrm{Steam} \cdot \Delta \mathrm{H}_{\mathrm{Ev,H_2O}}^{3.5\mathrm{bara}} \tag{22.75}$$

In Eq. (22.75), $\Delta H_{Ev,\mathrm{H_2O}}^{3.5\mathrm{bara}}$ is the mass latent heat of vaporization of water at 3.5 bara and its value is 2148 kJ/kg at a boiling temperature of 140°C used in the methodology by Langè et al. (2015), while it is 2187.55 kJ/kg at 121.11°C for the Maddox (1974) approach; K is the coefficient that indicates the steam consumption per cubic meter of lean circulating solution and its values are 140 kg/m (Langè et al., 2015) and 120 kg/m (Maddox, 1974) as previously indicated.

The LNG production is performed using the same configurations adopted for the other two process schemes, assuming, as previously discussed, that the dehydration of the produced gas is not taken into account energetically. Since from the top of the regeneration column CO_2 is obtained wet and at low pressure, to reach the same conditions as in the other schemes some additional treatments are necessary, which include a compression train, condensates separation and final cooling.

The intercooled compression has been designed considering three stages and the outlet pressure from each compression stage has been calculated as follows:

$$P_n = P_{n-1}\left(\frac{P_{\mathrm{out}}}{P_{\mathrm{in}}}\right)^{\frac{1}{n}} + \Delta P_{\mathrm{HE}} \tag{22.76}$$

where $\frac{P_{\mathrm{out}}}{P_{\mathrm{in}}}$ is the global compression ratio between the inlet and outlet pressures of the fluid in the total compression train, n is the number of compression stages, and ΔP_{HE} is the pressure drop in every intercooler (0.1 bar). The outlet temperature from intercoolers has been fixed at 30°C. Condensate at intercooler outlet is separated and collected. Since the flow rate of condensate is low, its relative heat flow has not been considered as process output in the global energy balance.

The three different processes have been compared considering the same operating conditions and specifications for both inlet and outlet streams. In this way, the comparison can be made only considering the differences regarding energy consumptions, since the enthalpy of feed and product streams are the same in all the considered cases.

Table 22.3 Energy Balance for the Ryan–Holmes Acid Gas Removal Process (Fig. 22.11) Used in the Liquefied Natural Gas Production

Thermal Energy Streams						
	Q_{c0}	Q_c	Q_{c1}	Q_{c3}	Q_{c4}	Q_{r1}
T [K]	243.15	185.72	267.62	188.15	111.77	415.18[a]
Power [kW]	5323.27	8187.33	9403.95	2079.12	5383.56	10,398.96
Eq. CH_4 [kg/s]	0.0730	0.3004	0.0650	0.0737	0.5440	0.2600
Mechanical Energy Streams						
	W_p		W_{p1}		W_{p2}	W_t
Power [kW]	0.0209		19.0121		68.2059	1640.3127
Eq. CH_4 [kg/s]	7.58E-07		6.91E-04		0.0025	0.0596

[a]*This temperature is one of the heating medium, determined from the outlet temperature on the cold side (known from simulations), considering a 5°C temperature approach.*

Results for the energy balance are reported in Table 22.3. For this process, the heating of the pressurized liquid CO_2 stream has been neglected since the heating occurs at 15°C and can be performed using nonenergy intensive utilities such as water at ambient conditions.

Regarding the second process solution, where the dual pressure low-temperature distillation process has been applied to LNG production, results are reported in Table 22.4.

For the second solution, the cooling of the feed is provided by energy recovery inside the process: the feed is cooled to the inlet temperature by heating the feed gas to the low-pressure section. The reboiler duty has been neglected since its temperature is 15°C and water can be used, without significant energy expenses.

The energy balance related to the third process scheme is reported in Table 22.5.

The duties of the regeneration column condenser and of the solvent recirculation cooler have been neglected because cooling water is used at ambient conditions, so their impact on the total energy

Table 22.4 Energy Balance for the Dual Pressure Low-Temperature Distillation Acid Gas Removal Process (Fig. 22.12) Used in the Liquefied Natural Gas Production

Thermal Energy Streams				
	Q_{c0}	Q_c	Q_{c1}	Q_{c2}
T [K]	245.42	190.98	185.72	111.77
Power [kW]	2556.20	7406.37	5171.30	5383.84
Eq. CH_4 [kg/s]	0.0333	0.2519	0.1897	0.5441
Mechanical Energy Streams				
		W_p		W_t
Power [kW]		308.37		1640.42
Eq. CH_4 [kg/s]		0.0112		0.0597

Table 22.5 Energy Balance for the Methyldiethanolamine Acid Gas Removal process (Fig. 22.13) Used in the Liquefied Natural Gas Production

Thermal energy Streams						
	Qreb (Langè et al., 2015)	**Qreb (Maddox, 1974)**	**Q_c**	**Q_{c1}**	**Qc2**	**Q_{c3}**
T [K]	412.15[a]	394.26	106.77	360.15	374.85	385.83
Power [kW]	109,872.18	95,898.35	8295.28	4072.41	3157.92	8762.25
Eq. CH_4 [kg/s]	2.7468	2.3975	0.9011	0.1018	0.0789	0.2191

Mechanical Energy Streams				
	Wc	**Wc1**	**W_{c2}**	**Wt**
Power [kW]	2963.13	2735.16	2574.59	3653.99
Eq. CH_4 [kg/s]	0.1078	0.0995	0.0936	0.1329

[a]*This temperature is the one of the heating medium, determined from the outlet temperature on the cold side (known from simulations), considering a 5°C temperature approach.*

balance is negligible. For the MDEA process, the estimation of the reboiler duty differs between the two adopted methodologies.

The main consumptions for the first process scheme are cooling duties and the reboiler heat required by the entrainer (assumed to be n-butane) regeneration column, so the only saving of the process in terms of equivalent CH_4 comes from the turbine power output. For the dual pressure low-temperature distillation process since no entrainer is used, only cooling duties account as energy expenses while power is produced by the expander. For the third process scheme, the main expenses are related to the reboiler of the solvent regeneration column, the LNG liquefaction, and the CO_2 compression. On the contrary, energy production terms come from the turbine output and the intercoolers after compression stages since the temperatures of the process streams to be cooled are suitable for the potential generation of LP steam. In this way, they can be interesting for a possible process energy intensification. The final results in terms of net equivalent CH_4 requirements are reported in Table 22.6. Results show that the second solution is the one which ensures the lowest consumption of equivalent CH_4, while the third process solution is the most energy-intensive technology if applied to high CO_2-content natural gas streams. The first solution remains in the middle since it depends on both cold and hot energy duties.

This example demonstrates the effective use of the net equivalent methane approach for purification processes evaluation and comparisons. As described in Section 22.4, the method is straightforward once the process flow sheet has been simulated/calculated including all the most relevant energy terms.

22.5.9 EXERGY ANALYSIS FOR THE OPTIMAL DESIGN OF REFRIGERATION CYCLES

In the natural gas processing industry, refrigeration cycles play an important role to provide energy for cryogenic separation processes (such as NGL recovery units and low-temperature purification processes) and for the production of LNG. The design of such energy systems should be optimal, since

Table 22.6 Final Comparison Among the Three Process Schemes for Liquefied Natural Gas Production: Energy Consumptions Are Given as Equivalent Methane

Process Scheme	Equivalent CH_4 Consumption [kg/s]	Equivalent CH_4 Savings [kg/s]	Equivalent net CH_4 Input [kg/s]
Ryan–Holmes	1.3192	0.0596	1.2596
Dual pressure low-temperature distillation	1.0302	0.0597	0.9705
Methyldiethanolamine (MDEA) unit (Langè et al., 2015)	3.9348	0.5327	3.4021
MDEA unit (Maddox, 1974)	3.5855	0.5327	3.0528

their performances are closely related to product quality, energy efficiency, and plant profitability. The degrees of freedom for the proper design of refrigeration systems can be numerous (temperature levels, working fluid mixture composition, pressure levels, number of refrigeration stages in a cascade system, *etc.*), increasing the complexity of the problem. A refrigeration system generally works by indirectly transferring thermal energy from low-temperature sources to high-temperature sinks by consuming electricity or mechanical work to lower or maintain the source temperature at a certain value. The complexity of refrigeration systems consists, mostly, in two fundamental aspects:

- An industrial refrigeration system usually needs to satisfy the cooling demands from many different units at different temperatures. Thus, a refrigeration system should simultaneously work at multiple temperature and pressure levels. As a result, proper considerations have to be made to satisfy multiple needs, minimizing electricity or mechanical work consumption.
- A complex refrigeration system may need to accomplish different refrigeration tasks in a wide temperature range, for example from 23°C to about −100/−160°C. Thermodynamically, it is impossible to achieve this result by using one single refrigerant only. Therefore, multiple refrigerants have to be employed in this situation. Each refrigerant has to satisfy its multiple temperature levels to handle the refrigeration tasks within a specific temperature range. Meanwhile, multiple temperature levels from multiple refrigerants may be optimally integrated in cascades to jointly accomplish some tough refrigeration tasks or to save energy.

An effective way to increase the performance of the refrigeration cycles is detecting the components with improvement potential. Conventional and advanced exergy analyses can be applied to refrigeration cycles for determining the components with high irreversibilities, as illustrated in the following examples.

22.5.9.1 Application of the Exergy Analysis for the Optimal Design of Cascade Vapor-Compression Refrigeration Cycles

To perform the optimal design of cascade refrigeration systems, Zhang and Xu (2011) have adopted the exergy analysis as the method to orient the definition of the best refrigeration cycle, coupling exergy analysis with economic evaluations of the defined solution. In this example, vapor compression

cycles are considered. These cycles are made by four main components (i.e., an evaporator, a compressor, a condenser, and an expansion valve, Fig. 22.14A). Some modifications can be made to increase the energy performances of the cycle, such as internal heat recovery to further reduce the temperature of the refrigerant after its condensation and prior to its expansion (if technically feasible). The main energy consumption for this kind of energy system is the mechanical energy to drive compressors. This energy can be supplied by means of turboexpanders or steam turbine, as well as electric engines.

In classical thermodynamic studies of energy cycles, the enthalpy–temperature diagram is typically used. By analogy, Zhang and Xu (2011) have adopted the equivalent exergy–temperature diagram to represent the behavior of the thermodynamic cycle. To do this, detailed steady-state simulations of the refrigeration systems are performed. An example of this exergy–temperature chart for a single-stage vapor-compression refrigeration cycle is shown in Fig. 22.14B.

In the graph shown in Fig. 22.14B, the red line corresponds to the saturated vapor line, hence the points of the cycle at the left of the red line are typical of a superheated vapor; the blue line corresponds to the saturated liquid line, and, so, all the points on the right side of this line correspond to a subcooled liquid. The intersection between the blue and the red lines is the equilibrium state at ambient temperature. The points lying between the red and the blue lines below the intersection point at ambient temperature are liquid + vapor mixtures. The region between the red and the blue lines above the intersection point (shadowed area) is still a single phase region that corresponds to states, or operating points, where the fluid exergy is identical for the superheated vapor as well as for the subcooled liquid. The green line is the pathway of the working fluid inside the refrigeration cycle:

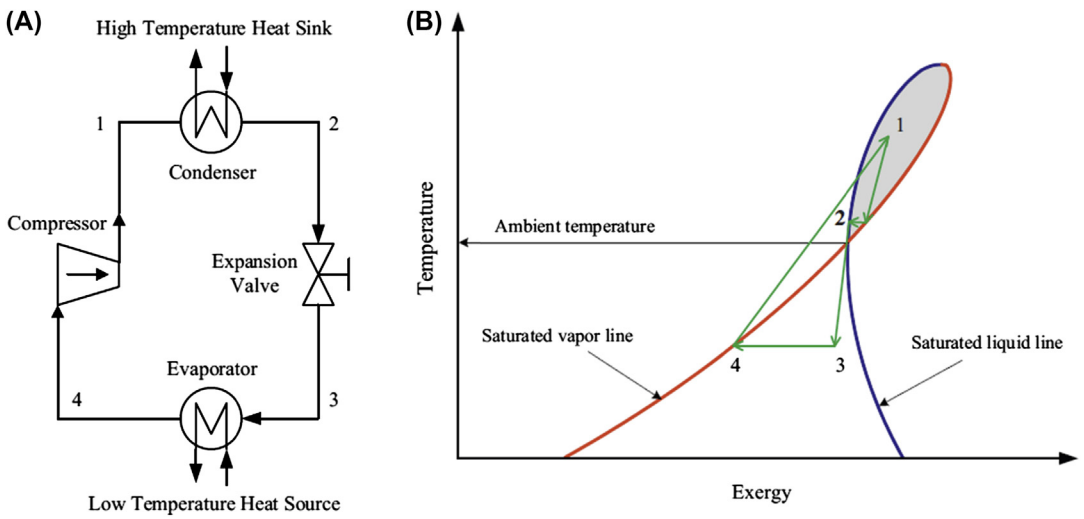

FIGURE 22.14

Process scheme of the single-stage vapor-compression refrigeration cycle (A) and the relative exergy–temperature diagram (B) (Zhang and Xu, 2011).

- 1 → 2: refrigerant condensation;
- 2 → 3: refrigerant expansion;
- 3 → 4: refrigerant evaporation;
- 4 → 1: refrigerant compression.

The expansion (2 → 3) is modeled as an adiabatic expansion: the valve is isenthalpic and so the enthalpy of the refrigerant across the valve remains constant, while temperature and pressure decrease. During this process entropy is increased and, so, exergy slightly decreases across the expansion valve. Evaporation (3 → 4) of the refrigerant occurs at constant temperature and pressure (if the working fluid is a pure compound or an azeotropic mixture). Since during evaporation, the refrigerant absorbs heat below the ambient temperature, its exergy is reduced. The compression (4 → 1) is not an isentropic process and the entropy level of the discharged pressurized gas is higher than the one of the feed gas: during this process, the exergy of the working fluid is increased. As it can be observed from Fig. 22.14B, the refrigeration cycle is divided into two main regions: the compression, where the exergy of the fluid is increased, and the condensation + expansion + evaporation, where the exergy of the fluid decreases. To boost the energy efficiency of the refrigeration cycle, the fluid should be able to absorb the largest amount of heat at a fixed work input; this means that the exergy change at the evaporator of the refrigeration cycle should be the maximum possible. Adding a subcooler to the refrigeration cycle, to further decrease the temperature of the working fluid leaving the condenser, can help to improve the energy efficiency of the cycle since it allows to reduce exergy losses across the expansion valve and to increase the exergy change at the evaporator. A graphic example of this effect is shown in Fig. 22.15.

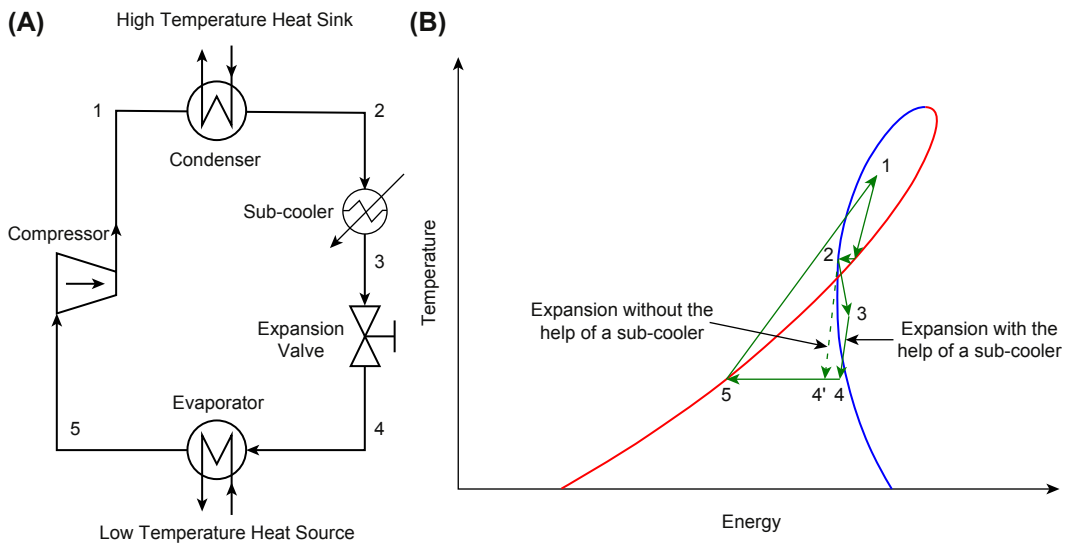

FIGURE 22.15

Process scheme of the single-stage vapor-compression refrigeration cycle with subcooling after condensation of the working fluid (A) and the relative exergy−temperature diagram (B) (Zhang and Xu, 2011).

The subcooling is the arrow 3 → 4, while the point 4′ represents the previous state (point 3 in Fig. 22.14B) of the refrigerant after expansion in the absence of a subcooler. This means that the lowest the vapor fraction of the refrigerant leaving the expansion valve, the highest the heat that the working fluid can absorb at the evaporator: if the refrigerant after expansion is in saturated liquid state at the lowest pressure of the cycle, it can absorb an amount of heat equal to its heat of evaporation, while for vapor fractions higher than zero, the refrigerant can absorb only a fraction of its heat of vaporization to completely pass from the mixed liquid + vapor state to the saturated vapor conditions. The same concept can be applied to a multiloop refrigeration cycle, where different refrigeration tasks are performed at different temperature levels. An example of a two-loop refrigeration cycle is provided in Fig. 22.16.

The two loops are connected via a flash drum that separates the liquid and the vapor refrigerant after the first heat exchange with the first low-temperature heat source (the process stream to be cooled at the first temperature level). In this case the refrigerant is firstly expanded (2 → 3) at an intermediate pressure level to provide the cooling duty to the first process stream (3 → 4). The stream leaving this first evaporator is a mixture of liquid + vapor and, so, it is separated inside the flash drum (4 → 5 for the liquid and 4 → 9 for the vapor). The liquid leaving the flash drum is a saturated liquid at the intermediate pressure and temperature levels and is further expanded to the lowest pressure of the refrigeration cycle (5 → 6). This portion of the total working fluid flow rate is used to provide cold at the lowest temperature needed by the process (6 → 7) and recompressed back to the intermediate pressure level (7 → 8). The vapor is then mixed with the vapor stream coming from the flash drum

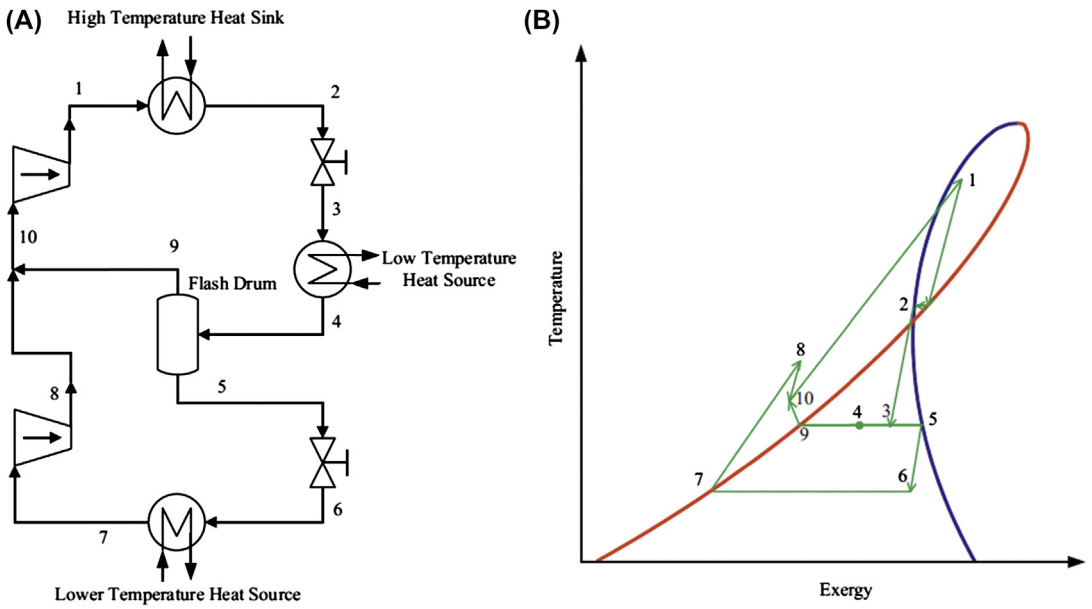

FIGURE 22.16

Process scheme of the two-loops vapor-compression refrigeration cycle (A) and the relative exergy−temperature diagram (B) (Zhang and Xu, 2011).

(8 + 9 → 10) and recompressed back to the highest pressure of the refrigeration cycle (10 → 1). The compressed gas is cooled and liquefied inside the condenser (1 → 2) and starts back the cycle again. The choice and the feasibility of this operation depend on the temperature levels at which the different tasks have to be performed: the working fluid should be chosen by consequence. Its properties should satisfy the constraints imposed by the cooling needs. Also in this case, the possibility of introducing subcoolings can be evaluated to improve the energy efficiency of the process. These concepts can be applied, in general, to a multistage cascade refrigeration cycle that operates with different refrigerants and each stage can present multiple loops working at different temperature levels. The aim for these complex systems is to accomplish several tasks in a wide range of temperature levels. An example is shown in Fig. 22.17, where a two-stage cascade refrigeration cycle is considered and each stage presents two loops.

In this cycle, the second refrigerant (refrigerant B) exchanges heat with both the temperature loops of the first refrigerant (refrigerant A) and the first stage (refrigerant A) is used to drive the operation of the second stage (refrigerant B) that exchanges heat with process streams at two different temperature levels. This solution is adopted for extremely low-temperature applications, where a single refrigerant cannot be used to perform the task due to a big difference between the cold temperature level to be reached and the possibility to define a suitable pressure level below the critical pressure of the working

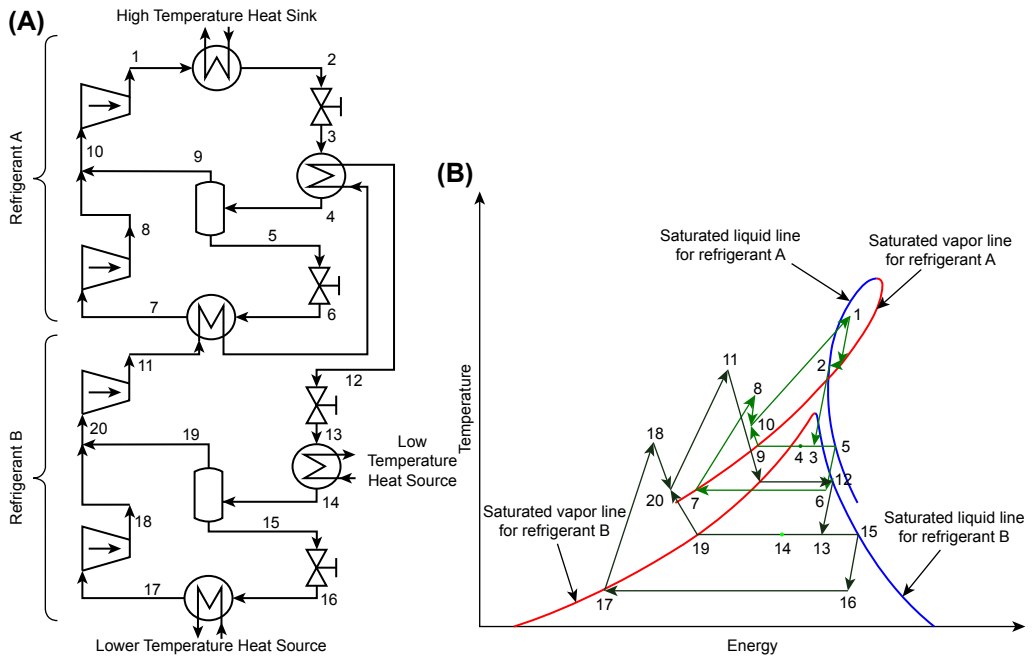

FIGURE 22.17

Process scheme of the two stages, two-loops vapor-compression refrigeration cycle (A) and the relative exergy−temperature diagram (B) (Zhang and Xu, 2011).

fluid to perform its condensation at ambient temperature. Examples of these applications can be found both in petrochemical plants (ethylene production units) and for LNG production (Kanoğlu, 2002; Mafi et al., 2009; Zhang and Xu, 2011).

22.5.10 PINCH TECHNOLOGY, EXERGY AND ENERGY ANALYSIS CASE STUDIES FOR CRYOGENIC NGL RECOVERY

The power consumption in the NGL recovery refrigeration system is always high and, as a result, its minimization is the most effective measure to reduce the cost associated to this process.

The exergy analysis is a powerful tool that can be used in the design, optimization, and performance evaluation of energy systems. It allows to determine how much of the usable work potential or of the exergy supplied as inlet has been consumed (lost) by the process. Also, the exergy destruction or irreversibility provides a general applicable quantitative measure of process inefficiency and shows the direction for potential improvement. The reader is referred to the works by Moran (1982), Kotas (1985), Bejan (1997), and Gaggioli (1998) for the general principles and methodology of the exergy analysis.

In this section, some case studies are reported which deal with the study of the refrigeration system employed in the NGL recovery process by means of pinch and exergy analysis.

22.5.10.1 Inefficiencies in NGL Recovery Processes

The following case study is taken from Shin et al. (2015) who have performed a thermodynamic analysis and optimization of NGL recovery processes aiming at identifying inefficient elements or subsystems for energy-saving purposes. They have taken into account three processes developed by Ortloff Engineers Ltd., namely:

- the gas subcooled (GS) process (Fig. 22.18);
- the recycle split vapor (RSV) process (Fig. 22.19);
- the cold residue reflux (CRR) process (Fig. 22.20).

All the abovementioned processes are turboexpansion-based NGL recovery processes.

For each scheme, two cases with different feed gas composition (lean gas and rich gas, as in Table 22.7) have been considered and for two sets of the number of tray of the demethanizer column (i.e., a 10-stage and a 30-stage column).

The variables selected for optimization (minimization) of the overall exergy loss (given by the sum of the exergy losses in heat exchanger, cooler, compressor, expander, column, and valve) of the NGL recovery processes taken into account are the precooled temperature after propane refrigeration cycle, column operating pressure, and vapor-split ratio after the flash drum. The recycling ratio of top product stream is additionally, considered as an optimization variable in the RSV and CRR processes since the recycled stream to the column influences its performance. The optimization has been subject to two constraints: one is to keep the pressure of off-the-shelf compressor higher than that of the demethanizer (feasibility condition in the heat exchanger) and the other is to have a minimum 90% ethane recovery.

Exergy loss obtained from the optimization of four cases is shown in Tables 22.8–22.10. One key feature in optimization results is to have high operating column pressures, compared with base cases, which result in lower entropy generation, leading to reduction in exergy loss associated with pressure change.

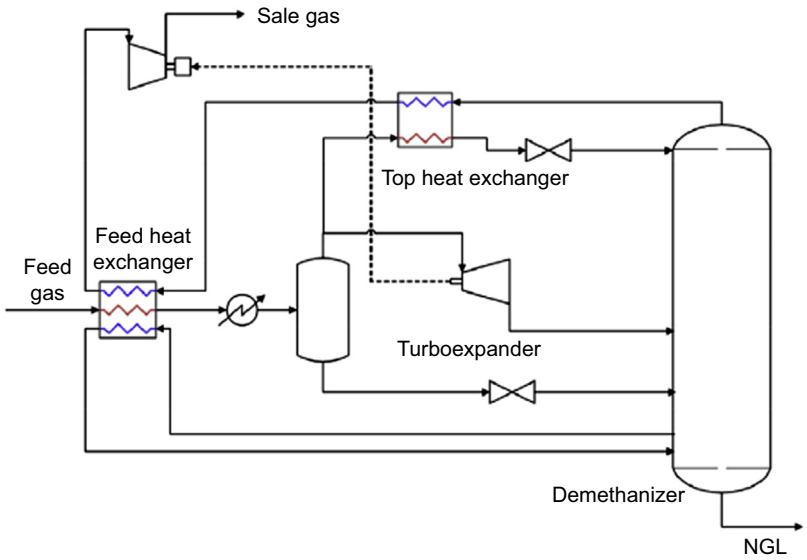

FIGURE 22.18

Schematic diagram of the gas subcooled process (Shin et al., 2015).

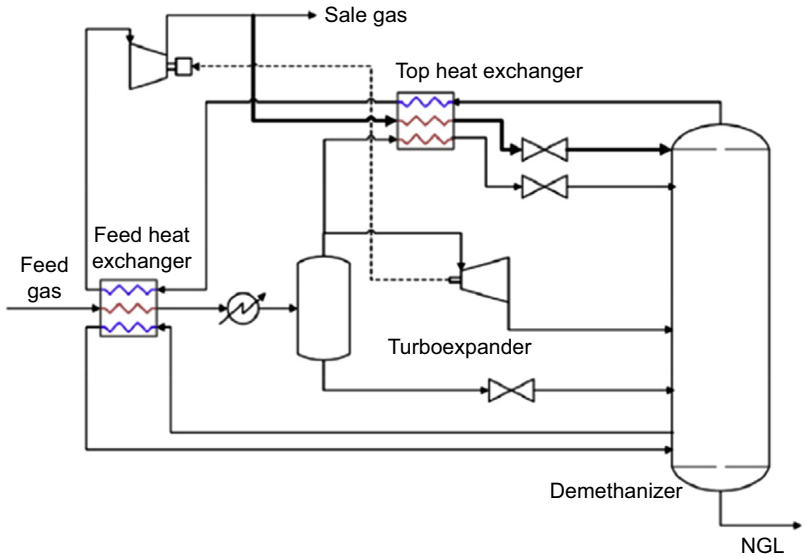

FIGURE 22.19

Schematic diagram of the recycle split vapor process (Shin et al., 2015).

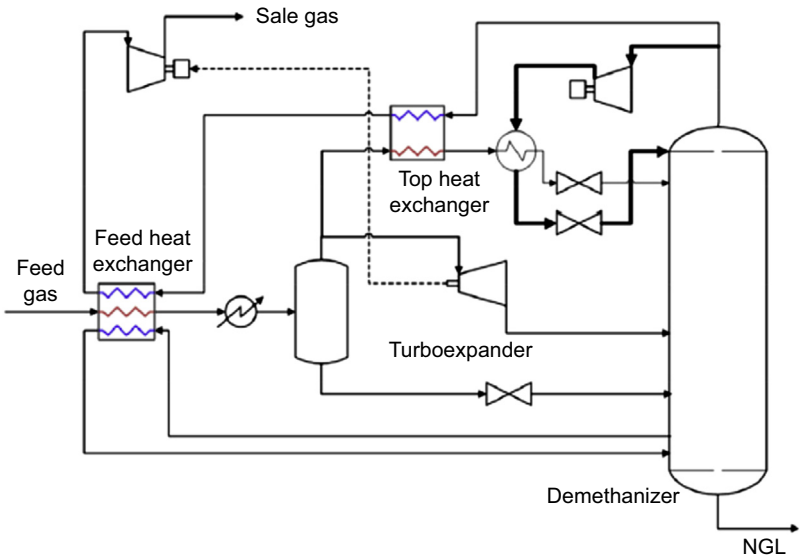

FIGURE 22.20

Schematic diagram of the CRR process (Shin et al., 2015).

22.5.10.2 Lean Feed Conditions

For lean feed conditions, total exergy loss is reduced about 8%−13% after optimization. Exergy loss of the compressor is reduced by about 2%−10% due to higher operating pressure for inlet stream, while the same reason contributes to a 26%−49% reduction in exergy loss for the valve through which upper vapor split stream is passed.

With a 30-stage column and lean feed, the overall exergy loss is reduced by about 16%−28% compared with the base case. In the GS process, exergy loss increases in rectifying section of the column but decreases in the section of the column near to side reboilers, compared with base case (Fig. 22.21). More vapor flow in the feed as well as in the rectifying section at the optimized condition improves the separation efficiency of the rectifying section but increases exergy loss. However, such

Table 22.7 Feed Conditions (Shin et al., 2015)

Components	Lean Feed	Rich Feed
Methane	0.93	0.69
Ethane	0.03	0.15
Propane	0.015	0.075
i-Butane	0.009	0.045
i-Pentane	0.003	0.015
i-Hexane	0.003	0.015
Nitrogen	0.01	0.01

Table 22.8 Optimization Results for Exergy Loss [kW] for the Gas Subcooled Process (Shin et al., 2015)

Stage	10				30			
Feed	Lean		Rich		Lean		Rich	
Case	Base	Opt	Base	Opt	Base	Opt	Base	Opt
Feed HX	41.5	41.3	51.2	55.8	37.8	43.2	55.5	54.8
C3 Cooler	9.4	4.2	63.8	90.2	4.5	1.9	66.5	80.6
Top HX	51	40.6	30.5	25.9	47.4	44.6	29.9	25.9
Expander	72.3	79.9	59.5	42.4	74.8	79.5	50.7	39.8
Compressor	166.3	162.1	183.3	158.6	159.4	156.7	168.5	150.5
VLV-1	41.8	27.3	28	25.3	34	25.9	25.3	25.4
VLV-2	4.6	3.4	132.6	117	3.1	2.7	123.2	107.6
Column	172.2	132.9	205.1	212.9	128.5	93.8	196.4	197.6
Total	559.2 (−12%)	491.9	754.2 (−3%)	728.6	489.4 (−8%)	448.6	716.1 (−4%)	682.2

change in operating conditions in the column leads to decrease in exergy loss for a stripping section. As exergy loss near sider reboilers in the stripping section is much larger than increase in exergy loss at the top of the column, overall exergy loss of the column is about 26% decreased. Similar characteristics related to exergy losses of columns for the RSV process (Fig. 22.22) and for the cold residue reflux

Table 22.9 Optimization Results for Exergy Loss [kW] for the Recycle Split Vapor Process (Shin et al., 2015)

Stage	10				30			
Feed	Lean		Rich		Lean		Rich	
Case	Base	Opt	Base	Opt	Base	Opt	Base	Opt
Feed HX	34.1	33.1	35.3	44.1	34.4	27.8	48.1	47.6
C3 Cooler	9.4	4.8	66.1	85.9	4.3	3.5	61.65	76.1
Top HX	66.8	57.4	46.1	44.3	60.6	60.1	38.6	39.8
Expander	71.1	80.1	57.8	37.9	62.7	57.1	55.1	37.7
Compressor	175.1	170.3	192.3	168.3	154.1	138.4	179.2	157.5
RF cooler	8.1	14.4	36.1	19.1	6.3	10.1	13.1	8.9
VLV-1	4.4	8.8	17.1	9.8	4.1	8.1	5.8	4.6
VLV-2	52.5	21.1	23.6	34.1	42.6	27.9	21.5	34.1
VLV-3	3.7	3.2	115.1	115.3	2.8	2.4	125.4	108.2
Column	176.7	152.7	234.2	231.4	119.5	97.4	201.8	193.1
Total	602.1 (−9%)	546.1	823.8 (−4%)	790.4	491.7 (−12%)	432.6	750.5 (−5%)	707.8

Table 22.10 Optimization Results for Exergy Loss [kW] for the CRR Process (Shin et al., 2015)

Stage	10				30			
Feed	Lean		Rich		Lean		Rich	
Case	Base	Opt	Base	Opt	Base	Opt	Base	Opt
Feed HX	35.1	37.3	47.6	52.6	41.1	43.6	45.4	55.1
C3 Cooler	5.2	3.4	72.1	75.9	7.2	5.6	66.2	78.4
Top HX 1	54.3	40.1	43.3	29.5	44.9	37.7	37.9	26.5
Top HX 2	13.5	0.5	1.1	0.4	4.2	6.1	1.1	0.1
Expander	78.4	80.7	41.9	46.5	62.8	60.8	43.5	37.4
Compressor	173.5	163.9	183.3	176.3	146.3	135.2	168.4	151.4
OTS comp	6.8	2.1	0.5	0.1	3.4	3.3	0.8	0.1
VLV-1	43.5	27.7	54.9	28.7	32.7	25.2	41.1	25.9
VLV-2	4.2	6.4	1.5	0.1	5.8	2.9	2.1	0.2
VLV-3	3.3	2.8	145.9	141.1	3.6	3.1	123.8	113.9
Column	151.2	130.8	216.7	223.9	132.2	104.3	188.4	195.5
Total	569.4 (−12%)	496.2	809.1 (−4%)	775.4	484.3 (−11%)	428.1	719 (−5%)	684.7

process (Fig. 22.23) are observed, with a reduction of about 18% and 20%, respectively, than base case.

Results for the case where a 10-stage column is considered show similar characteristics for the optimized processes. Exergy losses of the compressor, valve, and column are reduced by about 2%−5%, 34%−59%, and 13%−22%, respectively, and overall exergy loss is reduced by about 9%−12%.

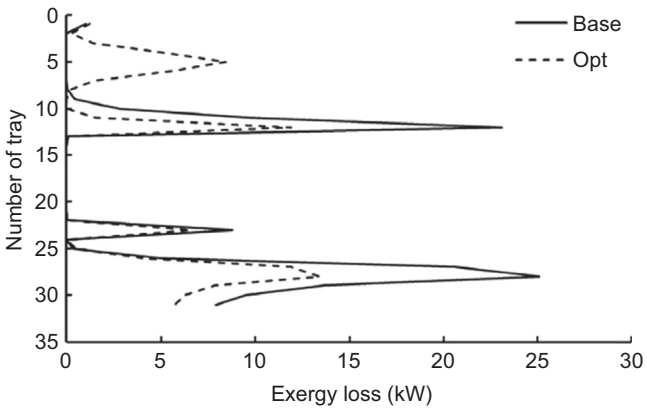

FIGURE 22.21

Exergy loss profile of gas subcooled process: lean feed and a 30-stage column (Shin et al., 2015).

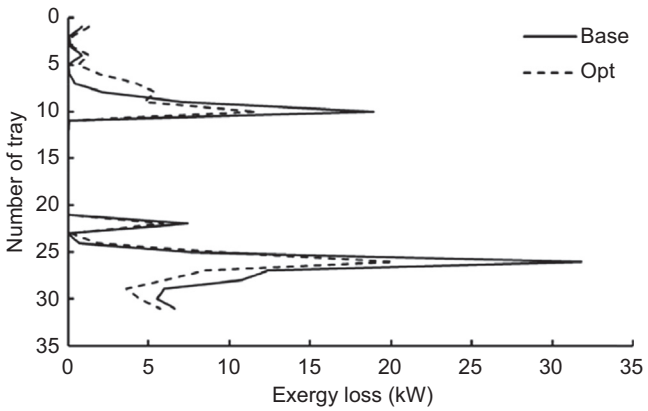

FIGURE 22.22

Exergy loss profile of recycle split vapor process: lean feed and a 30-stage column (Shin et al., 2015).

22.5.10.3 Rich Feed Conditions

For rich feed conditions, such as lean feed conditions, higher pressure, and temperature conditions of the column are found through optimization, leading to a reduction in total exergy loss of about 3%−5%.

Optimal operating conditions result in about 10%−12% reduction in exergy loss for the compressor and about 14%−31% reduction for the expander. However, exergy losses in the feed heat exchanger and refrigeration cycle are increased by about 18%−23% after optimization. This is because refrigeration duty for feed cooling is increased with respect to the base case, which leads to increase in exergy loss.

Unlike the case for the lean feed (Figs. 22.21−22.23), there is practically no change in exergy loss of a column through optimization for rich feed cases.

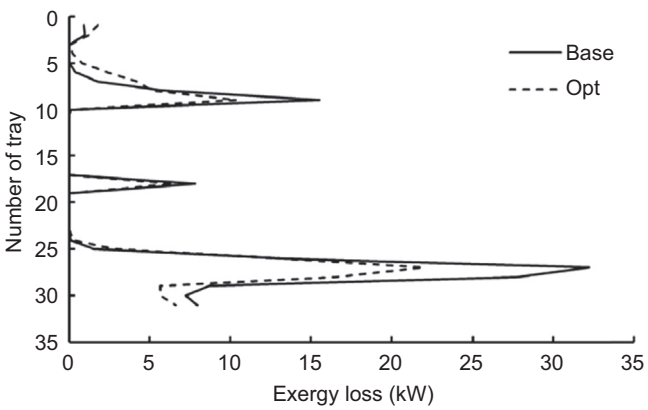

FIGURE 22.23

Exergy loss profile of cold residue reflux (CRR) process: lean feed and a 30-stage column (Shin et al., 2015).

22.5.10.4 Overall Comparison

Generally, it is known that RSV process and CRR process have better ethane recovery and less shaft power requirement than GS process (Pitman et al., 1998). Indeed, for these two processes in lean feed conditions with a 30-stage column, shaft power requirement is about 15% lower than GS process, and overall exergy loss is reduced by about 3% and 4% for RSV and CRR, respectively (Table 22.11). This result shows that the recycling concept applied to increase the methane fraction in the upper section of the column leads to lower shaft power requirement and less overall exergy loss.

However, other cases, except for cases of lean feed with a 30-stage column, show different results (Table 22.11). For lean feed cases with a 10-stage column, the recycle stream to the top of demethanizer is not effective in reducing the overall energy requirement and exergy loss, due to the low number of stages in the column, whereas recycling stream is effective for lean feed cases with the 30-stage column. For rich feed cases with columns having 10 and 30 stages, when the rich feed enters the demethanizer, more C_{2+} components are remained in the rectifying section of the column, compared

Table 22.11 Overall Comparison for Optimization Results (Shin et al., 2015)

Lean Feed						
	30 Stages			**10 Stages**		
	GSP	**RSV**	**CRR**	**GSP**	**RSV**	**CRR**
Recovery (%) C_2	90.12	90.14	90.14	90.15	90.17	90.14
Recovery (%) C_3	98.55	99.65	99.34	98.74	99.91	99.34
CW compressor (kW)	55.63	85.58	110.5	82.7	100.89	84.75
Main compressor[a] (kW)	805.32	679.86	682.68	839.51	871.54	856.29
Expander (kW)	162.96	118.5	122.95	160.16	159.8	161.97
Overall energy consumption (kW)	679.99	646.94	670.23	762.06	812.63	779.06
Overall exergy loss (kW)	448.66	432.63	428.11	491.98	546.17	496.2
Rich Feed						
	30 Stages			**10 Stages**		
	GSP	**RSV**	**CRR**	**GSP**	**RSV**	**CRR**
Recovery (%) C_2	90.11	90.13	90.17	90.13	90.13	90.15
Recovery (%) C_3	99.71	99.94	99.73	99.76	99.9	99.81
CW compressor (kW)	479.79	470.7	477.51	508.01	500.11	469.87
Main compressor[a] (kW)	819.93	856.46	826.94	877.88	917.99	1008.1
Expander (kW)	77.11	73.85	72.54	81.35	73.45	87.49
Overall energy consumption (kW)	1222.61	1253.31	1231.92	1304.54	1344.64	1390.48
Overall exergy loss (kW)	682.28	707.87	684.79	728.66	790.45	775.44

GSP, *gas subcooled process;* RSV, *recycle split vapor.*
[a]*CRR (cold residue reflux) process, main compressor duty includes off-the-shelf compressor duty.*

with conditions of lean feed cases. Such presence of heavy components in the rectifying section may lessen the benefit associated with a recycle stream which has a large fraction of methane.

22.5.10.5 Development of Energy-Efficient Processes for NGL Recovery

This case study is taken from Yoon et al. (2017) who have investigated and evaluated novel process configurations by considering several design modifications with the aim to develop a new process design to improve energy efficiency and product recovery. The new configuration (HY-NGL process shown in Fig. 22.24) implements two of the possible modifications that can be considered to improve NGL recovery efficiency: a side reboiler in the distillation column and integration with the cold box, and splitting of the feed stream after the cold box for additional heat recovery. These new configuration is compared with three conventional processes (GS, RSV, and CRR processes already considered in the previous example) in terms of energy requirements and product recovery at optimal conditions. The optimization has been carried out by minimizing power consumption given by the summation of the shaft power requirements that dominate the total energy costs: the shaft power required in the propane refrigeration cycle compressor, the shaft power required in the main compressor, and the shaft power generated in the turboexpander. The reader can refer to the original paper for major details about the choice of the optimization variables and associated bounds.

For the four configurations to be compared, a number of cases are considered including combinations of lean and rich feeds, two different column heights (either 10 or 30 stages) and two different ethane recoveries (either 85% or 90%).

For the case using the rich feed and a 30-stage column with an 85% minimum constraint applied to the ethane recovery, the results summarized in Table 22.12 suggest that power savings in the range

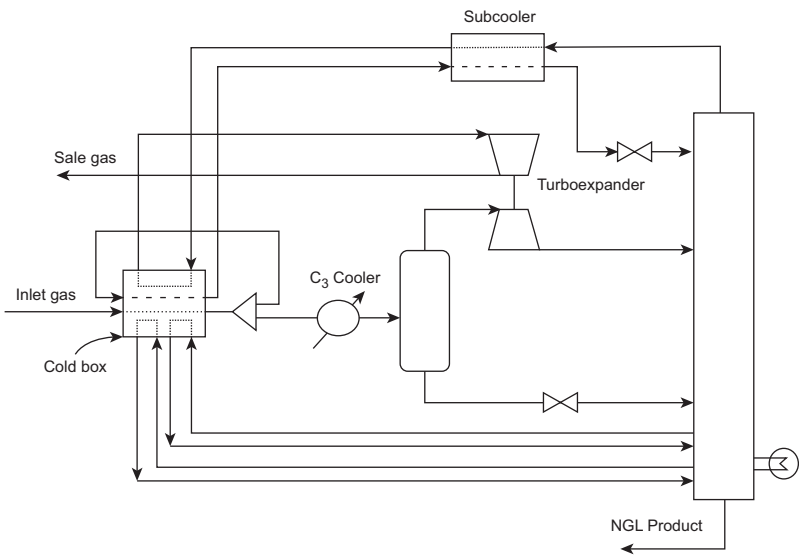

FIGURE 22.24

Schematic configuration of the HY-NGL process (Yoon et al., 2017).

0%−23% can be achieved through optimization and switching to the new HY-NGL configuration. Moreover, the new HY-NGL configuration is shown to be very energy efficient for most cases (Tables 22.12 and 22.13).

In particular, when considering a rich feed the new process configuration is able to give a significant reduction (18%) of energy consumption. However, for the case where there is a lean feed and a 30-stage column and 90% ethane recovery (Table 22.13), the CRR and RSV configurations are shown to give slightly better energy efficiency. In addition to these energy savings the optimal solutions are also able to give similar or higher ethane recovery (in some cases 0.1%−0.8% higher).

Table 22.12 Optimization Results for the Rich Feed Case Study (Yoon et al., 2017)

30 Trays, 85%						
	Recovery (%)		**C3 Compressor (kW)**	**Main Compressor (kW)**	**Expander (kW)**	**Total Power (kW)**
	C2	**C3**				
GSP	85.01	99.59	508.5	815.3	86.7	1237.1
CRR	85	99.64	420.2	840.9	78.2	1182.9
RSV	85.38	99.59	428.4	857.8	88.9	1197.3
HY-NGL	85.1	98.57	366.4	710.8	98.74	978.4
30 Trays, 90%						
	Recovery (%)		**C3 Compressor (kW)**	**Main Compressor (kW)**	**Expander (kW)**	**Total Power (kW)**
	C2	**C3**				
GSP	90.04	99.74	414.7	1080	113.2	1381.5
CRR	90.45	99.87	411.4	1032	90.4	1353
RSV	90.42	99.96	421.7	966.1	107.8	1280
HY-NGL	90.03	98.83	358.8	799.4	103.6	1054.6
10 Trays, 85%						
	Recovery (%)		**C3 Compressor (kW)**	**Main Compressor (kW)**	**Expander (kW)**	**Total Power (kW)**
	C2	**C3**				
GSP	85.01	99.71	504.7	822	87.5	1239.2
CRR	85.02	99.78	409.8	1001	100.4	1310.4
RSV	85.17	99.77	429.6	957.5	100.3	1286.8
HY-NGL	85.38	98.8	416.1	788.9	102.4	1102.6
10 Trays, 90%						
	Recovery (%)		**C3 Compressor (kW)**	**Main Compressor (kW)**	**Expander (kW)**	**Total Power (kW)**
	C2	**C3**				
GSP	90.13	99.75	538.3	842	62.4	1317.9
CRR	90.15	99.86	457.4	975.2	82.82	1349.8
RSV	90.13	99.96	424.1	1084	105.3	1402.8
HY-NGL	90.05	99.11	398.2	865.6	105.7	1158.1

GSP, *gas subcooled process;* RSV, *recycle split vapor.*

Table 22.13 Optimization Results for the Lean Feed Case Study (Yoon et al., 2017)

	Recovery (%)		C3 Compressor	Main Compressor	Expander	Total Power
	C2	C3	(kW)	(kW)	(kW)	(kW)
30 Trays, 85%						
GSP	85.05	97.89	81.2	693.0	135.3	638.9
CRR	85.06	98.75	45.6	730.4	143.3	632.7
RSV	85.02	99.81	82.1	657.4	111.6	627.9
HY-NGL	85.00	97.21	99.3	629.5	115.3	613.5
30 Trays, 90%						
	Recovery (%)		C3 Compressor	Main Compressor	Expander	Total Power
	C2	C3	(kW)	(kW)	(kW)	(kW)
GSP	90.98	98.78	110.9	866.5	150.3	827.1
CRR	90.08	98.90	40.1	818.4	159.0	699.5
RSV	90.13	99.70	77.3	742.5	122.0	697.8
HY-NGL	90.29	98.55	67.0	866.9	158.1	775.8
10 Trays, 85%						
	Recovery (%)		C3 Compressor	Main Compressor	Expander	Total Power
	C2	C3	(kW)	(kW)	(kW)	(kW)
GSP	85.06	98.18	123.9	734.3	128.6	729.6
CRR	85.14	97.86	106.0	738.2	123.5	720.7
RSV	85.08	99.30	107.7	952.4	149.2	910.9
HY-NGL	85.03	97.60	112.7	685.7	118.0	680.4
10 Trays, 90%						
	Recovery (%)		C3 Compressor	Main Compressor	Expander	Total Power
	C2	C3	(kW)	(kW)	(kW)	(kW)
GSP	90.13	98.65	108.4	844.4	148.1	804.7
CRR	90.26	98.75	93.80	903.9	156.1	841.6
RSV	90.01	99.72	122.6	1062.0	166.8	1017.8
HY-NGL	90.88	98.64	122.8	822.4	142.8	802.4

GSP, *gas subcooled process;* RSV, *recycle split vapor.*

Since the recovery of ethane is not always considered important depending on the operator's preference, market demands, and other reasons, Yoon et al. (2017) have also optimized the HY-NGL process with and without the inclusion of ethane recovery. Table 22.14 shows that operating in propane recovery mode (without considering ethane recovery) requires less energy due to the reduced separation requirements.

The HY-NGL process can be also modified to consider operational flexibility because operating conditions (e.g., the feed composition) and product specifications may change over time. This can be accomplished through the addition of an extra path connected to the separator vapor outlet, which

Table 22.14 Flexible Recovery Options With and Without Ethane Recovery (Yoon et al., 2017)

Rich Feed, 30 Tray						
	Recovery (%)		C_3 Compressor (kW)	Main Compressor (kW)	Expander (kW)	Total Power (kW)
	C_2	C_3				
C_2+C_3	85.1	98.57	366.4	710.8	98.7	978.4
C_3 only	73.74	95.13	365.5	552.3	71.2	846.6
Lean Feed, 30 Tray						
	Recovery (%)		C_3 Compressor (kW)	Main Compressor (kW)	Expander (kW)	Total Power (kW)
	C_2	C_3				
C_2+C_3	85	97.21	99.3	629.5	115.3	613.5
C_3 only	49.05	95.04	65.8	576.2	111.8	530.2

allows for two modes of operation, like either the GS process or the new HY-NGL process depending on the connections utilized (the reader can refer to the original work of Yoon et al. (2017) for this).

22.5.11 ENERGY SAVINGS THROUGH PROCESS INTENSIFICATION: CONDENSATE STABILIZATION

In the following, condensate stabilization is analyzed considering different literature case studies.

22.5.11.1 Condensate Stabilization

This case study is taken from Rabeau et al. (2007) who have analyzed the possibility to increase the efficiency on some process units, including condensate stabilization, to reduce CO_2 emissions. Thus, it shows a practical application of the benefit of process intensification for energy savings and for emissions reduction.

According to Rabeau et al. (2007), the consumptions of energy and the emissions of CO_2 for a typical LNG plant with production capacity of 25 million tonnes per year are located in the cold units (NGL recovery and liquefaction) and in the warm units (condensate stabilization, acid gas removal unit, dehydration unit), which account respectively for 82.0% and 14.0% of the total. Focusing on the warm units, the condensate stabilization one represents 20%−45% of the CO_2 emissions, the exact value depending on the heat power generation system used.

The simplest process scheme (Scheme 1) used for condensate stabilization is shown in Fig. 22.25. In this scheme, the high-pressure feed gas is expanded to the first high-pressure separator (V1). The liquid bottom of this first separator is further expanded to the middle-pressure level of the plant and fed to the middle-pressure vessel (V2). The liquid bottom from the middle-pressure separator (V2) is split into two parts: a first stream that is expanded to the low pressure of the system and fed (cold) on the first tray of the stabilizer, while the second part is expanded to the low pressure of the system, heated using the hot condensate coming from the bottom of the stabilizer and fed to the column. The stabilizer is operated at the lowest pressure of the system and is used to produce a bottom liquid stream rich in C_{5+} hydrocarbons and a top vapor stream rich in lighter hydrocarbons. The hot bottom stream from the stabilizer is used to preheat a part of the feed to the column, as previously said, while the light gases

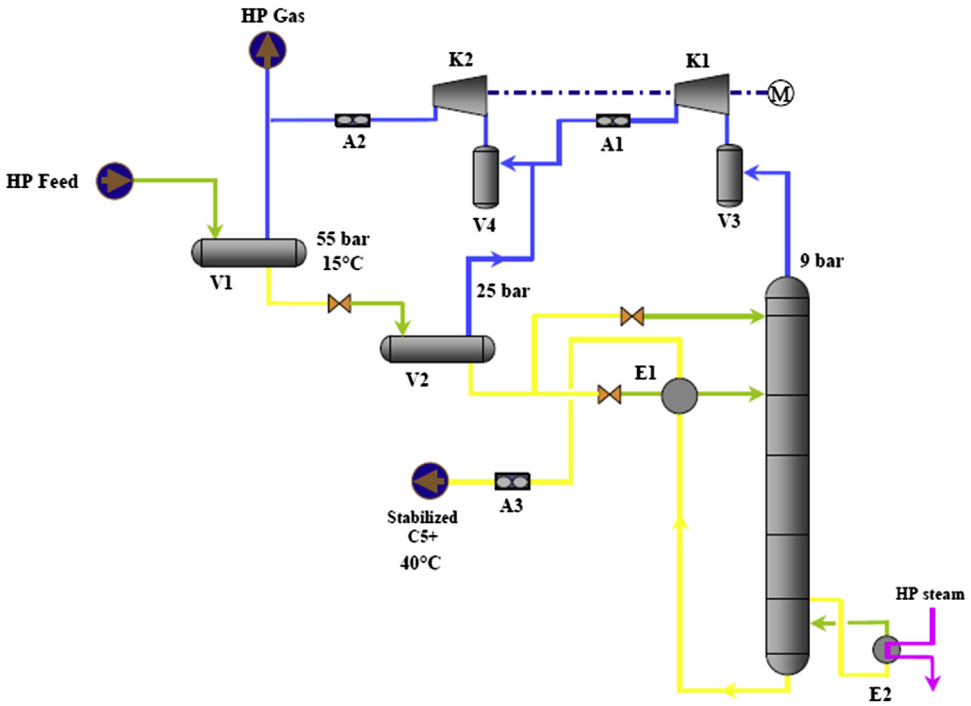

FIGURE 22.25

Process scheme of a condensate stabilization unit (Rabeau et al., 2007).

from the top of the stabilizer are compressed back to the middle-pressure of the process and mixed with the vapors coming from the middle-pressure vessel (V2). The resulting stream is compressed back to the high-pressure of the process and mixed with the vapors coming from the high-pressure vessel (V1).

Rabeau et al. (2007) have proposed different modifications for aiming at optimizing (1) the process scheme to obtain a better heat integration and (2) the operating parameters, mainly the pressure the stabilizer is operated at. The other process schemes are characterized by:

- Scheme 2: the addition of a reflux to the stabilizer to decrease the power of the off-gas compressor;
- Scheme 3: the addition of a side reboiler;
- Scheme 4: the addition of a second side reboiler.

The resulting process scheme after these modifications is shown in Fig. 22.26.

For each considered process scheme, Rabeau et al. (2007) have optimized the operating pressure of the stabilizer to obtain the lowest CO_2 emissions. Results of the investigation are reported in Table 22.15 together with reboiler duty, off-gas compressor power, and CO_2 emissions.

It can be concluded that 20% savings can be obtained by using heat integration and by optimization of the stabilizer pressure and that the reboiler duty can be reduced by about 28%. On the contrary, the

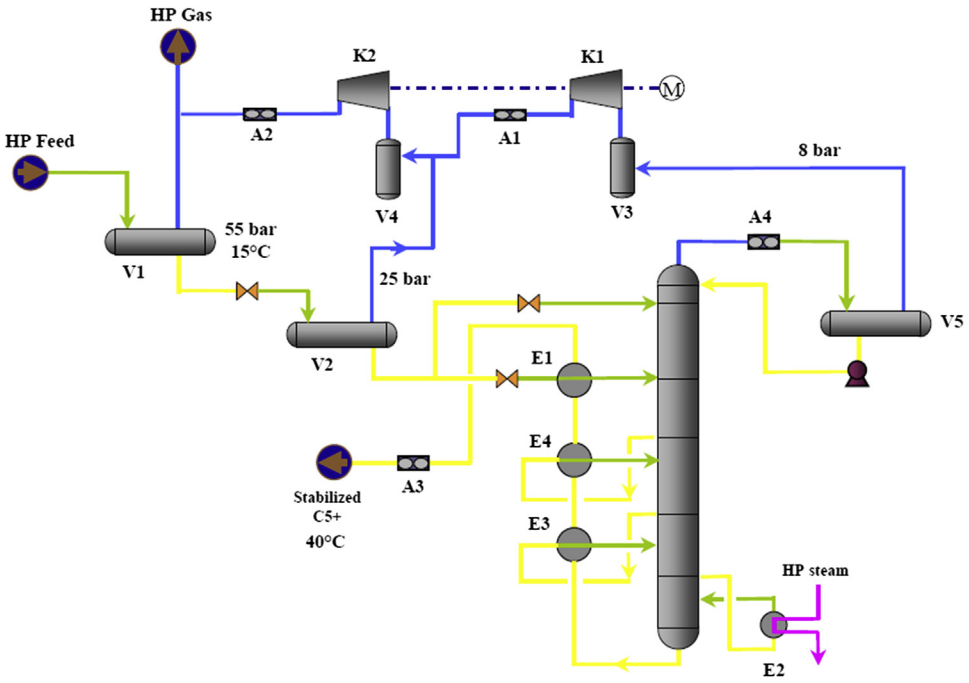

FIGURE 22.26

Process flow diagram for the condensate stabilization unit with heat integration (Rabeau et al., 2007).

off-gas compression work is not significantly affected by heat integration. Moreover, the use of side reboilers does not affect the operability of the system (Rabeau et al., 2007).

Considering Scheme 4, the numbers in Table 22.16 show how it is possible to reduce the amount of CO_2 emissions by optimization of the stabilizer pressure. In particular, going from 9.5 to 8 bar it is possible to reduce the reboiler duty by about 11%, but the compression work at the off-gas compressor will be increased by a similar amount. The reboiler duty decreases with pressure, while the compression work increases. The overall carbon dioxide emissions for the process units decrease by about 3.5% going from 9.5 to 8 bar, proving a positive benefit in terms of emissions. However, the

Table 22.15 Condensate Stabilization Heat Integration Results (Rabeau et al., 2007)

	Scheme 1	Scheme 2	Scheme 3	Scheme 4
Reboiler duty [kW]	53.6	54.5	42.2	38.4
Off-gas compression power [kW]	11.2	10.9	11.4	11.3
CO_2 emissions [T/h]	24	24	20.6	19.4
Stabilizer pressure [bar]	9	8.5	8	8

Table 22.16 Effect of the Stabilizer Operating Pressure on the Energy Consumptions and CO_2 Emissions of the Condensate Stabilization Unit for the Liquefied Natural Gas Plant, Considering Scheme 4 (Rabeau et al., 2007)

Stabilizer Pressure [bar]	9.5	9	8.5	8
Reboiler duty [kW]	43.3	41.8	40	38.4
Off-gas compression power [kW]	10.2	10.5	10.9	11.3
CO_2 emissions [T/h]	20.1	19.9	19.6	19.4

biggest contribution to energy savings and CO_2 emission mitigation comes from the process intensification strategy as it is possible to notice from Tables 22.15 and 22.16.

Therefore, this case study shows how the proper energy integration strategy in a process unit can significantly help to optimize the use of energy, reducing the consumptions and the emissions of carbon dioxide as well.

22.5.12 ANALYSIS OF ENERGY RECOVERY FROM TURBOEXPANDERS

The increasing demand for NGL, especially for ethane as a petrochemical feedstock, has resulted in the construction of turboexpander plants (TEPs) that recover ethane from natural gas streams at low temperatures, as low as −95°C. The TEPs involve gas turboexpansion cycles to attain, possibly without external refrigeration, the low temperatures desired for enhanced ethane recovery as high as 95%. Indeed, maintaining a high ethane recovery is crucial for the TEPs since even a less than 1% increase in recovery may lead to a significant increase in profits (Konukman and Akman, 2005). Since the earliest low-temperature expander plant was built 52 years ago, many alternative designs have been proposed to achieve higher ethane (and propane) recoveries. In the following, two literature case studies are presented about natural gas TEPs.

22.5.12.1 Flexibility and Operability Analysis of an HEN-Integrated Natural Gas Expander Plant

The first case study is taken from Konukman and Akman (2005) who refer to the simplified flow sheet of the TEP (Fig. 22.27) operating under ethane-recovery mode. With respect to it, the heat-integration efficiency is defined as the ability of the HEN to achieve chilling of the NG feed before entering the expander part of the plant with minimum external cooling requirement.

By starting from the TEP flow sheet/model available in the application-case library of HYSYS V2.4.1, Konukman and Akman (2005) have removed all the specifications to make it suitable for their performance-calculation purposes. In particular, the major changes have been made to the HEN part of the flow sheet. Fig. 22.28 illustrates the flow sheet of the HEN, which involves two rigorous (two-sided) heat exchangers (E-100 and E-103) and four nonrigorous (one-sided) ones (E-101, E-102, E-104, and E-105). Exchanger E-101 supplies heat to the reboiler of the demethanizer tower (DT), and exchangers E-102 and E-104 represent the side-stream reboilers of the DT. The major modification in the HEN part has been the addition of the two bypass streams (BP-1 and BP-2 in Fig. 22.28) around the

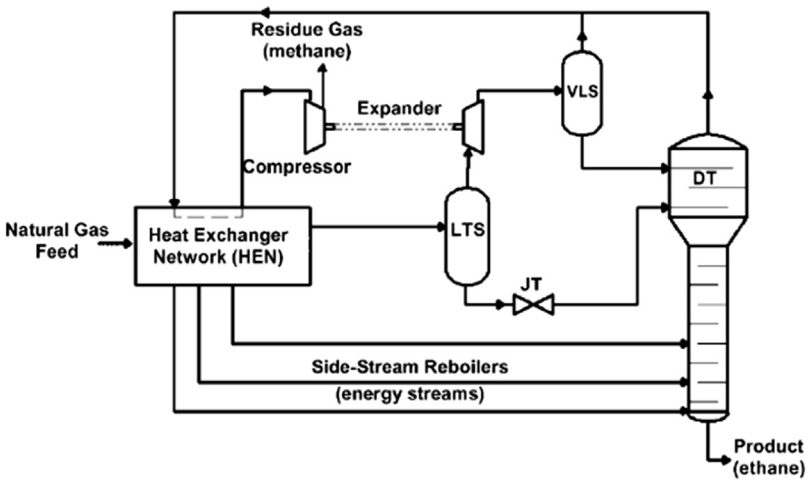

FIGURE 22.27

Simplified flow sheet of the turboexpander plant (Konukman and Akman, 2005).

two rigorous heat exchangers E-100 and E-103 to study the operability and flexibility of the HEN interacting with the plant. Indeed, this allows to manipulate the bypass flows in either the decreasing or increasing directions as dependent on the direction of the disturbance (e.g., decrease or increase in the feed gas temperature) at the expense of the UA values for the two exchangers E-100 and E-103.

Konukman and Akman (2005) have carried out the synthesis of the minimum-utility HEN structures at the base-case operating conditions summarized in Table 22.17, applying the superstructure-

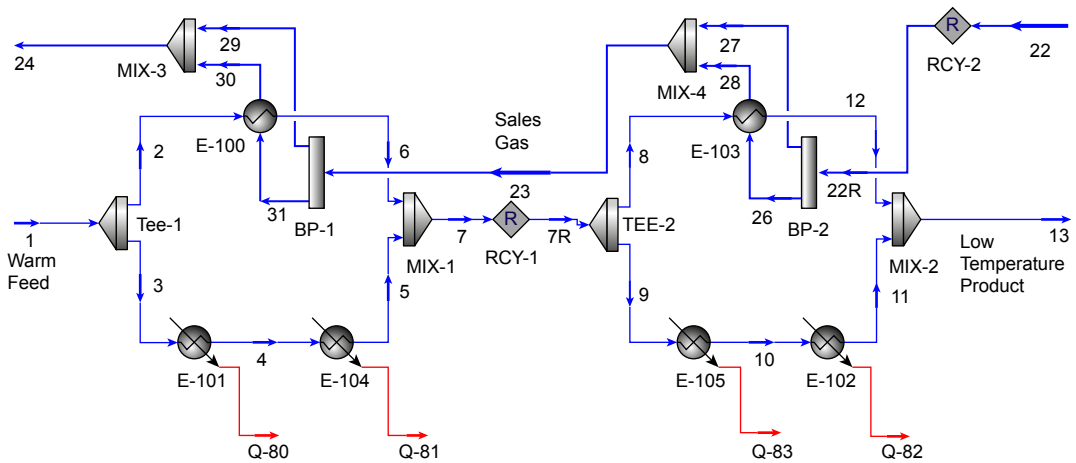

FIGURE 22.28

The HYSYS process subflow sheet diagram of the heat exchanger network (Konukman and Akman, 2005).

Table 22.17 Major Parameters Used for the Base-Case Solution (Konukman and Akman, 2005)

TEE-1	**Nominal Split Ratio (Stream 2 to Stream 1)**	**0.50**
TEE-2	Nominal split ratio (Stream 8 to Stream 7)	0.50
BP-1	Nominal bypass fraction (Stream 29 to Stream 6)	0.20
BP-2	Nominal bypass fraction (Stream 27 to Stream 22)	0.20
Q-80	Nominal heat duty	4.7322×10^6 kJ/h
Q-81	Fixed heat duty	1.5000×10^6 kJ/h
Q-82	Fixed heat duty	1.5000×10^6 kJ/h
Q-83	Fixed heat duty	5.0000×10^6 kJ/h
E−100	UA	1.5×10^6 kJ/°C-h
E−103	UA	1.0×10^6 kJ/°C-h
DT reboiler	Boil-up ratio ("boil-up" over Stream 21)	0.40

based simultaneous optimization formulation proposed by Yee and Grossmann (1990) and Yee et al. (1990). The final result has been that no external heating is required but only external cooling (load of 5×10^6 kJ/h) for minimum-approach-temperature less than 7°C.

Konukman and Akman (2005) have also investigated the effects of changing the NG feed temperature and pressure on ethane recovery, methane rejection, and on the mole fractions of methane and ethane in the residue and product. As a result, they have concluded that a 35°C nominal feed temperature seems to be optimal both considering the ethane recovery and methane recovery levels in the product streams (Fig. 22.29). Moreover, the methane mole fraction in the residue is not very sensitive

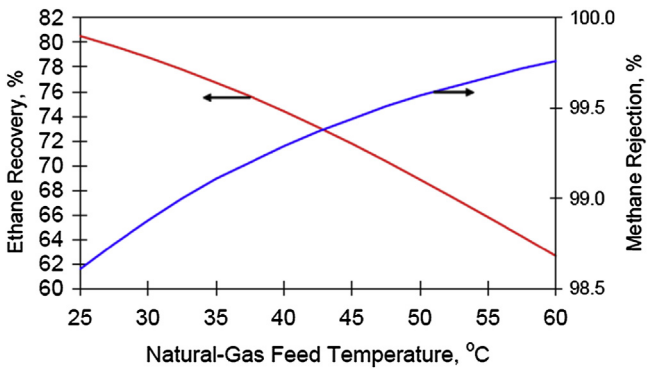

FIGURE 22.29

Ethane recovery and methane rejection as a function of the natural gas feed stream temperature (Konukman and Akman, 2005).

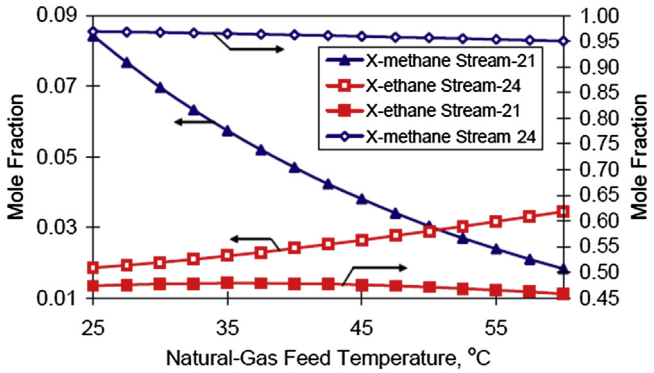

FIGURE 22.30

Mole fractions of ethane and methane in the residue and product streams as a function of the natural gas feed stream temperature (Konukman and Akman, 2005).

to the feed temperature, whereas the ethane mole fraction increases with increasing feed temperature indicating the increasing loss of ethane in the residue (Fig. 22.30).

As for the NG feed pressure, 60 atm nominal feed pressure seems to be optimal both considering the ethane recovery and methane rejection levels in the product stream (Fig. 22.31). Moreover, the methane mole fraction in the residue is not very sensitive to the feed pressure, whereas the ethane mole fraction decreases with increasing feed pressure, indicating the decreasing loss of ethane in the residue with increasing feed pressure (Fig. 22.32).

In investigating the operability and flexibility of the TEP, Konukman and Akman (2005) used the bypasses, the split fractions in the HEN, and the external cooling load as manipulated variables. To study the effects of the changes in these variables on ethane recovery, methane rejection, and on mole fractions of methane and ethane in the residue and product, they have made use of HYSYS's data book. The variables have been varied in the following range:

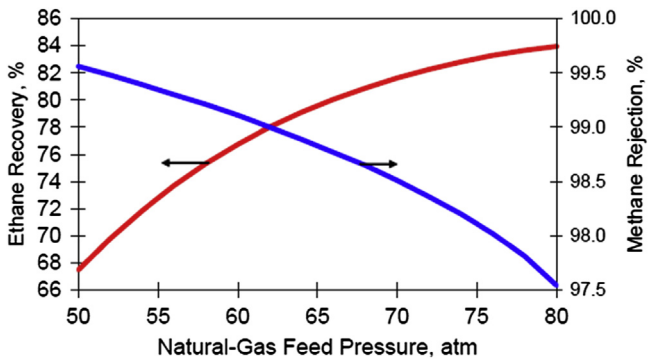

FIGURE 22.31

Ethane recovery and methane rejection as a function of the natural gas feed stream pressure (Konukman and Akman, 2005).

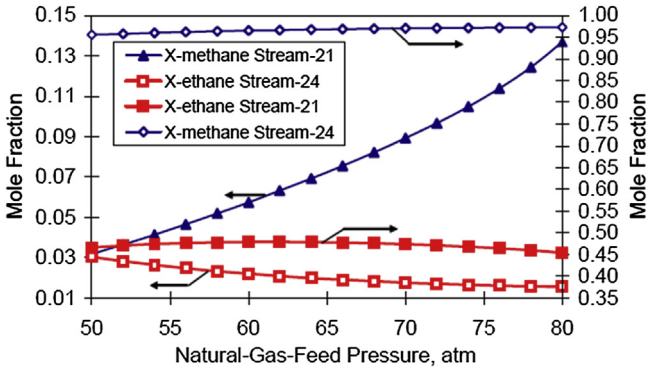

FIGURE 22.32

Mole fractions of ethane and methane in the residue and product streams as a function of the natural gas feed stream temperature (Konukman and Akman, 2005).

- 0.2−0.8 TEE-1 and TEE-2;
- 0−0.4 BP-1 and BP-2;
- 1×10^6−9×10^6 kJ/h external cooling load Q-83.

But these ranges have been normalized between [0,1] to facilitate the representation.
The following conclusions have been drawn by Konukman and Akman (2005):

- The control of the HEN outlet temperature should be done with the TEE-1 split fraction as the temperature decreases, for example, below −52°C (Fig. 22.33).

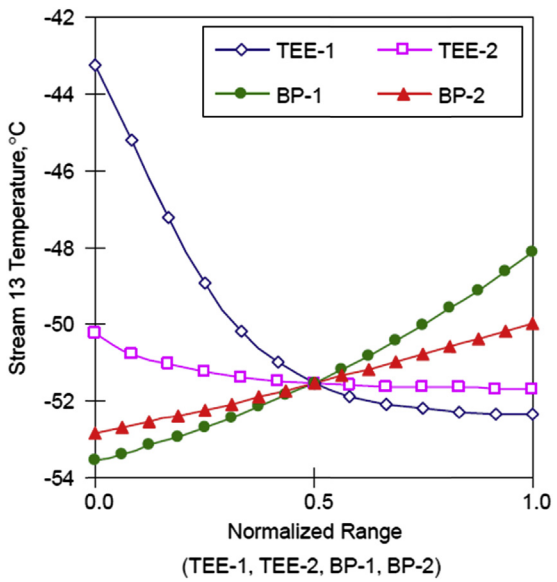

FIGURE 22.33

Temperature of the heat exchanger network outlet as a function of the normalized range of the manipulated variables (Konukman and Akman, 2005).

- The control of ethane recovery should be done with TEE-1 split for lower ethane recovery levels and with BP-1 bypass manipulation as the recovery increases, for example, below 75% (Fig. 22.34). Moreover, the external cooling load *Q-83* has more significant effect than other manipulated variables on ethane recovery.
- The control of ethane mole fraction should be done with the TEE-1 split fraction for lower ethane mole fraction levels and with BP-1 bypass manipulations as it increases, for example, above 0.5 (Fig. 22.35).
- The control of the methane rejection should be done with TEE-1 split and/or BP-1 bypass manipulations (Fig. 22.36).

In addition to this, Konukman and Akman (2005) have considered five disturbance scenarios (DS-1, DS-2, DS-3, DS-4, DS-5) characterized by a disturbance in the NG feed stream condition(s) and have dealt with the operability (steady-state control) problem aiming at determining how to keep the ethane recovery at its desired level (76.75% as in the base-case operating conditions) by using the four manipulated variables in the HEN of the TEP (i.e., all the previously mentioned variables except for the TEE-2 split, which has turned out to have a negligible effect on ethane recovery). They have concluded that TEE-1, BP-1, and BP-2 each alone are not able to keep the ethane recovery at its desired point for some disturbance scenarios. On the contrary, this has been possible for all scenarios using the external cooling load as the only manipulated variable, even if for some scenarios it has been greater than in the base case. This has led Konukman and Akman (2005) to state that the use of TEE-1, BP-1, and BP-2 accomplishes the ethane recovery control task without extra cooling.

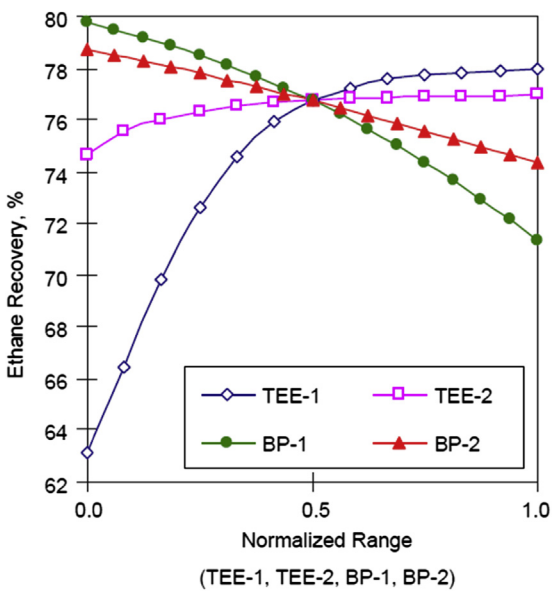

FIGURE 22.34

Ethane recovery as a function of the normalized range of the manipulated variables (Konukman and Akman, 2005).

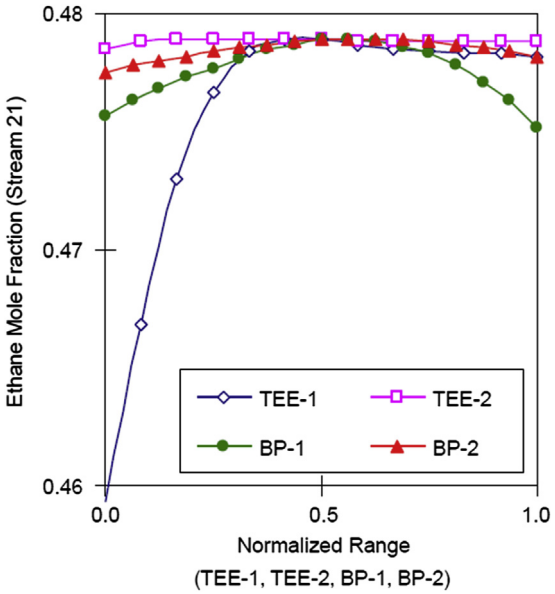

FIGURE 22.35

Ethane mole fraction as a function of the normalized range of the manipulated variables (Konukman and Akman, 2005).

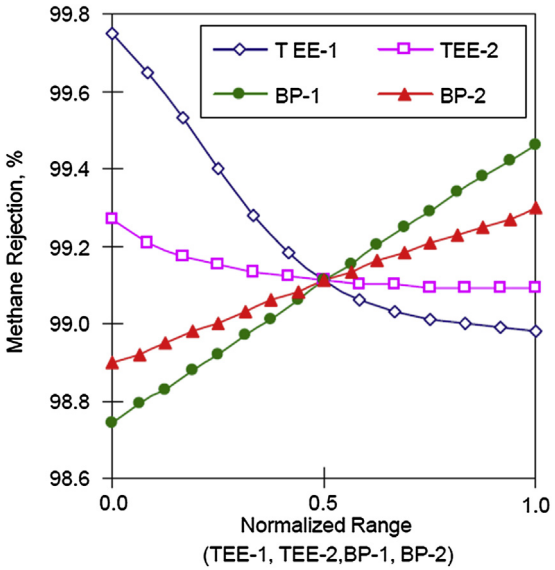

FIGURE 22.36

Methane rejection as a function of the normalized range of the manipulated variables (Konukman and Akman, 2005).

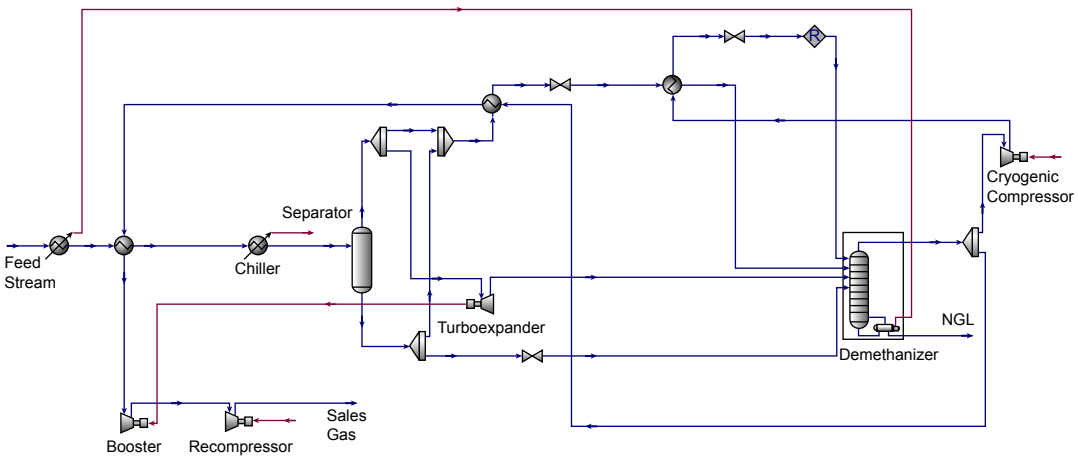

FIGURE 22.37

Cold residue reflux (CRR) process flow sheet (Kherbeck and Chebbi, 2015).

22.5.12.2 Optimizing Ethane Recovery in Turboexpander Processes

The following case study is taken from Kherbeck and Chebbi (2015) who have simulated the cold residue reflux (CRR) process (Fig. 22.37) to maximize ethane recovery at different demethanizer pressures (i.e., 100, 215, 335, and 450 psia) to cover the typical range, and for two different feeds (i.e., a lean gas with 6% C_{2+} content and a rich feed gas with 30% C_{2+} content).

The CRR process is built upon the GS process (Fig. 22.38). Results are compared with those of the optimized conventional process for ethane recovery (Fig. 22.39). The feed gas enters the NGL

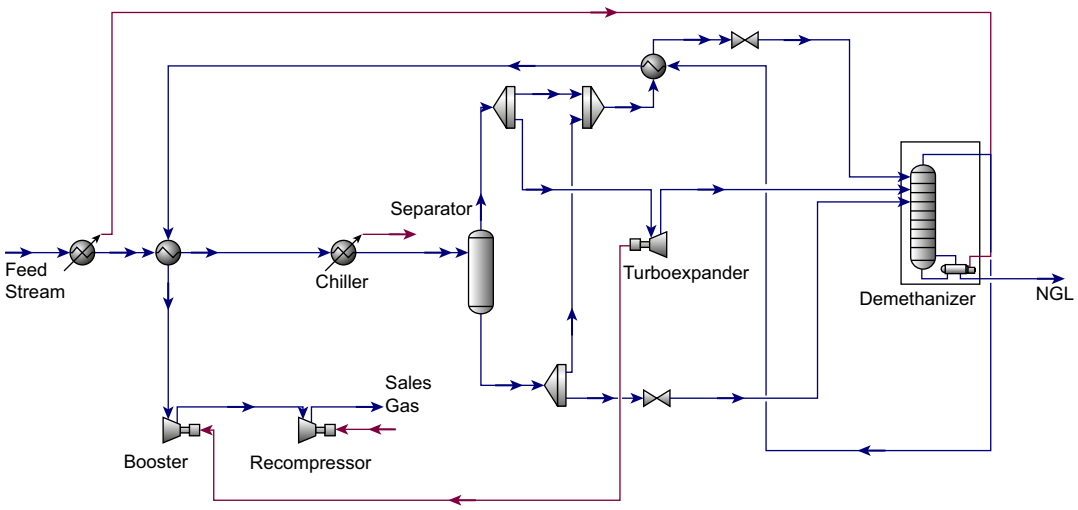

FIGURE 22.38

Gas subcooled (GS) process flow sheet (Kherbeck and Chebbi, 2015).

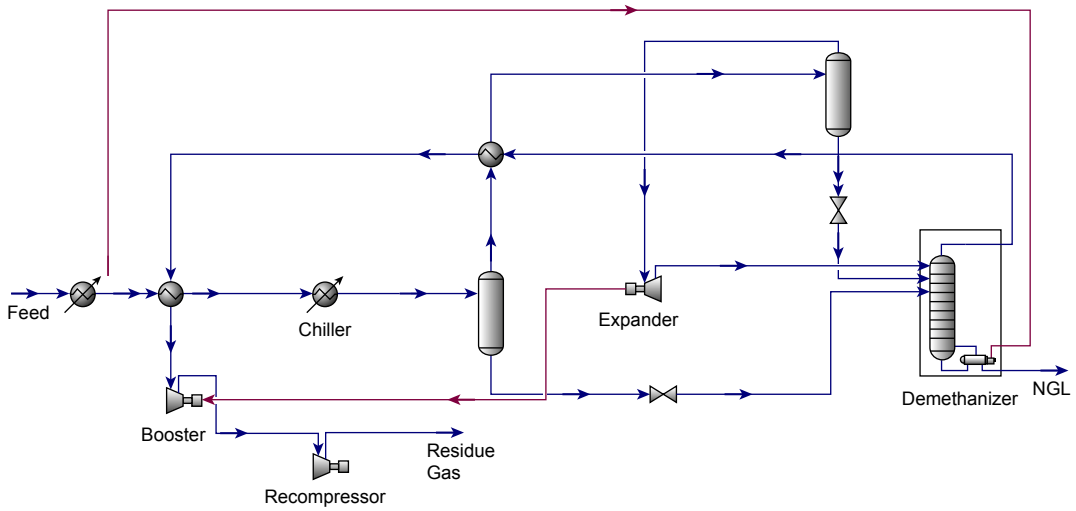

FIGURE 22.39

Conventional ethane recovery process optimized for maximum ethane recovery in Chebbi et al. (2008) and considered by Kherbeck and Chebbi (2015).

recovery unit with a flow rate of 10,980 lbmol/h and at 100°F and 882 psia and the residue gas is recompressed to 882 psia.

To maximize ethane recovery, Kherbeck and Chebbi (2015) have changed the following design variables: split ratios in all the splitters, the temperatures at the outlet of the heat exchangers following the mixer, and the cryogenic compressor outlet pressure. The optimization has been subject to the constraints set so as to prevent temperature cross in all the heat exchangers and to ensure that the reflux stream is colder than the flashed split-vapor stream as they enter the demethanizer.

The following conclusions can be drawn.

- For the lean gas, the CRR process, and hence the GS process, is not as effective at high demethanizer pressures, while the conventional one is not effective as the other two ones at low (100 psia) and intermediate (215 psia) demethanizer pressures (Fig. 22.40). By modifying the GS process, adding a cold separator, higher recoveries are obtained at high pressures.
- For the rich gas, the CRR process has been tested first and found to reduce to the GS one, which exhibits ethane recoveries close to the ones provided by the conventional turboexpander process at low and intermediate demethanizer pressures (Fig. 22.41). On the contrary, at high pressures the GS gives better recovery. As for the GS process with cold separator, Kherbeck and Chebbi (2015) have found that it gives recovery values similar to the other processes at low and intermediate pressures, while the recovery falls between the ones of the GS process and of the conventional turboexpansion process in the high-pressure range.
- For all the processes, the impact of the demethanizer pressure on ethane recovery is significantly less for the rich gas compared with the lean gas over the range 215−450 psia (Fig. 22.42 shows that for CRR/GS process, but the same has been obtained for the conventional turboexpander

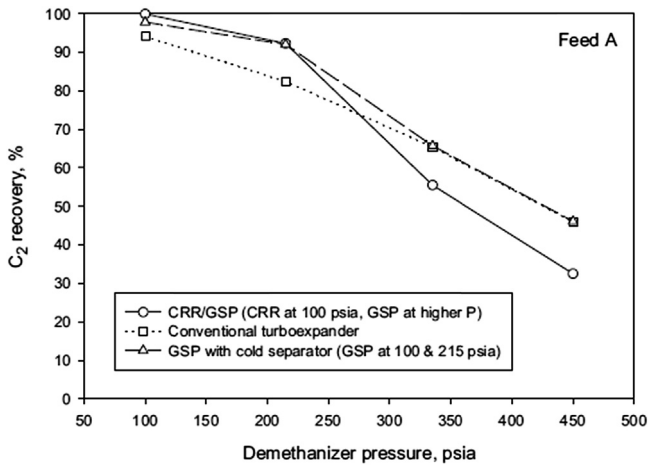

FIGURE 22.40

Effect of demethanizer pressure on ethane recovery for the lean feed gas A (1% nitrogen, 93% methane, 3% ethane, 1.5% propane, 0.9% butanes, 0.3% pentanes, 0.3% hexanes) (Kherbeck and Chebbi, 2015).

process (Chebbi et al., 2008) and GS process with cold separator). On the contrary, higher ethane recoveries are obtained for the lean gas at low pressures, whereas higher C_{2+} recoveries are obtained for the rich gas at intermediate and higher pressures.

22.5.13 RETROFIT OF EXISTING GAS PROCESSING PLANTS

Separation by distillation, the most widely used separation process in industry (Long and Lee, 2013), is known to be energy intensive (Hamidzadeh and Salehi, 2012): heat is supplied to the bottom reboiler

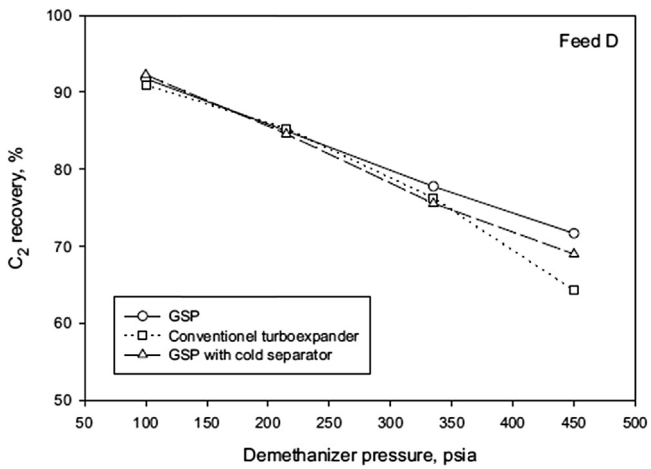

FIGURE 22.41

Effect of demethanizer pressure on ethane recovery for the rich feed gas D (1% nitrogen, 69% methane, 15% ethane, 7.5% propane, 4.5% butanes, 1.5% pentanes, 1.5% hexanes) (Kherbeck and Chebbi, 2015).

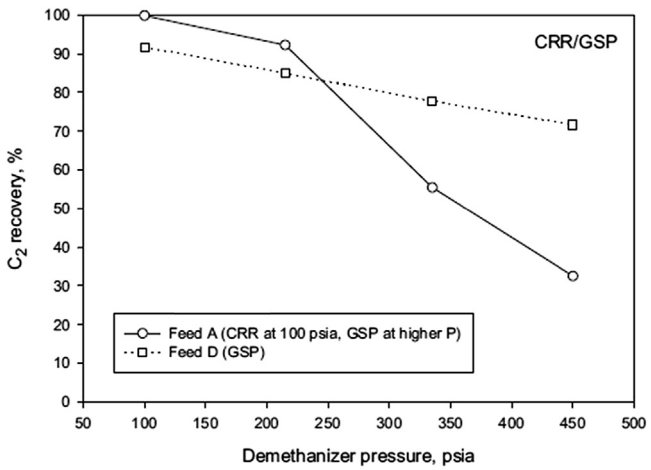

FIGURE 22.42

Effect of demethanizer pressure on ethane recovery for CRR/GSP process for feeds A and D (their composition is reported in the caption of Figs. 22.40 and 22.41, respectively) (Kherbeck and Chebbi, 2015).

(and sometimes to the feed heater) and the overhead stream is cooled in a condenser. Retrofits suggest modifications for existing distillation columns to reduce the costs of operations by increasing the efficiency in energy utilization.

Heat pumps in distillation allow to use the heat released at the condenser for evaporation in the reboiler: the vapor from the top of the column can be compressed to a certain pressure (increasing its temperature) and condensed in the reboiler through indirect contact with the liquid in the bottom of the column. This is an economic way of conserving energy when the difference in temperature between the overhead and bottom of the column is small and the heat load is high (Long and Lee, 2013). Heat pumps can be used in retrofitting designs because they are easy to introduce, and the plant operation is normally simpler than heat integration. However, they require high capital expenditure for compressors, which makes them industrially viable only for separation of substances with similar boiling points that require minimal compression costs (Long and Lee, 2013).

Self-heat recuperation technology is another way which helps to reduce the energy requirements of the process using compressors and self-heat exchangers based on energy recuperation (Long and Lee, 2013). Unlike the vapor recompression technology, which utilizes only the latent heat, it utilizes both the latent and sensible heat in the process, by recovering the cooling load by compressors and exchanging it with the heating load. Since it is imprudent to increase the pressure of the top vapor stream to a pressure that can boil the entire bottom liquid, the self-heat recuperation technology can be applied to a distillation process with a subsidiary reboiler (Long and Lee, 2013).

In the following, an application of the abovementioned concepts for retrofitting of distillation column(s) in gas separation plants is reported.

22.5.13.1 A Novel NGL Recovery Process Based on Self-Heat Recuperation

The following case study is taken from Long and Lee (2013) who have applied the self-heat recuperation technology to reduce the energy requirements of the deisobutanizing fractionation step of NGL processing. Conventionally, the distillation of C_2−C_4 from gasoline products (C_{5+}) is performed, followed by the distillation of iC_4 from nC_4, which is energy and capital intensive due to the low relative volatilities of these compounds.

Long and Lee (2013) have proposed two improved self-heat recuperative distillation processes:

- The *HES configuration* (heat exchangers in series), shown in Fig. 22.43: The compressed vapor is condensed in the column reboiler and then supplies heat to the feed stream, which also exchanges heat with the bottom product stream.
- The *HEP configuration* (heat exchangers in parallel), shown in Fig. 22.44: To maximize the heat recovery duty, the feed stream is divided into two parallel streams. A part of it is preheated by the bottom product stream, and the remaining part is preheated by the vapor from the top of the distillation column that has been compressed and condensed in the column reboiler. This stream is further cooled down before being divided into two streams: one is recycled back to the column as reflux, and the other is the final top product. The feed split ratio which allows to maximize the heat recovery duty and minimize the compressor power has been found to be 0.34.

The relative performances of the two processes are compared with those of the conventional column (Fig. 22.45) in Table 22.18. Savings in the condenser energy requirement and reboiler energy requirement compared with the conventional sequence are 83.23% and 93.95%, respectively, for the HES configuration, and 90.24% and 100.00%, respectively, for the HEP configuration. Thus, these sequences can be used in retrofit cases by installing new heat exchangers and compressors to reduce the energy consumption considerably.

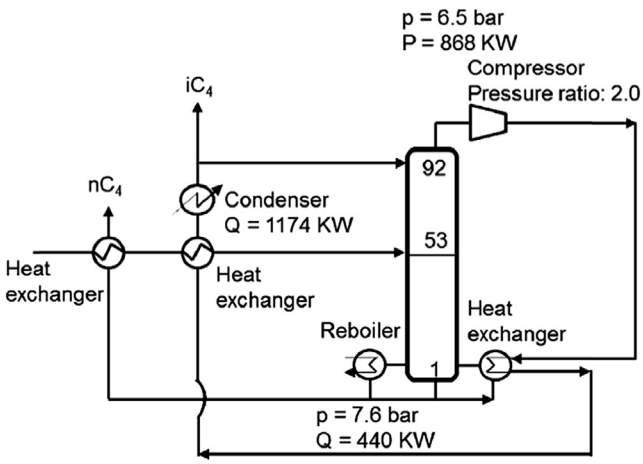

FIGURE 22.43

Simplified flow sheet illustrating the integrated distillation process (heat exchangers in series configuration) proposed by Long and Lee (2013).

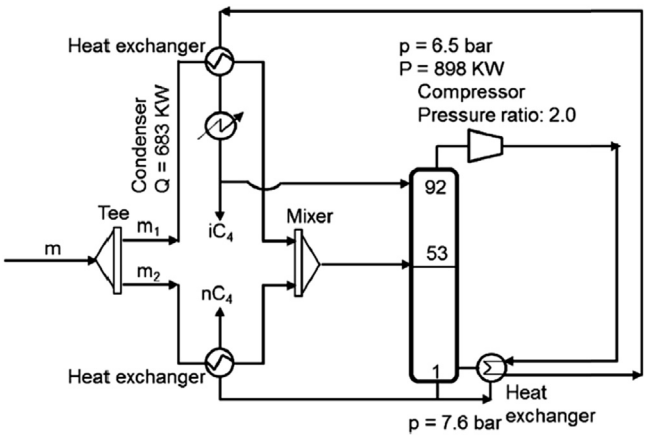

FIGURE 22.44

Simplified flow sheet illustrating the integrated distillation process (heat exchangers in parallel configuration) proposed by Long and Lee (2013).

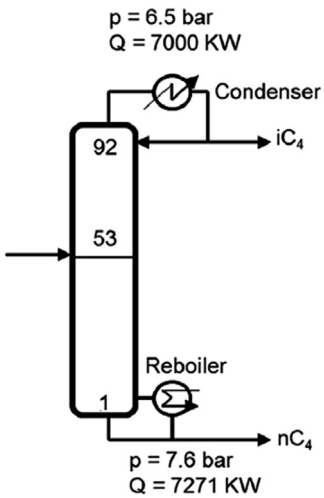

FIGURE 22.45

Simplified flow sheet illustrating the conventional deisobutanizer column (Long and Lee, 2013).

Table 22.18 Summary of Relative Performance for Conventional Deisobutanizer Column, the Heat Exchangers in Series (HES) and Heat Exchangers in Parallel (HEP) Configurations (Long and Lee, 2013)

	Conventional Column	HES Configuration	HEP Configuration
Energy requirement saving in condenser (%)	0.00	83.23	90.24
Energy requirement saving in reboiler (%)	0.00	93.95	100.00

REFERENCES

Addington, L., Ness, C., May 13−15, 2009. An evaluation of general rules of thumb in amine sweetening unit design and operation. Paper Presented at the GPA Europe Sour Gas Processing Conference, Sitges, Spain.

Baccanelli, M., Langé, S., Rocco, M.V., Pellegrini, L.A., Colombo, E., 2016. Low temperature techniques for natural gas purification and LNG production: an energy and exergy analysis. Applied Energy 180, 546−559.

Bejan, A., 1997. Advanced Engineering Thermodynamics. John Wiley & Sons, New York, NY, USA.

Bejan, A., 2002. Fundamentals of exergy analysis, entropy generation minimization, and the generation of flow architecture. International Journal of Energy Research 26 (7), 545−565.

Cápek, V., Sheehan, D.P., 2005. Challenges to the Second Law of Thermodynamics. Springer, Dordrecht, The Netherlands.

Carnot, S., 1978. Réflexions sur la puissance motrice du feu. Vrin, Paris.

Carnot, S., Carnot, H., Kelvin, W.T.B., 1897. Reflections on the Motive Power of Heat: From the Original French of N.-L.-S. Carnot, second ed. John Wiley & Sons, New York, NY, USA.

Cengel, Y.A., Boles, M.A., 2006. Thermodynamics: An Engineering Approach, fifth ed. McGraw-Hill, New York, NY, USA.

Chakma, A., 1997. CO_2 capture processes - opportunities for improved energy efficiencies. Energy Conversion and Management 38, S51−S56.

Chebbi, R., Al Mazroui, K.A., Abdel Jabbar, N.M., 2008. Study compares C2-Recovery for conventional turboexpander, GSP. Oil & Gas Journal 106 (46), 50−54.

Clausius, R., 1864. Abhandlungungen. uber die mechanische W. Armetheorie, vol. 2. F. Vieweg, Braunschweig, Germany.

CleaverBrooks, 2011. Boiler Efficiency Guide-facts about Firetube Boilers and Boiler Efficiency. Thomasville, GA, USA.

Demirel, Y., 2012. Energy and Energy Types. Energy, Springer, London, UK.

Gaggioli, R.A., 1998. Available energy and exergy. International Journal of Thermodynamics 1 (1−4), 1−8.

GPSA, 2004. Engineering Data Book, twelfth ed. Gas Processors Suppliers Association (GPSA), Tulsa, OK, USA.

Hamidzadeh, Z., Salehi, R., March 5-7, 2012. Retrofit of Distillation Columns in Gas Separation Plants. Paper Presented at the 3rd International Gas Processing Symposium, Doha, Qatar.

Holmes, A.S., Ryan, J.M., March 9, 1982a. Cryogenic Distillative Separation of Acid Gases from Methane. Patent No. US4318723 A.

Holmes, A.S., Ryan, J.M., September 21, 1982b. Distillative Separation of Carbon Dioxide from Light Hydrocarbons. Patent No. US4350511 A.

Holmes, A., Price, B., Ryan, J., Styring, R., 1983. Pilot tests prove-out cryogenic acid-gas/hydrocarbon separation processes. Oil & Gas Journal 81 (26), 85−91.

Ikoku, C.U., 1992. Natural Gas Production Engineering. Krieger Pub. Co, Malabar, FL, USA.

Kanoğlu, M., 2002. Exergy analysis of multistage cascade refrigeration cycle used for natural gas liquefaction. International Journal of Energy Research 26 (8), 763−774.

Kehlhofer, R., Hannemann, F., Rukes, B., Stirnimann, F., 2009. Combined-cycle Gas and Steam Turbine Power Plants, third ed. PennWell Books, Tulsa, OK, USA.

Kelvin, L., Thomson, W., 1882. Mathematical and Physical Papers. Cambridge University Press, Cambridge, UK.

Kent, R.L., Eisenberg, B., 1976. Better data for amine treating. Hydrocarbon Processing 55 (2), 87−90.

Kherbeck, L., Chebbi, R., 2015. Optimizing ethane recovery in turboexpander processes. Journal of Industrial and Engineering Chemistry 21, 292−297.

Kidnay, A.J., Parrish, W.R., 2006. Fundamentals of Natural Gas Processing, first ed. CRC Press, Boca Raton, FL, USA.

Konukman, A.E.S., Akman, U., 2005. Flexibility and operability analysis of a HEN-integrated natural gas expander plant. Chemical Engineering Science 60 (24), 7057−7074.

Kotas, T., 1985. The Exergy Method of Thermal Plant Analysis. Butterworths, London, UK.

Langé, S., Pellegrini, L.A., 2016. Energy analysis of the new dual-pressure low-temperature distillation process for natural gas purification integrated with natural gas liquids recovery. Industrial and Engineering Chemistry Research 55 (28), 7742−7767.

Langè, S., Pellegrini, L.A., Vergani, P., Lo Savio, M., 2015. Energy and economic analysis of a new low-temperature distillation process for the upgrading of high-CO_2 content natural gas streams. Industrial and Engineering Chemistry Research 54 (40), 9770−9782.

Linnhoff, B., 1998. Introduction to Pinch Technology. Linnhoff March Ltd, Northwich, Cheshire, England.

Long, N.V.D., Lee, M., 2013. A novel NGL recovery process based on self-heat recuperation. Energy 57, 663−670.

Maddox, R.N., 1974. Gas and Liquid Sweetening. Campbell Petroleum Series, Norman, OK, USA.

Mafi, M., Naeynian, S.M., Amidpour, M., 2009. Exergy analysis of multistage cascade low temperature refrigeration systems used in Olefin plants. International Journal of Refrigeration 32 (2), 279−294.

Moran, M.J., Shapiro, H.N., 2006. Fundamentals of Engineering Thermodynamics, fifth ed. John Wiley & Sons, Chichester, England.

Moran, M.J., 1982. Availability Analysis: A Guide to Efficient Energy Use. Prentice Hall PTR, New Jersey, NJ, USA.

Northrop, P.S., Valencia, J.A., 2009. The CFZ™ process: a cryogenic method for handling high-CO_2 and H_2S gas reserves and facilitating geosequestration of CO_2 and acid gases. Energy Procedia 1 (1), 171−177.

Pellegrini, L.A., October 1, 2015. Process for the Removal of CO_2 from Acid Gas. Patent No. US Patent 20150276308 A1.

Pellegrini, L.A., Langè, S., Baccanelli, M., De Guido, G., March 25−27, 2015. Techno-economic Analysis of LNG Production Using Cryogenic Vs Conventional Techniques for Natural Gas Purification. Paper Presented at the Offshore Mediterranean Conference and Exhibition, Ravenna, Italy.

Pellegrini, L.A., De Guido, G., Lodi, G., Mokhatab, S., September 24−27, 2017. CO_2 Capture from Natural Gas in LNG Production: Comparison of Low-temperature Purification Processes and Conventional Amine Scrubbing. Paper presented at the Cutting-Edge Technology for Carbon Capture, Utilization And Storage (CETCCUS), Clermont-Ferrand, France.

Pellegrini, L.A., De Guido, G., Langé, S., 2018. Biogas to liquefied biomethane via cryogenic upgrading technologies. Renewable Energy 124, 75−83.

Perry, R.H., Green, D.W., 2008. Perry's Chemical Engineers' Handbook, seventh ed. McGraw-Hill, New York, NY, USA.

Petela, R., 1964. Exergy of heat radiation. Journal of Heat Transfer 86 (2), 187−192.

Pitman, R.N., Hudson, H.M., Wilkinson, J.D., Cuellar, K.T., March 16−18, 1998. Next Generation Processes for NGL/LPG Recovery. Paper presented at the 77th Annual GPA Convention, Dallas, TX, USA.

Querol, E., Gonzalez-Regueral, B., Perez-Benedito, J.L., 2012. Practical Approach to Exergy and Thermoeconomic Analyses of Industrial Processes. Springer Science & Business Media, New York, NY, USA.

Rabeau, P., Paradowski, H., Launois, J., April 24−27, 2007. How to Reduce CO_2 Emissions in the LNG Chain. Paper Presented at the 15th International Conference & Exhibition on Liquefied Natural Gas (LNG 15), Barcelona, Spain.

Sciubba, E., Wall, G., 2007. A brief commented history of exergy from the beginnings to 2004. International Journal of Thermodynamics 10 (1), 1−26.

Shin, J., Yoon, S., Kim, J.-K., 2015. Application of exergy analysis for improving energy efficiency of natural gas liquids recovery processes. Applied Thermal Engineering 75, 967−977.

Szargut, J., 1980. International progress in second law analysis. Energy 5 (8−9), 709−718.

Voldsund, M., 2014. Exergy Analysis of Offshore Oil and Gas Processing. PhD Thesis, Norwegian University of Science and Technology, Trondheim, Norway.

Wall, G., 1977. Exergy-a Useful Concept within Resource Accounting. Chalmers Tekniska Högskola, Göteborgs Universitet, Göteborg, Sweden.

Yee, T.F., Grossmann, I.E., 1990. Simultaneous optimization models for heat integration—ii. Heat exchanger network synthesis. Computers and Chemical Engineering 14 (10), 1165−1184.

Yee, T.F., Grossmann, I.E., Kravanja, Z., 1990. Simultaneous optimization models for heat integration—I. Area and energy targeting and modeling of multi-stream exchangers. Computers and Chemical Engineering 14 (10), 1151−1164.

Yoon, S., Binns, M., Park, S., Kim, J.K., 2017. Development of energy-efficient processes for natural gas liquids recovery. Energy 128, 768−775.

Zhang, J., Xu, Q., 2011. Cascade refrigeration system synthesis based on exergy analysis. Computers and Chemical Engineering 35 (9), 1901−1914.

CHAPTER

MAXIMIZING PROFITABILITY OF GAS PLANT ASSETS 23

23.1 INTRODUCTION

Maximizing the return on gas plant assets becomes increasingly difficult because of the rising cost of energy in some cases and the increased demand for operations agility in most cases. On top of these demands, there is the constant need to increase the availability and utilization of these plants. It is worthwhile to consider techniques and the profit improvement of some of the world's best gas plants. This analysis identifies some key manufacturing and business strategies that appear to be necessary and are feasible for many facilities to achieve and sustain satisfactory performance. The essential nature of operating a gas plant is dealing with change. Disturbances such as slugging, trips of gathering compressors, weather changes, and changes in market demands make it challenging to operate reliably let alone profitably. A stabilization strategy is necessary but insufficient for most gas plants; it is necessary to sustain a degree of flexibility. A useful objective can be tracking desired changes and withstanding undesired changes in a manner that is safe, environmentally sound, and profitable (DeVries et al., 2001).

The main challenges to gas plant profitability are:

- continuous energy, yield, and throughput inefficiency due to providing operating margin for upsets and plant swings,
- continuous energy, yield, and throughput inefficiency due to not operating at optimum conditions,
- energy, yield, and throughput inefficiency due to the consumption during plant swings,
- labor costs to operate and support a gas plant—a poorer performing plant requires more personnel with a higher average salary,
- plant integrity,
- process and equipment reliability,
- poor throughput due to low availability,
- maintenance,
- safety.

Poorer performance compounds the cost challenges in most gas plants. To ensure these problems are avoided, it is essential to develop a fundamental understanding of all the technical factors impacting the performance of the plant, how they interact, and how they manifest themselves in business performance. This can only be achieved through the application of an integrated approach using the diverse skills of a multidisciplined team of engineers combined with the application of a robust performance-modeling tool. Technical assessments allow an understanding of technical risks to

Handbook of Natural Gas Transmission and Processing. https://doi.org/10.1016/B978-0-12-815817-3.00023-X

which the facility is exposed, ranging from deterioration of equipment due to exposure to corrosive environments to poor process efficiency as a result of poor design. Integration of expertise within a single team, which covers the broad range of technical fields involved in the operation of the gas-processing plant, ensures that all the technical risks and interactions are identified.

The following are the other business questions that asset managers are asking themselves (Howell, 2004):

- Are the assets performing according to plan, and how do we know?
- Are we choosing the optimal plans for developing the assets over their lifetime?
- Are we achieving the targeted return on capital employed for the assets?
- Are we meeting all the ever-growing health, safety, and environment guidelines?
- Can we forecast reliably, allocate with confidence, or optimize with knowledge?
- Do we derive enough value from the simulation and engineering model investments?
- How effective is the organization at capital avoidance?
- Are we drowning in data or are we knee-deep in knowledge?

Another area of opportunity is optimization of the process to maximize capacity or yields and minimize energy consumption while maintaining product qualities. Many tools have become available as powerful, inexpensive computing power has become available to run complex software quickly and reliably.

This chapter describes a vision of the integrated gas plant of the future and methods to identify solutions for attaining operational goals to maximize asset values.

23.2 THE PERFORMANCE STRATEGY OF THE INTEGRATED GAS PLANT

Successful gas plants have found that a combination of techniques is necessary:

1. a strategy to influence organizational behavior,
2. a strategy to integrate information,
3. an operations strategy that uses remote operations and support of unmanned plants,
4. process performance monitoring,
5. asset management,
6. process optimization implementation.

Merely adding technology without developing a new organizational behavior and operations strategy has often reduced gas plant performance instead of improving it.

The revolution in digital technologies could well transform the industry. Achieving the vision of the integrated gas plant of the future will require more than new technologies alone. It will require the alignment of strategy structure, culture, systems, business processes, and perhaps most importantly, the behaviors of people. Visionary companies who truly want to capture the "digital value" will need to create a climate for change, then maintain strong leadership through the change and use the skills and techniques from vendors to provide the technologies.

Gas plant operators are looking to integrate global operations and the energy supply chain into a cohesive picture. A global enterprise resource planning system gives companies the resources they need to better balance supply with demand, reduce inefficiencies and redundancies, and lower the total cost of information technology infrastructures. The challenge is to develop overlay solutions with

more domain content that can improve the knowledge inside the enterprise systems that producers depend on most for operations, planning, project management, workflow, document management, executive information and decision support, scheduling, database management, data warehousing, and much more.

The industry must capitalize on the opportunities provided by ever more capable and cost-effective digital technology.

23.3 STRATEGIES FOR ORGANIZATIONAL BEHAVIOR AND INFORMATION

Understanding and managing organizational behavior is an important element of effective operations. The effective management and coupling of technology to people is a crucial element in ensuring that the plant's culture will change to support modern manufacturing strategies. Four typical organizational cultures have been observed (Neumann, 1999). These cultures vary from cultures very resistant to change, which change for the sake of change.

23.4 ORGANIZATIONAL BEHAVIOR MODEL

It is worthwhile to review recent modeling attempts for organizational behavior. Two models, each focusing on different aspects of the organization, deserve exploration. Both attempt to explain the influence of information and management activities on organizational behavior. The first model, as shown in Fig. 23.1, attempts to identify and provide a structure for the various major influences on the organization.

The above mentioned model supports the following observations:

1. Unless constrained by their situation, people will improve their behavior if they have better information on which to act.

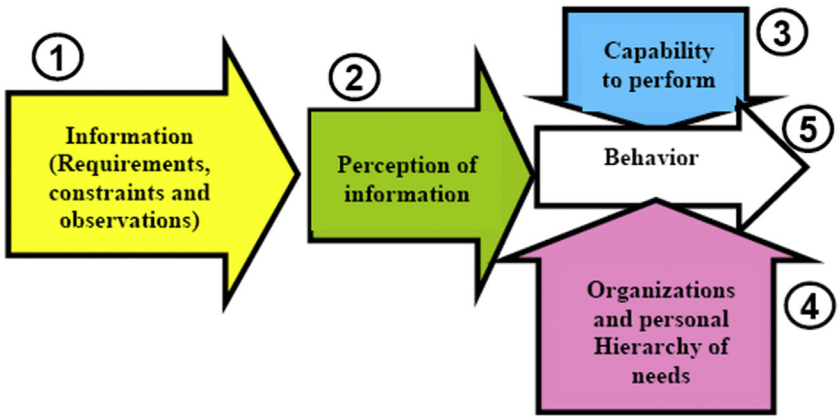

FIGURE 23.1

Major influences on the organization (DeVries et al., 2001).

2. Behavior is constrained by their capability to perform. This constraint is tied to the span of their control, their associated physical assets, and so forth, which is what the military calls "readiness".
3. The classical personal hierarchy of needs (Mazlow, 1968) that ranges as "survival," "hunger," and "need to belong" applies to organizations as well.

23.4.1 INFORMATION QUALITY

The natural gas–processing industry is unusual in its high degree of dependence on information technology to meet its business goals. With the enormous quantities of data that it generates and processes, an edge is gained by ensuring the quality of the data and using the information intelligently. Alongside this problem, the industry is addressing the changes required due to new and evolving working practices that the popularity of interdisciplinary asset teams has brought about.

This organizational model explains in part why people and organizations behave in a rebellious manner in spite of receiving "better" information. For example, operators and their supervisors are penalized for "tripping" units and major equipment; however, e-business decisions might require them to operate the plant in a manner that would increase the likelihood of trips. Another example is that a plant or unit's performance is broadcasted to a team of marketing and other plants while the plant or unit is chronically "under performing" based on the other organizations' expectations. This motivates the plant's managers to hide information and resist plans for performance improvement.

This model also points to a key issue in managing technology. Poor-quality information will be discarded, and information that is harder to use will not be used. This points to the need to define the quality of information. Suggested attributes of information quality include:

- available (is the information chain broken?)
- timely
- in the right context
- accurate
- to the right place
- easy to understand

It may be helpful to imagine a fuel gauge in the dashboard of a car. If the fuel gauge is working 75% of the time, the driver will not trust it and the gauge will be ignored. In process plants, information has to be much more reliable than that to be trusted.

Gas plants struggle to convert supply chain schedules into actual plans. Too often, the marketing department does not have appropriate feedback that equipment has failed or that a current swing in recovery mode is taking longer than expected to complete. Conversely, the operations department often lacks the tools to plan which resources and lineups to use while avoiding poor utilization of equipment. This gap between strategic and tactical scheduling is sometimes referred to as the "operations wall".

Much attention is given to networking information and knowledge software. So much attention is given to making as many components as possible accessible via the Web, to support virtual private networks and restructuring knowledge software using application service providers. This work is worthwhile, but the underlying information reliability issues are chronic and damage the credibility of major network and software installations.

The old expression "if garbage goes into the computer, then garbage will come out" is especially true for modern information technology strategies that end up with more than seven layers of components that process information. It is extremely important to note the following:

1. Much of the information used to enhance and change plant performance, as well as support supply chain management decisions, is based on sensors that degrade in accuracy and "fail" due to stresses or material that reduces their ability to produce a reliable measurement. A modern hydrocarbon-processing plant uses hundreds of these to support advanced control and advanced information software. Simply connecting digital networks to these sensors does not improve information reliability if the sensors do not have enough "intelligence" to detect and possibly compensate for failure or inability to measure.
2. Most components and software packages process online diagnostic information that gives some indication of the reliability of the information. However, most installations do not integrate these diagnostics with the calculations. If the information reliability of each of seven components from the sensor to the top e-business software is 95%, then on average the overall information reliability is no better than 69%. Raising the component reliability to 99% still only yields a maximum overall information reliability of 93%, which is unacceptable for supply chain management.

Therefore it is important to use as much "intelligence" as possible at all levels and maintain the integration of on-line quality statuses to maximize the quality and minimize the time to repair the failures.

23.4.2 PERCEPTION OF INFORMATION

Tables of menus and numbers do not help when a downsized team is asked to open multiple applications and "mine" for information. Most information displays are essentially number tables or bar graphs superimposed on plant flowsheets. Several plant examples exist to show how this interferes with improved performance.

23.4.2.1 Two-Dimensional Curves and Plots

As an example, compressors can be the main constraining factor in major hydrocarbon-processing facilities, and it is important to maintain the flow through each stage of compression sufficiently high to avoid surge. Too low pressure increase is inefficient and limits production throughput. The most efficient is higher pressure increases, but this yields operation closer to surge. Operators are normally given a pair of numbers or bar graphs for pressure and flow, and they need to recall from experience where the "operating point" is compared to the "surge line". To make matters worse, the "surge line" changes position as the gas's characteristics change. To solve this, plot the moving surge line and the operating point in real time. This is a suitable solution for distillation and reactor temperature profiles as well (Fig. 23.2).

23.4.2.2 Prediction Trends

The same operators who avoid trips tend to shut off advanced control software when the software is driving the plant toward undesirable states. But often the software is only using a spike to accelerate the transition for best performance, and the top of the spike still keeps the plant in the desirable state.

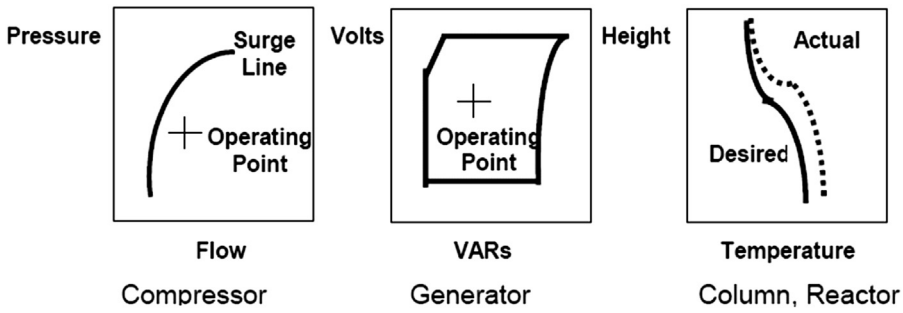

FIGURE 23.2

Examples of two-dimensional curves and plots (DeVries et al., 2001). *VARs*, volt-amperes reactive.

Prediction trends allow operators to see the remainder of the curve, so that if the curve looks safe, they will allow the software to continue with the spike.

23.4.2.3 Dynamic Performance Measures

Operators and their supervisors are given performance information and targets, but often the information is not "actionable", i.e., they cannot directly influence the information (Fig. 23.3). Furthermore, as manufacturing strategies change, they receive e-mails with a set of numbers. Ideally, the senior operators and their chain of management are seeing the targets and acceptable bands along with each actionable performance measure. In this way, coordination of a change in manufacturing tactic is faster and easier. A common example is changing from maximum throughput (at the expense of efficiency) to maximum efficiency (at the expense of throughout) to take advantage of market opportunities and minimize costs when the demand is reduced.

23.4.2.4 Performance Messages

Operators who monitor long batches, especially batches that will cover a shift change, tend to have lower productivity, especially during times that the main support staff is not available. Ingredients that exhibit quality problems can be used in applications such as in-line blending of fuels and batch

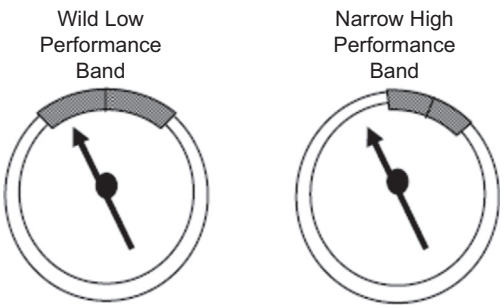

FIGURE 23.3

Dynamic performance dashboard examples (DeVries et al., 2001).

blending with on-line analyzers to support a performance model with a set of messages and procedures that allow operators to modify the batch during the run, avoiding a rework.

23.4.3 CAPABILITY TO PERFORM

When the organization can more accurately perceive their performance and the distance away from targets, they can develop a culture of learning how to improve. This is different than monthly accounting reports that show shadow costs and prices. This requires a condensed set of reliable information that supports factors that they can change. Examples include reliability, yield, quality, and throughput, and often it might be expressed in a different way. For example, reliability may be more "actionable" when expressed as "cycle time," "turnaround time," and so forth. Cutting the setup time from an overall 5%−2.5% is actually cutting the time by 50%; this is far more vivid than showing availability changing from 95% to 97.5%.

Research has been conducted on complex operations where a unit is several steps away from the true customer, and attempts to establish internal costs and prices of feedstock, utilities, and internal products have had insufficient credibility or even ability to effect a change. Some attempts at activity-based costing have tried to increase the percentage of direct costs, with the result that the cost per unit of product is so weighted with costs outside of the unit, that the unit manager cannot effect a useful improvement or is motivated to maximize throughput. Maximizing throughput is the only degree of freedom because the "costs" are relatively fixed. This is incompatible with modern manufacturing strategies that require precise, timely changes in prioritization of throughput, efficiency, and specific formulations to attract and retain key customers and more lucrative long-term contracts.

A key element of an organization's capability to perform is its ability to handle both planned and unplanned disturbances. Modern manufacturing strategies become a nightmare if the organization and facilities cannot cope with the accelerated pace of change brought on by the tight coupling with suppliers and customers. The following model, as shown in Fig. 23.4, helps to describe different levels of readiness.

Containment is the lowest level of readiness, and at this level, unplanned disturbances stop production or cause product rework, but the damage is "contained", i.e., no injury, equipment damage, or environmental release. Unplanned disturbances include operator errors, equipment failures, and

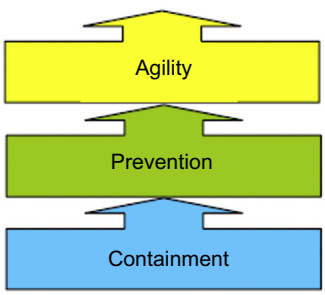

FIGURE 23.4

Levels of readiness (DeVries et al., 2001).

deviations in feedstock quality, as well as other factors. This level of readiness can be achieved with conventional information strategies:

- loose or no integration between components, from sensors to supply chain software,
- minimal integration of diagnostics of information quality,
- minimal performance information,
- minimal coordination between units or assets to withstand disturbances,
- reactive or scheduled maintenance strategies.

Prevention is a level of readiness where unplanned disturbances rarely affect production availability or product quality. However, this operation cannot consistently support planned disturbances to production rates, feedstock quality, or changes in yield or product mix. It is usually a case of stabilizing the plant as much as possible to achieve this level of performance. This level of readiness requires more advanced information strategies:

- moderate integration between components and a reliable connection to supply chain software,
- good management of information quality,
- good coordination between units and assets,
- scheduled maintenance at all levels,
- better performance information.

Agility is a level of readiness where the plant can consistently support wider and faster changes in feedstock quality, production rates, and output mix without reducing production availability or quality. This operation consistently achieves "prevention" readiness so that it can outperform other plants because of its agility. This level of readiness requires the most advanced information strategies:

- the tightest integration of all levels of software and sensors,
- good models that drive performance information and on-line operations advice,
- a reliability-centered maintenance strategy for information technology,
- good coordination with knowledge workers, who will likely come from key suppliers of catalysts, process licensors, information, and automation technologies, and workers at other sites of the company.

There is a tendency in many operations to try to jump from "containment" to an "agility" level of readiness by adding more information technology, but with the characteristics of "containment" such as minimal integration. This is potentially disastrous. Supporting modern manufacturing strategies can mean that the quality of integration is as important as or more important than the quality of the information components themselves.

Owing to the complexity of the interactions between technical factors affecting asset performance and the difficulty in converting technical understanding into a business context, the traditional approach has been to try and simplify the problem. Benchmarking, debottlenecking studies, maintenance, and integrity criticality reviews have all been applied to enhance process plant performance.

Each of these approaches tends to focus on a particular element of an assets' operation. As a result, enhancement decisions are made without a full understanding of the impact on the assets' performance and the overall business impact. This can result in opportunities being missed, capital being poorly invested, and delivery of short-term benefits, which are unsustainable. In the worst cases, this can result in a net reduction in plant performance and increased life cycle costs.

23.4.4 ORGANIZATIONAL HIERARCHY OF NEEDS

Attempts to develop plant culture by transplanting methods and equipment have not only failed but actually eroded performance. Key observations include the following:

1. Personnel may not associate performance or knowledge with increased security, wealth, and sense of belonging or esteem. They observe promotion and compensation practices and evaluate the effectiveness of improving their situation against new expectations for better performance.
2. Risk-adverse cultures dread the concept of visual management, benchmarking, or any other strategy that is designed to help a broader teamwork together to continually improve performance. Information that shows performance can be used to support rivalries rather than inspire teams to improve.
3. Organizations and personnel worry about surviving, resulting in questions such as will the plant be shut down? Will the staffing be reduced? Efforts to change behavior using information have to be coupled to the hierarchy of needs, and then the information can evolve as the organization evolves (thereby improving performance).

Research on dynamic performance measures has uncovered an effective model of organizational behavior that is especially appropriate for manufacturing. Two of the key issues that have been addressed are overcoming over 85 years of traditional organization structure that tries to isolate units and departments and the 20 years of cost and performance accounting.

The challenge with cost accounting is assigning costs in the correct manner. A plant manager or operations manager might face an insurmountable fixed cost. This motivates him/her to maximize production, which might be opposite to the current manufacturing requirements. The poor credibility of internal prices for utilities, feedstocks, and products also has motivated middle management to drive performance in the wrong way. These point to the need to redefine key performance indicators (KPIs). The group of research efforts to deal with this is called dynamic performance measures. The US Department of Labor and many large corporations embrace dynamic performance measures.

Vollman et al. (1998) have developed a model that associates the manager's strategy and actions to their measures of performance. This combination is called the Vollman Triangle, as shown in Fig. 23.5.

The manager's subordinates will develop their own triangles to support their supervisor's measures, within the constraints of their capability to perform, as outlined in Fig. 23.6.

This occurs at all levels of the organization. The goal is to ensure that a small group of measures (no more than 4), which can be consistently affected by that level of operations, is maintained with suitable quality.

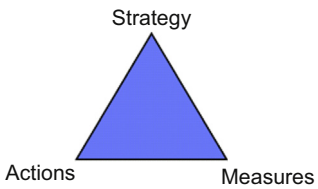

FIGURE 23.5

Vollman triangle.

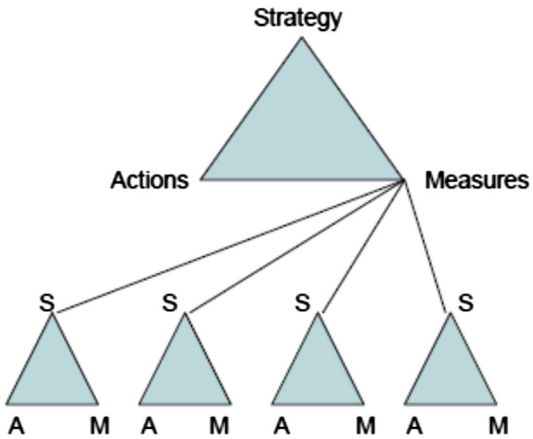

FIGURE 23.6

Application of Vollman triangle to subordinates (DeVries et al., 2001).

If this structure is maintained, then it is easier for the top management and modern manufacturing strategies to effect the change.

The "actionable" measures tend to conflict with each other. Higher throughput or quality often comes at the expense of efficiency, or each has a different optimum. Each person learns how these interact. Discussions on performance improvement become more effective because personnel can now describe this behavior. The discussion is vastly different than reviewing monthly reports. As far as operations are concerned, something that occurred several days or weeks ago is ancient history.

23.4.5 BEHAVIOR

The most important variables for performance are the work culture, job security, and career mobility. In many parts of the world, knowledge, experience, or skill is not sufficient to achieve promotion. Many cultures do not embrace an openness of sharing performance information, visual management techniques, and so forth. Therefore the information strategy needs to be adjusted to reflect the current human resources strategy, and ideally both will evolve in phases to achieve world-class performance.

Another strong issue is traditions at the plant. It is often much easier to initiate new teamwork and performance initiatives to a new plant with a new organization. Nevertheless, the right information strategy becomes a catalyst of change. Everyone can see the performance against the current targets, and everyone can understand the faster change of priorities, such as changing from maximum production to minimum, where maximum efficiency is desired.

23.5 THE SUCCESSFUL INFORMATION STRATEGY

Technology makes it easier to measure variables such as pressure, speed, weight, flow, and so forth. But, many operations achieve profitability with very complex equipment, and the key characteristics

are properties, not basic measurements. A notable example is found in oil refining. The basic manufacturing strategy is to improve yield by converting less valuable components from crude oil (molecules that are too short or too long) into valuable components (medium-length molecules). However, the essential measurement to determine the proportion of different molecules is chronically unreliable. New technology now exists to reliably indicate a property called "carbon aromaticity" that helps the operations team ensure that the process will be effective and that the feedstock will not degrade the expensive catalyst materials and erode production.

Reliable property measurement is the key. This also helps to improve the plant's culture from thinking about pressures and flows to thinking about properties. The information strategy becomes the following:

1. Assess the organization's readiness to support the desired manufacturing strategy and use information to evolve the plant culture.
2. Depending on the organization's hierarchy of needs, develop a phased evolution of the information strategy.
3. Develop appropriate measures that will directly support the actions needed to implement the strategy at all levels.
4. Develop the appropriate information to maximize its quality, reliability, and perception.
5. Manage the quality and reliability of information.

Data integration and visualization will continue to be a key area of focus throughout the next few years in digitizing the asset. Many new applications will bring knowledge gleaning ability from the data collected.

23.6 THE IMPACT OF LIVING WITH INFORMATION TECHNOLOGY

If the organization invests in "intelligent" components that enable advanced maintenance strategies such as reliability-centered maintenance or performance-monitoring centers, then the organization is committing to the advanced strategy. Otherwise, the flood of extra information will be disruptive. Intelligent sensors deliver up to 10 times as much information as conventional ones; a typical downsized organization, with as little as one-fifth the staffing of 10 years ago, would have to deal with 50 times the volume of information, which is too much. The information is only useful if it is coupled with appropriate software and methods to use the information to optimize the maintenance and maximize overall information and plant availability.

If the organization invests in supply chain management technology, then the organization is committing to an "agility" level of operations readiness and a team-based performance culture. The organization is also committing to business measurement changes—cost per unit of product gets in the way of profitability measures of reducing procurement costs or increasing return on sales using modern manufacturing strategies.

The organization develops a new language and starts to use new terminology. Furthermore, managers start focusing on managing the higher levels of information. The following model, as shown in Fig. 23.7, suggests a new terminology for dealing with information.

This terminology can be defined as follows:

- Data: the raw information from sensors and personnel keyboard entry;
- Information: the validated data obtained using diagnostics and techniques to enhance the quality and reliability of information;

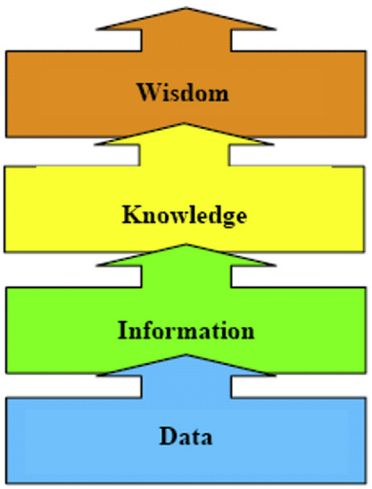

FIGURE 23.7

Hierarchy of information (DeVries et al., 2001).

- Knowledge: a comparison of information to targets and constraints. This answers the set of "how are we doing?" questions;
- Wisdom: guidance for best practices, customer satisfaction, supply chain management, and any other performance guidelines.

Many organizations have managers spending much of their time dealing with the "information" function rather than focusing on "knowledge" and "wisdom". It is extremely important to maximize the quality and type of information to ensure that management can support the "agility" demands of modern manufacturing strategies.

23.7 VISION OF THE MODERN PLANT OPERATION

There are four different groups of activities that require consistent information for most effective operations:

- operational decisions on an hourly or more frequent basis by operators, shift supervisors, or engineers;
- tactical decisions on a one- to 30-day basis by shift supervisors, engineers, purchasing, trading, and accounting;
- strategic decisions made on a 1-month to 5-year basis by plant management, purchasing, and accounting;
- monitoring on at least an hourly, weekly, and monthly basis by all parties involved.

Operational decisions include determination of set points for the equipment and switching equipment on or off. These decisions need to consider current pricing for commodities such as fuel and electricity, equipment availability, and environmental constraints. Furthermore, environmental constraints might be accumulative.

Tactical decisions include maintenance scheduling, demand forecasting, production planning, emissions forecasting, and trading. Strategic decisions require evaluation of future investment, budgeting, and long-term contract negotiations with suppliers and customers. Monitoring requirements include tracking plan versus target versus actual performance such as process energy use, cost accounting based on real costs, emissions accounting, and performance monitoring of utilities equipment.

Given that the quality and perception of information has to be improved to be used effectively to change an organization's culture, there are five key issues highlighted by the abovementioned model that must be addressed:

1. capability to perform,
2. operations readiness,
3. organizational hierarchy of needs,
4. establishing "actionable" information to act as a catalyst of change,
5. measuring the right things.

Technology can be the most effective tool used to improve plant culture. The speed of distributing reliable, timely, and easy-to-use performance and supply information changes the level of discussion and the dynamic behavior of the organization. But, the organization needs to have the right set of performance measures, a persistent effort to enhance operations readiness, an appropriate human resources strategy, and, above all, appropriate quality of information. The impact of these on changing a plant culture can be dramatic; as soon as the team realizes the ability and need to improve, they learn quickly how to improve their work methods to achieve it.

Modern manufacturing strategies are viable, and information technology strategies can transform the plant culture to achieve manufacturing success. The evidence of a change in the level of dialog and team dynamics confirms the success. But, several key strategies must be consistently maintained to sustain this success.

23.8 OPERATIONS STRATEGY

Major installations have been able to consolidate up to 10 control rooms and improve plant output by up to 15%. The goal was not to reduce personnel but was to improve flexibility because it is easier for a small team to drive change than a large one. This has been consistently proven in remote jungle sites in Southeast Asia, remote mountain sites in the United States and Canada, and remote sites in northern Africa. There are several techniques necessary to make this feasible:

- remote, secure, and online computer access to all control and monitoring equipment;
- advanced alarm management that dynamically filters alarms during upsets so that "alarm showers" are avoided as they blur the visibility to key cause and effect alarms;
- stabilization techniques to help units withstand upstream and downstream disturbances.

23.9 MODEL-BASED ASSET MANAGEMENT

Facility simulation has developed quickly over the last several decades. The integrated oil and gas field with production facilities is a complicated system with a high degree of interaction and dynamics that make it impossible for the human mind to control and optimize both technical and business parameters. Integrated discipline workflow and the development of model-based asset management are necessary to effectively deal with these complexities.

Model-based asset management techniques will begin to play a major role in the integrated gas plant of the future in bringing the predictive power of the production engineering toolset to the real-time data platforms. The analysis and prediction of near-real-time and future asset performance becomes a reality in the world of model-based asset management. For this, the complete integrated asset will be modeled dynamically in real time for both slow rigorous and fast proxy loop modes.

Facility simulation has come of age. The ability to predict very complex facility simulations in both steady state and dynamic mode has been achieved by continued integration of thermodynamic methods, hydraulic simulations, and unit operations. Facility simulation has progressed such that dynamic start up and shut down simulations have become routine and trusted among the engineering community. One can begin to think of dynamic simulation as a "virtual plant" for operational, advanced process control, and business analysis by a number of different departments.

Facilities simulation, control, optimization, operator training, collaborative engineering, and planning disciplines have a rather fragmented application of a number of associated technologies. To overcome this fragmentation, the first step is the adoption of integrated asset models that use comprehensive existing applications that are integrated together by a common 'glue' layer allowing a full model of the entire operation.

New concepts are appearing from the software community in the form of workflow solutions that enable assets to be modeled from a suite of selected software adaptors and can bring data from disperse and third-party tools into one common environment, creating the integrated asset model. One can then use engineering and business applications to identify asset-wide improvement opportunities.

A portal environment can be built which will allow multiple asset models to be visualized, compared and analyzed with distributed data sharing and events management, via proven and accepted enterprise platform message bus technologies. Key visualization and workflow technologies required include look-forward analytics, production scorecard, workflow management, production reporting, capital planning, and scheduling that can be performed on a uniform, company-wide basis and allow for rapid, informed decision-making.

23.10 OPTIMIZATION

Maximizing the profit contribution of natural gas—processing facilities is challenging given the fluctuating economics, changing ambient conditions, and feed variations that processors must address.

New dynamic markets for gas components lead to a need for stronger analytical capabilities of decision-support tools. Also the supply situation becomes more variable as the gas companies respond to market opportunities. The result is a more rapidly changing environment, and as a consequence, processing plants need to be reconfigured more often. There is a need for better

understanding on how to make plant-wide production plans and implement these through process management.

Decision-support tools have to combine both optimization and simulation capabilities to analyze the consequence of different scenarios. Advanced modeling and optimization is needed to address the new following challenges in plant control and optimization systems, which have an impact on the optimal design of gas-processing plants:

- Many of the processing plants are short of capacity. It is more important than before to maximize flow through the plants or the profit from final products.
- New opportunities exist because of recent advances in modern control technology, e.g., model predictive control lifts the level of automation and gives better opportunities for process optimization systems at higher levels.
- Integration of tasks and systems in operation-support centers. E-fields give a new perspective on operation of the oil and gas production, and this mode of operation must be prepared for in gas-processing plants.
- The Man-Technology-Organization perspective provides relevant information for the personnel involved.
- The use of models for planning and process control plays a central role.
- Modeling the dynamics of the markets and incorporation of it in contingent plans. The plans should reflect capacities and production possibilities of the plant. This again depends on the design and operation of the plant control system.
- Structuring of the information flow between layers and systems in the process control hierarchy, the real-time optimization level, and the planning and scheduling levels.
- Self-regulating and robust systems, which optimizes the other parameters.
- Limitations imposed by the process design.

23.10.1 TOOLS FOR OPTIMIZATION

Many of the tools mentioned in Chapter 20 could become integral elements of the operations strategy for maximizing profitability. A steady-state process model is necessary to determine the capability and current performance of the operation. Ideally, a dynamic model would be available to train operators and investigate control options. These models can then be used in a real-time mode to report the capability of the plant under different conditions.

Predictive equipment models can be used to determine when maintenance will yield long-term benefits that more than offset the short-term costs. These models can be an extension of existing steady-state models. These steady-state models can also be key elements of an on-line optimization strategy.

Real-time control models can be constructed from perturbations of a high-fidelity dynamic model. It is necessary to validate these models constructed from models against actual plant data. Often the control models require detuning to provide adequate and robust control.

23.10.2 OPTIMIZATION ALTERNATIVES

Some optimization alternatives for natural gas—processing plants include:

- advanced regulatory control
- multivariable predictive control
- neural network controllers
- offline process simulators
- on-line sequential simulation
- on-line equation-based optimization
- linear programs
- Web-based optimization

Advanced regulatory control and multivariable predictive control are discussed in Chapter 20.

Neural network—based controllers are similar to multivariable controls except that they gather plant data from the DCS and use the data to "learn" the process. Neural network controllers are said to handle nonlinearities better than multivariable controllers and are less expensive to commission and maintain.

Neural network—based models are only valid within the range of data in which they were trained. Conditions outside the range of data that were used to train a neural network model may be suspected. For example, if a neural network model was trained on data collected while a Joule—Thomson (JT) valve was closed, then the predictions from the model are invalid when the JT valve is open.

Refining and chemical companies have attempted using neural networks for control many times over the last 10 years. The technology has not proven to be viable compared with the other approaches such as advanced regulatory control and multivariable control.

Offline process simulators are used to develop a rigorous steady-state or dynamic model of the process. They are used by process engineering personnel to design and troubleshoot processes. Offline simulations allow for what-if case studies to evaluate process enhancements and expansion opportunities.

Offline simulators are typically not used to support daily operational decisions. They must be updated and calibrated to actual plant conditions for every use. They are not as robust as equation-based optimizers and can have difficulty converging large problems reliably and quickly.

A few of the offline simulation companies offer an inexpensive, sequential optimization system. The optimizer is based on a rigorous steady-state model of the process and is typically less expensive than equation-based systems. They leverage the work done to develop the offline model for online purposes. The extended convergence times inherent in these systems bring into question the robustness of the technology. The sequential nature of the solving technology also can limit the scope of the system. These systems require hardware and software to be purchased, installed, commissioned, and maintained onsite and require specialized resources to support them.

Equation-based optimizers use a rigorous steady-state model of the process as the basis for optimization and include an automatic calibration of the model with each optimization run. The equation-based solving technology allows optimizers to execute quickly and robustly making them viable for larger scale problems, i.e., multiplant load optimization for plants on a common gathering system.

Equation-based optimizers require a hardware platform, a costly software component, and highly specialized engineering services to install, commission, and maintain the technology. Closed-loop implementation requires a multivariable controller to be installed to effectively achieve the optimal targets.

Online equation-based optimizers, when coupled with a multivariable controller, represent the standard in optimization technology for refining and petrochemical industries. Most refineries and petrochemical companies are rapidly deploying this technology to improve the profit contribution of their larger scale processing facilities. Unfortunately, for gas processors, this technology is justifiable only for very large gas-processing facilities and is not scalable across their asset base.

Linear programs are used for evaluating feed and supply chain options. Linear programs are an offline tool that allows for what-if case studies and evaluation of supply chain alternatives. They are relatively inexpensive. Linear programs provide a linear representation of the plant process and do not provide guidance for operators (Roop et al., 2002).

Web-based optimization has been applied to cost effectively supply equation-based optimization to the natural gas—processing industry. However, the time lag in collecting data, calculating the optimum, and providing advice to the operators to implement the advice may not be fast enough to keep up with the constantly changing conditions experienced in natural gas—processing plants.

Another option is online performance-monitoring tools that predict the optimum operating point under all conditions (Ralph et al., 2011). These tools usually provide dashboards and graphical indicators to show the operator the gap between current plant performance and optimum performance. They may or may not provide advice on what parameters to change to reach optimum performance.

23.11 INDUSTRIAL RELEVANCE

In the upcoming decade, there will be large investments in gas production and in facilities for transportation and processing. Optimal utilization of all these facilities is vital to maximize the value from produced natural gas. Advanced process control and operation has raised the level of automation in the process industry significantly in the last decades. For example, in the refinery industry, methods such as model-based predictive control (MPC) and real-time optimization (RTO) have become widely used (Qin and Badgwell, 2003). The focus on these technologies has given large benefits to the industry in the form of increased throughput and more robust operation. The improvements obtained by the use of better control and decision-support tools ends up directly on the bottom line for the operating companies. The substance of these tools is in fact software realization of process knowledge, control, and optimization methods. MPC and RTO are now more or less off-the-shelf products, although for complex processes, the adoption of this technology requires specialist competence. However, there are significant potentials for further improvements in this area. One challenge for the gas-processing plants is being able to quickly adapt the plant operation to dynamic changes in the markets, thus the plant's flexibility and ability to perform rapid production changes becomes more important. It is also required to know accurately the plant's production capability, both on very short term (today—tomorrow) and on weekly, monthly, and even longer horizons. This requires the use of advanced optimization tools and efficient process calculations. It is important to consider these issues related to dynamic operation also in the design of new processing plants and for modification projects. Investments in this type of project have typically short payback time (Moen, 2004).

Combination of individual units into an integrated plant gives a large-scale control problem that is more than just the sum of the units. Cross-connections, bypasses, and recycling of streams give more flexibility, but at the same time, the operation becomes significantly more complicated, and it is almost impossible to use the full potential of a complex plant without computer-based decision-support tools. Thus there is a need for development of new decision-support tools that combine optimization technology, realize process calculation models at a suitable level of speed and accuracy, and structure the information flow, both from the process measurements and deduced variables and from the support tool down to the manipulated variables in the control system. It is also needed to develop further the methodology related to plant-wide control in this context (Skogestad, 2004).

23.12 THE TECHNOLOGY INTEGRATION CHALLENGE

There are three likely scenarios of the deployment of the integrated gas plant:

Scenario 1: Business as Usual—Digital technology, information, data, and models are used in an incremental way to reduce costs, increase recovery, and improve production, but no fundamental changes are made in business models, competitive strategies, or structural relationships.

Scenario 2: Visionary—Those who can best adopt and apply digital technologies and concepts will use them to gain significant competitive advantage. This will involve significant investment in software and IT technologies along with culture and management change. The industry will need to demand leaders in the highly technical processes, and modeling software contributes new and innovative solutions.

Scenario 3: Symbiotic Relationships—Those who use the availability of turnkey solutions to optimize production and leverage into larger industry positions. This will involve the use of third-party technology consultants and solution partners in an unprecedented way.

For most companies, an evolution approach that blends all three scenarios may well be the chosen route.

The foundation of the integrated gas plant of the future is engineering simulation, with integrated asset models and portfolio views of the business built on top. At the heart of the digital revolution in the upstream energy industry is a shift from historic, calendar-based serial processes to real-time, parallel processes for finding, developing, and producing oil and gas assets. Real-time data streams, combined with breakthrough software applications and ever-faster computers, are allowing the creation of dynamic, fast-feedback models. These dynamic models, running in conjunction with remote sensors, intelligent wells, and automated production and facility controls, will allow operators to visualize, like never before, what is happening in the facility and accurately predict what needs to happen next to maximize production and efficiently manage field development.

23.13 SCIENTIFIC APPROACH

Optimal operation of gas-processing plants is a challenging multidisciplinary task. Large-scale process optimization is challenging in itself. Thus when we also will consider dynamic conditions in the market and on the supply side, the operation will most certainly run into problems that must be solved. Some will arise from the size of the problem, some from complex process behavior, and some from requirements to solution of complex optimization problems.

The starting point in this project is the need for decision support as seen from the personnel in a plant-operating company. This defines a set of tasks that requires optimization calculations, process calculations, and measurement data handling. The personnel in question can be plant operators, production planners, sales personnel, maintenance planners, process engineers, managements, and so forth. Experience from other applications such as gas transportation will be used (Rømo et al., 2003).

The inclusion of market factors, capacity planning, and scheduling shall be focused, as this sets new requirements to vertical integration of process control and the optimization layers. We may in fact have several such layers, where, for example, the classical RTO is just one element. In planning and capacity assessment, the RTO layer may be accessed by superior layers to compute the optimal process targets over a certain horizon.

The requirements to process calculations for each type of task shall be classified. This may result in a set of optimization problems with different properties and requirements to solution and to the underlying process calculations and data handling, e.g., one approach from the planning side is to start with empty or extremely simple process models and to refine the models based on the requirements to the planning.

Segmentation into suitable process sections and control hierarchies are central issues. Here we can apply methods from plant-wide control to structure the control of the plant units in a way so that the influence from unknown disturbances and model uncertainties are minimized (Skogestad, 2004). A very important output in the first phase is to define high-level targets for the process control. The next important issue is to develop methods to select the variables that should be exchanged between the optimization and the process control layers. This is a control structure design task where the focus is on selecting the variables that are best suited for set point control to fulfill the process optimization targets in the presence of unknown disturbances and model parameters and measurement errors. Segmentation of the control into suitable sections and layers is also a part of this task.

Recent advances in process control technology also give a new perspective. For example, with an active MPC controller, information about active and inactive process constraints is of high-level importance which can be exchanged with the optimization layer, instead of representing the constraint equations at the optimization layer.

Efficient use of models is a so wide area that this issue can be subject to extended research in separate programs. For example, in process design, it is industrial practice to use quite detailed process models, including rigorous thermodynamics and representation of detailed phenomena within each process unit. In operator training simulators, detailed dynamic models are used, but these are rarely the same models as used in design, and the built-in process knowledge in form of model configurations and parameters is usually not interchangeable because of different modeling approaches and different model data representation. The models used in MPCs are normally captured from experiments on the process itself and are not connected to the other two types of models. For RTO, steady-state models are normally used, and in some cases, model tools with rigorous models are used there too. For capacity assessment, correct representation of potential bottlenecks is important.

23.14 OTHER MISCELLANEOUS INITIATIVES

Maintenance management, field information handling, work process optimization, compensation design, and procurement initiatives are several of the current gas-processing management initiatives.

In field information projects, companies considering upgrade should understand that technical support must also be upgraded and that care should be taken to select systems with an eye toward ensuring ongoing availability of support over a reasonable period.

In an effort to determine how they are doing against the competition as well as discovering new areas of potential, some processors have become involved in industry benchmarking activities. Benchmarking tools with a reasonable level of analytical content provide benchmarking against a select peer group as well as individual analysis of various cost components. Most organizations that persevere in the benchmarking process and are diligent to follow up on findings testify that benchmarking is a useful tool.

A company that fully uses second-wave technologies to streamline its back-office and process support technologies could reap a reduction in selling, general, and administrative (SG&A) costs in the range of 8%−10%. For a typical large firm, SG&A costs represent an estimated 10% of the total enterprise costs. Thus a 10% reduction in SG&A outlays would reduce overall corporate spending by 1%, which is a major gain, given that these savings would drop to the bottom line.

23.15 CONCLUSION

The goal of an integrated operations environment is to enable direct translation of management strategies into manufacturing performance. The vision is that:

- Utilization of raw materials is optimal.
- Overall margin and yield of product(s) is maximized.
- Planning, operational, and monitoring cycles are fully integrated.
- Identification and correction of problems occur rapidly.
- Operational (short and long term) factors are fully understood.
- The work force is well informed and aligned for a common purpose.

The most effective system is an integrated platform for computing and information processing at the production level. It is built around the premise that information is not to be isolated and that better information, when made widely available, will help people operate the facility closer to the optimum. A key principle is to empower everyone to maximize the value of their activities. The production management system provides the tools to help personnel do their job better.

A fully functional system will enable the quality cycle of planning, measuring, analyzing, correcting, and then planning again. To make improvements, the staff must be able to see and measure progress.

The integrated production/management system provides the data and the means to analyze situations, define solutions, and track progress. It is an integrated platform of computers, networks, and applications. It brings together the many individual automated systems that exist today and fills any gaps to bring the overall system to a high level of performance. The production/management system spans the gulf between process control and corporate business systems to support the day-to-day operations.

To achieve these goals: the production management system must achieve the following:

- It must be a single, comprehensive source of real-time and business data, addressing all operations and available to all appropriate personnel. This means providing long-term storage of all data (e.g., historical process, laboratory, plan, production, and shipment data), merging of these data, and retrieving data.

- It must provide information-retrieval tools for the full range of users. This usually means highly graphical tools that provide ease of use and a consistent look and feel to minimize the burden of finding and accessing information.
- It must integrate a wide range of computer systems and applications. No one system or set of tools will provide all the functionality needed. Instead, the production management system should allow for the use of the best products from different vendors.
- It must provide standard screens and reports that focus attention on problems and opportunities. The system should report by exception, highlighting the unusual, exceptions, and opportunities. It should compare actual results with the established plans and economic KPIs.
- It must maximize information content while minimizing data volume. This is achieved by the use of performance indices and other numerical, measurable indicators and the presentation of this information in graphical form whenever possible.
- It must present operational data in economic terms whenever possible. Opportunities, problems, and deviations from an operating plan should be prioritized based on their impact on overall profitability, and where possible, include an indication to the action or follow-up activity that alleviates the deviation.
- It must provide analytical tools that enable users to explore and pursue their own ideas. Much of the value of integrated operations comes not from presenting data about current operations, but from people looking for ways to improve current operations.
- It must facilitate plant-wide communications and workflow. For instance, plans and economic KPIs set in the planning group should flow automatically to operations to help operate the plant. Beyond the manufacturing issues, implementing a project with the scale and complexity of an integrated production/management system creates several management-of-technology issues.

These create the need to:

- balance the selection of individual applications with the need to integrate applications across departmental boundaries;
- provide a single, accessible look and feel, which is particularly important for users accessing data that originate in systems that belong to other departments (“single pane of glass”);
- use the latest proven information system technology as it becomes available and at the pace the operator can assimilate and manage.

Integration is a true example of the total being greater than the sum of the parts. A gas plant can profoundly affect the nature, quality, and profitability of its operations throughout the life of the gas plant with a truly integrated production management system.

Several operations have adopted some or all of the discussed strategies to improve their performance. A couple of these plants are discussed in Kennedy et al. (2002). Other examples include gas-processing operations in Tunisia, Norway, Nigeria, and Indonesia.

The future seems to belong to those who will be able to mix vision, intelligence, and understanding of human nature, technology, and the processing business into a formula for success in the new world of natural gas gathering and processing!

REFERENCES

DeVries, S., Lennox, K., Poe, W., September 26–28, 2001. Maximize the profitability of your gas plant assets - the integrated gas plant of the future. Paper Presented at the GPA Europe Annual Conference. Amsterdam, the Netherlands.

Howell, A., May 19–21, 2004. Obtaining value from oil & gas model based asset management. Paper Presented at the GPA Europe Spring Meeting, Dublin, Ireland.

Kennedy, J.M., Saunders, A., Poe, W.A., March 11–13, 2002. Reducing human intervention in gas processing. Paper Presented at the 81st Annual GPA Convention, Dallas, TX, USA.

Mazlow, A.H., 1968. Toward a Psychology of Being, second ed. Van Nostrand Reinhold Company, New York, NY, USA.

Moen, Ø., May 16–19, 2004. Machine Means for Design, Control and Economic Optimization of Polyolefin Production Processes and Their Products. Keynote at Escape-14, Lisbon, Portugal.

Neumann, R.W., March 1–3, 1999. Managing your gas processing plant fundamentalist, fashionable, farsighted or fantastic! Paper Presented at the 78th Annual GPA Convention, Nashville, TN, USA.

Qin, S.J., Badgwell, T.A., 2003. A survey of industrial model predictive control technology. Control Engineering Practice 11, 733–764.

Ralph, B., Hughes, J., Sigal, R., Morrison, R., Poe, W., April 3–6, 2011. Gas plant process manager application at Williams mobile bay plant. Paper Presented at the 90th Annual GPA Convention, San Antonio, TX, USA.

Rømo, F., Tomasgard, A., Røvang, L.B., Pedersen, B., 2003. Optimal Routing of Natural Gas in Pipeline Networks. SINTEF Report, SINTEF Industrial Management, Trondheim, Norway.

Roop, M., Leger, J., Hendon, S., March 11–13, 2002. Alternatives to optimize gas processing operations. Paper Presented at the 81st Annual GPA Convention, Dallas, TX, USA.

Skogestad, S., 2004. Control structure design for complete chemical plants. Computers and Chemical Engineering 28, 219–234.

Vollman, T.E., Berry, W.L., Whybark, C., 1998. In: Richard, D. (Ed.), Manufacturing Planning and Control Systems, third ed. Irwin Inc., Homewood, IL, USA.

CHAPTER

GAS PLANT PROJECT MANAGEMENT

24

24.1 INTRODUCTION

Project management is the application of knowledge, skills, tools, and techniques to project activities in order to meet or exceed stakeholder needs and expectations of a project. The project manager, sometimes referred to as the project coordinator or leader, coordinates project activities on a day-to-day basis. This is an ongoing challenge that requires an understanding of the broader contextual environment of the project and the ability to balance conflicting demands between (1) available resources and expectations (especially with respect to quality, time, and cost); (2) differing stakeholder priorities; (3) identified needs and project scope; and (4) quality and quantity of the project's deliverables. Project management for engineering and construction projects requires the application of principles and techniques of project management from the feasibility study through design and construction to completion. Good project management during the early stages of project development greatly influences the achievement of quality, cost, and schedule.

There must be a particular focus on predictability, transparency, and reliability, including managing the costs associated with these projects. With more joint venture projects, there is often the need to manage these relationships and preserve reputations.

This chapter covers many aspects of managing capital projects in the gas processing business. For the most part, best practice management for gas plant projects follows generic project management principles applicable to most industrial engineering and construction projects. This chapter reviews many of the standard and accepted practices that lead to successful installations as well as some of the unique considerations for gas plant projects, which arise from relatively complex processes employed in typically remote locations.

24.2 PROJECT MANAGEMENT OVERVIEW

One or more parties can perform the design and/or completion of a project. Regardless of the method that is used to handle a project, the management of a project generally follows these steps:

- **Step 1**: Project Definition—Determine the conceptual configurations and components to meet the intended use.
- **Step 2**: Project Scope—Identify the tasks that must be performed to fulfill the project definition. It also clarifies what the project does not include.

Handbook of Natural Gas Transmission and Processing. https://doi.org/10.1016/B978-0-12-815817-3.00024-1

- **Step 3**: Project Budgeting—Define the permissible budget plus contingencies to match the project definition and scope.
- **Step 4**: Project Planning—Determine the strategy and tasks to accomplish the work.
- **Step 5**: Project Scheduling—Formalizing the product of planning.
- **Step 6**: Project Execution and Tracking—Complete project tasks and measure work, time, and costs that are expended to ensure that the project is progressing as planned.
- **Step 7**: Project Close-out—Final testing, inspection, and payment upon owner satisfaction.

Successful projects require effective management, which means: (1) clear objectives, (2) a good project plan, (3) excellent communication, (4) a controlled scope, and (5) stakeholder support. Project management in today's organizations demands multiskilled persons who can handle and manage far more than their predecessors and requires competencies that span all of the critical management fields.

24.3 INDUSTRY PERSPECTIVE

The gas plant project management includes the planning, design, engineering, construction, and commissioning of the plant. Key elements are covered under the general headings of Engineering, Procurement, and Construction (EPC). Today in many large organizations there has been a trend away from the owner company performing the whole project management function toward the delegation of EPC in part or whole to Engineering Consultant organizations. At the same time, smaller companies have almost always subcontracted EPC activities. Most companies, however, specify and procure the major equipment themselves (or at least oversee those activities) to assure technical compatibility and adequate lead times for delivery, and so on. For example, the compressors and drivers will be specified and selected by the owner company as a priority.

A successful project in the gas processing industry is not only one that is profitable, but one that leads to the safe, reliable, predictable, stable, and environmentally friendly operational characteristics.

Gas processing is a service to the oil and gas production business. Oil and gas operations desire to produce into a system that has high availability and can produce saleable product in a safe, quality-consistent, and environmentally friendly manner. Gas processors must, of course, provide this service in a profitable manner. Flexibility to operate in various modes to respond to the markets and provide various processing alternatives should provide competitive advantages for a plant.

In many cases, the gas processing facilities are owned by the oil and gas producers as first facilities to enable the production of oil and gas and secondly as a value added operation. In some cases, particularly in the present state of the business in the United States, independent gas processors compete for gas that can be produced into a number of gas gathering systems. Several types of contracts exist, but the prevalent contract type is a "percent of proceeds" arrangement. Processors, who can offer the greatest revenue to the oil and gas producers, have an advantage in any case. The key is recovery of the greatest percentage of feedstock at the highest availability and at the lowest cost.

Adoption of integrated plant design and engineering is allowing gas processors, licensors, as well as engineering and construction firms to streamline workflows to improve efficiency and execute projects faster (Mullick and Dhole, 2007). Integrated models and toolsets allow rapid learning and ensure reuse of information and knowledge throughout the life cycle of the operation.

Engineering and construction firms are also utilizing their Information Technology infrastructure to support collaborative engineering environments to manage and execute projects around the clock and

across the globe. This global execution capability allows companies to fully utilize available talent in a cost-effective manner and to improve project schedules.

Rapid deployment of new engineering tools across the organization through a "virtualized" environment is another emerging trend.

24.4 THE PROJECT MANAGEMENT PROCESS

At the onset of a project, the owner company will undertake the required economic and business analysis regarding new or expanded facilities in order to receive board approval and budget allocation. Based on this approval and funding, the project definition will be refined. The owner company will initiate the project and set out design objectives, usually embodied in the Design Basis Memorandum (DBM), which will lay down the operating parameters and any key design guidelines and specifications. The owner company will solicit bids from EPC contractors and from these will select the successful bidder. In some cases, owner companies will have a partnership with an EPC contractor for certain types and sizes of projects. Pricing will be prenegotiated according to a range of possible contract models (fixed price, cost-plus, risk-sharing, etc.) or performed on a reimbursable basis. Both parties, owner and contractor, will set up teams to do the work. The EPC company may be asked to be completely responsible for all aspects of engineering, procurement, and construction or may only be required to do engineering and some procurement with the construction carried out by another company. Estimates and schedules will be set up by the EPC company in consultation with the owner.

Consultants and contract personnel will fill areas where the EPC company lacks resources or expertise. The owner also embeds staff in the contractor company to ensure oversight of the management process and also may include specialist engineering personnel to monitor progress against the plan including quality assurance as well as training of the owner staff on major projects.

For more complex, large projects that involve elements of innovation or requirements to build a gas facility in a region or country where such projects have not previously been conducted it is not unusual for the process to include feasibility studies and Front-End Engineering and Design (FEED) studies conducted prior to awarding the EPC contract. The feasibility and FEED studies are usually conducted by competent engineering consulting companies, capable of conducting the EPC work themselves. The deliverable from a FEED study may form the basis of a competitive tender for the EPC contract in which a number of prequalified contractors may compete.

A successful project requires the owner and EPC company to work very closely together. Typically, the owner will bring in operation staff at an early stage in the project to ensure that these staff members contribute to the project specifications and review deliverables as they unfold. In this way commissioning and operation proceed without serious problems. Companies with experienced staff often prefer to have the operating people closely integrated with the construction work from the outset. Similarly with the controls people, it is essential that the owners control philosophy is conveyed to the engineers of the contractor and that the machinery suppliers are brought into the loop so that engineering specifications and machine products reflect these perspectives. The owner company will undertake the required economic and business analysis regarding new or expanded facilities to receive board approval and budget allocation. From this the project will be defined.

24.4.1 DEFINING BUSINESS AND PROJECT OBJECTIVES

The first step in the project management process is to align the business and project objectives. A project can be installed on time and on budget, but if it does not meet the defined business objects, then the project cannot be deemed to be a success. Some of the questions that the business owners must be asked by the project team include:

- How much gas is available for processing (ultimate reserves and daily deliverable quantities)?
- What is the market demand for gas and gas products that can be met by this project?
- What is a realistic gas production schedule?
- What are the production pressure, temperature, and composition of the gas?
- How will the gas pressure, temperature, and composition change over time?
- What products can be sold and at what price?
- What are the product specifications?
- How will the products be delivered to market?
- What are the local environmental policies?
- What are the local safety policies?
- What infrastructure such as roads, bridges, loading and unloading facilities, personnel housing, etc. are required? and
- What is the skill level of the available operations and maintenance personnel?

Since most gas processing plants are services to the oil and gas producers, then collaboration between reservoir and production engineers and gas marketers to obtain answers to these questions is imperative. In cases where processors compete, then collaboration with those responsible for obtaining the processing and sales contracts (e.g., economists, lawyers, and negotiators) can be critical.

24.4.1.1 The Project Charter

The project charter is a document that demonstrates management support for the project. In particular, it authorizes the project manager to lead the project and allocate resources as required. It simply states the name and purpose of the project, the project manager's name, and a statement of support by management. Senior managers of the responsible organization and the partner organizations sign it. The project charter should be distributed widely—to anyone with an interest in the project. This will help build momentum, encourage questions and concerns early in the project's evolution, reinforce the project manager's authority, and possibly draw other interested and valuable stakeholders into the project.

The project owner may be a joint venture of oil and gas companies, with one designated as the project operator. The project charter is then usually signed off by all joint venture partners together with an authority for expenditure (AFE) approving the project budget and/or initial stages of expenditure.

24.4.1.2 Project Team Roles and Responsibilities

Project team size and make-up is dependent on the complexity of the project, however, the basic composition of the project team and their responsibilities are recommended for all projects including:

1. **Project Manager**
   The project manager is responsible for project development, developing schedule, budget, and deliverables definitions; evaluation of alternatives; determining return on investment; adherence to company policies; obtaining funding; acquiring internal and external project resources; contractor selection; maintaining project schedules and budgets; evaluating quality of project deliverables as they evolve; identifying and mitigating downside risks; identifying and exploiting upside opportunities; reporting to business owners; and creating project close-out reports.
2. **Business Owner Representative**
   The business owner representative is responsible for assuring that the project adheres to business objectives as objectives may change or require alteration during the project.
3. **Plant Manager**
   A plant manager should be appointed as early as possible to address operability and maintainability issues.
4. **Project Engineer/Construction Engineer/Start-up Engineer**
   A project/construction/start-up engineer can be a one role in smaller projects and multiple roles in larger projects. This engineer (or engineers) is responsible for technical specifications for contract bidding purposes, technical evaluation of contractor bids, owner's representative during construction, management of construction inspectors, turnover of facility to operations, training of operators, determination of plant performance and identification of any project deficiencies.
5. **Purchasing Representative**
   The purchasing representative is responsible for commercial evaluation of contractor bids and negotiation of contract.
6. **Process Engineer**
   A process engineer is recommended for evaluating alternative processing schemes during project development, assistance with technical specifications, and evaluation of contractor bids, and assistance with operator training and start-up issues.
7. **Environmental Engineer**
   An environmental engineer is recommended to review and provide advice on environmental issues encountered during the project including technical specifications and obtaining environmental permits.
8. **Safety Engineer**
   A safety engineer is recommended to review and advise on safety issues encountered during the project including technical specifications and participating on hazard analysis evaluations.
9. **Production or Reservoir Engineer**
   A production or reservoir engineer is recommended to be available to evaluate any oil and gas production issues that may be encountered during the project.
10. **Facilities Planner**
    For larger projects a facilities planner should be available to assist with project economics and to serve as a liaison for economic premises and marketing issues.

24.4.2 CONTRACTING STRATEGY

There are several alternative contracting stages and strategies. The first stage of contracting may be a front-end engineering design. With this approach, a contract is entered based on the design objectives

for an engineering contractor to evaluate process and construction alternatives as well as develop technical specifications for the project. In some cases, the owner's engineers may accomplish the front-end engineering design tasks. The second stage of contracting is for engineering, procurement, and construction services. Either stage can be contracted as a lump sum, fixed fee price also known as a turn-key project or on a reimbursable basis also known as a time and expense contract. In some cases more complex contracts, such as risk-sharing or gain-sharing, will divide risks and rewards more evenly between the contractors and project owners.

24.4.3 CONCEPTUAL ESTIMATES AND SCHEDULES

Most operating companies have developed estimating tools for budgeting of plants similar to those they are currently operating. Many operating companies have the capabilities and resources to evaluate alternative process and mechanical designs with budgetary or conceptual level estimates. These estimates typically have an accuracy of $\pm 30\% - 40\%$.

Under other circumstances such as when proprietary processes are in use, unique locations are to be selected, or there is a lack of available resources, an engineering firm may be hired to evaluate alternatives and determine budgetary estimates. After evaluation and selection of a conceptual process and mechanical design, the operating or engineering company will undertake a front-end engineering design. The detailed specifications and request for proposals will be the deliverable from the front-end engineering design.

Conceptual estimates and schedules should take the following into consideration:

- location,
- operators and operability,
- constructability, and
- special materials.

The availability of fresh water and electricity are considerations in determining location. Port facilities, roadways, and waterways are another consideration. A qualified and available work force is always a consideration when determining location. In some locations qualified operating personnel are difficult to find, so inexperienced and poorly educated operators may be hired. In order to overcome their lack of qualifications, intensive training is required. Generally, it is good to include in the project training using high fidelity simulators particularly where inexperienced operators are to be hired. In addition, plants with novel processes with which even experienced and highly educated operators are not familiar should include additional training provisions. Such training will impact the project's cost and schedule.

Regardless of schedule, the project team's capability to construct the facility must be addressed. For instance, vessels of large diameter and height will require shop facilities that have appropriate size capacity, as well as trucking and rail facilities that accommodate the finished products. In some cases, the vessel may require field fabrication or multiple vessels will be needed if shop fabricated. Alternatives for prime mover drivers such as electric motors, steam turbines, gas turbines, and gas engines may be influenced by the availability of infrastructure to support these devices. If electrical service is not provided by a utility, then generation or cogeneration facilities may be required. These must be addressed in the project cost estimates and schedules.

Special materials are often required in gas processing plant construction due to components such as hydrogen sulphide, carbon dioxide, mercury, water, etc. The availability of these materials and their

delivery should be considered. Sometimes cladding or linings may be alternatives to expensive and scarce alloys. In addition, approved welding procedures may not be available or the work force may not have the expertise to perform certain procedures. Addressing such obstacles must be part of the project plans.

During the proposal solicitation and award of the construction contract, the cost estimates and project schedule for the prime contractor will be focused on construction activities and therefore fairly detailed and inclusive. However, the overall project schedule from an operating company point of view must consider nonconstruction activities such as permits, licenses, and other government requirements; staffing, accounting, other internal issues, as well as contracts with suppliers and customers to name a few.

As project definition improves so the uncertainties associated with cost estimates should decrease to a funding level of accuracy of approximately +15%/−10% with a 10% contingency identified. A probabilistic approach to cost estimating identifying percentiles (P90, P50, and P10) is also widely used to illustrate cost uncertainties (McIntire, 2001).

24.4.3.1 HAZOP Analysis

A hazards and operability (HAZOP) analysis or equivalent is good practice even when not a statutory requirement. Such an analysis will most likely recommend the addition or deletion of valves, lines, instrumentation, and equipment needed for safe and reliable operation.

Fig. 24.1 illustrates a stages and gates approach to oil and gas facilities project management that emphasizes the importance of the planning stages (feasibility and FEED) leading into EPC

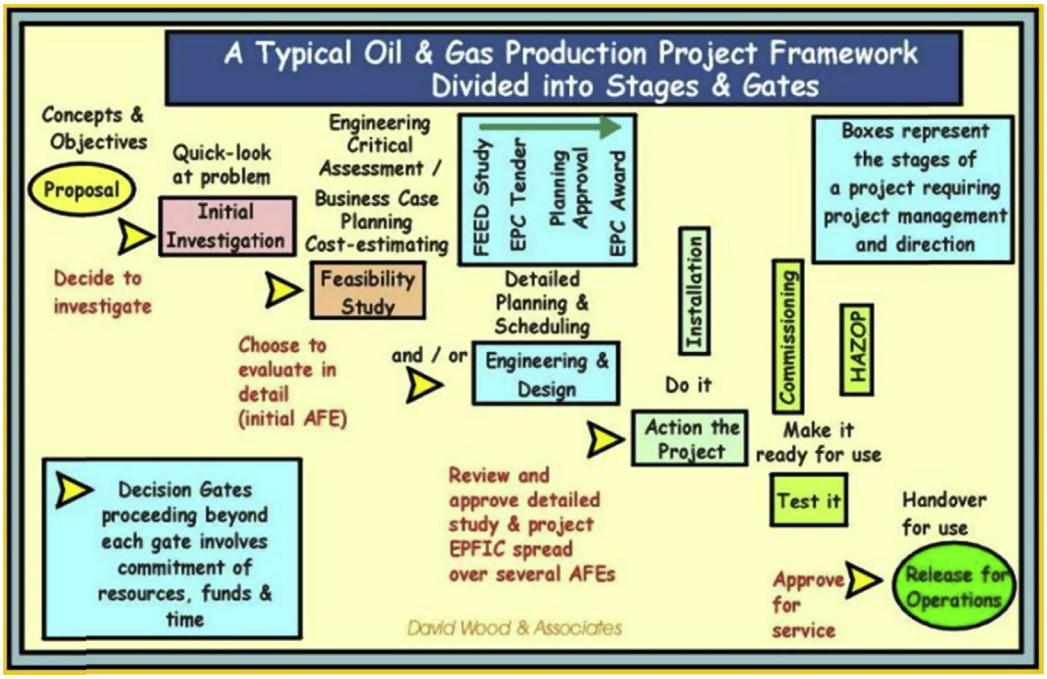

FIGURE 24.1

Stages and gates approach to project management (Wood and Mokhatab, 2006).

contracting, construction, and fabrication activity, on to HAZOP and ultimately plant commissioning. Moving from one stage to another requires a gate to be passed where decisions and approvals have to be made associated with funding, technical design, and project priority. Such approvals are usually structured in the form of authorities for expenditure (AFEs) to be signed-off by the project owners (and often other stakeholders—e.g., government authorities) as positive approval to proceed under stages of a project budget. Although the diagram for simplicity suggests a linear process proceeding from one stage to another, in practice there are often loops and feedbacks to the work of earlier stages that require adjustments to design, etc.

24.4.3.2 Scheduling and Cost Estimating Software

Software exists to assist with both conceptual cost and time estimates as well as detailed estimates and complex project networks involving the optimization of project networks with critical path analysis. Most major Engineering, Procurement, and Construction contractors have their own custom tools. Smaller contractors and operating companies may use products supplied by a vendor specializing in these tools. For larger projects it is increasingly common for Monte Carlo simulation analysis to be used in conjunction with critical path identification to yield probabilistic estimates of cost and time associated with each project activity and for the project as a whole (Wood, 2001).

24.4.4 PROJECT EXECUTION PLANNING

A project must be planned and tracked against the plan to assure successful execution. A project plan sets the ground rules and states them in a clear fashion. The project plan helps to control and measure progress and helps to deal with any changes that may occur. Previous experience is the best guide for determining the necessary tasks and the time to complete them. Many engineering and operating companies maintain databases that include previous project plans with actual time to completion and costs. To be able to benefit from such an approach requires good quality record keeping both during a project and following its completion.

Although, no two projects are identical no matter how similar they appear, these databases of past experience contain valuable information on which to plan. It is necessary to understand any unique requirements that previous projects met and how the current project compares. Some dissimilarities may include:

- location which impacts the government regulatory bodies, remoteness, cost of labor, etc.,
- make-up of the project team, including expertise, time available, geographic dispersion of team members, cultural differences, and organizational affiliations/loyalties,
- project scope, and
- current economic conditions, which affect inflation and employee availability.

The project plan should be relevant, understandable, and complete, and reflect the size and complexity of the unique project. The project plan should include the following elements (Hauge and Cramer, 2002):

- a project charter,
- a project timeline,
- a responsibility matrix,

- a project plan budget,
- major milestones with target dates, and
- a risk management strategy.

24.4.5 PREPROJECT PLANNING MEASUREMENT

The project objectives, or the measure for project success or failure, are often defined in terms of cost, schedule, and technical performance. In order to serve as a baseline for project execution, measurements should be in place to identify target completion dates, budgets, and expected technical performance. These measures should be included in a system that allows tracking of actual, target, and projected dates and costs with variances highlighted. The technical expectations should be tracked as well and checked for compliance as the project proceeds.

24.4.6 THE RESPONSIBILITY MATRIX

Projects are a collaborative effort between a number of individuals and organizations working together toward a common goal. Managing a diverse team, often spread over several locations (and countries), can present some special challenges. A responsibility matrix is a valuable project management tool to help meet these challenges. The matrix ensures that someone accepts responsibility for each major project activity. It also encourages accountability. The responsibility matrix should correspond with the project timeline. An example is shown in Table 24.1.

The left hand column lists all the required tasks for a project while the team members (e.g., project manager, project engineer, safety engineer, plant manager, purchasing agent, etc.) are listed across the top. A code is entered in each cell that represents that team member's involvement in the task in that row. For example, choose codes appropriate to the project; the key is to clearly identify who has a role in every activity, who is accountable, and who must sign off. Make sure the matrix is included in the project plan so that every participant is clearly aware of his or her responsibilities.

When developing the construction phase site staffing plan, the contractor's site organization should be analyzed for strengths and weaknesses that can affect the success of the project. In some cases, it is

Table 24.1 Typical Responsibility Matrix

	Project Team Members				
Task	**Contractor**	**Owner/Operator**	**1**	**2**	**3**
1	A	S	P	–	–
2	–	A	S	P	I
3	–	A	S	P	–
4	A	S	P	–	–
5	A	S	P	I	I
6	A	S	P	–	I
7	–	A	S	–	P

A, *accountable;* I, *input;* S, *sign-off;* P, *primary responsible.*

necessary to supplement the contractor's organization with project sponsor's own personnel or specialist independent contractors. The need for these adjustments generally is not known until a vulnerability assessment is performed on the contractor. Normally this is done during the evaluation phase in advance of the final project investment decision and award of the main EPC contracts. Upon completion of such an assessment, project sponsor staffing adjustments should be made to supplement and leverage the contractor's weaknesses and strengths, respectively. This approach helps to reduce project execution risks and improve constructability performance (Wood et al., 2008a).

For project contracts such as reimbursable contracts where the project sponsor is bearing most of the risk exposure, the project sponsor's site teams are commonly developed and aligned to match the structure and function of the contractor's site team. For lump sum and unit price contracts the project sponsor and contractor's site teams generally do not match.

A well-disciplined and managed team can make the difference to a project. Fig. 24.2 highlights that the time it takes to build a highly performing cohesive project team can be crucial, as project teams do not have time to waste. A focus on early team building initiatives can pay off as it is difficult to assemble a group of skilled staff and expect them to perform as a team without progressing through team building and integration phases. This becomes even more important in multicultural teams (Safakish and Wood, 2011).

In order to maximize team performance and motivation, team building and development must be given time and priority as well as careful project management attention at an early phase in the execution of any significant project. This is especially the case for mega-scale facilities projects with

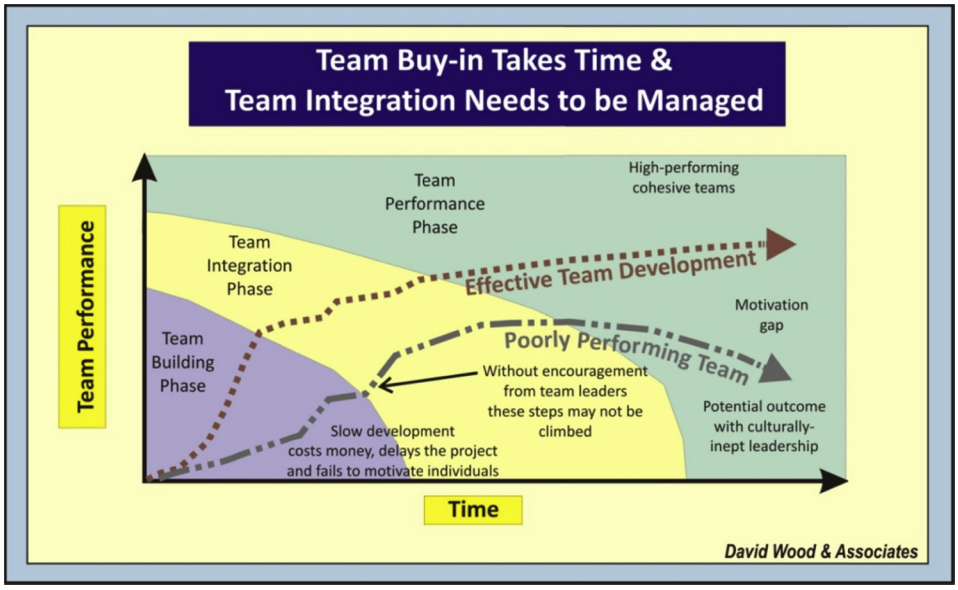

FIGURE 24.2

Team integration phases (Wood et al., 2011).

activities conducted at multiple sites in several countries separated by large time differences and cultural barriers (Safakish and Wood, 2010).

The key team attributes to achieve targets by overcoming obstacles are:

- being well-trained,
- highly-motivated,
- integrated,
- collaborative,
- led by a focused project plan,
- having a strong leadership,
- shared values (through buy-in and alignment), and
- being adequately resourced.

24.5 PROJECT CONTROLS

The two main elements of a project plan are: timeline and cost control. A timeline assures that the project is scheduled properly to meet the anticipated and promised dates. For projects that involve several parallel or overlapping activities the timeline becomes a network. Cost control assures that the project meets its budget.

A checklist approach has been proposed to provide a structured process for incorporating construction and other discipline knowledge that should enhance project safety, quality, schedule, cost, and risk management objectives (Wood et al., 2008a).

This checklist considers 10 key facets of project execution:

1. schedule,
2. design factors: simplicity, standardization, and ease of construction,
3. facilities layouts and arrangements,
4. safety, environment, security, community, and regulation,
5. specifications,
6. plans and logistics,
7. cost estimates,
8. construction execution issues,
9. modularization, and
10. risk mitigation and opportunity exploitation.

24.5.1 PROJECT TIMELINE

By dividing a project into the individual tasks required for completion, the project timeline (Greer, 2002):

- provides a detailed view of the project's scope,
- allows monitoring of what has been completed and what remains to be done,
- allows tracking of labor, time, and costs for each task,
- allows assigning of responsibility for specific tasks to team members, and
- allows team members to understand how they fit into the "big picture".

This timeline can take on a variety of formats and philosophies. The most prevalent philosophy is to determine the date for project completion and work backwards to identify key dates when certain milestones require completion. In practice, the project completion date is first determined through iterations of what is possible going forward with contingencies and identifying an end date. This usually involves establishing a critical path of activities which must be completed on time for a project not to fall behind its scheduled end date. If this end date is not acceptable, then acceleration plans should be explored. Most methods of acceleration require additional expense to accomplish objectives. These methods may include parallel tasking, overtime, and contractor bonuses for meeting an aggressive date to name a few.

Once the project milestones are set, then subtasks and assignments are identified. On large projects, certain tasks and subtasks will be assigned to an assistant project manager. The overall project manager will become responsible for coordinating the activities of the assistant project managers. The milestones, major tasks, and subtasks are commonly shown in a Gantt chart. This type of presentation presents dependencies in a graphical display such as predecessors (tasks that must be completed prior to commencing the next task) and successors (tasks that cannot be started until a previous task is completed). Milestones are significant events in a project, usually the completion of a major deliverable or tied to vendor or contractor payments. A very good method to analyze subtasks is to consult with an expert on accomplishing the subject task. And the very best way is to receive an estimate with commitment from the person responsible for executing the task. This is where contractors and their bids contribute to the best task analysis possible.

Note, as the project progresses, there may be tasks that were not foreseeable in the original plan, or tasks are added to enhance the overall project outcome. The impact of the additional tasks, delays, or even acceleration requires consideration of the impact on both the time schedule and resources. When changes to the schedule are warranted and feasible, the project manager should get a written agreement for the revised plan from all the key stakeholders in the project. A regular update of the time schedule is recommended as part of a routine project status report. The time period for such reporting may be weekly or monthly depending upon the project or the stage of the project.

24.5.2 RISK MANAGEMENT

Risk is inherent in all projects. In project management terms, "risk" refers to an uncertain event or condition that has a cause and, that if it occurs, has a positive or negative effect on a project's objectives, and a consequence on project cost, schedule, or quality. As discussed in the previous sections, the measure for project success or failure is defined in terms of cost, schedule, and technical performance. Project risk management is intended to increase the likelihood of attaining these project objectives by providing a systematic approach for analyzing, controlling, and documenting identified threats and opportunities both during the planning and execution of a project. The application of project risk management will vary from the operator (owner) or the contractor side. The term risk management is used to lump together different activities. These activities may be divided into (Hauge and Cramer, 2002):

1. Activities related to the day-to-day identification, assessment, and control of uncertainties, i.e., risk management activities related to understanding and controlling the most important risks

threatening the achievement of well-defined project objectives. This type of risk management may be based on a qualitative approach where each risk is assessed separately.

2. Activities related to the periodic assessment of achieving project objectives, i.e., assessing the probability of achieving well defined project objectives with respect to schedule, budget, or performance. The periodic assessment must use a quantitative approach based on the aggregation of most critical uncertainties.
3. Activities related to the ranking of a set of alternative decision options/system solutions, i.e., ranking different alternatives with respect to their desirability measured in terms of the corresponding project objectives. Such ranking is typically performed at major decision gates during the conceptual design stage.

A good risk management system identifies, assesses, and controls uncertainties during all phases of the project. This allows the project team to mitigate risks and take advantage of opportunities. The selected system should properly assess all project risks, causes, and consequences including (Wood et al., 2008b):

- technical and technological,
- financing and funding,
- joint venture and alliance,
- contractor and vendor performance,
- contract,
- health, safety, and security,
- community and public relations,
- environmental,
- statutory planning and regulation,
- capital and operations costs,
- construction, installation, and assembling schedules, and
- completion and commissioning.

The above risks should be addressed holistically to include all stakeholders, involved parties, all phases, and all types of project exposure and uncertainties. The system should be developed to properly address all actions necessary to fulfill the requirements of any and all contractual obligations, and to incorporate the results from all risk assessments into the requisite project plans.

Risk management is a key to success for project execution, but is often constrained by inadequate work processes and tools. An overall understanding of the different risk factors and how these affect the defined project performance goals is critical for successful project management and decision making. Project risk management is a systematic approach for analyzing and managing threats and opportunities associated with a specific project and will increase the likelihood of attaining project objectives. The usage of project risk management will also enhance the understanding of major risk drivers and how these affect the project objectives. Through this insight, the decision-makers can develop suitable risk strategies and action plans to manage and mitigate potential project threats and exploit potential project opportunities. Project risk management is based upon a number of different analysis techniques. The choice between these techniques is dependent on the quality of the information available and what kind of decisions project risk management should support. Day-to-day usage of project risk management is typically based on using risk-matrices, accounting for both threats and opportunities. With sufficient uncertainty information, the project risk management analysis can be extended to provide more direct decision support through probabilistic cost-benefit analyses.

Gas processing projects are often characterized by large investments, tight time schedules, and the introduction of technology or construction practices under unproven conditions. These challenges can result in a high-risk exposure but also opportunities that bring great rewards.

24.5.2.1 Project Risk Management Methodology

It is important to perform risk management in a structured manner. Indeed transparent risk management frameworks are becoming statutory requirements for many companies obliging them to demonstrate how they are managing risks throughout their organizations (enterprise risk management—ERM) or on an enterprise-wide basis (e.g., the COSO framework in the United States). It is important to ensure that the project risk management methodology is consistent with ERM frameworks (Wood and Randall, 2005). The project risk management process is often broken down into the following five general steps (Hauge and Cramer, 2002):

1. Initiation and focusing; initiate risk management process including identifying project objectives. The initiation should also assign personnel to the main risk management roles such as risk manager.
2. Uncertainty identification; identifying risks affecting the project objectives. Assign responsibility for assessing and mitigating each risk.
3. Risk analysis; assess for each risk the probability of occurring and the corresponding objective consequences, given that the risk occurs. Based on the risk assessment, classify each risk in terms of criticality.
4. Action planning; identify risk mitigating actions so that the most critical risks are mitigated. Assign responsibility and due dates for each action.
5. Monitoring and control; review and, if necessary, update risk assessments and corresponding action plans once new and relevant information becomes available.

The "initiation and focusing" step is normally performed once at the start of the project whereas the four other steps are performed in an iterative manner. The initiation of project risk management in projects has the following set of goals (Hauge and Cramer, 2002):

- Identify, assess, and control risks that threaten the achievement of the defined project objectives, like schedule, cost targets, and performance of project delivery. These risk management activities should support the day-to-day management of the project as well as contribute to efficient decision making at important decision points.
- Develop and implement a framework, processes, and procedures that ensure the initiation and execution of risk management activities throughout the project.
- Adapt the framework, processes, and procedures so that the interaction with other project processes flow in a seamless and logical manner.

The project risk management process should be assisted by a set of tools that support these processes.

24.5.2.2 Risk Response Planning

A risk response plan can help maximize the probability and consequences of positive events and minimize the probability and consequences of events adverse to the project objectives. It identifies the risks that might affect the project, determines their effect on the project, and includes responses to each

risk. The first step in creating a risk response plan is to identify risks, which might affect the project. The project team members should collaborate referring to the project charter, project timeline, and budget to identify potential risks. Those involved in the project can often identify risks on the basis of experience. Common sources of risks include:

- technical risks—such as unproven technology,
- project management risks—such as a poor allocation of time or resources,
- organizational risks—such as resource conflicts with other activities,
- external risks—such as changing priorities in partner or contractor organizations, and
- construction risks—such as labor shortages or stoppages and weather.

24.5.2.3 Developing Risk Response Strategies

There is no preparation for mitigating all possible risks, but risks with a high probability and high impact are likely to merit immediate action. The effectiveness of planning determines whether risk increases or decreases for the project's objectives. Several risk response strategies are available (HRDC, 2003):

- Avoidance—changing the project plan to eliminate the risk or protect the objectives from its impact. An example of avoidance is using a familiar technology instead of an innovative one.
- Transference—shifting the management and consequence of the risk to a third party. Risk transfer almost always involves payment of a premium to the party taking on the risk. An example of transference is using a fixed-price contract.
- Mitigation—reducing the probability and/or consequences of an adverse risk event to an acceptable threshold. Taking early action is more effective than trying to repair the consequences that occurred. An example of mitigation is seeking additional project partners to increase the financial resources of the project.
- Acceptance—deciding not to change the project plan to deal with a risk. Passive acceptance requires no action. Active acceptance may include developing contingency plans for action should the risk occur. An example of active acceptance is creating a list of alternative vendors who can supply materials with little notice.

Since not all risks will be evident at the outset of the project, periodic risk reviews should be scheduled at project team meetings. It is also important not to view risk with a negative mind set. In addition to the downside consequences associated with many risks lie opportunities, which should be identified and strategies developed to exploit them where possible. Risks that do occur should be documented, along with their response strategies in a risk register that assigns responsibilities for specific risks.

24.5.2.4 Qualitative Project Risk Management

The routine day-to-day identification, assessment, and control of project risks are similar to hazard and operability identification techniques. The identification of risks consists of collecting and examining information on potential events that may influence the achievement of the project objectives. Each such event is categorized as a risk or an opportunity. The identification of these events should involve expertise from all main project competencies to reduce the possibility of important risks being overlooked. These risks will normally be prioritized so that only the most likely and consequential

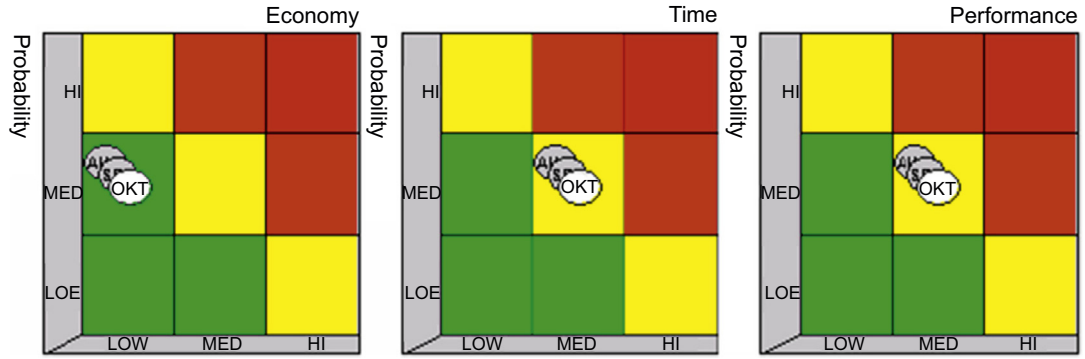

FIGURE 24.3

Risk matrices (Hauge and Cramer, 2002).

risks will be entered into a formal risk management process. The prioritization of risks should only be performed after thorough assessments and discussions among the project team. New information could mean that risks that have previously been determined as a lower likelihood must be inserted into the risk management process.

The assessment of each risk or opportunity is made in terms of scores for probability of occurrence and for consequence, given that it occurs, for each project objective. Based on the probability and consequence scores, the criticality of each risk with respect to achieving the project objectives can be assessed. Typically, a classification consisting of several possible probability scores and several possible consequence scores leads to several different classes of criticality, e.g., "critical", "significant", and "negligible". Fig. 24.3 is an example of how risks can be classified in relation to probability, project cost (economy), project effort or duration (time), and project performance.

The control of each risk event is normally based on its risk classification. A risk that is classified as "critical" will normally result in actions being identified in order to reduce the risk classification to either "significant" or "negligible". The risk reduction can be caused by either preventive measures (reducing the probability that the event will occur) or corrective measures (lessening the consequences of the event) or both.

24.5.2.5 Quantitative Project Risk Management Assessment

A periodic assessment of the probability of meeting project objectives must be based on quantitative calculation of the aggregated effect of the most important risks on the project objectives. The aggregation must also take into account sequences of scenarios and risk events, as well as the project structures given by the budget, the schedule, and operability. There exist several methodologies with supporting tools that can be used for risk assessment of the total budgets and schedules. The challenge is to apply a methodology and find a tool that supports this methodology so that the integration of risks in the different domains can take place, their mutual independence can be represented, and their aggregate effect on the project objectives can be assessed. Fortunately, the usage of influence diagrams enables such a methodology and there exist several influence diagram tools. In an influence diagram each risk is represented as a symbol (or "node") in a graphical diagram. The diagram represents the structural relationship between the different risks and their aggregate effect on the project objectives.

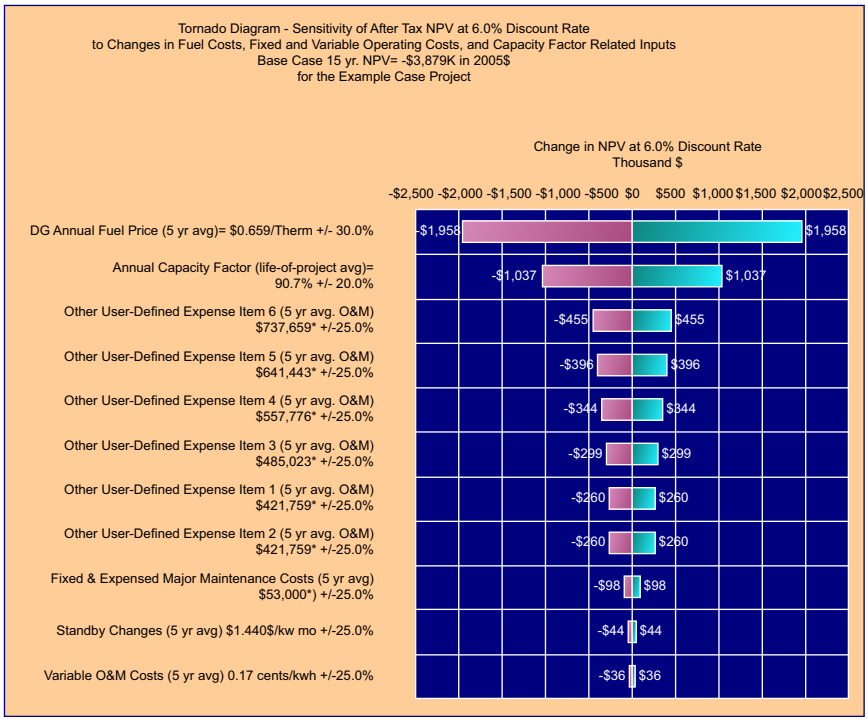

FIGURE 24.4

Typical Tornado diagram (generated with Palisade @Risk Software).

In this manner, influence diagrams are well suited to represent risk scenarios. The mathematics used for assessing the aggregate effect is hidden away "behind" the diagram. In this way the influence diagram also represents a methodology to split a risk management model into two: (1) the structural relationship between the various risks and (2) the mathematics of the risk model such as probabilistic distribution functions for the risks. Other quantification methods to identify criticality and rank risks include Monte Carlo simulations and presentation through "Tornado diagrams". Tornado diagrams (an example is shown in Fig. 24.4) help to identify which input parameters, if they were to change, would have most consequential impacts on the analysis. They help to establish materiality of potential outcomes and to illustrate how the project will be impacted by changes, in order or significance, of those selected inputs. This provides valuable insight into which parameters might warrant further investigation to determine how changes would impact the objectives.

24.5.2.6 Risk Process Modeling

The model of the general risk management process is by no means complete. The two most important omissions are (Hauge and Cramer, 2002):

- no direct representation of the interaction with external organizations and their processes and
- no direct representation of the interaction with other internal processes.

The interaction with other processes should be designed so that the (new) risk management process is integrated as seamlessly as possible into the existing organizations and its already existing other processes (e.g., Enterprise Risk Management—ERM-framework). Any required modifications should be as small as possible. Hence, this risk management process is integrated into the organization by having the already existing weekly management meeting also assessing the weekly risk report. Hence, no new forum for management review of risk is established, only an additional item is added to an existing agenda.

Since different parties in the risk management process have different interest, these interests should correspond to different views into the risk management process. Risk mitigation (and/or exploitation) strategies themselves involve costs to instigate and may lead to secondary risks. It is important to reconcile such costs and secondary risks with the risk management objectives, materiality of the risks being addressed, the project budget, and resources available.

24.5.2.7 Project Risk Management in Interaction With Other Management Processes

It is important to note that risk management has major similarities with other common management processes. Examples of such processes are (HRDC, 2003):

- management of project changes,
- management of public permits,
- management of health, safety, and environmental issues, and
- management of decision gates.

Similarities exist in the identification of items, the assessment of their criticality, the identification of corresponding mitigating actions, and the follow-up of criticality assessment and corresponding mitigation plans. These similarities should be exploited when setting up the risk management processes and establishing the tools for the management of these processes.

The risk management process will remain constant over the different project phases throughout the life-cycle of a construction project. The different risk management techniques for assessing day-to-day risks, calculating the ability to meet defined project objectives and ranking different decision alternatives, will also remain the same. In the ranking of different investment opportunities for a gas processing project, a number of issues will in general need to be looked into:

- revenue,
- costs (costs of different activities: capital expenditures—CAPEX and operational costs—OPEX),
- schedule (of project tasks and completion of milestones),
- taxes and depreciation,
- health, safety, and environment (meeting regulations and company requirements),
- structural reliability (design that meets requirements), and
- on-stream factor (design that meets availability requirements).

What will vary, however, over the life-cycle is the quality of the available risk related information, the kind of competence that is needed to compile and prioritize this information, and the kind of decisions that are supported by the risk management activities. A believable risk management process must be conducted by personnel with domain knowledge of the project phase in which decisions are to be made. Since the required competence will vary with the project phase, it is unlikely that the same person can fill the risk manager role throughout the project. Whether one or more risk managers or a

team are involved in managing risks it is crucial that analysis, actions, and outcomes are documented in a risk register and widely communicated both within the project team and to project stakeholders.

24.5.2.8 Other Risk Mitigation Concepts

Other methods of risk mitigation include (Hauge and Cramer, 2002):

- Cost Overrun Protection—Cost over-run insurance can be purchased. This insurance is most often used for infrastructures like bridges, islands, etc. that may be required to access or locate the facility.
- Regulatory Risk—A wide-ranging form of insurance covering political or regulatory risks is available. This is designed to provide an indemnity in the event when any changes occur to the regulatory requirements or political stance perceived at the conception of the project during construction and into commercial operations.
- Revenue Stream Stabilization—In addition to the historic insurance market places, capital markets are available that enable industry to transfer risks to financial vehicles and through structures different from traditional insurance policies. This market convergence has produced a wide range of creatively devised financial products, which can be applied to uninsurable risks. Hedging the sale prices for specific volumes of products is now widely used, particularly in the initial years of plant production prior to project pay-back, to help to reduce project finance risks.
- Blended Risk Solution—It is an integrated risk solution, which will result in a more comprehensive package of protection than the traditional set of policies providing limited but specific coverage addressing different areas of risk.

24.6 QUALITY ASSURANCE

An important part of defining the result and performance of the project is the specification of its quality related features, which the project must then aim to deliver. Quality assurance has been an issue at the forefront of organizational concerns for decades. The development of quality conscious construction practices has been identified as being of the utmost importance in gaining and retaining a competitive edge. In the context of a project that aims to deliver a complex result, the quality aspects of that result will need to be planned, designed, aspired, and monitored. Quality assurance is a term used to incorporate the quality policy, quality management, and quality control functions, which combine to assure that the end result will be consistently achieved to the required condition. Its aim is to attain and assure quality through the adoption of a cost effective quality control system and through external inspections and audits. Quality planning is an integral part of the planning activity. It manifests itself in the descriptions and in the scheduling of quality related activities. The results of the quality planning activities are reflected in the resource and technical plans, at each level of the project. Quality control is concerned with ensuring that the required qualities are built into all of the tasks throughout their development life cycles. Quality control utilizes measurable quality criteria and is exercised via quality reviews, project reviews, and by the testing of products. Quality assurance requires agreement on the level of quality controls to be adopted, both specifically relating to the project and to the overall organizational policy. It is important that all three interests represented by the project owner are taken into account when deciding the mechanisms to be adopted.

The task descriptions should describe the purpose, form, and components of a task. It should also list, or refer to, the quality criteria applicable to that task.

Task descriptions should be created as part of the planning process, to shadow the identification of the tasks that are required by the project. Each task description may either apply to a specific item or to all the tasks of a given type. The component tasks of a complex task may be described in separate descriptions, giving rise to a hierarchy of task descriptions for that task.

Quality criteria should be used to define the characteristics of a task in terms that are quantifiable, and therefore allow it to be measured at various points in its development life cycle, if required. The criteria effectively define quality in the context of the product and are used as a benchmark against which to measure the finished task. Quality criteria should be established by considering what the important characteristics of a result or task are in satisfying the need that it addresses, and they should always be stated objectively. Subjective or descriptive criteria such as "quick response" or "maintainable" are unsatisfactory—as they do not permit meaningful measurement.

Quality planning should ensure that all quality related activities are planned and incorporated into the project schedule. The tasks required to ensure the quality of the delivered result are often overlooked, with the result that the project schedule fails to represent quality related work. This can have serious consequences on either the quality levels achieved or the overall budget, or both.

Quality control is concerned with ensuring that the required qualities are built into all of the tasks throughout the construction cycle. It defines the method of inspection, in-process inspection, and final inspection to determine if the result has met its quality specification. Quality control utilizes measurable quality criteria and is exercised via change control, quality reviews, project reviews, and by the testing of products.

Reviews should be scheduled prior to key decision dates and important milestones such as shipment of rotating equipment and major equipment. For instance, modifications to a gas turbine are more easily made in the shop prior to shipment rather than in the field after transit. Modifications required that could have been found with shop inspections can cause significant delays.

Many of the top engineering consulting companies operate integrated Quality, Health, Safety, and Environmental (QHSE) management systems which they apply generically across their operations. This is appropriate as it makes clear to their staff that all four of its components are important to ensure successful outcomes and that QHS&E all influence each other as well as the budgetary, schedule, and risk issues that drive project decisions. The adage that one should expect what you inspect applies to gas processing project management. Management and technical peer reviews are good practice. Inspection reports monitor not only quality but progress and should be used liberally for best results.

24.7 COMMISSIONING AND START-UP

Commissioning and start-up of a new facility or unit is a very important phase of any processing project. These activities can be very expensive from a standpoint of project costs as well as deferral of operating revenues, if delays are encountered. For this reason, it is good practice to assign a start-up engineer to plan and coordinate these activities. Operators and maintenance personnel should be hired well before the start-up date and trained on the equipment and process basics. Familiarity with the particular control system can be accomplished through the use of Operator Training Simulators. These simulators can pay off easily by reducing the start-up time. More detailed training on particular aspects

of the equipment and process can be given to select individuals. Indeed many now argue that it is important to have operations and maintenance personnel involved in the design and engineering phase of a project as it is much easier to sort out operational control logistics at the planning stage than later on.

Thorough check-out of the equipment should be conducted by the owner and operator of the facility. Punch lists of all deficiencies should be prepared, reviewed with the constructor, and updated on a daily basis. Purging of the equipment is quite important for a safe start-up. Process gas or an inert gas, such as nitrogen, can be introduced to remove pockets of oxygen, which could lead to explosions. All high point vents should be opened and checked with a portable oxygen analyzer. These vents should only be closed when oxygen is no longer detected. Excess water and other liquids should also be removed from the system by opening low point drains until purge gas escapes through the drains.

Start-up should be a joint effort between the constructor, operator, and process designers. The constructor should be advised of any deficiencies in the equipment and instrumentation as they are identified by operations and have personnel readily available to resolve the issues. It is not uncommon for construction contracts to include a retention portion of the plant cost that the owner will withhold for a period (e.g., six months or 1 year) following start-up to motivate the contractor to deal promptly with any teething problems.

24.8 OPERATE AND EVALUATE

The final phase of a processing plant project is continuous operation and evaluation of the project results including plant capability over a finite period of time. Before the plant is turned over to operation, the performance of the plant should be measured. Sometimes this is required by the contractor or process licensor to meet performance guarantees. The capability of each process and equipment should be calculated and it becomes the baseline for operation. At this point you may discard the design capability as this was used only as a basis for sizing equipment. Many times equipment is sized with a contingency giving better than design capability. Other times, the equipment may not be capable of design. For example, a difference in the actual inlet gas composition from the design basis is a common culprit.

After detailed measurement of the plant's capabilities and deficiencies, these items should be well documented. The capability information is valuable should the plant require expansion in the future. Deficiencies become the basis for possible debottleneck and retrofit projects.

Capturing and transferring highly detailed and specific knowledge of a new plant, its machinery, its suppliers, and its commercial contracts is important for ensuring safety, reliability, and sustained plant performance.

Training and retaining operations staff is very important and in remote facilities where local skills may be in short supply it is not an easy task. An operator training simulator (OTS) can also be developed and maintained for training of new plant operators and analyzing plant performance under specific conditions relevant to planned operations. The OTS may be based on a dynamic simulation developed during the plant design. The long-term benefits of investing in an operator training simulator according to KBR (2012) are:

- Operator best practices are reinforced through refresher training.
- Workforce flexibility is increased through cross-trained operators.

- An opportunity to test trial modifications to the plant's control and automation systems and process configurations is provided.
- Development and refinement of operating procedures are facilitated.
- An OTS ensures that plant operators receive plant specific and realistic hands-on training ahead of plant start-up and throughout plant operation.

24.9 PROJECT CLOSE-OUT

In addition to the evaluation activities mentioned in the previous section, the project activities should be reviewed. This review should comprise:

- What worked well?
- What did not work well?
- What were the actual costs?
- What was the actual schedule?
- What assumptions need revision?
- What risks materialized and required attention? (as documented in the project risk register)
- Did risk mitigation strategies employed achieve their objectives?
- What are the project economics as constructed and operated?

As a result of this review or project postmortem, the Project Manager should write a project close-out report that includes the results of the project close-out review and recommendations for future similar projects.

24.10 CONCLUSION

Planning is critical to project success. Detailed, systematic, team-involved plans are the foundation for such success. When events cause a change to the plan, project managers must make a new one to reflect the changes. So continuous planning is a requirement of project management. Project managers must focus on three dimensions of project success. Project success means completing all project deliverables on time, within budget, and to a level of quality that is acceptable to sponsors and stakeholders. The project manager must keep the team's attention focused on achieving these broad goals and the stakeholders aligned to the project objectives. It is essential that the project team be comprised of all key disciplines that create or use the deliverables. The responsibilities of all team members should be clearly defined. Project managers must feel, and transmit to their team members, a sense of urgency. Because projects are endeavors with limited time, money, and other resources available, they must be kept moving toward completion. Since most team members have lots of other priorities, it's up to the project manager to keep their attention on project deliverables and deadlines. Regular status checks, meetings, and reminders are essential. All project deliverables and all project activities must be visualized and communicated in vivid detail. The project manager and project team must create a picture of the finished deliverables in the minds of everyone involved so that all effort is focused in the same direction. Avoid vague descriptions and make sure everyone understands what the final product will be.

Projects require clear approvals and sign-off by sponsors. Clear approval points, accompanied by formal sign-off by sponsors and key stakeholders, should be demarcation points in the evolution of project deliverables. Anyone who has the power to reject or to demand revision of deliverables after they are complete must be required to examine and approve them as they are being built.

Risk management is an essential responsibility of project management. All risks should be identified and a contingency plan should accompany all critical risks.

A gas processing project is not complete until the plant, unit or equipment is placed in service. An evaluation of the operability should be a deliverable upon completion of the project.

REFERENCES

Greer, M., 2002. The Project Manager's Partner: A Step-by-step Guide to Project Management, second ed. Human Resource Development Press, Amherst, MA, USA.

Hauge, L.H., Cramer, E., November 13–15, 2002. Project Risk Management in Deepwater Field Developments. Paper presented at the Deep Offshore Technology Conference, New Orleans, LA, USA.

HRDC, 2003. Introduction to Project Management Principles, Learning Module, Office of Learning Technologies. Human Resources Development Canada (HRDC), Canada.

KBR, 2012. Operator Training Simulators. http://www.kbr.com/Services/Advanced-Chemical-Engineering-Services/Operator-Training-Simulators.

McIntire, P.B., 2001. Cost estimating challenges face frontier projects. Oil & Gas Journal 99 (33), 30–34.

Mullick, S., Dhole, V., 2007. Consider integrated plant design and engineering. Hydrocarbon Processing 86 (12), 81–85.

Safakish, G., Wood, D., 2010. Cultural issues in multi-cultural mega-projects. Journal of Information, Intelligence and Knowledge 2 (1), 27–34.

Safakish, G., Wood, D., 2011. Approaches to communication and cultural issues to aid planning and execution of oil and gas sector mega-projects. Energy Sources Part B 6, 126–135.

Wood, D., 2001. Probabilistic methods with simulation help predict timing, costs of projects. Oil & Gas Journal 99 (46), 79–83.

Wood, D., Mokhatab, S., 2006. Challenges, risks can be managed in deepwater oil and gas projects. Oil & Gas Journal 104 (44), 37–42.

Wood, D., Randall, S., 2005. Implementing ERM. Oil & Gas Journal, Part 1: 8-23, 103, 11 (March 21) and Part 2: 20–26, 103, 12 (March 28).

Wood, D., Lamberson, G., Mokhatab, S., 2008a. Project execution risk management for addressing constructability. Hydrocarbon Processing 87 (12), 35–42.

Wood, D., Lamberson, G., Mokhatab, S., 2008b. Better manage risks of gas-processing projects. Hydrocarbon Processing 87 (6), 124–128.

Wood, D., Lamberson, G., Mokhatab, S., 2011. Staffing strategies for large projects must tackle many diverse issues. Oil & Gas Financial Journal 8 (9), 35–40.

Appendix 1

CONVERSION FACTORS

Length
1 m = 39.37 in. = 10^6 μm = 10^{10} A°
1 in. = 2.54 cm
1 ft = 30.48 cm = 0.3048 m
1 mile = 5280 ft = 1760 yds = 1609.344 m

Mass
1 lbm = 453.6 gr = 0.4536 kg = 7000 grain
1 kg = 1000 gr = 2.2046 lbm
1 slug = 1 lbf s^2/ft = 32.174 lbm
1 US ton = 2000 lbm (also called short ton)
1 long ton = 2240 lbm (also called British ton)
1 tonne = 1000 kg (also called metric ton)

Force
1 lbf = 4.448 N = 4.448 × 10^5 dyn = 32.174 poundals = 32.174 lbm ft/s^2 = 1 lbw

Pressure
1 atm = 14.696 psia = 2116 lbf/ft^2 = 29.92 in Hg
= 760 mm Hg
= 760 Torr = 1.013 bar = 33.9 ft H_2O = 1.013 × 10^5 Pa = 101.3 kPa
1 Pa = 1 N/m^2 = 10^{-5} bars

Volume
1 ft^3 = 7.4805 US gal = 6.23 Imperial gal
= 28.317 lit
1 m^3 = 1000 lit = 264.2 US gal = 35.31 ft^3
1 bbl = 42 US gal (oil) = 5.615 ft^3
1 lit = 1000 cc

Density
Water = 62.43 lbm/ft^3 = 1000 kg/m^3 = 1 gr/cm^3

Temperature
°F = 1.8 (°C) + 32
°R = °F + 459.67 = 1.8 (°K)

Energy
1 J = 1 W s = 1 kg m^2/s^2 = 1 N m^3 = 10^7 dyne cm = 10^7 erg
1 Btu = 778 ft lbf = 252 cal = 1055 J = 10.41 lit atm
1 HP h = 2545 Btu
1 kW h = 3412 Btu = 1.341 HP h

Power
1 HP = 550 ft lbf/s = 33000 ft lbf/min = 746 W = 0.746 kW

Gas Constant
R = 1.9859 Btu/lbmole °R.
= 1.9859 cal/grmole °K.
= 0.73024 atm ft^3/lbmole °R.
= 1545.3 ft.lbf/lbmole °R.
= 10.732 psia.ft^3/lbmole °R.
= 0.082057 lit. atm/grmole °K.
= 82.057 atm cm^3/grmole °K.
= 8314.5 Pa m^3/kgmole °K.
= 8.3145 kJ/kgmole °K

Dynamic Viscosity
1 cp = 0.01 Poise = 0.01 g/cm s = 0.01 dyne s/cm^2 = 0.001 kg/m s = 0.001 Pa s = 0.001 N s/m^2 = 2.42 lbm/ft h = 0.0752 slug/ft h = 6.72 × 10^{-4} lbm/ft s = 2.09 × 10^{-5} lbf s/ft^2
1 Pa s = 0.0209 lbf s/ft^2 = 0.672 lbm/ft s

Kinematic Viscosity
1 St = 1 cm^2/s = 0.0001 m^2/s
1 ft^2/s = 929 St = 0.0929 m^2/s

Force-mass conversion factor
g_c = 1 kg m/s^2 N =
1 g cm/s^2 dyne = 32.174 lbm ft/s^2 lbf = 1 slug ft/s^2 lbf

Acceleration due to gravity
g = 32.2 ft/s^2 = 9.81 m/s^2 = 981 cm/s^2 (varies very slightly with longitude and elevation)

Appendix 2

NORMAL AND STANDARD GAS CONDITIONS

Gas volumes given are for ideal gas only.

1. Normal: continental and scientific applications
   0°C, 1.01325 bar, gas volume = 22.4136 m^3/kg-mol
   32°F, 14.696 psia, gas volume = 359.031 ft^3/lb-mol
2. Standard: US engineering applications
   15.5556°C, 1.01325 bar, gas volume = 23.6900 m^3/kg-mol
   60°F, 14.696 psia, gas volume = 379.49 ft^3/lb-mol
3. Standard: API 2564, SI, 15°C, 101.325 kPa, gas volume = 23.6444 m^3/kg-mol

Appendix 3

PHYSICAL PROPERTIES OF FLUIDS

Tables 3.1 Properties of Hydrocarbons and Common Gases (GPSA, 2004)

Component	Formula	Molecular Weight	Boiling Point °F (1 atm)	Vapor Pressure at 100°F, Psia	Critical		Liquid Specific Gravity 60/60°F	Volume Ratio, Scf Gas per gal Liquid
					Pressure, Psia	Temperature, °F		
Methane	CH_4	16.043	−258.73	(5000)[a]	666.4	−116.67	0.3[a]	59.135[a]
Ethane	C_2H_6	30.070	−127.49	(800)[a]	706.5	89.92	0.35619[c]	37.476[c]
Propane	C_3H_8	44.097	−43.75	188.64	616.0	206.06	0.50699[c]	36.375[c]
Isobutane	C_4H_{10}	58.123	10.78	72.581	527.9	274.46	0.56287[c]	30.639[c]
n-Butane	C_4H_{10}	58.123	31.08	51.706	550.6	305.62	0.58401[c]	31.790[c]
Isopentane	C_5H_{12}	72.150	82.12	20.445	490.4	369.10	0.62470	27.393
n-Pentane	C_5H_{12}	72.150	96.92	15.574	488.6	385.8	0.63112	27.674
n-Hexane	C_6H_{14}	86.177	155.72	4.960	436.9	453.6	0.66383	24.371
n-Heptane	C_7H_{16}	100.204	209.16	1.620	396.8	512.7	0.68820	21.729
n-Octane	C_8H_{18}	114.231	258.21	0.537	360.7	564.2	0.70696	19.580
n-Decane	$C_{10}H_{22}$	142.285	345.48	0.061	305.2	652.0	0.73421	16.326
Nitrogen	N_2	28.013	−320.45	___	493.1	−232.51	0.80940[d]	91.413[c]
Oxygen	O_2	31.999	−297.33	___	731.4	−181.43	1.1421[d]	112.93[c]
Carbon Dioxide	CO_2	44.010	−109.26[b]	___	1071	87.91	0.81802[c]	58.807[c]
Hydrogen sulfide	H_2S	34.08	−76.50	394.59	1300	212.45	0.80144[c]	74.401[c]
Water	H_2O	18.0115	212.00	0.950	3198	705.16	1.00000[d]	175.62[c]
Air	Mixture	28.9625	−317.8	___	546.9	−221.31	0.87476[d]	95.557[c]

Continued

Tables 3.1 Properties of Hydrocarbons and Common Gases (GPSA, 2004)—cont'd

Component	Acentric Factor, ω	Flammability Limits, vol% in Air Mix		Heating Value at 60°F, 1 atm, Btu/scf		Freezing Point at 1 atm, °F	Heat of Vaporization at 1 atm, Btu/lb	
		Lower	Upper	Net	Gross			
Methane	0.0104	5.0	15.0	909.4	1010.0	−296.44[e]	219.45	
Ethane	0.0979	2.9	13.0	1618.7	1769.6	−297.04[e]	211.14	
Propane	0.1522	2.0	9.5	2314.9	2516.1	−305.73[e]	183.01	
Isobutane	0.1852	1.8	8.5	3000.4	3251.9	−255.82	157.23	
n-Butane	0.1995	1.5	9.0	3010.8	3262.3	−217.05	165.93	
Isopentane	0.2280	1.3	8.0	3699.0	4000.9	−255.82	147.12	
n-Pentane	0.2514	1.4	8.3	3706.9	4008.9	−217.05	153.57	
n-Hexane	0.2994	1.1	7.7	4403.8	4755.9	−139.58	143.94	
n-Heptane	0.3494	1.0	7.0	5100.8	5502.5	−131.05	136.00	
n-Octane	0.3977	0.8	6.5	5796.1	6248.9	−70.18	129.52	
n-Decane	0.4898	0.7	5.4	7189.6	7742.9	−21.36	119.65	
Nitrogen	0.0372	___	___	___	___	−346.00[f]	85.59	
Oxygen	0.0216	___	___	___	___	−361.82[f]	91.59	
Carbon dioxide	0.2667	___	___	___	___	−69.83	246.47	
Hydrogen sulfide	0.0948	4.3	45.5	586.8	637.1	−121.88[f]	235.63	
Water	0.3442	___	___	___	___	32.00	970.18	
Air	___	___	___	___	___	___	88.20	

[a] *Above critical point, extrapolated or estimated.*
[b] *Sublimation point.*
[c] *At saturation pressure, 60°F.*
[d] *At normal boiling point.*
[e] *Gas at 60 °F, liquid at normal boiling point.*
[f] *At the triple point pressure.*
GPSA, 2004. Engineering Data Book, 12th Edition, Gas Processors Suppliers Association (GPSA), Tulsa, OK, USA.

Table 3.2 Approximate Ratio of Specific Heats ("k" values) for Various Gases[b]

Gas	Symbol	Molecular Weight	k at 14.7 Psia		Density at 14.7 psi and 60°F Lbs/cu. ft
			60°F	150°F	
Monatomic	He, Kr, Ne, Hg	—	1.67	—	—
Most diatomic	O_2, N_2, H_2, and so on	—	1.4	—	—
Acetylene	C_2H_2	26.03	1.3	1.22	0.0688
Air	—	28.97	1.406	1.40	0.0765
Ammonia	NH_3	17.03	1.317	1.29	0.451
Argon	A	—	1.667	—	0.1056
Benzene	C_6H_6	78.0	1.08	1.09	0.2064
Butane	C_4H_{10}	58.1	1.11	1.08	0.1535
Isobutane	C_4H_{10}	58.1	1.11	1.08	0.1578
Butylene	C_4H_8	56.1	1.1	1.09	0.1483
Isobutene	C_4H_8	56.1	1.1	1.09	0.1483
Carbon dioxide	CO_2	44.0	1.3	1.27	0.1164
Carbon monoxide	CO	28.0	1.4	1.4	0.0741
Carbon tetrachloride	CCl_4	153.8	1.18	—	0.406
Chlorine	Cl_2	70.9	1.33	—	0.1875
Dichlorodifluoromethane	CCl_2F_2	120.9	1.13	—	—
Dichloromethane	CH_2Cl_2	84.9	1.13	—	0.2215
Ethane	C_2H_6	30.0	1.22	1.17	0.0794
Ethylene	C_2H_4	28.1	1.25	1.21	0.0741
Ethyl chloride	C_2H_5Cl	64.5	1.13	—	0.1705
Flue gas	—	—	1.4	—	—
Helium	He	4.0	1.667	—	0.01058
Hexane	C_6H_{14}	88.1	1.08	1.05	0.2276
Heptane	C_7H_{16}	100.2	—	1.04	0.264
Hydrogen	H_2	2.01	1.41	1.40	0.0053
Hydrogen chloride	HCl	36.5	1.48	—	0.09650
Hydrogen sulfide	H_2S	34.1	1.30	1.31	0.0901
Methane	CH_4	16.03	1.316	1.28	0.0423
Methyl chloride	CH_3Cl	50.5	1.20	—	0.1336
Natural gas (approximately)	—	19.5	1.27	—	0.0514
Nitric oxide	NO	30.0	1.40	—	0.0793
Nitrogen	N_2	28.0	1.41	1.40	0.0743
Nitrous oxide	N_2O	44.0	1.311	—	0.1163
Oxygen	O_2	32.0	1.4	1.39	0.0846
Pentane	C_5H_{12}	72.1	1.06	1.06	0.1905
Propane	C_3H_8	44.1	1.15	1.11	0.1164
Propylene	C_3H_6	42.0	1.16	—	0.1112
Sulfur dioxide	SO_2	64.1	1.256	—	0.1694
Water vapor (steam)	H_2O	18.0	1.33[a]	1.32	0.04761

[a] *At 212° F.*

[b] *Compiled from: "Plain Talks on Air and Gas Compression, Fourth of Series," Worthington Corp. and "Reciprocating Compressor Calculation Data Cooper–Bessemer Corp (1956).*

Table 3.3 Physical Properties of Selected Amines (GPSA, 2004)

Compound	Monoethanol-amine	Diethanol-amine	Methyldiethanol-amine	Diglycol-amine	Diisopropanol-amine
Formula	$HOC_2H_4NH_2$	$(HOC_2H_4)_2NH$	$(HOC_2H_4)_2NCH_3$	$H(OC_2H_4)_2NH_2$	$(HOC_3H_6)_2NH$
Molecular weight	61.08	105.14	119.16	105.14	133.19
Boiling point at 760 mmHg, °C	170.5	269	247	221	248.7
Freezing point, °C	10.5	28.0	−23	−12.5	42
Critical constants					
Pressure, kPa (abs)	5985	3273		3772	3770
Temperature, °C	350	442.1		402.6	399.2
Density at 20°C, gr/cc	1.018	1.095		1.058 at 15.6°C	0.999 at 30°C
Weight, kg/m^3	1016 at 15.6°C	1089 at 15.6°C	1040	1057 at 15.6°C	
Relative density 20°C/20°C	1.0179	1.0919 at 30°C/20°C	1.0418	1.0572	0.989 at 45°C/20°C
Specific heat at 15.6°C, kJ/(kg °C)	2.55 at 20°C	2.51	2.24	2.39	2.89 at 30°C
Thermal conductivity at 20°C, W/(m °C)	0.256	0.220	0.275	0.209	—
Latent heat of vaporization, kJ/kg	826 at 760 mmHg	670 at 73 mmHg	476	510 at 760 mmHg	430 at 760 mmHg
Heat of reaction, kJ/kg of acid gas					
H_2S				−1568	—
CO_2				−1977	—
Viscosity, mPa.sec	24.1 at 20°C	350 at 20°C (at 90% wt. solution)	1.3×10^{-6} m^2/s at 10°C	40 at 16°C	870 at 30°C, 198 at 45°C, 86 at 54°C
Refractive index, N_d 20°C	1.4539	1.4776	1.469	1.4598	1.4542 at 45°C
Flash point, COC, °C	93	138	129.4	127	124

Table 3.4 Physical Properties of Selected Glycols and Methanol (GPSA, 2004)

Compound	Ethylene Glycol	Diethylene Glycol	Triethylene Glycol	Tetraethylene Glycol	Methanol
Formula	$C_2H_6O_2$	$C_4H_{10}O_3$	$C_6H_{14}O_4$	$C_6H_{18}O_5$	CH_3OH
Molecular mass	62.1	106.1	150.2	194.2	32.04
Boiling Point at 760 mmHg, °C	197.3	244.8	285.5	314	64.5
Vapor Pressure at 77°F (25°C), mmHg	0.12	<0.01	<0.01	<0.01	120
Density at 77°F (25°C), kg/m^3	1110	1113	1119	1120	790
Freezing Point, °C	−13	−8	−7	−5.5	−97.8
Pour Point, °C	—	−54	−58	−41	—
Viscosity in centipoise at 77°F (25°C); and at 140°F (60°C)	16.5; 4.68	28.2; 6.99	37.3; 8.77	44.6; 10.2	0.52
Specific Heat at 77°F (25°C), kJ/(kg.K)	2.43	2.30	2.22	2.18	2.52
Flash Point, °C (PMCC)	116	124	177	204	12
Approximate decomposition temperatures, °C[a]	165	164	207	238	—

Note: These properties are laboratory results on pure compounds or typical of the products but should not be confused with or regarded as specifications.

[a]*Glycols decompose at temperatures below their atmospheric boiling point.*

Index

'*Note:* Page numbers followed by "f" indicate figures, "t" indicate tables.'

A

B

C

D

E

F

G

H

I

M

N

O

P

Q

R

S

T

U

V

W

Y

Z

HANDBOOK OF NATURAL GAS TRANSMISSION AND PROCESSING

PRINCIPLES AND PRACTICES FOURTH EDITION

SAEID MOKHATAB, WILLIAM A. POE, AND JOHN Y. MAK

Written by an internationally-recognized team of natural gas industry experts, the fourth edition of *Handbook of Natural Gas Transmission and Processing* is a unique, well-researched, and comprehensive work on the design and operation aspects of natural gas transmission and processing. Six new chapters have been added to include detailed discussion of the thermodynamic and energy efficiency of relevant processes, and recent developments in processing super-rich gas, high CO_2 content gas, and high nitrogen content gas with other contaminants. The new material describes technologies for processing today's unconventional gases, providing a fresh approach in solving today's gas processing challenges including greenhouse gas emissions. The updated edition is an excellent platform for gas processors and educators to understand the basic principles and innovative designs necessary to meet today's environmental and sustainability requirement while delivering acceptable project economics.

KEY FEATURES

- Covers all technical and operational aspects of natural gas transmission and processing.
- Provides pivotal updates on the latest technologies, applications, and solutions.
- Helps to understand today's natural gas resources, and the best gas processing technologies.
- Offers practical advice for the optimal design and operation of gas plants.

ABOUT THE AUTHORS

Saeid Mokhatab is a world class expert in the field of natural gas processing whose contributions to the industry have shaped the evolution of technology over the years. His numerous publications, which are widely read and highly respected, have set the technical standards in the natural gas and LNG industry.

William A. "Bill" Poe is a Senior Principal Technical Consultant at the Invensys Division of Schneider Electric, USA, where he has developed advanced process control and optimization master plans for international companies such as Saudi Aramco, ADNOC, Statoil, and PDVSA, as well as automation and advanced process control feasibility studies for over a hundred natural gas processing plants.

John Y. Mak is a Senior Fellow and Technical Director at Fluor, USA and leads the technology and design development for the chemical and energy sectors at Fluor. He has been with Fluor for over forty years and has been leading domestic and global oil and gas and refinery projects from conceptual design, feasibility study, FEED, and detailed engineering to plant startup and operations.

RELATED TITLES

Mokhatab, Mak, Valappil, and Wood, *Handbook of Liquefied Natural Gas*, 978-0-12-404585-9
Poe and Mokhatab, *Modeling, Control and Optimization of Natural Gas Processing Plants*, 978-0-12-802961-9
Stewart and Arnold/*Surface Production Operations, Volume I, Third Edition*, 978-0-7506-7853-7
Stewart and Arnold/*Surface Production Operations, Volume 2, Third Edition*, 978-0-12-382207-9

PETROLEUM AND PETROCHEMICAL ENGINEERING

ISBN 978-0-12-815817-3
9 780128 158173

ELSEVIER

G P P

Gulf Professional Publishing
An imprint of Elsevier
elsevier.com/books-and-journals